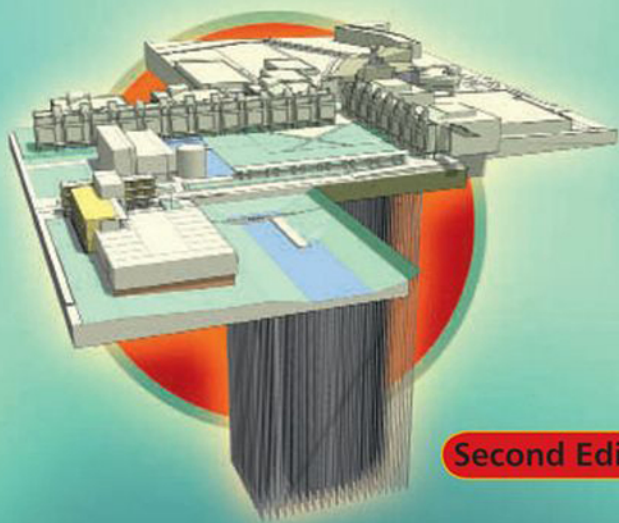


Ibrahim Dincer

Marc A. Rosen

# THERMAL ENERGY STORAGE SYSTEMS and APPLICATIONS



Second Edition

 WILEY



# **THERMAL ENERGY STORAGE**



# THERMAL ENERGY STORAGE

## SYSTEMS AND APPLICATIONS, SECOND EDITION

**İbrahim Dincer**

**and**

**Marc A. Rosen**

*Professor of Mechanical Engineering*

*Faculty of Engineering and Applied Science*

*University of Ontario Institute of Technology*

*Ontario, Canada*

 **WILEY**

A John Wiley and Sons, Ltd., Publication

This edition first published 2011  
Copyright © 2011, John Wiley & Sons, Ltd

First Edition published in 2002

*Registered office*

John Wiley & Sons Ltd, The Atrium, Southern Gate, Chichester, West Sussex, PO19 8SQ, United Kingdom

For details of our global editorial offices, for customer services and for information about how to apply for permission to reuse the copyright material in this book please see our website at [www.wiley.com](http://www.wiley.com).

The right of the author to be identified as the author of this work has been asserted in accordance with the Copyright, Designs and Patents Act 1988.

All rights reserved. No part of this publication may be reproduced, stored in a retrieval system, or transmitted, in any form or by any means, electronic, mechanical, photocopying, recording or otherwise, except as permitted by the UK Copyright, Designs and Patents Act 1988, without the prior permission of the publisher.

Wiley also publishes its books in a variety of electronic formats. Some content that appears in print may not be available in electronic books.

Designations used by companies to distinguish their products are often claimed as trademarks. All brand names and product names used in this book are trade names, service marks, trademarks or registered trademarks of their respective owners. The publisher is not associated with any product or vendor mentioned in this book. This publication is designed to provide accurate and authoritative information in regard to the subject matter covered. It is sold on the understanding that the publisher is not engaged in rendering professional services. If professional advice or other expert assistance is required, the services of a competent professional should be sought.

***Library of Congress Cataloguing-in-Publication Data***

Dincer, Ibrahim, 1964-

Thermal energy storage : systems and applications / Ibrahim Dincer, Marc A. Rosen. – 2nd ed.  
p. cm.

Rev. ed. of: Thermal energy storage systems and applications / [edited by] Ibrahim Dincer, and Marc Rosen. c2002.  
Includes index.

ISBN 978-0-470-74706-3 (cloth)

1. Heat storage. I. Rosen, Marc (Marc A.) II. Thermal energy storage systems and applications. III. Title.  
TJ260.T493 2010  
621.402'8–dc22

2010020654

A catalogue record for this book is available from the British Library.

Print ISBN: 978-0-470-74706-3

ePDF ISBN: 978-0-470-97073-7

oBook ISBN: 978-0-470-97075-1

Set in 9/11 Times by Laserwords Private Limited, Chennai

Front cover image: Borehole thermal energy storage system at the University of Ontario Institute of Technology, Oshawa, Ontario, Canada. The companies involved in the design and construction were Diamond and Schmitt Architects Incorporated and Keen Engineering with Brian Beatty and Associates.

*To my wife, Gülşen, and my children,  
Meliha, Miray, İbrahim Eren,  
Zeynep, and İbrahim Emir  
for their inspiration.*

*And to those who have helped and supported  
me in any way throughout  
my education and professional life.*

İbrahim Dinçer

*To my wife, Margot, and my children,  
Allison and Cassandra for their inspiration.  
And to Frank C. Hooper and David S. Scott,  
two giants in the field of energy and wonderful mentors.*

Marc A. Rosen





# Contents

<b>About the Authors</b>	<b>xv</b>
<b>Preface</b>	<b>xvii</b>
<b>Acknowledgements</b>	<b>xix</b>
<b>1 General Introductory Aspects for Thermal Engineering</b>	<b>1</b>
1.1 Introduction	1
1.2 Systems of Units	2
1.3 Fundamental Properties and Quantities	2
1.3.1 Mass, Time, Length, and Force	2
1.3.2 Pressure	2
1.3.3 Temperature	4
1.3.4 Specific Volume and Density	6
1.3.5 Mass and Volumetric Flow Rates	6
1.4 General Aspects of Thermodynamics	7
1.4.1 Thermodynamic Systems	7
1.4.2 Process	7
1.4.3 Cycle	7
1.4.4 Thermodynamic Property	7
1.4.5 Sensible and Latent Heats	7
1.4.6 Latent Heat of Fusion	8
1.4.7 Vapor	8
1.4.8 Thermodynamic Tables	8
1.4.9 State and Change of State	9
1.4.10 Specific Internal Energy	10
1.4.11 Specific Enthalpy	10
1.4.12 Specific Entropy	11
1.4.13 Pure Substance	11
1.4.14 Ideal Gases	11
1.4.15 Energy Transfer	15
1.4.16 Heat	16
1.4.17 Work	16
1.4.18 The First Law of Thermodynamics	17
1.4.19 The Second Law of Thermodynamics	17
1.4.20 Reversibility and Irreversibility	18
1.4.21 Exergy	18
1.5 General Aspects of Fluid Flow	20
1.5.1 Classification of Fluid Flows	20
1.5.2 Viscosity	22

1.5.3	<i>Equations of Flow</i>	23
1.5.4	<i>Boundary Layer</i>	29
1.6	General Aspects of Heat Transfer	32
1.6.1	<i>Conduction Heat Transfer</i>	33
1.6.2	<i>Convection Heat Transfer</i>	34
1.6.3	<i>Radiation Heat Transfer</i>	36
1.6.4	<i>Thermal Resistance</i>	37
1.6.5	<i>The Composite Wall</i>	38
1.6.6	<i>The Cylinder</i>	38
1.6.7	<i>The Sphere</i>	39
1.6.8	<i>Conduction with Heat Generation</i>	40
1.6.9	<i>Natural Convection</i>	42
1.6.10	<i>Forced Convection</i>	43
1.7	Concluding Remarks	45
<b>2</b>	<b>Energy Storage Systems</b>	<b>51</b>
2.1	Introduction	51
2.2	Energy Demand	52
2.3	Energy Storage	53
2.4	Energy Storage Methods	54
2.4.1	<i>Mechanical Energy Storage</i>	54
2.4.2	<i>Chemical Energy Storage</i>	62
2.4.3	<i>Biological Storage</i>	75
2.4.4	<i>Magnetic Storage</i>	75
2.4.5	<i>Thermal Energy Storage (TES)</i>	76
2.5	Hydrogen for Energy Storage	77
2.5.1	<i>Storage Characteristics of Hydrogen</i>	77
2.5.2	<i>Hydrogen Storage Technologies</i>	77
2.5.3	<i>Hydrogen Production</i>	78
2.6	Comparison of ES Technologies	80
2.7	Concluding Remarks	80
<b>3</b>	<b>Thermal Energy Storage (TES) Methods</b>	<b>83</b>
3.1	Introduction	83
3.2	Thermal Energy	84
3.3	Thermal Energy Storage	85
3.3.1	<i>Basic Principle of TES</i>	86
3.3.2	<i>Benefits of TES</i>	89
3.3.3	<i>Criteria for TES Evaluation</i>	90
3.3.4	<i>TES Market Considerations</i>	96
3.3.5	<i>TES Heating and Cooling Applications</i>	99
3.3.6	<i>TES Operating Characteristics</i>	103
3.3.7	<i>ASHRAE TES Standards</i>	104
3.4	Solar Energy and TES	104
3.4.1	<i>TES Challenges for Solar Applications</i>	105
3.4.2	<i>TES Types and Solar Energy Systems</i>	105
3.4.3	<i>Storage Durations and Solar Applications</i>	106
3.4.4	<i>Building Applications of TES and Solar Energy</i>	107
3.4.5	<i>Design Considerations for Solar Energy-Based TES</i>	108
3.5	TES Methods	109
3.6	Sensible TES	109
3.6.1	<i>Thermally Stratified TES Tanks</i>	111

3.6.2	<i>Concrete TES</i>	114
3.6.3	<i>Rock and Water/Rock TES</i>	114
3.6.4	<i>Aquifer Thermal Energy Storage (ATES)</i>	118
3.6.5	<i>Solar Ponds</i>	124
3.6.6	<i>Evacuated Solar Collector TES</i>	125
3.7	Latent TES	127
3.7.1	<i>Operational Aspects of Latent TES</i>	128
3.7.2	<i>Phase Change Materials (PCMs)</i>	129
3.8	Cold Thermal Energy Storage (CTES)	142
3.8.1	<i>Working Principle</i>	142
3.8.2	<i>Operational Loading of CTES</i>	143
3.8.3	<i>Design Considerations</i>	144
3.8.4	<i>CTES Sizing Strategies</i>	146
3.8.5	<i>Load Control and Monitoring in CTES</i>	147
3.8.6	<i>CTES Storage Media Selection and Characteristics</i>	148
3.8.7	<i>Storage Tank Types for CTES</i>	152
3.8.8	<i>Chilled-Water CTES</i>	153
3.8.9	<i>Ice CTES</i>	158
3.8.10	<i>Ice Forming</i>	174
3.8.11	<i>Ice Thickness Controls</i>	174
3.8.12	<i>Technical and Design Aspects of CTES</i>	178
3.8.13	<i>Selection Aspects of CTES</i>	179
3.8.14	<i>Cold-Air Distribution in CTES</i>	180
3.8.15	<i>Potential Benefits of CTES</i>	183
3.8.16	<i>Electric Utilities and CTES</i>	184
3.9	Seasonal TES	185
3.9.1	<i>Seasonal TES for Heating Capacity</i>	185
3.9.2	<i>Seasonal TES for Cooling Capacity</i>	186
3.9.3	<i>Illustration</i>	186
3.10	Concluding Remarks	187
<b>4</b>	<b>Thermal Energy Storage and Environmental Impact</b>	<b>191</b>
4.1	Introduction	191
4.2	Energy and the Environment	192
4.3	Major Environmental Problems	193
4.3.1	<i>Acid Rain</i>	194
4.3.2	<i>Greenhouse Effect (Global Climate Change)</i>	195
4.3.3	<i>Stratospheric Ozone Depletion</i>	196
4.4	Environmental Impact and TES Systems and Applications	198
4.5	Potential Solutions to Environmental Problems	198
4.5.1	<i>General Solutions</i>	198
4.5.2	<i>TES-Related Solutions</i>	199
4.6	Sustainable Development	199
4.6.1	<i>Conceptual Issues</i>	200
4.6.2	<i>The Brundtland Commission's Definition</i>	200
4.6.3	<i>Environmental Limits</i>	201
4.6.4	<i>Global, Regional, and Local Sustainability</i>	201
4.6.5	<i>Environmental, Social, and Economic Components of Sustainability</i>	201
4.6.6	<i>Energy and Sustainable Development</i>	202
4.6.7	<i>Environment and Sustainable Development</i>	202
4.6.8	<i>Achieving Sustainable Development in Larger Countries</i>	203
4.6.9	<i>Essential Factors for Sustainable Development</i>	203

4.7	Illustrative Examples and Case Studies	204
4.7.1	<i>The South Coast Air Quality Management District (California)</i>	204
4.7.2	<i>Anova Verzekering Co. Building (Amersfoort, The Netherlands)</i>	204
4.7.3	<i>The Trane Company's Technology Center (La Crosse, WI)</i>	205
4.7.4	<i>The Ministry of Finance Building (Bercy, France)</i>	206
4.7.5	<i>The City of Saarbrucken (Saarbrucken, Germany)</i>	207
4.8	Concluding Remarks	207
<b>5</b>	<b>Thermal Energy Storage and Energy Savings</b>	<b>211</b>
5.1	Introduction	211
5.2	TES and Energy Savings	212
5.2.1	<i>Utilization of Waste or Surplus Energy</i>	213
5.2.2	<i>Reduction of Demand Charges</i>	214
5.2.3	<i>Deferring Equipment Purchases</i>	215
5.3	Additional Energy Savings Considerations for TES	215
5.3.1	<i>Energy for Heating, Refrigeration, and Heat Pump Equipment</i>	215
5.3.2	<i>Storage Size Limitations</i>	216
5.3.3	<i>Thermal Load Profiles</i>	216
5.3.4	<i>Optimization of Conventional Systems</i>	217
5.4	Energy Conservation with TES: Planning and Implementation	217
5.5	Some Limitations on Increased Efficiency	218
5.5.1	<i>Practical and Theoretical Limitations</i>	218
5.5.2	<i>Efficiency Limitations and Exergy</i>	219
5.6	Energy Savings for Cold TES	219
5.6.1	<i>Economic Aspects of TES Systems for Cooling Capacity</i>	221
5.6.2	<i>Energy Savings by Cold TES</i>	221
5.6.3	<i>Case Studies for TES Energy Savings</i>	225
5.7	Concluding Remarks	230
<b>6</b>	<b>Energy and Exergy Analyses of Thermal Energy Storage Systems</b>	<b>233</b>
6.1	Introduction	233
6.2	Theory: Energy and Exergy Analyses	234
6.2.1	<i>Motivation for Energy and Exergy Analyses</i>	235
6.2.2	<i>Conceptual Balance Equations for Mass, Energy, and Entropy</i>	235
6.2.3	<i>Detailed Balance Equations for Mass, Energy, and Entropy</i>	236
6.2.4	<i>Basic Quantities for Exergy Analysis</i>	238
6.2.5	<i>Detailed Exergy Balance</i>	240
6.2.6	<i>The Reference Environment</i>	241
6.2.7	<i>Efficiencies</i>	243
6.2.8	<i>Properties for Energy and Exergy Analyses</i>	244
6.2.9	<i>Implications of Results of Exergy Analyses</i>	245
6.2.10	<i>Steps for Energy and Exergy Analyses</i>	246
6.3	Thermodynamic Considerations in TES Evaluation	246
6.3.1	<i>Determining Important Analysis Quantities</i>	246
6.3.2	<i>Obtaining Appropriate Measures of Efficiency</i>	246
6.3.3	<i>Pinpointing Losses</i>	247
6.3.4	<i>Assessing the Effects of Stratification</i>	248
6.3.5	<i>Accounting for Time Duration of Storage</i>	248
6.3.6	<i>Accounting for Variations in Reference-Environment Temperature</i>	249
6.3.7	<i>Closure</i>	249

---

6.4	Exergy Evaluation of a Closed TES System	249
6.4.1	<i>Description of the Case Considered</i>	250
6.4.2	<i>Analysis of the Overall Process</i>	251
6.4.3	<i>Analysis of Subprocesses</i>	253
6.4.4	<i>Alternative Formulations of Subprocess Efficiencies</i>	255
6.4.5	<i>Relations between Performance of Subprocesses and Overall Process</i>	256
6.4.6	<i>Example</i>	257
6.4.7	<i>Closure</i>	260
6.5	Appropriate Efficiency Measures for Closed TES Systems	260
6.5.1	<i>TES Model Considered</i>	261
6.5.2	<i>Energy and Exergy Balances</i>	261
6.5.3	<i>Energy and Exergy Efficiencies</i>	262
6.5.4	<i>Overall Efficiencies</i>	262
6.5.5	<i>Charging-Period Efficiencies</i>	263
6.5.6	<i>Storing-Period Efficiencies</i>	263
6.5.7	<i>Discharging-Period Efficiencies</i>	264
6.5.8	<i>Summary of Efficiency Definitions</i>	265
6.5.9	<i>Illustrative Example</i>	266
6.5.10	<i>Closure</i>	267
6.6	Importance of Temperature in Performance Evaluations for Sensible TES Systems	269
6.6.1	<i>Energy, Entropy, and Exergy Balances for the TES System</i>	269
6.6.2	<i>TES System Model Considered</i>	269
6.6.3	<i>Analysis</i>	270
6.6.4	<i>Comparison of Energy and Exergy Efficiencies</i>	271
6.6.5	<i>Illustration</i>	272
6.6.6	<i>Closure</i>	272
6.7	Exergy Analysis of Aquifer TES Systems	272
6.7.1	<i>ATES Model</i>	273
6.7.2	<i>Energy and Exergy Analyses</i>	274
6.7.3	<i>Effect of a Threshold Temperature</i>	277
6.7.4	<i>Case Study</i>	277
6.7.5	<i>Closure</i>	281
6.8	Exergy Analysis of Thermally Stratified Storages	281
6.8.1	<i>General Stratified TES Energy and Exergy Expressions</i>	282
6.8.2	<i>Temperature-Distribution Models and Relevant Expressions</i>	284
6.8.3	<i>Discussion and Comparison of Models</i>	289
6.8.4	<i>Illustrative Example: The Exergy-Based Advantage of Stratification</i>	289
6.8.5	<i>Illustrative Example: Evaluating Stratified TES Energy and Exergy</i>	290
6.8.6	<i>Increasing TES Exergy-Storage Capacity Using Stratification</i>	293
6.8.7	<i>Illustrative Example: Increasing TES Exergy with Stratification</i>	297
6.8.8	<i>Closure</i>	297
6.9	Energy and Exergy Analyses of Cold TES Systems	298
6.9.1	<i>Energy Balances</i>	299
6.9.2	<i>Exergy Balances</i>	301
6.9.3	<i>Energy and Exergy Efficiencies</i>	301
6.9.4	<i>Illustrative Example</i>	302
6.9.5	<i>Case Study: Thermodynamic Performance of a Commercial Ice TES System</i>	304
6.9.6	<i>Closure</i>	309
6.10	Exergy-Based Optimal Discharge Periods for Closed TES Systems	309
6.10.1	<i>Analysis Description and Assumptions</i>	309

6.10.2	<i>Evaluation of Storage-Fluid Temperature During Discharge</i>	310
6.10.3	<i>Discharge Efficiencies</i>	311
6.10.4	<i>Exergy-Based Optimum Discharge Period</i>	312
6.10.5	<i>Illustrative Example</i>	312
6.10.6	<i>Closure</i>	314
6.11	Exergy Analysis of Solar Ponds	314
6.11.1	<i>Experimental Solar Pond</i>	315
6.11.2	<i>Data Acquisition and Analysis</i>	316
6.11.3	<i>Energy and Exergy Assessments</i>	320
6.11.4	<i>Potential Improvements</i>	322
6.12	Concluding Remarks	323
	Appendix: Glossary of Selected Exergy-Related Terminology	332
<b>7</b>	<b>Numerical Modeling and Simulation of Thermal Energy Storage Systems</b>	<b>335</b>
7.1	Introduction	335
7.2	Approaches and Methods	336
7.3	Selected Applications	337
7.4	Numerical Modeling, Simulation, and Analysis of Sensible TES Systems	340
7.4.1	<i>Modeling</i>	340
7.4.2	<i>Heat Transfer and Fluid Flow Analysis</i>	343
7.4.3	<i>Simulation</i>	344
7.4.4	<i>Thermodynamic Analysis</i>	347
7.5	Case Studies for Sensible TES Systems	349
7.5.1	<i>Case Study 1: Natural Convection in a Hot Water Storage Tank</i>	349
7.5.2	<i>Case Study 2: Forced Convection in a Stratified Hot Water Tank</i>	355
7.5.3	<i>General Discussion of Sensible TES Case Studies</i>	365
7.6	Numerical Modeling, Simulation, and Analysis of Latent TES Systems	366
7.6.1	<i>Modeling</i>	366
7.6.2	<i>Heat Transfer and Fluid Flow Analysis</i>	366
7.6.3	<i>Simulation</i>	368
7.6.4	<i>Thermodynamic Analysis</i>	368
7.7	Case Studies for Latent TES Systems	369
7.7.1	<i>Case Study 1: Two-Dimensional Study of the Melting Process in an Infinite Cylindrical Tube</i>	369
7.7.2	<i>Case Study 2: Melting and Solidification of Paraffin in a Spherical Shell from Forced External Convection</i>	376
7.8	Illustrative Application for a Complex System: Numerical Assessment of Encapsulated Ice TES with Variable Heat Transfer Coefficients	391
7.8.1	<i>Background</i>	391
7.8.2	<i>System Considered</i>	392
7.8.3	<i>Modeling and Simulation</i>	392
7.8.4	<i>Numerical Determination of Heat Transfer Coefficients for Spherical Capsules</i>	397
7.8.5	<i>Heat Transfer Coefficients and Correlations</i>	398
7.8.6	<i>Closing Remarks for Illustrative Application for a Complex System</i>	404
7.9	Concluding Remarks	406
<b>8</b>	<b>Thermal Energy Storage Case Studies</b>	<b>413</b>
8.1	Introduction	413
8.2	Ice CTES Case Studies	414
8.2.1	<i>Rohm and Haas, Spring House Research Facility, PA</i>	414
8.2.2	<i>A Cogeneration Facility, California</i>	416

8.2.3	<i>A Power Generation Plant, Gaseem, Saudi Arabia</i>	421
8.2.4	<i>Channel Island Power Station, Darwin, Australia</i>	427
8.2.5	<i>The Abraj Atta'awuneya Ice CTES Project, Riyadh, Saudi Arabia</i>	429
8.2.6	<i>Alitalia's Headquarters Building, Rome, Italy</i>	431
8.3	Ice-Slurry CTES Case Studies	432
8.3.1	<i>The Stuart C. Siegel Center at Virginia Commonwealth University, VA</i>	432
8.3.2	<i>A Slurry Ice Rapid Cooling System, Boston, UK</i>	435
8.4	Chilled Water CTES Case Studies	436
8.4.1	<i>The Central Chilled Water System at the University of North Carolina, NC</i>	436
8.4.2	<i>Chilled Water CTES in a Trigeneration Project for a World Fair (EXPO'98), Lisbon, Portugal</i>	438
8.4.3	<i>TES at a Federal Facility, TX</i>	444
8.5	PCM-Based CTES Case Studies	446
8.5.1	<i>Minato Mirai 21, Yokohama</i>	446
8.5.2	<i>Harp Brewery, Dundalk, Ireland</i>	447
8.5.3	<i>Korean Development Bank, Seoul</i>	449
8.5.4	<i>Museum of Sciences and Industry, La Villette, France</i>	450
8.5.5	<i>Rueil Malmaison Central Kitchen, France</i>	451
8.5.6	<i>The Bangsar District Cooling Plant, Malaysia</i>	453
8.5.7	<i>Dairy TES Application Using Eutectic Solutions, Dorset, UK</i>	454
8.6	PCM-Based Latent TES for Heating Case Studies	455
8.6.1	<i>Solar Power Tower in Sandia National Laboratories, NM</i>	455
8.7	Sensible TES Case Studies	457
8.7.1	<i>New TES in Kumamoto, Kyushu</i>	457
8.7.2	<i>The World's First Passive Annual Heat Storage Home, MT</i>	458
8.8	Other Case Studies	459
8.8.1	<i>Potential for TES in a Hotel in Bali</i>	459
8.8.2	<i>Integrated TES Community System: Drake Landing Solar Community</i>	464
8.8.3	<i>The Borehole TES System at the University of Ontario Institute of Technology</i>	471
8.9	Concluding Remarks	479
<b>9</b>	<b>Recent Advances in TES Methods, Technologies, and Applications</b>	<b>483</b>
9.1	Introduction	483
9.2	Recent TES Investigations	483
9.3	Developments in TES Types and Performance	486
9.3.1	<i>Developments in PCM/HTF Material Selection</i>	486
9.3.2	<i>Shape</i>	491
9.3.3	<i>Nano- to Macro-Size Storage Media or PCM Particles and Capsules</i>	493
9.3.4	<i>Recent Advances in TES Types and Storage Techniques</i>	497
9.4	Micro- and Macro-Level Advances in TES Systems and Applications	504
9.5	Micro-Level Advances in TES Systems	504
9.5.1	<i>Modeling Methods</i>	504
9.5.2	<i>Contact Melting Driven by Temperature and Pressure Differences</i>	505
9.5.3	<i>Supercooling, Superheating, and Hysteresis</i>	509
9.5.4	<i>Geometry and Performance Optimization</i>	512
9.5.5	<i>Other Micro-Level Phenomena Affecting TES Performance</i>	512
9.5.6	<i>Developments in Stratification Analysis</i>	513
9.6	Macro-Level Advances in TES Systems and Applications	514
9.6.1	<i>Mode of Cooling/Heating: Passive or Active</i>	514
9.6.2	<i>Operating Strategies and Installation Configurations</i>	520
9.6.3	<i>Modeling, Control, Programming, and Optimization Methods</i>	524

---

9.6.4	<i>Measurement and Visualization Methods</i>	527
9.6.5	<i>Auxiliaries</i>	529
9.7	Performance Enhancement Techniques	530
9.7.1	<i>Conductivity-Enhancing Techniques</i>	530
9.7.2	<i>Thermal Batteries</i>	530
9.7.3	<i>Other Techniques</i>	534
9.8	Innovative Applications of TES Systems	535
9.9	Advanced Applications of Exergy Methods	542
9.10	Illustrative Examples	545
9.10.1	<i>Use of Effectiveness to Complement TES Energy and Exergy Efficiencies</i>	545
9.10.2	<i>Thermal Battery Ice-Storage System</i>	554
9.10.3	<i>Use of Artificial Neural Networks in TES</i>	560
9.11	Future Outlook for TES	566
<b>Appendix A Conversion Factors</b>		<b>585</b>
<b>Appendix B Thermophysical Properties</b>		<b>587</b>
<b>Appendix C Glossary</b>		<b>593</b>
<b>Index</b>		<b>595</b>



# About the Authors

**İbrahim Dinçer** is a full professor of mechanical engineering in the Faculty of Engineering and Applied Science at University of Ontario Institute of Technology (UOIT). Renowned for his pioneering works in the area of sustainable energy technologies, he has authored and co-authored numerous books and book chapters, more than 600 refereed journal and conference papers, and many technical reports. He has chaired many national and international conferences, symposia, workshops, and technical meetings. He has delivered more than 200 keynote and invited lectures. He is an active member of various international scientific organizations and societies, and serves as editor-in-chief (for *International Journal of Energy Research* by Wiley, and *International Journal of Exergy* and *International Journal of Global Warming* by Inderscience), associate editor, regional editor, and editorial board member on various prestigious international journals. He is a recipient of several research, teaching, and service awards, including a Premier's Research Excellence award in Ontario, Canada, in 2004. He has made innovative contributions to the understanding and development of sustainable energy technologies and their implementation, particularly through exergy. He has actively been working in the areas of hydrogen and fuel cell technologies, and his group has developed various novel technologies and methods.

**Marc A. Rosen** is a professor of mechanical engineering at the University of Ontario Institute of Technology in Oshawa, Canada, where he served as founding Dean of the Faculty of Engineering and Applied Science from 2002 to 2008. Dr. Rosen has served as President of the Engineering Institute of Canada and of the Canadian Society for Mechanical Engineering. He has acted in many professional capacities, including founding editor-in-chief of the journal *Sustainability* and a member of the Board of Directors of Oshawa Power and Utilities Corporation. With over 60 research grants and contracts and 500 technical publications, Dr. Rosen is an active teacher and researcher in thermodynamics, energy technology, sustainable energy, and the environmental impact of energy systems. Much of his research has been carried out for industry. Dr. Rosen has worked for such organizations as Imatra Power Company in Finland, Argonne National Laboratory near Chicago, the Institute for Hydrogen Systems near Toronto, and Ryerson University in Toronto, where he served as chair of the Department of Mechanical, Aerospace and Industrial Engineering. Dr. Rosen has received numerous awards and honours, including an Award of Excellence in Research and Technology Development from the Ontario Ministry of Environment and Energy, the Engineering Institute of Canada's Smith Medal for achievement in the development of Canada, and the Canadian Society for Mechanical Engineering's Angus Medal for outstanding contributions to the management and practice of mechanical engineering. He is a Fellow of the Engineering Institute of Canada, the Canadian Academy of Engineering, the Canadian Society for Mechanical Engineering, the American Society of Mechanical Engineers, and the International Energy Foundation.



# Preface

Thermal energy storage (TES) is an *advanced energy technology* that is attracting increasing interest for thermal applications such as space and water heating, cooling, and air conditioning. TES systems have enormous potential to facilitate more effective use of thermal equipment and large-scale energy substitutions that are economic. TES appears to be the most appropriate method for correcting the mismatch that sometimes occurs between the supply and demand of energy. It is therefore a very attractive technology for meeting society's needs and desires for more efficient and environmentally benign energy use.

This book is research oriented, and therefore includes some practical features often not included in other, solely academic textbooks. This book is essentially intended for use by advanced undergraduate and graduate students in various disciplines ranging from mechanical to chemical engineering, and as a basic reference for practicing energy engineers. Analyses of TES systems and their applications are undertaken throughout this comprehensive book, providing new understanding, methodologies, models, and applications, along with descriptions of several experimental works and case studies. Some of the material presented has been drawn from recent information available in the literature and elsewhere. The coverage is extensive, and the amount of information and data presented can be sufficient for several courses, if studied in detail. We strongly believe that this book will be of interest to students, engineers, and energy experts and that it provides a valuable and readable reference text for those who wish to learn more about TES systems and applications.

Chapter 1 addresses general aspects of thermodynamics, fluid flow, and heat transfer to furnish the reader with background information that is of relevance to the analysis of TES systems and their applications. Chapter 2 discusses the many types of energy storage technologies available. Chapter 3 deals extensively with TES methods, including cold TES. Chapter 4 addresses several environmental issues that we face today, and discusses how TES can help solve these problems. Several successful case studies are presented. Chapter 5 describes how TES is a valuable tool in energy conservation efforts that can help achieve significant energy savings. Chapter 6 covers energy and exergy analyses of a range of TES systems, along with various practical examples. Chapter 7 delves into both sensible and latent TES systems and their modeling, simulation, and numerical analyses; numerous case studies and illustrative examples are incorporated into this chapter, including heat transfer with phase change in simple and complex geometries. Chapter 8 discusses many practical TES applications and case studies along with their technical features and potential benefits. As the final unit, Chapter 9 reflects current developments in TES systems and applications, technologies, methods and techniques, and thereby seeks to provide thoughts on the future of thermal energy storage.

Incorporated throughout this book are many wide-ranging, illustrative examples that provide useful information for practical applications. Conversion factors and thermophysical properties of various materials are listed in the appendices in the International System of Units (SI). Complete references and a bibliography are included with each chapter to direct the curious and interested reader to further information.

The second edition of this book includes updated materials, new chapters, and questions/problems for each chapter. We feel that the enhanced content makes this edition of *Thermal Energy Storage: Systems and Applications* the best candidate as a text for senior level undergraduate and/or graduate level courses in the area.

İbrahim Dincer  
Marc A. Rosen  
*August 2010*

# Acknowledgements

Many people and organizations provided assistance that helped greatly in bringing this edition of our book to fruition.

We are most grateful to the following colleagues, postdoctoral fellows, and graduate students of ours for the time and effort they dedicated to assist in the preparation of some chapters, sections, figures, and problems:

- Mr. Hooman Abdi
- Mr. Mustafa Tolga Balta
- Dr. Aytunc Ereğ
- Mr. Othman Jaber
- Dr. Mehmet Karakilcik
- Mr. David MacPhee
- Mr. Bayu Susila

Their assistance helped us enhance the content and make it more focused as a comprehensive resource and textbook on thermal energy storage.

We are particularly thankful to the many companies and agencies that contributed documents and illustrations for use in this book. These valuable materials permit us to cover many recent developments and to provide a high degree of industrial relevance and practicality. Most such materials from the first edition are retained in this edition, because of their continuing illustrative nature and relevance. Furthermore, new materials from industry are included in this edition to enhance the coverage of practical applications. The relevant companies and agencies are acknowledged throughout the book where elements of the materials they provided are utilized.

We are grateful to several reviewers, colleagues, friends, and graduate students of ours for the feedback and suggestions they provided during the preparation of the first and current editions of this book.

We acknowledge the support provided by our former and current academic institutions.

In this second edition, several externally contributed chapters from the first edition have been replaced in order to provide a more unified and cohesive presentation. We nonetheless acknowledge with sincere thanks the chapters that were contributed to the first edition by Professors Adrian Bejan, Afshin J. Ghajar, Kamal A.R. Ismail, Marcel Lacroix, and Yousef H. Zurigat.

Also, we sincerely appreciate the encouragement of our publisher and their recognition of the increasing importance of thermal energy storage. In addition, we are grateful for the exemplary support provided by Nicky Skinner and Debbie Cox of John Wiley & Sons in the development of this second edition of the book, from the initial review phase to the final product.

Last, but not least, we thank our wives, Gülşen Dinçer and Margot Rosen, and our children Meliha, Miray, İbrahim Eren, Zeynep, and İbrahim Emir Dinçer, and Allison and Cassandra Rosen. They have been a great source of support and motivation, and their patience and understanding throughout this project have been most appreciated.



# 1

## General Introductory Aspects for Thermal Engineering

### 1.1 Introduction

Thermal energy storage (TES) is one of the key technologies for energy conservation, and therefore, it is of great practical importance. One of its main advantages is that it is best suited for heating and cooling thermal applications. TES is perhaps as old as civilization itself. Since recorded time, people have harvested ice and stored it for later use. Large TES systems have been employed in more recent history for numerous applications, ranging from solar hot water storage to building air conditioning systems. The TES technology has only recently been developed to a point where it can have a significant impact on modern technology.

In general, a coordinated set of actions has to be taken in several sectors of the energy system for the maximum potential benefits of thermal storage to be realized. TES appears to be an important solution to correcting the mismatch between the supply and demand of energy. TES can contribute significantly to meeting society's needs for more efficient, environmentally benign energy use. TES is a key component of many successful thermal systems, and a good TES should allow little thermal losses, leading to energy savings, while permitting the highest reasonable extraction efficiency of the stored thermal energy.

There are mainly two types of TES systems, that is, sensible (e.g., water and rock) and latent (e.g., water/ice and salt hydrates). For each storage medium, there is a wide variety of choices depending on the temperature range and application. TES via latent heat has received a great deal of interest. Perhaps, the most obvious example of latent TES is the conversion of water to ice. Cooling systems incorporating ice storage have a distinct size advantage over equivalent capacity chilled water units because of the ability to store large amount of energy as latent heat. TES deals with the storing of energy, usually by cooling, heating, melting, solidifying, or vaporizing a substance, and the energy becomes available as heat when the process is reversed. The selection of a TES is mainly dependent on the storage period required, that is, diurnal or seasonal, economic viability, operating conditions, and so on. In practice, many research and development activities related to energy have concentrated on efficient energy use and energy savings, leading to energy conservation. In this regard, TES appears to be an attractive thermal application. Furthermore, exergy analysis is an important tool for analyzing TES performance.

We begin this chapter with a summary of fundamental definitions, physical quantities, and their units, dimensions, and interrelations. We consider introductory aspects of thermodynamics, fluid flow, heat transfer, energy, entropy, and exergy.

## 1.2 Systems of Units

There are two main systems of units: the *International System of Units* (*Le Système International d'Unités*), which is normally referred to as *SI units*, and the *English System of Units*. SI units are used most widely throughout the world, although the English System is traditional in the United States. In this book, SI units are primarily employed. Note that the relevant unit conversions and relationships between the International and English unit systems concerning fundamental properties and quantities are listed in Appendix A.

## 1.3 Fundamental Properties and Quantities

In this section, we briefly cover several general aspects of thermodynamics to provide adequate preparation for the study of TES systems and applications.

### 1.3.1 Mass, Time, Length, and Force

Mass is defined as a quantity of matter forming a body of indefinite shape and size. The fundamental unit of mass is the kilogram (kg) in SI units and the pound mass (lb<sub>m</sub>) in English units. The basic unit of time for both unit systems is the second.

In thermodynamics, the unit *mole* (mol) is commonly used and defined as a certain amount of a substance as follows:

$$n = \frac{m}{M} \quad (1.1)$$

where  $n$  is the number of moles,  $m$  is the mass, and  $M$  is the molecular weight. If  $m$  and  $M$  are given in units of gram and gram per mole, we obtain  $n$  in moles. For example, one mole of water, having a molecular weight of 18 (compared to 12 for carbon-12), has a mass of 0.018 kg.

The basic unit of length is the meter (m) in SI units and the foot (ft) in the English system.

A force is a kind of action that brings a body to rest or changes its speed or direction of motion (e.g., a push or a pull). The fundamental unit of force is the Newton (N).

The four aspects, for example, mass, time, length, and force, are related by the Newton's second law of motion, which states that the force acting on a body is proportional to the mass and the acceleration in the direction of the force, as given in Equation 1.2:

$$F = ma \quad (1.2)$$

Equation 1.2 shows the force required to accelerate a mass of one kilogram at a rate of one meter per second per second as  $1 \text{ N} = 1 \text{ kg m/s}^2$ .

It is important to note that the value of the earth's gravitational acceleration is  $9.80665 \text{ m/s}^2$  in the SI system and  $32.174 \text{ ft/s}^2$  in the English system, and it indicates that a body falling freely toward the surface of the earth is subject to the action of gravity alone.

### 1.3.2 Pressure

When we deal with liquids and gases, pressure becomes one of the most important quantities. Pressure is the force exerted on a surface, per unit area, and is expressed in bar or Pascal (Pa). The related expression is

$$P = \frac{F}{A} \quad (1.3)$$



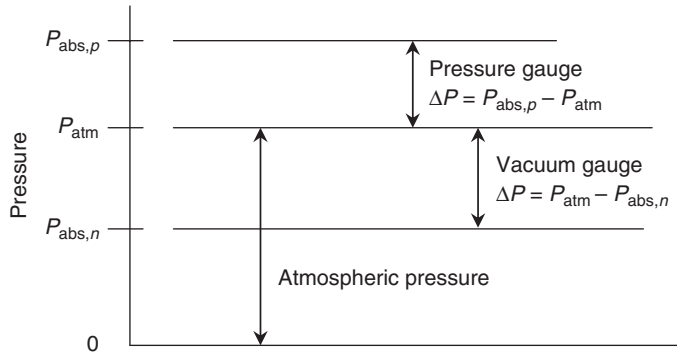


**Figure 1.1** Illustration of pressures for measurement

The SI unit for pressure is the force of one Newton acting on a square meter area (or the *Pascal*). The unit for pressure in the English system is pound-force per square foot,  $\text{lb}_f/\text{ft}^2$ .

Here, we introduce basic pressure definitions, and a summary of basic pressure measurement relationships is shown in Figure 1.1.

**Atmospheric Pressure** The atmosphere that surrounds the earth can be considered a reservoir of low-pressure air. Its weight exerts a pressure which varies with temperature, humidity, and altitude. Atmospheric pressure also varies from time to time at a single location because of the movement of weather patterns. While these changes in barometric pressure are usually less than one-half inch of mercury, they need to be taken into account when precise measurements are required.

**Gauge Pressure** The *gauge pressure* is any pressure for which the base for measurement is atmospheric pressure expressed as kPa (gauge). Atmospheric pressure serves as a reference level for other types of pressure measurements, for example, gauge pressure. As shown in Figure 1.1, the gauge pressure is either positive or negative depending on its level above or below atmospheric level. At the level of atmospheric pressure, the gauge pressure becomes zero.

**Absolute Pressure** A different reference level is utilized to obtain a value for absolute pressure. The absolute pressure can be any pressure for which the base for measurement is a complete vacuum, and is expressed in kPa (absolute). Absolute pressure is composed of the sum of the gauge pressure (positive or negative) and the atmospheric pressure as follows:

$$\text{pressure (gauge)} + \text{atmospheric pressure} = \text{pressure (absolute)} \quad (1.4)$$

For example, to obtain the absolute pressure, we simply add the value of atmospheric pressure to gauge pressure. The absolute pressure is the most common one used in thermodynamic calculations, despite the fact that what is read by most pressure gauges and indicators is the pressure difference between the absolute pressure and the atmospheric pressure existing in the gauge.

**Vacuum** A vacuum is a pressure lower than atmospheric pressure and occurs only in closed systems, except in outer space. It is also called *negative gauge pressure*. In fact, a vacuum is the pressure differential produced by evacuating air from the closed system. A vacuum is usually divided into four levels: (i) low vacuum representing pressures above 1 Torr absolute (a large number of

mechanical pumps in industries are used for this purpose; flow is viscous), (ii) medium vacuum varying between 1 and  $10^{-3}$  Torr absolute (most pumps serving this range are mechanical; fluid is in transition between viscous and molecular phases), (iii) high vacuum ranging between  $10^{-3}$  and  $10^{-6}$  Torr absolute (nonmechanical ejector or cryogenic pumps are used; flow is molecular or Newtonian), and (iv) very high vacuum representing absolute pressure below  $10^{-6}$  Torr (primarily for laboratory applications and space simulation).

It is important to note an additional term, the *saturation pressure*, which is the pressure of a liquid or vapor at saturation conditions.

### 1.3.3 Temperature

Temperature is an indication of the thermal energy stored in a substance. In other words, we can identify hotness and coldness with the concept of temperature. The temperature of a substance may be expressed in either relative or absolute units. The two most common temperature scales are Celsius ( $^{\circ}\text{C}$ ) and Fahrenheit ( $^{\circ}\text{F}$ ). The Celsius scale is used with the SI unit system and the Fahrenheit scale with the English system of units. There are two additional scales, the Kelvin scale (K) and the Rankine scale (R), which are absolute temperature scales and are often employed in thermodynamic applications.

The degree Kelvin is a unit of temperature measurement; zero kelvin (0 K) is absolute zero and is equal to  $-273.15^{\circ}\text{C}$ . Increments of temperature in units of K and  $^{\circ}\text{C}$  are equal. For instance, when the temperature of a product is decreased to  $-273.15^{\circ}\text{C}$  (or 0 K), known as *absolute zero*, the substance contains no thermal energy and all molecular movement stops.

Temperature can be measured in a large number of ways by devices. In general, the following devices are commonly used:

- **Thermometers.** Thermometers contain a volume of fluid which expands when subjected to heat, thereby raising its temperature. In practice, thermometers work over a certain temperature range. For example, the common thermometer fluid, mercury, becomes solid at  $-38.8^{\circ}\text{C}$  and its properties change dramatically at that condition.
- **Resistance thermometers.** A resistance thermometer (or detector), also known as a wire-wound thermometer, has great accuracy for wide temperature ranges. The wire used has to have known, repeatable, electrical characteristics so that the relationship between the temperature and resistance value can be predicted precisely. The measured value of the resistance of the detector can then be used to determine the value of an unknown temperature. Among metallic conductors, pure metals exhibit the greatest change of resistance with temperature. For applications requiring higher accuracy, especially where the temperature measurement is between  $-200$  and  $+800^{\circ}\text{C}$ , the resistance thermometer comes into its own. The majority of such thermometers are made of platinum. In industries, in addition to platinum, nickel ( $-60$  to  $+180^{\circ}\text{C}$ ) and copper ( $-30$  to  $+220^{\circ}\text{C}$ ) are frequently used to manufacture resistance thermometers. Resistance thermometers can be provided with two, three, or four wire connections, and for higher accuracy at least three wires are required.
- **Averaging thermometers.** An averaging thermometer is designed to measure the average temperature of bulk stored liquids. The sheath contains a number of elements of different lengths, all starting from the bottom of the sheath, The longest element that is fully immersed is connected to the measuring circuit to allow a true average temperature to be obtained. For this type of thermometer, several parameters are significant, namely, sheath material (stainless steel for the temperature range from  $-50$  to  $+200^{\circ}\text{C}$  or nylon for the temperature range from  $-50$  to  $+90^{\circ}\text{C}$ ), sheath length (to suit the application), termination (flying leads or terminal box), element length, element calibration (to copper or platinum curves), and operating temperature

ranges. In many applications, where a multielement thermometer is not required, such as in air ducts, cooling water and gas outlets, a single-element thermometer stretched across the duct or pipe work can provide a true average temperature reading. Despite the working range from 0 to 100 °C, the maximum temperature may reach 200 °C. To maintain high accuracy, these units are normally supplied with three-wire connections. However, up to 10 elements can be mounted in the averaging bulb fittings, and they can be made of platinum, nickel, or copper, and fixed at any required position.

- **Thermocouples.** A thermocouple consists of two electrical conductors of different materials connected together at one end (the so-called *measuring junction*). The two free ends are connected to a measuring instrument, for example, an indicator, a controller, or a signal conditioner, by a reference junction (the so-called *cold junction*). The thermoelectric voltage appearing at the indicator depends on the materials of which the thermocouple wires are made and on the temperature difference between the measuring junction and the reference junction. For accurate measurements, the temperature of the reference junction must be kept constant. Modern instruments usually incorporate a cold junction reference circuit and are supplied ready for operation in a protective sheath, to prevent damage to the thermocouple by any mechanical or chemical means. Table 1.1 lists several types of thermocouples along with their maximum absolute temperature ranges. As can be seen in Table 1.1, a copper–constantan thermocouple has an accuracy of  $\pm 1$  °C, and is often employed for control systems in refrigeration and food processing applications. The iron–constantan thermocouple with its maximum of 850 °C is used in applications in the plastics industry. The chromel–alumel-type thermocouples, with a maximum of about 1100 °C, are suitable for combustion applications in ovens and furnaces. In addition, it is possible to reach about 1600 or 1700 °C using platinum rhodium–platinum thermocouples, which are particularly useful in steel manufacturing. It is worth noting that one advantage that the thermocouple has over most other temperature sensors is that it has a small thermal capacity, and thus a prompt response to temperature changes. Furthermore, its small thermal capacity rarely affects the temperature of the body under examination.
- **Thermistors.** These devices are made of semiconductors and act as thermal resistors with a high (usually negative) temperature coefficient. In use, thermistors are either self-heated or externally heated. Self-heated units employ the heating effect of the current flowing through them to raise and control their temperature and thus their resistance. This operating mode is useful in such devices as voltage regulators, microwave power meters, gas analyzers, flow meters, and automatic volume and power level controls. Externally heated thermistors are well suited for precision temperature measurement, temperature control, and temperature compensation due to the large changes in resistance versus temperature. These are generally used for applications in the range

**Table 1.1** Some of the most common thermocouples

Type	Common names	Temperature range (°C)
T	Copper–constantan (C/C)	–250 to 400
J	Iron–constantan (I/C)	–200 to 850
E	Nickel chromium–constantan or Chromel–constantan	–200 to 850
K	Nickel chromium–nickel aluminum or Chromel–alumel (C/A)	–180 to 1100
–	Nickel 18% molybdenum–nickel	0 to 1300
N	Nicrosil–nasil	0 to 1300
S	Platinum 10% rhodium–platinum	0 to 1500
R	Platinum 13% rhodium–platinum	0 to 1500
B	Platinum 30% rhodium–platinum 6% rhodium	0 to 1600

–100 to +300 °C. Despite early thermistors having tolerances of  $\pm 20$  or  $\pm 10\%$ , modern precision thermistors are of a higher accuracy, for example,  $\pm 0.1$  °C (less than  $\pm 1\%$ ).

- **Digital display thermometers.** A wide range of digital display thermometers, for example, hand-held battery-powered displays and panel-mounted mains or battery units, are available commercially. Displays can be provided for use with all standard thermocouples or platinum resistance thermometers with several digits and 0.1 °C resolution.

It is important to emphasize that before temperature can be controlled, it must be sensed and measured accurately. For temperature measurement devices, there are several potential sources of error, including not only sensor properties but also contamination effects, lead lengths, immersion, heat transfer, and controller interfacing. In temperature control, there are many sources of error that can be minimized by careful consideration of the type of sensor, its working environment, the sheath or housing, extension leads, and the instrumentation. An awareness of potential errors is vital in many applications dealt with in this book. Selection of temperature measurement devices is a complex task and has been discussed only briefly here. It is important to remember the following: “choose the right tool for the right job.”

### 1.3.4 Specific Volume and Density

The *specific volume*  $v$  is the volume per unit mass of a substance, usually expressed in cubic meters per kilogram ( $\text{m}^3/\text{kg}$ ) in the SI system and in cubic feet per pound ( $\text{ft}^3/\text{lb}$ ) in the English system. The *density*  $\rho$  of a substance is defined as the mass per unit volume, and is therefore the inverse of the specific volume:

$$\rho = \frac{1}{v} \quad (1.5)$$

The units of density are  $\text{kg}/\text{m}^3$  in the SI system and  $\text{lb}/\text{ft}^3$  in the English system. Specific volume is also defined as the volume per unit mass, and density as the mass per unit volume, that is,

$$v = \frac{V}{m} \quad (1.6)$$

$$\rho = \frac{m}{V} \quad (1.7)$$

Both specific volume and density are intensive properties and are affected by temperature and pressure.

### 1.3.5 Mass and Volumetric Flow Rates

Mass flow rate is defined as the mass flowing per unit time ( $\text{kg}/\text{s}$  in the SI system and  $\text{lb}/\text{s}$  in the English system). Volumetric flow rates are given in  $\text{m}^3/\text{s}$  in the SI system and  $\text{ft}^3/\text{s}$  in the English system. The following expressions can be written for the flow rates in terms of mass, specific volume, and density:

$$\dot{m} = \dot{V} \rho = \frac{\dot{V}}{v} \quad (1.8)$$

$$\dot{V} = \dot{m} v = \frac{\dot{m}}{\rho} \quad (1.9)$$

## 1.4 General Aspects of Thermodynamics

In this section, we briefly introduce some general aspects of thermodynamics that are related to energy storage systems and applications.

### 1.4.1 Thermodynamic Systems

A thermodynamic system is a device or combination of devices that contains a certain quantity of matter. It is important to carefully define a system under consideration and its boundaries. We can define three important types of systems as follows:

- **Closed system.** This is defined as a system across the boundaries of which no material crosses. It, therefore, contains a fixed quantity of matter. In some books, it is also called a *control mass*.
- **Open system.** This is defined as a system in which material (mass) is allowed to cross its boundaries. The term open system is also called a *control volume*.
- **Isolated system.** This is a closed system that is not affected by the surroundings. No mass, heat, or work crosses its boundary.

### 1.4.2 Process

A process is a physical or chemical change in the properties of matter or the conversion of energy from one form to another. In some processes, one property remains constant. The prefix “iso” is employed to describe such a process, for example, isothermal (constant temperature), isobaric (constant pressure), and isochoric (constant volume).

### 1.4.3 Cycle

A cycle is a series of thermodynamic processes in which the end-point conditions or properties of the matter are identical to the initial conditions.

### 1.4.4 Thermodynamic Property

This is a physical characteristic of a substance, which is used to describe its state. Any two properties usually define the state or condition of a substance, from which all other properties can be derived. Some examples are temperature, pressure, enthalpy, and entropy. Thermodynamic properties are classified as intensive properties (independent of the mass, e.g., pressure, temperature, and density) and extensive properties (dependent on the mass, e.g., mass and total volume). Extensive properties on a per unit mass basis, such as specific volume, become intensive properties. Property diagrams of substances can be presented in graphical form and summarize the main properties listed in property tables, for example, refrigerant tables.

### 1.4.5 Sensible and Latent Heats

It is known that all substances can hold a certain amount of heat; this property is their thermal capacity. When a liquid is heated, its temperature rises to the boiling point. This is the highest temperature that the liquid can reach at the measured pressure. The heat absorbed by the liquid in raising the temperature to the boiling point is called *sensible heat*. The heat required to convert the liquid to vapor at the same temperature and pressure is called *latent heat*. This is the change in

enthalpy during a state change (the amount of heat absorbed or rejected at constant temperature at any pressure, or the difference in enthalpies of a pure condensable fluid between its dry saturated state and its saturated liquid state at the same pressure).

### 1.4.6 Latent Heat of Fusion

Fusion is associated with the melting and freezing of a material. For most pure substances, there is a specific melting/freezing temperature, relatively independent of the pressure. For example, ice begins to melt at 0°C. The amount of heat required to melt one kilogram of ice at 0°C to one kilogram of water at 0°C is called the *latent heat of fusion* of water, and equals 334.92 kJ/kg. The removal of the same amount of heat from one kilogram of water at 0°C changes it back to ice.

### 1.4.7 Vapor

A vapor is a gas at or near equilibrium with the liquid phase – a gas under the saturation curve or only slightly beyond the saturated vapor line. *Vapor quality* is theoretically assumed; that is, when vapor leaves the surface of a liquid, it is pure and saturated at the particular temperature and pressure. In actuality, tiny liquid droplets escape with the vapor. When a mixture of liquid and vapor exists, the ratio of the mass of the liquid to the total mass of the liquid and vapor mixture is called the *quality*, and is expressed as a percentage or decimal fraction. *Superheated vapor* is the saturated vapor to which additional heat has been added, raising the temperature above the boiling point. Let us consider a mass  $m$  with a quality  $x$ . The volume is the sum of the volumes of both the liquid and the vapor, as defined below:

$$V = V_{liq} + V_{vap} \quad (1.10)$$

Equation 1.10 can also be written in terms of specific volumes as

$$mv = m_{liq}v_{liq} + m_{vap}v_{vap} \quad (1.11)$$

Dividing all terms by the total mass yields

$$v = (1 - x)v_{liq} + xv_{vap} = v_{liq} + xv_{liq,vap} \quad (1.12)$$

where  $v_{liq,vap} = v_{vap} - v_{liq}$ .

### 1.4.8 Thermodynamic Tables

The thermodynamic tables were first published in 1936 as steam tables by Keenan and Keyes, and later in 1969 and 1978, these were revised and republished. The use of thermodynamic tables of many substances ranging from water to refrigerants is very common in process design calculations. In the literature, they are also called either *steam tables* or *vapor tables*. In this book, we will refer to the thermodynamic tables. These tables are normally given as different distinct phases (parts), for example, four different parts for water, such as saturated water, superheated vapor water, compressed liquid water, saturated solid-saturated vapor water; and two distinct parts for R-134a, such as saturated and superheated. Each table is listed according to the values of temperature and pressure, with the remainder containing values of various other thermodynamic parameters such as specific volume, internal energy, enthalpy, and entropy. Normally, when we have values for two independent variables, we may obtain other data from the respective table. In learning how to use these tables, an important point is to specify the state using any two independent parameters. In some design calculations if we do not have the exact values of the parameters, we use interpolation to find the necessary values.

Beyond thermodynamic tables, recently, much attention has been paid to computerized tables for such design calculations. Although computerized tables can eliminate several reading problems for data, they may not provide students with an understanding of the concepts and a good comprehension of the subject. That is why in thermodynamics courses, it is important for the students to know how to obtain thermodynamic data from the appropriate thermodynamic tables. The *Handbook of Thermodynamic Tables* by Raznjevic (1995) is one of the most valuable sources for several solids, liquids, and gaseous substances.

### 1.4.9 State and Change of State

The state of a system or substance is defined as the condition of the system or substance characterized by certain observable macroscopic values of its properties, such as temperature and pressure. The term *state* is often used interchangeably with the term *phase*, for example, solid phase or gaseous phase of a substance. Each of the properties of a substance in a given state has only one definite value, regardless of how the substance reaches the state. For example, when sufficient heat is added or removed at a certain condition, most substances undergo a state change. The temperature remains constant until the state change is complete. This can be from solid to liquid, liquid to vapor, or vice versa. Figure 1.2 depicts typical examples of ice melting and water boiling.

A clearer presentation of solid, liquid, and vapor phases of water is provided on a temperature–volume ( $T$ - $v$ ) diagram in Figure 1.3. The constant pressure line ABCD represents the states that water passes through as follows:

- **A–B.** Represents the process where water is heated from the initial temperature to the saturation temperature (liquid) at constant pressure. At point B, the water is a fully saturated liquid with a quality  $x = 0$ , but no water vapor has formed.
- **B–C.** Represents a constant-temperature vaporization process in which there is only phase change from a saturated liquid to a saturated vapor. As this process proceeds, the vapor quality

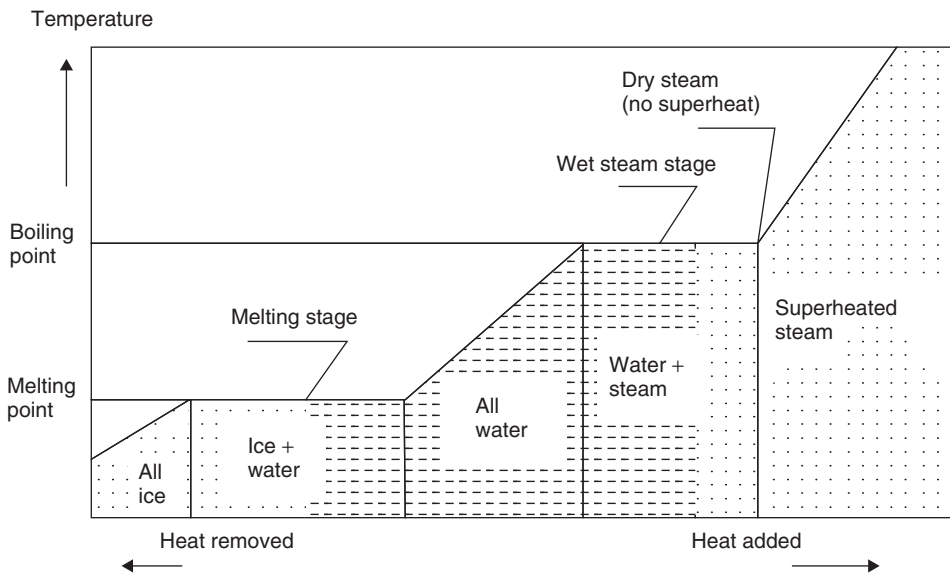
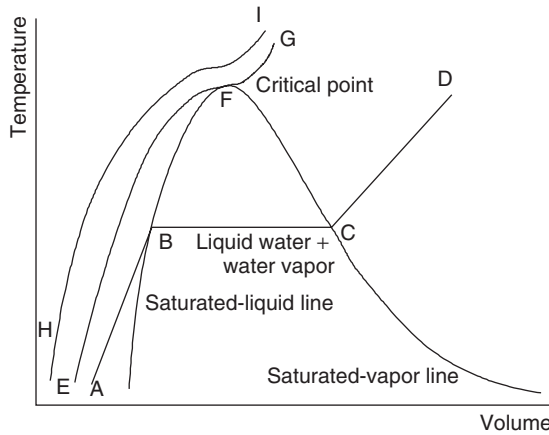


Figure 1.2 The state-change diagram of water



**Figure 1.3** Temperature–volume diagram for the phase change of water

varies from 0 to 100%. Within this zone, the water is a mixture of liquid and vapor. At point C, we have a completely saturated vapor and the quality is 100%.

- **C–D.** Represents the constant-pressure process in which the saturated water vapor is superheated with increasing temperature.
- **E–F–G.** Represents a nonconstant-temperature vaporization process. In this constant-pressure heating process, point F is called the *critical point* where the saturated liquid and saturated vapor states are identical. The thermodynamic properties at this point are called *critical thermodynamic properties*, for example, critical temperature, critical pressure, and critical specific volume.
- **H–I.** Represents a constant-pressure heating process in which there is no change from one phase to another (only one is present). However, there is a continuous change in density during this process.

The other process which may occur during melting of water is *sublimation*, in which the ice directly passes from the solid phase to the vapor phase. Another important point is that the solid, liquid, and vapor phases of water may be present together in equilibrium, leading to the *triple point*.

#### 1.4.10 Specific Internal Energy

Internal energy represents a molecular state type of energy. Specific internal energy is a measure per unit mass of the energy of a simple system in equilibrium as a function of  $c_p dT$ . For many thermodynamic processes in closed systems, the only significant energy changes are internal energy changes, and the significant work done by the system in the absence of friction is the work of pressure–volume expansion, such as in a piston–cylinder mechanism. The specific internal energy of a mixture of liquid and vapor can be written in a form similar to Equation 1.12:

$$u = (1 - x)u_{liq} + xu_{vap} = u_{liq} + xu_{liq,vap} \quad (1.13)$$

where  $u_{liq,vap} = u_{vap} - u_{liq}$ .

#### 1.4.11 Specific Enthalpy

Enthalpy is another measure of the energy per unit mass of a substance. Specific enthalpy, usually expressed in kJ/kg or Btu/lb, is normally expressed as a function of  $c_p dT$ . Since enthalpy is a



state function, it is necessary to measure it relative to some reference state. The usual practice is to determine the reference values that are called the *standard enthalpy of formation* (or the heat of formation), particularly in combustion thermodynamics. The specific enthalpy of a mixture of liquid and vapor components can be written as Equation 1.12:

$$h = (1 - x)h_{liq} + xh_{vap} = h_{liq} + xh_{liq,vap} \quad (1.14)$$

where  $h_{liq,vap} = h_{vap} - h_{liq}$ .

### 1.4.12 Specific Entropy

Entropy is the ratio of the heat added to a substance to the absolute temperature at which it was added, and is a measure of the molecular disorder of a substance at a given state. The specific enthalpy of a mixture of liquid and vapor components can be written as Equation 1.12:

$$s = (1 - x)s_{liq} + xs_{vap} = s_{liq} + xs_{liq,vap} \quad (1.15)$$

where  $s_{liq,vap} = s_{vap} - s_{liq}$ .

### 1.4.13 Pure Substance

A pure substance is defined as the one that has a homogeneous and invariable chemical composition. Despite having the same chemical composition throughout, it may be in more than one phase, namely, liquid, a mixture of liquid and vapor (e.g., steam), and a mixture of solid and liquid. Each phase has the same chemical composition. However, a mixture of liquid air and gaseous air cannot be considered a pure substance because the composition of each phase differs from that of the other. A thorough understanding of the pure substance is of significance, particularly for TES applications. Thermodynamic properties of water and steam can be obtained from tables and charts that are present in most thermodynamics books, based on experimental data or real-gas equations of state, or obtained through computer calculations. It is important to note that the properties of low-pressure water are of great significance in TES systems for cooling applications, since water vapor existing in the atmosphere typically exerts a pressure less than 1 psi (6.9 kPa). At such low pressures, it is known that water vapor exhibits ideal-gas behavior.

### 1.4.14 Ideal Gases

In many practical thermodynamic calculations, gases such as air and hydrogen can often be treated as ideal gases, particularly for temperatures much higher than their critical temperatures and for pressures much lower than their saturation pressures at given temperatures. An ideal gas can be described in terms of three parameters: the volume that it occupies, the pressure that it exerts, and its temperature. In fact, all gases or vapors, including water vapor, at very low pressures exhibit ideal-gas behavior. The practical advantage of treating real gases as ideal is that a simple equation of state with only one constant can be applied in the following form:

$$Pv = RT \quad (1.16)$$

and

$$PV = mRT \quad (1.17)$$

The ideal-gas equation of state was originally established from experimental observations, and is also called a *P-v-T relationship* for gases. It is generally considered as a concept rather than a

reality. It requires only a few data values to define a particular gas over a wide range of its possible thermodynamic equilibrium states.

The gas constant  $R$  is different for each gas depending on its molecular weight  $M$ :

$$R = \frac{\bar{R}}{M} \quad (1.18)$$

where  $\bar{R} = 8.314 \text{ kJ/kg K}$ .

Equations 1.17 and 1.18 may be written on a mole-basis as follows:

$$P\bar{v} = RT \quad (1.19)$$

and

$$PV = n\bar{R}T \quad (1.20)$$

The other simplifying feature of ideal-gas behavior is that, if assumed that the constant-pressure and constant-volume specific heats are constant, changes in specific internal energy and specific enthalpy can be calculated simply without referring to thermodynamic tables and graphs from the following expressions:

$$\Delta u = (u_2 - u_1) = c_v(T_2 - T_1) \quad (1.21)$$

$$\Delta h = (h_2 - h_1) = c_p(T_2 - T_1) \quad (1.22)$$

The following is another useful relation for ideal gases obtained from the expression,  $h = u + Pv = u + RT$ :

$$c_v - c_p = R \quad (1.23)$$

For the entire range of states, the ideal-gas model may be found unsatisfactory. Therefore, the compressibility factor ( $Z$ ) is introduced to measure the deviation of a real substance from the ideal-gas equation of state. The compressibility factor is defined by the relation:

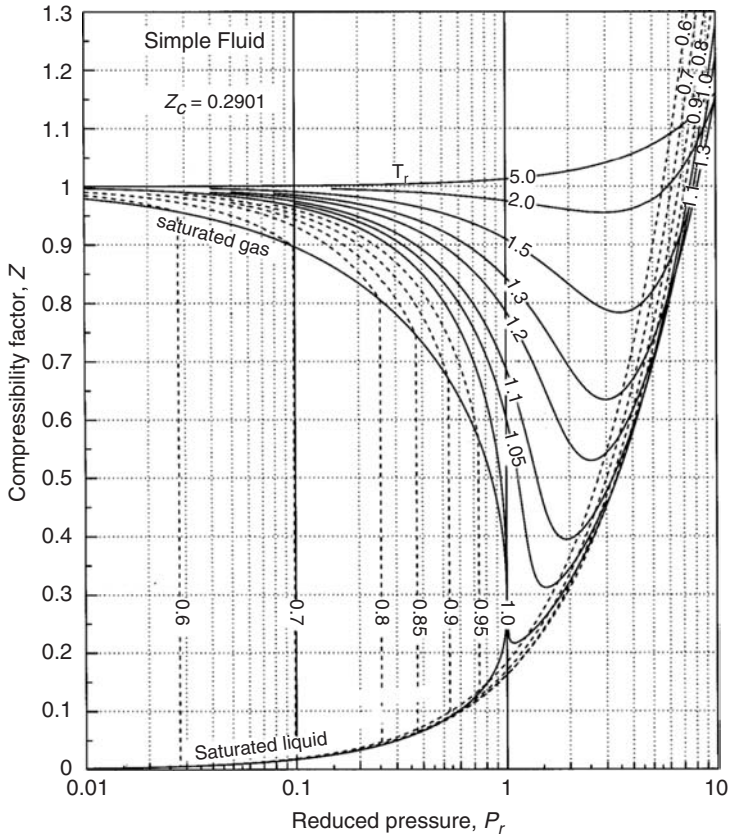
$$Pv = ZRT \quad \text{or} \quad Z = \frac{Pv}{RT} \quad (1.24)$$

Figure 1.4 shows a generalized compressibility chart for simple substances. In the chart, we have two important parameters: the reduced temperature ( $T_r = T/T_c$ ) and the reduced pressure ( $P_r = P/P_c$ ). To calculate the compressibility factor, the values of  $T_r$  and  $P_r$  should be calculated using the critical temperature and pressure values of the respective substance, which can easily be obtained from thermodynamics books. As can be seen in Figure 1.4, at all temperatures  $Z \rightarrow 1$  as  $P_r \rightarrow 0$ . This means that the behavior of the actual gas closely approaches ideal-gas behavior, as the pressure approaches zero. For real gases,  $Z$  takes on values between 0 and 1. If  $Z = 1$ , Equation 1.24 becomes Equation 1.16. In the literature, there are also several equations of state for accurately representing the  $P-v-T$  behavior of a gas over the entire superheated vapor region, for example, the Benedict–Webb–Rubin equation, the van der Waals equation, and the Redlich and Kwong equation. However, some of these equations of state are complicated due to the number of empirical constants they contain, and are more conveniently used with computer software to obtain results.

There are some special cases if one of  $P$ ,  $v$ , and  $T$  is constant. At a fixed temperature, the volume of a given quantity of ideal gas varies inversely with the pressure exerted on it (in some books, this is called *Boyle's law*), describing compression as

$$P_1 V_1 = P_2 V_2 \quad (1.25)$$

where the subscripts refer to the initial and final states.



**Figure 1.4** Generalized compressibility chart for simple substances (Borgnakke and Sonntag, 2008)

Equation 1.25 is employed by designers in a variety of situations: when selecting an air compressor, for calculating the consumption of compressed air in reciprocating air cylinders, and for determining the length of time required for storing air. Nevertheless, use of Equation 1.25 may not always be practical due to temperature changes. If temperature increases with compression, the volume of a gas varies directly with its absolute temperature in K as:

$$\frac{V_1}{T_1} = \frac{V_2}{T_2} \tag{1.26}$$

If temperature increases at constant volume, the pressure of a gas varies directly with its absolute temperature in K as:

$$\frac{P_1}{T_1} = \frac{P_2}{T_2} \tag{1.27}$$

Equations 1.26 and 1.27 are known as *Charles' law*. If both temperature and pressure change at the same time, the combined ideal-gas equation can be written as:

$$\frac{P_1 V_1}{T_1} = \frac{P_2 V_2}{T_2} \tag{1.28}$$

For a given mass, the internal energy of an ideal gas can be written as a function of temperature, since  $c_{v0}$  is constant, as shown below:

$$dU = mc_{v0}dT \quad (1.29)$$

and the specific internal energy becomes

$$du = c_{v0}dT \quad (1.30)$$

The enthalpy equation for an ideal gas, based on  $h = u + Pv$ , can be written as

$$dH = mc_{p0}dT \quad (1.31)$$

and the specific enthalpy then becomes

$$dh = c_{p0}dT \quad (1.32)$$

The entropy change of an ideal gas, based on the general entropy equation in terms of  $Tds = du + Pdv$  and  $Tds = dh - v dP$  as well as on the ideal-gas equation  $Pv = RT$ , can be obtained in two ways by substituting Equations 1.29 and 1.30:

$$s_2 - s_1 = c_{v0} \ln \left( \frac{T_2}{T_1} \right) + R \ln \left( \frac{v_2}{v_1} \right) \quad (1.33)$$

$$s_2 - s_1 = c_{p0} \ln \left( \frac{T_2}{T_1} \right) - R \ln \left( \frac{P_2}{P_1} \right) \quad (1.34)$$

For a reversible adiabatic process, the ideal-gas equation in terms of the initial and final states under  $Pv^k = \text{constant}$  can be written as:

$$Pv^k = P_1v_1^k = P_2v_2^k \quad (1.35)$$

where  $k$  denotes the adiabatic exponent (the *specific heat ratio*) as a function of temperature:

$$k = \frac{c_{p0}}{c_{v0}} \quad (1.36)$$

On the basis of Equation 1.35 and the ideal-gas equation, the following expression can be obtained:

$$\frac{P_2}{P_1} = \left( \frac{T_2}{T_1} \right)^{k/k-1} = \left( \frac{v_1}{v_2} \right)^k = \left( \frac{V_1}{V_2} \right)^k \quad (1.37)$$

Consider a closed system containing an ideal gas, undergoing an adiabatic reversible process. The gas has constant specific heats. The work can be derived from the first law of thermodynamics (FLT) as follows:

$$W_{1-2} = \frac{mR(T_2 - T_1)}{1 - k} = \frac{(P_2V_2 - P_1V_1)}{1 - k} \quad (1.38)$$

Equation 1.38 can also be derived from the general work relation,  $W = PdV$ .

For a reversible polytropic process, the only difference is the polytropic exponent  $n$  which shows the deviation in a log  $P$  and log  $V$  diagram, leading to the slope. Equations 1.35, 1.37, and 1.38 can be rewritten with the polytropic exponent under  $Pv^n = \text{constant}$  as:

$$Pv^n = P_1v_1^n = P_2v_2^n \quad (1.39)$$

$$\frac{P_2}{P_1} = \left(\frac{T_2}{T_1}\right)^{n/n-1} = \left(\frac{v_1}{v_2}\right)^n = \left(\frac{V_1}{V_2}\right)^n \quad (1.40)$$

$$W_{1-2} = \frac{mR(T_2 - T_1)}{1 - n} = \frac{(P_2V_2 - P_1V_1)}{1 - n} \quad (1.41)$$

To provide a clear understanding of the polytropic exponent, it is important to show the values of  $n$  for four types of polytropic processes for ideal gases (Figure 1.5):

- $n = 0$  for isobaric process ( $P = \text{constant}$ )
- $n = 1$  for isothermal process ( $T = \text{constant}$ )
- $n = k$  for isentropic process ( $s = \text{constant}$ )
- $n = \infty$  for isochoric process ( $v = \text{constant}$ )

As can be seen in Figure 1.5, there are two quadrants where  $n$  varies from zero to infinity and where it has a positive value. The slope of any curve is an important consideration when a reciprocating engine or compressor cycle is under consideration.

In thermodynamics, a number of problems involve the mixture of pure substances (e.g., ideal gases). In this regard, it is important to understand related aspects accordingly. Tables 1.2 and 1.3 summarize the relevant expressions and two ideal-gas models: the Dalton model and the Amagat model. In the comparison presented, it is assumed that each gas is unaffected by the presence of other gases, and each is treated as an ideal gas. With respect to entropy, it is noted that an increase in entropy is dependent only upon the number of moles of ideal gases, and is independent of the chemical composition. Of course, when the gases in the mixture are distinguished, the entropy increases.

### 1.4.15 Energy Transfer

Energy can be viewed as the capacity for doing work. Energy can take a number of forms during transfer such as thermal (heat), mechanical (work), electrical, and chemical. Thermal energy flows only from a higher to a lower temperature level unless external energy is added to reverse the process. The rate of energy transfer per unit time is called *power*.

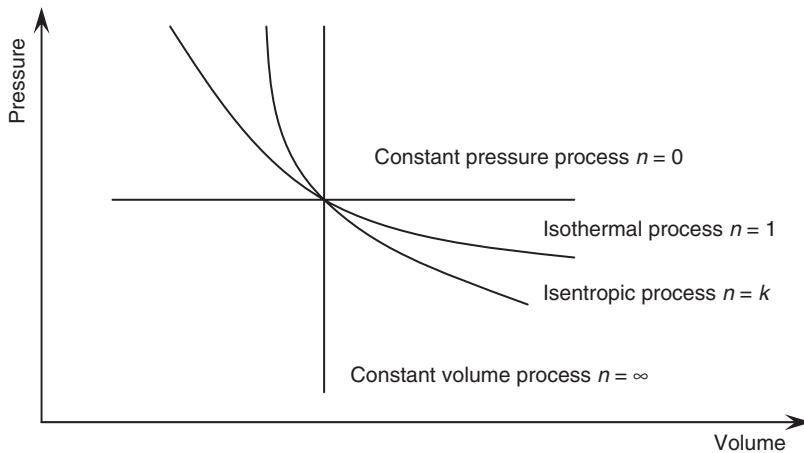


**Figure 1.5** Representation of four polytropic processes on a pressure–volume diagram

**Table 1.2** Equations for gas and gas mixtures and relevant models

Definition	Dalton model and Amagat model
Total mass of a mixture of $N$ components	$m_{tot} = m_1 + m_2 + \dots + m_N = \sum m_i$
Total number of moles of a mixture of $N$ components	$n_{tot} = n_1 + n_2 + \dots + n_N = \sum n_i$
Mass fraction for each component	$c_i = m_i/m_{tot}$
Mole fraction for each component	$y_i = n_i/n_{tot} = P_i/P_{tot} = V_i/V_{tot}$
Molecular weight of the mixture	$M_{mix} = m_{tot}/n_{tot} = \sum n_i M_i/n_{tot} = \sum y_i M_i$
Internal energy of the mixture	$U_{mix} = n_1 \bar{U}_1 + n_2 \bar{U}_2 + \dots + n_N \bar{U}_N = \sum n_i \bar{U}_i$
Enthalpy of the mixture	$H_{mix} = n_1 \bar{H}_1 + n_2 \bar{H}_2 + \dots + n_N \bar{H}_N = \sum n_i \bar{H}_i$
Entropy of the mixture	$S_{mix} = n_1 \bar{S}_1 + n_2 \bar{S}_2 + \dots + n_N \bar{S}_N = \sum n_i \bar{S}_i$
Entropy difference for the mixture	$S_2 - S_1 = -\bar{R}(n_1 \ln y_1 + n_2 \ln y_2 + \dots + n_N \ln y_N)$

**Table 1.3** Comparison of Dalton and Amagat models

Definition	Dalton model	Amagat model
$P, V, T$ for the mixture	$T$ and $V$ are constant $P_{tot} = P = P_1 + P_2 + \dots + P_N$	$T$ and $P$ are constant $V_{tot} = V = V_1 + V_2 + \dots + V_N$
Ideal-gas equation for the mixture	$PV = n\bar{R}T$	
Ideal-gas equations for the components	$P_1 V = n_1 \bar{R}T$ $P_2 V = n_2 \bar{R}T$ : $P_N V = n_N \bar{R}T$	$P V_1 = n_1 \bar{R}T$ $P V_2 = n_2 \bar{R}T$ : $P V_N = n_N \bar{R}T$

### 1.4.16 Heat

The definitive experiment that showed that heat was a form of energy convertible into other forms was carried out by a Scottish physicist, James Joule. Heat is the thermal form of energy, and heat transfer takes place when a temperature difference exists within a medium or between different media. Heat always requires a difference in temperature for its transfer. Higher temperature differences provide higher heat transfer rates. The units for heat are joules or kilojoules in the International system and the foot pound-force or British thermal unit (Btu) in the English system. Following a common convention in thermodynamic calculations, heat transfer to a system is considered *positive*, while heat transfer from a system is *negative*. If there is no heat transfer involved in a process, it is called *adiabatic*.

### 1.4.17 Work

Work is the energy that is transferred by a difference in pressure or force of any kind and is subdivided into shaft work and flow work. Shaft work is the mechanical energy used to drive a mechanism such as a pump, compressor, or turbine. Flow work is the energy transferred into a system by fluid flowing into, or out of, the system. Both forms are usually expressed in kilojoules and on a unit mass basis as kJ/kg. By usual convention, work done by a system is considered positive and work done on a system (work input) is considered negative. The unit for power or rate of work is joule per second, which is a Watt (W).

### 1.4.18 The First Law of Thermodynamics

Thermodynamics is the science of energy and entropy, and the basis of thermodynamics is experimental observation. In thermodynamics, such observations were formed into four basic laws: the zeroth, first, second, and third laws of thermodynamics. The first and second laws of thermodynamics are the most common tools in practice due to fact that transfers and conversions of energy are governed by these two laws, and in this chapter, we focus on these two laws.

The FLT can be defined as the law of conservation of energy and states that in a closed system energy can be neither created nor destroyed. For a change of state from an initial state 1 to a final state 2 with a constant amount of matter, the first law can be formulated as follows:

$$Q_{1-2} = (E_2 - E_1) + W_{1-2} = (U_2 - U_1) + (KE_2 - KE_1) + (PE_2 - PE_1) + W_{1-2} \quad (1.42)$$

where  $(U_2 - U_1) = mc_v(T_2 - T_1)$ ,  $(KE_2 - KE_1) = m(V_2^2 - V_1^2)/2$ ,  $(PE_2 - PE_1) = mg(Z_2 - Z_1)$ .

As is clear in Equation 1.42, we broaden the definition of energy to include kinetic and potential energies in addition to internal energy. An important consequence of the first law is that the internal energy change resulting from a process is independent of the thermodynamic path followed by the system, and of the paths followed by the processes, for example, heat transfer and work. In turn, the rate at which the internal energy content of the system changes is dependent only on the rates at which heat is added and work is done (when kinetic and potential energies are neglected).

### 1.4.19 The Second Law of Thermodynamics

As mentioned earlier, the first law is the energy-conservation principle. The second law of thermodynamics (SLT) is instrumental in determining the inefficiencies of practical thermodynamic systems, and indicates that it is impossible to have 100% efficiency in energy conversion. The classical statements, such as the Kelvin–Plank statement and the Clausius statement, help us formulate the second law:

- **The Kelvin–Plank statement.** It is impossible to construct a device operating in a cycle (e.g., heat engine), that accomplishes only the extraction of heat from some source and its complete conversion to work. This statement describes the impossibility to have a heat engine with a thermal efficiency of 100%.
- **The Clausius statement.** It is impossible to construct a device operating in a cycle (e.g., refrigerator and heat pump), that transfers heat from a low-temperature (cooler) region to a high-temperature (hotter) region.

A simple way to illustrate the implications of both the first and second laws is a desktop game that consists of several pendulums (made of metal balls), one in contact with the other. When you raise the first of the balls, you give energy to the system in the form of potential energy. Releasing this ball allows it to gain kinetic energy at the expense of potential energy. When this ball hits the second ball, a small elastic deformation transforms the kinetic energy again into a form of potential energy. The energy is transferred from one ball to the other. The last ball again gains kinetic energy, which allows it to rise. The cycle continues, with the ball rising every time to a slightly lower level, until it finally stops. The first law concerns why the balls keep moving, while the second law explains why they do not do it forever. In this game, the energy is lost in the form of sound and heat, as the motion declines.

The second law also states that the entropy in the universe always increases. As mentioned before, entropy is a measure of degree of disorder, and every process happening in the universe increases the entropy of the universe to a higher level. The entropy of a state of a system is proportional to (depends on) its probability, which gives us an opportunity to define the second

law in a broader manner as “the entropy of a system increases in any heat transfer or conversion of energy within a closed system.” That is why all energy transfers or conversions are irreversible. From the entropy perspective, the basis of the second law is the statement that the sum of the entropy of a system changes and that of its surroundings must always be positive. Recently, much effort has been invested in minimizing the entropy generation (irreversibilities) in thermodynamic systems and applications.

Moran and Shapiro (2007) noted that the second law and deductions from it are useful because they provide a means for

- predicting the direction of processes;
- establishing conditions for equilibrium;
- determining the best performance of thermodynamic systems and applications;
- quantitatively evaluating the factors that preclude the attainment of the best theoretical performance level;
- defining a temperature scale, independent of the properties of the substance; and
- developing tools for evaluating some thermodynamic properties, for example, internal energy and enthalpy, using available experimental data.

Consequently, the second law is the linkage between entropy and the usefulness of energy. The second law analysis has found applications in a wide variety of disciplines, for example, chemistry, economics, ecology, environment, and sociology, far removed from engineering thermodynamics applications.

#### 1.4.20 Reversibility and Irreversibility

These two concepts are highly important to thermodynamic processes and systems. *Reversibility* is defined by the statement that only for a reversible process can both a system and its surroundings be returned to their initial states. Such a process is only theoretical. The irreversibility during a process describes the destruction of useful energy or availability. Without new inputs, both the system and its surroundings cannot be returned to their initial states because of the irreversibilities that have occurred, for example, friction, heat transfer or rejection, and electrical and mechanical effects. For instance, an actual system provides an amount of work that is less than the ideal reversible work, so the difference between these two values gives the irreversibility of that system. In real applications, there are always such differences, and therefore real processes and cycles are always irreversible.

#### 1.4.21 Exergy

Exergy is defined as the maximum amount of work (also called *availability*, see Table 1.4) that can be produced by a stream of matter or energy (heat, work, etc.) as it comes to equilibrium with a reference environment. Exergy is a measure of the potential of a flow or system to cause change as a consequence of not being in complete stable equilibrium relative to a reference environment. For exergy analysis, the state of the reference environment, or the reference state, must be specified completely. This is commonly done by specifying the temperature, pressure, and chemical composition of the reference environment. Exergy is not subject to a conservation law. Rather exergy is consumed or destroyed because of irreversibilities in any process. Table 1.5 compares energy and exergy from a thermodynamics point of view.

As pointed out by Dincer and Rosen (1999, 2007), exergy is a measure of the usefulness, quality or potential of a flow or system to cause change, and is therefore a type of measure of the potential of a substance to impact on the environment.

Exergy analysis is a method that uses the conservation of mass and conservation of energy principles together with the second law of thermodynamics for the design and analysis of systems and processes. The exergy method can be suitable for furthering the goal of more efficient



**Table 1.4** Relations among essergy, availability, exergy, and free energy

Name	Function	Remarks
Essergy	$E + P_0V - T_0S - \sum_i \mu_{i0}N_i$	Formulated for the special case in 1878 by Gibbs and in general in 1962, and changed from available energy to exergy in 1963, and from exergy to essergy (i.e., essence of energy) in 1968 by Evans.
Availability	$E + P_0V - T_0S - (E_0 + P_0V_0 - T_0S_0)$	Formulated by Keenan in 1941 as a special case of the essergy function.
Exergy	$E + P_0V - T_0S - (E_0 + P_0V_0 - T_0S_0)$	Introduced by Darrieus in 1930 and Keenan in 1932; called the availability in steady flow by him, and exergy by Rant in 1956 as a special case of essergy.
Free Energy	Helmholtz: $E - TS$ Gibbs: $E + PV - TS$	Introduced by von Helmholtz and Gibbs in 1873 as the Legendre transforms of energy to yield useful alternate criteria of equilibrium, as measures of the potential work of systems representing special cases of the essergy function.

Source: Szargut *et al.* (1988).

**Table 1.5** Comparison between energy and exergy

Energy	Exergy
<ul style="list-style-type: none"> <li>• Dependent on the parameters of matter or energy flow only, and independent of the environment parameters.</li> <li>• Has values different from zero (which is equal to <math>mc^2</math> in accordance with Einstein's equation).</li> <li>• Guided by the first law of thermodynamics for all processes.</li> <li>• Limited by the second law of thermodynamics for all processes (including reversible ones).</li> <li>• Conserved in all processes.</li> </ul>	<ul style="list-style-type: none"> <li>• Dependent both on the parameters of matter or energy flow and on the environment parameters.</li> <li>• Equal to zero (in dead state by virtue of being in equilibrium with the environment).</li> <li>• Guided by the first and second laws of thermodynamics for reversible processes only (in irreversible processes, it is destroyed partly or completely).</li> <li>• Not limited for reversible processes owing to the second law of thermodynamics.</li> <li>• Not conserved in all processes.</li> </ul>

energy-resource use, for it enables the locations, types, and true magnitudes of wastes and losses to be determined. Therefore, exergy analysis can reveal whether or not, and by how much, it is possible to design more efficient energy systems by reducing the sources of inefficiency in existing systems. In the past, exergy was called *essergy*, *availability*, and *available energy*. Table 1.4 lists some relations among essergy, availability, exergy, and free energy.

From the point of view of energy and exergy efficiency, it is important to note that if a fossil fuel-based energy source is used for a low-temperature thermal application like space heating or cooling, there would be a great difference between the corresponding energy and exergy efficiencies, perhaps by as much as 50–70% for the energy efficiency and 5% for the exergy efficiency (Dincer, 1998). One may ask why, and to address that question, we provide the following:

- High quality (e.g., high temperature) energy sources such as fossil fuels are often used for relatively low-quality (e.g., low-temperature) processes like water and space heating or cooling.

- Exergy efficiency permits a better matching of energy sources and uses, leading to high-quality energy being reserved for performing high-quality tasks and not used for low-quality end uses.

## 1.5 General Aspects of Fluid Flow

For a good understanding of the operation of thermal energy storage systems and their components, as well as the behavior of fluid flows, an extensive background on fluid mechanics is essential. In addition to learning the principles of fluid flow, the student and/or engineer should develop an understanding of the properties of fluids and be able to solve practical thermodynamic problems.

In practice, engineers are regularly faced with a large variety of fluid-flow problems:

- subcooled liquids, like water and brine;
- mixtures of boiling liquids and the ensuing vapor;
- mixtures of refrigerants and absorbents;
- mixtures of air and water vapor as humid air; and
- low- and high-pressure gases.

To deal effectively with fluid-flow systems, it is necessary to identify flow categories, defined in predominantly mathematical terms, that allow the appropriate analysis to be undertaken by identifying suitable and acceptable simplifications. Examples of the categories to be introduced include variation of the flow parameters with time (steady or unsteady) or variations along the flow path (uniform or nonuniform). Similarly, compressibility effects may be important in high-speed gas flows, but may be ignored in many liquid flow situations.

### 1.5.1 Classification of Fluid Flows

Various criteria allow fluid flows to be classified into the following categories:

- uniform or nonuniform,
- one-, two-, or three-dimensional,
- steady- or unsteady-state,
- laminar or turbulent, and
- compressible or incompressible.

Also, liquids flowing in open channels may be classified according to their regions, for example, subcritical, critical, or supercritical, and gas flows may be categorized as subsonic, transonic, supersonic, or hypersonic.

#### Uniform Flow and Nonuniform Flow

If the velocity and cross-sectional area are constant in the direction of flow, the flow is uniform. Otherwise, the flow is nonuniform.

#### One-, Two-, and Three-Dimensional Flow

The flow of real fluids occurs in three dimensions. However, in the analysis the conditions are often simplified to either one- or two-dimensional, depending on the flow problem under consideration. If all fluid and flow parameters (velocity, pressure, elevation, temperature, density, viscosity, etc.) are considered to be uniform throughout any cross-section and vary only along the direction of

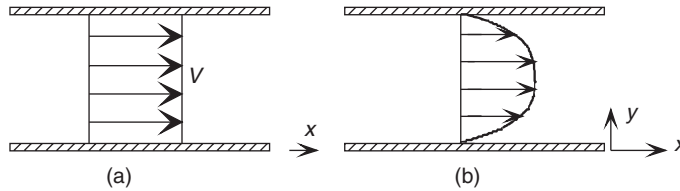


**Figure 1.6** Velocity profiles for flows: (a) one-dimensional flow, (b) two-dimensional flow

flow (Figure 1.6a), the flow is one-dimensional. Two-dimensional flow occurs when the fluid and flow parameters have spatial gradients in two directions, that is,  $x$  and  $y$  axes (Figure 1.6b). In three-dimensional flow, the fluid and flow parameters vary in three directions, that is,  $x$ ,  $y$ , and  $z$  axes, and the gradients of the parameters occur in all three directions.

### Steady Flow

Steady flow is defined as a flow in which the flow conditions do not change with time. However, we may have a steady flow in which the velocity, pressure, and cross-section of the flow vary from point to point but do not change with time. This requires us to distinguish by dividing such a flow into *steady, uniform flow* and *steady, nonuniform flow*. In a steady, uniform flow, all conditions (e.g., velocity, pressure, and cross-sectional area) are uniform and do not vary with time or position. For example, uniform flow of water in a duct of constant cross-section is considered a steady, uniform flow. If the conditions (e.g., velocity and cross-sectional area) change from point to point (e.g., from cross-section to cross-section) but not with time, we have a steady, nonuniform flow. For example, a liquid flows at a constant rate through a tapering pipe running completely full.

### Unsteady Flow

If the conditions vary with time, the flow becomes unsteady. If at a given time the velocity at every point in the flow field is the same, but the velocity changes with time, we have an *unsteady, uniform flow*. An example is an accelerating flow of a fluid through a pipe of uniform bore running full. In an unsteady, uniform flow, the conditions in cross-sectional area and velocity vary with time from point to point, for example, a wave traveling along a channel.

### Laminar Flow and Turbulent Flow

This classification is one of the most important in fluid flow and depends primarily upon the arbitrary disturbances, irregularities, or fluctuations in the flow field, based on the internal characteristics of the flow. In this regard, there are two significant parameters such as velocity and viscosity. If the flow occurs at a relatively low velocity and/or with a highly viscous fluid, resulting in a fluid flow in an orderly manner without fluctuations, the flow is referred to as laminar. As the flow velocity increases and/or the viscosity of fluid decreases, the fluctuations take place gradually, referring to a *transition state* which is dependent on the fluid viscosity, the flow velocity, and geometric details. The Reynolds number  $Re$  is introduced to represent the characteristics of the flow conditions relative to the transition state. As the flow conditions deviate more from the transition state, a more chaotic flow field, that is, turbulent flow, occurs. Increasing Reynolds number increases the chaotic nature of the turbulence. Turbulent flow is, therefore, defined as a characteristic representative of the irregularities in the flow field.

The differences between laminar flow and turbulent flow can be distinguished by the Reynolds number, which is expressed as

$$\text{Re} = \frac{VD}{\nu} = \frac{\rho VD}{\mu} \quad (1.43)$$

The Reynolds number indicates the ratio of inertial force to viscous force. At high Reynolds numbers the inertia forces dominate, resulting in turbulent flow, while at low Reynolds numbers the viscous forces become dominant, making the flow laminar. In a circular duct, the flow is laminar when  $\text{Re}$  is less than 2100 and turbulent when  $\text{Re}$  is greater than 4000. In a duct with a rough surface, the flow is turbulent at  $\text{Re}$  values as low as 2700.

### Compressible Flow and Incompressible Flow

All actual fluids are normally compressible, leading to a change in their density with pressure. However, in many cases it is assumed during analysis that changes in density are negligibly small. This refers to incompressible flow.

#### 1.5.2 Viscosity

Viscosity is one of the most significant fluid properties, and is defined as a measure of the fluid's resistance to deformation. In gases, the viscosity increases with increasing temperature, resulting in a greater molecular activity and momentum transfer. The viscosity of an ideal gas is a function of molecular dimensions and absolute temperature only, based on the kinetic theory of gases. However, in fluids, molecular cohesion between molecules considerably affects the viscosity, and the viscosity decreases with increasing temperature because of the fact that the cohesive forces are reduced by increasing the temperature of the fluid (causing a decrease in shear stress). This phenomenon results in an increase in the rate of molecular interchange, leading to a net result of a reduction in viscosity. The coefficient of viscosity of an ideal fluid is zero, meaning that an ideal fluid is inviscid, so that no shear stresses occur in the fluid, despite the fact that shear deformations are finite. Nevertheless, all real fluids are viscous.

As a fluid moves past a solid boundary or wall, the velocity of the fluid particles at the wall must equal the velocity of the wall; the relative velocity between the fluid and the wall at the surface of the wall is zero, which is called the *no-slip* condition, and results in a varying magnitude of the flow velocity (e.g., a velocity gradient), as one moves away from the wall (see Figure 1.7).

There are two types of viscosities, namely, *dynamic viscosity*, which is the ratio of a shear stress to a fluid strain (velocity gradient), and *kinematic viscosity*, which is defined as the ratio of dynamic viscosity to density.

The dynamic viscosity, based on a two-dimensional boundary layer flow and the velocity gradient  $du/dy$  occurring in the direction normal to the flow, as shown in Figure 1.7, leading to the shear

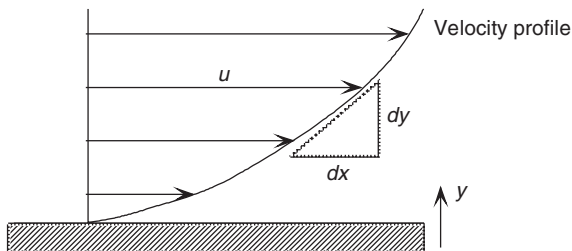


**Figure 1.7** Schematic of velocity profile moving away from a wall (i.e., as  $y$  increases)

stress within a fluid being proportional to the spatial rate of change of fluid strain normal to the flow, is expressed as

$$\mu = \frac{\tau}{(du/dy)} \quad (1.44)$$

where the units of  $\mu$  are  $\text{Ns/m}^2$  or  $\text{kg/ms}$  in the SI system and  $\text{lb}_f\text{s/ft}^2$  in the English system.

The kinematic viscosity then becomes

$$\nu = \frac{\mu}{\rho} \quad (1.45)$$

where the units of  $\nu$  are  $\text{m}^2/\text{s}$  in the SI system and  $\text{ft}^2/\text{s}$  in the English system.

From the viscosity perspective, the types of fluids may be classified into the two groups that follow below.

### Newtonian Fluids

These fluids have a dynamic viscosity dependent upon temperature and pressure and independent of the magnitude of the velocity gradient. For such fluids, Equation 1.44 is applicable. Some examples are water and air.

### Non-Newtonian Fluids

Fluids that cannot be represented by Equation 1.44 are called *non-Newtonian fluids*. These fluids are very common in practice and have a more complex viscous behavior due to the deviation from Newtonian behavior. There are several approximate expressions to represent their viscous behavior. Some examples of such fluids are slurries, polymer solutions, oil paints, toothpaste, and sludges.

## 1.5.3 Equations of Flow

The basic equations of fluid flow may be derived from important fundamental principles, namely, conservation of mass, conservation of momentum (i.e., Newton's second law of motion), and conservation of energy. Although general statements of these laws can be written (applicable to all substances, e.g., solids and fluids), in fluid flow these principles can be formulated as a function of flow parameters, namely, pressure, temperature, and density. The equations of motion may be classified into two general types: the equations of motion for inviscid fluids (i.e., frictionless fluids) and the equations of motion for viscous fluids. In this regard, we deal with the Bernoulli equations and Navier–Stokes equations.

### Continuity Equation

This is based on the *conservation of mass* principle. The requirement that mass be conserved at every point in a flowing fluid imposes certain restrictions on the velocity  $u$  and density  $\rho$ . Therefore, the rate of mass change is zero, so that for a steady flow, the mass of fluid in the control volume remains constant, and therefore the mass of fluid entering per unit time is equal to the mass of fluid exiting per unit time. We now apply this idea to a steady flow in a stream tube (Figure 1.8). The continuity equation for the flow of a compressible fluid through a stream tube is

$$\rho_1 \delta A_1 u_1 = \rho_2 \delta A_2 u_2 = \text{constant} \quad (1.46)$$

where  $\rho_1 \delta A_1 u_1$  is the mass entering per unit time (at section 1) and  $\rho_2 \delta A_2 u_2$  is the mass exiting per unit time (at section 2).

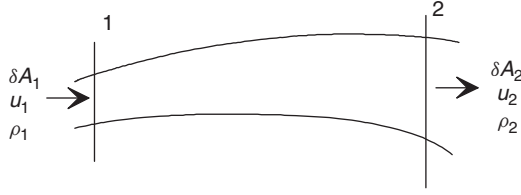


**Figure 1.8** Fluid flow in a stream tube

In practice, for the flow of a real fluid through a pipe or a conduit, the mean velocity is used since the velocity varies from wall to wall. Then, Equation 1.46 can be rewritten as

$$\rho_1 A_1 \bar{u}_1 = \rho_2 A_2 \bar{u}_2 = \dot{m} \quad (1.47)$$

where  $\bar{u}_1$  and  $\bar{u}_2$  are the mean velocities at sections 1 and 2.

For fluids that are considered as incompressible, Equation 1.47 is simplified to the following, since  $\rho_1 = \rho_2$ :

$$A_1 \bar{u}_1 = A_2 \bar{u}_2 = \dot{V} \quad (1.48)$$

The various forms of the continuity equation for steady-state and unsteady-state cases are summarized below:

- The steady-state continuity equation for an incompressible fluid in a stream tube:

$$V \cdot A = \dot{V} \quad (1.49)$$

- The unsteady-state continuity equation for an incompressible fluid in a stream tube:

$$\left( \frac{dm}{dt} \right)_{sys} = \frac{d}{dt} \int_{cv} \rho dV + \int_{cs} \rho \bar{V} d\bar{A} \quad (1.50)$$

- The steady-state continuity equation for an incompressible fluid in cartesian coordinates:

$$\frac{\partial u}{\partial x} + \frac{\partial v}{\partial y} + \frac{\partial w}{\partial z} = 0 \quad (1.51)$$

- The unsteady-state continuity equation for an incompressible fluid in cartesian coordinates:

$$\frac{\partial(\rho u)}{\partial x} + \frac{\partial(\rho v)}{\partial y} + \frac{\partial(\rho w)}{\partial z} = \frac{\partial \rho}{\partial t} \quad (1.52)$$

- The steady-state continuity equation for an incompressible fluid in cylindrical coordinates:

$$\frac{\partial v_r}{\partial r} + \frac{1}{r} \frac{\partial v_\theta}{\partial \theta} + \frac{\partial v_z}{\partial z} + \frac{v_r}{r} = 0 \quad (1.53)$$

- The steady-state continuity equation for a compressible fluid in a stream tube:

$$\rho V \cdot A = \dot{m} \quad (1.54)$$

- The steady-state continuity equation for a compressible fluid in cartesian coordinates:

$$\frac{\partial(\rho u)}{\partial x} + \frac{\partial(\rho v)}{\partial y} + \frac{\partial(\rho w)}{\partial z} = 0 \quad (1.55)$$

- The steady-state continuity equation for a compressible fluid in cylindrical coordinates:

$$\frac{\partial(\rho v_r)}{\partial r} + \frac{1}{r} \frac{\partial(\rho v_\theta)}{\partial \theta} + \frac{\partial(\rho v_z)}{\partial z} + \frac{\rho v_r}{r} = 0 \quad (1.56)$$

- The unsteady-state continuity equation for a compressible fluid in a stream tube:

$$\frac{\partial(\rho A)}{\partial t} + \frac{\partial(\rho V \cdot A)}{\partial s} = 0 \quad (1.57)$$

- The unsteady-state continuity equation for a compressible fluid in cartesian coordinates:

$$\frac{\partial \rho}{\partial t} + \frac{\partial(\rho u)}{\partial x} + \frac{\partial(\rho v)}{\partial y} + \frac{\partial(\rho w)}{\partial z} = 0 \quad (1.58)$$

- The unsteady-state continuity equation for a compressible fluid in cylindrical coordinates:

$$\frac{\partial \rho}{\partial t} + \frac{\partial(\rho v_r)}{\partial r} + \frac{1}{r} \frac{\partial(\rho v_\theta)}{\partial \theta} + \frac{\partial(\rho v_z)}{\partial z} + \frac{\rho v_r}{r} = 0 \quad (1.59)$$

### Momentum Equation

The analysis of fluid-flow phenomena is fundamentally dependent on the application of Newton's second law of motion, which is more general than the momentum principle, stating that when the net external force acting on a system is zero, the linear momentum of the system in the direction of the force is conserved in both magnitude and direction (the so-called *conservation of linear momentum*). In fact, the momentum principle is concerned only with external forces, and provides useful results in many situations without requiring much information on the internal processes within the fluid. The momentum principle finds applications in various types of flows (e.g., steady or unsteady, compressible or incompressible).

The motion of a particle must be described relative to an inertial coordinate frame. The one-dimensional momentum equation at constant velocity can be written as follows:

$$\Sigma F = \frac{d}{dt}(mV) \quad (1.60)$$

where  $\Sigma F$  stands for the sum of the external forces acting on the fluid, and  $mV$  stands for the kinetic momentum in that direction. Equation 1.60 states that the time rate of change of the linear momentum of the system in the direction of  $V$  equals the resultant of all forces acting on the system in the direction of  $V$ . The linear momentum equation is a vector equation and is therefore dependent on a set of coordinate directions.

The rate of change of momentum of a control mass can be related to the rate of change of momentum of a control volume via the continuity equation. Then, Equation 1.60 becomes

$$\Sigma F_t = \Sigma F_{cv} + \Sigma F_{cs} = \frac{d}{dt} \int_{cv} V \rho dV - \int_{cs} V(\rho \bar{V} d\bar{A}) \quad (1.61)$$

Here, the sum of forces acting on the control volume in any direction is equal to the rate of change of momentum of the control volume in that direction plus the net rate of momentum flux from the control volume through its control surface in the same direction.

For a steady flow, if the velocity across the control surface is constant, the momentum equation in scalar form becomes

$$\Sigma F_x = (\dot{m} V_x)_e - (\dot{m} V_x)_i \quad (1.62)$$

If the mass flow rate  $\dot{m}$  is constant, Equation 1.62 can be written as

$$\Sigma F_x = \dot{m}(V_{x_e} - V_{x_i}) \quad (1.63)$$

Similar expressions can be written for the  $y$  and  $z$  directions.

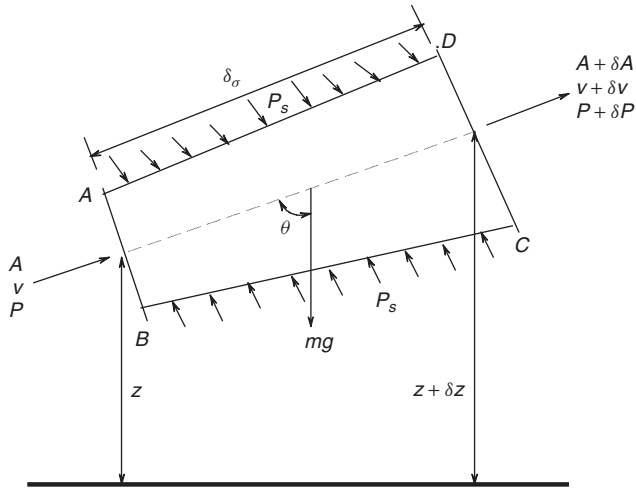


**Figure 1.9** Relationship between velocity, pressure, elevation, and density for a stream tube

### Euler's Equation

Euler's equation is a mathematical statement of Newton's second law of motion, and finds application in an inviscid fluid continuum. This equation states that the product of mass and acceleration of a fluid particle can be equated vectorially with the external forces acting on the particle. Consider a stream tube, as shown in Figure 1.9, with a cross-sectional area small enough for the velocity to be considered constant along the tube.

The following is a simple form of Euler's equation for a steady flow along a stream tube, representing the relationship in differential form between pressure  $p$ , velocity  $v$ , density  $\rho$ , and elevation  $z$ , respectively:

$$\frac{1}{\rho} \frac{dp}{ds} + v \frac{dv}{ds} + g \frac{dz}{ds} = 0 \quad (1.64)$$

For an incompressible fluid ( $\rho$  is constant), the integration of the above equation gives the following expression along the streamline (with respect to  $s$ ) for an inviscid fluid:

$$\frac{p}{\rho} + \frac{v^2}{2} + gz = \text{constant} \quad (1.65)$$

For a compressible fluid, the integration of Equation 1.64 can only be completed to provide the following:

$$\int \frac{dp}{\rho g} + \frac{v^2}{2g} + z = H \quad (1.66)$$

Note that the relationship between  $\rho$  and  $p$  needs to be known for the given case, and that for gases the relationship can be in the form  $p\rho^n = \text{constant}$ , varying from adiabatic to isothermal conditions, while for a liquid,  $\rho(dp/d\rho) = K$ , which is an adiabatic modulus.

### Bernoulli's Equation

This equation can be written for both incompressible and compressible flows. Under certain flow conditions, Bernoulli's equation for incompressible flow is often referred to as a *mechanical-energy*



*equation* because of the fact that there is similarity to the steady-flow energy equation obtained from the FLT for an inviscid fluid with no external heat transfer and no external work. It is necessary to point out that for inviscid fluids viscous forces and surface tension forces are not taken into consideration, leading to negligible viscous effects. The Bernoulli equation is commonly used in a variety of practical applications, particularly in flows in which the losses are negligibly small, for example, in hydraulic systems. The following is the general Bernoulli equation per unit mass for inviscid fluids between any two points:

$$\frac{u_1^2}{2g} + \frac{p_1}{\rho g} + z_1 = \frac{u_2^2}{2g} + \frac{p_2}{\rho g} + z_2 = H \quad (1.67)$$

Here, each term has a dimension of a length or head scale. In this regard,  $u^2/2g$  (kinetic energy per unit mass) is referred to as the *velocity head*,  $p/\rho g$  (pressure energy per unit mass) as the *pressure head*,  $z$  (potential energy per unit mass) as the *potential head* (constant total head), and  $H$  (total energy per unit mass) as the *total head* in meters. Subscripts 1 and 2 denote where the variables are evaluated on the streamline.

The terms in Equation 1.67 represent energy per unit mass and have the unit of length. Bernoulli's equation can be obtained by dividing each term in Equation 1.65 by  $g$ . These terms, both individually and collectively, indicate the quantities that may be directly converted to produce mechanical energy.

In summary, if we compare Equation 1.67 with the general energy equation, we see that the Bernoulli equation contains even more restrictions than might first be realized, due to the following main assumptions:

- steady flow (common assumption applicable to many flows);
- incompressible flow (acceptable if the Mach number is less than 0.3);
- frictionless flow along a single streamline (highly restrictive);
- no external shaft work or heat transfer occurs between 1 and 2.

### Navier–Stokes Equations

The Navier–Stokes equations are the differential expressions of Newton's second law of motion, and are known as constitutive equations for viscous fluids. These equations were named after C.L.M.H. Navier and Sir G.G. Stokes, who are credited with their derivation.

For viscous fluids, two force aspects, namely, a body force and a pressure force on their surface, are taken into consideration. The solution of these equations is dependent upon what flow information is known. The solutions evolving now for such problems have become extremely useful. Recently numerical software packages have been developed in the field of fluid flow for many engineering applications.

Exact solutions to the nonlinear Navier–Stokes equations are limited to a few cases, particularly for steady, uniform flows (either two-dimensional or with radial symmetry) or for flows with simple geometries. However, approximate solutions may be undertaken for other one-dimensional simple flow cases which require only the momentum and continuity equations in the flow direction for the solution of the flow field. Here, we present a few cases: uniform flow between parallel plates, uniform free surface flow down a plate, and uniform flow in a circular tube.

**Uniform Flow between Parallel Plates** Consider a two-dimensional uniform, steady flow between parallel plates, which extend infinitely in the  $z$  direction, as shown in Figure 1.10. We also consider the plates to be oriented at an angle  $\theta$  to the horizontal plane, which results in a body force per unit mass as the gravitational term  $g \sin \theta$ . Therefore, the pressure gradient is specified as  $(\partial p / \partial y) = \text{constant} = P^*$ . After making necessary simplifications and integrating, we find the total

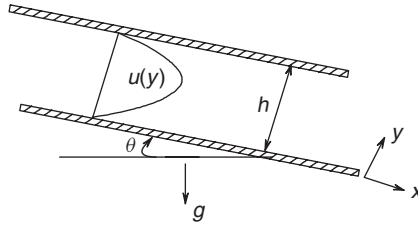


**Figure 1.10** Uniform flow between two stationary parallel plates

flow rate per unit width and the velocity profile as follows:

$$q_f = \frac{h^3}{12\mu} (-P^* + \rho g \sin \theta) \quad (1.68)$$

$$u = \frac{1}{2\mu} (-P^* + \rho g \sin \theta) (hy - y^2) \quad (1.69)$$

If the plates are horizontally located (i.e.,  $\sin \theta = 0$ ), the above equations reduce to

$$q_f = -\frac{P^* h^3}{12\mu} \quad (1.70)$$

$$u = -\frac{P^*}{2\mu} (hy - y^2) \quad (1.71)$$

**Uniform Free Surface Flow Down a Plate** This case is, by nature, similar to the previous case, except that the upper plate has been removed, as shown in Figure 1.11. The boundary condition at the lower boundary is the same no-slip boundary condition as before, so that the velocity is zero. However, the boundary condition at the free surface can no longer be specified as no-slip. The total flow rate per unit width becomes

$$q_f = \frac{\rho g d^3 \sin \theta}{3\mu} \quad (1.72)$$

while the flow velocity is

$$u = \frac{\rho g \sin \theta}{\mu} (yd - y^2/2) \quad (1.73)$$

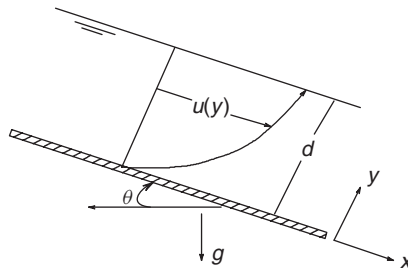


**Figure 1.11** Uniform flow down a plate

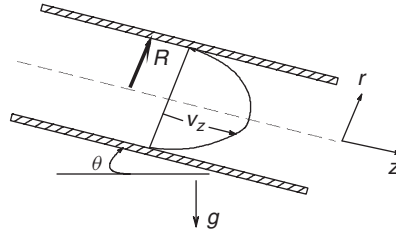


**Figure 1.12** Uniform flow in a pipe

Furthermore, the average velocity can be obtained by dividing the discharge by the flow area or depth as follows:

$$V = \frac{\rho g d^2 \sin \theta}{3\mu} \quad (1.74)$$

**Uniform Flow in a Circular Tube** This case concerns uniform fluid flow in a pipe of radius  $R$ , as shown in Figure 1.12, which is the most common example in practical applications associated with pipe flows. Despite having the flow field as three-dimensional, the assumption of radial symmetry makes the problem two-dimensional. Therefore, the parabolic velocity distribution with the maximum velocity at the center of the pipe can be found as follows:

$$v_z = \frac{(R^2 - r^2)}{4\mu} (-P^* + \rho g \sin \theta) \quad (1.75)$$

which is known as the Hagen-Poiseuille equation. The total volumetric flow rate can be calculated if the pressure gradient along with other flow conditions is specified and vice versa, as follows:

$$Q = \frac{\pi R^4}{8\mu} (-P^* + \rho g \sin \theta) \quad (1.76)$$

If the pipe is horizontally located (i.e.,  $\sin \theta = 0$ ), the above equations result in

$$v_z = \frac{(R^2 - r^2)}{4\mu} \quad (1.77)$$

$$Q = \frac{\pi R^4}{8\mu} \quad (1.78)$$

### 1.5.4 Boundary Layer

If there is an equivalence between fluid and surface velocities at the interface between a fluid and a surface, it is called a “no-slip” condition, which is entirely associated with viscous effects, as mentioned earlier. In practice, any real fluid flow shows a region of retarded flow near a boundary in which the velocity relative to the boundary varies from zero at the boundary to a value that may be estimated by the potential-flow solution some distance away. This region of retarded flow is known as the *boundary layer*, which was first introduced by Prandtl in 1904. His hypothesis of a boundary layer was arrived at by experimental observations of the flow past solid surfaces.

Of course, the boundary layer can be taken as that region of the fluid that is close to the surface immersed in the flowing fluid, and the boundary layer development takes place in both internal and external flows. In internal flows, it occurs until the entire fluid is encompassed, such as in pipe flow and open-channel flow. Boundary layer development is important for external flows, which

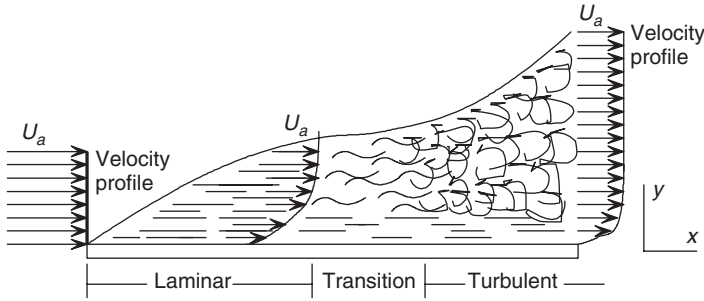


**Figure 1.13** Development of boundary layer in a viscous flow along a plate

exhibit a continued growth due to the absence of a confining boundary, such as a flow along a flat plate. It is, therefore, important to assume that the velocity at some distance from the boundary is unaffected by the presence of the boundary, referring to the free-stream velocity  $u_s$ .

We now consider a uniform flow of incompressible fluid at a free-stream velocity approaching the plate, as shown in Figure 1.13. Since the plate is stationary with respect to the earth, when the fluid is in contact with the plate surface, it has zero velocity (i.e., the “no-slip” condition). Later, the boundary layer thickens in the direction of flow, and a velocity gradient at a distance  $\delta$  over an increasingly greater distance normal to the plate takes place between the fluid in the free stream and the plate surface. The rate of change of velocity determines the velocity gradient at the surface as well as the shear stresses. The shear stress for the laminar boundary layer becomes

$$\tau = \mu \left( \frac{du}{dy} \right)_{y=0} \quad (1.79)$$

which varies with distance along the plate by the change in velocity. Further along the plate, the shear force is gradually increased, as the laminar boundary layer thickens, because of the increasing plate surface area affected, and the fluid becomes retarded, so that a turbulent boundary layer occurs as instabilities set in. Thus, the shear stress for the turbulent flow can be approximated as

$$\tau = (\mu + \epsilon) \left( \frac{du}{dy} \right)_{y=0} \quad (1.80)$$

Experimental studies indicate that there are two boundary layer flow regimes; a *laminar flow regime* and a *turbulent flow regime*, which can be characterized by the Reynolds number, as pointed out earlier. The transition from a laminar to a turbulent boundary layer is dependent mainly upon the following:

- $Re = u_s x_c / \nu$ ;
- the roughness of the plate; and
- the turbulence level in the free stream.

There are various boundary-layer parameters to be considered, such as boundary-layer thickness, the local wall shear stress (or local friction or drag coefficient), and the average wall shear stress (or average friction or drag coefficient). The boundary-layer thickness may be expressed in several ways. The simplest approach is that the velocity  $u$  within the boundary layer approaches the free-stream velocity  $u_s$ . From experimental measurements, it was observed that the boundary-layer thickness  $\delta$  can be defined as the distance from the boundary to the point at which  $u = 0.99u_s$ .

Table 1.6 gives the values of the boundary-layer thicknesses for laminar flow along a flat plate as a function of dimensionless coordinates  $\eta = y(u_s/\nu x)$ . These values are of practical interest in momentum analysis of fluid flow.

The momentum equations for velocity profiles can be summarized with respect to the momentum thickness, the average skin-drag coefficient, and the displacement thickness (see Table 1.7 for a flat plate). As can be pointed out from the table, the laminar boundary-layer thickness increases with  $x^{1/2}$  from the leading edge and inversely with  $u_s^{1/2}$ , the local and average skin-drag coefficients change inversely with  $x^{1/2}$  and  $u_s^{1/2}$ , and the total drag force,  $F = C_f \rho u_s^2 x/2$  per unit width, changes as the 1.5 power of  $u_s$  and the square root of the length  $x$ . Normally, fluid flow along a flat plate is laminar for Reynolds number values up to about 300,000–500,000, depending on the plate roughness and the level of turbulence in the free stream, as mentioned earlier.

Table 1.8 presents additional momentum equations for a boundary turbulent layer along a flat plate, including additional pipe flow velocity profiles, and summarizes the following for a turbulent boundary layer on a flat plate:

- The boundary-layer thickness increases as the 4/5 power of the distance from the leading edge, as compared with  $x^{1/2}$  for a laminar boundary layer.
- The local and average skin-friction coefficients vary inversely as the fifth root of both  $x$  and  $u_s$ , as compared with the square root for a laminar boundary layer.
- The total drag varies as  $u_s^{9/5}$ , and  $x^{4/5}$ , as compared with values of corresponding parameters for a laminar boundary layer.

**Table 1.6** Values of laminar boundary-layer thicknesses for laminar flow over a flat plate

$\eta$	0.0	0.6	1.2	1.8	2.4	3.0	3.6	4.2	4.8	5.4	6.0
$\delta$	0.000	0.200	0.394	0.575	0.729	0.846	0.924	0.967	0.988	0.996	0.999

Source: Olson and Wright (1991).

**Table 1.7** Momentum equations for laminar boundary layer

Velocity profile	$\delta/x$	$C_f$	$\delta^*/x$
$u/u_s = y/\delta$	$3.46/\text{Re}_x^{1/2}$	$1.156/\text{Re}_x^{1/2}$	$1.73/\text{Re}_x^{1/2}$
$u/u_s = 2(y/\delta) - (y/\delta)^2$	$5.48/\text{Re}_x^{1/2}$	$1.462/\text{Re}_x^{1/2}$	$1.83/\text{Re}_x^{1/2}$
$u/u_s = 1.5(y/\delta) - 0.5(y/\delta)^3$	$4.64/\text{Re}_x^{1/2}$	$1.292/\text{Re}_x^{1/2}$	$1.74/\text{Re}_x^{1/2}$
$u/u_s = \sin \pi y/2\delta$	$4.80/\text{Re}_x^{1/2}$	$1.310/\text{Re}_x^{1/2}$	$1.74/\text{Re}_x^{1/2}$
Blasius exact solution	$4.91/\text{Re}_x^{1/2}$	$1.328/\text{Re}_x^{1/2}$	$1.73/\text{Re}_x^{1/2}$

Source: Olson and Wright (1991).

**Table 1.8** Momentum equations for a turbulent boundary layer for flat plate flow and for pipe flow

$\text{Re}_D$	$F$	$u/u_s$	$V/u_s$	$C_f$	$\text{Re}_x$
$<10^5$	$0.316/\text{Re}_D^{1/4}$	$(y/R)^{1/7}$	49/60	$0.074/\text{Re}_x^{1/5}$	$5 \times 10^5 - 10^7$
$10^4 - 10^6$	$0.180/\text{Re}_D^{1/5}$	$(y/R)^{1/8}$	128/153	$0.045/\text{Re}_x^{1/6}$	$1.8 \times 10^5 - 4.5 \times 10^7$
$10^5 - 10^7$	$0.117/\text{Re}_D^{1/6}$	$(y/R)^{1/10}$	200/231	$0.0305/\text{Re}_x^{1/7}$	$2.9 \times 10^6 - 5 \times 10^8$

Source: Olson and Wright (1991).

Initially, as the boundary layer develops, it will be laminar in form. The boundary layer will become turbulent, based on the ratio of inertial and viscous forces acting on the fluid, referring to the value of the Reynolds number. For example, in pipe flow, for the values of  $Re < 2300$  the flow is laminar. If the Reynolds number increases, the flow becomes turbulent. Compared to flow along a flat plate, the major difference in pipe flow is that there is a limit to the growth of the boundary-layer thickness because of the pipe radius.

Many empirical pipe flow equations have been developed, particularly for water. The velocity  $V$  and volumetric flow rate  $\dot{V}$  equations of Hazen–Williams are the most widely used, and are as follows:

$$V = 0.850C R_h^{0.63} S^{0.54} \quad (1.81)$$

$$\dot{V} = 0.850C R_h^{0.63} S^{0.54} A \quad (1.82)$$

where  $R_h$  is the hydraulic radius of the pipe,  $P$  is wetted perimeter ( $A/P$ , for example,  $R_h = D/4$  for a round pipe),  $S$  is the slope of the total head line,  $h_f/L$ ,  $A$  is the pipe cross-sectional area, and  $C$  is the roughness coefficient. The coefficient  $C$  takes different values for the pipes, for example,  $C = 140$  for very badly corroded iron or steel pipes.

## 1.6 General Aspects of Heat Transfer

Thermal processes involving the transfer of heat from one point to another are often encountered in industries. The heating and cooling of gases, liquids, and solids, the evaporation of water, and the removal of heat liberated by chemical reaction are common examples of processes that involve heat transfer. Engineers, scientists, technologists, researchers, and others need to understand the physical phenomena and practical aspects of heat transfer, and have a good knowledge of the basic laws, governing equations, and related boundary conditions.

In order to transfer heat, there must be a driving force, which is the temperature difference between the locations where heat is taken and where the heat originates. For example, consider that a long slab of food product is subjected to heating on the left side; the heat flows from the left side to the right side, which is colder. Heat tends to flow from a point of high temperature to a point of low temperature, owing to the temperature difference driving force.

Many of the generalized relationships used in heat transfer calculations have been determined by means of dimensional analysis and empirical considerations. It has been found that certain standard dimensionless groups repeatedly appear in the final equations. It is necessary for people working in heat transfer to recognize the more important of these groups. Some of the most commonly used dimensionless groups that appear frequently in the heat transfer literature are given in Table 1.9.

**Table 1.9** Some of the most important heat transfer dimensionless parameters

Name	Symbol	Definition	Application
Biot number	Bi	$hY/k$	Steady- and unsteady-state conduction
Fourier number	Fo	$at/Y^2$	Unsteady-state conduction
Graetz number	Gz	$GY^2c_p/k$	Laminar convection
Grashof number	Gr	$G\beta\Delta TY^3/\nu^2$	Natural convection
Rayleigh number	Ra	$Gr \times Pr$	Natural convection
Nusselt number	Nu	$hY/k_f$	Natural or forced convection, boiling, or condensation
Peclet number	Pe	$UY/a = Re \times Pr$	Forced convection (for small Pr)
Prandtl number	Pr	$c_p\mu/k = \nu/a$	Natural or forced convection, boiling, or condensation
Reynolds number	Re	$UY/\nu$	Forced convection
Stanton number	St	$h/\rho U c_p = Nu/Re Pr$	Forced convection

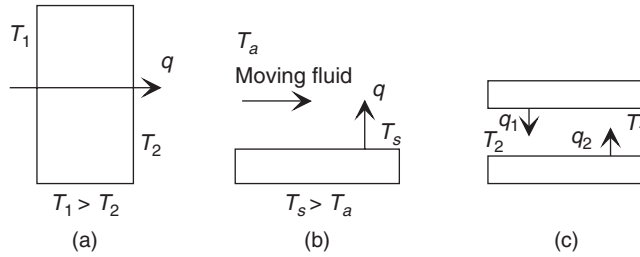


**Figure 1.14** Representations of heat transfer modes: (a) conduction through a solid, (b) convection from a surface to a moving fluid, (c) radiation between two surfaces

In the utilization of these groups, care must be taken to use equivalent units so that all the dimensions cancel out. Any system of units may be used in a dimensionless group as long as all units cancel in the final result.

Basically, heat is transferred in three ways: conduction, convection, and radiation (the so-called modes of heat transfer). In many cases, heat transfer takes place by all three of these methods simultaneously. Figure 1.14 shows the different types of heat transfer processes as modes. When a temperature gradient exists in a stationary medium, which may be a solid or a fluid, the heat transfer occurring across the medium is by conduction, the heat transfer occurring between a surface and a moving fluid at different temperatures is by convection, and the heat transfer occurring between two surfaces at different temperatures, in the absence of an intervening medium (or presence of a non-obscuring medium), is by radiation, where all surfaces of finite temperature emit energy in the form of electromagnetic waves.

### 1.6.1 Conduction Heat Transfer

Conduction is a mode of transfer of heat from one part of a material to another part of the same material, or from one material to another in physical contact with it, without appreciable displacement of the molecules forming the substance. For example, the heat transfer in a solid object subject to cooling in a medium is by conduction. In solid objects, the conduction of heat is partly due to the impact of adjacent molecules vibrating about their mean positions and partly due to internal radiation. When the solid object is a metal, there are also large numbers of mobile electrons that can easily move through the matter, passing from one atom to another, and they contribute to the redistribution of energy in the metal object. The contribution of the mobile electrons predominates in metals, which explains the relation that is observed between the thermal and electrical conductivities of such materials.

#### Fourier's Law of Heat Conduction

Fourier's law states that the instantaneous rate of heat flow through a homogeneous solid object is directly proportional to the cross-sectional area  $A$  (i.e., the area at right angles to the direction of heat flow) and to the temperature difference driving force across the object with respect to the length of the path of the heat flow,  $dT/dx$ . This is an empirical law based on observation.

Figure 1.15 presents an illustration of Fourier's law of heat conduction. Here, a thin slab object of thickness  $dx$  and surface area  $F$  has one face at a temperature  $T$  and the other at a lower temperature  $(T - dT)$ . Heat flows from the high-temperature side to the low-temperature side,

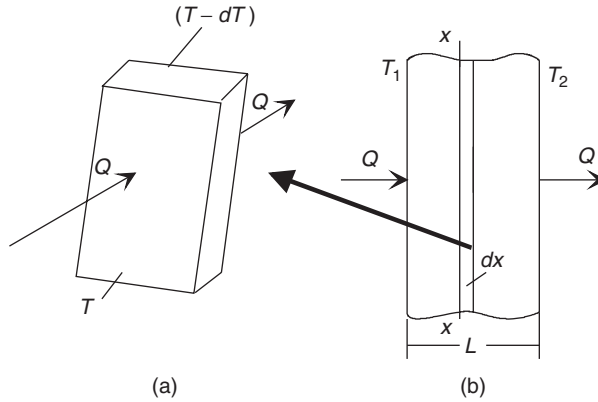


**Figure 1.15** Conduction in a slab (a) and in a thin slice of the slab (b)

with a temperature change  $dT$  in the direction of the heat flow. Therefore, under Fourier's law we obtain the heat transfer as

$$Q = -kA \frac{dT}{dx} \quad (1.83)$$

Here, we have a term *thermal conductivity*,  $k$ , of the object, which can be defined as the heat flow per unit area per unit time when the temperature decreases by one degree over a unit distance. The SI units of thermal conductivity are usually  $\text{W/m } ^\circ\text{C}$  or  $\text{W/m K}$ .

Integrating Equation 1.83 from  $T_1$  to  $T_2$  for  $dT$  and 0 to  $L$  for  $dx$  yields

$$Q = -k \frac{A}{L} (T_2 - T_1) = k \frac{A}{L} (T_1 - T_2) \quad (1.84)$$

Equation 1.84 can be solved when the variation of thermal conductivity with temperature is known. For most solids, thermal conductivity values are approximately constant over a broad range of temperatures, and can be taken as constants.

### 1.6.2 Convection Heat Transfer

Convection is the heat transfer mode that occurs within a fluid by mixing one portion of the fluid with another. Convection heat transfer may be classified according to the nature of the flow. When the flow is caused by some mechanical or external means such as a fan, a pump, or atmospheric wind, it is called *forced convection*. On the other hand, for *natural (free) convection* the flow is induced by buoyancy forces in the fluid that arise from density variations caused by temperature variations in the fluid. For example, when a hot object is exposed to the atmosphere, natural convection occurs, whereas in a cold place with a fan-driven air flow, forced-convection heat transfer takes place between air flow and the object subject to this flow. The transfer of heat through solid objects is by conduction alone, whereas the heat transfer from a solid surface to a liquid or gas takes place partly by conduction and partly by convection. Whenever there is an appreciable movement of the gas or liquid, the heat transfer by conduction in the gas or liquid becomes negligibly small compared with the heat transfer by convection. However, there is always a thin boundary layer of fluid on a surface, and through this thin film the heat is transferred by conduction. The convection heat transfer occurring within a fluid is due to the combined effects of conduction and bulk fluid motion. In general, the heat that is transferred is the *sensible* or internal thermal heat of the fluid. However, there are convection processes for which there is also *latent*



heat exchange, which is generally associated with a phase change between the liquid and vapor states of the fluid.

### Newton's Law of Cooling

Newton's law of cooling states that the heat transfer from a solid surface to a fluid is proportional to the difference between the surface and fluid temperatures, and the surface area. This is a particular type of convection heat transfer, and is expressed as

$$Q = hA(T_s - T_f) \quad (1.85)$$

where  $h$  is referred to as the *convection heat transfer coefficient* (the *heat transfer coefficient*, the *film coefficient*, or the *film conductance*). It encompasses all effects that influence the convection mode and depends on conditions in the boundary layer, which is affected by factors such as surface geometry, the nature of the fluid motion, and thermal and physical properties (Figure 1.16).

In Equation 1.85, a radiation term is not included. The calculation of radiation heat transfer is discussed later. In many heat transfer problems, the radiation effect on the total heat transfer is negligible compared with the heat transferred by conduction and convection from a surface to a fluid. When the surface temperature is high, or when the surface loses little heat by natural convection, then the heat transfer due to radiation is often of a similar magnitude to that lost by convection.

To better understand Newton's law of cooling, consider the heat transfer from a high-temperature fluid A to a low-temperature fluid B through a wall of thickness  $x$  (Figure 1.16). In fluid A, the temperature decreases rapidly from  $T_A$  to  $T_{s1}$  in the region of the wall, and similarly in fluid B from  $T_{s2}$  to  $T_B$ . In most cases, the fluid temperature is approximately constant throughout its bulk, apart from a thin film ( $\Delta_A$  or  $\Delta_B$ ) of fluid near each solid surface. The heat transfer per unit surface area from fluid A to the wall and that from the wall to fluid B can be expressed as

$$q = h_A(T_A - T_{s1}) \quad (1.86)$$

$$q = h_B(T_{s2} - T_B) \quad (1.87)$$

Also, the heat transfer in thin films is by conduction only, as given below:

$$q = \frac{k_A}{\Delta_A}(T_A - T_{s1}) \quad (1.88)$$

$$q = \frac{h_B}{\Delta_B}(T_{s2} - T_B) \quad (1.89)$$

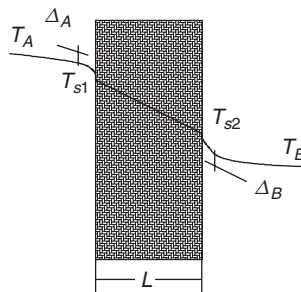


**Figure 1.16** A wall subject to convection heat transfer on both sides

Equating Equations 1.86–1.89, the convection heat transfer coefficients can be found to be  $h_A = k_A/\Delta_A$ , and  $h_B = k_B/\Delta_B$ . Thus, the heat transfer in the wall per unit surface area becomes

$$q = \frac{k}{L}(T_{s1} - T_{s2}) \quad (1.90)$$

For the case of steady-state heat transfer, Equation 1.86 is equal to Equation 1.87, and hence to Equation 1.90:

$$q = h_A(T_A - T_{s1}) = h_B(T_{s2} - T_B) = \frac{k}{L}(T_{s1} - T_{s2}) \quad (1.91)$$

which yields

$$q = \frac{(T_A - T_B)}{(1/h_A + L/k + 1/h_B)} \quad (1.92)$$

An analogy can be made with Equation 1.85, allowing Equation 1.92 to become

$$Q = HA(T_A - T_B) \quad (1.93)$$

where  $1/H = (1/h_A + L/k + 1/h_B)$ .  $H$  is the overall heat transfer coefficient and includes various heat transfer coefficients.

### 1.6.3 Radiation Heat Transfer

An object emits radiant energy in all directions unless its temperature is absolute zero. If this energy strikes a receiver, part of it may be absorbed, part may be transmitted, and part may be reflected. Heat transfer from a hot to a cold object in this manner is known as *radiation heat transfer*. The higher the temperature, the greater is the amount of energy radiated. If, therefore, two objects at different temperatures are placed so that the radiation from each object is intercepted by the other, then the body at the lower temperature will receive more energy than it radiates, and thereby its internal energy will increase; in conjunction with this, the internal energy of the object at the higher temperature will decrease. Radiation heat transfer frequently occurs between solid surfaces, although radiation from gases also takes place. Certain gases emit and absorb radiation at certain wavelengths only, whereas most solids radiate over a wide range of wavelengths. The radiative properties of many gases and solids may be found in heat transfer books.

Radiation striking an object can be absorbed by the object, reflected from the object, or transmitted through the object. The fractions of the radiation absorbed, reflected, and transmitted are called the *absorptivity*  $a$ , the *reflectivity*  $r$ , and the *transmissivity*  $t$ , respectively. By definition,  $a + r + t = 1$ . For many solids and liquids in practical applications, the transmitted radiation is negligible, and hence  $a + r = 1$ . A body that absorbs all radiation striking it is called a *blackbody*. For a blackbody,  $a = 1$  and  $r = 0$ .

#### The Stefan–Boltzman Law

This law was found experimentally by Stefan, and proved theoretically by Boltzmann. It states that the emissive power of a blackbody is directly proportional to the fourth power of its absolute temperature. The Stefan–Boltzmann law enables calculation of the amount of radiation emitted in all directions and over all wavelengths simply from the knowledge of the temperature of the blackbody. This law is expressible as follows:

$$E_b = \sigma T_s^4 \quad (1.94)$$

where  $\sigma$  denotes the Stefan–Boltzmann constant, which has a value of  $5.669 \times 10^{-8} \text{ W/m}^2 \text{ K}^4$ , and  $T_s$  denotes the absolute temperature of the surface.

The energy emitted by a non-blackbody becomes

$$E_{\text{nb}} = \varepsilon \sigma T_s^4 \quad (1.95)$$

Then, the heat transferred from an object's surface to its surroundings per unit area is

$$q = \varepsilon \sigma (T_s^4 - T_a^4) \quad (1.96)$$

Note that if the emissivity of the object at  $T_s$  is much different from the emissivity of the object at  $T_a$ , then this gray object approximation may not be sufficiently accurate. In this case, it is a good approximation to take the absorptivity of object 1 when receiving radiation from a source at  $T_a$  as being equal to the emissivity of object 1 when emitting radiation at  $T_a$ . This results in

$$q = \varepsilon_{T_s} \sigma T_s^4 - \varepsilon_{T_a} \sigma T_a^4 \quad (1.97)$$

There are numerous applications for which it is convenient to express the net radiation heat transfer (radiation heat exchange) in the following form:

$$Q = h_r A (T_s - T_a) \quad (1.98)$$

After combining Equations 1.97 and 1.98, the radiation heat transfer coefficient can be found as follows:

$$h_r = \varepsilon \sigma (T_s + T_a) (T_s^2 + T_a^2) \quad (1.99)$$

Here, the radiation heat transfer coefficient is seen to strongly depend on temperature, whereas the temperature dependence of the convection heat transfer coefficient is generally weak.

The surface within the surroundings may also simultaneously transfer heat by convection to the surroundings. The total rate of heat transfer from the surface is the sum of the convection and radiation modes:

$$Q_t = Q_c + Q_r = h_c A (T_s - T_a) + \varepsilon \sigma A (T_s^4 - T_a^4) \quad (1.100)$$

### 1.6.4 Thermal Resistance

There is a similarity between heat flow and electricity flow. While electrical resistance is associated with the conduction of electricity, thermal resistance is associated with the conduction of heat. The temperature difference providing heat conduction plays a role analogous to that of the potential difference or voltage in the conduction of electricity. Below we give the *thermal resistance for heat conduction*, based on Equation 1.84, and similarly the *electrical resistance for electrical conduction* according to Ohm's law:

$$R_{t,cd} \equiv \frac{(T_1 - T_2)}{Q_{cd}} = \frac{L}{kA} \quad (1.101)$$

$$R_e \equiv \frac{(E_1 - E_2)}{I} = \frac{L}{\sigma A} \quad (1.102)$$

It is also possible to write the *thermal resistance for convection*, based on Equation 1.85, as follows:

$$R_{t,c} \equiv \frac{(T_s - T_f)}{Q_c} = \frac{1}{hA} \quad (1.103)$$

In a series of connected objects through which heat is transferred, the total thermal resistance can be written in terms of the overall heat transfer coefficient. The heat transfer expression for a composite wall is discussed next.

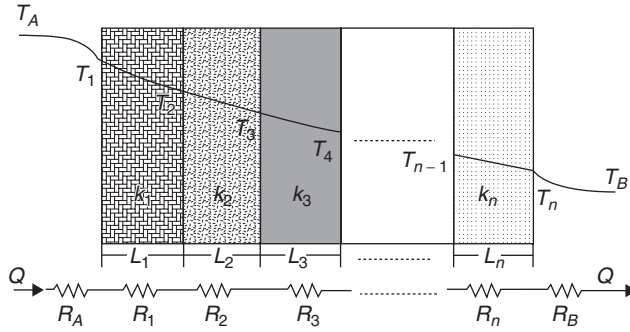


**Figure 1.17** A composite wall with many layers in series

### 1.6.5 The Composite Wall

In practice, there are many cases in the form of a composite wall, for example, the wall of a cold storeroom. Consider that we have a general form of the composite wall as shown in Figure 1.17. Such a system includes any number of series and parallel thermal resistances because of the existence of layers of different materials. The heat transfer rate is related to the temperature difference and resistance associated with each element as follows:

$$Q = \frac{(T_A - T_1)}{(1/h_1A)} = \frac{(T_1 - T_2)}{(L_1/k_1A)} = \dots = \frac{(T_n - T_B)}{(1/h_nA)} \quad (1.104)$$

Therefore, the one-dimensional heat transfer rate for this system can be written as

$$Q = \frac{(T_A - T_B)}{\Sigma R_t} = \frac{\Delta T}{\Sigma R_t} \quad (1.105)$$

where  $\Sigma R_t = R_{t,t} = 1/HA$ . Therefore, the overall heat transfer coefficient becomes

$$H = \frac{1}{R_{t,t}A} = \frac{1}{(1/h_1 + L_1/k_1 + \dots + 1/h_n)} \quad (1.106)$$

### 1.6.6 The Cylinder

A practical common object is a hollow cylinder, and a commonly encountered problem is the case of heat transfer through a pipe or cylinder. Consider that we have a cylinder of internal radius  $r_1$  and external radius  $r_2$ , whose inner and outer surfaces are in contact with fluids at different temperatures (Figure 1.18). In a steady-state form with no heat generation, the governing heat conduction equation is written as

$$\frac{1}{r} \frac{d}{dr} \left( kr \frac{dT}{dr} \right) = 0 \quad (1.107)$$

Based on Fourier's law, the rate at which heat is transferred by conduction across the cylindrical surface in the solid is expressed as

$$Q = -kA \frac{dT}{dr} = -k(2\pi rL) \frac{dT}{dr} \quad (1.108)$$

where  $A = 2\pi rL$  is the area normal to the direction of heat transfer.

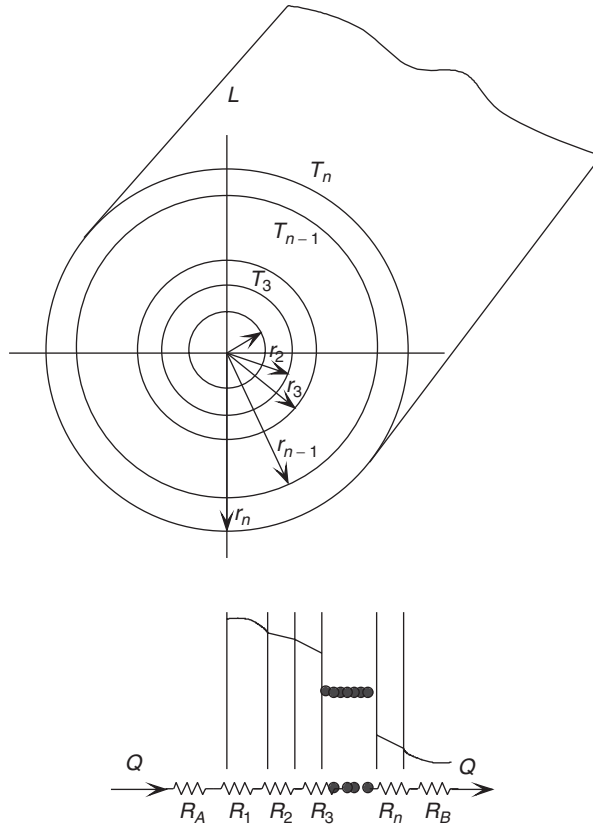


Figure 1.18 A hollow cylinder

To determine the temperature distribution in the cylinder, it is necessary to solve Equation 1.107 under appropriate boundary conditions, by assuming that  $k$  is constant. By integrating Equation 1.107 twice, the following heat transfer equation is obtained:

$$Q = \frac{k(2\pi L)(T_1 - T_2)}{\ln(r_1/r_2)} = \frac{(T_1 - T_2)}{R_t} \tag{1.109}$$

If we now consider a composite hollow cylinder, the heat transfer equation is found to be as follows, where interfacial contact resistances are neglected:

$$Q = \frac{(T_1 - T_n)}{R_{t,t}} = HA(T_1 - T_n) \tag{1.110}$$

where  $R_{t,t} = (1/2\pi r_1 L h_1) + (\ln(r_2/r_1)/2\pi k_1 L) + (\ln(r_3/r_2)/2\pi k_2 L) + \dots + (1/2\pi r_n L h_n)$ .

### 1.6.7 The Sphere

The case of heat transfer through a sphere is not as common as the cylinder problem. Consider a hollow sphere of internal radius  $r_1$  and external radius  $r_2$  (Figure 1.19). Also, consider the inside and outside temperatures to be  $T_1$  and  $T_2$ , respectively, and constant thermal conductivity with

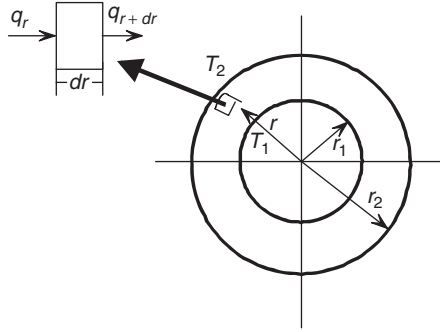


**Figure 1.19** Heat conduction in a hollow sphere

no heat generation. We can express the heat conduction across the sphere wall in the form of Fourier's law:

$$Q = -kA \frac{dT}{dr} = -k(4\pi r^2) \frac{dT}{dr} \quad (1.111)$$

where  $A = 4\pi r^2$  is the area normal to the direction of heat transfer.

After integrating Equation 1.111, we obtain the following expression:

$$Q = \frac{k(4\pi)(T_1 - T_2)}{(1/r_2 - 1/r_1)} = \frac{k(4\pi r_1 r_2)(T_1 - T_2)}{(r_2 - r_1)} = \frac{(T_1 - T_2)}{R_t} \quad (1.112)$$

If we now consider a composite hollow sphere, the heat transfer equation is determined to be as follows, neglecting interfacial contact resistances:

$$Q = \frac{(T_1 - T_n)}{R_{t,t}} = HA(T_1 - T_n) \quad (1.113)$$

where  $R_{t,t} = (1/4\pi r_1^2 h_1) + (r_2 - r_1)/(4\pi r_1 r_2 k_1) + (r_3 - r_2)/(4\pi r_2 r_3 k_2) + \dots + (1/4\pi r_2^2 h_2)$ .

## 1.6.8 Conduction with Heat Generation

### The Plane Wall

Consider a plane wall, as shown in Figure 1.20a, in which there is uniform heat generation per unit volume. The heat conduction equation becomes

$$\frac{d^2 T}{dx^2} + \frac{q_h}{k} = 0 \quad (1.114)$$

By integrating Equation 1.114 with the prescribed boundary conditions,  $T(-L) = T_1$  and  $T(L) = T_2$ . The temperature distribution can be obtained as

$$T(x) = \left( \frac{q_h L^2}{2k} \right) \left( 1 - \frac{x^2}{L^2} \right) + \left( \frac{T_2 - T_1}{2} \right) \left( \frac{x}{L} \right) + \left( \frac{T_2 + T_1}{2} \right) \quad (1.115)$$

The heat flux at any point in the wall can be found, depending on  $x$ , by using Equation 1.115 with Fourier's law.

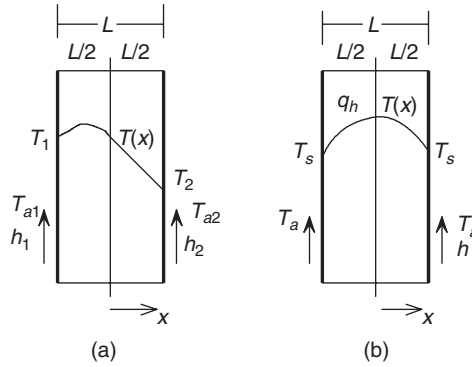


**Figure 1.20** Heat conduction in a slab with uniform heat generation: (a) asymmetrical boundary conditions, (b) symmetrical boundary conditions

If  $T_1 = T_2 \equiv T_s$ , the temperature distribution is symmetrical about the midplane (Figure 1.20b). Then,

$$T(x) = \left( \frac{q_h L^2}{2k} \right) \left( 1 - \frac{x^2}{L^2} \right) + T_s \tag{1.116}$$

At the plane of symmetry  $dT/dx = 0$ , and the maximum temperature at the midplane is

$$T(0) \equiv T_m = \left( \frac{q_h L^2}{2k} \right) + T_s \tag{1.117}$$

After combining Equations 1.116 and 1.117, we find the dimensionless temperature as follows:

$$\frac{(T(x) - T_m)}{(T_s - T_m)} = \left( \frac{x}{L} \right)^2 \tag{1.118}$$

### The Cylinder

Consider a long cylinder (Figure 1.18) with uniform heat generation. The heat conduction equation can be rewritten as

$$\frac{1}{r} \frac{d}{dr} \left( r \frac{dT}{dr} \right) + \frac{q_h}{k} = 0 \tag{1.119}$$

By integrating Equation 1.119, with the boundary conditions,  $dT/dr = 0$ , for the centerline ( $r = 0$ ) and  $T(r_1) = T_s$ , the temperature distribution can be obtained as

$$T(r) = \left( \frac{q_h r_1^2}{4k} \right) \left( 1 - \frac{r^2}{r_1^2} \right) + T_s \tag{1.120}$$

After combining terms, the dimensionless temperature equation results:

$$\frac{(T(r) - T_m)}{(T_s - T_m)} = 1 - \left( \frac{r}{r_1} \right)^2 \tag{1.121}$$

The approach mentioned previously can also be used for obtaining the temperature distributions in solid spheres and spherical shells for a wide range of boundary conditions.

### 1.6.9 Natural Convection

Heat transfer by natural (or free) convection involving motion in a fluid is due to differences in density and the action of gravity, which causes a natural circulation flow and leads to heat transfer. For many problems involving fluid flow across a surface, the superimposed effect of natural convection is negligibly small. The heat transfer coefficients for natural convection are generally much lower than that for forced convection. When there is no forced velocity of the fluid, heat is transferred entirely by natural convection (when there is negligible radiation). For some practical cases, it is necessary to consider the radiative effect on the total heat loss or gain. Radiation heat transfer may be of the same order of magnitude as natural convection in some circumstances even at room temperatures. Hence, wall temperatures in a room can affect the comfort of occupants.

It is pointed out that in many systems involving multimode heat transfer effects, natural convection provides the largest resistance to heat transfer, and therefore plays an important role in the design or performance of the system. Moreover, when it is desirable to minimize the heat transfer rates or to minimize operating costs, natural convection is often preferred to forced convection.

Natural convection is of significance in a wide variety of heating, cooling, and air-conditioning equipments. Natural convection heat transfer is influenced mainly by the gravitational force from thermal expansion, viscous drag, and thermal diffusion. For this reason, the gravitational acceleration, the coefficient of performance, the kinematic viscosity, and the thermal diffusivity directly affect natural convection. As shown in Table 1.8, these parameters depend on the fluid properties, the temperature difference between the surface and the fluid, and the characteristic length of the surface, which are involved in the Nusselt, Grashof, and Prandtl equations.

The natural convection boundary layers are not restricted to laminar flow. In many cases, there is a transition from laminar to turbulent flow. This is schematically shown in Figure 1.21 for a heated vertical plate.

Transition in a natural convection boundary layer is dependent on the relative magnitude of the buoyancy and viscous forces in the fluid. It is customary to correlate its occurrence in terms of the Rayleigh number. For example, for vertical plates the critical Rayleigh number is  $Ra \approx 10^9$ . As in forced convection, transition to turbulence has a strong effect on the heat transfer. Numerous natural convection heat transfer correlations for several plates, pipes, wires, cylinder, and so on, along with a list of heat transfer coefficients, which were compiled from the literature, are given in Table 1.10. To calculate the natural convection heat transfer coefficient, one evaluates the Rayleigh number to determine whether the boundary layer is laminar or turbulent, and then applies the appropriate equation from this table.

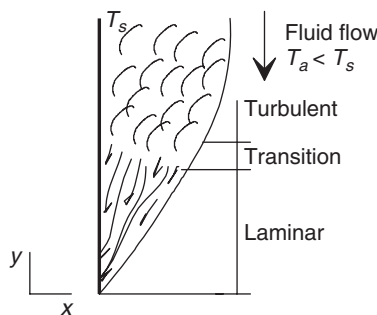


**Figure 1.21** Natural convection on a vertical plate



**Table 1.10** Natural convection heat transfer equations and correlations

Equation or correlation

- *General equations*

$$\text{Nu} = hY/k_f = c\text{Ra}^n \quad \text{and} \quad \text{Ra} = \text{Gr Pr} = g\beta(T_s - T_a)Y^3/\nu\alpha$$

where  $n$  is  $1/4$  for laminar flow and  $1/3$  for turbulent flow.  $Y$  denotes the height for vertical plates or pipes, diameter for horizontal pipes, and radius for spheres.  $T_{fm} \equiv (T_s + T_a)/2$ .

- *Correlations for vertical plates (or inclined plates, inclined up to  $60^\circ$ )*

$$\begin{aligned} \text{Nu} &= [0.825 + 0.387\text{Ra}^{1/6}/(1 + (0.492/\text{Pr})^{9/16})^{4/9}]^2 && \text{for an entire range of Ra} \\ \text{Nu} &= 0.68 + 0.67\text{Ra}^{1/4}/(1 + (0.492/\text{Pr})^{9/16})^{4/9} && \text{for } 0 < \text{Ra} < 10^9 \end{aligned}$$

- *Correlations for horizontal plates ( $Y \equiv A_s/P$ )*

For upper surface of heated plate or lower surface of cooled plate:

$$\text{Nu} = 0.54\text{Ra}^{1/4} \quad \text{for } 10^4 \leq \text{Ra} \leq 10^7$$

$$\text{Nu} = 0.15\text{Ra}^{1/3} \quad \text{for } 10^7 \leq \text{Ra} \leq 10^{11}$$

For lower surface of heated plate or upper surface of cooled plate:

$$\text{Nu} = 0.27\text{Ra}^{1/4} \quad \text{for } 10^5 \leq \text{Ra} \leq 10^{10}$$

- *Correlations for horizontal cylinders*

$$\text{Nu} = hD/k = c\text{Ra}^n$$

where

$$c = 0.675 \quad \text{and} \quad n = 0.058 \quad \text{for } 10^{-10} < \text{Ra} < 10^{-2}$$

$$c = 1.020 \quad \text{and} \quad n = 0.148 \quad \text{for } 10^{-2} < \text{Ra} < 10^2$$

$$c = 0.850 \quad \text{and} \quad n = 0.188 \quad \text{for } 10^2 < \text{Ra} < 10^4$$

$$c = 0.480 \quad \text{and} \quad n = 0.250 \quad \text{for } 10^4 < \text{Ra} < 10^7$$

$$c = 0.125 \quad \text{and} \quad n = 0.333 \quad \text{for } 10^7 < \text{Ra} < 10^{12}$$

$$\text{Nu} = [0.60 + 0.387\text{Ra}^{1/6}/(1 + (0.559/\text{Pr})^{9/16})^{8/27}]^2 \quad \text{for an entire range of Ra}$$

- *Correlations for spheres*

$$\text{Nu} = 2 + 0.589\text{Ra}^{1/4}/(1 + (0.469/\text{Pr})^{9/16})^{4/9} \quad \text{for } \text{Pr} \geq 0.7 \quad \text{and} \quad \text{Ra} \leq 10^{11}$$

- *Heat transfer correlations*

$$\text{Gr Pr} = 1.6 \times 10^6 Y^3 (\Delta T)$$

with  $Y$  in m;  $\Delta T$  in  $^\circ\text{C}$ .

$$h = 0.29(\Delta T/Y)^{1/4} \quad \text{for vertical small plates in laminar range}$$

$$h = 0.19(\Delta T)^{1/3} \quad \text{for vertical large plates in turbulent range}$$

$$h = 0.27(\Delta T/Y)^{1/4} \quad \text{for horizontal small plates in laminar range (facing upward when heated or downward when cooled)}$$

$$h = 0.22(\Delta T)^{1/3} \quad \text{for vertical large plates in turbulent range (facing downward when heated or upward when cooled)}$$

$$h = 0.27(\Delta T/Y)^{1/4} \quad \text{for small cylinders in laminar range}$$

$$h = 0.18(\Delta T)^{1/3} \quad \text{for large cylinders in turbulent range}$$

Source: Dincer, 1997.

### 1.6.10 Forced Convection

The study of forced convection is concerned with the heat transfer occurring between a forced moving fluid and a solid surface. To apply Newton's law of cooling as given in Equation 1.85, it is necessary to determine the heat transfer coefficient. For this purpose, the Nusselt–Reynolds

**Table 1.11** Forced-convection heat transfer equations and correlations

Equation or correlation		
• <i>Correlations for flat plate in external flow</i>		
$Nu = 0.332Re^{1/2}Pr^{1/3}$	for $Pr \geq 0.6$	for laminar; local; $T_{fm}$
$Nu = 0.664Re^{1/2}Pr^{1/3}$	for $Pr \geq 0.6$	for laminar; average; $T_{fm}$
$Nu = 0.565Re^{1/2}Pr^{1/2}$	for $Pr \leq 0.05$	for laminar; local; $T_{fm}$
$Nu = 0.0296Re^{4/5}Pr^{1/3}$	for $0.6 \leq Pr \leq 60$	for turbulent; local; $T_{fm}$ , $Re \leq 10^8$
$Nu = (0.037Re^{4/5} - 871)Pr^{1/3}$	for $0.6 < Pr < 60$	for mixed flow; average; $T_{fm}$ , $Re \leq 10^8$
• <i>Correlations for circular cylinders in cross-flow</i>		
$Nu = cRe^nPr^{1/3}$	for $Pr \geq 0.7$	for average; $T_{fm}$ ; $0.4 < Re < 4 \times 10^6$
where		
$c = 0.989$ and $n = 0.330$ for $0.4 < Re < 4$		
$c = 0.911$ and $n = 0.385$ for $4 < Re < 40$		
$c = 0.683$ and $n = 0.466$ for $40 < Re < 4,000$		
$c = 0.193$ and $n = 0.618$ for $4,000 < Re < 40,000$		
$c = 0.027$ and $n = 0.805$ for $40,000 < Re < 400,000$		
$Nu = cRe^nPr^s(Pr_a/Pr_s)^{1/4}$	for $0.7 < Pr < 500$	for average; $T_a$ ; $1 < Re < 10^6$
where		
$c = 0.750$ and $n = 0.4$ for $1 < Re < 40$		
$c = 0.510$ and $n = 0.5$ for $40 < Re < 1,000$		
$c = 0.260$ and $n = 0.6$ for $10^3 < Re < 2 \times 10^5$		
$c = 0.076$ and $n = 0.7$ for $2 \times 10^5 < Re < 10^6$		
$s = 0.37$ for $Pr \leq 10$		
$s = 0.36$ for $Pr > 10$		
$Nu = 0.3 + [(0.62Re^{1/2}Pr^{1/3})/(1 + (0.4/Pr)^{2/3})^{1/4}][1 + (Re/28,200)^{5/8}]^{4/5}$ for $RePr > 0.2$ for average; $T_{fm}$		
• <i>Correlations for spheres in cross-flow</i>		
$Nu/Pr^{1/3} = 0.37Re^{0.6}/Pr^{1/3}$		for average; $T_{fm}$ ; $17 < Re < 70,000$
$Nu = 2 + (0.4Re^{1/2} + 0.06Re^{2/3})Pr^{0.4}(\mu_a/\mu_s)^{1/4}$		for $0.71 < Pr < 380$
for average; $T_a$ ; $3.5 < Re < 7.6 \times 10^4$ ; $1 < (\mu_a/\mu_s) < 3.2$		
• <i>Correlation for falling drop</i>		
$Nu = 2 + 0.6Re^{1/2}Pr^{1/3}[25(x/D)^{-0.7}]$		for average; $T_a$

Source: Dincer, 1997.

correlations may be used. The definitions of the Nusselt and Reynolds numbers have been given in Table 1.9. Forced air and water coolers, forced air and water evaporators and condensers, and heat exchangers are examples of equipments commonly involved in forced convection heat transfer.

The various kinds of forced convection, such as flow in a tube, flow across a tube, and flow across a flat plate, may be solved mathematically when certain assumptions are made with regard to the boundary conditions. It is extremely difficult to obtain exact solutions to such problems, especially in the event of turbulent flow, but approximate solutions can sometimes be obtained using appropriate assumptions.

The essential first step in the solution of a convection heat transfer problem is to determine whether the boundary layer is *laminar* or *turbulent*. These conditions affect the convection heat transfer coefficient and hence the convection heat transfer rates.

The conditions of laminar and turbulent flows on a flat plate are shown in Figure 1.13. In the laminar boundary layer, fluid motion is highly ordered and it is possible to identify streamlines

along which particles move. Fluid motion in the turbulent boundary layer, on the other hand, is highly irregular, and is characterized by velocity fluctuations that begin to develop in the transition region (after this, the boundary layer becomes completely turbulent). These fluctuations enhance the transfer of momentum, heat, and species, and hence increase surface friction as well as convection transfer rates. In the laminar sublayer, which is nearly linear, transport is dominated by diffusion and the velocity profile. There is an adjoining buffer layer in which diffusion and turbulent mixing are comparable. In the turbulent region, transport is dominated by turbulent mixing.

The *critical Reynolds number* is the value of  $Re$  for which transition begins, and for external flow it is known to vary from  $10^5$  to  $3 \times 10^6$ , depending on the surface roughness, the turbulence level of the free stream, and the nature of the pressure variation along the surface. A representative value of  $Re$  is generally assumed for boundary layer calculations:

$$Re_c = \frac{\rho U_a X_c}{\mu} = \frac{U_a X_c}{\nu} = 5 \times 10^5 \quad (1.122)$$

For smooth circular tubes, when the Reynolds number is less than 2100, the flow is laminar, and when it is greater than 10,000, the flow is turbulent. The range between these values represents the transition region.

We give a list of various forced-convection heat transfer correlations (the Nusselt–Reynolds correlations), direct convection heat transfer coefficient equations, along with the relevant parameters and remarks, which are compiled from literature in Table 1.11. In many of these equations, the *film temperature* is used, and is defined as  $T_{fm} = (T_s + T_a)/2$ .

## 1.7 Concluding Remarks

In this chapter, a summary is presented of general introductory aspects of thermodynamics, fluid flow, and heat transfer, and related fundamental definitions and physical quantities, to provide a sufficient thermal sciences background for understanding thermal energy storage systems and applications, and their operations. The background provided here is also useful in the energy, exergy, and other analyses presented subsequently.

### *Nomenclature*

$a$	acceleration, $m/s^2$ ; thermal diffusivity, $m^2/s$ ; absorptivity
$A$	cross-sectional area, $m^2$ ; surface area, $m^2$
$Bi$	Biot number
$c$	mass fraction; constant in Tables 1.10 and 1.11
$c_p$	specific heat at constant pressure, $kJ/kg\ K$
$c_v$	specific heat at constant volume, $kJ/kg\ K$
$C_f$	average skin-friction coefficient
$d$	diameter, $m$ ; depth normal to flow, $m$
$D$	diameter, $m$
$E$	energy, $J$ or $kJ$ ; electric potential, $V$ ; constant
$\dot{E}$	energy rate, $W$ or $kW$
$F$	force; drag force, $N$
$Fo$	Fourier number
$g$	acceleration due to gravity ( $= 9.81\ m/s^2$ )
$G$	mass flow velocity, $kg/s\ m^2$
$Gz$	Graetz number
$Gr$	Grashof number
$h$	specific enthalpy, $kJ/kg$ ; heat transfer coefficient, $W/m^2\ ^\circ C$ ; head, $m$
$H$	enthalpy, $kJ$ ; overall heat transfer coefficient, $W/m^2\ ^\circ C$ ; head, $m$

$I$	electric current, A
$k$	thermal conductivity, W/m °C
$K$	adiabatic modulus
KE	kinetic energy, J or kJ
$L$	thickness, m
$m$	mass, kg; constant
$\dot{m}$	mass flow rate, kg/s
$M$	molecular weight, kg/kmol
$n$	mole number, kmol; constant exponent in Tables 1.9 and 1.10
Nu	Nusselt number
$P$	perimeter, m; pressure, Pa or kPa
$P^*$	constant-pressure gradient, Pa or kPa
Pe	Peclet number
PE	potential energy, J or kJ
Pr	Prandtl number
$q$	heat rate per unit area, W/m <sup>2</sup> ; flow rate per unit width or depth
$q_h$	heat generation rate per unit volume, W/m <sup>3</sup>
$Q$	heat transfer, J or kJ
$\dot{Q}$	heat transfer rate, W or kW
$r$	reflectivity; radial coordinate; radial distance, m
$R$	gas constant, kJ/kg K; radius, m
$\bar{R}$	universal gas constant, kJ/kg K
$R_t$	thermal resistance, °C/W
Ra	Rayleigh number
Re	Reynolds number
$s$	specific entropy, kJ/kg; streamline direction; distance, m; constant exponent in Tables 1.10 and 1.11
$S$	entropy, kJ/K
St	Stanton number
$t$	time, s; transmissivity
$T$	temperature, °C or K
$T_s$	absolute temperature of object surface, K
$u$	specific internal energy, kJ/kg; velocity in $x$ direction, m/s; variable velocity, m/s
$U$	internal energy, kJ; flow velocity, m/s
$x$	quality, kg/kg; cartesian coordinate; variable
$X$	length for plate, m
$v$	specific volume, m <sup>3</sup> /kg; velocity in $y$ direction, m/s
$\bar{v}$	molal specific volume, kmol/kg
$V$	volume, m <sup>3</sup> ; velocity, m/s
$V_x$	velocity in $x$ direction, m/s
$V_r$	velocity in radial direction, m/s
$V_y$	velocity in $y$ direction, m/s
$V_z$	velocity in $z$ direction, m/s
$V_\theta$	tangential velocity, m/s
$\dot{V}$	volumetric flow rate, m <sup>3</sup> /s
$w$	velocity in $z$ direction, m/s
$y$	mole fraction; cartesian coordinate, variable; coordinate normal to flow
$Y$	characteristic dimension (length), m
$z$	cartesian coordinate, variable
$Z$	compressibility factor (Equation 1.24); elevation, m

*Greek Letters*

$\phi$	temperature difference, °C or K
$\theta$	angle
$\beta$	volumetric coefficient of thermal expansion, 1/K
$\delta$	increment; difference
$\mu$	dynamic viscosity, kg/ms; root of the characteristic equation
$\rho$	density, kg/m <sup>3</sup>
$\nu$	kinematic viscosity, m <sup>2</sup> /s
$\Delta$	thickness of the stagnant film of fluid on the surface, m
$\Delta T$	temperature difference, K; overall temperature difference, °C or K
$\sigma$	Stefan–Boltzmann constant, W/m <sup>2</sup> K <sup>4</sup> ; electrical conductivity, 1/ohm
$\varepsilon$	surface emissivity, eddy viscosity
$\tau$	shear stress, N/m <sup>2</sup>
$\Sigma$	summation
$\pi$	number (= 3.14159)

*Subscripts and Superscripts*

<i>a</i>	air; medium; surroundings
<i>av</i>	average
<i>A</i>	fluid A
<i>b</i>	black
<i>B</i>	fluid B
<i>c</i>	convection, critical
<i>cd</i>	conduction
<i>cs</i>	control surface
<i>cv</i>	control volume
<i>D</i>	diameter
<i>e</i>	electrical; end; exit
<i>f</i>	fluid; final; flow; force; friction
<i>fm</i>	film condition
<i>h</i>	heat generation
<i>H</i>	high temperature
<i>hs</i>	heat storage
<i>i</i>	component; input
<i>ie</i>	internal energy
<i>liq</i>	liquid
<i>l</i>	liquid
<i>L</i>	low temperature
<i>m</i>	midplane for plane wall; centerline for cylinder
<i>mix</i>	mixture
<i>n</i>	nth value
<i>nb</i>	nonblack
<i>p</i>	previous
<i>r</i>	radiation
<i>s</i>	surface; near surface; saturation; free stream; in direction parallel to streamline
<i>t</i>	total; thermal
<i>tot</i>	total
<i>x</i>	x direction

$v$	vapor
$vap$	vapor
$y$	$y$ direction
$z$	$z$ direction
0	surroundings; ambient; environment; reference
1	first value; 1st state; initial
1, 2, 3	points

## References

- Borgnakke, C. and Sonntag, R.E. (2008). *Fundamentals of Thermodynamics*, 7<sup>th</sup> edition, Wiley, New York.
- Dincer, I. (1997). *Heat Transfer in Food Cooling Applications*, Taylor & Francis, Washington, DC.
- Dincer, I. (1998). Thermodynamics, exergy and environmental impact, *Proceedings of the ISTP-11, The Eleventh International Symposium on Transport Phenomena*, pp. 121–125, 29 November–3 December, Hsinchu, Taiwan.
- Dincer, I. and Rosen, M.A. (1999). Energy, environment and sustainable development, *Applied Energy* 64, 427–440.
- Dincer, I. and Rosen, M.A. (2007). *Energy: Energy, Environment and Sustainable Development*, Elsevier, New York.
- Moran, M.J. and Shapiro, H.N. (2007). *Fundamentals of Engineering Thermodynamics*, 6<sup>th</sup> edition, Wiley, New York.
- Olson, R.M. and Wright, S.J. (1991). *Essentials of Engineering Fluid Mechanics*, Harper & Row, New York.
- Raznjevic, K. (1995). *Handbook of Thermodynamic Tables*, 2<sup>nd</sup> edition, Begell House, New York.
- Szargut, J., Morris, D.R. and Steward, F.R. (1988). *Exergy Analysis of Thermal, Chemical, and Metallurgical Processes*, Hemisphere, New York.

## Study Questions/Problems

### Introduction, Thermodynamic Properties

- 1.1 Why are SI units most widely used throughout the world?
- 1.2 What is the difference between mass and weight?
- 1.3 What is specific heat? Define two commonly used specific heats. Is specific heat a function of temperature?
- 1.4 Explain the operating principle of thermocouples. List some typical applications for different types of thermocouples. What is the main advantage of thermocouples over other temperature sensors?
- 1.5 Consider the flow of a refrigerant vapor through a compressor, which is operating at steady-state conditions. Do mass flow rate and volume flow rate of the refrigerant across the compressor remain constant?
- 1.6 Consider a refrigeration system consisting of a compressor, an evaporator, a condenser, and an expansion valve. Is it best to evaluate each component as a closed system or as a control volume, and as a steady-flow system or unsteady-flow system? Explain.
- 1.7 What is the difference between an adiabatic system and an isolated system?
- 1.8 Define intensive and extensive properties. Identify the following properties as intensive or extensive: mass, volume, density, specific volume, energy, specific enthalpy, total entropy, temperature, pressure.
- 1.9 Define the terms system, process, and cycle.

- 1.10** What is the difference between gauge pressure, absolute pressure, and vacuum? Define atmospheric pressure.
- 1.11** What is the difference between mass flow rate and volumetric flow rate? How are these related?
- 1.12** Define the critical point and explain the difference between critical point and triple point.
- 1.13** Define sensible and latent heats, and latent heat of fusion. What are their units?
- 1.14** What is the weight of a 10-kg substance in N, kN, kgf, and lbf?
- 1.15** The vacuum pressure of a tank is given to be 40 kPa. If the atmospheric pressure is 95 kPa, what is the gauge pressure and absolute pressure in kPa, kN/m<sup>2</sup>, lbf/in<sup>2</sup>, psi, and mm Hg.
- 1.16** Express the temperature  $-40^{\circ}\text{C}$  in units of Fahrenheit ( $^{\circ}\text{F}$ ), Kelvin (K), and Rankine (R).
- 1.17** The temperature of air changes by  $10^{\circ}\text{C}$  during a process. Express this temperature change in Kelvin (K), Fahrenheit ( $^{\circ}\text{F}$ ), and Rankine (R) units.
- 1.18** The specific heat of water at  $25^{\circ}\text{C}$  is given to be  $4.18\text{ kJ/kg }^{\circ}\text{C}$ . Express this value in kJ/kg K, J/g  $^{\circ}\text{C}$ , kcal/kg  $^{\circ}\text{C}$ , and Btu/lbm  $^{\circ}\text{F}$ .
- 1.19** A 0.2-kg mass of R134a at 700 kPa pressure and at  $4^{\circ}\text{C}$  is heated until 50% of mass is vaporized. Determine the temperature at which the refrigerant is vaporized, and the sensible heat and the latent heat are transferred to the refrigerant.
- 1.20** A 0.5-lbm mass of R134a at 100 psia pressure and  $40^{\circ}\text{F}$  is heated until 50% of mass is vaporized. Determine the temperature at which the refrigerant is vaporized, and the sensible heat and the latent heat are transferred to the refrigerant.
- 1.21** A 2-kg mass of ice initially at  $-18^{\circ}\text{C}$  is heated until 75% of the mass is melted. Determine the sensible heat and the latent heat transferred to the water. The specific heat of ice at  $0^{\circ}\text{C}$  is  $2.11\text{ kJ/kg }^{\circ}\text{C}$ , and the latent heat of fusion of water at  $0^{\circ}\text{C}$  is  $334.9\text{ kJ/kg}$ .
- 1.22** A 2-kg mass of ice initially at  $-18^{\circ}\text{C}$  is heated until it becomes liquid water at  $20^{\circ}\text{C}$ . Determine the sensible heat and the latent heat transferred to the water. The specific heat of ice at  $0^{\circ}\text{C}$  is  $2.11\text{ kJ/kg }^{\circ}\text{C}$ , and the latent heat of fusion of water at  $0^{\circ}\text{C}$  is  $334.9\text{ kJ/kg}$ .
- 1.23** Refrigerant 134a enters the evaporator of a refrigeration system at  $-24^{\circ}\text{C}$  with a quality of 25% at a rate of  $0.22\text{ kg/s}$ . If the refrigerant leaves the evaporator as a saturated vapor, determine the rate of heat transfer to the refrigerant. If the refrigerant is heated by water in the evaporator, which experiences a temperature rise of  $16^{\circ}\text{C}$ , determine the mass flow rate of water.

#### **Ideal Gases and the First Law of Thermodynamics**

- 1.24** What is the compressibility factor?
- 1.25** When can we invoke the ideal gas assumption for real gases?
- 1.26** Define isothermal, isobaric, and isochoric processes.
- 1.27** What is an isentropic process? Is a constant-entropy process necessarily reversible and adiabatic?
- 1.28** What is the difference between heat and work?
- 1.29** An elastic tank contains 0.8 kmol of air at  $23^{\circ}\text{C}$  and 600 kPa. Determine the volume of the tank. If the volume is doubled at the same pressure, what is the temperature at the new state?
- 1.30** A 50-L piston–cylinder device contains oxygen at  $52^{\circ}\text{C}$  and 170 kPa. If the oxygen is heated until its temperature reaches  $77^{\circ}\text{C}$ , what is the amount of heat transfer during the process?
- 1.31** A 50-L rigid tank contains oxygen at  $52^{\circ}\text{C}$  and 170 kPa. If the oxygen is heated until its temperature reaches  $77^{\circ}\text{C}$ , what is the amount of heat transfer during the process?

- 1.32 A 50-L rigid tank contains oxygen at 52 °C and 170 kPa. If the oxygen is heated until the temperature reaches 77 °C, what is the entropy change during the process?
- 1.33 A rigid tank contains 2.5 kg of oxygen at 52 °C and 170 kPa. If the oxygen is heated in an isentropic process until it reaches 77 °C, what is the pressure at the final state? What is the work interaction during this process?
- 1.34 A piston–cylinder device contains 2.5 kg oxygen at 52 °C and 170 kPa. If the oxygen is heated until it reaches 77 °C, what is the work done and the amount of heat transfer during the process?

### Exergy

- 1.35 What is the Kelvin–Planck statement of the second law of thermodynamics?
- 1.36 What is the Clausius statement of the second law of thermodynamics?
- 1.37 Define the terms energy, exergy, entropy, and enthalpy.
- 1.38 What is the second-law efficiency? How does it differ from the first-law efficiency?
- 1.39 What is the relationship between entropy generation and irreversibility?
- 1.40 What are the two common causes of irreversibility?
- 1.41 During an irreversible process, do the parameters mass, energy, entropy, and exergy decrease or increase or remain conserved?
- 1.42 How does an exergy analysis help the goal of more efficient energy-resource use? What are the advantages of using exergy analysis?

### General Aspects of Fluid Flow

- 1.43 What is the physical meaning of the Reynolds number? What makes the flow laminar and what makes it turbulent?
- 1.44 What is viscosity? How does viscosity change with temperature for gases and for liquids?

### General Aspects of Heat Transfer

- 1.45 What is the difference between heat conduction and heat convection?
- 1.46 Define the terms forced convection and natural convection, and explain the difference between them.
- 1.47 Define the term heat generation. Give some examples.
- 1.48 What are the modes of heat transfer? Explain the physical mechanism of each mode.
- 1.49 How much energy does it take to convert 10.0 kg of ice at 0 °C to water at 25 °C?
- 1.50 A 20-cm thick wall of a house made of brick ( $k = 0.72 \text{ W/m} \cdot \text{°C}$ ) is subjected to inside air at 22 °C with a convection heat transfer coefficient of  $15 \text{ W/m}^2 \cdot \text{°C}$ . The temperature of the inner surface of the wall is 18 °C and the outside air temperature is  $-1 \text{ °C}$ . Determine the temperature of the outer surface of the wall and the heat transfer coefficient at the outer surface.
- 1.51 A satellite is subjected to solar energy at a rate of  $300 \text{ W/m}^2$ . The absorptivity of the satellite surface is 0.75 and its emissivity is 0.60. Determine the equilibrium temperature of the satellite.
- 1.52 An 80-cm-diameter spherical tank made of steel contains liquefied natural gas (LNG) at  $-160 \text{ °C}$ . The tank is insulated with a 4-cm thickness of insulation ( $k = 0.015 \text{ W/m} \cdot \text{°C}$ ). The tank is subjected to ambient air at 18 °C with a convection heat transfer coefficient of  $20 \text{ W/m}^2 \cdot \text{°C}$ . How long will it take for the temperature of the LNG to decrease to  $-150 \text{ °C}$ . Neglect the thermal resistance of the steel tank. The density and the specific heat of LNG are  $425 \text{ kg/m}^3$  and  $3.475 \text{ kJ/kg} \cdot \text{°C}$ , respectively.



# 2

## Energy Storage Systems

### 2.1 Introduction

Energy storage (ES) has only recently been developed to a point where it can have a significant impact on modern technology. In particular, ES is critically important to the success of any intermittent energy source in meeting demand. For example, the need for storage for solar energy applications is severe, especially when solar energy is least available, namely, in winter.

ES systems can contribute significantly to meeting society's needs for more efficient, environmentally benign energy use in building heating and cooling, aerospace power, and utility applications. The use of ES systems often results in such significant benefits as

- reduced energy costs;
- reduced energy consumption;
- improved indoor air quality;
- increased flexibility of operation; and
- reduced initial and maintenance costs.

In addition, Dincer (1997) point out some further advantages of ES:

- reduced equipment size;
- more efficient and effective utilization of equipment;
- conservation of fossil fuels (by facilitating more efficient energy use and/or fuel substitution); and
- reduced pollutant emissions (e.g., CO<sub>2</sub> and chlorofluorocarbons (CFCs)).

ES systems have an enormous potential to increase the effectiveness of energy-conversion equipment use and for facilitating large-scale fuel substitutions in the world's economy. ES is complex and cannot be evaluated properly without a detailed understanding of energy supplies and end-use considerations. In general, a coordinated set of actions is needed in several sectors of the energy system for the maximum potential benefits of ES to be realized. ES performance criteria can help in determining whether prospective advanced systems have performance characteristics that make them useful and attractive and, therefore, worth pursuing through the advanced development and demonstration stages. The merits of potential ES systems need to be measured, however, in terms of the conditions that are expected to exist after research and development is completed. Care should be taken not to apply too narrow a range of forecasts to those conditions. Care also should be taken to evaluate specific storage system concepts in terms that account for their full potential impact. The versatility of some ES technologies in a number of application areas should be accounted for in such assessments.

Today's industrial civilizations are based upon abundant and reliable supplies of energy. To be useful, raw energy forms must be converted to energy currencies, commonly through heat release. For example, steam, which is widely used for heating in industrial processes, is normally obtained by converting fuel energies to heat and transferring the heat to water. Electricity, increasingly favored as a power source, is generated predominately with steam-driven turbogenerators, fueled by fossil or nuclear energy. Power demands, in general, whether thermal or electrical, are not steady. Moreover, some thermal and electrical energy sources, such as solar energy, are not steady in supply. In cases where either supply or demand is highly variable, reliable power availability has in the past generally required energy-conversion systems to be large enough to supply the peak-demand requirements. The results are high and partially inefficient capital investments, since the systems operate at less than full capacity much of the time.

Alternatively, capital investments can sometimes be reduced if load-management techniques are employed to smooth power demands, or if ES systems are used to permit the use of smaller power-generating systems. The smaller systems operate at or near peak capacity, irrespective of the instantaneous demand for power, by storing the excess converted energy during reduced-demand periods for subsequent use in meeting peak-demand requirements. Although some energy is generally lost in the storage process, ES often permits fuel conservation by utilizing more plentiful but less flexible fuels such as coal and uranium in applications now requiring relatively scarcer oil and natural gas. In some cases, ES systems enable the waste heat accompanying conversion processes to be used for secondary purposes.

The opportunities for ES are not confined to industries and utilities. Storage at the point of energy consumption, as in residences and commercial buildings, will likely be essential to the future use of solar heating and cooling systems, and may prove important in lessening the peak-demand loads imposed by conventional electrical, space-conditioning systems. In the personal transportation sector, now dominated by gasoline-powered vehicles, adequate electrical storage systems might encourage the use of large numbers of electric vehicles, reducing the demand for petroleum.

The concept of ES using flywheels is not new. The ability of flywheels to smooth intermittent power impulses was recognized shortly after the invention of reciprocating engines in the 18th century. Special purpose locomotives have been operated with stored, externally supplied steam for about 100 years. Electric cars were early automobile competitors.

The marked increases in fuel costs in recent years, the increasing difficulty in acquiring the large amounts of capital required for power-generation expansions, and the emergence of new storage technologies has led to a recent resurgence of interest in the possibilities for ES systems. To the energy supplier, energy is a commodity whose value is determined by the cost of production and the marketplace demand. For the energy consumer, the value of energy is in its contribution to the production of goods and services or to personal comfort and convenience. Although discussions about the merits of alternative national energy production and consumption patterns in the future, it is likely that energy decisions, in general, will continue to be made based on evaluations of the costs of alternative means to attain these needs. In particular, decisions on whether to use ES systems will likely be made on the basis of prospective cost savings in the production or use of energy, unless legislative or regulatory constraints are imposed. Thus, among criteria necessary for the commercialization of ES systems, potential economic viability is a major consideration.

## 2.2 Energy Demand

Energy demand in the commercial, industrial, public, residential, and utility sectors varies on a daily, weekly, and seasonal basis. Ideally, these demands are matched by various energy-conversion systems that operate synergistically. Peak hours are the most difficult and expensive to supply. Peak electrical demands are generally met by conventional gas turbines or diesel generators, which are reliant on costly and relatively scarce oil or gas. ES provides an alternative method of supplying peak energy demands. Likewise, ES systems can improve the operation of cogeneration, solar, wind, and run-of-river hydro facilities. Some details on these ES applications follow:

- **Utility.** Relatively inexpensive base-load electricity can be used to charge ES systems during evening or off-peak weekly or seasonal periods. The electricity is then used during peak periods, reducing the reliance on conventional gas and oil peaking generators.
- **Industry.** High-temperature waste heat from various industrial processes can be stored for use in preheating and other heating operations.
- **Cogeneration.** Since the closely coupled production of heat and electricity by a cogeneration system rarely matches demand exactly, excess electricity or heat can be stored for subsequent use.
- **Wind and run-of-river hydro.** Conceivably, these systems can operate around the clock, charging an electrical storage system during low-demand hours and later using that electricity for peaking purposes. ES increases the capacity factor for these devices, usually enhancing their economic value.
- **Solar energy systems.** By storing excess solar energy received on sunny days for use on cloudy days or at night, ES systems can increase the capacity factor of solar energy systems.

## 2.3 Energy Storage

Mechanical and hydraulic ES systems usually store energy by converting electricity into energy of compression, elevation, or rotation. Pumped storage is proven, but quite limited in its applicability by site considerations. Compressed-air ES has been tried successfully in Europe, although limited applications appear in the United States. This concept can be applied on a large scale using depleted natural gas fields for the storage reservoir. Alternatively, energy can be stored chemically as hydrogen in exhausted gas fields. Energy of rotation can be stored in flywheels, but advanced designs with high-tensile materials appear to be needed to reduce the price and volume of storage. A substantial energy penalty of up to 50% is generally incurred by mechanical and hydraulic systems in a complete storage cycle because of inefficiencies.

Reversible chemical reactions can also be used to store energy. There is a growing interest in storing low-temperature heat in chemical form, but practical systems have not yet emerged. Another idea in the same category is the storage of hydrogen in metal hydrides (lanthanum, for instance). Tests of this idea are ongoing.

Electrochemical ES systems have better turnaround efficiencies but very high prices. Intensive research is now directed toward improving batteries, particularly by lowering their weight-to-storage capacity ratios, as needed in many vehicle applications. As a successor to the lead–acid battery, sodium–sulfur and lithium–sulfide alternatives, among others, are being tested. A different type of electrochemical system is the redox flow cell, so named because charging and discharging is achieved through reduction and oxidation reactions occurring in fluids stored in two separate tanks. To make the leading candidate (an iron redox system) competitive with today’s batteries, its price would have to be at least halved.

Thermal energy storage (TES) systems are varied, and include designed containers, underground aquifers and soils and lakes, bricks and ingots. Some systems using bricks are operating in Europe. In these systems, energy is stored as sensible heat. Alternatively, thermal energy can be stored in the latent heat of melting in such materials as salts or paraffin. Latent storages can reduce the volume of the storage device by as much as 100 times, but after several decades of research many of their practical problems have still not been solved. Finally, electric energy can be stored in superconducting magnetic systems, although the costs of such systems are high.

There are a number of promising areas of research in ES technology. Given the cost gap that needs to be spanned and the potential beneficial ES applications, it is clear that a sustained ES development effort is in order. For solar energy applications, advanced ES systems may not be needed for years and decades. For the near term, many less expensive ES alternatives are available that should allow for the growth of solar energy use.

Some current research and development areas in the field of ES are as follows:

- advanced ES and conversion systems with phase transformation, chemical and electrochemical reactions;

- fundamental phenomena inside a single cell as well as engineering integration of whole battery packs into vehicles;
- high-dielectric-constant polymers;
- high K composites for capacitors;
- polymer electrode interfaces (low- and high-frequency effects);
- integrated polymer capacitors.

## 2.4 Energy Storage Methods

For many energy technologies, storage is a crucial aspect. If we consider the storage of fuels as the storage of the energy embedded in them, then oil is an excellent example. The massive amounts of petroleum stored worldwide are necessary for the reliable, economic availability of gasoline, fuel oil, and petrochemicals.

Electric utilities also store energy using a scheme called *pumped storage*. Electricity generated by thermal power plants drives large electric motors to pump water uphill to elevated reservoirs during periods of low electric demand. During periods of peak demand, the water is allowed to flow back downhill to redeliver the energy through hydroelectric generation. Also, electricity can be stored in batteries. However, the present-day conventional automobile battery, to use an important and common example, is used for starting the internal combustion engine and not for locomotion. Nonetheless, progress is being made on automotive batteries for storage of energy for moving vehicles.

ES includes heat storage. In thermodynamic terms, such storages hold transferred heat before it is put to useful purposes. A conventional example is hot water storage in residences and industry. Such heat storage smoothes out the delivery of hot water or steam, but it is not usually considered for periods longer than one day.

Advanced new storage devices are often an integral part of other new technologies, and these sometimes can be made more feasible by innovations in storage. Advances in storage especially benefit wind and solar energy technologies. Also, new storage technologies may facilitate the development of electric-powered automobiles.

A large variety of ES techniques are under development. We shall discuss them by categories, grouping together those techniques that store energy in the following forms: mechanical, thermal, chemical, biological, and magnetic, as shown in Figure 2.1. Of course, ES devices can be classified and categorized in other ways. Here, each category considers the storage of one form of energy. Below, we examine briefly several possible storage options (Dincer, 1999).

### 2.4.1 Mechanical Energy Storage

Mechanical energy may be stored as the kinetic energy of linear or rotational motion, as the potential energy in an elevated object, as the compression or strain energy of an elastic material, or as the compression energy in a gas. It is difficult to store large quantities of energy in linear motion because one would have to chase after the storage medium continually. However, it is quite simple to store rotational kinetic energy. In fact, the potter's wheel, perhaps the first form of ES used by man, was developed several thousand years ago and is still being used. As seen in Figure 2.1, there are three main mechanical storage types that we discuss in this section: hydrostorage, compressed-air storage, and flywheels.

#### Hydrostorage (Pumped Storage)

Hydrostorage is a simple ES method. At night, when energy demand is low, pumps pump water upward from the river (Figure 2.2). The water is pumped through a pipe to a reservoir. During the day, when energy demand is high, the reservoir releases water, allowing it to flow downhill. The

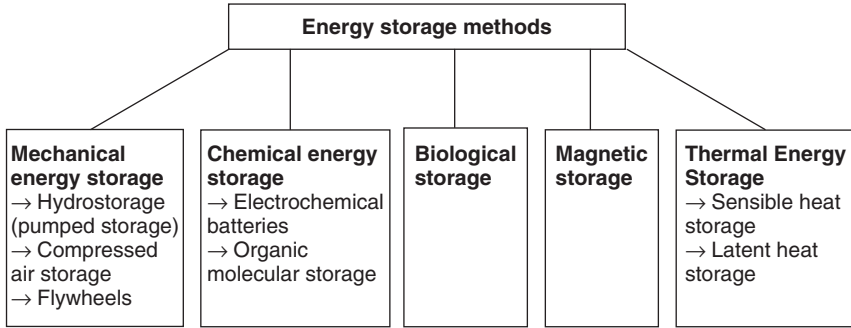


**Figure 2.1** A classification of energy storage methods

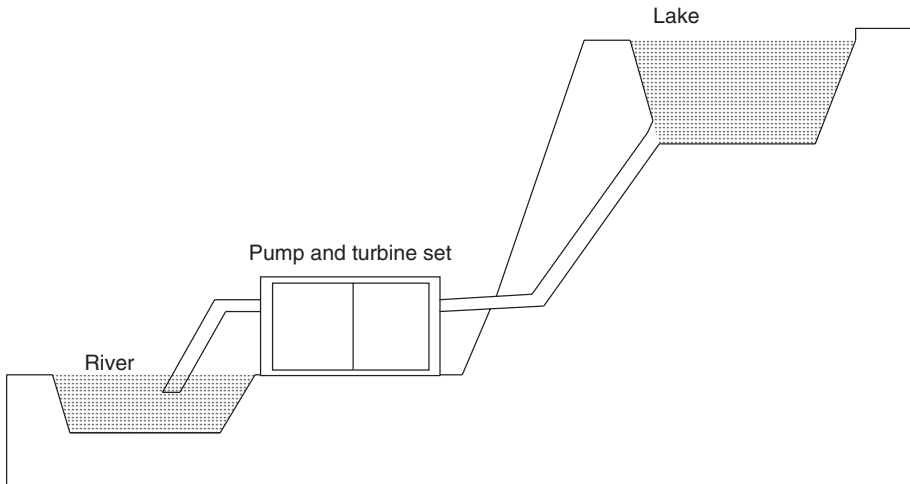


**Figure 2.2** A pumped hydrostorage plant

flowing water turns the turbine to generate electricity. The pump that pumps the water upward from the river can be powered by solar energy during the day. At night, when there is no solar energy, the stored water turns the turbine to generate electricity. The efficiency of a pumped water storage plant is about 50%. When water is pumped uphill, about 30% of the energy is lost. When the water flows down, another 20% of the energy is lost. A pumped water storage plant operates for more than 20 years. When the energy is needed, the plant only needs 30 s to reach 100% of its power.

In this storage type, reversible devices like pump/turbines pump water upward into a storage reservoir and after a period of time operate as turbines, driving generators, when the water runs back down through them. Hydrostorage has been proved economically viable, but its use is geographically limited to only a few percentage of the total hydroelectric capacity. Pumped storage is now considered important with wind machines. The best alternative to building expensive new storage systems in the near term is often to use existing storage systems, especially those of hydroelectric installations. By holding back water that would otherwise flow from a hydroelectric dam, energy can be stored in one part of an electric network while a solar electrical energy or wind system produces energy in another part. The United States currently has 59,000 MW of hydroelectric capacity, and an additional 10,000 MW of pumped storage capacity. Pumped storage facilities consist of a

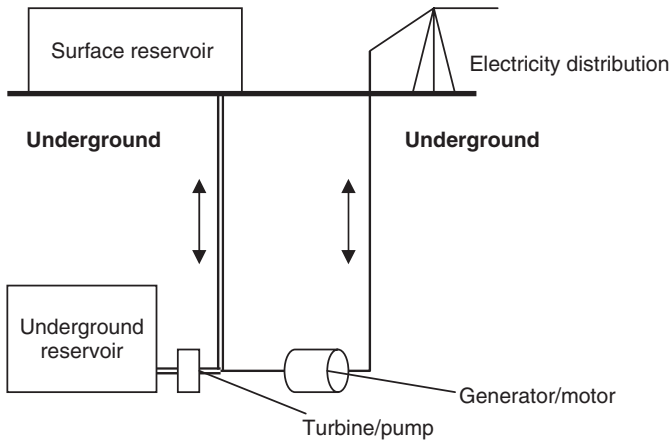


**Figure 2.3** Representation of underground pumped hydrostorage

pair of reservoirs; the upper one is filled with water pumped up from lower levels at times of low electricity usage.

Hydrostorage is widely used in the power industry to store off-peak power for peak load periods. This technique utilizes a dam that has sufficient hydrostatic head to drive a hydroelectric power plant. Water is pumped into the reservoir in off-peak periods and drawn out during peak periods. The basic requirement is a dam with a large quantity of water at its base or two dams with a height difference between them. Hydrostorage is relatively efficient. The energy used to pump water upward is recovered in a storage cycle with about 65–75% efficiency. Hydrostorage is often ideal for solar power storage. The solar plant produces power at the maximum rate during the day and is on standby during the night, maintaining only system temperatures so that it is ready to turn out power the next day as soon as the collector subsystem reaches operating temperature.

Pumped storage is the only well-established ES concept that is available on a large scale. The concept is simple. Energy is stored during evening hours by pumping water from a lower body of water to an upper reservoir behind a conventional dam. During peak demand hours, the water flows down from the upper reservoir through a hydroelectric turbine back into the lower body of water. Because of the environmental concerns associated with large-scale hydroelectric facilities, however, it is questionable if many conventional pumped hydro plants will be constructed in the future.

Underground pumped hydrostorage is a variation of this concept that has significant potential. Still in the planning stage, it would use an upper surface reservoir in conjunction with an artificially made lower reservoir (Figure 2.3). The upper surface reservoir can be an existing body of water or an artificial lake formed by dikes and dams. The lower reservoir is a large cavern excavated in hard solid rock. The two reservoirs are hydraulically connected by a waterway (pen-stock) that passes through a powerhouse with a dual purpose turbine/pump and generator/motor. Except for the artificial lower reservoir, pumped hydrostorage operates in the same manner as a conventional system. The power produced from a hydro facility is directly related to the hydraulic head (elevation difference between the reservoirs) available to the plant. Therefore, since the lower reservoir can be positioned to obtain high heads of approximately 1400 m (compared to the heads of usually less than 300 m for natural conventional hydro facilities), comparable power outputs can be achieved with significantly smaller reservoirs. Underground systems can be more acceptable since environmental impact is decreased. The area in underground pumped storage needing greatest development and having the greatest cost is the lower reservoir.

The primary criteria for location are the geological conditions for the lower reservoir. The subsurface material should be of solid hard rock, and should not be located in areas that have

- predominantly loose sedimentary rock;
- volcanic rock;
- complex geological structures with widely varying conditions over short distances;
- high seismic activity; or
- major faults.

As an example of an underground pumped storage, consider the following from Diamant (1984). Although in Great Britain nuclear power accounts for only about 3–4% of the country's total electrical generating capacity, nuclear energy supplies about 15% of the annual output of electricity. The reason for these different values is that nuclear power stations, whose main cost is the capital invested in them, are best operated at a very steady rate. Fuel costs for nuclear stations are smaller than those for fossil-fuel-fired electrical generating stations. Thus, since it is difficult to vary the output from nuclear power stations significantly over short time periods, these stations are often used for generating the base-load power. The outputs of power stations fueled by coal, gas, and oil can be more easily adjusted to match changing loads; but even so, it is best to steady the load if possible. Sometimes, there are very high peak load requirements which may only last a few minutes during a day. To satisfy these demands, it would be necessary to have costly stand-by stations that operate for only very short periods over the year. Yet not satisfying such loads may mean voltage reductions and the accompanying dangers of motors and other equipment burning out due to overheating.

If the nuclear capacity increases relative to the country's total installed electrical generating capacity, these problems will be accentuated. A first attempt to address this issue is the pumped storage scheme at Dinorwic in North Wales. The two lakes that exist near the town of Llanberis are the Llyn Peris lake, which lies in a valley, and the Marchlyn Mawr lake, which lies about 500 m higher on a mountain. Both lakes were enlarged and connected by a system of tunnels with enough capacity to drive six 313 MW turbine generators. When the turbine generators are driven in the opposite direction, powered by electricity from the national grid, they act as motor pumps which consume 281 MW of electricity per unit. When in operation, the Dinorwic station will be able to provide a constant output of 1680 MW for 5 h during peak demand periods, using the potential energy in the difference in water levels between the upper and lower reservoirs to drive the generators. The pumps require 6 h to transfer the water from the Llyn Peris lake at the bottom back to the Marchlyn Mawr lake at the top, an operation normally done at night using inexpensive off-peak electricity. The Dinorwic station can be put into operation to meet sudden surges in power demand far more rapidly than almost any alternative system. It is claimed that the station can ramp up from zero to an output of 1320 MW within 10 s, allowing it to be engaged extremely quickly to correct sudden voltage drops due to power consumption, momentarily outstripping production (Diamant, 1984).

### **Compressed-Air Storage**

In a compressed-air ES system, air is compressed during off-peak hours and stored in large underground reservoirs, which may be naturally occurring caverns, salt domes, abandoned mine shafts, depleted gas and oil fields, or man-made caverns. During peak hours, the air is released to drive a gas turbine generator.

The technique used by such a system to compress air to store energy is relatively straightforward. In a conventional gas turbine, high-pressure hot gas is supplied, and about two-thirds of the gross power output is used to drive the compressor. A compressed-air ES system decouples the compressor and the turbine and operates the former during off-peak hours to produce compressed air, which is stored in natural caverns, old oil or gas wells, or porous rock formations. Such ES storage is advantageous when an appreciable part of the power load is carried by nuclear stations, and where suitable spent salt caverns make it easy to build the compressed gas reservoirs.



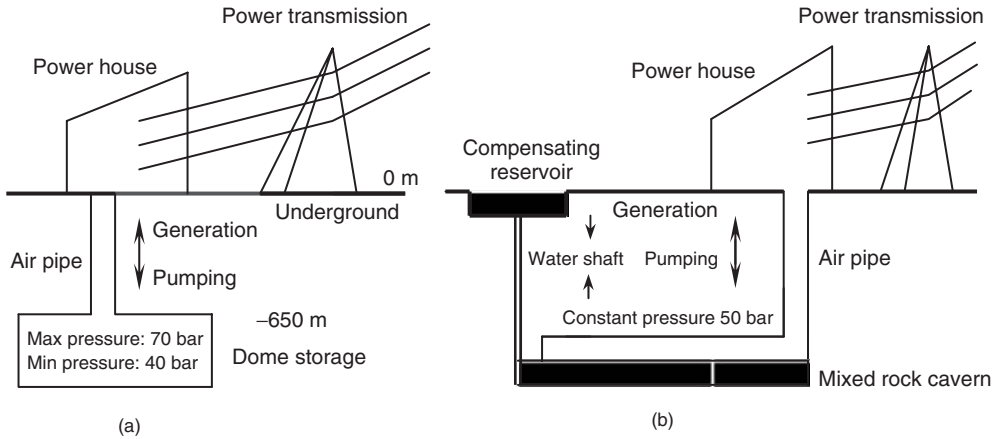


**Figure 2.4** Compressed-air ES systems: (a) sliding pressure system, (b) compensated pressure system

The compressed air storage technique in general takes advantage of off-peak electrical generating capacity using gas turbines in the same way that pumped storage does using water turbines. However, with gas systems, the heat generated when the air is compressed may be stored and used to preheat the expanding air, thus increasing efficiency.

Significant amounts of energy can be stored in the form of compressed air in underground caverns. Early studies indicate system costs to be comparable to those for hydrostorage, but the requirement of a large cavern limits the usefulness of this approach to regions where natural caverns exist or where caverns can be easily formed, as in salt domes. The air in such a storage facility is normally compressed in a device that later serves as expander or turbine.

In practice, two general categories of compressed-air ES systems are possible, depending on the storage pressure (see Figure 2.4). In sliding pressure systems (see Figure 2.3a), pressure increases as the store is charged and decreases as the stored air is released, between maximum and minimum pressures. In compensated pressure systems (see Figure 2.3b), an external force is used to keep the storage pressure constant throughout the operation.

The world's first compressed-air ES facility became operational in 1978 at Huntorf in Hamburg, Germany. The plant is connected to the local electric utility grid. During off-peak hours, air is compressed to approximately 47,780 Pa and stored in two caverns leached out of a salt dome. The combined storage capacity is 283,179 m<sup>3</sup>. During peak-demand periods, the air is released, heated by natural gas, and expanded through high- and low-pressure turbines. The system can generate 290 MW for up to about 2 h. The Huntorf facility requires an electric energy input of 0.8 kWh for air compression and 5600 kJ of natural gas input for reheating, for each 1.0 kWh of plant output. Heat recuperation from the compressed air for subsequent addition to the expanding air can reduce fuel consumption by about 25% (Sheahan, 1981).

Conventional power stations could include a compressed-air ES system. In one practical design, ambient air is compressed during off-peak operation by an axial flow compressor, intercooled and boosted to a pressure of approximately 70 bar by a high-speed centrifugal blower. Heat produced during compression is removed with conventional cooling devices. The compressed air is stored underground (ideally in leached-out salt domes or similar spaces). The pressure of the soil serves to resist the appreciable gas pressure. At peak demand periods, air passes from the underground compressed-air storage cavern through a control valve, where the pressure is throttled down to 43 bar at full load. After being heated, the compressed air drives gas turbines, effectively releasing the stored off-peak electricity.

The Brown Boveri company developed the ASSET (air storage system of energy transfer) plant for this purpose. The first plant of this type was ordered by NWK (Nordwestdeutsche Kraftwerke)



of Hamburg in June 1974. In 1980, the various power stations operated by this utility had a total electricity capacity of 4515 MW, broken down as follows (Diamant, 1984):

- fossil-fueled steam plants: 3000 MW,
- nuclear plants: 1210 MW,
- gas turbines plants: 305 MW.

The installed system is the one described earlier at Huntorf. In this system, the storage capacity is sufficient for 2 h of full peak load for the entire NWK system. No electric power is needed to start the unit. The compressed air is heated to 540°C in the high-pressure combustion chamber of the gas turbine plant and expanded in the gas turbine. When the gas turbine rotational speed reaches 3000 rpm, the generator connects to it via a “synchro-self-shifting clutch.” The total cold start-up time to full load is normally 11 min, but as short as 6 min in an emergency. All operations are controlled remotely. Since in this plant the heat of compression is rejected as a waste before storage, and then re-supplied using fuel before the air drives the gas turbine, the system has a relatively poor thermodynamic efficiency of approximately 46%. This ES method appears to be particularly advantageous when an appreciable part of the power load is met by nuclear stations, and where suitable compressed gas reservoirs such as spent salt caverns exist.

## Flywheels

The flywheel, a wheel of relatively large mass that stores rotational kinetic energy, has long been used to smooth out the shaft power output from one- or two-cycle (stroke) engines and to adjust for uneven loads. New uses of this device, and of the other two mechanical storage techniques discussed in this section, take advantage of the ability of the electric motor/generator operation to reverse. Such a device can be designed to work both as a motor when driven by electric power and as a generator when driven by mechanical power.

In such places as islands or isolated communities, where support from a larger area electrical grid is not possible, local electric generators are installed to meet local needs. Because variation in system loading is greater when the number of customers is small, and because maintenance of system voltage requires sufficient on-line capacity to meet load, such systems are typically operated at only a fraction of nameplate capacity. For example, a large diesel motor/generator (M/G) set is run at half capacity so that if several customers switch on loads at once, the extra load can be carried at full voltage. The excess capacity is spinning reserve. The use of on-line fuel-based capacity has several disadvantages. First, when a generator is operated at partial capacity, it operates inefficiently. Excess fuel is consumed, and the price per kWh of supplied electricity rises. Second, especially in the case of such advanced modular generation technologies as fuel cells and microturbines, variation of load causes variations in thermal stress on the generator, shortening its useful life. Both these problems can be addressed by using flywheel ES as the spinning reserve, and operating the fuel-based generators at peak efficiency.

Flywheels can be used for transportation ES, particularly in road vehicles (e.g., buses). Flywheels can have a significant advantage in vehicles that undergo frequent start/stop operations as in urban traffic. The basic idea is that with flywheels, decelerating does not convert mechanical energy into waste heat via friction brakes. Instead, the kinetic energy is stored by setting a flywheel spinning. Then, the power surge needed for vehicle acceleration is provided from the spinning flywheel. In petrol-driven test vehicles using flywheel ES, operational economies on the order of 50% have been achieved. It is expected that similar economies would be obtainable with electric vehicles. Figure 2.5 shows a flywheel that was successfully designed and constructed at the Pennsylvania Transportation Institute, PA. Research is ongoing to improve the practical aspects of these devices.

The most important use of flywheel ES will probably be regenerative braking. A subway train, for instance, may use a flywheel to decelerate by transferring energy to it from the wheels. The transfer can be made electrically; a conducting flywheel is rotated in a magnetic field, and the generated



**Figure 2.5** A flywheel (Courtesy of Prof. Charles E. Bakis, The Pennsylvania State University)

electrical energy stored in a battery for subsequent use. Work is required to move a conductor in a magnetic field, producing this work to slow the vehicle. In subway stop-and-start operations, energy savings as high as 30% may be realized through ES. A secondary benefit is that the subway tunnels remain more comfortable in summer due to less heat dissipation by friction braking.

Flywheel systems for electrical ES have two properties that differentiate them from present state rechargeable batteries: (i) a high power mass density specified by the maximum charge (discharge) power per system mass and (ii) a high life cycle.

In utility applications, a large flywheel located near an electric power demand could be set spinning by a motor using off-peak power and then drive the motor as a generator when additional electricity is needed. Although flywheels offer 80–90% cyclic efficiency, further research and development (e.g., on new materials and shapes) is needed to make them practical for large-scale ES.

Flywheels have also received attention elsewhere as potential ES devices. They have found practical application in storing the energy temporarily released from the large magnets of synchrotrons; the energy is recovered within a few seconds to re-energize the magnets. One can manage an energy system of this type simply by means of a switch. One polarity uses the dynamo as a motor, accelerating the flywheel; the other uses the dynamo as a generator, drawing energy from the kinetic energy of the flywheel.

The quantity of energy stored in a flywheel is usually small. One watt-hour of energy is equivalent to 1.8 kg of mass on a 2 m-diameter flywheel rotating at 600 rpm (Genta, 1985). New materials, such as carbon fiber composites, can withstand large centrifugal forces, and at high rotational speeds store much more energy than steel. The energy  $E_k$  stored in a flywheel (or kinetic energy of the rotor) is given by

$$E_k = \frac{1}{2}\Theta\omega^2 = \frac{1}{2}(kmr^2)\omega^2 = \frac{1}{2}(k\rho\Delta Vr^2)\omega^2 \quad (2.1)$$

where  $\Theta$  is the moment of inertia of the flywheel,  $\omega$  is its rotational speed (rad/s),  $k$  is its inertial constant,  $m$  is its mass (kg),  $r$  is its radius (m),  $\rho$  is its density ( $\text{kg/m}^3$ ), and  $\Delta V$  is the increment of the volume. The inertial constant depends on the shape of the rotating object. For a flywheel loaded at the rim, such as a bicycle wheel or hollow cylinder rotating on its axis,  $k$  is taken as 1, while for a solid disk of uniform thickness or a solid cylinder,  $k$  is taken as  $\frac{1}{2}$ .

An equivalent way of viewing the energy stored in a flywheel is as the energy in the “spring” formed by the tension created in the rim of the flywheel by the centrifugal force, which slightly

expands the diameter of the flywheel. As is the case for all types of ES, the potential of the stored energy to accidentally cause damage is appreciable.

The power  $P$  of the flywheel system is determined by the size of the electrical machine, not by that of the flywheel. The time  $t$  ideally required for the flywheel to be charged or discharged can be expressed as

$$t = \frac{E_k}{P} \quad (2.2)$$

Using the material-specific strength, the maximum circumferential speed  $v_{circ}$  of a thin rim can be determined as

$$v_{circ} = \left( \frac{2\sigma_{ult}}{\rho} \right)^{1/2} \quad (2.3)$$

where  $\sigma_{ult}$  denotes the ultimate strength of the material.

The specific energy or energy density of a flywheel can then be expressed as

$$\frac{E_k}{m} = \frac{1}{2} v_{circ}^2 = \frac{\sigma_{ult}}{\rho} \quad (2.4)$$

For a rotating thin ring, therefore, the maximum energy density is dependent on the specific strength of the material and not on the mass. The energy density of a flywheel is normally the first criterion for the selection of a material. Regarding specific strength, composite materials have significant advantages compared to metallic materials. Table 2.1 lists some flywheel materials and their properties.

The burst behavior is a deciding factor for choosing a flywheel material. With circumferential speeds of up to 2000 m/s, the bursting of a metallic rotor causes large fragments to be projected. Composite-material rotors can be designed to have benign failure modes with almost no penetration of pieces into the housing (Genta, 1985).

The stored energy in flywheels has a destructive potential when released uncontrolled. Some efforts have been made to design rotors such that, in the case of a failure, many thin and long fragments are released. These fragments have little translateral energy and the rotor burst can be relatively benign. However, even with careful design, a composite rotor still can fail dangerously. The safety of a flywheel ES system is not related only to the rotor. The housing, and all components and materials within it, can influence the result of a burst significantly.

Many kinds of bearing can also be running under vacuum conditions. Precision ball bearings are probably the most economic type presently. Active magnetic bearings have numerous technical benefits but are much more costly. Passive permanent magnet bearings in combination with another bearing can expand the limits of conventional bearings without the penalty of active magnetic

**Table 2.1** Some materials for flywheels and their properties

	Density (kg/m <sup>3</sup> )	Strength (MN/m <sup>2</sup> )	Specific strength (MNm/kg)
Steel (AISI 4340)	7800	1800	0.22
Alloy (AlMnMg)	2700	600	0.22
Titanium (TiAl <sub>6</sub> Zr <sub>5</sub> )	4500	1200	0.27
GFRP (60 vol% E-glass)	2000	1600	0.80
CFRP (60 vol% HT C)	1500	2400	1.60

GFRP, glass fiber reinforced polymer; CFRP, carbon fiber-reinforced polymer; HT C, heat treated carbon;

Source: ASPES Engineering AG.

bearings. Passive magnetic bearings using superconducting materials may prove useful in the future for high-speed applications.

Choosing the most appropriate bearing system depends very much on the specific application, including such factors as lifetime, maintenance interval, rotational speed and rotor weight, vibration monitoring needs, and cost.

Since we deal only with high-speed flywheels operating under vacuum conditions, mechanical shafts with gearboxes are considered beyond the scope of this discussion. The flywheel is coupled with an electrical motor/generator on a common shaft. In general, flywheel ES systems use synchronous electrical machines, with permanent or dynamic excitation. Based on the rotational speed, variable frequency can be converted to the constant grid frequency with an inverter.

To facilitate mechanical ES by flywheel, low-loss and long-life bearings and suitable flywheel materials need to be developed. Some new materials are steel wire, vinyl-impregnated fiberglass, and carbon fiber. Recently, a series of industrial flywheel ES systems using magnetic bearings have been employed. A typical example of those flywheels is capable of storing up to 3 kW of power, and consists of a series of discs, 400 mm in diameter and 200-mm deep, with a spinning mass of about 240 kg. The system is suspended on six magnetic bearings that support the unit when it is in operation, and two roller bearings that are used when accelerating the unit to working speed. Such flywheels can operate at speeds between 7500 and 15,000 rpm. A larger unit can be designed for practical applications for a maximum power storage of 10 kW with a maximum speed of 24,000 rpm. Both the flywheel and its ball bearings should be kept under vacuum.

Feasibility studies have shown that an economic single-family flywheel ES unit capable of storing up to 30 kWh of energy could be built. Inexpensive electricity would be used during off-peak periods to set the flywheel spinning. During peak-demand periods, the energy from the spinning flywheel would be discharged to generate electricity. A combined electric motor/generator is used in both operations. The entire flywheel motor system is arranged with a vertical axis in a special underground chamber such as the garage of a dwelling. A high vacuum would be maintained within the container housing the flywheel and bearings.

Some research and development areas in the field of flywheel ES are as follows:

- development of high-speed, low-cost manufacturing methods for composite rotors and hubs having high specific energy densities;
- development and experimental evaluation of novel composite rotor concepts (e.g., elastomeric matrix and elastomeric interlayer);
- evaluation of the durability of new composite rotor materials, considering properties such as fatigue and creep.

In the future, flywheels will be used to store energy for discharge over longer periods. These applications will become a reality when flywheel power systems can be made with both acceptably low cost and acceptably low losses. Among the applications which are considered of great potential benefit by energy futurists are the all-electric vehicle operated on flywheel power, the use of flywheel systems as the ES medium to couple with photovoltaics, and the use of flywheel systems in lieu of chemical batteries for backup power at telecommunication nodes.

### 2.4.2 Chemical Energy Storage

Energy may be stored in systems composed of one or more chemical compounds that release or absorb energy when they react to form other compounds. The most familiar chemical ES device is the battery. Energy stored in batteries is frequently referred to as *electrochemical energy* because chemical reactions in the battery are caused by electrical energy and subsequently produce electrical energy.

Some chemical storage systems are thermally charged and discharged. Many chemical reactions are endothermic and proceed forward with absorption of thermal energy. Then, when the temperature

of the system falls below a certain value, the energy stored in the system during the original reaction is released as the reaction is reversed. Thus, energy is stored by utilizing the heats of chemical reactions. Such chemical storage is considered for solar thermal applications, but is still at the developmental stage.

Production of a storable chemical using electricity or heat is a technical possibility. The simplest chemical to produce is considered to be hydrogen. Hydrogen can be produced electrochemically by the electrolysis of water or thermochemically by direct chemical reactions in multistage processes. This hydrogen then can be used as a fuel to drive some energy devices. In the meantime, the hydrogen acts as an ES medium. An important use of hydrogen fuel is to generate electricity in fuel cells. Fuel cells have proved useful in manned space missions and have demonstrated good reliability using hydrogen. Fuel cells using pipeline natural gas have not proved reliable to date. The use of a hydrogen fuel cell in conjunction with hydrogen production devices using solar energy has technical benefits, but costs appear to be prohibitive. The main reason is that hydrogen produced from solar electricity or other solar energy systems would be several times as costly as the hydrogen used today, which is produced primarily by reforming hydrocarbons. Oxidizing the hydrogen in a fuel cell further increases the cost of the final output due to the high costs of fuel cells. So, although such ES schemes are technically possible, their economics are questionable.

Another way to use hydrogen as a fuel, which involves more conventional technology, is direct burning in an engine. Combustion in a thermal cycle incurs significant thermodynamic losses. For example, hydrogen can be burned in a combined cycle consisting of a Rankine cycle and a Brayton topping cycle, with an overall cycle efficiency in the vicinity of 60%. This efficiency is near that of a fuel cell, but again the capital costs of the system are high and thus create implementation barriers.

Other chemical fuels also have the potential to act as storage media and to be produced with solar-derived (or other) electricity. One interesting possibility is aluminum. A large quantity of energy can be stored in a small mass of aluminum. Aluminum in granular form can easily be stored in open piles, not needing the complex storage containers used for other chemicals, such as cryogenic tanks for liquid hydrogen or containers for other hydrogen and carbon substances. The aluminum can be readily oxidized in air in a fluidized-grate burner, like powdered coal. The combustion product, aluminum oxide, is solid and can be recovered from the stacks with high efficiency. The aluminum oxide can be stored until it is needed for reprocessing into aluminum, closing the cycle. A significant disadvantage, again, is economics.

Any reversible chemical reaction may be considered for storing energy. The driving force for the reaction is generally thermal or electrical energy. When the reaction is reversed, the driving input commodity is released.

### **Electrochemical Batteries**

Batteries chemically store energy and release it as electric energy on demand. Batteries are a stable form of storage and can provide high energy and power densities, such as those needed for transportation. The lead-sulfuric acid battery has long been considered to be advantageous and has been widely applied. Recently, fuel cells have demonstrated the ability to act as large-scale chemical storages like batteries.

There are three main categories of energy applications for which batteries are potentially attractive: electric utility load management, electric vehicles, and storage for renewable energy systems (e.g., photovoltaic and wind systems). In the first of these applications, batteries are preferable to pumped hydro and compressed-air systems when the storage capacities needed are not great, and lead to savings in transmission system costs and construction lead time. Battery facilities can be modular in construction, making it easier to match storage capacity with utility system requirements. Batteries have higher energy efficiencies than mechanical systems (70–80% versus 50–70%), but do not benefit as much from economies of scale. For large utility systems, the simultaneous use of two or more types of storage may be desirable. For example, the compressed-air option could meet the needs for electricity generation over an 8–12 h period, while a battery facility may suffice only

over a 3–5 h period. For batteries used in utility systems, lifetime costs and service life are important characteristics, while weight or mass, volume, and power density are of secondary importance.

It is difficult to use the power generated by solar, wind, or hydropower sources directly, and so the electricity is usually stored in special batteries for use when it is needed. These batteries are often similar in chemistry to car batteries, but are designed differently. Car and truck batteries are designed to give short bursts of very high current to start the engine. They are not suited for use as storage batteries because they are made to be fully charged all the time, and have a very short life if subjected to the deep discharge cycles that are required with solar electric storage systems. Deep discharge cycles involve most of the energy stored in the battery being used before recharging.

Solar storage batteries are often made from large individual 2-V cells connected together, although smaller 6- and 12-V batteries are also available. The most common type of battery is the lead–acid battery, and these are usually of the flooded-cell type, though sealed lead–acid batteries are becoming more popular.

Nickel–cadmium (nicad) batteries are also available, and while expensive, do have the advantages of very long life and more stable voltage during discharge.

The amount of energy that can be stored in a battery is called its *capacity*, and is measured in amp hours (Ah). A 100-Ah battery will deliver 1 A of current for 100 h, or 4 A for 25 h, and so on, although battery capacity will decrease with increasing discharge rates. Battery capacities ranging from 1 to 2000 Ah or more are available.

For long battery life, it is desirable to use only a small part of the total battery capacity before recharging. Each time the batteries are run down and charged up, the batteries undergo a charge/discharge cycle. If more than half the battery's stored energy is discharged before it is recharged, this is called *deep cycling*. For example, lead–acid deep-cycle batteries designed for solar storage will last anywhere from 300 to 5000 cycles (and up to 50,000 cycles for nicad batteries), provided the discharge is limited to about 20% per cycle. Solar energy systems normally undergo one shallow cycle per day, but during “low sun” periods may undergo deeper discharges. For long battery life, the shallow cycle should be less than 20% of battery capacity and the deep cycle less than 80%.

It is possible to damage batteries by overcharging them. The maximum voltage that a battery should be charged to is about 2.5 V per cell, or 15.0 V for a 12-V battery. Some solar panels have an output voltage which is claimed to be low enough to stop charging above 15 V and to be self-regulating. However, because their open circuit voltage is still 18 V or so, they will actually continue to charge, with a much reduced current, until about 17 V. Most conventional panels deliver full power up to about 17 V and so need an external regulator. It is in general difficult to store significant quantities of electrical energy practically. Conventional battery designs can store in rechargeable batteries only very small amounts of the high-voltage alternating current (AC) power generated by either conventional or nuclear power plants. The difficulties include the following:

- The amount of energy which can be stored per unit weight or mass is small.
- The power density per unit weight or mass is low.
- All reversible batteries can withstand only a limited number of charge/discharge cycles before they are discarded. The lead–sulfuric acid cell is still the most economic option and is the battery used in many designs for electric cars.

The cost of battery systems is uncompetitive at present for large-scale ES applications. For example, battery storage of electricity may cost up to 50% more than pumped hydropower. The goal of the developers of advanced batteries for utilities is to reduce costs to about half of those of present heavy-duty lead–acid batteries.

**Characteristics of Batteries** Some chemical changes are readily reversed upon the application of a voltage, and form the basis of chemical batteries. Batteries have undergone development and experimentation since the late 19th century, but even then were not ready for immediate application.



**Table 2.2** Some batteries and their capacities

Type	Specific ES capacity (Wh/kg)	Lifetime cycles
Lead–acid (automotive)	33	300–1000
Lead–acid (commercial)	29	1600
NiCd	24	2000–3000
NiFe (Edison cell)	23	2000
AgZn	185–220	200
AgCd	110–165	500
NaS (250–350°C)	220	–
LiCl <sub>2</sub> (600°C)	440	–

Source: Meinel and Meinel (1977).

Articles written around 1900 suggested that inexpensive and long-lived batteries were just around the corner. Unfortunately, that corner has not yet been turned, in terms of all desired battery characteristics, but some claim that such advanced batteries are “almost here.” The batteries that come closest to having the lifetime characteristics and ES capacities needed for many modern applications are sodium or lithium batteries, which have recently been the subject of intensive development at a number of laboratories. These batteries must be maintained at high temperatures (several hundred degrees Celsius) to operate, but exhibit high ES capacities per unit mass. Sodium batteries can, in principle, store more than 200 Wh/kg, compared to the storage capacity of nickel–cadmium batteries of about 24 Wh/kg. In addition to having high storage capacity, a battery for utility functions must be able to tolerate repeated, full charge/discharge cycles. One thousand such cycles is a major challenge for today’s batteries; yet a lifetime of 10,000 cycles is desirable. A comparison of storage capacity and lifetime cycles for different types of batteries is given in Table 2.2.

Several terms are used to distinguish the characteristics of batteries in practical applications. These characteristics are significant in determining which battery is appropriate for a particular application. Five measures of merit for batteries for electric vehicles follow (Cassedy and Grossman, 1998):

- **Specific energy (or specific ES).** This is an important factor in determining the range of the battery, and can be defined as the amount of energy stored per unit weight or mass of a storage technology in a particular vehicle application (often measured in Wh/kg).
- **Energy density.** Energy density refers to the amount of energy of a battery in direct relation to its size, and can be defined as the total amount of energy a battery can store per liter of its volume for a specified rate of discharge (Wh/L or Wh/m<sup>3</sup>). High energy density batteries have a smaller size.
- **Specific power or power density.** This measure is an important factor for determining the acceleration of the battery, and can be defined as the rate of energy delivery or power for the storage per weight or mass of a storage technology in a particular vehicle application (often measured in W/kg). Specific power is at its highest when the battery is fully charged. As the battery is discharged, the specific power decreases, and acceleration also decreases. Specific power is usually measured at 80% of the depth of discharge. The driving range of a vehicle is roughly proportional to its specific energy, whereas the speed capability is nearly proportional to its specific power.
- **Cycle life.** The cycle life is total number of times a battery can be discharged and charged during its life. When the battery can no longer hold a charge over 80%, its cycle life is considered finished. The cycle of discharge and recharge for a battery can only be repeated a limited number of times due to electrode and electrolyte deterioration, which determines the life of the battery. For lead–acid batteries in automobiles, the life is around 300 cycles. If lead–acid batteries were

used in a solar application with daily cycling, they clearly would last less than a year. Industrial-grade lead–acid batteries can tolerate over five times the number of life cycles, but cost more than twice as much as automobile units, and would not be economically viable for such service.

- **Battery cost.** This economic factor is expressed in dollars per kilowatt-hour (\$/kWh).

Batteries are commercially available in many types and sizes. Although the most common type is lead–acid batteries, there are other promising batteries that are explained later. Present-day batteries generally are not suitable for most large-scale energy applications because of their weight, cost, and/or performance characteristics.

**Lead–Acid Batteries** For years, the “lead–acid” battery has dominated the field. In this battery, a lead compound (lead dioxide) at one electrode interacts with the sulfuric acid solution (the electrolyte) that fills each cell. Electrons are released and flow through the circuit to the other electrode (made of lead), providing the electric power. In the process, the lead compound reacts to form sulfate and the sulfuric acid is diluted with water. The battery can be recharged by forcing electric current through it (causing electrons to flow in the reverse direction). This process restores both electrodes and the sulfuric acid at an energy-conversion efficiency of about 80%.

The specific ES capacity of a typical lead–acid battery is only 126 kJ/kg, assuming 100% efficient conversion to electrical energy. The ES capacity of petrol is about 35,000 kJ/kg gross. After considering that only about 18% of this energy can be converted to mechanical energy, the net ES capacity is 6300 kJ/kg or 50 times as much as for the lead–acid battery.

The lead–acid battery operates on the principle of the galvanic cell, whose discovery goes back to the 18th century. A single-cell battery consists of two electrodes immersed in an electrolyte (Figure 2.6). Chemical reactions of the electrolyte with the substances at each of the two electrodes release electrons with the potential to do electrical work. In the lead–acid battery, one electrode is made of lead (Pb), the other electrode is of lead dioxide (PbO<sub>2</sub>), and the electrolyte is sulfuric acid (H<sub>2</sub>SO<sub>4</sub>). For the battery to deliver electricity, electrons are supplied to the lead dioxide electrode from the lead electrode. But as the energy is discharged, the chemical composition changes, as can be seen by writing the electrochemical equation:



The products of the discharge appear on the right side. The lead sulfate (PbSO<sub>2</sub>) product is deposited on the electrodes, while water goes into the solution of the electrolyte. These products build up, of course, as the discharge progresses, and eventually the battery no longer produces electricity. However, the reaction can be reversed. A storage battery can be recharged by a direct current (DC) source (generator). The charge flow in the cell reverses and so do the reactions from PbSO<sub>2</sub> back to PbO<sub>2</sub> on the positive electrode, to lead on the negative electrode, and to sulfuric acid in the electrolyte.

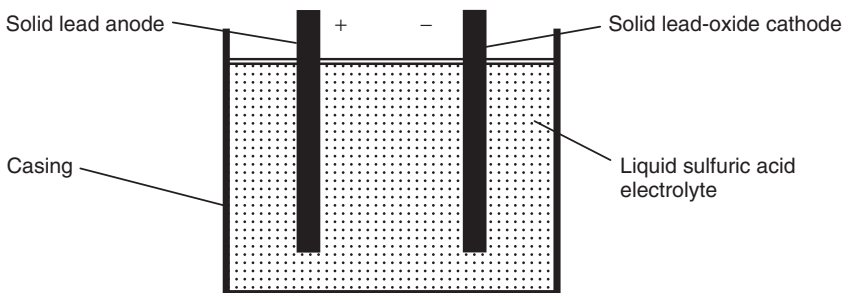


**Figure 2.6** Schematic of a liquid-acid battery



The lead–acid storage battery is generally too short-lived for many of the new applications envisaged. It is also too heavy and bulky for many uses, especially electric vehicle applications. Although proposed advanced batteries operate on the same galvanic principle as conventional batteries, major innovations have been attempted in their construction and operation. In an effort to avoid deposits and corrosion of solid electrodes, liquid electrodes were mostly designed and tested in practical applications. In the experimental battery described earlier, the two electrodes are comprised of molten sodium and a molten sulfur–carbon mixture. The use of these liquid electrodes in the sodium–sulfur battery not only reduces corrosion but also increases the allowable life cycles of the electrodes. But this battery has drawbacks in that it must operate at temperatures of 300–350 °C, which can present a safety risk in electric vehicles, and it is too heavy and costly for many practical uses.

Deep-cycle lead–acid batteries are available in three voltage sizes: 6-, 8-, and 12-V. For range, 6-V batteries are recommended because their specific energy is apparently higher. For performance, 12-V batteries are recommended, and these are popular with the newer components being used in cars with 144-V systems. The new 8-V battery offers a good balance between the range of the 6-V and the acceleration capabilities of the 12-V batteries.

Temperature has a direct effect on the performance of a lead–acid battery. The concentration of sulfuric acid inside the battery varies with temperature. A battery being used in 0 °C weather operates at only 70% of its capacity. Likewise, a battery being used in 43.3 °C weather operates at 110% of its capacity. The most efficient temperature that battery manufacturers recommend is 25.5 °C. Because the temperature factor is more important in colder climates, insulated battery boxes or thermal-management systems are highly recommended.

Maintaining batteries is very simple and requires little time. Each battery has three “flooded” cells, or six, which require watering with distilled water once a month. In addition, batteries need to be cleaned once every month with a solution of distilled water and baking soda to prevent ion tracking. Ion tracking is a condition in which dirt or moisture on top of the battery forms a conductive path from one terminal to another, or to a metal such as a battery rack. This can cause the ground-fault interrupter to trip on some battery chargers when the car is charging. Ion tracking is more prominent when the batteries are not stored in a protective enclosure or battery box.

Electrosource, a company in Austin, Texas, developed a horizon lead–acid battery. To develop this battery, Electrosource invented a patented process to extrude lead onto fiberglass filaments that are woven into grids in the battery’s electrode plates. The results are greater power capacity, longer life cycle, deep discharge without degeneration, rapid recharge, and high specific energy. The battery is sealed and maintenance free. Each battery is 12 V and costs about \$440. Table 2.3 compares the conventional sealed lead–acid battery with the horizon lead–acid battery technology.

**Nickel–Zinc (Ni–Zn), Nickel–Iron (Ni–Fe), and Nickel–Cadmium (Ni–Cd) batteries** In addition to improved lead–acid batteries, two other batteries with metallic electrodes (Ni–Zn and Ni–Fe batteries) are in advanced stages of development. The Ni–Zn battery uses dilute potassium hydroxide as an electrolyte. The present weakness of this battery is its lifetime, which is limited to 200 to

**Table 2.3** Comparison of conventional sealed lead–acid battery with the horizon lead–acid battery<sup>a</sup>

Characteristics	Conventional lead–acid battery	Horizon lead–acid battery
Specific energy (Wh/kg)	33	42
Energy density (Wh/L)	92	93
Specific power (W/kg)	75	240
Recharge time (hours)	8–16	<5
Cycle life (cycles)	400	800

<sup>a</sup>Adapted from Electrosource Inc.

300 cycles. Research is directed toward extending this value to 300 to 500 cycles. Such lifetimes may be sufficient for short-range urban driving where complete recharging is not often necessary. This battery's energy density of 65 Wh/kg is expected to be improved to at least 80 Wh/kg in the future, while its power density of 175 W/kg is already excellent.

The Ni–Fe battery is similar to the Ni–Zn unit and, in fact, was first invented by Thomas Edison in 1901 and only supplanted by the lead–acid battery in the 1920s. Currently, Ni–Fe batteries have storage capacities of 50–55 Wh/kg and power densities of 100 W/kg. They have excellent lifetimes (900 cycles have been demonstrated) but are somewhat bulky. A troublesome additional problem with this battery is that hydrogen gas is evolved from the electrode, which both reduces battery efficiency and creates a potential safety problem. Another difficulty with the Ni–Fe battery is that its power output drops drastically at temperatures below 10 °C and it is inoperable at 0 °C or below. Heaters may therefore be needed to make these batteries operable in cold climates. Nonetheless, the Ni–Fe battery will probably be an attractive power source for trucks and buses.

The Ni–Fe and Ni–Cd batteries are viewed as near-term batteries. Ni–Cd batteries are already in use in some countries, for example, Japan and Europe. They are apparently more expensive than lead–acid batteries because nickel is costly. The advantages of Ni–Cd batteries are higher energy density and higher cycle lives over 1000 charges. Although they can be recharged very quickly, they have a tendency to overheat; also Cd is highly toxic and so recycling efforts have to be managed very carefully. Although cadmium supplies are not large, it can be produced from sources such as copper, lead, zinc, and cadmium recycling.

Ni–Fe batteries have high energy densities and are capable of over 1000 deep discharge cycles before recharging. They need to be 11% overcharged to be charged. The result of the overcharging is water loss and a build-up of hydrogen, which is a safety concern. Efforts are on to improve the battery's efficiency, which will reduce these problems.

**Lithium–Iron Sulfide Batteries** The lithium–iron sulfide battery has as a negative electrode an alloy of aluminum and lithium, and iron sulfide as a positive electrode. The electrolyte is a molten salt that must be kept well above its melting point of about 350 °C. This battery is potentially one of the most suitable for electric vehicles. It is compact, with an energy/volume ratio projected at better than 200 Wh/L, and has a correspondingly high energy density of 100 Wh/kg and a power density of at least 100 W/kg. Despite the use of lithium, which is a fairly unstable metal that reacts with water to release hydrogen, safety tests in which prototype cells were crushed produced no combustion. Some significant engineering problems must be solved before the battery has a more adequate life expectancy than its present value of only about 200 cycles. Commercialization of a battery with a 1000 cycle lifetime is expected.

Although the lithium-ion battery was predicted to be a long-term battery, it is likely to be available soon for lease to fleets. The promising aspects of the battery are its low memory effect, high specific energy of 100 Wh/kg, high specific power of 300 W/kg, and a battery life of 1000 cycles. The battery has 28.8 V and consists of eight metal cylindrical cells encased in a resin module. Each battery has a built-in cell controller to ensure that each cell is operating within a specified voltage range of 2.5–4.2 V during charging and discharging. The cell controller communicates with the vehicle's battery controller to optimize power and energy usage. The disadvantages of the lithium-ion battery are its high cost and the ventilation system required to keep the batteries cool. The manufacturing costs are high because the battery uses an oxidized cobalt material for the anode, a highly purified organic material for the electrolyte, and a complex cell control system.

The lithium (metal) sulfide battery is an elevated temperature battery based on a lithium alloy/molten salt/metal sulfide electrochemical system. This system provides high specific power for better acceleration. Other advantages include its small size, low weight, and low cost per kilowatt-hour. The battery is composed of iron disulfide and lithium–aluminum alloy, which is completely recyclable.

The lithium–polymer battery is based on thin film technology. The battery is expected to cost 20% more than lead–acid but deliver twice the energy, with a lifespan of 50,000 miles. It has an

operating temperature between 65 °C and 120 °C. It can be fast charged in less than 90 min, but can be damaged by overcharging. The major challenge confronting this technology is scaling up its size to properly power an electric car.

**Sodium–Sulfur (Na–S) Batteries** The Na–S battery (Figure 2.7), like the lithium–iron sulfide battery, requires high-temperature operation. It differs significantly from other advanced batteries in that the electrodes are liquid (molten sodium or sulfur) and the electrolyte is a solid. The two electrodes are separated by a ceramic material (beta-alumina), which allows passage of (or conducts) sodium ions but not sodium atoms. The Na–S battery has adequate energy and power densities of 90 Wh/kg and 100 W/kg, respectively. Its volumetric energy density is expected to be at least 110 Wh/L. The major advantage of the liquid electrodes should be a long lifetime, because liquids are much easier to reconstitute than solids. Lifetimes of greater than 1000 cycles are expected, and the target for a sodium–sulfur battery for utility application is 2000 cycles. The Na–S battery has durability and safety problems that are yet to be solved. Sodium is a very reactive metal, and the necessary safety systems to protect an Na–S battery in case of a crash may make it too bulky for electric vehicle use. However, the battery may turn out to be of interest to utilities.

The requirement that the lithium–iron sulfide and Na–S batteries be maintained at 400 °C may appear to be a serious disadvantage. But because they are not 100% efficient, they do give off heat on charging. If carefully insulated, this heat is sufficient most of the time. A small auxiliary heater may be needed after long periods of inactivity.

The Na–S battery uses a ceramic beta-alumina electrolyte tube with sodium negative electrodes and molten sulfur positive electrodes within a sealed insulated container. To keep the sulfur in a molten state, the battery must be kept at a temperature of 300–350 °C. The batteries have built-in heaters to keep the sodium and sulfur from solidifying. The battery costs seven times more than the lead–acid batteries, but the price is expected to decrease during high volume production because the materials to build the battery are plentiful and inexpensive. Na–S battery research is currently being supported by various companies in the United States, United Kingdom, Canada, Germany, Sweden, and so on.

The main disadvantage of the Na–S battery is the high temperature, which has raised safety concerns. Also, the battery must be charged every 24 h to keep the sodium and sulfur from solidifying.

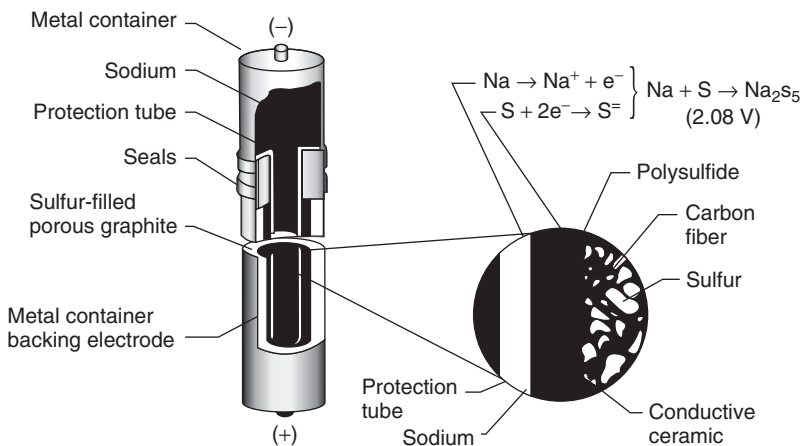


**Figure 2.7** High-temperature sodium–sulfur battery (Wilbur, 1985)

**Other Batteries** Other batteries that are even more advanced are also under investigation. One, a sodium–sulfur battery with a glass electrolyte, looks promising. There is interest in an aluminum–air battery that anticipates a high energy density. Because of its inexpensive components, this battery also offers the potential advantage of mechanical replacement of the aluminum plates instead of recharging.

One of the most promising battery technologies is the nickel–metal hydride (NiMH) battery. It is composed of nontoxic recyclable materials and is environmentally friendly. The NiMH battery has twice the range and cycle life of today’s lead–acid batteries. It is composed of nickel hydroxide and a multicomponent engineered alloy consisting of vanadium, titanium, nickel, and other metals. It is sealed, maintenance free, and can be charged in as quickly as 15 min. It can withstand overcharging and over discharge abuse. Ovonic Battery of Troy, MI, is currently manufacturing NiMH batteries.

Sodium–nickel chloride (NaNiCl<sub>2</sub>) batteries are under development by AEG Anglo Batteries. The battery operates at a temperature of 300 °C and is claimed by its manufacturer to be safe in accidents, and operates even if one of its cells fails. The NaNiCl<sub>2</sub> battery currently meets the future goals for both energy and power density. The battery can be cooled and reheated without damage; however, no current can be drawn from the battery if the temperature is below 270 °C. Costs to produce the battery remain a challenge. Various car making companies, for example, Bavarian Motor Works (BMW), Mercedes Benz, Opel, and Volkswagen (VW), are or have been testing their electric cars with NaNiCl<sub>2</sub> batteries.

The zinc–air battery developed by the Israeli firm Electric Fuel, Inc. is being used to power 40 test vans. After the battery pack or cassette is discharged, it is taken out of the vehicle and replaced with another cassette. The cassette replacement is done in a matter of minutes with highly automated equipment set up at various geographical locations. The discharged cassette has its electrodes replaced with fresh ones and the cassette is used for another vehicle. The spent electrodes are recycled and used to make new electrodes. The battery has an energy density 10 times that of lead–acid batteries.

The aluminum–air battery has aluminum plates added every 200 miles to replenish the used aluminum. The aluminum plates react with oxygen in sodium hydroxide electrolyte solution to form sodium aluminate. The sodium aluminate produces a byproduct of aluminum, aluminum trihydroxide, which is removed and replaced with fresh aluminum. The aluminum–air battery will probably be used by larger vehicles because of its size.

The nickel–hydrogen battery is currently under development by Johnson Controls. It is very expensive but has a long life and is safe to operate. It is currently being used in spacecraft and deep-water vehicles.

The nickel–zinc battery has more power than lead–acid batteries, but has a shorter discharge cycle, making it useful only for short commutes.

The zinc–chloride battery has high energy but must have a complex system to recapture the chlorine released during recharging.

The zinc–bromide battery developed by Johnson Controls stores electricity by plating zinc onto a surface and then unplating it. A bromide electrolyte solution that is 80% water is pumped through the battery to cause the plating and unplating reactions. Pure bromide is extremely toxic. Safety issues were raised about the battery in a 1992 electric vehicle race when it was involved in an accident. A hose that carried the bromide electrolyte became unconnected from the battery and leaked onto the race track, releasing irritating fumes.

The nickel–zinc, zinc–chloride, and zinc–bromide batteries will probably not be used commercially.

In the near future, electric vehicles are expected to be using advanced lead–acid batteries such as the horizon sealed lead–acid battery. One of the most promising battery technologies is the nickel–metal hydride battery. Although these batteries are expensive today, the price is expected to decrease. Also, electric vehicles might be powered by lithium batteries such as the lithium-ion battery now under development.

***Developments in Batteries*** We discuss below some new developments in batteries. Our understanding of batteries is about as old as our knowledge of electricity. In the not-too-distant future, “advanced” lead–acid batteries with new design breakthroughs may achieve ES capacities of 60 Wh/kg and 1000 cycle lifetimes. However, these figures of merit, which seem to be near the limit for lead–acid batteries, are still insufficient for satisfactory vehicular range and acceleration. Hence, battery researchers have begun to look at alternative materials, especially lighter elements.

During the past decades, research and development has been undertaken on batteries of untraditional designs. The leading contenders for commercial success among these are the lithium–metal sulfide, the zinc–chloride, and the sodium–sulfur batteries. All three of these (i) use light elements in one or both electrodes to achieve higher energy densities and (ii) operate at elevated temperatures. The zinc–chloride system must be at about 40 °C for its electrolyte to work properly; the other two need to be at the 300 to 400 °C range to operate. Development of the zinc–chloride battery was originally slowed because of the dangers of chlorine gas. A system that stores the chlorine in a frozen form (as a chlorine hydrate) seems to have solved that problem. The zinc–chloride battery will probably not be a candidate for most vehicular use because of its bulk, although it may be useful in trucks and vans if its size and shape do not cause severe design problems.

New developments in batteries are important for the stand-alone operation of solar photovoltaic and wind generators, for utilities as an alternative to pumped hydropower, and for electric vehicles. All of these applications require major technical improvements and cost reductions for storages. Advance battery concepts are typically variations on the conventional lead–acid battery.

It is clear that extending the lifetimes of batteries can make them more cost competitive. Developers of advanced batteries try to attain life cycles in excess of 2000 and lifetimes of over 10 years. To put these values into context, it is noted that daily cycling would require 3650 cycles over a 10-year lifetime. For comparison, note that the lifetime of a conventional pumped storage plant can be as high as 50 years, and the number of charge/discharge cycles presents no additional limitation to that technology. This observation has important economic ramifications because the capital cost of equipment is usually amortized over periods no longer than the working life of the equipment. The relatively shorter lifetimes of present-day batteries mean that the projected costs of delivered energy are more than 50% higher for batteries than for pumped hydropower. Thus, the cost to the utility ratepayer is correspondingly higher for that fraction of the electric energy delivered by batteries. In stand-alone processes utilizing batteries, such as remote wind generation, cost can be considered in a similar manner, but with different operational parameters if high availability is the objective. Regardless, achieving economic viability for large-scale wind or solar generation will require significantly greater ES capacities. That is, such systems must be capable of storing the equivalent of several days’ worth of energy usage so that they can deliver the energy at the normal rate of daily consumption during periods of limited sunlight or wind.

To bring advanced batteries to market, a coordinated effort is now underway to improve the development of battery technology. This effort has been undertaken by the United States Advanced Battery Consortium (USABC), whose members include Ford, Chrysler, General Motors (GM), utilities, the Department of Energy, national laboratories, and battery companies. The USABC established a time line that includes goals for battery development. The time line established around the year 2000 is divided into midterm and long-term goals as shown in Table 2.4.

Finally, there is a general need for the weight (or mass) and volume characteristics for batteries to be relatively competitive with those for other conventional ES technologies. Weight is often the most important technical requirement for batteries in such applications as electric vehicles where the alternative storage is a tank of gasoline.

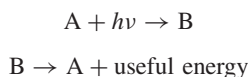
### **Organic Molecular Storage**

The intermittent availability of solar radiation, its seasonal and geographical variations, and its relatively low intensity, will limit the exploitation of that resource until it can be converted to forms of energy that can be efficiently stored and transported. However, most technologies that

**Table 2.4** The mid- and long-term goals of the USABC

Characteristic	Midterm goal	Long-term goal
Specific energy (Wh/kg)	80 (100 is desirable)	200
Specific power (W/kg)	150 (200 is desirable)	400
Recharge time (hours)	<6	3–6
Cycle life (cycles)	600	1000
Price (\$/kWh)	<150	<100

are presently available for the utilization of solar energy depend on the direct conversion of solar radiation to low-grade heat or electricity, both of which are difficult to store. The process of photosynthesis shows that endergonic photoreactions can convert radiative energy into storable chemical energy and, for at least a century, there have been attempts to find biological systems for the conversion of solar energy. In general, these efforts have been aimed at finding cyclic processes in which an endergonic photochemical reaction is followed by exergonic regeneration. After the second reaction, initial material is regenerated:



The general requirements for photochemical ES and conversion are discussed extensively elsewhere (Wilbur, 1985). Here, we restrict our discussion to selected aspects of six requirements that significantly affect the performance of organic systems for delivering heat. We point out the interdependence of these factors, and indicate areas where conflicting demands arise when trying to optimize them independently.

The efficiency of converting light into chemical energy by an endergonic photoreaction is subject to limitations that arise from the quantum nature of photochemical processes. These limitations apply to all quantum converters, including biological photosynthetic systems and photoelectric devices.

As shown in Figure 2.8, the photoreaction  $A \rightarrow A^* \rightarrow B$  can be initiated only by photons whose energies  $E_n$  match or exceed the energy  $E^*$  of the excited state  $A^*$  which is involved in the photoreaction. Therefore, only the fraction  $E^*/E_n$  of the absorbed radiation is available for the photoreaction. When this threshold effect is combined with the distribution of spectral intensities in the terrestrial solar spectrum, one finds that the maximum possible efficiency of a quantum process utilizing solar radiation depends on  $E^*$ , and reaches a maximum of about 44% at a value of  $E^*$  corresponding to a radiation wavelength of  $\sim 1100$  nm. At wavelengths that are more effective photochemically but less abundant, this efficiency decreases (e.g., to 25% at about 550 nm and 10% at about 390 nm). These efficiencies represent upper limits for any quantum converter operating with solar radiation (for details, see Sasse (1977)).

The potential for ES in an organic photoreaction depends on the difference in the energy contents of A and B, which can generally be recognized qualitatively by inspection of the structures involved. For the reactions considered here, ES requires the formation of strained structures (i.e., photoproducts with bond lengths and angles that differ from “normal” values) and/or an appreciable loss of “resonance energy” (i.e., a decrease in stabilization by  $\pi$ -electron delocalization) in the molecules concerned. The effects of strain and loss of resonance energy on the energy contents of A and B can be qualitatively compared and quantitatively predicted.

The overall performance of a photochemical ES system delivering heat depends critically on the temperature at which the exothermic reaction occurs, which in turn depends on the method used to induce the release of heat from ES compound B. Traditionally, heat release is caused by heating photoproduct B until the desired rate of heat evolution has been reached.



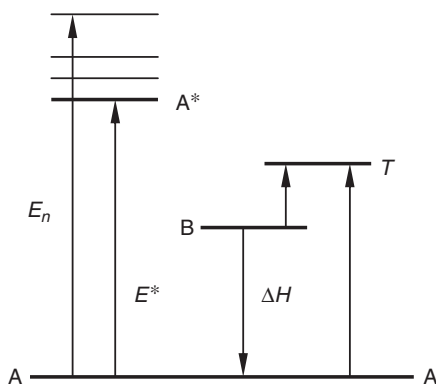


**Figure 2.8** Representation of energy levels in a cyclic system converting light to heat. Only the fraction  $E^*/E_n$  of the absorbed radiation can be used in the reaction  $A + h\nu \rightarrow A^* \rightarrow B$ .  $T$  denotes the transition state of the exothermic reaction  $B \rightarrow A = \Delta H$

In general, the temperature ranges for heat evolution are mainly between 100 °C and 200 °C. Thermal damage is a problem with compounds containing olefinic double bonds at these temperatures, although aromatic dimers function without detectable damage at higher temperatures. Unless especially stable compounds can be developed, for example, photochemically reactive aromatic fluorocarbons, heat-release temperatures in excess of approximately 220 °C probably cannot be routinely employed. However, photochemical storage systems operating between 100 °C and 200 °C may be sufficiently applicable in solar heating, and cooling at the upper temperature limits may not prevent the development of further interest in photochemical ES systems. Major improvements in storage capacity are possible for all of the systems described here by improving and better understanding the photophysical and photochemical characteristics of the ES compounds. Although much quantitative work has been done on individual compounds, more research is needed into the effects of structural modifications on photochemical and photophysical characteristics.

Some recognized areas for future investigation are the design of molecules that react sequentially with photons of different energies, and the use in ES of molecules that store energy. Also, the development of heterogeneous sensitizers is likely to offer important advantages both by extending the useful range of the solar spectrum and by simplifying the thermal steps involved.

### Chemical Heat Pump Storage

The system is based on a discontinuously working solid state absorption heat pump incorporating a storage function. The operating principle is as follows: two chambers are connected, as shown in Figure 2.9. Chamber I is the energy accumulator containing the vapor-absorbing salt ( $\text{Na}_2\text{S}$ ), and chamber II is the condenser/evaporator containing the working fluid ( $\text{H}_2\text{O}$ ). For the reversible chemical reaction in this case, sodium sulfide and water are used as a working pair and the reaction is



The system is charged by supplying heat from a heat source to chamber I so the vapor is driven from the salt to chamber II, where the vapor condenses. The heat of condensation has to be removed from chamber II, then called a condenser. If the system is completely charged, the discharge reaction starts on the right side of the reaction balance. When the system starts to discharge, heat is supplied to chamber II, then called an evaporator, to provide the latent heat of evaporation. At the same time, heat is released in chamber I when the vapor is absorbed by the hygroscopic salt. The result

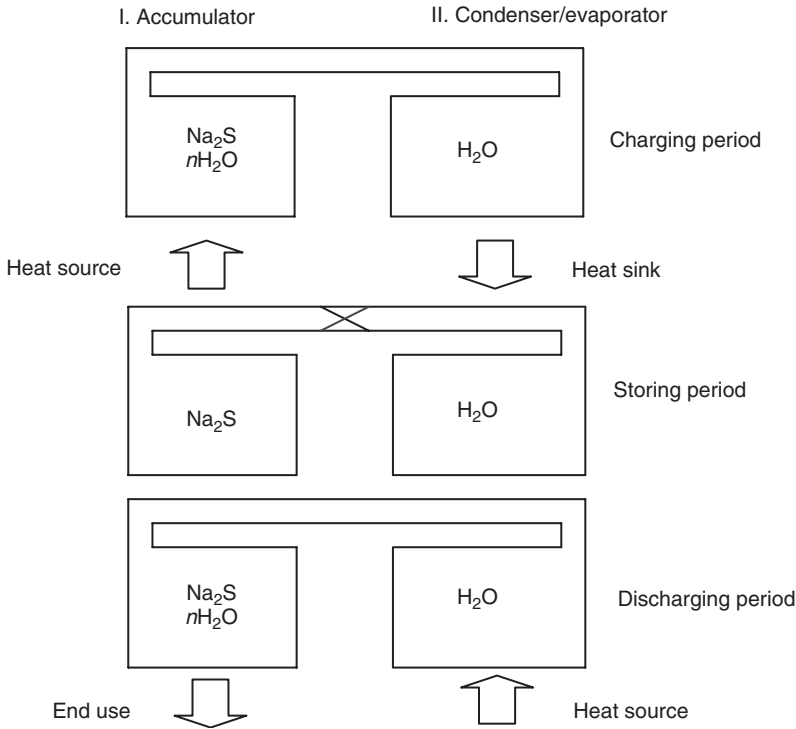


**Figure 2.9** Operating principle of a chemical heat pump system (Adapted from de Beijer, 1993)

is that chamber II can be used to produce cold, while chamber I can produce heat. The discharge process stops when the fluid is completely evaporated, the reaction balance is then on the left side, and the system must be charged again. The pressure–temperature curve above the sorption reaction between  $\text{Na}_2\text{S}$  and  $\text{H}_2\text{O}$  lies about  $55^\circ\text{C}$  from the vapor pressure curve of water. This temperature difference is defined as the equilibrium temperature difference. This is the temperature difference between the hot and the cold chamber in pressure equilibrium, that is, when no vapor is moving from one chamber to the other and no heat is taken from or supplied to one of the chambers. If the connection between the chambers is shut when the system is completely charged, the energy can be stored for an indefinite period. Both chambers may then reach equal temperatures without vapor moving from the evaporator to the accumulator; the losses are restricted to the loss of sensible heat, which is about 3–5% of the total heat stored. Details on this technology are provided by Beijer and Klein (1992) and de Beijer (1993).

The system also works with other absorbers and working fluids. Although the power output level is usually of the same order of magnitude, the storage capacity depends on the physical and chemical properties of the absorber and working fluid used. For applications where heat storage is an important qualification, the use of  $\text{Na}_2\text{S}$  and  $\text{H}_2\text{O}$  leads to the highest possible ES density.

On a per kilogram basis,  $\text{Na}_2\text{S}$  can store 1.1 kWh of energy. During the discharge process, about 1.05 kWh of heat can be released per kilogram of  $\text{Na}_2\text{S}$ . The cooling capacity of the system is about 0.75 kWh per kilogram of  $\text{Na}_2\text{S}$ , so the theoretical cooling factor is about 0.7. Cooling can be provided from ambient to  $0^\circ\text{C}$ ; below this point, the water in the evaporator freezes. By using heat exchangers in which the vapor absorbing salt is not integrated, like those used in comparable systems in the past, maximum power outputs of about 40 W/kg salt can be attained. By integration and optimization of the heat exchanger and the crystal structure of the salt, the system



has considerably improved power output per kilogram of salt. Power outputs of over 1.5 kW of heat and 1 kW/kg of Na<sub>2</sub>S have been achieved (de Beijer, 1993).

If there is a demand for high powers only and the internal temperature step of the heat pump or the evaporation temperature must be adapted to an application, the use of other absorbers and working fluids is recommended.

When used for air-conditioning in office and residential buildings, the system has the following advantages (de Beijer, 1993):

- saving of energy and costs by using residual or waste heat;
- exploitation of the difference in the electricity rates between peak and nonpeak periods (e.g., the day/night rate differential);
- reduction of the peak power payment to energy distribution companies;
- less capital investment in comparison to conventional systems;
- cooling of buildings using district heating, combined with heat or cold storage; and
- low maintenance cost, in large part because the system has no moving parts.

Some of the advantages which make the system suitable for applications in vehicles are

- high power density (150–220 W/kg);
- low specific system weight (4.5 kg per kWh); and
- low specific system volume (6 dm<sup>3</sup> per kWh).

However, several basic problems which are encountered in these systems, include

- poor stability and side reactions of the working materials;
- low power output; and
- low efficiency.

Despite such challenges, the system has proved its technical applicability for heating, cooling, and air-conditioning applications with low cost and thus exhibits strong market potential. There is good opportunity to use alternative absorbents and working fluids in chemical heat pump storage systems, and such systems look promising for the future, particularly for energy-conversion systems.

### 2.4.3 *Biological Storage*

Biological storage is the storage of energy in chemical form by means of biological processes and is considered an important method of storage for long periods of time. In this book, we do not discuss bioconversion, as it is not presently of practical interest, and limited information is available on biological ES. Note that if the quantum efficiency of biological processes can be increased by a factor of 10 over its present efficiency of about 1%, interest in bioconversion for ES will likely increase.

### 2.4.4 *Magnetic Storage*

Energy can be stored in a magnetic field (e.g., in a large electromagnet). An advanced scheme that employs superconducting materials is under development. At temperatures near absolute zero, certain metals have almost no electrical resistance and thus large currents can circulate in them with almost no losses. Because this scheme stores DC electricity, some losses are incurred in converting standard AC power to and from DC, and some energy is used to drive the refrigeration device to maintain the requisite low temperatures. Overall storage efficiencies of 80–90% are anticipated for these superconducting magnetic ES systems.

Magnetic storage is considered for two main purposes. First, large superconducting magnets capable of storing 1000–10,000 MWh of electricity could be attractive as load-leveling devices for central power stations, and may be cost-effective at such capacities. Second, smaller magnets with storage capacities in the 10-kWh range may be cost-effective in smoothing out transmission line loads, to better match short-term customer demands and generating equipment characteristics. A small superconducting magnet that can help in meeting customer peak needs at the far end of a transmission line could increase the effective load that the line can serve by as much as 25%, producing cost savings that could offset in whole or part the additional costs of expanding the transmission line capability.

The potential for highly efficient electrical ES is especially attractive for utilities, particularly when energy costs increase. The storage coil in a superconducting magnetic ES would likely be helical and located below ground. In order to obtain high current densities in the coil, and thereby reduce the quantity of costly superconductor needed, one proposed storage system is recommended for operation at 1.85 K. The storage unit could be charged during off-peak hours, with the electricity discharged back to the grid at a later time to meet peaking needs. The unit would generally operate on one charging and discharging cycle per day and would be connected to a three-phase utility transmission line. As noted earlier, the storage system requires the conversion of alternating to direct current for storage in the superconducting coil. An ES capacity of 1 GWh is typical of the size that is considered commonly. As the costs are projected to be high, no large-scale superconducting magnetic ES device is expected to be built in the foreseeable future. However, a small prototype system is now being built for use on transmission lines to dampen rapid voltage variations that occur with a periodicity on the order of seconds. The system has an ES capacity of 10 kWh and is designed to respond in fractions of a second. If line variations are reliably damped, the effective total capacity of the transmission system increases. The value of this increase in capacity is expected to more than compensate for the cost of the storage system. The stabilization unit itself is similar to the large-scale system for daily ES, but operates at the normal boiling point of helium.

#### 2.4.5 Thermal Energy Storage (TES)

Thermal energy may be stored by elevating or lowering the temperature of a substance (i.e., altering its sensible heat), by changing the phase of a substance (i.e., altering its latent heat) or through a combination of the two. Both TES forms are expected to see extended applications as new energy technologies are developed. TES is the temporary storage of high- or low-temperature energy for later use. Examples of TES are the storage of solar energy for overnight heating, of summer heat for winter use, of winter ice for space cooling in summer, and of the heat or cool generated electrically during off-peak hours for use during subsequent peak demand hours. Solar energy, unlike fossil fuels, is not available at all times. Even cooling loads, which nearly coincide with maximum levels of solar radiation, are often present after sunset. TES can be an important means of offsetting the mismatch between thermal energy availability and demand.

ES in the form of sensible heat changes appears very promising for the high-temperature storage of large quantities of energy at fossil-fired power plants. Oil will likely be used as the storage medium for this type of system.

The ES types discussed in the preceding sections of this chapter are applicable to electrical energy. In thermal electrical generating systems, TES offers the possibility of storing energy before its conversion to electricity.

Energy quality as measured by the temperatures of the materials entering, exiting, and stored within a storage is an important consideration in TES. For example, one kilowatt-hour of energy can be stored by heating one metric ton of water at 0.86 °C, or by heating 10 kg of water at 86 °C. The latter case is more attractive in terms of energy quality as a wider range of tasks can be accomplished with the higher temperature medium upon discharging the storage. For comparison, it is pointed out that the quality of energy stored in mechanical ES is higher still as, for example,

one kilowatt-hour of energy can also be stored by lifting one metric ton of water to a height of about 314 m.

Energy demands in the commercial, industrial, utility, and residential sectors vary on a daily, weekly, and seasonal basis. The use of TES in such varied sectors requires that the various TES systems operate synergistically and that they be carefully matched to each specific application. The use of TES for such thermal applications as space heating, hot water heating, cooling, air-conditioning, and so on has recently received much attention. A variety of new TES techniques has been developed over the past four or five decades in industrial countries. TES systems have enormous potential for making the use of thermal equipment more effective and for facilitating large-scale substitutions of energy resources economically. In general, a coordinated set of actions is needed in several sectors of the energy system for the maximum potential benefits of thermal and other types of ES to be realized.

Sensible heat changes in a material are dependent on its specific heat capacity and the temperature change. Latent heat changes are the heat interactions associated with a phase change of a material and occur at a constant temperature. Sensible heat storage systems commonly use rocks or water as the storage medium. Latent heat storage systems can utilize a variety of phase change materials, and usually store heat as the material changes from a solid to a liquid phase. We discuss each TES type in detail separately in Chapter 3.

## 2.5 Hydrogen for Energy Storage

Energy can be stored in chemical form as hydrogen. The potential versatility of this low-density gas for storing and transmitting energy has made it the subject of extensive research over the last few decades and brought it increasingly into the energy news. The variety of end uses for which hydrogen is well adapted includes being a fuel for electricity and/or heat production in fuel cells or combustion engines and for powering transportation devices, in addition to being a chemical commodity.

### 2.5.1 Storage Characteristics of Hydrogen

Hydrogen is not a source of energy. It does not exist in pure form to an appreciable extent on this planet. Rather, hydrogen is useful as an intermediate energy form (an “energy carrier”), much as electric energy is used today. Hydrogen has many advantages over electricity and thus is often considered a complementary intermediate energy form. In particular, hydrogen can be stored more easily and transported more inexpensively than electricity, and can deliver a much greater variety of end-use forms (including electricity). Hydrogen is less advantageous than electricity in terms of production costs.

Hydrogen has advantages and disadvantages as a medium for storing energy. Its energy density on a mass basis is high (116,300 kJ/kg), compared, for instance, with a value of 46,520 kJ/kg for jet aviation fuel and liquid methane. Hydrogen has a very low volumetric energy density, however, and thus usually requires a large storage volume. For example, the volumetric energy density of liquid hydrogen is only  $20.9 \times 10^6$  kJ/m<sup>3</sup>, compared to a value of  $34.84 \times 10^6$  kJ/m<sup>3</sup> for gasoline.

### 2.5.2 Hydrogen Storage Technologies

It is more difficult to store hydrogen than most conventional chemical fuels. For example, whereas gasoline can be stored in a relatively inexpensive tank, hydrogen requires either an expensive high-pressure tank in which the steel is 100 times heavier than the hydrogen stored or a refrigerated, vacuum-insulated dewar system which is both expensive and energy consuming. An alternative hydrogen storage system absorbs hydrogen in metallic powders, forming hydrogen metallic compounds (metal hydrides). These can be decomposed by the application of heat, releasing hydrogen.

An additional favorable property of metal hydrides is that they release hydrogen steadily at approximately a constant pressure. In a given volume, metal hydrides can hold an amount of hydrogen about the same as can be stored as a liquid. However, metal hydrides are dense, so that most of the weight in a storage system is due to the metal, not the hydrogen. A good candidate for metal hydride storage is iron–titanium.

### 2.5.3 Hydrogen Production

Most commercially available hydrogen is produced at present from such hydrocarbons as methane or other gases, and oil or similar petroleum products. The raw material from which most hydrogen is likely to be produced in the future is water, which is abundantly available. By the application of the required amount and form of energy, water can be separated into hydrogen and oxygen. A significant amount of hydrogen is already produced by the electrolysis of water. Water electrolysis is a relatively simple process in which positive and negative electrodes are immersed in water and a voltage is applied. Gas bubbles then appear – hydrogen at the negative electrode and oxygen at the positive electrode. The gases are prevented from diffusing to the other electrode by diaphragms that allow electric current to pass, but not gas. In a perfectly efficient electrolytic cell, 94 kWh of energy is needed to produce 28.3 m<sup>3</sup> of hydrogen (at atmospheric pressure). Only 79 kWh of that energy has to be electrical; the other 15 kWh of energy can be heat. This latter requirement can be exploited by power engineers, as a large electric power plant can provide an electrolysis plant with both electrical and thermal energy, the latter being otherwise unused. At present, most electrolysis cells operate at energy efficiencies of about 60–75%, although it is noted that they use a high-quality form of energy (electricity) to make a slightly lower quality form (chemical energy as hydrogen). The prospects for large-scale electrolysis as a future process are not great. A process that generates inexpensive electricity will likely make electrolytic production of hydrogen more commercially attractive.

Water can be decomposed directly by thermal energy, but the temperature required for a reasonable yield, approximately 2500 °C, is not readily available from nuclear reactors or other thermal sources. It is possible, though not likely, that fusion reactors or even high-temperature gas-cooled fission reactors could provide such temperatures in the future.

A more practical approach for using heat to dissociate water is through a thermochemical process. In such a process, a series of chemical reactions takes place where the required energy is supplied as heat. Most of the chemical products of the reactions are consumed in the other reactions, and the net reaction is the decomposition of water into hydrogen and oxygen. However, practical thermochemical reactions (e.g., those that produce at least half as much hydrogen per unit of primary energy as electrolysis) appear to need temperatures of 900 °C or higher. Research is nonetheless ongoing on thermochemical hydrogen production processes that utilize heat at significantly lower temperatures (approximately 500 °C), like the copper–chlorine cycle, in hopes that the lower temperature thermal requirement can make them more viable.

Direct thermal dissociation or these more complicated thermochemical water decomposition processes are attractive because they upgrade heat to hydrogen. By bypassing the less efficient production of electricity needed for electrolysis, they have a thermodynamic advantage. Unfortunately, this advantage depends on temperature, and the routine availability of such temperatures from suitable energy source may necessitate the successful development of advanced nuclear reactors or large-scale solar installations using lenses or mirrors to concentrate energy.

Another technique for hydrogen production that is undergoing laboratory development and which holds some future promise is photoelectrolysis. In this process, the electrodes are semiconductors which are immersed in an aqueous solution, and which produce an electric current and voltage when exposed to sunlight. This current then drives an electrolysis process. The process works well at the laboratory scale, but some difficulties need to be resolved. For instance, a physical separation process needs to be developed for the hydrogen and oxygen generated, as these gases are presently mixed in the electrolyte, posing an explosion hazard.

**Table 2.5** A technical comparison of ES technologies

ES technology	ESD) (kJ/m <sup>3</sup> )	MPD) (kW/m <sup>3</sup> )	SE (kJ/kg)	MSP (kW/kg)	CSL	TDT (s)	UL	AA
● Mechanical ES								
–Flywheels	$5 \times 10^4$	$5 \times 10^3$	6	0.6	Days	$1-10^3$	20 years	RB/SA
–Compressed air <sup>a</sup>	$10^4$	1	–	–	Weeks	$10^4-10^5$	20 years	EU
–Pumped hydrostorage <sup>b</sup>	$10^3$	0.1	1	$1 \times 10^{-4}$	Weeks	$10^4-10^5$	20 years	EU
● Thermal ES								
–Sensible heat								
High-temperature oil	$10^5$	10	100	0.01	Days	$10^4-10^5$	20 years	EU
Low-temperature	$3 \times 10^4$	3	10	0.001	Days	$10^4-10^5$	20 years	RH
rocks								
–Latent heat								
Various salts	$3 \times 10^5$	30	100	0.01	Weeks	$10^4-10^5$	$10^2-10^3$ cycles	RH
● Electromagnetic ES								
–Capacitors <sup>c</sup>	100	$10^8$	0.3	$3 \times 10^5$	Days	$10^{-6}-10^{-3}$	$10^4$ cycles	SA
–Magnets/coils <sup>d</sup>	$10^5$	10	1000	0.1	Days	$10^{-3}-10^5$	20 years	EU/SA
● Chemical ES								
–Batteries <sup>e</sup>								
Pb acid	$5 \times 10^4$	5	100	10	Weeks	$10-10^4$	$10^3$ cycles	ES/SLI/AP
Others <sup>f</sup>	10	10	500	–	Weeks	$10-10^5$	$10^3-10^5$ cycles	EU/SA/AP
–Hydrogen <sup>g</sup>	$9 \times 10^6$	–	$10^5$	–	Months	$10^4-10^5$	20 years	EU/SA/AP
–Methanol	$2 \times 10^7$	–	$3 \times 10^4$	–	Months	$10^4-10^5$	20 years	EU/SA/AP

ESD, energy storage density; MPD, maximum power density (based on minimum possible discharge times, except for those technologies where the device is for electric utility diurnal storage applications); SE, specific energy; MSP, maximum specific power (based on minimum possible discharge times, except for those technologies where the device is for electric utility diurnal storage applications); CSL, charged shelf life; TDT, typical discharge time (minimum discharge times are usually for partial discharges, but for specific technologies, smaller units can be discharged faster than larger units); UL, useful life in cycles and years (for economic considerations, a lifetime of 20 years is equivalent to an infinite life, but there is no indication that the various devices given a 20-year life expectancy in the table will wear out in 20 years); AA, application area; EU, electric utility diurnal storage; ES, emergency service for electric power system failure, and so on; SLI, automotive-starting, lighting, and ignition; RB, regenerative braking; RH, residential heating; SA, special applications; AP, automotive propulsion.

<sup>a</sup>Data for compressed gas are based on the plant installed at Huntorf, Germany.

<sup>b</sup>Data for pumped hydrostorage are based on the facility at Ludington, Michigan.

<sup>c</sup>Data are for oil-impregnated-paper capacitive ES systems.

<sup>d</sup>Most data are for a 104-MWh superconducting coil constructed underground and used for diurnal storage in an electric power system. Energy density is based on excavated volume.

<sup>e</sup>Most data are based on a diurnal ES application. Automotive propulsion batteries will have higher power rating.

<sup>f</sup>Several advanced battery systems were proposed for automotive propulsion and electric utility applications.

<sup>g</sup>Storage efficiency depends on the type of hydrogen storage, and storage cost depends on the medium used. Liquid hydrogen storage is less efficient but less expensive than metal hydride storage. Power and storage capacities are almost unrelated for hydrogen storage.

Source: Hassenzahl (1981).

Other hydrogen production processes that are being researched or are at the early stages of development, and therefore are of uncertain practicality, are being considered; for example, another hydrogen production process is biophotolysis. In this process, enzymes from algae help split water.

In general, for hydrogen to compete with electricity as an intermediate energy form, it appears that highly efficient water electrolysis systems using very inexpensive base-load electricity will have to become available or technological breakthroughs in other hydrogen production processes will have to occur.

**Table 2.6** Capital costs and efficiencies for ES devices

Technology	State-of-the-art technology		Future technology goal	
	Capital cost (\$/kW)	Efficiency (%)	Capital cost (\$/kW)	Efficiency (%)
● Pumped hydro				
–Above ground	300–500	71–74	–	–
–Underground	–	–	500 <sup>a</sup>	75
● Compressed air	770	50–52	600 <sup>b</sup>	65–70
● Superconducting magnetic	–	–	2600 <sup>c</sup>	80–90
● Batteries	600	75	35–55 <sup>d</sup>	50–60
● Flywheels	–	–	1200	70
● Thermal				
–Residential low temperature	200	100	150	100
–Industrial high temperature <sup>b</sup>	400	70	200	85–95
–Commercial cooling	400	85–100	100	85–95
–Seasonal storage	–	–	200	60–70
● Hydrogen				
–Daily storage	40–50	68–84	45	68
–Electrolytic production <sup>e</sup>	400–500	60–65	200–300	80–85

<sup>a</sup>Single high-head pump turbine.

<sup>b</sup>Cost basis is system with 8-h storage capacity (with no fuel consumption).

<sup>c</sup>Cost basis is system with 11-h storage capacity.

<sup>d</sup>Cost basis is vehicle battery with 2-h storage capacity.

<sup>e</sup>Efficiencies for electrolysis plant only.

Source: (Wilbur, 1985).

An indirect use of hydrogen as an ES medium is through hydrogen-derived fuels. These are chemical commodities that are produced using hydrogen, and their production processes often include hydrogen production as one part of the overall process. Examples of hydrogen-derived fuels include methanol and ammonia. These commodities have some advantages over hydrogen (e.g., methanol is a liquid at atmospheric conditions and thus easily handled). However, these fuels can also have disadvantages relative to hydrogen.

## 2.6 Comparison of ES Technologies

Many attempts have been made in the past to compare ES technologies based on such factors as efficiency, cost, application, and numerous other technical characteristics. Two such comparisons are presented in Tables 2.5 and 2.6. These tables consider the main ES technologies discussed in this chapter, as well as others, which, for several reasons, were not mentioned. The uncertainties about many ES technologies are evident in the tables, regarding present capabilities and future prospects and expectations.

## 2.7 Concluding Remarks

The different ES systems discussed in this chapter have their own advantages and disadvantages and are suitable for different energy forms. Where thermal energy is available and thermal demands exist, but these are not necessarily coincident, TES is the most direct means of ES as it avoids the need to convert energy from one form to another and the ensuing conversion losses. For the case of solar energy in particular, TES appears to be the most efficient and effective means of storage. Thus, TES is likely to have solar thermal applications in the future.

## References

- de Beijer, H.A. (1993). The economic analysis of the salt water energy accumulation and transformation (SWEAT) system, HPC Workshop Proceedings on Heat Pumps and Thermal Storage, pp. 111–118, 24-25 May, Fukuoka, Japan.
- de Beijer, H.A. and Klein, J.W. (1992). SWEAT-a chemical heat pump for heat or cold storage, *IEA Heat Pump Center Newsletter* 10 (1), 11–12.
- Cassedy, E.S. and Grossman, P.Z. (1998). *Introduction to Energy, Resources, Technology, and Society*, Cambridge University Press, Cambridge.
- Diamant, R.M.E. (1984). *Energy Conservation Equipment*, The Architectural Press, London.
- Dincer, I. (1997). *Heat Transfer in Food Cooling Applications*, Taylor & Francis, Washington, DC.
- Dincer, I. (1999). Evaluation and selection of energy storage systems for solar thermal applications, *International Journal of Energy Research* 23, 1017–1028.
- Genta, G. (1985). *Kinetic Energy Storage, Theory and Practice of Advanced Flywheel Systems*, Butterworths Co., London.
- Hassenzahl, W.V. (1981). *Mechanical, Thermal, and Chemical Storage of Energy*, Hutchinson Ros. Publ. Co., Stroudsburg, Pennsylvania.
- Meinel, A.B. and Meinel, M.P. (1977). *Applied Solar Energy*, Addition-Wesley, New York.
- Sasse, W.H.F. (1977). Organic molecular energy storage reactions, In: *Solar Power and Fuels* (Ed. J.R. Bolton), Academic Press, New York, pp. 227–245.
- Sheahan, R.T. (1981). *Alternative Energy Sources*, Aspen Publication Corp., Rockville.
- Wilbur, L.C. (1985). *Handbook of Energy Systems Engineering*, John Wiley & Sons, New York.

## Study Questions/Problems

- 2.1 What benefits do energy storage systems offer?
- 2.2 List some of the potential applications of energy storage options.
- 2.3 Classify energy storage methods and explain each in brief.
- 2.4 What are the primary criteria in selecting the location for underground pumped storage?
- 2.5 Classify compressed-air storage systems and explain each.
- 2.6 Explain how a flywheel works.
- 2.7 A flywheel is intended for a storage application. It has a weight of 10 kg, a diameter of 10 m, a rotational speed of 1000 rad/s, a density of 3200 kg/m<sup>3</sup>, and a volume change of 0.80 m<sup>3</sup>. For the system,  $k$  can be taken as  $\frac{1}{2}$ . Evaluate how much energy this flywheel can store.
- 2.8 List the key measures of merit for batteries.
- 2.9 What are the potential uses of hydrogen and its connection to energy storage options?
- 2.10 List the essential criteria for comparing energy storage methods.
- 2.11 Select a conventional car and estimate the specific fuel consumption for city driving, with and without regenerative braking using an appropriate energy storage. Re-evaluate for highway driving and comment on how the results differ from those for city driving.
- 2.12 Determine the capacity for electricity generation from pumped hydro at Niagara Falls, assessing Canadian and American capacities separately. Determine the actual electricity generated over a recent annual period from the pumped hydro facilities at Niagara Falls.

- 2.13** What are the more important and common factors for selecting an energy storage for a transportation application, and how do these differ from the more important factors for a static application?
- 2.14** List and describe the processes for hydrogen production, and explain the advantages and disadvantages of each.
- 2.15** Identify possible hydrogen-derived fuels and explain their advantages and disadvantages as energy storage media, relative to each other and relative to hydrogen.
- 2.16** Why does thermochemical storage often involve little if any thermal losses?



# 3

## Thermal Energy Storage (TES) Methods

### 3.1 Introduction

Energy demands in the commercial, industrial, and utility sectors vary on daily, weekly, and seasonal bases. These demands can be matched with the help of thermal energy storage (TES) systems that operate synergistically. The use of TES for thermal applications such as space and water heating, cooling, air-conditioning, and so on has recently received much attention. A variety of TES techniques have developed over the past four or five decades as industrial countries have become highly electrified. Such TES systems have an enormous potential to make the use of thermal energy equipment more effective and for facilitating large-scale energy substitutions from an economic perspective. In general, a coordinated set of actions in several sectors of the energy system is needed if the potential benefits of thermal storage are to be fully realized.

Many types of energy storage play an important role in energy conservation. In processes which yield waste energy that can be recovered, energy storage can result in savings of premium fuels.

Energy may be stored in many ways, as pointed out in Chapter 2, but since in much of the economy in many countries, energy is produced and transferred as heat, the potential for thermal energy storage warrants study in detail.

Chemically charged batteries became common in the mid-19th century to provide power for telegraphs, signal lighting, and other electrical devices. By the 1890s, central stations were providing both heating and lighting, and many did both. Electric systems were almost all direct current (dc); so, incorporating batteries was relatively easy. In 1896, Toledo inventor Homer T. Yaryan installed a thermal storage tank at one of his low-temperature hot-water district-heating plants in that city to permit the capture of excess heat when electric demand was high. Other plants used steam storage tanks, which were generally not as successful. Other forms of TES were used to power street cars in the 1890s, including compressed air and high-temperature water that was flashed into steam to drive a steam engine. Electric cars and trucks were quite common prior to World War I, after which gasoline-powered internal combustion engines became prevalent.

TES deals with the storage of energy by cooling, heating, melting, solidifying, or vaporizing a material; the thermal energy becomes available when the process is reversed.

Storage by causing a material to rise or lower in temperature is called *sensible heat storage*; its effectiveness depends on the specific heat of the storage material and, if volume is important, on its density. Storage by phase change (the transition from solid to liquid or from liquid to vapor with no change in temperature) is a mode of TES known as *latent heat storage*. Sensible storage systems commonly use rocks, ground, or water as the storage medium, and the thermal energy is stored by increasing the storage-medium temperature. Latent heat storage systems store energy in

phase change materials (PCMs), with the thermal energy stored when the material changes phase, usually from a solid to a liquid. The specific heat of solidification/fusion or vaporization and the temperature at which the phase change occurs are of design importance. Both sensible and latent TES also may occur in the same storage material. In this chapter, TES is considered to include the storage of heat through the reversible scission or reforming of chemical bonds.

PCMs are either packaged in specialized containers such as tubes, shallow panels, plastic bags, and so on, or contained in conventional building elements (e.g., wall board and ceiling) or encapsulated as self-contained elements.

The oldest form of TES probably involves harvesting ice from lakes and rivers and storing it in well-insulated warehouses for use throughout the year for almost all tasks that mechanical refrigeration satisfies today, including preserving food, cooling drinks, and air-conditioning. The Hungarian parliament building in Budapest is still air-conditioned, with ice harvested from Lake Balaton in the winter.

TES has always been closely associated with solar installations, including both solar heating and photovoltaic applications. Today, compressed-air storage, batteries, chilled and hot water storage, ice storage, and flywheels are used, all designed to meet one or more of the purposes listed above. Many utilities provide direct incentives for energy storage applications, while time-of-day rates and high demand charges indirectly entice customers to consider these opportunities.

TES generally involves a temporary storage of high- or low-temperature thermal energy for later use. Examples of TES are storage of solar energy for overnight heating, of summer heat for winter use, of winter ice for space cooling in summer, and of heat or coolness generated electrically during off-peak hours for use during subsequent peak demand hours. Solar energy, unlike energy from fossil fuels, is not available all the time. Cooling loads, which nearly coincide with maximum levels of solar radiation, are often present after sunset. This phenomenon is largely due to the time lag between when objects are heated by solar energy and when they release the heat to the surrounding air. TES can help offset this mismatch of availability and demand.

Energy plays a major role in the economic prosperity and the technological competitiveness of a nation. Because predicting future availability, demand, and price of energy forms is at best approximate and often imprecise, it is important to have a broad array of technologies available to meet the energy needs of the future. Furthermore, the technologies developed should be those that ensure energy security, efficiency, and environmental quality for a nation. TES is one such technology, and it is being promoted because it can substantially reduce total energy consumption, thereby conserving indigenous fossil fuels and reducing costly oil imports. As technical and economic problems and risks are reduced through proven performance, TES is expected to be accepted as an attractive option in the industrial and commercial sectors that will lead to, among other benefits, increased energy efficiency and environmental benefits. TES has been identified as a method for substantially reducing peak electrical demands, thereby helping to ameliorate predicted peak-power shortages in the future. TES provides a potentially economic means of using waste heat and climatic energy resources to meet a significant portion of our growing needs for heating and cooling, especially for industrial facilities and commercial buildings. Environmental benefits also accompany the use of TES in many applications.

TES technology has been used in various forms and applications. Some of the more common applications include the use of sensible TES (oils, molten salts) or latent TES (ice, phase change material) for refrigeration and/or space heating and cooling needs. Research activities on TES are continuing at various national laboratories, universities, and research centers throughout the world, as well as at industrial facilities.

## 3.2 Thermal Energy

Thermal energy quantities differ in temperature. As the temperature of a substance increases, the energy content also increases. The energy required  $E$  to heat a volume  $V$  of a substance from a

temperature  $T_1$  to a temperature  $T_2$  is given by

$$E = mC(T_2 - T_1) = \rho VC(T_2 - T_1)$$

where  $C$  is the specific heat of the substance. A given amount of energy may heat the same weight or volume of other substances, and increase the temperature to a value greater or lower than  $T_2$ . The value of  $C$  may vary from about 1 kcal/kg °C for water to 0.0001 kcal/kg °C for some materials at very low temperatures. Further information on such materials is available in Section 3.6.

The energy released by a material as its temperature is reduced, or absorbed by a material as its temperature is increased, is called the *sensible heat*.

Latent heat is associated with the changes of state or phase change of a material. For example, energy is required to convert ice to water, to change water to steam, and to melt paraffin wax. The energy required to cause these changes is called the *heat of fusion* at the melting point and the *heat of vaporization* at the boiling point. To illustrate, let us consider water, and suppose that we wish to evaporate 1 kg of ice by converting it to liquid and then heating it until it boils. In this case, 80 kcal is required to melt the ice at 0 °C to water at 0 °C; then, about 100 kcal is needed to raise the temperature of the water to 100 °C; finally, 540 kcal is needed to boil the water, giving a total energy need of 720 kcal. The sensible heat for a given temperature change varies from one material to another. The latent heat also varies significantly between different substances for a given type of phase change.

It is relatively straightforward to determine the value of the sensible heat for solids and liquids, but the situation is more complicated for gases. If a gas restricted to a certain volume is heated, both the temperature and the pressure increases. The specific heat observed in this case is called the *specific heat at constant volume*,  $C_v$ . If, instead the volume is allowed to vary and the pressure is fixed, the specific heat at constant pressure,  $C_p$ , is obtained. The ratio  $C_p/C_v$  and the fraction of the heat produced during compression can be saved, significantly affecting the storage efficiency.

### 3.3 Thermal Energy Storage

As an *advanced energy technology*, TES has attracted increasing interest for thermal applications such as space heating, hot water, cooling, and air-conditioning. TES systems have the potential for increasing the effective use of thermal energy equipment and for facilitating large-scale fuel switching. Of most significance, TES is useful for addressing the mismatch between the supply and demand of energy.

There are mainly two types of TES systems, sensible (e.g., water and rock) and latent (e.g., water/ice and salt hydrates). The selection of a TES system mainly depends on the storage period required, for example, diurnal or seasonal, economic viability, operating conditions, and so on. Many research and development activities on energy have concentrated on efficient energy use and energy conservation, and TES appears to be one of the more attractive thermal technologies that has been developed.

TES is basically the temporary “holding” of energy for later use. The temperature at which the energy is held in part determines the potential application. Examples of TES systems are storage of solar energy for night and weekend use, of summer heat for winter space heating, and of ice from winter for space cooling in summer. In addition, the heat or cool generated electrically during off-peak hours can be used during subsequent peak demand hours. Solar energy, unlike energy from fossil, nuclear, and some other fuels, is not available at all times. Even cooling loads, which coincide somewhat with maximum levels of solar radiation but lag by a time period, are often present after sunset. TES can provide an important mechanism to offset this mismatch between times of energy availability and demand.

Increasing societal energy demands, shortages of fossil fuels, and concerns over environmental impact are providing impetus to the development of renewable energy sources such as solar, biomass, and wind energies. Because of their intermittent nature, effective utilization of these

and other energy sources is in part dependent on the availability of efficient and effective energy storage systems.

TES involves the storage of energy by heating (or cooling) or melting or vaporizing (or solidifying or liquefying) a material, or through thermochemical reactions. The energy is recovered as heat or cool when the process is reversed. Storage by causing a temperature rise is known as *sensible TES*, and by causing a phase change as *latent TES*. Thermochemical thermal storage, in which a chemical reaction that can be reversed absorbs energy, is described in detail in Chapter 2.

TES has a wide variety of applications, the majority of which relate to heating and cooling. TES provides a link and buffer between a heat source and a heat user. A common example of a TES is the solar hot water storage system. The energy source is solar radiation and the heat user is the person demanding hot water. In this situation, storage is required because the energy supply rate is small compared with the instantaneous demand, and because solar radiation is not always available when hot water is demanded.

As an example of the cost savings and increased efficiency achievable through the use of TES, consider the following case. In some climates, it is necessary to provide heating in winter and cooling in summer. Typically, these services are provided by using energy to drive heaters and air-conditioners. With TES, it is possible to store heat from the warm summer months for use in winter, while the cold ambient temperatures of winter can charge a cool store and subsequently provide cooling in summer. This is an example of seasonal storage, which can be used to help meet the energy needs caused by seasonal fluctuations in temperature. Obviously, such a scheme requires a great deal of storage capacity because of the large storage timescales. The same principle can be applied on a smaller scale to smooth out daily temperature variations. For instance, solar energy can be used to heat tiles on a floor during the day. At night, as the ambient temperature falls, the tiles release their stored heat to slow the temperature drop in the room. Another example of a TES application is the use of thermal storage to take advantage of off-peak electricity tariffs. Chiller units can be run at night when the cost of electricity is relatively low. These units are used to cool a thermal storage, which then provides cooling for air-conditioning throughout the day. Not only are electricity costs reduced, but the efficiency of the chiller is increased because of the lower night-time ambient temperatures, and the peak electricity demand is reduced for electrical-supply utilities.

### 3.3.1 Basic Principle of TES

The basic principle is the same in all TES applications. Energy is supplied to a storage system for removal and use at a later time. What mainly varies is the scale of the storage and the storage method used. Seasonal storage requires immense storage capacity. One seasonal TES method involves storing heat in underground aquifers. Another suggested method is circulating warmed air into underground caverns packed with solids to store sensible heat. The domestic version of this concept is storing heat in hot rocks in a cellar. At the opposite end of the storage-duration spectrum is the storage of heat on an hourly or daily basis. The previously mentioned use of tiles to store solar radiation is a typical example, which is often applied in passive solar design.

#### TES Processes

A complete storage process involves at least three steps: charging, storing, and discharging. A simple storage cycle can be illustrated as in Figure 3.1, in which the three steps are shown as distinct. In practical systems, some of the steps may occur simultaneously (e.g., charging and storing), and each step may occur more than once in each storage cycle.

In terms of storage media, a wide variety of choices exists depending on the temperature range and application. For sensible heat storage, water is a common choice because, among its other positive attributes, it has one of the highest specific heats of any liquid at ambient temperatures.

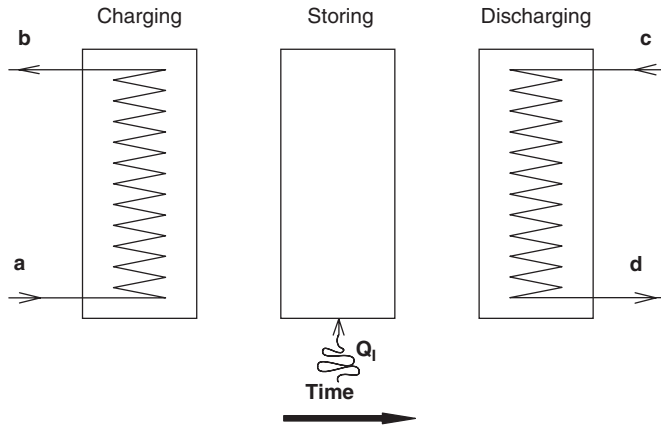


**Figure 3.1** The three processes in a general TES system: charging (left), storing (middle), and discharging (right). Here the heat  $Q_I$  is infiltrating and is positive in value for a cold thermal storage. If it is released, it will be toward the surroundings and  $Q_I$  will be negative. The heat flow is illustrated for the storing process, but can occur in all three processes

While the specific heat of water is not as high as that for many solids, it has the advantage of being a liquid that can easily be pumped to transport thermal energy. Being a liquid, water also allows good heat-transfer rates. Solids have the advantage of higher specific heat capacities, which allow for more compact storage units. When higher temperatures are involved, such as for preheating furnace air supplies, solids become the preferred sensible heat stores. Usually refractories are then used as the storage material. If the storage medium needs to be pumped, liquid metals are often used.

TES using latent heat changes has received a great deal of attention. The most common example of latent heat storage is the conversion of water to ice. Cooling systems incorporating ice storage have a distinct size advantage over equivalent-capacity chilled-water units because of the relatively large amount of energy that is stored through the phase change. Size is the major advantage of latent heat thermal storage. NASA has considered using lithium fluoride salts to store heat in the zero-gravity environment of the space shuttle. Another interesting development is the use of PSMs in wall paneling. These panels incorporate compounds that undergo solid-to-solid structural phase changes. With the appropriate choice of material, phase change occurs at ambient temperature. Then, these materials, when incorporated into the panels, act as high-density heat sinks/sources that resist changes in ambient room temperature.

The other category of storing heat is through the use of reversible endothermic chemical reactions, and in some literature this method is considered TES. However, we include it in Chapter 2 separately as chemical heat storage technology. In this method, the reactions involve the breaking and forming of chemical bonds; so, a great deal of energy can be stored per unit mass of storage material. Although not currently viable, a variety of reactions are being explored. These include catalytic reactions such as the steam reforming reaction with methane and the decomposition of sulfur trioxide, and thermal dissociation reactions involving metal oxides and metal hydrides. These reactions are expected to be useful in high-temperature nuclear cycles and solar-energy systems, and as topping cycles for industrial boilers. At present, lower temperature reactions ( $<300^\circ\text{C}$ ) have not proven promising. TES can be an effective way of reducing costs and increasing efficiency. While effective thermochemical storage is still some way off, latent and sensible heat storage are already well established. In these cases, TES has the potential to produce significant benefits, particularly for low-temperature heating and cooling applications. These benefits should allow TES to gain wider acceptance.

## Topics of Investigation

TES systems combined with heating, cooling, and air-conditioning applications have attracted much interest in recent years. Many related studies have been carried out in a variety of countries, particularly in the United States, Europe, and Japan. These studies address technical issues arising from new TES concepts and the improvements required in the performance of existing TES systems. Studies have also investigated the design of compact TES systems and the use of TES in solar applications. TES research and development has been broad based and productive, and directed toward both the resolution of specific TES issues and the potential for new TES systems and storage materials. The following discussions summarize many investigations and indicate the scope of TES studies.

During the past few decades, many articles have appeared in the literature reporting investigations of TES systems and their applications (especially with solar energy), field performance characteristics and evaluations, design fundamentals, transient behavior and thermal analyses, and system and process optimization. In addition, theoretical, experimental, and numerical studies have been undertaken on the thermophysical properties of new TES materials, TES selection criteria, the integration of TES systems into solar power plants, and the economics and environmental effects of TES. Some details on these studies are given below:

- For sensible heat storage, the performance and thermal characteristics of packed-bed storage systems, the use of different storage materials, and uses for aquifer TES, water TES, and solar ponds have been investigated, as have operating conditions, effectivenesses, economics, and so on, for these systems.
- Thermal analyses of PCMs and their use for energy conservation in buildings have been carried out. Experimental and theoretical investigations and performance evaluations of the PCMs in latent heat storage applications have also been undertaken.
- Aspects of TES systems and materials during operation have been studied, including heat and mass transfer, and transient behavior, and second-law optimization and performance.
- Many practical applications of solar heating using TES have also been reported.
- Numerous investigations have considered specific TES systems and applications, as well as the general objectives of TES and the energy conservation, and related benefits of different TES methods.

There is a growing interest in the use of diurnal, or daily, TES for electrical load management in both new and existing buildings. TES technologies allow electricity consumption costs to be reduced by shifting electrical heating and cooling demands to periods when electricity prices are lower, usually during the night. Load shifting can also reduce demand charges, which can represent a significant proportion of total electricity costs for commercial buildings.

Many TES studies aim to inform professionals concerned with heating and cooling systems in buildings about the characteristics of TES, and to examine the development of relevant technologies and assess their application in the field using data from case studies in different countries. Other studies also consider factors influencing technology adoption.

Space heating using electric TES has been used extensively in Europe and North America. The storage media can include ceramic brick, crushed rock, water, and building mass, and systems can be either room or centrally based. Many improvements have been introduced in such systems in the past few years, including the development of new PSMs for latent heat storage, which have recently become available commercially.

Cool storage using ice, water, or eutectic salts as the storage media are widely applied in the United States, where summertime cooling requirements are high. This technology is also used in Europe, often in combination with heat recovery and hot water storage, and in Australia, Canada, Korea, Japan, Taiwan, and South Africa.

TES systems can be installed in both residential and commercial buildings, and can be cost effective. Results from many of the monitored projects demonstrate payback periods of less than



three years. If time-of-use tariffs exist, electricity costs to the consumer can be reduced by shifting the main electrical loads to periods when electricity prices are lower. If demand charges are implemented, a shifting or spreading of the load can reduce these significantly. To be effective, each storage system must be sized and controlled to minimize electricity costs and other system costs.

District heating and cooling systems often also incorporate TES and can benefit from its careful integration into the overall system.

Benefits from TES also accrue to the electricity utilities. The shifting of loads to off-peak periods not only spreads the demand over the generating period, but may also enable electricity output from the more expensive generating stations to be reduced. Worldwide, electrical utility incentive programs promoting the use of storage technologies exist, many of them within demand-side management programs. Such programs can greatly influence the economic feasibility of installing thermal storage by offering financial rebates, information, or special electricity rates for consumers.

Research and development programs for TES are needed in a number of areas, including the following related to utility-based TES applications:

- Establishing quantitative models for ascertaining the effects and benefits of changes in storage-capacity levels on service reliabilities, optimum generation mixes, and reserve margins. These models need to incorporate detailed demand projections for the future that reflect probable changes in utility load characteristics.
- Establishing the benefits of dispersed storage as a function of the geographic land use and demand characteristics of utilities. The work should be carried out on a regional basis where possible, and on an average national basis where necessary.
- Establishing the possible interactions between storage and load control for areas of differing load characteristics.
- Relating dispersed storage to dispersed generation, particularly in the context of total energy systems.

In parallel with such studies, there is a need for research and development support of promising storage concepts in order to ensure their timely availability and that they include a wide range of operating characteristics.

### 3.3.2 *Benefits of TES*

Although TES is used in a wide variety of applications, all are designed to operate on a cyclical basis (usually daily, occasionally, seasonally). The systems achieve benefits by fulfilling one or more of the following purposes:

- **Increase generation capacity.** Demand for heating, cooling, or power is seldom constant over time, and the excess generation available during low-demand periods can be used to charge a TES in order to increase the effective generation capacity during high-demand periods. This process allows a smaller production unit to be installed (or to add capacity without purchasing additional units), and results in a higher load factor for the units.
- **Enable better operation of cogeneration plants.** Combined heat and power, or cogeneration, plants are generally operated to meet the demands of the connected thermal load, which often results in excess electrical generation during periods of low electricity use. By incorporating TES, the plant need not be operated to follow a load. Rather, it can be dispatched in more advantageous ways (within some constraints).
- **Shift energy purchases to low-cost periods.** This measure constitutes the demand-side application of the first purpose listed, and allows energy consumers subject to time-of-day pricing to shift energy purchases from high- to low-cost periods.

- **Increase system reliability.** Any form of energy storage, from the uninterruptable power supply of a small personal computer to a large pumped storage project, normally increases system reliability.
- **Integration with other functions.** In applications where on-site water storage is needed for fire protection, it may be feasible to incorporate thermal storage into a common storage tank. Likewise, equipment designed to solve power-quality problems may be adaptable to energy-storage purposes.

One may ask: what is the most significant benefit of a TES system? A common answer is reducing electric bills by using off-peak electricity to produce and store energy for daytime cooling. Indeed, TES is successfully operating in offices, hospitals, schools, universities, airports, and other facilities in many countries, shifting energy consumption from periods of peak electricity rates to periods of lower rates. This benefit is accompanied by the additional advantage of lower demand charges.

### 3.3.3 *Criteria for TES Evaluation*

There are numerous criteria to evaluate TES systems and applications such as technical, environmental, economic, energetic, sizing, feasibility, integration, and storage duration. Each of these criteria should be considered carefully to ensure successful TES implementation.

#### **Technical Criteria for TES**

Independent technical criteria for storage systems are difficult to establish, since they are usually case specific and are closely related to and generally affected by the economics of the resultant systems. Nevertheless, certain technical criteria are desirable, although appropriate trade-offs must be made with such other criteria as

- storage capacity,
- lifetime,
- size,
- cost,
- resources use,
- efficiency,
- commercial viability,
- safety,
- installation, and
- environmental standards.

Before proceeding with a project, a TES designer should possess or obtain technical information on TES such as the types of storage appropriate for the application, the amount of storage required, the effect of storage on system performance, reliability and cost, and the storage systems or designs available.

TES is difficult to employ at sites that have severe space restrictions. Also, TES tanks often have significant first capital costs. Financial analysis for TES-based projects can be complex, although most consulting energy engineers are now capable of performing financial calculations and evaluating TES benefits.

#### **Environmental Criteria for TES**

The basic design, materials, and operational practices that are used for TES should preferably not overly impair public health or the natural ecology and environment. Materials should not be used that are toxic or dangerous if released, or that could adversely affect the environment during the manufacture, distribution, installation, or operation of the storage system.



### **Economic Criteria for TES**

The economic justification for storage systems normally requires that the annualized capital and operating costs for TES be less than those required for primary generating equipment supplying the same service loads and periods. In general, TES systems accrue fuel cost savings relative to primary generating equipment, but often at the expense of higher initial capital costs.

The key performance characteristics involved in the evaluation of the cost effectiveness of TES include

- hourly thermal loads for the peak day;
- the electrical load profile of the base-case system against which TES is being compared; and
- the size of the storage system and the control methods used.

Economic information that is needed includes

- electricity demand charges and time-of-use costs;
- the costs of the storage; and
- financial incentives available.

Economic evaluation and comparison parameters often determined include the simple payback period. Other methods are also used to compare the annualized investment cost of a TES with annual electricity cost savings.

### **Energy Savings Criteria for TES**

The past few years have seen a significant shift in understanding about the economics and environmental impact of TES. Today, well-designed TES systems can in some cases reduce the first costs on some projects. Moreover, they can reduce the amount of electricity that a facility uses, not just the amount it pays. Many project engineers now find that TES technology can significantly reduce energy use and demand, which translates into lower operating costs.

In addition, TES provides environmental advantages by using electricity produced at night, when utilities are generally operating their most efficient plants. As a result, significant savings of “source energy” (coal, natural gas, oil, or nuclear fuel) accrue to electric utilities and reduce pollutant emissions.

Air-conditioning typically accounts for a large portion of a building’s energy use. One or more chillers are usually used to match the cooling load, which rises during the day and peaks in mid-afternoon. With TES, peak electric use can be reduced, so that smaller chillers can handle the load. In addition, air-cooled equipment can take advantage of lower night-time ambient temperatures to increase operating efficiency. Also, since water from TES systems may be colder than conventional chilled water, smaller pipes, pumps, and air handlers may be integrated into the building design.

Stored cooling capacity can be used alone to meet the entire cooling load (so chillers remain off during the day) or to supplement chillers by satisfying part of the load.

Perhaps the greatest shift in thinking about the potential uses of TES comes from the growing use of cold-air distribution. Cold-air distribution typically requires 30% less cold air than conventional cooling systems for a similar load, resulting in smaller fans, ducts, and risers. The related cost savings often offset the first-cost premium of TES.

The ability of cool storage to shift large amounts of peak electric demand to off-peak periods usually leads to the greatest interest in TES. When combined with cold-air distribution, TES systems can yield significant cost savings and improve a building’s energy efficiency and comfort level. Yet, building owners often hesitate to use TES, erroneously believing that installing it is expensive. TES paired with cold-air distribution offers a more efficient, and often more cost-effective, cooling option, which is competitive with conventional technology and which offers promising payback

periods. By integrating TES with cold-air distribution during the design and construction of office and other buildings, building owners add floor space for useful purposes or rental. This space becomes available because such systems require smaller air-handling units and often do not need a mechanical room.

Careful designing of a TES often yields first-cost savings by permitting the use of

- smaller air-handling units,
- smaller ducts, and
- smaller variable air volume (VAV) boxes.

Cold-air distribution can increase the capacity of existing air-conditioning systems or be used to replace older chillers. In general, existing fans and ductwork can be used, although in some cases more duct insulation and upgraded diffusers or mixing boxes may be needed.

Fan energy usage in cold-air distribution is typically reduced by 30–40%. Actual long-term energy-cost savings can often be even greater because compressor energy consumption is shifted to less expensive, off-peak hours. Research by the Electric Power Research Institute (EPRI) in the United States indicates that overall heating, ventilating and air conditioning (HVAC) operating costs can be lowered by 20–60% by combining TES with cold-air distribution. In such combined systems, conditioned spaces are maintained at 35–45% relative humidity, as compared to the 50–60% relative humidity often found with conventional systems. At lower humidity, occupants perceive improved air quality. In humid climates, the cooling energy requirement may increase slightly, but this is often offset by the inherent efficiencies of cold-air distribution.

### Sizing Criteria for TES

A need exists for improved TES-sizing techniques as analyses of projects reveal both undersized and oversized systems. Undersizing can result in poor levels of indoor comfort, while oversizing results not only in higher than necessary initial costs, but also in the potential wasting of electricity if more energy is stored than is required. Another requirement for successful TES that affects sizing is proper installation and control. Using state-of-the-art equipment, properly designed and controlled storage systems often do not use more energy than conventional heating and cooling equipments.

Performance data describing the use of TES for heating and cooling by shifting peak loads to off-peak periods are limited, although the potential for such technologies is substantial. The initial costs of such systems can be lower than those for other systems. To yield the benefits, new construction techniques are required together with the use of more sophisticated thermal-design calculations that are, as yet, unfamiliar to many designers.

The costs of TES systems for heating range from US\$ 20 to US\$ 60/kWh in Canada. A major development over the last decade or so has been improved controls. Modern storage systems can shift nearly all of the space-heating energy use to off-peak hours, whereas, with conventional systems, only about 50% of the energy for heating is consumed during off-peak periods. Off-peak periods typically last for more than 7 h (CADET, 1997).

Energy use for conventional heating systems tends to be less than that for storage heaters for rooms but greater than that for central brick- and water-storage systems. Base-case heating systems vary greatly and include direct electric-resistance baseboard heating, heat pumps, and electric central furnaces. Detailed comparisons of energy use for TES and base-case systems are often complicated by variations in other parameters such as the age and thermal integrity of buildings and homes.

The use of off-peak storage for heating in commercial buildings is growing as manufacturers produce more sophisticated storage equipment that is suited to larger buildings. Sizing of systems can, however, be difficult because of the more complex energy considerations and variable occupancy patterns for such buildings. Developments in energy control systems are enabling building operators to control HVAC and lighting systems more effectively. These improvements, in turn,

allow better integration of thermal energy storage with other energy systems. The payback periods for such systems often range from one to ten years, depending on the capacity and application.

TES systems for cooling capacity have been most successful in larger buildings, although research is underway on the development of smaller units. Unlike heat storage, part of the cost of cold storage can be paid for through savings derived from the installation of a smaller chiller than would be required for a conventional cooling system. Costs for cold TES often range from about US\$ 15 to US\$ 50/kWh, and many designers claim that initial costs for cold storage systems are below those for conventional cooling (CADDET, 1997). Cold TES systems for most buildings use ice or chilled-water on floor mass as the storage medium. The systems may include full, partial, and demand-side storage. Payback periods for some systems, based on measured data and/or estimates, vary from less than one year to 15 years.

### Feasibility Criteria for TES

A variety of factors are known to dramatically influence the selection, implementation, and operation of a TES system. Therefore, it is necessary to carry out a comprehensive feasibility assessment that takes into consideration all parameters that impact on the cost and the benefits of the TES systems considered. However, it is not always possible to follow all steps in a feasibility study for an application and, in such instances, as many items should be considered and studied as possible. In such TES feasibility studies, a checklist can be helpful in ensuring that significant issues related to the project are addressed and details regarding the evaluation, selection, implementation, and operation of the system are assessed correctly. Figure 3.2 provides a checklist that can be beneficial to the TES industry and analysts involved in TES projects. A checklist completed in the preliminary stages of the project guides the technical staff.

### Integration Criteria for TES

When considering the integration of TES into an existing thermal facility, an additional checklist (Figure 3.3) can assist in conducting the feasibility study for the TES system and its incorporation into the facility. For a facility under design, the information required is generally the same as in Figure 3.3, except that the database must be developed or estimated since there is lack of actual operating data.

### Storage Duration Criteria for TES

In practice, it is useful to characterize different types of TES depending on the storage duration: short-, medium- or long-term.

Short-term storage is used to address peak power loads lasting a few hours to a day in order to reduce the sizing of systems and/or to take advantage of energy-tariff daily structures. Short-term is often called *diurnal storage*.

Medium- or long-term storage is recommended when waste heat or seasonal energy loads can be transferred with a delay of a few weeks to several months. Long-term storages that take advantage of seasonal climatic variations are often referred to as *annual or seasonal storage*.

TES can be separated into high- and low-temperature systems, where low-temperature TES is the storage where heat enters and leaves at temperatures below approximately 120°C. The storage of cold or cooling capacity is also considered within this category. Low-temperature storage often permits efficient utilization of heat that otherwise would have been partially or entirely wasted. Low-temperature TES also permits the storage of heat obtained from solar radiation from day to night or from summer to winter, and permits the storage of heat from central power plants, from times of low-demand to hours of high-demand on both diurnal and seasonal bases.

TES also permits the storage of cold for air-conditioning purposes, from night to day and from winter to summer. On a diurnal basis, the storage energy efficiency can exceed 90%, while on a

<b>Checklist for evaluating a general TES project</b>	
Please tick (√) items which are available or known.	
( )	1. Management objectives
( )	2. Economic objectives
( )	3. Financial parameters of the project
( )	4. Available utility incentives
( )	5. Status of TES system (a) New ( ) (b) Existing ( )
( )	6. Net heating or cooling storage capacity
( )	7. Utility rates and associated energy charges
( )	8. Loading type of TES system (a) Full ( ) (b) Partial ( )
( )	9. Best possible TES system options
( )	10. Anticipated operating strategies for each TES system option
( )	11. Space availability for TES system (e.g. tank)
( )	12. Type of TES system (a) Open ( ) (b) Closed ( )
( )	13. General implementation logistics of TES system under consideration
( )	13.1. Status of TES system
( )	13.2. TES system location
( )	13.3. Structural impact
( )	13.4. Heat exchanger requirements
( )	13.5. Piping arrangement
( )	13.6. Automatic control requirements
( )	13.7. New electrical service requirements
( )	13.8. Others
Signature:	
Project Leader:	
Date:	
Project Title and Number:	

**Figure 3.2** Checklist for evaluating a TES project

seasonal basis it usually is not much above 70%. Low-temperature TES has wide applicability in domestic hot-water systems.

Another kind of diurnal TES is the use of electric heaters that produce heat at night using low-cost electricity and store the thermal energy in the mass of bricks.

Table 3.1 provides information on diurnal and seasonal TES techniques for small- and large-scale applications. Diurnal storage equipment often reduces HVAC costs or avoids the need for backup heating or cooling equipment. Diurnal storage is increasingly used as a demand-side management technology (especially with cold storage in air-conditioned buildings). Wider use of air-conditioning in buildings combined with a need to reduce peak energy demands is motivating TES development.

Nonenergy regulations are rather neutral toward TES, although large-scale seasonal storage is subject to a large number of codes and standards that may conflict with plans of building managers. For short-term storage, safety (e.g., related to PCM handling), or hygiene regulations may to a

<b>Checklist for integrating TES into an existing thermal facility</b>	
Please tick (√) items which are available or known.	
<b>Database</b>	
( )	1. Utility's maximum incentive
( )	2. Facility occupancy hours
( )	3. Facility operating requirements
( )	4. Existing physical constraints
( )	5. Facility peak-day load and monthly average requirements
( )	6. Historic energy consumption rates
<b>Analysis</b>	
( )	1. Best possible TES system options
( )	2. General implementation logistics of each TES system under consideration
( )	3. Plant's yearly energy consumption with or without a TES system
( )	4. Size utilization factor for TES
( )	5. Projected operating cost reduction for each TES system under consideration
<b>Conclusion</b>	
( )	1. Financial analysis
( )	2. System implementation recommendation
( )	3. Others
Signature:	
Project Leader:	
Date:	
Project Title and Number:	

**Figure 3.3** Checklist for integrating TES into an existing thermal facility

**Table 3.1** Storage durations for small- and large-scale applications

	Small-scale/decentralized storage		Large-scale/centralized storage	
	New	Existing	New	Existing
Diurnal latent TES (e.g., salt hydrates)	++	++	-	-
Diurnal sensible TES	++	+	-	++
Seasonal latent TES	-	-	-	-
Seasonal sensible TES (e.g., aquifers, rocks)	+++	-	+++	+

+++ , high probability; ++ , medium probability; + , low probability.

certain extent hinder the development of TES markets. Insurance companies are often reluctant to support the incorporation of products or equipments that have not received appropriate certification, as is often the case with innovative devices.

### 3.3.4 TES Market Considerations

Since TES is an energy efficiency option that complements other energy conservation strategies, government support could enhance the development of such technologies. At present, TES products or equipments do not contribute significantly to international trade. A good level of knowledge of TES exists in developed countries. The main area where trade could grow is ice storage, which is already widely marketed in the United States.

Widespread implementation of large seasonal storage appears unlikely in the near future. In France and other southern European countries, large-scale TES applications will likely remain limited in part, because there are few district-heating (or cooling) networks. TES can be a valuable complement to such networks. Table 3.2 compares TES application potential in France and the United States. In practice, large-scale TES will face implementation challenges similar to those for district heating, due to its complementary nature. Another challenge for TES technology is the absence of an industry support group that can extol the benefits of TES, promote its use, and provide information. Such support groups are common and important in other sectors.

#### Barriers to TES Adoption

Although TES technology is proven and economically viable, it is sometimes not readily accepted. Barriers to TES adoption can be categorized into several types:

- lack of proper information;
- lack of commercial options;
- high initial cost; and
- infrastructure constraints.

The first of these barriers can be overcome with appropriate information dissemination and related activities (on-site visits, publication of independent monitoring results, etc.). High initial costs as a barrier can only be overcome by establishing reimbursable funds dedicated to large-project investments. In the near term, TES developments are not likely to significantly reduce TES initial costs. For example, the European community could arrange with banks a third-party financing scheme for TES investment. Infrastructure constraints, such as the types of buildings and energy infrastructures largely in place, seem to be the most difficult to overcome, because they are linked to wider policy considerations, especially in the case of large-scale TES. For short-term TES, support of renewable energy technologies in the building sector and of passive solar design can help overcome this barrier.

**Table 3.2** Comparison of potential TES implementation in France and the United States

Country	Market area	Predicted maximum potential deployment by 2010	Units in which deployment is measured
France	Seasonal storage	25–30	Number of sites
	Diurnal storage	500,000	Number of dwellings
United States	Diurnal storage	50	GW

Source: (Anon, 1990; Piette, 1990).

Other barriers that hinder greater use of TES can be summarized as follows:

- decision makers often do not think about using TES, with the possible exception of ice storage in air-conditioned buildings;
- long-term (seasonal) TES is perceived to be high risk;
- demonstration of economic long-term TES systems of local interest is lacking (e.g., in the immediate future emphasis is likely to be on aquifer and borehole storage);
- short-term TES using PCMs is not fully developed, and safety and hygiene concerns exist for PCMs; and
- insurance companies are not enthusiastic about systems using innovative products like TES that have not yet received certification, and obtaining certification is expensive.

To overcome these barriers, priority should be given to the following:

- developing appropriate information packages on commercially developed TES systems aimed at those with no previous knowledge of storage systems;
- carrying out technical development to improve performance and reduce costs;
- focusing in the short term on technologies for which local experience has been gained and keeping systems as simple as possible;
- providing training on these systems for designers, operators, and builders;
- providing risk capital for construction of systems close to commercialization; and
- carrying out research and development on financially promising TES systems, including PCMs suitable for use in the building industry, and innovative systems suitable for solar applications.

### **Maturity of TES**

A large amount of TES technology has reached a level of maturity and begun to establish markets. PCMs are still undergoing research and development, but they, nevertheless, have been demonstrated and are commercially available. Thus, TES is mature and its lack of dissemination mostly relates to barriers other than technical (e.g., financial). For large-scale seasonal storage, cost reductions can likely be obtained (e.g., by improving excavating techniques and large-store construction methods). Demonstrations are needed of the use of PCMs in diurnal applications, especially by integrating them into building components (ceiling, tiles, wallboards, shutters, etc.). A comparison of TES system characteristics for diurnal applications is given in Table 3.3.

### **Market Position of TES**

TES applications are at various states of development, depending on the country considered. Diurnal heat storage has not taken on a large market share in any country, with the exception of cold storage in air-conditioned buildings for demand-side management purposes (mostly in the United States, Canada, and Japan, and in some commercial premises in Europe and pilot-project “zero energy” houses in Finland). Diurnal cool storage in the United States has allowed about 15 GW of cooling power to be shifted to off-peak periods. Seasonal storage has been investigated and tested in the 1980s, and the main sites are located in northern European countries (especially Sweden) and are associated with district-heating networks. Seasonal storage in aquifers is well developed in China.

Large-seasonal TES facilities have been installed either to complement solar collection systems in large-scale building projects or in association with district-heating plants. Long-term seasonal TES development is thus linked to the market status of these technologies.

Individual houses or commercial (including office) buildings can use diurnal TES for either heating or cooling applications. Demonstration projects and information dissemination are, nevertheless, needed to increase building managers’ awareness of these options. The needs of passive, hybrid,

**Table 3.3** Thermal and technical data for selected TES techniques

Thermal and technical data	Concrete or steel tank	Basin with total insulation	Basin with top insulation	Rock cavern	Aquifer	Earth bed	Vertical tubes in clay	Drilled wells
Specific thermal capacity (kWh/m <sup>3</sup> K)	1.16	1.16	1.16	1.16	0.75	0.70	0.80	0.63
Reference $\Delta T$ (°C)	55	55	55	55	55	55	15	55
Typical storage efficiency	0.90	0.85	0.70	0.80	0.75	0.60	0.70	0.70
Conversion factor (kWh/m <sup>3</sup> )	57	54	45	51	31	23	8	24
Size range (m <sup>3</sup> )	0–100,000	0–75,000	0–50,000	50,000–300,000	50,000–500,000	0–100,000	50,000–300,000	50,000–400,000
Investment cost (ECU <sup>a</sup> /m <sup>3</sup> )	150–250	120–220	40–60	80–120	20	50–100	5–8	30–40
Cost of energy supplied by TES (ECU/kWh)	0.2–0.4	0.15–0.25	0.05–0.1	0.12–0.20	<0.05	0.16–0.40	0.05	0.09–0.12

<sup>a</sup>1 ECU was approximately 0.85 US\$ in 1990.

Source: (Anon, (1990); Piette, 1990).



and other low-energy cooling techniques for some type of short-term cold TES should foster the development of this kind of TES.

Market demands for TES are linked to general energy policy. For example, increased support for and use of renewable energy would lead to large efforts to inform designers of active solar technologies and others of the possibilities offered by TES.

Relatively high risks are perceived as existing for seasonal TES (especially when used with an aquifer). Possible technical difficulties with pumps and exhaust water systems (clogged pump strainers, choked filters) can lead to performance and safety problems, which in turn can induce higher initial costs.

Ice storage is an exception to these concerns as many systems have been implemented and have demonstrated a high cost effectiveness. When economic evaluations of TES are based on current energy-price structures, risks are associated with modified price structures. Widely disseminated information on successful operations can help reduce the perceived risks. Transfer and exchange of knowledge internationally through detailed specifications can limit the risks of projects that have been encountered in the past, and thus foster the development of TES.

Environmental legislation that directly controls the development of TES does not exist, but growing concern for the water quality in aquifers and the use of various PCMs has caused some TES technologies to be scrutinized and hindered decision makers from adopting them. Governments are also concerned about ensuring that appropriate regulations are in place to ensure that TES implementations do not cause environmental problems.

Financial factors affect TES marketability. For example, access to funds or the ability to raise funds at reasonable interest rates may hinder potential investors. Access to funds does not constitute a major barrier for TES technology, but the projected payback periods are often not appealing to many decision makers in the building sector. Sometimes, a financial consortium is needed for large TES facilities. Such consortia may include local authorities, which may or may not have access to funds, and energy utilities, which can usually obtain necessary funding.

Long-term TES systems with large storage capacities (>1000 MWh) have been in use since the 1980s. The storage medium is generally water or rocks, and the “container” is often aquifers, rock caverns, and underground boreholes. The main markets for long-term (seasonal) TES have been located in northern European countries, particularly Sweden, where it is used in association with large-scale district-heating schemes.

Short-term cool storage for air-conditioning has been found to be cost effective in applications in the United States and Canada; Japan and Europe have also used these systems. PCMs are not yet fully developed for the building sector, although they have been used for certain industrial applications.

In the future, TES appears to be able to help reduce the amount of heating and cooling systems by 50–70%, which in turn can yield energy savings because of better efficiency of systems working near to reference values. But TES losses can curtail some of the savings potential, lowering the energy conservation potential of TES to approximately 5–10%.

### *3.3.5 TES Heating and Cooling Applications*

The use of TES systems for thermal applications such as heating and cooling has recently received much attention. In various energy sectors, the potential benefits of TES for heating and cooling applications have been fully realized. In the following two subsections, we describe heating TES and cooling TES in detail.

#### **Heating TES**

Electricity, natural gas, propane, or fuel oils can produce space heating. Heating TES using electricity operates resistance heaters at night when electricity rates are low to produce heating

capacity for use during the day. Electric-resistance efficiencies (near 100% on an energy basis) combined with lower off-peak electric rates can produce heating at a fraction of the cost of conventional systems. Heat produced by electrical resistance heaters at night is stored in such storage media as earth materials or ceramic bricks in insulated containers. The production of heat at night takes advantage of electric off-peak rates, which are generally 33–75% less expensive than peak rates. When heat demand rises (e.g., for space heating), heat is recovered from the storage unit and transferred into the room.

The use of earth as a TES medium is usually restricted to new construction, since the application requires that electric resistance grids be placed 0.5 to 1 m in the ground, beneath a structure. The need to place the grids under a building makes retrofit work extremely difficult for any facility without a basement or crawlspace. For new construction applications, approximately 2 m of earth directly below the structure is used for storage of heat produced by the grid. A rigid and waterproof insulating material is placed vertically around the perimeter of the building and extends approximately four feet below the earth grade level. The insulation ensures that heat stored in the ground is radiated mainly into the structure and not into the surrounding earth. The electric resistance grid is covered with about two inches of sand and earth materials.

Ceramic bricks provide an excellent heat storage medium for retrofit as well as new construction applications because of their modular sizes, ease of installation, and high heat-retention abilities. These units are normally manufactured in various sizes and transported to building sites. The construction of this type of TES normally consists of an insulated box, about the size of a conventional radiant hot water or steam heating unit, filled with ceramic bricks. The number of bricks in a module depends on the heat storage requirement. The unit also includes a small fan. The ceramic bricks contain electric resistance strip heaters in their holes. During charging, the strip heating units produce heat, which is absorbed by the ceramic bricks. The insulation surrounding the bricks restricts heat losses from them. During the day, a conventional thermostat is used to control the fractional horsepower fan that circulates air from the room across the ceramic bricks to recover the stored heat and transports it into the room. The thermostat controller shuts the circulating fan when the room temperature is acceptable.

Heating TES systems can be justified economically for most facilities which have significant space heating needs and are billed under time-of-use electric rate schedules that have large differentials between peak and off-peak electric consumption.

## Cooling TES

Cooling TES can reduce cooling energy costs while maintaining a comfortable environment. Summer air-conditioning bills have two components: an electric demand charge and an electric usage charge. The usage and demand charges are often further divided into peak and off-peak periods. The peak operating period of electric air-conditioning systems normally occurs during the high-cost demand and usage periods (i.e., the summer afternoon). TES systems are designed to shift the peak operating period of electric air-conditioning systems to the less expensive night periods.

Air-conditioning systems cool by removing heat via a chilled-water network or directly from an air stream. Most air-conditioning systems produce a cooling effect precisely when cooling is needed in a building or room. Cool TES-based air-conditioning systems operate similarly, but remove heat from an intermediate substance when the building does not need cooling, producing a cool reservoir that is stored until there is a need for cooling. The intermediate substance is normally water, ice, or eutectic salt solutions.

The most popular thermal storage medium is ice. The conversion of 1 kg of water to ice at 0°C requires the removal of 152 kJ of heat. Similarly, adding 152 kJ of heat to the ice causes water at 0°C to be formed. Ice TES operates in this fashion. At night, heat is removed from water to produce ice (i.e., charging of the storage occurs). During the day when the building requires cooling, heat is removed from the building and added to the ice (i.e., discharge occurs). The melted ice is reused during the next charging period. The advantage of this cooling scheme is that

the main electrically driven device in cooling systems, namely, the compressor motor, is operated during low-electrical cost periods.

The previous example illustrates one design possibility. In another common design, the compression system operates for the whole day to provide stored cooling at night and to partially meet the cooling load during the day. This design usually requires the least investment.

Many cooling TES systems use chilled-water systems to transfer the cooling capacity from the storage to the building air-distribution system. Although chilled-water distribution systems are usually confined to large buildings with conventional air-conditioning, chilled water distribution systems with TES are now being designed for smaller buildings.

Cooling TES systems are generally advantageous for a new facility that has large daytime cooling loads and little or no cooling load at night. For retrofit situations, cooling TES is usually difficult to justify unless the cooling system is being replaced because of old age or inadequate capacity.

TES can be a beneficial component of the refrigeration-based cooling technologies. TES can significantly reduce the size of a refrigeration system and its electrical use during peak demand periods. TES is typically employed at power plants that mainly meet peak loads or that have significantly differing revenue structures for off-peak versus peak power.

For example, if a peaking gas turbine operates only 4 h per day, it usually does not make much sense to build a refrigeration plant that also operates at full load for only 4 h per day. This is because cooling capacity, unlike electricity, can be easily stored. It is usually more sensible to size the refrigeration system to meet about 20% of the peak cooling load and, slowly, to make and store cooling capacity during other periods so that it can be discharged during peak conditions.

### **TES and Gas Cooling**

An alternative to cold TES is the use of gas engine-driven chillers or gas-fired absorption chillers for peak cooling loads. The higher first cost of these refrigeration systems is comparable to the high capital costs of TES tanks and infrastructure. The high-electrical load of a standard vapor-compression refrigeration system is displaced by either of these gas-cooling alternatives. A gas-engine chiller is often advantageous for a site that has limited operating hours per day per year. A gas-fired absorption chiller can make sense for sites that have longer operating hours.

An additional benefit of TES and gas-cooling technologies is that they permit changes to a site's electrical infrastructure to be minimized. One challenge to back-fitting electric vapor-compression systems to most sites is the placement and connection of a large transformer for the new electrical loads. With TES and gas-cooling technologies, the electrical load of the new equipment is significantly reduced, and there may be sufficient capacity in the plant's existing control centers for the smaller loads.

During the past decade there has been increasing interest in gas cooling with TES in power generation industries, and cold TES and gas-cooling technologies are both expected to take more prominent roles in advanced cooling projects in the future.

A combustion-turbine inlet-air cooling system, with and without storage, is shown in Figure 3.4. The main components are the chiller, the cooling tower, the air coil, and interconnecting piping. Cold fluid from the chiller is pumped through the air coil, where the coolant is heated and returned to the chiller, while the inlet air is cooled prior to entering the compressor. The cooling tower provides cooling water to the chiller condenser. Alternatively, an evaporative condenser can be used with some types of chillers. Including storage and its associated piping loop increases the number of system components, but allows the chiller and cooling tower components to be downsized, assuming that cooling is not conducted for the whole day. Storage also significantly reduces peak power consumption for electrically driven chiller systems.

The fundamental benefit of inlet-air cooling is that it can increase the efficiency of the gas turbine system (see Figure 3.4). However, the technique entails additional costs. The main cost is for the purchase and periodic maintenance of the inlet-air cooling system hardware. The energy used to drive the chiller also results in a significant expense, although the cost varies significantly

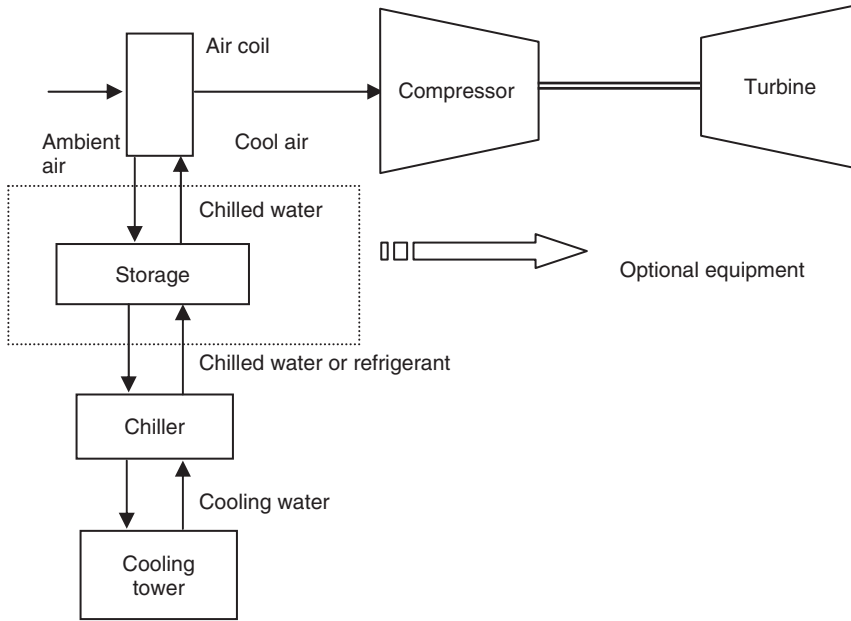


**Figure 3.4** Generic inlet-air cooling system. (The cold storage inside the dotted line is optional.) (Adopted from Brown *et al.*, 1996)

depending on whether the chiller is thermally or electrically driven and the source of the thermal or electric energy. Inclusion of an air-cooling coil within the inlet duct to the compressor causes an additional pressure loss, with negative consequences to gas-turbine power output and efficiency, but the impacts are generally less than 0.5% (Brown *et al.*, 1996).

A common alternative to the inlet-air cooling system in Figure 3.4 is evaporative cooling. Direct-contact evaporative cooling, accomplished by passing the inlet air through a wet media can be particularly effective in drier climates. Analyses of inlet-air cooling normally consider evaporative cooling as an option. Note that evaporative and refrigeration-based approaches should be considered independently. Direct evaporative cooling followed by refrigerative cooling does not reduce the refrigeration cooling load. Rather, it substitutes latent load for sensible load.

Incorporating storage into an inlet-air cooling system is desirable for downsizing the chiller and heat-rejection components and significantly reducing peak electricity consumption for electrically driven systems. The chiller is usually the most expensive component of such systems; so, reducing its size and cost at the expense of adding storage and related piping can be cost effective. Reducing peak electricity consumption is important because increasing peak power output is usually the primary objective of combustion-turbine inlet-air cooling. Chilled water and ice are the preferred storage media for inlet-air cooling systems. Both are applicable to diurnal storage, and ice storage is also applicable to weekly storage cycles. Seasonal storage of ice via engineered ice or snow ponds or of chilled water in naturally occurring aquifers is also possible for inlet-air cooling, but these concepts suffer from site-specific limitations, and have had only limited successful applications. Eutectic salts are another storage medium possibility, but the salts are more expensive than water, suffer availability losses on charge and discharge, and also suffer from limited application experience. Steel or concrete cylindrical tanks can be used for water or ice storage. External insulation is usually sufficiently thick to avoid condensation. Chilled water is normally added and removed from the bottom of water storage tanks, while warm water is added or removed from the top, so as to form a thermally stratified tank. The preferred ice-making method uses a harvesting approach that

periodically passes hot refrigerant from the compressor through the evaporator to release ice from the evaporator surface. The ice falls from the evaporator and makes a pile within the tank. Several evaporators are used to aid in distributing the ice. An alternative approach is to build up logs of ice around evaporator coils that run back and forth throughout the tank. Although its defrost cycle increases the effective cooling load by about 15%, the ice harvester is less costly to build because it requires much less evaporator surface and refrigerant inventory.

Selection of the storage media for inlet-air cooling depends partly on the chiller type. Lithium-bromide absorption chillers can only use water storage. Either water or ice storage is possible for vapor-compression chillers. The principal advantage of ice is its greater cold storage density, and the advantage of water is the mechanical simplicity of the storage system. Ice storage generally allows the inlet air to be cooled to a lower temperature than that of water storage, but ice generation requires a lower chiller evaporator temperature, which results in poorer chiller efficiency and higher chiller cost.

### 3.3.6 TES Operating Characteristics

A major factor in determining the feasibility of TES is the shape of the daily electrical load curve for a utility and its impact on the availability of energy for charging a TES. For example, an urban utility with a summer peak demand may have a peak of moderate duration during the day and a much reduced load for a short duration at night. Thus, the storage device may be required to supply energy for 10 h during the day, while significant charging capacity is only available for 6 h at night. Such a storage device would either have to be charged at a faster rate than it is discharged, or operate on a weekly cycle with part of the charge taking place over the weekend.

The diverse operating conditions for different utilities cause substantial variations in the duty cycles of TES systems. Table 3.4 summarizes the typical range of cycle characteristics for different applications. The values assume a storage efficiency of 75%.

#### Diurnal versus Seasonal TES

The primary characteristic of a seasonal storage system is the very large capacity that is required (in the order of a hundred times the capacity of a daily storage). Thermal losses become very important for such long-term storage. More care is, therefore, taken to prevent thermal losses in a seasonal system than in a system for daily storage. While diurnal systems can generally be installed within a building, seasonal storage requires such large storage volumes that separate, or requires frequent additional locations.

**Table 3.4** Sample TES cycle characteristics

Duty-cycle characteristic	Type of operation			
	Peaking duty		Regular duty	
	Daily cycle	Weekly cycle	Daily cycle	Weekly cycle
Discharge time (h/day)	2–8	2–8	9–14	9–14
Charge time (h/day)				
Weekday	5–9	5–9	5–9	5–9
Weekend	–	14–34	–	14–34
Charge/discharge ratio	0.8–2.1	0.1–2.1	1.3–3.7	0.8–2.4
Storage period (h)	2–8	4–26	9–14	17–47
Annual operating time (h) (discharge time)	350–1600	350–1600	2300–3600	2300–3600

Source: Dinter *et al.* (1991).

The capital costs associated with the size and insulation necessary for seasonal storage systems have generally kept them from becoming economical. New technologies, increased energy costs, and the general desire to conserve scarce energy sources may warrant a review of seasonal storage systems. However, diurnal and other short-term storage will probably find broader application, and in many instances will have greater impact in a country at any given time.

### **Individual versus Aggregate TES Systems**

A size relationship similar to that for diurnal/seasonal applications results from the consideration of individual versus aggregate use of TES systems. When individual units are aggregated into a system large enough for buildings, the total storage volume becomes the sum of the volumes of the individual units. With a larger volume, the lower surface–volume ratio of the aggregate unit reduces the thermal losses for identical storage periods.

Lower unit-storage costs also generally result as size is increased by the aggregation of individual systems. Depending on building and load density, however, thermal transmission costs and losses can eliminate any savings arising from aggregation. Control can be more difficult when a single aggregate storage system is used for several buildings. If individual accounts are maintained, cost billings can be difficult as allocation of energy costs in an aggregated situation requires a fair and inexpensive way of prorating thermal energy consumption.

Preferences for individual or aggregate systems depend on the circumstances of each particular case. For applications characterized by small loads, building ownership, and a wide diversity in consumption patterns, such as single family residences, aggregate systems are unlikely to be favored.

### **3.3.7 ASHRAE TES Standards**

The American Society of Heating, Refrigerating and Air-conditioning Engineers (ASHRAE) provides testing standards for TES systems. ASHRAE TES standard 943 is called the “Method of Testing Active Sensible TES Devices Based on Thermal Performance.” This sensible TES standard (ASHRAE, 2000) is the second half of a revision of ASHRAE’s first TES standard, 94-77, “Methods of Testing Thermal Storage Devices Based on Thermal Performance.” The first half was issued as ANSI/ASHRAE 94.1-1985, “Method of Testing Active Latent Heat Storage Devices Based on Thermal Performance.” Sensible TES usually applies to heat storage in water or rocks or cool storage in chilled water. This standard was prepared by a group of volunteers representing users, design engineers, manufacturers, scientists, and the US federal government. Research sponsored by the US Department of Energy and the Electric Power Research Institute in solar and off-peak energy programs at government laboratories and universities has assisted TES standards development. The major change in the new standards is to provide wider freedom to the supplier of the test device in the choice of cycling time, capacity, maximum flow rate, and temperature range. Another important revision is in making the stand-by heat loss test more practical and accurate.

Since storage is usually part of a system, total performance depends on more than just the performance of the storage component. However, the results of this test procedure are intended to provide stand-alone specification of the storage-components’ performance. The Standards Project Committee that developed these TES standards hopes they will be used by manufacturers and others.

## **3.4 Solar Energy and TES**

Solar energy is an important alternative energy source that will more likely be utilized in the future. One main factor that limits the application of solar energy is that it is a cyclic, time-dependent energy resource. Therefore, solar energy systems require energy storage to provide energy during



the night and overcast periods. Although the need for TES also exists for many other thermal applications, it is particularly notable for solar applications.

### 3.4.1 *TES Challenges for Solar Applications*

TES is important to the success of many intermittent energy sources in meeting demand. This problem is especially severe for solar energy, because it is usually needed most when solar availability is lowest, namely, in winter. TES complicates solar energy systems in two main ways. First, a TES subsystem must be large enough to permit the system to operate over periods of inadequate sunshine. The alternative is to have a backup energy supply, which adds a capital cost and provides a unit that remains idle. In the short run, solar energy can and probably needs to be integrated into systems that also use conventional energy sources, such as fossil fuels. In the long run, however, stand-alone solar energy systems may be desired.

The second major complication imposed by TES is that the primary collecting system must be sufficiently large to build the supply of stored energy during periods of adequate insolation. Thus, additional collecting area (and its additional capital cost) is needed. Examinations of typical sunshine records show that even in the desert, the periods of cloudy and clear weather are about equally spaced, a few days of one followed by a few days of the other. Partly cloudy days can greatly affect performance and make the difference between practical and impractical energy storage. If the total energy of a partly cloudy day can be collected, then the periods requiring energy storage are greatly reduced.

Concentrating solar systems must cope with the intermittent nature of direct sunlight on a cloudy day. Consequently, absorbers and boilers must be designed with care to avoid burn-out problems when the sun suddenly returns with full brilliance. Non-concentrating systems face the fundamental problem of trying to provide sufficiently high efficiency at medium temperatures to yield energy output at a reasonable cost. Thus, TES costs must be reasonable.

### 3.4.2 *TES Types and Solar Energy Systems*

In solar energy applications, TES can provide savings in systems involving either simultaneous heating and cooling, or heating and cooling at different times of the year. Most TES applications involve a diurnal storage cycle; however, weekly and seasonal storage is also used. Solar energy applications require storage of thermal energy for periods ranging from very short durations (e.g., buffer storage of minutes for solar thermal power plants) to annual cycle timescales. Most solar energy systems use diurnal storage, where energy is stored for at most a day or two. Diurnal storage offers a number of advantages, such as

- capital investments for storage and energy loss are usually low;
- devices are smaller and can easily be manufactured offsite; and
- sizing of daily storage for an application is not as critical as sizing for larger annual storages.

Seasonal storages do, nevertheless, have some advantages. Larger storages have lower heat losses because of their lower surfacetovolume ratios. The need for backup systems can be eliminated, since periods of adverse weather have little effect on the long-term thermal energy availability. Collector areas can consequently be reduced. Also, annual TES systems complement well-designed energy management systems in which excess heat or coolness from the environment or adjacent structures is saved for later use.

A TES designed primarily for the storage of solar energy is not necessarily restricted to that source. It may be used to store surplus energy from the power plants, usually in the form of waste

water, waste energy from air-conditioners or industrial processes, and so on. Such storage use may not be applicable for small houses, but could be useful for largescale central heating systems.

A variety of active and passive systems for storage have been developed for the effective utilization of solar energy. Passive systems, which do not need pumps are often suitable for smallscale domestic applications, and are widely used throughout Europe and the United States. The five main types of such passive systems are:

- direct heat gain,
- heat collection and storage,
- sun space,
- roof-top heat storage,
- thermosyphon.

Effective use of solar energy relies to such an extent on TES that solar systems without TES facilities are probably only utilizable in the most rudimentary applications. Some examples of solar thermal applications that do not need storage include solar grain driers, solar distillers, and solar kilns. In these systems the solar heat is used immediately as it becomes available. However, in solar space-heating applications the situation is different, because the solar system normally provides more heat than demanded by the building during the collection period. Storage is required to make such solar energy systems viable and attractive, in the long- or short-term.

### 3.4.3 Storage Durations and Solar Applications

Annual solar energy TES systems are designed to collect solar energy during the summer months and retain the heat in storage for use during the following winter. Although the technology exists to construct annual storage systems, and some have been demonstrated, it is challenging to make these systems cost effective. The main impediment is the lack of a cost-effective means to contain heat for long periods (e.g., three months). Ground-based TES has successfully been used in some jurisdictions. Economic breakthroughs in TES are of course possible, possibly via annual storage on a community-wide scale, which could reduce costs and dramatically improve the reliability of solar heating.

Short-term solar energy TES systems are designed to store heat for up to a few days. Although solar energy systems utilizing annual storage can contribute close to 100% of building heating needs, short-term TES systems rarely contribute in excess of 60%. Nevertheless, short-term solar energy TES systems can operate on a competitive basis with conventional fuels (Dincer *et al.*, 1997a, b).

Any solar energy system has some degree of TES, either deliberately provided as a device in which to store energy, or through the thermal inertia of the extensive system of collectors and heat-transfer fluid. TES is considered cost effective only for short periods (hours to days), which is generally not enough to carry a system through much winter weather. Making TES capacity large enough is normally economically prohibitive. One exception is the special case of saline solar ponds, which act as both solar collectors and TESs having weeks of storage capacity.

TES is often thought of in conjunction with solar energy, because the latter is often associated only with technologies that translate sunlight directly into thermal energy or electricity. Solar technology today includes a broad spectrum of concepts that differ greatly in their requirements for storage. Plant matter, or biomass, is ideally storable for long periods. Wind power is another form of indirectly derived solar energy that, even though is intermittent, is available more continuously through the day and night than direct sunlight in many regions. TES is often important for solar water heating, heating of buildings, and industrial heating processes.

A factor that may facilitate storage applications and the resolving of challenges is the movement of the energy economy toward greater coordination of energy supplies and demands. Although many people will not readily give up energy choices, the flexibility of use that occurred in the eras



of inexpensive energy may be changing. Time-of-day electric pricing, already introduced in some areas, is one example. The use of computer systems that automatically manage the energy load in large office buildings is another. Such changes occur gradually and tend to create a social climate in which solar energy is more acceptable.

Solar energy may also develop without storage in the future as there exist some configurations in which solar power sources can be integrated with energy systems, particularly electric systems, without bulk storage. Nevertheless, even with optimistic rates of growth, solar energy's contribution will remain relatively small in the near future. Thus, traditional energy systems can be used to compensate for the fluctuations in solar energy supply. Solar energy can also be used to match the fluctuating energy demand, particularly for electricity, without endangering the stability of electrical networks. Since large quantities of electric power are routinely transmitted through long distances, the electric network is particularly well-suited for smoothing and balancing solar-source power fluctuations. If solar-derived energy grows to too large a fraction of the total, the overall stability of an electric network might be adversely affected, but many studies indicate that this limitation is unlikely to be a problem until solar power penetration reaches 15–20%.

### 3.4.4 *Building Applications of TES and Solar Energy*

The ability to store thermal energy is important for effective use of solar energy in buildings. Today, much interest is focused on passive systems for space heating and active systems for water heating. For building heating, conventional passive TES materials include water, rocks, masonry, and concrete. To perform well, these storage materials must be massive because their allowable temperature swings are limited by comfort conditions that must be maintained inside the building.

With lightweight-building construction practices commonplace in the United States, a lightweight latent TES system which is easily installed in a building could be beneficial. One problem is the effective and economic containment of a PCM in its liquid phase. Tubes, rods, bottles, and canisters containing PCMs that melt in the room-temperature range have been studied with varying degrees of success; most have proved uneconomical. A more interesting approach is a wallboard containing a PCM. With the wallboard providing PCM containment as well as serving an architectural function, the economics are improved. Further, the large heat-transfer area of the wallboard supports large heat fluxes driven by small temperature differences.

Seasonal storage has been pilot-tested and used in a number of countries to store solar energy for providing winter space heating, in conjunction with district-heating systems. Sweden has implemented many such systems. A TES system examined by the University of Massachusetts at Amherst (Tomlinson and Kannberg, 1990) started using a long-term seasonal thermal storage of solar heat in a subsurface clay formation for heating a local athletic center. Use of seasonal storage can substantially reduce the cost of providing solar energy systems that can supply 100% of energy needs because of the reduced collector area required. In high latitudes, storage is virtually essential to provide a large percentage of heating from solar energy. The economics of scale favors relatively large systems.

Commercial buildings are now becoming more complex. Not only are architectural features such as atriums and skylights common, but sophisticated controls on HVAC equipment are being used in an attempt to provide superior comfort and lower energy costs. These situations make it difficult to determine the economic feasibility of TES systems and require computer simulation programs to model the complex systems, controls, and economic parameters of commercial buildings.

The storage system is the heart of a solar heating and cooling system. Storage evens out the extremes of temperature caused by the daily cycle of solar availability, permitting indoor temperatures to remain comfortable during the day while providing heat at night. The storage component of a solar energy system significantly affects the design and construction and therefore cost. The storage medium and the "reliability" required of a system determine the size of the storage and, to some degree, its location. Most storage systems are not sized to provide 100% of heating needs when sunshine is not available. Since solar unavailability and availability are difficult to predict

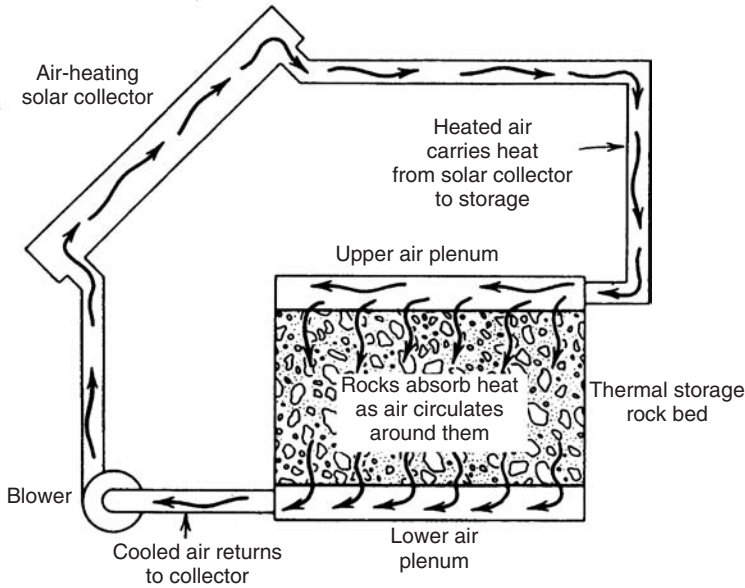


Figure 3.5 A solar rock-bed TES system (Harris *et al.*, 1985)

in most cases, 100% storage systems would be very large, but most of the capacity would remain unused most of the time. Being willing to tolerate some daily temperature swings can reduce the size of such TES.

All substances have a thermal capacity and ability to hold a certain amount of heat. Water can store large amounts of heat. Rock has about one-fifth the thermal capacity of water, but like brick and concrete, it is more dense. Rock, when used as a storage medium, is usually placed in an insulated bed under or attached to a building. Figure 3.5 illustrates a solar rock-bed TES system with air-heating collectors. As can be seen from the figure, the air from the collectors carries the absorbed solar heat to the rocks. As the heated air flows around the rocks, they absorb the heat, and the cooled air returns to the solar collectors to be heated again.

### 3.4.5 Design Considerations for Solar Energy-Based TES

The energy from solar collectors tends to be at low temperatures and requires a large storage mass when stored as sensible heat. Although the energy efficiency of solar collectors increases (and the collector cost probably decreases) as the temperature of the collector output reduces toward the space-conditioning comfort range of 20–25 °C, the overall mass and volume of the storage device increase further. For most locations, however, a space-conditioning system using solar energy needs to be supplemented by an electric- or fuel-powered auxiliary energy source. Thus, optimal and synergistic use of both energy sources via TES is important in designing building structures and TES systems.

A major question in the design of solar TES systems involves the quantity of solar energy to be stored. The storage system must be adequate to supply heat not only during the night, but also for several consecutive cloudy days if complete independence from external energy sources is desired. In many regions, winter periods without sunshine are so long that complete independence is not feasible. Furthermore, the solar-collector system, to achieve independence, must be sufficiently large to heat the structure even while storing more heat for the next sunless period. Days can span

less than 8 h during northern winters, and under such conditions, the costs of the combined collector and storage system may effectively limit the extent to which the solar system can economically supply the needed energy. If an alternate heating system with another energy source is needed as a backup for extended sunless periods, then solar energy use may be even further limited. However, if a storage system is economically justified, perhaps because it takes advantage of low off-peak electricity prices, then storage of solar energy in addition may enhance that benefit.

The energy from solar collectors need not be used directly in space-conditioning systems. One alternative and promising application is to use it as a heat source for a heat pump in a solar-augmented heat-pump system. For such uses, the solar-collector outlet temperatures can be lower than those achieved with direct heating, thereby increasing energy efficiency and probably reducing cost. In addition, having higher source temperatures available for the heat pump increases its coefficient of performance (COP) and reduces its electricity consumption. How the solar-augmented heat-pump system operates depends, in part, on the energy storage provisions. With minimum or no storage, the solar collector only improves the heat-pump efficiency during hours of sunlight. With greater storage, the solar input also provides a reservoir of higher source temperatures for heat-pump operations during sunless periods. If the overall system is designed to limit the heat-pump operation to off-peak hours, then a dual storage system is necessary (one system for the solar input storage and a second to store the heat-pump output energy for round-the-clock use in space conditioning).

### 3.5 TES Methods

TES can aid in the efficient use and provision of thermal energy whenever there is a mismatch between energy generation and use. Various subsets of TES processes have been investigated and developed for building heating and cooling, industrial applications, and utility and space power systems. The period of storage is an important factor. Diurnal storage systems have certain advantages: capital investment and energy losses are usually low, and units are smaller and can easily be manufactured offsite. The sizing of daily storage for each application is not nearly as critical as it is for larger annual storage. Annual storage, however, may become economic only in multidwelling or industrial park designs, and often requires expensive energy distribution systems and novel institutional arrangements related to ownership and financing. In solar TES applications, the optimum energy storage duration is usually the one which offers the final delivered energy at minimum cost when integrated with the collector field and backup into a final application.

Some of the media available for sensible and the latent TESs are classified in Table 3.5.

### 3.6 Sensible TES

In sensible TES, energy is stored by changing the temperature of a storage medium such as water, air, oil, rock beds, bricks, sand, or soil. The amount of energy input to TES by a sensible heat device

**Table 3.5** Available media for sensible and latent TES systems

Sensible		Latent
Short term	Long term (annual)	Short term
Rock beds	Rock beds	Inorganic materials
Earth beds	Earth beds	Organic materials
Water tanks	Large water tanks	Fatty acids
–	Aquifers	Aromatics
–	Solar ponds	–

is proportional to the difference between the storage final and initial temperatures, the mass of the storage medium, and its heat capacity. Each medium has its own advantages and disadvantages. For example, water has approximately twice the specific heat of rock and soil. The high heat capacity of water ( $\sim 4.2 \text{ kJ/kg}^\circ\text{C}$ ) often makes water tanks a logical choice for TES systems that operate in a temperature range needed for building heating or cooling. The relatively low heat capacity of rocks and ceramics ( $\sim 0.84 \text{ kJ/kg}^\circ\text{C}$ ) is somewhat offset by the large temperature changes possible with these materials, and their relatively high densities (Tomlinson and Kannberg, 1990).

Sensible TES consists of a storage medium, a container, and input/output devices. Containers must both retain the storage material and prevent losses of thermal energy. Thermal stratification, the existence of a thermal gradient across storage, is desirable. Maintaining stratification is much simpler in solid storage media than in fluids.

Sensible TES materials undergo no change in phase over the temperature range encountered in the storage process. The amount of heat stored in a mass of material can be expressed as

$$Q = mc_p \Delta T = \rho c_p V \Delta T$$

where  $c_p$  is the specific heat of the storage material,  $\Delta T$  is the temperature change,  $V$  is the volume of storage material, and  $\rho$  is the density of the material.

The ability to store sensible heat for a given material strongly depends on the value of the quantity  $\rho c_p$ . Water has a high value and is inexpensive but, being liquid, must be contained in a better quality container than a solid.

Some common TES materials and their properties are presented in Table 3.6. To be useful in TES applications, the material normally must be inexpensive and have a good thermal capacity. Another important parameter in sensible TES is the rate at which heat can be released and extracted. This characteristic is a function of thermal diffusivity. For this reason, iron shot is an excellent thermal storage medium, having both high heat capacity and high thermal conductance.

For high-temperature sensible TES (i.e., up to several hundred degrees Celsius), iron and iron oxide have thermal properties that are comparable to those of water per unit volume of storage. The cost is moderate for either pellets of the oxide or metal balls. Since iron and its oxide have similar thermal characteristics, the slow oxidation of the metal in a high-temperature liquid or air system would not degrade its performance.

**Table 3.6** Thermal capacities at  $20^\circ\text{C}$  of some common TES materials

Material	Density ( $\text{kg/m}^3$ )	Specific heat ( $\text{J/kg K}$ )	Volumetric thermal capacity ( $10^6 \text{ J/m}^3 \text{ K}$ )
Clay	1458	879	1.28
Brick	1800	837	1.51
Sandstone	2200	712	1.57
Wood	700	2390	1.67
Concrete	2000	880	1.76
Glass	2710	837	2.27
Aluminum	2710	896	2.43
Iron	7900	452	3.57
Steel	7840	465	3.68
Gravelly earth	2050	1840	3.77
Magnetite	5177	752	3.89
Water	988	4182	4.17

Source: Norton (1992).

Rock is a good sensible TES material from the standpoint of cost, but its volumetric thermal capacity is only half that of water. Past studies have shown that rock storage bins are practical, their main advantage being that they can easily be used for heat storage at above 100°C.

### 3.6.1 Thermally Stratified TES Tanks

TES tanks for use in heating, air-conditioning, and other applications have, in general, received increasing attention in recent years. Thermally stratified storage tanks, which have gradually seen more widespread use recently, are now described.

Figure 3.6 shows, for a thermally stratified storage tank, the positions of the inlet and outlet for well and poorly designed cases. Also shown is the thermally effective quantity of water that results from these positions. Since the tank stores thermal energy for periods of at least several hours, heat loss/gain occurs from the tank. The thermal-retaining performance of a tank is an important factor in its design.

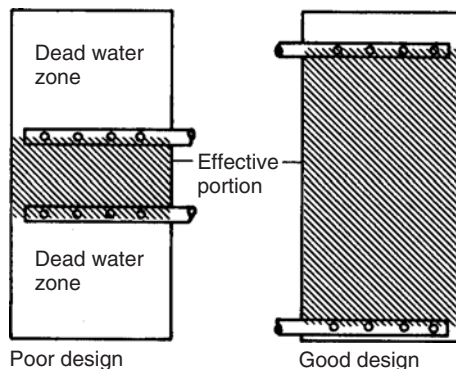
#### Types and Features of Various Stratified TES Tanks

The TES system most commonly employed at present is sensible TES utilizing water as the storage medium. The term “thermal” storage is used instead of “heat” storage because the former implies storage of heat or cold and the latter just heat. An effective TES tank utilizing water as the storage medium satisfies the following three general requirements:

- The tank should be stratified, that is, it should hold separate volumes of water at different temperatures. Mixing of the volumes should be minimal, even during charging and discharging periods.
- The effective storage capacity should minimize the amount of dead water volume in the tank (see Figure 3.6).
- The heat loss/gain from the tank should be minimized.

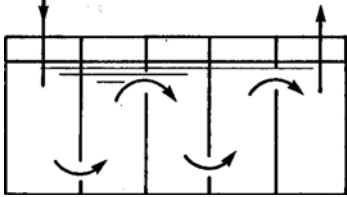
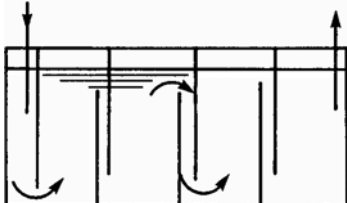
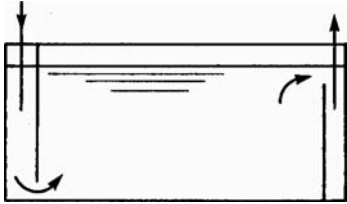
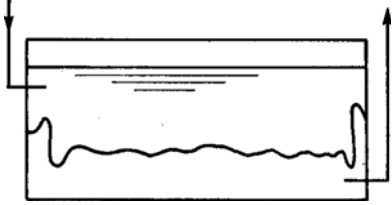
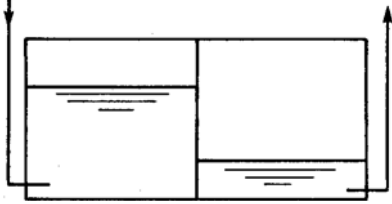
Many types of TES tanks have been developed to satisfy these requirements, the principal ones being listed in Table 3.7.

A thermally naturally stratified storage tank has no inside partitions and has the following principle of operation. Warm water has low density and floats to the top of the tank, while cooler water



**Figure 3.6** Position of inlet and outlet, and effective quantity of water (hatched regions), for a thermally stratified TES (Shimizu and Fujita, 1985)

**Table 3.7** Types and features of various stratified TES tanks

Type	Schematic representation of cross section	Efficiency	Remarks
Continuous multitank type		Medium	Underground beam space can be used effectively. Insulation is difficult to install.
Improved dipped weir type		Medium } High	Construction is difficult
Thermally stratified type		High	Best suited for large-size tank built aboveground
Movable diaphragm type		High	Diaphragm material is problematical. Not easily adapted to tanks with internal pillars and beams
Multitank water renewing type		High	Underground beam space can be utilized to some extent. Heat loss is large

Shimizu and Fujita (1985).

with higher density sinks to the bottom. The storage volume with this type of system is reduced relative to other systems, because the dead water volume is relatively low and the energy efficiency relatively high.

### Design Considerations for Stratified TES Tanks

When designing a thermally stratified thermal storage tank, the following criteria can guide the design process:

- **Geometrical considerations.** A deep water-storage container is desirable to improve thermal stratification. The water inlet and outlet should be installed in a manner that produces a uniform flow of water to avoid mixing. To minimize dead water volume, the outlet and inlet connections should be located as close as possible to the top and bottom of the storage volume, respectively. The surface area in contact with the storage water should be minimized.
- **Operating considerations.** The temperature difference between the upper and lower parts of the tank should be large, at least 5–10 °C. Controls can be used to maintain fixed water temperatures in the upper and lower parts of the tank if desired. The velocity of the water flowing into and out of the tank should be low.
- **Other considerations.** The insulating and water-proofing characteristics of the tank should be designed to meet appropriate specifications.

### Stratified TES Tank Configurations

Several possible stratified storage concepts are depicted in Figure 3.7. The advantage of the single-medium storage systems, in which the heat-transfer fluid is also the storage medium, is that no internal heat exchange between the transfer fluid and the storage medium is necessary, thus avoiding the consequential temperature losses. If the liquid has low thermal conductivity and permits good thermal stratification (e.g., for water or thermal oil), the one tank thermocline concept requires

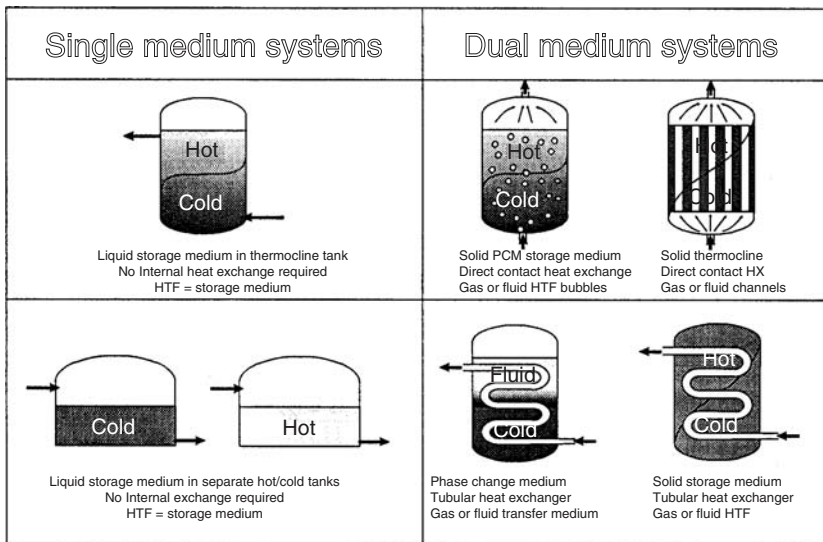


**Figure 3.7** Schematics of various tank configurations (HX: heat exchanger; HF: heat-transfer fluid) (Dinter *et al.*, 1991)



the least tank volume, since the hot and cold media are contained in a single vessel. When the storage-medium thermal conductivity is higher, as in molten salts or sodium, rapid equilibration of hot and cold temperature regions occurs, making separate hot and cold tanks necessary. Since in that case, twice as much tank volume as fluid content is required, a three-tank system in which there is only 1.5 times as much tank volume as fluid content is often recommended. However, such systems are difficult to control, involve extensive piping, and are subject to increased heat losses from higher surface-to-volume ratios. Dual-medium concepts employ different transfer and storage media often, because the storage medium (usually solid) is less expensive than the transfer fluid. The transfer medium exchanges heat through direct or indirect contact with the storage medium, forming a thermocline. Apart from the temperature drop between charging and discharging due to the intermediate heat exchange, the dual-medium concept has another operational drawback relative to single-medium hot/cold tank systems. While the latter keeps constant outlet temperatures at charging and discharging until the tank is empty, in a dual medium storage system, the outlet temperature of the heat-transfer medium increases the more it is charged and decreases the more it is discharged, leading to unusable storage capacities (Dinter *et al.*, 1991).

### 3.6.2 Concrete TES

Concrete is sometimes chosen because of its low cost, availability throughout the world, and easy processing. Inexpensive aggregates to the concrete are widely available. Concrete has the following characteristics as a storage medium:

- high specific heat;
- good mechanical properties (e.g., compressive strength);
- a thermal expansion coefficient near that of steel (pipe material); and
- high mechanical resistance to cyclic thermal loading.

When concrete is heated, a number of transformations and reactions take place which influence its strength and other physical properties. When concrete is heated to about 100 °C, water is expelled (up to 130 kg of water per m<sup>3</sup> of concrete). The remaining water (50 to 60 kg of water per m<sup>3</sup> concrete), either physically bound in smaller pores or held by chemisorption, is expelled as temperatures rise from 120 to 600 °C. Most dehydration occurs between 30 and 300 °C. This water loss reduces the weight of concrete by 2–4%. The specific heat decreases in the temperature range between 20 and 120 °C, and the thermal conductivity decreases between 20 and 280 °C. The mechanical properties are also slightly influenced by the loss of water; compressive strength decreases by about 20% at 400 °C compared to that at ambient temperature. Resistance to thermal cycling depends on the thermal expansion coefficients of the materials used in the concrete. To minimize such problems, a basalt concrete is sometimes used. Steel needles and reinforcement are sometimes added to the concrete to impede cracking. By doing so, the thermal conductivity is increased by about 15% at 100 °C and 10% at 250 °C (Dinter *et al.*, 1991).

Such concrete storage can be supplied as prefabricated plates. Alternatively, the concrete may be poured on-site into large blocks, leading to easier and more economic construction. Whether prefabricated plates or on-site pouring is advantageous depends on local conditions.

### 3.6.3 Rock and Water/Rock TES

Rock is an inexpensive TES material from the standpoint of cost, but its volumetric thermal capacity is much less than that of water. Rock storage bins in home air-heating systems are practical (Dincer, 1999). The advantage of rock over water is that it can easily be used for TES above 100 °C. Rock-bed and water storage types can both be utilized in many ways. For example,



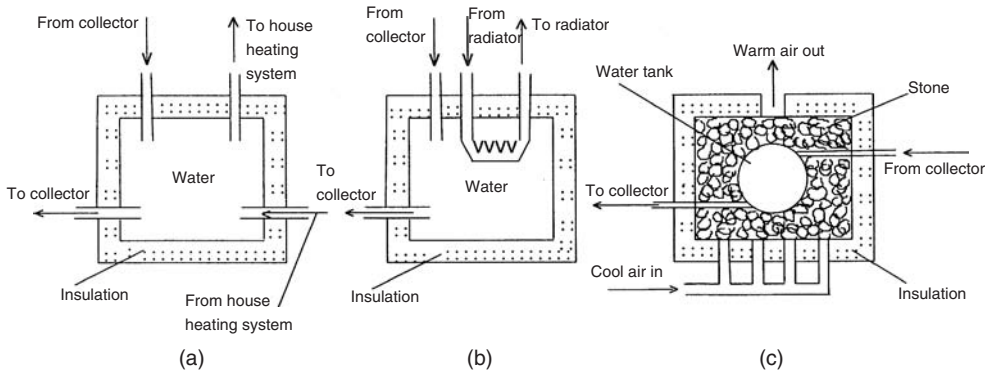


**Figure 3.8** Solar storage tanks: (a) heat storage tank directly tied to both the collector and the house heating system, (b) sensible TES system using a heat exchanger to extract solar heat from a storage tank, and (c) Harry Thomason's technique using both water and stone as storage media

they may be used in conjunction with heat pumps to improve the efficiency of heat recovery, or with more elaborate heat exchangers, or with each other.

Eldighidy (1991) conducted extensive theoretical and experimental investigations on solar storage tanks with TES and indicated that water, rock beds, and PCMs are the most suitable storage media. Three different configurations of storage tanks (Figure 3.8) for TES applications were examined. The most common TES system has a water-filled container in direct contact with both the solar collector and the house heating system (Figure 3.8a). Cool water from the bottom of the tank is circulated to the collector for solar heating and then returned to the top of the tank. Warm water from the top of the tank is circulated directly through baseboard radiators or radiant heating panels inside the rooms. Figure 3.8(b) shows another system which consists of a copper coiled finned tube immersed in the tank of solar heated water. Rocks are the most widely used storage medium for air collectors.

One attractive storage method that uses both water and rocks as storage media is known as *Harry Thomason's method* (Figure 3.8c). In this system, heated water from the solar collector enters a water tank at the top, sinks as it cools, and finally leaves at the tank bottom as it is recirculated to the collectors. The water tank is surrounded by river rock through which air is circulated to carry the heat into the house; the entire rock and water tank assembly is contained within insulated walls. The advantage of this system is the high heat capacity of the water, and the extensive area of the rock's container leads to efficient transfer of heat to the air.

Rocks are sometimes the preferred storage medium over water for solar energy systems situated in northern latitudes. However, air/rock solar systems can, and in some instances do, make provision for partial heat storage in water for domestic hot water use. Storage of heat in rocks requires approximately three times as much space as an equivalent amount of heat in water. This disadvantage is often overcome by cost advantages. Water containment in a TES or a swimming pool is expensive. Combined with the higher capital and maintenance costs of a liquid collector, the economics quickly favor the use of air collectors with rock storage for domestic heating applications. Liquid solar energy systems were chosen during the early stages of solar energy development because of the superior heat-transfer characteristics of liquid over air. Initial solar energy collection systems were able to capture slightly more than 50% of the incident solar radiation with liquid collectors but barely 30% with air type collectors. Present air collectors, which incorporate developments in selective coatings, are beginning to match the energy efficiency of liquid collectors while retaining simplicity, minimal maintenance, and low costs. The volume occupied by a rock store is equal to approximately  $1.6 \text{ m}^3$  per  $\text{m}^2$  of collector. The average collector array for a typical residence occupies an area of  $30.4 \text{ m}^2$ . A rock store for a collector of this size occupies a volume

equal to  $4.6 \text{ m}^3$  (e.g., rectangle of dimensions  $1.5 \text{ m} \times 1.5 \text{ m} \times 2 \text{ m}$ ). Such a size usually does not present a significant design problem with respect to interior living spaces.

### Design Considerations for TES in Rocks

The rule of thumb for determining the size of a storage rock bed specifies that a collector area of  $1 \text{ m}^2$  is needed for an amount of rock of  $1.6 \text{ m}^3$ . This rule assumes a home insulated to high standards and situated in regions experiencing average levels of solar radiation. Regions experiencing significantly higher levels of radiation may benefit from increasing store size if there is no corresponding decrease in ambient temperature. An increase in store size in proportion to an increase in solar radiation enables the system to store more heat for use during nonsolar periods of little or no solar insolation. However, if the increase in solar radiation is accompanied by colder weather, such as that experienced in mountainous terrain, there is probably no advantage in increasing the size of the store. This is because the additional heat gain as a result of the increased radiation is dissipated faster because of the accelerated heat loss caused by the lower ambient temperatures.

Storage configurations that are nearly cubic or slightly rectangular generally perform well. This type of geometry allows for a high ratio of volume to surface area of containment. In heat stores, an increase in surface area produces a corresponding increase in heat loss. Thus, heat retention can be enhanced by keeping the surface area of the store to a minimum. A way of further reducing surface area is to utilize cylindrical containment.

Washed gravel is preferable to crushed stone as a storage medium, because the resistance to air flow of crushed stone is up to three times greater than that of washed gravel. The major constraint associated with rock beds is that the rock should be uniform in size, which requires some sort of screening. The recommended particle diameter is 2.5 cm.

The air flow through a vertical heat store should be from top to bottom while charging and from bottom to top while recuperating heat. By reversing the flow in this manner, we are able to stratify the store. Stratification can provide a warmer air supply for the home and a cooler air supply to a solar collector or other heat source. With this arrangement, efficiency is increased.

The pressure drop through a rock store should be significantly higher (minimum five times) than that in the plenums leading to the store, so as to assure a good flow distribution through the bed. One rock bed installation, for example, is designed for a  $21.2 \text{ m}^2$  single glazed, selective coated, back-pass collector array. The air stream is designed for two stages with a maximum air flow rate of  $4.65 \text{ m}^3/\text{s}$ . A store for this configuration with 2.5-cm diameter would have a pressure drop of 5.84 mm of water. Additional facts pertaining to pressure drop that are worth noting are as follows (Dincer and Dost, 1996):

- Pressure drop through a rock bed is directly proportional to air speed.
- Pressure drop through a rock bed is inversely proportional to the area of cross section.
- A  $0.028\text{-m}^3$  store containing 2.5-cm-diameter rock has approximately  $0.82 \text{ m}^2$  of surface area.
- A  $0.093 \text{ m}^2$  store containing 7.6 cm diameter rock has about  $1.3 \text{ m}^2$  of surface area.

Pressure drop and heat-transfer coefficients can be altered by adjusting these parameters.

### Water–Rock Beds

One study (Moschatos, 1993) discussed in detail a type of TES that combines rock-bed and water storage. The configuration consists of a water storage surrounded by a rock-bed storage instead of insulation, as shown in Figure 3.9. The basic concept is that, for a house heated by solar collectors, heat losses could be offset by the thermal energy of water storage, or by auxiliary energy. Part of the ventilation thermal losses can be recovered by passing fresh air through the bed storage.

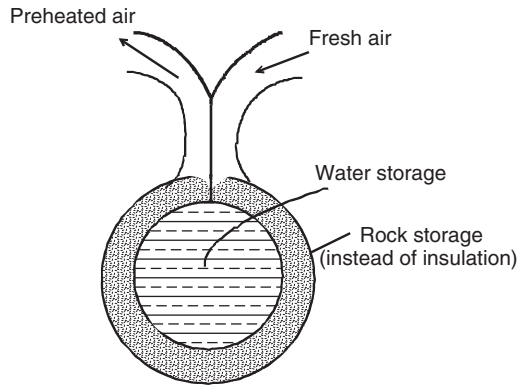


**Figure 3.9** Schematic of a cylindrical combined water-rock storage (Moschatos, 1993)

The general idea of combined storage was developed for a number of houses by Thomason (1960). The differences between the storage combination of Thomason (see Figure 3.8c) and that in Figure 3.9 are

- Thomason utilizes both water and rock storage to hold solar energy, with the thermal load of the house mainly met by rock storage. The main solar TES is the water storage, which is covered by a rock bed instead of insulation. In this way, water-storage thermal losses preheat the cold fresh air for ventilation.
- Thomason's bed storage has no specific geometrical shape.

With the combined storage, (a) fresh air is preheated, (b) low-temperature thermal energy contained in the bed storage is utilized, and (c) water storage thermal losses are partially recovered.

Combining water with air/rock storage systems is becoming common for solar energy applications. Such systems aim to provide a portion of the energy needs for domestic hot water without a significant reduction in the solar energy supply for space heating needs. Conventional air–rock solar systems for space heating are pressed into service during the heating season only. Consequently, the amortization period is lengthened, because the solar energy system is inoperative for approximately six months of the year. Adding domestic hot water capability to the basic air/rock system increases the capital costs by a small fraction. So, for a relatively small additional investment, the solar energy system can provide 100% of the domestic hot water during summer and less during other seasons. The configuration for heating domestic hot water with an air/rock solar energy system can be as simple as placing a steel tank in the rock store. For such systems, tanks with glass linings, which are readily available at low prices since they are mass produced for conventional hot water heating, are often used. The glass-lined water storage tank is preferred for its long life expectancy, often greater than 20 years in solar applications.

There is relatively little thermal shock on storages associated with solar use. In conventional use, the sudden application of high-grade heat to a water store can harm the tank over time, depending on the mineral content of the water and other related factors. Compared to oil, gas, or electric heated water, which is at a very high temperature for a short period of time, solar heated water is at a low temperature for a long period of time. The actual firing or heat supply temperatures are approximately 60 °C for solar energy and over 800 °C for conventional systems.

It is advisable to provide access for visual monitoring and replacement of storage. The latter may never be needed but, if it is, it is easier to gain access through a panel than to have to destroy the storage.

In certain instances, solar collection efficiency can be improved by placing a second water reservoir in the cold end of the store. This option is sometimes considered when the water supply to the home is at a fairly low temperature (5 °C). The effect is to preheat the water entering the tank situated in the hot end of the store, and to keep the cold end of the store below the average temperature. This increases the solar heat gain and the efficiency of the collector. An additional benefit of the second water tank is an increase in thermosyphoning (natural convection) within the store, which transfers heat from the rocks to the water reservoir during periods when the solar house fan is inoperative.

There are two potential disadvantages to using this type of system. First, it may prove difficult to provide access to a water tank located under a pile of rocks. Second, the air from the house returning to the store during the heating season may nullify all or part of the preheating effect. Consequently, the addition of the secondary water reservoir should be considered for select applications only.

Storage bins may be constructed utilizing containers of water as a replacement for rocks. The containers have to be small, 1 gal or less, in order to have effective heat transfer between the air stream and the contained water. Also, the container must be of a type that withstands thermal degradation.

The most important advantage of a hybrid heating system with a water-to-air heat exchanger and storage unit is its multiple applications, including water heating, drying, space heating, and space cooling (by letting cold water flow through the system) during different times of the year. A rock-bed heat exchanger and storage unit has been successfully used for heat transfer (from water to air) and heat storage in the Thomason residential heating systems. Such systems can operate for several years, but few design investigations and parametric studies have been conducted. In one work, Choudhury and Garg (1995) conducted a performance evaluation of the system with optimized design parameters, both with and without a domestic hot water load on the system. The load is the standard hot water demand of a four person (two adults and two children) residential building in India. The system has been evaluated under both continuous and intermittent air circulation conditions (i.e., air flow rate becomes zero, when the room temperature exceeds 27 °C, which is taken to the upper limit of the comfortable range for residential buildings). No auxiliary energy is used to satisfy the space heating and the hot water demand.

### 3.6.4 *Aquifer Thermal Energy Storage (ATES)*

An aquifer is a groundwater reservoir. The word aquifer derives from the Latin words “aqua” meaning water and “ferre” meaning to carry. The material in an aquifer is highly permeable to water, and the boundary layer consists of more impermeable materials such as clay or rock. Aquifers are found throughout the world. For example, two types of aquifers are found in Sweden. The most common type consists of sand and gravel deposits left by retreating ice from the Ice Age. The second type consists of sandstone or limestone, and can be found mainly in the southern part of Sweden. Water from precipitation continuously seeps down to an aquifer and flows slowly through it until finally reaching a lake or the sea. Aquifers are often used as fresh water sources.

Aquifers often have large volumes, often exceeding millions of cubic meters, and as they consist of about 25% water they have a high TES capacity. When heat extraction and charging performances are good, high heating and cooling powers can be achieved. The amount of energy that can be stored in an aquifer depends on local conditions, such as

- allowable temperature change;
- thermal conductivity; and
- natural groundwater flows.

ATES is a concept that has been known for several decades. Aquifer systems have received worldwide attention because of their potential for large-scale and long-term TES. In its most common form, the technique involves storing excess heat in an aquifer and recovering it later

during periods of heat demand. With growing concerns about global warming, the concept is receiving renewed attention as a viable means of conserving energy and reducing fossil fuel use. This increasing interest is reflected in accelerated research activities in northern European countries and Canada. In developing ATEs systems, the physical processes governing the behavior of thermal energy transport in groundwater must be well understood. Numerical simulation models serve a key role in contributing to this understanding, and are thus indispensable in the design of efficient ATEs facilities.

The injection of heated water into an aquifer may also be necessary for reasons other than energy conservation. For example, where water rights issues or concerns about land or water quality arise, water extracted for cooling purposes may be reinjected into the aquifer. In these situations, it is important to understand the effect of heat on the groundwater system, and to be able to predict consequences such as the accelerated precipitation of dissolved substances, or changes in the biological regime.

Research into ATEs has been ongoing for several decades in North America and in Europe. Work in Denmark, for example, shows a high level of development. In the United States, pioneering research has been done at Auburn University and at the General Electric Center for Advanced Studies at Santa Barbara, California. Research into ATEs is also being conducted in many other European countries, including Sweden, Germany, Denmark, and France.

Figure 3.10 illustrates the operating principle of simple ATEs systems. Both heating and cooling cycles for a building are considered. Wells have been drilled to transport water to underground aquifers (underground areas of water-bearing rock, sand, or gravel). Well spacing, depth, and size are functions of the aquifer.

An aquifer storage system can be used for storage periods ranging from long to short, including daily, weekly, seasonal, or mixed cycles. To avoid undesired permanent changes of the temperature level in the aquifer, the input and output of heat must be of the same magnitude at least after a number of cycles. The system should be designed to be adjustable in case the long-term energy flows do not balance. The TES capacity should be appropriate to the heating/cooling loads.

Extensive investigations and test runs are usually needed to predict the performance of an ATEs before the design of the energy system. Such preparatory work can in some cases be relatively costly.

Aquifers with groundwater, or the ground itself (soil, rock), can be used as a storage medium in ATEs systems. Aquifer stores are most suited to high capacity systems. The existing capacities range in size from less than 50 to over 10,000 kW.

### Utilization of ATEs

ATEs or groundwater energy systems utilize groundwater, and do not necessarily deplete nonrenewable resources. In some systems, external thermal energy is stored in an ATEs. In others, the

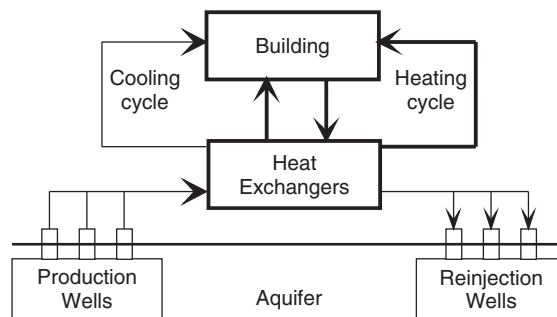


**Figure 3.10** Schematic of the operation of an ATEs system

natural groundwater temperatures are used. In the latter case, the system requires production wells to supply groundwater to a series of heat exchangers. In winter, heat from underground is used to preheat outside building air. In summer, direct cooling is achieved by transferring heat from buildings to the groundwater using the same principle in reverse. In both cases, the groundwater is returned to the subsurface aquifer through reinjection wells without having been exposed to any form of contamination. Over time, a thermal balance is maintained in the aquifer.

These groundwater systems can be applied to new and existing heating and cooling systems in such facilities as government buildings, business parks, residential complexes, educational institutions, hospitals, and industrial complexes. In addition, groundwater systems can be integrated into industrial process plants such as paper and textile mills, and pharmaceutical manufacturing, mining, and food processing facilities.

Groundwater energy systems provide an efficient and reliable supply of low-cost energy that can complement conventional heating and cooling systems. Furthermore, the groundwater systems are environmentally benign technology and can reduce stack emissions (e.g., carbon dioxide) and the use of chlorofluorocarbon CFCs, and can reduce electrical usage during peak demand periods.

ATES has been used successfully around the world for the seasonal storage of heat and cold energy for the purpose of heating and cooling buildings. Domestic and large-scale ATES systems are used quite widely in some countries, for example, Canada and Germany.

When heat storage is needed to match thermal demand and supply, the ground has proven to be a useful storage medium, especially for large quantities of heat and long storage durations, like seasons. Many plants use ATES to store summer solar heat for use in winter heating, and ATES for waste heat is now emerging. The efficiency of heat storage depends upon the temperature level achieved and upon the quantity of thermal losses. While heat storage in ATES in the range of 10–40°C has been demonstrated successfully, storage at higher temperatures (e.g., up to about 150°C) was shown to cause many problems in experimental and pilot plants in the 1980s.

### Deep Confined Aquifers

Traditionally, deep confined aquifers have been preferred for ATES facilities. Some suggest that such aquifers are advantageous because (i) regional groundwater flow usually being negligible, the injected hot water is not displaced, (ii) the thickness of overburden is such that the storage is not disturbed by seasonal surface temperature variations, and (iii) the initial temperature is higher (due to the natural geothermal gradient), thus significantly reducing heat losses to confining layers. Nonetheless, unconfined aquifers are being used for ATES systems in Sweden, France, and the United States. Shallow, unconfined aquifers are easier to delineate. They are more common in many regions, and can be inexpensive when it comes to well installation and monitoring. Therefore, the use of unconfined aquifers for ATES can be advantageous, provided the energy recovery efficiency is adequate.

The aquifers used in ATES are permeable, water-bearing rock formations. Where aquifers are unavailable, a network of plastic tubing inserted into boreholes drilled into the earth can be used as underground storage, usually with water. With an aquifer system, two well fields are often tapped: one for cold storage and the other for heat. These wells, which are usually around 200 m deep, are capable of maintaining storage temperatures between 4 and 90°C.

During the summer months, cool groundwater is extracted from one aquifer and circulated through building systems to lower the air temperature. The water, which is heated during the process, is then returned to the other aquifer for eventual use in heating in winter – a cyclic process that can be repeated indefinitely. An ATES system typically reduces cooling costs by 80% and heating costs by 40% or more, while significantly reducing emissions of greenhouse gases and ozone-depleting substances.

Environment Canada (1999) in the Atlantic region of Canada has developed a variety of tools and procedures for implementing this energy-efficient technology – including tests to determine the thermal properties of boreholes, water-treatment technologies for high-temperature applications,

and environmental screening techniques – and plays an active role in the transfer of ATEs technologies, both nationally and internationally.

In the mid-1990s, Environment Canada teamed up with the New Brunswick Department of the Environment, New Brunswick Power, the Canadian Electricity Association, the Panel of Energy Research and Development, and the local community to launch an aquifer-based ATEs demonstration project at the Sussex Hospital in New Brunswick. The first hospital in Canada and the second in North America to adopt such a system, it has saved nearly \$50,000 annually in energy consumption costs since the project began, and reduced carbon dioxide emissions by 720,000 kg annually. These savings were accomplished after the hospital had already cut its energy consumption in half by installing an energy management system. During an emergency, only small auxiliary generators are required to operate the water pumps used in heating and cooling using the ATEs system.

ATEs is commonly used in China and parts of Western Europe – particularly the Netherlands and Sweden, where its use is growing by 25% a year. Although office buildings remain the primary market for the technology, it is gaining ground in industrial and agricultural applications, and a new market is developing in the de-icing and cooling of roads and bridges.

The environmental benefits of ATEs are illustrated in Figure 3.11, focusing on important global problems. The sizes of the circles represent the relative impact of the use of ATEs technology on the emissions indicated.

The success of the Sussex Hospital ATEs and other ATEs projects in Canada, such as those at Saskatoon Airport and Carleton University in Ottawa, has spurred the development of several new initiatives in Ontario, Nova Scotia, and British Columbia. Other situations exist where a system of this kind can yield considerable long-term environmental benefits and reduced use of fossil fuels for heating and electricity.

Annual ATEs systems use aquifers which are found near the Earth’s surface. These water-bearing rocks are large geological formations that can be tapped by wells. Although some technical

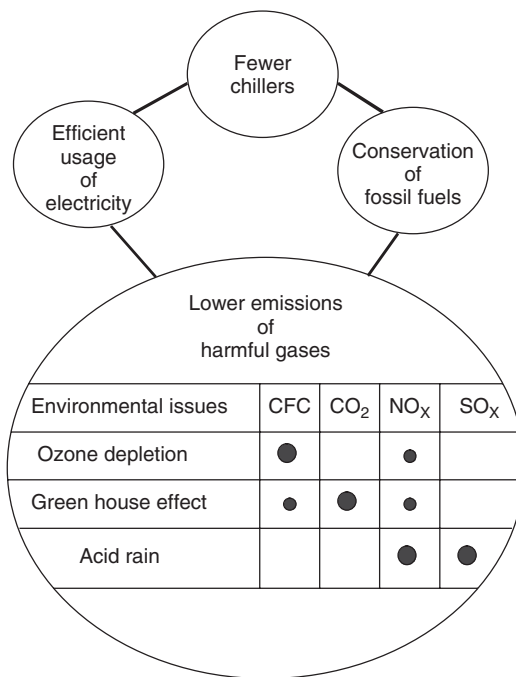


Figure 3.11 Some environmental benefits of ATEs (Environment Canada, 1999)



challenges (e.g., biofouling and clogging of pipes and wells) remain to be solved, aquifers potentially offer low-cost storage for large-scale systems. The main cost is associated with access wells. However, relatively low cyclic ATEs efficiencies (~70%), depending on the storage duration, may limit their use to the storage of such low-cost energy supplies as industrial waste heat.

### Performance of ATEs

The viability and cost effectiveness of an ATEs system depend on the mechanical design and thermodynamic efficiency of the aboveground installation, as well as on the physical, chemical, and biological processes within the aquifer. The spatial and temporal variations of temperature, as well as total energy, have been found to be critical factors in determining ATEs performance.

Physical processes affecting heat transport within a storage aquifer include advection, dispersion, and diffusion. The diffusion of heat depends on the thermal conductivity and heat capacity of the aquifer. In a composite medium such as an aquifer, the properties of both the fluid phase and the solid phase play important roles in heat transport, and ultimately control the recovery efficiency of stored energy. In addition, heat transfer from the aquifer system to adjacent aquitards or through the unsaturated zone to the atmosphere can be a significant process for removing heat from the ATEs system. An aquitard is a zone within the earth adjacent to an aquifer that has low permeability and thus restricts the flow of groundwater from one aquifer to another. An aquitard may serve as a storage unit for groundwater.

Chemical reactions resulting from changes in temperature and from mixing of the injection water with the resident groundwater can change the porosity and permeability of the aquifer, decrease well efficiency, and increase the cost of operation and maintenance of the heat exchangers. Temperature changes can also affect the activity of subsurface microorganisms, which can lead to a decrease in permeability and increased maintenance costs.

### Expansion of ATEs Applications

Possible heat sources and heat users for ATEs applications are listed in Table 3.8. The heat sources for many promising systems can be divided into two main groups:

- **Renewable energy sources.** Solar heat can be used with ATEs to supply heat to district-heating networks, along with backup auxiliary heating systems. Solar heat can also be used with heat pumps, avoiding the need for auxiliary heating. Another ATEs use may be for geothermal heating, allowing storage of excess production in summertime and to cover peaks in winter, or for storing waste heat from geothermal power plants.
- **Waste or excess heat.** The storage of waste heat from cogeneration or industrial processes (Table 3.8) may be needed on a seasonal or other cycle. ATEs can also be applied as a backup for processes that use industrial waste heat, to cover heat load during periods when the industrial process is stopped (for production breaks, repairs, etc.). Similarly, ATEs can be used for load leveling in a district-heating system, where the store is always charged at times of low heat demand and unloaded during peak heating periods.

The IEA study mentioned in the previous subsection shows that technical problems related to higher temperatures in ATEs system may be overcome (IEA, 1990). A remaining issue is the changes in water chemistry with the drastically changing temperatures in ATEs systems, resulting in clogging, scaling, corrosion, and leaching. It is possible to design and build reliable ATEs plants today, but caution is necessary when working with groundwater. In the future, a range of suitable methods for various hydrogeological/hydrochemical situations and system requirements are desirable. Many opportunities exist, for promising ATEs system concepts yield energy savings and reduced emissions.



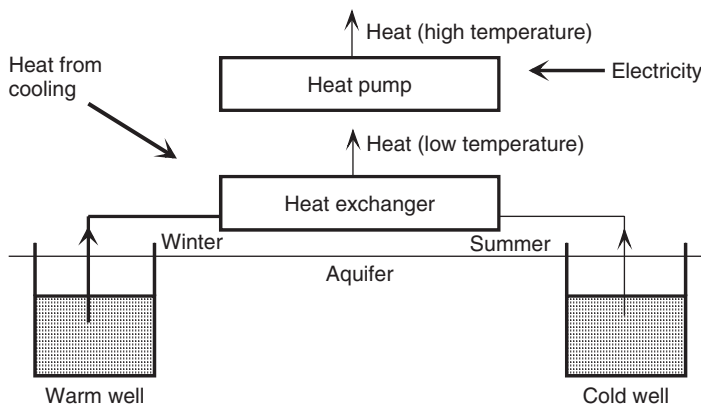
**Table 3.8** Some possible heat sources and heat users for ATEs

Possible heat sources	Possible heat users
Renewable energy <ul style="list-style-type: none"> <li>• Solar thermal (solar collectors, but also road surfaces, etc.)</li> <li>• Geothermal (hydrogeothermal, but also waste heat from geothermal power plants, e.g., hot dry rock)</li> <li>• Others (e.g., biomass combustion)</li> </ul>	Space heating <ul style="list-style-type: none"> <li>• District heating</li> <li>• Large buildings (houses, offices, hospitals, hotels, airports, etc.)</li> </ul>
Waste heat <ul style="list-style-type: none"> <li>• Heat and power cogeneration (likely only with high electrical efficiency)</li> <li>• Industrial process heat (e.g., from paper mills, steel works, etc.)</li> <li>• Waste incineration</li> <li>• Others</li> </ul>	Industrial heat <ul style="list-style-type: none"> <li>• Batch or seasonal processes such as those in sugar refineries</li> <li>• Drying in the food industry</li> <li>• Miscellaneous heat needs in many industries</li> </ul>
Load leveling <ul style="list-style-type: none"> <li>• In district-heating systems (for short- to medium-term periods)</li> </ul>	Agriculture <ul style="list-style-type: none"> <li>• Greenhouse heating</li> <li>• Food drying applications</li> <li>• Aquaculture</li> </ul>
	De-icing and snow-melting <ul style="list-style-type: none"> <li>• On roads, sport centers, airports, runways, etc.</li> </ul>

### ATES Using Heat Pumps

The concept of TES in an aquifer combined with a heat pump is relatively simple (see Figure 3.12). During the summer, cold water is extracted from a cold well and warmed by cooling a building, and then returned to a warm well in the aquifer. A heat pump can be used to chill the cold water further, if necessary. The warmed water diffuses out from the warm well, gradually raising the temperature of the aquifer. During the winter the process is reversed, with heat drawn from the warm well and the temperature boosted with the heat pump, if necessary.

The basic operational scheme of a ground-coupled heat pump with seasonal cold storage is shown in Figure 3.13 (Sanner and Chant, 1992). During heating, the ground or groundwater is cooled, while heat is supplied to the building. At the end of the heating season, enough cold is stored to run a

**Figure 3.12** An ATES system combined with a heat pump

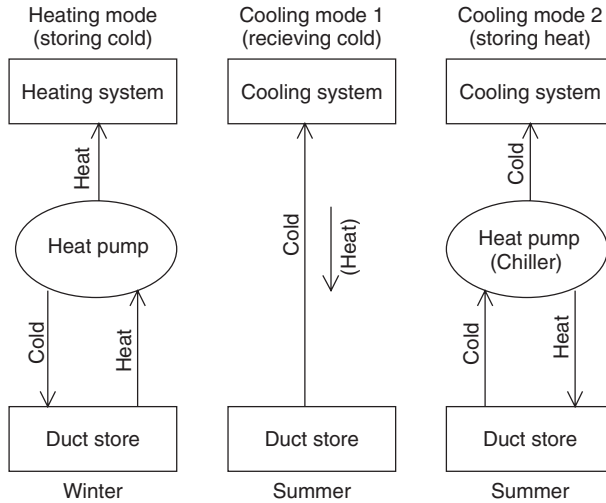


**Figure 3.13** Operational principles for ATEs systems using heat pumps

cooling system directly (mode 1), with cold groundwater from the injection well or cold brine from earth heat exchangers. For peak cooling loads, a backup system using the heat pump in reversed mode can be operated (mode 2). After continuously running the heat pump for space cooling for more than a few hours, temperatures in the ground may be too high for mode 1 cooling. The system should then be operated only as a conventional heat pump plant, storing heat in the ground until the beginning of the next heating season. The most cost-effective and efficient energy performance can usually be obtained by running the system in heating mode and cooling mode 1 only.

The cost effectiveness of seasonal storage depends significantly on the thermal and seasonal characteristics of the load. Storage for cooling is more cost effective for cooling systems with relatively high operating temperatures (up to 15 °C) than with more conventional temperatures (6–8 °C). By operating at higher temperatures, storage for cooling experiences reduced thermal losses, increased loading availability in winter, and reduced climatic influences on performance.

### 3.6.5 Solar Ponds

A salinity-gradient solar pond is an integral collection and storage device of solar energy. By virtue of having built-in TES, it can be used irrespective of time and season. In an ordinary pond or lake, when the sun's rays heat up the water, this heated water, being lighter, rises to the surface and loses its heat to the atmosphere. The net result is that the pond water remains at nearly atmospheric temperature. The solar pond technology inhibits this phenomenon by dissolving salt into the bottom layer of this pond, making it too heavy to rise to the surface, even when hot. The salt concentration increases with depth, thereby forming a salinity gradient. The sunlight which reaches the bottom of the pond remains entrapped there. The useful thermal energy is then withdrawn from the solar pond in the form of hot brine. The pre-requisites for establishing solar ponds are a large tract of land (it could be barren), a lot of sunshine, and cheaply available salt (e.g., NaCl) or bittern.

Salt-gradient solar ponds may be economically attractive in climates with less snow and in areas where land is readily available. In addition, sensible cooling storage can be added to existing facilities by creating a small pond or lake on the site. In some installations, this can be done as part of property landscaping. Cooling takes place by surface evaporation and the rate of cooling can be increased with a water spray or fountain. Ponds can be used as an outside TES system or as a means of rejecting surplus heat from refrigeration or process equipment.

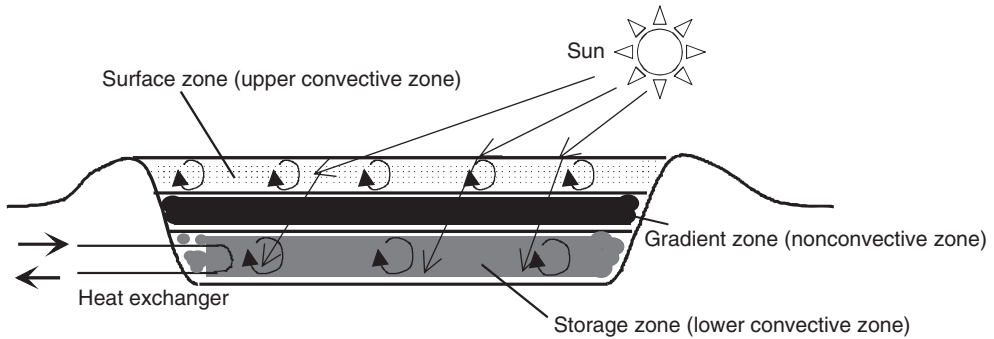


**Figure 3.14** A cross-section representation of a typical salinity-gradient solar pond

Being large, deep bodies of water, solar ponds are usually sized to provide community heating. Solar ponds differ in several ways from natural ponds. Solar ponds are filled with clear water to ensure maximum penetration of sunlight. The bottom is darkened to absorb more solar radiation. Salt is added to make the water denser at the bottom and to inhibit natural convection. The cooler water on top acts as insulation and prevents evaporation. Salt water can be heated to high temperatures, even above the boiling point of fresh water.

Figure 3.14 represents a cross-section view of a typical salinity-gradient solar pond which has three regions. The top region is called the *surface zone, or upper convective zone*. The middle region is called the *gradient zone, or nonconvective zone*. The lower region is called the *storage zone or lower convective zone*. The lower zone is a homogeneous, concentrated salt solution that can be either convecting or temperature stratified. Above it, the nonconvective gradient zone constitutes a thermally insulating layer that contains a salinity gradient. This means that the water closer to the surface is always less concentrated than the water below it. The surface zone is a homogeneous layer of low-salinity brine or fresh water. If the salinity gradient is large enough, there is no convection in the gradient zone even when heat is absorbed in the lower zone, because the hotter, saltier water at the bottom of the gradient remains denser than the colder, less salty water above it. Because water is transparent to visible light but opaque to infrared radiation, the energy in the form of sunlight that reaches the lower zone and is absorbed there can escape only via conduction. The thermal conductivity of water is moderately low, and if the gradient zone has substantial thickness, heat escapes upward from the lower zone very slowly. This makes the solar pond both a thermal collector and a long-term storage device.

Solar ponds were pioneered in Israel in the early 1960s, and are simple in principle and operation. They are long-lived and require little maintenance. Heat collection and storage are accomplished in the same unit, as in passive solar structures, and the pumps and piping used to maintain the salt gradient are relatively simple. The ponds need cleaning, like a swimming pool, to keep the water transparent to light. A major advantage of solar ponds is the independence of the system. No backup is needed, because the pond's high heat capacity and enormous thermal mass can usually buffer a drop in solar supply that would force a single-dwelling unit to resort to backup heat.

### 3.6.6 Evacuated Solar Collector TES

Selection of a storage medium is often based on availability, durability, and cost, and tends to favor solar TES using water or rocks. One of the most promising applications of sensible TES is for solar heated residential and commercial buildings.

As mentioned earlier, in some cases rocks are preferred to water for solar energy systems. However, air/rock solar systems can allow for partial heat storage in water for domestic hot water

use. Heat stored in rocks, compared with an equivalent amount of heat stored in water, occupies approximately three times as much volume. However, liquid containment systems have higher initial and maintenance costs. Economics usually favor the use of air collectors with rock storage for domestic heating applications. Water and air/rock systems are often combined for solar energy applications (Dincer *et al.*, 1997a), so as to provide a portion of energy needs for domestic hot water and space heating. Conventional air/rock solar systems for space heating are used only during the heating season, which usually lasts no more than half of the year. Hybrid hot water and air/rock systems have slightly increased the capital costs, but operate round the year by providing domestic hot water during summer.

Active solar energy systems with standard flat-plate solar heat collectors for domestic and commercial applications have some technical and operational problems. Evacuated-tube solar collectors have some advantages, and since 1980, several million tubes have been installed in over thirty countries. In 1991, the Thermomax Mazdon evacuated solar collector (Figure 3.15a) was developed. Its manifold configuration is particularly suited to North American conditions and plumbing practices. These collectors avoid many of the thermal and operational problems that occur in the flat-plate collectors and have better efficiencies (up to 80%), mainly because of their thermophysical properties (e.g., their heat-transfer rate is thousands of times greater than that of the best solid heat conductors of the same size). Some of the features of these solar collectors are as follows:

- high efficiency;
- low heat capacity and high heat-transfer rate;
- control of maximum temperature;
- high durability;
- a wide range of availability for thermal applications ranging from hot water to industrial process heat;
- free of corrosion, maintenance, and cold weather/frost problems;
- easy installation.

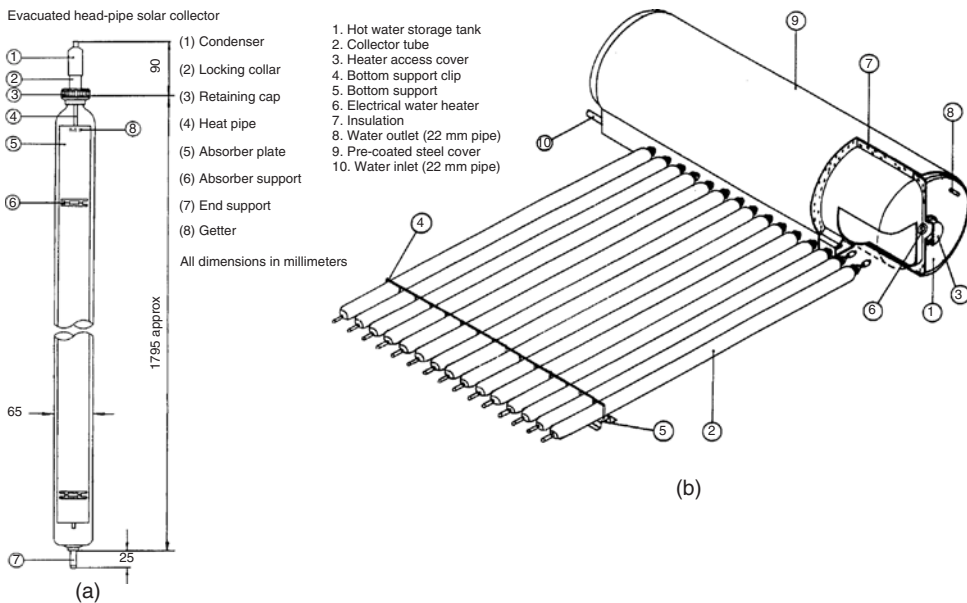


**Figure 3.15** Evacuated solar collector TES system. (a) Evacuated solar collector, (b) an integrated tank system

Figure 3.15(b) shows an integrated tank system, consisting of 15 evacuated solar collector tubes and a 170-L hot water storage tank. The tank is made from a high-grade stainless steel, having at least 2.5% molybdenum content, sealed in a weather-resistant metal cover. There is a thick polyurethane foam insulation jacket that lies between the tank and the steel cover. This solar energy system produces high water temperatures, eliminating the need for large and cumbersome water storage tanks. A large volume of warm water can be obtained by mixing cold water with the hot water from the unit. During the operation, the maximum chloride concentration of the water in the tank should not exceed 40 ppm in order to avoid corrosive effects.

### 3.7 Latent TES

Effective utilization of time-dependent energy resources requires appropriate TES methods to reduce the time and rate mismatch between energy supply and demand. TES provides a high degree of flexibility since it can be integrated with a variety of energy technologies, for example, solar collectors, biofuel combustors, heat pumps, and off-peak electricity generators.

The heat transfer which occurs when a substance changes from one phase to another is called the *latent heat*. The latent heat change is usually much higher than the sensible heat change for a given medium, which is related to its specific heat. When water turns to steam, the latent heat change is of the order of 2 MJ/kg.

Most practical systems using phase-change energy storage involve solutions of salts in water. Several problems are associated with such systems, which includes the following:

- Supercooling of the PCM may take place, rather than crystallization with heat release. This problem can be avoided partially by adding small crystals as nucleating agents.
- It is difficult to build a heat exchanger capable of dealing with the agglomeration of varying sizes of crystals that float in the liquid.
- The system operation cannot be completely reversed.

Any latent heat TES system must possess at least the following three components (Abhat, 1983):

- A heat storage substance that undergoes a phase transition within the desired operating temperature range, and wherein the bulk of the heat added is stored as latent heat.
- A containment for the storage substance.
- A heat-exchange surface for transferring heat from the heat source to the storage substance and from the latter to the heat sink, for example, from a solar collector to the latent TES substance to the load loop.

Some systems use either  $\text{Na}_2\text{SO}_4 \cdot 10 \cdot \text{H}_2\text{O}$  or  $\text{CaCl}_2 \cdot 6\text{H}_2\text{O}$  crystals as their storage media, and employ a heat-exchange oil. The oil is pumped in at the bottom of the storage and rises in globules through the fluid without mixing. Other promising latent TES reactions are those of intercrystalline changes. Many of these take place at relatively high temperatures.

Solar energy applications require large TES capacities in order to cover a minimum of 1–2 days of thermal demand. This capacity is commonly achieved by sensible heat storage in large water tanks. An alternative is offered by latent heat storage systems, where thermal energy is stored as latent heat in substances undergoing a phase transition, for example, the heat of fusion in the solid–liquid transition. The main advantages of latent TES systems are high TES capacities per unit mass compared to those of sensible heat systems, and a small temperature range of operation since the heat interaction occurs at constant temperature. There is no gradual decline in temperature as heat is removed from the PCM.

Salt compounds that absorb a large amount of heat during melting are useful for energy storage. Eutectic salts and salt hydrates are widely used. Glauber's salt (sodium sulfate decahydrate)

is a leading PCM, because it has a high heat-storage capacity (280 kJ/kg) and a phase-change temperature that is compatible with solar energy systems (31.5 °C).

PCM can be contained in rods or plastic envelopes to facilitate the freeze–thaw cycle. These small modules, and the small number of modules required for storage, make phase-change storage especially suitable for use in conventional design and for retrofitting.

In the Mattapoisett house in Massachusetts, which is 60% heated by passive solar gain, 8.5 m<sup>3</sup> of Glauber's salt is located in the ceiling. The phase-change storage has been demonstrated to lower the peak indoor temperatures. Table salt (NaCl) can be added to the PCM, lowering the melting point to about 22.7 °C. Because heat is then absorbed at a lower temperature, the house only reaches about 26.6 °C on a clear winter's day instead of the 29.4 °C or as often seen in passive solar structures (Lane, 1988).

The three most favored storage media for solar energy systems, water, rock, and Glauber's salt, vary considerably in price and required volume. For 9 m<sup>2</sup> of collector area (assuming a 20 °C temperature swing), the storage cost for water is \$54 and for Glauber's salt it is \$146. However, only 0.18 m<sup>3</sup> of Glauber's salt is required, which is one-quarter of the necessary 0.72 m<sup>3</sup> of water. Rock storage for the same collector would cost \$217 at \$8/t for the required 2.46 m<sup>3</sup>. This option would seem the least appealing, but it is nonetheless established and widely used. For example, the Lof home in Denver has been heated by a rock storage system for several decades (Tomlinson and Kannberg, 1990).

Latent TES is a promising storage technique, since it provides a high energy storage density, second only to chemical energy storage, and can store and release heat at a constant temperature corresponding to the phase transition temperature of the heat-storage medium.

Another important material category capable of storing energy through phase change is paraffin waxes. These have the advantage of very high stability over repeated cycles of latent TES operation without degradation. Several types of heat exchangers have been used to retrieve the energy from this storage medium: a cylindrical pipe, a single radial-finned pipe, and a multiple radial-finned pipe. Experimental tests have been performed for each of the different configurations, and the relative merits of each discussed in terms of heat-exchange properties and total energy exchanged.

### 3.7.1 Operational Aspects of Latent TES

At present, problems concerning the inability to completely reverse the storing process limit the practical applications of chemical storage media. On the other hand, storage media that undergo physical processes can usually have the storage process totally reversed, but involve less TES per unit weight of the device than chemical storage. Latent TES systems thus have the advantage of compactness in comparison with sensible TES devices (as well as the operational advantage of a nearly constant storage-cycle temperature).

Among the thermodynamic phase changes at a constant temperature with the absorption or release of latent heat, the most suitable ones for TES are the solid–liquid and solid–solid transitions. Solid–gas transitions, even though they often involve the largest heat interactions per unit weight, present the disadvantage of very large volume changes.

The most important criteria to be met by the storage material for a latent TES in which the material undergoes a solid–liquid or a solid–solid phase transition are as follows:

- high transition enthalpy per unit mass;
- ability to fully reverse the transition;
- adequate transition temperature;
- chemical stability and compatibility with the container (if present);
- limited volume change with the transition;
- nontoxicity;
- low cost, in relation to the foreseen application.

### 3.7.2 Phase Change Materials (PCMs)

When a material melts or vaporizes, it absorbs heat; when it changes to a solid (crystallizes) or to a liquid (condenses), it releases this heat. This phase change is used for storing heat in PCMs. Typical PCMs are water/ice, salt hydrates, and certain polymers. Since energy densities for latent TES exceed those for sensible TES, smaller and lighter storage devices and lower storage losses normally result.

Like ice and water, eutectic salts have been used as storage media for many decades. Perhaps the oldest application of a PCM for TES was the use of seat warmers for British railroad cars in the late 1800s. During cold winter days, a PCM, sodium thiosulfate pentahydrate, that melts and freezes at 44.4 °C was used. The PCM was filled into metal or rubber bags.

Other early applications of PCMs included “eutectic plates” used for cold storage in trucking and railroad transportation applications. Another important application of PCMs was in association with space technology, with NASA sponsoring a project on PCM applications for thermal control of electronic packages.

The first experimental application of PCMs for cool storage occurred in the early 1970s at the University of Delaware. The University’s Institute of Energy Conversion undertook the design and construction of a solar energy laboratory that became known as Solar One, located on the Newark, Delaware, campus. Dr. Maria Telkes, a leader in the research and development of eutectic salts, was selected to direct the institute’s Thermal Energy Applications program. The design of the Solar One building incorporated several hydrate-based storage systems. One material was used in association with solar collectors for heat storage. In the same sheet metal bin were placed containers of a Glauber’s salt mixture that melts and freezes at 12.7 °C.

During the late 1970s and 1980s, several organizations offered phase change products for solar heat storage. For instance, Dow Chemical provided a technically successful product that melts and freezes at 27.2 °C, whose market presence declined in the 1980s with the solar industry in general.

In 1982, Transphase Systems Inc. installed the first eutectic salt storage system for cool storage to serve a commercial or industrial building (Ames, 1989).

Like chilled-water storage systems, the 8.3 °C eutectic phase change temperature requires conventional chilled-water temperatures (5.5 °C) to charge the TES system. These temperatures allow new or existing centrifugal, screw, or reciprocating chillers to be used to charge the TES system, and make eutectics particularly appropriate for retrofit applications. The 5.5 °C charging temperature also enables the chiller to operate at high suction temperatures and compressor efficiencies as low as 0.55 kW/t.

Advantageous use of a PCM’s latent heat of fusion allows a TES to be moderate in size (about 0.155 m<sup>3</sup> per ton for the entire TES system, which includes piping headers and water in the tank). The storage capacity is based upon the amount of PCM frozen, and is not a temperature difference across the cooling coils.

The PCM is often contained in rugged, self-stacking, water-impermeable containers made of a high-density polyethylene. In Ames (1989), the containers measure 0.6 m × 0.2 m × 0.045 m, and are hermetically and redundantly sealed. The containers are designed with a surface-to-volume ratio of 24 m<sup>-1</sup> for maximum heat transfer; and provide 0.00635 m<sup>3</sup> of space for water to pass between the containers in a meandering flow pattern. The eutectic salt does not expand or contract when it freezes and melts; so, there is no fatigue on the plastic container. The eutectic salt-filled containers are placed in a tank, typically in a below-grade concrete or gunitite structure. The containers occupy about two-thirds of the tank’s volume, so that one-third of the tank is occupied by the water used as the heat-transfer medium. No glycol or other water-freezing-point depressant is used. The eutectic salt density is about 1.5 times that of water, so that the containers do not float or expand when the PCM freezes and the heat transfer/container spacing arrangement is maintained throughout the melt/freeze cycle. The top of the tank is designed for heavy truck traffic, and used as a parking lot. Thus, the tank does not use or alter above-grade space and may be placed away from the chiller plant.



Longevity, or the repeated use of a containerized PCM over 20 or more years and thousands of freeze/thaw cycles is one of eutectic salt's greatest strengths as a thermal storage medium. Because it is a passive system with no mechanical parts, the storage system is maintenance-free (apart from water treatment).

For the PCM with the 8.3 °C phase change temperature, the eutectic has been cycled in the field for 6.5 years with complete retention of thermal storage capacity. Also, the PCM has been subjected to accelerated life cycling equivalent to 12 years of performance with no loss of capacity. With the physical equilibrium of the PCM established after the first few cycles, the phase change appears to be stable and the TES capacity constant indefinitely, or at least as long as the life of chiller equipment used to freeze the PCM.

### Paraffins

A large number of organic compounds suitable to be storage media for solar heating have been investigated in recent decades. The most promising candidates seem to be the normal paraffins. Their solid–liquid transitions (fusions) satisfactorily meet seven important criteria for PCMs. For example, the heat of fusion has a mean value of 35–40 kcal/kg, there are no problems in reversing the phase change, and the transition points vary considerably with the number of carbon atoms in the chains. Also, the normal paraffins are chemically inert, nontoxic, and available at reasonably low cost. The change of volume with the transition, which is in the order of 10%, could represent a minor problem.

### Zeolites

The zeolites are naturally occurring minerals. Their high heat of adsorption and ability to hydrate and dehydrate, while maintaining structural stability have been found to be useful in various thermal storage and solar refrigeration systems. This hygroscopic property coupled with the rapid exothermic reaction that occurs when zeolites are taken from a dehydrated to a hydrated form (when the heat of adsorption is released) makes natural zeolites an effective storage material for solar and waste heat energy.

Low energy density and time of availability have been key problems in the use of solar energy and waste heat. Commercial TES systems have been developed incorporating GSA (2000) zeolites to overcome these problems. These systems are capable of utilizing solar heat, industrial waste heat, and heat from other sources, thereby converting underutilized resources into useful energy. A typical means of using zeolites as a heat storage medium is illustrated in Figure 3.16. The capacity of natural zeolites to store thermal energy and adsorb the water vapor used in that energy interaction comes from their honeycomb structure and resultant high internal surface area.

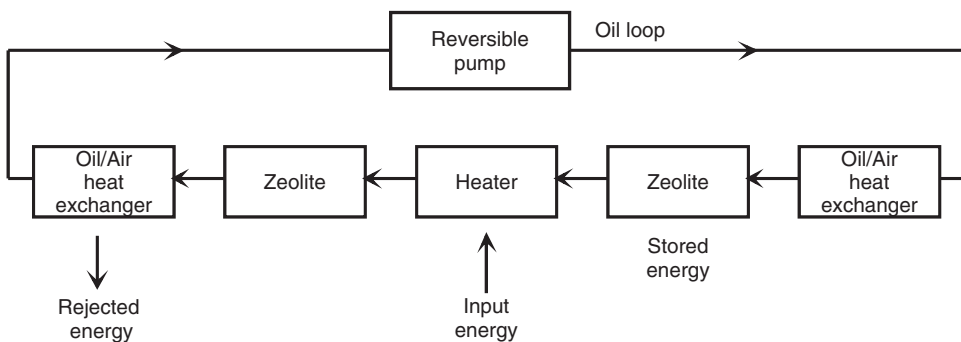


**Figure 3.16** A process for using GSA zeolites as a heat storage media (GSA, 2000)



When charged, GSA zeolites can store energy as latent heat indefinitely if maintained in a controlled environment and not exposed to water vapor. This stored energy can be liberated as needed simply through the addition of controlled amounts of water vapor, which initiates the exothermic reaction. Most other storage media do not possess this property. TES units using natural zeolites can reduce the dependence on secondary/backup heating systems, and allow for efficient and safe use of waste heat.

### Requirements of PCMs

Latent TES in the temperature range 0–120 °C is of interest for a variety of low-temperature applications, such as space heating, domestic hot water production, heat-pump-assisted space heating, greenhouse heating, solar cooling, and so on. The development of dependable TES systems for these and other applications requires a good understanding of heat-of-fusion storage materials and heat exchangers.

Knowledge of the melting and freezing characteristics of PCMs, their ability to undergo thermal cycling, and their compatibility with construction materials is essential for assessing the short- and long-term performance of a latent TES. Using two different measurement techniques (e.g., differential scanning calorimetry and thermal analysis), the melting and freezing behavior of PCMs can be determined. Commercial paraffins are characterized by two phase transitions (solid–liquid and solid–solid) that occur over a large temperature range, depending on the paraffin concerned. *n*-paraffins are usually preferred in comparison to their iso-counterparts, as the desired solid-to-liquid phase transition is generally restricted to a narrow temperature range. Fatty acids are organic materials with excellent melting and freezing characteristics and may have a good future potential, if their costs can be reduced. Inorganic salt hydrates, on the other hand, must be carefully examined for congruent, “semi-congruent,” or incongruent melting substances with the aid of phase diagrams. Incongruent melting in a salt hydrate may be “modified” to overcome decomposition by adding suspension media, or extra water, or other substances that shift the peritectic point. The use of salt hydrates in hermetically sealed containers is normally recommended. Also, the use of metallic surfaces to promote heterogeneous nucleation in a salt hydrate is seen to reduce the supercooling of most salt hydrates to a considerable extent. Thermal cycling and corrosion behavior are also of importance in the appropriate choice of materials as they affect the life of a latent heat store.

### Characterization of PCMs

Many characteristics are desired of a PCM. Since no material can satisfy all of the desires, the choice of a PCM for a given application requires careful examination of the properties of the various candidates, weighing of their relative merits and shortcomings, and, in some cases, a certain degree of compromise. The properties of many PCMs were investigated and reported earlier (Lane, 1988). It should be noted, however, that properties of industrial-grade products, which are used in practical applications, may deviate broadly from reported values because of the presence of impurities, composition variations (mixtures, distillation cuts), and chain-length distribution (in the case of polymers). Dilution by additives, such as the stabilizing agents required by salt hydrates, also modify thermal properties and, in particular, TES capacity. Selections should be based on assayed values of fully formulated products, whenever feasible.

### Difficulties with PCMs

Although significant advances have been made, some major hurdles still remain in the development of reliable and practical storage systems utilizing salt hydrates and similar inorganic substances:

- Difficulties in obtaining an optimal match between transition zone and operating range, because of the small number of materials available in the temperature range of interest.

- Uncertainties concerning the long-term thermal behavior, despite testing over a number of cycles generally much below the number of cycles that can be expected during the useful life of a storage system.
- Increased costs and reduced effective storage capacities because of the diluting effect of stabilizing additives.
- The potential for slow loss from water for encapsulated hydrates, and a resulting drift in thermal behavior.

During the last decades, attention was focused on a new class of materials: low-volatility, anhydrous organic substances such as polyethylene glycol, fatty acids and their derivatives, and paraffins. Those materials were not viewed as high-potential candidates in early studies, because they were costlier than common salt hydrates, they have somewhat lower heat storage capacities per unit volume, and, possibly, because of a bias against petroleum derivatives. Recent studies have shown that some of these materials have advantages that outweigh these shortcomings. The advantages include physical and chemical stability, good thermal behavior, and an adjustable transition zone. Paraffins appear particularly well suited for applications related to energy conservation in buildings and solar energy.

### Expectations of PCMs

Numerous organic and inorganic PCMs melt with a high heat of fusion in the temperature range 0–120°C. However, for their employment as heat storage materials in TES systems, PCMs must also possess certain desirable thermodynamic, kinetic, chemical, technical, and economic characteristics. Some of the criteria considered in evaluating PCMs follow (Abhat, (1983); Dincer *et al.*, 1997b):

#### Thermodynamic criteria:

- a melting point at the desired operating temperature;
- a high latent heat of fusion per unit mass, so that less amount of material stores a given amount of energy;
- a high density, so that less volume is occupied by the material;
- a high specific heat, so that significant sensible TES can also occur;
- a high thermal conductivity, so that small temperature differences are needed for charging and discharging the storage;
- congruent melting, that is, the material should melt completely, so that the liquid and solid phases are homogeneous (this avoids the difference in densities between solid and liquid that causes segregation, resulting in changes in the chemical composition of the material); and
- small volume changes during phase transition, so that a simple containment and heat exchanger can be used.

#### Kinetic criterion:

- little or no supercooling during freezing, that is, the melt should crystallize at its freezing point. This criterion can be achieved through a high rate of nucleation and growth rate of the crystals. Supercooling may be suppressed by introducing a nucleating agent or a cold trigger into the storage material.

#### Chemical criteria:

- chemical stability;
- no susceptibility to chemical decomposition, so that a long operation life is possible;

- noncorrosive behavior to construction materials; and
- nontoxic, nonflammable, and nonexplosive characteristics.

**Technical criteria:**

- simplicity,
- applicability,
- effectiveness,
- compactness,
- compatibility,
- viability, and
- reliability.

**Economic criteria:**

- commercial availability, and
- low cost.

**Applications of PCMs**

There are many different methods of using PCM storage systems for heating or cooling buildings, as demonstrated by the following concepts (Lane, 1988):

- A PCM melting at 5–15 °C could be used for cool TES. The PCM is frozen by operating a chiller at night, when electricity demand and prices are low, and melted during the day to cool the building.
- A PCM melting near room temperature, for example,  $\text{CaCl}_2 \cdot 6\text{H}_2\text{O}$ , which has a melting point (m.p.) of 27 °C, could be incorporated into a building structure to temper diurnal swings in ambient temperature.
- A building could be heated and cooled using heat pumps that are connected to circulating water tempered by a PCM melting at 20–35 °C, for example,  $\text{CaCl}_2 \cdot 6\text{H}_2\text{O}$  (m.p. = 27 °C).
- A solar hot-air heating system could use a PCM melting at 25–30 °C, for example,  $\text{CaCl}_2 \cdot 6\text{H}_2\text{O}$ , to provide night-time heating and as a preheat for daytime heating.
- A solar hot-air heating system could use a PCM melting at 40–60 °C, for example,  $\text{Mg}(\text{NO}_3)_2 \cdot 6\text{H}_2\text{O} - \text{MgCl}_2 \cdot 6\text{H}_2\text{O}$  eutectic (m.p. = 58 °C), for day and night heating.
- Domestic hot water could be preheated in a tank filled with an encapsulated PCM melting at 55–70 °C, for example,  $\text{Mg}(\text{NO}_3)_2 \cdot 6\text{H}_2\text{O} - \text{MgCl}_2 \cdot 6\text{H}_2\text{O}$  eutectic.
- A solar hot-water baseboard system could employ a PCM melting at 60–95 °C, for example,  $\text{Mg}(\text{NO}_3)_2 \cdot 6\text{H}_2\text{O}$  (m.p. = 89 °C).
- Off-peak electricity could be used to melt a PCM (with m.p. above 25 °C) to heat a building during later periods.
- Concentrated solar energy could be used with a PCM melting at 100–175 °C, for example,  $\text{Mg}(\text{NO}_3)_2 \cdot 6\text{H}_2\text{O}$  (m.p. = 117 °C), to drive an absorption air-conditioner.

**Evaluation of PCMs**

In the evaluation and selection of a PCM, a good understanding of various aspects, including freezing or solidification, supercooling, nucleation, thermal cycling, encapsulation, and compatibility is needed.

- **Freezing or solidification.** Many materials are not suitable as PCMs because of their freezing or solidification behavior. Some have incongruent freezing behavior. Others crystallize exceedingly

slowly, form viscous mixtures, or are not stable over the range of temperatures. Some materials have near-congruent freezing behavior and so may be suitable as PCMs. To overcome the solidification problem, the nucleation rate can be increased by two methods: homogeneous nucleation and heterogeneous nucleation.

- **Supercooling.** A major problem associated with salt hydrates as PCMs is the fact that they tend to supercool considerably. This behavior is of major importance, and has not always received sufficient attention from workers in the field. The reason for the high degree of supercooling is the fact that either the rate of nucleation (of crystals from the melt) or the rate of growth of these nuclei (or both) is very slow. Therefore, as the melt is cooled, it does not solidify at the thermodynamic melting point. Thus, the advantage of the material for heat storage is reduced. The reason for the strong tendency to supercool is well understood. Some empirical evidence connects the tendency to supercool with the viscosity of the melt at the melting point. Materials with high viscosity in the liquid state have low diffusion coefficients for their constituent atoms (or ions), and these may be unable to rearrange themselves to form a solid; instead the liquid supercools. Supercooling occurs when, in attempting to freeze the material, the temperature drops well below the melting point before freezing initiates. Once the freezing process begins, the temperature rises to the melting point where it remains until the material is entirely frozen. Supercooling behavior is undesirable in heat storage systems. If excessive, it can prevent the withdrawal of stored heat from the PCM.
- **Nucleation.** Supercooling can often be mitigated by adding nucleating materials. Some success has been attained by using additives with a crystal structure similar to that of the PCM. Often this fails. Usually nucleating additives are discovered by trial and error. Using these approaches, effective nucleating additives have been discovered for zinc nitrate hexahydrate, calcium chloride hexahydrate, magnesium chloride hexahydrate, magnesium nitrate hexahydrate and its eutectics with magnesium chloride hexahydrate or ammonium nitrate. In homogeneous nucleation, the rate of nucleation of crystals from the melt is increased without adding any foreign materials. One way in which this can be done is to use ultrasonic waves in which we stir the liquid, and thus increase the diffusion of ions in the melt; they also create cavities that act as nucleation centers and, finally, they break up the forming crystals and distribute them through the melt, creating new nucleation centers. Many crystals, such as sodium thiosulfate and potassium alums, have been nucleated from more dilute solutions. Also, other classes of materials, such as metals and organic crystals, have been nucleated by ultrasonic waves. In heterogeneous nucleation, the walls of the container, or some impurity present within the melt, act as a catalyst for nucleation by providing a substrate on which the nuclei can form. In order for an impurity to be an effective nucleating agent, it should satisfy the following criteria:
  - have a melting point higher than the highest temperature reached by the energy storage material in the storage cycle;
  - be insoluble in water at all temperatures;
  - not form solid solutions with the salt hydrate;
  - have a crystal structure similar to that of the salt hydrate;
  - have unit cell dimensions that do not vary by more than 10% from those of the salt hydrate; and
  - not chemically react with the hydrate.
- **Thermal cycling.** Practical heat storage PCMs must be able to undergo repetitive cycles of freezing and thawing. Some unsuitable materials exhibit changes within a relatively short time. Some experimental results demonstrate this. After 21 cycles from 95 to 20 °C, palmitic acid, normally white, takes on a yellowish color, and the melting point diminishes by 2 °C. The eutectic of 25.1% propionamide and 74.9% palmitic acid progressively discolors from white to yellow, orange, and then black, although little change occurs in the freezing curve (Lane, 1988).
- **Encapsulation.** Successful utilization of a PCM requires a means of containment. For active solar systems with a liquid heat-transfer medium, tanks with coil-type heat exchangers are appropriate. For passive or air-cooled active solar systems, much effort has centered on the packaging of a mass of PCM in a sealed container, which itself serves as the heat exchange surface.

Potential containers include steel cans, plastic bottles, polyethylene, and polypropylene bottles, high-density polyethylene pipe, flexible plastic film packages, and plastic tubes. The choice of the construction material for the container of a PCM is important. Appropriate tests that are realistic and representative of usage conditions are needed in any product development. The container material should be an effective barrier that prevents loss of material or water or, when the PCM is hygroscopic, gain water. Oxygen penetration and subsequent oxidization may also be detrimental. The encapsulating material should also be a good heat conductor, so that it facilitates effective heat transfer, and be mechanically resistant to damage from handling, processing, and transport. Systems based on salt hydrates may sometimes have encapsulation problems, particularly in early designs, because of corrosion and fatigue for metals, or water loss through plastics.

- **Compatibility.** To determine the suitability of encapsulant materials, PCMs are subject to compatibility tests with packaging materials. For example, a plastic–aluminum foil laminate is not suitable for use with organic PCMs, because the heat-sealed seam is attacked by the organic material, and it is unsuitable for temperatures above 70 °C. Paraffins are compatible with most metals and alloys, but they can impregnate and soften some plastics.

### Characteristics and Thermophysical Properties of PCMs

The precise determination of the transition zone at fusion and at solidification is essential for the optimal design of a latent TES unit, since the transition zone of the PCM must match, sometimes exactly, the intended operating temperature span of the latent TES unit. Pure substances have exact melting and freezing points, but they are affected by impurities even in small amounts. Polymers and mixtures have a more complex behavior, with a true, and sometimes very broad, transition zone over which fusion or solidification is progressive. Salt hydrates, when pure, behave as pure substances and afford little design flexibility. Design options based on salt hydrates are rather limited in the range 15–65 °C, because their fusion–solidification behavior cannot be easily modified. Thermophysical properties of paraffins generally change monotonously as a function of chain length (e.g., melting temperature). An important advantage of paraffins is that neighboring homologs are totally compatible and that stable, homogeneous mixtures can be readily prepared. It is thus possible to design paraffin-based PCMs meeting a wide variety of transition-zone specifications (Paris *et al.*, 1993). Formulating a compound PCM for a given transition range is a key task in which composition, thermophysical properties, and most other characteristics are fixed. However, properties of mixtures cannot be calculated from simple interpolation of properties of pure components, and therefore experimental characterization is required.

The heat storage capacity of a latent TES is primarily a function of the heat of fusion of the PCM. The heat of fusion of paraffins increases with chain length until 24 and is generally higher than that of salt hydrates. The heat of fusion of salt hydrates increases with the degree of hydration, but higher hydration often comes with incongruent or semicongruent fusion (Lane, 1988).

The specific heats of solid and liquid PCMs are not critical factors in the performance of a system unless the operating span of the storage unit far exceeds the transition zone of the PCM. Then, the mode of operation tends toward sensible heat storage and the relative contribution of latent heat to its performance diminishes. Since a PCM changes temperature during operation, heat transfer over a charge (or discharge) cycle includes sensible heat. Paraffins generally have higher specific heats in both the solid and liquid states than salt hydrates.

Heat transfer to and from a storage unit strongly depends on the thermal conductivities of the solid and liquid PCM. The higher the conductivities, the more efficient the heat transfer for a given design. However, the heat-transfer phenomena during fusion or solidification of a PCM are very complex because of the moving solid–liquid interface, the density and conductivity differences between the two phases, and the induced movements in the liquid phase. Salt hydrates have higher thermal conductivities than those of paraffins.

The density of a PCM is important, because it affects its storage effectiveness per unit volume. Salt hydrates are generally more dense than paraffins, but are slightly more effective on a per volume

basis, despite a slightly lower heat of fusion. The rate of crystallization of a salt hydrate can be low, and can become the limiting factor in the rate of heat storage and restitution. Crystallization is generally more rapid for paraffins, and heat-transfer mechanisms are then the limiting factors. In addition, paraffins exhibit little or no supercooling, which is frequent and often significant in magnitude with salt hydrates.

Paraffins have very low vapor pressures, which leads to low long-term loss of material and flammability. Salt hydrates have significantly higher vapor pressures, which induce water loss and progressive changes of thermal behavior. The vapor pressure of salt hydrates increases with the degree of hydration, and salt hydrates exhibit variable chemical stability and can be subject to long-term degradation by oxidization, hydrolysis, thermal decomposition, and other reactions. Some salt hydrates are very corrosive in the presence of water. Paraffins are very stable and unreactive, but slow oxidization may occur when they are exposed to air at elevated temperatures over extended periods. Paraffins are not corrosive.

Salt hydrates are neither toxic nor flammable. They can be irritants, and contact with skin and eyes should be avoided. Paraffins are innocuous, being neither toxic nor irritants. Although paraffins are flammable in the presence of oxygen and at elevated temperatures, because of their low vapor pressure they are considered low fire hazards. Compliance with safety codes for products containing paraffin-based PCMs should not present particular difficulties if this point is properly addressed in the design stage.

Table 3.9 presents experimental data on melting temperature, heat of fusion, thermal conductivity and density data for several organic and inorganic compounds, aromatics, and fatty acids.

Latent TES using PCMs provides an effective way to store thermal energy from a range of sources, high storage capacity, and heat recovery at almost constant temperatures. The relatively constant temperature of storage can maximize solar collector efficiency, where relevant.

### Performance of Latent TES with PCMs

To improve the performance of latent TES with PCMs, nucleating agents and thickeners have been used to prevent supercooling and phase separation. Also, extended heat-transfer surfaces can be used to enhance the heat transfer from PCM to the heat-transfer tubes. While many studies on the latent TES systems have been performed at relatively low temperatures (below 100 °C) for TES in home heating and cooling units, few studies have been undertaken for higher temperature heat (above 200 °C), as is applicable for some solar energy systems and intermediate-temperature latent TES. Magnesium chloride hexahydrate ( $\text{MgCl}_2 \cdot 6\text{H}_2\text{O}$ ), with a melting temperature of 116.7 °C, is an attractive high-temperature PCM in terms of cost, material compatibility, and thermophysical properties (a specific latent heat of 168.8 kJ/kg, a specific heat of 2.25 kJ/kgK in the solid state and 2.61 kJ/kgK in the liquid state, a thermal conductivity of 0.704 W/mK in the solid state and 0.570 W/mK in the liquid state, and a density of 1570 kg/m<sup>3</sup> in the solid state and 1450 kg/m<sup>3</sup> in the liquid state) (Choi and Kim, 1995).

Sharma *et al.* (1992) showed that the acetamide–sodium bromide eutectic is a promising latent TES material that could find use in such applications as commercial and laundry water heating, process heating, domestic water and air heating, crop drying, and food warming. Vaccarino *et al.* (1985) conducted an experimental study on the low-temperature latent TES and found that two mixtures containing  $\text{Ca}(\text{NO}_3)_2 \cdot 4\text{H}_2\text{O}$  and  $\text{KNO}_3$  or  $\text{Mg}(\text{NO}_3)_2 \cdot 6\text{H}_2\text{O}$  are suitable PCMs for passive heating of such facilities as buildings and greenhouses in the temperature range 15–35 °C, and for domestic hot water production and active space heating in the range 25–55 °C.

Although PCMs must usually be placed in capsules or other vessels to prevent them from mixing with heat carriers after melting, concepts have recently been developed that permit PCMs to come into direct contact with heat carriers, thereby providing good heat exchange without the usual heat exchangers or capsules. In such a system, an immiscible fluid is bubbled into the storage bottom

**Table 3.9** Measured thermophysical data of some PCMs

Compound	Melting temp. (°C)	Heat of fusion (kJ/kg)	Thermal conductivity (W/mK)	Density (kg/m <sup>3</sup> )
<b>Inorganics</b>				
MgCl <sub>2</sub> · 6H <sub>2</sub> O	117	168.6	0.570 (liquid, 120 °C)	1450 (liquid, 120 °C)
			0.694 (solid, 90 °C)	1569 (solid, 20 °C)
Mg(NO <sub>3</sub> ) <sub>2</sub> · 6H <sub>2</sub> O	89	162.8	0.490 (liquid, 95 °C)	1550 (liquid, 94 °C)
			0.611 (solid, 37 °C)	1636 (solid, 25 °C)
Ba(OH) <sub>2</sub> · 8H <sub>2</sub> O	78	265.7	0.653 (liquid, 85.7 °C)	1937 (liquid, 84 °C)
			1.255 (solid, 23 °C)	2070 (solid, 24 °C)
Zn(NO <sub>3</sub> ) <sub>2</sub> · 6H <sub>2</sub> O	36			1828 (liquid, 36 °C)
CaBr <sub>2</sub> · 6H <sub>2</sub> O	34	146.9	0.464 (liquid, 39.9 °C)	1937 (liquid, 84 °C)
			–	1956 (liquid, 35 °C)
CaCl <sub>2</sub> · 6H <sub>2</sub> O	29	115.5	–	2194 (solid, 24 °C)
			–	1562 (liquid, 32 °C)
		190.8	0.540 (liquid, 38.7 °C)	1802 (solid, 24 °C)
			1.088 (solid, 23 °C)	
<b>Organics</b>				
<b>Paraffin wax</b>				
Paraffin wax	64	173.6	0.167 (liquid, 63.5 °C)	790 (liquid, 65 °C)
			0.346 (solid, 33.6 °C)	916 (solid, 24 °C)
Polyglycol E400	8	99.6	0.187 (liquid, 38.6 °C)	1125 (liquid, 25 °C)
			–	1228 (solid, 3 °C)
Polyglycol E600	22	127.2	0.187 (liquid, 38.6 °C)	1126 (liquid, 25 °C)
			–	1232 (solid, 4 °C)
Polyglycol E6000	66	190.0	–	1085 (liquid, 70 °C)
			–	1212 (solid, 25 °C)
<b>Fatty acids</b>				
<b>Stearic acid</b>				
Stearic acid	69	202.5	–	848 (liquid, 70 °C)
				965 (solid, 24 °C)
Palmitic acid	64	185.4	0.162 (liquid, 68.4 °C)	850 (liquid, 65 °C)
			–	989 (solid, 24 °C)
Capric acid	32	152.7	0.153 (liquid, 38.5 °C)	878 (liquid, 45 °C)
			–	1004 (solid, 24 °C)
Caprylic acid	16	148.5	0.149 (liquid, 38.6 °C)	901 (liquid, 30 °C)
			–	981 (solid, 13 °C)
<b>Aromatics</b>				
<b>Biphenyl</b>				
Biphenyl	71	119.2	–	991 (liquid, 73 °C)
			–	991 (liquid, 73 °C)
Naphthalene	80	147.7	0.132 (liquid, 83.8 °C)	976 (liquid, 84 °C)
			0.341 (solid, 49.9 °C)	1145 (solid, 20 °C)

Source: Lane (1980).

of the fused PCM and heat is transferred as the droplets rise. Here, the immiscible fluid agitates the PCM so that the disadvantage of supercooling is minimized (Sokolov and Keizman, 1991).

Over 20,000 compounds and/or mixtures have been considered as PCMs, including single-component systems, congruent mixtures, eutectics, and peritectics. Criteria being investigated include melting point, phase-diagram characteristics, toxicity, stability, corrosivity, flammability, safety, availability, and cost. Over 200 compositions, organic and inorganic compounds, eutectics, and other mixtures have been considered as promising (Lane, 1988).

Sokolov and Keizman (1991) developed an attractive PCM application for hot water heating. The system contains a solar pipe consisting of two concentric pipes with the space between them filled with PCM (Figure 3.17). Solar radiation is directly absorbed on the outer surface and then



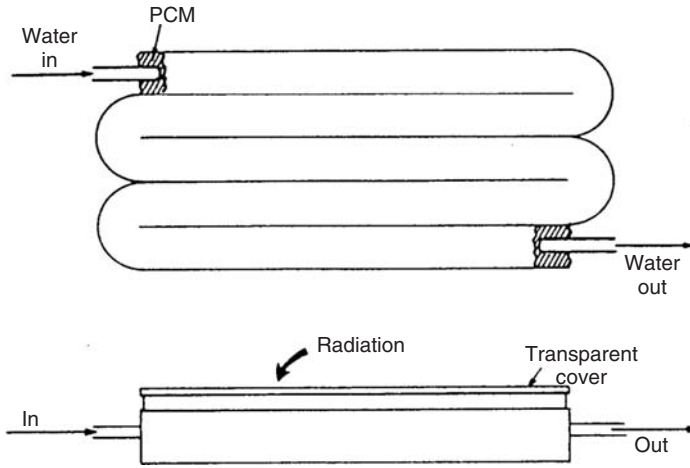


Figure 3.17 A solar TES pipe using a PCM (Sokolov and Keizman, 1991)

transmitted to the PCM, where it is stored as sensible and latent heat. During energy release, heat is exchanged between a water flow through the inner tube and the PCM storage, and hot water is delivered at the discharge of the solar pipe.

In this system, direct solar radiation absorption onto the PCM container and direct heating of water eliminate the need for energy transport media. Some advantages of the system include

- simple construction;
- efficient and compact latent heat storage;
- elimination of expensive components such as a water tank, pump, and control devices;
- suitability of the system for modular construction and installation;
- protection against freezing.

Solar TES as latent heat has an enormous potential. With latent heat, the temperature of the phase change medium stays fixed. The most common PCM for solar applications is Glauber's salt ( $\text{Na}_2\text{SO}_4 \cdot 10\text{H}_2\text{O}$ ).

Two approaches are under development to improve the performance of phase change storage. One approach is to increase the temperature at which PCMs such as salts change phase, and the other is to employ the use of a heat pump. The heat pump raises the temperature of the heat extracted from the phase change storage to a temperature high enough to satisfy the thermal needs.

A further advantage of using a PCM is its capability to store up to nine times more energy for the same volume of containment occupied by rocks. This characteristic is particularly advantageous for retrofits (e.g., adding a solar energy system to an existing dwelling). One of the prime difficulties in solar retrofits is locating and charging the store. The volume and mass of sensible TES in rocks or water limit applications. On the other hand, the relatively low mass and volume of PCM often makes it a good choice for retrofits. These characteristics permit latent TES to be located in attic spaces, closets, or even sandwiched between floors and ceilings.

### Selection of PCMs for Latent TES

No material has all the optimal characteristics for a PCM, and the selection of a PCM for a given application requires careful consideration of the properties of various substances. Among PCMs, sodium acetate trihydrate deserves special attention for its large latent heat of fusion–crystallization



(264–289 kJ/kg) and its melting temperature of 58–58.4 °C. However, this substance exhibits significant subcooling, preventing most practical large-scale applications, even though attempts have been made to find ways of suppressing or reducing this phenomenon.

Energy balance simulations of a PCM wall as a TES in a passive direct gain solar house suggest that the PCM melting temperature should be adjusted from the climate-specific optimum temperature to achieve maximum performance of the storage. A nonoptimal melting temperature significantly reduces the latent heat storage capacity, for example, a 3 °C nonoptimality temperature causes a 50% loss (Dincer and Dost, 1996).

Of practical importance in the selection of PCMs for solar and other thermal applications are thermophysical properties such as

- heat of fusion,
- heat capacity of solid and liquid,
- thermal conductivity of solid and liquid, and
- density of solid and liquid.

Another important factor in PCM selection is supercooling and nucleation. Several PCMs exhibit supercooling, that is, on attempting to freeze the material the temperature drops well below the melting point before freezing initiates. Although the temperature rises to the melting point once freezing begins, supercooling is nevertheless undesirable in latent TES because it can prevent the withdrawal of stored heat. For this reason, nucleative materials are sometimes used.

### The STL system

Peak cooling loads for buildings are often at a level two or more times higher than the average daily load. Some industrial processes also have load peaks that are much greater than the average load. Since many electric utilities impose demand charges based on a customer's highest power demand during on-peak hours and/or during the entire billing cycle, TES can be beneficial. The STL (*le stockage latent* in French, or latent heat storage) latent TES can be an efficient solution for these applications. The STL is composed of a tank filled with spherical nodules. The tank has upper manholes to allow the filling with nodules. A lower manhole allows emptying. Inside the tank two diffusers (inlet and outlet) spread the heat-transfer fluid along the tank. The pressure drop through the tank is 2.5 mWG. The inlet in charge mode must be via the lower diffuser in order to ensure the natural stratification.

The tanks are manufactured with black steel (test pressure between 4.5 to 10 bar), are delivered empty and positioned on site or, if access to the site is impossible, constructed on site. The nodules are spherical with a diameter of 77 mm, 78 mm, or 98 mm (depending on the nodule type).

The nodules (Figure 3.18a) contain the PCM. The mechanical and chemical characteristics of the nodule shell (manufactured with polyolefin) are well adapted to the conditions encountered in

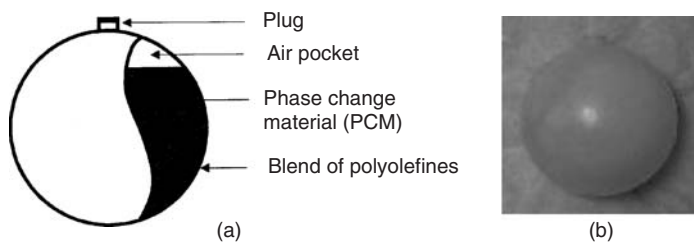


**Figure 3.18** (a) The nodule for STL system (Courtesy of Cristopia Energy Systems), and (b) a capsule for the new STL latent TES (Courtesy of Mitsubishi Chemical Co.)

air-conditioning or refrigeration systems. Once filled with PCM, the nodule plugs are sealed by ultrasonics to ensure perfect water tightness. The nodules are delivered in 22-kg bags. Tanks are filled on site. The filling is regular and homogeneous. Filling procedures are described elsewhere (for details, see Cristopia, 2000).

The shape of the tank is usually cylindrical in order to withstand service pressure higher than 3 bar. The test pressure varies between 4.5 and 10 bar. The spherical shape also allows an easy filling. The nodule diameter has been calculated to meet economical and technical requirements. The size allows high exchanges until the end of the cycle.

The use of modern technologies permits quality control. The materials used are completely neutral to the PCMs and heat-transfer fluid. This product development work has led to a very high reliability of the STL. The temperature range offered is  $-33$  to  $+27$  °C.

It is important to mention that in the STL system the quantity of energy stored for each type of nodule is proportional to the storage volume. The number of nodules in a system determines the heat exchange rate between the nodules and the heat-transfer fluid.

In the terminology, an STL is determined by the phase change temperature and the volume (i.e., the storage capacity and the heat exchange rate). There are three types of nodules characterized by their diameter: AC (98 mm), IC, and IN (78 mm) (Cristopia, 2000), such as

- **STL-AC.00-15.** Where AC: 98-mm diameter nodules, 00: phase change temperature in OC, and 15: tank volume in  $m^3$ .
- **STL-IN.15-50.** Where IN: 78-mm diameter nodules for negative temperature, 15: the phase change temperature (melting) is  $-15$  °C, and 50: tank volume in  $m^3$ .
- **STL-IC.27-100.** Where IC: 78-mm diameter nodules, 27: the phase change temperature (melting) is  $+27$  °C, and 100: tank volume in  $m^3$ .

The features and characteristics of the nodules can be summarized as follows (Cristopia, 2000):

- material is a blend of polyolefins;
- chemically neutral toward eutectics and heat-transfer fluid;
- thickness is 1.0 mm; there is no migration of the heat-transfer fluid;
- sphere is obtained by blow moulding and there is no leakage;
- sealing of the cap is by ultrasonic welding;
- exterior diameter is 98 mm for air-conditioning and 78 or 77 mm for industrial cooling or backup;
- exchange surface diameter is 78 or 77 mm for  $1.0 m^2/kWh$  stored and the diameter is 98 mm for  $0.6 m^2/kWh$  stored;
- air pocket for expansion; no stress on the nodule shell;
- useful number of nodules per  $m^3$ ; diameter is 77 mm for 2548 nodules per  $m^3$ , 78 mm for 2444 nodules per  $m^3$ , and 98 mm for 1222 nodules per  $m^3$ .

The characteristics of the STL tanks can be summarized as follows (Cristopia, 2000):

- black steel,
- horizontal or vertical,
- outside, inside, buried, built on-site,
- rustproof exterior paint,
- insulation on-site,
- efficient diffuser system,
- high service pressure,
- pressure drop of 2.5 mWG,
- made to measure according to site requirements.

The Energy Research Group in Japan in collaboration with Mitsubishi Chemical Co. is investigating the performance of the STL system in combination with storage tanks developed for solar energy utilization. The STL system consists of salts and hydrates contained in plastic capsules (Figure 3.18b), where the thermal energy is stored during hydration of the thermally dehydrated salt. Different PSMs that operate at a wide range of storage temperatures are suitable for various applications such as domestic hot water, space heating, and cooling.

Traditional refrigeration systems are designed to satisfy the peak cooling demand, which occurs only a few hours per year, and thus spend most of their operational lives working at reduced capacity and lower efficiency. The STL system, which is suitable for any air-conditioning system or refrigeration plant, allows installed chiller capacity (and the size of other components) to be significantly reduced – typically between 40 and 60%. The STL system provides the shortfall of the energy when demand exceeds chiller capacity. Thus, chiller operation is continuous and at maximum efficiency. The result is reduced operating costs for refrigeration and building air-conditioning by taking advantage of lower cost off-peak electricity and reducing demand charges. The STL system allows real management of the cooling energy according to the demand. In addition, the STL allows the consumption of night-time electricity produced with a higher efficiency (2300 kcal/kWh compared to 3500–4000 kcal/kWh at peak hours), resulting in a reduction in CO<sub>2</sub> emissions and energy consumption. The reduction in the chiller size also reduces the quantity of refrigerant used, which is important with increasingly strict laws on refrigerants.

### Heat Pump Latent TES

A heat pump was integrated with latent TES to enable quick room temperature increases and defrosting. This inverter-aided room air-conditioner/heat pump was put on the market by Daikin Industries Ltd. in Japan in 1989. The latent TES consists of the PCM, polyethylene glycol, which surrounds a rotary compressor, as shown in Figure 3.19. Heat released from the compressor is transferred to the TES through a finned-tube heat exchanger. The TES is used during start-up and during defrosting. During start-up, the TES reduces the time required to reach a 45 °C discharge air temperature by 50%. During defrosting, a heating capacity of 3.5 kW is made available by the TES, which avoids a drop in room temperature. Integrating the system improved heat capacity by about 10% and COP by 5%. The characteristics of the system were also improved with TES. The installation space required is the same as that for a conventional heat pump/air-conditioner.

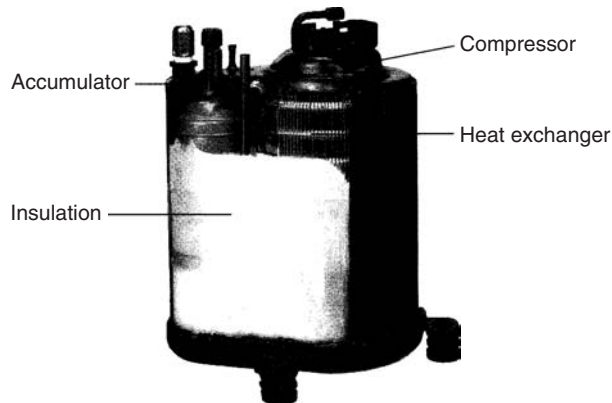


**Figure 3.19** A latent TES integrated with a heat pump (IEA, 1990)

### 3.8 Cold Thermal Energy Storage (CTES)

Cooling capacity can be stored either by chilling or freezing water (or such other materials as glycol and eutectic salts). Water is the storage material of choice for a variety of practical and thermodynamic reasons, including its ready availability, relative harmlessness, and its compatibility with a wide availability of equipments for its storage and handling. The choice of whether the water should be used in sensible or latent types, which equipment should be used, if eutectic salts should be applied to raise freezing temperatures, and so on, is often not simple. Options are numerous, and answers are not clear-cut. Ultimately, the CTES method selected must meet the particular needs and constraints of the specific facility in which it is installed.

CTES is an innovative way of storing night-time off-peak energy for daytime peak use. In many locations, demand for electrical power peaks during summer. Air-conditioning is the main reason, in some areas accounting for as much as half of the power demand during the hot mid-day hours when electricity is most expensive. Since, at night, utilities have spare electrical generating capacity, electricity generated during this “off-peak” is much less expensive.

In essence, one can air-condition during the day using electricity produced at night. CTES has become one of the primary means of addressing the electrical power imbalance between high daytime demand and high night-time abundance. If properly designed, installed, operated, and maintained, CTES systems can be used to shift peak cooling loads to off-peak periods, thereby evenly distributing the demand for electricity and avoiding shortages usually encountered during peak periods.

Although the phrase “cool TES” may appear to be contradictory, it is not. The phrase TES is widely used to describe storage of both heating and cooling energy. TES for heating capacity usually involves using heat at above environment temperatures from a variety of sources to heat a storage medium for later use. In contrast, cold TES uses off-peak power to provide cooling capacity by extracting heat from a storage medium, such as ice, chilled water, or PCMs. Typically, a CTES system uses refrigeration equipment at night to create a reservoir of cold material, which is tapped during the day to provide cooling capacity. In this book, the abbreviation CTES represents both cool and cold TES.

CTES has many advantages. Lower night-time temperatures allow refrigeration equipment to operate more efficiently than during the day, reducing energy consumption. Lower chiller capacity is required, which leads to lower equipment costs. Also, using off-peak electricity to store energy for use during peak demand hours, daytime peaks of power demand are reduced, sometimes deferring the need to build new power plants.

CTES systems are presently operational in many commercial and industrial buildings in various countries. Some are not achieving expected design performance, often because TES design engineers and construction companies in the past lacked experience. Now, package-type TES systems are available and are commonly used, which involve more straightforward design and installation for conventional air-conditioning systems. Therefore, the economic and other benefits of TES operating performance at design conditions for system owners are more likely to be attained.

#### 3.8.1 Working Principle

CTES systems, which have the potential to provide substantial operating cost savings, are most likely to be cost effective in situations where

- a facility’s maximum cooling load is much greater than the average load;
- the utility rate structure has higher demand charges for peak demand periods;
- an existing cooling system is being expanded;
- an existing tank is available;
- limited on-site electric power is available;
- backup cooling capacity is desirable;
- cold air distribution is desirable or advantageous.

It is difficult to generalize about when cool storage systems will be cost effective, but if one or more of the above criteria are satisfied, a detailed analysis may prove worthwhile.

Some CTES systems generate ice during off-peak hours and store it for use in daytime cooling. Until recently, decreasing electricity costs and an abundance of reliable cooling equipment had slowed the development of this technology, which has existed for more than half a century. Today, increases in maximum power demands, major changes in electric rate structures, and the emergence of utility-sponsored incentive programs have inspired a renewed interest in CTES. For instance, utility companies often experience peak electrical demands for 4 to 6 h on hot summer afternoons, when air-conditioning loads also peak, and apply time-of-use rates to discourage energy consumption during these peak demand periods. One objective is for the air chiller to be shut down during peak-load hours and to have a TES system that provides cooling for the facility at those times.

An ice-ball system uses chillers to build ice at night. The ice balls float in a glycol solution that runs through chillers in the evening. These chillers, which are set at  $-7.5$  to  $-6.5$  °C, freeze the ice balls in the storage tanks, and the glycol circulates around the ice balls. Chilled glycol is pumped into the bottom of the tank to freeze the ice balls, and warms as it rises and extracts heat from the ice balls. Later, the cycle is reversed and the glycol is pumped into the top of the tank and past the ice balls. The cold glycol solution then passes through heat exchangers and is connected to the building's chilled-water system, which interfaces with the air handler. Cooling is thus obtained while only operating the fans on the air handlers, but cooling is the same if chillers are operated with the air-handling units.

### 3.8.2 Operational Loading of CTES

Several strategies are available for charging and discharging a storage to meet cooling demand during peak hours. The main strategies are full storage and partial storage.

#### Full-Storage CTES

A full-storage strategy shifts the entire peak cooling load to off-peak hours (Figure 3.20a). The system is typically designed to operate on the hottest anticipated days at full capacity during all nonpeak hours in order to charge the storage. This strategy is most attractive when peak demand charges are high or the peak period is short.

Full-storage (load-shifting) designs are those that use storage to fully decouple the operation of the heating or cooling generating equipment from the peak heating or cooling load. The peak heating

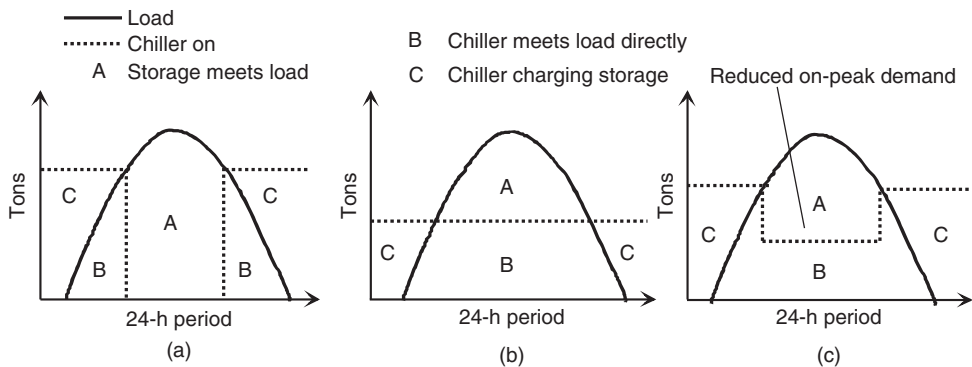


**Figure 3.20** Operating strategies: (a) full-storage, (b) partial-storage load leveling, and (c) partial-storage demand limiting

or cooling load is met through the use (i.e., discharging) of the storage while the heating or cooling generating equipment is idle. Full-storage systems are likely to be economically advantageous only under one or more of the following conditions:

- spikes in the peak load curve are of short duration;
- time-of-use energy rates are based on short-duration peak periods;
- there are short overlaps between peak loads and peak energy periods;
- large cash incentives are offered for using TES;
- high peak-demand charges apply.

For example, a school or business whose electrical demand drops dramatically after 5 p.m. in an electric utility territory where peak energy and demand charges apply between 1 p.m. and 9 p.m. can usually economically apply a full CTES. Cooling during the 4-h period between 1 p.m. and 5 p.m. can be fully shifted, that is, can be met with a relatively small and cost-effective CTES system and without oversizing the chiller equipment.

### Partial-Storage CTES

In a partial-storage method, the chiller operates to meet part of the peak-period cooling load, and the rest is met by drawing from storage. The chiller is sized at a smaller capacity than the design load. Partial-storage systems may operate as load-leveling or demand-limiting operations. In a load-leveling system (Figure 3.20b), the chiller is sized to run at its full capacity for 24 h on the hottest days. The strategy is most effective where the peak cooling load is much higher than the average load. In a demand-limiting system, the chiller runs at reduced capacity during peak hours, and is often controlled to limit the facility's peak demand charge (Figure 3.20c). Demand savings and equipment costs are higher than they would be for a load-leveling system, and lower than those for a full-storage system.

Partial storage is more often the most economic option, and therefore represents the majority of thermal storage installations. Although partial storage does not shift as much load (on a design day) as a full-storage system, partial-storage systems can have lower initial costs, particularly if the design incorporates smaller equipment by using low-temperature water and cold-air distribution systems.

For many applications, a form of partial storage known as *load leveling* can be used with minimum capital cost. A load-leveling system is designed with the heating or cooling equipment sized to operate continuously at or near its full capacity to meet design-day loads. Thus, equipment having minimum capacity (and cost) can be used. During operation at less than peak design loads, partial-storage designs can function as full-storage systems. For example, a system designed as a load-leveling partial storage for space heating at winter design temperatures may function as a full storage (with a full demand shift) on mild spring or autumn days.

### 3.8.3 Design Considerations

CTES can take many forms to suit a variety of applications. This section addresses several groups of CTES applications: off-peak air-conditioning, industrial/process cooling, off-peak heating, and other applications.

Selecting a storage system and its characteristics usually requires a detailed feasibility study. An analysis is involved, and is best accomplished following an established procedure. Data needed for feasibility analysis can include (i) an hour-by-hour 24-h building-load profile for the design day, and (ii) a description of a baseline non-storage system, including chiller capacity, operating conditions, and efficiency. The description of a CTES often stipulates the following:

- the sizing basis (full storage, or load leveling, or demand limiting);

- sizing calculations showing chiller capacity and storage capacity, and considering the required supply temperature;
- the design operating profile, showing load, chiller output, and amount of heat added to or taken from storage for each hour of the design day;
- chiller operating conditions while charging the storage, and, if applicable, when meeting the load directly;
- the chiller efficiency under each operating condition;
- a description of the system control strategy, for the design-day and part-load operation.

An operating-cost analysis includes

- an evaluation of demand savings;
- a determination of changes in energy consumption and cost;
- a description and justification of the assumptions used for annual energy demand and use estimates.

Storage equipment manufacturers often provide simulations of storage performance for a given load profile and chiller temperature to assist design efforts.

Although applications and technologies vary significantly, certain characteristics and design options are common to all TES systems. Whether for heat or cool storage, and whether for storing sensible or latent heat, storage designs follow one of two control strategies: full storage or partial storage (Figure 3.21).

The following steps should be considered for all ice TES refrigeration systems:

- **Design for part-load operation.** Refrigerant flow rates, pressure drops, and velocities are reduced during part-load operation. Components and piping must be designed so that, at all load conditions, control of the system can be maintained and the working fluid can be returned to the compressors.
- **Design for pull-down load.** Because ice-making equipment is designed to operate at water temperatures approaching 0°C, a higher load is imposed on the refrigeration system during the initial start-up, when the inlet water is warmest. The components must be sized to handle this higher load.

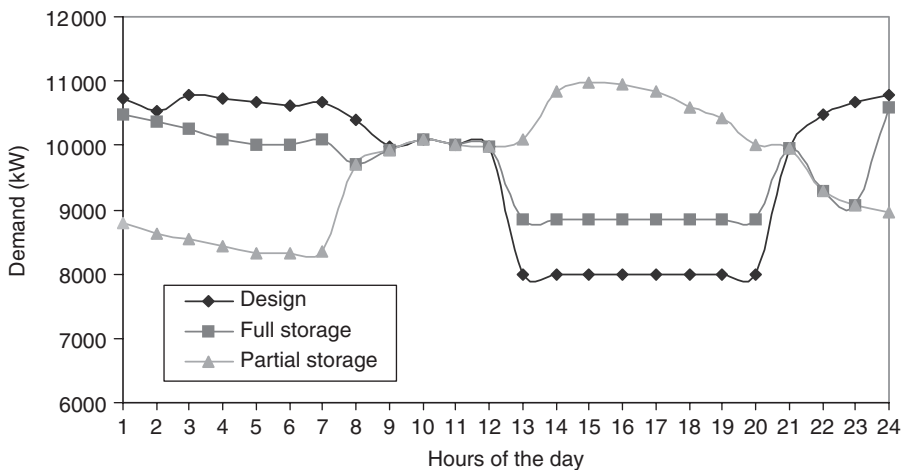


Figure 3.21 Sample demand profiles for the design, full-storage and partial-storage systems



- **Plan for chilling versus ice making.** Most ice-making equipment has a much higher instantaneous chilling capacity than ice-making capacity. This higher chilling capacity can be used advantageously if the refrigeration equipment and interconnecting piping are properly sized to accommodate alternative modes of operation.
- **Protect compressors from liquid slugging.** Ice producers and ice harvesters tend to contain more refrigerant than chillers of similar capacity used for nonstorage systems. The opportunity, therefore, exists for compressor liquid slugging. Care should be taken to oversize suction accumulators and equip them with high-level compressor cutouts and suction heat exchangers to evaporate any remaining liquid.
- **Oversize the receivers.** The system should be made easy to maintain and service. Maintenance flexibility may be provided in a liquid overfeed system by oversizing the low-pressure receiver and in a direct-expansion system by oversizing the high-pressure receiver.
- **Prevent oil trapping.** Refrigerant lines should be arranged to prevent the trapping of large amounts of oil anywhere in the system, and to ensure its return to compressors under all operating conditions, especially during periods of low compressor loads. All suction lines should slope toward the suction line accumulators, and all discharge lines should pitch toward the oil separators. Oil tends to collect in the evaporator because that is the location at the lowest temperature and pressure. Because refrigerant accumulators trap oil as well as liquid refrigerant, the larger accumulators needed for ice storage systems require special provisions to ensure adequate oil return to the compressors.

It is important to fully analyze design trade-offs; comparisons of CTES to other available cost- and energy-saving opportunities should be fair. For example, if energy-efficient motors are assumed for a CTES design, they should be assumed for the nonstorage system being compared. Current designs should be considered in comparisons, whether based on hydrochlorofluorocarbons (HCFCs), hydrofluorocarbon (HFCs), or ammonia refrigerants, or on any of the proven refrigeration techniques (e.g., direct expansion, flooded, liquid overfeed).

Means are often sought to reduce electrical costs. One way to do this is to lower electrical consumption at peak times of the day. Conventional air-conditioning systems often contribute a large percentage to this peak load, because they typically run during peak hours. Shifting air-conditioning loads to off-peak times when demand costs are lower cuts demand costs significantly. CTES can help shift air-conditioning loads in this way.

CTES is a proven and workable technology. Over 10,000 CTES systems currently operate in the USA. TES relies on an inexpensive storage medium using high specific or latent heat to store cooling. The most common types of storage units use chilled water or ice. Because of the difference in energy density of the storage, ice storage units are smaller.

### 3.8.4 CTES Sizing Strategies

The decision of which sizing strategy to use for a CTES is generally an economic rather than a technical one. There are three basic storage-sizing strategies:

- full storage,
- load-leveling partial storage, and
- demand-limiting partial storage.

The full-storage strategy supplies all of a facility's peak cooling needs using a storage unit by shifting all of the electrical demand caused by cooling to off-peak hours. Calculating the design-day cooling requirement (tons per hour) during peak times and dividing that by the tank's efficiency factor determines the size of storage tank needed. Initial costs are usually expected to be high.



The load-leveling partial-storage strategy supplies only part of a building's cooling load during peak hours. This method levels the building's electrical demand caused by cooling over the design day. Compared to the other two strategies, this method minimizes the size of storage and refrigeration equipment needed to cool a building, resulting in lower equipment costs. However, this strategy does not create as great operating savings as the others.

Demand-limited partial storage requires less storage capacity than full storage, but more than load-leveling strategies, and lowers a building's peak electrical demand to a predetermined level. This level is normally equal to the peak demand imposed by noncooling loads. To effectively keep the total electric demand below the predetermined level, real-time controllers are required to monitor the building's non-cooling loads and control the ratio of storage- and chiller-supplied cooling.

Reduced operating costs are the primary benefit derived from using CTES. Energy cost can be reduced for cooling a facility by as much as 70%. Typical payback periods using CTES usually range from 2 to 6 years. Prediction of cost savings from using CTES requires the following building-specific information:

- hour-by-hour power usage;
- performance of the proposed cool storage system;
- the local electrical utility's rate structure.

Particularly in the United States, utility companies sometimes offer incentive programs, reduced rates, or free feasibility studies related to saving energy. Incentive payments for installing a functional TES unit can be in the form of cash subsidies or rebates to the customer. Retrofits are usually eligible for higher incentives than new construction. Feasibility studies are an indirect inducement that may be offered free or at a reduced rate by the utility.

### 3.8.5 *Load Control and Monitoring in CTES*

Two key control issues unique to CTES systems are monitoring and regulating the water or ice temperature and controlling tank-water level (Maust, 1993). Temperature sensors inside chilled-water storage tanks provide data which the control system uses to evaluate the tank's cooling capacity. Temperature monitoring also gives the operator information to make load-management and chiller-operation decisions. For instance, encapsulated ice systems evaluate cooling capacity by monitoring tank liquid level and the amount of ice that remains. By trend-logging the cooling demand and the rate at which stored cold is used, an operator can operate a chiller plant and the storage system to achieve the desired objectives.

It is also important to monitor the tank water level, because it can indicate faulty operation. Large volumes of water are often involved, and a leak or break in the treated-water system could lead to large and expensive losses. Sensors monitoring tank level, performance of the makeup water system and pressure regulating components provide important diagnostic information.

Small ice CTES systems have built-in control systems. For large ice storage systems, such as the encapsulated systems, control systems are integrated into the building automation system that controls chillers, pumps, and air-handling units. These control systems are normally custom designed and constructed on site. Systems typically consist of a set of microprocessors connected to a high-speed, local-area network and an operator's workstation. Network control systems usually require minimal operator training. Software continuously monitors building load, storage capacity, and outdoor conditions and compares them with historical data. The program determines the best use of chillers and stored cool water. A control system also can provide troubleshooting capabilities.

Monitoring and control of CTES systems are generally straightforward. For example, consider two basic modes of operation such as near-full storage and partial storage. In near-full storage, chillers are permitted to operate as little as possible during peak hours. In partial storage, chillers

are allowed to operate up to a pre-determined load limit during peak hours, with storage making up the remainder of a daily load.

### 3.8.6 CTES Storage Media Selection and Characteristics

The storage medium determines how large the storage tank will be and the size and configuration of the HVAC system and components. The main options include chilled water, ice, and eutectic salts. Ice systems offer the densest storage capacity, but have the most complex charge and discharge equipment. Water systems offer the lowest storage density, and are the least complex. Eutectic salts have intermediate characteristics. Some details on each storage medium are as follows:

- **Chilled water.** Chilled-water systems require the largest storage tanks, but can easily interface with existing chiller systems. Chilled-water CTES systems use the sensible heat capacity of water to store cooling capacity. They operate at temperature ranges (3.3–5.5 °C) compatible with standard chiller systems and are most economical for systems greater than 2000 ton-hours in capacity.
- **Ice.** Ice systems use smaller tanks and offer the potential for the use of low-temperature air systems, but require more complex chiller systems. Ice CTES systems use the latent heat of fusion of water (335 kJ/kg) to store cooling capacity. Storage of energy at the temperature of ice requires refrigeration equipment that provides charging fluids at temperatures below the normal operating range of conventional air-conditioning equipment. Special ice-making equipment or standard chillers modified for low-temperature service are used. The low chilled-water-supply temperatures available from ice storage allow the use of cool-air distribution, the benefits of which include the ability to use smaller fans and ducts and the introduction of less humid air into occupied spaces. With ice as the storage medium, there are several technologies available for charging and discharging the storage: ice harvesting systems feature an evaporator surface on which ice is formed and periodically released into a storage tank that is partially filled with water. External melt ice-on-coil systems use submerged pipes through which a refrigerant or secondary coolant is circulated. Ice accumulates on the outside of the pipes. The storage is discharged by circulating the warm return water over the pipes, melting the ice from the outside. Internal melt ice-on-coil systems also feature submerged pipes on which ice is formed. The storage is discharged by circulating warm coolant through the pipes, melting the ice from the inside. The cold coolant is then pumped through the building cooling system or used to cool a secondary coolant that circulates through the building's cooling system. Encapsulated ice systems use water inside submerged plastic containers that freeze and thaw as cold or warm coolant is circulated through the storage tank holding the containers. Ice slurry systems store water or water/glycol solutions in a slurry state (a partially frozen mixture of liquid and ice crystals that looks like slush). To meet a cooling demand, the slurry may be directly pumped to the load or to a heat exchanger cooling a secondary fluid that circulates through the building's chilled-water system. Internal melt ice-on-coil systems are the most commonly used type of ice storage technology in commercial applications. External melt and ice-harvesting systems are more common in industrial applications, although they can also be applied in commercial buildings and district-cooling systems. Encapsulated ice systems are also suitable for many commercial applications. Ice slurry systems have not been widely used in commercial applications.
- **Eutectic salts.** Eutectic salts can use existing chillers but usually operate at warmer temperatures than ice or chilled-water systems. Eutectic salts use a combination of inorganic salts, water, and other elements to create a mixture that freezes at a desired temperature. The material is encapsulated in plastic containers that are stacked in a storage tank through which water is circulated. The most commonly used mixture for thermal storage freezes at 8.3 °C, which allows the use of standard chilling equipment to charge storage, but leads to higher discharge temperatures. These temperatures, in turn, limit the operating strategies that may be applied. For example, eutectic salts may only be used in full-storage operation if dehumidification requirements are low.

**Water versus Ice CTES**

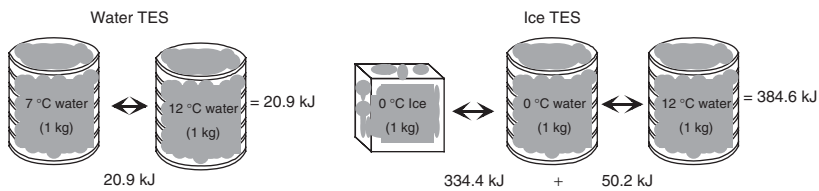
To increase compactness, CTES systems have been developed that utilize the latent heat of in-phase changes (usually solid–liquid) of substances. Presently in practice, latent storage utilizing water and ice is employed most widely.

Figure 3.22 shows that the cooling capacity of an ice CTES system under total freezing is 18 times as high as that of a water CTES operating between 12 and 7 °C. Consequently, the thermal storage volume can be substantially reduced. However, because of practical difficulties in melting ice, it is often not advantageous to turn all the water into ice. Figure 3.23 shows how the ice packing factor (IPF) affects the tank volume for ice CTES in comparison to water CTES. As shown, if 10% of the water is converted to ice, the tank volume is 32% of that for a water storage tank.

Currently, buildings in Japan have a cooling load to heating load ratio of approximately 2 : 1 to 3 : 1 due to the heating load of office equipment. If a TES tank is used as a hot water tank in winter, the same tank can be used with an IPF of about 10% for balanced service in winter. As a result of the reduced tank volume, it is possible to install it on the roof. A further advantage of the reduced volume of ice storage is lower surface area, which leads to lower heat losses relative to a water CTES.

Conventional water CTES systems utilize sensible heat and thus need large tanks. These are often located under a building. In many cases, however, it is difficult to secure such a large tank space, and the use of conventional systems is thus restricted. The design and development of more compact thermal storage tanks has therefore become important.

A major drawback of ice thermal storage is that, since ice must be produced, the chiller evaporator temperature must be lower than that for a water CTES, so chiller capacity and COP are decreased. For water CTES, the evaporation temperature of an ordinary chiller is in the vicinity of 0 °C. For ice CTES, however, evaporator temperatures are often below –10 °C so that the capacity and COP are reduced to about 56 and 71%, respectively, of those of a water CTES system. A capacity drop leads to an increase in the size and cost of the chiller, while a COP reduction leads to an increase in energy costs. To control both of these costs, it is desirable to store the minimum of ice required by the available space.



**Figure 3.22** The capacity of an ice CTES is 18 times as high as that of water CTES (Kuroda, 1993)

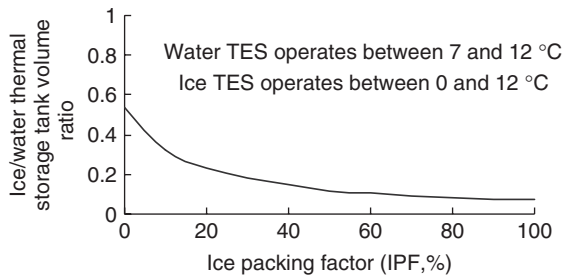


**Figure 3.23** Variation in tank volume (expressed as the ratio between ice and water thermal storage tank volume) with ice packing factor (Kuroda, 1993)

Two basic types of commercial ice storage exist: static (ice building) and dynamic (ice shucking) systems. In the static system, ice is formed on the cooling coils within the storage tank itself (ice-on-coil). Such systems are normally manufactured in packaged units and connected to the building's chilled-water system. Dynamic systems, which are becoming popular, make ice in chunks or crushed (so-called *ice harvesting*) form and deliver it for storage in large pits similar to those used in chilled-water systems. Dynamic systems may also include the formation of ice glycol slurry, which can be stored in a tank. Static ice storage systems are designed to form ice on the surface of evaporator tubes, and to store it until chilled water is needed for cooling. The ice is melted by the warm return water, thereby re-cooling the water before it is pumped back to the coils in the building. Other static systems use brine that circulates through tubes in an ice block or around containers filled with frozen water. These systems have the advantage of being closed and not open to the atmosphere. An examination of the relative costs of ice CTES systems versus comparable water storage systems sometimes indicates that the ice CTES system costs less, mainly because of the considerably reduced storage volume requirements. Ice CTES has the disadvantage of lower evaporator temperatures and higher electrical energy requirements to achieve the necessary freezing of the water.

On the basis of years of experience, many companies believe that chilled water and encapsulated ice are the most practical storage methods. Chilled CTES requires a large vertical tank with a capacity of approximately  $0.283 \text{ m}^3$  per ton-hour of storage. Encapsulated ice requires a much smaller storage capacity, approximately  $0.071 \text{ m}^3$  per ton-hour stored.

Both systems have advantages that are site specific. In general, chilled-water storage becomes practical in capacities exceeding 25,000 ton-hours. In addition, companies note the following:

- Encapsulated ice CTES systems produce much colder water, so pumps, piping, heat exchangers, and cooling coils can be smaller. Chiller compressors must be of the positive displacement type, such as rotary screws or reciprocating. Centrifugal compressors are not practical for this application.
- Chilled CTES systems may use any type of system as long as there is a  $20^\circ\text{C}$  difference during the discharge cycle between supply and return water. Each cooling coil should be equipped with a dedicated pump and a direct digital control (DDC) system.

### PCMs (Eutectic Salts) for CTES

PCMs have recently received significant attention for CTES, although they have been considered for heating since the early 1980s. PCMs suitable for CTES are eutectic salts that undergo liquid/solid phase changes at temperatures as high as  $8.3^\circ\text{C}$ , and absorb and release large amounts of energy during the phase change. Stored in hermetically sealed plastic containers, PCMs change to solids as they release heat to water, or to another fluid that flows around them. At these temperatures (up to  $8.3^\circ\text{C}$ ), chillers can operate more efficiently than at the low temperatures required by ice CTES systems. PCMs also have about three times the storage capacity of a typical chilled-water CTES system. The choice of ice, chilled water, or PCMs depends on the services needed. If low temperatures are needed, ice is likely preferable. If more conventional temperatures are needed and space is available, chilled-water CTES can be installed. If space is limited, but low temperatures are not required and a passive, easy-to-maintain system is desired, PCM may be a good choice.

Ice CTES is one example of using the latent heat characteristic of a storage medium. The significance of latent heat is that far more energy may be added or removed from a storage material as it undergoes a change of phase than can be added or removed from a material that remains in a single liquid phase, such as water, or a single solid phase, such as rock or brick.

Two commercially available materials that enhance the phase change process that ordinarily occurs between water and ice are eutectic salts and gas hydrates. Eutectic salts are mixtures of inorganic salts, water, and additives. Gas hydrates are produced by mixing gas with water. Both of these materials work by raising the temperature at which water freezes. These materials have the advantage of a freezing point of  $8.3$  or  $8.8^\circ\text{C}$ , which reduces energy requirements for freezing.

PCMs can, therefore, provide a highly desirable TES storage medium for cooling purposes. PCMs also provide most of the storage space advantages associated with ice storage systems. By freezing and melting at 8.3 or 8.8 °C, the PCMs can be easily used in conventional chilled-water systems with centrifugal or reciprocating chillers. The storage tank can be placed above or below grade. In addition, chiller power requirements are reduced when PCMs are used for TES because evaporative temperatures remain fairly constant.

Gas hydrates, still in the development stage for large, commercial installations, have some advantages over eutectic salts. Gas hydrates have high latent heat values, which lead to size and weight advantages. Gas hydrates require only one-half to one-third of the space, and are approximately one-half the weight of an equivalent eutectic salt system.

Like ice and chilled-water storage systems, hydrated salts have been in use for many decades. PCMs with various phase-change points have been developed. To date, the hydrated salt most commonly used for CTES applications changes phase at 8.3 °C, and is often encapsulated in plastic containers. The material is a mixture of inorganic salts, water, and nucleating and stabilizing agents. It has a latent heat of fusion of 95.36 kJ/kg and a density of 1489.6 kg/m<sup>3</sup>. A CTES using the latent heat of fusion of this PCM requires a capacity of about 0.155 m<sup>3</sup>/ton-hour for the entire tank assembly, including piping headers.

**PlusICE™ PCMs** The disadvantages of conventional ice CTES (low temperature chillers to build ice) and water CTES (large volume of water storage) can be overcome by utilizing the latent heat capacity of various eutectic salts, otherwise known as *PCMs*. Table 3.10 lists several types of commercially available PlusICE™ substances and their thermophysical data. For different phase change temperatures, some other types of substances are also available. PlusICE™, mixtures of nontoxic eutectic salts, have freezing and melting points higher than those of water, and the temperature range offered by this concept provides the following benefits:

- space-efficient coolness and heat recovery CTES;
- utilization of existing chiller and refrigeration equipment for new and retrofit CTESs;
- elimination of low-temperature glycol chillers;
- improvement of system efficiency due to higher evaporation temperatures and possible charging by means of free cooling (i.e., without operating the chiller).

**Table 3.10** Commercially available PlusICE™ substances

PlusICEtype	Phase change temperature (°C)	Density (kg/m <sup>3</sup> )	Heat of fusion (kJ/kg)	Latent heat (MJ/m <sup>3</sup> )
A4	4	766	227	174
E7	7	1542	120	185
E8	8	1469	140	206
A8	8	773	220	170
E10	10	1519	140	213
E13	13	1780	140	245
E21	21	1480	150	222
A22	22	775	220	171
A28	28	789	245	193
E30	30	1304	201	262
E32	32	1460	186	272
E48	48	1670	201	336
E58	58	1280	226	289
E89	89	1550	163	253
E117	117	1450	169	245

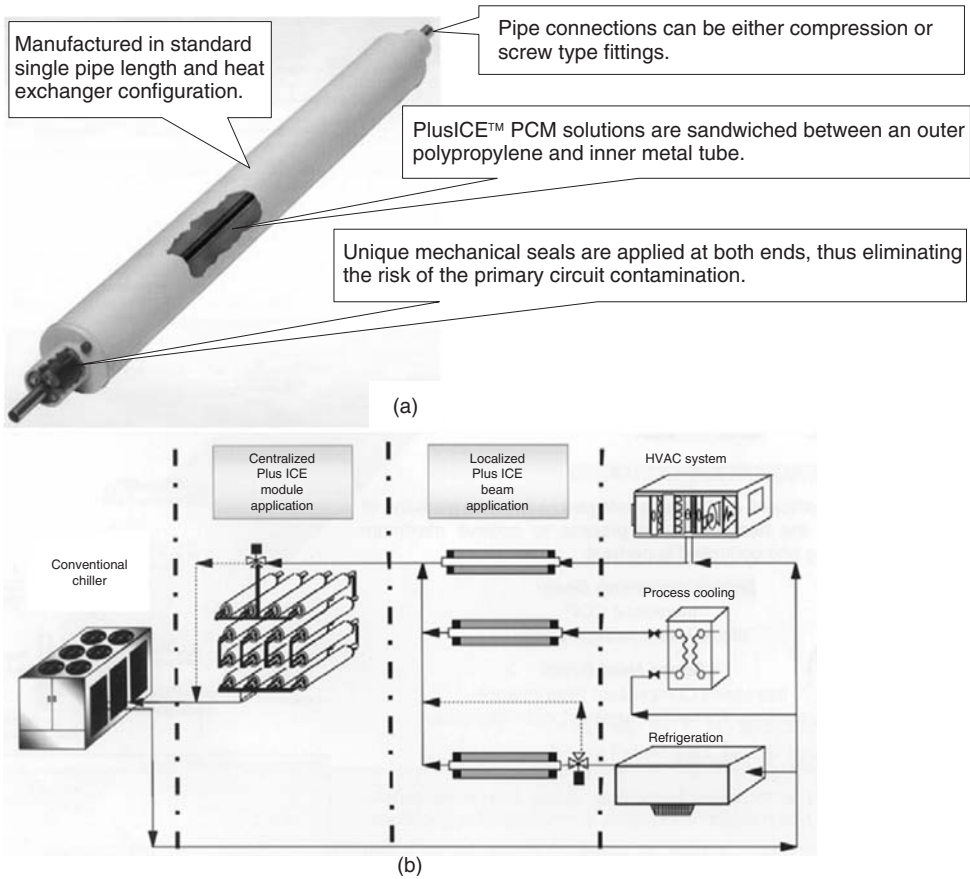


**Figure 3.24** (a) PlusICE™ beam for CTES applications, (b) centralized and localized PlusICE™ applications (Courtesy of Environmental Process Systems Limited)

PlusICE™ beams (Figure 3.24a) provide a static CTES system, and the self-stacking modular tube concept offers flexibility for the size and location. They can be manufactured either as a single or multi-pass arrangement for the most economical capacity and duty balancing for any given new and retrofit application. Site-assembled modular self-stacking design offers flexibility and simple installation. Future capacity increases can be easily accommodated by simply adding more beams into an existing module with minimal modification. In the operation of the system, water or refrigerant is circulated within the inner tube and the excess capacity from this fluid is stored in the form of latent heat by the eutectic salts during the charging mode. This operation is reversed during the discharge mode to supplement the system load. Beams can be applied as either a totally centralized CTES, similar to a conventional storage tank, or totally localized, that is, spread over the system as part of the pipe runs, or a combination of the two (Figure 3.24b). This enables a reduction or even elimination of the central storage module.

### 3.8.7 Storage Tank Types for CTES

Storage tanks must have the strength to withstand the pressure of the storage medium, and be watertight and corrosion resistant. Aboveground outdoor tanks must be weather resistant. Buried



tanks must withstand the weight of the soil covering and any other loads that might occur above the tank, such as the parking of cars. Tanks may also be insulated to minimize thermal losses (which are typically 1–5% per day).

The options for tank materials include the following:

- **Steel.** Large steel tanks, with capacities up to several million cubic meters, are typically cylindrical in shape and field-erected of welded plate steel. Corrosion protection, such as an epoxy coating, is usually required to protect the tank interior. Small tanks, with capacities of less than 100 m<sup>3</sup>, are often rectangular in shape and typically made of galvanized sheet steel. Cylindrical pressurized tanks are generally used to hold between 10 and 200 m<sup>3</sup>.
- **Concrete.** Concrete tanks may be precast or cast-in-place. Precast tanks are most economical in sizes of one million gallons or more. Cast-in-place tanks can often be integrated with building foundations to reduce costs. However, cast-in-place tanks are more sensitive to thermal shock. Large tanks are usually cylindrical in shape, while smaller tanks may be rectangular or cylindrical.
- **Plastic.** Plastic tanks are typically delivered as prefabricated modular units. Ultraviolet (UV) stabilizers or an opaque covering is required for plastic tanks used outdoors to provide protection against the UV radiation in sunlight.

Steel and concrete are the most commonly used types of tanks for chilled-water storage. Most ice harvesting systems and encapsulated ice systems use site-built concrete, while external melt systems usually use concrete or steel tanks, internal melt systems usually use plastic or steel, and concrete tanks with polyurethane liners are common for eutectic salts.

CTES tanks often use insulation. Because of the low temperatures associated with ice storage, insulation is a high priority. Ice storage tanks located above ground are normally insulated to limit standby losses. For external melt ice-on-coil systems and some internal melt ice-on-coil systems, the insulation and vapor barrier are part of the factory-supplied containers; most other storage tanks require field-applied insulation and vapor barriers. Belowground tanks used with ice harvesters sometimes do not need insulation beyond 1 m below grade. Because the tank temperature does not drop below 0°C at any time, there is no danger of freezing and thawing groundwater. All belowground tanks using fluids below 0°C during the charge cycle should have insulation and a vapor barrier system, generally on the exterior. Interior insulation is susceptible to damage from the ice and should be avoided.

Exposed tank surfaces should be insulated to help maintain the temperature in the tank. Insulation is especially important for smaller storage tanks, because the ratio of surface area to stored volume is relatively high. Heat transfer between the stored water and the tank contact surfaces (including divider walls) is a primary source of loss. Not only does the stored fluid lose heat to (or gain heat from) the ambient by conduction through the floor and wall, but heat also flows vertically along the tank walls from the warmer to the cooler region. Exterior insulation of the tank walls does not inhibit this heat transfer.

The cost of chemicals for water treatment may be significant, especially if the tank is filled more than once during its life. A filter system helps keep the stored water clean. Exposure of the stored water to the atmosphere may require the occasional addition of biocides. While tanks should be designed to prohibit leakage, the designer should account for the potential impact of leakage on the selection of chemical water treatment. Storage circulating pumps should be installed below the minimum operating water level to ensure flooded suction. The required net positive suction pressure must be maintained to avoid sub-atmospheric pressure conditions at the pumps.

### 3.8.8 Chilled-Water CTES

A chilled-water CTES system uses the sensible heat in a body of water to store energy. Given its specific heat of 4.187 kJ/kg °C, about 0.2 m<sup>3</sup> of water is needed to absorb 12,000 kJ and provide 1 ton-hour of cooling if the coil raises the water temperature by 20°C.

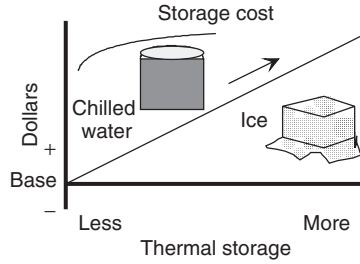


Figure 3.25 CTES cost relationship (AEP, 2001)

By contrast, the same ton-hour of cooling can be provided with just 0.042 m<sup>3</sup> of ice, since each kilogram of ice absorbs 152 kJ as it melts. Therefore, a CTES system that uses chilled water rather than ice requires six to seven times more installed storage volume. Figure 3.25 shows a plot of the cost of CTES components as a function of the ton-hours of cooling stored. The sizable cost penalty imposed by the significantly larger storage tank volume required for chilled water is readily apparent compared with ice storage. Note, however, that the cost of the water storage tank is mainly a function of its surface area, while the capacity of the tank is mainly a function of its volume. Therefore, as the size required of a chilled-water storage tank increases, the per-ton-hour cost of the storage tank actually decreases. Consequently, it appears that chilled water may be competitive with ice in applications that require more than 10,000 ton-hours of thermal storage.

A chilled-water storage system can be viewed as a simple variation of a decoupled chiller system. Since the same fluid water is used both to store and to transfer heat, few accessories are needed and the system is simple. As shown in Figure 3.26, a decoupled system separates the production and distribution of chilled water. The balance of flow between the constant-volume production of chilled water and its variable-volume distribution is handled with a bypass pipe commonly called a *decoupler*. The decoupler redirects surplus chilled water to storage when production exceeds distribution and withdraws storage water when distribution exceeds supply.

Chilled-water CTES systems offer a number of benefits, especially for larger systems. In addition, the large storage volume of water can be incorporated into fire safety systems, and in fact, some sprinkler systems use storage water in their design. The disadvantages of chilled-water storage, which relate to the tank design, weight, location, and space requirements, can pose challenges.

The relative installed cost of a chilled-water CTES (see Figure 3.27) shows the significance of storage tank expense. While somewhat prohibitive for most applications under 10,000 ton-hours,

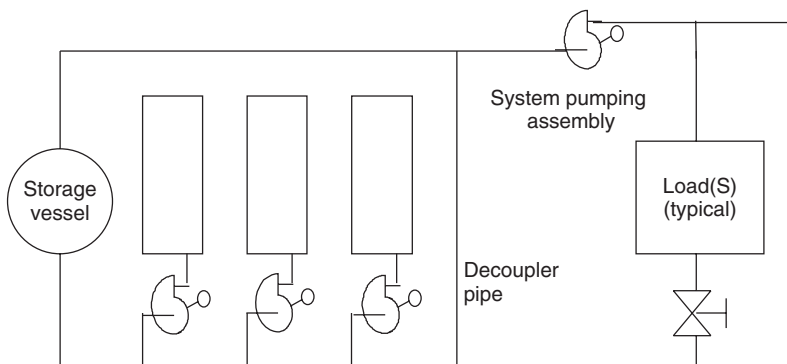
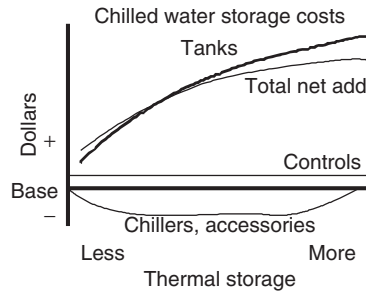


Figure 3.26 Schematic of a chilled-water production and distribution system (AEP, 2001)





**Figure 3.27** Advantages and disadvantages of tank configuration (AEP, 2001)

the decreasing unit cost of chilled-water CTES systems can be very attractive for large central plants and industrial installations.

### Series Storage Tanks for Chilled-Water CTES

The simplest form of chilled-water storage places one or more tanks in series. This concept is illustrated in Figure 3.28 as a single baffled tank. When the chillers produce more chilled water than the system requires, the excess is diverted to the series tank where it displaces the warmer water already present there. Likewise, when chilled water demand exceeds the quantity produced, chilled water is drawn from the tank by displacing it with warm return water.

A number of chilled-water CTES systems with designs similar to that in Figure 3.28 have been installed and proven to be effective in reducing peak electrical demand. However, series-tank designs can cause the water to stratify or become stagnant. Stagnation is the tendency of some water to shortcut through the tank, and renders large volumes of tank water ineffective for storage. Also, intercompartmental mixing can raise the tank-water exit temperature, reducing the tank effectiveness during its final hours of discharge.

### Parallel Storage Tanks for Chilled-Water CTES

The problems of mixing and stratification can be reduced with a multiple-tank parallel design (see Figure 3.29). This arrangement replaces the bypass pipe or decoupler with a number of separate tanks piped in parallel between the 14.5 °C return water from the cooling coils and the 4.5 to 5.5 °C supply water from the chiller(s). Each of these tanks has individually controlled drain and fill valves.

In practice, one of the parallel-piped tanks is empty when the storage is changed, and that tank's drain and fill valves are closed. When the discharge cycle starts (i.e., when the system starts to use

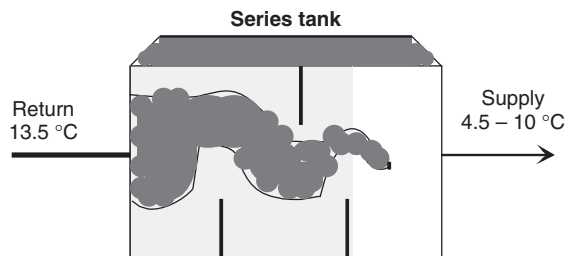


**Figure 3.28** Series tank configuration for chiller-water CTES (AEP, 2001)

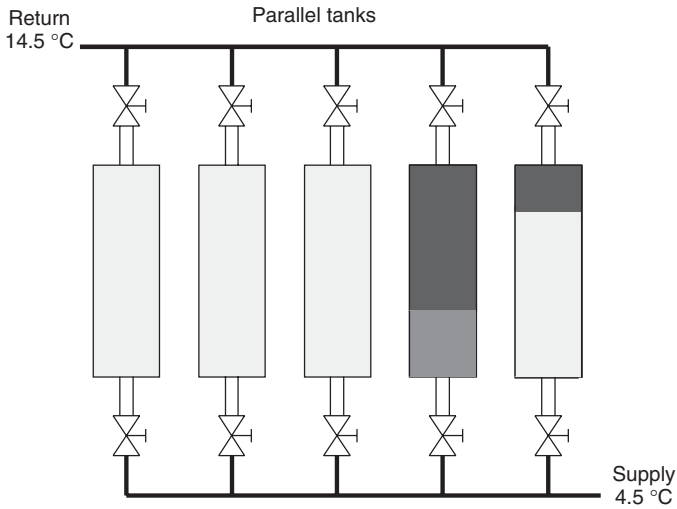


**Figure 3.29** Parallel tank configuration for chilled-water CTES (AEP, 2001)

chilled water), the empty tank's fill valve opens to allow it to receive warm return water. The drain valve on any one of the tanks filled with previously chilled water opens so that, as warm return water fills the empty tank, an equal flow of cold water is drawn from the tank with the open drain valve.

Proper valve sequencing is especially important when the receiving tank is nearly full and the draining tank is almost depleted. In this valve control sequence:

1. The drain valve on a new tank previously filled with chilled water must open.
2. The drain valve on the just-emptied tank must close as its fill valve opens, allowing the tank to receive warm return water.
3. The fill valve on the once-empty tank that is now full of warm return water must close. (This tank is now ready for off-peak recharging.)

A building of automation system and an accurate method of measuring tank volume are required to facilitate this control task. Although the multiple-parallel-tank scheme eliminates many of the problems associated with mixing and tank stratification, its complexity can add to the cost of a chilled-water CTES system.

### Stratified Storage Tanks for Chilled-Water CTES

Most chilled-water storage systems installed today are based on designs that exploit the tendency of warm and cold water to stratify. Cold water is then added to or drawn from the bottom of the tank, while warm water is returned to or drawn from the top. A boundary layer, or thermocline, often 0.2 to 0.4 m in height, is established between the resultant warm and cold zones (Figure 3.30). Specially engineered diffusers or any array of nozzles can ensure laminar flow within the tank. This laminar flow is necessary to avoid mixing and promote stratification, since the respective densities of the 15.5 °C return water and 4.5 to 5.5 °C supply water are almost identical.

### Advantages of Chilled-Water CTES

The most important advantage of water thermal storage is the fact that water is a well understood and familiar medium. No danger is associated with handling water as a TES material. Basically,

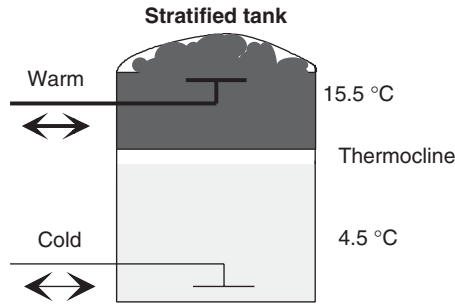


**Figure 3.30** Stratified tank configuration (AEP, 2001)

heating and cooling applications require only a moderate temperature range (5 to 45 °C). Water can be used as a storage medium for both cooling and heating, allowing the same TES material to be used throughout the year. The relatively high thermal capacity of water is also attractive for TES applications. These advantages give water CTES economic advantages over other air-conditioning systems, including those using ice CTES systems.

For example, an economic comparison between water CTES and ice CTES for a model building of 10,000 m<sup>2</sup> situated in Tokyo indicates the following ( Narita, 1993):

- The initial cost of water thermal storage is approximately 20% less than that of ice CTES. The main reason is the cost of the ice-making unit in the TES tank.
- In the ice-making mode, the COP is approximately 20% lower than that for the water cooling mode because of the lower evaporating temperature. Consequently, more electricity is consumed in ice CTES.
- The ice CTES system has little thermal storage capacity for potential use in the heating season.
- The operating cost of water thermal storage is approximately 20% less than that of ice CTES.

A major disadvantage of water CTES is volume. For the same amount of thermal capacity, a water CTES system requires approximately three times as much tank volume as ice CTES. To somewhat circumvent this problem, alternative design configurations are sometimes considered.

### Heat Pumps and Chilled-Water CTES

The heat pump is an important technology for energy conservation. Combining heat pumps and water CTES has many advantages, including the economic operation of the heat pump as well as a load-leveling effect on electricity demand. Such combined systems can overcome some of the disadvantages of water CTES that have been introduced in actual plants.

In conventional air-conditioning systems using heat pumps, the heat pump must be operated during the day when cooling demand exists. This operation contributes to electricity demand during the same period. Cooling demand is often responsible for approximately one-third of the electricity demand at the peak period. In a typical water CTES system, half of the daily cooling load can be covered by night operation of the heat pumps.

The combination of a heat pump and a water CTES can provide the following benefits:

- **Load leveling of electricity demand for air-conditioning.** If 50% of the air-conditioning load is shifted to the night on the peak day, the annual dependence on night-time electricity can be as high as 70% for cooling and 90% for heating. Thus, the CTES system achieves peak shifting on the peak day and improves the annual load factor of electricity-supply facilities. At

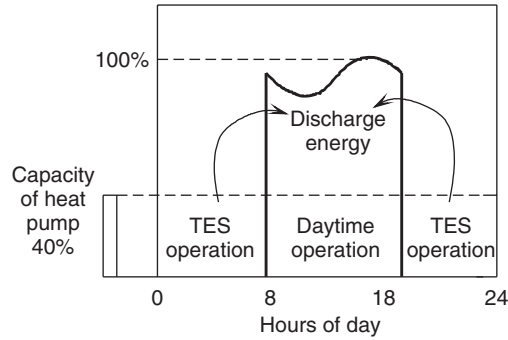


Figure 3.31 Operation of heat pump CTES

the same time, customers accrue economic advantages with a CTES system when electric power companies provide discount rates for night-time electricity.

- Efficient operation of the heat pump unit.** Heat pumps and other such devices as chillers and boilers have a maximum efficiency point of operation. In commercial and residential applications of heat pumps, heat pump operation cannot be maintained at the most efficient point because the cooling and heating loads vary temporally. This variation reduces the seasonal efficiency of heat pumps. CTES can help to avoid this problem by allowing operation of heat pumps at the most efficient point, because heat pumps can operate independent of the cooling and heating loads of buildings.
- Reduction of heat pump capacity.** As Figure 3.31 shows, for the same amount of air-conditioning load, the longer operating hours allow for smaller size of heat pump, which leads to a reduction in demand for electricity. Thus both initial and operating costs decrease.

### 3.8.9 Ice CTES

Ice CTES systems can be economically advantageous and require less space than water CTES systems. This space advantage often allows heating and cooling capacity to be enlarged within the often restricted area of existing machine rooms.

An ice CTES system with heat pump is composed of a heat pump, an ice-making system, a storage tank, and an air-conditioning system that can be a conventional central system.

Ice CTES systems are often classified as static or dynamic, according to the way ice is delivered to the storage tank. Each of these ice CTES types are discussed below.

- Static systems.** In static systems, an ice-making pipe is installed in the storage tank where ice is formed and later melted. Ice-in-tube systems produce ice inside the ice-making coil. Ice-on-coil systems produce ice outside the coil. The ice may be melted using either an external melting system that melts ice from the outer side, or an internal melting system (for ice-on-coil only). Internal melting may be achieved by feeding the warmed brine returning from the air-conditioning equipment into the coil. Alternatively, a refrigerant subcooling system can pass high-temperature and high-pressure refrigerant from the condenser through the coil. Another type of static system is the ice-tube float system that uses a polyurethane tube filled with water.
- Dynamic systems.** In the dynamic type of ice CTES system, ice is produced outside the storage tank and removed from the ice-making surface continuously or intermittently by various means. The ice harvest system feeds refrigerant that has passed through the expansion valve into an ice-making plate where ice is peeled off and dropped into a storage tank. The ice chip system continuously produces ice, which is scraped off as ice chips. In the liquid-ice system, fine



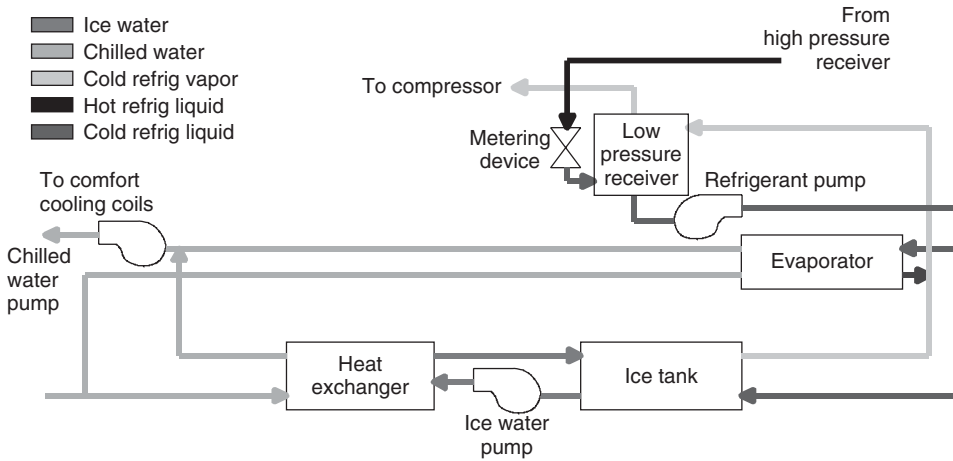


Figure 3.33 Low-pressure portion of an ice-on-pipe CTES for process refrigeration (AEP, 2001)

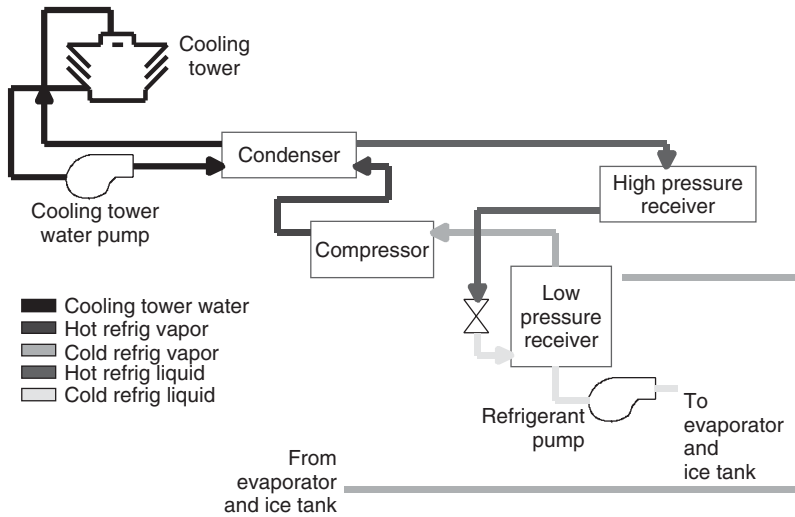


Figure 3.34 High-pressure portion of an ice-on-pipe CTES (AEP, 2001)

exits the condenser and enters a high-pressure receiver, where it is stored for later use. Refrigerant flow from the high-pressure receiver is regulated by a refrigerant metering device to ensure that a minimum liquid level is maintained in the low-pressure receiver.

The ice produced by an ice-on-pipe system forms on the exterior surfaces of an “ice coil.” This coil is actually a series of steel pipes immersed in a tank of water. Cold refrigerant (usually HCFC-22) is then pumped through these pipes to freeze the water that surrounds them. Bubbles flow around the steel pipes to agitate the water in the tank, sometimes by injecting air at the bottom. The rising air bubbles promote dense, even ice formation during the freezing cycle and uniform melting when the tank is discharged.

The low-pressure receiver plays a critical role in liquid-overfeed ice-on-pipe systems: it separates the two-phase refrigerant solution returning from the ice coil (or chiller evaporator) into liquid and

vapor. Gravity induces this separation, causing the liquid refrigerant and oil to settle at the bottom of the receiver while pure refrigerant vapor collects at the top. As the compressor draws this vapor from the receiver, the liquid level falls. To ensure that there is always sufficient liquid in this vessel, a liquid level control adds refrigerant from the high-pressure receiver as needed.

Liquid-overfeed systems require a separate oil return/recovery system. This is because the preferred compressor type (helical rotary/screw) expels significant amounts of oil into the discharge line. Entrained in the refrigerant, the oil makes its way through the condenser and high-pressure receiver, eventually ending up in the low-pressure receiver. There, the oil collects at the bottom of the tank (along with the liquid refrigerant) and cannot return to the compressor through the suction line. A separate oil-recovery system is needed to capture, distill, and return the oil to the compressor. This must be carefully addressed in the system design. The complexity of the liquid overfeed ice-on-pipe system translates into significant fixed costs that are independent of the quantity of ice produced and stored. The refrigerant and oil inventory control systems, refrigerant pumps and other system accessories, plus the field labor required to install them, constitute a sizable investment.

Depending on the system size, the tank can be either premanufactured to include both the ice coil and tank, or field-assembled by installing the ice coil in a field-erected concrete tank. While the latter option makes the per-ton-hour cost of the tank attractive, it only partially offsets the combined cost of field labor and accessories, even when the lower compressor cost is considered. Liquid overfeed ice-on-pipe systems are expensive because they require not only large inventories of oil and refrigerant, but refrigerant containment equipment as well. The high costs of engineering and installing liquid-overfeed ice-on-pipe systems typically limit their use to larger applications.

Ice-on-pipe systems offer a number of benefits over chilled-water storage. The storage volume required is considerably less, since each ton-hour of cooling stored can occupy as little volume as  $0.085 \text{ m}^3$ . Also, unlike their chilled-water counterparts, ice storage systems can operate at any return-water temperature.

### Ice Harvesters

Ice harvesters circumvent the problems associated with liquid-overfeed ice-on-pipe systems by combining all of the components and accessories required for ice production in a single manufactured package. This device, called an ice harvester (see Figure 3.35), is installed above an open tank that stores a combination of water and flakes of ice.

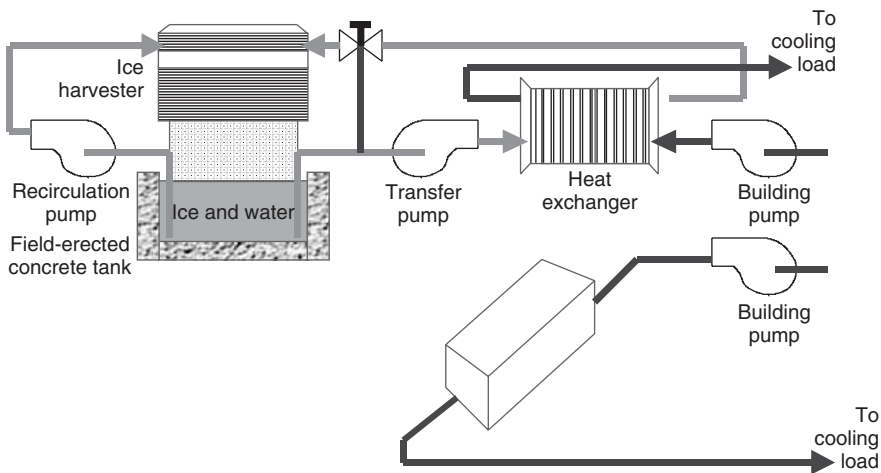


Figure 3.35 Ice harvester system (AEP, 2001)

To produce ice, 0°C water is drawn from the storage tank and delivered to the ice harvester by a recirculation pump at a flow rate of 1.75 to 2.75 m<sup>3</sup>/h per ton of ice-producing capacity. Once inside the ice harvester, the recirculated water flows into a drain pan positioned over a series of refrigerated plates. Each of these plates is constructed of two stainless steel sheets welded together at their circumference. A refrigeration system integral to the ice harvester maintains the plates at a temperature of -9.5 to -6.5°C.

As the water leaves the drain pan, it flows freely over both sides of the refrigerated plates, where it freezes to a thickness of 0.3 to 1.0 cm. On reaching a given thickness (or at the initiation of a time), the ice is dislodged from the plates by a hot-gas defrost cycle, and falls into the tank below. When cooling is required, a transfer pump draws iced water from the storage tank and delivers it to a building heat exchanger.

It is possible to use the ice harvester as a water chiller by raising the suction temperature of the refrigeration system and pumping warm water from the building heat exchanger over the refrigerated plates. In fact, operating at this higher suction temperature improves the ice harvester's efficiency. Unfortunately, the ice harvester cannot produce chilled water without melting ice stored in the storage tank.

This inability to operate as a true water chiller in a chilled-water system poses a significant efficiency penalty on ice storage systems with ice harvesters. To address this inefficiency, ice harvesters are commonly used in tandem with conventional water chillers. Ice harvesting systems separate ice formation from ice storage. Ice is typically formed on both sides of a hollow flat plate, or on the outside or inside (or both) of a cylindrical evaporator surface. The evaporators are arranged in vertical banks located above the storage tank. Ice is formed to thicknesses between 0.5 and 1 cm. This ice is then harvested, often through the introduction of hot refrigerant gas into the evaporator; the gas warms the evaporator, which breaks the bond between the ice and the evaporator surface and allows the ice to drop into the storage tank below. Other types of ice harvesters use a mechanical means of separating the ice from the evaporator surface.

Ice is generated by circulating 0°C water from the storage tank over the evaporators for a 600–1800 s build cycle. The defrost time is a function of the amount of energy required to warm the system and break the bond between the ice and the evaporator surface. Depending on the control methods, the evaporator configuration, and the discharge conditions of the compressor, defrost can usually be accomplished in 20–90 s. Typically, the evaporators are grouped in sections that are defrosted individually so that the rejected heat from the active sections provides the energy for defrost.

In load-leveling applications, ice is generated and the storage tank charged when there is no building load. When a building load is present, the return chilled water flows directly over the evaporator surface, and the ice generator functions either as a chiller or as both an ice generator and a chiller. Cooling capacity as a chiller is a function of the water velocity on the evaporator surface and the entering water temperature. The defrost cycle must be energized any time the exit water from the evaporator is within a few degrees of freezing. In chiller operation, maximum performance is obtained with minimum system-water flows and highest entering-water temperatures. In load-shifting applications, the compressors are turned off during the electric utility on-peak period.

Positive displacement compressors are usually used with ice harvesters, and saturated suction temperatures are usually between -7.5 and -5.5°C. Condensing temperatures should be kept as low as possible to reduce energy consumption. The minimum allowable condensing temperature depends on the type of refrigeration system used and the defrost characteristics of the system. Several systems with evaporatively cooled condensers have operated with a compressor-specific power consumption of 0.9 to 1.0 kW/ton.

Ice-harvesting systems can melt stored ice quickly. Individual ice fragments are characteristically less than 15.5 × 15.5 × 0.65 cm, and provide a minimum of 1.5 m<sup>2</sup> of surface area per ton-hour of ice stored. When properly wetted, a 24-h charge of ice can be melted in less than 30 min for emergency cooling demands.



During the ice-generation mode of operation, the system is energized if the ice is below the high ice level. A partial-storage system is energized only when the entering water is at or above a temperature that will permit chilling during the discharge mode; otherwise, the system does not operate, and the ice tank is discharged during the peak period to meet the load. The high-ice level sensor can be mechanical, optical, or electronic. The entering-water temperature thermostat is usually electronic.

When ice is floating in a tank, the water level remains nearly constant, rendering it difficult to measure ice inventory by measuring water level. The following general methods are used to determine ice inventory:

- **Water conductivity method.** As water freezes, dissolved solids are forced out of the ice into the liquid, thus increasing their concentration in the water. Accurate ice-inventory information can thus be maintained by measuring conductivity and evaluating the ice level.
- **Heat balance method.** The cooling effect of a system may be determined by measuring the mechanical power input to, and heat of rejection from, the compressor. The cooling load on the system is determined by measuring coolant flow and temperature. The ice inventory is then determined by integrating cooling input minus load and evaluating the ice level. A variant of the heat balance method involves a heat balance on the compressor only, using performance data from the compressor manufacturer and measured load data.

Optimal performance of ice-harvesting systems may be achieved by recharging the ice storage tank over a maximum amount of time with minimum compressor capacity. Ice inventory measurement and the known recharge time are used to determine such specifications. Efficiency can also be increased with proper selection of multiple compressors and unloading controls.

Design of the storage tank is important to the operation of the system. The amount of ice stored in a storage tank depends on the shape of the storage, the location of the ice entrance to the tank, the angle of repose of the ice (which normally is between 15 and 30°, depending on the shape of the ice fragments), and the water level in the tank. If the water level is high, voids occur below the water surface because of the buoyancy of the ice. Ice–water slurries have been reported to have a porosity of 0.50 and typical specific storage volumes of 0.08 m<sup>3</sup> per ton-hour.

**Cost** A cost analysis of ice harvester systems indicates increasing costs for both the tank and the harvester as the quantity of ice stored increases (see Figure 3.36). Given their high dollar-per-ton cost, ice harvester systems are usually used to provide additional capacity in retrofit applications, or in large installations.

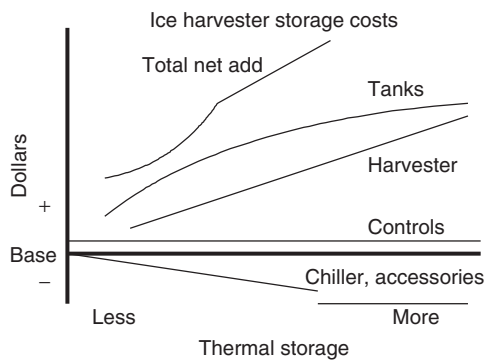


Figure 3.36 Cost relationship for ice harvesters (AEP, 2001)

**Advantages** Ice harvesters present the system designer with a number of benefits. As with other ice storage systems, the space requirement and cost of the volume stored are less than those for chilled-water systems. In addition, the ice harvester is a packaged device, leading to simplified installation, reduced installed costs, and, in most cases, factory-tested performance.

**Disadvantages** Ice harvesters have some limitations, particularly since the harvester and tank are open to the atmosphere. For example, the plates and chassis of the ice harvester are normally constructed of stainless steel, a material that adds significantly to the ice harvester's already high cost. Water treatment is also necessary because of the open nature of the tank and drain pan. The complexities of evenly distributing the ice in the bin and the prevention of piling and bridging add to the cost and operation of this system. Finally, the ice harvester's inability to produce chilled water without depleting the ice in the storage tank may be an economic deterrent.

### CTES glycol systems

Glycol systems freeze water by circulating ethylene or propylene glycol through storage tanks (Figure 3.37). The glycol ice storage system is simple. Few accessories are needed, and conventional water chillers are used. Instead of water, a glycol solution (in this case, 25% ethylene glycol) is pumped through the chiller coils and ice storage tanks in the chilled-water loop. The  $-5.5$  to  $-4.5$  °C ethylene glycol produced by the packaged chiller freezes the water contained inside the ice storage tanks.

Glycol ice storage systems are available from all major chiller manufacturers. Though similar in concept, they may be packaged differently. Glycol ice storage systems can generally be divided into two major categories: modular and encapsulated ice storage.

**Cost** Glycol ice storage systems have low installed costs since the same packaged chiller that provides space cooling also doubles as the ice maker. The storage tanks themselves are the only significant additional cost in these systems. In fact, glycol ice storage systems sometimes reduce chiller costs.

**Advantages** Glycol ice storage systems present numerous benefits, including the ability to use a standard packaged chiller. They also offer an opportunity to reduce pump work, and require few ancillary devices. The choice of modular storage tanks or encapsulated ice systems offers not only application flexibility, but cost choices and reliable performance as well. Simple control schemes

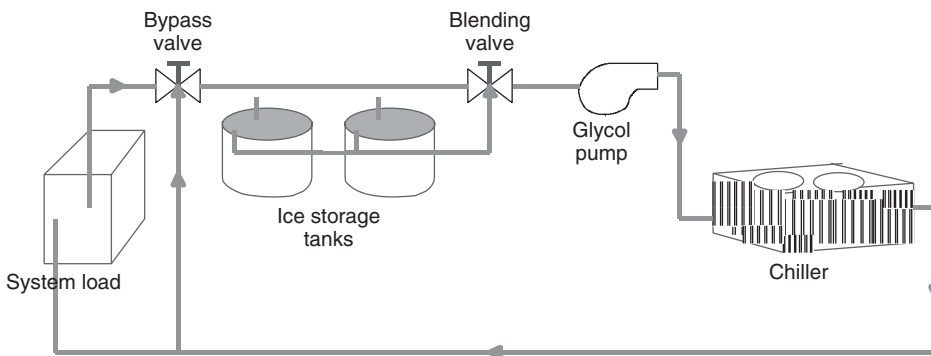


Figure 3.37 Glycol ice CTES system (AEP, 2001)

can be used and, as for all ice storage systems, volume and space requirements per ton-hour of storage are considerably lower than those for chilled-water storage.

**Disadvantages** Glycol ice storage systems have some problems, the most significant of which is the need for a heat-transfer system that uses ethylene (or propylene) glycol rather than water.

**Types of Systems** Glycol ice-storage systems presently enjoy a great deal of market popularity because of their simplicity and low installed cost. They can operate a wide variety of CTES technologies and equipment, and these are now discussed.

**Modular Ice Storage for Glycol Systems** Modular ice storage tanks can be constructed in many sizes or shapes. Two designs are common: a cylindrical polyethylene tank with circular polyethylene heat exchangers; and a rectangular metal tank with polypropylene heat exchangers. Some modular ice storage tanks are illustrated in Figure 3.38, along with some details of their storage capacities and key physical characteristics. In both modular ice storage designs, the heat exchanger separates the glycol solution from the water in the tank. The water is frozen by circulating  $-6.5$  to  $-4.5$  °C glycol through the heat exchanger. The differences in tank geometry and heat exchanger design pose different problems for the design engineer. For example, the shape of circular ice storage tanks allows heat exchangers with fewer circuits of longer length, and permits freezing or melting at lower flow rates and higher temperature differences. Low flow-rate freeze cycles enable the designer to better match the capacities of the storage tanks and chiller. Rectangular tank designs, on the other hand, incorporate high flow-rate, low pressure-drop heat exchangers that operate with a lower temperature difference during freezing. These characteristics not only place additional design constraints on chiller selection, but require individual flow balancing for each storage tank.

Both modular ice storage tank designs share the advantage of pre-engineering and factory manufacture. Factory design and testing increase the likelihood of reliable performance. Piping two or more modular tanks in parallel can increase capacity as required.

**Encapsulated Ice Storage for Glycol System** The other class of glycol-system storage, encapsulated ice, offers a wide degree of latitude in the design of the ice containment vessel. Various construction materials and geometries can be exploited and designed to conform to the space available and building architecture.

Encapsulated ice designs store the water to be frozen in a number of plastic containers. These containers may be thin and rectangular, spherical, or annular. Figure 3.39 illustrates some encapsulated ice storage containers, and provides information on their storage capacities and design-related characteristics. The number of containers or units required for an application depends on their

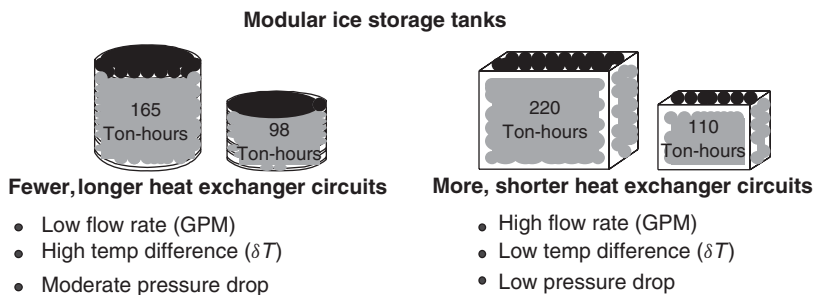


**Figure 3.38** Modular ice storage tanks and some of their characteristics (AEP, 2001)

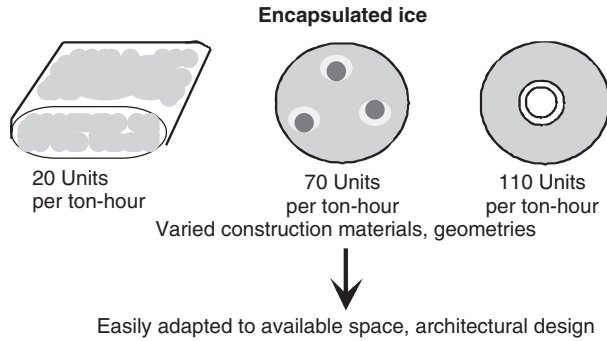


**Figure 3.39** Encapsulated ice storage tanks (AEP, 2001)

individual storage capacities. For example, as seen in Figure 3.38, 1 ton-hour of storage can be provided with approximately 20 ice “trays” or by 70 of the 10-cm-diameter spheres, called *ice balls*. Some commercially available rectangular containers are approximately  $3.5 \times 30.5 \times 76.5$  cm. Other designs are also available.

Perhaps the greatest advantage of this type of glycol system is the degree of application flexibility it affords the system designer. By selecting or designing a specifically adapted containment vessel, the storage system can be customized to the application. If desirable, it can even be placed below ground.

Encapsulated ice units consist of plastic containers filled with ionized water and an ice nucleating agent. These primary containers are placed in storage tanks, which may be either steel pressure vessels, open concrete tanks, or fiberglass or polyethylene tanks. In tanks with spherical containers, water usually flows vertically through the tank, and in tanks with rectangular containers, water flows horizontally. The type, size, and shape of the storage tank are limited only by the need to achieve an even flow of heat-transfer fluid between the containers.

A fluid coolant (e.g., 25% ethylene glycol or propylene glycol and 75% water) is cooled to  $-4.5$  to  $-3.5$  °C by a liquid chiller, and circulates through the tank and over the outside surface of the plastic containers, causing ice to form inside the containers. The chiller must be capable of operating at this reduced temperature. The plastic containers must be flexible to allow for change of shape during ice formation; the spherical type has preformed dimples in the surface, and the rectangular type is designed for direct flexure of the walls. During discharge, coolant flows directly either to the system load or to a heat exchanger, thereby removing heat from the load and melting the ice within the plastic containers. As the ice melts, the plastic containers return to their original shape.

Ice inventory is measured and controlled by an inventory/expansion tank normally located at the high point in the system and connected directly to the main storage tank. As ice forms, the flexing plastic containers force the surrounding secondary coolant into the inventory tank. The liquid level in the inventory tank may be monitored to account for the ice available at any point during the charge or discharge cycle.

### Ice-Slurry CTES Systems

Ice slurry is a very versatile cooling medium. The handling characteristics, as well as the cooling capacities, can be matched to suit any application by means of simply adjusting the percentage of ice concentration. At 20–25% ice concentration, ice slurry flows like conventional chilled water while providing five times the cooling capacity. At 40–50% ice concentration, an ice-slurry flow demonstrates thick slurry characteristics, and at a 65–75% concentration, slurry ice has the consistency

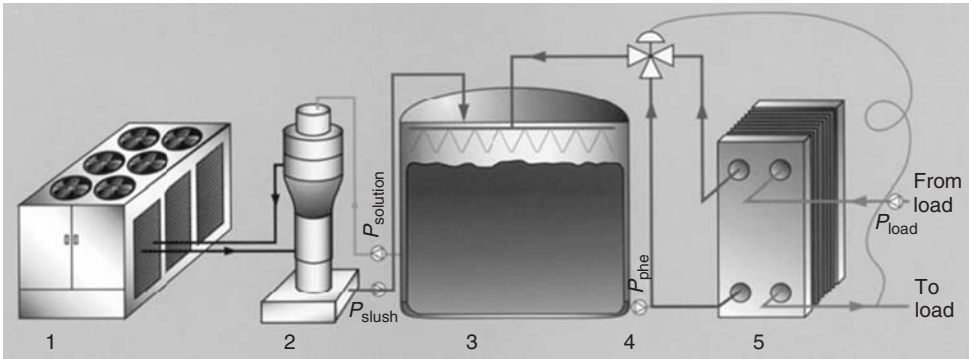


**Figure 3.40** A MaximICE ice-slurry system (Courtesy of Paul Mueller Company)

of soft ice cream. When slurry ice is produced in dry form (i.e., 100% ice), it takes the form of nonstick pouring ice crystals, which can be directly used in various products and processes.

Ice slurry is a crystallized water-based ice solution that can be pumped, and offers a secondary cooling medium for CTES while remaining fluid enough to pump. It flows like conventional chilled water while providing five to six times higher cooling capacity. The ice-slurry system is a dynamic type of ice CTES system that offers a pumpable characteristic advantage over any other type of dynamic systems. Compact equipment design and the pumpable characteristics offer tremendous flexibility for the location of the storage tank(s) and the most economic capacity and duty balancing for any given application. The storage tank can be placed under, beside, inside, or on top of a building, and can be in any shape and size to match the building, and architectural requirements. Multiple small storage tanks can be used instead of a single large static-type ice storage tank.

Figure 3.40 shows a MaximICE ice-slurry CTES system and its components. In the operation of such a system, a compressor/condenser (1) supplies refrigerant to the evaporator. A MaximICE orbital rod evaporator (2) uses a freeze-depressant solution to produce a pumpable ice slurry. Low-temperature slurry makes MaximICE ideal for use with low-temperature air systems. An insulated ice storage tank (3) separates ice manufacturing from ice usage. The tank contains a freeze-depressant solution that is converted to an ice slurry in the MaximICE evaporator. The slurry melts as the stored ice absorbs the heat of the cooling load. A load control pump and valve (4) control the supply temperature to the load. A plate heat exchanger (5) separates the storage tank from the cooling load and prevents cross-contamination between the ice-melting loop and the cooling load. It is important to note that the solution can be supplied from the ice storage tank to the load at various temperatures to satisfy specific application needs.

Ice-slurry CTES systems offer a large number of advantages:

- **Higher energy efficiency.** These systems provide relatively high energy efficiency. Unlike static ice systems, where ice adheres to the heat-transfer surface, ice slurry produced by the ice-slurry generator does not adhere to the heat-transfer surfaces, and unlike ice harvesters, defrost is not required to harvest the ice for storage in tanks.
- **Cost-effective tank design.** Ice slurry can be pumped into storage tanks, reducing the need for extra structural support, as required for ice harvesters located above the storage tanks.
- **Compact equipment.** The systems have a small evaporator footprint, which leads to space savings in the refrigeration equipment room.
- **Lower supply temperature.** Such systems offer lower supply water temperature compared to other ice systems.

- **Flexible ice storage tank design.** Ice slurry can be stored in tanks of any shape. For example, the height of an ice storage tank can be increased, resulting in a reduction of the tank footprint that leads to often valuable floor space savings. This is difficult to achieve in static and other dynamic ice storage systems.
- **Maintenance-free ice tank design.** Unlike ice-on-coil systems, ice-slurry systems do not require extensive lengths of pipe or tubing in the storage tanks, sometimes on the order of kilometers. This characteristic eliminates the need for repairing leaking pipes or tubing inside the tank.
- **Satisfies large loads.** Large loads for short durations can be met by ice-slurry systems because of the quick melting of ice that is achieved by a large area of contact between the warm return solution and stored ice.
- **Ease of modification.** The systems can be easily adapted to changing needs, which can occur. for example, when facility expansion takes place and facility use and/or utility rates change.

### CYFLIP as a new CTES system

Among the various systems to facilitate night-time power usage, the CHIYODA Corp. has developed the CYFLIP CTES system, which reduces 40% of the refrigerator duty of a normal air-conditioning system. CYFLIP is a static CTES system that makes ice in a polyethylene tube filled with water. These tubes are placed in a TES vessel where low-temperature brine is circulated. CYFLIP has a simple design and low equipment costs. The total investment can be less than that for a conventional air-conditioning system, since the capacity of the refrigerator becomes smaller. The CYFLIP system is regarded as reliable, because of its ease of operation and durability. The CYFLIP system is illustrated in Figure 3.41, where several operating parameter values are given.

### Practical Example I: Performance Curves for an Ice TES

In this section, a practical design application for a school is given to point out the design and technical aspects of ice TES.

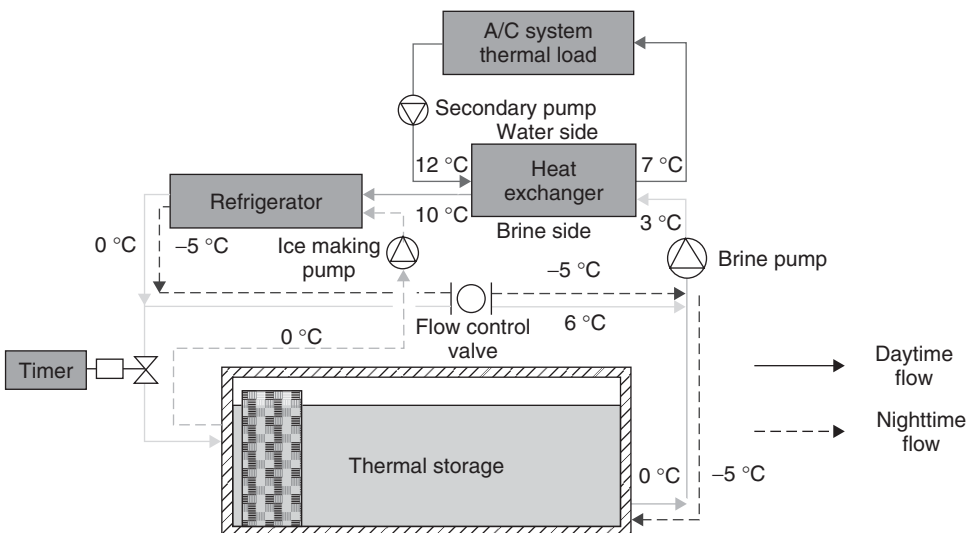


Figure 3.41 The CYFLIP ice CTES (Courtesy of CHIYODA Corp.)

In this project, the chiller capacity of 225 t is the capacity at ice-making conditions. At the lower temperatures required to make ice, the chiller is derated to 225 t.

The 288 t listed in the example is the chiller when operating at supplemental chiller capacity. This means that the chiller is running to supply cooling to the load directly, and not making ice. In this mode, the chiller would be running at standard conditions, at the higher normal air-conditioning temperatures. A chiller that is capable of producing 225 t at ice-making conditions would be capable of approximately 320 t at standard conditions.

Because this is a partial storage example, the chiller supplies cooling directly to the load between the hours of 6:00 am and 1:00 pm (supplemental chiller operation) The thermal storage system then takes over and supplies cooling during the peak electrical period from 1:00 to 8:00 pm (storage discharge-ice melting). Finally, during off-peak hours, the chiller operates at the reduced capacity of 225 t to replace the ice consumed during the day. The final hour of the charge is lower as the chiller unloads at the end of the cycle.

During the ice-making mode, we have modified the table to provide for a chiller running at 225 t for 7 h and at 97 t for 1 h. This provides a total ice build of 1672 ton-hours. This is the same amount of energy that is removed from the storage system during storage discharge. This is also known as the *rated capacity*.

The nominal capacity of the system is 1800 ton-hours. Therefore, following the discharge of 1672 ton-hours from storage, there is an unused capacity of 128 ton-hours still remaining. This difference between nominal and rated capacity, and the unused ice left in storage, is normal for all thermal storage systems. Indeed, it is impossible to discharge 100% of the ice in storage at useful rates, because the discharge rates fall off rapidly as we approach 100% discharge. It is normally not possible for thermal storage to melt 100% of the ice at rates that are high enough to satisfy a typical load. Unfortunately, there are still manufacturers and designers who insist that thermal storage is 100% efficient. This myth leads them to install smaller and less expensive thermal storage systems wherein the nominal and rated capacities are the same. Such systems usually run out of ice before the end of the discharge period and the discharge temperatures from storage climb prematurely (Ott, V.J. (2001). *Personal communication*, President of CRYOGEL Ice Ball Thermal Storage, San Diego.).

Figures 3.42 and 3.43 illustrate performance curves for charging (freezing) and discharging (melting) for Cryogel ice balls. The details of a CTES using Cryogel ice balls for a typical application (a sample input/output design report), along with a load profile table, follow:

<b>Project:</b>	Typical Elementary School	
<b>Storage rating:</b>		
	Rated capacity:	1,672 ton-hours
	Nominal capacity:	1,800 ton-hours
<b>Charge-cycle specifications:</b>		
	Entering-fluid temperature:	-5.55 °C
	Leaving-fluid temperature:	-1.66 °C
	Tank temperature difference:	-13.88 °C
	Tank LMTD:	-14.55 °C
	Chiller capacity:	225 t
	Charging period:	8 h
	Chiller shut-off temperature:	-6.66 °C
<b>Discharge-cycle specifications:</b>		
	Entering-fluid temperature:	12.22 °C
	Leaving-fluid temperature:	3.33 °C
	Tank temperature difference:	-8.8 °C
	Tank LMTD:	-10.94 °C
	Peak discharge rate:	288 t

**Load profile:**

Hour	Building Load	Supplemental Chiller	Storage		Ice Making Charge	Net Storage Inventory
			Discharge	Ton-hours		
Mid to 1	0	0	0	0	225	1,028.00
1 to 2	0	0	0	0	225	1,253.00
2 to 3	0	0	0	0	225	1,478.00
3 to 4	0	0	0	0	225	1,800.00
4 to 5	0	0	0	0	97	1,800.00
5 to 6	0	0	0	0	0	1,800.00
6 to 7	118.00	118.00	0	0	0	1,800.00
7 to 8	205.00	205.00	0	0	0	1,800.00
8 to 9	257.00	257.00	0	0	0	1,800.00
9 to 10	252.00	252.00	0	0	0	1,800.00
10 to 11	255.00	255.00	0	0	0	1,800.00
11 to 12	279.00	279.00	0	0	0	1,800.00
12 to 1	288.00	288.00	0	0	0	1,800.00
1 to 2	285.00	0	285.00	285.00	0	1,515.00
2 to 3	287.00	0	287.00	572.00	0	1,228.00
3 to 4	262.00	0	262.00	834.00	0	966.00
4 to 5	216.00	0	216.00	1,050.00	0	750.00
5 to 6	208.00	0	208.00	1,258.00	0	542.00
6 to 7	207.00	0	207.00	1,465.00	0	335.00
7 to 8	207.00	0	207.00	1,672.00	0	128.00
8 to 9	0	0	–	1,672.00	0	128.00
9 to 10	0	0	–	1,672.00	245	353.00
10 to 11	0	0	–	1,672.00	245	578.00
11 to Mid	0	0	–	1,672.00	245	803.00
<b>TOTAL</b>	<b>3,326.00</b>	<b>1,654.00</b>	<b>1,672.00</b>		<b>1,921.00</b>	

*Note:* Chiller must run fully loaded at storage entering fluid temperature as specified above. Estimated sizing may change with actual load profile. All units are tons, except the totals across the bottom and the data under the columns “storage-ton hours” and “net storage inventory” which are in ton-hours (*Courtesy of CRYOGEL Ice Ball Thermal Storage*).

The curves in Figures 3.42 and 3.43 are based on typical heat exchanger sizing methods using log mean temperature differences (LMTDs). Indeed, ice CTES systems are like large heat exchangers but the surface area of the thermal storage media changes as ice is frozen or melted. Therefore, a degradation is observed in Figures 3.42 and 3.43 in instantaneous performance as ice melts during discharge. Also observed is a reduction in instantaneous performance as ice gets thicker and impedes the heat-transfer process during charging. This behavior is typical of all ice-based CTES systems.

The LMTD is calculated using the storage tank inlet ( $T_i$ ) the storage outlet ( $T_o$ ) and the ice temperature ( $T_c$ ) as follows:

$$\text{LMTD} = \frac{[(T_i - T_c) - (T_o - T_c)]}{\ln[(T_i - T_c)/(T_o - T_c)]}$$

Using LMTD together with the performance curves allows one to predict instantaneous capacity at any point during the discharge of the storage system. This assessment is critical to be certain that a system has sufficient ice to meet the most demanding periods of each daily cycle. In a similar manner, although less critical, one can determine proper chiller sizing to match the ability of the ice balls to release heat during the charge process. Although the CTES market is generally not interested



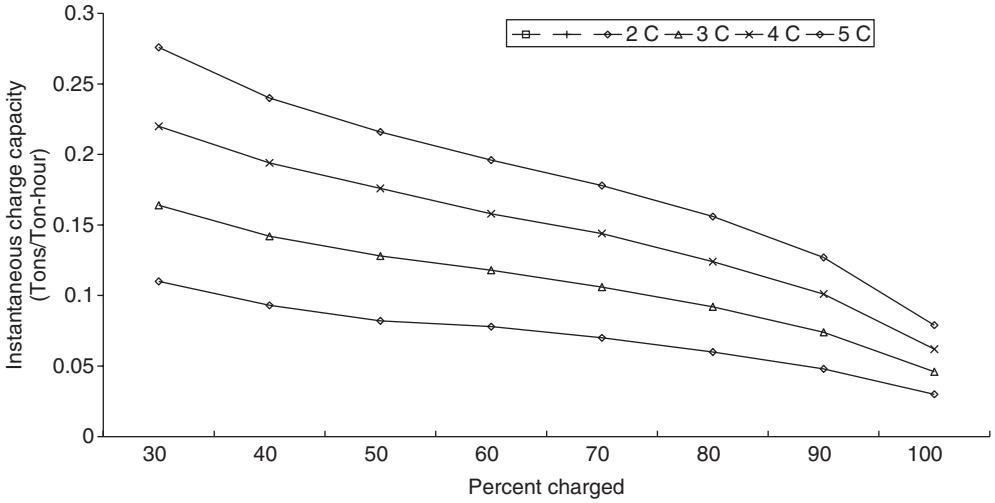


**Figure 3.42** Instantaneous charge capacity of Cryogel ice balls (in tons per ton-hour of storage capacity), as a function of storage inlet and outlet LMTDs (Courtesy of CRYOGEL Ice Ball Thermal Storage)

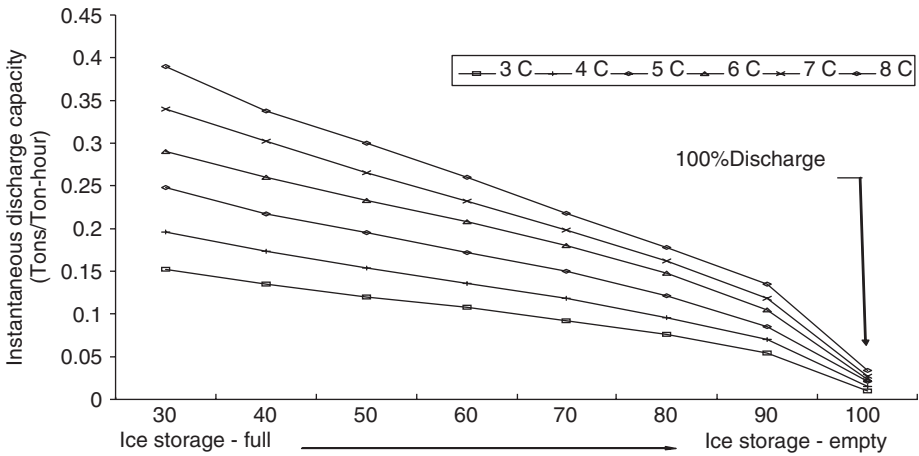


**Figure 3.43** Instantaneous discharge capacity of Cryogel ice balls (in tons per ton-hour of storage capacity), as a function of storage inlet and outlet LMTDs (Courtesy of CRYOGEL Ice Ball Thermal Storage)

in this level of detail, and focuses on the practical output of the sizing methodology, this information helps understand some of the design details for ice CTES systems (e.g., Figures 3.44 and 3.45).

**Practical Example II: Design and Operational Loads**

The following design example is taken from Baltimore Aircoil Company (BAC, 1985). The analysis is performed using ice chiller Thermal Storage Unit Selection (TSU-M) software. The selected TES, substance, and chiller are

- BAC thermal storage: 1 TSU-476M 1 TSU-761M
- Glycol charge: 4776 L of 25% ethylene glycol
- Specified chiller: Model A-chiller 12 at approximately 514 kW  
(for details, see Table 3.11).

Before providing details, it is necessary to introduce some definitions which are important in design calculations:

- **LBT.** Chiller-leaving brine temperature.
- **EDB.** Dry-Bulb air temperature (for air-cooled chillers used in ice building).
- **CWT.** Condenser water temperature (for water-cooled chillers used in ice building).
- **Parasitic load(s).** The heat input to the thermal storage device from other devices in the TES system. Internal melt ice-on-coil systems do not have such parasitic loads. However, for external melt ice-on-coil systems, the parasitic auxiliary device is the air pump used for agitation of the storage media. In this case, the parasitic heat gain must include the heat input to the thermal storage device as the air is cooled from its source temperature to the temperature of the storage media.
- **Operational modes.** Status of the thermal devices in the cooling system in relation to meeting the required load. Modes include cooling with chillers (compressor) only, cooling with TES device plus chiller (in partial-storage systems), building ice without cooling, building ice with cooling, cooling with ice only (full-storage systems), and no chiller plus no TES (in the case of no cooling load).
- **Chiller load.** Cooling load supplied by the chiller compressor.

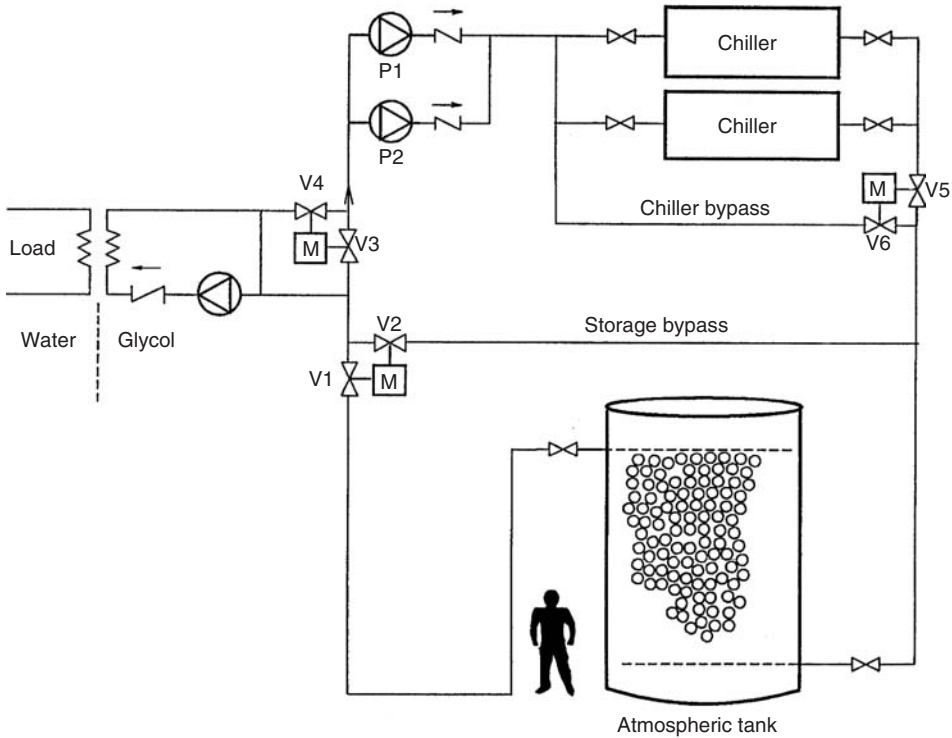


**Figure 3.44** An atmospheric ice ball, single tank (series) TES system (Courtesy of CRYOGEL Ice Ball Thermal Storage)

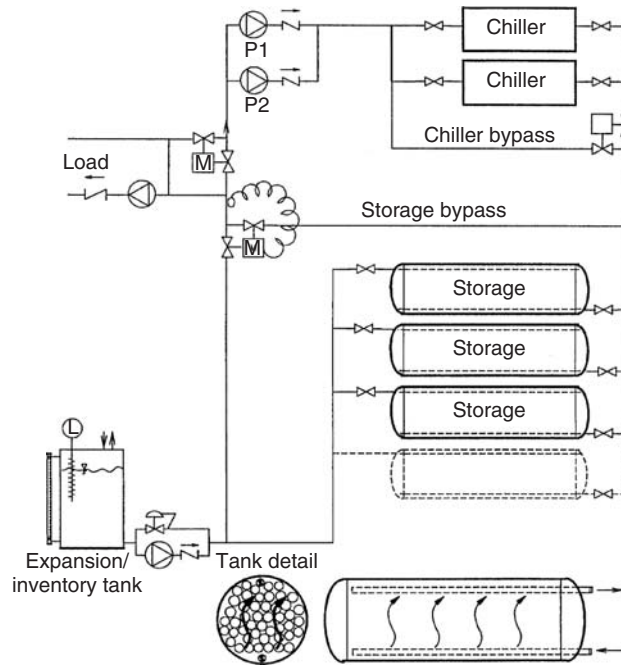


**Figure 3.45** A pressurized ice ball, single tank (series) TES system (Courtesy of CRYOGEL Ice Ball Thermal Storage)

**Table 3.11** Details for chiller A (38 L/s)

LBT (°C)	EDB (°C)	Capacity (kW)	Power (kW)	COP
-5.6	23.9	374	154	2.43
-5.6	35.0	331	166	2.00
6.7	23.9	568	180	3.15
6.7	35.0	513	199	2.57

Courtesy of Baltimore Aircoil International N.V.

- **Base load.** Load to be met completely by the chillers. Selection of base load chillers should be done so that the chillers are running at maximum efficiency.
- **Total load.** Total thermal load of the building/process to be delivered by the cooling system (chillers and ice TES system).
- **Heat rejection.** Heat dissipated by the condenser of the chiller to achieve the cooling required from the chiller.
- **Charge and discharge rates.**
  - *Charge rate.* The rate (typically expressed in tons or kW) at which energy (heat) is removed from the storage device during the charge period.
  - *Discharge rate.* The rate (typically expressed in tons or kW) at which energy (heat) is added to the storage device during the discharge period.
- **Ambient loss.** Sum of conduction, convection, and radiation heat escaping from the thermal energy storage tank to the surroundings.
- **Net storage.** Actual quantity of ice present in the ice TES tank at a particular time.
- **Flow rate.** Brine flow rate within the ice TES system.

- **Inlet temperature.**
  - *Inlet temperature for the thermal storage device.* Temperature of the brine entering the ice thermal energy storage tank.
  - *Inlet Temperature for the thermal storage system.* Temperature of the brine entering the ice thermal energy storage system (chiller and tank).
- **Exit temperature.**
  - *Exit temperature for the thermal storage device.* Temperature of the brine leaving the ice thermal energy storage tank.
  - *Exit temperature for the thermal storage system.* Temperature of the brine leaving the ice thermal energy storage system (chiller and tank).
- **Pressure drop.** Pressure loss due to brine flow through the coil of the ice thermal energy storage system.
- **Chiller peak load.** Maximum load delivered by the chiller at certain ambient and brine temperatures.
- **Chiller average load.** Average load delivered by the chiller at certain ambient and brine temperatures.
- **COP.** Coefficient of performance.

On the bases of the load profile and operating strategy, the selection will deliver a peak of 1000 kW at design conditions of 38 L/s of 25% by weight ethylene glycol from 10.2 to 3.4 °C. The maximum pressure drop across the storage unit is 79.1 and 75.3 kPa in the ice build and melt modes, respectively. Summaries for the loads, flow, temperature, and pressure parameters, and energy demand and use are presented in Tables 3.12–3.14.

### 3.8.10 Ice Forming

The ice-making equipment is expected to form ice and deliver it to the storage tank accordingly. Three main systems are available for forming ice:

- direct expansion, which forms ice by directly feeding refrigerant into the ice-making heat exchanger;
- the brine system, which exchanges heat between refrigerant and brine in the heat pump evaporator to produce low-temperature liquid brine that is fed to the ice-forming coil, and
- the heat pipe system, which exchanges heat between the refrigerant evaporator and water, and forms ice on the heat pipe surface.

In the United States, direct expansion is used in the majority of large-scale systems, while the brine system is mainly used for medium- and small-scale equipment. In Japan, the brine system is favored regardless of building size.

Compared to the other types, brine systems require more space and special materials, and have lower COPs because of the additional temperature difference between refrigerant and brine, and the power consumption by the brine pump. However, they do have the advantage that the tank and heat pump can be located separately. Direct expansion systems require a much larger refrigerant charge, are more expensive, and are difficult to maintain.

### 3.8.11 Ice Thickness Controls

The oldest type of ice storage is the refrigerant-fed ice builder, which consists of refrigerant coils inside a storage tank filled with water. The tank water freezes on the outside of the chiller evaporator coils to a thickness of up to 0.065 m. Ice is melted from the outside of the formation (hence the

**Table 3.12** Design and operational loads and TES system parameters

Hour	Mode	EDB (°C)	Chiller load (kW)	Base load (kW)	Total load (kW)	Chiller load (kW)	Heat rejection rate	Charge rate (kW)	Discharge rate (kW)	Ambient loss rate (kW)	Net storage (kWh)
0:00	B	38	0	0	0	347	520	347	–	1.8	2,081
1:00	B	38	0	0	0	345	518	345	–	1.8	2,426
2:00	B	37	0	0	0	346	517	346	–	1.8	2,769
3:00	B	36	0	0	0	346	517	346	–	1.8	3,113
4:00	B	36	0	0	0	345	516	345	–	1.8	3,457
5:00	B	36	0	0	0	344	514	344	–	1.8	3,801
6:00	B	36	0	0	0	215	375	215	–	1.8	4,143
6:37	S	36	0	0	0	–	–	–	–	1.8	4,357
7:00	S	37	0	0	0	–	–	–	–	1.8	4,357
8:00	I	38	800	0	800	464	661	–	336	1.8	4,354
9:00	I	39	840	0	840	460	661	–	380	1.8	4,016
10:00	I	41	860	0	860	466	673	–	394	1.8	3,635
11:00	I	43	890	0	890	465	675	–	425	1.8	3,239
12:00	I	45	950	0	950	463	679	–	487	1.8	2,812
13:00	I	47	980	0	980	459	679	–	521	1.8	2,323
14:00	I	47	1,000	0	1,000	458	679	–	542	1.8	1,800
15:00	I	48	990	0	990	455	677	–	535	1.8	1,256
16:00	I	47	880	0	880	444	662	–	436	1.8	719
17:00	I	47	660	0	660	414	623	–	246	1.8	281
18:00	B	45	0	0	0	339	526	339	–	1.8	33
19:00	B	44	0	0	0	340	524	340	–	1.8	371
20:00	B	42	0	0	0	342	523	342	–	1.8	709
21:00	B	41	0	0	0	345	523	345	–	1.8	1,049
22:00	B	39	0	0	0	346	522	346	–	1.8	1,392
23:00	B	38	0	0	0	347	522	347	–	1.8	1,736

Since storage device(s) is passive, there are no parasitic loads.

mode, mode of operation; B, ice build; S, standby; I, cooling (ice with compressor); C, cooling (compressor only) (Courtesy of Baltimore Aircoil International N.V.).

term *external melt*) by circulating water through the tank, causing it to become chilled. Air bubbled through the tank agitates the water to promote uniform ice buildup and melting.

Instead of a refrigerant, a secondary coolant (e.g., 25% ethylene glycol and 75% water) can be pumped through the coils inside the storage tank. The coolant has the advantage of greatly decreasing the refrigerant inventory. However, a refrigerant-to-coolant heat exchanger between the refrigerant and the storage tank is required in such instances.

Some major concerns specific to the control of ice-on-coil systems are

- limiting ice thickness (and thus excess compressor energy) during the build cycle and
- minimizing the bridging of ice between individual tubes in the ice bank.

Bridging is avoided because it restricts the free circulation of water during the discharge cycle. While not being physically damaging to the tank, this blockage reduces performance, raising the water exit temperature because of reduced heat-transfer surface.

Regardless of the refrigeration method (direct-expansion or secondary coolant), the compressor is controlled by (i) a timer or controller that restricts operation to periods dictated by the utility rate structure, and (ii) an ice-thickness override control, which stops the compressor(s) at a predetermined ice thickness. At least one ice-thickness controller should be installed per ice bank. If there are multiple refrigeration circuits per ice bank, one ice-thickness control per circuit should be installed.

**Table 3.13** Flow, temperature, and pressure parameters

Hour	Mode	Charge rate (kW)	Discharge rate (kW)	Flow rate (L/s)	Inlet temp. (°C)	Exit temp. (°C)	Pressure drop (kPa)	Total load (kW)	Flow rate (L/s)	Inlet temp. (°C)	Exit temp. (°C)	Net storage (kWh)
0:00	B	347	—	38.0	−3.9	−1.5	78.6	—	0	—	—	2,081
1:00	B	345	—	38.0	−4.0	−1.7	78.6	—	0	—	—	2,426
2:00	B	346	—	38.0	−4.2	−1.8	78.6	—	0	—	—	2,769
3:00	B	346	—	38.0	−4.3	−2.0	78.6	—	0	—	—	3,113
4:00	B	345	—	38.0	−4.4	−2.1	78.6	—	0	—	—	3,457
5:00	B	344	—	38.0	−4.5	−2.2	78.6	—	0	—	—	3,801
6:00	B	215	—	38.0	−4.6	−2.2	78.6	—	0	—	—	4,143
6:37	S	—	—	—	—	—	—	—	—	—	—	4,357
7:00	S	—	—	—	—	—	—	—	—	—	—	4,357
8:00	I	—	336	38.0	4.3	2.0	75.2	800	38.0	7.4	2.0	4,354
9:00	I	—	380	38.0	4.6	2.0	75.1	840	38.0	7.7	2.0	4,016
10:00	I	—	394	38.0	5.5	2.8	74.8	860	38.0	8.6	2.8	3,635
11:00	I	—	425	38.0	5.9	3.0	74.7	890	38.0	9.1	3.0	3,239
12:00	I	—	487	38.0	6.5	3.2	74.5	950	38.0	9.7	3.2	2,812
13:00	I	—	521	38.0	6.8	3.3	74.4	980	38.0	9.9	3.3	2,323
14:00	I	—	542	38.0	7.1	3.4	74.4	1,000	38.0	10.2	3.4	1,800
15:00	I	—	535	38.0	7.1	3.4	74.4	990	38.0	10.1	3.4	1,256
16:00	I	—	436	38.0	5.9	3.0	74.7	880	38.0	8.9	3.0	719
17:00	I	—	246	38.0	3.7	2.0	75.3	660	38.0	6.5	2.0	281
18:00	B	339	—	38.0	−2.3	0.0	77.6	—	0	—	—	33
19:00	B	340	—	38.0	−2.6	−0.3	77.8	—	0	—	—	371
20:00	B	342	—	38.0	−3.0	−0.6	78.0	—	0	—	—	709
21:00	B	345	—	38.0	−3.2	−0.9	78.2	—	0	—	—	1,049
22:00	B	346	—	38.0	−3.5	−1.2	78.3	—	0	—	—	1,392
23:00	B	347	—	38.0	−3.7	−1.4	78.5	—	0	—	—	1,736

Since storage device(s) is passive, there are no parasitic loads.

Mode, mode of operation; B, ice build; S, standby; I, cooling (ice with compressor); C, cooling (compressor only) (*Courtesy of Baltimore Aircoil International N.V.*).

Placement of the ice-thickness controller(s) should be determined by the ice-bank manufacturer, on the basis of circuit geometry and flow pressure drop to minimize bridging.

Ice-thickness controls are either mechanically or electrically operated. Mechanical controls typically consist of a fluid-filled probe positioned at a desired distance from the coil. As ice builds, it encapsulates the probe, causing the fluid to freeze and apply pressure. The pressure signal controls the refrigeration system via a pneumatic–electric switch. Electric controls operate by sensing difference between electrical conductivities of ice and water. Multiple probes are installed at the desired thickness, and the change in current flow between probes provides a control signal. Consistent water treatment is essential to maintaining constant conductivity and thus accurate control.

An ice logic ice quantity (ILIQ) controller (Figure 3.46) is commonly used, allowing accurate setting of the minimum and maximum ice quantity as a function of the expected cooling load. This enables maximum control, system efficiency, and operating flexibility of the cooling equipment. The setting can easily be done manually on the ILIQ controller or automatic (remote) control can be used. Ice quantities are measured and displayed, often as 0, 20, 40, 60, 80, and 100% of nominal storage capacity. The ILIQ controller has the necessary output contacts that can be connected to a building management control system to allow automatic control of the cooling system. As an option, a 4–20 mA output signal is possible. The ILIQ controller contains the necessary logic to prevent unwanted chiller cycling after the desired ice build is complete. Between the control box and the sensors, the intermediate cabling has steel reinforcement and a poly(vinyl chloride (PVC)

**Table 3.14** Energy demand and usage

	Mode	Chiller used	Loading (%)	Chiller peak load (kW)	Chiller average load (kW)	Electric rate
0:00	B	A	100	173	173	1
1:00	B	A	100	173	173	1
2:00	B	A	100	172	172	1
3:00	B	A	100	171	171	1
4:00	B	A	100	170	170	1
5:00	B	A	100	170	170	1
6:00	B	A	100	170	104	1
6:37	S	–	–	–	–	–
7:00	S	–	–	–	–	–
8:00	I	A	100	197	197	1
9:00	I	A	100	201	201	1
10:00	I	A	100	206	206	1
11:00	I	A	100	210	210	1
12:00	I	A	100	216	216	1
13:00	I	A	100	220	220	1
14:00	I	A	100	221	221	1
15:00	I	A	100	222	222	1
16:00	I	A	100	218	218	1
17:00	I	A	100	209	209	1
18:00	B	A	100	186	186	1
19:00	B	A	100	184	184	1
20:00	B	A	100	181	181	1
21:00	B	A	100	178	178	1
22:00	B	A	100	176	176	1
23:00	B	A	100	174	174	1

Electric rate structure: 1, peak demand period; 2 shoulder peak demand; 3, off-peak period; mode, mode of operation (*Courtesy of Baltimore Aircoil International N.V.*).

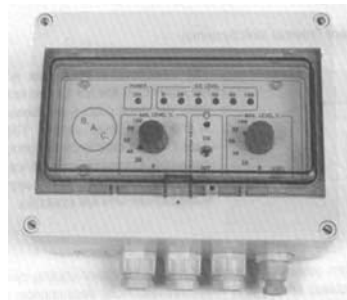


**Figure 3.46** ILIQ controller for manual control (*Courtesy of Baltimore Aircoil International N.V.*)

cover. The cables possess a screening against interference. Ice TES units can be designed for two different TES system concepts: external or internal melt (the ILIQ controller is the same for both except that for each concept a specific sensor (Figure 3.47) is designed).

- **Ice thickness sensor for external melt systems.** A series of accurately positioned electrodes detect the ice thickness on the coil tube. The measurement is based on difference in electrical

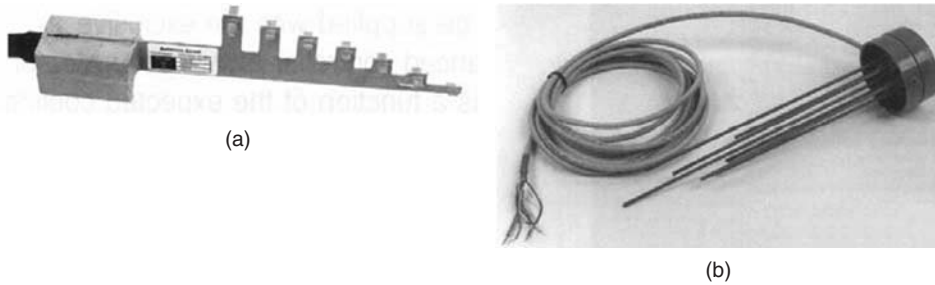


**Figure 3.47** (a) Ice thickness sensor for external melt systems, and (b) water level sensor for internal melt systems (Courtesy of Baltimore Aircoil International N.V.)

conductivity between ice and water. Combined with this sensor, the ILIQ controller limits the maximum ice thickness to the desired level.

- Water level sensor for internal melt systems.** The water level in the sensor is proportional to the ice quantity in the ice chiller tank. A series of specially designed probes measure the water level in the water level sensor. The measurement is based on the difference of conductivity between air and water. Combined with the ILIQ controller, output signals to control the operations of the ice chiller unit are also available.

Because energy use is related to ice thickness on the coil, a partial-load ice inventory management system is often considered. This system keeps the ice inventory at the minimum level needed to supply immediate future cooling needs, rather than topping off the inventory after each discharge cycle. It also helps prevent bridging by ensuring that the tank is completely discharged at regular intervals, thereby allowing ice to build evenly.

The most common method of measuring ice inventory is based on the fact that ice has a greater volume than water. Thus, a sensed change in water level indicates a change in the amount of stored ice. Because water increases 9% in volume when it changes to ice, the water level varies directly with the amount of ice in the tank as long as all of the ice remains submerged. This water displaced by the ice must not be frozen, or it freezes above the original water level. Therefore, no heat exchange surface area can be above the original water level. The change in water level in the tank due to freezing and thawing is typically 0.153 m. This change can be measured with either a pressure gauge or a standard electrical transducer. For projects with multiple tanks, a reverse-return piping system ensures uniform flow through all the tanks; so, measuring the level in one tank is sufficient to determine the overall proportion of ice remaining.

### 3.8.12 Technical and Design Aspects of CTES

While conventional cooling systems operate chillers to satisfy predictable, instantaneous cooling loads, CTES systems operate chillers to produce cold during off-peak hours. Conventional chillers typically operate 8–12 h per day to meet cooling requirements, representing a large portion of a building's daytime electrical demand. Shifting electrical use through thermal energy storage reduces high peak demand charges. Utilities benefit from lower peak demand and gain off-peak load, often allowing a shift from less efficient to more efficient equipment. Thus, utilities increase plant efficiencies and delay the need for future expansion.

The selection of a specific type of CTES system is dependent on many factors. The first issue is usually whether CTES is appropriate for a facility. If so, the next question usually concerns the most appropriate type. System options often include ice or water storage, but the most appropriate choice depends on project characteristics. Some other key factors that affect system choices include building type, utility rate structure, and energy-conservation grants and incentives.



Building type, not building size, normally determines whether CTES is cost effective. A building with a fairly even load demand 24 h per day is not a good candidate. Office buildings or schools that close at night, or buildings with short, intense power demands, such as convention centers, sports facilities, and religious buildings, are often good candidates. In general, the higher the peak load, the more likely a candidate the facility is to benefit from CTES. Local energy rates also play a key role in determining CTES cost effectiveness. Most utilities charge for peak demand and have significantly higher rates for electricity used during peak, daytime hours. Therefore, careful analysis of rates and load distribution is essential when considering CTES.

Client attitudes can also affect technology choices. Although CTES systems are not entirely new, some clients may not be familiar and therefore comfortable with this technology, or may not have staff willing to take on different operating and maintenance tasks. In some applications, system redundancy is required (at least for an initial period) to overcome apprehension about CTES.

Therefore, when considering and selecting a CTES system for a client or facility, an engineer should have or obtain a thorough understanding of the following design issues (Maust, 1993):

- Is CTES economically and physically feasible?
- Is there room on-site for a chilled-water or ice or other CTES systems?
- Does the local utility have peak-demand charges, low off-peak rates or rebates for avoiding peak demand?
- Is the building-load profile flat or is there a strong peak?
- Will the client be comfortable maintaining and operating a CTES?

CTES is often best considered relatively later in the design process. While CTES must be integrated with many other aspects of building design (e.g., heating or cooling loads, mass, layout, and HVAC equipment), other efficiency measurements may level cooling loads and/or heating needs sufficiently that otherwise attractive storage schemes no longer make economic sense.

Most efficiency and many load management options cost less than CTES in retrofits, and should therefore be implemented first where appropriate. In new buildings, however, installation of an ice storage or a water tank can be synergistic with other design choices that reduce both energy consumption and peak load. Such benefits are especially achievable using fully integrated and computer-aided design.

For CTES, full storage is sometimes preferable to partial storage. Similarly, ice storage sometimes has advantages over chilled-water storage (when equally well designed). Skill and experience are needed to ensure appropriate implementation.

Significant recent progress has been made in improving the cost effectiveness and reliability of CTES equipment, especially for ice harvesters and stratified storages.

Ice storage uses more energy because of the lower temperatures needed compared to chilled-water systems and higher heat leaks through tank insulation. But ice storage uses less energy for several other reasons: the chiller always runs at its design efficiency or not at all (rather than varying continually in response to changing building loads); the ambient dry and wet bulb temperatures in contact with the condenser are lower at night; and the very cold melt water from the ice greatly reduces the energy needed for both chilled-water pumping and air handling. The net effect is usually a net decrease in electrical energy consumption with ice CTES as low as a few percent to a few tens of percent.

The economics of CTES in buildings of all types and sizes frequently hinge on two nonenergy factors: (i) the expected political and economic stability of utilities time-of-use rates; and (ii) demand charges, and the physical space available, and structural load tolerance for the storage tank.

### *3.8.13 Selection Aspects of CTES*

Selecting a CTES for a particular application is often difficult. International standards have not yet been fully developed to provide a basis for the rating and performance testing of these systems.

In general, however, it is clear that a CTES system must cool a building in the same way as the chiller it replaces or supplements.

The selection of a CTES system should account for the load, as should its operating characteristics, that is, the discharge rate, the energy discharged at all times during the discharge cycle, and required storage inlet and outlet temperatures. Information on temperatures, energy stored, and energy discharged versus discharge cycle time describes the performance of a CTES system well. With this information, a performance data schedule should be established to fully describe the system needs (Bishop, 1992). Clearly, rating a CTES system on only energy storage capacity does not accurately describe the system needs. All aspects of the system must be such that overall the system has the capability to provide performance roughly equivalent to that for the conventional chiller supplemented or replaced. In particular, CTES must provide stored energy when the building requires it. Performance specifications that recognize this complexity can help in achieving successful CTES projects.

The selection among available system options depends upon site-specific factors. Some of the factors that can enter into this decision are as follows (Wylie, 1990):

- **Space availability.** Ice storage systems require approximately one-third to one-quarter of the space of chilled-water systems. PCMs also have similar storage advantages over chilled-water systems.
- **Efficiency.** Water chillers use less energy than ice-makers because of higher evaporating temperatures. PCMs require slightly less energy than chilled-water systems.
- **Chilled-water temperatures.** Ice storage systems can supply lower water temperatures, and systems can be designed for larger supply/return temperature differences, resulting in lower flow rates and pumping costs and smaller central plants.
- **Refrigeration compressor size.** Reciprocating compressors associated with ice storage are size limited. The use of multiple units in large plants is usually uneconomic, requiring the use of screw-type compressors instead.
- **Maintenance costs.** In general, chilled-water storage tanks have lower maintenance costs. Maintenance personnel are usually more familiar with chilled-water systems.
- **Experience of contractor and operator.** Contractors and building operation engineers are usually weakly familiar if not totally unfamiliar with the large, built-up, field-erected direct-expansion or flooded coil refrigeration systems required for ice storage.

### 3.8.14 Cold-Air Distribution in CTES

Reducing the temperature of the distribution air in an air-conditioning system is attractive because smaller air-handling units, ducts, pumps, and piping can be used, resulting in lower initial costs. In addition, the reduced ceiling space required for ductwork can significantly reduce building height, particularly in high-rise construction. These cost reductions can make thermal storage systems competitive with nonstorage systems on an initial cost basis.

The optimum supply air temperature is usually determined through an analysis of initial and operating costs for various design options. Depending on the load, the additional latent energy removed at the lower discharge-air temperature may be offset by the reduction in fan energy associated with the lower air flow rate.

The minimum achievable supply air temperature is determined by the chilled-water temperature and the temperature rise between the cooling plant and the terminal units. With some ice storage systems, the fluid temperature may rise during discharge; therefore the supply temperatures normally achievable with various types of ice storage plants should be carefully investigated with the equipment supplier.

A heat exchanger is sometimes required with storage tanks that operate at atmospheric pressure or between a secondary coolant and a chilled-water system. The rise in chilled-water temperature

between the cooling-plant discharge and the chilled-water coil depends on the length of piping and the amount of insulation. A smaller temperature difference can be achieved with more cooling-coil rows or a larger surface area on the cooling coil, but extra heat-transfer surface is often uneconomic.

A blow-through configuration provides the lowest supply air temperature and the minimum supply air volume. The lowest temperature rise achievable with a draw-through configuration is 2–3 °C because heat from the fan is added to the air. A draw-through configuration should be used if space for flow straightening between the fan and coil is limited. A blow-through unit should not be used with a lined duct because air with high relative humidity enters the duct.

Face velocity determines the size of the coil for a given supply air volume, and the coil size determines the size of the air-handling unit. A lower face velocity generates a lower supply air temperature, whereas a higher face velocity results in smaller equipment and lower initial costs. The face velocity is limited by moisture carry-over from the coil. The face velocity for cold-air distribution systems is usually 1.5–2.5 m/s. Cold primary air can be tempered with room air or plenum return air by using fan-powered mixing boxes or induction boxes. The primary air should be tempered before it is supplied to the space. The energy use of fan-powered mixing boxes is significant, and negates the savings from downsizing central supply fans.

Diffusers designed for cold-air distribution can provide supply air directly to the space without causing drafts, thereby eliminating the need for fan-powered boxes. If the supply air flow rate to occupied spaces is expected to be below 0.02 m<sup>3</sup>/s per m<sup>2</sup> of floor area, fan-powered or induction boxes should be used to boost the air circulation rate. At supply air rates of 0.02 to 0.03 m<sup>3</sup>/s per m<sup>2</sup>, a diffuser with a high ratio of induced room air to supply air should be used to ensure adequate dispersion of ventilation air throughout the space. A diffuser that relies on turbulent mixing rather than induction to temper the primary air may not be effective at these flow rates.

Cold-air distribution systems normally maintain space humidity between 30 and 45% as opposed to the 50–60% generally maintained by other systems. At this lower humidity level, equivalent comfort conditions are provided at higher dry-bulb temperatures. The increased dry-bulb set point generally results in decreased energy consumption.

The surfaces of any equipment that may be cooled below the ambient dew point, including air-handling units, ducts, and terminal boxes need to be insulated. Any vapor-barrier penetrations should be sealed to prevent migration of moisture into the insulation. Prefabricated, insulated round ducts are normally insulated externally at joints where internal insulation is not continuous. If ducts are internally insulated, access doors also need to be insulated.

Duct leakage is undesirable because it represents cooling capacity that is not delivered to the conditioned space. In cold-air distribution systems, leaking air can cool nearby surfaces to the point at which condensation forms. Designers should specify acceptable methods of sealing ducts and air-handling units, and establish allowable leakage rates and test procedures. These specifications must be checked through on-site supervision and inspection during construction.

A thorough commissioning process is important for the optimal operation of any large space conditioning system, particularly thermal storage and cold-air distribution systems. Reductions in initial and operating costs are the major features for cold-air distribution, but successful performance can be compromised by reducing initial costs by avoiding commissioning. In fact, comprehensive commissioning can decrease costs by reducing future system malfunctions and troubleshooting expenses, and provide increased value by ensuring optimal system operation.

### Advantages of Cold-Air Distribution and TES

- **Demand reduction.** Cooling load is often the largest contributor to the peak electrical demand in a building. Since many electric utilities experience their peak electrical demands in the summer months, attributable mainly to building cooling loads, electric utilities often promote the use of CTES systems to shift the electrical demand in buildings from peak to off-peak periods. Continually increasing peak demands from customers require the utilities to either build additional generating capacity or rely on less efficient peaking plants. With higher demand charges and

seemingly high “ratchet clauses” associated with electric utility rates, building owners can find CTES options attractive in retrofit situations. This advantage is especially significant when incentive or rebate programs are offered toward CTES.

- **Lower capital costs.** Thermal storage and cold-air distribution systems require considerably less volume to meet a cooling load relative to conventional systems that use 12.7°C supply air. Thus, the mechanical system including chillers, air-handling units, pumps, fans, fan motors, and ductwork can be downsized and still satisfy the same cooling load as a conventional system. Reduced equipment size results in significant capital cost savings.
- **Lower operating costs.** The reduced size of the mechanical equipment associated with a thermal storage and cold-air distribution system leads to significant savings in the operating costs associated with running the system. Because the chillers, fans, and pumps used in the system consume less electricity than their counterparts in conventional systems, the thermal storage and cold-air distribution systems consume less energy over the operating life of the equipment, and thus provide additional operating cost savings to building owners.
- **Improved comfort.** Thermal storage and cold-air distribution systems typically provide 5.5–7.5°C supply air into the space for comfort cooling. This low-temperature supply air improves comfort levels by lowering the relative humidity in the occupied areas. Typically, the dry bulb temperature is 5.5°C off the coil, and results in a relative humidity of about 36% in the occupied areas, compared to about 50% for a conventional system. This reduction in relative humidity along with room conditions of 25.5°C (typical for low-temperature primary air systems) results in a cool feeling in the occupied zone.
- **Reduced noise.** The smaller air-handling equipment and insulated ductwork associated with cold-air distribution and TES usually reduce the transmission of noise to the occupied zones, and thus reduce potential annoyances to occupants.
- **Increased usable space.** Typically, in a retrofit project, the architectural impact resulting from a modification to a conventional HVAC system is significant. The increased cooling load associated with increased occupancy loads or computer and equipment loads requires additional chiller capacity, air-handling capacity, and ductwork (or a combination of these). A low-temperature air-distribution system allows for small equipment and use of existing vertical shafts to carry low-temperature air to occupied zones, thereby reducing major architectural impacts due to modifications associated with the HVAC system. The smaller mechanical equipment frees up some existing space in the mechanical room for other systems or purposes.
- **Increased leaseability and marketability.** Reductions in the demand charges and energy costs associated with operating a thermal storage and cold-air distribution system may attract tenants, because these savings can be passed on to them through leasing-cost reductions or lower utility bills. Similarly, when the owner of a building sells the property, the CTES increases the marketability of the building.
- **Minimum disruption.** Because thermal storage and cold-air distribution systems can utilize existing ductwork in the building, this option minimizes work disruption, inconvenience to building occupants, and sometimes, the costs associated with occupant relocations.

### Disadvantages of Cold-Air Distribution and TES

- **Condensation.** The main difficulty in using thermal storage and cold-air distribution is the condensation that may occur because of the low-temperature air passing through the ductwork, causing ceiling damage and mold. Properly insulated and sealed ductwork, sealed plenum spaces, and special collars at the duct connection to the VAV boxes (if used) or diffusers can prevent condensation and ensure proper operation of the cold-air distribution system.
- **Insufficient air.** The reduction in volume of air supplied to the occupied space may cause feelings of stuffiness and stagnation in those in the room. At the present time, building

owners/designers have two alternatives to address this problem. First, fan-powered VAV boxes can be used in conjunction with the low-temperature air to mix proper amounts of ceiling plenum (return) air with low-temperature supply air to produce 12.7°C and to maintain minimum air circulation in the room. Second, low-temperature diffusers that are offered by some manufacturers can be used. These low-temperature diffusers have unique thermal characteristics that can prevent the condensation problems mentioned above, and provide high induction rates to maintain room air circulation. The noise levels produced by such high-induction unit diffusers are within acceptable limits.

- **Dumping of air.** Because of the decrease in supply air temperature and the low buoyancy of cold air jet, air from the outlets may be dumped into the occupied zone causing occupant discomfort due to concentrations of cold air. Dumping is simply the discharge of an air jet with little velocity. This problem can be addressed by using the two methods discussed earlier (fan-powered VAV boxes or high-induction diffusers).

### 3.8.15 *Potential Benefits of CTES*

During the past two decades, CTES technology has matured and is now accepted by many as a proven energy-conservation technology. However, the predicted payback period of a potential cool storage installation is often not sufficiently attractive to give it priority over other technology options. This determination often is reached because full advantage is not made of the many potential benefits of CTES, or because the CTES sizing is not optimized.

Several steps can be taken to optimize the payback period of cold TES systems. In general, cool storage should be closely integrated with the overall building and its energy systems to take full advantage of its potential benefits. These benefits depend on whether the application is for a new or existing facility.

For new facilities, the potential benefits include

- use of low-temperature chilled-water distribution to reduce pipe and pump sizes and operating costs;
- use of low-temperature air distribution to reduce duct and fan sizes and operating costs;
- use of smaller chillers and electrical systems to reduce initial costs;
- a gain in usable building space due to less space being required for the mechanical system components.

For existing facilities, the potential benefits that should be evaluated include

- the possible advantages of modifying the existing chillers to make ice versus the purchase of a new machine;
- the use of spare chiller capacity in a chilled-water CTES system;
- the use of cold storage to gain more cooling capacity in situations where the chiller and electrical service capacities are fully utilized;
- the possibility of using low-temperature air to advantage, where practical.

For both new and existing facilities, the sizing of the cool storage system should be optimized, as opposed to the typical process of considering full storage and one or two levels of partial storage versus a conventional system. A practical method to assist in determining the optimum system size should be developed. Also, the value should be accounted for of the gain in usable building space due to less space being required for mechanical system components when cool TES is used.

Most CTES systems reduce electricity demand during peak times by reducing (or eliminating) the need to run the air-conditioning compressor during the day when electricity costs are highest.

Thus, buildings can be cooled effectively during the day, while taking advantage of lower off-peak electricity rates. The chilled medium remains in storage until needed, typically during the day when the building is occupied. Then, the water or ice is used to cool the building. Cold-air distribution can be used with CTES to allow the user to take advantage of the colder temperatures supplied by some CTES systems. With cold-air distribution, the size of ductwork can be reduced, lowering construction costs.

Consequently, a CTES system can be of benefit to users in three main ways:

- **Lower electricity rates.** With CTES, chillers can operate at night to meet the daytime cooling needs, taking advantage of lower off-peak electricity consumption rates.
- **Lower demand charges.** Many commercial customers pay a monthly electrical demand charge on the basis of the largest amount of electricity used during any 30-minute period of the month. CTES reduces peak demands by shifting some of those demands to off-peak periods. Furthermore, some utilities provide a rebate for shifting electrical demand to night or other off-peak periods.
- **Lower air-conditioning system and compressor costs.** Without CTES, large compressors capable of meeting peak cooling demands are needed, whereas smaller and less expensive units are sufficient when CTES is used. Also, since water from a CTES may be colder than conventional chilled water, smaller pipes, pumps, and air handlers may be integrated into the building design to reduce costs further.

In some situations, one can reduce air-conditioning costs by up to one-half with CTES.

### 3.8.16 *Electric Utilities and CTES*

Electric utilities are placing increased emphasis on peak-load pricing strategies, such as time-of-day rates and marginal cost-based rates. These rate strategies present consumers with significant opportunities for cost control through load management in building design and operation. Consumers can take advantage of peak-load time-of-use rates, while reducing cooling and heating costs and maintaining comfort by installing a CTES system for space conditioning.

CTES systems can reduce HVAC equipment sizes, and lower air supply temperature (to as low as 8.3 °C, with 30% relative humidity). This low humidity can provide adequate comfort with a 26.6 °C ambient thermostat setting. By comparison, the supply air for conventional systems is at 12.7 °C and 50% relative humidity, which permits a 23.3 °C thermostat setting. CTES systems can also lower the first cost of equipment for energy distribution (e.g., pumps, pipes, fans, air ducts) and the operating costs for fans and pumps. The chilled-water storage media in some systems can also provide backup for fire control systems. The 30% relative humidity supply air can in some instances be passed through heat exchangers to cool incoming outdoor air from 35 to as low as 20 °C using direct evaporative cooling. Chiller condenser water (especially during ice making) can also be used in winter to reduce heating requirements.

Actual CTES systems are designed, evaluated, and approved in situations where the concerns and preferences of the electric utility are of considerable importance, since utilities often provide financial incentives to promote the inclusion of CTES in new and retrofitted air-conditioning systems. Special off-peak rate schedules are also sometimes available to larger customers for which separate metering of air-conditioning loads is practical. Rebates are normally predicated on electrical demand (in kW) shifted to off-peak periods. Substantial payments are common. Some examples from relatively recent years: southern California Edison's CTES-rebate limit was \$300,000, based on \$200 per kW shifted, while at Wisconsin Electric, rebates were variable, typically \$350 per kW shifted and \$0.08 per kWh shifted during the May to September cooling period. The combined effect of such rebates and the reduced operating costs achieved with a properly designed CTES system typically leads to simple payback periods of 2–5 years based on the CTES implementation cost.



### 3.9 Seasonal TES

Many heating systems, notably those using heat pumps, and including virtually all active solar space-heating systems, incorporate TES systems capable of storing heat from times when excess amounts are available to times when they are unavailable or expensive. The period of storage can vary from a few hours for diurnal storage cycles, to many months for seasonal (annual) cycles. Seasonal TES in solar heating systems is particularly favored in high-latitude locations, where

- solar energy is available more during the long summer days, when it is not needed, than during the short winter days, when heating demands must be met and
- cold ambient conditions, often below 0°C, are available during the winter with its short days, when cooling is not needed, than during the long summer days, when space cooling demands must be met.

The potential exists for seasonal storage of heating capacity from summer until winter in the former case, while the potential exists for seasonal storage of cooling capacity from winter until summer in the latter case.

#### 3.9.1 Seasonal TES for Heating Capacity

Water is often favored as the storage medium in seasonal TES systems because it can function as both the heat transport medium and the heat storage medium, eliminating the cost and thermodynamic losses of one heat exchange operation, and also meeting the engineering preferences for a low-cost, nontoxic, nonflammable, noncorrosive, chemically stable, nonviscous, high-specific-heat fluid with known characteristics.

Many storage containers are used for seasonal TES, including tanks, caverns, and aquifers. Seasonal storage requirements for heating capacity are often met by large, insulated-tank, hot-water systems. They are typically of substantial size, usually above 500,000 L, because the decreasing surface-to-volume ratio with increasing size reduces both the cost and the heat loss on a unit of storage capacity basis.

The optimal form for such large tanks appears to be the right circular cylinder with vertical axis. Tanks of this form have low surface-to-volume ratios. They can be built to rest on the ground surface, or to be partially or fully buried. Often the tops of the tanks in buried configurations are modified for other purposes (e.g., paved for use as a parking lot or landscaped for use as a park). All heat losses or infiltrations from buried tanks flow through the soil and ultimately reach one of the two heat sinks: the ground–air interface and the water table. It is noted for this cylindrical geometry that the condition where height and radius are approximately equal tends to minimize the overall tank heat loss, since it gives the minimum surface-to-volume ratio. The inside of the tank is often covered with a layer of insulation.

In some cases, tanks that are partially buried can have some or all of the excavated material bermed against the side walls (see Figure 3.48), to provide both physical support and a degree of insulation for the upper part of the tank wall. This configuration also provides for good surface water drainage, often has hydraulic advantages associated with the lift requirements of the system pumps, and avoids the need to haul and dispose of excavated soil from the site.

Methodologies for the analysis of the heat loss characteristics of several long-term storages have been studied (Hooper *et al.*, 1980; Rosen, 1990, 1998a). In particular, the fully buried tank, with its top flush with the surface of the ground, and the on-ground tank have already received attention, and design methodologies for these cases have been developed. The thermal properties of the soil surrounding the tank are sometimes dependent on position, time, and temperature. For example, changes in soil moisture content can occur during rains or melting of snow and ice, and can significantly alter the soil's thermal properties. Some additional energy interactions that are present

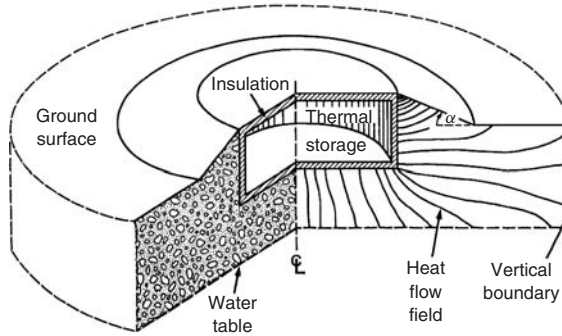


**Figure 3.48** Illustration of partially buried, bermed heat storage tank. Approximate lines of heat flow outside the tank are shown

include the latent heat of fusion of soil moisture during freezing and thawing, and the latent heat of vaporization during surface drying. The structural materials of the tank walls, often reinforced concrete, sometimes have similar thermal properties as the soil regime.

### 3.9.2 Seasonal TES for Cooling Capacity

Several systems for seasonal storing of cold have been proposed and tested. Most of these are based on ice storage, and are applicable in climates where temperatures are below  $0^{\circ}\text{C}$  for much of the winter.

In one system, an ice store is built up throughout the winter by spraying water into a tank that is exposed to the ambient atmosphere when conditions are suitable for freezing water. During other times, the tank, which is insulated, is closed. In the summer, when space cooling is needed, the ice is allowed to melt and the cold water is circulated as required for cooling. The tank is designed to permit enough ice to be created in the winter to meet most or all of the summer cooling needs. Such a system has been tested in Ottawa, Canada.

### 3.9.3 Illustration

A seasonal thermal storage for heating capacity was installed at the Aylmer Senior Citizens residence in Ontario, Canada. That storage is a cylindrical tank, with its axis vertical and with a height of 6.7 m and a radius of 7.5 m. The tank is uniformly insulated with 0.15 m of foamed polyurethane having a conductivity of  $0.0346\text{ W/m K}$ , and is buried. The storage fluid, water, ranges in temperature from about  $80^{\circ}\text{C}$  at the end of summer when the storage is almost fully charged, to about  $30^{\circ}\text{C}$  at the end of winter when the storage has been for the most part discharged.

The surrounding conditions of the Aylmer area are typical of south-western Ontario. The seasonal mean temperatures of the ambient air are about  $21^{\circ}\text{C}$  in summer,  $-7^{\circ}\text{C}$  in winter, and  $7^{\circ}\text{C}$  in both spring and autumn. The water table is relatively constant when the temperature is about  $7^{\circ}\text{C}$ , and the thermal conductivity of the soil is about  $1.73\text{ W/m K}$ .

In a preliminary economic analysis of cylindrical tanks such as the one considered here (Rosen, 1998b), tanks that are buried and have soil berms applied were shown, in most instances, to be superior to other tank configurations. This analysis determined whether the initial cost savings derived from using a bermed tank, instead of an in-ground tank, are greater or less than the additional costs associated with the greater heat losses for the bermed tank over the life of the tank. The factors considered in the analysis included the increased excavation cost associated with an in-ground tank, the increased wall thickness required for an in-ground tank, the haulage of excavated



soil for an in-ground tank compared to the cost of placing the soil into a berm, and the increased heat loss associated with a bermed tank.

### 3.10 Concluding Remarks

Although energy may be stored in many ways (e.g., in mechanical, kinetic or chemical forms), since much of the economy involves thermal energy, the storage of thermal energy warrants careful attention. TES deals with the storing of energy by cooling, heating, melting, solidifying, or vaporizing a material, the energy becoming available as heat when the process is reversed. TES is a temporary storage of high – or low – temperature energy for later use. There are mainly two types of TES systems: sensible (e.g., water and rock) and latent (e.g., ice and salt hydrates). Storage by causing a material to increase or decrease in temperature is called *sensible heat storage*. Its effectiveness depends on the specific heat of the material and, if volume is important, the density of the storage material. Storage by phase change, the transition from solid to liquid or from liquid to vapor with no change in temperature, is known as *latent heat storage*.

Short-term storage (diurnal storage) is used to manage peak power loads of a few hours to a day, in order to reduce the sizing of systems and/or to take advantage of energy tariffs. Medium- or long-term storage is more common when waste heat or seasonal energy loads can be transferred, with a delay of a few weeks to several months, to cover seasonal needs. This type of TES is called *seasonal or annual storage*.

The selection of TES systems mainly depends on the storage period required (e.g., diurnal or seasonal), economic viability, operating conditions, and so on. Some specific parameters that influence the viability of a TES include facility thermal loads, thermal and electrical load profiles, availability of waste or excess thermal energy, electrical costs and rate structures, type of thermal generating equipment, and building type and occupancy. The economic justification for TES systems usually requires that annual capital and operating costs are less than the costs for primary generating equipment supplying the same service loads and periods. Substantial energy savings can be realized by taking advantage of TES to facilitate using waste energy and surplus heat, reducing electrical demand charges, and avoiding heating, cooling, or air-conditioning equipment purchases.

Today TES is considered as an advanced energy technology. The use of TES systems has been attracting increasing interest in several thermal applications, for example, active and passive solar heating, water heating, cooling, and air-conditioning. TES is often the most economic storage technology for HVAC applications.

For solar thermal applications, the use of TES systems is essential because of fluctuations in the solar energy input. Several classes of storage may be required for a single installation, depending on the type and scale of the solar power plant, and the nature of its integration with conventional utility systems.

TES can help correct the mismatch between supply and demand of energy, and can significantly contribute to meeting society's needs for more efficient, environmentally benign energy use. TES thus plays an important role in energy conservation, and can yield significant saving of premium fuels.

TES exhibits an enormous potential to make the use of thermal energy equipment more effective, and for facilitating large-scale energy substitutions economically. A coordinated set of actions is needed in several sectors of energy systems in order to realize the maximum benefits of storage.

### References

- Abhat, A. (1983). Low temperature latent heat thermal energy storage: heat storage materials, *Solar Energy* 30(4), 313–332.
- AEP (2001). *HVAC Central System-Thermal Storage*, American Electric Power, [http://www.aep.com/EnergyInfo/ces\\_html](http://www.aep.com/EnergyInfo/ces_html)

- Ames, D. (1989). The past, present and future of eutectic salt storage systems, *ASHRAE Journal*, May 1989, 2, 26–27.
- Anon. (1990). *Guide to Seasonal Storage*, Swiss Federal Energy Office.
- ASHRAE (2000). *Standard 943*, American Society of Heating, Refrigerating and Air-Conditioning Engineers, Inc., Atlanta, Georgia.
- BAC (1985). *Ice Chiller Thermal Storage Unit Selection*, Baltimore Aircoil International N.V., Belgium.
- Bishop, D. (1992). How to select thermal storage, *Heating/Piping/Air-conditioning*, January 1992, 87–88.
- Brown, D.R., Katipamula, S. and Koynenbelt, J.H. (1996). *A Comparative Assessment of Alternative Combustion Turbine Cooling Systems*, Pacific Northwest National Laboratory, Project Report: PNNL-10966/UC-202, Richland.
- CADDET (1997). *Learning from Experiences with Thermal Energy Storage: Managing Electrical Loads in Buildings*, Analyses Series 4, Center for the Analysis and Dissemination of Demonstrated Energy Technologies (CADDET), Paris.
- Choi, J.C. and Kim, S.D. (1995). Heat transfer in latent heat-storage system using  $MgCl_2 \cdot 6H_2O$  at the melting point, *Energy* 29, 13–25.
- Choudhury, C. and Garg, H.P. (1995). Integrated rock bed heat exchanger-cum-storage unit for residential-cum-water heating, *Energy Conversion and Management* 36(10), 999–1006.
- Cristopia (2000). *Thermal Energy Storage Technical Manual*, Cristopia Energy Systems, Venice.
- Dincer, I. (1999). Evaluation and selection of thermal energy storage systems for solar thermal applications, *International Journal of Energy Research* 23(12), 1017–1028.
- Dincer, I. and Dost, S. (1996). A perspective on thermal energy storage systems for solar energy applications, *International Journal of Energy Research* 20(6), 547–557.
- Dincer, I., Dost, S. and Li, X. (1997a). Performance analyses of sensible heat storage systems for thermal applications, *International Journal of Energy Research* 21(10), 1157–1171.
- Dincer, I., Dost, S. and Li, X. (1997b). Thermal energy storage applications from an energy saving perspective, *International Journal of Global Energy Issues* 9(4-6), 351–364.
- Dinter, F., Ger, M. and Tamme, R. (1991). *Thermal Energy Storage for Commercial Applications*, Springer-Verlag, Berlin.
- Eldighidy, S.M. (1991). Insulated solar storage tanks, *Solar Energy* 47, 253–268.
- Environment Canada (1999). The Earth for storing energy, *Science and the Environment Bulletin*, No. 14, 6.
- GSA (2000). *Heat Storage*, GSA Resources Inc., <http://www.gsaresources.com/heat.htm>
- Harris, N.C., Miller, C.E. and Thomas, I.E. (1985). *Solar Energy Systems Design*, John Wiley & Sons, Ltd., New York.
- Hooper, F.C., McClenahan, J.D. and Williams, G.T. (1980). *Solar Space Heating Systems using Annual Heat Storage*. Final Report No. DOE-CS-32939-12 prepared for U.S. Department of Energy, by Department of Mechanical Engineering, University of Toronto.
- IEA (1990). Thermal storage, *IEA Heat Pump Center Newsletter* 8(2), 10.
- Kuroda, H. (1993). Ice thermal storage systems, *IEA Heat Pump Center Newsletter* 11(4), 22–24.
- Lane, G.A. (1980). Low temperature heat storage with phase change materials, *International Journal of Energy Research* 5, 155–160.
- Lane, G.A. (1988). *Solar Heat Storage: Latent Heat Materials, Vol. 1: Background and Scientific Principles*, CRC Press, Florida.
- Maust, D. (1993). A tale of two systems: ice versus cold water thermal storage, *Heating/Piping/Air-conditioning*, September 1993, 30–36.
- Moschatos, A.E. (1993). Combined thermal storage, *Solar Energy* 51(5), 391–399.
- Narita, K. (1993). Combined system of heat pump and water thermal storage, *Proceedings of the Heat Pumps and Thermal Storage*, pp. 69–75, 24-25 May 1993, Fukuoka, Japan.
- Norton, B. (1992). *Solar Energy Thermal Technology*, Springer-Verlag, London.
- Paris, J., Falardeau, M. and Villeneuve, C. (1993). Thermal storage by latent heat: a viable option for energy conservation in buildings, *Energy Sources* 15, 85–93.
- Piette, M.A. (1990). *Learning from Experience with Diurnal Thermal Energy Storage Managing Electric Loads in Buildings*, CADDET Analysis Support Unit, June 1990.
- Rosen, M.A. (1990). Evaluation of the heat loss from partially buried, bermed heat storage tanks, *International Journal of Solar Energy* 9(3), 147–162.

- Rosen, M.A. (1998a). A semi-empirical model for assessing the effects of berms on the heat loss from partially buried heat storage tanks, *International Journal of Solar Energy* 20, 57–77.
- Rosen, M.A. (1998b). The use of berms in thermal energy storage systems: energy-economic analysis, *Solar Energy* 63(2), 69–78.
- Sanner, B. and Chant, V.G. (1992). Seasonal cold storage in the ground using heat pumps, *IEA Heat Pump Center Newsletter* 10(1), 4–7.
- Sharma, S.K., Sethi, P.B.S. and Chopra, S. (1992). Kinetic and thermophysical studies of acetamide sodium bromide eutectic for low temperature storage applications, *Energy Conversion and Management* 33(2), 145–150.
- Shimizu, M. and Fujita, K. (1985). Actual efficiencies of thermally-stratified thermal storage tanks, *IEA Heat Pump Center Newsletter* 3 (1/2), 20–25.
- Sokolov, M. and Keizman, Y. (1991). Performance indicators for solar pipes with phase change storage, *Solar Energy* 47(5), 339–346.
- Thomason, H.E. (1960). Solar space heating and air conditioning in the Thomason house, *Solar Energy* 4, 11–19.
- Tomlinson, J.J. and Kannberg, L.D. (1990). Thermal energy storage, *Mechanical Engineering* 112, 68–72.
- Vaccarino, C., Cimino, G., Frusteri, F. and Barbaccia, A. (1985). A new system for heat storage utilizing salt hydrates, *Solar Energy* 34(2), 171–173.
- Wylie, D. (1990). Evaluating and selecting thermal energy storage, *Energy Engineering* 87(6), 6–17.

### Study Questions/Problems

- 3.1 How much energy is needed to heat a volume of  $10\text{ m}^3$  of water from  $25$  to  $75^\circ\text{C}$ ? Take the density of water as  $1000\text{ kg/m}^3$  and the specific heat as  $4.2\text{ kJ/kg}^\circ\text{C}$ .
- 3.2 List the various TES processes and explain each.
- 3.3 What are the benefits of TES systems?
- 3.4 What criteria should be considered in TES evaluation?
- 3.5 Modify the TES evaluation checklist to cover current environmental issues.
- 3.6 What are the barriers to TES adoption?
- 3.7 Define the storage period and the types of classifications used for them for applications.
- 3.8 Are there any standards available for TES? If so, identify and describe them.
- 3.9 What kinds of storage options are available for solar energy applications?
- 3.10 Discuss the types and features of various stratified TES tanks.
- 3.11 What are the differences between single- and dual-medium systems?
- 3.12 Explain how an aquifer TES works.
- 3.13 List the environmental benefits of TES.
- 3.14 Identify potential heat sources for an aquifer TES, in general, and specifically in your community.
- 3.15 Describe the operation of an aquifer-based heat pump.
- 3.16 What are the main advantages of evacuated solar collectors?
- 3.17 What are the main expectations of PCMs?
- 3.18 What is nucleation?
- 3.19 What is thermal cycling?

- 3.20 What aspects are necessary to evaluate and select a PCM?
- 3.21 Explain how the performance of a PCM is assessed.
- 3.22 What are the selection criteria for latent TES?
- 3.23 Explain the working principle of a cold TES.
- 3.24 Show the possible TES operating strategies on a chart and explain each.
- 3.25 What are the main design considerations for a cold TES?
- 3.26 Compare the storage volumes of water and ice for 1000 kJ of heat capacity.
- 3.27 List the classifications for ice TES and describe them.
- 3.28 Describe the operation and technical details of ice-on-pipe CTES system.
- 3.29 Describe the operation and technical details of a ice harvester system.
- 3.30 Describe the operation and technical details of a glycol CTES system.
- 3.31 Describe the operation and technical details of CTES systems with encapsulated storage media.
- 3.32 Describe the operation and technical details of an ice-slurry CTES system.
- 3.33 What are the advantages offered by ice-slurry CTES?
- 3.34 What are the main systems for ice formation?
- 3.35 What are the options to control the ice thickness?
- 3.36 Why is it important in many ice CTES systems that the ice buildup does not become extensive in all parts of the system?
- 3.37 List and explain the CTES selection factors.
- 3.38 What is seasonal TES? Describe how it works for cooling and heating options.

# 4

## Thermal Energy Storage and Environmental Impact

### 4.1 Introduction

Energy supply and use are related not only to problems such as global warming but also to such environmental concerns as air pollution, ozone depletion, forest destruction, and emissions of radioactive substances. These and other environmental issues must be taken into consideration if human society is to develop in the future while maintaining a healthy and clean environment. Much evidence suggests that the future will be negatively impacted if people and societies continue to degrade the environment.

There is an intimate connection between energy, the environment, and sustainable development. A society seeking sustainable development ideally must utilize only energy resources that cause no environmental impact (e.g., which release no emissions or only harmless emissions to the environment). However, since all energy resources lead to some environmental impact, it is reasonable to suggest that some (but not all) of the concerns regarding the limitations imposed on sustainable development by environmental emissions and their negative impacts can be overcome through increased energy efficiency. A strong correlation clearly exists between energy efficiency and environmental impact since, for the same services or products, less resource utilization and pollution is normally associated with higher efficiency processes.

Thermal energy storage (TES) systems can contribute significantly to meeting society's needs and desires for more efficient, environmentally benign energy use in such applications as building heating and cooling and electric power generation and distribution. The use of TES systems often results in significant benefits, such as the following (Dincer *et al.*, 1997; Rosen *et al.*, 2000):

- reduced energy costs;
- reduced energy consumption;
- improved indoor air quality;
- increased flexibility of operation;
- decreased initial and maintenance costs;
- reduced equipment size;
- more efficient and effective utilization of equipment;
- conservation of fossil fuels (by facilitating more efficient energy use); and
- reduced pollutant emissions (e.g., CO<sub>2</sub>).

In this chapter, anticipated patterns of future energy use and consequent environmental impacts (focusing on acid precipitation, stratospheric ozone depletion, and the greenhouse effect) are

comprehensively discussed. Also, some solutions to current environmental issues are identified, including energy conservation, increased efficiency, and use of renewable energy technologies, and some theoretical and practical limitations to increased efficiency are explained. The relations between energy and sustainable development and between the environment and sustainable development are described, and several illustrative examples are presented. Throughout the chapter, several issues relating to energy, environment, and sustainable development are examined from both current and future perspectives. Finally, several conclusions are drawn and recommendations are made, which are useful to scientists, researchers, engineers, and policy makers in the field of TES.

## 4.2 Energy and the Environment

Achieving solutions to the environmental problems that we face today requires long-term planning and actions, particularly if we are to approach sustainable development. In this regard, renewable energy resources appear to represent one of the most advantageous solutions. Hence, a strong connection is often reported between renewable energy and sustainable development.

Energy is in many ways the convertible currency of technology. Without energy resources, our societies cannot function and would crumble. The effect of only a 24-h disruption in electricity supply to a city shows how totally dependent we are on that particularly useful form of energy. Computers and elevators cease to function, hospitals reduce to a basic care and maintenance level, and lights go out.

The average annual growth rate in world population is approximately 2%, and many countries exceed that level. As populations grow, the need for more and more energy resources is exacerbated. Enhanced lifestyles and energy demand usually rise together. Presently, there is a great disparity between the populations of countries and their wealth and energy use. The wealthy industrialized economies of the world which contain 25% of the world's population consume about 75% of the world's energy supply (Dincer, 1998).

World population is expected to double by the middle of the 21st century and economic development will almost certainly continue to grow. Global demand for energy services is expected to increase by as much as an order of magnitude by 2050, while primary energy demands are expected to increase by 1.5–3 times. Simultaneously, concern will likely increase regarding energy-related environmental issues such as acid precipitation, stratospheric ozone depletion, and global climate change (Dincer, 2000).

Environmental considerations have been given increasing attention in recent decades by energy industries and the public. The concept that consumers share responsibility for pollution and its impact and cost has been increasingly accepted. In some jurisdictions, the prices of many energy resources have increased over the last 20 years, in part to account for environmental costs.

An often-proposed solution to possible energy-resource shortage is increased use of TES technologies, and the application of TES technologies can be quite advantageous in many instances. To achieve the benefits, engineers and designers must carefully consider the practicality, reliability, applicability, and economics of TES. Scarcity of energy supply and public acceptability should also be considered accordingly.

More broadly, it is pointed out that energy is one of the main factors that must be considered in discussions of sustainable development. Several definitions of sustainable development have been put forth, including the following common one: "development that meets the needs of the present without compromising the ability of future generations to meet their own needs" (Anon, 1987). Thus, to achieve sustainable development, a supply of energy resources is required that is fully sustainable (i.e., in the long term, it is readily and sustainably available at reasonable cost and can be utilized for all required tasks without causing negative societal impacts) (Norton, 1991; MacRae, 1992; Rosen, 1996; Dincer and Rosen, 1998). Although a secure supply of energy resources is generally agreed to be a necessary but not sufficient requirement for development within a society, sustainable development further demands a sustainable supply of energy resources and effective and efficient utilization of energy resources. In this regard, the advantages of TES utilization are clear.

### 4.3 Major Environmental Problems

During the past few decades, the risks and reality of environmental degradation have become increasingly apparent. The environmental impact of human activities has grown dramatically due to a combination of factors such as increasing world population, energy consumption, industrial activity, and so on. Throughout the 1970s, most environmental analysis and control instruments concentrated on conventional pollutants such as SO<sub>2</sub>, nitrogen oxides (NO<sub>x</sub>), particulates, and CO. Recently, environmental concern has extended to the control of micro- or hazardous air pollutants, which are usually toxic chemical substances that are harmful in small doses, as well as globally significant emissions such as CO<sub>2</sub>. Despite advances in environmental science, developments in industrial processes and structures have led to new environmental problems such as an increase in the effects of NO<sub>x</sub> and volatile organic compound (VOC) emissions. Details on these gaseous and particulate pollutants and their impacts on the environment and human bodies may be found elsewhere (Dincer, 1998).

Environmental problems span a continuously growing range of pollutants and hazards, and include ecosystem degradation over ever-wider areas. The major areas of environmental concern may be classified as follows (Dincer, 1998):

- acid rain,
- stratospheric ozone depletion,
- global warming and climate change,
- hazardous air pollutants,
- poor ambient air quality,
- water and maritime pollution,
- land use and siting impact,
- radiation and radioactivity,
- solid waste disposal, and
- major environmental accidents.

Among these environmental issues, the most internationally known and most significant ones are usually considered to be acid precipitation, stratospheric ozone depletion, and global climate change. Consequently, we focus on these in this section.

Some gaseous pollutants are listed in Table 4.1, along with their environmental impacts.

**Table 4.1** Main gaseous pollutants and their impacts on the environment

Gaseous pollutant	Greenhouse effect	Stratospheric ozone depletion	Acid precipitation	Smog
Carbon monoxide (CO)	•	•	•	•
Carbon dioxide (CO <sub>2</sub> )	+	+/-	•	•
Methane (CH <sub>4</sub> )	+	+/-	•	•
Nitric oxide (NO) and nitrogen dioxide (NO <sub>2</sub> )	•	+/-	+	+
Nitrous oxide (N <sub>2</sub> O)	+	+/-	•	•
Sulfur dioxide (SO <sub>2</sub> )	-	+	•	•
Chlorofluorocarbons (CFCs)	+	+	•	•
Ozone (O <sub>3</sub> )	+	•	•	+

*Note:* + denotes a contributing effect, - denotes that the substance exhibits an impact which varies with conditions and chemistry and may not be a general contributor, and • denotes no impact.

*Source:* Speight (1996).

### 4.3.1 Acid Rain

Acid rain (acid precipitation) refers to the end result of certain pollutants that are produced by the combustion of fossil fuels, particularly from both stationary devices such as smelters for nonferrous ores and industrial boilers, and transportation vehicles, and that are transported over great distances through the atmosphere and deposited via precipitation on the earth. In the atmosphere, these substances react to form acids, which are often deposited on ecosystems that are exceedingly vulnerable to damage from excessive acidity. This acid rain is mainly attributable to emissions of  $\text{SO}_2$  and  $\text{NO}_x$ . These gases react with water and oxygen in the atmosphere to form such substances as sulfuric and nitric acids (Figure 4.1). The control of acid precipitation requires appropriate control of mainly  $\text{SO}_2$  and  $\text{NO}_x$  emissions.

These pollutants have caused only local concerns related to health in the past. However, awareness of their contributions to the regional and transboundary problem of acid precipitation has recently grown, and attention has also begun focusing on other contributing substances such as VOCs, chlorides, ozone, and trace metals. These substances may participate in the complex set of chemical transformations in the atmosphere that result in acid precipitation and the formation of other regional air pollutants. The types of damage caused by acid precipitation are as follows (Dincer and Rosen, 1998):

- acidification of lakes, streams, and ground waters;
- damage to forests, agricultural crops, and plants due to the toxicity of excessive acid concentration;
- damage to fish and aquatic life;
- deterioration of materials, for example, buildings, metal structures, and fabrics; and
- alterations of the physical and optical properties of clouds due to the influence of sulfate aerosols.

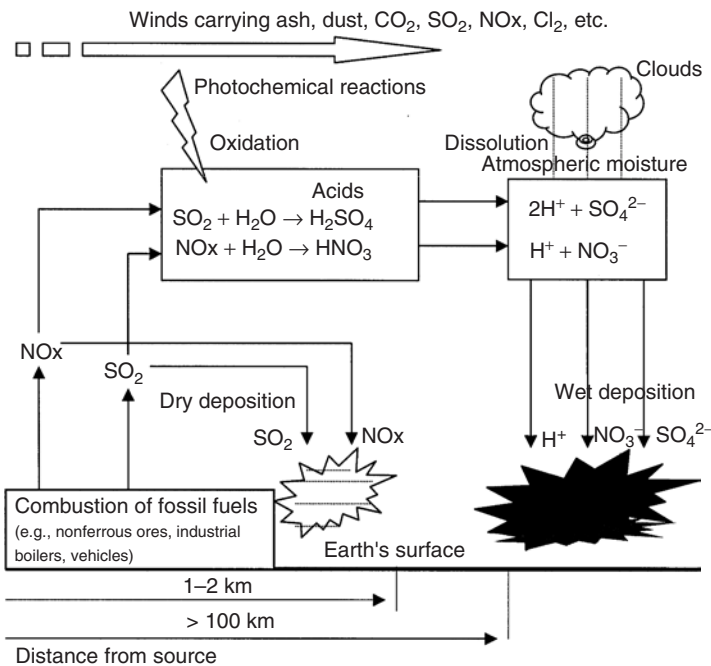


**Figure 4.1** Illustration of the formation, transport, and impact of acid precipitation (Dincer, 2000)



Some energy-related activities are major sources of acid precipitation. For example, electric power generation, residential heating, and industrial energy use account for 80% of  $\text{SO}_2$  emissions. Another source of acid precipitation is sour gas treatment, which releases  $\text{H}_2\text{S}$  that reacts to form  $\text{SO}_2$  when exposed to air. Most of the  $\text{NO}_x$  emissions are due to fossil fuel combustion in stationary sources and road transport. VOCs, which are generated by a variety of sources and comprise a large number of diverse compounds, also contribute to acid precipitation. Countries in which these energy-related activities occur widely are significant contributors to acid precipitation. The largest contributors are the United States, the countries from the former Soviet Union, and China.

The problem of acid precipitation is very contentious because the acid precipitation produced by some countries' emissions often falls on other countries, where it exhibits its damaging effects on the ecology of water systems and forests, and on historical and cultural artifacts.

### 4.3.2 Greenhouse Effect (Global Climate Change)

Although the term the *greenhouse effect*, also known as *global warming* and which leads to global climate change, has generally been used in the past to refer to the role of the atmosphere (mainly water vapor and clouds) in keeping the surface of the earth warm, it is now associated with the warming contribution of  $\text{CO}_2$  and certain other gases. Currently, it is estimated that  $\text{CO}_2$  emissions are responsible for about 50% of the anthropogenic greenhouse effect. Other gases, such as  $\text{CH}_4$ , CFCs, halons,  $\text{N}_2\text{O}$ , ozone, and peroxyacetylnitrate, produced by industrial and domestic activities, also contribute to the greenhouse effect, which, most agree, is causing an increase in the earth's mean temperature and climatic changes (Figure 4.2).  $\text{CO}_2$  and these other gases are often referred to as *greenhouse gases* (GHGs).

The greenhouse effect is potentially the most important environmental problem relating to energy utilization. The greenhouse effect is associated with increasing atmospheric concentrations of GHGs, which increase the manner in which the atmosphere traps heat radiated from the earth's surface, thereby raising the surface temperature of the earth. The earth's surface temperature has increased by about  $0.6^\circ\text{C}$  over the last century, and as a consequence, the sea level is estimated to have risen by perhaps 20 cm (Colonbo, 1992). Such changes can have wide-ranging effects on human

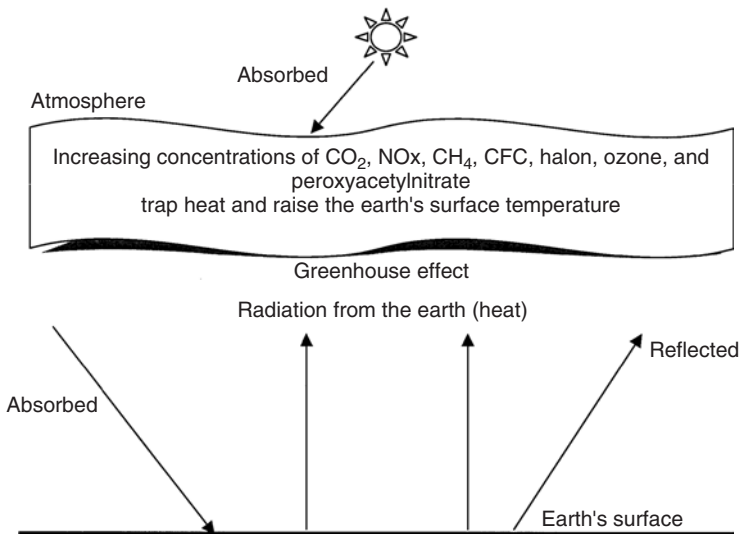


Figure 4.2 Illustration of the greenhouse effect (Dincer, 2000)

activities all over the world. Current knowledge of the role of various GHGs is summarized in Dincer and Rosen (1998).

Humankind is contributing through many of its economic and other activities to the increase in atmospheric concentrations of various GHGs. For example, CO<sub>2</sub> releases from fossil fuel combustion, methane emissions from increased human activity, CFC releases, and deforestation all contribute to the greenhouse effect. Most scientists agree that there is a cause–effect relationship between the observed emissions of GHGs and global warming. Furthermore, many scientists predict that if atmospheric concentrations of GHGs continue to increase, as present trends in fossil fuel consumption suggest, the earth's temperature may increase in the next century by another 2 °C, and perhaps by 4 °C or more. If this prediction is realized, the sea level could rise between 30 and 60 cm before the end of the 21st century (Colonbo, 1992). The impact of such a phenomenon could be dramatic, including flooding of coastal settlements, displacement of fertile zones for agriculture and food production toward higher latitudes, and decreasing availability of freshwater for irrigation and other essential uses. Such consequences could jeopardize the survival of entire populations.

Discussions on averting global climate change must consider the costs of reducing carbon emissions. From a developing country perspective, discussions of costs and benefits should account for the need for policies promoting rapid economic growth. Achieving a balance between economic development and emissions abatement requires domestic policies aimed at improving the efficiency of energy use and facilitating fuel switching, and international policies enabling easier access to advanced technologies and external resources.

Arguments about the magnitude of the greenhouse effect at present and the possible levels in the future have gone on for some time. Some believe that the earth is doomed to a rise in temperature, while others believe that we can go polluting the atmosphere without consequence. However, most agree that GHG emissions are harmful to the environment (Bradley *et al.*, 1991), although some contradictory reports have been published, making the issue complicated to study. Many state that the environment should be considered to be an extremely limited resource, and the discharge of chemicals into it should be subject to severe constraints.

In Table 4.2, the role of various GHGs in the processes involved in the greenhouse effect is summarized.

### 4.3.3 Stratospheric Ozone Depletion

It is known that the ozone present in the stratosphere, roughly between altitudes of 12 and 25 km, plays a natural, equilibrium-maintaining role for the earth, through absorption of ultraviolet (UV) radiation of wavelengths 240–320 nm and absorption of infrared radiation (Dincer, 1998). A global

**Table 4.2** Roles of some substances in the greenhouse effect

Substance	ARIRR <sup>a</sup>	Atmospheric concentration (ppm)		AGR <sup>b</sup> (%)	SGEHA <sup>c</sup> (%)	SGEIHA <sup>d</sup> (%)
		Pre-industrial	In 1990s			
CO <sub>2</sub>	1	275	346	0.4	71	50 ± 5
CH <sub>4</sub>	25	0.75	1.65	1	8	15 ± 5
N <sub>2</sub> O	250	0.25	0.35	0.2	18	9 ± 2
R-11	17,500	0	0.00023	5	1	13 ± 3
R-12	20,000	0	0.00040	5	2	13 ± 3

<sup>a</sup>Ability to retain infrared radiation relative to CO<sub>2</sub>.

<sup>b</sup>Annual growth rate.

<sup>c</sup>Share in the greenhouse effect due to human activities.

<sup>d</sup>Share in the greenhouse effect increase due to human activities.

Source: Dincer and Rosen (1999).

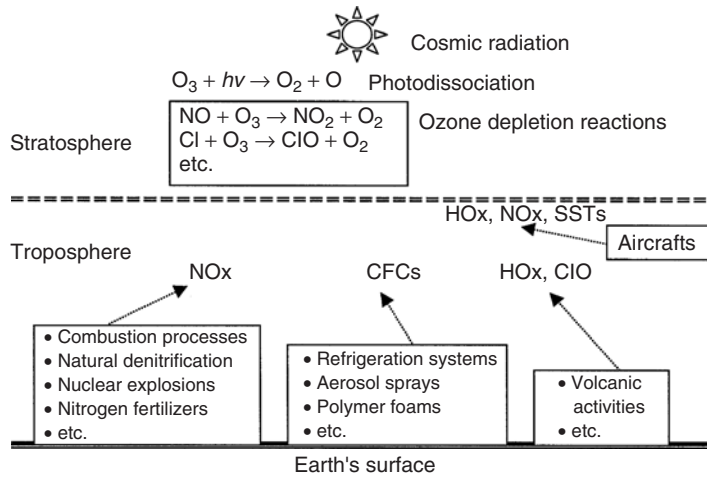


**Figure 4.3** Illustration of sources of natural and anthropogenic ozone-depleting substances (Dincer, 2000)

environmental problem is the distortion and regional depletion of the stratospheric ozone layer, which has been shown to be caused by emissions of CFCs, halons (chlorinated and brominated organic compounds), and NO<sub>x</sub> (Figure 4.3). Ozone depletion in the stratosphere can lead to increased levels of damaging UV radiation reaching the ground, causing increased rates of skin cancer, eye damage, and other harm to many biological species.

Energy- and non-energy-related activities are only partially responsible (directly or indirectly) for the emissions that lead to stratospheric ozone depletion. CFCs, which are used in air-conditioning and refrigerating equipment as refrigerants and in foam insulation as blowing agents, and NO<sub>x</sub> emissions, which are produced from fossil fuel and biomass combustion processes, natural denitrification, nitrogen fertilizers, and aircraft, play the most significant role in ozone depletion. Although scientific debate on ozone depletion has occurred for over two decades, only in 1987 was an international landmark protocol signed in Montreal to reduce the production of CFCs and halons. Much scientific evidence confirming the destruction of stratospheric ozone by CFCs and halons has recently been gathered, and commitments for more drastic reductions in their production were undertaken at many international conferences (e.g., the 1990 London Conference). Many researchers and scientists have undertaken comprehensive studies on the current status of the stratospheric ozone layer. Topics that have been investigated include the history of the problem, chemical and physical phenomena associated with ozone depletion, mapping of ozone losses in the stratosphere, and hypotheses for the causes of the problem and its impacts.

Replacement equipment and technologies that do not use CFCs are increasingly coming to the fore and may ultimately allow for a total ban of CFCs. An important consideration in such a CFC ban is the need to distribute fairly the economic burdens deriving from the ban, particularly with respect to developing countries, some of which have invested heavily in CFC-related technologies. In order to eliminate or minimize the impacts of NO<sub>x</sub> emissions, the solutions mentioned in the previous section can be implemented accordingly.

To conduct a successful environmental study, a clear outline of activities is needed, including the following significant steps:

- definition of the main goals, both short- and long-term;
- measurement or estimation of the data needed with as much accuracy as desired and possible;
- evaluation and assessment of the data;

- processing of the data to generate new and reliable information and knowledge, as well as conclusions and recommendations; and
- reporting of the results without exaggeration or bias.

## 4.4 Environmental Impact and TES Systems and Applications

TES systems can contribute significantly to meeting society's desire for more efficient, environmentally benign energy use, particularly in the areas of building heating and cooling and electric power generation. By reducing energy consumption, the utilization of TES systems results in two significant environmental benefits:

- the conservation of fossil fuels through efficiency increases and/or fuel substitution; and
- reductions in emissions of such pollutants as CO<sub>2</sub>, SO<sub>2</sub>, NO<sub>x</sub>, and CFCs.

TES can impact air emissions at building sites by reducing (i) the amount of ozone-depleting CFC and hydrochlorofluorocarbon (HCFC) refrigerants in chillers, and (ii) the amount of combustion emissions from fuel-fired heating and cooling equipment. Each of these impacts is considered. TES helps reduce CFC use in two main ways. First, since cooling systems with TES require less chiller capacity than conventional systems, they use fewer or smaller chillers with less refrigerant. Second, using TES can offset the lost cooling capacity that can sometimes occur when existing chillers are converted to more benign refrigerants, making building operators more willing to switch refrigerants.

The potential aggregate air-emission reductions at power plants due to TES have been shown to be significant. For example, TES systems have been shown to reduce CO<sub>2</sub> emissions in the United Kingdom by 14–46% by shifting electric load to off-peak periods (Beggs, 1994), while an Electric Power Research Institute (EPRI) co-sponsored analysis found that TES could reduce CO<sub>2</sub> emissions by 7% compared to conventional electric cooling technologies (Reindl, 1994). Also, using California Energy Commission data indicating that existing gas plants produce about 0.06 kg of NO<sub>x</sub> and 15 kg of CO<sub>2</sub> per 293,100 kWh of fuel burned, and assuming that TES installations save an average of 6% of the total cooling electricity needs, TES could possibly eliminate annual emissions of about 560 t of NO<sub>x</sub> and 260,000 t of CO<sub>2</sub> statewide (CEC, 1996).

## 4.5 Potential Solutions to Environmental Problems

In this section, we list a number of general potential solutions to environmental issues. Then, TES-related solutions and their consequences are explained in detail.

### 4.5.1 General Solutions

Various potential solutions to the current environmental problems associated with harmful pollutant emissions have recently evolved, including

- use of TES technologies;
- use of renewable energy technologies;
- energy conservation and increasing the efficiency of energy utilization;
- cogeneration and district heating and cooling;
- use of alternative energy forms and sources for transport;
- energy-source switching from fossil fuels to environmentally benign energy forms;
- use of coal-cleaning technologies;

- optimum monitoring and evaluation of energy indicators;
- policy integration;
- recycling;
- process change and sectoral modification;
- acceleration of forestation;
- application of carbon and/or fuel taxes;
- material substitution;
- promoting public transport;
- changing lifestyles;
- increasing public awareness of energy-related environmental problems;
- increased education and training.

#### 4.5.2 *TES-Related Solutions*

Among the potential solutions listed earlier, the most important to the present discussions is the use of TES technologies. TES and its role in reducing environmental impact are discussed here.

An important step in moving toward the implementation of TES technologies is to identify and remove barriers. Several barriers to the development and introduction of cleaner energy processes, devices, and products have been identified in the past. These barriers must be removed for TES and associated technologies to be more widely used. The barriers can also affect the financing of efforts to augment the supply of TES technologies. Although there are a number of barriers in practice, each TES project or application has its own difficulties and obstacles.

Some of the barriers faced by many TES technologies include (Dincer, 1999)

- technical constraints;
- financial constraints;
- limited information and knowledge of options;
- lack of necessary infrastructure for recycling, recovery, and re-use of materials and products;
- lack of facilities;
- lack of expertise within industry and research organizations, and/or lack of coordinated expertise;
- poorly coordinated and/or ambiguous national aims related to energy and the environment;
- uncertainties in government regulations and standards;
- lack of adequate organizational structures;
- lack of varied electrical rates to encourage off-peak electricity use;
- mismanagement of human resources;
- lack of societal acceptability of new TES technologies; and
- absence of, or limited consumer demand for, TES products and processes.

Establishing concrete methods for promoting TES technologies requires analysis and clarification about how to combine environmental objectives, social and economic systems, and technical developments to attain effective solutions. It is important to create and employ tools that encourage technological development and diffusion, and to align government policies in such areas as energy and environmental standards and government purchasing.

## 4.6 Sustainable Development

Energy resources are needed for societal development, and sustainable development requires a supply of energy resources that is sustainably available at reasonable cost and which causes no negative societal impacts. Thus, energy resources such as fossil fuels that are finite lack sustainability, while

others such as renewable energy sources, often supplemented by TES, are sustainable over the relatively long term.

Environmental concerns also factor into sustainable development, as activities that degrade the environment are not sustainable. As much environmental impact is associated with energy, sustainable development requires the use of energy resources that cause as little environmental impact as possible. Clearly, limitations on sustainable development due to environmental emissions can in part be overcome through increased efficiency, as it leads to less environmental impact for the same services or products.

Consequently, there is a diversity of choices and TES technologies often play an important role in the context of sustainable development.

### 4.6.1 Conceptual Issues

*Sustainability* has become a fashionable word in the 1990s, a legacy of concerns about the environment expressed during the 1970s and 1980s. Also common is *sustainable development* – another term made fashionable. The media often refer to sustainable architecture, sustainable diets, sustainable fisheries, sustainable food production, sustainable futures, sustainable communities, sustainable economic development, sustainable economic growth, sustainable policies, and even sustainable debt.

*Sustainable* has come to mean something good. Part of the problem with sustainable is that it is oftentimes unclear or ambiguous, at least in political discourse. One meaning of sustainable is supportable. But the originators of the term *sustainable development* had another meaning in mind: *capable of being continued*. Thus, sustainable development is politically supportable development, on the one hand, or development that is capable of being continued on the other hand.

Further uncertainty in meaning arises from consideration of what is *unsustainable*, that is, cannot be continued. If transportation trends are stated to be unsustainable (to anticipate later parts of this chapter), does this mean that the transportation trends cannot be continued or that society as we know it cannot continue if the transportation trends continue?

*Development* is also a somewhat ambiguous word. It can mean both progress and happening. The former use has the connotation of movement to a better state; the latter use is less laden with value. Consequently, a minimal, value-free meaning of sustainable development might be “activity that is capable of being continued” (OECD, 1996).

### 4.6.2 The Brundtland Commission’s Definition

The term sustainable development was introduced in 1980, popularized in the 1987 report of the World Commission on Environment and Development (the Brundtland Commission), and given the status of a global mission by the United Nations Conference on Environment and Development (UNCED) in Rio de Janeiro in 1992.

The Brundtland Commission defined sustainable development as “development that meets the needs of the present without compromising the ability of future generations to meet their own needs.” The Commission noted that its definition contains two key concepts: *needs*, meaning “in particular the essential needs of the world’s poor,” and *limitations*, meaning “limitations imposed by the state of technology and social organization on the environment’s ability to meet present and future needs” (OECD, 1996).

The Brundtland Commission’s definition was thus not only about sustainability and its various aspects but also about equity – equity among present inhabitants of the planet, and equity among generations. Sustainable development for the Brundtland Commission includes environmental, social, and economic aspects, but considers remediation of current social and economic aspects an initial priority. The chief tools cited for remediation were “more rapid economic growth in both industrial and developing countries, freer market access for the products of developing countries,

lower interest rates, greater technology transfer, and significantly larger capital flows, both concessional and commercial.” Such growth was said to be compatible with recognized environmental constraints, but the extent of the compatibility was not explored.

### 4.6.3 *Environmental Limits*

The report of the Brundtland Commission stimulated debate about the environmental impacts of industrialization and about the legacy of present activities for coming generations. The report also increased interest in what might be the physical or ecological limits to economic growth.

Further definitions of sustainability proposed give priority to such limits. One business writer, Paul Hawken, suggested the following (OECD, 1996): “The word sustainability can be defined in terms of carrying capacity of the ecosystem, and described with input–output models of energy and resource consumption. Sustainability is an economic state where the demands placed on the environment by people and commerce can be met without reducing the capacity of the environment to provide for future generations. It can also be expressed in the simple terms of an economic golden rule for the restorative economy: Leave the world better than you found it, take no more than you need, try not to harm life or the environment, make amends if you do.”

The author of the above quotation and others have drawn on the work of Herman Daly, formerly of the World Bank, in considering how environmental limits might be characterized. Daly suggested that the limits on society’s material and energy throughputs might be set as follows (OECD, 1996):

- The rates of use of renewable resources should not exceed their rates of regeneration.
- The rates of use of nonrenewable resources should not exceed the rates at which renewable substitutes are developed.
- The rates of pollution emissions should not exceed the assimilative capacity of the environment.

### 4.6.4 *Global, Regional, and Local Sustainability*

Sustainability – or unsustainability – must also be considered in terms of its geographic scope. Activity may be globally unsustainable. For example, it may result in climate change or depletion of the stratospheric ozone layer and so affect several geographic regions, if not the whole world. Activity may be regionally unsustainable, perhaps by producing and dispersing tropospheric ozone or acidifying gases that can kill vegetation and cause famine in one region but not in other parts of the world. Activity may be locally unsustainable, perhaps because it results in hazardous ambient levels of carbon monoxide locally, or because the noise it produces makes habitation impossible. In the long term, sustainability appears to be more a global concern than a regional or local one. If an environmental impact exceeds the carrying capacity of the planet, then life as we know it is threatened. If it is beyond the carrying capacity of one area, then that area may become uninhabitable, but life can most likely continue elsewhere.

### 4.6.5 *Environmental, Social, and Economic Components of Sustainability*

The focus of this discussion on physical limits does not deny the social and economic aspects of sustainability. A way of life may not be worth sustaining under circumstances of extreme oppression or deprivation. Moreover, oppression or deprivation can interfere with efforts to make human activity environmentally benign. Nonetheless, if ecosystems are irreparably altered by human activity, then subsequent human existence may become not merely unpalatable, but impossible. Thus, the environmental component of sustainability is essential.



The heterogeneity of the environmental, social, and economic aspects of sustainability should also be recognized. Environmental and social considerations often refer to *ends*, the former having perhaps more to do with the welfare of future generations and the latter with the welfare of present people. Economic considerations, often taken to refer to ends, can perhaps more helpfully be seen as a *means* to the various ends implied by the environmental and social considerations.

The environmental aspects of sustainability, particularly those of a global nature, are often not focused on by spokespeople for the world's poorer countries. They argue that a preoccupation with the environment ignores their real needs to eliminate poverty and may be associated with plans to prevent development in general and industrialization in particular. The reality is that the poorer half of the world's human population has contributed relatively little to the degradation of global and regional environments. Of the remaining 2–3 billion people whose activities significantly degrade global and regional environments, the several hundred millions who live in OECD member countries contribute a disproportionately large share. They are also the people who can more afford the luxury of thinking about the future. Thus, a focus within the OECD on the environmental aspects of sustainability may be viewed as appropriate (OECD, 1996).

#### 4.6.6 *Energy and Sustainable Development*

A secure supply of energy resources is generally agreed to be a necessary but not sufficient requirement for development within a society. Furthermore, sustainable development demands a sustainable supply of energy resources. The implications of these statements are numerous and depend on how sustainable is defined.

One important implication of these statements is that sustainable development within a society requires a supply of energy resources that, in the long term, is readily and sustainably available at reasonable cost and can be utilized for all required tasks without causing negative societal impacts. Supplies of such energy resources as fossil fuels (coal, oil, and natural gas) and uranium are generally acknowledged to be finite; other energy sources such as sunlight, wind, and falling water are generally considered renewable and therefore sustainable over the relatively long term. Wastes (convertible to useful energy forms through, for example, waste-to-energy incineration facilities) and biomass fuels are also usually viewed as sustainable energy sources.

A second implication of the initial statements in this section is that sustainable development requires that energy resources be used as efficiently as possible (MacRae, 1992; Rosen, 1996). In this way, society maximizes the benefits it derives from utilizing its energy resources, while minimizing the negative impacts (such as environmental damage) associated with their use. This implication acknowledges that all energy resources are to some degree finite, so that greater efficiency in utilization allows such resources to contribute to development over a longer period of time, that is, to make development more sustainable. Even for energy sources that may eventually become inexpensive and widely available, increases in energy efficiency will likely remain sought after to reduce the resource requirements (energy, material, etc.) to create and maintain systems and devices to harvest the energy and to reduce the associated environmental impacts.

The first implication, clearly being essential to sustainable development, has been and continues to be widely discussed. The second implication, which relates to the importance and role of efficiency in achieving sustainable development, is somewhat less discussed and understood.

#### 4.6.7 *Environment and Sustainable Development*

Environmental concerns are an important factor in sustainable development. For a variety of reasons, activities which continually degrade the environment are not sustainable over time, for example, the cumulative impact on the environment of such activities often leads over time to a variety of health, ecological, and other problems.



A large portion of the environmental impact in a society is associated with its utilization of energy resources. Ideally, a society seeking sustainable development utilizes only energy resources that cause no environmental impact (e.g., which release no emissions to the environment). However, since all energy resources lead to some environmental impact, it is reasonable to suggest that some (not all) of the concerns regarding the limitations imposed on sustainable development by environmental emissions and their negative impacts can be in part overcome through increased efficiency. Clearly, a strong relation exists between efficiency and environmental impact since, for the same services or products, less resource utilization and pollution is normally associated with increased efficiency.

Improved energy efficiency leads to reduced energy losses. Most efficiency improvements produce direct environmental benefits in two ways. First, operating energy input requirements are reduced per unit output, and pollutants generated are correspondingly reduced. Second, consideration of the entire life cycle for energy resources and technologies suggests that improved efficiency reduces environmental impact during most stages of the life cycle.

#### 4.6.8 *Achieving Sustainable Development in Larger Countries*

Can sustainable development be pursued by larger countries with varied political and administrative systems? Wealth and advanced technology may make it easier for the industrialized countries to strive for sustainable development, but as the reversal in the trend toward declining carbon emissions after the oil-price decline in 1986 illustrates, the basic motivations, dreams, and desires which require higher energy use (and yield corresponding increases in emissions) have not changed. Transforming these behavioral and decision-making patterns requires the recognition that current development paths are not sustainable. History suggests that such recognition occurs only when short-term consequences are obvious, as in the case of an “oil-price shock” or a drought. In order to successfully mobilize the resources necessary to reduce the risks posed by a changing global climate, the public must perceive the potential long-term consequences associated with present behavior patterns. Translating the future threats associated with continual increases in energy use and carbon emissions into immediate priorities is and will be one of the most difficult challenges faced by policy analysts.

#### 4.6.9 *Essential Factors for Sustainable Development*

The main concept of sustainability, which often inspires local and national authorities to incorporate environmental considerations into their energy program, and which has different meanings in different contexts, embodies a long-term perspective. Future energy systems will largely be shaped by broad and powerful trends that have their roots in basic human needs. Combined with increasing world population, the need will become more apparent for successful implementation of sustainable development.

Various parameters are important to achieving sustainable development in a society, some of which are as follows (Dincer, 1999):

- **Public awareness.** A fundamental step in making a sustainable energy program successful is improving public awareness of its need. This step should be carried out through the media and by public and/or professional organizations.
- **Information.** Necessary information on energy utilization, environmental impact, renewable energy resources, and so on should be provided to the public through public and government channels.
- **Environmental education and training.** This activity complements the provision of information. Any approach that does not include as integral education and training is likely to fail, so

this activity can be considered as necessary to a sustainable energy program. For this reason, a wide scope of specialized agencies and training facilities should be made available to the public.

- **Innovative energy strategies.** Such strategies should be included where appropriate in an effective sustainable energy program. In parallel, efficient dissemination of information is required of the new methods through public relations, training, and counseling.
- **Renewable energy resources and cleaner technologies.** In developing an environmentally benign sustainable energy program, renewable energy sources and cleaner technologies (including TES) should be promoted at every stage. Such activities form a basis for short- and long-term policies.
- **Financing.** Financing is an important tool for achieving the main goal of sustainable energy development in a country and accelerating the implementation of environment friendly energy technologies.
- **Monitoring and evaluation tools.** In order to assess how successfully a program has been implemented, it is of great importance to monitor each step and evaluate the data and findings obtained. In this regard, appropriate monitoring and evaluation tools should be used.

## 4.7 Illustrative Examples and Case Studies

Five examples are considered of energy systems that incorporate TES and, by so doing, mitigate some environmental impacts. The examples are drawn from actual cases.

### 4.7.1 *The South Coast Air Quality Management District (California)*

The South Coast Air Quality Management District (SCAQMD) identifies TES as one way to reduce site emissions, and TES can also significantly reduce combustion air emissions from power plants. Indeed, in California, where natural gas is usually the fuel used for marginal power generation, the reductions in power plant emissions are comparable to emission reductions due to the energy savings from TES. Assuming 20% market penetration by 2005, TES was estimated to be able to avoid 260,000 t of CO<sub>2</sub> emissions annually, statewide. Just as importantly, TES could eliminate about 1.6 t of NO<sub>x</sub> emissions per day in the SCAQMD. These NO<sub>x</sub> emission reductions are equivalent to the reductions achieved by using almost 100,000 electric vehicles (CEC, 1996). At the building site, TES can help reduce CFCs and combustion emissions. TES can also help in the transition to non-CFC air-conditioning refrigerants. For example, when existing chillers are converted to a non-CFC refrigerant, the chillers' effective cooling capacity may be reduced. Some key facility managers see TES as making up the cooling-capacity difference. In addition, use of partial-storage TES often can reduce the required chiller capacity by half, which means, half as much refrigerant is necessary.

### 4.7.2 *Anova Verzekering Co. Building (Amersfoort, The Netherlands)*

This application shows how an aquifer TES system provides energy savings and reductions in environmental pollutants. This seasonal system was introduced in the Netherlands by an insurance company, Anova Verzekering, in its newly renovated office in Amersfoort (IEA-HPC, 1994). The system is considered an innovative space-conditioning system. A schematic diagram of the system for both heating and cooling modes of operation is shown in Figure 4.4. In winter, an electric heat pump is utilized within a hydronic heating and cooling distribution system, which uses a warm ground water aquifer as a heat source. In the heating mode, the ground water is cooled to 8°C and stored in a second water layer location. At the end of the heating season, sufficient cool water has been stored to meet the office cooling needs in summer without requiring operation of the heat pump or any other active cooling system. When cooling is needed, the cooled ground water is

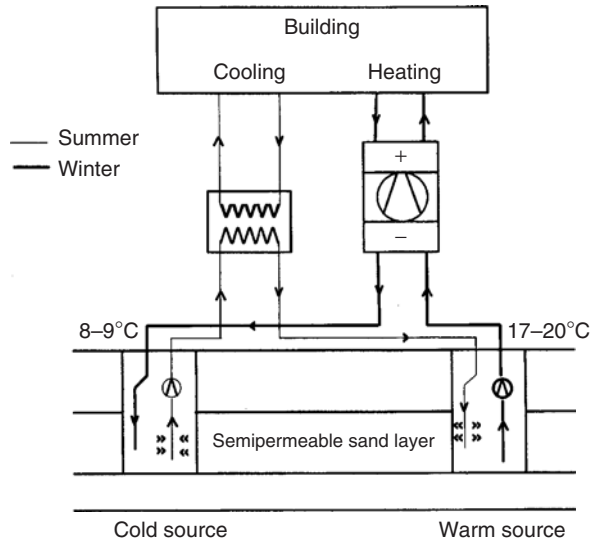


**Figure 4.4** An aquifer TES space air-conditioning system (*Adapted from IEA-HPC, 1994*)

pumped up and used to extract heat from the hydronic system. The ground water then returns to the warm well at temperatures between 17°C and 20°C, thus providing a useful source of stored heat. Very efficient heat pump operation is expected, since the system uses a warm heat source coupled with a heat-distribution temperature of 35–40°C.

A key issue in the success of this design is the utilization of an advanced ceiling-mounted hydronic heating and cooling distribution system. This system offers significant energy savings (as detailed in Section 5.6.3) and environmental benefits, as shown in Table 4.3. With a subsidy of US\$212,000 from the Dutch government, representing over 20% of the total installation cost, the savings in energy costs will pay back the additional investment costs within 6.5 years. This assessment is relative to the conventional alternative technology of gas heating and electric air conditioning.

#### 4.7.3 The Trane Company's Technology Center (La Crosse, WI)

In 1994, the US Environmental Protection Agency (EPA) launched the Energy Star Showcase Buildings Program to encourage and highlight improved building energy efficiency and reduce the environmental pollution.

The Trane Company's Technology Center in La Crosse, WI, was selected as one of 24 charter participants in the program. Under the terms of an agreement signed at EPA headquarters in July 1994, Trane committed to making major improvements in its 18,580 m<sup>2</sup> Technology Center. Built

**Table 4.3** Environmental benefits of the aquifer TES system\*

Emission	Conventional system	TES-based system	Reduction for TES-based system
CO <sub>2</sub> (kg)	608,000	346,000	262,000 (43%)
NO <sub>x</sub> and SO <sub>2</sub>	—	—	(40%)

\*Adapted from IEA-HPC (1994), where further details are available.

in 1954, this building contains laboratories, product design facilities, and offices. The strategy was to first make all the appropriate improvements in the building shell, lighting systems, and heating, ventilating and air conditioning (HVAC) distribution system, and then to make necessary changes in the chillers and chilled water system.

HVAC improvements under the Energy Star Program consisted of improving the air distribution system in the building by evaluating and tuning up fans, dampers, and actuators to make sure they were working properly. It turned out that only minimal structural changes to the air distribution system were necessary. After these changes were made, the chilled water system was assessed.

The existing cooling system for the building used two chillers with 17 modular ice storage containers. The chillers were a two-stage 300-t centrifugal (rated at 1.0 kW/t) and a 1984 three-stage 250-t centrifugal (0.70 kW/t). The newer chiller had been used as the lead chiller and the older machine in a backup capacity. In the ice-making mode, the 250-t machine was rated at 150 t (0.85 kW/t). The new chiller configuration featured a 230-nominal-ton chiller used for ice making, with a duty capacity of 152 t at  $-4.5^{\circ}\text{C}$  leaving water, and a second 400-nominal-ton machine with a rated efficiency of 0.497 kW/t at 100% load. The second chiller was equipped with an adaptive frequency drive to further reduce demand under part-load conditions.

The total cost of the building improvement project was \$350,000. Of this, \$62,000 was rebated by the local utility, Northern States Power Company. The forecast savings from the improvements were \$63,125 per year. In 1995, during which only a part of the improvements were complete, the actual savings were \$36,835. The summer of 1995 was exceptionally warm, with cooling degree days over 50% higher than the previous summer. Yet actual energy performance of the building met expected levels, and a projected simple payback of 4.5 years was confirmed. This represents an internal rate of return on investment of 21.4% for the Trane Company.

From an environmental perspective, the reduced energy requirements by building improvements over 30 years represented a reduction in utility emissions as follows:

- 24.5 million kg of  $\text{CO}_2$ ,
- 313,000 kg of  $\text{SO}_2$ , and
- 115,000 kg of  $\text{NO}_x$ .

Additionally, the project represented an electric demand reduction of over 300 kW, one-third of a megawatt of generating capacity that would not need to be built or purchased over the lifetime of the building. Further details on this system are provided by Trane (1997).

#### 4.7.4 *The Ministry of Finance Building (Bercy, France)*

In 1987, the French government decided to build the new Ministry of Finance on the site of Bercy. The new building ( $260,000\text{ m}^2$ ) is occupied by 5000 persons. It includes restaurants, banks, a post office, a nursery, and so on. It is well equipped with high technologies (security systems, automatic document carrier, etc.). The building is air conditioned by five chillers of 1100 kW each (25,000 kWh stored daily in eight tanks of  $56\text{ m}^3$  each). The STL (*le stockage latent* in French, or latent heat storage) is used to shave the peak demand in summer. Technical data can be summarized as follows:

- Daily cooling energy consumption: 120,000 kWh
- Maximum cooling demand: 9000 kW
- Cooling energy stored: 25,000 kWh
- Store type: STL - 00 - 448
- Number of tanks: 8

The STL is used to shave the peak demand between 8 h and 19 h. The STL is comprised of eight tanks in parallel. The STL is charged during the night by three chillers (2500 kW at  $-5.5/-1^{\circ}\text{C}$ ).

The STL allows the Ministry of Finance to save on operating costs and to have a backup system. The technical advantages of the TES system include

- chiller size reduced by 40%;
- higher electrical generation plant efficiency;
- smaller heat rejection plant;
- increased lifetime of equipment;
- reduced electrical installation;
- backup at disposal; and
- reduced maintenance.

The financial advantages of the TES system can be listed as follows:

- lower operating costs,
- use of low-cost electricity,
- savings on demand charge, and
- savings on maintenance.

Consequently, the environmental advantages of the TES system can be highlighted as follows:

- reduced use of refrigerant by 40%, leading to ozone layer protection; and
- reduced emission of CO<sub>2</sub>, SO<sub>2</sub>, and N<sub>2</sub>O, lowering contributions to the greenhouse effect and other environmental concerns.

Further information on the application may be found elsewhere (Cristopia, 1999).

#### 4.7.5 *The City of Saarbrücken (Saarbrücken, Germany)*

This case study considers the city of Saarbrücken, Germany, which implemented a new energy and environment strategy in the 1980s to reduce energy consumption and CO<sub>2</sub> emissions. The strategy mainly involved district heating, seasonal energy storage, and the use of renewable energies. The city's achievements were classified into energy savings (as detailed in Section 5.6.3) and CO<sub>2</sub> emission reductions as follows: a 15% reduction in CO<sub>2</sub> emissions for the heating and electrical requirements of the municipality. As a result of this successful implementation, the city of Saarbrücken received a Local Government Honor at the UNCED in Rio de Janeiro in June 1992. For further details on this case study, see OECD (1995).

## 4.8 Concluding Remarks

Several concluding remarks can be drawn from this chapter.

There are a number of environmental problems that we face today. These problems span a continuously growing range of pollutants, hazards, and ecosystem degradation over ever-wider areas. The most significant problems are acid precipitation, stratospheric ozone depletion, and global climate change. The latter is potentially the most important environmental problem relating to energy utilization. Rising atmospheric concentrations of GHGs are increasing the manner in which these gases trap heat radiated from the earth's surface, thereby raising the surface temperature of the earth and, as a consequence, sea levels.

Recently, a variety of potential solutions to the current environmental problems associated with the harmful pollutant emissions have evolved. TES appears to be one effective solution and plays a significant role in environment policies.

Sustainable development demands a sustainable supply of energy resources that, in the long term, is readily and sustainably available at reasonable cost and can be utilized for all required tasks without causing negative societal impacts. TES systems can contribute significantly to meeting society's desire for more efficient, environmentally benign energy use and for sustainable development, particularly in the areas of building heating and cooling and electric power generation. By reducing energy consumption, the utilization of TES systems results in two significant environmental benefits: (i) the conservation of fossil fuels through efficiency increases and/or fuel substitution and (ii) reductions in emissions of such pollutants as CO<sub>2</sub>, SO<sub>2</sub>, NO<sub>x</sub>, etc.

## References

- Anon. (1987). *Our Common Future*, World Commission on Environment and Development, Oxford University Press, Oxford.
- Beggs, C.B. (1994). Ice thermal storage: impact on United Kingdom carbon dioxide emissions, *Building Services Engineering Research and Technology* 15(1), 756–763.
- Bradley, R.A., Watts, E.C. and Williams, E.R. (1991). *Limiting Net Greenhouse Gas Emissions in the United States*, US Department of Energy, Washington, DC.
- CEC. (1996). *Source Energy and Environmental Impacts of Thermal Energy Storage*, California Energy Commission, Technical Report No. P500-95-005, California.
- Colonbo, U. (1992). Development and the global environment, In: *The Energy-Environment Connection* (ed. J.M. Hollander), Island Press, Washington, DC, pp. 3–14.
- Cristopia. (1999). *An STL Application: French Ministry of Finance*, Cristopia Energy Systems Catalog, Vence, France.
- Dincer, I. (1998) Energy and environmental impacts: present and future perspectives, *Energy Sources* 20(4/5), 427–453.
- Dincer, I. (1999). Environmental impacts of energy, *Energy Policy* 27(14), 845–854.
- Dincer, I. (2000). Renewable energy and sustainable development: a crucial review, *Renewable and Sustainable Energy Reviews* 4(2), 157–175.
- Dincer, I., Dost, S. and Li, X. (1997). Performance analyses of sensible heat storage systems for thermal applications, *International Journal of Energy Research* 21(10), 1157–1171.
- Dincer, I. and Rosen, M.A. (1998). A worldwide perspective on energy, environment and sustainable development, *International Journal of Energy Research* 22(15), 1305–1321.
- Dincer, I. and Rosen, M.A. (1999). Energy, environment and sustainable development, *Applied Energy* 64(1-4), 427–440.
- International Energy Agency Heat Pump Centre (IEA-HPC). (1994). Energy storage, *International Energy Agency, IEA-Heat Pump Center Newsletter* 12(4), 8.
- MacRae, K.M. (1992). *Realizing the Benefits of Community Integrated Energy Systems*, Canadian Energy Research Institute, Alberta.
- Norton, R. (1991). An Overview of a Sustainable City Strategy, Report Prepared for the Global Energy Assessment Planning for Cities and Municipalities, Montreal, Quebec.
- OECD. (1995). *Urban Energy Handbook*, Organization for Economic Co-Operation and Development, Paris.
- OECD. (1996). *Pollution Prevention and Control: Environmental Criteria for Sustainable Transport*, Organization for Economic Co-Operation and Development, Report: OECD/GD(96)136, Paris.
- Reindl, D.T. (1994). *Characterizing the Marginal Basis Source Energy Emissions Associated with Comfort Cooling Systems*, Thermal Storage Applications Research Center, Report No. TSARC 94-1, USA.
- Rosen, M.A. (1996). The role of energy efficiency in sustainable development, *Technology and Society* 15(4), 21–26.
- Rosen, M.A., Dincer, I. and Pedinelli, N. (2000). Thermodynamic performance of ice thermal energy storage systems, *ASME-Journal of Energy Resources Technology* 122(4), 205–211.
- Speight, J.G. (1996). *Environmental Technology Handbook*, Taylor & Francis, Washington, DC.
- Trane. (1997). *Energy Star Building Performance Showcased at Trane Technology Center*, Trane Commercial/Industrial Case Studies Catalog, USA.

## Study Questions/Problems

- 4.1 What kinds of environmental benefits are offered by TES?
- 4.2 List the major environmental problems faced by people and societies.
- 4.3 Classify the environmental problems faced by the society into local, regional, and global.
- 4.4 What are the primary greenhouse gases?
- 4.5 What is the CO<sub>2</sub> equivalent in terms of greenhouse gas potential of the various greenhouse gases?
- 4.6 Find estimates for future global population levels, and describe qualitatively and quantitatively the impact that increasing global population is anticipated to have on environmental challenges in the future.
- 4.7 Describe the physical and chemical processes that lead to global warming and climate change.
- 4.8 Describe the physical and chemical processes that lead to stratospheric ozone depletion.
- 4.9 Describe the physical and chemical processes that lead to acid precipitation.
- 4.10 Describe the mechanisms that lead to the possibility that the source of acid precipitation in one region may be in another country.
- 4.11 Explain the physical mechanisms that cause climate change to be considered a global problem, considering how the sources of climate change in one country affect other countries.
- 4.12 Describe sustainability and how it is connected to energy use. Explain how utilization of TES can contribute to making human activity more sustainable.
- 4.13 What is the Brundtland Commission's definition for sustainable development?
- 4.14 Explain how the local and global context of sustainability can be assessed.
- 4.15 Explain how one can contribute to achieving sustainable development through TES.
- 4.16 What are the key parameters in achieving sustainable development? Rank the various parameters important to achieving sustainable development in a society from most to least important, justifying your rankings as much as possible.





# 5

## Thermal Energy Storage and Energy Savings

### 5.1 Introduction

Thermal energy storage (TES) is a key component of many successful thermal systems. TES should allow for the minimum reasonable thermal energy losses and the corresponding energy savings, while permitting the highest appropriate extraction efficiency of the stored thermal energy. This chapter deals with the methods for describing and assessing TES systems, and practical energy-saving applications provided by using TES systems. The design and selection criteria for TES systems are examined. Further, energy-saving techniques and applications are discussed and highlighted with illustrative examples.

TES is considered by many to be an *advanced energy technology*, and there has been increasing interest in using this essential technology for thermal applications such as hot water, space heating, cooling, air-conditioning, and so on. TES systems have enormous potential for permitting more effective use of thermal energy equipment and for facilitating large-scale energy substitutions. The resulting benefits of such actions are especially significant from an economic perspective. In general, a coordinated set of actions has to be taken in several sectors of an energy system for the maximum potential benefits of TES to be realized. TES appears to be the best means of correcting the mismatch that often occurs between the supply and demand of thermal energy. More broadly, TES can contribute significantly to meeting society's needs for more efficient, environmentally benign energy use. The two main types of TES systems, sensible (e.g., water and rock) and latent (e.g., water/ice and salt hydrates), offer economic and other advantages, depending on the application. The selection of a TES system mainly depends on the storage period required, that is diurnal or seasonal, and such other factors as economic viability, operating conditions, and so on. In practice, many research and development activities have concentrated and continue to concentrate on efficient energy use and energy savings, leading to a broad array of energy conservation measures. In this regard, TES appears to have a major role to play as it is an attractive thermal technology.

TES generally involves the temporary storage of high- or low-temperature thermal energy for later use. Examples of TES applications include the storage of solar energy during the day for overnight heating, of summer heat for winter use, of winter ice for space cooling in summer, and of heat or cool generated electrically during off-peak hours for use during subsequent peak demand hours. Solar energy, unlike energy from fossil fuels, is not available at all times. Even cooling loads, which nearly coincide with maximum levels of solar radiation, are often present after sunset. TES provides an important mechanism to offset the mismatch between thermal energy availability and demand in this application.

TES can also aid in the efficient use and provision of thermal energy in other situations where there is a mismatch between energy generation and use. Various TES processes have been investigated and developed for building heating and cooling, industrial energy-efficiency improvement, and utility power systems. The period of storage is clearly an important factor. Diurnal storage systems have certain advantages: capital investment and energy losses are usually low, units are smaller and can easily be manufactured off-site, and the sizing of daily storage for each application is not nearly as critical as it is for larger annual storage systems. Annual storage systems are likely to be economical only in multi-dwelling or industrial park designs. Such systems often require expensive energy distribution networks and novel institutional arrangements related to ownership and financing. In solar TES applications, the optimum energy storage duration is usually the one that offers the final delivered thermal energy at minimum cost, when integrated with the collection system and backup in the final application.

The economic justification for TES systems usually requires that the annualized capital and operating costs be less than the annualized costs of primary generating equipment supplying the same service loads and periods. TES is usually installed for two major reasons: (i) to lower initial costs and (ii) to lower operating costs. Lower initial costs are usually possible when the thermal load is of short duration and there is a long time gap before the load returns, because a small storage is adequate in such instances. Secondary capital costs may also be lower for systems incorporating TES. For example, the electrical service capacity can sometimes be reduced because energy demand is lower.

In order to perform a comprehensive economic analysis of TES, the initial costs must be determined. Equipment costs can be obtained from relevant manufacturers, and estimates of installation costs can be made. The cost savings and the net capital costs can be analyzed using the life-cycle cost method, or other applicable methods, to determine which system is most suitable for a given application.

Other items to be considered in TES economic analyses are space requirements and system reliability, and the interface to the delivery system for the application. An optimal energy storage application achieves a balance between maximizing the savings accrued in utility charges and minimizing the initial cost of the installation needed to achieve the savings. Consequently, the decision to install a storage system must be based on anticipated system loads, load characteristics, and generating capacity mix for an extended period. Uncertainty about the future economic outlook, life-style changes, and the availability of low-cost energy charging the storage system may lead to differing investment decisions if alternative technical solutions are feasible. These uncertainties may vary temporally and spatially. The technical characteristics of alternative technologies for situations in which TES systems are potentially attractive may also affect decisions.

In this chapter, TES systems and their applications are examined from an energy savings perspective, and possible energy-saving technologies are discussed in detail and highlighted with illustrative case studies of actual systems.

## 5.2 TES and Energy Savings

TES systems are an important element of many energy-saving programs in a variety of sectors, residential, commercial, industrial, and utility, as well as in the transportation sector.

TES can be employed to reduce energy consumption or to transfer an energy load from one period to another. The consumption reduction can be achieved by storing excess thermal energy that would normally be released as waste, such as heat produced by equipment and appliances, by lighting, and even by occupants. Energy-load transfer can be achieved by storing energy at a given time for later use, and can be applied to TES for either heating or cooling capacity.

The main objective of most TES systems, which is often to alter energy-use patterns so that financial savings occur, can be achieved in several ways (Dincer *et al.*, 1997a):

- The consumption of purchased energy can be reduced by storing waste or surplus thermal energy available at certain times for use at other times. For example, solar energy can be stored during the day for heating at night.
- The demand of purchased electrical energy can be reduced by storing electrically produced thermal energy during off-peak periods to meet the thermal loads that occur during high-demand periods. There has been an increasing interest in the reduction of peak demand or transfer of energy loads from high- to low-consumption periods. For example, an electric chiller can be used to charge a chilled water storage system at night to reduce the electrical demand peaks usually experienced during the day.
- The use of TES can defer the need to purchase additional equipment for heating, cooling, or air-conditioning applications and reduce equipment sizing in new facilities. The relevant equipment is operated when thermal loads are low to charge the TES, and energy is withdrawn from storage to help meet the thermal loads that exceed equipment capacity.

Each of these points is discussed separately in the following three subsections

### 5.2.1 Utilization of Waste or Surplus Energy

If a TES system is installed and charged using waste heat otherwise released to the environment, and if the energy is held and later used in place of added primary energy, overall energy consumption is reduced. To be economically feasible, the cost of the replaced primary energy should exceed the capitalization, maintenance, and operating costs of the TES system. The stored energy can in a sense be considered free, since it would otherwise be lost.

Useful waste or surplus thermal energy is available from many sources. Some examples are (i) hot or cold water drained to a sewer, (ii) hot flue gases, (iii) exhaust air streams, (iv) hot or cold gases or waste gases, (v) heat collected from solar panels, (vi) ground source thermal energy, (vii) heat rejected from the condenser of refrigeration and air-conditioning equipment, and (viii) the cooling effect from the evaporator of a heat pump.

Many of the TES applications in this category are designed for load leveling rather than waste energy recovery. The thermal energy stored is then in a higher grade rather than waste condition, being drawn from the conversion equipment during periods of low end-use demand for thermal energy. Such TES systems do not reduce energy use, and may actually cause it to increase because of TES inefficiencies. For example, the overall energy consumption for a task supplied using a storage, having an overall energy efficiency of 75%, will be one-third (i.e.,  $1/0.75 - 1$ ) greater than the energy consumption using a direct primary energy supply. The objectives of such systems are clearly not to reduce energy consumption, but rather to either reduce costs or allow the displacement of scarce fuels by more abundant fuels in an energy process.

Tomlinson and Kannberg (1990) point out that industrial production uses about one-third of the total energy consumed in the United States, much of it as hydrocarbon fuels. Therefore, energy-efficiency improvements in the industrial sector can have a substantial impact on national energy consumption levels. TES represents an important option for improving industrial energy efficiency. By storing and then using thermal energy that would otherwise be discharged in flue gases to the environment, less purchased fuel is used, plant thermal emissions are reduced, and product costs associated with fuel use are decreased. The following six industries, which account for approximately 80% of total US industrial energy use, have the highest potential for energy savings through implementation of TES: aluminum, brick and ceramic, cement, food processing, iron and steel, and paper and pulp. Most existing TES systems in an industry are found in iron and steel plants where they are used as regenerators to preheat air to about 600 °C. Opportunities exist for the reclamation of waste heat from stack gases in other industries as well. Estimates have shown that TES can result in potential energy savings in US industries of as much as 3 EJ per year.

In general, TES can reduce the time or rate mismatch between energy supply and energy demand, thereby playing a vital role in improved energy management. TES use can lead to savings of

premium fuels and make a system more cost effective by reducing waste energy. TES can improve the performance of thermal systems by smoothing loads and increasing reliability. Therefore, TES systems are becoming increasingly important in many utility systems.

### 5.2.2 Reduction of Demand Charges

A major application of TES is to lower electrical demand and thus reduce electrical demand charges. Reduction in demand charges is accomplished by eliminating or limiting electrical input to electrically operated heating or cooling devices during the peak electrical demand periods for a facility. The devices are operated before the peak occurs (e.g., overnight) to charge TES systems. During the peak demand period, the heating or cooling equipment does not operate or operates at reduced levels, and the thermal loads are met with the heating or cooling capacity of the storage.

The electrical source that powers the heating or cooling equipment can be shut off, or have power limiters installed, to reduce electrical demand during the peak periods. A number of devices can be energized and de-energized in accordance with TES operating strategies. Some examples are equipment for building heating, cooling and air-conditioning, domestic water heating, process heating and cooling, refrigeration, snow melting, drying, ice-making, and so on.

The fundamental purpose of cool storage is to provide a buffer between the chiller and the building cooling load, thereby decoupling the chiller capacity and operating schedule from the building load profile, leading to energy consumption and demand savings and economic benefits through electrical load management. This application of TES can be beneficial in several ways, regardless of the chiller energy source. In many practical applications, the intention is to maximize the utilization of efficient base load generating plants and avoid the need for additional capacity. The benefits often justify offering rate structures that favor load shifting and peak shaving, and sometimes, financial incentives to reduce the cost of storage.

Figure 5.1 provides an example of daily load profiles for a building, with and without cool storage. Figure 5.1(a) represents the case with no storage, and Figure 5.1(b) shows a full-storage case. In the latter case, the TES provides enough storage capacity to meet the peak (i.e., 9:00 a.m. to 9:00 p.m.) cooling load, shifting the entire electrical demand for cooling to off-peak hours when there is little cooling load. This particular application achieves maximal benefits

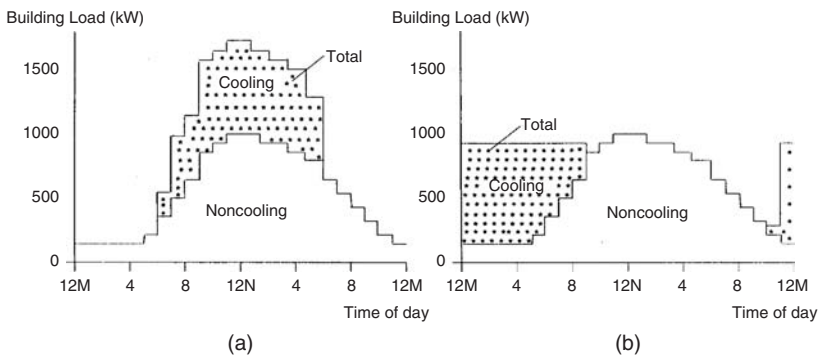


**Figure 5.1** Daily load profiles of a building energy load: (a) no storage and (b) full storage (Dincer *et al.*, 1997b)

in terms of demand charge reduction and use of favorable off-peak rates, both of which lower operating costs.

### 5.2.3 Deferring Equipment Purchases

The capacity of heating and cooling equipment is normally selected to match the part of the design-day load when the requirements for heating and cooling are close to maximum. These peak design loads occur for only short periods of time, resulting in excess capacity on average days. TES systems take advantage of the difference between the peak and average thermal loads to provide an opportunity to defer equipment purchases in a retrofit application, or reduce the equipment size in a new installation.

For example, consider a building with an average cooling load of 500 kW and a peak cooling load of 650 kW. The capacity of the existing chiller is 750 kW. A proposed expansion will increase the average cooling load to 700 kW and the peak to 850 kW. The new average load could be satisfied with the existing equipment, but the peak load could not be satisfied. An additional chiller with a capacity of 100 kW is required, based on the conventional method. As an alternative to providing a new chiller, a TES system could be incorporated to satisfy the peak cooling load. During off-peak hours, when the thermal load is less than the capacity of the existing chiller, the chiller would operate to maintain the desired building or process conditions, and excess capacity would be used to charge a chilled-water TES system (or other cool TES). When the cooling load exceeds the chiller capacity, chilled water would be drawn from storage. The benefits of the TES option can include capital savings and reduced operating costs. The reduced operating costs result from limiting the peak electrical load (and corresponding demand charge) to that required to provide only 750 kW of cooling instead of 850 kW, and from having less chilling equipment to maintain. Note that in either case the annual electrical consumption for cooling increases roughly in proportion to the new cooling loads (Anon, 1985).

The technique illustrated in the above example can also be used in new facilities. Then, TES permits the capacity of the thermal equipment to be selected closer to the average rather than the peak condition.

## 5.3 Additional Energy Savings Considerations for TES

The complete assessment of a TES application in a given facility requires an appreciation of several other criteria: energy requirements for heating, refrigeration and heat pump equipment, storage size limitations, thermal load profiles, and optimization of conventional systems (Anon., 1985; Dincer *et al.*, 1997b). These topics are discussed in the following subsections.

### 5.3.1 Energy for Heating, Refrigeration, and Heat Pump Equipment

Electricity can be converted to thermal energy by electric resistance elements or by mechanical means. In resistance heating systems, each unit of electricity (1 kWh) is converted to heat (1 kWh), and the conversion efficiency is at or very near to 100%. Typical examples are electric baseboard heaters, electric water heaters, and slab heating systems.

Where refrigeration and/or heat pump systems are used to produce heating and/or cooling, the conversion efficiency, which is referred to as a *coefficient of performance* (COP), is normally greater than 100%. Heat pump systems require a heat source, which can be the outdoor environment or a waste heat stream. In many typical systems, the COP is approximately 3.5, where each unit of electrical input (e.g., 1 kWh) to the equipment produces about 3.5 kWh of heating or cooling. For

example, a refrigeration system with a COP of 3.5 producing cooling at a rate of 350 kW has an electric power requirement of 100 kW (350 kWh/3.5). This behavior is important when TES systems, which aim at demand reduction, are being considered. When existing systems are being considered for conversion to TES arrangements, actual equipment COPs should be obtained from the manufacturers. Note that high-efficiency heat pump and refrigeration systems can have COP values in excess of 3.5.

Refrigeration system energy consumption per unit of cooling capacity increases as the evaporator temperature is reduced and as the condenser temperature increases. Producing ice at 0°C, therefore, requires more energy than producing chilled water at 4°C. Conversely, a heat pump requires more electrical power to produce hot water at 50°C than at 35°C. When the temperature variations are minor, the variations in electrical consumption can be approximated as negligible in many practical applications.

### 5.3.2 Storage Size Limitations

TES systems find application possibilities in a range of capacities, from only a few hours to seasonal storage. An example of seasonal storage is the collection of solar energy available during the summer for use in winter heating. Practical limitations such as space requirement and capital cost often restrict TES schemes to storage durations of a few hours to a few days.

As an example of these difficulties, consider a building or process requiring 1000 kW of chilling capacity for 900 h of full-load operation. For a TES, the annual cooling energy that must be stored (ignoring losses) is  $900 \text{ h} \times 1000 \text{ kW} = 900,000 \text{ kWh}$ . If ice is used as the storage medium, the quantity of ice required is 9,720,000 kg or 9720 m<sup>3</sup>, since about 3 kg of ice is required to store 1 MJ of cooling capacity. Assuming a perfect tank with no standby heat losses and no oversize margin, a tank 2 m deep would cover an area the size of a football field. A water storage system would be at least 10 times larger. Costs for such large systems are unacceptable. For reasons illustrated in this example, greater attention has been paid in many instances to short term or diurnal TES systems, especially latent heat TES systems using phase change materials (PCMs).

### 5.3.3 Thermal Load Profiles

When thermal loads fluctuate, the potential exists for storing thermal energy to meet later energy requirements. Many buildings and units have load profiles conducive to TES.

Office buildings with low cooling requirements overnight and during the morning, and high cooling demands in the late afternoon, exhibit the optimum profile for TES. Often, the air-conditioning systems of these buildings are shut off at night. The combination of daytime part loads and nighttime shutdown provides the daily equivalent of 15–20 h when a chilled water storage could be charged to meet the demand period.

Busy facilities, for example, hotels, hospitals, and industrial plants, are less likely candidates for full-storage systems as their load profiles are flatter. Less time is, therefore, available for charging the storage between the long cooling periods. However, these facilities are often suited to partial TES and peak shaving systems. For example, the base thermal load may be met by a chiller, and load peaks reduced using a combination of chiller and storage operation. In this case, the chiller contributes to the peak electrical demand, but by a lower amount than without TES.

The return on capital investment for a TES system can be maximized by careful sizing of the equipment. Often, compressor waste heat can be used for preheating domestic or process hot water. This by-product utilization can further improve the economics of a system.

Weather also affects the thermal load profile of a building, and is consequently a major factor in determining the feasibility of TES. Cooling storage is often advantageous in facilities where the summer weather profile includes a limited number of peak demand days and large temperature



variations during a given 24-h period. Where TES for heating is considered, a minimum of 2200 degree days below 18 °C are usually required to make the project viable (Dincer *et al.*, 1997b).

### 5.3.4 Optimization of Conventional Systems

Existing heating and cooling systems should be upgraded where possible and properly maintained to reduce energy inefficiencies before implementing an active TES system. When reviewing conventional systems, the possibility of heat recovery from exhaust streams should be considered, for example, from boiler flue gases. The possibility of changing from batch to continuous industrial processes should also be examined so that direct heat recovery, without intermediate TES, can be used. This mode of operation often results in more effective heat recovery, no standby thermal losses, and reduced capital expenditure.

Control flexibility is an important tool for optimizing building TES systems, because exact operating modes and schedules vary continuously and are difficult to predict accurately. Systems designed either with manual control or with state-of-the-art computerized controls can be equally effective, provided system operation can be readily adjusted to meet actual site conditions.

Monitoring of TES system operation is required to track system performance and to identify operating problems and potential areas for future improvements. Small systems can be monitored with standard meters, gauges, and manual entry logs. Electronic instrumentation and control systems with automatic data logging, trend analysis, and other features are generally used in larger systems.

## 5.4 Energy Conservation with TES: Planning and Implementation

TES plays an important role in many energy conservation initiatives. In processes with large energy wastes, energy storage can result in a saving of fuels.

Energy may be stored in many ways, for example, mechanical and chemical energy storage. However, since in many economies, energy is produced and transferred as heat, the potential benefits of TES in energy conservation warrant detailed study. Thermal energy can be stored by cooling, heating, melting, solidifying, or vaporizing a material, the thermal energy becoming available when the process is reversed. Thermal storage by causing a rise or drop in material temperature is called *sensible heat storage*. Its effectiveness depends on the specific heat of the material and, if volume is important, the density of the storage material. Storage by phase change (solid to liquid or liquid to vapor) with no change in temperature is known as *latent heat storage*. Short-term storage is often used to manage peak power loads of a few hours to all day long in order to reduce the sizing of systems and/or to take advantage of the daily structure of energy tariffs. Long-term storage is possible when seasonal energy loads can be transferred over periods of weeks to several months, to cover seasonal needs. This type of storage is also called *seasonal storage*.

TES has a significant role to play in energy conservation efforts, and the following are the main steps in implementing an energy conservation strategy involving TES:

1. **Defining the main direct goals.** It is important to start by identifying clearly the goals of the project in a systematic way. This step should use an organized framework that facilitates deciding priorities and identifying the resources needed to achieve the goals.
2. **Identifying community goals.** Community priorities and issues involving energy use, energy conservation, the environment, and other local issues should be identified. Also, the institutional structures and barriers, and financial instruments should be identified.
3. **Scanning the environment.** The main objective in this step is to develop a clear picture of the community and to identify energy- and resource-related problems facing the community and its electrical and gas utilities, the existing organizational structures, and base data for evaluating the future progress of the program. Communication with local and international financial institutions,

project developers, and bilateral aid agencies can help capture new initiatives and explain lessons learned and viewpoints on problems and potential solutions.

4. **Increasing public awareness.** Governments can increase potential customers' awareness and acceptance of energy conservation programs by entering into performance contracts for government activities and publicizing the results. Also, international workshops to share experiences help to overcome the initial barrier of unfamiliarity in countries where TES applications have not been introduced.
5. **Building community support.** Obtaining the participation and support of local industries and public communities for an initiative requires understanding the nature of conflicts and barriers between given goals and local stakeholders, improving information flows, promoting education and advice activities, identifying institutional barriers, and involving a broad spectrum of citizen and government agencies.
6. **Analyzing information.** This step includes defining available options and comparing possible options in terms of factors, for example, program implementation costs, funding availability, utility capital deferral, potential for energy efficiency, compatibility with community goals, environmental benefits, and so on.
7. **Adopting policies and strategies.** High-priority projects need to be identified through approaches that are the best for the community. The decision process should evaluate options in terms of savings in energy costs, generation of businesses and tax revenues, and the number of jobs created, as well as their contribution to energy sustainability and other community and environmental goals.
8. **Developing the plan.** A specific plan of measures and activities should be developed. Once the draft plan has been adopted, it is important for the community to review it and comment on it. The public consultation process may vary, but a high level of approval should be sought.
9. **Implementing future programs.** This step involves deciding which future programs to concentrate on, with long-term aims being preferred over short-term aims. The options that have the greatest impact should be focused on, and all details defined. Potential financial resources need to be identified to implement the programs.
10. **Evaluating success.** The final stage involves evaluating and assessing how well the strategy performs, and helps detect its strengths and weaknesses and determine who is benefiting from it.

## 5.5 Some Limitations on Increased Efficiency

In terms of increased energy efficiency, there are a number of theoretical and practical limitations that apply to TES as well as to other processes.

### 5.5.1 Practical and Theoretical Limitations

The contributions that increased energy efficiency can make toward sustainable development are theoretically limited, because there exists a limit on the maximum efficiency attainable for any process. Such limitations are a consequence of the laws of thermodynamics (Moran, 1989). This concept, when applied to TES, implies that an ideal storage is one in which all of the input energy is restored after storage with no degradation of quality (i.e., temperature) and with complete recovery of energy used to drive the process (e.g., electricity to pumps).

In conventional engineering, the goal when selecting energy sources and utilization processes is not to achieve maximum efficiency. Rather, the goal is to achieve an optimal trade-off between efficiency and such factors as economics, sustainability, environmental impact, safety, and societal and political acceptability. Consideration of these factors leads to practical limitations on increased energy efficiency. For energy efficiency to have an increased contribution toward sustainable development, the position of the optimum among these factors will have to shift toward increased energy utilization efficiency (while recognizing the theoretical limitations on increased energy efficiency).



To assess the potential of increased energy efficiency as a measure for promoting sustainable development, the limits imposed by the existence of maximum theoretical energy efficiencies must be clearly understood. Lack of clarity on this issue has, in the past, often led to confusion and misunderstanding. Part of the reason for this problem is that conventional energy analysis often does not evaluate efficiencies as a measure of how nearly the performance of a process approaches the ideal, or maximum possible. The difficulties inherent in energy analysis are in part attributable to the fact that such an analysis methodology considers only energy quantities, and ignores energy quality and the fact that energy quality is continually degraded during processes. Here, higher quality energy forms are taken to be those that can be used for a wider range of tasks; for example, high-temperature steam is more useful than lower temperature steam as the hotter steam can satisfy all the heating uses of the lower temperature steam and more.

### 5.5.2 *Efficiency Limitations and Exergy*

One way to deal with energy forms of different qualities is to consider exergy. The exergy of a quantity of energy or a substance is a measure of its usefulness or quality, or a measure of its potential to cause change. Exergy analysis has recently been proposed by many scientists and engineers as a technique for thermodynamic assessment that overcomes most, if not all, of the problems associated with energy analysis (e.g., Moran, 1989; Rosen and Dincer, 1997a; 1997b). In practice, the authors feel that a thorough understanding of exergy and how exergy analysis can provide insights into the efficiency and performance of energy systems is required for the engineer or scientist working in the area of energy systems and the environment.

As environmental concerns such as pollution, ozone depletion, and global climate change became major issues in the 1980s, environmental concerns come to represent another factor related to efficiency limit. Consequently, interest developed in the link between energy utilization and the environment. Since then, there has been increasing attention to this linkage. Many scientists and engineers suggest that the impact of energy-resource utilization on the environment is best addressed by considering exergy. Exergy appears to be an effective measure of the potential of a substance to impact the environment. Although many studies exist concerning the close relationship between energy and the environment, there have been limited works on the link between exergy and environment concepts (Rosen and Dincer, 1996; 1997a).

Another use of exergy in TES work is in comparisons. TES systems have been investigated and applied for many years. These experiences have shown that although many technically and economically successful TES systems exist, no broadly valid basis for comparing the achieved performance of one storage with that of another operating under different conditions has found general acceptance. The development of such a basis for comparison has been receiving increasing attention, especially using exergy methods. Exergy analysis, which is identified as one of the most powerful ways of evaluating the thermal performance of TES systems, is based primarily on the second law of thermodynamics, as compared to energy analysis, which is based on the first law, and takes into account the quality of the energy transferred.

## 5.6 Energy Savings for Cold TES

In a TES for cooling capacity, “cold” is stored in a thermal storage mass. As shown in Figure 5.2, the storage can be incorporated in an air-conditioning or cooling system in a building. In most conventional cooling systems, there are two major components (Dincer and Rosen, 2001):

- a chiller – to cool a fluid such as water, and
- a distribution system – to transport the cold fluid from the chiller to where it cools air for the building occupants.

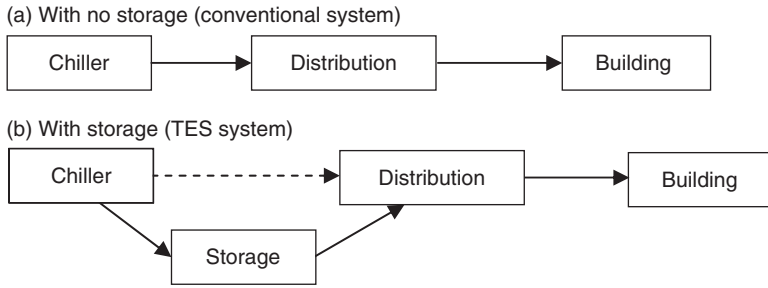


**Figure 5.2** Representation of two cooling TES systems for buildings: (a) with no storage and (b) with storage

In conventional systems, the chiller operates only when the building occupants require cold air. In a cooling system incorporating TES, the chiller also operates at times other than when the cooling is needed.

During the past two decades, much TES technology, especially cold storage, has matured and is now accepted by many as a proven energy conservation technology. However, the predicted payback period of a potential cold storage installation is often not sufficiently attractive to give it priority over other energy-efficient technologies. This determination is often made, because full advantage is not made of the many potential benefits of cold storage, or because the cold storage sizing is not optimized. Some recommendations for optimizing the payback period of cold TES systems follow.

For new facilities, cold storage should be carefully integrated into the overall building and its energy systems so that full advantage is taken of the potential benefits of cold TES, including

- reduced pipe and pump sizes for chilled water distribution;
- reduced duct and fan sizes for low-temperature air distribution;
- reduced operating and maintenance costs;
- reduced electricity consumption and therefore energy costs; and
- increased flexibility of operation.

Smaller chiller and electrical systems lead to initial cost advantages. The sizing of the cold storage system should be optimized, as opposed to the typical process of considering full storage and one or two levels of partial storage versus a conventional system. A practical method to assist in determining the optimum system size should be developed. Also, the value should be accounted for of the gain in usable building space due to less space being required for mechanical system components when cold TES is used.

For existing facilities, potential advantages of cold TES that should be evaluated include

- modifying the existing chillers to make ice versus the purchase of a new machine;
- using spare chiller capacity by adding a cold TES system;
- using cold storage to increase cooling capacity in situations where chiller and electrical service capacity are fully utilized;
- sizing the cold storage system optimally as opposed to taking the best of only a few options; and
- using available low-temperature air and water to advantage through “free cooling,” where practical.

In summary, a cold TES system can benefit users in three ways:

- **Lower electricity rates.** With cold TES, chillers can operate at night to meet the daytime cooling needs, taking advantage of lower off-peak electricity consumption rates.

- **Lower demand charges.** Many commercial customers pay a monthly electrical demand charge based on the largest amount of electricity used during any 30-min period of the month. Cold TES reduces peak demands by shifting some of those demands to off-peak periods. Furthermore, some utilities provide a rebate for shifting electrical demand to nighttime or other off-peak periods.
- **Lower air-conditioning system and compressor costs.** Without cold TES, large compressors capable of meeting peak cooling demands are needed, whereas smaller and less expensive units are sufficient when cold TES is used. Also, since water from a cold TES may be colder than conventional chilled water, smaller pipes, pumps, and air handlers may be integrated into the building design to reduce costs further.

### 5.6.1 *Economic Aspects of TES Systems for Cooling Capacity*

TES-based systems are usually economically justifiable when the annualized capital and operating costs are less than those for primary generating equipment supplying the same service loads and periods. TES is mainly installed to lower initial costs of the other plant components and operating costs. Initial equipment costs are usually lower when intervals between periods of energy demand are large. Secondary capital costs may also be lower for TES-based systems. For example, the electrical service equipment size can sometimes be reduced when energy demand is lowered.

In complete economic analyses of systems including and not including TES, the initial equipment and installation costs must be determined, usually from manufacturers, or else they must be estimated. Operating cost savings and the net overall costs should be assessed using life-cycle costing or other suitable methods to determine which system is the most beneficial.

Utilizing TES can enhance the economic competitiveness of both energy suppliers and building owners. For example, one study for California indicates that, assuming 20% statewide market penetration of TES, the following financial benefits can be achieved in the state (CEC, 1996):

- For energy suppliers, TES leads to lower generating equipment costs (30 to 50% lower to serve air-conditioning loads), reduced financing requirements (US\$1–2 billion), and improved customer retention.
- For building owners statewide, TES leads to lower energy costs (over one-half billion US dollars annually), increased property values (US\$5 billion), increased financing capability (US\$3–4 billion), and increased revenues.

### 5.6.2 *Energy Savings by Cold TES*

Cold TES has been shown to be able to reduce building cooling costs, which can be significant. Stored cooling capacity can be used either to meet the total air-conditioning load so that chillers remain off during the day, or to supplement the chiller so that it only has to satisfy part of the load.

Numerous cities throughout the world, including many in the United States, are faced with increasingly high energy costs. Often, these costs are in large part due to electrical demand charges in addition to energy consumption costs. Many electrical utilities experience difficulties in maintaining sufficient capacity to meet the peak customer demand while at the same time supplying reasonably priced electricity. One way to defer or avoid the construction of new power plants is to level local electrical loads over time. Such leveling can be achieved in part by shifting the electrical loads in buildings due to heating, ventilating, and air-conditioning equipment to periods of lower overall electrical usage. This load shifting can be accomplished by applying TES technologies, and utility companies and governments in many countries offer incentives to encourage such uses of TES.

Strong interest in TES systems for commercial buildings led the Air-Conditioning and Refrigeration Institute (ARI) in the United States to establish in May 1997 a new product section, Thermal Storage Equipment, to promote the attributes of TES and to develop a standard for rating the efficiency of TES equipment. Members of the product section have identified many TES case

studies illustrating the technical impacts and financial benefits of TES use. The ARI is the national trade association representing manufacturers of more than 90% of United States, which produce central air-conditioning and commercial refrigeration equipment.

### Energy-Saving Strategies for Cold TES

Three basic strategies are typically employed for reducing peak electricity use with TES, as shown in Figure 5.3: full, near-full, and partial storage. With full storage, the chiller and storage tank are sized so that the chiller does not run during the peak hours even on the hottest days, while with partial storage that equipment is downsized and the smaller chiller runs continuously on hot days. Thus full storage allows electricity costs to be lowered significantly, while partial storage reduces TES system capital costs. To achieve some of the benefits of both modes of operation, one can also utilize a near-full storage strategy, in which the chiller runs at a reduced level during peak hours.

With these strategies, five major types of TES system are usually utilized, as shown in Table 5.1. The first type, which uses chilled water as the storage medium, has the advantage of being compatible with existing chillers, and is usually more efficient than the other types. However, this TES type requires larger storage tanks than the other types, which use different storage media. The second type of TES, which uses a “eutectic salt” water solution as the storage medium, stores cooling capacity by freezing the storage solution at a temperature typically near 8.3 °C. The main advantages of this TES type are that (i) by storing cold through a phase change (freezing), tanks smaller than that used for chilled water are required, and (ii) by freezing at 8.3 °C, standard chillers producing 5 °C chilled water in commercial facilities can be used. The main disadvantage is that the tank typically cools the water for the distribution system to only 8.5–10 °C, which accomplishes less building dehumidification and requires more pumping energy.

The last three types in Table 5.1 have ice as the storage medium, and differ in how the “cold” from the ice is distributed throughout the building. Before the differences in the distribution systems are considered, the features of their common components (ice storage and chiller) are taken into consideration.

The main advantage of ice storage is compactness, which can be a significant benefit where space is a premium, as ice tanks often are 10 to 20% of the size of comparable chilled water tanks, and 30

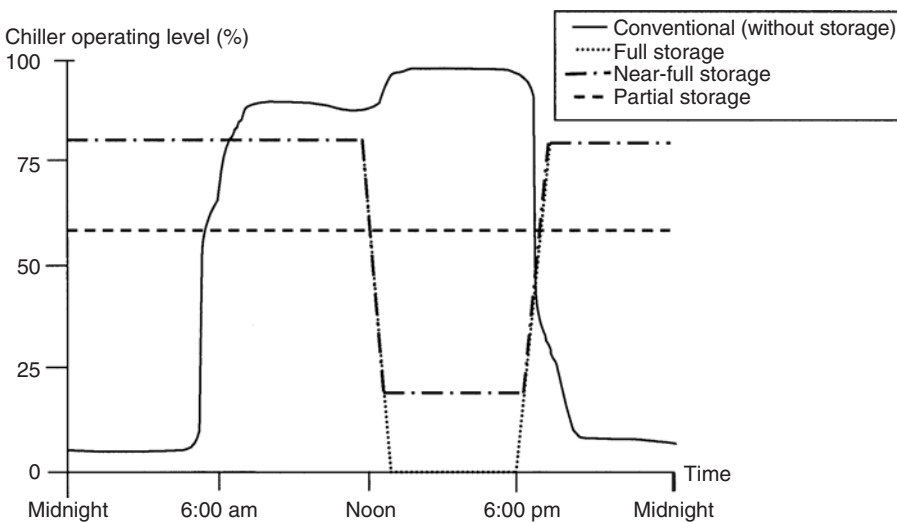


**Figure 5.3** Comparison of conventional and cold TES systems for electricity use

**Table 5.1** Major types of TES cooling systems

Chiller	Storage	Distribution
Conventional	Chilled water	Conventional water
Conventional	Eutectic salt/water solution	Conventional water
Ice-making	Ice	Conventional water
Ice-making	Ice	Cold air
Ice-making	Ice	Unitary (Rooftop) 1

Source: CEC (1996).

to 50% of the size of eutectic salt tanks. Additional benefits of ice storage systems, when used with cold air or rooftop distribution systems, are increased dehumidification and fan energy savings. The major disadvantage of ice systems is that they are not compatible with most conventional chillers that use cold water, and so ice-making chillers must be used, which use more electricity than conventional water chillers because of the lower temperatures required to freeze water.

Although ice storage systems can be used with conventional chilled-water distribution systems, they are particularly beneficial when the distribution system (fans and ducts) is designed to take advantage of the lower temperatures available to produce cold air, and correspondingly downsized. The benefits of such downsizing include lower distribution-system initial costs, lower distribution-system energy use for fans and pumps (by 40% or more), and smaller duct passages, which can mean lower floor-to-floor heights in buildings, allowing architects to design additional floors without increasing building height, and lower net costs per unit area of floor space.

The first four TES types listed in Table 5.1 are used mostly with typical chilled-water distribution systems in larger buildings. The last type is used with unitary systems, including those used in typical single-family residences having an outdoor condensing unit and indoor coil as well as gas or electric heating, or having heat pumps and related air handlers. Unitary systems also include single-package systems that are roof mounted on low-rise commercial buildings and, in certain geographical locations, some residences. These unitary systems use a “direct-expansion” process in which the refrigerant, not chilled water, cools the air that is delivered directly to the structure. Unitary systems are typically small, air cooled, and not as efficient as most of the water-cooled chilled water systems used in larger buildings. Because of their lower efficiencies, air-cooled unitary systems may undergo significant improvement efforts in the near future.

### Analysis of TES Savings

A major focus of this study is on determining the increase or decrease in energy use and demand due to TES. TES generally reduces the fuel or energy required and changes the time at which electricity is used. In order to quantify the source energy impact of TES and to calculate the source energy savings, the incremental energy method (or marginal plant method) can be used (CEC, 1996). The incremental energy method is consistent with evaluation methods for several TES programs. In this method, decisions about which resource to use are based on how the costs of providing power change for a marginal or incremental change in electricity use from current levels. Many believe that marginal costs should be used in the design of electric rates so that they lead energy users to utilize energy resources prudently.

Following these concepts, a standard practice methodology (SPM) is commonly used for evaluating the cost effectiveness of both new supply resources and demand-side management (DSM) measures (CEC, 1996). DSM measures include programs for energy efficiency (often aimed at reducing electrical energy use) and load management (primarily aimed at reducing electrical peak demand), and are often considered as a special type of supply-side resources in resource planning decisions. The SPM evaluates DSM programs by comparing electrical energy and demand savings

to the marginal costs for providing those quantities. This methodology has gained international acceptance as a rational way to evaluate DSM programs – including TES. With the SPM approach, DSM program saving can be expressed as follows:

$$D = \sum_{i=1}^n [(kWh \text{ savings})_i (\text{marginal cost of kWh})_i] + \sum_{i=1}^n (kWh \text{ savings}) \quad (5.1)$$

where  $n$  denotes the number of time periods in the program. In other words, DSM program cost savings are evaluated by determining the energy consumption and demand savings in each of  $n$  time periods, multiplying each of those savings by the marginal costs for that time period, and then summing the cost savings over all time periods. Using the SPM, the year can be divided into  $n$  time periods, each with different marginal costs (for both kW and kWh). Note that utility companies often define the summer peak period as working weekdays from noon to 6:00 p.m., and that the winter peak period is much less dominant than the summer peak in determining new (marginal) capacity decisions.

The “marginal electrical energy cost” (in \$/kWh), referred to in Equation 5.1 as “the marginal cost of a kWh,” for a time period equals the cost of fuel (in \$/kWh) multiplied by the average heat rate (or the incremental energy rate  $R$ ). Thus,  $R$  can be expressed (in kWh fuel/kWh electricity):

$$R = \text{marginal electrical energy cost (\$/kWh)} / \text{marginal cost of plant's fuel (\$/kWh)} \quad (5.2)$$

Equation 5.2 can be substituted into the energy terms in Equation 5.1, after dividing all marginal energy cost terms in Equation 5.1 by the marginal fuel cost, to develop an expression for source energy savings:

$$DS = \sum_{i=1}^n [(kWh \text{ savings})_i R_i] \quad (5.3)$$

When evaluating source energy savings with Equation 5.3 or other benefits of TES, care should be taken to account appropriately for the difference between utility source energy use (i.e., fuel used at the power plant to generate electricity), the electricity generated at the power plant, and the electrical energy provided to the user site. While transferring electricity over power lines from the power plant to the user, energy is lost because of resistance in the power lines (line losses). Line losses are often neglected even though they are sometimes significant (e.g., 10%). Of particular significance in TES assessments are the facts that line losses vary temporally, being greater when the lines are more fully loaded and when the ambient temperature is higher. Thus, line losses are often higher during summer peak hours, so TES can reduce energy use by shifting electricity use to times of lower line losses.

Assessments do not always account for line losses as utilities are concerned about marginal costs sometimes at the power plant (or generation) level, and at other times at the user site (or distribution) level. When evaluating the marginal energy cost  $M$  at the distribution level, the generation-level marginal costs are increased to reflect the line losses to the distribution level, as follows:

$$M (\$/kWh \text{ at site}) = MFP \times R \times LLF \quad (5.4)$$

where MFP is the fuel marginal price at the power plant (in \$/kWh of fuel) and LLF is the line loss factor, evaluated as the ratio of kWh electric exiting the power plant to the kWh electric delivered to the site.

Finally, the TES-derived source energy savings  $T$  can be determined considering all assessment periods and accounting for line losses as

$$T = \sum_{i=1}^n [(kWh \text{ electric savings})_i \times R_i \times LLF_i] \quad (5.5)$$

An alternate method that air-conditioning engineers can use to characterize this information involves evaluating the fractional source energy savings due to TES. This fraction can be calculated as

$$F_{\text{TES}} = F_{\text{ES}} \times F_{\text{EST}} \quad (5.6)$$

where  $F_{\text{TES}}$  is fractional source energy savings due to TES for the annual cooling load,  $F_{\text{ES}}$  is fractional source energy savings per kWh electric shifted, and  $F_{\text{EST}}$  is the fraction of the annual kWh electric shifted by TES.

In Equation 5.6, the second term on the right-hand side varies with the TES system, typically ranging from about 0.40 for hospitals with partial storage systems to about 0.65 for office buildings with full-storage systems (CEC, 1996).

### 5.6.3 Case Studies for TES Energy Savings

Thousands of cold TES systems have been operating in the world, particularly in developed countries, for years in hospitals, public and private schools, universities, airports, government facilities and private office buildings, and in industrial process cooling applications. Described below are several case studies reported by the IEA-HPC (1994), OECD (1995), CEC (1996), ARI (1997), Mathaudhu (1999), and Dincer and Rosen (2001), which demonstrate how TES systems provide energy savings and reduce the environmental impact, and which illustrate some clever applications of TES equipment in new buildings to reduce initial costs. In this section, several examples are given to illustrate the energy savings achievable through TES.

#### TES Energy Conservation Project (California, USA)

This case study considers a project incorporating TES and other energy conservation features into systems for using electricity and water and into the design of the building envelope. The TES project was applied to a Center in California, USA. The Center's major areas include a central operations control center and computer room (which operate throughout the day), administrative and engineering offices, and clerical and conference rooms (all of which have 10 hours per day operation). To comply with California State energy efficiency standards, packaged rooftop heat pump units were selected for the base mechanical system. A 20-year life-cycle analysis was performed to review alternate mechanical systems using a variable-air-volume (VAV) system with electric reheat; with shut-off VAV boxes; and with fan-powered VAV boxes. This analysis determined that fan-powered VAV boxes with electric reheat using an air-cooled chiller were the most cost effective, with a 5.5-year payback period.

At the design stage, the client requested a study to consider incorporating a TES system. The selected system consisted of a fan-powered, variable-volume system with electric reheat, low-temperature supply air (6 °C), a chilled water plant, air handlers with variable speed drives, and ice storage tanks. This system resulted in 30% greater energy savings than mandated by the California State Energy Efficiency Standards and ANSI/ASHRAE/IESNA Standard 90.1.

Designing the HVAC system for the building (Figure 5.4) efficiently is considered a challenge because of the constant fluctuation in the number of people present (50 to 370). Some of the areas have 24-h occupancy, and many employees are dispatched to the field after coming to work in the morning and then meet at the end of the day for reporting.

In this application, seven thermal ice storage tanks, with a total capacity of 1330 ton-hours, provide 1095 ton-hours of full-load off-peak cooling. Other energy conservation measures used to increase efficiency include the following (Mathaudhu, 1999):

- Low-temperature air supply at 6 °C is used instead of conventional air supply at 13 °C to help reduce the supply fan size from 20,760 L/s to 14,745 L/s.



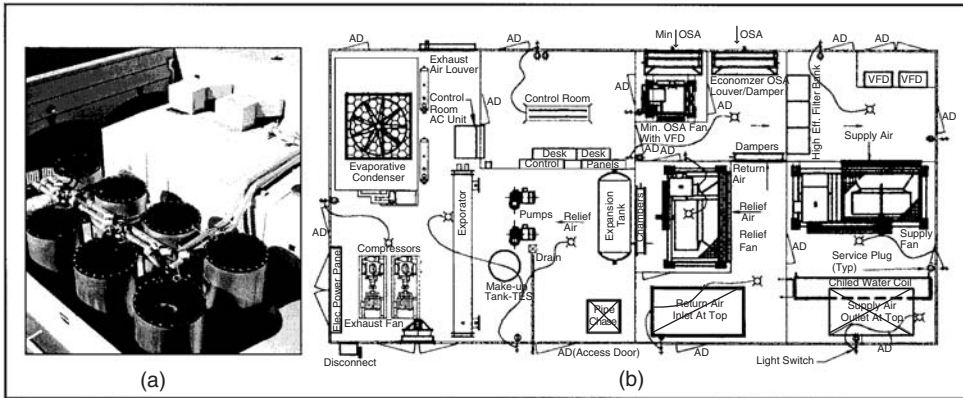


**Figure 5.4** Custom-built unit and sensible ice storage tanks (a) and custom-built unit layout (b) (Reprinted from Mathaudhu (1999) by permission of ASHRAE)

- Variable speed drives are provided for supply, return/relief, and outside air fans. All air-handling unit fans and pumps have high-efficiency motors. The outside air fan speed is controlled by CO<sub>2</sub> sensors located in the main return-air duct.
- Fan-powered VAV boxes mix filtered plenum air with primary air supplied at 6°C. Additional heating requirements are provided by three-stage electric heaters in VAV boxes. The secondary fan in the VAV box has a variable-speed controller to fine-tune the plenum air quantity for recirculation.
- A direct digital control energy management system helps optimize the system operation.
- A high-efficiency heat pump unit maintains comfort level after normal operating hours in the evenings, on weekends and holidays, and for the continuously occupied central control room.
- An evaporative condenser is used rather than a cooling tower to increase system efficiency.

Further, energy conservation features include R-19 wall insulation, R-30 roof insulation, low-emissivity glass windows, high-efficiency T-8 lamps, daylight sensors, occupancy light sensors, skylights, and low-water-consumption plumbing fixtures and metering faucets.

Locating the air-handling unit, chiller, pumps, and cooling tower became a challenge, because the architect had counted on the HVAC system being packaged rooftop heat pump units, and had not planned for the additional space. The installed cost for all of the central plant equipment with an architectural enclosure, but excluding the energy management controls, was over budget by at least \$130,000. An alternate plan including a custom unit to house all the equipment was determined to be more cost effective. The unit would be factory-piped and wired with a complete energy management control system. The custom unit consists of a supply fan (plug type), a return/relief fan (plug type), minimum outside air fan (FC fan), prefilters and high-efficiency filters, two multiple-stage reciprocating compressors, evaporative condenser cooler, variable speed drives for supply, return/relief, and outside air fans, water/glycol circulating pumps, and a control room with complete direct digital control panels and a computer. The control room within the custom unit is designed to be accessible at all times so that clients can observe the system operation. This control room is cooled by a through-the-wall air conditioner that is factory-mounted on the common wall to the evaporative condenser area and the control room.

Although the application of packaged roof-mounted heat pumps would have been the least costly option for installation, the client preferred using a chiller system with a VAV system. Therefore, this system was used as the base case. For the TES system, the time-of-use load leveling strategy provided a payback period of 3.5 years. The time-of-use peak-hour shift option provided a payback



period of 7.8 years, and the time-of-use mid- and peak-hour shift provided a payback period of 17.7 years, compared to the conventional base case of off-peak cooling. A 20-year life-cycle analysis was used to project these payback periods. The client chose to use the time-of-use peak-hour shift strategy. The supply air temperature of 6 °C helped reduce the sizes and related costs for the supply fan, return fan, air-distribution duct, duct insulation, fan motors, and variable frequency drives, resulting in about \$56,000 savings per year. The custom air-handler/chiller system helped reduce mechanical central plant costs by about \$150,000, to \$550,000 from \$700,000.

The seven thermal ice storage tanks (Figure 5.4) provide the flexibility to isolate a tank in case of any failure and still provide over 85% off-peak cooling. The system installed in the facility has demonstrated overall a high level of occupant comfort, while proving itself as an energy-efficient and cost-efficient choice. On the basis of data for building operation for almost 3 years (in the late 1990s), its performance was observed to be slightly better than projected. In other words, the study predicted annual electrical consumption of 623,400 kWh, while the actual value observed was 566,900 kWh.

### **California Energy Commission's TES Program (California, USA)**

In this section, we consider the California Energy Commission's "Opportunity Technology Commercialization (OTCOM)" program to increase the market penetration of energy technologies such as TES that offer, among other factors, significant energy benefits. OTCOM's TES Systems Collaborative Program Commission requested an analysis of the source energy (power plant fuel) savings of electric TES systems in California and of other TES impacts. Besides environmental and economic development benefits, the study identified significant potential for energy savings. In many California TES installations, 40–80% of the annual electricity used for air-conditioning can be shifted from day to night, yielding source energy savings per kWh shifted ranging from 12–43%, depending on the estimation method employed. The results predicted that if TES achieves 20% market penetration by the year 2005, enough source energy would be saved from load shifting (ignoring energy impacts) to supply the energy needs of over a fifth of all new air-conditioning growth projected by the Commission during the next decade. When the site energy savings are combined with the TES source energy savings from shifting load noted above, TES can achieve even greater energy savings. Again, assuming 20% market penetration by 2005, TES was predicted to be able to, in total, save enough energy to supply over a third of the new air-conditioning load projected by the Commission. Of course, the source energy savings for a particular TES system in a particular building depend on a number of factors that are related to the system and its environment (CEC, 1996).

### **Anova Verzekering Co. Building (Amersfoort, The Netherlands)**

This relatively recent TES provided energy savings and reductions in pollutant emissions (Table 5.2). In the application, a groundwater aquifer TES system was installed as part of a space-conditioning unit in a newly renovated office building of Anova Verzekering Co. An electric heat pump is used to supply hydronic heating and cooling. Accounting for the subsidy of US\$212,000 received from the Dutch government, which is equivalent to 20% of the total initial system costs, the reduced energy costs due to TES are expected to lead to a payback period of 6.5 years for the additional investment costs due to TES. In the case study, primary energy consumption decreases because of TES by over 40%, even though electricity use increases.

### **City of Saarbrücken (Saarbrücken, Germany)**

The city of Saarbrücken, Germany, implemented a strategy in the 1980s to reduce energy consumption through seasonal TES, district heating, and by increasing the use of renewable energy (e.g., solar thermal, solar photovoltaic energy, and small hydropower). Between 1980 and 1990, the city achieved significant energy use savings, including a 15% reduction in overall heating demand

**Table 5.2** Annual energy savings and emission reductions for the case study<sup>a</sup>

Commodity	Conventional system	TES-based system	Reduction for TES-based system
<b>Consumptions</b>			
Natural gas (m <sup>3</sup> )	215,800	95,500	120,300 (56%)
Electricity (kWh)	395,550	511,500	-84,000 (-21%)
Primary energy (m <sup>3</sup> ) <sup>b</sup>	322,000	179,000	143,000 (44%)

<sup>a</sup>Adapted from IEA-HPC (1994), where further details are available.

<sup>b</sup>Primary energy is calculated as the equivalent amount of natural gas on the basis of the assumption that 0.25 m<sup>3</sup> gas is used in the generation of 1 kWh of electricity.

and a 45% reduction in heating consumption for the municipal buildings. Some of the energy savings resulting from this successful energy program are attributable to TES (OECD, 1995).

### **Kraft General Foods Headquarters Building (Northfield, Illinois, USA)**

All daytime air-conditioning loads are presently being met at this facility by melting ice that is made and stored overnight. It is anticipated that additional loads from future expansion will be met by operating some of the chillers during the day as well as at night. The building was designed to pump 2.2 °C water to the air-handling units, which in turn provide 7.2 °C air to the building. These temperatures, which are lower than that required for non-TES-based systems, permit the use of smaller pipes, pumps, air-handling units, and ductwork, resulting in lower initial capital costs for the system. Annual electric bills for this building are nearly US\$200,000 lower than that for an almost identical building just three miles away, which does not use a TES system.

### **Chrysler Motors Technology Development Center (Auburn Hills, Michigan, USA)**

Since opening in 1990, the Chrysler Motors Corporation's new technology development center has achieved both equipment and operating cost savings by using a 68,000 ton-hour chilled-water TES system. The TES capacity allowed the center's chiller plant to be downsized from 17,710 tons, which would have been needed to meet peak cooling loads, to 11,385 tons. Chilled water is stored in the TES system at night and supplements chiller operation during peak cooling conditions the following day. Reduced chiller costs more than offset the cost of the TES installation, resulting in initial savings of US\$3.6 million. In addition, the TES system shifts over 5000 kW of peak electrical demand to off-peak periods, saving over US\$1 million per year.

### **San Francisco Marriott Hotel (San Francisco, California, USA)**

Using a TES system in tandem with a real-time pricing strategy from the local utility, this hotel is expected to save US\$135,000 in annual cooling costs. Only 1800 ton-hours of ice storage are needed, enough to satisfy the 450 ton cooling load during the daily peak-rate time period, which lasts only 2 to 3 h under the real-time pricing schedule. Over one-third of the installed cost of the TES system will be covered by a rebate from the utility; the rest is expected to be recouped in less than two years of operation.

### **Texas A&M University (Corpus Christi, Texas, USA)**

In August 1997, the Central Power & Light (CPL) Co. presented Texas A&M University-Corpus Christi with a US\$431,800 incentive award for the university's participation in a TES program that

is resulting in substantial energy savings. The university system uses the bulk of its electricity during off-peak evening hours, allowing CPL to shift some of its electric load from peak usage times and to share the annual cost savings of up to US\$150,000 with the university. Texas A&M-Corpus Christi invested approximately US\$900,000 to purchase and install the TES equipment, which became operational in January 1995, and was predicted to recover that cost through energy savings within five years. The US\$431,800 incentive includes US\$20,400 for installing high-efficiency equipment for cooling and heating the campus. The remaining incentive was provided through CPL's energy efficiency program, wherein the university was offered US\$200 for every kW of electricity load shift from CPL's peak daytime load to off-peak evening hours. The university reduced electric peak demand by approximately 2057 kW, earning a US\$411,400 incentive. CPL worked with the university to install an 11,800 ton-hour thermal storage system with a water storage capacity of 5300 m<sup>3</sup>. The university also installed a 500-ton industrial heat pump for heating, which CPL estimated, would save the university approximately US\$90,000 annually in energy costs. The heat pump captures waste heat from the university's 3000-ton chiller plant, and recirculates it into areas of the campus needing heating. The TES tank stores chilled water, which is produced by the conventional air-conditioning system during the night, and is then used to cool buildings during the day, when the highest demand is placed on the air-conditioning system.

#### **Gillette Capital Corporation (Gaithersburg, Maryland, USA)**

The addition of 1050 ton-hours of latent ice storage to this facility in August 1994 saved the building owners both initial system costs and subsequent operating expenses. The project cost just over US\$121,000, with 57% of this expense paid for by utility incentives, including a US\$350 per kW demand-reduction rebate. An air-cooled reciprocating chiller was originally used to cool the 5760 m<sup>2</sup> building, with the chiller operating 14–15 hours per day during the hottest summer months. With the full-storage system, the cooling load from 8:00 a.m. to 5:30 p.m. is now supplied by ice alone, with the chiller normally running only 5 h during the night to replenish the ice supply. The peak electrical load during the four-month summer peak period is reduced by 198 kW, avoiding the US\$12.95 per kW demand charge, and resulting in over US\$2500 in monthly operating savings. Accounting for initial financial incentives as well as operating savings, a simple payback period of 3.5 years is expected for the TES system.

#### **Miller Electric Company (Appleton, Wisconsin, USA)**

In 1990, this industrial manufacturer of welding equipment converted its cooling system from once-through well-water coolers and conventional rooftop direct-expansion units to ice thermal storage. Conversion eliminated the owner's concerns with the high sewer costs associated with the well-water units and the pending phase-out of the chlorofluorocarbons (CFCs) used in the direct-expansion units. The 46,450 m<sup>2</sup> of conditioned space has an air-conditioning peak design capacity of 3000 t. The cooling load is handled by 1380 t of ice harvesting equipment using ammonia as the refrigerant and operating on a weekly load-shift strategy in which ice is made only during the off-peak weekend and weeknight hours. The owner received a US\$905,000 rebate from the local electric utility, and realizes a 65% (US\$140,000) reduction in annual air-conditioning costs.

#### **Kirk Produce Company (Placentia, California, USA)**

In operation since 1987, two TES units are charged with 465 tons of ice cooling capacity during weekends and an additional 360 tons during off-peak weekday times. The ice is stored with 605.6 m<sup>3</sup> of water in a 1161.2-m<sup>3</sup> storage tank. The water at 0 °C is pumped from the tank through spray nozzles to cool air to 1 °C, for use in cooling fresh-picked strawberries prior to storage and shipping.

Beyond controlling humidity, which is vital to the preservation of strawberries, this process cooling system annually saves \$153,000, or more than half of the refrigeration plant operating costs.

These case studies demonstrate that TES technology offers to owners and regions compelling energy savings as well as environmental, diversity, and economic benefits. As TES now seems poised for wider commercialization, institutional policies, such as those previously identified, should be considered for implementation to increase the market penetration of TES beneficially.

## 5.7 Concluding Remarks

The main advantages of using TES can be summarized as follows:

- Substantial energy savings can be realized by taking advantage of TES when implementing the techniques such as using waste energy and surplus heat, reducing electrical demand charges, and avoiding heating, cooling, or air-conditioning equipment purchases. These savings in energy can be realized despite the fact that the storage energy efficiency, the ratio of thermal energy withdrawn from storage to the amount input, is less than 100%. Storage energy losses are often small, for example, energy efficiencies up to 90% can be achieved in well-stratified water tanks that are fully charged and discharged on a daily cycle.
- TES plays a significant role in meeting society's needs for more efficient use in various sectors as it permits mismatches between supply and demand of energy to be addressed.
- With TES, peak-period demand for electrical energy can be reduced by storing electrically produced thermal energy during off-peak periods and using it to meet the thermal loads that occur during high-demand periods. For example, a chiller can charge TES at night to reduce the peak electrical demands experienced during the day.
- TES exhibits enormous potential for more effective use of TES equipment, and for facilitating large-scale energy substitutions economically. The economic justification for TES systems normally requires the annual income needed to cover capital and operating costs to be less than that required for primary generating equipment supplying the same service loads and periods. A coordinated set of actions is required in several energy sectors to realize the maximum benefits of storage.

## References

- Anon (1985). *Thermal Storage*, Energy Management Series No. 19, Energy, Mines and Resources, Canada.
- ARI (1997). *Thermal Energy Storage: A Solution for Our Energy, Environmental and Economic Challenges*, The Air-Conditioning and Refrigeration Institute, Arlington.
- CEC (1996). *Source Energy and Environmental Impacts of Thermal Energy Storage*, Technical Report No. P500-95-005, California Energy Commission, California.
- Dincer, I., Dost, S. and Li, X. (1997a). Performance analyses of sensible heat storage systems for thermal applications, *International Journal of Energy Research* 21, 1157–1171.
- Dincer, I., Dost, S. and Li, X. (1997b). Thermal energy storage applications from an energy saving perspective, *International Journal of Global Energy Issues* 9, 351–364.
- Dincer, I. and Rosen, M.A. (2001). Energetic, environmental and economic aspects of thermal energy storage systems for cooling capacity, *Applied Thermal Engineering* 21, 1105–1117.
- IEA-HPC (1994). Energy storage, international energy agency, *Heat Pump Center Newsletter* 12(4), 8.
- Mathaudhu, S.S. (1999). Energy conservation showcase, *ASHRAE Journal*, April, 44–46.
- Moran, M.J. (1989). *Availability Analysis: A Guide to Efficient Energy Use*, revised edition, American Society of Mechanical Engineers, New York.
- OECD (1995). *Urban Energy Handbook*, Organization for Economic Co-Operation and Development, Paris.
- Rosen, M.A. and Dincer, I. (1996). Linkages between energy and environment concepts, In *Proceedings of TIEES-96, The First Trabzon International Energy and Environment Symposium* (eds T. Ayhan, I. Dincer, H. Olgun, S. Dost and B. Cuhadaroglu), Vol. 3, 29-31 July, Karadeniz Technical University, Trabzon, Turkey, pp. 1051–1057.

Rosen, M.A. and Dincer, I. (1997a). On Exergy and environmental impact, *International Journal of Energy Research* 21(7), 643–654.

Rosen, M.A. and Dincer, I. (1997b). Sectoral energy and exergy modelling of Turkey, *ASME Journal of Energy Resources Technology* 119(3), 200–204.

Tomlinson, J.J. and Kannberg, L.D. (1990). Thermal energy storage, *Mechanical Engineering* 112, 68–72.

## Study Questions/Problems

- 5.1 What kinds of energy-saving opportunities are offered by TES?
- 5.2 Compare the daily energy load profiles of a conventional building with no storage and full storage options.
- 5.3 Compare the economics (in terms of payback period) for a building in a local city if TES is introduced with full storage and partial storage. Estimate costs for a TES system at your location and utilize local utility rate structures.
- 5.4 How does TES contribute to resolving space limitations that may be present in a building?
- 5.5 Describe possible energy conservation strategies with TES.
- 5.6 Explain the major benefits of a cold TES.
- 5.7 What kinds of financial benefits are expected from TES?
- 5.8 In what situation might the main financial savings from introducing TES be due to reduced demand charges, rather than reduced energy consumption?
- 5.9 In what situation might the main financial savings from introducing TES be due to reduced energy consumption, rather than reduced demand charges?
- 5.10 Explain how a demand-side management option is used with TES for better savings.
- 5.11 Describe how one would determine if it is economically justified to use different sources of heat (industrial waste heat, solar thermal energy, cogenerated thermal energy, etc.) in a TES system for heating capacity.
- 5.12 Describe how one would determine whether it is economically justified to use different sources of cold (chiller generated, heat-pump generated, winter cold, etc.) in a TES system for cooling capacity.
- 5.13 Summarize the key advantages of using TES after reading the case studies.



# 6

## Energy and Exergy Analyses of Thermal Energy Storage Systems

### 6.1 Introduction

Thermal energy storage (TES) systems for heating or cooling capacity are often utilized in applications where the occurrence of a demand for energy and that of the economically most favorable supply of energy are not coincident. Thermal storages are an essential element of many energy conservation programs – in industry, commercial building, and solar energy utilization. Numerous reports on TES applications and studies have been published (Hahne, 1986; Kleinbach *et al.*, 1993; Dincer *et al.*, 1997a, 1997b; Dincer, 1999; Beckman and Gilli, 1984; Bejan, 1982, 1995; Jansen and Sorensen, 1984).

Many types of TES systems exist for storing either heating or cooling capacity. The storage medium often remains in a single phase during the storing cycle (so that only sensible heat is stored), but sometimes undergoes phase change (so that some of the energy is stored as latent heat). Sensible TES systems (e.g., liquid water systems) exhibit changes in temperature in the store as heat is added or removed (Ismail and Stuginsky, 1999; Ismail *et al.*, 1997). In latent TES systems (e.g., liquid water/ice systems and eutectic salt systems), the storage temperature remains fixed during the phase-change portion of the storage cycle (Adebiyi *et al.*, 1996; Laouadi and Lacroix, 1999; Brousseau and Lacroix, 1999; Costa *et al.*, 1998). The storage medium can be located in storage “containers” of various types and sizes, including storage tanks, ponds, caverns, and underground aquifers.

Many researchers have investigated methodologies for TES evaluation and comparison (Rosen, 1991, 1992b, 1999b; Rosen and Dincer, 1999a), and concluded that, while many technically and economically successful thermal storages are in operation, no generally valid basis for comparing the achieved performance of one storage with that of another operating under different conditions has found broad acceptance. The energy efficiency of a TES system, the ratio of the energy recovered from storage to that originally input, is conventionally used to measure TES performance. The energy efficiency, however, is an inadequate measure because it does not take into account all the considerations necessary in TES evaluation (e.g., how nearly the performance of the system approaches the ideal, the storage duration, the temperatures of the supplied and recovered thermal energy and of the surroundings).

Exergy analysis is a thermodynamic analysis technique based on the second law of thermodynamics, which provides an alternative and illuminating means of assessing and comparing TES



systems rationally and meaningfully. In particular, exergy analysis yields efficiencies that provide a true measure of how nearly actual performance approaches the ideal and identifies more clearly than energy analysis the causes and locations of thermodynamic losses. Consequently, exergy analysis can assist in improving and optimizing TES designs. Increasing application and recognition of the usefulness of exergy methods by those in industry, government, and academia has been observed in recent years (Moran, 1989, 1990; Kotas, 1995; Edgerton, 1982; Ahern, 1980; Morris *et al.*, 1988; Dincer and Rosen, 2007). Some researchers have examined exergy-analysis methodologies (Rosen and Horazak, 1995; Rosen, 1999a) and applied them to industrial systems (Rosen and Scott, 1998; Rosen and Horazak, 1995), countries (Rosen and Dincer, 1997b; Rosen, 1992a), environmental impact assessments (Crane *et al.*, 1992; Rosen and Dincer, 1997a, 1999b; Gunnewiek and Rosen, 1998), and TES. To date, however, few exergy analyses of TES systems have been performed (Badar *et al.*, 1993; Bascetincelik *et al.*, 1998; Bejan, 1978, 1982, 1995; Bjurstrom and Carlsson, 1985; Hahne *et al.*, 1989; Krane, 1985, 1987; Krane and Krane, 1991; Mathiprakasham and Beeson, 1983; Moran and Keyhani, 1982; Rosenblad, 1985; Taylor, 1986). Exergy analysis is described extensively elsewhere (Gaggioli, 1983; Maloney and Burton, 1980; Moran and Shapiro, 2000; Rosen, 1999a; Kestin, 1980; Dincer and Rosen, 2007), and background material is provided on energy and exergy analyses that is relevant to applications to TES systems in the next section.

The main objectives of this chapter are to describe how energy and exergy analyses of TES systems are performed and to demonstrate the usefulness of such analyses in providing insights into TES behavior and performance. In the presentation, the thermodynamic considerations and challenges involved in the evaluation of TES systems are discussed, and recent advances in addressing these challenges are described in the hope that standardized exergy-based methodologies can evolve for TES evaluation and comparison.

The topics covered in this chapter can be summarized as follows: First, theoretical and practical aspects of energy and exergy analyses are described (Section 6.2) and general thermodynamic considerations in TES evaluation are discussed (Section 6.3). Then, the use of exergy in evaluating a closed TES system is detailed (Section 6.4), with in-depth discussions of two critical evaluation factors: appropriate TES efficiency measures (Section 6.5) and the importance of temperature in performance evaluations for sensible TES systems (Section 6.6). Next, applications of exergy analysis to a wide range of TES systems are considered, including aquifer TES systems (Section 6.7), thermally stratified storage systems (Section 6.8), and cold TES systems (Section 6.9). Finally, uses of exergy analysis in optimization and design activities are illustrated by examining exergy-based optimal discharge periods for closed TES systems (Section 6.10), and a solar pond is also examined (Section 6.11). Many illustrative examples are given in all the above-listed sections.

## 6.2 Theory: Energy and Exergy Analyses

This section reviews the aspects of thermodynamics that are most relevant to energy and exergy analyses. Fundamental principles and such related issues as reference environment selection, efficiency definition, and material properties acquisition are discussed. These issues were also discussed by others (Moran and Shapiro, 2000; Moran, 1989, 1990; Kotas, 1995; Gaggioli, 1983; Dincer and Rosen, 2007). General implications of exergy analysis results are discussed, and a step-by-step procedure for energy and exergy analyses is given.

A note on terminology is in order here. A relatively standard terminology and nomenclature has evolved for conventional classical thermodynamics. However, at present, there is no generally agreed-upon terminology and nomenclature for exergy analysis. A diversity of symbols and names exist for basic and derived quantities (Kotas *et al.*, 1987; Lucca, 1990). For example, exergy is often called available energy, availability, work capability, essergy, and so on; and exergy consumption is often called irreversibility, lost work, dissipated work, dissipation, and so on. The exergy analysis nomenclature used here follows that proposed by Kotas *et al.* (1987) as a standard exergy analysis nomenclature. For the reader unfamiliar with exergy, a glossary of selected exergy terminology is included (see Appendix at the end of this chapter).



### 6.2.1 *Motivation for Energy and Exergy Analyses*

Thermodynamics permits the behavior, performance, and efficiency to be described for systems for the conversion of energy from one form to another. Conventional thermodynamic analysis is based primarily on the first law of thermodynamics, which states the principle of conservation of energy. An energy analysis of an energy-conversion system is essentially an accounting of the energies entering and exiting. The exiting energy can be broken down into products and wastes. Efficiencies are often evaluated as ratios of energy quantities and are often used to assess and compare various systems. Conventional thermal storages, for example, are often compared on the basis of their energy efficiencies.

However, energy efficiencies are often misleading in that they do not always provide a measure of how nearly the performance of a system approaches ideality. Further, the thermodynamic losses that occur within a system (i.e., those factors that cause performance to deviate from ideality) are often not accurately identified and assessed with energy analysis. The results of energy analysis can indicate the main inefficiencies to be within the wrong sections of the system and a state of technological efficiency different than what actually exists.

Exergy analysis helps to overcome many of the shortcomings of energy analysis. Exergy analysis is based on the second law of thermodynamics and is useful in identifying the causes, locations, and magnitudes of process inefficiencies. The exergy associated with an energy quantity is a quantitative assessment of its usefulness or quality. Exergy analysis acknowledges that, although energy cannot be created or destroyed, it can be degraded in quality, eventually reaching a state in which it is in complete equilibrium with the surroundings and hence of no further use for performing tasks. This statement is of particular importance to TES systems in that, from a thermodynamic perspective, one would wish to recover as much thermal energy as is reasonably possible after the input energy is stored, with little or no degradation of temperature toward the environmental state.

For TES systems, exergy analysis allows one to determine the maximum potential associated with the incoming thermal energy. This maximum is retained and recovered only if the thermal energy undergoes processes in a reversible manner. No further useful thermal energy or exergy can be extracted by allowing a system and its environment to interact if they are in equilibrium. Losses in the potential for exergy recovery occur in the real world because actual processes are always irreversible.

The exergy flow rate of a flowing commodity is the maximum rate at which work may be obtained from it as it passes reversibly to the environmental state, exchanging heat and materials only with the surroundings. In essence, exergy analysis states the theoretical limitations imposed upon a TES system, clearly pointing out that no real system can conserve thermal exergy and that only a portion of the input thermal exergy can be recovered. Also, exergy analysis quantitatively specifies practical TES limitations by providing losses in a form in which they are a direct measure of lost thermal exergy.

### 6.2.2 *Conceptual Balance Equations for Mass, Energy, and Entropy*

A general balance for a quantity in a system may be written as

$$\text{Input} + \text{Generation} - \text{Output} - \text{Consumption} = \text{Accumulation} \quad (6.1)$$

Input and output refer respectively to quantities entering and exiting through system boundaries. Generation and consumption refer respectively to quantities produced and consumed within the system. Accumulation refers to build-up (either positive or negative) of the quantity within the system.

Versions of the general balance equation above may be written for mass, energy, entropy, and exergy. Mass and energy, being subject to conservation laws (neglecting nuclear reactions), can be

neither generated nor consumed. Consequently, the general balance (Equation 6.1) written for each of these quantities becomes

$$\text{Mass input} - \text{Mass output} = \text{Mass accumulation} \quad (6.2)$$

$$\text{Energy input} - \text{Energy output} = \text{Energy accumulation} \quad (6.3)$$

Before giving the balance equation for exergy, it is useful to examine that for entropy:

$$\text{Entropy input} + \text{Entropy generation} - \text{Entropy output} = \text{Entropy accumulation} \quad (6.4)$$

Entropy is created during a process because of irreversibilities, but cannot be consumed. By combining the conservation law for energy and nonconservation law for entropy, the exergy balance can be obtained as follows:

$$\text{Exergy input} - \text{Exergy output} - \text{Exergy consumption} = \text{Exergy accumulation} \quad (6.5)$$

Exergy is consumed owing to irreversibilities. Exergy consumption is proportional to entropy creation. Equations 6.3 and 6.5 demonstrate an important and main difference between energy and exergy: energy is conserved while exergy, a measure of energy quality or work potential, can be consumed.

These balances describe what is happening in a system between two instants of time. For a complete cyclic process where the initial and final states of the system are identical, the accumulation terms in all the balances are zero.

### 6.2.3 Detailed Balance Equations for Mass, Energy, and Entropy

Two types of systems are normally considered: open (flow) and closed (nonflow). In general, open systems have mass, heat, and work interactions, and closed systems have heat and work interactions. Mass flow “into,” heat transfer “into,” and work transfer “out of” the system are defined to be positive. Mathematical formulations of the principles of mass and energy conservation and entropy nonconservation can be written for any system, following the general physical interpretations in Equations 6.2–6.4.

Consider a nonsteady flow process in a time interval  $t_1$  to  $t_2$ . Balances of mass, energy, and entropy, respectively, can be written for a control volume as

$$\sum_i m_i - \sum_e m_e = m_2 - m_1 \quad (6.2a)$$

$$\sum_i (e + Pv)_i m_i - \sum_e (e + Pv)_e m_e + \sum_r (Q_r)_{1,2} - (W')_{1,2} = E_2 - E_1 \quad (6.3a)$$

$$\sum_i s_i m_i - \sum_e s_e m_e + \sum_r (Q_r/T_r)_{1,2} + \Pi_{1,2} = S_2 - S_1 \quad (6.4a)$$

Here,  $m_i$  and  $m_e$  denote respectively the amounts of mass input across port  $i$  and exiting across port  $e$ ;  $(Q_r)_{1,2}$  denotes the amount of heat transferred into the control volume across region  $r$  on the control surface;  $(W')_{1,2}$  denotes the amount of work transferred out of the control volume;  $\Pi_{1,2}$  denotes the amount of entropy created in the control volume;  $m_1$ ,  $E_1$ , and  $S_1$  denote respectively the amounts of mass, energy, and entropy in the control volume at time  $t_1$ , and  $m_2$ ,  $E_2$ , and  $S_2$  denote respectively the same quantities at time  $t_2$ ; and  $e$ ,  $s$ ,  $P$ ,  $T$ , and  $v$  denote specific energy, specific entropy, absolute pressure, absolute temperature, and specific volume, respectively. The total work  $W'$  done by a system excludes flow work, and can be written as

$$W' = W + W_x \quad (6.6)$$

where  $W$  is the work done by a system owing to change in its volume and  $W_x$  is the shaft work done by the system. The term *shaft work* includes all forms of work that can be used to raise a weight (i.e., mechanical work, electrical work, etc.), but excludes work done by a system because of change in its volume. The specific energy  $e$  is given by

$$e = u + ke + pe \quad (6.7)$$

where  $u$ ,  $ke$ , and  $pe$  denote respectively specific internal, kinetic, and potential (due to conservative force fields) energies. For irreversible processes,  $\Pi_{1,2} > 0$ , and for reversible processes,  $\Pi_{1,2} = 0$ .

The left sides of Equations 6.2a, 6.3a, and 6.4a represent the net amounts of mass, energy, and entropy transferred into (and in the case of entropy created within) the control volume, while the right sides represent the amounts of these quantities accumulated within the control volume.

For the mass flow  $m_j$  across port  $j$ ,

$$m_j = \int_{t_1}^{t_2} \left[ \int_j (\rho V_n dA)_j \right] dt \quad (6.8)$$

Here,  $\rho$  is the density of matter crossing an area element  $dA$  on the control surface in time interval  $t_1$  to  $t_2$  and  $V_n$  is the velocity component of the matter flow normal to  $dA$ . The integration is performed over port  $j$  on the control surface. One-dimensional flow (i.e., flow in which the velocity and other intensive properties do not vary with position across the port) is often assumed. Then, the previous equation becomes

$$m_j = \int_{t_1}^{t_2} (\rho V_n A)_j dt \quad (6.8a)$$

It has been assumed that heat transfers occur at discrete regions on the control surface and the temperature across these regions is constant. If the temperature varies across a region of heat transfer,

$$(Q_r)_{1,2} = \int_{t_1}^{t_2} \left[ \int_r (q dA)_r \right] dt \quad (6.9)$$

and

$$(Q_r/T_r)_{1,2} = \int_{t_1}^{t_2} \left[ \int_r (q/T)_r dA_r \right] dt \quad (6.10)$$

where  $T_r$  is the temperature at the point on the control surface where the heat flux is  $q_r$ . The integral is performed over the surface area of region  $A_r$ .

The quantities of mass, energy, and entropy in the control volume (denoted by  $m$ ,  $E$ , and  $S$ ) on the right sides of Equations 6.2a, 6.3a, and 6.4a, respectively, are given more generally by

$$m = \int \rho dV \quad (6.11)$$

$$E = \int \rho e dV \quad (6.12)$$

$$S = \int \rho s dV \quad (6.13)$$

where the integrals are over the control volume.

For a closed system,  $m_i = m_e = 0$  and Equations 6.2a, 6.3a, and 6.4a become

$$0 = m_2 - m_1 \quad (6.2b)$$

$$\sum_r (Q_r)_{1,2} - (W')_{1,2} = E_2 - E_1 \quad (6.3b)$$

$$\sum_r (Q_r/T_r)_{1,2} + \Pi_{1,2} = S_2 - S_1 \quad (6.4b)$$

### 6.2.4 Basic Quantities for Exergy Analysis

Several quantities related to the conceptual exergy balance are described here, following the presentations by Moran (1989), Kotas (1995), and Dincer and Rosen (2007).

#### Exergy of a Closed System

The exergy  $\Xi$  of a closed system of mass  $m$ , or the nonflow exergy, can be expressed as

$$\Xi = \Xi_{ph} + \Xi_o + \Xi_{kin} + \Xi_{pot} \quad (6.14)$$

where

$$\Xi_{pot} = PE \quad (6.15)$$

$$\Xi_{kin} = KE \quad (6.16)$$

$$\Xi_o = \sum_i (\mu_{io} - \mu_{i00})N_i \quad (6.17)$$

$$\Xi_{ph} = (U - U_o) + P_o(V - V_o) - T_o(S - S_o) \quad (6.18)$$

where the system has a temperature  $T$ , pressure  $P$ , chemical potential  $\mu_i$  for species  $i$ , entropy  $S$ , energy  $E$ , volume  $V$ , and number of moles  $N_i$  of species  $i$ . The system is within a conceptual environment in an equilibrium state with intensive properties  $T_o$ ,  $P_o$ , and  $\mu_{i00}$ . The quantity  $\mu_{io}$  denotes the value of  $\mu$  at the environmental state (i.e., at  $T_o$  and  $P_o$ ). The terms on the right side of Equation 6.14 represent respectively physical, chemical, kinetic, and potential components of the nonflow exergy of the system.

The exergy  $\Xi$  is a property of the system and conceptual environment combining the extensive properties of the system with the intensive properties of the environment.

Physical nonflow exergy is the maximum work obtainable from a system as it is brought to the environmental state (i.e., to thermal and mechanical equilibrium with the environment), and chemical nonflow exergy is the maximum work obtainable from a system as it is brought from the environmental state to the dead state (i.e., to complete equilibrium with the environment).

#### Exergy of a Flowing Stream of Matter

The exergy of a flowing stream of matter  $\epsilon$  is the sum of nonflow exergy and the exergy associated with the flow work of the stream (with reference to  $P_o$ ), that is,

$$\epsilon = \Xi + (P - P_o)V \quad (6.19)$$

Alternatively,  $\epsilon$  can be expressed following Equation 6.14 in terms of physical, chemical, kinetic, and potential components:

$$\epsilon = \epsilon_{ph} + \epsilon_o + \epsilon_{kin} + \epsilon_{pot} \quad (6.20)$$

where

$$\epsilon_{pot} = PE \quad (6.21)$$

$$\epsilon_{kin} = KE \quad (6.22)$$

$$\epsilon_o = \Xi_o = \sum_i (\mu_{io} - \mu_{ioo}) N_i \quad (6.23)$$

$$\epsilon_{ph} = (H - H_o) - T_o (S - S_o) \quad (6.24)$$

### Exergy of Thermal Energy

Consider a control mass, initially at the dead state, being heated or cooled at constant volume in an interaction with some other system. The heat transfer experienced by the control mass is  $Q$ . The flow of exergy associated with the heat transfer  $Q$  is denoted by  $X$ , and can be expressed as

$$X = \int_i^f (1 - T_o/T) \delta Q \quad (6.25)$$

where  $\delta Q$  is an incremental heat transfer, and the integral is from the initial state ( $i$ ) to the final state ( $f$ ). This “thermal exergy” is the minimum work required by the combined system of the control mass and the environment in bringing the control mass to the final state from the dead state.

Often, the dimensionless quantity in parentheses in this expression is called the *exergetic temperature factor* and is denoted by  $\tau$ :

$$\tau = 1 - T_o/T \quad (6.26)$$

The relation between  $\tau$  and the temperature ratio  $T/T_o$  is illustrated in Figure 6.1.

If the temperature  $T$  of the control mass is constant, the thermal exergy transfer associated with a heat transfer is

$$X = (1 - T_o/T) Q = \tau Q \quad (6.25a)$$

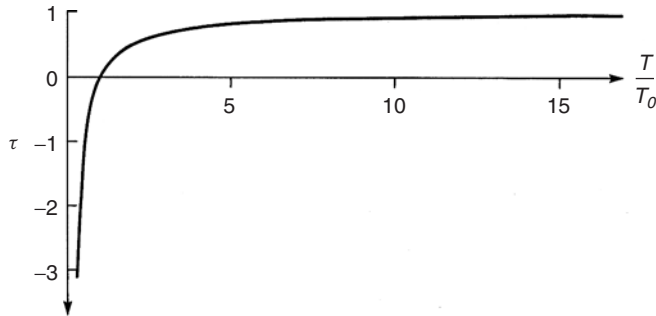


**Figure 6.1** The relation between the exergetic temperature factor  $\tau$  and the absolute temperature ratio  $T/T_o$ . The factor  $\tau$  is equal to zero when  $T = T_o$ . For heat transfer at above-environment temperatures (i.e.,  $T > T_o$ ),  $0 < \tau \leq 1$ . For heat transfer at subenvironment temperatures (i.e.,  $T < T_o$ ),  $\tau < 0$ , implying that exergy and energy flow in opposite directions in such cases. Note that the magnitude of exergy flow exceeds that of the energy flow when  $\tau < -1$ , which corresponds to  $T < T_o/2$

For heat transfer across a region  $r$  on a control surface for which the temperature may vary,

$$X = \int_r [q (1 - T_o/T) dA]_r \quad (6.25b)$$

where  $q_r$  is the heat flow per unit area at a region on the control surface at which the temperature is  $T_r$ .

### Exergy of Work and Electricity

Equation 6.6 separates total work  $W'$  into two components:  $W_x$  and  $W$ . The exergy associated with shaft work  $W_x$  is by definition  $W_x$ . Similarly, the exergy associated with electricity is equal to the energy.

The exergy transfer associated with work done by a system due to volume change is the net usable work due to the volume change, and is denoted by  $W_{NET}$ . Thus, for a process in time interval  $t_1$  to  $t_2$ ,

$$(W_{NET})_{1,2} = W_{1,2} - P_o (V_2 - V_1) \quad (6.27)$$

where  $W_{1,2}$  is the work done by the system due to volume change ( $V_2 - V_1$ ). The term  $P_o(V_2 - V_1)$  is the displacement work necessary to change the volume against the constant pressure  $P_o$  exerted by the environment.

### Exergy Consumption

For a process occurring in a system, the difference between the total exergy flows into and out of the system, less the exergy accumulation in the system, is the exergy consumption  $I$ , expressible as

$$I = T_o \Pi \quad (6.28)$$

Equation 6.28 points out that exergy consumption is proportional to entropy creation, and is known as the Gouy–Stodola relation.

### 6.2.5 Detailed Exergy Balance

An analogous balance to those given in Equations 6.2a, 6.3a, and 6.4a can be written for exergy, following the physical interpretation of Equation 6.5. For a nonsteady flow process during time interval  $t_1$  to  $t_2$

$$\sum_i \varepsilon_i m_i - \sum_e \varepsilon_e m_e + \sum_r (X_r)_{1,2} - (W_x)_{1,2} - (W_{NET})_{1,2} - I_{1,2} = \Xi_2 - \Xi_1 \quad (6.5a)$$

where  $(W_{NET})_{1,2}$  is given by Equation 6.27 and

$$(X_r)_{1,2} = \int_{t_1}^{t_2} \left[ \int_r (1 - T_o/T_r) q_r dA_r \right] dt \quad (6.29)$$

$$I_{1,2} = T_o \Pi_{1,2} \quad (6.30)$$

$$\Xi = \int \rho \xi dV \quad (6.31)$$

Here,  $I$  and  $\Pi$  respectively denote exergy consumption and entropy creation,  $\Xi$  denotes specific nonflow exergy, and the integral for  $\Xi$  is performed over the control volume. The first two terms on the left side of Equation 6.5a represent the net input of exergy associated with matter; the third term, the net input of exergy associated with heat; the fourth and fifth terms, the net input of exergy associated with work; and the sixth term the exergy consumption. The right side of Equation 6.5a shows the accumulation of exergy.

For a closed system, Equation 6.5a simplifies to

$$\sum_r (X_r)_{1,2} - (W_x)_{1,2} - (W_{NET})_{1,2} - I_{1,2} = \Xi_2 - \Xi_1 \quad (6.5b)$$

When volume is fixed,  $(W_{NET})_{1,2} = 0$  in Equations 6.5a and b. Also, when the initial and final states are identical as in a complete cycle, the right sides of Equations 6.5a and b are zero.

### 6.2.6 The Reference Environment

Exergy is evaluated with respect to a reference environment. The intensive properties of the reference environment determine the exergy of a stream or system. The exergy of the reference environment is zero. The exergy of a stream or system is zero when it is in equilibrium with the reference environment. The reference environment is in stable equilibrium, with all parts at rest relative to one another. No chemical reactions can occur between the environmental components. The reference environment acts as an infinite system, and is a sink and source for heat and materials. It experiences only internal reversible processes in which its intensive state remains unaltered (i.e., its temperature  $T_o$ , pressure  $P_o$ , and the chemical potentials  $\mu_{i00}$  for each of the  $i$  components present remain constant).

The natural environment does not have the theoretical characteristics of a reference environment. The natural environment is not in equilibrium and its intensive properties exhibit spatial and temporal variations. Many chemical reactions in the natural environment are blocked because the transport mechanisms necessary to reach equilibrium are too slow at ambient conditions. Thus, the exergy of the natural environment is not zero; work could be obtained if it were to come to equilibrium. Consequently, models for the reference environment are used that try to achieve a compromise between the theoretical requirements of the reference environment and the actual behavior of the natural environment.

One important class of the reference-environment model is the natural-environment-subsystem type. These models attempt to simulate realistic subsystems of the natural environment. One such model consisting of saturated moist air and liquid water in phase equilibrium was proposed by Baehr and Schmidt (1963). An extension of the above model, which allowed sulphur-containing materials to be analyzed, was proposed by Gaggioli and Petit (1977) and Rodriguez (1980). The temperature and pressure of this reference environment (see Table 6.1) is normally taken to be 25 °C and 1 atm, respectively, and the chemical composition is taken to consist of air saturated with water vapor, and the following condensed phases at 25 °C and 1 atm: water ( $H_2O$ ), gypsum ( $CaSO_4 \cdot 2H_2O$ ), and limestone ( $CaCO_3$ ). The stable configurations of C, O, and N, respectively, are taken to be those of  $CO_2$ ,  $O_2$ , and  $N_2$  as they exist in air saturated with liquid water at  $T_o$  and  $P_o$ ; of hydrogen is taken to be in the liquid phase of water saturated with air at  $T_o$  and  $P_o$ ; and of S and Ca, respectively, are taken to be those of  $CaSO_4 \cdot 2H_2O$ ; and  $CaCO_3$  at  $T_o$  and  $P_o$ .

The analyses in this chapter use the natural-environment-subsystem model described in Table 6.1, but with a temperature modified to reflect the approximate mean ambient temperature of the location of the TES for the time period under consideration (e.g., annual, seasonal, monthly). Other classes of reference-environment models have been proposed.

- **Reference-substance models.** These are models in which a “reference substance” is selected and assigned a zero exergy for every chemical element. One such model in which the reference

**Table 6.1** A reference-environment model

Temperature:	$T_o = 298.15 \text{ K}$	
Pressure:	$P_o = 1 \text{ atm}$	
Composition:	(i) Atmospheric air saturated with $\text{H}_2\text{O}$ at $T_o$ and $P_o$ having the following composition:	
	Air constituents	Mole fraction
	$\text{N}_2$	0.7567
	$\text{O}_2$	0.2035
	$\text{H}_2\text{O}$	0.0303
	Ar	0.0091
	$\text{CO}_2$	0.0003
	$\text{H}_2$	0.0001
	(ii) Condensed phases at $T_o$ and $P_o$ :	
	Water ( $\text{H}_2\text{O}$ )	
	Limestone ( $\text{CaCO}_3$ )	
	Gypsum ( $\text{CaSO}_4 \cdot 2\text{H}_2\text{O}$ )	

Source: Adapted from Gaggioli and Petit (1977).

substances were selected as the most valueless substances found in abundance in the natural environment was proposed by Szargut (1967). The criteria for selecting such reference substances are consistent with the notion of simulating the natural environment, but are primarily economic in nature, and are vague and arbitrary with respect to the selection of reference substances. Part of this environment is the composition of moist air, including  $\text{N}_2$ ,  $\text{O}_2$ ,  $\text{CO}_2$ ,  $\text{H}_2\text{O}$  and the noble gases, gypsum (for sulphur), and limestone (for calcium). Another model in this class, in which reference substances are selected arbitrarily, was proposed by Sussman (1980, 1981). This model is not similar to the natural environment, consequently absolute exergies evaluated with this model do not relate to the natural environment, and cannot be used rationally to evaluate efficiencies. Since exergy-consumption values are independent of the choice of reference substances, they can be rationally used in analyses.

- Equilibrium models.** A model in which all the materials present in the atmosphere, oceans, and a layer of the crust of the earth are pooled together and an equilibrium composition is calculated for a given temperature was proposed by Ahrendts (1980). The selection of the thickness of crust considered is subjective, and is intended to include all materials accessible to technical processes. Ahrendts considered thicknesses varying from 1 m to 1000 m, and a temperature of 25 °C. For all thicknesses, Ahrendts found that the model differed significantly from the natural environment. Exergy values obtained using these environments are significantly dependent on the thickness of crust considered, and represent the absolute maximum amount of work obtainable from a material. Since there is no technical process available that can obtain this work from materials, Ahrendts' equilibrium model does not give meaningful exergy values when applied to the analysis of real processes.
- Constrained-equilibrium models.** Ahrendts (1980) also proposed a modified version of his equilibrium environment in which the calculation of an equilibrium composition excludes the possibility of the formation of nitric acid ( $\text{HNO}_3$ ) and its compounds. That is, all chemical reactions in which these substances are formed are in constrained equilibrium, and all other reactions are in unconstrained equilibrium. When a thickness of crust of 1 m and temperature of 25 °C were used, the model was similar to the natural environment.
- Process-dependent models.** A model which contains only components that participate in the process being examined in a stable equilibrium composition at the temperature and total pressure of the natural environment was proposed by Bosnjakovic (1963). This model is dependent on the process examined, and is not general. Exergies evaluated for a specific process-dependent model



are relevant only to the process; they cannot rationally be compared with exergies evaluated for other process-dependent models.

Many researchers have examined the characteristics of and models for reference environments (Wepfer and Gaggioli, 1980; Sussman, 1981; Ahrendts, 1980), and the sensitivities of exergy values to different reference-environment models (Rosen and Scott, 1987).

### 6.2.7 *Efficiencies*

#### **General Efficiency Concepts**

Efficiency has always been an important consideration in decision making regarding resource utilization. Efficiency is defined as “the ability to produce a desired effect without waste of, or with minimum use of, energy, time, resources, and so on,” and is used by people to refer to the effectiveness with which something is used to produce something else, or the degree to which the ideal is approached in performing a task.

For general engineering systems, nondimensional ratios of quantities are typically used to determine efficiencies. Ratios of energy are conventionally used to determine efficiencies of engineering systems whose primary purpose is the transformation of energy. These efficiencies are based on the first law of thermodynamics. A process has maximum efficiency according to the first law if energy input equals recoverable energy output (i.e., if no “energy losses” occur). However, efficiencies determined using energy are misleading, because, in general, they are not measures of “an approach to an ideal.”

To determine more meaningful efficiencies, a quantity is required for which ratios can be established that do provide a measure of an approach to an ideal. Thus, the second law must be involved, as this law states that maximum efficiency is attained (i.e., ideality is achieved) for a reversible process. However, the second law must be quantified before efficiencies can be defined.

The “increase of entropy principle,” which states that entropy is created because of irreversibilities, quantifies the second law. From the viewpoint of entropy, maximum efficiency is attained for a process in which entropy is conserved. Entropy is created for nonideal processes. The magnitude of entropy creation is a measure of the nonideality or irreversibility of a process. In general, however, ratios of entropy do not provide a measure of an approach to an ideal.

A quantity that has been discussed in the context of meaningful measures of efficiency is negentropy (Hafele, 1981). Negentropy is defined such that the negentropy consumption due to irreversibilities is equal to the entropy creation due to irreversibilities. As a consequence of the “increase of entropy principle,” maximum efficiency is attained from the viewpoint of negentropy for a process in which negentropy is conserved. Negentropy is consumed for nonideal processes. Negentropy is a measure of order. Consumptions of negentropy are therefore equivalent to degradations of order. Since the abstract property of order is what is valued and useful, it is logical to attempt to use negentropy in developing efficiencies. However, general efficiencies cannot be determined based on negentropy because its absolute magnitude is not defined.

Negentropy can be further quantified through the ability to perform work. Then, a maximum efficiency is attainable only if, at the completion of a process, the sum of all energy involved has an ability to do work equal to the sum before the process occurred. Exergy is a measure of the ability to perform work and, from the viewpoint of exergy, maximum efficiency is attained for a process in which exergy is conserved. Efficiencies determined using ratios of exergy do provide a measure of an approach to an ideal. Exergy efficiencies are often more intuitively rational than energy efficiencies, because efficiencies between 0 and 100% are always obtained. Measures that can be greater than 100% when energy is considered, such as coefficient of performance, are normally between 0 and 100% when exergy is considered. In fact, some researchers (Gaggioli, 1983) call exergy efficiencies “real” or “true” efficiencies, while calling energy efficiencies “approximations to real” efficiencies.

### Energy and Exergy Efficiencies

Many researchers (Sussman, 1981; Hevert and Hevert, 1980; Alefeld, 1990) have examined efficiencies and other measures of performance. Different efficiency definitions generally answer different questions.

Energy ( $\eta$ ) and exergy ( $\psi$ ) efficiencies are often written for steady-state processes occurring in systems as

$$\eta = \frac{\text{Energy in product outputs}}{\text{Energy in inputs}} = 1 - \frac{\text{Energy loss}}{\text{Energy in inputs}} \quad (6.32)$$

$$\psi = \frac{\text{Exergy in product outputs}}{\text{Exergy in inputs}} = 1 - \frac{\text{Exergy loss plus consumption}}{\text{Exergy in inputs}} \quad (6.33)$$

Two other common exergy-based efficiencies for steady-state devices are as follows:

$$\text{Rational efficiency} = \frac{\text{Total exergy output}}{\text{Total exergy input}} = 1 - \frac{\text{Exergy consumption}}{\text{Total exergy input}} \quad (6.34)$$

$$\text{Task efficiency} = \frac{\text{Theoretical minimum exergy input required}}{\text{Actual exergy input}} \quad (6.35)$$

Exergy efficiencies often give more illuminating insights into process performance than energy efficiencies because (i) they weigh energy flows according to their exergy contents, and (ii) they separate inefficiencies into those associated with effluent losses and those due to irreversibilities. In general, exergy efficiencies provide a measure of potential for improvement.

### 6.2.8 Properties for Energy and Exergy Analyses

Many material properties are needed for energy and exergy analyses of processes. Sources of conventional property data are abundant for many substances, for example, steam, air and combustion gases (Keenan *et al.*, 1992), and chemical substances (Chase *et al.*, 1985).

Energy values of heat and work flows are absolute, while the energy values of material flows are relative. Enthalpies are evaluated relative to a reference level. Since energy analyses are typically concerned only with energy differences, the reference level used for enthalpy calculations can be arbitrary. For the determination of some energy efficiencies, however, the enthalpies must be evaluated relative to specific reference levels (e.g., for energy-conversion processes, the reference level is often selected so that the enthalpy of a material equals its higher heating value (*HHV*)).

If, however, the results from energy and exergy analyses are to be compared, it is necessary to specify the reference levels for enthalpy calculations such that the enthalpy of a compound is evaluated relative to the stable components of the reference environment. Thus, a compound that exists as a stable component of the reference environment is defined to have an enthalpy of zero at  $T_o$  and  $P_o$ . Enthalpies calculated with respect to such conditions are referred to as *base enthalpies* (Rodriguez, 1980). The base enthalpy is similar to the enthalpy of formation. While the latter is the enthalpy of a compound (at  $T_o$  and  $P_o$ ) relative to the elements (at  $T_o$  and  $P_o$ ) from which it would be formed, the former is the enthalpy of a component (at  $T_o$  and  $P_o$ ) relative to the stable components of the environment (at  $T_o$  and  $P_o$ ). For many environment models, the base enthalpies of material fuels are equal to their *HHV* s.

The base enthalpies for many substances, corresponding to the reference-environment model in Table 6.1, are listed in Table 6.2 (Rodriguez, 1980). It is required to determine chemical exergy values for exergy analysis. Many researchers have developed methods and tabulated values for evaluating chemical exergies (Rodriguez, 1980; Szargut, 1967; Sussman, 1980). Included are methods for evaluating the chemical exergies of solids, liquids, and gases. For complex materials (e.g., coal, tar, and ash), approximation methods have been developed. By considering environmental air

**Table 6.2** Base enthalpy and chemical exergy values of selected species

Species	Specific base enthalpy (kJ/g-mol)	Specific chemical exergy <sup>a</sup> (kJ/g-mol)
Ammonia (NH <sub>3</sub> )	382.585	2.478907 ln y + 337.861
Carbon (graphite) (C)	393.505	410.535
Carbon dioxide (CO <sub>2</sub> )	0.000	2.478907 ln y + 20.108
Carbon monoxide (CO)	282.964	2.478907 ln y + 275.224
Ethane (C <sub>2</sub> H <sub>6</sub> )	1564.080	2.478907 ln y + 1484.952
Hydrogen (H <sub>2</sub> )	285.851	2.478907 ln y + 235.153
Methane (CH <sub>4</sub> )	890.359	2.478907 ln y + 830.212
Nitrogen (N <sub>2</sub> )	0.000	2.478907 ln y + 0.693
Oxygen (O <sub>2</sub> )	0.000	2.478907 ln y + 3.948
Sulphur (rhombic) (S)	636.052	608.967
Sulphur dioxide (SO <sub>2</sub> )	339.155	2.478907 ln y + 295.736
Water (H <sub>2</sub> O)	44.001	2.478907 ln y + 8.595

<sup>a</sup>y represents the molal fraction for each of the respective species.

Source: Compiled from data in Rodriguez (1980) and Gaggioli and Petit (1977).

and gaseous process streams as ideal gas mixtures, chemical exergy can be calculated for gaseous streams using component chemical exergy values, that is, values of  $(\mu_{io} - \mu_{ioo})$  listed in Table 6.2.

### 6.2.9 Implications of Results of Exergy Analyses

The results of exergy analyses of TES systems have direct implications on application decisions and on research and development (R&D) directions.

Further, exergy analyses provide insights into the “best” directions for R&D effort more than energy analyses. Here, “best” is loosely taken to mean “most promising for significant efficiency gains.” There are two main reasons for this statement:

- Exergy losses represent true losses of the potential that exists to generate the desired product (recovered thermal energy with little temperature degradation, here) from the given driving input (input thermal energy and electricity, here). In general, this is not true for energy losses. Thus, if the objective is to increase TES efficiency while accounting for temperature degradation, focusing on exergy losses permits R&D to focus on reducing losses that will affect the objective.
- Exergy efficiencies always provide a measure of how nearly the operation of a system approaches the ideal or theoretical upper limit. In general, this is not true for energy efficiencies. By focusing R&D effort on those plant sections or processes with the lowest exergy efficiencies, the effort is being directed to those areas that inherently have the largest margins for efficiency improvement. By focusing on energy efficiencies, on the other hand, one can expend R&D effort on topics for which small margins for improvement, even theoretically, exist.

Exergy analysis results typically suggest that R&D efforts should concentrate more on internal rather than external exergy losses, based on thermodynamic considerations, with a higher priority for the processes having larger exergy losses. Although this statement suggests focusing on those areas for which margins for improvement are greatest, it does not indicate that R&D should not be devoted to those processes having low exergy losses, as simple and cost-effective ways to increase efficiency by reducing small exergy losses should certainly be considered when identified.

More generally, it is noted that application and R&D allocation decisions should not be based exclusively on the results of energy and exergy analyses, even though these results provide useful

information to assist in such decision making. Other factors must also be considered, such as economics, environmental impact, safety, and social and political implications.

### 6.2.10 Steps for Energy and Exergy Analyses

A simple procedure for performing energy and exergy analyses involves the following steps:

- Subdivide the process under consideration into as many sections as desired, depending on the depth of detail and understanding desired from the analysis.
- Perform conventional mass and energy balances on the process, and determine all basic quantities (e.g., work, heat) and properties (e.g., temperature, pressure) (Section 6.2.3).
- Based on the nature of the process, the acceptable degree of analysis complexity and accuracy, and the questions for which answers are sought, select a reference-environment model (Section 6.2.6).
- Evaluate energy and exergy values, relative to the selected reference-environment model (Sections 6.2.4 and 6.2.8).
- Perform exergy balances, including the determination of exergy consumptions (Section 6.2.5).
- Select efficiency definitions depending on the measures of merit desired, and evaluate values for the efficiencies (Section 6.2.7).
- Interpret the results and draw appropriate conclusions and recommendations relating to such issues as design changes, retrofit plant modifications, and so on. (Section 6.2.9).

## 6.3 Thermodynamic Considerations in TES Evaluation

Several of the more important thermodynamic factors to be considered during the evaluation and comparison of TES systems are discussed in this section (Rosen and Dincer, 1999a).

### 6.3.1 Determining Important Analysis Quantities

The two most significant quantities to consider when evaluating TES systems are energy and exergy. Exergy analysis involves the examination of the exergy at different points in a series of energy-conversion steps, and the determination of meaningful efficiencies and of the steps having the largest losses (i.e., the largest margin for improvement). The authors and others feel that the use of exergy analysis circumvents many of the problems associated with conventional TES evaluation and comparison methodologies by providing a more rational basis.

Exergy analysis permits more rational and convenient evaluation than energy analysis of TES systems for cooling capacity as well as heating capacity. Exergy analysis applies equally well to systems for storing thermal energy at temperatures above and below the temperature of the environment, because the exergy associated with such energy is always greater than or equal to zero. Energy analysis is more difficult to apply to such storage systems because efficiency definitions have to be carefully modified when cooling capacity, instead of heating capacity, is stored, or when both warm and cool reservoirs are included.

### 6.3.2 Obtaining Appropriate Measures of Efficiency

The evaluation of a TES system requires a measure of performance that is rational, meaningful, and practical. The conventional energy storage efficiency, as pointed out earlier, is an inadequate measure. A more perceptive basis for comparison is apparently needed if the true usefulness of thermal storages is to be assessed, and so permit maximization of their economic benefit. Efficiencies

based on ratios of exergy do provide rational measures of performance, since they can measure the approach of the performance of a system to the ideal.

That the energy efficiency is an inappropriate measure of thermal storage performance can best be appreciated through a simple example. Consider a perfectly insulated thermal storage containing 1000 kg of water, initially at 40 °C. The ambient temperature is 20 °C.

A quantity of 4200 kJ of heat is transferred to the storage through a heat exchanger from an external body of 100 kg of water cooling from 100 °C to 90 °C (i.e., using Equation 6.168,  $(100 \text{ kg})(4.2 \text{ kJ/kg K})(100 - 90)^\circ\text{C} = 4200 \text{ kJ}$ ). This heat addition raises the storage temperature from 1.0 °C to 41 °C (i.e., with Equation 6.181,  $(4200 \text{ kJ})/((1000 \text{ kg})(4.2 \text{ kJ/kg K})) = 1.0^\circ\text{C}$ ). After a period of storage, 4200 kJ of heat are recovered from the storage through a heat exchanger that delivers it to an external body of 100 kg of water, raising the temperature of that water from 20 °C to 30 °C (i.e., with Equation 6.168,  $\Delta T = (4200 \text{ kJ})/((100 \text{ kg})(4.2 \text{ kJ/kg K})) = 10^\circ\text{C}$ ). The storage is returned to its initial state at 40 °C.

For this storage cycle, the energy efficiency, the ratio of the heat recovered from the storage to the heat injected, is  $4200 \text{ kJ}/4200 \text{ kJ} = 1$ , or 100%. But, the recovered heat is at only 30 °C, and of little use, having been degraded even though the storage energy efficiency was 100%. With Equation 6.170a, the exergy recovered in this example is evaluated as  $(100 \text{ kg})(4.2 \text{ kJ/kg K})[(30 - 20)^\circ\text{C} - (293 \text{ K}) \ln (303/293)] = 70 \text{ kJ}$ , and the exergy supplied as  $(100 \text{ kg})(4.2 \text{ kJ/kg K})[(100 - 90)^\circ\text{C} - (293 \text{ K}) \ln (373/363)] = 856 \text{ kJ}$ . Thus the exergy efficiency, the ratio of the thermal exergy recovered from storage to that injected, is  $70/856 = 0.082$ , or 8.2%, a much more meaningful expression of the achieved performance of the storage cycle.

In most TES investigations, the energy and exergy efficiency definitions in Equations 6.32 and 6.33 are used. These efficiency definitions are dependent on what quantities are considered to be products and inputs. Two possible sets of efficiency definitions are presented in Table 6.3. The energy or exergy initially in the store is neglected in the first definition, and considered to be an “input” in the second definition. Depending on the particular circumstances, the energy efficiency definitions in Table 6.3 can yield values that are identical or radically different. The same statement can be made for the exergy efficiencies. Regardless of definition, however, the authors feel that the use of exergy analysis is necessary for evaluating TES systems.

### 6.3.3 Pinpointing Losses

With energy analysis, all losses are attributable to energy releases across system boundaries. With exergy analysis, losses are divided into two types: those associated with releases of exergy from the system and those associated with internal consumptions of exergy (Alefeld, 1990). For a TES system, the total exergy loss is the sum of the exergy associated with heat loss to the surroundings and the exergy loss due to internal exergy consumptions, such as by reductions in availability of the stored heat through mixing of warm and cool fluids. The division of losses associated with exergy analysis allows the causes of inefficiencies to be more accurately identified than does energy analysis, and R&D effort to be more effectively allocated. The analysis of the heat flows from

**Table 6.3** Two overall energy ( $\eta$ ) and exergy ( $\psi$ ) TES efficiencies

Efficiency	Definition 1	Definition 2
$\eta$	$\frac{\text{Energy recovered from TES}}{\text{Energy input to TES}}$	$\frac{\text{Energy recovered from and remaining in TES}}{\text{Energy input to and originally in TES}}$
$\psi$	$\frac{\text{Exergy recovered from TES}}{\text{Exergy input to TES}}$	$\frac{\text{Exergy recovered from and remaining in TES}}{\text{Exergy input to and originally in TES}}$

or into TES systems is often investigated (Rosen, 1990, 1998a, 1998b), and is discussed in the first chapter.

#### 6.3.4 Assessing the Effects of Stratification

Water tanks are one of the most economic devices for TES. For many TES applications, performance is strongly dependent on the temperature required to meet the thermal energy demand, and stratification within the tank can play a significant role (Yoo *et al.*, 1998; Homan *et al.*, 1996; Mavros *et al.*, 1994; Nelson *et al.*, 1999; Gretarsson *et al.*, 1994). In practice, in most cases, a vertical cylindrical tank with a hot water inlet (outlet) at the top and a cold water inlet (outlet) at the bottom is used. The hot and cold water in the tank are usually stratified initially into two layers, with a mixing layer in between. The degree of stratification is dependent on the volume and configuration of the tank, the size, location, and design of the inlets and outlets, the flow rates of the entering and exiting streams, and the durations of the charging, storing, and discharging periods.

Four primary factors contribute to the loss of stratification and hence the degradation of the stored energy:

- heat losses to (or leakages from) the surrounding environment;
- heat conduction from the hot portions of the storage fluid to the colder portions;
- vertical conduction in the tank wall; and
- mixing during charging and discharging periods.

Among these, the last item generally is the major cause of loss of stratification, with particularly significant mixing losses occurring during lengthy storing periods. Improving stratification often leads to substantial improvement in TES efficiency relative to a system incorporating a thermally mixed-storage tank.

TES evaluation methodologies must quantitatively and clearly assess the effects of stratification on system performance. The effects of stratification are more clearly assessed with exergy analysis than with energy analysis because of the internal spatial temperature variations that stratified storages exhibit (Hahne *et al.*, 1989; Krane and Krane, 1991; Rosen and Tang, 1997). Through carefully managing the injection, recovery, and holding of heat (or cold) during a storage cycle so that temperature degradation is minimized, better storage-cycle performance can be achieved (as measured by better thermal energy recovery and temperature retention). This improved performance is accounted for explicitly with exergy analysis through increased exergy efficiencies. Some relatively simple approaches for stratified TES evaluation have been developed (Hooper *et al.*, 1988; Rosen and Hooper, 1991a, 1991b, 1992, 1994), which take into consideration the second-law concerns, and which assess the performance of real stratified storages with an accuracy acceptable for most purposes, and certainly superior to that from assessments based only on the first law.

#### 6.3.5 Accounting for Time Duration of Storage

Rational measures of merit for the evaluation and comparison of TES systems must account for the length of time thermal energy is in storage. The length of time that thermal energy is retained in a TES does not enter into the expressions for thermal efficiency and exergy efficiency for thermal storages, although it is clearly a dominant consideration in the overall effectiveness for such systems. The authors have examined the relation between the length of time thermal energy is held in storage and storage effectiveness, and have developed an approach for comparing TES systems using a time parameter (Barbaris *et al.*, 1988).

### 6.3.6 Accounting for Variations in Reference-Environment Temperature

Over the time periods involved in some TES cycles (up to six months for seasonal systems), the value of the reference-environment temperature  $T_o$  varies with time. The value of  $T_o$  also varies with location. Since the results of TES evaluations based on energy and exergy analyses depend on the value of  $T_o$ , the temporal and spatial dependencies must be considered in such evaluations.

The value of  $T_o(t)$  can often be assumed to be the same as the ambient temperature variation with time,  $T_{amb}(t)$ . On an annual basis, the ambient temperature varies approximately sinusoidally with time  $t$  about the annual mean:

$$T_{amb}(t) = \bar{T}_{amb} + \Delta T_{amb} \left[ \sin \frac{2\pi t}{\text{period}} + (\text{phase shift}) \right] \quad (6.36)$$

where  $\bar{T}_{amb}$  is the mean annual ambient temperature and  $\Delta T_{amb}$  is the maximum temperature deviation from the annual mean. The values of the parameters in Equation 6.36 vary spatially and the period is one year.

In evaluating the performance of most storages (particularly of long-term storages), a constant value of  $T_o$  can be assumed. Some possible values for  $T_o$  are:

- the appropriate seasonal mean value of the temperature of the atmosphere;
- the appropriate annual mean value of the temperature of the atmosphere;
- the temperature of soil far enough below the surface that the temperature remains approximately constant throughout the year, that is, near the water table (this temperature is usually near to that specified in the previous point); and
- the lowest value of the atmosphere temperature during the year, for heat storage processes, and the highest value of the atmosphere temperature during the year, for cooling capacity storage processes.

### 6.3.7 Closure

The factors discussed here that significantly impacts on the evaluation and comparison of TES systems are summarized in Table 6.4.

## 6.4 Exergy Evaluation of a Closed TES System

The use of exergy analysis in the evaluation of a specific TES system (a simple closed tank storage with heat transfers by heat exchanger) is described in this section, following an earlier report (Rosen *et al.*, 1988). A complete storing cycle, as well as the individual charging, storing, and discharging

**Table 6.4** Some exergy-related thermodynamic considerations in TES system evaluations

- 
- Determining important analysis quantities.
  - Evaluating storages for cooling as well as heating capacity.
  - Obtaining appropriate measures of efficiency.
  - Pinpointing losses.
  - Assessing the effects of stratification.
  - Assessing the performance of subprocesses.
  - Accounting for temporal and spatial variations in  $T_o$ .
  - Accounting for the time duration of storage.
-



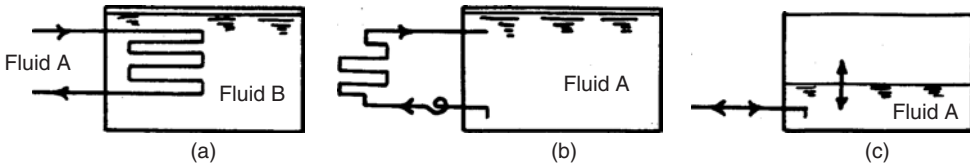


**Figure 6.2** Three basic types of thermal storage. (a) A closed system in which heat transfer occurs between the transport fluid A and the storage fluid B. (b) An open system of constant mass in which the same fluid is used for both transport and storage of heat. (c) An open system of variable mass

periods, is considered. A numerical example for a simple case is given (see Section 6.4.6). This application highlights the fact that, although energy is conserved in an adiabatic system, mixing of the high- and low-temperature portions of the storage medium causes a consumption (or destruction) of exergy, which is conserved only in fully reversible processes.

A clear understanding of the TES type under consideration and a clear declaration of the assumptions used are important in establishing a consistent basis for TES analysis and comparison. Three basic sensible heat storage types are shown in Figure 6.2. The first type, which is considered here, represents a closed system storing heat in a fixed amount of storage fluid B, to or from which heat is transferred through a heat exchanger by means of a heat transport fluid A. The second type is also of fixed mass, but is open, and the transport and storage fluids are of the same substance. No heat exchanger is involved. The third type uses an open system storing a variable amount of the combined heat transport and storage fluid. For each of these storage types, further characteristics can yield additional cases and conditions (e.g., adiabatic or nonadiabatic boundaries, complete or incomplete cycles, fully mixed or stratified storage fluid, steady or intermittent fluid flows, steady or variable ambient conditions, short or long storage periods, constant or variable physical properties, and one-, two-, or three-dimensional heat flows).

### 6.4.1 Description of the Case Considered

A specific, simple case is considered in which a TES system undergoes a complete storage cycle, ending with the final state identical to the initial state. Figure 6.3 illustrates the three periods in the overall storage process considered. The TES may be stratified. Other characteristics of the considered case are:

- nonadiabatic storage boundaries;
- finite charging, storing, and discharging time periods;
- surroundings at constant temperature and pressure;
- constant storage volume;
- negligible work interactions (e.g., pump work); and
- negligible kinetic and potential energy terms.

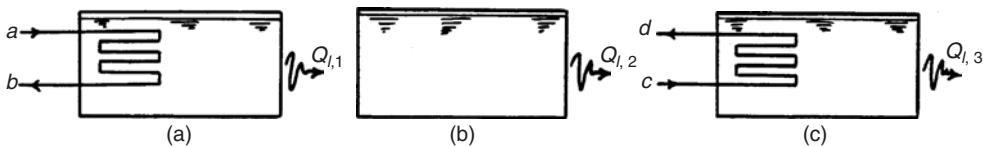


**Figure 6.3** The three stages in a simple heat storage process: charging period (a), storing period (b), and discharging period (c)



The operation of the heat exchangers is simplified by assuming that there are no heat losses to the surrounding environment from the charging and discharging fluids. That is, it is assumed for the charging period that all heat removed from the charging fluid is added to the storage medium, and for the discharging period that all heat added to the discharging fluid originated in the storage medium. This assumption is valid if heat losses from the charging and discharging fluids are small compared with heat losses from the storage medium. This assumption can be extended by lumping actual heat losses from the charging and discharging fluids together with heat losses from the TES. Also, as is often done for practical systems, the charging- and discharging-fluid flows are considered steady and with time-independent properties, and modeled as one-dimensional.

### 6.4.2 Analysis of the Overall Process

For the cases considered (Figure 6.3), energy and exergy balances and efficiencies are provided for the overall process.

#### Overall Energy Balance

Following Equations 6.3 and 6.3a, an energy balance for the overall storage process can be written as

$$\text{Energy input} - (\text{Energy recovered} + \text{Energy loss}) = \text{Energy accumulation} \quad (6.37)$$

or

$$(H_a - H_b) - [(H_d - H_c) + Q_l] = \Delta E \quad (6.37a)$$

where  $H_a$ ,  $H_b$ ,  $H_c$ , and  $H_d$  are the total enthalpies of the flows at states  $a$ ,  $b$ ,  $c$ , and  $d$ , respectively;  $Q_l$  denotes the heat losses during the process and  $\Delta E$  the accumulation of energy in the TES. In Equation 6.37a,  $(H_a - H_b)$  represents the net heat delivered to the TES and  $(H_d - H_c)$  the net heat recovered from the TES. The quantity in square brackets represents the net energy output from the system. The terms  $\Delta E$  and  $Q_l$  are given by

$$\Delta E = E_f - E_i \quad (6.38)$$

$$Q_l = \sum_{j=1}^3 Q_{l,j} \quad (6.39)$$

Here  $E_i$  and  $E_f$  denote the initial and final energy contents of the storage, and  $Q_{l,j}$  denotes the heat losses during the period  $j$ , where  $j = 1, 2, 3$  corresponds to the charging, storing, and discharging periods, respectively. In the case of identical initial and final states,  $\Delta E = 0$ , and the overall energy balance simplifies.

#### Overall Exergy Balance

Following Equations 6.5 and 6.5a, an overall exergy balance can be written as

$$\begin{aligned} &\text{Exergy input} - (\text{Exergy recovered} + \text{Exergy loss}) - \text{Exergy consumption} \\ &= \text{Exergy accumulation} \end{aligned} \quad (6.40)$$

or

$$(\epsilon_a - \epsilon_b) - [(\epsilon_d - \epsilon_c) + X_l] - I = \Delta \Xi \quad (6.40a)$$

where  $\epsilon_a, \epsilon_b, \epsilon_c$ , and  $\epsilon_d$  are the exergies of the flows at states  $a, b, c$ , and  $d$ , respectively; and  $X_l$  denotes the exergy loss associated with  $Q_l$ ;  $I$  is the exergy consumption; and  $\Delta \Xi$  is the exergy accumulation. In Equation 6.40a,  $(\epsilon_a - \epsilon_b)$  represents the net exergy input and  $(\epsilon_d - \epsilon_c)$  is the net exergy recovered. The quantity in square brackets represents the net exergy output from the system. The terms  $I, X_l$ , and  $\Delta \Xi$  are given respectively by

$$I = \sum_{j=1}^3 I_j \quad (6.41)$$

$$X_l = \sum_{j=1}^3 X_{l,j} \quad (6.42)$$

$$\Delta \Xi = \Xi_f - \Xi_i \quad (6.43)$$

Here,  $I_1, I_2$ , and  $I_3$  denote respectively the consumptions of exergy during the charging, storing, and discharging periods;  $X_{l,1}, X_{l,2}$ , and  $X_{l,3}$  denote the exergy losses associated with heat losses during the same periods; and  $\Xi_i$  and  $\Xi_f$  denote the initial and final exergy contents of the storage. When the initial and final states are identical,  $\Delta \Xi = 0$ .

The exergy content of the flow at the states  $k = a, b, c, d$  is evaluated as

$$\epsilon_k = (H_k - H_o) - T_o (S_k - S_o) \quad (6.44)$$

where  $\epsilon_k, H_k$ , and  $S_k$  denote the exergy, enthalpy, and entropy of state  $k$ , respectively, and  $H_o$  and  $S_o$  the enthalpy and the entropy at the temperature  $T_o$  and pressure  $P_o$  of the reference environment. The exergy expression in Equation 6.44 only includes physical (or thermomechanical) exergy. Potential and kinetic exergy components are, as pointed out earlier, considered negligible for the devices under consideration. The chemical component of exergy is neglected because it does not contribute to the exergy flows for sensible TES systems. Thus, the exergy differences between the inlet and outlet for the charging and discharging periods are, respectively:

$$\epsilon_a - \epsilon_b = (H_a - H_b) - T_o (S_a - S_b) \quad (6.45)$$

and

$$\epsilon_d - \epsilon_c = (H_d - H_c) - T_o (S_d - S_c) \quad (6.46)$$

Here it has been assumed that  $T_o$  and  $P_o$  are constant, so that  $H_o$  and  $S_o$  are constant at states  $a$  and  $b$ , and at states  $c$  and  $d$ .

For a fully mixed tank, the exergy losses associated with heat losses to the surroundings are evaluated following Equation 6.25 as

$$X_{l,j} = \int_i^f \left(1 - \frac{T_o}{T_j}\right) dQ_{l,j} \text{ for } j = 1, 2, 3 \quad (6.47)$$

where  $j$  represents the particular period. If  $T_1, T_2$ , and  $T_3$  are constant during the respective charging, storing, and discharging periods, then  $X_{l,j}$  may be written with Equation 6.25a as follows:

$$X_{l,j} = \left(1 - \frac{T_o}{T_j}\right) Q_{l,j} \quad (6.47a)$$

Sometimes when applying Equation 6.47a to TES systems,  $T_j$  represents a mean temperature within the tank for period  $j$ .

### Overall Energy and Exergy Efficiencies

Following Equations 6.32 and 6.33, the energy efficiency  $\eta$  can be defined as

$$\eta = \frac{\text{Energy recovered from TES during discharging}}{\text{Energy input to TES during charging}} = \frac{H_d - H_c}{H_a - H_b} = 1 - \frac{Q_l}{H_a - H_b} \quad (6.48)$$

and the exergy efficiency  $\psi$  as

$$\psi = \frac{\text{Exergy recovered from TES during discharging}}{\text{Exergy input to during charging}} = \frac{\epsilon_d - \epsilon_c}{\epsilon_a - \epsilon_b} = 1 - \frac{X_l + I}{\epsilon_a - \epsilon_b} \quad (6.49)$$

The efficiency expressions in Equations 6.48 and 6.49 do not depend on the initial energy and exergy contents of the TES.

If the TES is adiabatic,  $Q_{l,j} = X_{l,j} = 0$  for all  $j$ . Then, the energy efficiency is fixed at unity and the exergy efficiency simplifies to

$$\psi = 1 - \frac{I}{\epsilon_a - \epsilon_b} \quad (6.49a)$$

emphasizing the point that even when TES boundaries are adiabatic and there are therefore no energy losses, the exergy efficiency is less than unity due to internal irreversibilities.

### 6.4.3 Analysis of Subprocesses

Many different efficiencies based on energy and exergy can be defined for the charging, storing, and discharging periods (as discussed in Section 6.5). In the present analysis of the subprocesses (see Figure 6.3), only one set of efficiencies is considered.

#### Analysis of Charging Period

An energy balance for the charging period can be written as follows:

$$\text{Energy input} - \text{Energy loss} = \text{Energy accumulation} \quad (6.50)$$

$$(H_a - H_b) - Q_{l,1} = \Delta E_1 \quad (6.50a)$$

Here,

$$\Delta E_1 = E_{f,1} - E_{i,1} \quad (6.51)$$

and  $E_{i,1}$  and  $E_{f,1}$  denote the initial and the final energy of the TES for the charging period. Note that  $E_{i,1} \equiv E_i$  (see Equation 6.38). A charging-period energy efficiency can be defined as

$$\eta_1 = \frac{\text{Energy accumulation in TES during charging}}{\text{Energy input to TES during charging}} = \frac{\Delta E_1}{H_a - H_b} \quad (6.52)$$

An exergy balance for the charging period can be written as

$$\text{Exergy input} - \text{Exergy loss} - \text{Exergy consumption} = \text{Exergy accumulation} \quad (6.53)$$

$$(\epsilon_a - \epsilon_b) - X_{l,1} - I_1 = \Delta \Xi_1 \quad (6.53a)$$

Here,

$$\Delta \Xi_1 = \Xi_{f,1} - \Xi_{i,1} \quad (6.54)$$

and  $\Xi_{i,1}$  and  $\Xi_{f,1}$  are the initial and the final exergy of the TES for the charging period. Note that  $\Xi_{i,1} \equiv \Xi_i$  (see Equation 6.43). A charging-period exergy efficiency can be defined as

$$\psi_1 = \frac{\text{Exergy accumulation in TES during charging}}{\text{Exergy input to TES during charging}} = \frac{\Delta \Xi_1}{\epsilon_a - \epsilon_b} \quad (6.55)$$

The charging efficiencies in Equations 6.52 and 6.55 indicate the fraction of the input energy/exergy that is accumulated in the store during the charging period.

### Analysis of Storing Period

An energy balance for the storing period can be written as

$$-\text{Energy loss} = \text{Energy accumulation} \quad (6.56)$$

$$-Q_{l,2} = \Delta E_2 \quad (6.56a)$$

Here,

$$\Delta E_2 = E_{f,2} - E_{i,2} \quad (6.57)$$

and  $E_{i,2} (\equiv E_{f,1})$  and  $E_{f,2}$  denote the initial and final energy contents of the TES for the storing period. An energy efficiency for the storing period can be defined as

$$\eta_2 = \frac{\text{Energy accumulation in TES during charging and storing}}{\text{Energy accumulation in TES during charging}} = \frac{\Delta E_1 + \Delta E_2}{\Delta E_1} \quad (6.58)$$

Using Equation 6.56a, the energy efficiency can be rewritten as

$$\eta_2 = \frac{\Delta E_1 - Q_{l,2}}{\Delta E_1} \quad (6.58a)$$

An exergy balance for the storing period can be written as

$$-\text{Energy loss} - \text{Exergy consumption} = \text{Exergy accumulation} \quad (6.59)$$

$$-X_{l,2} - I_2 = \Delta \Xi_2 \quad (6.59a)$$

Here,

$$\Delta \Xi_2 = \Xi_{f,2} - \Xi_{i,2} \quad (6.60)$$

and  $\Xi_{i,2} (\equiv \Xi_{f,1})$  and  $\Xi_{f,2}$  denote the initial and the final exergies of the system for the storing period. An exergy efficiency for the storing period can be defined as

$$\psi_2 = \frac{\text{Exergy accumulation in TES during charging and storing}}{\text{Exergy accumulation in TES during charging}} = \frac{\Delta \Xi_1 + \Delta \Xi_2}{\Delta \Xi_1} \quad (6.61)$$

Using Equation 6.59a, the exergy efficiency can be rewritten as

$$\psi_2 = \frac{\Delta \Xi_1 - (X_{l,2} + I_2)}{\Delta \Xi_1} \quad (6.61a)$$

The storing efficiencies in Equations 6.58 and 6.61 indicate the fraction of the energy/exergy accumulated during charging that is still retained in the store at the end of the storing period.

### Analysis of Discharging Period

An energy balance for the discharging period can be written as

$$-(\text{Energy recovered} + \text{Energy loss}) = \text{Energy accumulation} \quad (6.62)$$

$$-[(H_d - H_c) + Q_{l,3}] = \Delta E_3 \quad (6.62a)$$

Here,

$$\Delta E_3 = E_{f,3} - E_{i,3} \quad (6.63)$$

and  $E_{i,3}(= E_{f,2})$  and  $E_{f,3}(= E_f$  in Equation 6.38) denote the initial and final energies of the store for the discharging period. The quantity in square brackets represents the energy output during discharging. An energy efficiency for the discharging period can be defined as

$$\eta_3 = \frac{\text{Energy recovered from TES during discharging}}{\text{Energy accumulation in TES during charging and storing}} = \frac{H_d - H_c}{\Delta E_1 + \Delta E_2} \quad (6.64)$$

Using Equation 6.56a, the energy efficiency can be rewritten as

$$\eta_3 = \frac{H_d - H_c}{\Delta E_1 - Q_{1,2}} \quad (6.64a)$$

An exergy balance for the discharging period can be written as follows:

$$-(\text{Exergy recovered} + \text{Exergy loss}) - \text{Exergy consumption} = \text{Exergy accumulation} \quad (6.65)$$

$$-[(\epsilon_d - \epsilon_c) + X_{l,3}] - I_3 = \Delta \Xi_3 \quad (6.65a)$$

Here,

$$\Delta \Xi_3 = \Xi_{f,3} - \Xi_{i,3} \quad (6.66)$$

and  $\Xi_{i,3}(= \Xi_{f,2})$  and  $\Xi_{f,3}(= \Xi_f$  in Equation 6.43) denote the initial and final exergies of the store for the discharging period. The quantity in square brackets represents the exergy output during discharging. An exergy efficiency for the discharging period can be defined as

$$\psi_3 = \frac{\text{Exergy recovered from TES during discharging}}{\text{Exergy accumulation in TES during charging and storing}} = \frac{\epsilon_d - \epsilon_c}{\Delta \Xi_1 + \Delta \Xi_2} \quad (6.67)$$

Using Equation 6.59a, the exergy efficiency can be rewritten as

$$\psi_3 = \frac{\epsilon_d - \epsilon_c}{\Delta \Xi_1 - (X_{l,2} + I_2)} \quad (6.67a)$$

The discharging efficiencies in Equations 6.64 and 6.67 indicate the fraction of the energy/exergy input during charging and still retained at the end of storing that is recovered during discharging.

### 6.4.4 Alternative Formulations of Subprocess Efficiencies

Several alternative subprocess efficiency formulations, which can be useful depending upon the inclination of the analyst and the application addressed, are given here.

In the expressions for the subprocess energy and exergy efficiencies, that is, in Equations 6.52, 6.55, 6.58a, 6.61a, 6.64a, and 6.67a, the terms  $\Delta E_1$  and  $\Delta \Xi_1$  can be eliminated using Equations

6.50a and 6.53a, respectively. After substitutions for  $\Delta E_1$  and  $\Delta \Xi_1$  and minor rearrangement of the equations, the following are obtained:

$$\eta_1 = \frac{(H_a - H_b) - Q_{l,1}}{(H_a - H_b)} = 1 - \frac{Q_{l,1}}{H_a - H_b} \quad (6.52a)$$

$$\psi_1 = \frac{(\epsilon_a - \epsilon_b) - (X_{l,1} + I_1)}{(\epsilon_a - \epsilon_b)} = 1 - \frac{X_{l,1} + I_1}{\epsilon_a - \epsilon_b} \quad (6.55a)$$

$$\eta_2 = \frac{[(H_a - H_b) - Q_{l,1}] - Q_{l,2}}{(H_a - H_b) - Q_{l,1}} = \frac{(H_a - H_b) - \sum_{j=1}^2 Q_{l,j}}{(H_a - H_b) - Q_{l,1}} = 1 - \frac{Q_{l,2}}{(H_a - H_b) - Q_{l,1}} \quad (6.58b)$$

$$\begin{aligned} \psi_2 &= \frac{[(\epsilon_a - \epsilon_b) - (X_{l,1} + I_1)] - [X_{l,2} + I_2]}{(\epsilon_a - \epsilon_b) - (X_{l,1} + I_1)} = \frac{(\epsilon_a - \epsilon_b) - \sum_{j=1}^2 (X_{l,j} + I_j)}{(\epsilon_a - \epsilon_b) - (X_{l,1} + I_1)} \\ &= 1 - \frac{X_{l,2} + I_2}{(\epsilon_a - \epsilon_b) - (X_{l,1} + I_1)} \end{aligned} \quad (6.61b)$$

$$\eta_3 = \frac{H_d - H_c}{[(H_a - H_b) - Q_{l,1}] - Q_{l,2}} = \frac{H_d - H_c}{(H_a - H_b) - \sum_{j=1}^2 Q_{l,j}} \quad (6.64b)$$

$$\psi_3 = \frac{\epsilon_d - \epsilon_c}{[(\epsilon_a - \epsilon_b) - (X_{l,1} + I_1)] - (X_{l,2} + I_2)} = \frac{\epsilon_d - \epsilon_c}{(\epsilon_a - \epsilon_b) - \sum_{j=1}^2 (X_{l,j} + I_j)} \quad (6.67b)$$

The above equations for  $\eta_3$  and  $\psi_3$  can be further modified if the terms in the numerators are eliminated using Equations 6.37a and 6.40a with  $\Delta E = \Delta \Xi = 0$ . Then,

$$\eta_3 = \frac{(H_a - H_b) - Q_l}{(H_a - H_b) - \sum_{j=1}^2 Q_{l,j}} = \frac{(H_a - H_b) - \sum_{j=1}^3 Q_{l,j}}{(H_a - H_b) - \sum_{j=1}^2 Q_{l,j}} = 1 - \frac{Q_{l,3}}{(H_a - H_b) - \sum_{j=1}^2 Q_{l,j}} \quad (6.64c)$$

$$\begin{aligned} \psi_3 &= \frac{(\epsilon_a - \epsilon_b) - (X_l + I)}{(\epsilon_a - \epsilon_b) - \sum_{j=1}^2 (X_{l,j} + I_j)} = \frac{(\epsilon_a - \epsilon_b) - \sum_{j=1}^3 (X_{l,j} + I_j)}{(\epsilon_a - \epsilon_b) - \sum_{j=1}^2 (X_{l,j} + I_j)} \\ &= 1 - \frac{X_{l,3} + I_3}{(\epsilon_a - \epsilon_b) - \sum_{j=1}^2 (X_{l,j} + I_j)} \end{aligned} \quad (6.67c)$$

### 6.4.5 Relations between Performance of Subprocesses and Overall Process

The total energy and exergy efficiencies can be written as the products of the energy and exergy efficiencies of the charging, storing, and discharging periods. That is,

$$\eta = \prod_{j=1}^3 \eta_j \quad (6.68)$$

$$\psi = \prod_{j=1}^3 \psi_j \quad (6.69)$$

The energy efficiency relationship can be verified by multiplying together Equations 6.52, 6.58a, and 6.64a and comparing the result to Equation 6.48. Similarly, the exergy efficiency relationship can be verified by comparing the product of Equations 6.55, 6.61a, and 6.67a to Equation 6.49a. Equations 6.68 and 6.69 can also be shown to hold when using the alternative formulations of the subprocess efficiencies.

In addition, it can be shown that the summations of the energy or exergy balance equations, respectively, for the three subprocesses give the energy or exergy balance equations for the overall process. This statement can be verified by noting that,

$$\sum_{j=1}^3 \Delta E_j = E_{3,f} - E_{1,i} = E_f - E_i = \Delta E \quad (6.70)$$

$$\sum_{j=1}^3 \Delta \Xi_j = \Xi_{3,f} - \Xi_{1,i} = \Xi_f - \Xi_i = \Delta \Xi \quad (6.71)$$

and by comparing the sum of Equations 6.50a, 6.56a, and 6.62a with Equation 6.37a for energy, and by comparing the sum of Equations 6.53a, 6.59a, and 6.65a with Equation 6.40a for exergy. In writing Equations 6.70 and 6.71, it has been noted that for period  $j$ ,

$$\Delta E_j = E_{f,j} - E_{i,j} \quad (6.72)$$

$$\Delta \Xi_j = \Xi_{f,j} - \Xi_{i,j} \quad (6.73)$$

and that  $E_{i,1} = E_i$ ,  $E_{f,3} = E_f$ , and  $E_{i,j+1} = E_{f,j}$  for  $j = 1, 2$ , while analogous expressions hold for the  $\Xi$  terms.

### 6.4.6 Example

Consider two different thermal storages, each of which undergoes a similar charging process. In each charging operation, heat is transferred to a closed thermal storage from a stream of 1000 kg of water that enters at 85 °C and leaves at 25 °C (see Figure 6.4). Consider Cases A and B, representing two different modes of operation. For Case A, heat is recovered from the storage after 1 day by a stream of 5000 kg of water entering at 25 °C and leaving at 35 °C. For Case B, heat is recovered from the storage after 100 days by a stream of 1000 kg of water entering at 25 °C and leaving at 75 °C.

Energy and exergy analyses of the overall processes are performed for both cases using superscripts *A* and *B* to denote Cases A and B, respectively. In both cases, the temperature of the surroundings remains constant at 20 °C, and the final state of the storage is the same as the initial state. Water is taken to be an incompressible fluid having a specific heat at constant pressure of  $c_p = 4.18$  kJ/kg K, and heat exchanges during charging and discharging are assumed to occur at constant pressure.

The numerical values used in the example were selected to illustrate the concepts discussed in this section, and to resemble values for possible practical system configurations. Several physical implications of the selected numerical values are as follows. First, the inlet and outlet temperatures for the charging and discharging fluids imply that a stratified temperature profile exists in the TES after charging. Secondly, the higher discharging-fluid temperature for Case B implies that a greater degree of stratification is maintained during the storing period for Case B (or that greater internal mixing occurs for Case A). Thirdly, the quantities of discharging fluid and the associated temperatures imply that the discharging fluid is circulated through the TES at a greater rate for Case A than for Case B.

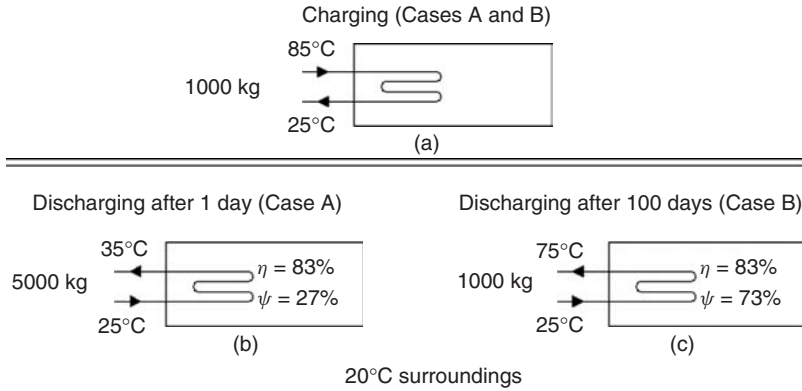


**Figure 6.4** An example in which two cases are considered. Shown are the charging process, which is identical for Cases A and B (a), the discharging process for Case A (b), and the discharging process for Case B (c)

### Energy Analysis for the Overall Process

The net heat input to the storage during the charging period for each case is

$$H_a - H_b = m_1 c_p (T_a - T_b) = 1000 \text{ kg} \times 4.18 \text{ kJ/kg K} \times (85 - 25) \text{ K} = 250,800 \text{ kJ}$$

For Case A, the heat recovered during the discharging period is

$$(H_d - H_c)^A = 5000 \text{ kg} \times 4.18 \text{ kJ/kg K} \times (35 - 25) \text{ K} = 209,000 \text{ kJ}$$

The energy efficiency of storage is (see Equation 6.48)

$$\eta^A = \frac{\text{Heat recovered}}{\text{Heat input}} = \frac{(H_d - H_c)^A}{H_a - H_b} = \frac{209,000 \text{ kJ}}{250,800 \text{ kJ}} = 0.833$$

The heat lost to the surroundings during storage is (see Equation 6.37a with  $\Delta E = 0$ )

$$Q_l^A = (H_a - H_b) - (H_c - H_d)^A = 250,000 \text{ kJ} - 209,000 \text{ kJ} = 41,800 \text{ kJ}$$

For Case B, the heat recovered during discharging, the energy efficiency, and the heat lost to the surroundings can be evaluated similarly:

$$(H_d - H_c)^B = 1000 \text{ kg} \times 4.18 \text{ kJ/kg K} \times (75 - 25) \text{ K} = 209,000 \text{ kJ}$$

$$\eta^B = \frac{209,000 \text{ kJ}}{250,800 \text{ kJ}} = 0.833$$

$$Q_l^B = 250,800 \text{ kJ} - 209,000 \text{ kJ} = 41,800 \text{ kJ}$$

The values of the three parameters evaluated above for Case B are the same as the corresponding values for Case A.

### Exergy Analysis for the Overall Process

The net exergy input during the charging period ( $\epsilon_a - \epsilon_b$ ) can be evaluated with Equation 6.45. In that expression, the quantity  $(H_a - H_b)$  represents the net energy input to the store during charging,



evaluated as 250,800 kJ in the previous subsection. Noting that the difference in specific entropy can be written assuming incompressible substances having a constant specific heat as

$$s_a - s_b = c_p \ln \frac{T_a}{T_b} = 4.18 \frac{\text{kJ}}{\text{kg K}} \times \ln \frac{358 \text{ K}}{298 \text{ K}} = 0.7667 \frac{\text{kJ}}{\text{kg K}}$$

the quantity  $T_o(S_a - S_b)$ , which represents the unavailable part of the input heat, is

$$T_o(S_a - S_b) = T_o m_1 (s_a - s_b) = 293 \text{ K} \times 1000 \text{ kg} \times 0.7667 \text{ kJ/kg K} = 224,643 \text{ kJ}$$

where  $m_1$  denotes the mass of the transport fluid cooled during the charging period. Then, the net exergy input is

$$\epsilon_a - \epsilon_b = 250,800 \text{ kJ} - 224,643 \text{ kJ} = 26,157 \text{ kJ}$$

The net exergy output during the discharging period ( $\epsilon_d - \epsilon_c$ ) can be evaluated using Equation 6.46 and denoting the mass of the transport fluid circulated during the discharging period as  $m_3$ , in a similar three-step fashion for Cases A and B. For Case A,

$$\begin{aligned} (s_d - s_c)^A &= c_p \ln \frac{T_d^A}{T_c^A} = 4.18 \frac{\text{kJ}}{\text{kg K}} \times \ln \frac{308 \text{ K}}{298 \text{ K}} = 0.1379 \frac{\text{kJ}}{\text{kg K}} \\ T_o(S_d - S_c)^A &= T_o m_3^A (s_d - s_c)^A = 293 \text{ K} \times 5000 \text{ kg} \times 0.1379 \text{ kJ/kg K} = 202,023 \text{ kJ} \\ (\epsilon_d - \epsilon_c)^A &= 209,000 \text{ kJ} - 202,023 \text{ kJ} = 6977 \text{ kJ} \end{aligned}$$

For Case B,

$$\begin{aligned} (s_d - s_c)^B &= c_p \ln \frac{T_d^B}{T_c^B} = 4.18 \frac{\text{kJ}}{\text{kg K}} \times \ln \frac{348 \text{ K}}{298 \text{ K}} = 0.6483 \frac{\text{kJ}}{\text{kg K}} \\ T_o(S_d - S_c)^B &= T_o m_3^B (s_d - s_c)^B = 293 \text{ K} \times 1000 \text{ kg} \times 0.6483 \text{ kJ/kg K} = 189,950 \text{ kJ} \\ (\epsilon_d - \epsilon_c)^B &= 209,000 \text{ kJ} - 189,950 \text{ kJ} = 19,050 \text{ kJ} \end{aligned}$$

Thus, the exergy efficiency (see Equation 6.49) for Case A is

$$\psi^A = \frac{(\epsilon_d - \epsilon_c)^A}{\epsilon_a - \epsilon_b} = \frac{6977 \text{ kJ}}{26,157 \text{ kJ}} = 0.267$$

and for Case B

$$\psi^B = \frac{(\epsilon_d - \epsilon_c)^B}{\epsilon_a - \epsilon_b} = \frac{19,050 \text{ kJ}}{26,157 \text{ kJ}} = 0.728$$

which is considerably higher than for Case A.

The exergy losses (total) can be evaluated with Equation 6.40a (with  $\Delta \Xi = 0$ ) as the sum of the exergy loss associated with heat loss to the surroundings and the exergy loss due to internal exergy consumptions:

$$\begin{aligned} (X_l + I)^A &= (\epsilon_a - \epsilon_b) - (\epsilon_d - \epsilon_c)^A = 26,157 \text{ kJ} - 6977 \text{ kJ} = 19,180 \text{ kJ} \\ (X_l + I)^B &= (\epsilon_a - \epsilon_b) - (\epsilon_d - \epsilon_c)^B = 26,157 \text{ kJ} - 19,050 \text{ kJ} = 7107 \text{ kJ} \end{aligned}$$

Here, no attempt has been made to evaluate the individual values of the two exergy loss parameters. If it is assumed that heat is transferred at  $T_o$  to the surroundings, then  $X_l^A = X_l^B = 0$ , and all the exergy losses are internal consumptions.

**Table 6.5** Comparison of the performance of a TES for two cases

	Case A	Case B
<i>General parameters</i>		
Storing period (days)	1	100
Charging-fluid temperatures (in/out) (°C)	85/25	85/25
Discharging-fluid temperatures (in/out) (°C)	25/35	25/75
<i>Energy parameters</i>		
Energy input (kJ)	250,800	250,800
Energy recovered (kJ)	209,000	209,000
Energy loss (kJ)	41,800	41,800
Energy efficiency (%)	83.3	83.3
<i>Exergy parameters</i>		
Exergy input (kJ)	26,157	26,157
Exergy recovered (kJ)	6,977	19,050
Exergy loss (kJ)	19,180	7,107
Exergy efficiency (%)	26.7	72.8

### Comparative Summary

The two cases are summarized and compared in Table 6.5. Although the same quantity of energy is discharged for Cases A and B, a greater quantity of exergy is discharged for Case B. In addition, Case B stores the energy and exergy for a greater duration of time.

### 6.4.7 Closure

This section demonstrates the application of exergy analysis to closed TES systems. The use of exergy analysis clearly takes into account the external and temperature losses in TES operations, and hence it more correctly reflects their thermodynamic behavior. Exergy and energy analyses do not quantitatively assess the value associated with the length of time the heat is held in storage, so this factor must be considered separately. Other TES types are considered in subsequent sections.

## 6.5 Appropriate Efficiency Measures for Closed TES Systems

Generally accepted standards have not been established for TES evaluation and comparison for at least two reasons. First, many different but valid efficiency measures can be defined. As shown in Table 6.3, for example, TES energy efficiency can be defined as the ratio of energy recovered to energy input, or as the ratio of energy recovered and remaining in a TES to energy input and originally in the TES; both definitions are reasonable but can yield different values in some circumstances. Secondly, while most TES efficiency definitions are based on energy, more meaningful efficiencies can be defined based on exergy, which takes into account temperature level (and hence quality) of the energy transferred.

In this section, several categories of TES energy and exergy efficiencies are discussed, following an earlier analysis (Rosen, 1992b). The overall storage process and the charging, storing, and discharging subprocesses are considered. An illustrative example is presented. This section is an extension of the previous one where a limited set of TES efficiencies are considered and helps determine which efficiencies are most appropriate in different circumstances.

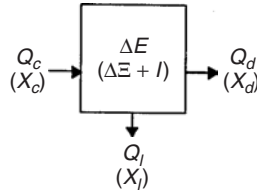


**Figure 6.5** The overall heat storage process, showing energy parameters (terms not in parentheses) and exergy parameters (terms in parentheses)

### 6.5.1 TES Model Considered

As in Section 6.4, a simple TES model is considered, which undergoes a storage process (Figure 6.5) involving distinct charging, storing, and discharging periods (Figure 6.6). The model is described in Section 6.4.1. Heat is transferred at specified temperatures to and from the TES. For simplicity, only the net thermal energy and thermal exergy transfers associated with material flows are considered here, rather than the energy and exergy values of the material flows themselves.

### 6.5.2 Energy and Exergy Balances

Energy and exergy balances for the overall storage process (Figure 6.5) can be expressed, following Equations 6.37 and 6.40, respectively, as

$$Q_c - (Q_d + Q_l) = \Delta E \tag{6.74}$$

$$X_c - (X_d + X_l) - I = \Delta \Xi \tag{6.75}$$

where  $Q_c$ ,  $Q_d$ , and  $Q_l$  denote respectively the heat input during charging, recovered during discharging, and lost during the entire process; and  $X_c$ ,  $X_d$ , and  $X_l$  denote respectively the exergy transfers associated with  $Q_c$ ,  $Q_d$ , and  $Q_l$ . For the case of a complete cycle (i.e., a process with identical initial and final states),  $\Delta E = \Delta \Xi = 0$ . The exergy  $\Xi$  can be written with Equation 6.18 which, for a tank of constant volume and a working fluid that behaves ideally, becomes

$$\Xi = mc_v[(T - T_o) - T_o \ln(T/T_o)] \tag{6.76}$$

where  $T$ ,  $c_v$ , and  $m$  respectively denote for the TES temperature, specific heat at constant volume, and mass. The terms  $Q_l$ ,  $X_l$ ,  $I$ ,  $\Delta E$ , and  $\Delta \Xi$  can be written in terms of subprocess values as in Equations 6.39, 6.42, 6.70, and 6.71, respectively.

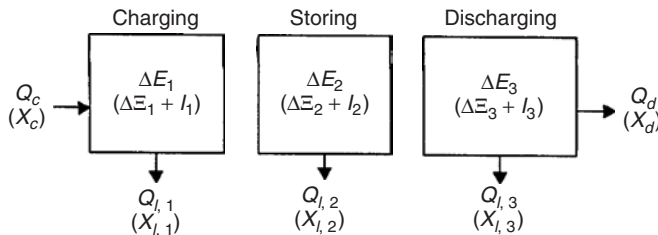


**Figure 6.6** The three periods in the overall heat storage process (charging, storing, and discharging), showing energy parameters (not in parentheses) and the exergy parameters (in parentheses)

Energy and exergy balances, respectively, can be written for the charging period as in Equations 6.50a (with  $Q_c$  replacing  $H_a - H_b$ ) and 6.53 (with  $X_c$  replacing  $\epsilon_a - \epsilon_b$ ), for the storing period as in Equations 6.56a and 6.59a, and for the discharging period as in Equations 6.62a (with  $Q_d$  replacing  $H_d - H_c$ ) and 6.65a (with  $X_d$  replacing  $\epsilon_d - \epsilon_c$ ).

By introducing the definition  $E' \equiv E - E_o$ , where  $E'$  represents the TES energy content, Equations 6.70 and 6.72 can be written as

$$\Delta E = (E_f - E_o) - (E_i - E_o) = E'_f - E'_i \quad (6.70a)$$

$$\Delta E_j = (E_{f,j} - E_o) - (E_{i,j} - E_o) = E'_{f,j} - E'_{i,j} \quad (6.72a)$$

The terms  $\Xi$  and  $E'$  are analogous (e.g., both are equal to zero at the dead state, i.e.,  $\Xi_o = E'_o = 0$ ).

### 6.5.3 Energy and Exergy Efficiencies

Since several quantities can be considered to be products and inputs for TES systems, various efficiency definitions are possible. For each subprocess and the overall storage process, energy and exergy efficiencies are evaluated here based on the quantities of heat transferred to and from a TES, the temperatures at which the heat transfers occur, and the initial and final TES states. Furthermore, for each energy and exergy efficiency, four cases are considered (where possible). The initial energy or exergy in the store is neglected in Cases *A* and *B*, and accounted for in Cases *C* and *D*, while the net accumulation of energy or exergy in the store is treated as a loss for Cases *A* and *C*, and as a product for Cases *B* and *D*. Here, efficiency cases are denoted by superscripts and, following the notation introduced earlier, efficiencies with subscripts denote period efficiencies while efficiencies without subscripts denote overall efficiencies. Other efficiency cases are possible but not considered here.

### 6.5.4 Overall Efficiencies

The following four overall energy efficiency  $\eta$  definitions are considered:

$$\eta^A = \frac{\text{Energy recovered}}{\text{Energy input}} = 1 - \frac{\text{Energy loss} + \text{Energy accumulation}}{\text{Energy input}}$$

$$\eta^A = \frac{Q_d}{Q_c} = 1 - \frac{Q_l + \Delta E}{Q_c} \quad (6.77)$$

$$\eta^B = \frac{\text{Energy recovered} + \text{Energy accumulation}}{\text{Energy input}} = 1 - \frac{\text{Energy loss}}{\text{Energy input}}$$

$$\eta^B = \frac{Q_d + \Delta E}{Q_c} = 1 - \frac{Q_l}{Q_c} \quad (6.77a)$$

$$\eta^C = \frac{\text{Energy recovered}}{\text{Energy input} + \text{Initial energy in store}} = 1 - \frac{\text{Energy loss} + \text{Final energy in store}}{\text{Energy input} + \text{Initial energy in store}}$$

$$\eta^C = \frac{Q_d}{Q_c + E'_i} = 1 - \frac{Q_l + E'_f}{Q_c + E'_i} \quad (6.77b)$$

$$\eta^D = \frac{\text{Energy recovered} + \text{Final energy in store}}{\text{Energy input} + \text{Initial energy in store}} = 1 - \frac{\text{Energy loss}}{\text{Energy input} + \text{Initial energy in store}}$$

$$\eta^D = \frac{Q_d + E'_f}{Q_c + E'_i} = 1 - \frac{Q_l}{Q_c + E'_i} \quad (6.77c)$$

Four overall exergy efficiencies, analogous to those in Equations 6.77–6.77c, respectively, are defined:

$$\psi^A = \frac{X_d}{X_c} = 1 - \frac{X_l + I + \Delta \Xi}{X_c} \quad (6.78)$$

$$\psi^B = \frac{X_d + \Delta \Xi}{X_c} = 1 - \frac{X_l + I}{X_c} \quad (6.78a)$$

$$\psi^C = \frac{X_d}{X_c + \Xi_i} = 1 - \frac{X_l + I + \Xi_f}{X_c + \Xi_i} \quad (6.78b)$$

$$\psi^D = \frac{X_d + \Xi_f}{X_c + \Xi_i} = 1 - \frac{X_l + I}{X_c + \Xi_i} \quad (6.78c)$$

Note that  $\eta^A = \eta^B = \eta^C = \eta^D$  if  $E'_i = E'_f = 0$ , and  $\psi^A = \psi^B = \psi^C = \psi^D$  if  $\Xi_i = \Xi_f = 0$ , while  $\eta^A = \eta^B$  if  $\Delta E = 0$ , and  $\psi^A = \psi^B$  if  $\Delta \Xi = 0$ . Also, if  $\Delta E < 0$  and  $\Delta \Xi < 0$ , the definitions for Cases *A* and *B* do not provide rational measures of performance for normal applications, while those for Cases *C* and *D* do. Furthermore, if the store is adiabatic,  $Q_{l,j} = X_{l,j} = 0$ , and all the efficiencies simplify (e.g., the energy efficiencies in Equations 6.77a and c become 100%).

### 6.5.5 Charging-Period Efficiencies

The following two energy efficiency definitions for the charging period are considered:

$$\eta_1^B = \frac{\text{Energy accumulation}}{\text{Energy input}} = 1 - \frac{\text{Energy loss}}{\text{Energy input}}$$

$$\eta_1^B = \frac{\Delta E_1}{Q_c} = 1 - \frac{Q_{l,1}}{Q_c} \quad (6.79)$$

$$\eta_1^D = \frac{\text{Final energy in store}}{\text{Energy input} + \text{Initial energy in store}} = 1 - \frac{\text{Energy loss}}{\text{Energy input} + \text{Initial energy in store}}$$

$$\eta_1^D = \frac{E'_{f,1}}{Q_c + E'_{i,1}} = 1 - \frac{Q_{l,1}}{Q_c + E'_{i,1}} \quad (6.79a)$$

Two analogous exergy efficiencies are defined:

$$\psi_1^B = \frac{\Delta \Xi_1}{X_c} = 1 - \frac{X_{l,1} + I_1}{X_c} \quad (6.80)$$

$$\psi_1^D = \frac{\Xi_{F,1}}{X_c + \Xi_{I,1}} = 1 - \frac{X_{L,1} + I_1}{X_c + \Xi_{I,1}} \quad (6.80a)$$

Meaningful charging-period efficiencies cannot be defined for Cases *A* and *C*, since accumulations are treated as losses for these cases, resulting in the efficiencies reducing to zero.

### 6.5.6 Storing-Period Efficiencies

As for the charging period, only two sets of storing-period efficiencies can be defined. The two energy efficiencies are

$$\eta_2^B = \frac{\text{Energy accumulation during charging and storing}}{\text{Energy accumulation during charging}}$$

$$= 1 - \frac{\text{Energy loss during storing}}{\text{Energy accumulation during charging}}$$

$$\eta_2^B = \frac{\Delta E_1 + \Delta E_2}{\Delta E_1} = 1 - \frac{Q_{l,2}}{\Delta E_1} \quad (6.81)$$

$$\eta_2^D = \frac{\text{Final energy in store}}{\text{Initial energy in store}} = 1 - \frac{\text{Energy loss during storing}}{\text{Initial energy in store}}$$

$$\eta_2^D = \frac{E'_{f,2}}{E'_{i,2}} = 1 - \frac{Q_{l,2}}{E'_{i,2}} \quad (6.81a)$$

and the two corresponding exergy efficiencies are

$$\psi_2^B = \frac{\Delta \Xi_1 + \Delta \Xi_2}{\Delta \Xi_1} = 1 - \frac{X_{l,2} + I_2}{\Delta \Xi_1} \quad (6.82)$$

$$\psi_2^D = \frac{\Xi_{f,2}}{\Xi_{i,2}} = 1 - \frac{X_{l,2} + I_2}{\Xi_{i,2}} \quad (6.82a)$$

It can be shown that  $\eta_2^B = \eta_2^D$  if  $E'_{i,1} = 0$ , and  $\psi_2^B = \psi_2^D$  if  $\Xi_{i,1} = 0$ .

### 6.5.7 Discharging-Period Efficiencies

Four discharging-period energy efficiencies are considered:

$$\eta_3^A = \frac{Q_d}{\Delta E_1 + \Delta E_2} = 1 - \frac{\Delta E + Q_{l,3}}{\Delta E_1 + \Delta E_2} \quad (6.83)$$

where  $Q_d$  is energy recovered,  $\Delta E_1$  and  $\Delta E_2$  are energy accumulation during charging and storing,  $\Delta E$  is overall energy accumulation, and  $Q_{l,3}$  is energy loss.

$$\eta_3^B = \frac{Q_d + \Delta E}{\Delta E_1 + \Delta E_2} = 1 - \frac{Q_{l,3}}{\Delta E_1 + \Delta E_2} \quad (6.83a)$$

where  $Q_d$  is energy recovered,  $\Delta E_1$  and  $\Delta E_2$  are energy accumulation during charging and storing,  $\Delta E$  is overall energy accumulation, and  $Q_{l,3}$  is energy loss.

$$\eta_3^C = \frac{\text{Energy recovered}}{\text{Initial energy in store}} = 1 - \frac{\text{Final energy in store} + \text{Energy loss}}{\text{Initial energy in store}}$$

$$\eta_3^C = \frac{Q_d}{E'_{i,3}} = 1 - \frac{E'_{f,3} + Q_{l,3}}{E'_{i,3}} \quad (6.83b)$$

$$\eta_3^D = \frac{\text{Energy recovered} + \text{Final energy in store}}{\text{Initial energy in store}} = 1 - \frac{\text{Energy loss}}{\text{Initial energy in store}}$$

$$\eta_3^D = \frac{Q_d + E'_{f,3}}{E'_{i,3}} = 1 - \frac{Q_{l,3}}{E'_{i,3}} \quad (6.83c)$$

Four analogous exergy efficiencies are defined:

$$\psi_3^A = \frac{X_d}{\Delta \Xi_1 + \Delta \Xi_2} = 1 - \frac{\Delta \Xi + X_{l,3} + I_3}{\Delta \Xi_1 + \Delta \Xi_2} \quad (6.84)$$

$$\psi_3^B = \frac{X_d + \Delta \Xi}{\Delta \Xi_1 + \Delta \Xi_2} = 1 - \frac{X_{l,3} + I_3}{\Delta \Xi_1 + \Delta \Xi_2} \quad (6.84a)$$

$$\psi_3^C = \frac{X_d}{\Xi_{i,3}} = 1 - \frac{X_{l,3} + I_3 + \Xi_{f,3}}{\Xi_{i,3}} \quad (6.84b)$$

$$\psi_3^D = \frac{X_d + \Xi_{f,3}}{\Xi_{i,3}} = 1 - \frac{X_{l,3} + I_3}{\Xi_{i,3}} \quad (6.84c)$$

### 6.5.8 Summary of Efficiency Definitions

The efficiency definitions in the four preceding subsections are summarized in Table 6.6. Although all the efficiencies are useful in specific applications, the choice of definition depends on the specific application and the aspect of performance considered critical. Many of the efficiencies discussed here are applied in practice and some are used in Section 6.4, but with  $Q_c$  (or  $X_c$ ) given as the difference between the total enthalpy (or exergy) of the fluid passing into and out of the store during charging, and  $Q_d$  (or  $X_d$ ) as the corresponding difference during discharging.

For the assumptions considered in this section, it can be shown for Cases *B* and *D* that the overall efficiency is the product of the three corresponding subprocess efficiencies, that is,

$$\eta^B = \prod_{j=1}^3 \eta_j^B \quad (6.85)$$

$$\eta^D = \prod_{j=1}^3 \eta_j^D \quad (6.86)$$

$$\psi^B = \prod_{j=1}^3 \psi_j^B \quad (6.87)$$

$$\psi^D = \prod_{j=1}^3 \psi_j^D \quad (6.88)$$

**Table 6.6** Summary of possible efficiency definitions for closed TES systems<sup>a</sup>

Period	Energy Efficiency, $\eta$			
	Case A	Case B	Case C	Case D
Overall	$\frac{Q_d}{Q_c}$	$\frac{Q_d + \Delta E}{Q_c}$	$\frac{Q_d}{Q_c + E'_i}$	$\frac{Q_d + E'_f}{Q_c + E'_i}$
Charging (1)	–	$\frac{\Delta E + 1}{Q_c}$	–	$\frac{E'_{f,1}}{Q_c + E'_{i,1}}$
Storing (2)	–	$\frac{\Delta E_1 + \Delta E_2}{\Delta E_1}$	–	$\frac{E'_{f,2}}{E'_{i,2}}$
Discharging (3)	$\frac{Q_d}{\Delta E_1 + \Delta E_2}$	$\frac{Q_d + \Delta E}{\Delta E_1 + \Delta E_2}$	$\frac{Q_d}{E'_{i,3}}$	$\frac{Q_d + E'_{f,3}}{E'_{i,3}}$
Period	Exergy Efficiency, $\psi$			
	Case A	Case B	Case C	Case D
Overall	$\frac{X_d}{X_c}$	$\frac{X_d + \Delta \Xi}{X_c}$	$\frac{X_d}{X_c + \Xi_i}$	$\frac{X_d + \Xi_f}{X_c + \Xi_i}$
Charging (1)	–	$\frac{\Delta \Xi_1}{X_c}$	–	$\frac{\Xi_{f,1}}{X_c + \Xi_{i,1}}$
Storing (2)	–	$\frac{\Delta \Xi_1 + \Delta \Xi_2}{\Delta \Xi_1}$	–	$\frac{\Xi_{f,2}}{\Xi_{i,2}}$
Discharging (3)	$\frac{X_d}{\Delta \Xi_1 + \Delta \Xi_2}$	$\frac{X_d + \Delta \Xi}{\Delta \Xi_1 + \Delta \Xi_2}$	$\frac{X_d}{\Xi_{i,3}}$	$\frac{X_d + \Xi_{f,3}}{\Xi_{i,3}}$

<sup>a</sup>Charging and storing efficiencies are not defined for Cases A and C. The cases listed across the top are denoted by superscripts, and the periods along the left side by subscripts (e.g., the lower left entry corresponds to  $\eta_3^A$  and the upper right entry to  $\psi^D$ ).

By noting the similarities between Cases *A* and *B* and between Cases *C* and *D*, it can also be shown that

$$\eta^A = \eta_1^B \eta_2^B \eta_3^A \quad (6.89)$$

$$\eta^C = \eta_1^D \eta_2^D \eta_3^C \quad (6.90)$$

$$\psi^A = \psi_1^B \psi_2^B \psi_3^A \quad (6.91)$$

$$\psi^C = \psi_1^D \psi_2^D \psi_3^C \quad (6.92)$$

### 6.5.9 Illustrative Example

#### Problem Statement

A TES that undergoes discrete charging, storing, and discharging processes is considered. Three modes of operation are considered and defined according to the sign of the energy and exergy accumulations during the overall storing process:

- I.  $\Delta E > 0$  and  $\Delta \Xi > 0$ ;
- II.  $\Delta E = \Delta E \Xi = 0$ , that is, a complete storage cycle; and
- III.  $\Delta E < 0$  and  $\Delta \Xi < 0$ .

For all modes of operation, and with values in kilojoules,  $Q_c = 100$ ,  $Q_{l,1} = Q_{l,3} = 5$ ,  $Q_{l,2} = 10$ ,  $E'_{i,1} = 20$ ,  $X_{l,j} = 0$  for all  $j$ ,  $\Xi_{i,1} = 1$ ,  $I_1 = 4$ , and  $I_2 = I_3 = 1$ . For modes I, II, and III, respectively,  $Q_d$  is 60, 80, and 100 kJ. Also,  $X_c = 0.1 \times Q_c$  and  $X_d = 0.05 \times Q_d$ . Note that the specification of the exergy parameters involves assumptions regarding the temperatures associated with the heat transfers  $Q_c$ ,  $Q_d$ , and  $Q_{l,j}$  (e.g., the fact that  $X_{l,j} = 0$  and  $Q_{l,j} \neq 0$  for all  $j$ , implies that heat transfers  $Q_{l,j}$  occur at the environmental temperature  $T_o$ ). The specified parameter values are chosen so as to represent a realistic but simple case.

#### Results and Discussion

Unknown parameter values are evaluated using the previously specified values and energy and exergy balances. Following the format of Figure 6.6, all relevant values are summarized illustratively in Figure 6.7 for energy parameters and in Figure 6.8 for exergy parameters. Since the charging and storing processes are identical for all three modes of operation, they are illustrated only once, while the discharging process is shown for each operation mode. Values for  $\Delta E$  and  $\Delta \Xi$  are not shown in Figures 6.7 and 6.8, but by substituting subprocess values for  $\Delta E_j$  and  $\Delta \Xi_j$  from Figures 6.7 and 6.8 into Equations 6.70 and 6.71, can be shown to be (in kJ) as follows:  $\Delta E = 20$  and  $\Delta \Xi = 1$  for mode of operation I,  $\Delta E = \Delta \Xi = 0$  for mode II, and  $\Delta E = -20$  and  $\Delta \Xi = -1$  for mode III. The exergy values associated with all heat transfers in Figure 6.8 are significantly less than the corresponding energy values in Figure 6.7, reflecting the fact that for most TES applications, the temperatures associated with all heat transfers are relatively low (between  $T_o$  and  $2T_o$ ). These values indicate that the usefulness of thermal energy transferred at a practical temperature is significantly less than an equal quantity of any work-equivalent energy form.

Efficiencies are evaluated according to the expressions in Table 6.6, and tabulated in the same format in the top, middle, and bottom sections of Table 6.7 for operation modes I, II, and III, respectively. The corresponding efficiencies for modes I to III are the same for charging and storing since these processes are independent of mode of operation. Several points are demonstrated in Table 6.7. First, all exergy efficiency values are less than the corresponding energy efficiency values, due to the degradation of temperature as heat is transferred and stored. Since this degradation is reflected in efficiencies based on exergy and not in those based on energy, exergy efficiencies are



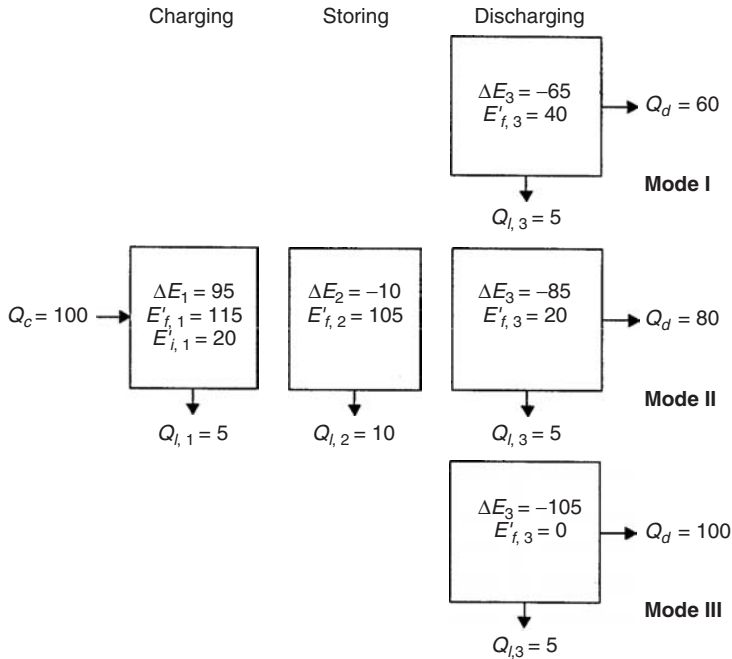


**Figure 6.7** Energy values (in kJ) for the example, showing the three modes of operation (I, II, and III) and the three storing periods (charging, storing, and discharging)

considered more meaningful. Second, for energy and exergy efficiencies for all periods, the values of the calculated efficiencies are different for Cases *A* to *D*. The achievement of consistent comparisons and evaluations of performance requires that care be exercised in selecting efficiency definitions. Third, some efficiency values are not meaningful because they are not based on rational measures of performance for the operation mode considered. For example, consider, for Case *A* and operation mode III, the overall energy efficiency ( $\eta^A = 100\%$ ), the discharging energy efficiency ( $\eta_3^A = 118\%$ ), and the discharging exergy efficiency ( $\psi_3^A = 100\%$ ). These efficiency values consider the percentage of the input energy or exergy that is discharged, but are not rational measures because they do not account for the fact that part of the discharged energy and exergy is attributable to energy and exergy in the TES before the charging process began. Thus, the efficiency definitions presented for Cases *B* to *D* are more meaningful for mode of operation III.

Several generalizations can be made for each of the three modes of operation with respect to the validity and meaningfulness of the efficiency definitions for the different cases. For mode I, the definitions for Cases *B* and *D* are preferred. The definitions for Cases *A* and *C*, although valid, can be misleading because they neglect the fact that some of the charging energy or exergy increases the internal energy or exergy of the TES. For mode II (the complete storage cycle), the definitions for all cases are valid and meaningful. For mode III, the definitions for Cases *B* and *D* are preferred. As discussed in the previous paragraph, the definition for Case *A* is not rational for mode III, while that for Case *C*, although valid, can be misleading.

### 6.5.10 Closure

Several key points are discussed in this section. First, many valid and meaningful TES efficiency definitions exist. Differences in definitions normally depend on which quantities are considered to

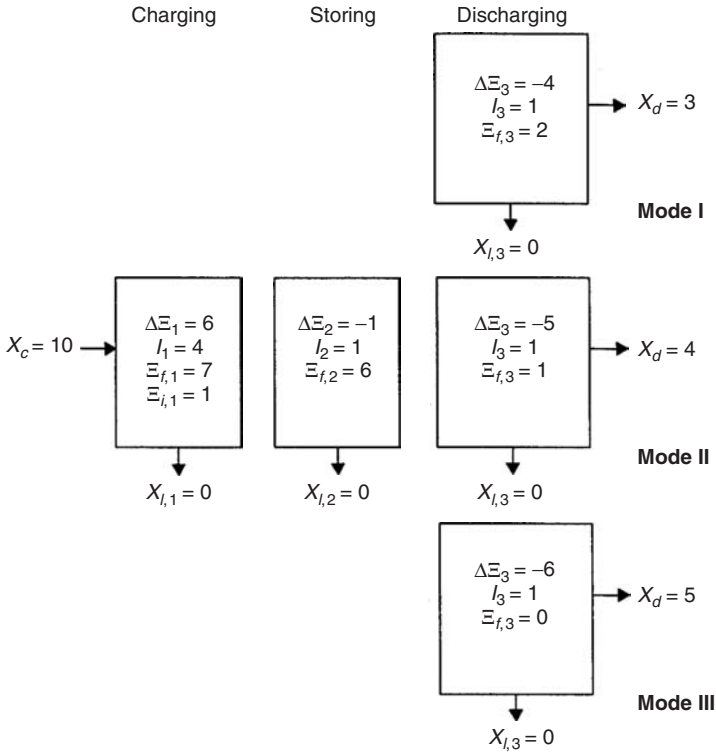


**Figure 6.8** Exergy values (in kJ) for the example, showing the three modes of operation and the three storing periods

**Table 6.7** Efficiency values (in %) for the illustrative example

Period	Energy efficiency, $\eta$				Exergy efficiency, $\psi$			
	A	B	C	D	A	B	C	D
<i>Mode of operation I</i>								
Overall	60	80	50	83	30	40	27	45
Charging (1)	–	95	–	96	–	60	–	64
Storing (2)	–	89	–	91	–	83	–	86
Discharging (3)	71	94	57	95	60	80	50	83
<i>Mode of operation II</i>								
Overall	80	80	67	83	40	40	36	45
Charging (1)	–	95	–	96	–	60	–	64
Storing (2)	–	89	–	91	–	83	–	86
Discharging (3)	94	94	76	95	80	80	67	83
<i>Mode of operation III</i>								
Overall	100	80	83	83	50	40	45	45
Charging (1)	–	95	–	96	–	60	–	64
Storing (2)	–	89	–	91	–	83	–	86
Discharging (3)	118	94	95	95	100	80	83	83

be products and inputs. Second, different efficiency definitions are appropriate in different situations and when different aspects of performance are being evaluated. Of course, efficiency comparisons for different TES systems are logical only if the efficiencies are based on common definitions. Third, exergy efficiencies, because they measure how nearly a system approaches ideal performance and account for the loss of temperature in TES systems, are generally more meaningful and illuminating than energy efficiencies, and may prove useful in establishing standards for TES evaluation and comparison.

## 6.6 Importance of Temperature in Performance Evaluations for Sensible TES Systems

Being energy-based, most existing TES evaluation measures disregard the temperatures associated with the heat injected into and recovered from a TES. Examining energy efficiencies alone can result in misleading conclusions because such efficiencies weight all thermal energy equally. Exergy efficiencies acknowledge that the usefulness of thermal energy depends on its quality, which is related to its temperature level, and are therefore more suitable for determining how advantageous is one TES relative to another.

This section discusses the importance of temperature in TES performance evaluations, following an earlier report (Rosen, 1991). The energy and exergy efficiencies for a simple sensible TES system are compared and the differences between them highlighted. It is demonstrated that exergy analysis weights the usefulness of thermal energy appropriately, while energy analysis tends to present overly optimistic views of TES performance by neglecting the temperature levels associated with thermal energy flows. The concepts are illustrated by examining several TES systems.

### 6.6.1 Energy, Entropy, and Exergy Balances for the TES System

Consider a process involving only heat interactions and occurring in a closed system for which the state is the same at the beginning and end of the process. Balances of energy and exergy, respectively, can be written for the system using Equations 6.3b and 6.5b as follows:

$$\sum_r Q_r = 0 \quad (6.93)$$

$$\sum_r X_r - I = 0 \quad (6.94)$$

where  $I$  denotes the exergy consumption, and  $X_r$  denotes the exergy associated with  $Q_r$ , the heat transferred into the system across region  $r$  at temperature  $T_r$ . Note that the exergetic temperature factor  $\tau$  is illustrated as a function of the temperature ratio  $T/T_o$  in Figure 6.1, and these parameters are compared with the temperature  $T$  in Table 6.8 for above-environmental temperatures (i.e., for  $T \geq T_o$ ), the temperature range of interest for most heat storages.

### 6.6.2 TES System Model Considered

Consider the overall storage process for the general TES system shown in Figure 6.9. Heat  $Q_c$  is injected into the system at a constant temperature  $T_c$  during a charging period. After a storing period, heat  $Q_d$  is recovered at a constant temperature  $T_d$  during a discharging period. During all periods, heat  $Q_l$  leaks from the system at a constant temperature  $T_l$  and is lost to the surroundings.

For normal heating applications, the temperatures  $T_c$ ,  $T_d$ , and  $T_l$  exceed the environment temperature  $T_o$ , but the discharging temperature cannot exceed the charging temperature. Hence, the exergetic temperature factors for the charged and discharged heat are subject to the constraint  $0 \leq \tau_d \leq \tau_c \leq 1$ .

**Table 6.8** Relation between several temperature parameters for above-environment temperatures<sup>a</sup>

$T/T_o$	$T$ (K)	$\tau$
1.00	283	0.00
1.25	354	0.20
1.50	425	0.33
2.00	566	0.50
3.00	849	0.67
5.00	1415	0.80
10.00	2830	0.90
100.00	28,300	0.99
Infinity	Infinity	1.00

<sup>a</sup>The reference-environment temperature is  $T_o = 10\text{ }^\circ\text{C} = 283\text{ K}$ .

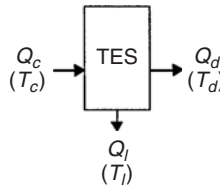


**Figure 6.9** The overall heat storage process for a general TES system. Shown are heat flows and associated temperatures at the TES boundary (terms in parentheses). The corresponding energy and exergy parameters are shown for this system in Figure 6.5

### 6.6.3 Analysis

The energy and exergy balances in Equations 6.93 and 6.94, respectively, can be written for the modeled system as

$$Q_c = Q_d + Q_l \tag{6.93a}$$

and

$$X_c = X_d + X_l + I \tag{6.94a}$$

With Equation 6.25a, the exergy balance can be expressed as

$$Q_c \tau_c = Q_d \tau_d + Q_l \tau_l + I \tag{6.94b}$$

Following the general energy and exergy efficiency statements in Equations 6.32 and 6.33, the energy efficiency can be written for the modeled system as

$$\eta = \frac{Q_d}{Q_c} \tag{6.95}$$

and the exergy efficiency (with Equations 6.25a and 6.95) as

$$\psi = \frac{X_d}{X_c} = \frac{Q_d \tau_d}{Q_c \tau_c} = \frac{\tau_d}{\tau_c} \eta \tag{6.96}$$

### 6.6.4 Comparison of Energy and Exergy Efficiencies

An illuminating parameter for comparing the efficiencies is the ratio  $\psi/\eta$ . For the general TES system above, Equation 6.96 implies that the energy-efficiency-to-exergy-efficiency ratio can be expressed as

$$\frac{\psi}{\eta} = \frac{\tau_d}{\tau_c} \quad (6.97)$$

With Equation 6.25a, Equation 6.97 can be alternatively expressed as

$$\frac{\psi}{\eta} = \frac{(T_d - T_o)T_c}{(T_c - T_o)T_d} \quad (6.97a)$$

The ratio  $\psi/\eta$  is plotted against  $\tau_d$  for several values of  $\tau_c$  in Figure 6.10. It is seen that  $\psi/\eta$  varies linearly with  $\tau_d$  for a given value of  $\tau_c$ . Also, if the product heat is delivered at the charging temperature (i.e.,  $\tau_d = \tau_c$ ),  $\psi = \eta$ , while if the product heat is delivered at the temperature of the environment (i.e.,  $\tau_d = 0$ ),  $\psi = 0$  regardless of the charging temperature. In the first case, there is no loss of temperature during the entire storage process, while in the second there is complete loss of temperature. The largest deviation between values of  $\psi$  and  $\eta$  occurs in the second case.

The deviation between  $\psi$  and  $\eta$  is significant for most present day TES systems. This can be seen by noting that (i) most TES systems operate between charging temperatures as high as  $T_c = 130^\circ\text{C}$  and discharging temperatures as low as  $T_d = 40^\circ\text{C}$ , and (ii) a difference of about  $30^\circ\text{C}$  between charging and discharging temperatures is utilized in most TES systems (i.e.,  $T_c - T_d = 30^\circ\text{C}$ ). With Equation 6.26 and  $T_o = 10^\circ\text{C}$ , the first condition can be shown to imply for most present day systems that  $0.1 \leq \tau_d \leq \tau_c \leq 0.3$ . Since it can be shown with Equation 6.26 that

$$\tau_c - \tau_d = \frac{(T_c - T_d)T_o}{T_c T_d} \quad (6.98)$$

the difference in exergetic temperature factor varies roughly between 0.06 and 0.08. Then the value of the exergy efficiency is nearly 50–80% of that of the energy efficiency.

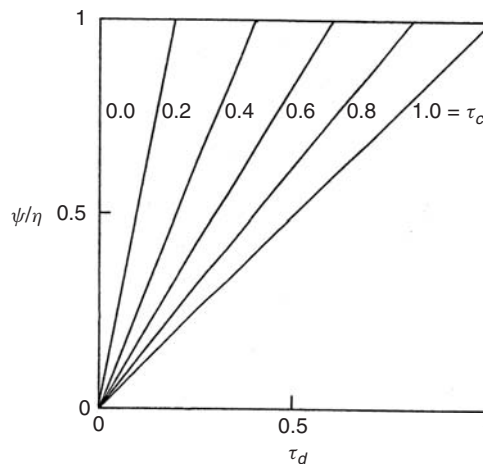


**Figure 6.10** Energy-efficiency-to-exergy-efficiency ratio,  $\psi/\eta$ , as a function of the discharging exergetic temperature factor  $\tau_d$ , for several values of the charging exergetic temperature factor  $\tau_c$

**Table 6.9** Values of the ratio  $\psi/\eta$  for a range of practical values for  $T_d$  and  $T_c$ <sup>a</sup>

Discharging temperature, $T_d$ (°C)	Charging temperature, $T_c$ (°C)			
	40	70	100	130
40	1.00	0.55	0.40	0.32
70	–	1.00	0.72	0.59
100	–	–	1.00	0.81
130	–	–	–	1.00

<sup>a</sup>The reference-environment temperature is  $T_o = 10$  °C = 283 K.

### 6.6.5 Illustration

The ratio  $\psi/\eta$  is illustrated in Table 6.9 for a simple TES having charging and discharging temperatures ranging between 40 °C and 130 °C, and a reference-environment temperature of  $T_o = 10$  °C. The energy and exergy efficiencies differ (with the exergy efficiency always being the lesser of the two) when  $T_d < T_c$ , and the difference becomes more significant as the difference between  $T_c$  and  $T_d$  increases. The efficiencies are equal only when the charging and discharging temperatures are equal (i.e.,  $T_d = T_c$ ), and no values of the ratio  $\psi/\eta$  are reported for the cases when  $T_c < T_d$ , since such situations are not physically possible. Unlike the exergy efficiencies, the energy efficiencies tend to appear overly optimistic, in that they only account for losses attributable to heat leakages but ignore temperature degradation.

### 6.6.6 Closure

This section demonstrates the importance of temperature in TES performance evaluations. Exergy efficiencies are seen to be more illuminating than energy efficiencies because they weight heat flows appropriately, being sensitive to both the fraction of the heat injected into a TES that is recovered and the temperature at which heat is recovered relative to the temperature at which it is injected. Energy efficiencies are only sensitive to the first of the above factors. TES energy efficiencies are good approximations to exergy efficiencies when there is little temperature degradation, as thermal energy quantities then have similar qualities. In most practical situations, however, thermal energy is injected and recovered at significantly different temperatures, making energy efficiencies both poor approximations to exergy efficiencies and prone to lead to erroneous interpretations and conclusions.

## 6.7 Exergy Analysis of Aquifer TES Systems

Underground aquifers are the storage type considered in this section (Jenne, 1992). The storage medium in many aquifer thermal energy storage (ATES) systems remains in a single phase during the storing cycle, so that temperature changes are exhibited in the store as thermal energy is added or removed. To assess ATES systems and to integrate them into larger thermal systems properly, their characteristics must be accurately expressed. As for TES systems, standards have not been established for evaluating and comparing the performance of different ATES systems, and conventional energy-based performance measures are often misleading. Exergy methods are advantageous in this regard.

In this section, the application of exergy analysis to ATES systems is described, following a previous assessment (Rosen, 1999b). For an elementary ATES model, expressions are presented for the

injected and recovered quantities of energy and exergy and for efficiencies. The impact is examined of introducing a threshold temperature below which residual heat remaining in the aquifer water is not considered worth recovering. ATES exergy efficiencies are demonstrated to be more useful and meaningful than energy efficiencies because the former account for the temperatures associated with thermal energy transfers and consequently assess how nearly ATES systems approach ideal thermodynamic performance. ATES energy efficiencies do not provide a measure of approach to ideal performance and, in fact, are often misleadingly high because some of the thermal energy can be recovered at temperatures too low for useful purposes. A case study using realistic ATES parameter values is presented.

### 6.7.1 ATES Model

Charging of the ATES occurs over a finite time period  $t_c$  and after a holding interval discharging occurs over a period  $t_d$ . The working fluid is water, having a constant specific heat  $c$ , and assumed incompressible. The temperature of the aquifer and its surroundings prior to heat injection is  $T_o$ , the reference-environment temperature. Only heat stored at temperatures above  $T_o$  is considered, and pump work is neglected.

#### Charging and Discharging

During charging, heated water at a constant temperature  $T_c$  is injected at a constant mass flow rate  $\dot{m}_c$  into the ATES. Then, after a storing period, discharging occurs, during which water is extracted from the ATES at a constant mass flow rate  $\dot{m}_d$ . The fluid discharge temperature is taken to be a function of time, that is,  $T_d = T_d(t)$ . The discharge temperature after an infinite time is taken to be the temperature of the reference-environment, that is,  $T_d(\infty) = T_o$ , and the initial discharge temperature is taken to be between the charging and reference-environment temperatures, that is,  $T_o \leq T_d(0) \leq T_c$ .

Many discharge temperature–time profiles are possible. The discharge temperature may be taken to decrease linearly with time from an initial value  $T_d(0)$  to a final value  $T_o$ . The final temperature is reached at a time  $t_f$  and remains fixed at  $T_o$  for all subsequent times, that is,

$$T_d(t) = \begin{cases} T_d(0) - (T_d(0) - T_o)t/t_f, & 0 \leq t \leq t_f \\ T_o, & t_f \leq t \leq \infty \end{cases} \quad (6.99)$$

Alternatively, the discharge temperature can be expressed as

$$T_d(t) = T_o + (T_d(0) - T_o)e^{-\alpha t} \quad (6.99a)$$

Here, the discharge temperature decreases with time asymptotically toward the environment temperature  $T_o$ , at a rate controlled by the arbitrary constant  $\alpha$ . Of course, these and other models of discharging temperature–time profiles are simply elementary representations of events that are often more complicated in actual devices.

The simple linear discharge temperature–time profile (Equation 6.99) is used here because, for the purposes of this section, most of the other possible discharge temperature–time profiles are inconveniently complex mathematically. The linear profile is sufficiently realistic and simple to illustrate the importance of using exergy analysis in ATES evaluation and comparison, without obscuring the central ideas of the section. The temperature–time profiles considered in the present model for the fluid flows during the charging and discharging periods are summarized in Figure 6.11.

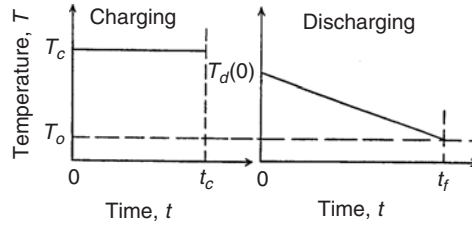


**Figure 6.11** Temperature–time profiles assumed for the charging and discharging periods in the ATES model considered

### Thermodynamic Losses

The two main types of thermodynamic losses that occur in ATES systems are accounted for in the model:

- **Energy losses.** Energy injected into an ATES that is not recovered is considered lost. Thus, energy losses include energy remaining in the ATES at a point where it could still be recovered if pumping were continued, and energy injected into the ATES that is convected in a water flow or is transferred by conduction far enough from the discharge point that it is unrecoverable, regardless of how much or how long water is pumped out of the ATES. The effect of energy losses is that less than 100% of the injected energy is recoverable after storage.
- **Mixing losses.** As heated water is pumped into an ATES, it mixes with the water already present (which is usually cooler), resulting in the recovered water being at a lower temperature than the injected water. In the present model, this loss results in the discharge temperature  $T_d$  being at all times less than or equal to the charging temperature  $T_c$ , but not below the reference-environment temperature  $T_o$  (i.e.,  $T_o \leq T_d(t) \leq T_c$  for  $0 \leq t \leq \infty$ ).

### 6.7.2 Energy and Exergy Analyses

To perform energy and exergy analyses of ATES systems, the quantities of energy and exergy injected during charging and recovered during discharging must be evaluated. The energy flow associated with a flow of liquid at a constant mass flow rate  $\dot{m}$ , for an arbitrary period of time with  $T$  a function of  $t$ , is

$$E = \int_t \dot{E}(t) dt \quad (6.100)$$

where the integration is performed over the time period, and the energy flow rate at time  $t$  is

$$\dot{E}(t) = \dot{m}c(T(t) - T_o) \quad (6.101)$$

Here  $c$  denotes the specific heat of the liquid. Combining Equations 6.100 and 6.101 for constant  $\dot{m}$ ,  $c$ , and  $T_o$ ,

$$E = \dot{m}c \int_t (T(t) - T_o) dt \quad (6.100a)$$

The corresponding exergy flow is

$$\epsilon = \int_t \dot{\epsilon}(t) dt \quad (6.102)$$



where the exergy flow rate at time  $t$  is

$$\dot{\epsilon}(t) = \dot{m}c[(T(t) - T_o) - T_o \ln(T(t)/T_o)] \quad (6.103)$$

Combining Equations 6.102 and 6.103, and utilizing Equation 6.100a,

$$\epsilon = \dot{m}c \int_t [(T(t) - T_o) - T_o \ln(T(t)/T_o)] dt = E - \dot{m}cT_o \int_t \ln(T(t)/T_o) dt \quad (6.102a)$$

### Charging

The energy input to the ATES during charging, for a constant water injection rate  $\dot{m}_c$  and over a time period beginning at zero and ending at  $t_c$ , is expressed by Equation 6.100a with  $T(t) = T_c$ . That is,

$$E_c = \dot{m}_c c \int_{t=0}^{t_c} (T_c - T_o) dt = \dot{m}_c c t_c (T_c - T_o) \quad (6.104)$$

The corresponding exergy input is expressed by Equation 6.102a, with the same conditions as for  $E_c$ . Thus, after integration,

$$\epsilon_c = \dot{m}_c c t_c [(T_c - T_o) - T_o \ln(T_c/T_o)] = E_c - \dot{m}_c c t_c T_o \ln(T_c/T_o) \quad (6.105)$$

### Discharging

The energy recovered from the ATES during discharging, for a constant water recovery rate  $\dot{m}_d$  and for a time period starting at zero and ending at  $t_d$ , is expressed by Equation 6.100a with  $T(t)$  as in Equation 6.99. Thus,

$$E_d = \dot{m}_d c \int_{t=0}^{t_d} (T_d(t) - T_o) dt = \dot{m}_d c [T_d(0) - T_o] \theta (2t_f - \theta) / (2t_f) \quad (6.106)$$

where

$$\theta = \begin{cases} t_d, & 0 \leq t_d \leq t_f \\ t_f, & t_f \leq t_d \leq \infty \end{cases} \quad (6.107)$$

The corresponding exergy recovered is expressed by Equation 6.102a, with the same conditions as for  $E_d$ . Thus,

$$\epsilon_d = \dot{m}_d c \int_{t=0}^{t_d} [(T_d(t) - T_o) - T_o \ln(T_d(t)/T_o)] dt = E_d - \dot{m}_d c T_o \int_{t=0}^{t_d} \ln(T_d(t)/T_o) dt \quad (6.108)$$

Here,

$$\int_{t=0}^{t_d} \ln(T_d(t)/T_o) dt = \int_{t=0}^{t_d} \ln(at + b) dt = [(a\theta + b)/a] \ln(a\theta + b) - \theta - (b/a) \ln b \quad (6.109)$$

where

$$a = [T_o - T_d(0)] / (T_o t_f) \quad (6.110)$$

$$b = T_d(0) / T_o \quad (6.111)$$

When  $t_d \geq t_f$ , the expression for the integral in Equation 6.109 reduces to

$$\int_{t=0}^{t_d} \ln(T_d(t)/T_o) dt = t_f \left[ \frac{T_d(0)}{T_d(0) - T_o} \ln \frac{T_d(0)}{T_o} - 1 \right] \quad (6.109a)$$

### Energy and Exergy Balances

An ATES energy balance taken over a complete charging–discharging cycle states that the energy injected is either recovered or lost. A corresponding exergy balance states that the exergy injected is either recovered or lost, where lost exergy is associated with both waste exergy emissions and internal exergy consumptions due to irreversibilities.

If  $f$  is defined as the fraction of injected energy  $E_c$  that can be recovered if the length of the discharge period approaches infinity (i.e., water is extracted until all recoverable energy has been recovered), then

$$E_d(t_d \rightarrow \infty) = fE_c \quad (6.112)$$

It follows from the energy balance that  $(1 - f)E_c$  is the energy irreversibly lost from the ATES. Clearly,  $f$  varies between zero for a thermodynamically worthless ATES and unity for an ATES having no energy losses during an infinite discharge period. (Note that even if  $f = 1$ , the ATES can still have mixing losses that reduce the temperature of the recovered water and consequently cause exergy losses.) Since  $E_c$  is given by Equation 6.104 and  $E_d(t_d \rightarrow \infty)$  by Equation 6.106 with  $\theta = t_f$ , Equation 6.112 may be rewritten as

$$\dot{m}_d c (T_d(0) - T_o) t_f / 2 = f \dot{m}_c c (T_c - T_o) t_c \quad (6.112a)$$

or, after rearranging,

$$f = \frac{t_f \dot{m}_d (T_d(0) - T_o)}{2 t_c \dot{m}_c (T_c - T_o)} \quad (6.112b)$$

Since  $T_d(0)$  can vary from  $T_o$  to  $T_c$ , the temperature-related term  $(T_d(0) - T_o)/(T_c - T_o)$ , like  $f$ , varies between zero and unity. The time ratio  $t_f/t_c$  and mass flow rate ratio  $\dot{m}_d/\dot{m}_c$  can both take on any positive values, subject to the above equality.

### Efficiencies and Losses

For either energy or exergy, efficiency is defined as the fraction, taken over a complete cycle, of the quantity input during charging that is recovered during discharging, while loss is the difference between input and recovered amounts of the quantity. Hence, the energy loss as a function of the discharge time period is given by  $[E_c - E_d(t_d)]$ , while the corresponding exergy loss is given by  $[\epsilon_c - \epsilon_d(t_d)]$ . It is emphasized that energy losses do not reflect the temperature degradation associated with mixing, while exergy losses do.

The energy efficiency  $\eta$  for an ATES, as a function of the discharge time period, is

$$\eta(t_d) = \frac{E_d(t_d)}{E_c} = \frac{\dot{m}_d (T_d(0) - T_o)}{\dot{m}_c (T_c - T_o)} \frac{\theta(2t_f - \theta)}{2t_f t_c} \quad (6.113)$$

and the corresponding exergy efficiency  $\psi$  by

$$\psi(t_d) = \epsilon_d(t_d) / \epsilon_c \quad (6.114)$$

Note that the energy efficiency in Equation 6.113 simplifies when the discharge period  $t_d$  exceeds  $t_f$ , that is,  $\eta(t_d \geq t_f) = f$ . Thus, for an ATES in which all injected energy is recoverable during an infinite discharge period, that is,  $f = 1$ , the energy efficiency can reach 100% if the discharge period  $t_d$  is made long enough. The corresponding exergy efficiency, however, remains less than 100% because due to mixing losses, much of the heat is recovered at near-environmental temperatures. Only a thermodynamically reversible storage, which would never be an objective since such other factors as economics must be considered, would permit the achievement of an exergy efficiency of 100%.

### 6.7.3 Effect of a Threshold Temperature

In practice, it is not economically feasible to continue the discharge period until as much recoverable heat as possible is recovered. As the discharge period increases, water is recovered from an ATES at ever-decreasing temperatures (ultimately approaching the reference-environment temperature  $T_o$ ), and the energy in the recovered water is of decreasing usefulness. Exergy analysis reflects this phenomenon, as the magnitude of the recovered exergy decreases as the recovery temperature decreases. To determine the appropriate discharge period, a threshold temperature  $T_i$  is often introduced, below which the residual energy in the aquifer water is not considered worth recovering from an ATES. For the linear temperature–time relation used here (see Equation 6.99), it is clear that no thermal energy could be recovered over a cycle if the threshold temperature exceeds the initial discharge temperature, while the appropriate discharge period can be evaluated using Equation 6.99 with  $T_i$  replacing  $T_d(t)$  for the case where  $T_o \leq T_i \leq T_d(0)$ . Thus,

$$t_d = \begin{cases} \frac{T_d(0) - T_i}{T_d(0) - T_o} t_f, & T_o \leq T_i \leq T_d(0) \\ 0, & T_d(0) \leq T \end{cases} \quad (6.115)$$

The effect of a threshold temperature in practice, therefore, is to place an upper limit on the allowable discharge time period. Utilizing a threshold temperature usually has the effect of decreasing the difference between the corresponding energy and exergy efficiencies.

### 6.7.4 Case Study

#### Background

In this case study, experimental data are used from the first of four short-term ATES test cycles, using the Upper Cambrian Franconia–Ironton–Galesville confined aquifer. The test cycles were performed at the University of Minnesota's St. Paul campus from November 1982 to December 1983 (Hoyer *et al.*, 1985). During the test, water was pumped from the source well, heated in a heat exchanger, and returned to the aquifer through the storage well. After storage, energy was recovered by pumping the stored water through a heat exchanger and returning it to the supply well. The storage and supply wells are located 255 m apart.

For the test cycle considered here, the water temperature and volumetric flow rate vary with time during the injection and recovery processes as shown in Figure 6.12. The storage period duration (13 days) is also shown. Charging occurred during 5.24 days over a 17-day period. The water temperature and volumetric flow rate were approximately constant during charging, and had mean values of 89.4 °C and 18.4 l/s, respectively. Discharging also occurred over 5.24 days, approximately with a constant volumetric flow rate of water and linearly decreasing temperature with time. The mean volumetric flow rate during discharging was 18.1 l/s, and the initial discharge temperature was 77 °C, while the temperature after 5.24 days was 38 °C. The ambient temperature was reported to be 11 °C.

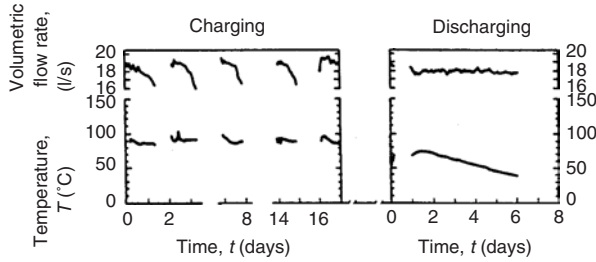


**Figure 6.12** Observed values for the temperature and volumetric flow rate of water, as a function of time during the charging and discharging periods, for the experimental test cycles used in the ATEs case study

### Assumptions and Simplifications

In subsequent calculations, mean values for volumetric flow rates and charging temperature are used. Also, the specific heat and density of water are both taken to be fixed, at  $4.2 \text{ kJ/kg K}$  and  $1000 \text{ kg/m}^3$ , respectively. Since the volumetric flow rate (in L/s) is equal to the mass flow rate (in kg/s) when the density is  $1000 \text{ kg/m}^3$ ,  $\dot{m}_c = 18.4 \text{ kg/s}$  and  $\dot{m}_d = 18.1 \text{ kg/s}$ . Also, the reference-environment temperature is fixed at the ambient temperature, that is,  $T_o = 11^\circ\text{C} = 284 \text{ K}$ .

### Analysis and Results

During charging, it can be shown using Equations 6.104 and 6.105, with  $t_c = 5.24 \text{ d} = 453,000 \text{ s}$  and  $T_c = 89.4^\circ\text{C} = 362.4 \text{ K}$ , that

$$E_c = (18.4 \text{ kg/s})(4.2 \text{ kJ/kg K})(453,000 \text{ s})(89.4^\circ\text{C} - 11^\circ\text{C}) = 2.74 \times 10^9 \text{ kJ}$$

and

$$\begin{aligned} \epsilon_c &= 2.74 \times 10^9 \text{ kJ} - (18.4 \text{ kg/s})(4.2 \text{ kJ/kg K})(453,000 \text{ s})(284 \text{ K}) \ln(362.4 \text{ K}/284 \text{ K}) \\ &= 0.32 \times 10^9 \text{ kJ} \end{aligned}$$

During discharging, the value of the time  $t_f$  is evaluated using the linear temperature–time relation of the present model and the observations that  $T_d(t = 5.24 \text{ d}) = 38^\circ\text{C}$  and  $T_d(0) = 77^\circ\text{C} = 350 \text{ K}$ . Then, using Equation 6.99 with  $t = 5.24 \text{ d}$ ,

$$38^\circ\text{C} = 77^\circ\text{C} - (77^\circ\text{C} - 11^\circ\text{C})(5.24 \text{ d}/t_f)$$

which can be solved to show that  $t_f = 8.87 \text{ d}$ . Thus, with the present linear model, the discharge water temperature would reach  $T_o$  if the discharge period was lengthened to almost 9 days. In reality, the rate of temperature decline would likely decrease, and the discharge temperature would asymptotically approach  $T_o$ .

The value of the fraction  $f$  can be evaluated with Equation 6.112b as

$$f = \frac{(8.87 \text{ d})(18.1 \text{ kg/s})(77^\circ\text{C} - 11^\circ\text{C})}{2(5.24 \text{ d})(18.4 \text{ kg/s})(89.4^\circ\text{C} - 11^\circ\text{C})} = 0.701$$

Thus, the maximum energy efficiency achievable is approximately 70%. With these values and Equations 6.110 and 6.111, it can be shown that

$$a = (11^\circ\text{C} - 77^\circ\text{C})/(284 \text{ K} \times 8.87 \text{ d}) = -0.0262/\text{d} \text{ and } b = (350 \text{ K})/(284 \text{ K}) = 1.232$$

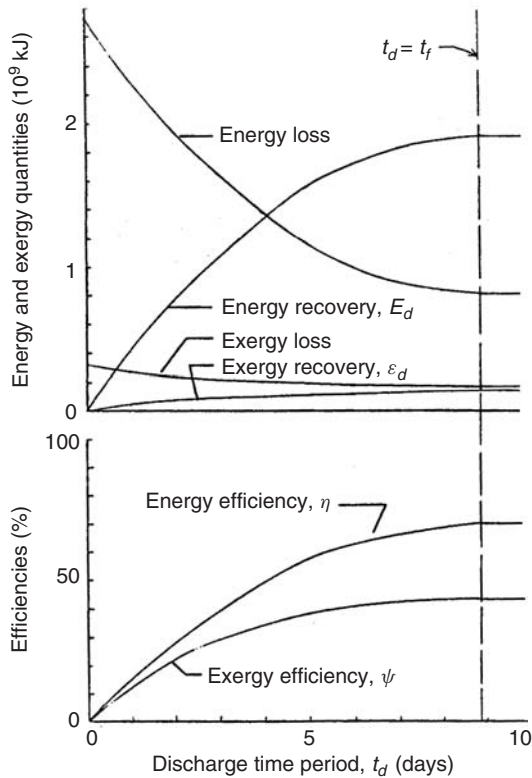


**Figure 6.13** Variation of several calculated energy and exergy quantities and efficiencies, as a function of discharge time period, for the ATEs case study

Consequently, expressions dependent on discharge time period  $t_d$  can be written and plotted (see Figure 6.13) for  $E_d$ ,  $\epsilon_d$ ,  $\eta$ , and  $\psi$  using Equations 6.106–6.111, 6.113, and 6.114, and for the energy loss ( $E_c - E_d$ ) and exergy loss ( $\epsilon_c - \epsilon_d$ ).

### Discussion

Both energy and exergy efficiencies in Figure 6.13 increase from zero to maximum values as  $t_d$  increases. Further, the difference between the two efficiencies increases with increasing  $t_d$ . This latter point demonstrates that the exergy efficiency gives less weight than the energy efficiency to the energy recovered at higher  $t_d$  values, since it is recovered at temperatures nearer to the reference-environment temperature.

Several other points in Figure 6.13 are worth noting. First, for the conditions specified, all parameters level off as  $t_d$  approaches  $t_f$ , and remain constant for  $t_d \geq t_f$ . Second, as  $t_d$  increases toward  $t_f$ , the energy recovered increases from zero to a maximum value, while the energy loss decreases from a maximum of all the input energy to a minimum (but nonzero) value. The exergy recovery and exergy loss functions behave similarly qualitatively, but exhibit much lower magnitudes.

**Importance of Temperature** The difference between energy and exergy efficiencies is due to temperature differences between the charging- and discharging-fluid flows. As the discharging time increases, the deviation between these two efficiencies increases (Figure 6.13) because the

temperature of recovered heat decreases (Figure 6.12). In this case, the energy efficiency reaches approximately 70% and the exergy efficiency 40% by the completion of the discharge period, even though the efficiencies are both 0% when discharging commences.

To further illustrate the importance of temperature, a hypothetical modification of the present case study is considered. In the modified case, all details are as in the original case except that the temperature of the injection flow during the charging period is increased from 89.4 °C to 200 °C (473 K), while the duration of the charging period is decreased from its initial value of 5.24 days (453,000 s) so that the energy injected does not change. By equating the energy injected during charging for the original and modified cases, the modified charging-period duration  $t'_c$  can be evaluated as a function of the new injection flow temperature  $T'_c$  as follows:

$$t'_c = t_c \frac{T_c - T_o}{T'_c - T_o} = (453,000 \text{ s}) \frac{(89.4^\circ \text{C} - 11^\circ \text{C})}{(200^\circ \text{C} - 11^\circ \text{C})} = 188,000 \text{ s}$$

The modified exergy input during charging can then be evaluated as

$$\begin{aligned} \epsilon'_c &= 2.74 \times 10^9 \text{ kJ} - (18.4 \text{ kg/s})(4.2 \text{ kJ/kg K})(188,000 \text{ s})(284 \text{ K}) \ln(473 \text{ K}/284 \text{ K}) \\ &= 0.64 \times 10^9 \text{ kJ} \end{aligned}$$

This value is double the exergy input during charging for the original case, so, since the discharging process remains unchanged in the modified case, the exergy efficiency (for any discharging time period) is half that for the original case. The altered value of exergy efficiency is entirely attributable to the new injection temperature, and occurs despite the fact that the energy efficiency remains unchanged.

**Effect of Threshold Temperature** If a threshold temperature is introduced and arbitrarily set at 38 °C (the actual temperature at the end of the experimental discharge period of 5.24 days), then the data in Figure 6.13 for  $t_d = 5.24 \text{ d}$  apply, and one can see that:

- the exergy recovered ( $0.127 \times 10^9 \text{ kJ}$ ) is almost all (91%) of the exergy recoverable in infinite time ( $0.139 \times 10^9 \text{ kJ}$ ), while the energy recovered ( $1.60 \times 10^9 \text{ kJ}$ ) is not as great a portion (83%) of the ultimate energy recoverable ( $1.92 \times 10^9 \text{ kJ}$ );
- the exergy loss ( $0.19 \times 10^9 \text{ kJ}$ ) exceeds the exergy loss in infinite time ( $0.18 \times 10^9 \text{ kJ}$ ) slightly (by 5.5%), while the energy loss ( $1.14 \times 10^9 \text{ kJ}$ ) exceeds the energy loss in infinite time ( $0.82 \times 10^9 \text{ kJ}$ ) substantially (by 39%); and
- the exergy efficiency (40%) has almost attained the exergy efficiency attainable in infinite time (43.5%), while the energy efficiency (58%) is still substantially below the ultimate energy efficiency attainable (70%).

**Verification of Results** To gain confidence in the model and the results, some of the quantities calculated using the linear model can be compared with the same quantities as reported in the experimental paper (Hoyer *et al.*, 1985):

- (i) the previously calculated value for the energy injection during charging of  $2.74 \times 10^9 \text{ kJ}$  is 1.1% less than the reported value of  $2.77 \times 10^9 \text{ kJ}$ ;
- (ii) the energy recovered at the end of the experimental discharge period of  $t_d = 5.24 \text{ d}$  can be evaluated with Equation 6.106 as

$$\begin{aligned} E_d(5.24\text{d}) &= (18.1)(4.2)(77 - 11)[5.24(2 \times 8.87 - 5.24)/(2 \times 8.87)](86,400 \text{ s/d}) \\ &= 1.60 \times 10^9 \text{ kJ} \end{aligned}$$

which is 1.8% less than the reported value of  $1.63 \times 10^9 \text{ kJ}$ ; and

(iii) the energy efficiency at  $t_d = 5.24$  d can be evaluated with Equation 6.113 as

$$\eta(5.24 \text{ d}) = (1.60 \times 10^9 \text{ kJ})(2.74 \times 10^9 \text{ kJ}) = 0.584$$

which is 1.0% less than the reported value of 0.59 (referred to as the *energy recovery factor*).

### 6.7.5 Closure

Although energy-based performance measures are normally used in ATEs assessments, it can be seen using an elementary ATEs model that ATEs performance measures based on exergy are more useful and meaningful than those based on energy. Exergy efficiencies account for the temperatures associated with energy transfers to and from an ATEs, as well as the quantities of energy transferred, and consequently provide a measure of how nearly ATEs systems approach ideal performance. Energy efficiencies account only for quantities of energy transferred and can often be misleadingly high, for example, in cases where heat is recovered at temperatures too low to be useful. The use of an appropriate threshold recovery temperature can partially avoid the most misleading characteristics of ATEs energy efficiencies. The analysis presented here for a simple ATEs cycle can be extended to more complex systems, and is applicable to a wide range of ATEs designs.

## 6.8 Exergy Analysis of Thermally Stratified Storages

Two key advantages of exergy analysis over energy analysis in TES applications are that exergy analysis recognizes differences in storage temperature, even for storages containing equivalent energy quantities, and evaluates quantitatively losses due to degradation of storage temperature toward the environment temperature (i.e., the cooling of heat storages and the heating of cold storages) and due to mixing of fluids at different temperatures. These advantages of the exergy method are particularly important for stratified storages because of the internal spatial temperature variations they exhibit. Since thermodynamic losses are incurred when storage fluids at different temperatures mix, the inhibition of mixing through appropriate temperature stratification is advantageous. By carefully managing the injection, recovery, and holding of heat (or cold) during a storage cycle so that temperature degradation is minimized, better storage cycle performance can be achieved (as measured by better thermal energy recovery and temperature retention and accounted for explicitly through exergy efficiencies) (Hahne *et al.*, 1989; Krane and Krane, 1991).

This section focuses on the energy and exergy contents of stratified storages, which are usually evaluated numerically for arbitrary temperature distributions. Since numerical methods can be effort consuming and often do not provide practical insights into the physical systems, the temperature distributions may alternatively be modeled so that the corresponding TES energy and exergy values can be evaluated analytically. However, accurate mathematical expressions are usually too complex to permit closed-form solutions, and their solutions again normally necessitate the use of computational techniques. As analytical expressions are usually more convenient and provide greater physical insights, temperature-distribution models that achieve an optimal balance between the needs for accuracy, convenience, and physical insight when evaluating storage energy and exergy contents are desirable. Such models can be particularly useful in economic design activities that are greatly simplified and enhanced if analytical expressions for storage energy and exergy contents are available.

In the first part of this section, which follows earlier reports (Rosen and Hooper, 1991b, 1992, 1994; Rosen *et al.*, 1991), several models are presented for the temperature distributions in vertically stratified thermal storages, which are sufficiently accurate, realistic, and flexible for use in engineering design and analysis, yet simple enough to be convenient, and which provide useful physical insights. One-dimensional gravitational temperature stratification is considered, and temperature is expressed as a function of height for each model. To reduce effort, only distributions for

which energy and exergy data can be obtained analytically are considered. Expressions are derived for TES energy and exergy contents in accordance with the models, which are discussed, compared, and illustrated.

In the second part of this section, following previous studies (Rosen and Tang, 1997; Rosen and Dincer, 1999a), the increase in exergy-storage capacity resulting from stratification is described.

### 6.8.1 General Stratified TES Energy and Exergy Expressions

The energy  $E$  and exergy  $\Xi$  in a TES can be found, following Equations 6.12 and 6.31, by integrating over the entire storage-fluid mass  $m$  within the TES as follows:

$$E = \int_m e \, dm \quad (6.116)$$

$$\Xi = \int_m \zeta \, dm \quad (6.117)$$

where  $e$  denotes specific energy and  $\xi$  specific exergy. For an ideal liquid, the  $e$  and  $\xi$  are functions only of temperature  $T$ , and can be expressed as follows:

$$e(T) = c(T - T_o) \quad (6.118)$$

$$\zeta(T) = c[(T - T_o) - T_o \ln(T/T_o)] = e(T) - cT_o \ln(T/T_o) \quad (6.119)$$

Both the storage-fluid specific heat  $c$  and reference-environment temperature  $T_o$  are assumed constant here.

Consider now a TES of height  $H$ , which has only one-dimensional stratification, that is, temperature varies only with height  $h$  in the vertical direction. The horizontal cross-sectional area of the TES is assumed constant. A horizontal element of mass  $dm$  can then be adequately approximated as

$$dm = \frac{m}{H} dh \quad (6.120)$$

Since temperature is a function of height only (i.e.,  $T = T(h)$ ), the expressions for  $e$  and  $\xi$  in Equations 6.118 and 6.119, respectively, can be written as

$$e(h) = c(T(h) - T_o) \quad (6.118a)$$

$$\zeta(h) = e(h) - cT_o \ln(T(h)/T_o) \quad (6.119a)$$

With Equation 6.120, the expressions for  $E$  and  $\Xi$  in Equations 6.116 and 6.117, respectively, can be written as

$$E = \frac{m}{H} \int_0^H e(h) dh \quad (6.116a)$$

$$\Xi = \frac{m}{H} \int_0^H \zeta(h) dh \quad (6.117a)$$

With Equation 6.118a, the expression for  $E$  in Equation 6.116a can be written as

$$E = mc(T_m - T_o) \quad (6.116b)$$



where

$$T_m \equiv \frac{1}{H} \int_0^H T(h) dh \quad (6.121)$$

Physically,  $T_m$  represents the temperature of the TES fluid when it is fully mixed. This observation can be seen by noting that the energy of a fully mixed tank  $E_m$  at a uniform temperature  $T_m$  can be expressed, using Equation 6.118 with constant temperature and Equation 6.116, as

$$E_m = mc(T_m - T_o) \quad (6.122)$$

and that the energy of a fully mixed tank  $E_m$  is by the principle of conservation of energy the same as the energy of the stratified tank  $E$ :

$$E = E_m \quad (6.123)$$

Comparing Equations 6.116b, 6.122, and 6.123 confirms that  $T_m$  represents the temperature of the mixed TES fluid.

With Equation 6.119a, the expression for  $\Xi$  in Equation 6.117a can be written as

$$\Xi = E - mcT_o \ln(T_e/T_o) \quad (6.117b)$$

where

$$T_e \equiv \exp \left[ \frac{1}{H} \int_0^H \ln T(h) dh \right] \quad (6.124)$$

Physically,  $T_e$  represents the equivalent temperature of a mixed TES that has the same exergy as the stratified TES. In general,  $T_e \neq T_m$ , since  $T_e$  is dependent on the degree of stratification present in the TES, while  $T_m$  is independent of the degree of stratification. In fact,  $T_e = T_m$  is the limit condition reached when the TES is fully mixed. This can be seen by noting (with Equations 6.117, 6.117b, 6.122, and 6.123) that the exergy in the fully mixed TES,  $\Xi_m$ , is

$$\Xi_m = E_m - mcT_o \ln(T_m/T_o) \quad (6.125)$$

The difference in TES exergy between the stratified and fully mixed (i.e., at a constant temperature  $T_m$ ) cases can be expressed with Equations 6.117b and 6.125 as

$$\Xi - \Xi_m = mcT_o \ln(T_m/T_e) \quad (6.126)$$

The change given in Equation 6.126 can be shown to be always negative. That is, the exergy consumption associated with mixing fluids at different temperatures, or the minimum work required for creating temperature differences, is always positive.

It is noted that when the temperature distribution is symmetric about the center of the TES such that

$$\frac{T(h) + T(H-h)}{2} = T(H/2) \quad (6.127)$$

the mixed temperature  $T_m$  is always equal to the mean of the temperatures at the top and bottom of the TES.

## 6.8.2 Temperature-Distribution Models and Relevant Expressions

Six stratified temperature-distribution models are considered: linear (denoted by a superscript  $L$ ), stepped ( $S$ ), continuous-linear ( $C$ ), general-linear ( $G$ ), basic three-zone ( $B$ ), and general three-zone ( $T$ ). For each model, the temperature distribution as a function of height is given, and expressions for  $T_m$  and  $T_e$  are derived. The distributions considered are simple enough in form to permit energy and exergy values to be obtained analytically, but complex enough to be relatively realistic. Although other temperature distributions are, of course, possible, these are chosen because closed-form analytical solutions can readily be obtained for the integrals for  $T_m$  in Equation 6.121 and  $T_e$  in Equation 6.124.

### Linear Temperature-Distribution Model

The linear temperature-distribution model (see Figure 6.14) varies linearly with height  $h$  from  $T_b$ , the temperature at the bottom of the TES (i.e., at  $h = 0$ ), to  $T_t$ , the temperature at the top (i.e., at  $h = H$ ), and can be expressed as

$$T^L(h) = \frac{T_t - T_b}{H}h + T_b \quad (6.128)$$

By substituting Equation 6.128 into Equations 6.121 and 6.124, it can be shown that

$$T_m^L = \frac{T_t + T_b}{2} \quad (6.129)$$

which is the mean of the temperatures at the top and bottom of the TES, and that

$$T_e^L = \exp\left[\frac{T_t(\ln T_t - 1) - T_b(\ln T_b - 1)}{T_t - T_b}\right] \quad (6.130)$$

### Stepped Temperature-Distribution Model

The stepped temperature-distribution model (see Figure 6.15) consists of  $k$  horizontal zones, each of which is at a constant temperature, and can be expressed as

$$T^S(h) = \begin{cases} T_1, & h_0 \leq h \leq h_1 \\ T_2, & h_1 < h \leq h_2 \\ \dots & \\ T_k, & h_{k-1} < h \leq h_k \end{cases} \quad (6.131)$$

where the heights are constrained as follows:

$$0 = h_0 \leq h_1 \leq h_2 \dots \leq h_k = H \quad (6.132)$$

It is convenient to introduce here  $x_j$ , the mass fraction for zone  $j$ :

$$x_j \equiv \frac{m_j}{m} \quad (6.133)$$

Since the TES-fluid density  $\rho$  and the horizontal TES cross-sectional area  $A$  are assumed constant here, but the vertical thickness of zone  $j$ ,  $h_j - h_{j-1}$ , can vary from zone to zone,

$$m_j = \rho V_j = \rho A(h_j - h_{j-1}) \quad (6.134)$$

and

$$m = \rho V = \rho AH \quad (6.135)$$

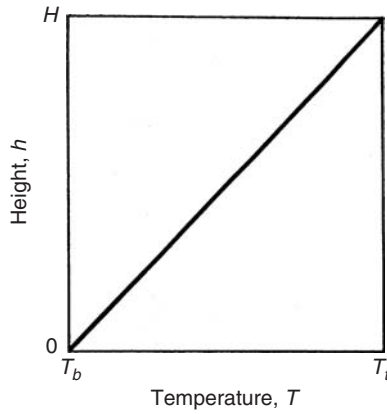


**Figure 6.14** A vertically stratified storage having a linear temperature distribution

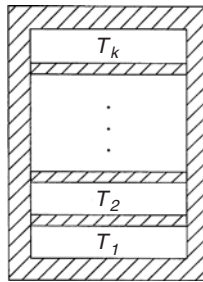


**Figure 6.15** A vertically stratified storage having a stepped temperature distribution

where  $V_j$  and  $V$  denote the volumes of zone  $j$  and of the entire TES, respectively. Substitution of Equations 6.134 and 6.135 into Equation 6.133 yields

$$x_j = \frac{h_j - h_{j-1}}{H} \tag{6.133a}$$

With Equations 6.121, 6.124, 6.131, and 6.133a, it can be shown that

$$T_m^S = \sum_{j=1}^k x_j T_j \tag{6.136}$$

which is the weighted mean of the zone temperatures, where the weighting factor is the mass fraction of the zone, and that

$$\begin{aligned} T_e^S &= \exp \left[ \sum_{j=1}^k x_j \ln T_j \right] \\ &= \prod_{j=1}^k T_j^{x_j} \end{aligned} \tag{6.137}$$

### Continuous-Linear Temperature-Distribution Model

The continuous-linear temperature distribution consists of  $k$  horizontal zones, in each of which the temperature varies linearly from the bottom to the top, and can be expressed as

$$T^C(h) = \begin{cases} \phi_1^C(h), & h_0 \leq h \leq h_1 \\ \phi_2^C(h), & h_1 < h \leq h_2 \\ \dots \\ \phi_k^C(h), & h_{k-1} < h \leq h_k \end{cases} \quad (6.138)$$

where  $\phi_j^C(h)$  represents the linear temperature distribution in zone  $j$ .

$$\phi_j^C(h) = \frac{T_j - T_{j-1}}{h_j - h_{j-1}}h + \frac{h_j T_{j-1} - h_{j-1} T_j}{h_j - h_{j-1}} \quad (6.139)$$

The zone height constraints in Equation 6.132 apply here. The temperature varies continuously between zones.

With Equations 6.121, 6.124, 6.133a, 6.138, and 6.139, it can be shown that

$$T_m^C = \sum_{j=1}^k x_j (T_m)_j \quad (6.140)$$

where  $(T_m)_j$  is the mean temperature in zone  $j$ , that is,

$$(T_m)_j = \frac{T_j + T_{j-1}}{2} \quad (6.141)$$

and that

$$\begin{aligned} T_e^C &= \exp \left[ \sum_{j=1}^k x_j \ln(T_e)_j \right] \\ &= \prod_{j=1}^k (T_e)_j^{x_j} \end{aligned} \quad (6.142)$$

where  $(T_e)_j$  is the equivalent temperature in zone  $j$ , that is,

$$(T_e)_j = \begin{cases} \exp \left[ \frac{T_j (\ln T_j - 1) - T_{j-1} (\ln T_{j-1} - 1)}{T_j - T_{j-1}} \right], & \text{if } T_j \neq T_{j-1} \\ T_j, & \text{if } T_j = T_{j-1} \end{cases} \quad (6.143)$$

### General-Linear Temperature-Distribution Model

For the general-linear model, there are  $k$  horizontal zones, in each of which the temperature varies linearly. The temperature does not necessarily vary continuously between zones. That is,

$$T^G(h) = \begin{cases} \phi_1^G(h), & h_0 \leq h \leq h_1 \\ \phi_2^G(h), & h_1 < h \leq h_2 \\ \dots \\ \phi_k^G(h), & h_{k-1} < h \leq h_k \end{cases} \quad (6.144)$$

where the zone height constraints in Equation 6.132 apply, and  $\phi_j^G(h)$  represents the temperature distribution (linear) in zone  $j$ :

$$\phi_j^G(h) = \frac{(T_t)_j - (T_b)_j}{h_j - h_{j-1}}h + \frac{h_j(T_b)_j - h_{j-1}(T_t)_j}{h_j - h_{j-1}} \quad (6.145)$$

Here,  $(T_t)_j$  and  $(T_b)_j$  denote respectively the temperatures at the top and bottom of zone  $j$ , and  $h_j$  and  $h_{j-1}$  the heights at the top and bottom of zone  $j$  (relative to the bottom of the TES).

For the general-linear temperature-distribution model,

$$T_m^G = \sum_{j=1}^k x_j (T_m^G)_j \quad (6.146)$$

$$T_e^G = \exp \left[ \sum_{j=1}^k x_j \ln(T_e^G)_j \right] = \prod_{j=1}^k (T_e^G)_j^{x_j} \quad (6.147)$$

where

$$(T_m^G)_j = \frac{(T_t)_j + (T_b)_j}{2} \quad (6.148)$$

$$(T_e^G)_j = \begin{cases} \exp \left[ \frac{(T_t)_j (\ln(T_t)_j - 1) - (T_b)_j (\ln(T_b)_j - 1)}{(T_t)_j - (T_b)_j} \right] & \text{if } (T_t)_j \neq (T_b)_j \\ (T_t)_j, & \text{if } (T_t)_j = (T_b)_j \end{cases} \quad (6.149)$$

### General Three-Zone Temperature-Distribution Model

Two three-zone temperature-distribution models are considered in this and the next subsection: general and basic. Both of the three-zone models are subsets of the continuous-linear model in which there are only three horizontal zones (i.e.,  $k = 3$ ). The temperature varies linearly within each zone and continuously across each zone.

The temperature distribution for the general three-zone model is illustrated in Figure 6.16(a), and can be expressed as follows:

$$T^T(h) = \begin{cases} \phi_1^C(h), & h_0 \leq h \leq h_1 \\ \phi_2^C(h), & h_1 < h \leq h_2 \\ \dots & \\ \phi_3^C(h), & h_2 < h \leq h_k \end{cases} \quad (6.150)$$

where  $\phi_j^C(h)$  represents the temperature distribution (linear) in zone  $j$  (see Equation 6.139), and where the heights are constrained as in Equation 6.132 with  $k = 3$ .

Expressions for the temperatures  $T_m$  and  $T_e$  can be obtained for the general three-zone model with Equations 6.121, 6.124, and 6.150 (or from the expressions for  $T_m$  and  $T_e$  for the continuous-linear model with  $k = 3$ ):

$$T_m^T = \sum_{j=1}^3 x_j (T_m^C)_j \quad (6.151)$$

$$T_e^T = \exp \left[ \sum_{j=1}^3 x_j \ln(T_e^C)_j \right] = \prod_{j=1}^3 (T_e^C)_j^{x_j} \quad (6.152)$$

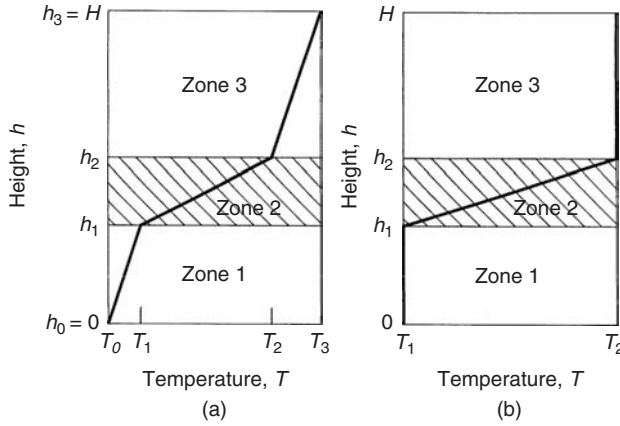


**Figure 6.16** The three-zone temperature-distribution models. (a) General (b) basic

where

$$(T_m^C)_j = \frac{T_j + T_{j-1}}{2} \tag{6.153}$$

$$(T_e^C)_j = \begin{cases} \exp \left[ \frac{T_j (\ln T_j - 1) - T_{j-1} (\ln T_{j-1} - 1)}{T_j - T_{j-1}} \right], & \text{if } T_j \neq T_{j-1} \\ T_j, & \text{if } T_j = T_{j-1} \end{cases} \tag{6.154}$$

**Basic Three-Zone Temperature-Distribution Model**

The basic three-zone temperature-distribution model (*B*) is a subset of the general three-zone model. In the top and bottom zones, the temperatures are constant at  $T_2$  and  $T_1$ , respectively, and in the middle zone, the temperature varies linearly between  $T_2$  and  $T_1$ . The temperature distribution for this model is illustrated in Figure 6.16(b), and can be expressed as

$$T^B(h) = \begin{cases} T_1, & 0 \leq h \leq h_1 \\ \frac{T_2 - T_1}{h_2 - h_1}h + \frac{h_2 T_1 - h_1 T_2}{h_2 - h_1}, & h_1 \leq h \leq h_2 \\ T_2, & h_2 \leq h \leq H \end{cases} \tag{6.155}$$

where  $0 \leq h_1 \leq h_2 \leq H$ .

By extension of the general three-zone model, it can be shown that

$$T_m^B = x_1 T_1 + x_2 \frac{T_1 + T_2}{2} + x_3 T_2 = f T_1 + (1 - f) T_2 \tag{6.156}$$

where  $f$  represents the mean height fraction in zone 2, expressible as

$$f \equiv \frac{h_1 + h_2}{2H} \tag{6.157}$$

It can also be shown that

$$T_e^B = \exp \left[ x_1 \ln T_1 + x_2 \frac{T_2 (\ln T_2 - 1) - T_1 (\ln T_1 - 1)}{T_2 - T_1} + x_3 \ln T_2 \right] \tag{6.158}$$

### 6.8.3 Discussion and Comparison of Models

Each of the six stratified temperature-distribution models has advantages and disadvantages, particularly with respect to ease of utilization and flexibility to approximate accurately different actual temperature distributions. The linear temperature-distribution model is simple to utilize but not flexible enough to fit the wide range of actual temperature distributions possible, while the stepped, continuous-linear, and general-linear distribution models are flexible and, if the zones are made small enough, can accurately fit any actual temperature distribution. However, the latter models are relatively complex to utilize when the number of zones is large. Although the continuous and general-linear models involve the more complex equations, they usually require fewer zones than the stepped model to achieve similar accuracy in results.

For most normal situations, the three-zone temperature-distribution models may be optimal in terms of achieving an appropriate compromise between such factors as result accuracy, computational convenience, physical insight, and so on. Both the three-zone models are relatively easy to utilize, yet are flexible enough to simulate well the stratification distribution in most actual TES fluids, which possess lower and upper zones of slightly varying or approximately constant temperature, and a middle zone (the thermocline region) in which temperature varies substantially. The intermediate zone, which grows as thermal diffusion occurs in the tank being modeled, accounts for the irreversible effects of thermal mixing. The basic three-zone model is simpler while the general three-zone model is more accurate.

It is noted that simplified forms of the expressions for  $T_m$  and  $T_e$  can be written for the multizone temperature-distribution models when all zone vertical thicknesses are the same, since in this special case, the mass fractions for each of the  $k$  zones are the same (i.e.,  $x_j = 1/k$  for all  $j$ ). Also, several relations exist between the model temperature distributions beyond those described earlier:

- The general-linear temperature distribution reduces to (i) the stepped distribution when  $(T_t)_j = (T_b)_j$  for all  $j$ ; (ii) the continuous-linear distribution when  $(T_t)_j = (T_b)_{j+1}$  for  $j = 1, 2, \dots, k - 1$ ; and (iii) the linear distribution when  $k = 1$ .
- The continuous-linear model with  $k = 1$  reduces to the linear model.

### 6.8.4 Illustrative Example: The Exergy-Based Advantage of Stratification

This example illustrates the advantage of stratification by showing that the exergy of a stratified storage is greater than the exergy for the same tank when it is fully mixed, even though the energy content does not change. The case considered is a perfectly insulated, rigid tank of volume  $V$ , divided by an adiabatic partition into two equal-size compartments. The tank is filled with an incompressible fluid. The temperatures of the fluids in each compartment ( $T_1$  and  $T_2$ ) are initially different.

The partition is removed and a new equilibrium state is attained. No chemical reactions occur. Clearly, the initial state corresponds to a stratified tank with a stepped temperature distribution, and the final state to a fully mixed tank containing an identical quantity of energy. Thus, the TES energy and exergy contents can be expressed with Equations 6.116b and 6.117b for the initial state (denoted by subscript  $i$ ) and Equations 6.122 and 6.125 for the final state ( $f$ ), using the stepped temperature-distribution expressions for  $T_m^S$  and  $T_e^S$  (Equations 6.136 and 6.137) with  $k = 2$  and  $x_1 = x_2 = 0.5$ .

Since neither work nor heat interactions occur, the total internal energy of the storage fluid does not change, that is,  $E_f - E_i = 0$ . The exergy change of the fluid can be expressed with Equation 6.126 as

$$\Xi_f - \Xi_i = -T_o mc \ln \frac{T_m}{T_e} \quad (6.159)$$

Equation 6.136 can be used to show that the final temperature of the store after adiabatic mixing is  $T_m = (T_1 + T_2)/2$ . Also, from Equation 6.137,  $T_e = \sqrt{T_1 T_2}$ . Equation 6.159 therefore simplifies for this case as follows:

$$\Xi_f - \Xi_i = -T_o m c_v \ln \frac{T_1 + T_2}{2\sqrt{T_1 T_2}} = -T_o m c_v \ln \frac{\sqrt{r} + \sqrt{1/r}}{2} \quad (6.159a)$$

where  $r = T_1/T_2$ , a positive quantity. The above expression can be further simplified by noting that, since the mixed temperature is given by the mean of the initial temperatures, the initial temperatures can be written as  $T_1 = T_m + \Delta T$  and  $T_2 = T_m - \Delta T$ , where  $\Delta T$  is an arbitrary temperature increment. Then,

$$\Xi_f - \Xi_i = T_o m c_v \ln \sqrt{1 - \alpha^2} \quad (6.159b)$$

where  $\alpha \equiv \Delta T/T_m$  and  $0 \leq \alpha \leq 1$ . Note that if  $T_m = T_o$ , the temperature of the store after mixing is  $T_o$  and the total exergy content of the store can be shown with Equation 6.116b to be zero. Noting that  $\sqrt{r} + \sqrt{1/r} \geq 2$  and  $\sqrt{1 - \alpha^2} \leq 1$ , that the natural logarithm of a quantity greater than one is always positive and less than one is always negative, and that the other terms in Equations 6.159a and b are positive, it can be seen that  $\Xi_f - \Xi_i$  is zero for  $r = 1$  and  $\alpha = 1$ , and negative for all other possible values of  $r$  and  $\alpha$ .

Thus, while the total energy contained in the store (the sum of the energy in each of the two sections) before and after mixing is equal, the total exergy contained in the store (the sum of the exergy in each of the two sections) before mixing is greater than that contained in the store after mixing. A corollary to this point is that to reverse the mixing process, no net energy need be added to the tank, while some net exergy must be added. The exergy change is zero only if  $T_1 = T_2$  (i.e., there are no exergy consumptions due to irreversibilities if fluids of the same temperature are mixed).

### 6.8.5 Illustrative Example: Evaluating Stratified TES Energy and Exergy

#### Problem Statement

Several energy and exergy quantities are determined for a realistic stratified temperature distribution, which was assembled by the authors based on many temperature observations for actual storages, using the linear, stepped, continuous-linear, general-linear, and general three-zone temperature-distribution models to approximate the actual distribution. For comparative purposes, the exact values for these quantities are determined by numerical integration of the integrals in Equations 6.121 and 6.124 for the actual temperature distribution. Three-stepped distribution cases are considered, each with a different numbers of zones. The actual distribution is shown in Figure 6.17, with most of the model distributions.

The TES fluid is taken to be water. Specified general data are listed in Table 6.10, and additional data specific to the temperature-distribution models are shown in Figure 6.17 and summarized below:

- **Continuous-linear.**  $k = 3$ ,  $h_1 = 1.8$  m,  $h_2 = 2.2$  m,  $T_1 = 318$  K,  $T_2 = 348$  K.
- **General-linear.**  $k = 2$ ,  $h_1 = 2.0$  m,  $(T_t)_1 = 318$  K,  $(T_b)_2 = 348$  K.
- **Stepped.**  $k = 2$ ,  $h_j - h_{j-1} = 2$  m for the first case;  $k = 20$ ,  $h_j - h_{j-1} = 0.2$  m for the second case;  $k = 200$ ,  $h_j - h_{j-1} = 0.02$  m for the third case. The temperatures for the stepped cases can be read from Figure 6.17.
- **General three-zone.**  $h_1 = 1.8$  m,  $h_2 = 2.2$  m,  $T_1 = 318$  K,  $T_2 = 348$  K. Note that this distribution is equivalent to the continuous-linear temperature distribution described earlier.



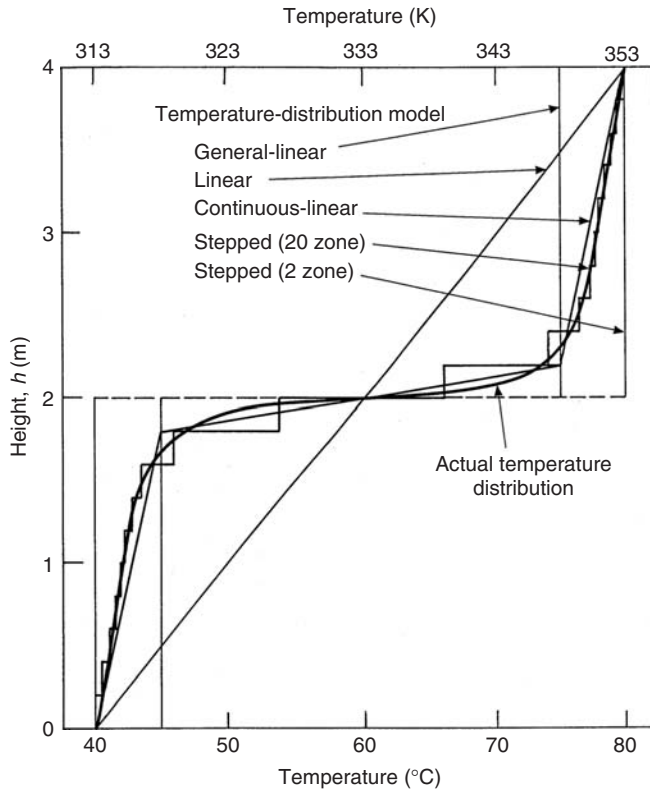


**Figure 6.17** The realistic vertically stratified temperature distribution considered in the example, and some of the temperature-distribution models used to approximate it (linear, continuous-linear, general-linear, stepped with two zones, and stepped with 20 zones). The continuous-linear distribution shown is equivalent to a general three-zone distribution

**Table 6.10** Specified general data for the example

• Temperatures (K)	
At TES top, $T(h = H)$	353
At TES bottom, $T(h = 0)$	313
Reference environment, $T_o$	283
• TES-fluid parameters	
Height, $H$ (m)	4
Mass, $m$ (kg)	10,000
Specific heat, $c$ (kJ/kg K)	4.18

## Results and Discussion

The results (see Table 6.11) demonstrate the following points for all temperature-distribution models considered:

- The TES energy and exergy contents differ significantly, the exergy values being more than an order of magnitude less than the energy values. This observation is attributable to the fact that

**Table 6.11** Results for the stratification example

	Temperature-distribution model						Results from numerical integration
	Linear	General-linear	Stepped			Continuous-linear <sup>a</sup>	
			$k = 200$	$k = 20$	$k = 2$		
Temperatures (K)							
$T_m$	333.000	333.000	333.000	333.000	333.000	333.000	333.000
$T_c$	332.800	332.540	332.550	332.560	332.400	332.570	332.550
Energy values (MJ)							
$E$	2090.000	2090.000	2090.000	2090.000	2090.000	90.000	2090.000
$E_m$	2090.000	2090.000	2090.000	2090.000	2090.000	2090.000	2090.000
$E - E_m$	0.000	0.000	0.000	0.000	0.000	0.000	0.000
Exergy values (MJ)							
$\Xi$	172.500	181.800	181.400	181.000	186.700	80.700	181.400
$\Xi_m$	165.400	165.400	165.400	165.400	165.400	165.400	165.400
$\Xi - \Xi_m$	7.100	16.400	16.000	15.600	21.300	15.300	16.000
Percentage errors							
In values of $T_e$	+0.075	-0.030	0.000	+0.003	-0.045	+0.006	-
In values of $\Xi$	-4.900	+2.000	0.000	-0.200	+2.900	-0.400	-
In values of $\Xi - \Xi_m$	-55.600	+22.500	0.000	-2.500	+33.100	-4.400	-

<sup>a</sup>This case is also a general three-zone temperature-distribution model.

the stored thermal energy, although great in quantity, is at near-environmental temperatures, and therefore low in quality or usefulness.

- Values vary among the models for  $T_e$ ,  $\Xi$ , and  $\Xi - \Xi_m$ , while values do not vary for  $T_m$ ,  $E$ ,  $E_m$ , and  $\Xi_m$ . The latter point is expected since the symmetry condition of Equation 6.127 holds for all model temperature distributions considered. As expected from Equation 6.123,  $E = E_m$ .

The effort required to evaluate the results in Table 6.11 and the accuracy of the results are different for each temperature-distribution model, as explained below:

- Accuracy can be measured by comparing the results for the model distributions with the results obtained by numerical integration (see Table 6.11). Percentage errors are given for the quantities in Table 6.11 that vary from model to model (i.e., for  $T_e$ ,  $\Xi$ , and  $\Xi - \Xi_m$ ), where

$$\% \text{ error} = \frac{(\text{Value}) - (\text{Numerical simulation value})}{(\text{Numerical simulation value})} 100 \tag{6.160}$$

In Table 6.11, the percentage errors for  $T_e$  values are very small (ranging from -0.045% to +0.075%) and for  $\Xi$  values are fairly small (ranging from -4.9% to +2.9%), but, for values of  $\Xi - \Xi_m$ , are in some cases large (ranging from -55.6% to +33.1%).

- Computational effort expended increases as the number of zones required in multizone distributions for acceptable approximations to the actual temperature distribution increases, and as the complexity of the calculations involved increases. Less computational effort is required to obtain the values in Table 6.11 for all the different temperature-distribution models considered, than for the values obtained by numerical integration.

In the present example, the general three-zone model has an acceptable accuracy and yet is simple to use. Although the stepped models (with 20 or 200 zones) are more precise, they are more complex to apply. The poor correlations between the actual and linear temperature distributions, and

between the actual and stepped (with  $k = 2$ ) distributions, cause these model distributions to provide results of significantly lower precision, although they are simpler to apply. Clearly, the selection of a particular distribution as a model involves a trade-off, and the three-zone temperature-distribution model appears to represent an appropriate compromise between high precision of results and an acceptable level of calculational effort.

### 6.8.6 Increasing TES Exergy-Storage Capacity Using Stratification

The increase in the exergy capacity of a thermal storage through stratification is described. A wide range of realistic storage-fluid temperature profiles is considered, and for each, the relative increase in exergy content of the stratified storage compared to the same storage when it is fully mixed is evaluated. It is shown that, for all temperature profiles considered, the exergy-storage capacity of a thermal storage increases as the degree of stratification, as represented through greater and sharper spatial temperature variations, increases. Furthermore, the percentage increase in exergy capacity is greatest for storages at temperatures near to the environment temperature, and decreases as the mean storage temperature diverges from the environment temperature (to either higher or lower temperatures).

#### Analysis

Thermal storages for heating and cooling capacity, having numerous temperature-distribution profiles, are considered. The general three-zone model, which, as discussed previously, is a suitable design-oriented temperature-distribution model for vertically stratified thermal storages, is utilized to evaluate storage energy and exergy contents. For each case, the ratio is evaluated of the exergy of the stratified storage  $\Xi$  to the exergy of the same storage when fully mixed  $\Xi_m$ . Using Equations 6.116b, 6.117b, and 6.125, this ratio can be expressed, after simplification, as

$$\frac{\Xi}{\Xi_m} = \frac{T_m/T_o - 1 - \ln(T_e/T_o)}{T_m/T_o - 1 - \ln(T_m/T_o)} \quad (6.161)$$

This ratio increases, from as low as unity when the storage is not stratified, to a value greater than one as the degree of stratification present increases. The ratio in Equation 6.161 is independent of the mass  $m$  and specific heat  $c$  of the storage fluid. The ratio is also useful as an evaluation, analysis, and design tool, as it permits the exergy of a stratified storage to be conveniently evaluated by multiplying the exergy of the equivalent mixed storage (a quantity straightforwardly evaluated) by the appropriate exergy ratio, where values for the exergy ratio can be determined separately (as is done here).

Several assumptions and approximations are utilized throughout this subsection:

- Storage horizontal cross-sectional area is taken to be fixed.
- The environmental temperature  $T_o$  is fixed at 20 °C for all cases (whether they involve thermal storage for heating or cooling capacity).
- Only one-dimensional gravitational (i.e., vertical) temperature stratification is considered.
- Only temperature distributions that are rotationally symmetric about the center of the storage, according to Equation 6.127, are considered. This symmetry implies that zone 2 is centered about the central horizontal axis of the storage, and that zones 1 and 3 are of equal size, that is,  $x_1 = x_3 = (1 - x_2)/2$ .

To model and then assess the numerous storage cases considered, two main relevant parameters are varied realistically:

- the principal temperatures (e.g., mean, maximum, minimum), and
- temperature-distribution profiles (including changes in zone thicknesses).

Specifically, the following characterizing parameters are varied to achieve the different temperature-distribution cases considered:

- The mixed-storage temperature  $T_m$  is varied for a range of temperatures characteristic of storages for heating and cooling capacity.
- The size of zone 2, which represents the thermocline region, is allowed to vary from as little as zero to as great as the size of the overall storage, that is,  $0 \leq x_2 \leq 1$ . A wide range of temperature profiles can thereby be accommodated, and two extreme cases exist: a single-zone situation with a linear temperature distribution when  $x_2 = 1$ , and a two-zone distribution when  $x_2 = 0$ .
- The maximum and minimum temperatures in the storage, which occur at the top and bottom of the storage, respectively, are permitted to vary about the mixed-storage temperature  $T_m$  by up to  $15^\circ\text{C}$ .

Using the zone numbering system in Figure 6.16(a) and the symmetry condition introduced earlier, the following expressions can be written for the temperatures at the top and bottom of the storage, respectively:

$$T_3 = T_m + \Delta T_{st} \text{ and } T_0 = T_m - \Delta T_{st} \quad (6.162)$$

while the following equations can be written for the temperatures at the top and bottom of zone 2, respectively:

$$T_2 = T_m + \Delta T_{th} \text{ and } T_1 = T_m - \Delta T_{th} \quad (6.163)$$

where the subscripts “th” and “st” denote thermocline region (zone 2) and overall storage, respectively, and where

$$\Delta T \equiv |T - T_m| \quad (6.164)$$

According to the last bullet above,  $0 \leq \Delta T_{th} \leq \Delta T_{st} = 15^\circ\text{C}$ . Also,  $\Delta T_{th}$  is the magnitude of the difference, on either side of the thermocline region (zone 2), between the temperature at the outer edge of zone 2 and  $T_m$ , while  $\Delta T_{st}$  is the magnitude of the difference, on either side of the overall storage, between the temperature at the outer edge of the storage and  $T_m$ . That is,

$$\Delta T_{th} = \Delta T_1 = \Delta T_2 \text{ and } \Delta T_{st} = \Delta T_0 = \Delta T_3 \quad (6.165)$$

where the  $\Delta T$  parameters in the above equations are defined using Equation 6.164 as follows:

$$\Delta T_j \equiv |T_j - T_m|, \text{ for } j = 0, 1, 2, 3 \quad (6.166)$$

### Effects of Varying Stratification Parameters

- **Effect of varying  $T_m$ .** The variation of thermal-storage exergy with storage temperature for a mixed storage is illustrated in Figure 6.18. For a fixed storage total heat capacity ( $mc$ ), storage exergy increases, from zero when the temperature  $T_m$  is equal to the environment temperature  $T_o$ , as the temperature increases or decreases from  $T_o$ . This general trend, which is illustrated here for a mixed storage, normally holds for stratified storages, since the effect on storage exergy of temperature is usually more significant than the effect of stratification.
- **Effect of varying minimum and maximum temperatures for a linear profile.** A linear temperature profile across the entire storage occurs with the three-zone model when  $x_2 = 1$ . Then, the upper and lower boundaries of zone 2 shift to the top and bottom of the storage, respectively,

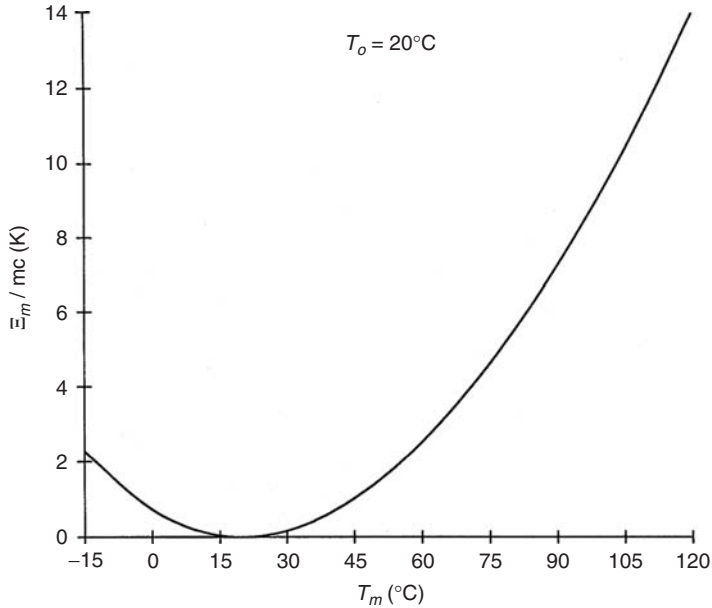


**Figure 6.18** Variation with the mixed-storage temperature  $T_m$  of the modified exergy quantity  $\Xi_m/mc$  (where  $m$  and  $c$  are constant) for a mixed storage. When  $T_m$  equals the environment temperature  $T_o = 20^\circ\text{C}$ ,  $\Xi_m = 0$

and correspondingly the temperature deviation  $\Delta T_{th}$  occurs at those positions. For a linear temperature profile, the ratio  $\Xi/\Xi_m$  is illustrated in Figures 6.19(a–c) for three temperature regimes, respectively:

- high-temperature thermal storage for heating capacity, that is,  $T_m \geq 60^\circ\text{C}$ ;
- low-temperature thermal storage for heating capacity, that is,  $20^\circ\text{C} \leq T_m \leq 60^\circ\text{C}$ ; and
- thermal storage for cooling capacity, that is,  $T_m \leq 20^\circ\text{C}$ .

The temperature range considered is above the environment temperature  $T_o = 20^\circ\text{C}$  for the first two cases, and below it for the third. Two key points are demonstrated in Figure 6.19. First, it is evident for all cases that, for a fixed mixed-storage temperature  $T_m$ , storage exergy content increases as the level of stratification increases (i.e., as  $\Delta T_{th}$  increases). Secondly, the percentage increase in storage exergy, relative to the mixed-storage exergy at the same  $T_m$ , is greatest when  $T_m = T_o$ , and decreases both as  $T_m$  increases from  $T_o$  (see Figures 6.19a and b) and decreases from  $T_o$  (see Figure 6.19c). The main reason for this second observation relates to the fact that the absolute magnitude of the mixed exergy for a thermal storage is small when  $T_m$  is near  $T_o$ , and larger when  $T_m$  deviates significantly from  $T_o$  (see Figure 6.18). In the limiting case where  $T_m = T_o$ , the ratio  $\Xi/\Xi_m$  takes on the value of unity when  $\Delta T_{th} = 0$  and infinity for all other values of  $\Delta T_{th}$ . Hence, the relative benefits of stratification as a tool to increase the exergy-storage capacity of a thermal storage are greatest at near-environment temperatures, and less for other cases.

- **Effect of varying thermocline-size parameter  $x_2$ .** The variation of the ratio  $\Xi/\Xi_m$  with the zone-2 size parameter and the temperature deviation at the zone-2 boundaries,  $\Delta T_{th}$ , is illustrated in Figure 6.20 for a series of values of the mixed-storage temperature  $T_m$ . For a fixed value of  $\Delta T_{th}$  at a fixed value of  $T_m$ , the ratio  $\Xi/\Xi_m$  increases as the zone-2 size parameter  $x_2$  decreases. This observation occurs because the stratification varies less smoothly and more sharp and pronounced as  $x_2$  decreases.

- Effect of varying temperature-distribution profile shape.** The temperature-distribution profile shape is varied, for a fixed value of  $T_m$ , primarily by varying values of the parameters  $x_2$  and  $\Delta T_{th}$  simultaneously. The behavior of  $\Xi/\Xi_m$  as  $x_2$  and  $\Delta T_{th}$  are varied for several  $T_m$  values is shown in Figure 6.20. For all cases considered, by varying these parameters at a fixed value of  $T_m$  (except for  $T_m = T_o$ ), the ratio  $\Xi/\Xi_m$  increases, from a minimum value of unity at  $x_2 = 1$  and  $\Delta T_{th} = 0$ , as  $x_2$  decreases and  $\Delta T_{th}$  increases. Physically, these observations imply that, for a fixed value of  $T_m$ , storage exergy increases as stratification becomes more pronounced, both by increasing the maximum temperature deviation from the mean storage temperature and by increasing the sharpness of temperature profile differences between storage zones.

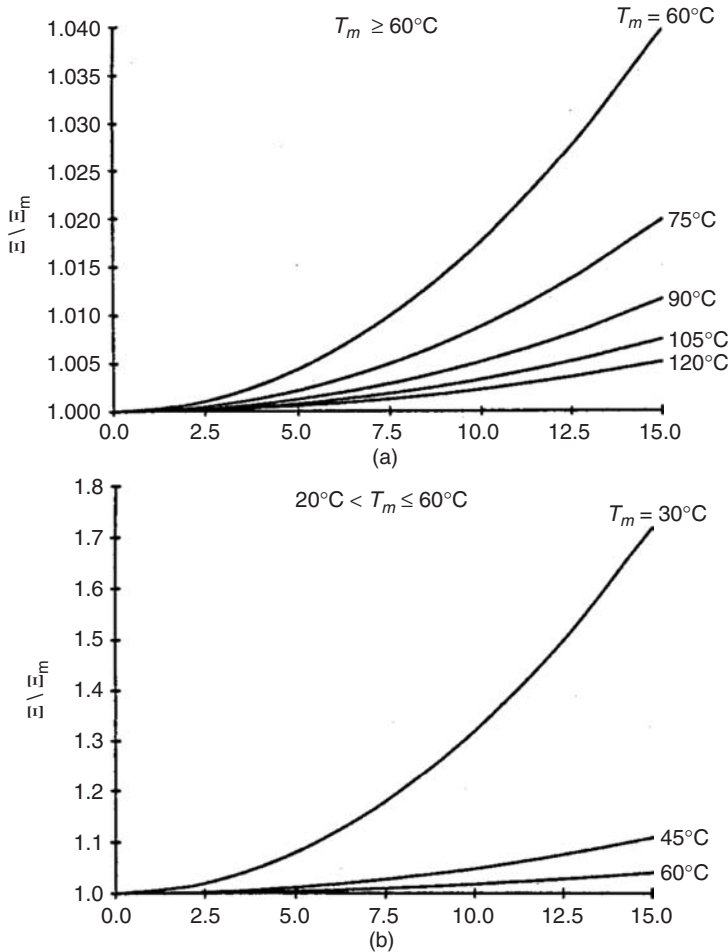


**Figure 6.19** Illustration for three ranges of values of the mixed-storage temperature  $T_m$  (each corresponding to a different graph) of the variation of the ratio of the exergy values for stratified and fully mixed storages,  $\Xi/\Xi_m$ , with temperature deviation from  $T_m$  at the upper and lower boundaries of the thermocline zone (zone 2),  $\Delta T_{th}$ . For all cases, a linear temperature profile is considered, that is, the zone-2 mass fraction is fixed at  $x_2 = 1$ . (a) High-temperature thermal storage for heating capacity, that is,  $T_m \geq 60^\circ\text{C}$ ; (b) low-temperature thermal storage for heating capacity, that is,  $20^\circ\text{C} \leq T_m \leq 60^\circ\text{C}$ ; (c) thermal storage for cooling capacity, that is,  $T_m \leq 20^\circ\text{C}$

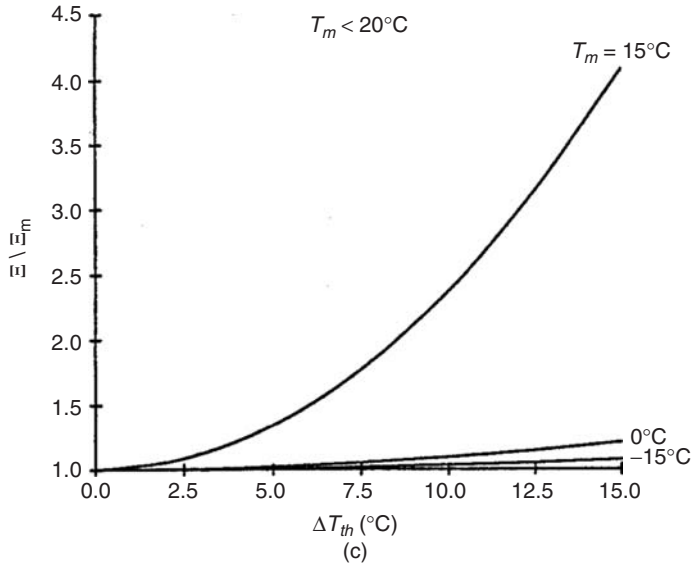


Figure 6.19 (continued)

### 6.8.7 Illustrative Example: Increasing TES Exergy with Stratification

In this example, several energy and exergy quantities relevant to the previous subsection are determined using the general three-zone model, for a thermal storage using water as the storage fluid and having a realistic stratified temperature distribution. The use of the data presented in this section as a design tool is also illustrated.

The actual distribution is taken to be that from the illustrative example in Section 6.8.5 for the general three-zone case. The temperature distribution is shown in Figure 6.17, along with the general three-zone model distribution used to approximate the actual distribution. Specified general data are listed in Table 6.10.

The results of the example (see Table 6.11) demonstrate that, for the case considered, the ratio  $\Xi/\Xi_m = 180.7/165.4 = 1.09$ . This implies that the exergy of the stratified storage is about 9% greater than the exergy of the mixed storage. In effect, therefore, stratification increases the exergy-storage capacity of the storage considered, relative to its mixed condition, by 9%.

Rather than determine values of the ratio  $\Xi/\Xi_m$  using the expressions in this section, values can be read from figures such as those in Figure 6.20 (although the case here of  $T_m = 60^\circ\text{C}$ ,  $x_2 = 0.1$ , and  $\Delta T_{th} = 20^\circ\text{C}$  falls slightly outside of the range of values covered in Figure 6.20 for the case of  $T_m = 60^\circ\text{C}$ ). Then, such diagrams can serve as design tools from which one can obtain a ratio that can be applied to the value of the exergy of the mixed storage to obtain the exergy of the stratified storage.

### 6.8.8 Closure

The temperature-distribution models described here (linear, stepped, continuous-linear, general-linear, basic three-zone, and general three-zone) facilitate the evaluation of energy and exergy contents of vertically stratified thermal storages. The selection of a particular distribution as a model involves a trade-off between result accuracy and calculational effort, and the three-zone models appear to provide the most reasonable compromise among these factors, and thus to be suitable as simple engineering aids for TES analysis, design, and optimization.

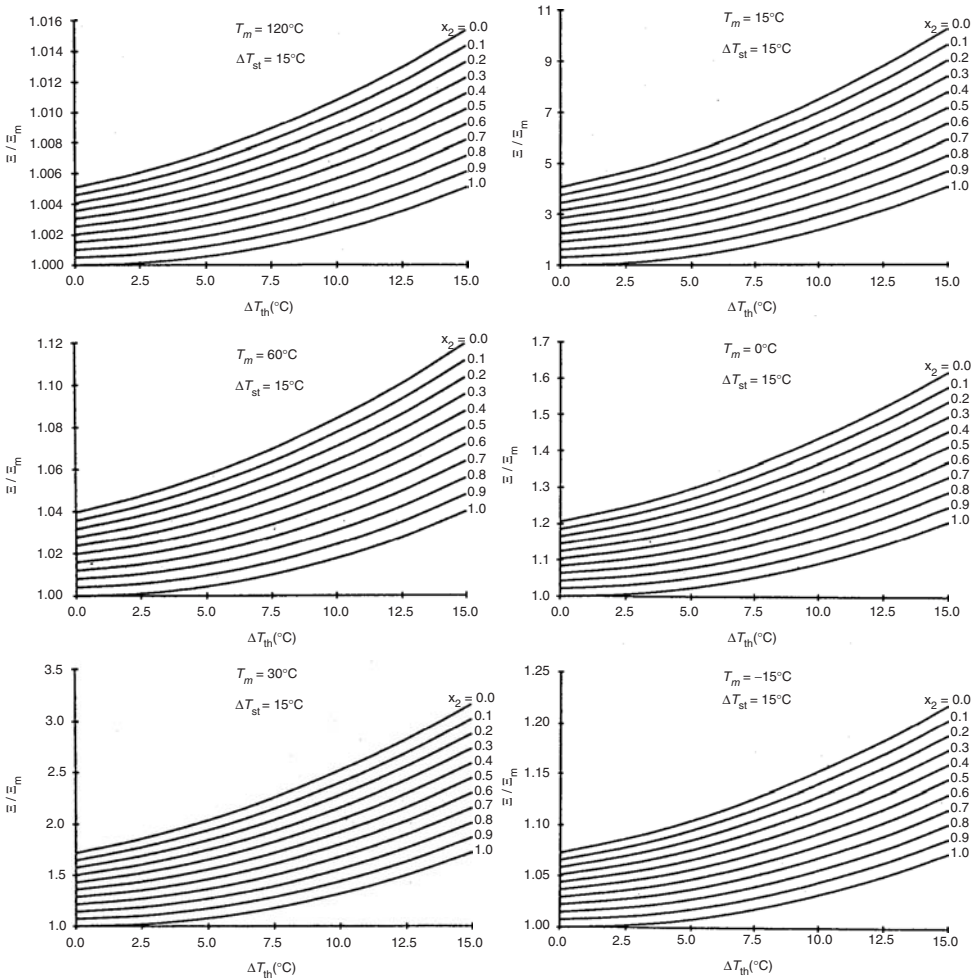


**Figure 6.20** Illustration for a series of values of the mixed-storage temperature  $T_m$  (each corresponding to a different graph) of the variation of the ratio of the exergy values for stratified and fully mixed storages,  $\Xi/\Xi_m$ , with temperature deviation from  $T_m$  at the upper and lower boundaries of the thermocline zone (zone 2),  $\Delta T_{th}$ , and with the zone-2 mass fraction  $x_2$ . The magnitude of the temperature deviation from  $T_m$  at the top and bottom of the storage,  $\Delta T_{st}$ , is  $15^\circ\text{C}$  for all cases

TES exergy values, unlike energy values, change due to stratification, giving a quantitative measure of the advantage provided by stratification. The examples considered illustrate how (i) the quantities of energy and exergy contained in a stratified TES differ, and (ii) the exergy content (or capacity) of a TES increases as the degree of stratification increases, even if the energy remains fixed. The use of stratification can therefore aid in TES design as it increases the exergy-storage capacity of a thermal storage.

### 6.9 Energy and Exergy Analyses of Cold TES Systems

An important application of TES is in facilitating the use of off-peak electricity to provide building heating and cooling. Recently, increasing attention has been paid in many countries to cold thermal



energy storage (CTES), an economically viable technology that has become a key component of many successful thermal systems. In many CTES applications, inexpensive off-peak electricity is utilized during the night to produce with chillers a cold medium, which can be stored for use in meeting cooling needs during the day when electricity is more expensive. CTES is applied mainly in building cooling, particularly for large commercial buildings that often need year-round cooling because of the heat released by occupants, lighting, computers, and other equipment. In most situations, CTES permits the mismatch between the supply and demand of cooling to be favorably altered (Dincer and Dost, 1996), leading to more efficient and environmentally benign energy use as well as reduced chiller sizes, capital and maintenance costs, and carbon dioxide and chlorofluorocarbon CFC emissions (Beggs, 1991).

To be economically justifiable, the annual costs needed to cover the capital and operating expenses for a CTES (and related systems) should be less than the costs for primary generating equipment supplying the same service loads and periods (Dincer, 1999). A CTES can lead to lower initial and operating costs for associated chillers when cooling loads are intermittent and of short duration. Secondary system capital costs may also be lower with CTES, for example, electrical service entrance sizes can sometimes be reduced because energy demand is lower.

Although CTES efficiency and performance evaluations are conventionally based on energy, energy analysis itself is inadequate for complete CTES evaluation because it does not account for such factors as the temperatures at which heat (or cold) is supplied and delivered. Exergy analysis overcomes some of these inadequacies in CTES assessments.

This section deals with the assessment using exergy and energy analyses of CTES systems, including sensible and/or latent storages, following earlier reports (Rosen *et al.*, (1999, 2000)). Several CTES cases are considered, including storages that are homogeneous or stratified and some that undergo phase changes. A full cycle of charging, storing, and discharging is considered for each case. This section demonstrates that exergy analysis provides more realistic efficiency and performance assessments of CTES systems than energy analysis, and conceptually is more direct since it treats cold as a valuable commodity. An example and case study illustrate the usefulness of exergy analysis in addressing cold thermal-storage problems.

### 6.9.1 Energy Balances

Consider a cold storage consisting of a tank containing a fixed quantity of storage fluid and a heat-transfer coil through which a heat-transfer fluid is circulated. Kinetic and potential energies and pump work are considered negligible. Energy balance for an entire cycle of a CTES can be written following Equation 6.3 in terms of “cold” as follows:

$$\text{Cold input} - [\text{Cold recovered} + \text{Cold loss}] = \text{Cold accumulation} \quad (6.167)$$

Here, “cold input” is the heat removed from the storage fluid by the heat-transfer fluid during charging; “cold recovered” is the heat removed from the heat-transfer fluid by the storage fluid; “cold loss” is the heat gain from the environment to the storage fluid during charging, storing, and discharging; and “cold accumulation” is the decrease in internal energy of the storage fluid during the entire cycle. Following Equation 6.3a, the overall energy balance for the simplified CTES system illustrated in Figure 6.21 becomes

$$(H_b - H_a) - [(H_c - H_d) + Q_l] = -\Delta E \quad (6.167a)$$

where  $H_a$ ,  $H_b$ ,  $H_c$ , and  $H_d$  are the enthalpies of the flows at points  $a$ ,  $b$ ,  $c$ , and  $d$  in Figure 6.21;  $Q_l$  is the total heat gain during the charging, storing, and discharging processes; and  $\Delta E$  is the difference between the final and initial storage-fluid internal energies. The terms in square brackets in Equations 6.167 and 6.167a represent the net “cold output” from the CTES, and  $\Delta E = 0$  if the CTES undergoes a complete cycle (i.e., the initial and final storage-fluid states are identical).

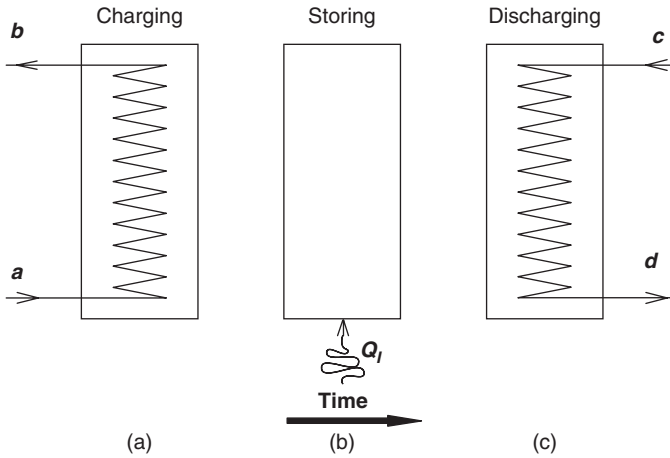


**Figure 6.21** The three processes in a general CTES system: charging (a), storing (b), and discharging (c). The heat leakage into the system  $Q_l$  is illustrated for the storing process, but can occur in all three processes

The energy transfer associated with the charging fluid can be expressed as

$$H_b - H_a = m_a c_a (T_b - T_a) \quad (6.168)$$

where  $m_a$  is the mass flow of heat-transfer fluid at point *a* (and at point *b*), and  $c_a$  is the specific heat of the heat-transfer fluid, which is assumed constant. A similar expression can be written for  $H_c - H_b$ . The energy content of a storage which is homogeneous (i.e., entirely in either the solid or the liquid phase) is

$$E = m(u - u_o) \quad (6.169)$$

which, for sensible heat interactions only, can be written as

$$E = mc(T - T_o) \quad (6.169a)$$

where, for the storage fluid,  $c$  denotes the specific heat (assumed constant),  $m$  the mass,  $u$  the specific internal energy, and  $T$  the temperature. Also,  $u_o$  is  $u$  evaluated at the environmental conditions.

For a mixture of solid and liquid, the energy content of the solid and liquid portions can be evaluated separately and summed as follows:

$$E = m[(1 - F)(u_s - u_o) + F(u_l - u_o)] \quad (6.169b)$$

where  $u_s$  and  $u_l$  are the specific internal energies of the solid and liquid portions of the storage fluid, respectively, and  $F$  is the melted fraction (i.e., the fraction of the storage-fluid mass in the liquid phase).

For a storage fluid that is thermally stratified with a linear temperature profile in the vertical direction, the energy content can be shown with Equations 6.116b and 6.129 to be

$$E = mc \left( \frac{T_t + T_b}{2} - T_o \right) \quad (6.169c)$$

where  $T_t$  and  $T_b$  are the storage-fluid temperatures at the top and bottom of the linearly stratified storage tank, respectively.

The change in CTES energy content from the initial (*i*) to the final state (*f*) of a process can be expressed as in Equation 6.38.

### 6.9.2 Exergy Balances

An exergy balance for a CTES undergoing a complete cycle of charging, storing, and discharging can be written as in Equations 6.40 and 6.40a. The exergy content of a flow of heat-transfer fluid at state  $k$  (where  $k = a, b, c,$  or  $d$  in Figure 6.21) can be expressed as in Equation 6.44. The exergy transfers associated with the charging and discharging of the storage by the heat-transfer fluid can be expressed by Equations 6.45 and 6.46, respectively.

The exergy loss associated with heat infiltration during the three storage periods can be expressed as in Equation 6.47a. The thermal exergy terms are negative for sub-environment temperatures, as is the case here for CTES, indicating that the heat transfer and the accompanying exergy transfer are oppositely directed. That is, the losses associated with heat transfer are due to heat infiltration into the storage when expressed in energy terms, but due to a cold loss out of the storage when expressed in exergy terms.

The exergy content of a homogeneous storage can be shown with Equation 6.116 to be

$$\Xi = m[(u - u_o) - T_o(s - s_o)] \quad (6.170)$$

where  $s$  is the specific entropy of the storage fluid and  $s_o$  is  $s$  evaluated at the environmental conditions. If only sensible heat interactions occur, Equation 6.170 can be written with Equation 6.119 as

$$\Xi = mc[(T - T_o) - T_o \ln(T/T_o)] \quad (6.170a)$$

For a mixture of solid and liquid, the exergy content can be written as

$$\Xi = m\{(1 - F)[(u_s - u_o) - T_o(s_s - s_o)] + F[(u_l - u_o) - T_o(s_l - s_o)]\} \quad (6.170b)$$

where  $s_s$  and  $s_l$  are the specific entropies of the solid and liquid portions of the storage fluid, respectively.

The exergy content of a storage that is linearly stratified can be shown with Equations 6.117b and 6.130 to be

$$\Xi = E - mcT_o \left[ \frac{T_t(\ln T_t - 1) - T_b(\ln T_b - 1)}{T_t - T_b} - \ln T_o \right] \quad (6.170c)$$

The change in TES exergy content can be expressed as in Equation 6.43.

### 6.9.3 Energy and Exergy Efficiencies

For a general CTES undergoing a cyclic operation, the overall energy efficiency  $\eta$  can be evaluated as in Equation 6.32, with the word *energy* replaced by *cold* for understanding. Then, following Figure 6.21, the overall and charging-period energy efficiencies can be expressed as in Equations 6.48 and 6.52, respectively.

Energy efficiencies for the storing and discharging subprocesses can be written respectively as

$$\eta_2 = \frac{\Delta E_1 + Q_l}{\Delta E_1} \quad (6.171)$$

$$\eta_3 = \frac{H_c - H_d}{\Delta E_3} \quad (6.172)$$

where  $\Delta E_1$  and  $\Delta E_3$  are the changes in CTES energy contents during charging and discharging, respectively.

The exergy efficiency for the overall process can be expressed as in Equation 6.49, and for the charging, storing, and discharging processes, respectively, as in Equations 6.55, 6.61, and 6.67.

### 6.9.4 Illustrative Example

#### Cases Considered and Specified Data

Four different CTES cases are considered. In each case, the CTES has identical initial and final states, so that the CTES operates in a cyclic manner, continuously charging, storing, and discharging. The main characteristics of the cold storage cases are as follows:

- sensible heat storage, with a fully mixed-storage fluid;
- sensible heat storage, with a linearly stratified storage fluid;
- latent heat storage, with a fully mixed-storage fluid;
- combined latent and sensible heat storage, with a fully mixed-storage fluid.

The following assumptions are made for each of the cases:

- Storage boundaries are nonadiabatic.
- Heat gain from the environment during charging and discharging is negligibly small relative to heat gain during the storing period.
- The external surface of the storage tank wall is at a temperature  $2^\circ\text{C}$  greater than the mean storage-fluid temperature.
- The mass flow rate of the heat-transfer fluid is controlled so as to produce constant inlet and outlet temperatures.
- Work interactions and changes in kinetic and potential energy terms, are negligibly small.

Specified data for the four cases are presented in Table 6.12 and relate to the diagram in Figure 6.21. In Table 6.12,  $T_b$  and  $T_d$  are the charging and discharging outlet temperatures of the heat-transfer fluid, respectively. The subscripts 1, 2, and 3 indicate the temperature of the storage fluid at the beginning of charging, storing, or discharging, respectively. Also,  $t$  indicates the liquid state and  $s$  indicates the solid state for the storage fluid at the phase-change temperature.

In addition, for all cases, the inlet temperatures are fixed for the charging-fluid flow at  $T_a = -10^\circ\text{C}$  and for the discharging-fluid flow at  $T_c = 20^\circ\text{C}$ . For cases involving latent heat changes (i.e., solidification),  $F = 10\%$ . The specific heat  $c$  is  $4.18\text{ kJ/kg K}$  for both the storage and heat-transfer fluids. The phase-change temperature of the storage fluid is  $0^\circ\text{C}$ . The configuration of the storage tank is cylindrical with an internal diameter of  $2\text{ m}$  and internal height of  $5\text{ m}$ . Environmental conditions are  $20^\circ\text{C}$  and  $1\text{ atm}$ .

**Table 6.12** Specified temperature data for the cases in the CTES example

Temperature ( $^\circ\text{C}$ )	Case			
	I	II	III	IV
$T_b$	4.0	15	-1	-1
$T_d$	11.0	11	10	10
$T_1$	10.5	19/2 <sup>a</sup>	0 (t)	8
$T_2$	5.0	17/-7 <sup>a</sup>	0 (s)	-8
$T_3$	6.0	18/-6 <sup>a</sup>	0 (t and s)	0 (t and s)

<sup>a</sup>When two values are given, the storage fluid is vertically linearly stratified and the first and second values are the temperatures at the top and bottom of the storage fluid, respectively.

**Table 6.13** Energy and exergy quantities for the cases in the CTES example

Period or quantity	Energy quantities				Exergy quantities			
	I	II	III	IV	I	II	III	IV
Efficiencies (%)								
Charging (1)	100	100	100	100	51	98	76	77
Storing (2)	82	82	90	90	78	85	90	85
Discharging (3)	82	100	100	100	38	24	41	25
Overall	100	82	90	90	15	20	28	17
Input, recovered and lost quantities (MJ)								
Input	361.1	361.1	5237.5	6025.9	30.9	23.2	499.8	575.1
Recovered	295.5	295.5	4713.8	5423.3	4.6	4.6	142.3	94.7
Loss (external)	65.7	65.7	523.8	602.6	2.9	2.9	36.3	48.9
Loss (internal)	–	–	–	–	23.3	15.6	321.2	431.4

## Results and Discussion

The results for the four cases are listed in Table 6.13, and include overall and subprocess efficiencies, input and recovered cold quantities, and energy and exergy losses. The overall and subprocess energy efficiencies are identical for Cases I and II, and for Cases III and IV. In all cases, the energy efficiency values are high. The different and lower exergy efficiencies for all cases indicate that energy analysis does not account for the quality of the “cold” energy, as related to temperature, and considers only the quantity of “cold” energy recovered.

The input and recovered quantities in Table 6.13 indicate the quantity of “cold” energy and exergy input to and recovered from the storage. The energy values are much greater than the exergy values because, although the energy quantities involved are large, the energy is transferred at temperatures only slightly below the reference-environment temperature, and therefore is of limited usefulness.

The cold losses during storage, on an energy basis, are entirely due to cold losses across the storage boundary (i.e., heat infiltration). The exergy-based cold losses during storage are due to both cold losses and internal exergy losses (i.e., exergy consumptions due to irreversibilities within the storage). For the present cases, in which the exterior surface of the storage tank is assumed to be 2 °C warmer than the mean storage-fluid temperature, the exergy losses include both external and internal components. Alternatively, if the heat-transfer temperature at the storage tank external surface is at the environment temperature, the external exergy losses would be zero and the total exergy losses would be entirely due to internal consumptions. If heat transfer occurs at the storage-fluid temperature, on the other hand, more of the exergy losses would be due to external losses. In all cases, the total exergy losses, which are the sum of the internal and external exergy losses, remain fixed.

The four cases demonstrate that energy and exergy analyses give different results for CTES systems. Both energy and exergy analyses account for the quantity of energy transferred in storage processes. Exergy analyses take into account the loss in quality of “cold” energy, and thus more correctly reflect the actual value of the CTES.

In addition, exergy analysis is conceptually more direct when applied to CTES systems because cold is treated as a useful commodity. With energy analysis, flows of heat rather than cold are normally considered. Thus, energy analyses become convoluted and confusing as one must deal with heat flows, while accounting for the fact that cold is the useful input and product recovered for CTES systems. Exergy analysis inherently treats any quantity that is out of equilibrium with the environment (be it colder or hotter) as a valuable commodity, and thus avoids the intuitive conflict in the expressions associated with CTES energy analysis. The concept that cold is a valuable commodity is both logical and in line with one’s intuition when applied to CTES systems.

### 6.9.5 Case Study: Thermodynamic Performance of a Commercial Ice TES System

One type of CTES is ice storage, which has been increasingly utilized recently. In an ice thermal energy storage (ITES) system, off-peak electricity is utilized to create a large mass of ice, and during the day, this ice store is melted by absorbing the heat from buildings needing cooling (De Lucia and Bejan, 1990; Beggs, 1991). ITES is a proven technology applicable to any plant that has a chilled water system.

Numerous economic studies of ITES systems and their applications have been undertaken (Althof, 1989; Beggs, 1991; Fields and Knebel, 1991). Chen and Sheen (1993) developed a model for a CTES system that evaluates the component size for a eutectic salt storage system. The related computer simulation determines energy consumption, and performs a cost/benefit analysis to estimate the system payback period. Chen and Sheen also determined the best system operating strategies for varying weather conditions and electricity rates, particularly in Taiwan. Wood *et al.* (1994) investigated TES technical and economic aspects, and presented a techno-economic feasibility evaluation method for new technologies in the commercial sector using a pseudo-data analysis approach. Some (Badar *et al.*, 1993; Domanski and Fellah, 1998) have applied thermoeconomic optimization techniques to TES systems that minimize the combination of entropy generation cost and annualized capital cost of the thermal component.

In this case study, which is based on an earlier analysis (Rosen *et al.*, 2000), energy and exergy analyses of a commercial encapsulated ITES are performed. A full cycle, with charging, storing, and discharging stages, is considered. The case study demonstrates the usefulness of exergy analysis in thermodynamic assessments of ITES systems, provides insights into their performances and efficiencies, and shows that energy analysis leads to misleadingly optimistic statements of ITES efficiency.

#### Types and Operation of ITES Systems

By making ice at night for use in the day when it is needed to provide cooling, ITES systems take advantage of low off-peak electricity rates and often permit building chillers to be shut down or operated at reduced levels during the day. Consequently, owners can realize lower utility bills, and electrical utilities attain a reduction in peak demand, which can defer or avoid the need for new power plants. Ice storage systems are capable of providing the same quantity and quality of cooling as conventional chillers.

There are two main cases of ice storage systems, differing in the levels of electrical load shifting achieved. With a "full storage," the entire cooling load is shifted, eliminating chiller operation during peak hours. In a "partial storage," part of the load is met from a downsized chiller, and part from the storage. In both cases, the sizes of the chiller and of the storage depend on the total amount of cooling needed to meet the building load over the entire day. Sizing is the main factor differentiating ice storage from conventional air-conditioning, since in the latter case, the chiller must be larger to meet the peak cooling load, which normally occurs during the hottest part of the day.

Four main types of ITES systems are commonly used in commercial and industrial applications (Beckman and Gilli, 1984; Beggs, 1991): ice-on-coil, static ice tank, ice harvesting, and encapsulated ice store. The most common ITES type is the encapsulated ice store (Figure 6.22), which is considered in this case study. Encapsulated ITES systems consist of an insulated storage tank (normally constructed from either steel or concrete) that is filled with small plastic capsules containing deionized water and a nucleating agent (Carrier, 1990). Circulating around the capsules is a glycol/water brine solution. During charging, the brine solution is circulated through the tank at a sub-freezing temperature, causing the water in the capsules to freeze to form the ice store. To discharge the store when cooling is needed, the same brine solution is circulated through the tank but at a temperature above the freezing point of water. The ice in the capsules then melts, cooling the brine solution that is subsequently circulated to the air-conditioning unit.

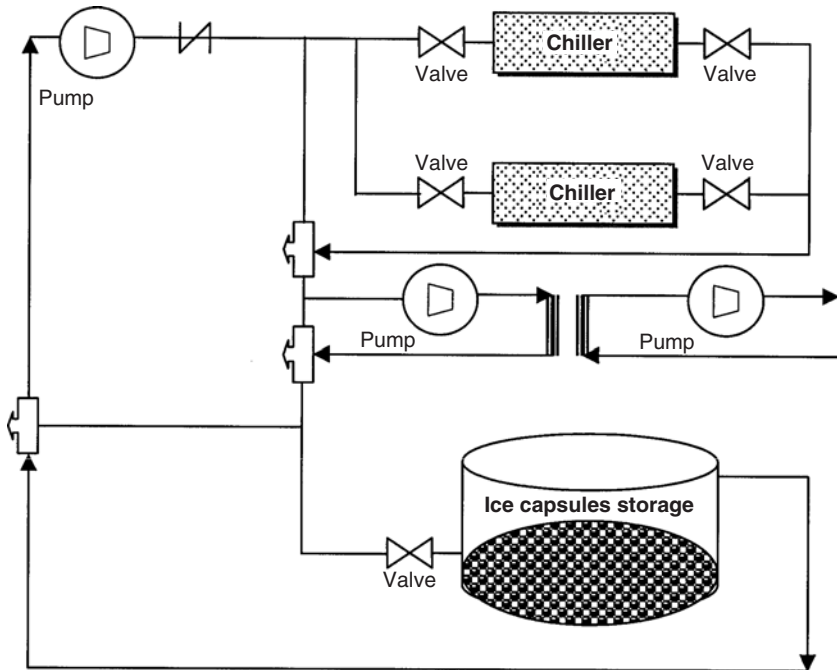


Figure 6.22 A schematic representation of an encapsulated ITES system

### Description of ITES Considered and its Operation

The ITES system considered in this study (Figure 6.22) is designed to have the chiller operate continuously during the design day, and utilizes three operating modes (Carrier, 1990):

- Charging.** The charging mode is the normal operating mode during no-load periods. The chiller cools the antifreeze solution to approximately  $-4^{\circ}\text{C}$ . The antifreeze solution flows through the storage module, freezing the liquid water inside the encapsulated units. The circulating fluid increases in temperature (to a limit of  $0^{\circ}\text{C}$ ), and returns to the chiller to be cooled again. During charging, the building loop is isolated so that full flow is achieved through the storage module.
- Chilling.** The chilling mode is the same as for a nonstorage (conventional) chiller system, with the entire building load being met directly by the chiller. The chiller operates at a warmer set point than for ice making, which results in an increased capacity and a higher coefficient of performance. In this mode, there is no flow through the storage module, and ice in the store is kept in reserve for use later in the day.
- Chilling and discharging.** Chilling and discharging is the normal operating mode during daytime hours. The chiller and storage module share the cooling load, often in a series configuration. Systems are normally designed with the chiller downstream of the storage. Then, the storage module pre-cools the building return fluid before it is further cooled to the design supply temperature by the chiller. This sequence gives a higher effective storage capacity, since the exit temperature from the storage can be higher. The ice melting rate is controlled by modulating valves that cause some flow to bypass the storage module, usually to hold constant the blended fluid temperature downstream of the storage throughout discharging.

The design-day cooling load profile of a typical office building is considered here (Figure 6.23). The circles and squares in Figure 6.23 indicate the cooling load required for the building and the

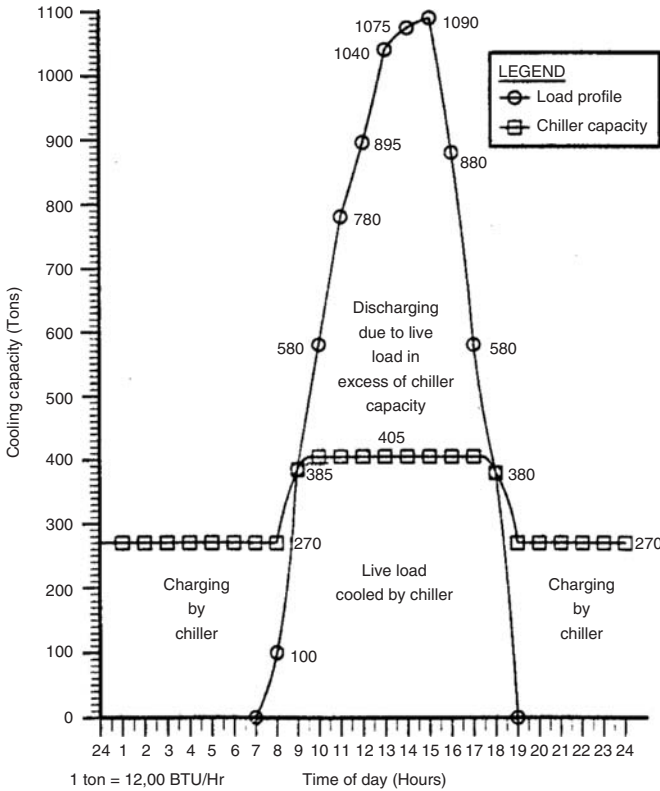


Figure 6.23 A load profile diagram for an encapsulated ITES system (see Rosen *et al.*, 2000)

chiller loads, respectively. Data for the case, taken from Carrier (1990), is presented in Table 6.14 for a full 24-h cycle. The ITES is designed for the chiller to operate continuously during the day (i.e., partial storage operation is used). The ITES module has nonadiabatic storage boundaries with a total thermal resistance of  $R_T = 1.98 \text{ m}^2 \text{ K/W}$ . The specific heat of the heat-transfer fluid (a glycol-based antifreeze solution) is  $3.22 \text{ kJ/kg K}$  at  $-6.6^\circ\text{C}$  and  $3.60 \text{ kJ/kg K}$  at  $15.5^\circ\text{C}$ , and the specific gravity is 1.13. The storage fluid (deionized water) has a freezing point of  $0^\circ\text{C}$ , a mass of  $144,022 \text{ kg}$ , and a density of  $1000 \text{ kg/m}^3$ . The storage module has a volume of  $181.8 \text{ m}^3$ , with  $144.0 \text{ m}^3$  occupied by the storage fluid, and a surface area  $A$  of  $241.6 \text{ m}^2$ . The reference-environment conditions are  $20^\circ\text{C}$  and 1 atm.

### Thermodynamic Analysis

To reduce analysis complexity and to emphasize the significant factors in ice storage operation, it is assumed that the storage fluid remains isothermal at its melting point, fluids are frictionless, the pumping power is zero, and kinetic and potential energy terms are negligibly small. These assumptions neglect some of the irreversibilities in the encapsulated ITES system, notably those associated with the temperature gradients close to the freezing or thawing surfaces in the storage. The net effect of these assumptions is to increase the apparent exergy efficiencies, but probably not their relative values. Hence, the results should be valid in ordering the performances of competitive systems in an optimization process. The analysis generally follows the discussions



**Table 6.14** Specified and evaluated data for the ITES case study

Hour	Process	Load (tons)			Melted fraction (%)	Efficiency (%)	
		Storage	Building	Chiller		Exergy	Energy
1	Charging	270	0	270	48.55	88.1	99.7
2	Charging	270	0	270	41.46	87.0	99.7
3	Charging	270	0	270	34.36	85.9	99.7
4	Charging	270	0	270	27.27	84.8	99.7
5	Charging	270	0	270	20.17	83.7	99.7
6	Charging	270	0	270	13.08	82.6	99.7
7	Charging	270	0	270	5.99	81.6	99.7
8	Charging	170	100	270	1.53	80.4	99.5
9	Storing	0	385	385	1.55	99.9	99.9
10	Discharging	175	580	405	6.12	66.0	99.7
11	Discharging	375	780	405	15.96	63.3	99.9
12	Discharging	490	895	405	28.83	59.9	99.9
13	Discharging	635	1040	405	45.53	58.5	99.9
14	Discharging	670	1075	405	63.15	57.1	99.9
15	Discharging	685	1090	405	81.16	55.7	99.9
16	Discharging	475	880	405	93.63	52.9	99.9
17	Discharging	175	580	405	98.21	63.9	99.7
18	Storing	0	380	380	98.22	99.9	99.9
19	Charging	270	0	270	91.13	93.5	99.7
20	Charging	270	0	270	84.03	92.6	99.7
21	Charging	270	0	270	76.94	91.8	99.7
22	Charging	270	0	270	69.84	90.9	99.7
23	Charging	270	0	270	62.74	90.1	99.7
24	Charging	270	0	270	55.65	89.3	99.7

earlier in this section. Also, losses due to heat gain from the environment,  $Q_l$ , are determined here as follows:

$$Q_l = \frac{A \Delta T}{R_T} \quad (6.173)$$

where  $\Delta T$  is the difference between the storage-fluid and environmental temperatures,  $A$  is the surface area through which the heat is transferred, and  $R_T$  is the unit total thermal resistance of the storage module. Following Figure 6.21, the overall energy and efficiencies can be written with Equations 6.32 and 6.49 for the ITES module as it undergoes a cyclic operation over a 24-h period, by summing over the 24 h:

$$\eta = \frac{\text{Product cold recovered}}{\text{Cold input}} = \frac{\sum_{j=1}^{24} (H_c - H_d)_j}{\sum_{j=1}^{24} (H_b - H_a)_j} \quad (6.174)$$

$$\psi = \frac{\text{Exergy recovered}}{\text{Exergy input}} = \frac{\sum_{j=1}^{24} (\epsilon_d - \epsilon_c)_j}{\sum_{j=1}^{24} (\epsilon_a - \epsilon_b)_j} \quad (6.175)$$

Energy and exergy efficiencies for charging, storing, and discharging are similarly evaluated, following Section 6.9.3.

## Results and Discussion

The overall energy and exergy efficiencies are 99.5% and 50.9%, respectively, and the hourly energy and exergy efficiencies are listed in Table 6.14. The hourly exergy efficiencies range from 80–94% and average 86% for the overall charging period, range from 53–66% and average 60% for the overall discharging period, and range from 99–100% for the overall storing period. The hourly energy efficiencies exceed 99% for all periods.

The marked differences in the energy and exergy efficiencies for the overall process and the subprocesses merit emphasis and explanation. The energy efficiencies are high, since they only account for heat gains from the environment, which are small. The exergy efficiencies are much lower since they account for the “usefulness” of the energy, which is related to the inlet and outlet temperatures and the mass flow rates of heat-transfer fluid. In the example, the charging fluid being at  $-4^{\circ}\text{C}$ , a much lower temperature than that of the environment, is a moderately high-quality cold flow. The cold flow recovered during discharging, however, is of much lower quality with a temperature much closer to that of the environment. Thus, the energy efficiencies, for each hour or for the entire cycle, are misleadingly high as they only account for energy recovery but neglect entirely the loss of quality of the flows. This quality loss is quantified with exergy analysis. Since the irreversibilities in an ITES process destroy some of the input exergy, ITES exergy efficiencies are always lower than the corresponding energy efficiencies.

Another interesting observation stems from the fact that exergy efficiencies provide a measure of how nearly a process approaches ideality, while energy efficiencies do not. Here, the energy efficiencies being over 99% for the overall process and all subprocesses erroneously imply that the ITES system is nearly ideal. The overall exergy efficiency of approximately 51%, as well as the subprocess exergy efficiencies, indicate that the ITES system is far from ideal, and has a significant margin for efficiency improvement. In this example, the same cooling capacity could be delivered from the ITES using about half of the input exergy if it were ideal. Thus, overall electrical use by the chillers could be greatly reduced while still maintaining the same cooling services. Such a reduction would reduce the necessary installed cooling power and electrical costs.

Further implications of the results follow:

- The fact that the exergy efficiencies are less than 100% implies that a mismatch exists between the quality of the thermal energy delivered by the ITES (and required by the cooling load) and the quality of the thermal energy input to the ITES. This mismatch, which is detectable through the temperature of the thermal energy flows across the ITES boundaries, is quantifiable with exergy analysis as the work potential lost during storage. The exergy loss, therefore, correlates directly with an additional use of electricity by the chillers than would occur without the exergy loss. When exergy efficiencies are 100%, there is no loss in temperature during storage.
- The nonideal exergy efficiencies imply that excessively high-quality thermal energy is supplied to the ITES than is required given the cooling load. Thus, exergy analysis indicates that lower quality sources of thermal energy could be used to meet the cooling load. Although economic and other factors must be taken into account when selecting energy resources, the exergy-based results presented here can assist in identifying feasible energy sources that have other desired characteristics (e.g., environmentally benign or abundant).

Consequently, the results demonstrate that a more perceptive measure of comparison than energy efficiency is needed if the true usefulness of an ITES is to be assessed and a rational basis for the optimization of its economic value established. Energy efficiencies ignore the quality (exergy) of the energy flows, and so cannot provide a measure of ideal performance. Exergy efficiencies provide more comprehensive and useful efficiency measures for practical ITES systems, and facilitate more rational comparisons of different systems. In addition, exergy analysis can assist in the optimization

of ITES systems, when combined with assessments of such other factors as resource-use reductions, environmental impact and emissions decreases, and economics.

### 6.9.6 Closure

Exergy analysis provides more meaningful and useful information than energy analysis about the efficiencies, losses, and performance for CTES systems. A prime justification for this view is that the loss of low temperature is accounted for in exergy – but not in energy-based performance measures. Furthermore, the exergy-based information is presented in a more direct and logical manner, as exergy methods provide intuitive advantages when CTES systems are considered. Consequently, exergy analysis can likely assist in efforts to optimize the design of CTES systems and their components, and to identify appropriate applications and optimal configurations for CTES in general engineering systems. Several additional key points can be drawn from this section: (i) exergy analysis can assist in selecting alternative energy sources for CTES systems, so that the potential role can be properly considered for CTES in meeting society's preferences for more efficient, environmentally benign energy use in various sectors; and (ii) the application of exergy analysis to CTES systems permits mismatches in the quality of the thermal energy supply and demand to be quantified, and measures to reduce or eliminate reasonably avoidable mismatches to be identified and considered. The material presented in this section for cold TES parallels that presented in the rest of this chapter for heat storage systems, although the advantages of the exergy approach appear to be more significant when CTES systems are considered due to manner in which “cold” is treated as a resource.

## 6.10 Exergy-Based Optimal Discharge Periods for Closed TES Systems

Since in many instances, energy-based performance measures can be misleading while exergy-based measures provide more realistic TES evaluations, exergy results can be useful in design and optimization activities. Some researchers (Bejan, 1978; Rosen, 1990) have attempted to obtain optimum design and operating parameters for sensible TES systems using exergy techniques. Bejan (1978) considered the charging process of a TES system. Krane (1987), considering the entire charging–discharging cycle, found that high-efficiency systems had charging–discharging time ratios of 1:4 or higher. It may not be possible to incorporate such charging–discharging time ratios into many TES applications. Optimal efficiencies and temperatures for the phase change in latent TES have also been investigated (Saborio-Aceves *et al.*, 1994).

In this section, which follows an earlier report (Gunnawiek *et al.*, 1993), the usefulness of using exergy-based measures in optimization and design is demonstrated for TES discharge processes. Analytical expressions are developed using energy and exergy methods for the storage-fluid temperature during discharging and the TES discharge efficiencies. Although in much of this chapter, pump work has been neglected with respect to thermal energy flows, one must account for work terms in optimization efforts. Thus pump work is accounted for in this section, and the optimum discharge period based on thermodynamic criteria is determined. An illustrative example is presented.

### 6.10.1 Analysis Description and Assumptions

A simple case is considered in which a sensible, closed, fully mixed TES undergoes a complete storage cycle where the final state of the TES is the same as the initial state. The TES system boundaries may be adiabatic or nonadiabatic, and the surroundings are at a constant temperature and pressure. Fluid flows are modeled as steady and one-dimensional. Kinetic and potential energy

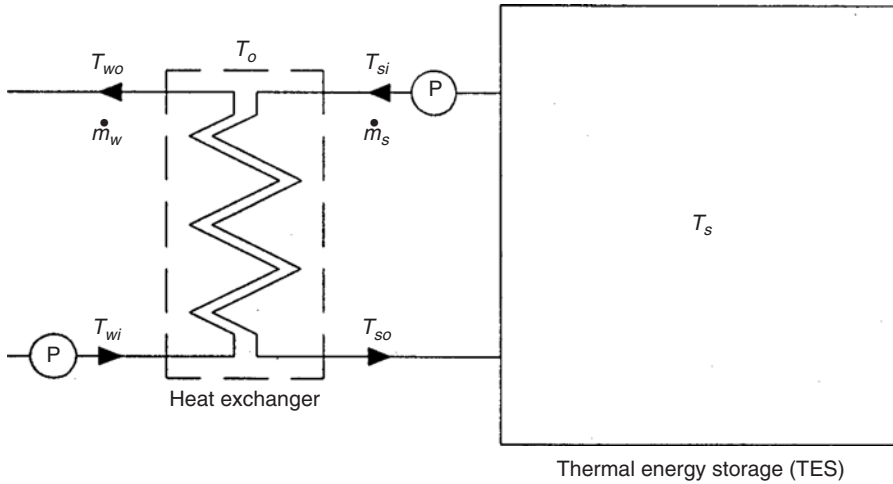


**Figure 6.24** The closed TES system considered in evaluating optimal discharge periods

terms are considered negligible, as is the chemical component of exergy, because it does not contribute to the exergy transfers for a sensible TES system.

### 6.10.2 Evaluation of Storage-Fluid Temperature During Discharge

It is assumed that the recovery of thermal energy from the TES system is achieved with a heat exchanger (Figure 6.24). The heat-recovery rate may be written as

$$\dot{Q} = \dot{m}_s c_s (T_{si} - T_{so}) \quad (6.176)$$

where  $\dot{m}_s$  and  $c_s$  are the mass flow rate and specific heat of the storage fluid, and  $T_{si}$  and  $T_{so}$  are the heat exchanger inlet and outlet storage-fluid temperatures, respectively.

Knowing the effectiveness  $\varepsilon$  of the heat exchanger, which is dependent on the heat-exchanger configuration and fluid flow conditions, and the minimum heat capacity rate  $C_{min}$  for the two fluids involved in the heat-transfer process, the heat-recovery rate may also be written as

$$\dot{Q} = C_{min} \varepsilon (T_{si} - T_{wi}) \quad (6.177)$$

Assuming that the temperature of the storage fluid entering the heat exchanger  $T_{si}$  is the same as the storage-fluid temperature  $T_s$ , and that the working-fluid temperature entering the heat exchanger  $T_{wi}$  is the same as the reference-environment temperature  $T_o$ , then it can be shown with Equations 6.176 and 6.177 that

$$T_{so} = T_s - \frac{C_{min} \varepsilon}{\dot{m}_s c_s} (T_s - T_o) \quad (6.178)$$

To evaluate the changing storage-fluid temperature during the discharge process, a mathematical model is introduced in which, for a finite time step of  $t^s$ , a mass of storage fluid at temperature  $T_s$  exits the TES while an equal mass of storage fluid at temperature  $T_{so}$  enters. The importance has recently been recognized of the time-step size used in the mathematical modeling and numerical simulation of TES systems (Fanny and Klein, 1988; Lightstone *et al.*, 1988). The accuracy of the results is partially dependent on the time-step size and flow rates. A decrease in the time-step size increases the accuracy of the solution to a certain point. In one particular study (Lightstone *et al.*, 1988), a decrease in a time step of 10 s resulted in no significant difference in the results.

### Adiabatic TES Case

After each time step of the discharging period, the new storage-fluid temperature  $T_{sa}$  for a fully mixed TES with adiabatic boundaries can be expressed as

$$T_{sa} = \frac{(m - \dot{m}_s t^s)T_s + (\dot{m}_s t^s)T_{so}}{m} \quad (6.179)$$

where  $m$  is the mass of the storage fluid and is constant for a closed TES system. Using Equation 6.178, Equation 6.179 becomes

$$T_{sa} = T_s - \frac{C_{min}\varepsilon t^s}{mc_s}(T_s - T_o) \quad (6.179a)$$

### Nonadiabatic TES Case

For a nonadiabatic TES with an overall heat-transfer coefficient  $U$  based on an outer-surface area  $A$ , the heat loss  $Q_l$  at any storage-fluid temperature  $T_s$ , for a finite time step  $t^s$ , is

$$Q_l = UA t^s (T_s - T_o) \quad (6.180)$$

and the TES energy content  $E_s$  is

$$E_s = mc_s(T_s - T_o) \quad (6.181)$$

Thus, after each finite time step during the discharging process, the new storage-fluid temperature  $T_{sn}$ , for a fully mixed TES with nonadiabatic boundaries, can be found with the following energy balance:

$$mc_s(T_{sn} - T_o) = mc_s(T_{sa} - T_o) - Q_l \quad (6.182)$$

After rearranging and substituting Equations 6.179a and 6.180, it can be shown that

$$T_{sn} = T_s - \frac{C_{min}\varepsilon t^s}{mc_s}(T_s - T_o) - \frac{UA t^s}{mc_s}(T_s - T_o) \quad (6.183)$$

Note that Equation 6.183 expresses the new storage-fluid temperature after a finite time step for any fully mixed, closed TES with adiabatic or nonadiabatic boundaries.

## 6.10.3 Discharge Efficiencies

### Energy Efficiency

The heat  $Q_3$  recovered from a TES during the  $i$ th finite time step  $t_s(i)$  can be written as

$$Q_3(i) = \dot{m}_s c_s t^s(i) [T_{sn}(i) - T_{so}(i)] \quad (6.184)$$

Equation 6.184 does not account for the work required to recover the heat. If pump work is considered, the net energy recovered from the TES system may be written as  $Q_3(i) - \dot{W} t^s(i)$ , where  $\dot{W}$  is the shaft power used by the pump, and the discharge energy efficiency after  $n$  time steps is defined as

$$\eta = \sum_{i=1}^n \frac{Q_3(i) - \dot{W} t^s(i)}{E_s(i=0)} \quad (6.185)$$

Here  $E_s(i=0)$  is the initial energy content of the storage, when the storage-fluid temperature is  $T_s$ . Note that the energy discharge efficiency is 100% when heat transfer is ideal and the TES is perfectly insulated.

### Exergy Efficiency

The thermal exergy  $X_3$  recovered from the TES during time step  $i$  can be written as

$$X_3(i) = \dot{m}_s c_s t^s(i) \left[ (T_{sn}(i) - T_{so}(i)) - T_o \ln \frac{T_{sn}(i)}{T_{so}(i)} \right] \quad (6.186)$$

Accounting for pump work, the net exergy recovered is  $X_3(i) - \dot{W}t^s(i)$  and the discharge exergy efficiency can be written as

$$\psi = \sum_{i=1}^n \frac{X_3(i) - \dot{W}t^s(i)}{\Xi_s(i=0)} \quad (6.187)$$

where  $\Xi_s(i=0)$  is the initial exergy content of the TES, expressible as

$$\Xi_s = mc_s [(T_s - T_o) - T_o \ln(T_s/T_o)] \quad (6.188)$$

#### 6.10.4 Exergy-Based Optimum Discharge Period

From a thermodynamic perspective, the optimum discharge period for a TES is that corresponding to the maximum discharge efficiency. The authors feel that the optimum discharge period is more meaningfully determined using exergy rather than energy efficiencies, because exergy analysis considers the quality or usefulness of storage-fluid energy, which is dependent on the fluid and ambient temperatures, and recognizes the difference in usefulness of pump work and recovered heat, whereas energy analysis treats these two energy forms as equal.

It is noted that the optimum discharge period here, which is constrained to being based solely on thermodynamic criteria, may not in general coincide with the optimum period when factors other than thermodynamics (e.g., economics, environmental impact) are taken into account.

#### 6.10.5 Illustrative Example

Consider an active solar space-heating system having a sensible, fully mixed TES that is charged during daylight hours and discharged at night. The storage medium, water, has a mass of  $m = 10,000$  kg, a constant specific heat of  $c_s = 4.18$  kJ/kg K, and a temperature at the beginning of the discharge period of  $T_s = 353$  K. Heat transfer between the storage fluid and working fluid (air, with  $c_w = 1.007$  kJ/kg K) occurs in a heat exchanger with a “number of transfer units” of  $NTU = 2.5$ , an effectiveness of  $\varepsilon = 0.7$ , and mass flow rates of  $\dot{m}_s = 0.22$  and  $\dot{m}_w = 1.2$  kg/s. The temperature of the reference environment is  $T_o = 293$  K. A time step of  $t^s = 600$  s is used.

Energy and exergy discharge efficiencies are evaluated as a function of discharge period duration for several cases. Figure 6.25 compares storages having adiabatic and nonadiabatic boundary conditions, that is,  $UA = 0$  and  $0.15$  kW/K, when the pump shaft power is  $\dot{W} = 0.745$  kW. Figure 6.26 considers the influence of pump shaft power ( $\dot{W} = 0$  and  $0.745$  kW) for a nonadiabatic TES ( $UA = 0.15$  kW/K).

In Figure 6.25, the top two curves show energy efficiencies for adiabatic and nonadiabatic storages, and the bottom two curves show the corresponding exergy efficiencies. The difference in discharge efficiencies for adiabatic and nonadiabatic TES systems is attributable to heat losses, which reduce the amount of heat that can be recovered in the heat-transfer process. Two points of significance are noted in the differences between the energy and exergy efficiency curves. First, the maximum exergy and energy discharge efficiencies differ and occur at different times, for example, for the nonadiabatic TES, the maximum exergy efficiency (28.7%) occurs at 13.5 h, while the maximum energy efficiency (72.1%) occurs at 57.3 h. Secondly, the net exergy recovered from a TES becomes negative (and consequently, the exergy discharge efficiency becomes negative) before the maximum energy discharge efficiency is attained.

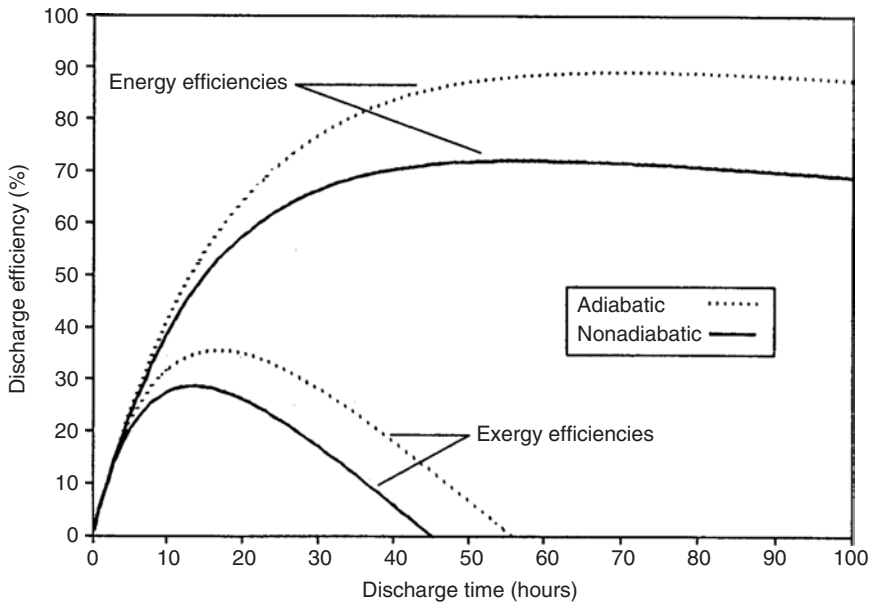


Figure 6.25 Discharge efficiencies, accounting for pump work, for adiabatic and nonadiabatic TES systems

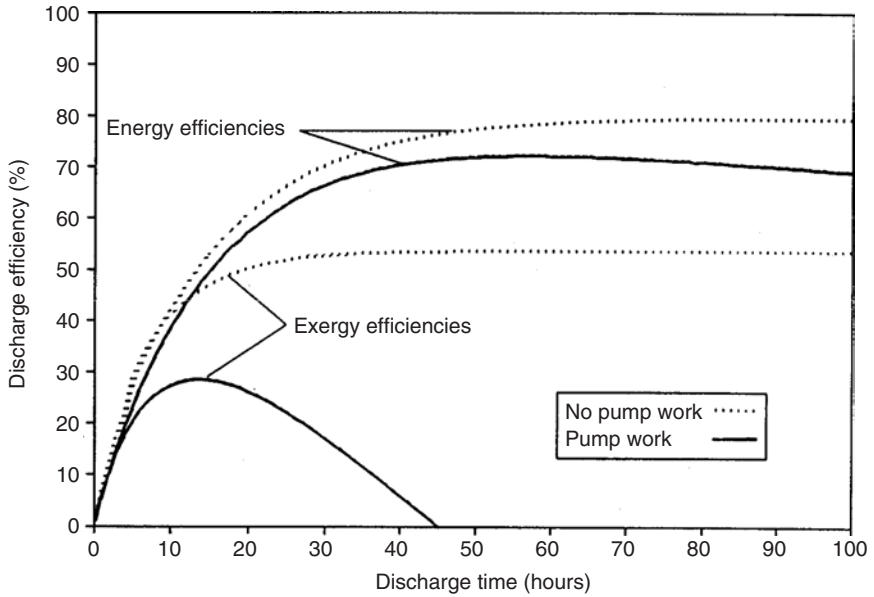


Figure 6.26 Discharge efficiencies for nonadiabatic TES systems with and without pump work

In Figure 6.26, it can be seen that if pump shaft power is considered negligible, maximum discharge efficiencies are higher for both energy and exergy analysis, relative to when the pump shaft power is considered nonzero. Also, with negligible pump shaft power, the maximum net energy recovery is not diminished by continued operation of the heat-exchanger pump. In addition, Figure 6.26 demonstrates that thermal energy and thermal exergy differ, depending on the temperatures involved, while pump shaft power is equivalent in energy and exergy terms. Hence in Figure 6.26, the difference between the exergy and energy efficiencies is much greater for the cases with pump work than without.

### 6.10.6 Closure

Using energy and exergy discharge efficiencies and a method for evaluating the changing storage-fluid temperature for the discharge process of a closed, fully mixed, sensible TES system, optimal discharge periods can be evaluated based on thermodynamic considerations. The results show that the difference between the results of energy and exergy analyses is significant, and that the impact of pump work on the optima can be important. The authors feel that, since exergy is a measure of the quality or usefulness of energy, exergy performance measures are more meaningful than energy performance measures, and should be considered in the evaluation of the optimum discharge period for TES systems and in related design activities.

## 6.11 Exergy Analysis of Solar Ponds

Solar ponds provide an interesting option for simultaneously collecting and storing solar energy and are viable in some regions (e.g., those with readily available land, much sunshine, little snow, and access to inexpensive salt – NaCl or bittern). The technology was developed in Israel in the 1960s. Solar ponds are usually large and deep, and sized to provide community heating. The pond acts as a sensible TES that can supply thermal energy for many applications. The ability to collect and store solar energy makes the solar pond somewhat akin to some passive solar energy technologies (e.g., trombe walls).

A solar pond (see Figure 6.27) differs from an ordinary pond or lake in one key way. In the latter, solar radiation warms the water and increases its buoyancy, causing it to rise to the surface where it loses heat to the atmosphere. This phenomenon is inhibited in a solar pond by dissolving salt into its bottom layer, making that water too dense to rise, even when hot. Thus, solar energy reaching the bottom of the pond is trapped, unlike the water in an ordinary pond that remains at nearly atmospheric temperature. The salt concentration increases with depth, forming a saline concentration gradient. The added salt also inhibits natural convection, allowing the cooler water on top to act as insulation and reduce evaporation. Salt water can be heated to high temperatures, even above the boiling point of fresh water. Solar ponds also differ in other ways from the ordinary ponds: solar ponds contain clear water to increase solar radiation penetration as much as possible, and the pond bottom is darkened to increase solar radiation absorption. Thermal energy is discharged from the solar pond as hot brine.

The three regions or zones of a typical solar pond can be seen in Figure 6.27 and have the following characteristics:

- The top region is the surface zone or upper convective zone (UCZ). This zone contains a homogeneous layer of low-salinity brine or fresh water. This zone is fed with fresh water of a density near to the density of fresh water in the upper part to maintain the cleanliness of the pond and replenish lost water due to evaporation.
- The middle region is the gradient zone or nonconvective zone (NCZ) or insulation zone. This zone acts as a thermally insulating layer. It contains a salinity gradient, implying water nearer the surface is less concentrated than water below it. That is, the brine density of the salty water in this



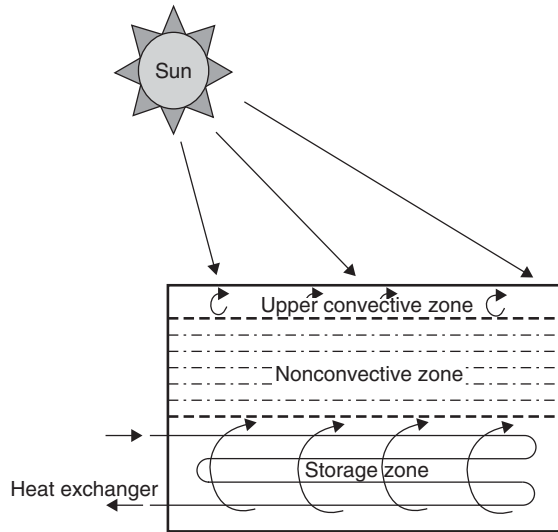


**Figure 6.27** Illustration of a solar pond

zone gradually increases toward the lower convective zone (LCZ). Hence, there is no convection in the gradient zone even when the lower zone is heated since the hotter, saltier water at the bottom of the gradient remains denser than the less salty water above it. The NCZ performs an important function in a solar pond: it allows solar radiation to penetrate into the storage zone but inhibits heat (long-wave thermal radiation) from escaping. This function is possible in part because water is opaque to infrared radiation.

- The lower region is the LCZ or heat storage zone (HSZ). This zone contains homogeneous, concentrated salty water that can be either convecting or thermally stratified. Much of the incident solar energy is absorbed and stored in this zone. This is because water transmits solar radiation well and infrared radiation poorly. Hence, solar energy that reaches and is absorbed in this zone can escape via conduction only. The thermal conductivity of water is moderately low and, if the gradient zone has substantial thickness, heat escapes upward from the lower zone slowly. The LCZ has the highest temperature, so the strongest thermal interactions occur between this zone and the adjacent insulated bottom and side walls.

Solar ponds are relatively simple devices that operate straightforwardly, require little maintenance (e.g., they need cleaning to maintain water transparency), and have long lifetimes. The pumps and piping used to maintain the salt gradient are not complex. The performance of a solar pond depends on its thermal-storage capacity, construction and maintenance, and the thermophysical properties of its components (especially the storage fluid) (Karakilcik *et al.*, 2006a, b). Solar ponds do not typically require backup systems because their high heat capacity and large thermal mass normally allow them to buffer periods of reduced solar intensity.

Various investigations of solar ponds have been reported, including modeling to facilitate examinations of performance, efficiency, and operation. The case study described here draws heavily on results reported previously (Karakilcik and Dincer, 2008).

### 6.11.1 Experimental Solar Pond

In this case study, we examine an experimental solar pond located in Adana, Turkey at Cukurova University (35°18' E longitude, 36°59' N latitude). Temperature distributions, energy and exergy



**Figure 6.28** A photo of experimental solar pond

losses, and efficiencies are measured or determined. The data allow pond performance to be obtained experimentally for 11 representative months (all but June). Significant factors affecting performance are described, for example, incident solar radiation, zone thicknesses, wall shading, and insulation.

The experimental solar pond considered in this case study (Figure 6.28) is 1.5 m deep and has a square horizontal profile of side lengths 2 m. The UCZ, NCZ, and HSZ thicknesses are 0.1 m, 0.6 m, and 0.8 m, respectively. The salt-water solution contains a NaCl reagent and fresh water. A salt gradient exists in the zones, with the pond water having a density of  $1000\text{--}1045\text{ kg/m}^3$  in the UCZ,  $1045\text{--}1170\text{ kg/m}^3$  in the NCZ and  $1170\text{--}1200\text{ kg/m}^3$  in HSZ. The bottom and the side walls of the pond are plated with 5-mm thick iron sheets, and contain a layer of glass wool insulation 50 mm thick. The solar pond has a steel base 0.5 m above the ground, which is somewhat insulated with 20 mm thick wood slats. The inner and outer side walls are covered with anti-corrosion paint. Figure 6.29 illustrates the inner zones of the solar pond and Figure 6.30 illustrates solar radiation entering the pond and the shading area by its south sidewall. The UCZ, NCZ, and HSZ thicknesses of the salt gradient solar pond are seen in Figure 6.30 to be  $X_1$ ,  $X_2 - X_1$ , and  $X_3 - X_2$ , respectively. Other property data for the solar pond parts and surroundings are listed in Table 6.15.

### 6.11.2 Data Acquisition and Analysis

#### Data Acquisition

The experimental unit used to obtain data is described in detail elsewhere, along with the experimental method and measurements (Karakilcik and Dincer, 2008; Karakilcik *et al.*, 2006a, b). The inner zones of the experimental unit (Figure 6.30) consist of three zones (eight saline water layers). The UCZ is 10 cm thick. The NCZ consists of six layers each of 10 cm thickness and having different density. The HSZ is 80 cm thick. Some details on data follow:

- Temperatures are sensed at heights from the bottom of the pond of 0.05, 0.30, 0.55, 0.70, 0.80, 1.05, 1.35, and 1.50 m, and, from the bottom of the pond downward into the insulated bottom,

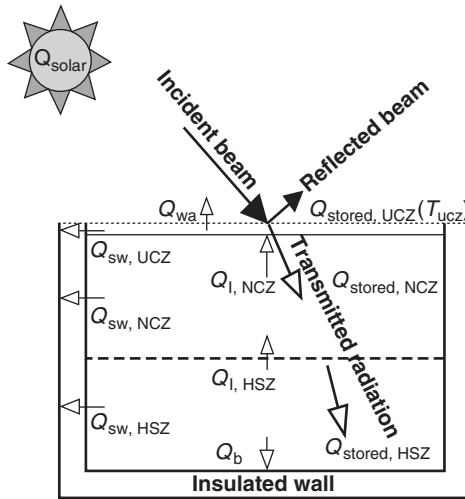


**Figure 6.29** Illustration of all heat transfers in experimental solar pond

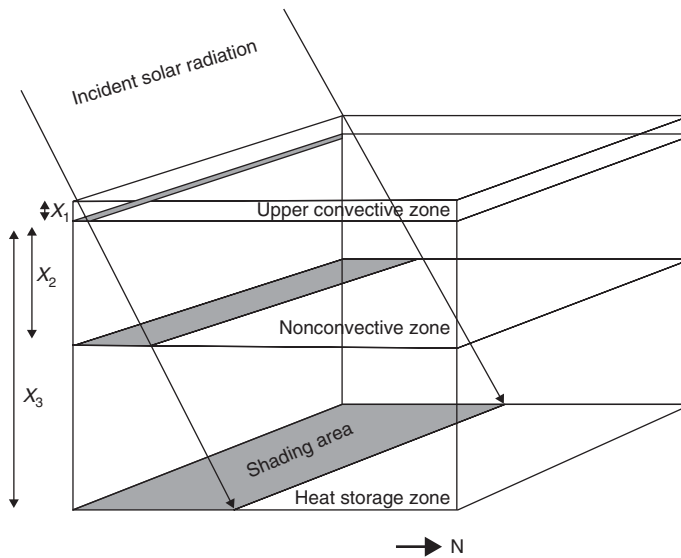


**Figure 6.30** Illustration of the three zones in the experimental solar pond

at 15 and 45 mm, and for heights from the bottom of the side wall of 0, 0.35, 0.65, 0.75, 1.00, and 1.35 m.

- Inner and wall temperatures of the pond are measured on an hourly basis during the day.
- Temperatures at the inner zones and insulated sidewall of the pond are measured by sensors with a range of  $-65^{\circ}\text{C}$  to  $+155^{\circ}\text{C}$ , and with an accuracy of  $\pm 0.1^{\circ}\text{C}$  for the temperature range of  $0^{\circ}\text{C}$  to  $120^{\circ}\text{C}$ . The sensors consist of 1N4148 semiconductor devices with coaxial cables lengths of 17 to 20 m.

**Table 6.15** Selected properties of materials comprising and surrounding experimental solar pond

Property	Storage substance		Experimental container		Surroundings
	Brine	Water	Insulation	Painted wall	Air
Density (kg/m <sup>3</sup> )	1185	998	200	7849	1.16
Specific heat (kJ/kg/K)	–	4.182	0.670	0.460	1.007
Thermal conductivity (kJ/m/K/h)	–	2.160	0.143	21.20	0.0947

Source: (Karakilcik, 2006a, b).

- Solar energy data are obtained using a pyranometer, and hourly and daily average air temperatures are obtained from a local meteorological station.
- The temperature-distribution profiles and other data are obtained using a data acquisition system (Karakilcik and Dincer, 2008).

### Data Analysis

To understand the thermal performance of a solar pond, the rates of absorption of the incident solar radiation by zone and the temperature distributions of its regions need to be determined. Part of the solar radiation incident on the solar pond is absorbed, part is reflected at the surface, and the remaining part is transmitted (see Figure 6.29). Most of the incident radiation is transmitted through the layers and part reaches the HSZ where it is converted to heat and stored.

The absorption by the salty water solutions changes with concentration of the solution. The fluid in the UCZ has uniform and low salinity (like seawater). Concentration and temperature both increase linearly with pond depth in the NCZ, while the fluid is stratified due in the LCZ to its high salinity and correspondingly varying density.

In this analysis, the pond and its three zones are separated into 30 inner layers or zones. The temperatures of the layers vary temporally and depend on various factors, such as incident solar radiation, transmission and absorption characteristics (by layer), pond dimensions, structure and insulation, shading, solar pond fluid thermophysical properties (e.g., thermal conductivity), and surrounding climate. Analysis of an experimental solar pond is generally complicated due to variations in these factors.

### Temperatures

To determine heat losses from the solar pond, experimental temperature distributions with pond height are obtained for the inner zones (see Table 6.16 and Figure 6.31). The temperatures at points in each zone are measured during the months and the monthly average temperatures are determined.

**Table 6.16** Mean monthly temperatures (in °C) of solar pond zones and surroundings

	January	February	March	April	May	July	August	September	October	November	December
Upper convective zone (UCZ)	10	12	14	18	27	33	34	33	28	20	18
Nonconvective zone (NCZ)	14	15	19	22	36	42	43	41	32	22	20
Heat storage zone (HSZ)	17	18	22	28	40	52	55	50	41	28	23
Surroundings	10	11	14	18	22	28	28	26	21	16	11

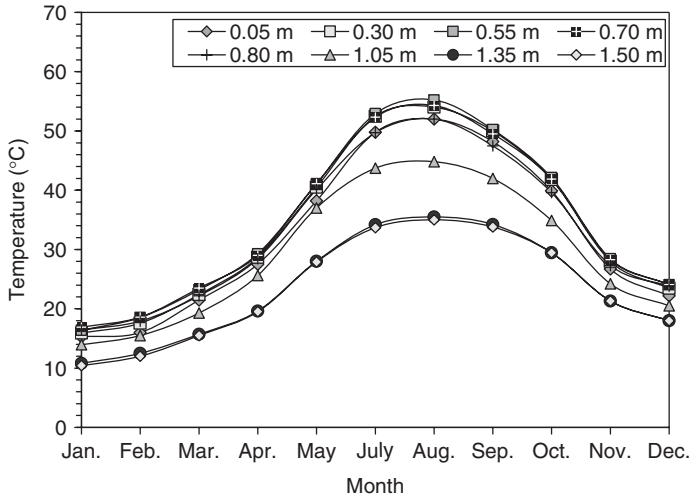


Figure 6.31 Monthly temperature distributions at various heights of the solar pond

Zone temperatures are clearly seen to vary with month, as the surrounding temperature and incoming solar radiation vary significantly monthly. Specifically, the temperature of each zone reaches a maximum in August and a minimum in January. These maximum and minimum temperatures, respectively, are 35°C and 10°C for the UCZ, 45°C and 14°C for the NCZ, and 55°C and 17°C for the HSZ. Generally, the temperatures of the zones increase with incident solar flux.

**Brine Density Gradient**

The vertical variation of brine density in the solar pond is illustrated in Figure 6.32 for each month. The monthly differences are likely attributable to the warmer conditions in summer, and are related

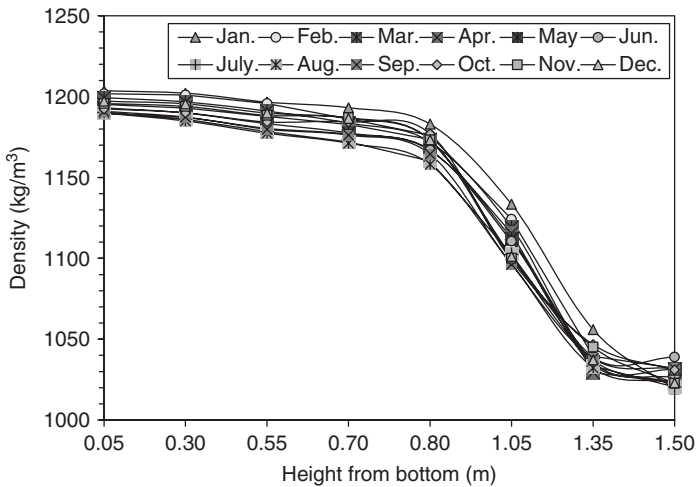


Figure 6.32 Density variation of water in the solar pond

to the absorption and reflection of incident solar radiation at the pond surface, surface heat losses to air, and the thermophysical properties of brine. As expected, increasing temperature reduces the density more in the summer months. The increase in saline density for the UCZ and the NCZ is caused by evaporation of water at the upper region. These changes can be reduced by continuously adding fresh water to the top of the pond. Significant changes are observed in the UCZ and the NCZ when salt gradient protection systems for cleaning purposes are not used.

### 6.11.3 Energy and Exergy Assessments

#### Energy Flows, Efficiencies, and Losses

Energy flows in the inner zones of the pond are illustrated in Figure 6.29. The thermal performance of the solar pond depends on incident solar radiation, shading and reflection, transmission and absorption, as well as heat flows to the surroundings and across the zones. The net energy stored in the zones is determined by using the property data in Table 6.15. Heat losses significantly affect performance; these are significant at the pond surface, but are kept very small by insulation from the sides and bottom.

The sunlit area and temperature of the zones, especially the HSZ, are affected by wall shading. The average sunny area and shaded areas, respectively, are determined to be  $3.93 \text{ m}^2$  and  $0.07 \text{ m}^2$  for the UCZ,  $3.13 \text{ m}^2$  and  $0.87 \text{ m}^2$  for the NCZ, and  $2.63 \text{ m}^2$  and  $1.37 \text{ m}^2$  for the HSZ.

The net average values of solar radiation incident on the zone sunny area during January, May, and August, respectively, are 439, 2077, and 2042 MJ for the UCZ, 352, 1662, and 1634 MJ for the NCZ, and 193, 914, and 899 MJ for the HSZ. Most of the incident solar radiation is transmitted to the NCZ through the UCZ, although some is absorbed in the NCZ. Furthermore, much of the incident solar radiation is transmitted from the NCZ to the HSZ. Little incident solar radiation is reflected from the NCZ to the UCZ. The majority of the incident radiation reaches the HSZ from the NCZ. This transmitted solar radiation from the NCZ is absorbed in the HSZ, while little of the incident solar radiation is reflected from the HSZ to the upper zones.

The energy stored in each of the zones is shown in Figure 6.33. For instance, the respective quantities of energy stored for January and August are 4 and 93 MJ in the UCZ, 311 and 225 MJ

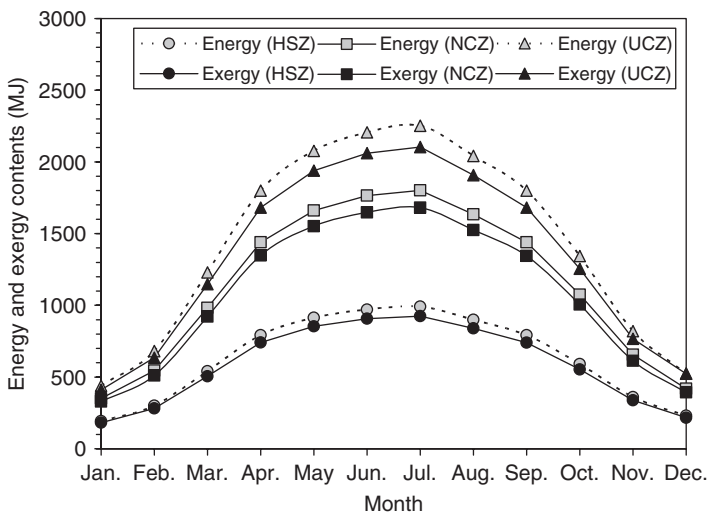


Figure 6.33 Monthly variation of energy and exergy contents of the solar pond zones

in the NCZ, and 19 and 253 MJ in the HSZ. Most of the energy is stored in the HSZ, which is responsible for the greatest heat loss.

Zone energy efficiencies are shown in Figure 6.34. The UCZ efficiencies vary from 0.9% to 4.5% for January and August, respectively. The NCZ energy efficiencies vary from 3.2% to 13.8% for January and August, respectively, while the HSZ efficiencies vary from 9.7% to 28.1% for January and August, respectively. Although the UCZ receives the greatest incident solar radiation, it exhibits the lowest zone efficiencies, mainly because of its small thickness and large surface heat losses to the surrounding air. The low UCZ efficiency is also attributable to shading. Shading significantly decreases the performance of the NCZ and the HSZ.

The performance of the solar pond as a TES depends upon the total radiation reaching its zones. In summer, much of the incident solar radiation is absorbed by the HSZ and little is reflected from the pond bottom wall. Increasing shading area from the top to the bottom of the pond reduces the solar radiation transmitted. In a solar pond, efficiencies are low since the stored energy is much smaller than the incident solar radiation on the zone surfaces. Energy losses from heat transfer to air from the UCZ reduce energy efficiency. Little of the incident solar radiation is stored in the pond and the UCZ efficiency has little impact on the overall performance of the pond compared to the NCZ. The efficiencies are dependent on the temperatures of the brine and surrounding air. The monthly temperature variations between the zones affect the diffusion of salt molecules from the pond bottom and heat losses.

To better understand the true magnitudes of thermodynamic efficiencies and losses for the solar pond and to potentially improve performance, exergy analysis is useful. This is the topic of the next section.

### Exergy Flows, Efficiencies, and Losses

By clarifying and correcting many of the weaknesses of energy analysis of solar pond systems, exergy analysis is useful for analysis, design, and improvement. For instance, exergy analysis assesses meaningful efficiencies and losses. Corresponding exergy flows for the energy flows in Figure 6.29 for each of the zones in the pond can be determined. Also, energy and exergy efficiencies are compared for the three pond zones. Here, the exergy of the solar radiation is expressed assuming a surface temperature for the sun of 6000 K, using an expression proposed by Petala (2003).

Monthly energy and exergy contents for the pond zones, determined using average temperatures in Table 6.16, are shown in Figure 6.33. The energy and exergy contents follow the solar irradiation annual profile, with the lowest exergy contents observed in January and the highest in July. The energy contents exceed the corresponding exergy contents. Energy is conserved, so the only energy losses are heat emissions to the surroundings. Exergy can also be lost to the surrounding but it is also destroyed in each zone due to irreversibilities and processes like mixing fluids of different temperatures. The temperature of the surroundings affects energy and exergy losses significantly since both involve losses to the ambient air.

Monthly variations in exergy input, exergy recovered and exergy destruction and losses for the zones are provided in Table 6.17 (except for June when maintenance was performed on the data acquisition system). The exergy recovered and the exergy destruction and losses sum to the exergy input. The exergy input for all zones is greatest in July when incoming solar irradiation is greatest, and the other exergy terms vary somewhat in proportion to the exergy input.

Exergy accumulation is assumed not to occur in the UCZ, since it is less than 1%. Exergy accumulation is also assumed negligible for the NCZ. The exergy recovered in the UCZ is transferred to the NCZ. The exergy recovered from the UCZ varies from 392 MJ in January to 1682 MJ in July. Similarly, exergy recovered in the NCZ is transferred to the HSZ. The exergy recovered from the NCZ varies from 18 MJ in January to 958 MJ in July. In the HSZ, exergy is stored rather than recovered, permitting solar ponds to perform daily or seasonal storage. Much less exergy is stored in the HSZ than the exergy input and the exergy destruction and losses. The exergy recovered from the NCZ varies from 170 MJ in January to 743 MJ in July.

**Table 6.17** Mean monthly exergy parameters (in MJ) for solar pond zones

	January	February	March	April	May	July	August	September	October	November	December
<b>Input</b>											
UCZ	417	644	1161	1700	1976	2168	1982	1740	1300	783	506
NCZ	335	517	931	1363	1588	1748	1601	1404	1049	629	408
HSZ	188	291	525	768	885	959	869	767	573	350	224
<b>Recovered or stored*</b>											
UCZ	329	511	920	1348	1553	1682	1525	1345	1005	614	393
NCZ	188	291	525	768	885	958	869	766	573	350	224
HSZ	17	27	53	89	141	204	218	181	133	57	28
<b>Loss**</b>											
UCZ	88	133	241	352	423	486	457	395	295	169	113
NCZ	147	226	406	595	703	790	732	638	476	279	184
HSZ	171	264	472	679	744	755	651	586	440	293	196

\*Values for HSZ are stored exergy and for UCZ and NCZ are recovered exergy.

\*\*Includes exergy destruction and waste exergy emission.

Monthly energy and exergy efficiencies for the zones of the solar pond are presented in Figure 6.34. The exergy efficiencies are lower than the energy efficiencies for each pond zone. The differences between energy and exergy efficiencies are smaller in winter than summer. The efficiencies for the HSZ are higher than the corresponding efficiencies for the UCZ and NCZ. The pond inner zones store more exergy in the summer than the winter. The exergy destruction and losses significantly affect the performance and detract from system efficiency.

### 6.11.4 Potential Improvements

The energy and exergy analyses using experimental data reported in this case study of a solar pond has demonstrated that performance is affected strongly by the variation of temperature with

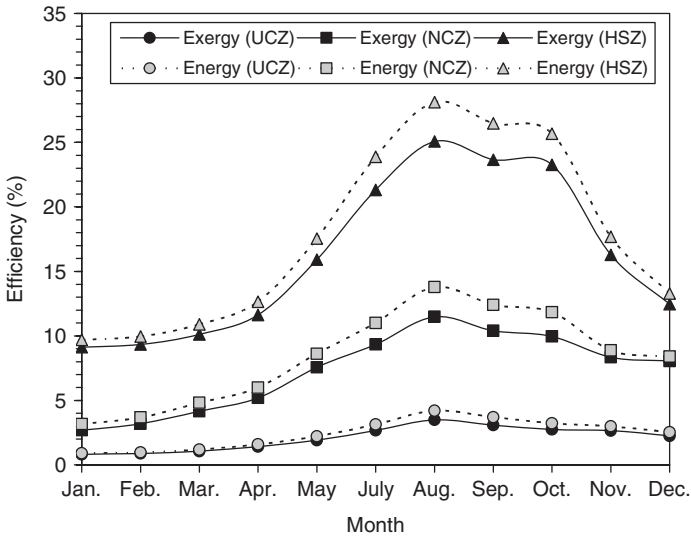


**Figure 6.34** Monthly variation of energy and exergy efficiencies of the solar pond zones



depth, especially the LCZ temperature, and that the temperature of the zones is affected by incident radiation, zone thickness, shading, and thermal losses.

To increase the pond efficiency, several modifications could be considered:

- Heat losses and solar radiation reflection from upper zone should be reduced, as should shading and thermal losses from the bottom and side walls.
- Zone thicknesses should be modified where practical. This modification would also enhance the stability of the pond.
- Energy and exergy efficiencies and losses of the pond zones should be applied to help determine the best operating state.

## 6.12 Concluding Remarks

This chapter has demonstrated that the use of exergy analysis is very important in developing a good understanding of the thermodynamic behavior of TES systems, and for rationally assessing, comparing, and improving their efficiencies.

Methods identified by exergy analysis as having high improvement potential for TES systems are only limited by the creativity and knowledge of engineers and designers, and can include:

- reducing thermal losses (heat leakage from hot TES systems and heat infiltration to cold TES systems) by improving insulation levels and distributions;
- avoiding temperature degradation by using smaller heat-exchanger temperature differences, ensuring that heat flows of appropriate temperatures are used to heat cooler flows, and increasing heat-exchanger efficiencies;
- avoiding mixing losses by retaining and taking advantage of thermal stratification; and
- reducing pumping power by using more efficient pumps, reduced-friction heat-transfer fluids, and appropriate heat-recovery threshold temperatures.

The authors feel that the development is required of standard TES evaluation methodologies which take into account the thermodynamic considerations discussed in this chapter. By accounting for these considerations, meaningful methodologies can be developed for assessing the comparative value of alternative storages. In particular, the use of exergy analysis (and related concepts) is important because it clearly takes into account the loss of availability and temperature of heat in storage operations, and hence it more correctly reflects the thermodynamic and economic value of the storage operation.

Without methodologies capable of providing perceptive measures of technical, and ultimately of competitive economic performance, the development of better technology will be unscientific and disorganized, and open to subjective assessments of accomplishment. The development of better assessment methodologies will ensure effective use of energy resources by providing the basis for identifying the more productive directions for development of TES technology, and identifying the better systems without the lengthy and inefficient process of waiting for them to be sorted out by competitive economic success in the marketplace.

### *Nomenclature*

$A$	surface area
$c$	specific heat
$c_p$	specific heat at constant pressure
$c_v$	specific heat at constant volume
$C$	heat capacity rate
$e$	specific energy

$E$	energy
$f$	fraction; mean height fraction
$F$	fraction of storage-fluid mass in liquid phase
$h$	specific enthalpy; specific base enthalpy; height (relative to TES bottom)
$H$	enthalpy; TES fluid height
$i$	time-step increment
$I$	exergy consumption due to irreversibilities
$ke$	specific kinetic energy
$m$	mass
$N$	moles
NTU	number of transfer units
$pe$	specific potential energy
$P$	absolute pressure
$Q$	heat
$R$	thermal resistance
$s$	specific entropy
$S$	entropy
$t$	time
$T$	temperature
$u$	specific internal energy
$U$	internal energy; overall heat-transfer coefficient
$v$	specific volume
$V$	volume
$W$	shaft work
$x$	mass fraction
$X$	thermal exergy (i.e., the exergy associated with heat $Q$ )
$y$	mole fraction

### *Greek Symbols*

$\alpha$	constant parameter
$\varepsilon$	specific flow exergy; heat-exchanger effectiveness
$\in$	flow exergy
$\eta$	energy efficiency
$\theta$	parameter
$\mu$	chemical potential
$\zeta$	specific exergy
$\Xi$	exergy
$\Pi$	entropy production
$\rho$	density
$\tau$	exergetic temperature factor
$\phi$	zone temperature distribution
$\psi$	exergy efficiency

### *Subscripts*

$a$	inlet flow during charging; adiabatic; parameter
$amb$	ambient
$b$	outlet flow during charging; bottom; parameter

<i>c</i>	injected during charging period; charging; inlet flow during discharging
<i>d</i>	recovered during discharging period; discharging; outlet flow during discharging
<i>e</i>	exit; equivalent
<i>f</i>	final
<i>i</i>	initial; <i>i</i> th constituent; inlet
<i>j</i>	zone
<i>jk</i>	number of zones
<i>min</i>	minimum
<i>kin</i>	kinetic component
<i>l</i>	loss
<i>m</i>	mixed
<i>n</i>	nonadiabatic
<i>net</i>	net
<i>o</i>	environmental state; chemical exergy; outlet
<i>oo</i>	dead state
<i>p</i>	product
<i>ph</i>	physical component
<i>pot</i>	potential component
<i>r</i>	region of heat interaction
<i>s</i>	solid state; storage fluid
<i>st</i>	storage (overall)
<i>t</i>	threshold; top; liquid state
<i>T</i>	total
<i>th</i>	thermocline zone (zone 2)
<i>w</i>	working fluid
1	charging period
2	storing period
3	discharging period

### *Superscripts*

.	rate with respect to time
–	mean
'	modified case
A	case A
B	case B; basic three-zone model
C	case C; continuous-linear model
D	case D
G	general-linear model
L	linear model
s	step
S	stepped model
T	general three-zone model

### *Acronyms*

ATES	aquifer thermal energy storage
CTES	cold thermal energy storage
ITES	ice thermal energy storage
TES	thermal energy storage

## References

- Adebiyi, G.A., Hodge, B.K., Steele, W.G., Jalalzadeh-Aza, A. and Nsofor, E.C. (1996). Computer simulations of a high temperature thermal energy storage system employing multiple families of phase-change storage materials, *Journal of Energy Resources Technology* 118, 102–111.
- Ahern, J.E. (1980). *The Exergy Method of Energy System Analysis*, Wiley, New York.
- Ahrendts, J. (1980). Reference states, *Energy-The International Journal* 5, 667–678.
- Alefeld, G. (1990). What are thermodynamic losses and how to measure them? *A Future for Energy: Proc. of the Florence World Energy Research Symposium*, Firenze, Italy, pp. 271–279.
- Althof, J. (1989). Economic feasibility of thermal storage, *Heating/Piping/Air Conditioning* September, 159–163.
- Badar, M.A., Zubair, S.M. and Al-Farayehdi, A.A. (1993). Second-law-based thermoeconomic optimization of a sensible heat thermal energy storage system, *Energy* 18, 641–649.
- Baehr, H.D. and Schmidt, E.F. (1963). Definition und berechnung von brennstoffexergien (Definition and calculation of fuel exergy), *Brennst-Waerme-Kraft* 15, 375–381.
- Barbaris, L.N., Hooper, F.C. and Rosen, M.A. (1988). The relationship between storage period duration and measures of the overall performance of sensible thermal energy storages, *Proceedings of the International Conference on Applied Geothermal Energy and Thermal Energy Storage*, France, pp. 723–727.
- Bascetincelik, A., Ozturk, H.H., Paksoy, H.O. and Demirel, Y. (1998). Energetic and exergetic efficiency of latent heat storage system for greenhouse heating, *Renewable Energy* 16, 691–694.
- Beckman, G. and Gilli, P.V. (1984). *Thermal Energy Storage*, Springer-Verlag, New York.
- Beggs, C. (1991). The economics of ice thermal storage, *Building Research and Information* 19, 342–355.
- Bejan, A. (1978). Two thermodynamic optima in the design and operation of thermal energy storage systems, *Journal of Heat Transfer* 100, 708–712.
- Bejan, A. (1982). Thermal energy storage, Chapter 8, In: *Entropy Generation through Heat and Fluid Flow*, Wiley, New York, pp. 158–172.
- Bejan, A. (1995). *Entropy Generation Minimization: The Method of Thermodynamic Optimization of Finite-Size Systems and Finite-Time Processes*, CRC Press, Boca Raton, Florida.
- Bjurstrom, H. and Carlsson, B. (1985). An exergy analysis of sensible and latent heat storage, *Heat Recovery Systems* 5, 233–250.
- Bosnjakovic, F. (1963). Bezugszustand der exergie eines reagierenden systems (Reference states of the exergy in a reacting system), *Forschung Im Ingenieurwesen* 20, 151–152.
- Brosseau, P. and Lacroix, M. (1998). Numerical simulation of a multi-layer latent heat thermal energy storage system, *International Journal of Energy Research* 22, 1–15.
- Carrier (1990). *Encapsulated Ice Store*, USA.
- Chase, M.W., Davies, C.A., Downey, J.R., et al., eds. (1985). *JANAF Thermochemistry Tables*, 3<sup>rd</sup> edition, American Chemical Society and American Inst. of Physics, Washington, DC.
- Chen, C.S. and Sheen, J.N. (1993). Cost benefit analysis of a cooling energy storage system, *IEEE Transactions on Power Systems* 8 (4), 1504–1510.
- Costa, M., Buddhi, D. and Oliva, A. (1998). Numerical simulation of a latent heat thermal energy storage system with enhanced heat conduction, *Energy Conversion and Management* 39, 319–330.
- Crane, P., Scott, D.S. and Rosen, M.A. (1992). Comparison of exergy of emissions from two energy conversion technologies, considering potential for environmental impact, *International Journal of Hydrogen Energy* 17, 345–350.
- De Lucia, M. and Bejan, A. (1990). Thermodynamics of energy storage by melting due to conduction or natural convection, *ASME Journal of Solar Energy Engineering* 112, 110–116.
- Dincer, I. (1999). Evaluation and selection of energy storage systems for solar thermal applications, *International Journal of Energy Research* 23, 1017–1028.
- Dincer, I. and Dost, S. (1996). A perspective on thermal energy storage systems for solar energy applications, *International Journal of Energy Research* 20, 547–557.
- Dincer, I., Dost, S. and Li, X. (1997a). Performance analyses of sensible heat storage systems for thermal applications, *International Journal of Energy Research* 21, 1157–1171.
- Dincer, I., Dost, S. and Li, X. (1997b). Thermal energy storage applications from an energy saving perspective, *International Journal of Global Energy Issues* 9, 351–364.

- Dincer, I. and Rosen, M.A. (2007). *Exergy: Energy, Environment and Sustainable Development*, Elsevier, Oxford, UK.
- Domanski, R. and Fellah, G. (1998). Thermoeconomic analysis of sensible heat, thermal energy storage systems, *Applied Thermal Engineering* 18 (8), 693–704.
- Edgerton, R.H. (1982). *Available Energy and Environmental Economics*, D.C. Heath, Toronto.
- Fanny, A.H. and Klein, S.A. (1988). Thermal performance comparisons for solar hot water systems subjected to various collector and heat exchanger flow rates, *Solar Energy* 40, 1–11.
- Fields, W.M.G. and Knebel, D.E. (1991). Cost effective thermal energy storage, *Heating/Piping/Air Conditioning*, July, 59–72.
- Gaggioli, R.A. (1983). Second law analysis to improve process and energy engineering, In *Efficiency and Costing: Second Law Analysis of Processes* (ed. R.A. Gaggioli), Vol. 235, ACS Symposium Series, American Chemical Society, Washington, DC, pp. 3–50.
- Gaggioli, R.A. and Petit, P.J. (1977). Use the second law first, *Chemtech* 7, 496–506.
- Gretarsson, S.P., Pedersen, C.O. and Strand, R.K. (1994). Development of a fundamentally based stratified thermal storage tank model for energy analysis calculations, *ASHRAE Transactions* 100, 1213–1220.
- Gunnawiek, L.H., Nguyen, S. and Rosen, M.A. (1993). Evaluation of the optimum discharge period for closed thermal energy storages using energy and exergy analyses, *Solar Energy* 51, 39–43.
- Gunnawiek, L.H. and Rosen, M.A. (1998). Relation between the exergy of waste emissions and measures of environmental impact, *International Journal of Environment & Pollution* 10, 261–272.
- Hafele, W. (ed.) (1981). Energy, negentropy, and endowments, Chapter 21, In *Energy in a Finite World: A Global Systems Analysis*, Ballinger, Toronto, pp. 693–705.
- Hahne, E. (1986). Thermal energy storage: some views on some problems, *Proceedings of the 8<sup>th</sup> International Heat Transfer Conference*, San Francisco, pp. 279–292.
- Hahne, E., Kubler, R. and Kallewit, J. (1989). The evaluation of thermal stratification by exergy, In *Energy Storage Systems* (ed. B. Kilikis and S. Kakac), Kluwer, Dordrecht, pp. 465–485.
- Hevert, H.W. and Hervert, S.C. (1980). Second law analysis: an alternative indicator of system efficiency, *Energy-The International Journal* 5, 865–873.
- Homan, K.O., Sohn, C.W. and Soo, S.L. (1996). Thermal performance of stratified chilled water storage tanks, *HVAC and R Research* 2 (2), 158–170.
- Hooper, F.C., Barbaris, L.N. and Rosen, M.A. (1988). An engineering approach to the evaluation of the performance of stratified thermal energy storages, *Proceedings of the International Conference on Applied Geothermal Energy and Thermal Energy Storage*, Versailles, France, pp. 155–160.
- Hoyer, M.C., Walton, M., Kanivetsky, R. and Holm, T.R. (1985). Short-term aquifer thermal energy storage (ATES) test cycles, St. Paul, Minnesota, U.S.A., *Proceedings of the 3<sup>rd</sup> International Conference on Energy Storage for Building Heating and Cooling*, Toronto, Canada, pp. 75–79.
- Ismail, K.A.R., Leal, J.F.B. and Zanardi, M.A. (1997). Models of liquid storage tanks, *Energy-The International Journal* 22, 805–815.
- Ismail, K.A.R. and Stuginsky, R. (1999). A parametric study on possible fixed bed models for PCM and sensible heat storage, *Applied Thermal Engineering* 19, 757–788.
- Jansen, J. and Sorensen B. (1984). *Fundamentals of Energy Storage*, Wiley, New York.
- Jenne, E.A. (ed.) (1992). *Aquifer Thermal Energy (Heat and Chill) Storage*, Pacific Northwest Lab, Richland, WA.
- Karakilcik, M. and Dincer, I. (2008). Exergetic performance analysis of a solar pond. *International Journal Thermal Sciences* 47, 93–102.
- Karakilcik, M., Dincer, I. and Rosen, M.A. (2006a). Performance investigation of a solar pond. *Applied Thermal Engineering* 26, 727–735.
- Karakilcik, M., Kiyamac, K. and Dincer, I. (2006b). Experimental and theoretical temperature distributions in a solar pond. *International Journal of Heat and Mass Transfer* 49, 825–835.
- Keenan, J.H., Chao, J. and Kayle, J. (1992). *Gas Tables International Version. Properties of Air Products of Combustion and Component Gases Compressible Flow Functions*, Krieger, Florida.
- Kestin, J. (1980). Availability: the concept and associated terminology, *Energy-The International Journal* 5, 679–692.
- Kleinbach, E.M., Beckman, W.A. and Klein, S.A. (1993). Performance study of one-dimensional models for stratified thermal storage tanks, *Solar Energy* 50, 155–166.
- Kotas, T.J. (1995). *The Exergy Method of Thermal Plant Analysis*, reprint edition, Krieger, Florida.

- Kotas, T.J., Raichura, R.C. and Mayhew, Y.R. (1987). Nomenclature for exergy analysis, In *Second Law Analysis of Thermal Systems* (ed. M.J. Moran E. Sciubba), ASME, New York, pp. 171–176.
- Krane, R.J. (1985). A second law analysis of a thermal energy storage system with Joulean heating of the storage element, *Paper 85-WA/HT-19, ASME Winter Annual Meeting*, 17-21 Nov., Miami.
- Krane, R.J. (1987). A second law analysis of the optimum design and operation of thermal energy storage systems, *International Journal of Heat and Mass Transfer* 30, 43–57.
- Krane, R.J. and Krane, M.J.M. (1991). The optimum design of stratified thermal energy storage systems, *Proceedings of the International Conference on the Analysis of Thermal and Energy Systems*, Greece, pp. 197–218.
- Laouadi, A. and Lacroix, M. (1999). Thermal performance of a latent heat energy storage ventilated panel for electric load management, *International Journal of Heat and Mass Transfer* 42, 275–286.
- Lightstone, M., Hollands, K.G.T. and Hassani, A.V. (1988). Effect of plume entrainment in the storage tank on calculated solar energy performance, *Energy Solutions for Today: Proceedings of the 14<sup>th</sup> Annual Conference of Solar Energy Society of Canada*, Canada, pp. 236–241.
- Lucca, G. (1990). The exergy analysis: role and didactic importance of a standard use of basic concepts, terms and symbols, *A Future For Energy: Proceedings of the Florence World Energy Research Symposium*, Firenze, Italy, pp. 295–308.
- Maloney, D.P. and Burton, J.R. (1980). Using second law analysis for energy conservation studies in the petrochemical industry, *Energy-The International Journal* 5, 925–930.
- Mathiprakasam, B. and Beeson, J. (1983). Second law analysis of thermal energy storage devices, *Proceedings of the AIChE Symposium Series, National Heat Transfer Conference*, Seattle, Washington, DC.
- Mavros, P., Belesiotis, V. and Haralambopoulos, D. (1994). Stratified energy storage vessels-characterization of performance and modeling of mixing behavior, *Solar Energy* 52, 327–336.
- Moran, M.J. (1989). *Availability Analysis: A Guide to Efficient Energy Use*, ASME, New York.
- Moran, M.J. (1990). Second law analysis. What is the state of the art? A future for energy, *Proceedings of the Florence World Energy Research Symposium*, Firenze, Italy, pp. 249–260.
- Moran, M.J. and Keyhani, V. (1982). Second law analysis of thermal energy storage systems, *Proceedings of the 7<sup>th</sup> International Heat Transfer Conference* Vol. 6, Munich, pp. 473–478.
- Moran, M.J. and Shapiro, H.N. (2000). *Fundamentals of Engineering Thermodynamics*, 4<sup>th</sup> edition, Wiley, Toronto.
- Morris, D.R., Steward, F.R., and Szargut, J. (1988). *Exergy Analysis of Thermal, Chemical and Metallurgical Processes*, Springer-Verlag, New York.
- Nelson, J.E.B., Balakrishnan, A.R. and Murthy, S.S. (1999). Experiments on stratified chilled water tanks, *International Journal of Refrigeration* 22 (3), 216–234.
- Petala, R. (2003). Exergy of undiluted thermal radiations. *Solar Energy* 74, 469–488.
- Rodriguez, L.S.J. (1980). Calculation of available-energy quantities, in *Thermodynamics: Second Law Analysis* (ed. R.A. Gaggioli), American Chemical Society, Washington, DC, pp. 39–60.
- Rosen, M.A. (1990). Evaluation of the heat loss from partially buried, bermed heat storage tanks, *International Journal of Solar Energy* 9, 147–162.
- Rosen, M.A. (1991). On the importance of temperature in performance evaluations for sensible thermal energy storage systems, *Proceedings of the Biennial Congress International Solar Energy Society* (ed. M.E. Arden, S.M.A. Burley and M. Coleman), Vol. 2, Part II, Pergamon, New York, pp. 1931–1936.
- Rosen, M.A. (1992a). Evaluation of energy utilization efficiency in Canada using energy and exergy analyses, *Energy-The International Journal* 17, 339–350.
- Rosen, M.A. (1992b). Appropriate thermodynamic performance measures for closed systems for thermal energy storage, *ASME Journal of Solar Energy Engineering* 114, 100–105.
- Rosen, M.A. (1998a). A semi-empirical model for assessing the effects of berms on the heat loss from partially buried heat storage tanks, *International Journal of Solar Energy* 20, 57–77.
- Rosen, M.A. (1998b). The use of berms in thermal energy storage systems: energy-economic analysis, *Solar Energy* 63 (2), 69–78.
- Rosen, M.A. (1999a). Second law analysis: approaches and implications, *International Journal of Energy Research* 23 (5), 415–429.
- Rosen, M.A. (1999b). Second-law analysis of aquifer thermal energy storage systems, *Energy-The International Journal* 24, 167–182.

- Rosen, M.A. and Dincer, I. (1997a). On exergy and environmental impact, *International Journal of Energy Research* 21, 643–654.
- Rosen, M.A. and Dincer, I. (1997b). Sectoral energy and exergy modeling of Turkey, *ASME Journal of Energy Resources Technology* 119, 200–204.
- Rosen, M.A. and Dincer, I. (1999a). Thermal storage and exergy analysis: the impact of stratification, *Transactions of CSME* 23 (1B), 173–186.
- Rosen, M.A. and Dincer, I. (1999b). Exergy analysis of waste emissions, *International Journal of Energy Research* 23 (13), 1153–1163.
- Rosen, M.A., Dincer, I. and Pedinelli, N. (2000). Thermodynamic performance of ice thermal energy storage systems, *ASME Journal of Energy Resources Technology* 122 (4), 205–211.
- Rosen, M.A. and Hooper, F.C. (1991a). A general method for evaluating the energy and exergy contents of stratified thermal energy storages for linear-based storage fluid temperature distributions, *Proceedings of the 17<sup>th</sup> Annual Conference of the Solar Energy Society of Canada*, Toronto, pp. 182–187.
- Rosen, M.A. and Hooper, F.C. (1991b). Evaluating the energy and exergy contents of stratified thermal energy storages for selected storage-fluid temperature distributions, *Proceedings of the Biennial Congress of International Solar Energy Society*, Denver, pp. 1961–1966.
- Rosen, M.A. and Hooper, F.C. (1992). Modeling the temperature distribution in vertically stratified thermal energy storages to facilitate energy and exergy evaluation, in *Thermodynamics and the Design, Analysis and Improvement of Energy Systems*, AES-Vol 27/HTD-Vol. 228 (ed. R.F. Boehm), American Society of Mechanical Engineers, New York, pp. 247–252.
- Rosen, M.A. and Hooper, F.C. (1994). Designer-oriented temperature-distribution models for vertically stratified thermal energy storages to facilitate energy and exergy evaluation, *Proceedings of the 6<sup>th</sup> International Conference on Thermal Energy Storage*, Espoo, Finland, pp. 263–270.
- Rosen, M.A., Hooper, F.C. and Barbaris, L.N. (1988) Exergy analysis for the evaluation of the performance of closed thermal energy storage systems, *ASME Journal of Solar Energy Engineering* 110, 255–261.
- Rosen, M.A. and Horazak, D.A. (1995). Energy and exergy analyses of PFBC power plants, Chapter 11, In *Pressurized Fluid Bed Combustion* (ed. M. Alvarez-Cuenca and E.J. Anthony), Chapman & Hall, London, pp. 419–448.
- Rosen, M.A., Nguyen, S. and Hooper, F.C. (1991). Evaluating the energy and exergy contents of vertically stratified thermal energy storages, *Proceedings of the 5<sup>th</sup> International Conference on Thermal Energy Storage*, Scheveningen, The Netherlands, pp. 7.4.1–7.4.6.
- Rosen, M.A., Pedinelli, N. and Dincer, I. (1999) Energy and exergy analyses of cold thermal storage systems, *International Journal of Energy Research* 23 (12), 1029–1038.
- Rosen, M.A. and Scott, D.S. (1987). On the sensitivities of energy and exergy analyses to variations in dead-state properties, In *Analysis and Design of Advanced Energy Systems*, AES-Vol. 3-1, ASME, New York, pp. 23–32.
- Rosen, M.A. and Scott, D.S. (1998). Comparative efficiency assessments for a range of hydrogen production processes, *International Journal of Hydrogen Energy* 23, 653–659.
- Rosen, M.A. and Tang, R. (1997). Increasing the exergy storage capacity of thermal storages using stratification, In *Proceedings of the ASME Advanced Energy Systems Division*, AES-Vol. 37 (ed. M.L. Ramalingam, J.L. Lage, V.C. Mei and J.N. Chapman), ASME, New York, pp. 109–117.
- Rosenblad, G. (1985). Quality loss from seasonal storage of heat in rock, magnitude and evaluation, *Proceedings of the 3<sup>rd</sup> International Conference on Energy Storage for Building Heating and Cooling*, Toronto, pp. 594–599.
- Saborio-Aceves, S., Nakamura, H. and Reistad, G.M. (1994). Optimum efficiencies and phase change temperature in latent heat storage systems, *Journal of Energy Resources Technology* 116, 79–86.
- Sussman, M.V. (1980). Steady-flow availability and the standard chemical availability, *Energy-The International Journal* 5, 793–804.
- Sussman, M.V. (1981). Second law efficiencies and reference states for exergy analysis, *Proceedings of the 2<sup>nd</sup> World Congress Chemical Engineering*, Canadian Society of Chemical Engineers, Montreal, pp. 420–421.
- Szargut, J. (1967). Grenzen fuer die anwendungsmoeglichkeiten des exergiebegriffs (Limits of the applicability of the exergy concept), *Brennstoff-Waerme-Kraft* 19, 309–313.
- Taylor, M.J. (1986). Second law optimization of a sensible heat thermal energy storage System with a distributed storage element, MS Thesis, Department of Mechanical and Aerospace Engineering, University of Tennessee, Knoxville.



- Wepfer, W.J. and Gaggioli, R.A. (1980). Reference datums for available energy, in *Thermodynamics: Second Law Analysis*, Vol. 122 (ed. R.A. Gaggioli), ACS Symposium Series, American Chemical Society, Washington, DC, pp. 77–92.
- Wood, L.L., Miedema, A.K. and Cates, S.C. (1994). Modeling the technical and economic potential of thermal energy storage systems using pseudo-data analysis, *Resource and Energy Economics* 16, 123–145.
- Yoo, H., Kim, C.-J. and Kim, C. (1998). Approximate analytical solutions for stratified thermal storage under variable inlet temperature, *Solar Energy* 66, 47–56.

## Study Questions/Problems

- 6.1 What is exergy and how is it different from energy?
- 6.2 What are the different types of exergy?
- 6.3 Describe the significance of the reference environment in exergy analysis.
- 6.4 The mean summer temperature in a particular location is  $26^{\circ}\text{C}$  and the mean winter temperature is  $-2^{\circ}\text{C}$ . What would be an appropriate reference-environment temperature for assessing the performance of a diurnal TES in winter? What would be an appropriate reference-environment temperature for assessing the performance of a diurnal TES in spring? What would be an appropriate reference-environment temperature for assessing the performance of a seasonal TES that collects heat during the summer and utilizes it during the winter?
- 6.5 What is the exergy transfer associated with a heat transfer of 1000 kJ at 400 K, in a reference environment at 300 K?
- 6.6 What is the exergy flow rate associated with a flow of electrical power of 1000 kW? Does the answer depend on the reference environment?
- 6.7 What is the exergy flow rate associated with a mass flow rate of water of 25 kg/s at 2 atm and 360 K, in a reference environment at 290 K and ambient pressure?
- 6.8 What are the two main types of exergy losses? Do they have energy-based counterparts?
- 6.9 Describe the steps involved in performing an exergy analysis of a TES system.
- 6.10 What is the energy loss for a TES in which 1000 kJ of thermal energy is injected during charging and 700 kJ of thermal energy is recovered during discharging? What is the energy efficiency of the TES?
- 6.11 For the previous question, if the thermal energy is injected at  $90^{\circ}\text{C}$  and recovered at  $55^{\circ}\text{C}$ , and if the reference-environment temperature is  $10^{\circ}\text{C}$ , what would be the exergy loss and the exergy efficiency of the TES? Estimate the breakdown of the exergy loss into exergy associated with waste heat emission and exergy loss due to internal exergy destruction.
- 6.12 Identify and compare several possible TES energy efficiencies. Repeat this task for TES exergy efficiencies. Then, compare and contrast the energy and exergy efficiencies.
- 6.13 How does stratification improve the exergy efficiency of a TES?
- 6.14 Describe at least four causes of loss of stratification in a TES.
- 6.15 If the heat loss from a TES during a period of operation is 20 kJ during charging, 80 kJ during storing, and 10 kJ during discharging, what is the heat loss from the TES during the overall period?
- 6.16 The exergy associated with surface heat losses from a TES is 200 kJ, but the overall exergy loss for the TES is 450 kJ. Explain why these values are not the same.
- 6.17 A closed TES undergoes a charging process in which heat is transferred to it from a stream of 4000 kg of water which enters at  $70^{\circ}\text{C}$  and leaves at  $55^{\circ}\text{C}$ . Heat is recovered from the storage



by a stream of 2500 kg of water entering at 20 °C and leaving at 40 °C. Determine for the TES, the energy input, the energy recovered, the energy lost, and the energy efficiency. Also, determine for the TES, the exergy input, the exergy recovered, the exergy lost, and the exergy efficiency. Compare the answers and explain the differences between the energy and exergy parameters. Assume an appropriate reference-environment condition.

- 6.18** A closed TES undergoes a charging process in which heat is transferred to it from a stream of fluid which enters at 80 °C and leaves at 40 °C, and heat is recovered from the storage by a stream of fluid entering at 20 °C. Could the heat-recovery fluid exit at a temperature above 80 °C? Could the heat-recovery fluid exit at a temperature above 40 °C but below 80 °C? The reference-environment temperature is 15 °C. Justify your answers.
- 6.19** If the exergy efficiency is equal to the energy efficiency for a closed TES which receives a heat flow during charging at a certain temperature, what must be the relation between the charging and discharging temperatures?
- 6.20** For an aquifer TES storing heating capacity, a threshold temperature below which heat is not recovered is sometimes applied. Is the energy or exergy efficiency of the ATES more affected by the application of this threshold? Explain why the exergy efficiency is only slightly affected by the threshold application.
- 6.21** As an underground water resource, there are concerns about the quality of waters in aquifers. Discuss the potential for contamination of aquifer water if it is used for thermal energy storage. Also, investigate environmental and other regulations that exist in your jurisdiction related to the use of aquifer as underground thermal energy storages.
- 6.22** Does thermal stratification increase or decrease the exergy efficiency of a TES containing a fixed quantity of energy? Does thermal stratification increase or decrease the energy efficiency of the TES? Justify your answers.
- 6.23** Determine the exergy content of a water storage which is stratified with an upper temperature of 60 °C and a lower temperature of 40 °C, assuming the stepped temperature-distribution model with two steps applies. The mass of water in the storage is 200 kg and the reference-environment temperature is 20 °C.
- 6.24** Determine the exergy content of a water storage which is stratified with an upper temperature of 40 °C and a lower temperature of 20 °C, assuming the linear temperature-distribution model applies. The mass of water in the storage is 200 kg and the reference-environment temperature is 20 °C.
- 6.25** Determine the exergy content of a water storage in the previous question after a long period of time has passed and the storage fluid becomes fully mixed, assuming no heat is lost from the TES. The mass of water in the storage is 200 kg and the reference-environment temperature is 20 °C.
- 6.26** What is the main weakness of the linear temperature distribution model for vertical thermal stratification in a TES?
- 6.27** Heat storages can exhibit vertical thermal stratification. Can cold storages be thermally stratified? Justify your answer.
- 6.28** What types of physical and other methods can be used to maintain thermal stratification of a TES? Discuss how they work. Explain how they contribute to increasing the exergy content of a TES.
- 6.29** To provide an equivalent amount of storage of cooling capacity, how does the volume of an ice-based cold TES compare to the volume of a liquid water-based cold TES? Justify your answer.
- 6.30** What is the thermocline in a TES?
- 6.31** Explain why the thermocline is important for retaining exergy in a vertically stratified TES.

- 6.32** Determine the cooling capacity of an ice TES of  $3 \text{ m}^3$  volume which undergoes only latent heat changes at  $0^\circ\text{C}$ . Then determine the cooling capacity of a water CTES of  $3 \text{ m}^3$  volume which undergoes only sensible heat changes between  $3^\circ\text{C}$  and  $9^\circ\text{C}$ . Compare the two answers.
- 6.33** Why is it important to consider pump work when evaluating the energy and exergy efficiencies for a TES system? Does the inclusion of pump work have a greater effect on the energy efficiency or the exergy efficiency?
- 6.34** For an insulated TES, describe the behavior of the energy efficiency with discharge period when pump work is accounted for and when it is neglected.
- 6.35** Describe the three zones of a solar pond.
- 6.36** Is energy and exergy stored in all zones of a solar pond? Explain.
- 6.37** Where in a solar pond is the fluid density the greatest?

## Appendix: Glossary of Selected Exergy-Related Terminology

This glossary identifies exergy-related terminology from the literature that is of relevance to the TES discussions in this chapter. Most exergy terminology has only recently been adopted, and is still evolving. Often more than one name is assigned to the same quantity, and more than one quantity to the same name. Only exergy-related definitions are given for terms having multiple meanings. The glossary is based in part on previously developed broader glossaries (Kotas *et al.*, 1987; Kotas, 1995; Kestin, 1980).

**Available Energy.** See exergy

**Available Work.** See exergy

**Availability.** See exergy

**Base Enthalpy.** The enthalpy of a compound (at  $T_o$  and  $P_o$ ) evaluated relative to the stable components of the reference environment (i.e., relative to the dead state).

**Chemical Exergy.** The maximum work obtainable from a substance when it is brought from the environmental state to the dead state by means of processes involving interaction only with the environment.

**Dead State.** The state of a system when it is in thermal, mechanical, and chemical equilibrium with a conceptual reference environment (having intensive properties of pressure  $P_o$ , temperature  $T_o$ , and chemical potential  $\mu_{i,oo}$  for each of the reference substances in their respective dead states).

**Degradation of Energy.** The loss of work potential of a system which occurs during an irreversible process.

**Dissipation.** See exergy consumption.

**Effectiveness.** See second-law efficiency.

**Energy Analysis.** A general name for any technique for analyzing processes based solely on the first law of thermodynamics. Also known as *first-law analysis*.

**Energy Efficiency.** An efficiency determined using ratios of energy. Also known as *thermal efficiency* or *first-law efficiency*.

**Energy Grade Function.** The ratio of exergy to energy for a stream or system.

**Entropy Creation.** See entropy production.

**Entropy Generation.** See entropy production.

**Entropy Production.** A quantity equal to the entropy increase of an isolated system (associated with a process) consisting of all systems involved in the process. Also known as *entropy creation* or *entropy generation*.

**Environment.** See reference environment.

**Environmental State.** The state of a system when it is in thermal and mechanical equilibrium with the reference environment, that is, at pressure  $P_o$  and temperature  $T_o$  of the reference environment.

**Essergy.** See exergy. Derived from essence of energy.

**Exergetic Temperature Factor.** A dimensionless function of the temperature  $T$  and environmental temperature  $T_o$  given by  $(1 - T_o/T)$ .

**Exergy.** (1) A general term for the maximum work potential of a system, stream of matter or a heat interaction in relation to the reference environment as the datum state. Also known as available energy, availability, essergy, technical work capacity, usable energy, utilizable energy, work capability, work potential, or xergy. (2) The unqualified term *exergy* or *exergy flow* is the maximum amount of shaft work obtainable when a steady stream of matter is brought from its initial state to the dead state by means of processes involving interactions only with the reference environment.

**Exergy Analysis.** An analysis technique in which process performance is assessed by examining exergy balances. A type of second-law analysis.

**Exergy Consumption.** The exergy consumed or destroyed during a process due to irreversibilities within the system boundaries. Also known as *dissipation*, *irreversibility*, or *lost work*.

**Exergy Efficiency.** A second-law efficiency determined using ratios of exergy.

**External Irreversibility.** The portion of the total irreversibility for a system and its surroundings occurring outside the system boundary.

**First-Law Analysis.** See energy analysis.

**First-Law Efficiency.** See energy efficiency.

**Ground State.** See reference state.

**Internal Irreversibility.** The portion of the total irreversibility for a system and its surroundings occurring within the system boundary.

**Irreversibility.** (1) An effect, making a process nonideal or irreversible. (2) See exergy consumption.

**Negentropy.** A quantity defined such that the negentropy consumption during a process is equal to the negative of the entropy creation. Its value is not defined, but is a measure of order.

**Nonflow Exergy.** The exergy of a closed system, that is, the maximum net usable work obtainable when the system under consideration is brought from its initial state to the dead state by means of processes involving interactions only with the environment.

**Physical Exergy.** The maximum amount of shaft work obtainable from a substance when it is brought from its initial state to the environmental state by means of physical processes involving interaction only with the environment. Also known as *thermomechanical exergy*.

**Rational Efficiency.** A measure of performance for a device given by the ratio of the exergy associated with all outputs to the exergy associated with all inputs.

**Reference Environment.** An idealization of the natural environment which is characterized by a perfect state of equilibrium, that is, absence of any gradients or differences involving pressure, temperature, chemical potential, kinetic energy, and potential energy. The environment constitutes a natural reference medium with respect to which the exergy of different systems is evaluated.

**Reference State.** A state with respect to which values of exergy are evaluated. Several reference states are used, including environmental state, dead state, standard environmental state, and standard dead state. Also known as *ground state* .

**Reference Substance.** A substance with reference to which the chemical exergy of a chemical element is calculated. Reference substances are often selected to be common, valueless environmental substances of low chemical potential.

**Resource.** A material found in nature or created artificially in a state of disequilibrium with the environment.

**Restricted Equilibrium.** See thermomechanical equilibrium.

**Second-Law Analysis.** A general name for any technique for analyzing process performance based solely or partly on the second law of thermodynamics. Abbreviated as SLA.

**Second-Law Efficiency.** A general name for any efficiency based on a second-law analysis (e.g., exergy efficiency, effectiveness, utilization factor, rational efficiency, task efficiency). Often loosely applied to specific second-law efficiency definitions.

**Task Efficiency.** See second-law efficiency.

**Technical Work Capacity.** exergy.

**Thermal Efficiency.** See energy efficiency.

**Thermal Exergy.** The exergy associated with a heat interaction, that is, the maximum amount of shaft work obtainable from a given heat interaction using the environment as a thermal energy reservoir.

**Thermomechanical Exergy.** See physical exergy.

**Thermomechanical Equilibrium.** Thermal and mechanical equilibrium.

**Unrestricted Equilibrium.** Complete (thermal, mechanical, and chemical) equilibrium.

**Usable and Useful Energy.** See exergy.

**Utilizable Energy.** See exergy.

**Utilization Factor.** See second-law efficiency.

**Work Capability.** See exergy.

**Work Potential.** See exergy.

**Xergy.** See exergy.

# 7

## Numerical Modeling and Simulation of Thermal Energy Storage Systems

### 7.1 Introduction

The numerical modeling of thermal energy storage (TES) systems has attracted considerable attention recently because of the increased feasibility of a wide array of TES applications. Although appropriate numerical procedures can vary widely depending on the system, the impetus for their use can almost always be attributed to cost and time constraints. For example, experimental methods to assess performance in TES systems can be quite costly. Additionally, analytical models can be subject to extensive assumptions that render models incomplete, but are necessary since the exclusion of such assumptions can make equations overly complicated and cumbersome to evaluate. Therefore, there has been a growing need for numerical models to describe TES systems, thereby allowing computational methods to help solve governing equations. As a result, much of the research regarding this subject reflects the advancement of numerical analysis as a very sophisticated field.

Over the past few decades, advances in computing technology have made numerical analysis much more of an acceptable technique. However, numerical methods have been in use for centuries; even prominent mathematicians such as Isaac Newton and Leonhard Euler developed algorithms that are still used today in optimization problems. Because of the complicated form of the governing equations used in heat transfer and fluid flow, solving numerical equations in TES applications is more tractable with modern computers.

Numerical analyses differ from analytical methods in that they do not solve governing equations explicitly; rather they use approximations that make the equations solvable to a certain tolerance. For fluid flow in three dimensions, for example, pipe flow, solving the Navier–Stokes and continuity equations results in a function that allows velocities and pressures to be specified continuously within the domain. However, for more complex situations, for example, a pipe elbow, the introduction of a complicated boundary condition results in a difficult problem, which, in most cases, is too cumbersome to solve analytically. In these cases, numerical methods are advantageous, and can approximate real-world behavior to a high degree of accuracy. Using an approximated function and a sophisticated algorithm, the fluid flow domain can be discretized so that a finite number of points or volumes can be solved to any desired tolerance, depending on computing power. Most fluid flow and heat transfer problems can be solved by using commercially available software, much of which has been developed over the past several decades. Consequently, numerical analysis and computational codes are now widely used to solve problems.

Perhaps, the most important use for numerical modeling is when experimental or analytical means are not feasible. Complicated dimensional analysis coupled with scale modeling can be expensive and time consuming, whereas with some commercially available software, modeling design platforms can be combined with computational solvers to simulate many processes accurately. Although analytical means can provide high accuracy in the form of continuous solutions, they usually do not represent real scenarios and, if they do, assumptions are usually made, which neglect certain effects, such as radiation or contact resistance. The need is also great for computational procedures for the optimization and improvement of existing systems, which permit cost to be lowered and energy resources to be used more efficiently. For new TES systems, numerical techniques can greatly aid design. For TES systems already in use, numerical techniques can be used to properly identify locations, causes, and magnitudes of losses and help develop more efficient operational strategies. Potential retrofits of existing systems can also be simulated and assessed using numerical techniques, saving money and time compared to experimental approaches.

This chapter describes and illustrates various numerical approaches and methods for the modeling, simulation, and analysis of sensible and latent TES systems. An overview of the approaches, methods, and applications in numerical analysis is presented, after which a more detailed description of the finite volume approach, which is commonly used, is provided. Several case studies are considered to illustrate numerical techniques for both sensible and latent systems. The chapter concludes with a summary of the methods used and the trends observed.

## 7.2 Approaches and Methods

For any problem, there is often more than one technique that will result in an adequate solution. Similarly, for numerical analysis, there are many techniques available to simulate real-world processes, with varying levels of success. This section provides a brief overview of several techniques used in typical analyses of TES applications, with an emphasis on numerical simulation.

Although there are hundreds – perhaps even thousands – of published works on numerical analysis in the realm of TES, they have many similarities. Generally, numerical analysis is the study of developing or using algorithms to solve continuous problems in mathematics. In most cases, an exact solution to an equation or system of equations is not obtainable and numerical analysis can provide approximate solutions to a high degree of accuracy.

Consider, for example, the problem of solving for the perimeter of a circle with diameter 1. While ancient mathematicians had varying success in approximating the now well-known irrational number  $\pi$ ; it was not until Archimedes of Syracuse (~250 BC) developed a numerical algorithm to approximate  $\pi$  that the accuracy was increased to three decimal places. By the method of exhaustion, he drew a large  $n$ -sided polygon outside of the circle, then another  $n$ -sided polygon just inside of the circle and calculated the perimeter of each. Since the value of  $\pi$  must lie between these two values, he deduced by drawing a 96-sided polygon that  $\pi$  must have a value between 3.1429 and 3.1408. Through methods such as this, mathematicians, scientists, and engineers have been using numerical analysis to approximate solutions for thousands of years.

For most numerical analysis problems in the real world, the challenge is not in solving a single value (such as  $\pi$ ) but a continuous function representing scalar and/or vector quantities in a finite domain. In these cases, unless the governing equations and boundary and initial conditions are in the simplest forms, the domain must be *discretized* in order to obtain meaningful results. Discretization refers to the segregation of a volume into a discrete number of nodes or volumes in order to approximate the solution as a series of finite values or vectors. Although some TES applications of numerical analysis do not rely on discretized schemes (see Section 7.3), the great majority of work in the literature is concerned with discretized problems.

Currently, there are many commercially available software programs that allow numerical analyses for TES applications. These are mainly of two types: finite element methods (FEMs) and finite volume methods (FVMs). Spectral methods as well as finite difference methods are also common in similar applications, but of the four, the FVM and the FEM are the most abundant in the

literature, since they are much more attractive in terms of versatility. At the simplest level, the main difference between the two is the method of discretization. The FEM divides the domain into a number of elements or nodes (points), while the FVM separates the domain into volumes or cells. Both the methods use various techniques in order to achieve convergence.

The FEM generally solves the system of equations (i.e., the strong form of the problem) by first transforming to an equivalent variational (or weak) form of the problem. Then, by employing a specific method (Galerkin methods are the most common), the system is ultimately converted to a system of linear equations represented by a matrix equation, which can be solved using a sparse matrix solver for larger systems. This is a rather simplistic description of the FEM method; for a much more effective treatment of the subject, the reader is referred to Hughes (2000). FEMs have the widest range of applications, since both solid and fluid mechanics can effectively be modeled; however, it is much more computationally expensive than other techniques, which is the main reason FVMs are most often used in TES applications.

In the FVM, the initial solution is essentially guessed, and a formal integration of each volume using the Gauss divergence theorem indicates the errors between cells. This theorem states that the outward flux through a surface equals the volume integral of the divergence inside the surface. In simpler terms, the net flow of any property out of a volume must equal the sum of sources less the sum of sinks in the volume. The computational domain is updated iteratively based on the errors in adjacent volumes and is converged to specified residual error limits.

Although there are advantages to both techniques, the FEM generally is the superior choice when dealing with changes in domain. For instance, the FEM is preferred in cases where elastic deformation, contraction, or expansion of the physical domain may occur, for example, in crash tests in automobiles. The FEM also allows for a varied tolerance according to geometry, so that higher precision can be obtained in areas of importance, reducing the overall cost of simulation. The FEM is often used on structural mechanics and other problems where a discontinuous trend is expected in the results.

The FVM has been used extensively in computational fluid dynamics (CFD), since its conservative nature allows for a good simulation of many fluid flow phenomena. Unstructured or abnormal meshings are readily created with the FVM and can be structured to increase cell density in areas of importance, which, like the FEM, reduces the cost of computation. For this reason, FVMs are normally used for the simulation of complex TES systems, especially since fluid motion and heat transfer equations can be coupled to achieve highly accurate solutions.

This chapter focuses on the utilization of FLUENT, an FVM commercial code, to simulate problems involving sensible and latent TES. A brief overview of selected applications in the literature follows, along with a more detailed examination of the simulation and modeling procedures and the algorithms used in this software.

### 7.3 Selected Applications

Some of the numerical techniques and applications in the literature are briefly reviewed here. Although the field of TES is broad, most TES research is concerned with space heating or cooling, so this review focuses on applications of these types. This review is not intended to be comprehensive, but rather covers selected informative applications of numerical analysis in both sensible and latent TES.

In sensible TES design, considerable research has been reported on such stores as stratified water tanks, cold and warm water storage, rock bed TES, packed-bed TES, and others. Numerical analysis can assist greatly in reducing costs that would otherwise be incurred to construct and perform experiments, and can model real processes accurately, often with relative ease. For example, Chen *et al.* (2006) considered a vapor compression refrigeration cycle with a cold water TES. Three system types with different water cycle patterns are theoretically analyzed and simulated using numerical techniques. Although the physical system was not simulated directly using a finite volume approach, the numerical solution involved solving a system of partial



differential equations, likely based on finite difference models. In such cases, the exact numerical procedure is not explicitly defined, but the usefulness of such methods is clear: performance investigations and efficiency comparisons can be computed without resorting to experiments, reducing investments of time and money. In another study using numerical optimization, Zohoor and Moosavi (2008) developed a numerical model for optimizing a solar TES system. The hybrid storage system consists of both a hot water tank acting as a sensible storage and a paraffin tank for latent heat storage. A computational approach is used to optimize the charging and storage time schedules that coincide with available solar radiation conditions.

In the two examples described, numerical approaches are used to solve systems of equations that rely on analytical approximations. For example, convective heat transfer rates or flow fields are solved using laminar flow principles. Another useful application of numerical analysis is to compare these approximations, as is done in a study by Ismail and Stuginsky (1999). Here, a packed-bed model for both sensible and latent storage is investigated, and groups of models are examined to determine their accuracy under various system criteria. Four groups of models with different energy expressions are monitored, using a porous-medium method when the heat transfer fluid is of concern. That approach demonstrates well the usefulness of numerical analysis: bed particle size, void fraction, and particle material can be varied to illustrate the advantageousness of some models, depending on TES conditions.

Another feature of numerical analysis is that all-encompassing models can be constructed to simulate the transient behavior of TES systems. Finite volume or finite difference models are usually used for this purpose and, depending on the user-defined boundary conditions, pressure, temperature, and phase change phenomena can be observed at any point in the system, depending on how grid structures are set. An example is presented by Ghaddar and Al-Maarafie (1997), who considered a thermally stratified solar TES tank. A spectral-element method is employed, which is an FEM with good convergence properties. Their two-dimensional model is used to analyze a cylindrical storage tank and compared with both experimental data and a one-dimensional plug flow model. The spectral-element model presented in Ghaddar and Al-Maarafie (1997) was found to be superior for representing experimental data. Similarly, Oliveski *et al.* (2003) applied numerical approaches to simulate experimental data, but they included more effects (e.g., turbulence) and considered both forced and free convection. The developed numerical model is observed to be accurate in simulating the experimental process, reinforcing the advantage of numerical over corresponding analytical techniques.

Numerical simulations via commercial codes are popular, and greatly facilitate computational assessments for TES and other applications. Shah and Furbo (2003) utilized FLUENT to determine entrance effects in a solar hot water tank. The finite volume approach incorporated in this software permitted the construction of three separate inlet jets and the evaluation of their first- and second-law efficiencies. The simulated results were validated with experimental data and aided an investigation of efficiencies when flow rate and thermal conditions were varied.

The above applications of the numerical approach generally simulate or numerically solve for parameters relating to sensible TES systems. Although the concepts for latent TES are similar, a number of other variables need to be addressed in latent TES and can greatly complicate calculations. For example, density changes during solidification and melting are difficult to model, especially when natural convection is taken into consideration. However, recent advances in computing and numerical codes have permitted the modeling of latent TES processes and the optimization of latent TES systems. These include ice-on-coil systems, packed-bed encapsulated phase change material (PCM) systems, ice slurry systems, and microencapsulated systems. The most useful and readily observed applications are concerned with the former two systems, and therefore are the focus of attention here.

Erek and Ezan (2007) reported a numerical and experimental study of the charging process in an external-melt ice-on-coil TES system. The numerical procedure was simplified by considering a small section of the tank and exploiting symmetries. The control-volume approach used described the system dynamics and accurately predicted the effects of heat transport fluid (HTF) flow rate



and inlet temperature on the storage characteristics of this cold storage tank. Such characteristics include heat transfer rate, total stored energy, and energy efficiency.

Kiatreungwattana and Krarti (2002) reported another numerical application on an ice-on-coil TES system, focusing on an internal melt system during both charging and discharging. The numerical scheme allows a parametric analysis, so that the brine HTF inlet flow rate and temperature as well as the duration of the charging and discharging cycles could be varied to indicate their effects on overall performance. Partial charging and discharging processes are also considered and the model was validated with experimental data.

An increasingly popular latent TES application is based on encapsulated PCMs. As with latent or ice-on-coil TES, these can be divided into two groups: those which use numerical techniques to solve problems concerned with the packed-bed encapsulates as a whole and those which are concerned with analyses involving single capsules.

Most of the numerical procedures observed in the recent literature concerning packed-bed encapsulated TES deal with warm TES using paraffin waxes. Zukowski (2007) analyzed the heat transfer characteristics in a ventilation duct filled with encapsulated paraffin wax in rectangular configurations. He considered a three-dimensional transient model, which is used to predict the effects of capsule geometry and configuration on heat storage. Introducing parallel connectors downstream from the inlet is found to make the heat storage and retrieval more uniform. Benmansour *et al.* (2006) provided a two-dimensional transient analysis of a cylindrical storage tank filled with uniformly sized spherical capsules. The paraffin wax in the randomly packed capsules exchanges heat with air, acting as a heat transfer fluid, and the resulting model is found to agree favorably with observations.

Kousksou *et al.* (2005) proposed a two-dimensional approach to simulate the temperature field in a cylindrical container containing spherical capsules for ice storage. Using the porous-medium model along with the average Nusselt number for such flows proposed by Churchill (1983), the charging and discharging processes are evaluated. Density variations within the HTF are considered and the system is run in both vertical and horizontal positions. The optimal case occurs with the tank in the vertical position, when natural convective currents coincide with forced convection currents.

In addition to macroscopic views of packed-bed encapsulated TES systems, microscopic views that more correctly describe the inner flow networks in such systems are also popular. These can be helpful in determining viscous dissipation and the effect of capsule size, configuration, and orientation. Ismail *et al.* (2003) proposed a finite difference method to simulate the solidification of water in a spherical capsule. A moving-grid scheme is used to enhance the accuracy of the algorithm. The effects of shell size, as well as PCM internal and exterior temperatures, are found to be related to liquid fraction and solidification times.

Other geometries besides spheres have been analyzed numerically. De Souza and Vielmo (2005) investigated the freezing and melting of water in tubes, accounting for natural convection and density changes during the phase change. This analysis is applicable to cylindrical capsule geometries. Wei *et al.* (2005) reported numerical and experimental simulations for spherical, cylindrical, plate, and tube geometries, using the finite volume approach. The capsules in this case are constructed of stainless steel and contain paraffin wax, and are packed in a bed-like geometry and exposed to a cross-flow heat transfer fluid. The model agrees well with the experimental heat transfer rates.

Pinelli and Piva (2003) used FLUENT to investigate a vertical cylindrical cavity heated from above. In this study, the top and bottom of the upright cylinder are maintained at temperatures higher and lower, respectively, than the solidification temperature of the PCM (*n*-octadecane, a paraffin wax). Convective heat transfer occurs from the sides of the cylinder to the atmosphere, defining the boundary conditions that permit the numerical code to solve the problem accurately and examine the flow fields, temperature distributions, and total energy stored. These parameters are also obtained experimentally with a heating and cooling system controlling the upper and lower parts of the cylinder and a Styrofoam belt across the sides. The two sets of results agree reasonably well.

Assis *et al.* (2007) demonstrated the ability of FLUENT to analyze complicated flows accurately. In this study, a sphere containing a commercially available paraffin PCM is monitored qualitatively

and quantitatively during melting, induced by maintaining its outer shell at a constant temperature above the melting temperature. The change in density from solid to liquid is accounted for, as are the minor density differences in the liquid state due to temperature variations, which lead to convective flows. The sphere diameter and wall temperature are varied, and the simulation is validated in large part by visual studies of the moving solid–liquid interface with time. Relationships between various dimensionless parameters are determined, and the model is tested for grid size and time step independence, with good results. However, the computational time ratio was found to be over 300:1, that is, 300 s of computational time is required for 1 s of real flow time. Thus, a typical simulation required several days, even using a powerful computer by the standards at the time of the investigation. This example demonstrates that computational accuracy often needs to be balanced against simulation computational cost. Although computing power continually increases, many phenomena are still better neglected or simplified in numerical codes, where only minor losses in accuracy are caused.

## 7.4 Numerical Modeling, Simulation, and Analysis of Sensible TES Systems

One of the most important aspects of a CFD code is its ability to incorporate governing equations and conservation laws. For example, a code must apply conservation of energy and momentum and continuity principles during simulations of steady state and transient behavior. Here, we explain how a commercially available computational heat transfer and fluid flow code, ANSYS FLUENT 6.3, handles these phenomena in TES applications.

Since TES stores thermal energy in a medium for later extraction, all computational codes relating to TES need to account for energy conservation. Additionally, both sensible and latent TES systems usually involve one or more fluids. For instance, many cold latent TES systems employ an HTF to deliver heat to or from the PCM, and sensible TES media like rock beds transfer heat to or from a surrounding fluid, often air. The finite volume techniques used in the solution algorithms in FLUENT 6.3 are shown in this section to be able to handle such situations and their complicated governing equations.

In this section, geometric modeling techniques in fixed-grid schemes are outlined, including grid size and boundary layer construction in two and three dimensions. Also, the governing equations are presented, which the various FLUENT algorithms solve to analyze heat transfer and fluid flow. Attention is focused on the more complicated models that allow for phase change, natural convection, and viscous heating. Then, the simulation procedures used in most TES simulations are briefly explained as is the post-processing of the obtained data. Finally, the use of the data for thermodynamic analysis is described, illustrating how it can help present information about performance criteria and efficiencies in an effective manner.

### 7.4.1 Modeling

Proper and effective modeling is essential for the accuracy of numerical simulations. The geometry that one models or creates for use in computational analysis must satisfy three main criteria. That is, it must

- be constructed so as to facilitate accurate simulation of real-world scenarios;
- be sufficiently simple and/or contain fewer volumes to permit simulations with available computing power and within time constraints; and
- be sufficiently complicated or contain sufficient computational volumes to achieve accurate results.

These criteria can be illustrated with a simple example. Using ANSYS GAMBIT software, we construct a two-dimensional duct of length 100 cm and width 20 cm, in which air flows from left

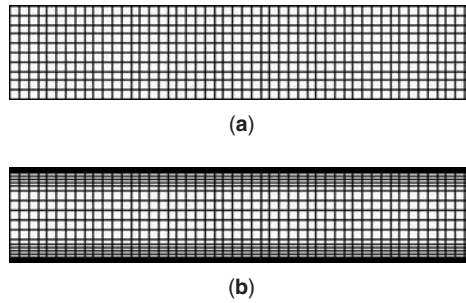


**Figure 7.1** Grid structuring for two flow cases. (a) 500 cells of equal size and (b) 1050 cells with increased cell density at wall boundaries

to right at a speed of 10 cm/s. Owing to the no-slip condition at the duct walls, a velocity boundary layer develops in the duct and a velocity profile exists. Note that due to the length of the duct, the flow is considered laminar so that no turbulence modeling is needed.

Two cases are examined (see Figure 7.1). The grid structure for the first case contains 500 rectangular volumes (cells) of equal size and for the second it contains 1050 rectangular volumes and a concentration of such volumes in the upper and lower boundary layers.

Both grid cases fit the system configuration but allow different results to be obtained. The duct is of the same size in each case, and the inlet and outlet criteria are identical. Thus, the first criterion mentioned earlier is satisfied for both the cases. The second criterion (the model should be sufficiently simple that the simulation can be carried out in a reasonable amount of time) is also satisfied. That is, both the cases were solved transiently in a matter of seconds using a somewhat outdated laptop with a Pentium M 1.6 GHz processor with 512 Mb DDR RAM, a time step of 0.5 s, 50 iterations, and a total of 25 s of flow time. The third criterion is significantly impacted by the grid structuring and cell density within the computational domain. In the first case, the flow is treated equally at all points and extra attention is not paid to those areas that experience the largest velocity gradients, that is, near the walls. The situation in the second case is different, as most of the cells in the computational domain are located along the walls. The finer grid near the walls ensures that information is not lost in these areas of the flow. Since all conservation laws are solved to a specific tolerance (as explained in more detail in Section 7.4.3), locating more cells in areas of higher gradients improves predictions in those areas.

Figure 7.2 depicts the simulated velocity profiles for the two cases. The velocity profiles in Figure 7.2(a) and (b) differ. The first (Figure 7.2a) exhibits a sharper increase in velocity as the

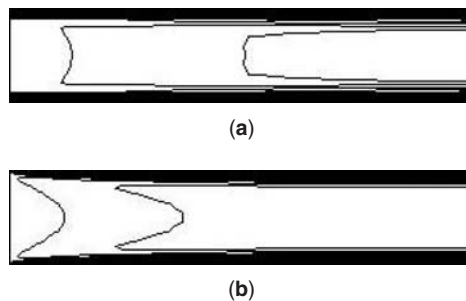


**Figure 7.2** Velocity profiles for two flow cases, characterized by the grid structures in Figure 7.1. Each solid line represents a contour of constant velocity

distance from the wall increases, with an almost constant boundary layer thickness. It is apparent from fluid mechanics principles that the first case (Figure 7.2a) does not accurately depict the process, since the boundary layer thickness should start at zero and increase gradually over the flat plate (see Section 1.5.6). Further, the transition in the first case from a zero velocity to the centerline velocity is not smooth, as should occur for laminar fluid flow. The second case (Figure 7.2b) characterizes the flow more accurately, with the velocity profiles transitioning smoothly across the duct and the boundary layer thickness changing in a more reasonable manner. Thus, the second case (case b) attains a more accurate numerical simulation than case a and thus better satisfies the third criterion above.

The previous example illustrates the need for care when constructing a computational domain for a TES simulation. Although heat transfer is not accounted for in the example, the same steps in terms of developing appropriate meshing or grid procedures must be taken to ensure that thermal boundary layers and temperature profiles are accurately depicted.

In addition to ensuring that the above three criteria are met, there is a need to develop independence tests with any numerical model. These include grid size, grid orientation, and time step independence tests, as well as in some cases far-field boundary independence tests. Furthermore, model validation is required before results generated by a numerical code are utilized.

A grid size and orientation test is needed to help in model validation and to assure accuracy. The need for a grid size test is illustrated in part by the above example. By adjusting the grid size slightly and, in some cases, the orientation in different ways with respect to temperature and velocity profiles, the dependence of numerical solutions on these small changes can be observed. If the simulation results change significantly, grid refinement is necessary. If the results do not change significantly, the numerical procedure is established to be independent of grid meshing changes and the geometric constraints for numerical simulation are satisfied.

The time step independence test is similar and is intended to ensure that time steps in simulation are as large as possible to reduce computation time while being sufficiently small to provide accurate solutions. If the time step in an unsteady flow problem is increased significantly, numerical solutions lose accuracy because information details are lost between time steps. For example, in the case considered earlier (see Figure 7.2b), if the time step is increased from 50 steps of 0.5 s to a single step of 25 s, the velocity profile that results can be seen in Figure 7.3. This profile differs qualitatively and quantitatively from the one in Figure 7.2(b), mainly because of the lack of information transferred from one time step to another. To ensure solutions are independent of time step, care should be taken to retain an adequate amount of flow information by decreasing time step, while decreasing computational time by increasing time step. In complicated problems, the choice of time step is often crucial, as it can mean the difference between simulation times ranging from a few hours to a few days.

In some cases, a far-field independence test is also required to assure the accuracy of a simulation. In those cases, a well-developed profile may be needed or assumed in the problem description, and care must be taken to ensure that the length or size of the boundary does not detract from the results. A simple example is provided by the cooling of a large, heated rock at the bottom of the ocean. Since it is not necessary to model the entire ocean, a smaller body of water can be created for modeling purposes, but the size of the water body would have to satisfy far-field independence tests. That is, the water body must be created so that its boundaries match the conditions, for

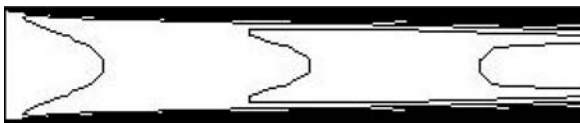


Figure 7.3 Velocity profile with a single time step of 25 s

example, temperature gradients, far from the system being assessed. If the size of the smaller water body is established correctly, loss of simulation data is avoided and, in this example, a “virtual” ocean is developed.

Together, the various independence tests ensure that a model achieves accurate results. The tests can help identify grid configurations, which increase computing speeds without significant loss of accuracy.

### 7.4.2 Heat Transfer and Fluid Flow Analysis

During TES numerical simulation, governing equations are solved to determine velocity, pressure, and temperature fields. In general, the governing equations involve energy and momentum balances and the continuity equation. Sometimes, simplifications can be made. For cases with no moving fluid, only the energy equation needs to be considered. For cases with fluid flow but no heat transfer or heat generation, the momentum and continuity equations must be invoked. For the case of combined fluid flow and heat transfer, all equations must be solved within specified tolerances (see Section 7.4.3).

For sensible TES, the energy equation in FLUENT is usually expressed as follows:

$$\frac{\partial}{\partial t} (\rho h - p) + \nabla \cdot (\vec{V} \rho h) = k \nabla^2 T + \Phi \quad (7.1)$$

Here,  $h$  denotes specific enthalpy,  $p$  pressure,  $\rho$  density, and  $\vec{V}$  the velocity vector, while  $k$  and  $T$  denote thermal conductivity and temperature, respectively. This equation expresses the principle of energy conservation, but is simplified somewhat by assuming that kinetic and potential energy effects, radiation effects, and source terms from chemical reactions or other heat sources are negligible and that the medium is homogenous. The last term on the right-hand side of Equation 7.1 accounts for viscous heating and can be expressed in three-dimensional Cartesian coordinates as follows:

$$\Phi = \mu \left[ 2 \left( \frac{\partial u}{\partial x} \right)^2 + 2 \left( \frac{\partial v}{\partial y} \right)^2 + 2 \left( \frac{\partial w}{\partial z} \right)^2 + \left( \frac{\partial v}{\partial x} + \frac{\partial u}{\partial y} \right)^2 + \left( \frac{\partial w}{\partial y} + \frac{\partial v}{\partial z} \right)^2 + \left( \frac{\partial u}{\partial z} + \frac{\partial w}{\partial x} \right)^2 \right] \quad (7.2)$$

This equation is used in all subsequent TES case studies. Care must be taken for media undergoing phase change. For media not subject to phase change, the sensible specific enthalpy from Equation 7.1 can be derived using incompressible assumptions as

$$h(T) = h_o + C(T - T_o) \quad (7.3)$$

where the subscript  $o$  refers to the reference state, which is typically at a temperature of 298.15 K. This assumption of incompressibility is normally reasonable since in most cases water or some liquid solution, which behaves like an incompressible fluid, is used as the heat transfer fluid and/or storage medium.

Aspects of computationally solving the flow field for the general energy equation are now outlined. Fluids must adhere to the principle of conservation of mass. For incompressible substances, the continuity equation can be written as

$$\nabla \cdot \vec{V} = 0 \quad (7.4)$$

The Navier–Stokes equations, or flow energy conservation equations, also apply:

$$\rho \frac{\partial \vec{V}}{\partial t} + \vec{V} \cdot \nabla \vec{V} = -\nabla p + \mu \nabla^2 \vec{V} + \rho \vec{g} \quad (7.5)$$

These equations depend primarily on the velocities and pressure differentials within the velocity field. The change in velocity at any point in the fluid depends on the pressure gradient at that point  $\nabla p$  as well as on the viscous dampening effect, represented by  $\mu \nabla^2 \vec{V}$ .

For temperature differences like the ones experienced in most TES applications, which normally would be considered “small,” it is often useful to consider natural convection as well, by accounting for the small density differences experienced when the temperature distribution in a fluid is nonuniform. Then, the *Boussinesq* model is often preferred, since it achieves faster convergence by solving the energy and continuity equations using a constant density. For the Navier–Stokes equations, the natural buoyancy term (the far right term of Equation 7.5) is solved using the Boussinesq density approximation:

$$(\rho - \rho_o) g \approx -\rho_o \beta (T - T_o) g \quad (7.6)$$

This approximation is valid provided density differences are not large, in which case  $\beta (T - T_o) \ll 1$ . This condition applies for TES heating and cooling applications, and is adopted throughout the case studies presented here, which take natural convection into consideration.

Although the above discussion simplifies the governing equations in many TES systems, the approach is sufficient in analyzing basic systems. These equations provide a useful and simple means to achieve an accurate simulation and analysis for some of the sensible TES systems included in the case studies in Section 7.5.

Note that FLUENT includes sophisticated turbulence modeling and combustion packages, which are not utilized here and are beyond the scope of this discussion.

### 7.4.3 Simulation

The computational procedures used in FLUENT are complex and much research has gone into developing the many algorithms used in FLUENT to solve the differential equations in complex fluid flow and heat transfer problems. As a result, numerous algorithms and discretization schemes are available in FLUENT. Only those pertinent to sensible heat storage are considered in this section.

As noted earlier, FLUENT uses a finite volume approach to solve for domain data. Grid and mesh construction splits each domain into a finite number of volumes (cells) and the relationships between adjacent cells are computed over their adjoining faces (facets). To solve the necessary governing equations from Section 7.4.2, several initial and boundary conditions must be established, including cell initializations (initial conditions) and wall or flow information concerning boundaries. If the energy balance (Equation 7.1) is enabled, each cell must be assigned an initial temperature and pressure by the user before computation for transient solutions begins. In the case of fluid flow, the velocity and pressure vectors in all cells must be initialized so that Equations 7.4 and 7.5 can be solved. The boundary conditions, which must be applied to all wall surfaces (denoted by  $W$  in the following equations) as well as inlet and outlet flows, are equally important. For geometries which have walls, a “no-slip” boundary condition is often employed, which establishes a zero velocity on the surface. In other words, for those wall facets  $\vec{f}$  that are part of the no-slip wall regime, the velocity vector is zero, or

$$\vec{V} (\vec{f} \subset W_{ns}) = 0 \quad (7.7)$$

All cell data is extrapolated from cell centers, for which information is stored, to cell facets by a linear interpolation scheme.

In many cases, the number of computational volumes can be greatly reduced by splitting flow regimes into symmetric segments, as is readily visible in Section 7.7.2, where a “slip” condition is applied.



The slip boundary condition requires zero-shear stress at points of flow symmetry:

$$\frac{d\vec{V}}{d\vec{n}} \left( \vec{f} \in W_s \right) = 0 \quad (7.8)$$

For outflow zones, where fluid is expected to flow out of the domain, FLUENT extrapolates the required information from the interior of the domain. A zero diffusion flux is assumed for all flow variables in outlet type flows. In other words, for any flow variable  $\gamma$ ,

$$\frac{d\gamma}{dz} \left( \vec{f} \in W_{out} \right) = 0 \quad (7.9)$$

where the subscript *out* refers to the outlet boundary region. The symbol  $\gamma$  can refer to any of the velocity, temperature, or pressure vectors. This criterion can create some problems with the robustness of simulations with respect to far-field boundary conditions, so care must be taken when choosing boundaries of this type.

Other boundary types include velocity inlet, where flow velocity and temperature at the inlet must be indicated. Convective and conductive walls, adiabatic walls, and constant-temperature walls are some of the many useful conditions that can be employed at boundaries as well. These conditions are explained in Section 1.6.

A pressure-based solver is used in the case studies investigated here, since all of the materials used are assumed incompressible. Flows are therefore governed solely by pressure differentials. However, for the case of natural convection using the Boussinesq model in Section 7.4.2, the pressure is discretized using a body-force-weighted scheme. In this scheme, facet pressures are computed assuming that the normal gradient of the difference between pressure and body forces is constant. This approach works well in most natural convection cases.

The pressure-based solver employs an algorithm that belongs to a general class of methods called *projection methods* (Chorin, 1968). In this method, continuity is achieved by solving a pressure correction equation. This equation is derived from the continuity and momentum equations, outlined earlier, in such a way that the pressure/velocity field satisfies the continuity equation. Since the differential equations that must be satisfied are nonlinear by nature and coupled, the solution must be obtained by iteration in a closed loop until convergence is achieved within the specified tolerances. A schematic of the general pressure-based solution process is shown in Figure 7.4.

The premise of the segregated pressure-based algorithm is that the variables ( $u$ ,  $v$ ,  $w$ ,  $p$ , and so on) are solved sequentially (segregated). Although this approach is somewhat tedious computationally, advances in computer speed and memory capacity make it an excellent choice for more simple problems. Then, the SIMPLE algorithm for pressure-based segregated solvers is used.

The SIMPLE (Semi-Implicit Method for Pressure-Linked Equations) algorithm follows the basic outline of the flow diagram in Figure 7.4, but each step is somewhat more complicated. Owing to the complexity of the algorithm when applied to discrete cell volumes, the general outline of the model is described in lieu of a more involved explanation, which is beyond the scope of this discussion.

Since all pertinent flow and energy information is stored in the centroid of each cell, the mass, continuity, and energy equations must be applied at cell facets. To do this, the momentum and continuity equations are discretized using projected face values from the centers of adjacent cells, using the Green–Gauss cell-based method:

$$\gamma_f = \frac{\gamma_{ca} + \gamma_{cb}}{2} \quad (7.10)$$

In other words, the facet values of all variables are taken as the average at the centers of the adjoining two cells, “*ca*” and “*cb*,” and all variables in the solution can be seen as piecewise linear at any time. But the overall solution appears continuous rather than discrete since the number of cells is large and each cell is small compared to the total volume.

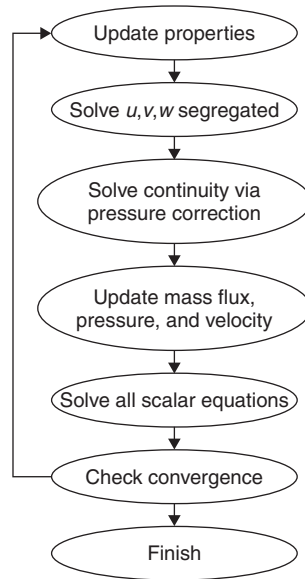


**Figure 7.4** Solution procedure flow chart for the coupled pressure-based solution algorithm, such as the one used in the SIMPLE method

The first step in the SIMPLE algorithm is to solve the momentum equations sequentially, by guessing the pressure field, say  $p^*$ . The pressure field must subsequently be improved, and much of this algorithm is devoted to that task. As the solution loop progresses, the algorithm updates the pressure field continuously until a solution is achieved within specified tolerances.

If the pressure field,  $p^*$ , is not initially correct, the continuity equation, which is evaluated next, is not satisfied. A correction factor is then introduced in order to correct the face fluxes so that continuity can be achieved. The corrected face fluxes for each cell are then substituted back into the discrete continuity equation to obtain a discrete equation for the pressure correction in each cell. The pressure correction equation is achieved by solving this discrete pressure correction equation using the algebraic multigrid (AMG) method. Details of this method are complex and are not discussed here, but it is noted that the AMG method does not depend on problem geometry and thus can be used for complicated problems like TES applications.

Once the pressure correction equation has been obtained, it is used, along with several user-defined under-relaxation factors, to correct all cell pressure values and face fluxes. The penultimate step in the algorithm is the solution of the energy equations using the corrected continuity and momentum equations. Once the energy equations, which are important in any heat transfer application and which differ from zone to zone, are solved, the residual error of the conservation equations is checked, completing the algorithm.

The residual error is the total summed differences in the governing equations from cell to cell. Since the equations cannot be solved perfectly using the cells in the computational domain, there are always errors when updating solutions. The error for each of the  $x$ ,  $y$ , and  $z$  velocities, along with the continuity and energy equation errors, are summed separately over the domain. If the result is below the specified tolerance, the solution is deemed to have converged. If the convergence criteria are not met, the solution has not converged and the corrected pressure field becomes the new pressure field guess in the first step of the algorithm. The process is then repeated iteratively.

The residual values are dependent on the scale of the problem. For example, a large system with many computational domains and a fast moving flow would typically have a much larger



residual error than a small system with little flow. If the total residual error tolerance is fixed at the same value in both cases, the simpler problem would lose much more information about these differences per cell. Hence, residual values are often scaled based on cell values. A simplification of the normalized or scaled residual can be obtained as follows. For any domain parameter,  $\gamma$ , a cell value is obtained by considering neighboring cells,  $nb$ , so that  $f(nb) = \gamma$ , at which the cell residual is  $|\gamma - f(nb)|$ . Then, the scaled residual over a domain of  $n$  cells is

$$Res^\gamma = \sum_{i=i}^n \frac{|\gamma_n - f(nb_n)|}{|\gamma_n|} \quad (7.11)$$

These residuals are applicable to the momentum, continuity, and energy equations, and are automatically implemented in FLUENT whenever the pressure-based algorithm is employed. The scaled residual approach allows for a more accurate solution convergence across a wide range of applications and is used throughout the TES applications herein.

#### 7.4.4 Thermodynamic Analysis

Although the heat transfer and fluid flow analysis allows for TES simulation, thermodynamic analysis is necessary to link the obtained information to physical phenomena. Thermodynamic analysis is concerned with evaluating the mass, energy, entropy, and exergy equations to provide performance and efficiency data. These quantities are described in this section, as is an associated balance equation used for control volume analysis. The method by which physical quantities are monitored using FLUENT for solving the balances is explained.

The mass balance for a control volume is shown in Equation 7.12. Mass can be transferred to or from the control volume, and the difference is the gain in mass of the system:

$$\Delta m_{CV} = m_{in} - m_{out} \quad (7.12)$$

The energy balance is similar. Since energy can be neither created nor destroyed according to the first law of thermodynamics, energy is conserved. For sensible TES applications, kinetic and potential energy effects are usually neglected. The energy balance equation for a single-inlet, single-outlet system is

$$\Delta E_{CV} = E_{in} - E_{out} = Q - W + H_{in} - H_{out} \quad (7.13)$$

The change in energy of the control volume is equal to the net heat added to the system, less the net work done by the system, plus the difference of the enthalpy flow into and out of the control volume with mass flows. The usual sign convention treats heat into a system as positive and work out as negative. Often substances are assumed incompressible, and enthalpy differences can be evaluated as follows:

$$\Delta H = H_2 - H_1 = m(h_2 - h_1) = mC(T_2 - T_1) \quad (7.14)$$

In contrast to mass and energy, entropy and exergy are not conserved. For a single-inlet, single-outlet case with  $j$  heat interactions with the surroundings, the entropy balance can be written as

$$\Delta S_{CV} = \sum_j \frac{Q_j}{T_j} + S_{in} - S_{out} + \Pi \quad (7.15)$$

The second law of thermodynamics implies that the entropy of a system increases because of irreversibilities, so the last term of Equation 7.15 is always greater than zero for real applications. The entropy transfer associated with a heat interaction is the ratio of the heat transfer across a

surface to the temperature  $T_j$  at which the interaction occurs. For incompressible substances, the entropy change can be simplified:

$$\Delta S = S_2 - S_1 = m(s_2 - s_1) = mC \ln \left( \frac{T_2}{T_1} \right) \quad (7.16)$$

Exergy analysis is useful in TES applications, providing assessments based on the first and second laws and assessing both the quantity and usefulness of energy. As an example, consider cold TES. Since exergy methods treat cold as a useful commodity relative to ambient conditions, more realistic performance assessments are obtained using exergy rather than energy efficiencies. Exergy, like entropy, is not conserved. For a single-inlet, single-outlet case with  $j$  heat interactions with the surroundings, an exergy balance can be written as

$$\Delta \Xi_{CV} = \sum_j \left( 1 - \frac{T_\infty}{T_j} \right) X_j - W + \epsilon_{in} - \epsilon_{out} \quad (7.17)$$

where the exergy difference for an incompressible substance is

$$\Delta \Xi = \epsilon_2 - \epsilon_1 = m(e_2 - e_1) = mC \left( T_2 - T_1 - T_\infty \ln \left( \frac{T_2}{T_1} \right) \right) \quad (7.18)$$

With these thermodynamic principles, energy (first law) and exergy (second law) efficiencies can be defined. In both cases, the efficiencies are often based on the ratio of the product (or desired) output to total input. Expressions for energy efficiency  $\eta$  and exergy efficiency  $\psi$  based on this definition, which are used in the case studies, are as follows:

$$\eta = \frac{\text{Product energy output}}{\text{Total energy input}} = \frac{E_{prod}}{E_{input}} \quad (7.19)$$

$$\psi = \frac{\text{Product exergy output}}{\text{Total exergy input}} = \frac{\Xi_{prod}}{\Xi_{input}} \quad (7.20)$$

To evaluate efficiencies, energy and exergy quantities must be obtained, in general and with FLUENT. For mass flows, the temperature of the flow on a mass-weighted average is preferred. The mass-weighted average temperature obtained by a surface monitor for an outflow containing  $n$  facets is defined as follows in FLUENT:

$$\bar{T}_{out} = \frac{\sum_{i=1}^n T_i \rho_i \left| \vec{V}_i \cdot \vec{A}_i \right|}{\sum_{i=1}^n \rho_i \left| \vec{V}_i \cdot \vec{A}_i \right|} \quad (7.21)$$

The mass flow rate is provided as the divisor of Equation 7.21. Surface integrals can also be computed, and are usually used for evaluating the total heat flow through a surface. For a heat flux  $q$ , the total surface heat flux for a surface containing  $n$  facets is calculated in FLUENT as:

$$Q = \int q dA = \sum_{i=1}^n q_i |A_i| \quad (7.22)$$

In addition, a volume monitor is often used to determine the average temperature in a specified material or section of the domain. For a volume comprised of  $n$  elements, the volume average temperature from a volume monitor is

$$\bar{T}_v = \frac{1}{V} \sum_{i=1}^n T_i |V_i| \quad (7.23)$$

The above two methods are used in the case studies and permit calculation of performance parameters for each case.

## 7.5 Case Studies for Sensible TES Systems

The thermodynamic analysis described in the previous section is applied to several TES case studies. The case studies are chosen to be illustrative and are therefore simple. They are easily repeated and provide useful insights into sensible and latent TES systems. The cases are simulated using FLUENT 6.3, using an IBM Thinkpad laptop with a Pentium M 1.60 GHz processor and equipped with 512 Mb of DDR RAM. This computer is sufficient for performing the calculations with the software (although more computing power is required to attain convergence for complex problems in a reasonable time).

In the following examples, typical uses for ANSYS FLUENT software are outlined. As one of the most popular finite volume solvers in the industry, it is adept at solving many computational fluid flow and heat transfer problems over a wide range of applications. Many examples are cited in the literature in which FLUENT simulates real scenarios, varying from simple to complex. FLUENT can implement a wide range of models, which can be toggled on or off, to handle phenomena such as multiphase flows (e.g., gas diffusion beds), viscous heating, radiation, solidification and melting, acoustics, turbulence, and others. The advantage of commercially available software is relatively straightforward problem setup and solution, although care must be exercised for more complicated applications to ensure that proper models are enabled, residual tolerances are within reason, and computational domains, including boundary and initial conditions, are properly constructed.

Two cases are investigated here, both involving relatively simple FLUENT simulations. The first is natural convection in a hot water storage tank, and is intended to simulate the cooling process for an uninsulated residential hot water tank in ambient conditions. The second case is forced convection in a stratified cylindrical storage tank, where hot water is pumped into the tank as in solar heating applications. Although grid and time step dependence tests are administered, because of the lengthy nature of such tests they are shown in more detail when a complicated case study is undertaken in Section 7.7.2. These examples are intended to provide the reader with an understanding of the usefulness of such software in sensible TES applications.

### 7.5.1 Case Study 1: Natural Convection in a Hot Water Storage Tank

In this case, natural convection is simulated using FLUENT. This simple case permits some of the basic aspects of the software to be understood and utilized. We consider an upright cylindrical storage tank with a radius of 30 cm and a height of 120 cm. These dimensions are typical of commercial hot water tanks. The tank is assumed to have negligible insulation on its walls and to exchange heat with its surroundings through convective heat transfer only. The hot water tank has an initial temperature higher than that at ambient conditions. The resulting convection and stratification within the tank are examined as time progresses over a 24-hour period. Various physical quantities are considered so as to provide sufficient information to calculate energy and exergy efficiencies.

The sole heat storage and transport medium is water, which provides the sensible thermal storage capacity. The water has an initial temperature of 60 °C and exchanges energy through convective heat transfer with the ambient surroundings at a temperature  $T_{\infty} = 20^{\circ}\text{C}$ . The simplistic modeling applied here permits the ambient atmosphere to be excluded from the physical domain and instead for a convective boundary condition to be imposed at the tank walls with a heat transfer coefficient of 10 W/m<sup>2</sup> K. This value compares well with that found in a similar study by Oliveski *et al.* (2003). The tank walls are uninsulated, and this lack of conductive thermal resistance allows the wall to be treated as very thin. The water is assumed to have constant thermophysical properties, including a density of 992.2 kg/m<sup>3</sup>, a specific heat of 4.182 kJ/kg K, a conductivity of 0.618 W/m K, a dynamic viscosity of 0.000653 kg/m s, and a thermal expansion coefficient of 0.000386/K. These values are taken at 40 °C, the mean temperature of the system and its surroundings.

To create the physical domain and segregate it into finite volumes, GAMBIT software is used. Special care is taken to ensure a higher concentration of cells in regions expected to experience higher thermal and velocity gradients, namely, the inside walls of the tank. This is done to ensure

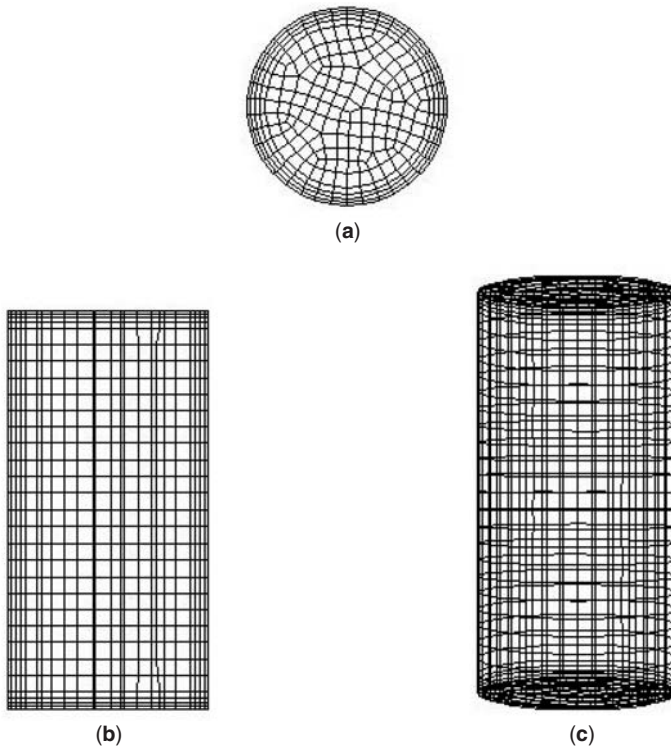


**Figure 7.5** Cross-sectional views of the cell density in the (a) radial plane, (b) axial plane, and (c) outer wall regions

greater simulation accuracy, as explained earlier. The cell configurations for horizontal and vertical cross sections through the tank are shown in Figure 7.5, along with a three-dimensional view of the cell distribution in the outer walls.

To establish this cell configuration, a boundary layer is first meshed in all inner faces (walls), using an initial spacing of 1 cm, with a growth factor of 1.2 and four layers in total, giving a total boundary layer thickness of 5.37 cm. Subsequently, the remainder of the volume is meshed using hex elements and a cooper meshing with a spacing of 5 cm, which corresponds to a total of 8580 elements. These configurations are simple to implement with a basic knowledge of GAMBIT, and are chosen because of the good convergence results they yield in the associated FLUENT simulations. No grid size or orientation tests are administered for this case study, but a comprehensive and detailed account of these procedures is given in Section 7.7.2.

Once the computational domain configuration is created, it can be read into FLUENT as a system of nodes and volume types. The remainder of the numerical setup involves setting initial and boundary conditions, temperature monitors, time steps, and residual tolerance values. For this case, the energy balance of Equation 7.1 is enabled, and water properties are set via the Boussinesq natural convection approximation in Equation 7.6. The entire volume is initialized to have zero gauge pressure and a temperature of 60 °C, and the convective heat transfer boundary condition is set using the “Boundary Conditions” panel. The SIMPLE solver is utilized, but the pressure discretization scheme is weighted by body forces, as required for natural convection cases. For natural convection to occur, gravity must be enabled. Here, gravitational acceleration is set to  $9.81 \text{ m/s}^2$  in the negative  $y$ -direction. Monitors are put in place to record the volume-averaged

temperature in the tank at 5-min intervals, and the residual tolerances are set to  $10^{-3}$  for the  $x$ ,  $y$ , and  $z$  velocities and continuity and  $10^{-6}$  for energy. The time step is set to 2 s, a coarse value that eases the simulation. As in grid construction, time step independence is not demonstrated in this case, but is explained in detail in Section 7.7.2. The simulation is then run. With a computational time ratio of about 1:3, the simulation required is about 10 h to complete.

### Performance Criteria

Since no mass flow crosses the tank walls and no work is done on the control volume, the energy balance from Section 7.4.4 can be simplified to

$$\Delta E_{\text{sys}} = Q \quad (7.24)$$

The energy efficiency, based on the ratio of product to input energies, can be computed at any time during the simulation, since monitors are in place to calculate the heat loss via the average change in water temperature. The product energy is defined as the recoverable energy in the tank at any time, while the total energy input is taken to be the recoverable energy in the tank at the beginning of the simulation. These two values are evaluated by monitoring the average temperature within the tank at each time step, and the energy efficiency becomes

$$\eta = \frac{E_{\text{prod}}}{E_{\text{input}}} = \frac{H(t)}{H(0)} = \frac{H(0) - Q}{H(0)} \quad (7.25)$$

where

$$H(t) = m [h_{\infty} + C (\bar{T}_v(t) - T_{\infty})] \quad (7.26)$$

The exergy efficiencies are similarly calculated, with no mass flows across the control volume. For simplicity, we assume reversible behavior in the tank with no viscous losses or volumetric changes, so the only system loss is the exergy loss associated with heat leakage:

$$\Delta \Xi_{\text{sys}} = X_l \quad (7.27)$$

The exergy content at each time step of the simulation can be similarly calculated by monitoring the volume-averaged temperature in the tank. Then, the exergy efficiency can be expressed as

$$\psi = \frac{\Xi_{\text{prod}}}{\Xi_{\text{input}}} = \frac{\Xi(t)}{\Xi(0)} = \frac{\Xi(0) - X_l}{\Xi(0)} \quad (7.28)$$

where

$$\Xi(t) = mC \left[ \bar{T}_v(t) - T_{\infty} - T_{\infty} \ln \left( \frac{\bar{T}_v(t)}{T_{\infty}} \right) \right] \quad (7.29)$$

The total volume of the system is calculated to be 339 L, corresponding to a mass  $m$  of 336 kg. The specific enthalpy of water at the reference-environment condition is given in thermodynamic tables as  $h_{\infty} = 83.93$  kJ/kg. Note that, although the tank is taken to undergo a reversible process for simplicity, all other cases have internal irreversibilities.

### Results and Discussion

Before considering the performance values calculated from the monitored simulation data, we utilize the field data visualization software in FLUENT. Views of the temperature and velocity (scalar)

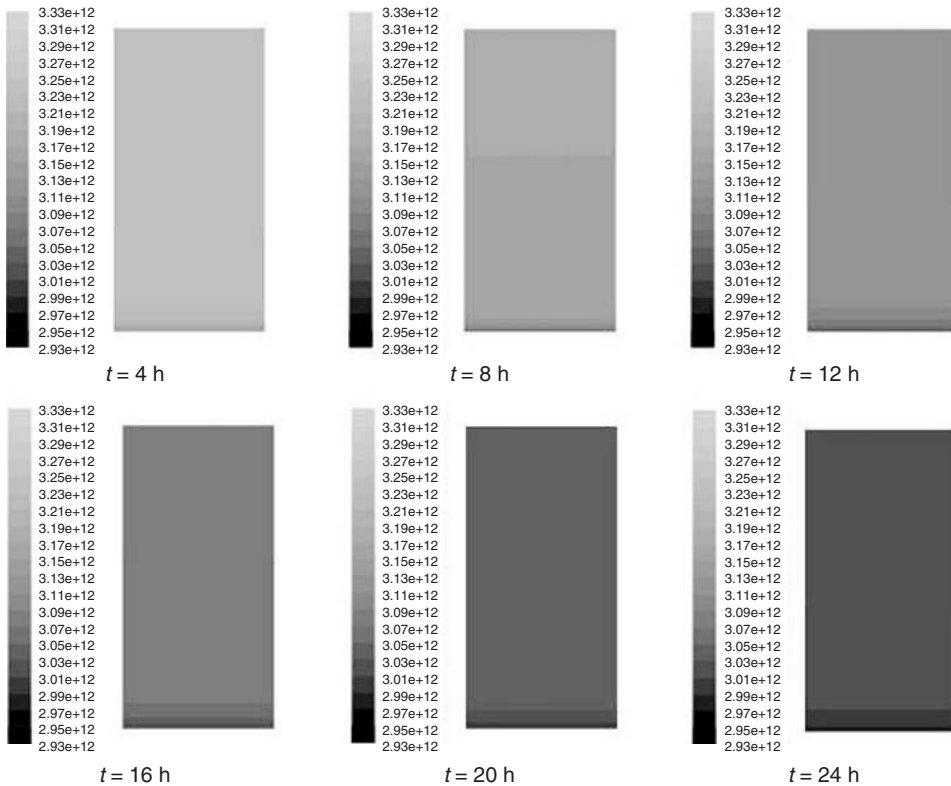


**Figure 7.6** Temperature distributions (in K) for the storage tank at 4-h intervals

fields are taken at 4-h intervals. These views are shown for an axial cross section (see Figure 7.5b) in Figures 7.6 and 7.7.

In the temperature fields in Figure 7.6, darker regions indicate cooler temperatures. It is seen that the tank cools considerably as time progresses, and that cooler temperatures exist in the lower parts of the tank, due to natural convection currents, as well as on the tank walls. This is not surprising since the natural convection model is employed and warmer fluids have a lower density than cooler fluids.

From the absolute velocity field of the tank in Figure 7.7, it is observed that the velocities, although small, vary as time progresses. Darker areas represent lower velocities. Two points are apparent in Figure 7.7: the velocity differences in the storage tank decrease with time and the velocities are highest along the tank walls and lowest at the tank bottom. These observations are attributable to natural convection. Since the tank walls experience the highest velocity gradients, the cells nearest to the walls exhibit the lowest temperatures in the domain and the greatest densities, leading to the greatest downward velocity. As time passes, the density variations within the tank decrease as the average temperature within the tank decreases toward the ambient temperature. If the simulation is continued for enough time, all velocity vectors would become zero. Note that small eddy currents are present in the tank interior due to the fact that FLUENT automatically uses a turbulence model for such situations. Compared to thermal energy losses, the losses due to viscous heating in both laminar and turbulent cases are extremely small and therefore are assumed negligible for this and all subsequent TES case studies.

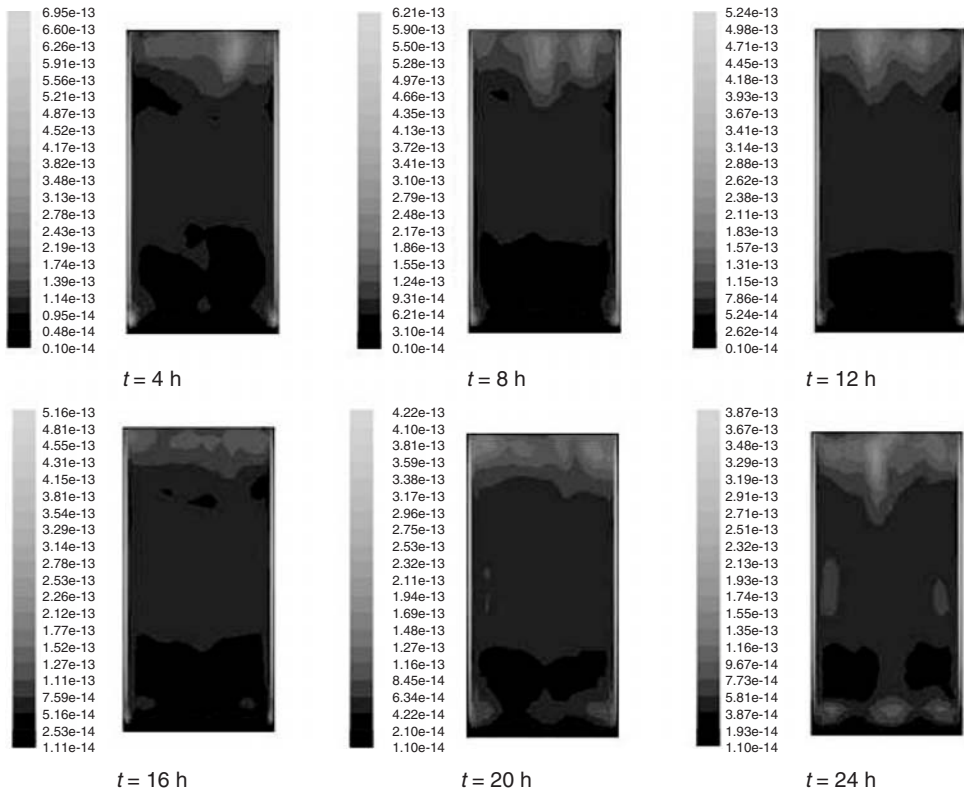


Figure 7.7 Velocity profiles (in m/s) for the storage tank at 4-h intervals

The tank temperature progression over 24 h is obtained with the volume-averaged temperature monitor (see Figure 7.8). A significant loss of temperature is observed over the period because of the lack of insulation surrounding the tank. The temperature decreases sharply at first and the rate of decrease levels off as time progresses. The temperature profile parallels the heat transfer from the tank, with the greatest heat transfer rate at high temperatures due to Newton’s law of cooling. The tank energy storage and thermal energy loss are shown over 24 h in Figure 7.9, while the tank exergy storage and thermal exergy loss are depicted in a similar format in Figure 7.10.

Several points concerning with the differences between energy and exergy values in TES applications can be noted by comparing Figures 7.9 and 7.10:

- First, the exergy storage and thermal exergy loss are much less than the corresponding energy quantities. This is due to the fact that the exergy of a substance is relative to the reference-environment state, and that thermal exergy is much less than thermal energy at near-reference-environment temperatures. In contrast, the energy of the thermal storage is considerable, reflecting incorrectly the usefulness of the TES.
- Second, while the energy storage and heat loss curves are almost linear, the corresponding exergy curves tend to change much more sharply with time. This observation indicates that the usefulness (or exergy content) of the thermal store is much greater at higher temperatures, that is, a high-temperature thermal storage contains much more exergy than a lower temperature storage. Clearly, exergy takes into consideration not only the quantity but also the quality of energy.

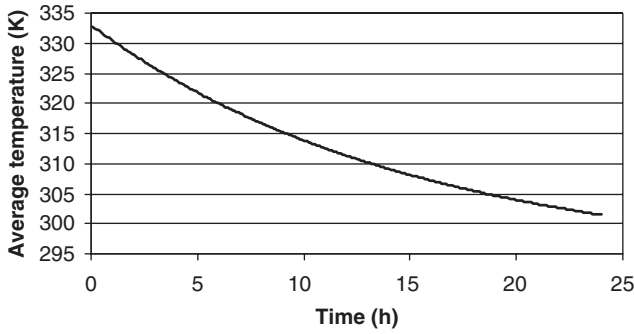


Figure 7.8 Volume-averaged temperature in the storage tank over the 24-h cooling period

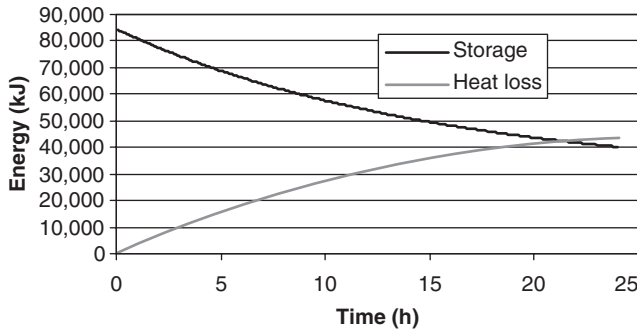


Figure 7.9 Total energy storage and thermal energy loss over the 24-h cooling period

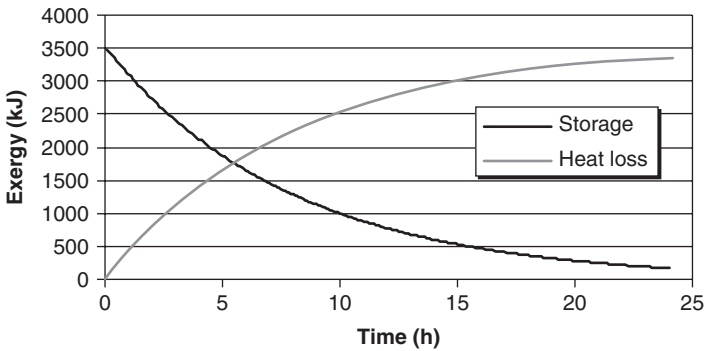
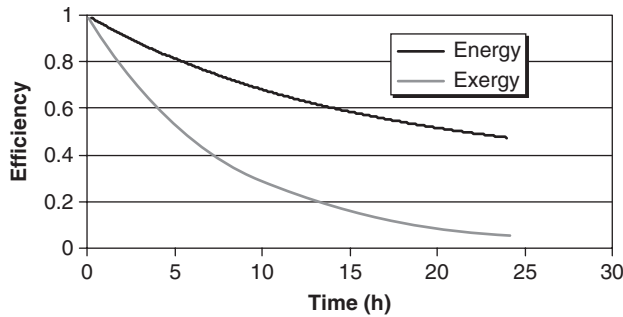


Figure 7.10 Total exergy storage and thermal exergy loss over the 24-h cooling period

These results demonstrate useful aspects of exergy analyses and explain in part why both energy and exergy efficiencies are often sought in evaluating the merit of TES systems.

The efficiencies for this case are shown as a function of time in Figure 7.11. As anticipated, the exergy efficiencies are much lower than the corresponding energy efficiencies, and represent a more realistic view of system performance. If the tank were left to cool for an infinite time, the exergy profile would asymptotically approach a zero efficiency value. However, the energy profile would





**Figure 7.11** Variation with time of the energy and exergy efficiencies of the cooling process

eventually decrease to a value of  $mh_{\infty}/E(0)$  or approximately 33.4%. The fact that a completely useless mass of water, with zero heating potential, still retains a recovery efficiency of 33.4% illustrates the inadequacies of using energy alone in TES system assessments and improvement efforts.

### Closure for Case Study 1

The cooling is investigated for a large tank of hot water initially at  $60^{\circ}\text{C}$  as it exchanges heat with its surroundings at  $20^{\circ}\text{C}$ , via convective heat transfer with a convective coefficient of  $10\text{ W/m}^2\text{ K}$ . The average temperature within the tank is monitored as time progresses, so that efficiencies and thermal losses can be recorded.

The process is observed to be highly efficient in both the energy and exergy senses at the beginning of the simulation, since most of the thermal energy or exergy can be recovered. As time progresses and the temperature of the storage tank drops due to heat losses, the efficiencies decrease and less recoverable thermal energy or exergy remains. The energy efficiency is 47.5% after the 24-h cooling period, while the exergy value is 4.79%. The differences between the two efficiencies demonstrate the usefulness of exergy analysis in TES applications: since the TES is at a temperature of just over  $23^{\circ}\text{C}$  after the 24-h period, it is misleading to deem that the thermal energy is almost half recoverable as the energy efficiency suggests since the quality of the thermal energy is neglected.

This case study is intended to give the reader an understanding of the usefulness of FLUENT in TES applications. Although this particular example is simple and incorporates many assumptions to simplify the modeling and simulation, it provides a good introduction for the more complicated simulations that are investigated in subsequent case studies. These include forced convection and stratification for sensible TES, as well as external flow, solidification, and melting for latent TES.

### 7.5.2 Case Study 2: Forced Convection in a Stratified Hot Water Tank

This case study is concerned with forced convection in a stratified, hot water storage tank. Whereas the study in the previous section is concerned with the losses due to only natural convection, this example examines the charging of a hot water tank with warm water. The tank considered is cylindrical, with a height of 100 cm and a radius of 15 cm, and is insulated along its walls with fiberglass. The tank is initially at a temperature of  $20^{\circ}\text{C}$ . A schematic of the system is shown in Figure 7.12. The physical model and variable inputs are chosen to be similar to those in an investigation by Ghaddar and Al-Maarafie (1997). FLUENT is used to investigate the charging process using hot water at  $70^{\circ}\text{C}$ .

The system is subject to convective heat loss to surroundings at  $20^{\circ}\text{C}$ , and has a surface convective heat transfer coefficient of  $4.5\text{ W/m}^2\text{ K}$ , which is taken to be constant. The inlet velocity

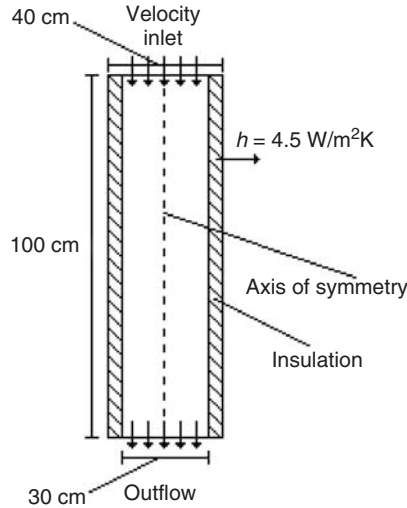


**Figure 7.12** Schematic of physical domain of a thermal storage, modified from Ghaddar and Al-Maarafie (1997)

is treated as uniform. The effect of flow rate on the resulting performance criteria is examined by considering two flow rates (9 L/min and 3 L/min). The water is taken to have a density of  $998.2 \text{ kg/m}^3$ , a specific heat of  $4.182 \text{ kJ/kg K}$ , a thermal conductivity of  $0.6 \text{ W/m K}$ , and a dynamic viscosity of  $0.00103 \text{ kg/m s}$ . Natural convection is considered negligible. As the Reynolds number for the flow cases considered here is between 200 and 650, which is in the laminar regime, the flows are treated as laminar. The insulation is a common fiberglass type, with a density of  $12.0 \text{ kg/m}^3$ , a specific heat of  $0.844 \text{ kJ/kg K}$ , and a thermal conductivity of  $0.04 \text{ W/m K}$  (Harris *et al.*, 2003).

The flow is considered to have a no-slip condition on the inner walls of the insulation, which is contained by a steel wall of thickness 3 mm. Although not shown in Figure 7.12, this boundary condition includes a “virtual” wall for simulation purposes; it does not occupy finite space, but still applies a conductive resistance to the heat flow as in a thin wall. The steel in this case is considered to be stainless steel, with a density of  $8030 \text{ kg/m}^3$ , specific heat of  $0.502 \text{ kJ/kg K}$ , and conductivity of  $16.27 \text{ W/m K}$ , based on FLUENT default values. The specified inlet temperature and velocity corresponding to each flow rate considered, along with the outflow boundary condition (discussed in Section 7.4.3) and convectively cooled tank walls, provide sufficient boundary and initial conditions for the simulation.

The model was created using GAMBIT software, with special attention at the inner walls of the flow regime. The computational domain, separated into finite volumes, can be seen in Figure 7.13. The cell densities on the inner walls of the tank can be seen in Figure 7.13(a) and (b), where longitudinal and cross sections of the volume, respectively, are shown. The top view in Figure 7.13(c) shows the cell distribution and shape of the outer tank wall more clearly. The meshing is developed by first creating a four-layer boundary region on the innermost cylinder, with an initial spacing of 0.5 cm and a growth factor of 1.2. With this boundary layer, the cells for the remainder of the volume, including the insulation, are created with hex/wedge elements in a cooper-type mesh, resulting in a total of 7718 computational volumes.

This physical domain, after specifying the appropriate zone and boundary types, is simulated with FLUENT. The inlet velocity is set to  $0.000707 \text{ m/s}$  and  $0.002121 \text{ m/s}$  for the flow rates of 3 L/min and 9 L/min, respectively. Simulations are run for 18 min of real flow time for the slower flow rate and 6 min for the faster, with three data samples of the temperature and velocity fields

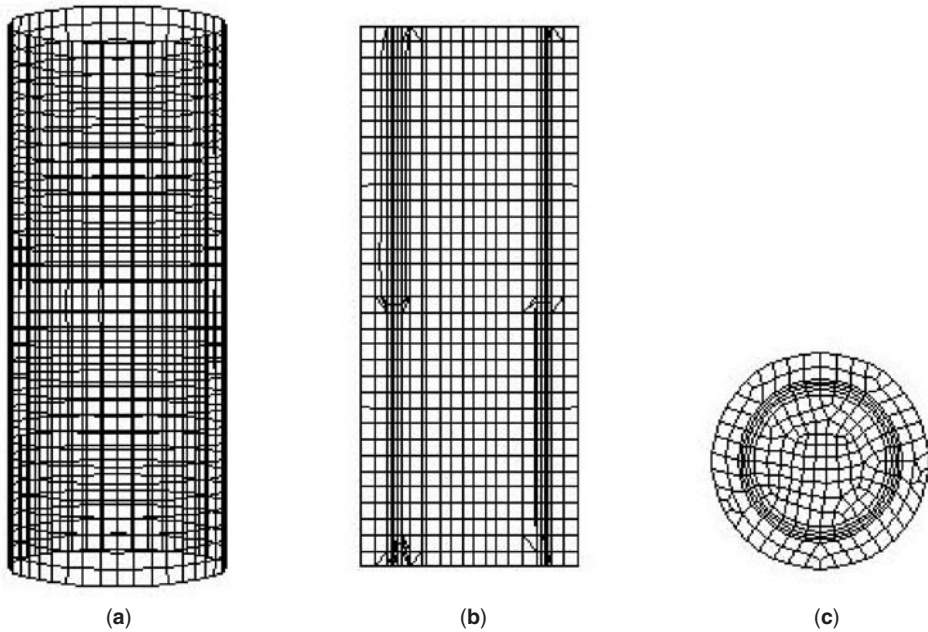


**Figure 7.13** Views of the computational grid for the hot water storage in the outer wall section (a), radial cross section (b), and axial cross section (c)

taken at equally spaced intervals in each case. The residual tolerances are set to  $10^{-3}$  for the  $x$ ,  $y$ , and  $z$  velocities and continuity and  $10^{-6}$  for energy.

To simulate the efficiency and performance equations correctly, the following quantities are monitored over the duration of the simulation: the outlet mass-weighted average temperature (see Equation 7.21), the volume-weighted water and insulation average temperatures (Equation 7.23), and the surface heat flux from the tank (Equation 7.22). The simulations are run with a time step of 1 s for the slower flow rate and 0.5 s for the faster, while temperature and heat flux data are taken at 5-s intervals. A comparison of the simulation results with experimental results from Ghaddar and Al-Maarafie (1997) shows good agreement. Time step independence is also verified, but the reader should consult the case study in Section 7.7.2 for an illustration of the methodology of independence verification. With the proper monitors in place and the computational domain initialized at  $20^\circ\text{C}$ , the simulation is then run with a computational time ratio of about 1:1, so that each simulation concludes in less than 20 min.

### Performance Criteria

The energy balance for the tank charging process at time  $t$  is as follows:

$$\Delta E_{sys} = \Delta E_{water} + \Delta E_{insulation} = \int_0^t \dot{m}C (T_{in} - \bar{T}_{out}) dt - Q(t) \quad (7.30)$$

where  $Q(t)$  is the total heat loss from the system at time  $t$ . Since the purpose is hot water storage, the energy product for the energy efficiency is taken to be the change in energy of the water in

the tank. The total required energy is the total flow energy difference in the flow, so the energy efficiency can be expressed as

$$\eta = \frac{E_{prod}}{E_{input}} = \frac{\Delta E_{water}}{\Delta E_{water} + \Delta E_{insulation} + Q(t)} \quad (7.31)$$

The total heat loss is evaluated by approximate integration over  $n$  time steps of equal length  $\Delta t$  as

$$Q(t) = \int_0^t Q dt = \sum_{i=0}^n Q_n \Delta t \quad (7.32)$$

Since kinetic and potential energy effects are neglected, the changes in energy in both the water and insulation portions of the domain are evaluated using incompressibility assumptions as

$$\Delta E_{water} = m_{water} C_{water} (\bar{T}_{v,water} - T_{\infty}) \quad (7.33)$$

$$\Delta E_{insulation} = m_{insulation} C_{insulation} (\bar{T}_{v,insulation} - T_{\infty}) \quad (7.34)$$

The ambient temperature in this case is set to 20°C, while the masses of water and insulation are 70.1 kg and 0.66 kg, respectively.

The exergy analysis reflects the losses associated with the mixing of fluids, which is an irreversible process. The exergy balance can be expressed as follows:

$$\Delta \Xi_{sys} = \Delta \Xi_{water} + \Delta \Xi_{insulation} = \epsilon_{in} - \epsilon_{out} - X_I - I \quad (7.35)$$

Before delving into entropy balances, which can be used to calculate the exergy destroyed because of irreversibility  $I$ , the exergy efficiency is defined in the same format as used for the energy efficiency. That is, the exergy efficiency is taken to be the ratio of product exergy to the thermal exergy stored in the tank, or the change in exergy in the storage medium, water. The required input exergy content is the difference in exergy from the inlet to outlet, so that

$$\psi = \frac{\Xi_{prod}}{\Xi_{input}} = \frac{\Delta \Xi_{water}}{\Delta \Xi_{water} + \Delta \Xi_{insulation} + X_I(t) + I(t)} \quad (7.36)$$

Here, the exergy change of the system at any time  $t$  is once again obtained from the instantaneous volume-averaged temperatures in the respective mediums:

$$\Delta \Xi_{water} = m_{water} C_{water} \left[ \bar{T}_{v,water} - T_{\infty} - T_{\infty} \ln \left( \frac{\bar{T}_{v,water}}{T_{\infty}} \right) \right] \quad (7.37)$$

$$\Delta \Xi_{insulation} = m_{insulation} C_{insulation} \left[ \bar{T}_{v,insulation} - T_{\infty} - T_{\infty} \ln \left( \frac{\bar{T}_{v,insulation}}{T_{\infty}} \right) \right] \quad (7.38)$$

The exergy loss due to heat leakage is again calculated with an approximated integral, assuming heat leakage takes place at the average temperature of the insulation:

$$X_I(t) = \int_0^t \left( 1 - \frac{T_{\infty}}{\bar{T}_{v,insulation}} \right) Q dt = \sum_{i=0}^n \left( 1 - \frac{T_{\infty}}{\bar{T}_{v,insulation,i}} \right) Q_i \Delta t \quad (7.39)$$

The remainder of the performance criteria determination is concerned with evaluating the exergy destroyed by irreversibilities. Entropy expressions are used, including an entropy balance at time  $t$ :

$$\Delta S_{sys} = \Delta S_{water} + \Delta S_{insulation} = (S_{in} - S_{out})(t) + S_Q(t) + \Pi(t) \quad (7.40)$$

where

$$\Delta S_{water} = m_{water} C_{water} \ln \left( \frac{\bar{T}_{v,water}}{T_{\infty}} \right) \tag{7.41}$$

$$\Delta S_{insulation} = m_{insulation} C_{insulation} \ln \left( \frac{\bar{T}_{v,insulation}}{T_{\infty}} \right) \tag{7.42}$$

$$S_Q(t) = \frac{Q(t)}{\bar{T}_{v,insulation}} \tag{7.43}$$

If the quantity  $\bar{T}_{out}$  is measured for the outflow, then the total difference in entropy flow at any time  $t$  is as follows:

$$(S_{in} - S_{out})(t) = \int_0^t \dot{m} C_{water} \ln \left( \frac{\bar{T}_{out}(t)}{T_{in}} \right) dt = \sum_{i=0}^n \dot{m} C_{water} \ln \left( \frac{\bar{T}_{out,t}}{T_{in}} \right) \Delta t \tag{7.44}$$

Finally, the exergy destroyed because of irreversibilities is evaluated:

$$I(t) = T_{\infty} \Pi(t) \tag{7.45}$$

and the exergy efficiency can now be determined.

### Results and Discussion

FLUENT allows for data sampling of the entire field at any time during the simulation. Here, the temperature and velocity fields are sampled at intervals of 6, 12, and 18 min for the flow rate of 3 L/min, and at intervals of 2, 4, and 6 min for the flow rate of 9 L/min. These sampling rates permit qualitative examinations of the intrinsic nature of the flow and temperature values in the tank. For a lengthwise cross-section of the tank, temperature distributions for the flow rates of 3 L/min and 9 L/min, respectively, can be seen in Figures 7.14 and 7.15, while corresponding velocity distributions are shown in Figures 7.16 and 7.17.

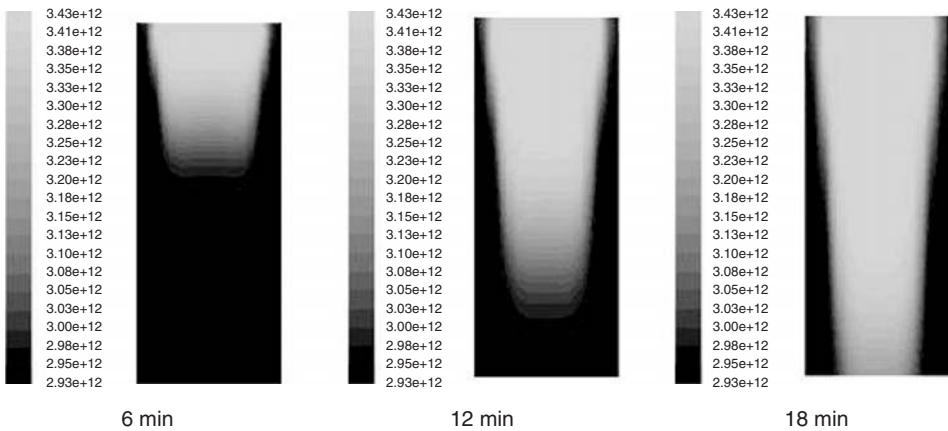


**Figure 7.14** Temperature distributions (in K) in a thermal storage tank at selected times for a flow rate of 3 L/min

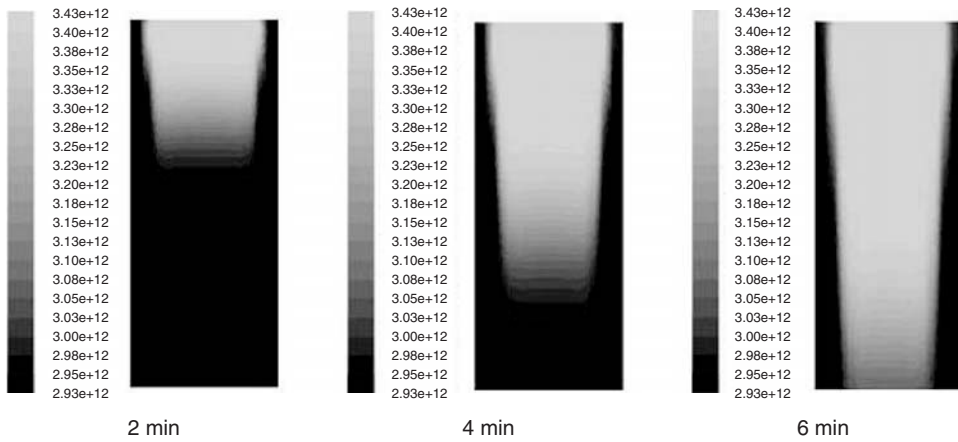


**Figure 7.15** Temperature distributions (in K) in a thermal storage tank at selected times for a flow rate of 9 L/min

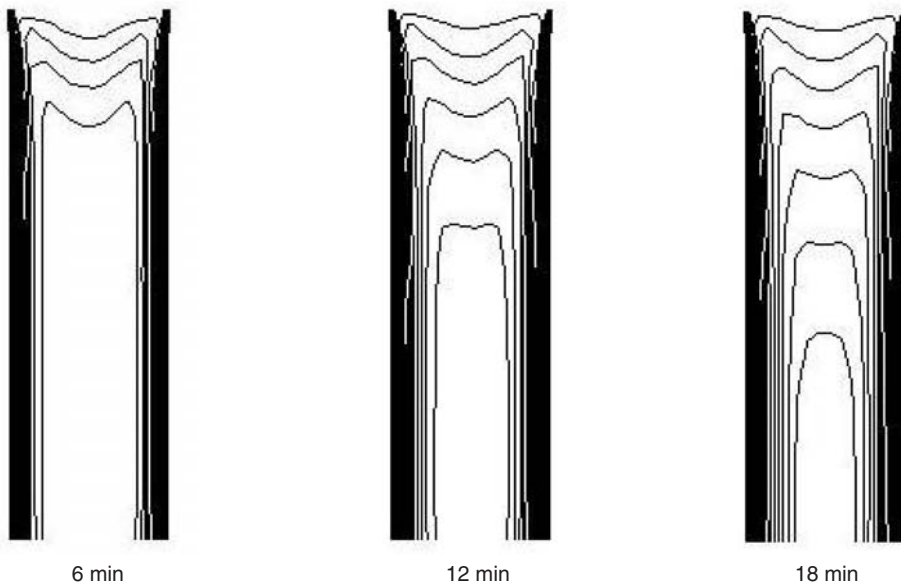


**Figure 7.16** Velocity contours in a thermal storage tank at selected times for a flow rate of 3 L/min

The distinct difference in temperature between the insulation and the flowing fluid is clearly evident in the temperature distributions. The insulation hinders the amount of heat transfer to the ambient air, and the dark color in this region, indicating a relatively low temperature, confirms that little heat escapes. As time progresses, however, especially for the slower flow rate case (Figure 7.14), the upper portion of the tank is seen to be losing some heat because of the increasing temperature difference between the ambient air and the warm inner fluid. It is also observed that a thermal boundary layer is developing in the flow and, although this case is not simulated for

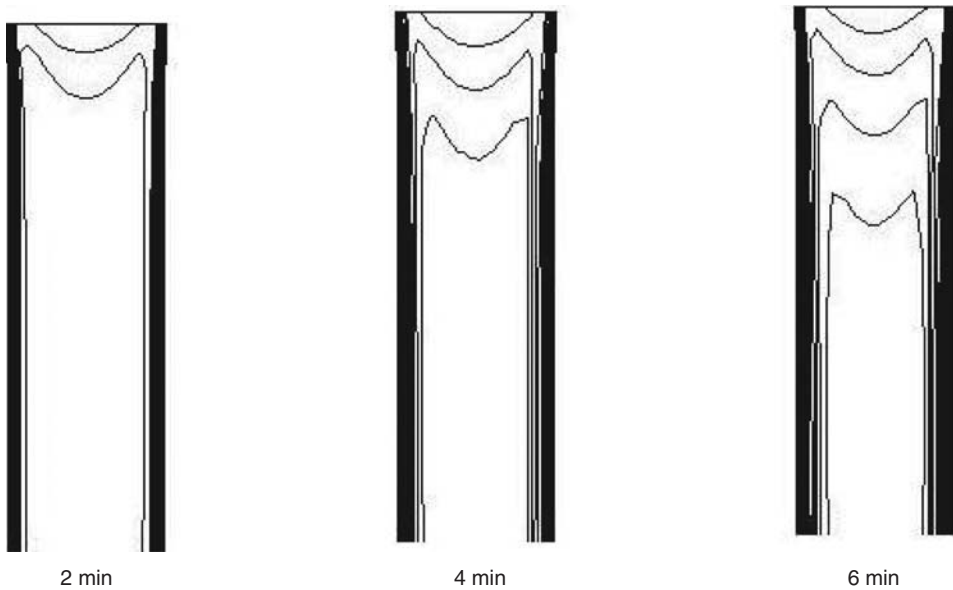


**Figure 7.17** Velocity contours in a thermal storage tank at selected times for a flow rate of 9 L/min

steady-state conditions, it is apparent that equilibrium would be reached after sufficient time with respect to thermal and velocity gradients within the computational domain.

The shapes of the temperature contours in Figures 7.14 and 7.15 are also interesting to compare. In the faster moving flow, the temperature contours at the edge of the warm flow appear to be much more sharply differentiated from the cold region. In contrast, the slower flow appears to have more rounded isotherms, mainly because of the fact that more time is available in the case of the slower flow rate for heat from the hot water to diffuse downstream. In both cases, the hot water travels the same distance along the tank, but less heat diffusion clearly occurs in the faster moving case, yielding less rounded isotherms.

The velocity contours also help explain the differences in the temperature profiles for the two flow rates. Since the computational domain is initialized at zero velocity, there is a trend as the fluid traverses the tank for the flow to become fully developed, as seen in Figures 7.16 and 7.17. There, the velocities become more representative of a continuous, fully developed regime as time progresses, and less like plug flow. Consequently, the corresponding isotherms also tend toward fully developed flow.

The types of contour plots shown here, which are easily accessible in FLUENT, help determine whether simulations are achieving good results, and in some cases can indicate problems in modeling and setup. For this reason, it is prudent when performing simulations to intermittently check the pressure, temperature, and flow fields to determine the accuracy or precision of the numerical progression.

After reviewing qualitative aspects of the simulation, the previously outlined performance criteria and their variations with time can be examined, including thermal energy and exergy losses, exergy destruction due to irreversibility, and energy and exergy efficiencies. The variation with time of the overall volume-averaged temperature of the tank and insulation are shown for the two flow rates considered in Figures 7.18 and 7.19. The two temperature profiles appear similar, but for the case with the slower flow rate (3 L/min), the temperature of the insulation is higher. This phenomenon is due to the increased wall conduction and correspondingly reduced heat loss to the surroundings associated with the longer charging time.

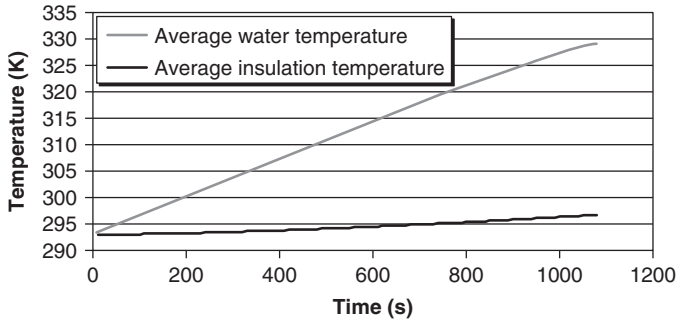


**Figure 7.18** Volume-averaged temperatures of the water and insulation for a flow rate of 3 L/min

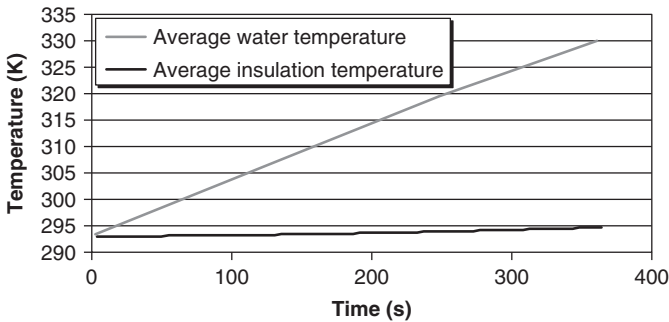


**Figure 7.19** Volume-averaged temperatures of the water and insulation for a flow rate of 9 L/min

The two flow rates exhibit similar trends and are compared in the remainder of the analysis by plotting them against a dimensionless time,  $t^* = t/t_{\max}$ , to better reveal their differences. For the 3 L/min case,  $t_{\max} = 1800$  s, and for the case where the flow rate is 9 L/min,  $t_{\max} = 360$  s.

The loss of heat to the environment,  $Q(t)$ , is plotted as a function of the dimensionless time  $t^*$  in Figure 7.20 for both flow rate cases. It is clear that the higher flow rate case experiences a greater heat loss, which is almost five times the heat loss of the 3 L/min flow rate case.

The energy efficiencies for both cases are presented in Figure 7.21. The energy efficiencies are very high for both cases, indicating that almost all of the injected heat is recovered. At the conclusion of each simulation, that is, when  $t^* = 1$ , the energy efficiencies are 99.93% and 99.84% for the flow rates of 9 L/min and 3 L/min, respectively. Furthermore, since the only mode of energy loss is heat leakage, the efficiencies are directly dependent on heat leakage. For the higher flow rate, the energy efficiency is higher since less heat leaks to the surroundings.

The energy efficiencies do not reflect the thermodynamic performance properly, and a more comprehensive view is provided when exergy considerations are taken into account. The exergy loss to the surroundings via heat loss is shown in Figure 7.22. A comparison of this figure with Figure 7.20 shows that the absolute magnitudes of the thermal energy and exergy losses differ greatly, with the heat leakage varying between 5 and 30 J, while the corresponding exergy values of these heat leakages are relatively insignificant (less than one-hundredth of a joule in all cases). These values indicate that the tank is well insulated, and are not a large factor in performance calculations. The thermal exergy loss is small because the heat loss occurs at a temperature near that of the reference environment. The exergy associated with the heat loss depends on the temperature



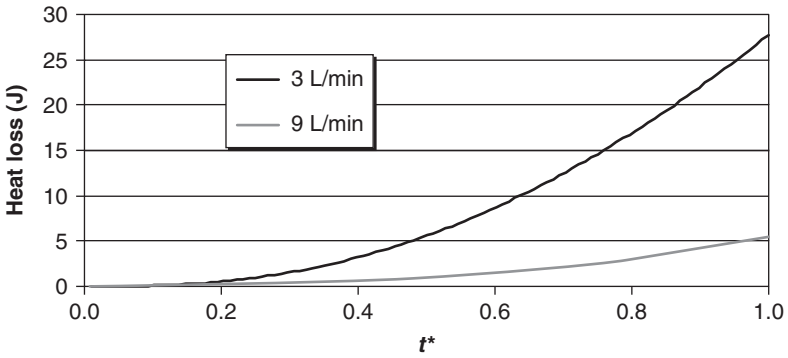


Figure 7.20 Loss of thermal energy from the storage to the surroundings, for the two flow rates

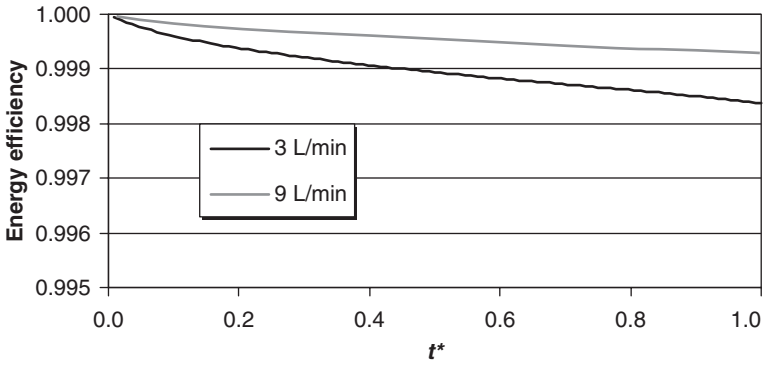


Figure 7.21 Energy efficiencies of the storage, for the two flow rates

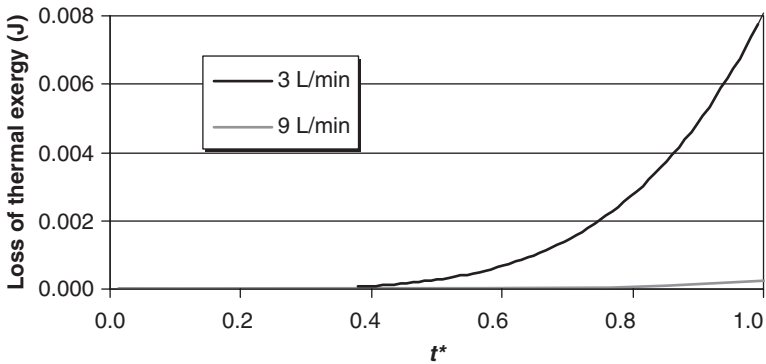
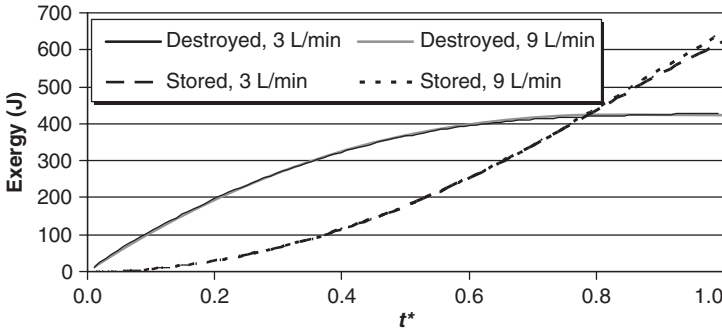
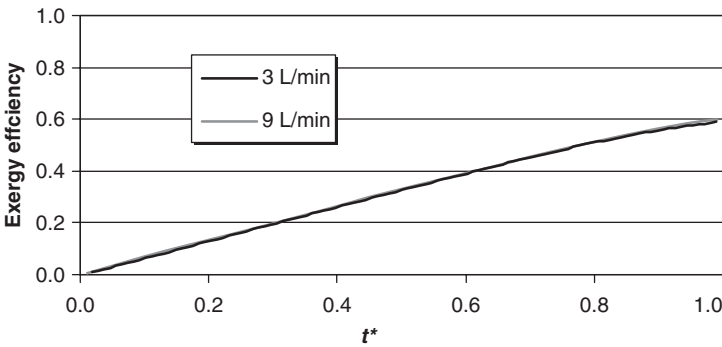


Figure 7.22 Exergy lost from the storage to the surroundings owing to heat leakage, for the two flow rates



**Figure 7.23** Exergy destruction in the storage due to irreversibilities and exergy of the stored hot water, for two flow rates



**Figure 7.24** Exergy efficiencies of the storage, for the two flow rates

ratio of heat loss to the reference environment in such a manner that these temperatures render the thermal exergy loss very small, especially in comparison to the overall thermal exergy of the tank.

The other component of the exergy loss, the destroyed exergy, is displayed in Figure 7.23. Also shown is the exergy of the stored hot water. This loss provides a much more perceptive picture of the overall performance of the charging process, since the destroyed and stored exergies both significantly affect the exergy efficiency. The exergy destroyed because of irreversibilities is much greater than the thermal exergy loss and is the main contributing factor to the exergy efficiency values (see Figure 7.24), which are approximately 60% at the conclusion of the simulation for both flow rate cases. The exergy efficiencies are clearly significantly lower than the energy efficiencies.

The exergy efficiencies are lower largely as a result of the recoverable thermal exergy. Near the beginning of the simulation, the overall water tank temperature is low and it can be shown with Equation 7.18 to have little exergy (see Figure 7.23). As the volume-weighted temperature of the tank increases, its recoverable exergy content becomes greater. Since the thermal energy input to the tank is of a much higher quality because of its relatively high temperature, the ratio of recovered to input exergy is initially almost zero and increases as the tank charges. However, it is apparent in Figure 7.23 that the increase in exergy destruction with time levels off after a period of time. This observation is mainly attributable to the fact that the outlet temperature increases with time, so less mixing with the colder fluid occurs. When the outlet temperature rises, the exergy difference between inlet and outlet drops sharply, so less of the quality of the charging fluid is wasted. The exergy efficiency consequently levels off also, as can be partly seen in Figure 7.24.

The result comparisons also reveal a similarity between the efficiencies of the two flow rates considered. The energy efficiencies, although of high magnitude, exhibit discernable differences, as seen in the profiles for the two flow rates. However, the exergy efficiencies are more similar. This observation reinforces the point made earlier that thermal leakage, which differs greatly for the two cases, does not affect exergy efficiency markedly. For both cases, heat leakage and the energy stored in the insulation are unimportant, and it is the exergy destruction (due to entropy generation) that affects performance significantly. The two storage cases are equally efficient at charging the thermal store.

Finally, it is noted that the results demonstrate that energy analysis creates confusion regarding the performance of this TES system. While energy analysis suggests to engineers that the process is nearly ideal, the exergy efficiencies indicate that this is not the case, and that there exists a significant margin for efficiency improvement. This important observation recurs in subsequent case studies.

### Closure for Case Study 2

In this sensible TES case study, the charging of an insulated, stratified hot water tank with forced convection is investigated. The tank considered contains around 72 L of water initially at the ambient temperature of 20 °C, and is charged using hot water at 70 °C. Heat loss to the surroundings is accounted for. Two flow rates (3 and 9 L/min) are considered, and the simulated charging times for the two cases are 18 min and 6 min, respectively. To facilitate performance calculations, average temperatures in the water and insulation regions are monitored, as are the total heat loss through the outer tank walls and the mass-weighted outlet temperature.

The main simulation results demonstrate that the energy and exergy efficiencies exhibit different trends. The energy efficiency of the process begins at 100% and gradually decreases over the course of the simulation to 99.9%, while the exergy efficiency begins at 0% and increases with time to a final value of approximately 60%. This result suggests that a thorough charging of hot water tanks provides one means of avoiding loss of energy quality. The energy and exergy losses due to heat leakage to the environment are found to affect performance values relatively insignificantly.

Although this sensible TES case study is more complex than the first in terms of thermodynamic analysis, the simulation of similar sensible TES processes is relatively straightforward. The ease of numerical solution has a cost – the need to understand the volume and surface monitors available (many of which are either not mentioned or addressed in Section 7.6.3) sufficiently well so that they can be used to achieve proper results.

### 7.5.3 General Discussion of Sensible TES Case Studies

The case studies in this section help illustrate the usefulness of FLUENT and, more generally, finite volume solvers. While the modeling and simulation algorithms are complex, commercially available software for TES purposes provides ease of use. Complex fluid flow problems coupled with heat transfer phenomena can be straightforwardly investigated.

In the first case study, natural convection is modeled in a large storage tank, with heat leakage via natural convection. The simulation results confirm the contribution of insulation to efficiency. Similarly, forced convection is modeled in the second case study for an insulated storage. The results show that the heat leakage to the surroundings detracts less from efficiency than internal irreversibilities. In both cases, energy efficiencies are misleadingly high, and second-law considerations need to be taken into account to better understand performance and efficiency.

The case studies presented provide a good introduction to the latent TES cases considered subsequently. Most latent TES systems involve some sensible heat interactions, for example, in a heat transfer fluid (HTF). In addition, to extract energy from a latent store like a PCM, temperature changes in the liquid or solid phases sometimes occur, and sensible considerations must be

accounted for. The main objective of the following section is to build upon the material introduced in this section and thereby explain how more complicated cases may be simulated using FLUENT. However, since many of the modeling, simulation, and analysis techniques are similar, repetition is avoided in the next section and only pertinent information provided.

## 7.6 Numerical Modeling, Simulation, and Analysis of Latent TES Systems

The modeling and simulation of latent TES systems is addressed in this section. Latent TES systems are finding increasing applications because of their high volumetric heat capacities. However, compared to sensible TES systems, which are usually water based, latent TES systems can be subject to more implementation difficulties. These include finding a material with a suitably high heat of fusion and a melting point near the desired temperature, and that is relatively benign and reliable, so that successive charging and discharging cycles can be carried out without replacement of equipment. Since solidification or melting occurs for a given storage material at a specified temperature and pressure, care must be exercised to ensure that proper conditions are in place for effective phase change, which is most desirable at the heat utilization temperature of the application.

Building on the modeling, simulation, and analysis of sensible TES systems in previous sections, much of the following material avoids unnecessary repetition. Nonetheless, several models and equations need to be introduced to permit the case studies to be studied properly. These include the volume of fluid (VOF) model, the solidification/melting model, and various ancillary equations for heat transfer and thermodynamic analysis. This treatment is intended to provide the reader with a good understanding of the modeling and simulation of latent TES systems and to facilitate practical and accurate representations of real scenarios.

### 7.6.1 Modeling

The modeling of latent TES systems does not differ greatly from the modeling of sensible systems, as explained in Section 7.4.1. The computational domains and grid meshing procedures are analogous to the material explained in the previous modeling section. In some cases, moving-grid schemes can be used for more accurate simulations, thereby allowing solid/liquid interfaces to contain a greater concentration of cells. However, the scope of this chapter allows only some options to be explained.

Throughout the analysis, the same principles as in Section 7.4.1 are applied. It is generally advantageous to place more cells (volumes) in areas where phase change is expected to occur. This practice is addressed in subsequent case studies.

### 7.6.2 Heat Transfer and Fluid Flow Analysis

The phase change that occurs in latent TES leads to slight differences in the heat transfer and energy equations used in the computational domain. For those volumes in liquid phase, however, the same expressions from Section 7.4.2 apply, for example, Navier–Stokes and continuity equations. The Boussinesq model for natural convection is not to be used because of the complexities it introduces, which greatly lengthens modeling, setup, and computational times. For example, Assis *et al.* (2007) investigated melting in a spherical enclosure with FLUENT, accounting for density changes from phase change and natural convective currents. The computational time ratio in this case is over 300:1, even with a markedly more powerful computer than the one used in these case studies. The resulting simulations can require several days, while the models used in this treatment have simulation durations of only a few hours, with little loss in result accuracy or validity. With FLUENT, modeling natural convection and density differences in phase change in an enclosed

volume requires knowledge of C+ programming to implement special user-defined functions in each phase. A detailed explanation of the implementation of C+ scripts into FLUENT is beyond the scope of this book, but is needed for assessments of natural convection.

As mentioned earlier, the continuity and momentum equations in Equations 7.4 and 7.5 are valid in the fluid regions. However, the energy balance in Equation 7.1 is modified to account for energy absorption during phase change. Utilizing a modified enthalpy, the energy equation can be written as follows:

$$\frac{\partial}{\partial t} (\rho h' - p) + \nabla \cdot (\vec{V} \rho h') = k \nabla^2 T + \Phi \quad (7.46)$$

where  $h'$  denotes a combined specific enthalpy, which is the sum of two contributions: the sensible enthalpy  $h$  and the latent enthalpy  $h_{latent}$ . That is,

$$h' = h + h_{latent} \quad (7.47)$$

The sensible enthalpy is calculated with Equation 7.3, and FLUENT uses the enthalpy/porosity method (Voller, 1987; Voller and Prakash, 1987; Voller *et al.*, 1987) to calculate the latent portion. In lieu of a solver that produces a specific melt interface position, this method is often chosen to solve problems with more complex geometries. Instead of tracking the solid/liquid interface position explicitly, the “liquid fraction,” that is, the fraction of the cell in liquid form, is determined. The liquid fraction  $\varphi$  is calculated as

$$\varphi = \frac{T - T_{solid}}{T_{melt} - T_{solid}} \quad (7.48)$$

where  $T_{solid}$  denotes the solidification temperature and  $T_{melt}$  the melting temperature. The liquid fraction is determined during each iteration to correctly define the temperature field and energy balance. The liquid fraction varies between  $\varphi = 0$  when  $T < T_{solid}$  and  $\varphi = 1$  when  $T > T_{melt}$ . Cells with a liquid fraction between 0 and 1 have a temperature of  $T_{solid} < T < T_{melt}$  and it is only when a cell has a temperature between  $T_{solid}$  and  $T_{melt}$  that the liquid fraction in Equation 7.48 is calculated.

The latent enthalpy can be written in terms of the latent heat of the material  $L$  and the liquid fraction  $\varphi$ :

$$h_{latent} = \varphi L \quad (7.49)$$

Once a cell has received or released all of its latent heat, it cools or warms in a sensible manner as either a solid or a liquid, depending on the process. Equations 7.46 through 7.49, when combined with the sensible enthalpy (Equation 7.3), allow the liquid fractions in all cells, and the temperature and latent energy absorbed in the entire domain, to be calculated.

Note that for the solidification and melting modeling used in FLUENT, there exists a “mushy” zone, which refers to the portion of the domain with a liquid fraction between 0 and 1. This zone is treated as a porous medium, creating a momentum sink. However, due to the lack of forced convection over solidifying or melting regions and the lack of natural convective currents, this momentum sink becomes negligible, and is consequently usually omitted from the momentum equations. For most cases, the solidification and melting temperatures can be set to be equal to facilitate computations and avoid the dampening effects of the mushy zone.

The VOF model also plays an important role. This model permits two or more fluids to be treated by specifying the interface and patching each phase once the domain has been initialized. This approach is important for phase change in an enclosed space, where compressible air is often present with a PCM, to allow for expansion. In the VOF model, the momentum equations are satisfied for the two fluids, and a quantity called the *volume fraction* is computed in each cell for each iteration. The volume fraction ranges from 0 to 1 for each fluid, where a volume fraction of 0 indicates that the cell is void of the fluid and 1 indicates that the cell contains only the fluid.

A volume fraction between 0 and 1 indicates that the cell contains an interface between the fluid and another substance. The momentum and energy equations can be chosen based solely on the volume fraction of each cell, allowing the simulation to proceed. While the VOF model is suitable for predicting phase change in the presence of a compressible gas, it involves some computational challenges, as shown for the case study in Section 7.7.1.

The models presented here, with the accompanying modifications to the heat transfer and fluid flow equations, allow latent TES systems to be well represented for simulation. Before applying these models in the case studies, changes in both simulation and thermodynamic analyses are described.

### 7.6.3 Simulation

For simplicity, the SIMPLE algorithm (Section 7.4.3) is utilized in the subsequent case studies. Although a pressure-based solver is not always the best choice when a simulation is concerned with density changes and natural convection during phase change, it nonetheless provides reasonable convergence characteristics for the cases considered.

### 7.6.4 Thermodynamic Analysis

The thermodynamic assessment discussed in Section 7.4.4 applies to latent TES systems, but with a few minor differences in the energy and entropy expressions to account for solidification and melting. The enthalpy change of a material as it undergoes phase change is expressible as

$$\Delta H = \pm mL \quad (7.50)$$

where the positive sign is associated with melting and the negative sign with solidification.

The entropy change during phase change can be expressed as

$$\Delta S = \frac{\Delta Q}{T_b} \quad (7.51)$$

where the subscript  $b$  denotes the boundary at which the heat transfer occurs. For a substance undergoing phase change with heat transfer with its surroundings at a temperature of  $T_{sf}$ , normally taken as the solidification temperature, the change in entropy can be written as

$$\Delta S = \frac{\pm mL}{T_{sf}} \quad (7.52)$$

To calculate entropy changes, which facilitate the evaluation of entropy and exergy balances, the heat added and the temperatures of the substances need to be known. In some cases, there are changes in the densities of the mediums due to phase change. To evaluate entropy changes in the system in such instances, the mass-weighted average temperature is used:

$$\bar{T}_m = \frac{\sum_{i=1}^n T_i \rho_i |V_i|}{\sum_{i=1}^n \rho_i |V_i|} \quad (7.53)$$

This parameter is similar to the volume-weighted quantity in Equation 7.23. Furthermore, an additional monitor is put in place to observe the heat dissipation from viscous sources. Hence, the

mass-weighted total pressures at the inlet and outlet are monitored:

$$\bar{p}_{out} = \frac{\sum_{i=1}^n p_i \rho_i \left| \vec{V}_i \cdot \vec{A}_i \right|}{\sum_{i=1}^n p_i \left| \vec{V}_i \cdot \vec{A}_i \right|} \quad (7.54)$$

With this parameter, changes in pressure can be translated to head generation from pressure.

## 7.7 Case Studies for Latent TES Systems

To build on the latent TES case studies in Section 7.5, two cases involving latent TES systems are examined here. The first case considers the melting of a PCM in an infinitely long cylinder, using a two-dimensional mesh representing the cross-section of such a cylinder. The second case considers melting and solidification in a spherical shell exposed to an external heat transfer fluid flow, and represents a more comprehensive analysis.

The first case demonstrates ways of using the VOF model. Since the PCM is modeled as in contact with a compressible gas, the density differences accompanying phase change are considered, and the sinking of the solid in the melting regime is observed. This particular case is computationally demanding, resulting in an extremely high computational time ratio. Although using the VOF model can help achieve more accurate results, especially when modeled with natural convective currents in the PCM volume, the second case study shows that simplifying assumptions can greatly reduce simulation time while retaining good results.

The second case study considers air as the heat transfer fluid that heats paraffin wax until it completely melts. The wax then cools until it completely solidifies. The model is subject to a complete validation and independence testing phase, after which it is considered accurate for similar simulations. This case presents a culmination of the first four case studies in this chapter, and serves as an example of proper comprehensive modeling and simulation using FLUENT of either latent or sensible TES systems.

Through these case studies and the techniques explained through them, the reader should be able to construct, model, and simulate various sensible and latent TES systems. As with any experiment or simulation, the main objective is to obtain useful results and to present them informatively. It is also demonstrated that simulation, while important, also requires sound analysis and interpretation of numerical data in order to achieve meaningful results.

### 7.7.1 Case Study 1: Two-Dimensional Study of the Melting Process in an Infinite Cylindrical Tube

This first latent TES case involves the melting process in a horizontal cylindrical duct. PCMs are often contained in cylindrical tubes because of the ease of manufacturing such enclosures as well as their ability to accommodate pressure changes induced by expansion or contraction of the PCM during phase change. A simplified approach is adopted in this case in which the tube is treated as infinitely long, resulting in a two-dimensional simulation.

The PCM is a paraffin blend, RT27, supplied by Rubitherm GmbH. Applications of RT27 in hot latent storage applications and experiments have been reported in the literature, for example, Assis *et al.* (2007). The paraffin fills 85% of the volume, while the VOF model (see Section 7.6.2) is used to account for the remaining 15%, which is filled with compressible air, acting as an ideal gas.



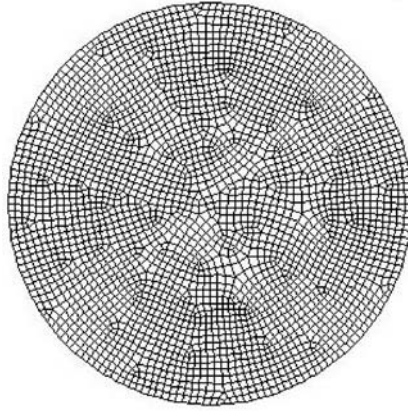


**Figure 7.25** Grid structure of the two-dimensional surface representing the infinite cylinder

Throughout the analysis, a two-dimensional cross section of the cylindrical duct of unit depth is considered. The cylinder has a diameter of 20 mm, and the volume can be created straightforwardly using GAMBIT software. The circular shape is constructed first, and then meshed with quadrilateral elements, in a paved meshing. The volume is discretized into 2890 cells, as shown in Figure 7.25. Since the melting front is not known *a priori*, no boundary layer meshings are created; consequently, the equations involving the melt front have equal accuracy, regardless of its position. Once the proper boundary (wall) condition and interior zones are identified, they are input to FLUENT for simulation.

The volume is assigned simple initial and boundary conditions to reduce the computational cost involving density changes with the VOF model. The entire volume, including both the PCM and air regions, is set initially to the ambient temperature of 25 °C (298 K). Then, a constant wall temperature boundary condition of 50 °C (333 K) is invoked to induce melting. This constant wall temperature is not intended to be a condition experienced in real scenarios, but rather is a simple boundary condition that allows for simpler calculations and thus permits the phase change process to be studied qualitatively. The small diameter of 20 mm is chosen to further reduce computational times, since the surface area to volume ratio decreases markedly as the diameter of the cylinder is decreased. Consequently, heat transfer from the cylinder increases, reducing the time required for complete melting of the PCM.

The solidification/melting model is enabled, as is the VOF model, to ensure that proper equations for phase change are used in the domain. Once initial and boundary conditions are set, the PCM is patched to the lower region to model the equilibrium initial state. A density contour diagram is presented in Figure 7.26, which shows the interface position of the PCM and air regions.

The PCM has a melting temperature of 30 °C and a solidification temperature of 28 °C. Many of the thermophysical properties are not held constant, but instead are considered to vary linearly between the two temperatures experienced during phase transition, to increase simulation accuracy. In the solid and liquid phases, respectively, the specific heats are taken to be 2.4 kJ/kg K and 1.89 kJ/kg K and the thermal conductivities 0.24 W/m K and 0.15 W/m K. The solid density is 870 kg/m<sup>3</sup> and the liquid density is 760 kg/m<sup>3</sup>. The decrease in density during melting indicates that expansion occurs during the process. In addition, the dynamic viscosity of the liquid is taken to be 0.0032 kg/m s. All thermophysical properties used here are taken from Assis *et al.* (2007). Air is modeled as an ideal gas, for which properties are obtained using FLUENT's built-in thermophysical properties.

With material properties and boundary conditions established, the melting progression is simulated using a time step of 0.005 s. Larger time steps can be shown in this case to result in a



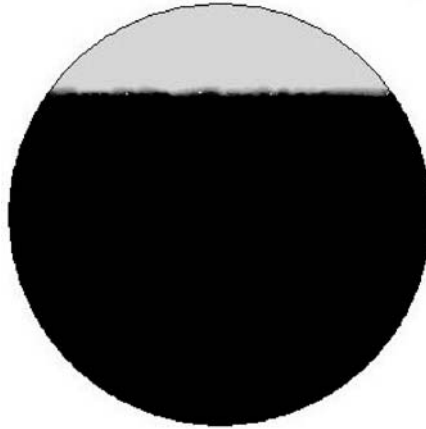


**Figure 7.26** Variation in density in the cylinder at time  $t = 0$ . The darker region represents the PCM and the lighter region above it represents air

diverging residual error, indicating the complexity of using the VOF model in conjunction with solidification/melting. To properly calculate the performance criteria, the heat flux to the region is monitored on an integral basis to determine the total heat addition to the volume as time progresses. To monitor quantitatively the solidification process, the liquid fraction is also monitored on a volume-averaged basis, and the mass-weighted temperature of the entire region is tracked to facilitate entropy calculations. All monitors sample at 1-s intervals throughout the melting process.

The residuals are set to default values of  $10^{-3}$  for the  $x$ ,  $y$ , and  $z$  velocities and continuity, and  $10^{-6}$  for energy. The total time to simulate the melting process is considerable; although the real time for the simulation was 173 s, the computational time required was over 4 h. These data indicate a computational time ratio of around 80:1. This result explains why a smaller volume is chosen for assessment here and demonstrates the increase in computational cost when changes in density are considered.

### Performance Criteria

With the data obtained from the monitors, the melting process can be evaluated on a thermodynamic basis. Energy, entropy, and exergy balances and efficiencies are presented and discussed.

The only energy input to the control volume is the heat added through the constant-temperature wall, so the energy balance can be written as

$$\Delta E_{sys} = Q_w \quad (7.55)$$

The energy efficiency is defined as the ratio of the energy stored in the volume, that is, the change in energy of the system, to the total input energy. Since no heat is assumed lost to the surroundings, the energy efficiency is

$$\eta = \frac{E_{prod}}{E_{input}} = \frac{\Delta E_{sys}}{Q_w} = 1 \quad (7.56)$$

The 100% energy efficiency is somewhat artificial because of the assumption regarding heat loss. For this system, all heat delivered to the PCM and used for melting is available for recovery on PCM solidification.

The exergy balance more effectively describes the behavior of this system. At any time  $t$  during the simulation, the exergy balance can be written as

$$\Delta \Xi_{sys} = X_w - I \quad (7.57)$$

where  $\Delta \Xi_{sys}$  denotes the change in exergy of the system,  $X_w$  the wall exergy addition associated with heat transfer, and  $I$  the exergy destroyed. Hence, we can examine the exergy efficiency progression during the melting process.

The total exergy transferred to the system via the heated wall over  $n$  sampling time periods of 1 s each from the start of the simulation to time  $t$  can be approximated as follows:

$$X_w = \int_0^t \left(1 - \frac{T_\infty}{T_w}\right) Q_w dt = \sum_{i=0}^t \left(1 - \frac{T_\infty}{T_w}\right) Q_{w,t} \quad (7.58)$$

Since the exergy destroyed due to irreversibilities is given by the relation

$$I = T_\infty \Pi \quad (7.59)$$

the exergy efficiency can be determined using the total entropy generated from the start of the simulation to time  $t$ , which can be obtained with an entropy balance:

$$\Delta S_{sys} = \frac{Q_w}{T_w} + \Pi \quad (7.60)$$

The entropy addition to the system by the heated wall is approximated using the sampled data from the monitors:

$$\frac{Q_w}{T_w} = \sum_{i=0}^n \frac{Q_{w,t}}{T_w} \quad (7.61)$$

The change in entropy of the system must account for the change in phase and a change in density in both regions. For an internally reversible process, the change in entropy can be evaluated as an integral of the ratio of heat transferred to the temperature of the heat transfer:

$$S_2 - S_1 = \left( \int_1^2 \frac{\delta Q}{T} \right)_{int, rev} \quad (7.62)$$

If the PCM/air region is assumed to receive heat at its average temperature, the change in entropy of the system at time  $t$  can be written as the incremental heat additions to the region divided by the mass-weighted temperature at which these incremental heat additions occur, that is,

$$\Delta S_{sys} = \int_0^t \frac{Q_w}{\bar{T}_m} = \sum_{i=0}^t \frac{Q_{w,t}}{\bar{T}_{m,t}} \quad (7.63)$$

The exergy efficiency is defined as the ratio of product to total input exergy, where the product exergy is the change in exergy of the system and the total input exergy is the exergy transferred to the system from the wall:

$$\eta = \frac{\Xi_{prod}}{\Xi_{input}} = \frac{\Delta \Xi_{sys}}{X_w} = \frac{\Delta \Xi_{sys}}{\Delta \Xi_{sys} + I} \quad (7.64)$$

## Results and Discussion

Using the visualization tools in FLUENT, the liquid and solid fractions can be viewed as time progresses (see Figure 7.27). It is clear that the solid gradually decreases in size and sinks as time progresses. Additionally, at the later stages of melting, the solid region takes on an unexpected shape from what is conventional in solidification problems. This shape is attributable to the omission of natural convection in the simulation. Currents in this case are based solely on the sinking solid PCM and very little motion occurs in the fluid regions as melting progresses. Since heat transfer occurs at the surface, the static liquid PCM region tends to act as an insulator to the melt front, causing the center region to melt less quickly than would be the case in a real scenario. It is not until the mushy zone is completely melted, between 120 and 165 s, that the solid region sinks to the bottom of the domain as expected.

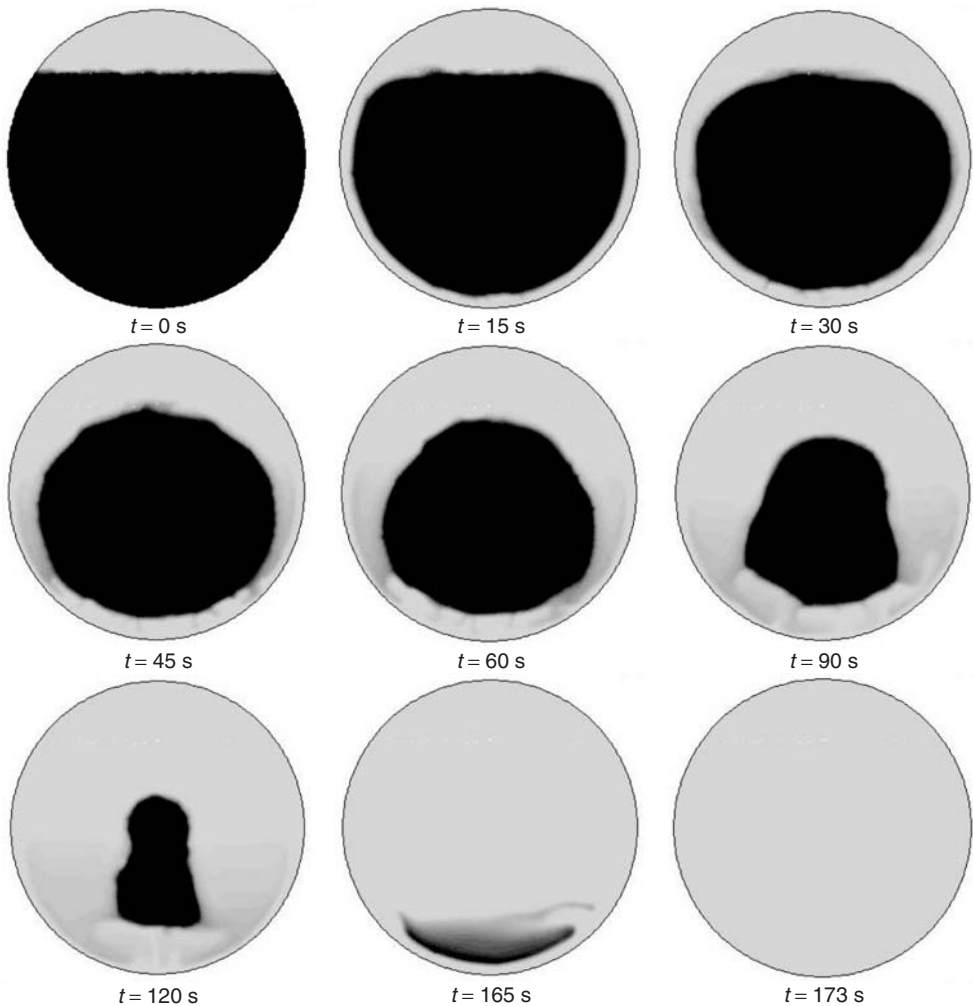


**Figure 7.27** Liquid and solid fractions in the storage domain at selected time intervals during melting. The darker image represents the solid material

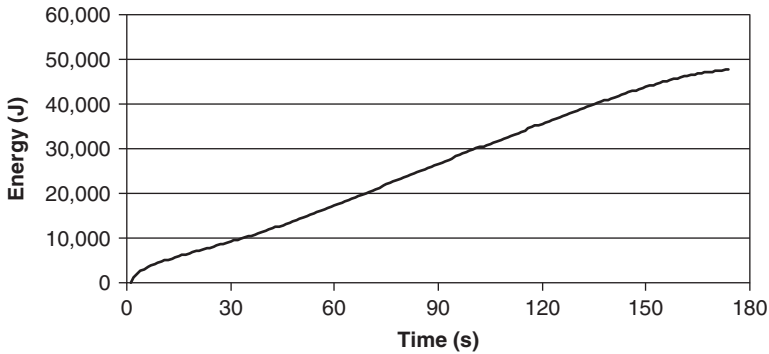


**Figure 7.28** Total energy transferred to the cylinder from the heated wall over time

Although the liquid/solid front exhibited in Figure 7.27 is only approximated in this case, the thermodynamic performance presented provides an understanding of the efficiency of melting processes using a high-temperature source.

The total heat transferred to the cylinder as time progresses is shown in Figure 7.28. As expected, the heat transfer from the wall increases sharply at first and then shifts to a nearly linear pattern. The initial heat addition is large at the beginning of the simulation because of the large temperature gradients, which become smaller as time progresses. The almost linear nature of the curve in Figure 7.28 indicates that the temperature gradients are somewhat constant in the cylinder, and suggests that the sinking motion of the PCM allows for some convection. The heat transfer in the domain is enhanced by considering the change in density, and mirrors the behavior of models with natural convection considered in the liquid portion of the PCM.

With energy analysis, the efficiency of the system is determined to be 100%, since all of the heat added to the system is recoverable. This value is not indicative of the actual thermodynamic behavior of the system, and exergy analysis provides a more perceptive assessment. The exergy efficiency of the system as time progresses is shown in Figure 7.29, along with the liquid fraction. The most significant difference between the exergy and energy efficiencies is magnitude. Whereas the energy efficiency is 100% at all times, the exergy efficiency is initially zero and gradually

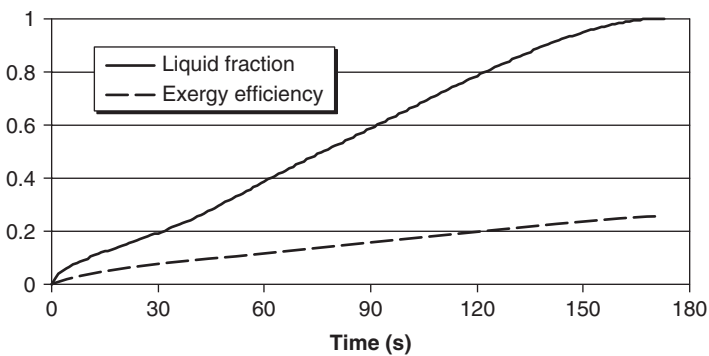


**Figure 7.29** Exergy efficiency and liquid fraction of the melting process with time for the cylindrical storage

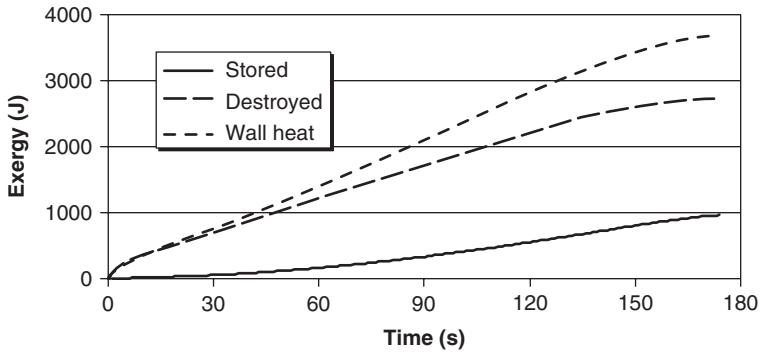


**Figure 7.30** Quantities of exergy stored, destroyed, and input with wall heat for the cylindrical storage

increases to 26% at the end of the 173-s simulation period. The result indicates that the heat addition is most efficient when the PCM temperature is hottest and least efficient when relatively high-temperature heat is added to a lower temperature medium. The change in exergy of the entire system is small at the initial stages of the simulation due to the low temperature (near-ambient conditions) in the cylinder, and the exergy added with wall heat is large in comparison. When the temperature of the thermal storage PCM rises appreciably, the difference between its temperature and that associated with the wall heat becomes smaller, and the efficiency increases.

Figure 7.30 depicts the stored and destroyed exergy as well as the exergy addition by wall heat. It can be seen in that figure that the stored exergy does not increase significantly until the later stages of melting. Also, the stored exergy is the difference between the wall thermal exergy and destroyed exergy, as indicated by the exergy balance of Equation 7.57. The exergy quantities are smaller than the corresponding energy quantities. Whereas almost 50 kJ of energy is stored in the PCM, the exergy content is well below 1 kJ for most of the melting process. This disparity highlights the usefulness of exergy analysis. Until the temperature of a substance reaches a useful level, the corresponding exergy is relatively small. This generality in the analysis of TES systems is also observed in the final case study in this chapter.

### Closure for Case Study 1

The present case study concerns the modeling of the melting process in a narrow, infinitely long cylinder containing a paraffin-blend PCM. A two-dimensional mesh is constructed in GAMBIT with a uniform meshing structure and simulated using FLUENT 6.3 with the VOF and solidification/melting models. The paraffin PCM initially occupies the bottom 85% of the cylinder volume and the top portion contains air modeled as an ideal gas. The paraffin/air region is initially set to 25 °C, and at time  $t > 0$  the wall surrounding the region is set to a constant temperature of 50 °C, allowing heat to be transferred from it to the contents of the cylinder.

The transient behavior of the PCM melting front exhibits unusual trends in terms of shape of the solid fraction due to the omission of natural convection modeling. However, the sinking motion of the solid region enhances heat transfer to a degree, somewhat offsetting the lack of natural convection.

The thermodynamic assessment based on energy and exergy shows the process to be 100% energy efficient at all times since all heat added to the cylinder is recoverable. However, the exergetic performance is much different, with an initial exergy efficiency of 0% that increases to approximately 26% after the 173-s simulation time. These differences indicate the importance of energy quality in TES assessments, particularly since substances at temperatures at or near the reference-environment temperature contain little exergy.

Although the physical configuration, assumptions, and methods used in this latent TES are not entirely based on real-world scenarios (e.g., the omission of natural convection and the use of a constant wall temperature), this case helps demonstrate the use of proper models for phase change with FLUENT. Although the next case study in this chapter is more comprehensive and realistic, the relatively simple case in this section shows how satisfactory results can sometimes be attained while using simplifications to avoid complicated modeling.

### 7.7.2 Case Study 2: Melting and Solidification of Paraffin in a Spherical Shell from Forced External Convection

This latent TES case study models the charging and discharging processes inside an encapsulated-paraffin latent TES sphere. Because of its complexity, the case is in some way a culmination of the first four case studies in this chapter. The results are validated with experimental data, and the model is subject to rigorous independence testing to ensure satisfactory behavior of the numerical simulation. Then, several input and boundary conditions are considered to determine their impacts on various performance criteria. A detailed discussion of the results is provided, along with a description of the importance of the data obtained.

The case simulated is similar to that reported by Ettouney *et al.* (2005). A paraffin blend is contained in a spherical, copper shell, and air is used as the heat transfer fluid. The paraffin is heated until it completely melts and then cooled to solidification using a fan, which blows air at 10 m/s through a vertical glass tube containing the copper sphere. The experimental apparatus is shown in Figure 7.31.

The glass column has a diameter of 20 cm and a height of 40 cm. The copper sphere, which is suspended by a thin supporting rod, has an outer diameter of 3 cm and a copper wall thickness of 1.2 mm, and is filled with a paraffin PCM. Thermocouples are located throughout the PCM to record temperature variations and also to estimate the energy stored in the capsule during the charging and discharging processes. Owing to the high velocity of the incoming air, heat transfer from the glass column to the ambient environment is neglected.

During charging of the latent store, the air is heated to a specified temperature above the melting point of the PCM, and the fan is used to force convective heat transfer to the sphere from the air. During discharging, the inlet air has a temperature below that of the PCM, so that heat is removed from it and solidification occurs.

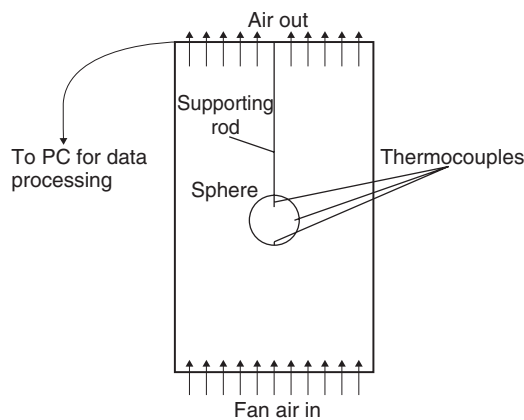


**Figure 7.31** Experimental apparatus used for the charging and discharging of the latent store using a forced air flow, modified from Ettouney *et al.* (2005)

The thermophysical properties used for the air and the PCM are taken for specified ranges from Ettouney *et al.* (2005), and in cases where variations exist between the solid and liquid states (e.g., density), the property is taken as the average of the two. Although this is not a precise approximation, its use as a simplifying assumption reduces the cost of computation. The impact on the results of this assumption is assessed subsequently.

The paraffin wax used as the PCM is thus assumed to have a constant density of  $820 \text{ kg/m}^3$ , a latent heat of fusion of  $210 \text{ kJ/kg}$ , and a melting temperature of  $48.51 \text{ }^\circ\text{C}$  ( $321.66 \text{ K}$ ). Its specific heat and thermal conductivity, taken as the average between solid and liquid states, are taken to be  $2.5 \text{ kJ/kg K}$  and  $0.195 \text{ W/m K}$ , while the viscosity of the paraffin wax in the liquid state is taken to be  $0.205 \text{ kg/m s}$ . The air used as a heat transfer fluid has a density of  $1.137 \text{ kg/m}^3$ , specific heat of  $1.005 \text{ kJ/kg K}$ , thermal conductivity of  $0.0249 \text{ W/m K}$ , and dynamic viscosity of  $2.15 \times 10^{-5} \text{ kg/m s}$ . The copper shell, in which the PCM is contained, has a FLUENT-defined density of  $8978 \text{ kg/m}^3$ , thermal conductivity of  $387.6 \text{ W/m K}$ , and specific heat of  $0.381 \text{ kJ/kg K}$ .

An analysis of the experiment of Ettouney *et al.* (2005) reveals an axis of symmetry, which can be exploited to reduce the computational effort. Consequently, the cylindrical column in Figure 7.31 is split into four quadrants, reducing the computational cost of simulation by 75%. This simplification does not change the validity of the results, as shown subsequently, and lowers simulation times significantly. The quarter-section considered of the physical domain, as created in GAMBIT, is shown in Figure 7.32.

In addition to assuming axisymmetric properties along the cuts made to the original domain, a number of other assumptions are also introduced to facilitate calculations. These include neglecting kinetic and potential energy effects, including buoyancy, and assuming a zero-shear wall (see Equation 7.8) for the symmetric walls in Figure 7.32. In addition, the outer walls, while exhibiting no-slip wall conditions, are assumed adiabatic. Since the heat transfer fluid passes rapidly through the volume, this assumption is both accurate and reasonable; it also simplifies modeling procedures greatly.

Since the HTF experiences drastic pressure, velocity, and temperature gradients in regions near the PCM capsule, the first step in the meshing procedure is to create a boundary layer on the outside of the PCM face. Seven rows of boundary layer meshing are created, with the first layer at a thickness of  $0.2 \text{ mm}$  and a growth factor of 1.3, resulting in a boundary layer thickness of about  $0.35 \text{ cm}$ . The cell density in this boundary layer is determined by the meshing of the copper shell. Since this material connects the PCM to the HTF regions, a small mesh spacing here results in a very small initial volume size in the boundary layer region. For this reason, a spacing of  $0.2 \text{ mm}$

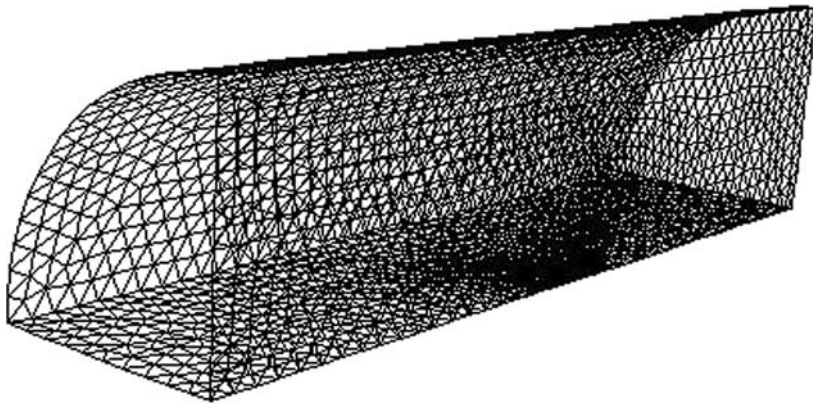


**Figure 7.32** Wall grid volumes for the computational domain considered for a latent TES. The PCM capsule volumes are shown in the darker center region



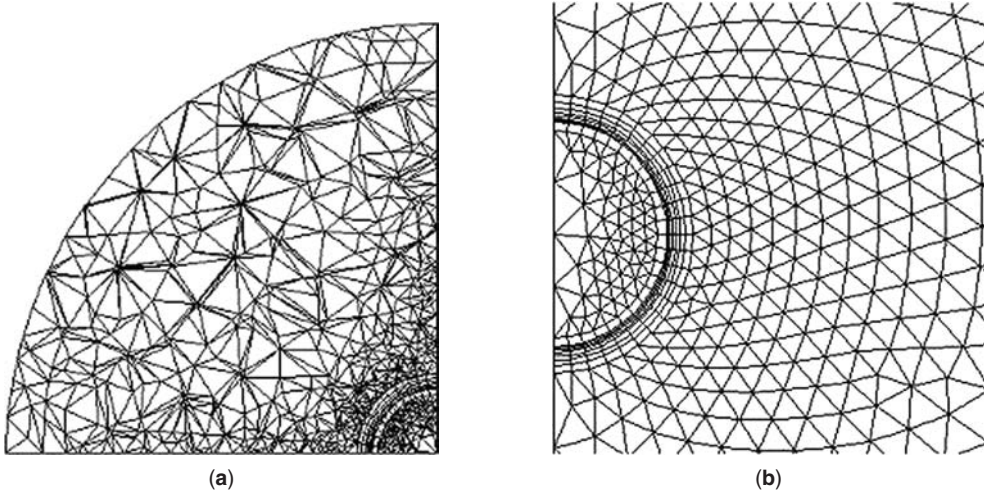


**Figure 7.33** Views of the grid cell distributions, for (a) the axial, or flow, direction, and (b) the view of the PCM/HTF cell distribution on the symmetric wall. Note that the view in (a) appears disproportional because of the three-dimensional nature of the grid

is used in the copper region, resulting in 200 volumes for the shell, and the rest of the domain is meshed using 1-cm spacing, resulting in 2048 and 29,616 volumes for the PCM and HTF regions, respectively. Therefore, a total of 31,864 volumes are used for the domain in Figure 7.32. A close-up view of the mesh volumes near the capsule region is shown in Figure 7.33, for lengthwise and axial cross-sections of the grids. The views of the cell densities in Figure 7.33 clearly show that large numbers of volumes are used in regions where computational accuracy is more important, namely, in and around the copper shell.

Once the geometric creation from GAMBIT is loaded into FLUENT, the remaining steps in the simulation setup are concerned with using the correct models, defining material properties, monitoring data for performance calculations, choosing a suitable time step, and setting the residual tolerances. Since these simulations involve phase change, the solidification/melting model is turned on, with the material properties for air, copper, and paraffin as previously described entered. The performance calculations in this case are more complicated than in the previous case studies in this chapter, so the monitors include such quantities as liquid fraction (average), inlet pressure, outlet pressure, temperatures within all domains, and heat flux to the PCM. These are explained in greater detail when the performance criteria are defined.

The case study investigates the effects of variations in the inlet air temperature on the performance of the system. In the study, four cases are considered: two charging and two discharging. For the charging (melting) cases, the initial temperature of the PCM is set to a subcooled temperature  $5^{\circ}\text{C}$  below its freezing point (i.e., at 316.66 K), while the inlet air temperature is set to either  $10^{\circ}\text{C}$  or  $20^{\circ}\text{C}$  above the melting point (i.e., to 331.66 K and 341.66 K). The resulting performance values help indicate which option is more efficient. For the discharging (solidification) cases, the initial temperature is set  $5^{\circ}\text{C}$  above the melting point (i.e., at 326.66 K) so that the PCM is completely melted. As with the charging case, the inlet air temperatures are set between  $10^{\circ}\text{C}$  and  $20^{\circ}\text{C}$  below the melting point (i.e., at 311.66 K and 301.66 K). The reference-environment temperature for exergy calculations in all cases is taken to be  $23^{\circ}\text{C}$ .

The residual tolerances for this case are set to the default values of  $10^{-3}$  for the  $x$ ,  $y$ , and  $z$  velocities and continuity, and  $10^{-6}$  for energy. The time step is determined to be most efficient for simulating the processes when set to 1.0 s, for which the computational time ratio is about



1:1. This case study includes independence testing in which variations are examined in simulation progression when the time step and the grid size change. These discussions are presented in the next section along with a validation of the model.

### Validation of Numerical Model and Model Independence Testing

To validate the numerical model, conditions from Ettouney *et al.* (2005) are mirrored so that the resulting temperature variations on the inner portion of the shell can be monitored and compared. The experimental steps are as follows: Air enters the glass column at 60 °C and with a velocity of 10 m/s. The PCM capsule, initially at a temperature of 23 °C, receives heat from the hot air until complete melting is achieved after 1120 s. Then, the air heater is removed and ambient air at 23 °C is used to resolidify the PCM, which occurs after 760 s. The PCM temperatures are recorded with thermocouples located just inside the copper shell at three locations: facing the flow direction, away from the flow direction, and at the side of the sphere where the air moves the fastest. That is, the thermocouples are located at the top, bottom, and side of the sphere as shown in Figure 7.31.

The FLUENT simulation is configured to match the above conditions, and the temperature profiles at the thermocouple locations are monitored by selecting a point in the PCM domain and recording the temperature in the corresponding volume or cell as time progresses. The resulting temperature profiles are shown in Figure 7.34.

Differences between the numerical and experimental temperature profiles are likely because of a number of factors, including contact resistance, effects caused by embedding thermocouples in the PCM, and convection effects in the PCM. However, the solidification and melting times, as well as the overall heat transfer rates, are important to this investigation, the purpose of which is to determine heat transfer characteristics between the PCM and HTF and associated performance criteria.

The time required for the PCM to completely melt is similar with both the experimental and numerical approaches. Complete melting is detected in 600 s experimentally, while the numerical approach quite accurately predicts complete melting in 615 s. A duration of 280 s is required to completely solidify the PCM after solidification is initiated in the experimental unit. This value is again in good agreement (within 1.5%) with the numerically obtained value of 285 s.

The similarities in the numerical and experimental results are encouraging and well within normal acceptable errors when validating a numerical model such as the one considered here. With these

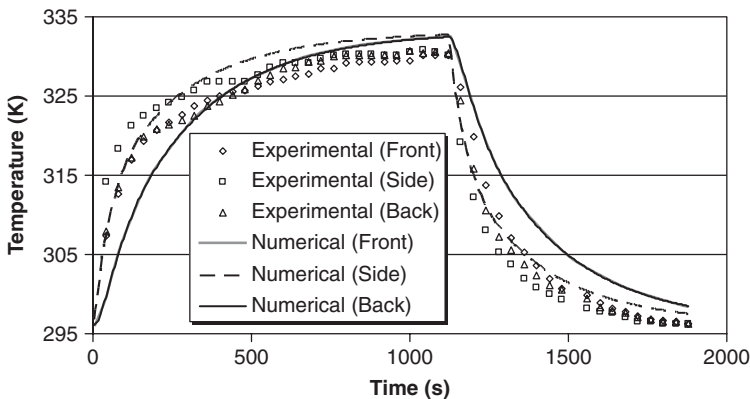


**Figure 7.34** Comparison of numerical temperature profiles at three locations in the sphere with the experimental results from Ettouney *et al.* (2005), for the model validation

results, the model can next be subject to grid size and time step validations, to improve confidence in the performance data.

The grid size performance independence tests are presented first. In any numerical model, if the results are to be taken as a realistic representation of actual behavior, the simulation results must be shown to be independent of small changes in the structure of the computational volume. Here, therefore, the mesh spacing is changed in the copper shell region, causing the spacing in the other connected regions of the domain to change correspondingly. The cell density throughout the region is varied so that more and fewer volumes are considered compared to the grid used in the base performance analysis. The cell distribution in all three cases is shown in Table 7.1.

To determine the dependence of the overall results on the small changes in cell distribution, simulations are performed using the same conditions as in the model validation tests in Figure 7.34, and the variation of the liquid fraction inside the PCM with time is monitored. The resulting liquid fraction variations are shown in Figure 7.35.

Since the liquid fraction is a good indicator of the heat transfer characteristics to and from the capsules, it is taken here to be a sufficient gauge of the overall grid performance. From Figure 7.35, it can be clearly observed that the changes in grid size have little impact on the overall solutions. Hence, the chosen grid size and orientation are deemed adequate. In general, care must be taken when initially choosing the cell distribution in a computational domain to ensure the model is not only able to model physical scenarios well but also capable of passing grid independence tests.

The time step independence is now tested. In the present case, the time step is set to 1.0 s. The dependence of the simulation progression on changes in time step can be evaluated straightforwardly

**Table 7.1** Cell distribution for the three cases considered in the grid independence tests for the sphere

Cell data	Grid size		
	Small	Base	Large
Mesh spacing in copper shell (cm)	0.21	0.20	0.18
Mesh volumes in copper region	164	200	221
Mesh volumes in PCM region	1,523	2,048	2,313
Mesh volumes in air (HTF) region	27,775	31,864	33,238
Total volumes	29,462	32,312	35,772

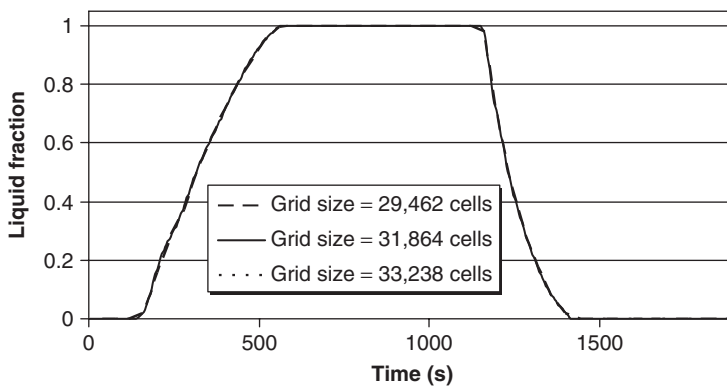


**Figure 7.35** Liquid fraction as a function of time for the grid size independence tests for the sphere

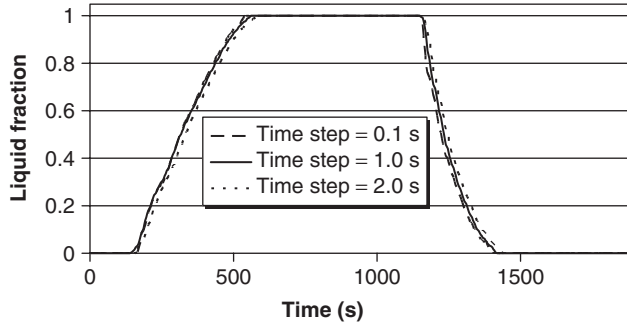


**Figure 7.36** Liquid fraction as a function of time for the time step independence tests for the sphere

by altering the time step in the FLUENT controls, and monitoring the changes in liquid fraction for the overall process. To illustrate, alternative time steps of 0.1 s and 2 s are considered, and the resulting liquid fraction variations with time are shown in Figure 7.36.

The liquid fraction variations in Figure 7.36 correlate very well for all time steps considered, suggesting that the step of 1.0 s used in the initial analysis is adequate. Although the smaller time step of 0.1 s may permit a more accurate representation of the physical domain and phenomena, the computational cost is increased tenfold, increasing the simulation time greatly and, depending on the computer resources available, perhaps unreasonably. For the time step of 2 s, little difference is observed in the variation of liquid fraction while computational cost is severely decreased but, although not shown here, it was found that increasing the time step beyond 2.0 s significantly influenced the validity of results. This test shows the importance of choosing the time step appropriately. The selection of time step and grid sizes can serve as a useful tool for determining the most computationally efficient scenario for any given problem.

With the model having been validated and passing time step and grid size independence testing, the remainder of the analysis focuses on the performance criteria.

### Performance Criteria

Since kinetic and gravitational potential energy effects are neglected, the energy balance for a system undergoing either charging or discharging processes can be written as follows:

$$\Delta E_{sys} = E_{in} - E_{out} = U_{in} - U_{out} \quad (7.65)$$

The change in energy of the system itself is comprised of the changes in energy of each material within the domain, namely, the air, copper, and PCM (paraffin) regions:

$$\Delta E_{sys} = \Delta E_{air} + \Delta E_{copper} + \Delta E_{pcm} \quad (7.66)$$

The change in energy of the air and copper regions at any time can be calculated using the change in volume-averaged temperature within each region:

$$\Delta E_{air} = m_{air} C_{air} (\bar{T}_{air} - T_{air,ini}) \quad (7.67)$$

$$\Delta E_{copper} = m_{copper} C_{copper} (\bar{T}_{copper} - T_{copper,ini}) \quad (7.68)$$

Owing to the complexities resulting from solid/liquid interfaces within the PCM, its energy change is evaluated by monitoring the heat transfer from the copper to the PCM on the inner surface of

the copper shell:

$$\Delta E_{pcm} = \int_0^t Q_w dt = \sum_{i=0}^t Q_{w,t} \quad (7.69)$$

The efficiency of the system in general differs for each process. First, we consider energy efficiencies. For the charging process, the purpose is to add heat to the PCM region. In other words, the energy content of the PCM and copper shell regions is increased, while the energy input to achieve this objective is the change in enthalpy from inlet to outlet of an HTF (air in the present case).

$$\eta_{ch} = \frac{E_{prod}}{E_{input}} = \frac{\Delta E_{sys}}{H_{in} - H_{out}} = \frac{\Delta E_{sys}}{U_{in} - U_{out} + V(p_{in} - p_{out})} \quad (7.70)$$

The term  $V(p_{in} - p_{out})$  can be written as follows:

$$V(p_{in} - p_{out}) = \frac{\dot{m}t}{\rho_{air}} \int_0^t (\bar{p}_{in} - \bar{p}_{out}) dt = \frac{\dot{m}t}{\rho_{air}} \sum_{i=0}^t (\bar{p}_{in,t} - \bar{p}_{out,t}) \quad (7.71)$$

During discharging, the purpose is to recover heat from the solidifying PCM, so that the total enthalpy received from the capsule is the product energy content. The total energy obtained is the change in energy of the PCM and its shell:

$$\eta_{dc} = \frac{E_{prod}}{E_{input}} = \frac{H_{in} - H_{out}}{\Delta E_{sys}} = \frac{U_{in} - U_{out} + V(p_{in} - p_{out})}{\Delta E_{sys}} \quad (7.72)$$

The change in energy of the system is negative during the discharging process, and there is a drop in pressure through the column. The energy efficiency varies between 0% and 100% for both discharging and charging cases. Although the dependence of the evaluated parameters on the progression time of the simulation is not written explicitly here, the energy and exergy efficiencies are examined as the simulation time progresses.

The exergy performance criteria can be similarly examined. For charging or discharging processes, the exergy balance can be expressed as follows:

$$\Delta \Xi_{sys} = \epsilon_{in} - \epsilon_{out} - I \quad (7.73)$$

Here,  $I$  denotes exergy destruction and includes exergy destroyed because of heat transfer and viscous dissipation in the flowing fluid. The exergy balance excludes thermal exergy flows across system boundaries, since the walls are assumed adiabatic. The exergy destruction can be determined with an entropy balance:

$$I = T_{\infty} \Pi \quad (7.74)$$

where

$$\Delta S_{sys} = S_{in} - S_{out} + \Pi \quad (7.75)$$

The change in entropy of the system is calculated as the summation of the changes in entropy for each of its three components:

$$\Delta S_{sys} = \Delta S_{pcm} + \Delta S_{copper} + \Delta S_{air} \quad (7.76)$$

where

$$\Delta S_{pcm} = \frac{\Delta E_{pcm}}{\bar{T}_{m,pcm}} = \sum_{i=0}^t \frac{Q_{w,t}}{\bar{T}_{m,pcm}} \quad (7.77)$$

$$\Delta S_{copper} = m_{copper} C_{copper} \ln \left( \frac{\bar{T}_{m,copper}}{T_{ini}} \right) \quad (7.78)$$

$$\Delta S_{air} = m_{air} C_{air} \ln \left( \frac{\bar{T}_{m,air}}{T_{ini}} \right) \quad (7.79)$$

The above expression for  $\Delta S_{pcm}$  presumes that no entropy generation occurs within the PCM. Further, it is assumed that heat transfer to the PCM occurs at its mean temperature. The expressions for  $\Delta S_{copper}$  and  $\Delta S_{air}$  assume incompressible fluid behavior and constant specific heats.

The difference between inlet and outlet entropy is dependent on the flow temperatures, so that after time  $t$  the entropy difference is

$$S_{in} - S_{out} = \sum_{i=0}^t \dot{m} C_{air} \ln \left( \frac{T_{in}}{\bar{T}_{out,t}} \right) \quad (7.80)$$

To solve the exergy balance, the total exergy change of the system is needed at each time  $t$ . The exergy balance depends on the change in energy of the system as well as the entropy change:

$$\Delta \Xi_{sys} = \Delta E_{sys} - T_{\infty} \Delta S_{sys} \quad (7.81)$$

With this information, the charging and discharging exergy efficiencies can be written analogously to their energy counterparts:

$$\psi_{ch} = \frac{\Delta \Xi_{sys}}{\epsilon_{in} - \epsilon_{out}} \quad (7.82)$$

$$\psi_{dc} = \frac{\epsilon_{in} - \epsilon_{out}}{\Delta \Xi_{sys}} \quad (7.83)$$

The energy and exergy efficiencies can now be assessed while the simulation progresses.

It is instructive to examine the nature of the irreversibilities, which are a result of viscous dissipation within the fluid and heat transfer. The exergy destruction associated with viscous dissipation can be expressed as follows:

$$I_{dissipative} = T_{\infty} \Pi_{dissipative} \quad (7.84)$$

The exergy destroyed via heat transfer during the melting and solidification processes can be written as the difference between the overall exergy destruction  $I$  and the exergy destruction associated with viscous dissipation:

$$I_{ht} = I - I_{dissipative} \quad (7.85)$$

## Results and Discussion

For the charging and discharging processes, many of the performance results as well as energy and exergy quantities are presented here as a function of a dimensionless time  $t^*$ , defined as

$$t^* = \frac{t}{t_{sf}} \quad (7.86)$$

where  $t_{sf}$  denotes the time for total solidification or melting.

The liquid fractions for solidification and melting are plotted against this dimensionless time in Figure 7.37. In this figure, as noted previously, inlet air temperatures 10°C and 20°C above the

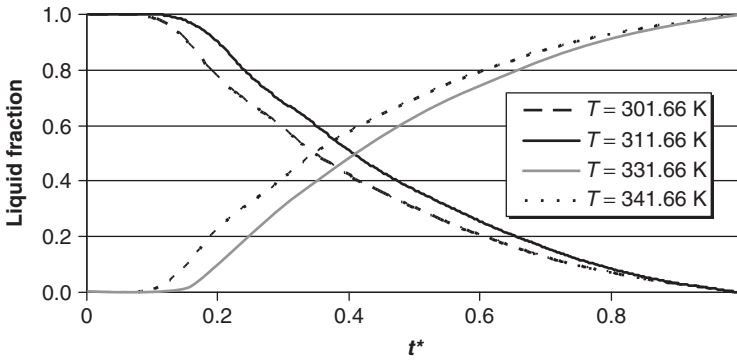


**Figure 7.37** Variation of liquid fraction for the charging and discharging cases with dimensionless time  $t^*$ , for several inlet air temperatures

melting point (i.e., at 331.66 K and 341.66 K) are considered for the charging (melting) cases, while inlet air temperatures 10 °C and 20 °C below the melting point (i.e., at 311.66 K and 301.66 K) are considered for the discharging (solidification) cases. It is observed in Figure 7.37 that inlet air temperatures, which are further removed from the phase change temperature, promote heat transfer more readily between the air and the copper capsule, causing the liquid fraction to decrease more rapidly for the solidification process and increase more rapidly for the melting process.

To illustrate the energy-related processes during charging and discharging, energy quantities for each case are shown in Figures 7.38 and 7.39. These include the heat generated through viscous dissipation, the energy stored during charging, and the energy recovered during discharging.

The heat generated through viscous dissipation for both the charging and discharging cases is small compared with the stored and recovered energy quantities. This result is expected, since heat generation through viscous dissipation is usually small compared to the input and recovered thermal energy quantities in most TES systems. In this case study, the high velocity of the heat transfer fluid (air) causes the heat generation through viscous dissipation to be somewhat larger than usual.

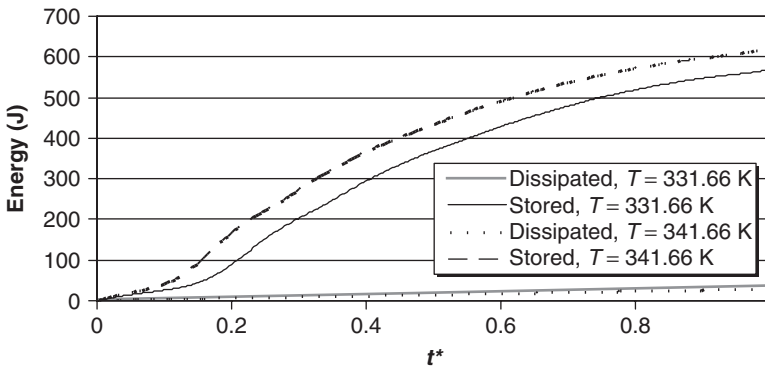


**Figure 7.38** Variation of the energy stored and the heat generated through viscous dissipation for the two charging cases, as represented by the two inlet air temperatures considered

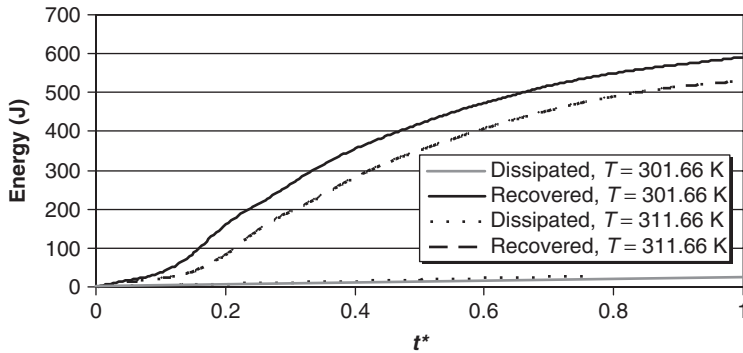


**Figure 7.39** Variation of the energy recovered and the heat generated through viscous dissipation for the two discharging cases, as represented by the two inlet air temperatures considered

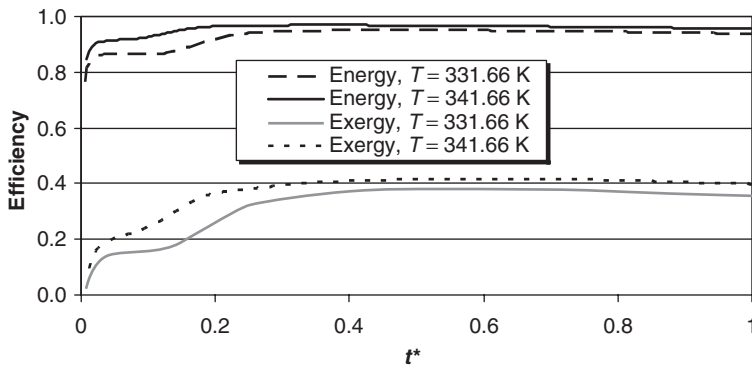


**Figure 7.40** Variation of energy and exergy efficiencies with dimensionless time  $t^*$  for the charging process, for two inlet air temperatures

Energy and exergy efficiencies are shown in Figures 7.40 and 7.41 for the charging and discharging cases, respectively. Note that there are no external heat losses from the system shown in Figure 7.31, so the energy efficiencies accounting for only external energy losses are always 100%. In this case study, the heat generated through viscous dissipation, which is relatively small, is assumed unrecoverable and thus treated as an energy loss. Hence, the energy efficiencies are somewhat less than 100%. The exergy efficiencies in Figures 7.40 and 7.41 are discussed further after the various exergy quantities (destroyed, stored, and recovered) are presented.

Energy efficiency varies with dimensionless time as observed because the stored and recovered energy quantities in the initial stages of the simulations are high because of the good heat transfer characteristics of the copper shell. The shell's high thermal conductivity permits it to convey heat readily when  $t^* < 0.1$ . As  $t^*$  increases, the paraffin must be heated or cooled to its fusion temperature, so little heat storage or retrieval occurs until melting or solidification begins. Heat storage or retrieval further increases the energy efficiency until  $t^* \approx 0.6$ , where a maximum is realized (although the efficiency is fairly constant for  $t^* > 0.3$ ). The existence of this energy efficiency maximum can be attributed to the superheating of the paraffin liquid state (or supercooling of the solid state), which reduces heat transfer significantly. Since the energy stored or retrieved is slightly curtailed, the energy efficiency decreases.

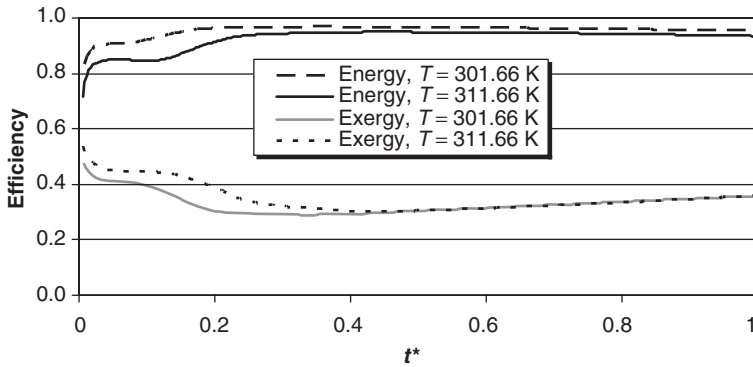


**Figure 7.41** Variation of energy and exergy efficiencies with dimensionless time  $t^*$  for the discharging process, for two inlet air temperatures

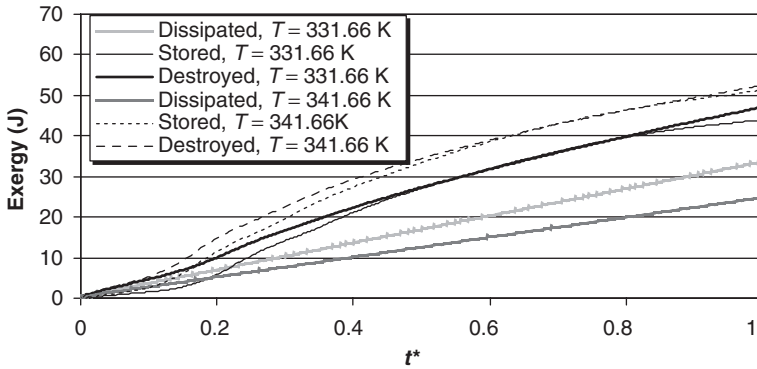


**Figure 7.42** Variation with dimensionless time  $t^*$  of exergy stored, destroyed via viscous dissipation, and destroyed via heat transfer during charging, for two inlet air temperatures

Another important observation in Figures 7.40 and 7.41 is that the energy efficiencies are higher for inlet air temperatures that lead to lower solidification or melting times. Inlet air temperatures that decrease the simulation time also decrease the energy loss, thereby increasing the energy efficiency.

To explain the behaviors of the exergy efficiencies, the quantities of exergy destroyed, stored, and recovered are shown in Figures 7.42 and 7.43. Two primary exergy destruction mechanisms occur, and both are considered: exergy destruction as a result of irreversibilities associated with viscous dissipation (referred to as *dissipated*) and exergy destruction due to irreversibilities associated with heat transfer (referred to as *destroyed*). This use of “dissipated” and “destroyed” is followed throughout the remainder of this case study.

The variations in exergy quantities with time for the charging and discharging cases are noteworthy. A complex balance exists between the magnitudes and modes of exergy destroyed and recovered (or stored), which affects the exergy efficiency. The balance suggests multiple interpretations of the most efficient scenario. The main factors involved are the entropy production associated with the two irreversibilities: viscous dissipation and heat transfer.

In Figures 7.42 and 7.43, the largest exergy quantity is the destroyed exergy due to heat transfer, followed by the stored (recovered) exergy, and then the exergy destruction due to viscous



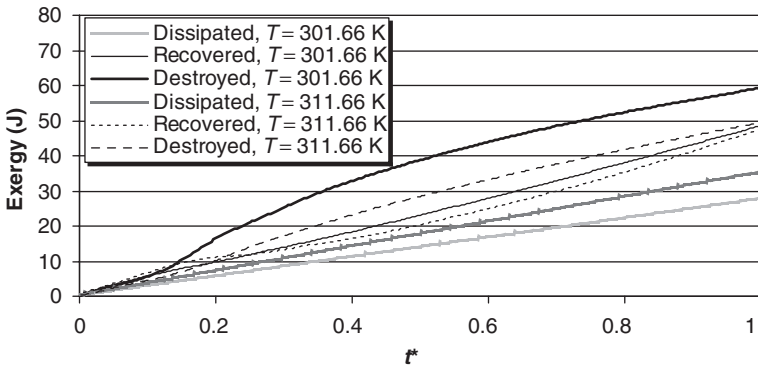


**Figure 7.43** Variation with dimensionless time  $t^*$  of exergy recovered, destroyed via viscous dissipation, and destroyed via heat transfer during discharging, for two inlet air temperatures

dissipation. This finding suggests that the temperature of the inlet air is an important factor when optimizing charging or discharging processes involving latent encapsulated PCMs. Note that when the inlet air temperature is further removed from the solidification temperature, the exergy destruction associated with heat transfer increases. However, since reducing the difference between the inlet air temperature and the PCM solidification temperature raises the charging/discharging time, the exergy destruction due to viscous dissipation is greatly increased in this instance, which reduces the exergy efficiency.

The destroyed exergy due to heat transfer and viscous dissipation, as well as the overall destroyed exergy, after solidification or melting is shown in Figure 7.44 for each air inlet temperature case.

An important inference from the results is that efficiencies increase as inlet temperatures are lowered for the discharging case and are raised for the charging case. This result can be attributed to the increased viscous dissipation in the computational domain as the air speed used to charge or discharge the capsule rises. Note that in most cases the heat transfer fluid used in macroencapsulated paraffin PCMs is not air, but rather a glycol-based refrigerant (for cold storage) or water (for warm storage). These fluids have advantageous thermophysical properties (e.g., relatively high specific heats), heat transfer characteristics, and low costs. Thus, the results of the current case study are most meaningful when a high pressure head is present during charging or discharging.

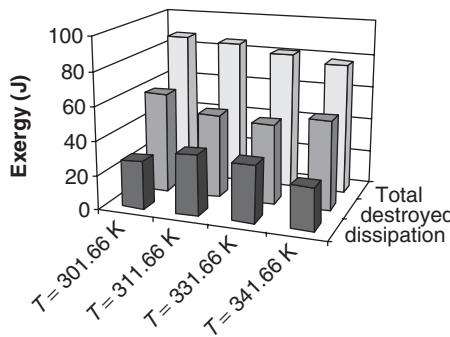


**Figure 7.44** Exergy destroyed via viscous dissipation and heat transfer, and the total exergy destruction, after the overall storage process, for all inlet air temperature cases

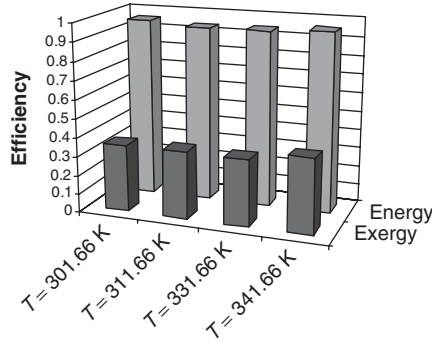


**Figure 7.45** Energy and exergy efficiencies at the completion of the overall storage process, for all inlet air temperature cases

In most other packed-bed analyses, the irreversibility associated with heat transfer usually is responsible for the dominant exergy loss. For example, consider the detailed TES investigation by MacPhee (2008) of the charging and discharging efficiencies over a wide range of inlet temperatures, flow rates, and geometries, including spherical, cylindrical, and slab capsules. The capsules are situated in a packed bed of similar capsules, and an ethylene glycol solution is the heat transfer fluid. The results indicate that all processes are more efficient at lower inlet velocities, which decreases the exergy destroyed due to viscous dissipation (rendering it almost negligible). As a result, the dominant exergy loss is the exergy destruction due to heat transfer, and this quantity decreases as inlet temperature approaches the solidification temperature.

For higher inlet velocities of the heat transfer fluid, the results suggest that it may be more efficient to consider inlet temperatures, which achieve solidification or melting more quickly, to decrease exergy destruction via viscous dissipation. This result could be useful for understanding TES using microencapsulated packed beds or any medium that normally experiences a high pressure drop in a flowing heat transfer fluid. Nonetheless, the irreversibility associated with heat transfer is likely to be of major importance for any space heating or cooling applications. This irreversibility is reduced when the two materials exchanging heat are at similar temperatures. When larger temperature differences exist, entropy generation and exergy destruction are greater. In most cases, like those reported by MacPhee (2008), it is beneficial in terms of efficiency to keep the inlet temperature close to the fusion temperature of the PCM.

The overall energy and exergy efficiencies after the solidification or melting processes are completed are shown in Figure 7.45.

An important outcome of this case study is the demonstration provided of the usefulness and versatility of exergy analysis. From an energy perspective, only heat generation through viscous dissipation is considered a loss (and usually even this is not treated as a loss), resulting in very high overall efficiencies. In Figure 7.45, exergy efficiencies are contrasted with their energy counterparts. The lower magnitudes of the exergy efficiencies reflect more accurately and comprehensively the actual efficiency of the TES system.

Since exergy analysis provides a detailed understanding of system performance and efficiency as well as the exergy destroyed and its breakdown by cause, the method allows designers to test different options and determine performance trends, ultimately facilitating system enhancements and optimization.

### Extension to Other Geometries

An advantageous aspect of TES numerical simulation is that once the numerical scheme is validated and found to be independent of grid and time step changes, it can be applied to a range of similar

applications. For the present case study, for instance, alternative geometries can be investigated to determine the most beneficial configuration of the PCM capsule. Further, the effect could be examined by varying physical properties and the inlet temperature and flow rate of the heat transfer fluid. Here, the effect of geometry variation is examined.

Two alternative capsule geometries are considered: cubic and cylindrical. Performance data are obtained for these cases and compared to those for the spherical capsule. The PCM volume is fixed at the same value for all geometries, and the quantities of energy and exergy stored and recovered are determined. For all cases, the capsule contains the same paraffin PCM, has the same shell material and thickness, and undergoes one charging and one discharging process. The inner length of the cubic capsule is therefore 2.225 cm and the outer length is 2.465 cm. The inner height and diameter for the cylindrical capsule are set to be equal, so the inner diameter (and height) is 2.411 cm, while the outer diameter (and height) is 2.651 cm. The grid meshing is developed in a similar manner as for the spherical capsules, with similar grid sizes and a higher density on the capsule outer surfaces.

After the geometries are properly created and segmented, the same simulation procedures are performed as for the spherical element. To properly compare the new geometries, one charging and one discharging process is simulated for each element, with the inlet temperature for charging and discharging set to 341.66 K and 301.66 K, respectively. The inlet air velocity is fixed at 10 m/s, while the initialization temperature in the PCM and copper regions for the charging and discharging case are 316.66 K and 326.66 K, respectively. Consequently, performance comparisons can be made for the spherical, cubic, and cylindrical cases.

The overall energy and exergy efficiencies are shown in Figure 7.46 for the three cases. Note that the overall efficiencies are obtained by multiplying the charging and discharging efficiencies.

The cylindrical capsule attains the highest efficiency from both energy and exergy perspectives. This result is due to a number of factors, most of which are more readily explained once the modes of exergy destruction are considered, as is done in Figure 7.47.

The exergy destruction values in Figure 7.47 can explain the overall efficiencies by separating the destroyed exergy by cause. First, the exergy destroyed due to viscous dissipation is greatest in the cubic capsule. This observation is expected based on aerodynamic considerations since a cubic capsule has the most drag of the three geometries and creates higher velocity gradients, especially at the edges. The spherical capsule experiences much lower dissipated exergy, while the lowest amount is experienced by the cylindrical capsule. Owing to the higher surface area to volume ratio of the cylindrical capsule, it experiences lower charging and discharging times, and as such realizes less total dissipation.

The energy efficiencies in Figure 7.46 indicate that the cylindrical capsule achieves the highest energy efficiency, followed by the spherical and cubic capsules.

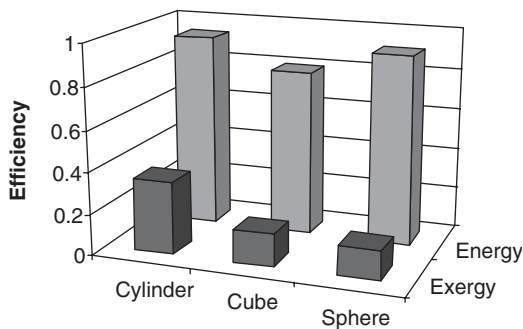


**Figure 7.46** Overall energy and exergy efficiencies for charging and discharging for the three storage capsule geometries

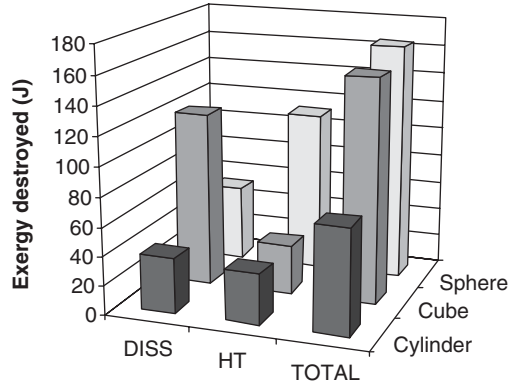


**Figure 7.47** Exergy destroyed for several storage capsule geometries by viscous dissipation (DISS), heat transfer (HT), and their combination (TOTAL)

The exergy destruction due to heat transfer is greatest for the spherical capsule, followed by the cylindrical and cubic capsules. The spherical capsule realizes the largest exergy destruction due to its poor heat transfer characteristics. The other geometries have higher surface areas and thus transfer heat more efficiently. When overall exergy destruction is considered, however, the cylindrical capsule is observed to be preferable, followed by the cubic and spherical capsules. These results are reflected in the exergy efficiencies, as greater exergy destruction results in lower efficiencies.

This brief assessment demonstrates the versatility of numerical simulations and supports their use in similar studies. Provided proper validation and independence tests are completed, a model may be run for other cases in lieu of experimentation. However, a more detailed analysis is required in this particular case before generalizations can be inferred about performance when geometry and heat transfer fluid flow conditions are varied.

#### Closure for Case Study 4

This latent TES case study addresses the charging and discharging of a paraffin wax storage contained in a copper shell, which is suspended in a glass column, while air is used as a heat transfer fluid to transfer heat convectively to and from the capsule. The inlet air velocity is set at 10 m/s, and four inlet air temperature cases are investigated: 341.66 K and 331.66 K for charging and 311.66 K and 301.66 K for discharging. The solidification temperature of the paraffin wax is 321.66 K, and trials are conducted until the liquid fraction reaches 1 in the charging case and 0 in the discharging case. Energy and exergy efficiencies, as well as the different modes of losses, are obtained as a function of time.

Before simulation data can be used reliably, a detailed model validation must be conducted. This validation demonstrated the accuracy of the numerical procedures. In addition, time step and grid size independence tests showed that the model provides an accurate representation of real-world scenarios.

The results indicated that energy analysis is incomplete and misleading for assessing TES losses. For the charging cases, the processes have energy efficiencies of 93.4% and 95.4% for inlet temperatures of 311.66 K and 301.66 K, respectively. The corresponding exergy efficiencies are 36.0% and 35.8%, indicating that the charging process is much less efficient than indicated considering energy. The lower efficiencies are due to the decreased exergy content of the PCM storage compared to its energy content, as well as the increased losses from two modes of entropy generation: viscous dissipation and heat transfer.

For the discharging processes, the inlet temperatures are 331.66 K and 341.66 K, respectively, and the corresponding energy efficiencies are 93.8% and 95.6%, while the corresponding exergy efficiencies are 35.2% and 39.8%. The differences between energy and exergy efficiency values for the discharging processes mirror those for the charging processes.

Following the spherical geometry simulations, two more geometry cases (cylindrical and cubic) are considered to assess their performances with identical PCM volumes. The cases demonstrate the versatility of numerical simulation and show the cylindrical capsule to have the highest overall energy and exergy efficiencies because of a smooth profile and a high surface area to volume ratio.

Although exergy destruction due to viscous dissipation is a major loss in all cases considered here, it is observed for most sensible or latent TES systems that viscous dissipation is not the major source of irreversibility. Viscous dissipation is important for quickly moving flows. Designers can use exergy analyses to perform detailed optimization and improve efficiency.

This case study is intended to give the reader a good understanding of the modeling, validation, testing, and simulation procedures necessary for all numerical simulations of latent TES. It is hoped that the four case studies considered to this point in this chapter allow the reader to conduct TES case assessments typical of those used by industry today. By using the techniques presented here in sensitivity or parametric analyses, optimization or loss minimization schemes can be realized relatively straightforwardly and inexpensively.

## 7.8 Illustrative Application for a Complex System: Numerical Assessment of Encapsulated Ice TES with Variable Heat Transfer Coefficients

Encapsulated ice storage systems are an effective type of TES in part because they have a large heat transfer area per unit storage volume, resulting in higher heat transfer rates. Such latent TES systems and the phase change that takes place within them in the PCM capsules are the focus of this illustrative application.

An average heat transfer coefficient is commonly used for heat transfer analysis, whether analytical or numerical, in encapsulated ice TES systems. In reality, the heat transfer coefficient changes along the flow path since the fluid flow around capsules is not hydrodynamically and thermally developed. In most instances, consequently, the results deviate significantly compared to experimental data. More accurate heat transfer coefficients and correlations are thus desirable, and are obtained in this illustrative application by simulating a series of 120 numerical “experiments” for encapsulated ice TES systems, considering various capsule diameters, mass flow rates, and temperatures of the heat transfer fluid. Changes in the heat transfer coefficient along the flow path are thus taken into account, avoiding the need to use the average heat transfer coefficients for encapsulated TES. We compare the numerical results with experimental data.

Only the charging process is examined in this section, which is adapted from a recent investigation (Erek and Dincer, 2009).

### 7.8.1 Background

Modeling and analytical assessments of latent TES systems have been reported for some time, as have experimental studies. More recently, latent TES systems have been investigated numerically, and often verified with experimental data. Some of these are reviewed here, as they pertain to this illustrative application.

Numerical assessments of many types have been reported for TES. Tao (1967) presented a numerical method, using constant values of heat capacity and thermal conductivity for the solid region and a constant heat transfer coefficient, for solidification inside both cylindrical and spherical containers. Shih and Chou (1971) describe an iterative method for predicting solidification in

spherical capsules, while Ismail and Henriquez (2000) apply a finite difference approximation and moving-grid approach to solidification in a spherical container. Ismail *et al.* (2003) numerically assessed heat transfer during the solidification of water inside a spherical nodule, and discussed the effect on solidification time and rate of container size and material and flow parameters. A numerical investigation of inward solidification of a PCM encapsulated in cylindrical and spherical containers yielded a correlation that expresses the dimensionless total solidification time in terms of Stefan number, Biot number, and a superheat parameter (Bilir and İlken, 2005). Kousksou *et al.* (2005) used a two-dimensional porous-medium approach to describe the effect of storage tank position and the flow pattern inside a tank containing spherical capsules.

Various experimental TES assessments have also been reported. Eames and Adref (2002) experimentally investigated the heat transfer characteristics for water in spherical elements during TES charging and discharging processes and introduced a method to measure interface position during solidification. Chen *et al.* (1999) examined experimentally the nucleation probability of supercooling, that is, cooling the contained liquid (water inside capsules) to below its freezing point prior to solidification and investigated the effect of different factors on the nucleation behavior. This information is important since encapsulated containers can be subject to supercooling, which can occur in fully discharged containers and reduces the heat transfer rate at the beginning of charging, but which can be significantly reduced by the addition of nucleating agents. Chen *et al.* (2000) examined the thermal behavior of an encapsulated cold TES during charging for varying inlet coolant temperatures and flow rates. An investigation of the thermal characteristics of paraffin wax in a spherical capsule during freezing and melting showed that the average heat transfer coefficient around capsules is affected by the inlet and initial temperature and Reynolds number more during melting than freezing due to the effect of natural convection during melting (Cho and Choi, 2000).

Numerical TES assessments often use experimental data for verification purposes. For instance, numerical and experimental investigations of the heat transfer characteristics associated with phase change in a horizontal cylindrical capsule containing a paraffin wax PCM demonstrated that melting is mainly governed by the Stefan number (Regin *et al.*, 2006). Also, Bedecarrats *et al.* (1996) introduced a model that accounts for supercooling and investigated experimentally and numerically the energy storage in a tank filled with PCM encapsulated in spherical capsules.

### 7.8.2 System Considered

The encapsulated ice TES considered is shown in Figure 7.48. The TES system consists of a cylindrical tank of height  $H$  and diameter  $D_{inf}$  and contains PCM spherical capsules. The tank is completely insulated and the PCM, which is pure water, is homogenous and isentropic. The thermal behavior of the TES system is investigated numerically for the charging process, in which a cold heat transfer fluid flows over capsules and the PCM in the capsules solidifies. Solidification begins at the capsule surface and moves toward the center with time.

### 7.8.3 Modeling and Simulation

The modeling of the heat transfer for the ice TES is described, along with assumptions and simplifications. Also, the numerical simulation process is explained, including initial and boundary conditions and the simulation procedure employed.

#### Assumptions

The following assumptions are considered in the numerical model:

- The temperature in the tank changes mainly along axial direction with time.
- Heat transfer within the container is dominated by conduction in the radial direction.

- The heat flux is isotropic over the PCM capsule area.
- Natural convection in the tank is negligible.
- Thermophysical properties of the container wall and the heat transfer fluid are independent of temperature.
- Thermophysical properties of the PCM in the solid and liquid phases differ.

**Heat transfer**

Since such a three-dimensional and time-dependent system is difficult to model and analyze numerically, the system is simplified using symmetry surfaces. The resulting system includes four quarter-sphere capsules and the heat transfer fluid around them, as shown in Figure 7.49. This three-dimensional view is utilized in the numerical simulation. Assuming that heat loss from the system is negligible, the heat transfer equation for the heat transfer fluid can be expressed as

$$\epsilon \rho_f c_f \frac{\partial T_f}{\partial t} + \rho_f c_f u \frac{\partial T_f}{\partial x} = \frac{\partial}{\partial x} \left( \epsilon k_f \frac{\partial T_f}{\partial x} \right) + \frac{q_{capsule}^0}{V_{CV}} \tag{7.87}$$

where  $q_{capsule}^0$  represents the heat transfer from the capsules to the heat transfer fluid. As seen in Figure 7.49, the fluid around the four quarter-capsules is taken as the control volume. This is done because the discretization of Equation 7.87 is simpler. The assumption of constant surface temperature and temperature distribution in only the radial direction leads to heat conduction inside the capsules. Heat transfer between the heat transfer fluid and the PCM inside the capsules can be determined using the following analogy:

$$q_{capsule}^0 = \frac{T_{s,i} - T_{f,i}}{R_{t,cond} + R_{t,conv}}$$

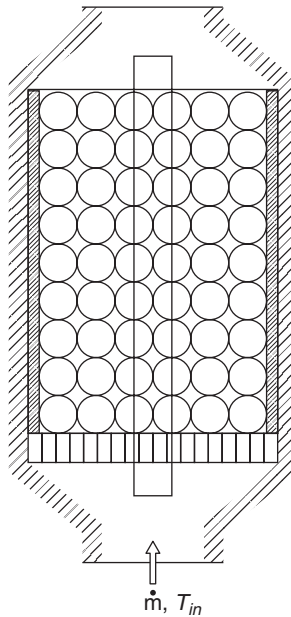


**Figure 7.48** Physical model of ice TES system

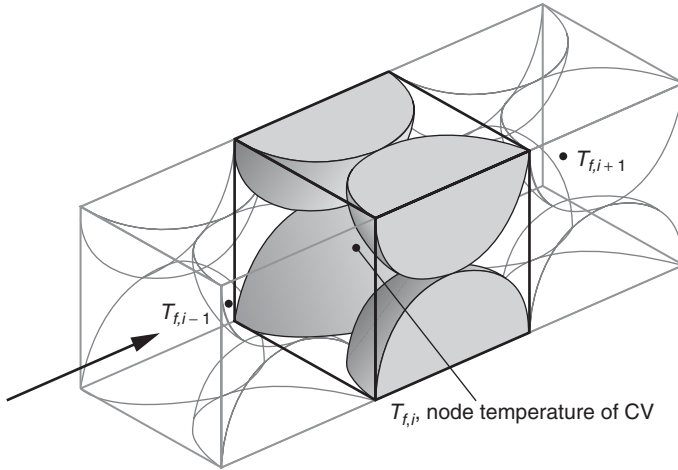


**Figure 7.49** Segment of ice TES system used for numerical simulation

Here,  $R_{t,cond}$  and  $R_{t,conv}$  represent thermal conduction and convection resistances, respectively. After substituting these terms, this expression can be written as

$$q_{capsule}^0 = \frac{T_{s,i} - T_{f,i}}{\frac{1}{h\pi D^2} + \frac{1}{2\pi k} \left( \frac{1}{D_i} - \frac{1}{D} \right)}$$

Rewriting Equation 7.87 in the dimensionless form,

$$\varepsilon C_f \frac{\partial \theta_f}{\partial Fo} + C_f \text{Re}_f \text{Pr}_f \frac{\partial \theta_f}{\partial X} = \frac{\alpha_l}{\alpha_f} \frac{\partial}{\partial X} \left( \varepsilon K_f \frac{\partial \theta_f}{\partial X} \right) + \frac{q_{capsule}'''}{Dk_f (T_m - T_{in})} \quad (7.88)$$

The heat transfer can then be written in dimensionless form as

$$q_{capsule} = \frac{\pi (\theta_{s,i} - \theta_{f,i})}{\frac{1}{\text{Nu}_f} + \frac{K_f}{K_w} \left( \frac{t_w}{1 - 2t_w} \right)} \quad (7.89)$$

Note that the relation between  $q_{capsule}$  and  $q_{capsule}^0$  is  $q_{capsule} = q_{capsule}^0 / Dk_f (T_m - T_{in})$ . The Nusselt number  $\text{Nu}_f$  is obtained using CFD. Details on the numerical analysis are given in the next section.

To link the heat transfer between capsules and the heat transfer fluid, the heat transfer equation for the PCM capsules must be solved. The heat transfer equation in the spherical capsules is described by a temperature transforming method using a fixed-grid numerical model (Cho and Choi, 2000). In this method, it is assumed that phase change occurs over a temperature range from  $T_m - \delta T_m$  to  $T_m + \delta T_m$ . This approach can also be used to simulate the solidification process occurring at a single temperature by taking a small range of phase change temperature,  $2\delta T_m$ . Where water is used as the PCM, there is a quick transition from solid to liquid and the value of the dimensionless semirange phase change temperature,  $\delta\theta_m$ , is taken as 0.001.

The dimensionless heat transfer equation for the PCM in the capsules can be written as

$$\frac{\partial(C\theta)}{\partial Fo} = \frac{\alpha_l}{\alpha_f} \frac{1}{R^2} \frac{\partial}{\partial R} \left( KR^2 \frac{\partial \theta}{\partial R} \right) - \frac{\partial S}{\partial \tau} \quad (7.90)$$



where

$$\begin{aligned}
 C = C(\theta) &= \begin{cases} C_{sl} & \theta < -\delta\theta_m & \text{Solid} \\ \frac{1}{2}(1 + C_{sl}) + \frac{1}{2Ste\delta\theta_m} & -\delta\theta_m \leq \theta \leq \delta\theta_m & \text{Mushy} \\ 1 & \theta > \delta\theta_m & \text{Liquid} \end{cases} \\
 S = S(\theta) &= \begin{cases} C_{sl}\delta\theta_m & \theta < -\delta\theta_m & \text{Solid} \\ \frac{1}{2}\delta\theta_m(1 + C_{sl}) + \frac{1}{2Ste} & -\delta\theta_m \leq \theta \leq \delta\theta_m & \text{Mushy} \\ C_{sl}\delta\theta_m + \frac{1}{Ste} & \theta > \delta\theta_m & \text{Liquid} \end{cases} \\
 K = K(\theta) &= \begin{cases} K_{sl} & \theta < -\delta\theta_m & \text{Solid} \\ K_{sl} + \frac{(1 - K_{sl})(\theta + \delta\theta_m)}{2\delta\theta_m} & -\delta\theta_m \leq \theta \leq \delta\theta_m & \text{Mushy} \\ 1 & \theta > \delta\theta_m & \text{Liquid} \end{cases}
 \end{aligned}$$

**Initial and Boundary Conditions**

The initial and boundary conditions can be written as follows:

- Initial condition (Fo = 0):

$$\text{At } 0 \leq R \leq R_i, \theta = \theta_i$$

- Boundary conditions (Fo > 0):

$$\text{At } R = 0, \frac{\partial\theta}{\partial R} = 0$$

$$\text{At } R = R_i, -K \left( \frac{\partial\theta}{\partial R} \right)_{R=R_i} = q''_{capsule}$$

**Physical Behavior**

The phase change process of solidification of water inside a capsule involves four stages (Chen *et al.*, 1999, 2000). The first stage, sensible heat extraction, is the process from the initial stage to the subcooling state before water nucleation occurs. The second stage, dendritic ice formation, is the process from the start of nucleation to the completion of dendritic ice formulation. The other two stages are latent heat transfer and sensible heat transfer in the solid. Since the time interval of the second stage is relatively small, the modeling of this stage is difficult. Here, the growth of ice crystals is not taken into account and the first two stages are combined into a sensible heat extraction process for liquid water.

The one-dimensional conduction equation is written for the PCM inside a capsule, and the effect of natural convection that takes place inside the encapsulated liquid PCM is taken into account using an effective thermal conductivity, as given elsewhere (Lacroix, 1993). The effective thermal

conductivity denotes the ratio of total heat transfer rate to heat transfer rate by conduction, and is expressible as

$$K_{effective} = \frac{Nu}{Nu_{cond}} \quad (7.91)$$

Limited studies have been reported on natural convection inside an encapsulated PCM. Here, the Nusselt number correlated experimentally by Ettouney *et al.* (2005) for a capsule during melting and solidification is used.

### Numerical Solution Procedure

The temperature distribution inside the problem domain is calculated by solving the heat transfer equations expressed by Equation 7.90. The solution procedure used for these energy equations is a control-volume approach described elsewhere (Patankar, 1980). The thermal conductivity  $K$  is calculated by a harmonic mean method at the control surface; the thermal conductivity for any control surface  $K_n$  results in

$$K_n = \frac{1}{\frac{1-f_n}{K_P} + \frac{f_n}{K_N}} \quad (7.92)$$

where the interpolation factor  $f_n$  is defined as

$$f_n = \frac{\frac{1}{R_n} - \frac{1}{R_N}}{\frac{1}{R_P} - \frac{1}{R_N}} \quad (7.93)$$

Here, the subscripts  $P$  and  $N$  denote control-volume nodes and  $n$  denotes the control surface.

A semi-implicit solver (Ettouney *et al.*, 2005) is employed for solving the discretized heat transfer equations. CPU time is greatly reduced for a single iteration using this solver, which requires less storage than other solvers (e.g., the Gauss–Seidel iteration method). Since the energy equation for the PCM is a nonlinear heat conduction equation, iterations are needed during each time step. For a given time step, convergence is deemed at iteration  $k + 1$  when  $|\theta_{i,j}^{k+1} - \theta_{i,j}^k| \leq 10^{-6}$ . The numerical results are then verified by testing the resulting predictions for independence relative to grid size, time step, and other parameters. The grid size used for the solution is 200 (radially) for each capsule with a time step  $\Delta t = 0.1$  s. Furthermore, the overall energy balance is checked during the calculation process to verify the numerical results. At a time step, the change in energy storage in the PCM and container wall must equal the total energy supplied by the heat transfer fluid as follows:

$$\int_0^\tau Pe_f C_f (\theta_{b,out} + 1) d\tau = \sum_{k=1}^N \int_{R=0}^{R_i} 4\pi R^2 (H - H_i) dR \quad (7.94)$$

Here,  $H = C \times T + S$  represents the total enthalpy of the control volume. The left side of Equation 7.94 represents the thermal energy supplied by the heat transfer fluid and the right side the thermal energy stored in the encapsulated PCM. In the calculation procedure, the numerical deviation between the two sides of Equation 7.94 is less than 1%.

### 7.8.4 Numerical Determination of Heat Transfer Coefficients for Spherical Capsules

In this section, we examine the variation in heat transfer coefficients using the simplified physical model in Figure 7.49. The heat transfer fluid flows past four quarter-spherical capsules that are kept at a constant temperature of 273.15 K for each segment. The side walls are taken along planes that are symmetric regarding heat transfer. At the inlet, fluid with a constant mass flow rate  $\dot{m}$  and a temperature  $T_{in}$  enters the TES system at a constant speed  $u_0$ . The flow is assumed to be developing and steady. Here, ethyl alcohol is taken as the heat transfer fluid. This selection allows the results obtained from the numerical analysis to be compared with experimental data provided by Chen and Yue (1991). In calculating the heat transfer coefficient, the density, thermal conductivity, and dynamic viscosity of the heat transfer fluid are assumed linear or a second-order polynomial, depending on temperature. Thermophysical properties of the heat transfer fluid are given in Table 7.2 and of the capsule wall and PCMs in Table 7.3.

The primitive volume mesh for the FLUENT CFD program used to obtain solutions is constructed with the aid of the GAMBIT program. Along the entire system, 20 separate zones for each capsule zone and an additional two zones for the inlet and the outlet are formed, as illustrated in Figure 7.49. These allow specification of uniform velocity for the inlet and outflow for the outlet. For each simulation, nearly 650,000 tetrahedral cells are used.

**Table 7.2** Properties of heat transfer fluids

Heat transfer fluid	Temperature, $T$ (°C)	Density, $\rho$ (kg m <sup>-3</sup> )	Specific heat, $c_p$ (J kg <sup>-1</sup> K <sup>-1</sup> )	Thermal conductivity, $k$ (W m <sup>-1</sup> K <sup>-1</sup> )	Thermal diffusivity, $\alpha$ (m <sup>2</sup> s <sup>-1</sup> )	Dynamic viscosity, $\mu$ (Pa.s)
Ethyl alcohol	-10	838.6	2253	–	$1.053 \times 10^{-7}$	0.0030
	-15	842.9	2209	0.199	$1.069 \times 10^{-7}$	0.0034
	-20	847.3	2149	–	$1.093 \times 10^{-7}$	0.0038
Ethylene glycol (40%)	-5	1068.3	3384	0.389	$1.08 \times 10^{-7}$	$7.18 \times 10^{-3}$
	-10	1069.6	3367	0.383	$1.06 \times 10^{-7}$	$9.06 \times 10^{-3}$
	-15	1070.9	3351	0.377	$1.05 \times 10^{-7}$	$11.7 \times 10^{-3}$

**Table 7.3** Properties of capsule wall and PCMs

Material	Phase	Density, $\rho$ (kg m <sup>-3</sup> )	Specific heat, $c_p$ (J kg <sup>-1</sup> K <sup>-1</sup> )	Thermal conductivity, $k$ (W m <sup>-1</sup> K <sup>-1</sup> )	Thermal diffusivity, $\alpha$ (m <sup>2</sup> s <sup>-1</sup> )	Enthalpy change, $\Delta H$ (J m <sup>-3</sup> )
Capsule wall: polyethylene	Solid	940	1900	0.35	$1.96 \times 10^{-7}$	–
PCM: <i>n</i> -tetradecane	Liquid	765	2100	0.211	$1.31 \times 10^{-7}$	$175.2 \times 10^6$
PCM: water	Solid	803	1800	0.273	–	–
	Liquid	999.8	4217	0.561	$1.33 \times 10^{-7}$	$333.5 \times 10^6$
	Solid	916.8	2040	2.2	–	–

For the heat transfer fluid, the continuity, momentum, and energy equations follow:

$$\begin{aligned}\frac{\partial}{\partial x_i}(\rho u_i) &= 0 \\ \frac{\partial}{\partial x_i}(\rho u_i u_j) &= -\frac{\partial P}{\partial x_i} + \frac{\partial \tau_{ij}}{\partial x_j} + \rho g_i + S_i \\ \frac{\partial}{\partial x_i}(\rho u_i h) &= \frac{\partial}{\partial x_i}\left(k \frac{\partial T}{\partial x_i}\right)\end{aligned}$$

Here,  $\rho$  denotes density,  $u_i$  velocity component in the  $i$  direction,  $p$  static pressure,  $g_i$  gravitational acceleration in the  $i$  direction,  $k$  thermal conductivity,  $T$  temperature, and  $t$  time. Also,  $x_i$  is a cartesian coordinate and  $\tau_{ij}$  is a stress tensor. Viscous heating is not taken into account since it is negligibly small.

The numerical solution is obtained using FLUENT 6.0 software. The governing equations for internal flow and heat transfer around the spherical capsules are solved with the control-volume method introduced by Patankar (1980). The SIMPLEC algorithm of Doormaal and Raithby (1984) is used to solve the coupling between velocity and pressure.

### 7.8.5 Heat Transfer Coefficients and Correlations

The variation of the heat transfer coefficient around the spherical capsules along the flow path is examined. The three-dimensional model shown in Figure 7.49 is applied for four capsule diameters ( $D = 40, 60, 70,$  and  $80$  mm). All capsules have a wall thickness of 1 mm. To focus better on heat transfer coefficient around the capsules, their surface temperature is taken to be constant as a result of the heat transfer fluid around them.

#### Heat Transfer Coefficients

A series of 120 numerical “experiments” are performed to calculate the heat transfer coefficients for various capsule diameters, mass flow rates, inlet heat transfer fluid temperatures, and capsule layers, as summarized in abbreviated form in Table 7.4. Numerical results are provided only for capsule diameters of 40 mm and 80 mm in this table. The heat transfer coefficient is seen to decrease markedly along the downstream flow. Furthermore, the heat transfer coefficient decreases as capsule diameter increases, as inlet temperature increases (or the temperature difference,  $T_m - T_{in}$ , decreases), and as mass flow rate decreases.

#### Velocities

Velocity vectors along the centerline are plotted in Figure 7.50, which shows that the flow characteristics around the capsules are different since the flow is developing. The heat transfer fluid enters the system with uniform velocity and the centerline velocity increases downstream, as is the case with internal flow in a channel. This observation supports the contention that the heat transfer coefficient changes along the flow path.

#### Correlations

The 120 numerical datasets are used to correlate the heat transfer coefficient via nonlinear regression using SPSS 10. The following correlation is developed by Erekan and Dincer (2009) for the heat

transfer coefficient:

$$Nu_X = 0.726(Re Pr)^{0.360} \left(\frac{T}{T_s}\right)^{-20.094} X^{\frac{-450.656}{Re.Pr}} \tag{7.95}$$

Here, the correlation coefficient obtained for this correlation is high, at  $R^2 = 0.950$ . The numerical data are plotted with correlation curves for comparison in Figure 7.51. It is seen that the correlation agrees well with the data, as almost all numerical data falls between the correlation curves for  $Pe = 500$  and  $Pe = 15,000$ . Since the exponent of the axial direction coordinate  $X$  is a function of the Peclet number, where  $Pe = Re Pr$ , two correlation curves are shown for two Peclet numbers, representing the lower and upper limits for the numerical data.

**Table 7.4** Numerically obtained parameters and heat transfer coefficients for two capsule outer diameters at various capsule rows

Capsule outer diameter (mm)	Mass flow rate (kg/s)	Inlet temperature (°C)	Heat transfer coefficient (W/m <sup>2</sup> K)					
			Row 1	Row 2	Row 3	Row 5	Row 10	Row 20
40	0.003	-5	59.65	36.20	32.19	26.33	16.49	7.56
40	0.003	-10	118.32	72.18	64.17	52.43	32.84	15.05
40	0.003	-15	175.85	107.74	95.70	78.11	48.92	22.41
40	0.003	-20	232.04	142.64	126.56	103.17	64.61	29.58
40	0.005	-5	76.18	50.59	45.92	39.07	26.76	14.66
40	0.005	-10	150.97	100.48	91.31	77.72	53.28	29.22
40	0.005	-15	224.21	149.44	135.92	115.68	79.37	43.58
40	0.005	-20	295.68	197.25	179.47	152.70	104.82	57.59
40	0.010	-5	99.53	74.08	68.99	61.50	47.17	31.76
40	0.010	-10	197.33	146.87	137.01	122.22	93.83	62.61
40	0.010	-15	293.32	218.23	203.79	181.88	139.66	94.19
40	0.010	-20	387.29	287.87	269.01	240.13	184.36	124.54
40	0.050	-5	151.28	134.39	131.98	126.55	115.48	98.75
40	0.050	-10	300.22	265.36	260.48	249.94	228.26	196.10
40	0.050	-15	446.62	393.02	385.66	370.11	338.24	292.27
40	0.050	-20	590.39	517.57	507.63	487.04	445.13	384.99
80	0.003	-5	20.20	11.35	9.58	7.32	4.00	1.33
80	0.003	-10	40.30	22.77	19.14	14.59	7.95	2.63
80	0.003	-15	60.23	34.15	28.61	21.74	11.80	3.89
80	0.003	-20	79.88	45.39	37.91	28.72	15.55	5.10
80	0.005	-5	26.92	16.18	14.05	11.29	6.89	2.92
80	0.005	-10	53.45	32.33	28.04	22.48	13.70	5.81
80	0.005	-15	79.51	48.33	41.85	33.51	20.41	8.64
80	0.005	-20	105.01	64.05	55.39	44.28	26.94	11.40
80	0.010	-5	37.90	25.61	22.85	19.48	13.43	7.29
80	0.010	-10	75.12	50.87	45.46	38.74	26.74	14.53
80	0.010	-15	111.58	75.66	67.69	57.66	39.83	21.67
80	0.010	-20	147.15	99.88	89.42	76.11	52.60	28.64
80	0.050	-5	65.19	55.26	51.96	48.75	42.11	33.30
80	0.050	-10	129.05	109.05	102.60	96.39	83.44	66.34
80	0.050	-15	191.66	161.50	152.01	142.95	123.85	98.90
80	0.050	-20	253.04	212.63	200.22	188.35	163.20	130.64

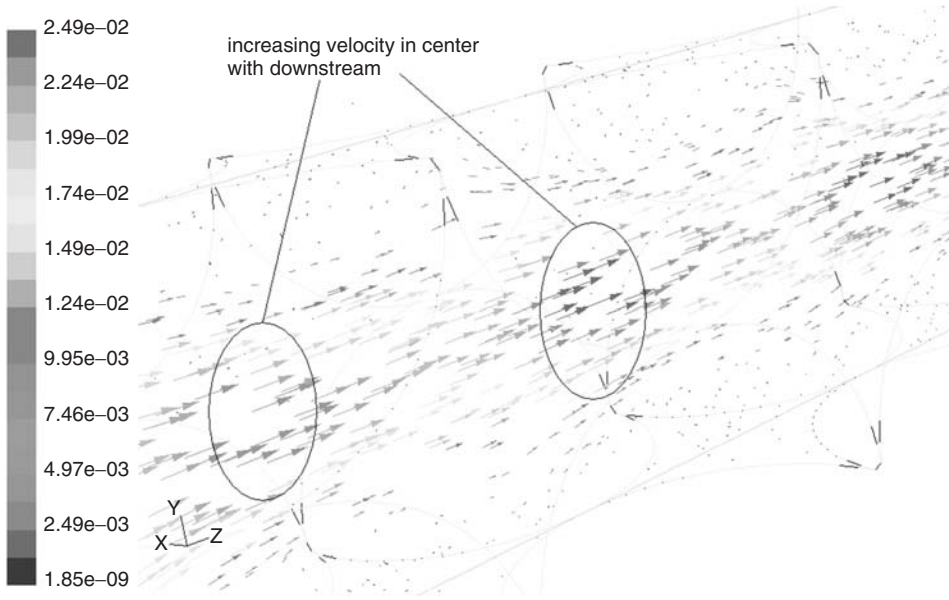


Figure 7.50 Fluid velocity vectors around the PCM capsules

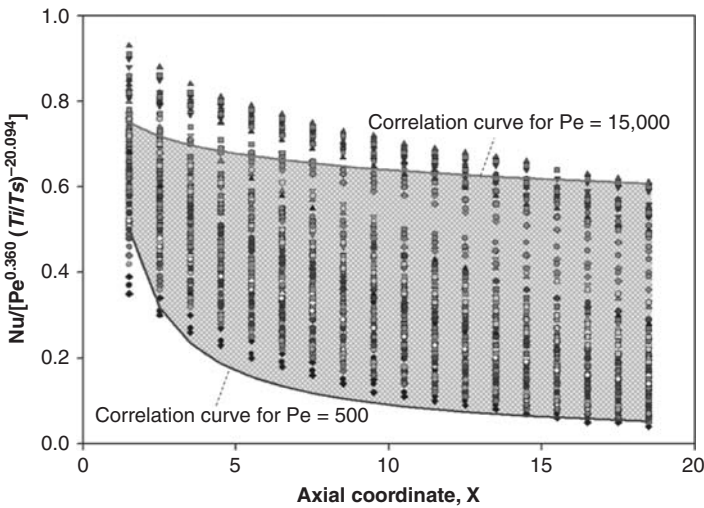
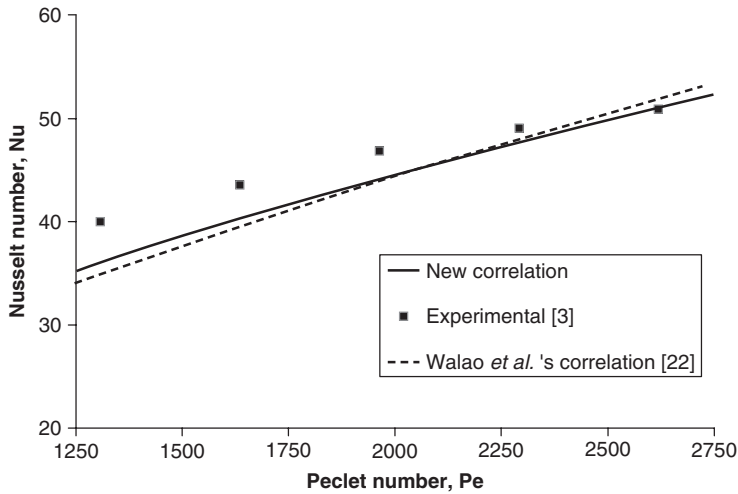


Figure 7.51 Variation with axial coordinate of the heat transfer correlations for two values of Peclet number (curves) and for numerically obtained data (dots)

To further confirm the results, we validate this correlation using experimental data from the literature. Chen and Yue (1991) proposed a correlation based on experimental data and numerical results for the heat transfer coefficient around spherical capsules. Kunii and Suzuki (1967) obtained time-averaged internal heat transfer coefficients by matching experimental measurements and theoretical results of the temperature profile for a coolant. Wakao *et al.* (1979) correlated heat transfer data published earlier for axial fluid thermal-dispersion coefficients. The corrected data for



**Figure 7.52** Variation of Nusselt number with Peclet number for correlation obtained here and in the literature (Wakao *et al.*, 1979) and for experimental data (Chen and Yue, 1991)

Reynolds numbers ranging from 15 to 8500 are correlated by an analogous form of mass correlation. Figure 7.52 compares the heat transfer coefficient obtained with the correlation determined here and from other studies (Chen and Yue, 1991; Wakao *et al.*, 1979). Satisfactory agreement is observed between the results in this figure.

The physical validity of the mathematical model is inspected by comparing it to predictions using experimental data. Cho and Choi (2000) determined the temperature variations inside and on the surface of a spherical capsule filled with *n*-tetradecane, along the centerline of the storage tank. To validate the numerical model with experimental data from Cho and Choi (2000), the numerical code is tested for the same geometrical and operational parameters and the same PCM (*n*-tetradecane), heat transfer fluid (40% aqueous solution of ethylene glycol), and container material (polyethylene). Properties for these materials are listed in Tables 7.2 and 7.3. The comparison of numerical results and experimental data from Cho and Choi (2000) is given in Figure 7.53(a) and (b). Although the present numerical model does not consider sensible storage in the container wall or supercooling, there is still good agreement between the numerical results and experimental data. A sharp decrease in the center temperature is more emphasized with the numerical analysis, as is also observed elsewhere (Ismail *et al.*, 2003). This decrease occurs at the end of solidification.

### Effect of Other Parameters

The variation of the local heat transfer coefficient along the flow path is significant, indicating that it should not be treated as constant. Figure 7.54(a) and (b) demonstrate clearly the importance of the  $x$ -dependent heat transfer coefficient. The variation of time (dimensionless) for complete solidification of each capsule for different Reynolds and Stefan numbers is shown in Figure 7.54(a) for the first layer of capsules and in Figure 7.54(b) for the seventh layer. The solidification time is not sensitive to variations in Reynolds number for the first capsule, but becomes very sensitive for the seventh capsule. Hence, the effect of inlet heat transfer fluid temperature and Stefan number on the solidification time is important for the two cases. Solidification time appears to be independent of capsule diameter.

The variation of the time-dependent heat transfer rate with capsule layer is shown in Figure 7.55 for  $Re = 20$  and  $Re = 60$ . As expected, the variation of the heat transfer rate along the flow path

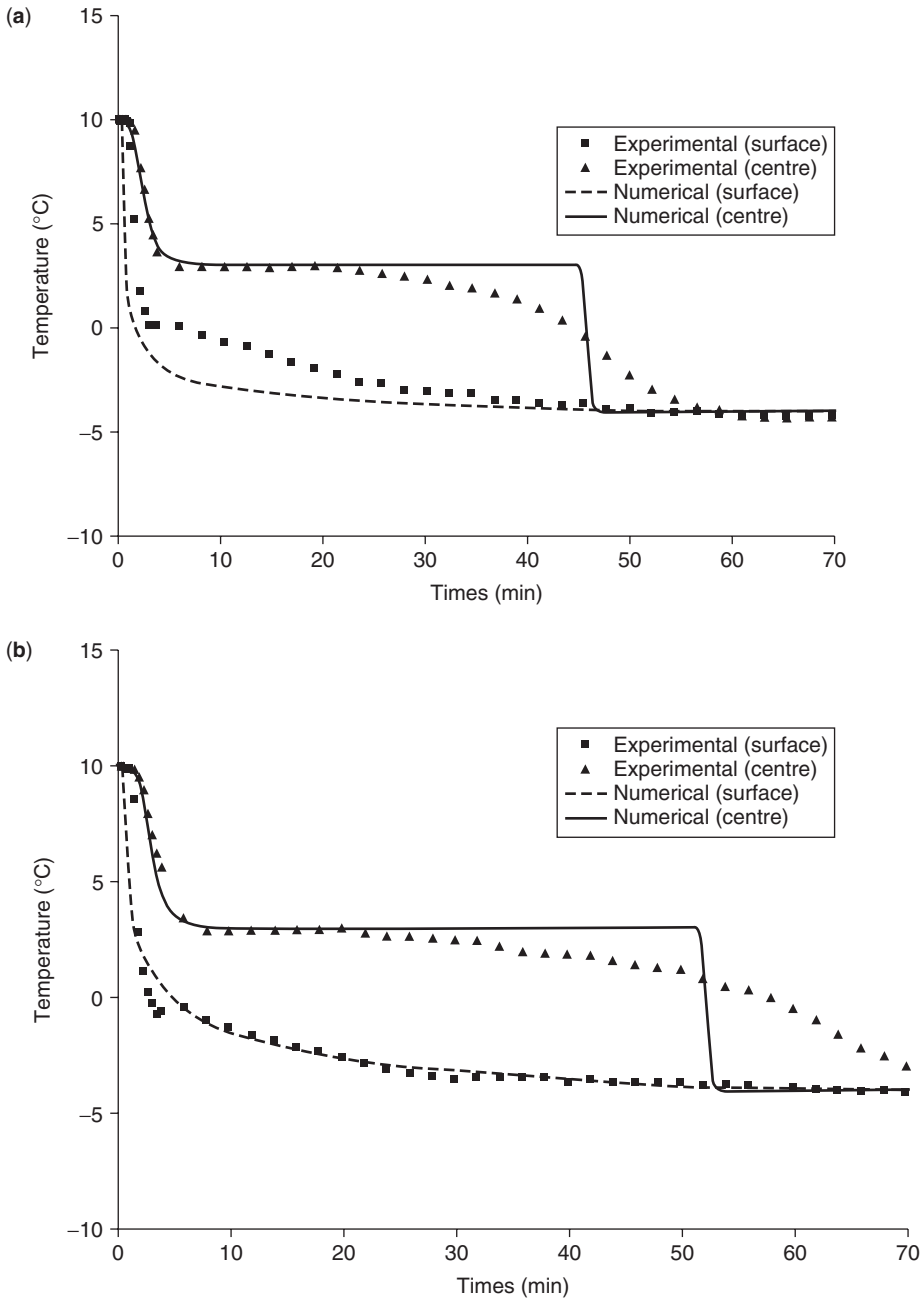


**Figure 7.53** (a) Variations of experimental and numerical temperatures at center and surface points with time for first capsule layer. (b) Variations of experimental and numerical temperatures at center and surface points with time for seventh capsule layer.



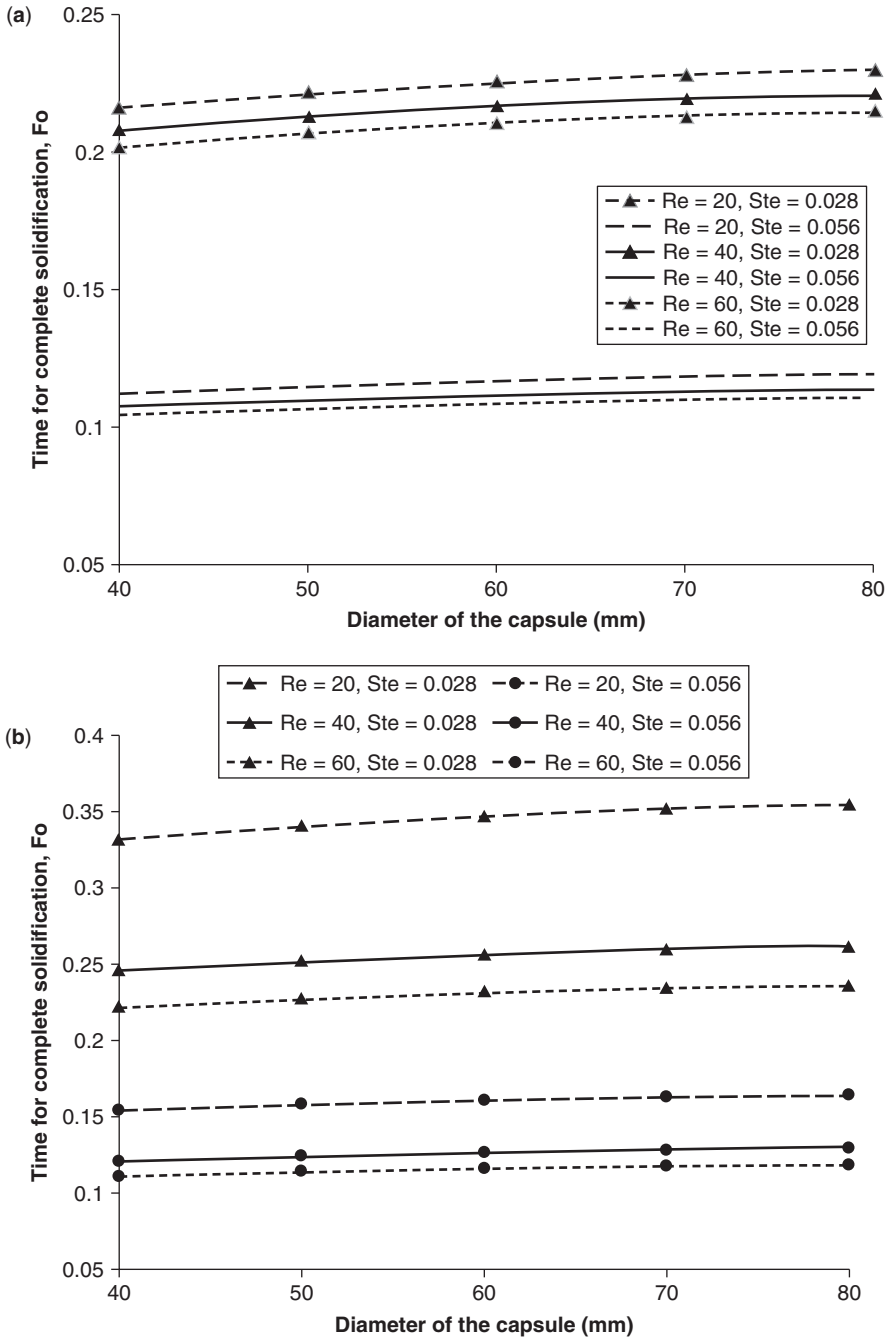


**Figure 7.54** (a) Variation of dimensionless time for complete solidification with capsule diameter for several values of Reynolds and Stefan numbers, for first capsule layer (b) Variation of dimensionless time for complete solidification with capsule diameter for several values of Reynolds and Stefan numbers, for seventh capsule layer

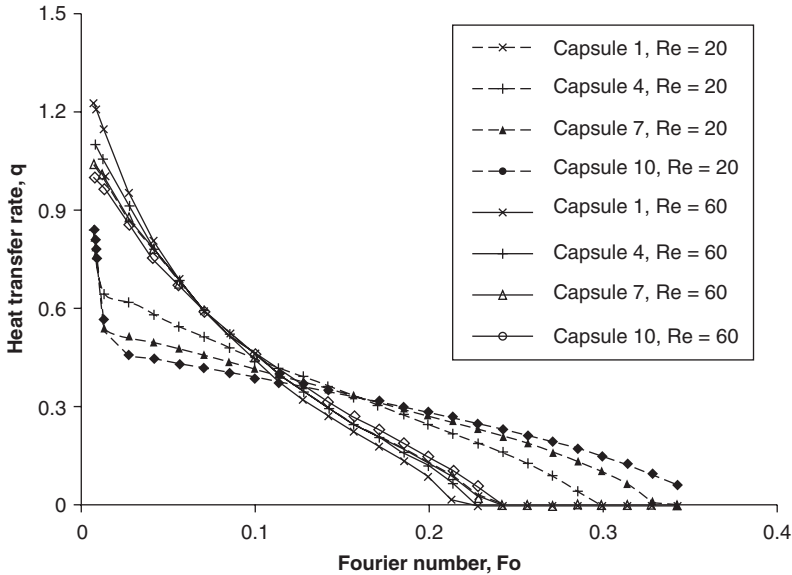


**Figure 7.55** Variation of heat transfer rate with Fourier number for several Reynolds numbers and capsule row numbers

is more marked at lower Reynolds numbers. The heat transfer rate varies little along the flow path for high Reynolds numbers. But increasing the Reynolds number increases the heat transfer rate.

The effect of Reynolds and Stefan numbers on the heat transfer rate is illustrated in Figure 7.56 for the case of a 60-mm diameter capsule. The heat transfer rate is observed to increase as Reynolds number increases and heat transfer fluid inlet temperature decreases. The effect of Stefan number is more significant than that of Reynolds number.

The total energy stored as a function of time for several Reynolds and Stefan numbers is shown in Figure 7.57 for a 60-mm diameter capsule. As Reynolds number and Stefan number increase, the total charging time decreases. Note that the total stored energy increases with Stefan number at the end of charging due to sensible heat gains.

### 7.8.6 Closing Remarks for Illustrative Application for a Complex System

Numerical simulation has been applied to develop a heat transfer coefficient correlation that varies along the flow path for heat transfer around a spherical capsule in a cold TES. A validation shows that the correlation demonstrates good agreement with experimental data from the literature. Numerical analysis of the heat transfer behavior of an encapsulated ice TES system is performed using a temperature-based fixed-grid solution with a control-volume approach. The results show that

- the effect of varying heat transfer coefficient on the heat transfer is significant and should be considered;
- the heat transfer rate increases as Reynolds number increases and heat transfer fluid inlet temperature decreases; and
- the solidification process is primarily dependent on Stefan number, capsule diameter, and capsule row number.

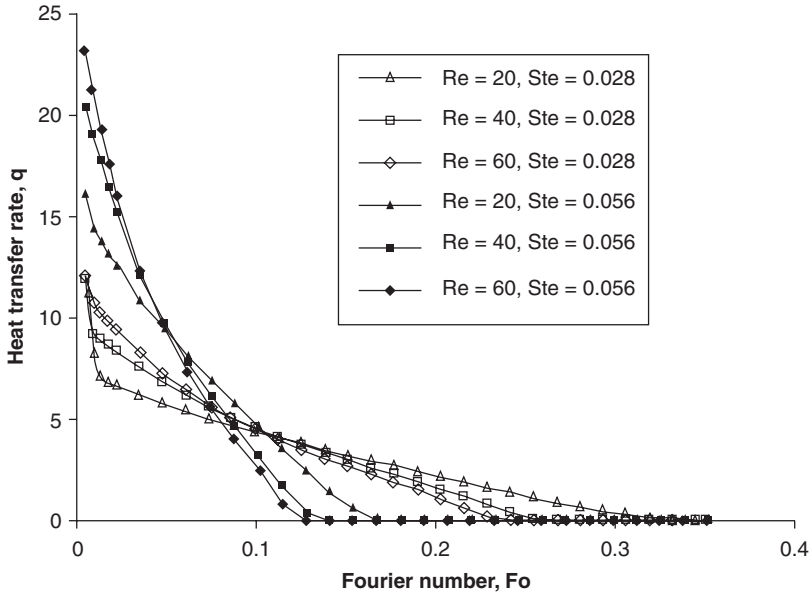


Figure 7.56 Variation of heat transfer rate with Fourier number for several Reynolds and Stefan numbers

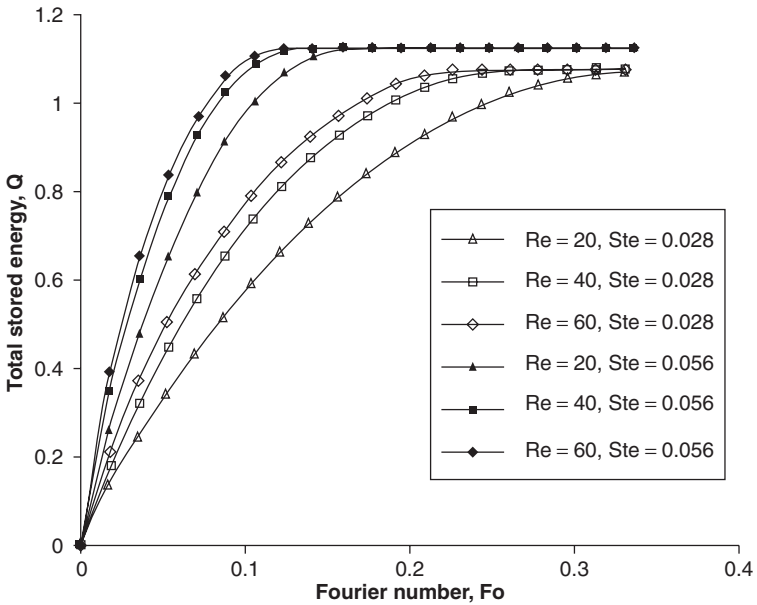


Figure 7.57 Variation of total energy stored with Fourier number for several Reynolds and Stefan numbers

## 7.9 Concluding Remarks

The usefulness of numerical modeling and simulation in TES applications has been demonstrated in this chapter. By considering heat transfer and thermodynamic analyses of sensible and latent TES systems, numerical simulations can provide meaningful insights into system behavior and the magnitudes of system losses.

Common practices for creating computational volumes using commercial software have been described, along with the significance of the number of volumes and the size of each. While care must be taken to ensure that a discretized volume behaves as expected, the grid should not overburden the computational algorithm with too much information. Hence a balance is sought between computational cost and complexity. A similar trade-off is required when choosing a time step size. An extremely small time step increases accuracy but increases computational cost greatly. Thus, an important factor in establishing a numerical simulation is to ensure the time step and discretization schemes are adequate for accuracy, but not overly complicated.

We have described and discussed fluid flow, which forms the basis of CFD codes, and the Navier–Stokes and continuity equations that must be solved in numerical TES simulations. The associated energy equations, including in some cases viscous dissipation, have also been described to provide a more complete understanding of the phenomena occurring in sensible and latent TES systems. An overview is included of the correct data monitoring processes for thermodynamic analyses, which are important for understanding efficiencies and losses, and which can be formulated on first- and second-law bases.

Four case studies are presented in this chapter, including two sensible and two latent TES cases. A commercial computational heat transfer and fluid dynamics software package, ANSYS FLUENT, is used. The cases incorporate various models including viscous dissipation, natural convection, and phase change. For all cases, the geometric construction and discretization of the domain into finite volumes is discussed, and simulation procedures are explained in detail. The results for all cases are examined, using FLUENT visualization tools where beneficial. Factors affecting performance criteria are explained. The fourth case study contains information about the validation and independence tests that a numerical study must satisfy. All simulations were run on a modest computer in a reasonable amount of time, and each gave insightful information into the operation of many TES systems and their components. The case studies provide examples that may prove useful for similar systems. In addition, an illustrative application for a more complex system is provided, which involves a numerical assessment of an encapsulated ice TES with variable heat transfer coefficients.

Numerical modeling and simulation of TES systems is relatively simple to perform and much less expensive than corresponding experimental investigations. The benefits of modern numerical practices are significant, since they decrease experimental costs and often provide enhanced information on the losses occurring in TES systems. Numerical investigations facilitate system optimization, and are likely to become increasingly important in the future, with the expected increase in long-term global demand for energy resources.

### *Nomenclature*

$A$	area, $\text{m}^2$
$c, C$	specific heat, $\text{J/kg K}$ ; dimensionless volumetric heat capacity ( $C^0/(c_l \rho_l)$ )
$C_{sl}$	ratio of solid–liquid volumetric heat capacity ( $C_s/C_l$ )
$D$	capsule outer diameter, $\text{m}$
$\text{Fo}$	Fourier number ( $\alpha_f t/D^2$ )
$\vec{f}$	wall facet
$\vec{g}$	gravitational force vector
$h$	specific enthalpy, $\text{J/kg}$
$h'$	latent enthalpy portion, $\text{J/kg}$

$H$	enthalpy, J; dimensionless enthalpy
$I$	destroyed exergy, J
$k$	thermal conductivity, W/m K
$K$	dimensionless thermal conductivity ( $k/k_l$ )
$K_{sl}$	ratio of solid–liquid thermal conductivity ( $k_s/k_l$ )
$L$	latent heat of fusion, J/kg
$m$	mass, kg
Nu	Nusselt number
$p$	static pressure, Pa
$\bar{p}$	average static pressure from monitors, Pa
$Pe_f$	fluid Peclet number ( $Re_f Pr_f$ )
$Pr_f$	fluid Prandtl number ( $\nu_f/\alpha_f$ )
$q$	heat flux, W/m <sup>2</sup>
$q^0$	heat transfer rate, W
$q$	dimensionless heat transfer rate ( $= q^0/(\alpha_l \Delta H D)$ )
$Q$	heat transfer, J; dimensionless total stored energy ( $= Q^0/(\Delta H D^3)$ )
$Q^0$	total stored energy, J
$r$	radial coordinate, m
$R$	dimensionless radial direction ( $r/D$ )
$R_i$	dimensionless inner radius
$Re_f$	fluid Reynolds number $\left(\frac{\rho \cdot u \cdot D}{\mu}\right)$
$Res$	residual error
$s$	specific entropy, J/kg K
$S$	entropy, J/K; dimensionless source term $\left(\frac{S^0}{\rho_l \cdot c_l (T_m - T_{in})}\right)$
$S^0$	source term
Ste	Stefan number $\left(\frac{\rho_s c_s (T_m - T_{in})}{\Delta H}\right)$
$t$	time, s
$t_w$	dimensionless wall thickness of capsules $\left(\frac{(D - D_i)}{2D}\right)$
$t^*$	dimensionless time
$T$	temperature, °C or K
$\bar{T}$	average temperature from monitors, K
$u$	$x$ -portion of velocity, m/s
$U$	internal energy, J
$v$	$y$ -portion of velocity, m/s
$V$	volume, m <sup>3</sup>
$\vec{V}$	velocity vector
$w$	$z$ -portion of velocity, m/s
$W$	work, J
$X$	exergy of heat transfer, J; dimensionless axial direction ( $x/D$ )

### Greek and Special Symbols

$\alpha$	thermal diffusivity, m <sup>2</sup> /s
$\rho$	density, kg/m <sup>3</sup>
$\delta\theta_m$	dimensionless semi phase change temperature range ( $\delta T_m/(T_m - T_{in})$ )
$\theta$	dimensionless temperature $\left(\frac{(T - T_m)}{(T_m - T_{in})}\right)$
$\Delta H$	latent heat of PCM, J/m <sup>3</sup>

$\Phi$	viscous heating term
$\mu$	dynamic viscosity, kg/m s
$\beta$	volumetric expansion coefficient, $K^{-1}$
$\gamma$	dummy variable
$\Pi$	entropy production
$\Xi$	exergy, J
$\in$	flow exergy, J
$\infty$	reference environment
$\phi$	liquid fraction
$\eta$	energy efficiency
$\psi$	exergy efficiency
$\tau$	dimensionless time ( $\alpha_f t / D^2$ )
$\nu$	kinematic viscosity, $m^2/s$

### Subscripts

0	reference state
1	initial state
2	final state
<i>air</i>	air region
<i>b</i>	boundary heat interaction temperature
<i>c</i>	center
<i>ca</i>	center value at cell "a"
<i>cb</i>	center value at cell "b"
<i>ch</i>	charging
<i>copper</i>	region filled with copper
<i>CV</i>	control volume
<i>dc</i>	discharging
<i>dissipative</i>	viscous dissipation
<i>f</i>	facet value; transfer fluid
<i>ht</i>	heat transfer
<i>i</i>	<i>initial</i>
<i>in</i>	inlet
<i>inf</i>	outside of the thermal storage tank
<i>ini</i>	initial
<i>input</i>	input quantity
<i>insulation</i>	insulation region
<i>j</i>	heat interaction <i>j</i>
<i>l</i>	latent; liquid PCM
<i>latent</i>	phase change
<i>m</i>	mass-weighted; mushy phase
<i>nb</i>	neighboring
<i>ns</i>	no-slip wall region
<i>out</i>	outlet
<i>pcm</i>	paraffin phase change material region
<i>prod</i>	product quantity
<i>s</i>	slip wall region; solid PCM; inner surface
<i>source</i>	source terms
<i>t</i>	time
<i>v</i>	volume-weighted
<i>w</i>	wall; container wall or surface
<i>water</i>	water region

## Acronyms

CFD	computational fluid dynamics
FEM	finite element method
FVM	finite volume method
HTF	heat transfer fluid
PCM	phase change material
SIMPLE	semi-implicit method for pressure-linked equations
TES	thermal energy storage
VOF	volume of fluid model

## References

- Assis, E., Katsman, L., Ziskind, G. and Letan, R. (2007). Numerical and experimental study of melting in a spherical shell, *International Journal of Heat and Mass Transfer* 50, 1790–1804.
- Bedecarrats, J.P., Strub, F., Falcon, B. and Dumas, J.P. (1996). Phase-change thermal energy storage using spherical capsules: performance of a test plant, *International Journal of Refrigeration-Revue Internationale Du Froid* 19, 187–196.
- Benmansour, A., Hamdan, M. and Bengueuddach, A. (2006). Experimental and numerical investigation of solid particles thermal energy storage unit, *Applied Thermal Engineering* 26, 513–518.
- Bilir, L. and İlken, Z. (2005). Total solidification time of a liquid phase change material enclosed in cylindrical/spherical containers, *Applied Thermal Engineering* 25, 1488–1502.
- Chen, S.L., Chen, C.L., Tin, C.C., Lee, T.S. and Ke M.C. (2000). An experimental investigation of cold storage in an encapsulated thermal storage tank, *Experimental Thermal and Fluid Science* 23, 133–144.
- Chen, Z., Qi, X., Cheng, W. and Hu, P. (2006). A theoretical study of new-style cool storage air-conditioning systems with high-temperature water, *Energy and Buildings* 38, 90–98.
- Chen, S.L., Wang, P.P. and Lee, T.S. (1999). An experimental investigation of nucleation probability of super-cooled water inside cylindrical capsules, *Experimental Thermal and Fluid Science* 18, 299–306.
- Chen, S.L. and Yue, J.S. (1991). Thermal performance of cool storage in packed capsules for air conditioning, *Heat Recovery Systems and CHP* 11 (6), 551–561.
- Cho, K. and Choi, S.H. (2000). Thermal characteristics of paraffin in a spherical capsule during freezing and melting processes, *International Journal of Heat and Mass Transfer* 43, 3183–3196.
- Chorin, A.J. (1968). Numerical solution of Navier–Stokes equations, *Mathematics of Computation* 22, 745–762.
- Churchill, S. (1983). Comprehensive theoretically based, correlating equations for free convection from isothermal spheres, *Chemical Engineering Communications* 24, 339–352.
- De Souza, S. and Vielmo, H. (2005). Numerical analysis of water melting and solidification in the interior of tubes, *Journal of the Brazilian Society of Mechanical Sciences and Engineering* 27, 119–131.
- Doormaal, J. and Raithby, G.D. (1984). Enhancements of the SIMPLE method for predicting incompressible flow problem, *Numerical Heat Transfer* 7, 147–158.
- Eames, I.W. and Adref, K.T. (2002). Freezing and melting of water in spherical enclosures of the type used in thermal (ice) storage systems, *Applied Thermal Engineering* 22, 733–745.
- Erek, A. and Dincer, I. (2009). Numerical heat transfer analysis of encapsulated ice thermal energy storage system with variable heat transfer coefficient in downstream, *International Journal of Heat and Mass Transfer* 52, 851–859.
- Erek, A. and Ezan, M. (2007). Experimental and numerical study on charging processes of and ice-on-coil thermal energy storage system, *International Journal of Energy Research* 31, 158–176.
- Ettouney, H., El-Dessouky, H. and Al-Ali, A. (2005). Heat transfer during phase change of paraffin wax stored in spherical shells, *Journal of Solar Energy Engineering* 127, 357–365.
- Ghaddar, N. and Al-Maarafie, A. (1997). Study of charging of stratified storage tanks with finite wall thickness, *International Journal of Energy Research* 21, 411–427.
- Harris, K., Roux, J. and McCarty, T. (2003). Phenolic binder content impact on total heat transfer for fibrous insulation batts, *Journal of Thermal Envelope and Building Science* 26, 237–257.
- Hughes, T. (2000). *The Finite Element Method*, Dover Publications, Mineola, New York.

- Ismail, K.A.R. and Henriquez, J. (2000). Solidification of PCM inside a spherical capsule, *Energy Conservation and Management* 41 (2), 173–187.
- Ismail, K., Henriquez, J. and Da Silva, T. (2003). A parametric study on ice formation inside a spherical capsule, *International Journal of Thermal Sciences* 42, 881–887.
- Ismail, K.A.R. and Stuginsky, Jr, R. (1999). A parametric study on possible fixed bed models for PCM and sensible heat storage, *Applied Thermal Engineering* 19, 757–788.
- Kiatreungwattana, K. and Krarti, M. (2002). Evaluation of an internal melt ice-on-coil storage tank during partial charging and discharging cycles, *ASHRAE Transactions* 108, 1061–1071.
- Kousksou, T., Bedecarrats, J., Dumas, J. and Mimet, A. (2005). Dynamic modeling of the storage of an encapsulated ice tank, *Applied Thermal Engineering* 25, 1534–1548.
- Kunii, D. and Suzuki, M. (1967). Particle-to-fluid heat and mass transfer in packed beds of fine particles, *International Journal of Heat and Mass Transfer* 10, 845–852.
- Lacroix, M. (1993). Numerical simulation of a shell-and-tube latent heat thermal energy storage unit, *Solar Energy* 50, 357–367.
- MacPhee, D. (2008). Performance investigation of various cold thermal energy storages. M.A.Sc. thesis. University of Ontario Institute of Technology, Oshawa, Ontario, Canada.
- Oliveski, R., Krenzinger, A. and Vielmo, H. (2003). Comparison between models for the simulation of hot water storage tanks, *Solar Energy* 75, 121–134.
- Patankar, S.V. (1980). *Numerical Heat Transfer and Fluid Flow*, McGraw-Hill, New York.
- Pinelli, M. and Piva, S. (2003). Solid/liquid phase change in presence of natural convection: a thermal energy storage case study, *Journal of Energy Resources Technology* 125, 190–198.
- Regin, A.F., Solanki, S.C. and Saini J.S. (2006). Latent heat thermal energy storage using cylindrical capsule: numerical and experimental investigations, *Renewable Energy* 31, 2025–2041.
- Shah, L. and Furbo, S. (2003). Entrance effects in solar storage tanks, *Solar Energy* 75, 337–348.
- Shih, Y.P. and Chou, T.C. (1971). Analytical solutions for freezing a saturated liquid inside or outside sphere, *Chemical Engineering Science* 26, 1787–1793.
- Tao, L.C. (1967). Generalized numerical solutions of freezing a saturated liquid in cylinders and spheres, *AIChE Journal* 13 (1), 165–169.
- Voller, V.R. (1987). *Modeling Solidification Processes, Mathematical Modeling of Metals Processing Operations Conference*, American Metallurgical Society.
- Voller, V.R., Brent, A.D. and Reid, K.J. (1987). Computational modeling framework for the analysis of metallurgical solidification processes and phenomena, *Proceedings of the Conference for Solidification Processing*, Sheffield, UK, pp. 378–380.
- Voller, V.R. and Prakash, C. (1987). A fixed-grid numerical modeling methodology for convection-diffusion mushy region phase-change problems, *International Journal of Heat and Mass Transfer* 30, 1709–1720.
- Wakao, N., Kaguei, S. and Funazkri T. (1979). Effect of fluid dispersion coefficient on particle-to-fluid heat transfer coefficient in packed beds: correlation of Nusselt numbers, *Chemical Engineering Science* 34, 325–336.
- Weï, J., Kawaguchi, Y., Hirano, S. and Takeuchi, H. (2005). Study on a PCM heat storage system for rapid heat supply, *Applied Thermal Engineering* 25, 2903–2920.
- Zohoor, H. and Moosavi, Z. (2008). Increase in solar thermal energy storage by using a hybrid energy storage system, *Proceedings of World Academy of Science, Engineering and Technology* 33, 582–587.
- Zukowski, M. (2007). Mathematical modeling and numerical simulation of a short term thermal energy storage system using phase change material for heating applications, *Energy Conversion and Management* 48, 155–165.

## Study Questions/Problems

- 7.1 How can numerical simulation help identify that energy-saving opportunities are offered by TES?
- 7.2 In many numerical schemes, most notably in finite difference schemes, the Courant number  $v = u(\Delta t/\Delta x)$  is an important nondimensional parameter when discussing both stability and accuracy



of a numerical method involving advection. For a one-dimensional application to TES systems, where  $u$  is the velocity,  $\Delta t$  is the time step, and  $\Delta x$  is the nodal distance between points, for what values of  $v$  would you expect the method to be stable or unstable? Why?

- 7.3** In the case study in Section 7.5.1, natural convection is investigated by simulating the cooling of a hot water storage tank. Based on the resulting efficiencies, what would you expect to happen if the temperature of the water were increased or decreased? Discuss several other possible storage tank geometries and their expected relative performances.
- 7.4** What are the three main criteria for ensuring accuracy when modeling the physical domain in a numerical scheme for TES applications? Discuss how these criteria are addressed in each of the case studies in this chapter.
- 7.5** The Peclet number  $Pe = VL/\alpha$  is a measure of the ratio between advection (convection) and diffusion for a particular problem, where  $V$  is the fluid velocity,  $L$  is the characteristic length, and  $\alpha = k/\rho C_p$  is the thermal diffusivity. What is the Peclet number for the HTF in the case study in Section 7.5.2? What is the Peclet number for the HTF in the case study in Section 7.7.2? Should either conduction or advection be neglected in either case?
- 7.6** Try to recreate the case study in Section 7.4.1, using commercially available CFD software. Comment on the relationship between your results and the ones found in Figures 7.2 and 7.3.
- 7.7** In encapsulated ice thermal energy storage systems, porosity rate is the most important parameter affecting the maximum storage rate. The capsules may either be installed staggered or aligned in the direction of flow in the TES system.
- Calculate the porosity rate for the two arrangements.
  - If the capsules are initially in the liquid phase at the phase change temperature  $T_m$  and at the end of the storage period are in the solid phase at the heat transfer temperature  $T_\infty$ , determine the maximum thermal storage rate per unit volume with respect to the porosity rate.
- 7.8** A nondimensional representation of governing equations makes it easier to solve equations in numerical methods. The energy equation for an encapsulated ice TES can be written as

$$\varepsilon \rho_f c_f \frac{\partial T_f}{\partial t} + \rho_f c_f u \frac{\partial T_f}{\partial x} = \frac{\partial}{\partial x} \left( \varepsilon k_f \frac{\partial T_f}{\partial x} \right) + \frac{q_{capsule}^0}{V_{CV}}$$

Using the nondimensional parameters

$$X = \frac{x}{D}, \tau = \alpha_f \frac{t}{D^2}, K = \frac{k}{k_l}, C = \frac{\rho c_p}{(\rho c_p)_l}, \alpha = \frac{k}{(\rho c_p)}, Pe = \frac{uD}{\alpha_f}, \theta = \frac{T - T_{in}}{T_m - T_{in}}$$

obtain the following nondimensional expression:

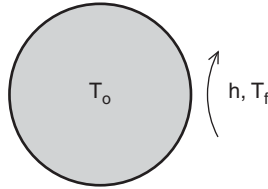
$$\varepsilon C_f \frac{\partial \theta_f}{\partial \tau} + C_f Pe_f \frac{\partial \theta_f}{\partial X} = \frac{\alpha_l}{\alpha_f} \frac{\partial}{\partial X} \left( \varepsilon K_f \frac{\partial \theta_f}{\partial X} \right) + \frac{q_{capsule}'''}{Dk_f (T_m - T_{in})}$$

- 7.9** The Nusselt number is a dimensionless temperature gradient on a surface and determines the convective heat transfer rate from that surface. For an encapsulated ice TES system, the Nusselt correlation is obtained as

$$Nu_x = 0.726 (\text{RePr})^{0.36} \left( \frac{T_i}{T_s} \right)^{-20.094} X^{\frac{-450.656}{\text{RePr}}}$$

For  $T_i/T_s = -10$  and  $X = 0$  to 20, show the variation of Nusselt number for three Peclet numbers ( $Pe = 500, 1000$ , and  $10,000$ ) on the same graph, noting that  $Pe = \text{Re Pr}$ . Discuss the effect of the Peclet number on the Nusselt number.

- 7.10** In the overall design process of a thermal system, the convective heat transfer rate is generally determined by the mean Nusselt number ( $\overline{Nu}$ ), rather than the local  $Nu_x$ . For the parameters given in Problem 2, obtain an expression for  $\overline{Nu}$ .
- 7.11** A spherical capsule filled with water at a temperature  $T_0$  is put in a refrigerated bath to observe the inward phase change process. The refrigerated bath consists of ethylene glycol at a constant temperature  $T_f$ . The bath provides a constant temperature around the capsule, and convection occurs at the interface with a heat transfer coefficient  $h$ . Assuming that the phase change process can be assumed to be one-dimensional for this scenario,
- obtain the appropriate dimensionless governing equation and boundary conditions; and
  - determine using numerical methods the surface temperature of the sphere, the solid/liquid interface position, and the total stored energy, all as a function of time.



- 7.12** In the case study in Section 7.8, it is emphasized that the heat transfer rate decreases and the required time for full solidification of the capsules increases as one moves downstream. What arrangements could be made in the system to achieve an almost uniform solidification for each capsule, and thereby have a more homogeneous storage? Conduct a detailed investigation, including a literature survey, on this topic.

# 8

## Thermal Energy Storage Case Studies

### 8.1 Introduction

Thermal energy storage (TES) systems have been employed to cool buildings since Roman Imperial times, when snow was raced from the mountains to provide short-term cooling in sweltering villas. In the early part of the industrial era, natural ice was used in theaters to cool the stage and portions of the audience. Air was blown over a pit full of ice to remove heat. With the advent of commercial air-conditioning equipment in the 1930s, some engineering practitioners used chilled water storage to supplement cooling and downsize compressors. Advances in manufacturing and an abundance of inexpensive power often encouraged designers and owners to rely on direct cooling equipment. These systems were cost-effective but consumed energy at the peak period of the day (when it was typically generated with oil). The 1973 oil embargo radically altered energy prices and perceptions of energy availability in the world. Many policies were developed that encouraged the use of TES to shift demand to evening and other off-peak hours (when nuclear and coal were the primary fuels for electrical generation). Electric utilities were encouraged to promote TES systems through rebates, design assistance, and demonstration. Now, TES finds use for heating and/or cooling purposes in a variety of applications.

Space heating using electric thermal storage has been used extensively in Europe and North America. The storage media include ceramic brick, crushed rock, water, and building mass, and systems can be either room or centrally based. Many improvements have been introduced in the past few years, including new phase-change materials (PCMs) for latent heat storage that have recently become available commercially.

Cold storage using ice, water, or eutectic salts as the storage media is widely applied where summer cooling requirements are high. It is also used in Europe, often in combination with heat recovery and hot water storage, and in Australia, Canada, Korea, Japan, Taiwan, and South Africa.

TES can be installed in both residential and commercial buildings, and can be cost-effective. Results from many of the monitored projects demonstrate payback periods of less than 3 years. If time-of-use tariffs exist, electricity costs to the consumer can be reduced by shifting the main electrical loads to periods when electricity prices are lower. If demand charges are implemented, a shifting or spreading of the load can reduce these significantly. To be effective, each storage system must be sized and controlled to minimize electricity costs.

Benefits from TES use also accrue to electricity utilities. The shifting of loads to off-peak periods not only spreads the demand over the generating period but may also enable output from the more expensive generating stations to be reduced.

Worldwide, there are many electricity-utility programs promoting the use of storage technologies – many of them are part of the demand-side management programs. Such programs can greatly influence the economic feasibility of installing thermal storage through offers of financial rebates for equipment, information programs, or special electricity rates for consumers.

In this chapter, a wide range of case studies are presented to illustrate the benefits, as well as drawbacks, of TES. The cases consider applications from the commercial and institutional building sector, industry, and groups within the utility sector representing electricity generation and district heating and cooling (DHC). The case studies illustrate the full context in which a given TES opportunity is viewed, rather than examining the TES in isolation. The types of TES represented by the case studies include both

- cold TES, using ice, chilled water, and PCMs; and
- heat TES, using both sensible and latent storage techniques.

The material presented here, based on actual applications, is drawn from various sources, for example, company reports and catalogs. In this regard, for the most part, the presentation and wording from the original sources is used to permit the views of the original writers to be provided.

## 8.2 Ice CTES Case Studies

### 8.2.1 Rohm and Haas, Spring House Research Facility, PA

In 1992, the manager of facilities and engineering, and the maintenance and utilities manager, Rohm and Haas, Spring House Research Facility, requested an in-depth energy review of the entire facility, considering both long- and short-term goals. The purpose of the study was to identify various ways to reduce electrical costs and optimize chilled water usage. The original chiller plant was built 32 years ago with 1200 ton-hour installed capacity and served two buildings. By 1987, the plant had grown to 4000 ton-hour installed capacity and served 13 buildings. The last research building was added in 1987. By 1990, the available cooling capacity at peak ambient conditions could barely meet the peak demand. Setting the supply chilled water temperature to 7.2 °C from 10 °C and hydraulically rebalancing the entire system permitted Rohm and Haas to meet cooling demands. Thus, more time was gained, permitting operation for the following 2 years; even 1991, which had unusually high ambient peak temperatures, presented only minor problems. This time allowed for a total re-evaluation and review of the chilled water plant, which uses almost 50% of the total electric demand. Therefore, an energy utilization study was done in 1992.

#### Scope of the Project

Rohm and Haas was concerned with the environmental impact of the refrigerant that was to be used for cooling, since additional refrigeration capacity was required. The existing four chillers' refrigerant is either CFC-11 or R-114, which mandated replacement. Another concern was the ever-increasing electric summer peak demands, largely derived from the chillers and their auxiliaries, with the corresponding increase in operating cost.

Many options were evaluated, including absorption refrigeration, high-efficiency centrifugal chillers, and cogeneration. After investigation and evaluation, a TES system was chosen, which produces ice during off-peak hours and, if elected, chilled water during the peak hours. The selection was reached based on the capability to shave in excess of 50% or more of the electric peak demand resulting from operating the chillers and auxiliaries.

Peco Energy, the electric company serving Spring House, has a cold thermal energy storage (CTES) rider, which reduces the peak demand hours from 12 to 10 Monday through Thursday and 6 on Friday. In addition, the peak demand for each peak month is averaged, and this results in a

lower annual peak billing demand. This provision is valid provided that the total cooling demand is reduced by 50% or more (preliminary results obtained during June and July 1995 indicate a reduction of about 70%).

In February 1994, Frank V. Radomski & Sons, Inc., a general contracting firm, was selected, and began preliminary engineering and cost estimate activities. By September 1994, all engineering services were selected and all major equipment vendors were chosen. In September 1994, the project was put on a fast track with strict scheduling and cost control, and construction commenced. The plant went into successful operation at the beginning of June 1995, exceeding all the peak demand shaving requirements during June and July.

The goal was to reduce peak electrical demand by a minimum of 1.6 MW. The payback calculations were based on 2.0-MW peak demand shaving and 10-month operation. An average peak demand shaving of about 2.3 MW, a 15% increase over the 2.0-MW design value, was achieved. All project aspects, including project management, architectural, electrical and mechanical design and engineering, and plant operation, were coordinated. All final decisions were open to review and solved cooperatively. This approach led to a well-designed, architecturally attractive addition to the utility plant, and the research facility began operation on time with a minimum of field changes and operating problems.

### Description of the System

The ice CTES system selected for the facility was an ice harvester-type system. A weekly load-shift strategy was incorporated in the system design to shift electric cooling load from the peak hours to the less expensive evening and weekend off-peak hours. The system consisted of four Mueller 250 ton-hour evaporators mounted on top of a rectangular poured-in-place concrete ice water storage tank. Completely assembled units were shipped to the plant.

The system was chosen over other TES technologies for the following reasons:

- the flexibility to optimize the system's efficiency under various load conditions;
- the ability to operate as a chiller as well as an ice maker;
- the ability to maintain consistent low water temperature from the ice storage, thus providing lower water temperatures to the existing air-handling units. This allows an increase in heat transfer and compensates for increased loads for some of the units and thus saves in replacement costs.

American Industrial Refrigeration (AIR) supplied the assembled high-side refrigeration package system, including a four-cell evaporator condenser furnished by Evapco, two-screw compressor packages, and a PC-based control system was supplied by Freezing Equipment Sales, Inc. (FES). The control system includes the integration and programming of the ice system's controls, compressor package controls, refrigeration system controls, and the ice and chilled water system controls.

This system is enclosed in an insulated double-wall enclosure, 12.8-m long by 8.5-m wide. The refrigeration high-side package, including all electrical switchgear, wiring, and pipe insulation, was completely fabricated at AIR's shop facilities. The work also included the installation of the compressor packages. The system was trucked from Minnesota to the Rohm and Haas plant site. The package was designed and built to be split into two halves and reassembled at the job site. The structure was designed to support the evaporative condensers, which were shipped directly in two packages. The condensers were installed and piped at the job site, using a preassembled structural steel catwalk assembly and piping. The on-site construction time for the assembly of these packages and evaporative condenser was 4 weeks. The refrigeration system is an HCFC-22 liquid recirculation system with a capacity of 1280 t of refrigeration during the ice-making mode and 1720 t of refrigeration during the water-chilling mode.

The goal of the project to reduce energy consumption economically was considered throughout the project. For example, the compressor packages were provided with oversized oil separators and suction valve assemblies to reduce pressure losses and allow operation at higher suction pressures

and lower discharge pressures. Thermosyphon oil cooling was selected for further economy of operation. The system utilizes the economizer cycle available on screw compressors. A flash-type economizer vessel is used to subcool the HCFC-22. The flash gas goes to a sideport connection on the screw compressor. This further increases the overall efficiency of the system. The evaporative condenser was oversized to allow overall operation at lower condensing temperatures. All equipment was selected with zero negative performance allowance. All electric motors were selected for high efficiency. The evaporator fan motors and one of the chilled water pumps have variable speed drives.

All operating functions are automatically controlled by the PC-based control system, which controls the ice harvesters and the water-side system. Compressors, condenser fans, condenser water pumps, refrigerant pumps, and control valves can all be operated on local control. In addition to its general features, such as dual pressure relief valves and high- and low-level alarms, the refrigeration high-side package also includes refrigerant detectors and an oxygen detector. All of the alarm signals are sent to the control system for operator display and acknowledgment.

The ice water storage tank includes a spray distribution system at the top of the tank to provide for an even melting of the ice. This produces low temperatures at the suction header. The suction channel is a 0.457 by 0.457 m formed channel in the bottom of the tank. This channel is covered by a 0.0127-m galvanized plate that has perforations to draw water evenly across the bottom of the tank. The mechanical equipment room is located between the ice storage tank and the existing utility building and is 7.62 by 24.38 m and 7-m high. Located in the mechanical equipment room are three ice water pumps nominally rated at  $0.157 \text{ m}^3/\text{s}$  each, circulating ice water through a single plate-type heat exchanger rated for  $0.466 \text{ m}^3/\text{s}$  and  $9.5^\circ\text{C}$  or 4625 ton-hour back to the ice harvesters. There are also three chilled water pumps rated at  $0.157 \text{ m}^3/\text{s}$ . One of the chilled water pumps has a variable speed drive. The electrical switchgear is located on the second floor.

The ice water storage tank is an above-ground concrete tank, poured in place to hold more than 45,000 ton-hour of latent cooling. The tank's nominal internal dimensions are 27.5-m long by 18.3 m with a usable height of 6.7 m. The tank floor is 0.3-m thick and the walls are 0.46 m. Galvanized structural steel, fully welded to wall channels, is anchored to the 0.46-m concrete tank walls. The tank top is designed to support the four 250 t/h harvester-type evaporators and two future evaporators. The tank interior is coated with a commercial industrial membrane, which is liquid applied urethane coating. All masonry exposed walls are insulated with 0.076 m of polyisocyanurate insulation and 0.1 m of split face block exterior. The roof insulation has 0.076 m of polyisocyanurate insulation with 0.46 by 0.46 m concrete pavers for ballast.

Further information on this project may be obtained from Kent (1996).

### 8.2.2 A Cogeneration Facility, California

Combustion gas turbines are constant-volume engines for which shaft horsepower is proportional to the combustion air mass flow. Engine output improves if the air temperature is depressed at the compressor inlet to increase the air density. When a combustion turbine generator is used in a power plant, increased engine output increases the electrical generating capacity. That is the concept presented in this case study of an inlet air chilling system installed in a cogeneration plant in California. The plant also uses a TES system with the inlet air chiller to optimize the plant's economic performance.

The facility considered here is a 36-MW gas turbine topping cycle cogeneration plant that began commercial operation in November 1991, producing electricity for sale to a regulated utility and generating steam for sale to an enhanced oil recovery operation in a local oil field.

The plant operates all year at base load. The summer season is when power sales are most valuable. The plant makes almost 80% of its electrical revenues between May 1 and October 31, yet the plant power output is substantially reduced by the high ambient temperature. Inlet air chilling

with TES was installed at the facility to increase output during critical peak hours in the summer when maximum unit performance is required.

The chiller/TES system consists of a mechanical vapor-compression refrigeration cycle driving an ice harvester that is operated in the evening hours to stockpile ice in a TES tank. Chilled water from the tank is circulated through cooling coils at the gas turbine air inlet during the heat of the day to increase the plant's electrical output.

### **Plant Description**

The plant's prime mover is a single-combustion gas turbine. It is an industrial-frame unit of single-shaft design driving a synchronous generator through a load gear. The compressor is of the 17-staged, axial-flow type with variable-inlet guide vanes. The turbine is three staged and is designed for an 1104.5 °C firing temperature. It has 10 combustion chambers arranged in can-annular design and, in this application, is fired on natural gas with nitrogen oxide (NO<sub>x</sub>) combustors for emission control. A heat recovery steam generator (HRSG) captures the 542.7 °C waste heat from the turbine exhaust to generate 61.6 MW of 75% quality steam for enhanced oil recovery. In new and clean conditions, the unit is rated for 36.24 MW gross output at the generator terminals with ambient air at ISO conditions (dry-bulb temperature 15 °C; relative humidity, RH, 60%). Approximately 1 MW is used for the plant's station light and power requirements. At the rated output, 132.4 m/s of air is consumed by the engine.

### **Inlet-Chilling Concept**

Electric power is sold to the utility under the terms of a purchase agreement. This agreement recognizes peak periods when high consumer demand places a premium value on generating capacity. Peak period occurs on weekdays from noon to 6 p.m. from May 1 through October 31 each year. During these periods, central California temperatures exceed 37.77 °C and air-conditioning units create the highest demand for power.

The power purchase agreement is structured so that the utility pays an energy payment for every kilowatt-hour delivered, a capacity payment for delivering power at no less than 85% of a dedicated firm capacity level, and a bonus payment based on how well the plant meets the remaining 15% of the dedicated firm capacity during peak hours. No bonus is earned on kilowatt-hour delivered above the dedicated firm capacity. The dedicated firm capacity level was set by a test of plant output at the time commercial operation began. That was, as it happened, in winter months when cool temperatures and the new and clean condition of the unit allowed a 35.5-MW dedicated firm capacity level to be set.

The gas turbine air-inlet system was originally equipped with an evaporative cooler to reduce inlet dry-bulb temperature. With the evaporative cooler operating at 85% effectiveness on a typical 35 °C day with 20% RH, the net output of the plant is at "best" 34 MW. Further reduction of output occurs because of unit degradation, for example, the effect of fouling, erosion, corrosion, and foreign object damage that inevitably degrades performance by reducing compressor airflow. Typically, such degradation will advance very rapidly during the first 2 or 3 years of operation to as much as 6% of output capability. Hence, performance of the plant would not meet the 35.5 MW dedicated capacity level, and was subject to the loss of a large share of potential bonus revenue.

To compensate for temperature and degradation effects, inlet air chilling was installed at a design temperature of 5.5 °C. In addition to increased output, chilled inlet air improves the gas turbine heat rate. The net plant heat rate is lowered when additional station power is used to generate ice at night, but the effect is almost completely mitigated by the heat rate improvement when chilling. Overall, net plant output with inlet air chilled to 5.5 °C during peak hours now satisfies the dedicated



capacity level. Operating points are indicated for typical summer peak ambient conditions (35 °C, 20% RH) with and without evaporative cooling and with chilling.

### Design Considerations

For the turbine generator, inlet air chilling is limited to 5.5 °C. Inlet air temperatures that were any lower at a nearly saturated condition could cause icing at the compressor inlet, resulting in damage to the engine. As air enters the bell mouth of the axial compressor, the velocity increases. Air enthalpy is transformed to kinetic energy in an adiabatic process as the velocity increases. Air at 5.5 °C accelerated to 106.7 m/s results in an approximate  $-12.2$  °C drop in temperature, to 0 °C. With this limitation in mind, three types of inlet air chilling were considered: direct mechanical refrigeration, absorption refrigeration, and TES.

The overall effect on net power produced for each scheme is shown in Table 8.1. Direct mechanical refrigeration consists of a vapor-compression refrigeration system to chill inlet air to 5.55 °C during the peak hours, without TES. This system has the added benefit of chilling capability during all hours of the day. Furthermore, there is a 1300-kW penalty associated with running the refrigeration compressor while chilling. The compressor load penalty would lower the net plant power output during peak hours. The plant would not meet 35.5 MW with 5.5 °C inlet air if an additional 1300-kW station load were subtracted from the net output. Furthermore, compared to TES, the installed refrigeration capacity required for direct refrigeration would be three times larger. Direct refrigeration would have to be sized to deliver the full instantaneous chilling duty for a turbine generator. With TES, the chilling duty for 6 h is accumulated and stored over 18 h, thus reducing the refrigeration required by a factor of 6/18, or one-third the size required for direct refrigeration.

Absorption refrigeration (e.g., a lithium bromide system) was considered. It would have required modifying the existing HRSG to provide low-pressure steam to drive the absorption system, thereby avoiding the power penalty associated with a direct mechanical refrigeration system. A drawback, however, is that there is no cooling water available at the site. A closed-loop cooling system would have been required, with the heat rejected to the air with an aerial cooler. As a result, during peak hours when the ambient temperature is above 32.22 °C, it would be difficult to chill the inlet air below 10.5 °C. This system would not maximize power output during peak hours.

TES was selected because it allows power output to be maximized during peak hours. The TES configuration allows operation of the refrigeration system when the value for power is lowest. In turn, the refrigeration system is turned off during peak hours to minimize station load, and inlet chilling is accomplished with the stored energy. The size of the refrigeration equipment is optimized with TES, since it is allowed 18 h of operation to store only 6 h of chilling capacity. The method of TES with ice was evaluated against cold water and cold brine storage. The latent heat of fusion for ice, 333.8 kJ/kg, substantially reduces the mass required to store energy, providing a more compact and economical system. After ice storage design considerations, such as air space and circulating water space, are accounted for, the volume required to store a given amount of energy with ice is about one-fifth the volume required to store an equivalent amount of energy with liquid. With ice

**Table 8.1** Plant performance data with inlet air cooling options

Ambient conditions (30 °C, 20% RH)	Evaporator cooler (85% efficiency)	Direct mechanical refrigeration	Absorption refrigeration	TES
Inlet air (°C)	21.1	5.5	10.5	5.5
Gross power (MW)	34.7	38.8	37.3	38.8
Station power (MW)	1.0	2.3	1.0	1.0
Net power (MW)	33.7	36.5	36.3	37.8
Heat rate (Btu/kWh)	11,190	10,900	10,980	10,900

Source: Hall *et al.* (1994).



storage, chilled water can be consistently supplied to the inlet air coil at  $0^{\circ}\text{C}$  to  $1.2^{\circ}\text{C}$ , whereas if storing chilled liquid, the temperature of the liquid gradually increases during the 6-h-per-day use cycle, creating a transient heat-transfer problem at the air inlet.

### System Design Basis

Weather data was analyzed to design the system. The inlet air chiller coil is designed to cool the inlet air for an average peak temperature condition of  $35^{\circ}\text{C}$  and 20% RH. This corresponds to a duty of 4.73 MW. Under these conditions, the refrigeration system will not totally replace the ice melted during a 6-h peak period overnight; however, the storage tank is sized for a 5-day weekly chilling cycle. The ice will be nearly depleted by the end of the week, but by operating over the weekend, the tank can again be filled with ice for the following week's cycle. The system was not designed to fully accommodate extreme weather conditions of more than  $37.7^{\circ}\text{C}$  with greater than 15% RH, which only periodically occur at the site. Under these conditions, the system may be operated to chill inlet air to a point above  $5.5^{\circ}\text{C}$  in order to maintain enough ice storage to last the week. The extra ice storage capacity, or refrigeration tonnage, necessary to accommodate extreme conditions was deemed too costly for optimum economic return on investment.

Another option, reducing the size of the refrigeration equipment to a capacity of 300–350 t, was considered. With this scenario, an ice storage tank 1.7 times larger than that selected would be required. The savings in the size of the refrigeration equipment did not offset the cost of the increased storage. For this reason, as well as for fear of ice/water distribution problems in a tank of this size, this option was not selected.

### Inlet Air Chiller Coil Design

The inlet air coils (Figure 8.1) were required to fit up to the existing inlet air-filter house for the gas turbine. This required a configuration that would add no new structural load, which could

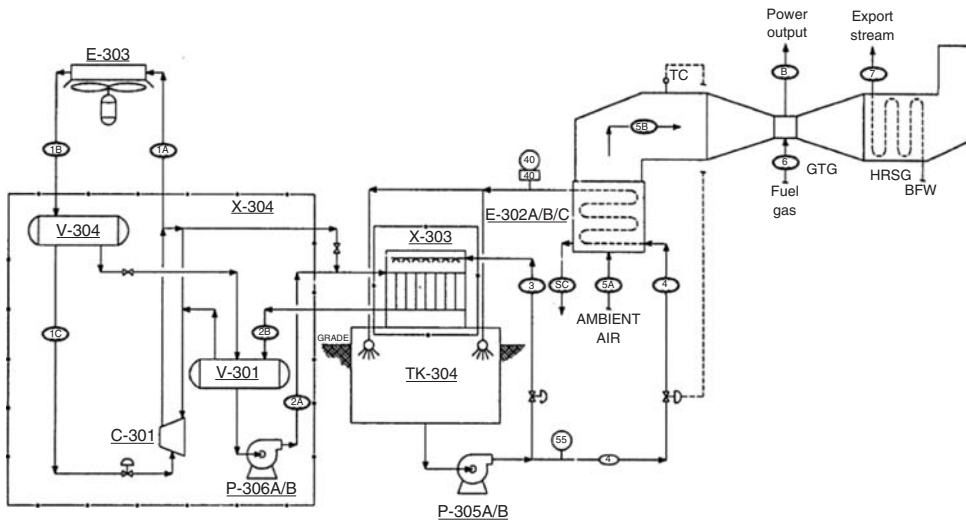


**Figure 8.1** Gas turbine inlet air cooling system (E-303  $\text{NH}_3$  condenser, V-304HP pilot receiver, P-306A/B refrigerant pumps, X-303 evaporator package, TK-304 ice water storage tank, C-301  $\text{NH}_3$  compressor, X-304 refrigeration package, V-301 liquefied petroleum (LP) receiver, P-305A/B chilled water pumps, E-302A/B/C inlet air cooling coils) (Reprinted from Hall *et al.* (1994) by permission of ASHRAE)

compromise the integrity of the existing structure. The design of the coils was also required to minimize the airflow pressure drop.

The resultant design was in three sections of horizontal tube bundles, with each bundle having a tube length of 8.12 m. The bundles are aluminum finned tubes with a diameter of 3.175 cm; the fin diameter is 6.35 cm with five fins per centimeter. Tubes are arranged four deep in a triangular pitch with 176 tubes per bundle. Each bundle is set in a galvanized steel framework that mounts on a concrete ring wall built around the outside perimeter of the inlet housing. The coils are supported by the ring wall on the front and sides of the filter house. Aluminum sheet metal was installed along the back of the filter house and between the coil housings and the filter house to prevent airflow from bypassing the coils. The coil arrangement allowed for ease of installation and a minimum reconfiguration of the existing plant. Pressure loss across the coils is only 1.27 cm H<sub>2</sub>O because of the low air velocity. There was concern about placing the coils upstream of the inlet air filters when chilling below the dew point, since this would expose the filters to possible carryover of condensed water droplets from the coils. Carryover has not proved to be a problem; condensate forms on the coils and falls into the basin formed inside the ring wall and is drained away.

### TES Design

The ice harvester selected for this project utilizes flat inflated stainless steel plates for the evaporator surface. Cold ammonia is circulated through the annular space inside the plates, and water is circulated out of the tank and over the outside surface of each plate. Ice is formed on both sides of the plate. When the ice reaches 1-cm thickness, hot gas is injected directly from the discharge of the compressor into the plate. The hot gas breaks the bond between the ice and the plate and the ice falls off (is harvested) into the tank. As ice falls into the tank, it forms a mound similar to sand in an hourglass. The angle of the mound, called the *angle of repose*, for ice built on the ice harvester is 15°. The location and size of the ice opening relative to the top area of the tank is critical. The evaporator plates for this application were positioned to minimize tank void volumes and optimize tank utilization. The size of the ice storage tank was determined based on the ice density of 916.22 kg/m<sup>3</sup> and the 560,926.08 kg of maximum ice storage required for the design condition. Assuming a 50% water/ice ratio below the water level and a 50% air/ice ratio above, the tank minimum volume requirement  $V$  was determined to be

$$V = 2 \times (560,926.08/916.22) = 1224.43 \text{ m}^3$$

Additional space allowance was included for the ice mounding at the top of the tank. The final internal dimensions of the tank are 14 by 12 by 8 m. The ice storage tank is cast-in-place concrete. The tank is installed partially in the ground on a hillside. One end of the tank is exposed from the hillside; this is where circulating pumps are installed, avoiding the need for a pump vault below ground. The tank is initially filled with water to the 60% level. As ice is dropped into the tank, it floats, with 91.7% of the ice below the water level and the remainder above. The water level remains constant in the initial stages of the charge cycle. When the ice level meets the bottom of the tank, the water level starts to drop. When the high ice level has been reached, the water is at the 20% level.

During the charging (ice-making) cycle, 0.126 m<sup>3</sup>/s of water is pumped over the evaporator. During the discharge (melting) cycle, 0.126–0.252 m<sup>3</sup>/s is pumped through the system as needed to meet the chilling demand. During the discharge cycle, when the chilled water feeds the turbine inlet air coil, the water bypasses the evaporator and flows directly into the tank. The “warm” return water is distributed in the tank via a spray header. The spray header is mounted at the top of the tank and evenly distributes the water over the ice pile. This even distribution of return water over the ice is necessary to maintain a constant supply water temperature to the coil through the entire discharge cycle.

## Refrigeration Design

The refrigeration system is a pumped liquid overfeed system. Liquid refrigerant is pumped from the low-pressure receiver into the evaporator plates. The plates are overfed with refrigerant at a rate of 3:1. Both liquid and gas refrigerants are then returned from the plates back to the low-pressure receiver. Gas is drawn out of the top of the low-pressure receiver and into the compressor. The gas is compressed and discharged into an air-cooled condenser. The condensed liquid refrigerant then flows through a high-side float and back into the low-pressure receiver. A diagram of the system is given in Figure 8.1. This type of refrigeration system was chosen because of its simplicity, high reliability, and low operating costs, as also the fact that it avoids slugging in the compressor.

Owing to the large size of the system, a single screw compressor was chosen over multiple reciprocating compressors. While in the ice-making mode, the compressor operates with a coefficient of performance (COP) of 2.8. Ammonia was chosen as the refrigerant because of the operators' familiarity with it (ammonia is stored on-site for a selective catalytic reduction system), and because it has environmentally benign qualities, including zero ozone depletion and greenhouse effect factors.

## System Operation

During the first 3 months of operation (June, July, and August 1993), the chiller/TES system maintained the plant's net electrical output above the dedicated firm capacity level of 35.5 MW for 100% of peak hours, fully satisfying its intended purpose of capturing full bonus revenues for the plant. A sister plant, a cogeneration plant situated two miles away, is identical to this facility in every respect except that it has evaporative cooling instead of an inlet -chilling/TES system. The sister plant experiences the same ambient air conditions, and thus provides an ideal yardstick by which to measure the benefit of inlet chilling at the original facility. During June, July, and August, the sister plant generated an average net output of 34.26 MW compared to the facility's average net output of 36.57 MW during peak hours. The inlet air temperature averaged 19.5 °C at the sister plant with the evaporative cooler. The inlet air temperature averaged 10.5 °C at this facility with the chiller/TES system. In future summer periods, the output of the sister plant will continue to degrade without the ability to make up the loss with chilled inlet air. The inlet temperature at this facility will be depressed further with the chiller/TES system, thus overcoming degradation in order to keep output above 35.5 MW.

## Closing Remarks

Inlet air chilling is a viable means to enhance turbine generator performance, provided revenues associated with the incremental output are cost-effective. This is particularly the case when hot summer weather conditions cause a peak power demand that raises generating capacity value to a premium, and at the same time inlet chilling can produce a significant performance improvement. TES provides a means to maximize chilled inlet air performance gains needed during peak hours by deferring the refrigeration parasitic load to night-time hours. TES allows optimized refrigeration equipment sizing, since it spreads chilling duty for weekday peak hours over nighttimes and weekends.

Further information is available elsewhere (Hall *et al.*, 1994).

### 8.2.3 A Power Generation Plant, Gaseem, Saudi Arabia

This case study provides some insight into a relatively new application of industrial refrigeration technology. Significant benefits can be realized by electricity-generating organizations employing gas turbine generators, particularly when located in regions of high ambient temperature, using the methods discussed here. Several systems are considered, including some that use CTES.

Some motivations for this project follow:

- The Middle East countries (e.g., Saudi Arabia) have a rapidly developing economy, with ever-increasing power use. There is presently a shortage of generating capacity to meet the peak demands of the summer period. Investment in new plants is expensive and the timescale to implement new plant is typically 18–24 months.
- Gas turbines are used for the majority of the power generation capacity throughout the Middle East and a large proportion of the world, particularly where gas or liquid fuels are readily available. These drivers are fixed-speed, constant inlet-air-volume machines, designed generally for steady-state operation. Whether operating on simple or combined cycles, their output power is directly linked to the rate of fuel that they can consume efficiently. This in turn is a function of air mass flow, which is a function of air density. It follows that if the air density can be increased, the turbine is likely to be able to burn more fuel and therefore produce more power.
- Owing to the high electricity load for air-conditioning in this region, the demand peaks between 12:00 and 17:00h. Outside these hours, particularly at night, demand drops considerably.
- At the time of the peak demand, the available capacity from the turbines is at its lowest because of the high ambient temperatures (and corresponding low air density).

The profile of the electricity demand, particularly in the Middle East, introduces opportunities for economically attractive, innovative plant designs. Thermal energy storage turbine inlet air cooling (TESTIAC) offers such an alternate design.

Cooling the combustion air to the turbines is beneficial because it increases the density and therefore increases the mass flow of air. This enables more power to be generated. Figures 8.2(a) and (b) illustrate the original process flow diagrams, and indicate the effect of turbine inlet air cooling on a typical gas turbine generating set, respectively.

Summer ambient design temperatures at the site under consideration are 50°C dry bulb, 10% RH. The site is at an altitude (relative to sea level) of 650 m, where the air density is approximately 1 kg/m<sup>3</sup>. If this air is cooled to 10°C, the density is increased to 1.15 kg/m<sup>3</sup>. This increases the mass flow by 15% and enables an increase in turbine output power of about 33%.

The improvement in output capacity has to be balanced against additional costs of the enhancements to the system. Normally, the costs of implementing TESTIAC to increase electricity production capacity are merited if they are less than the costs of new turbine equipment. The development of capacity enhancement of gas turbine power generation by TESTIAC has been progressing for about 20 years. In North America, there were approximately 10 plants in operation around 2002, of various sizes and designs, operating with varying degrees of success. The development process has stimulated many differing configurations, some of which are illustrated in Figures 8.3–8.5.

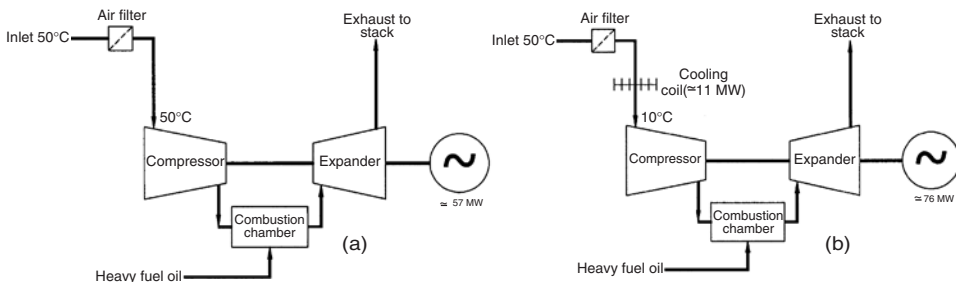


**Figure 8.2** Gas turbine generator system (a) without precooling and (b) with precooling (Courtesy of WS Atkins Consultants Limited)

The simplest example (Figure 8.3a) is where the refrigeration system is matched to the instantaneous cooling requirement. This involves no TES, but requires the greatest refrigeration capacity. This arrangement may be appropriate when the requirement for capacity enhancement is relatively small and the peak load duration is a large proportion of the available hours. Such a system will ordinarily employ centrifugal compressor-chiller packages. These are more efficient because of the small temperature differential across which they operate, and less expensive, per unit of cooling capacity. Because of the smaller water temperature differential available from this system, water flow rates and pumping costs are higher than with other systems.

The next example (Figure 8.3b) utilizes chilled water storage. This method uses only the sensible heat in the storage fluid. The method can be economic for small- to medium-sized loads, but the storage volumes involved can increase the cost dramatically for larger applications. The disadvantages of the previous example also apply if packaged chillers are used.

The third example as shown in Figure 8.4 uses an ice CTES system. This system requires a more expensive refrigeration plant because of the lower evaporating temperatures and specialized evaporator design configurations. The significant advantage is that the latent thermal storage capacity of the ice reduces the storage volume considerably, although this design requires extensive evaporator

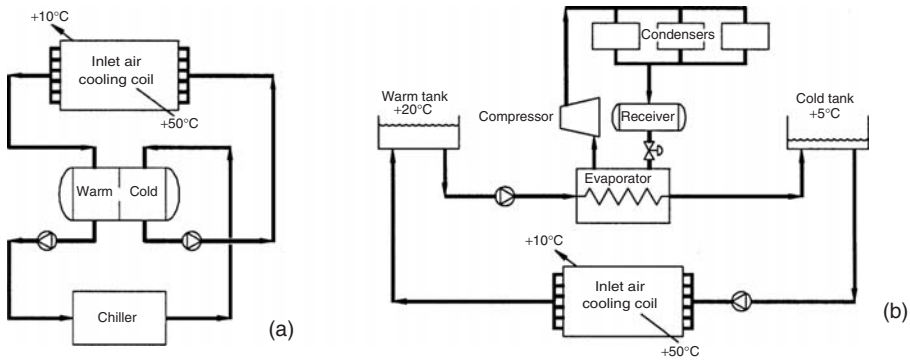


**Figure 8.3** A simple on-line inlet air cooling system (a) without TES (b) with TES using chilled water tanks (Courtesy of WS Atkins Consultants Limited)

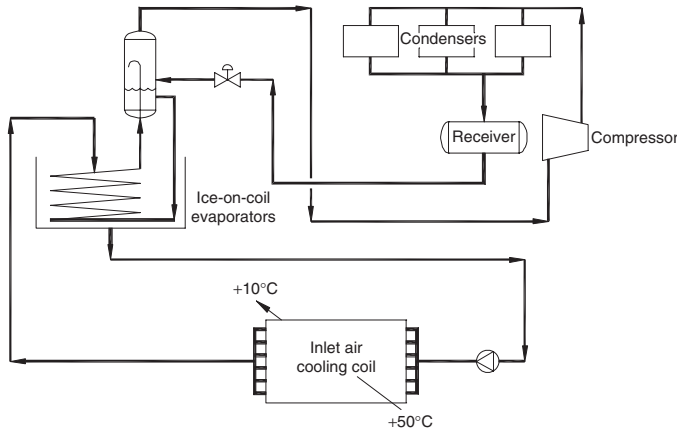


**Figure 8.4** A simple on-line inlet air cooling system with TES using ice-on-coil system (Courtesy of WS Atkins Consultants Limited)

surface area to handle the necessary ice storage volume. An additional advantage with some ice storage systems is that high peak loads can be readily managed. This is usually only possible with flake/slurry/sheet ice systems that offer high surface-area-to-volume ratios within the ice storage system. In practical applications, external or internal melt ice-on-coil systems cannot normally meet this requirement as effectively.

In this project, many systems were evaluated. These included ice-on-coil, panel (sheet), slurry ice, and various configurations of vacuum ice generators. In this particular evaluation, ice-on-coil systems were discounted as expensive, inflexible, and difficult to monitor in terms of available/residual storage capacity. Slurry ice systems had many advantages, but because of their relatively short development and application time, were discounted by the client. They also normally require the use of a eutectic solution, which adds cost. Ice slurry systems generally also offer advantages of two-phase pumping to the process load, which significantly lowers the parasitic pumping load. Vacuum ice generators offer the potential for large, future installations, pending the development of suitable compressors. On balance, the client's preferred option was the sheet-ice evaporator system, as indicated in Figure 8.5. This system represents a reasonable compromise between the competing factors of efficiency, flexibility, cost, and reliability. This design does, however, involve complex water and ice management, and also numerous solenoid valve actuations for the frequent defrosting of the plate packs. Another method, already operational in India, is to use the heat in the turbine exhaust gas to generate cooling via a lithium bromide (LiBr) absorption refrigeration plant. This approach would require that the system either be on line, as in Figure 8.3(a), or use water storage, as in Figure 8.3(b), because the chilled temperature is limited to around  $5^{\circ}\text{C}$ . Such systems may also require an intermediate steam generator because of control difficulties experienced to-date when applying the exhaust gases directly to the absorption plant generator.

A simple comparison of the main system types, relevant to this application, is provided in Table 8.2.

The overall client specification was of a functional nature. Six new turbines were to be installed, each having a nominal capacity of 342 MW at the summer design ambient condition. The cooling plant had to produce an air temperature of  $10^{\circ}\text{C}$  off the inlet air cooling coils, for the full 5-h peak period, across all six turbines. This precooling would enable a full load capacity of 455 MW with an increase of 113 MW.

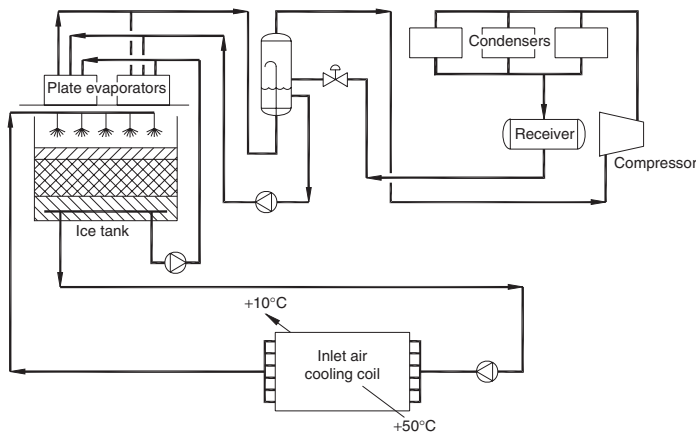


**Figure 8.5** A simple on-line inlet air cooling system with TES using flake or slurry ice in tank (Courtesy of WS Atkins Consultants Limited)

### Basis of Design

In order to enable the additional output power generation as specified by the gas turbine manufacturer, the inlet air cooling system was designed on the following basis:

- Ambient dry-bulb temperature: 50 °C
- Ambient air humidity: 10% RH
- Air mass flow rate per turbine (excluding air cooler): 275 kg/s
- Number of turbines: 6
- Required turbine inlet air dry-bulb temperature: 10 °C
- Peak load period: 5 h
- Ice regeneration period: 19 h

The plant configuration, as shown in Figure 8.6, is an integrated ammonia refrigeration plant, with four-screw compressors, multiple air-cooled condensers, four air-cooled oil coolers, and eight plate-pack sheet-ice evaporators arranged for pumped circulation from a single suction accumulator and a flash economizer vessel. The high ambient temperatures and the shortage of a water source precluded the use of conventional thermosyphon oil cooling and evaporative condensers. Instead, remote air-cooled oil coolers and air-cooled condensers were used.

The evaporators are multiple vertical stainless steel plate evaporators, located on the roof of an ice storage tank. Water is passed over the plates by a sparge system that ensures that an even film of water is applied to each side of each plate. During the ice-build period, some of this flow is frozen to the plate, which is maintained at approximately  $-8^{\circ}\text{C}$  by the recirculation of liquid ammonia

**Table 8.2** Comparison of three main types of TES systems for the project

System	Storage volume (m <sup>3</sup> )	Capital estimate (M£)	Daily energy use (MWh)
Chilled water	20,000	20	250
Ice-on-coil	10,000	18	350
Ice in tank	8,000	14	314

Source: Palmer (2000).

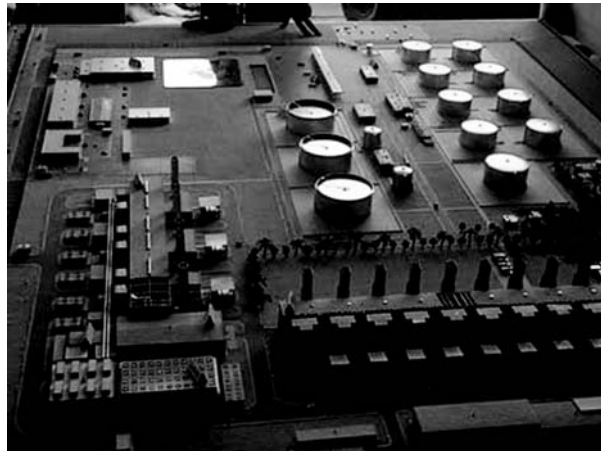


**Figure 8.6** The Gaseem TESTIAC system (Courtesy of MARCO)



from the suction accumulator. After a specified period of time, or on ice thickness measurement, a hot gas defrost cycle is initiated. This injects a flow of ammonia discharge vapor into a section of the plate pack, melting a small proportion of the ice and causing it to fall directly into the storage tank below. The cycle repeats for each of the evaporator units until the ice inventory is replenished.

The tank is a reinforced concrete structure, measuring  $34 \times 34 \times 13$  m externally and initially containing over  $8000 \text{ m}^3$  of water. The walls are 1200-mm thick at the base. There are sleeved perforations through the wall base, to allow the pump suction connections to join the inner ring header. The tank is lined internally with a plastic membrane to protect the concrete and to reduce the risk of leakage.

Two sets of water circulation pumps are provided. Each of them draws from the specially designed header within the tank. This header regulates the flow of water within the tank, to ensure even distribution through the ice inventory. The water flow diagram shows that during the accumulation period, water is collected via the inner ring pipework and circulated over the evaporators. The disposition of the ice buildup within the tank is an important factor. If the ice store becomes unevenly distributed, water bypassing can result. This will prevent sufficient cooling contact between warm water and ice and cause over-temperature water to be circulated to the cooling coils. For this reason, during the accumulation period, circulation of water to the evaporators is controlled by motorized valves and sensors, ensuring that the ice within the tank is evenly distributed. This generation process continues over the 19-h build period, or until the desired ice storage volume has been achieved. The refrigeration plant is then turned off. During the 5-h demand period, the second set of water pumps are run, also drawing from the inner ring and then circulating to the inlet air cooling coils. Flow to each turbine is controlled locally to maintain the desired air temperature. Flow to the coils in general is regulated by control of the pumps and a bypass control valve. Return water is routed back to the ice tank and distributed through a matrix of nozzles, controlled by motorized valves to ensure even distribution over the ice within the tank. The warm return water passes through the broken sheet ice, melting it in the process of being cooled. The cooled water is then collected in the internal header and recirculated.

The pipework system was comprehensively analyzed for stress during the design period, to determine the range of forces to which the foundations, support structures, pipework, and fittings would be subjected, over the range of operational temperatures. The complete water and refrigerant pipework systems and all the necessary structural supports, anchor points, and spring hangers, were designed on the basis of these analyses and site surveys.

The ammonia refrigerant is to be circulated by hermetic pumps from the suction accumulator. These operate constantly during the build cycle. Evaporated vapor is drawn off by the four-screw compressor packages. These operate through a centralized controller to maintain a constant evaporating temperature by slide valve control and off cycling, as required by the system demand. The discharge vapor from these is condensed in the air-cooled condensers. Condensate is collected in a control level receiver, which modulates a control valve and feeds the liquid into the combined flash economizer/liquid storage vessel. Vapor from this is taken to the compressor economizer port and the liquid is fed to the suction accumulator to maintain a working level.

The refrigeration plant has been designed not only to work at the maximum average ambient condition when required but also to take advantage of the diurnal swing in ambient temperature. Owing to these temperature swings, more capacity is available at night than during the day. The parasitic power consumption is also reduced. Over the 19 h of ice-build time, accumulation of the maximum requirement of ice can be achieved.

The operating economics are less significant than the capital cost of such a plant. The cost of fuel (and hence electricity) is low during off-peak periods. The benefit gained by increasing the net peak capacity is of great significance, whereas the cost of the energy expended in enabling it during the off-peak period is low. In this example, the energy cost of operating the plant to accumulate the ice capacity is about 304 MWh (16 MW for 19 h) per day (during the peak ambient conditions). The additional energy cost of circulating the chilled water to the cooling coils during the peak 5-h



period (a direct parasitic cost) is about 10 MWh. The generating benefit gained during this period is about 565 MWh (113 MW for 5 h). This illustrates that the net benefit of this system, during peak, is an increase in generating capacity of 555 MWh per day, equivalent to two additional turbines. Even over the whole day, the net benefit is 251 MWh. The plant began operation in June 2000.

Since this project was initiated, there have been continuing developments in the technologies that contribute to the TESTIAC concept. In particular, slurry ice production and handling systems have been developed. Suitable alternative eutectic materials have also been developed that lower costs. Test rigs have been constructed, from which the pumping characteristics of various ice concentrations of these materials can be determined. Investigations are continuing and, as a result, the probability of slurry ice displacing sheet-ice systems is increasingly likely.

Further details can be obtained from Palmer (2000) and Abusaa (2000).

### 8.2.4 Channel Island Power Station, Darwin, Australia

The power demand since the early 1990s in the city of Darwin, Australia, due to a dramatic population increase in the city has been met by the introduction of an ammonia ice TES system at the city's Channel Island power station.

#### Motivation

The power station was built in 1985, and is operated by a Northern Territory Government utility. The electricity consumption of Darwin has been steadily monitored over the years by the Power and Water Authority (PAWA). An assessment in 1995 showed that demand was growing at a faster rate than earlier projections had identified, and that action was needed to avoid electricity shortages before 2000. The decision made to utilize an ice TES has not only eased the pressure but also resulted in considerable savings for PAWA and the government. The TES system cost is one-third the installation cost of an extra turbine. In order to fully appreciate the actions taken, it is essential to study the background of the power station's previous capability.

#### Background

Channel Island has five gas-fired General Electric "Frame 6" combustion turbines. Each turbine has a nominal capability of 40 MW when operating at 15 °C air-inlet temperature. The gas is piped from a distance of almost 1500 km from the city of Alice Springs, Australia. Two of the five gas turbines recover heat from the exhaust gas, passing it across heat exchangers to generate steam under pressure. The steam drives a steam-turbine generator, providing additional electrical power through this combined cycle operation. Darwin's power demand is dominated by air-conditioning usage, which accounts for 70% of the peak load, a higher ratio than in cooler climates. In part, this high demand ratio can be attributed to population growth, increasing affluence, and more widespread use of air-conditioning. Peak load customarily occurs around 2:00 p.m., when the ambient temperature (summer average 35 °C) is warmest, and the air-conditioning requirement is greatest.

#### Power Production Challenges and Options

A challenge to be addressed in the overall system is that gas turbine output is affected significantly by changes in climatic conditions. An increase in inlet air temperature results in an output drop of the turbine. This loss can be as high as 8 MW per turbine when electricity demand is peaking. Considerable studies by PAWA to solve these problems and meet adjusted anticipated demands identified three major options. One option was for consumers to employ TES systems, allowing ice

to build overnight. The daytime ice melt would provide the necessary cooling, and would avoid the need for a larger refrigeration plant. As a result, the Northern Territory University retrofitted some facilities to include TES. For PAWA, the second option was to purchase extra turbines to increase output. This cost was estimated at \$40 million Australian dollars. The third option, ultimately chosen and successful in other hot climatic conditions, was to cool the inlet air to the turbines. This had the dual advantages of cost-effectiveness and quick installation and operation.

### Description of the Selected System

The final system chosen by PAWA employs an ammonia ice TES system plant (Figure 8.7), supplying ice water during peak periods to wet air coolers on the inlets of three turbines. The first stage of the project included the following major equipment:

- five 500kW Sullair screw compressors, of 1500kW (426 t) capacity each;
- five BAC Model CXV 435 evaporative condensers;
- 96 BAC ice-builder coils, capacity of building 1400 t of ice that provide 130,000 kWh (36,932 ton-hours) of storage;
- three BAC wet air cooler modules, cooling inlet air from 37 °C to 9 °C;
- two concrete tanks 15 × 15 × 7 m.

The system has a simple operation. During the night and morning off-peak periods, the refrigeration plant builds ice on the ice-builder coils. At peak demands (customarily from noon to 4:00 p.m.), ice water is pumped from the storage tanks and across a direct-contact heat exchanger medium to cool air before it enters the turbine. The ultimate cost of the installation was approximately \$12 million Australian dollars. The system was expected to be running by 1998, and to yield considerable financial savings by PAWA and a gain of 20 MW extra power production at peak periods. The ice-build period is off-peak, and has no effect on the daily maximum demand. Also, the control of ice build can be coordinated with spinning reserve needs. The wet air cooler provides extra benefits in washing the air, removing dust, insects, and smoke. The dirt is collected in a sump that is easily accessible for filtration or cleaning. There are no finned coils to clog. The use of ammonia leads to an environmentally benign system that does not contribute to the greenhouse effect and has very little effect on the ozone layer. The use of natural gas system rather than a coal-fired station also reduced greenhouse gas (GHG) production. A final benefit is that the ice TES system can be activated in minutes, allowing operating flexibility.

Further information is available elsewhere (BAC, 1999a).

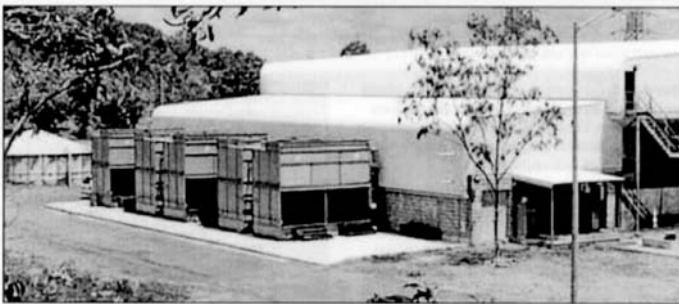


**Figure 8.7** Evaporative condensers, plant room, and ice TES system (Courtesy of Baltimore Aircoil International N.V.)

### 8.2.5 The Abraj Atta'awuneya Ice CTES Project, Riyadh, Saudi Arabia

A state-of-the-art ice CTES system that has been designed to perform under all circumstances has been installed at the Abraj Atta'awuneya, which is an impressive example of contemporary architectural design. It comprises twin 17-storey triangle-shaped towers joined together by two bridges. The building, located on a 7440 m<sup>2</sup> site, is the first high-rise building in Saudi Arabia. The architectural marvel provides 44,500 m<sup>2</sup> of office space, a 5200 m<sup>2</sup> business center, and 600 car spaces.

TES was required because of the Saudi Consolidated Electric Company's (SCECO) new regulations regarding power supply for large retail areas and office buildings, limiting the power supply to the building to only 50% of the total connection capacity between 1:00 and 5:00 p.m. Therefore, building owners had to limit the power supply for chillers to 50% and have a system that is capable of handling the remaining 50% of the cooling load by other means. A well-accepted technique is the use of TES. With a TES system, it is possible to produce and store cooling capacity during periods of low cooling demands and when sufficient electrical power to operate the chillers is available during the night. The accumulated energy is then used during the next cooling cycle the following day.

Figure 8.8 shows the daily cooling requirements for the Abraj Atta'awuneya. Also shown in the diagram is the cooling delivered by the chillers during the day and the cooling to be delivered by the TES system, which should deliver daily 26 MWh. During nighttime, the chillers operate and accumulate this cooling capacity. Various TES techniques were available on the market, and it was a task for the designers to integrate a TES system that could meet the following design criteria:

- minimum occupied space,
- low initial cost,
- possibility of use in high-rise buildings,
- maximum use of standard components,
- easy maintenance of the system and low operating cost,
- user-friendly and full integration in the building management system (BMS), and
- reliable operation and thermal performance.

Detailed comparisons between different types of TES systems to fully assess their overall impact on the initial costs of the complete installation and future operation were made with the help of value engineering techniques.

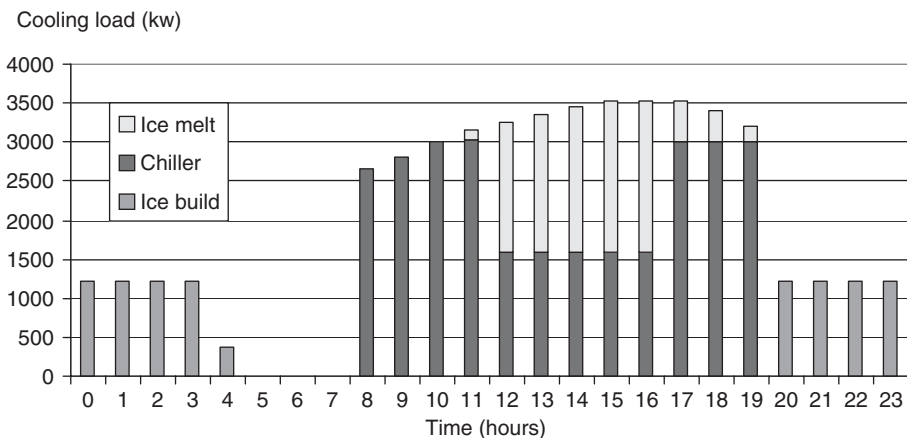


**Figure 8.8** Daily building cooling requirements (Courtesy of Baltimore Aircoil International N.V.)

- **Minimum occupied space.** Two different TES techniques for cooling capacity are available: chilled water CTES and ice CTES. Chilled water CTES systems make use of the sensible cooling capacity of water. For normal air-conditioning applications, the cool storage capacity of chilled water is limited to 8 kWh per m<sup>3</sup> of storage volume. Ice CTES systems make use of the latent storage capacity of water/ice. Therefore, ice CTES systems can accumulate about 48 kWh per m<sup>3</sup> of storage volume. Depending on the type of CTES system selected for the Abraj Atta'awuneya, the occupied space could vary from 600 m<sup>3</sup> for an ice CTES system, that is, a room of 20 by 10 m and 3-m high to 4000 m<sup>3</sup> for a system using chilled water storage, that is, a room of 20 m by 10 m and 20-m high. As space is costly in this high-quality type of building, the owner's preference went rather quickly to an ice CTES concept.
- **Low first cost.** The selected CTES system made full use of the full concrete basement that was used as the tank for the thermal storage units. By doing this, factory-assembled tanks could be eliminated and strong heavy-gauge hot dip galvanized steel coils were used. The low glycol temperature coming from ice CTES units allowed the designer to design the glycol loop with a maximum temperature difference reducing glycol flows, pipe sizes, and pumps. The chillers will first cool the warm glycol from the heat exchanger, which allows them to operate in the most favorable conditions.
- **Possible use in high-rise buildings.** All the mechanical heating, ventilating, and air-conditioning (HVAC) equipment located in the building basement had to be able to withstand the pressures caused by the total static height in the system. Since the building is 21 floors high and the mechanical equipment was installed in the basement at the minus 3 level, all equipment including the TES heat exchangers and TES units required a design pressure of 16 bar. This had to be considered when selecting the equipment for the thermal storage system.
- **Maximum use of standard components.** An important criterion was the maximum use of materials that are commonly used in air-conditioning systems. This was done not only to keep the initial cost reasonable but also to assure controllable maintenance and replacement costs in the future. The final selection included pumps, standard valves, and control equipment of a standard range made of materials suitable for glycol/water mixtures. The chillers used in the CTES system are standard air-cooled packaged chillers.
- **Easy maintenance and low operating cost.** The aim was to have a system not requiring any additional special skills of the operators or maintenance staff. Ice CTES systems, making use of standard products, can be maintained as any other piece of mechanical equipment. Chilled water storage systems, with their large water volumes, would have required expensive and complicated maintenance of the stored water and storage tanks. The system design was to be executed in a manner that operating costs were at a lowest possible level.
- **User-friendly and full integration in the BMS.** To keep the complete TES system manageable, a full automated control system for the TES system was needed. To assure a reliable communication between the BMS and the TES, it was decided to fully integrate the TES system controls within the overall BMS. Uniform communication language and single source responsibility for the system control was obtained.
- **Reliable operation and thermal performance.** In a building of such a high standard, it was an absolute must that the air-conditioning system should perform under all circumstances. Detailed analyses of the hourly cooling loads were made and the performance of every piece of equipment including the ice storage (Figure 8.9) was scrutinized.

The design had to be developed in such a way that all possible operating modes, including ice building at night and cooling, were possible. Also any potential risk for freezing the heat exchangers had to be eliminated. The performance of the TES system on an hourly basis was fully guaranteed by the manufacturer. The owner made the manufacturer of the TES units, Baltimore Aircoil, responsible for design, selection of all TES components, and commissioning. This was to ensure that the performance for the complete TES system was guaranteed by a reputable manufacturer.

Detailed information can be found in BAC (1999b).

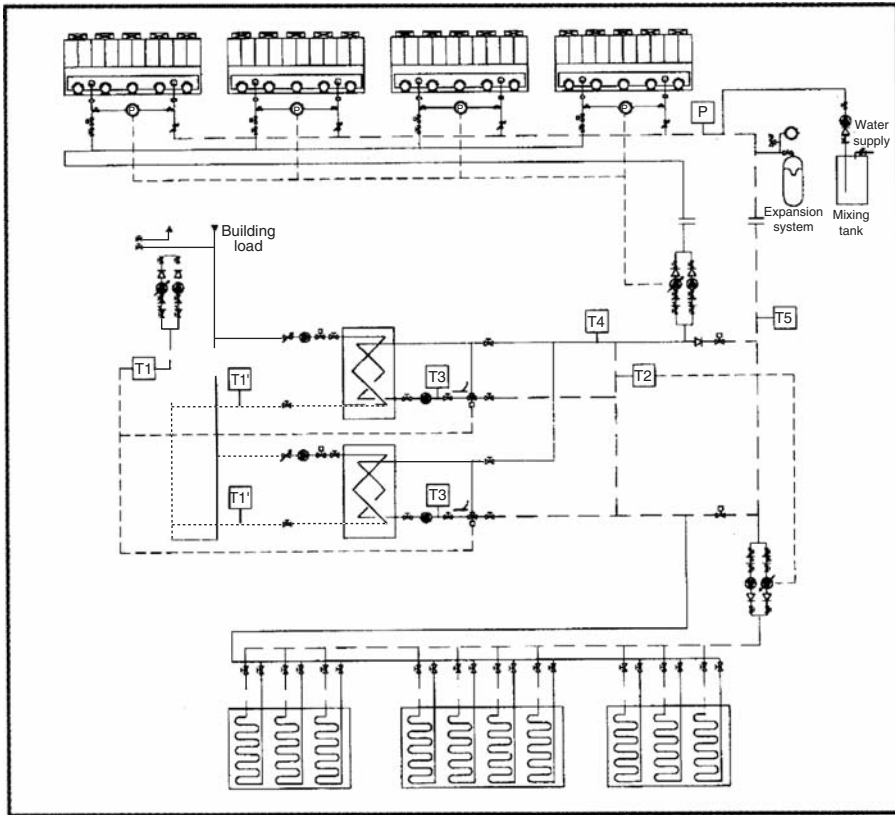
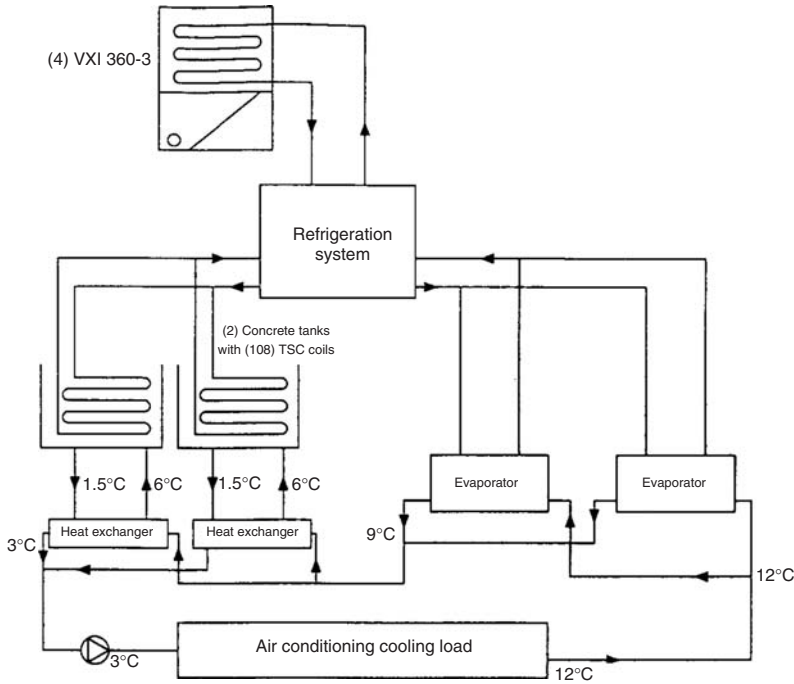


Figure 8.9 A schematic of ice CTES system (Courtesy of Baltimore Aircoil International N.V.)

### 8.2.6 Alitalia's Headquarters Building, Rome, Italy

In June 1991, Alitalia, Italy's largest airline company, officially opened its new headquarters building in the southwest area of Rome. With a total plan area of 130,000 m<sup>2</sup>, this building contains 55,000 m<sup>2</sup> of office space, 72,000 m<sup>2</sup> of service and technical rooms, and 26 conference rooms, surrounded by a large parking area for more than 3000 cars. For the air-conditioning and computer cooling needs of the entire complex, ice chiller thermal storage coils (Figure 8.10) were selected to meet a total storage capacity of 65,000 kWh. This makes Alitalia the largest ice storage installation in Europe, and one of the largest in the world. Owing to the magnitude of this project, the designers opted to install thermal storage coils in two concrete tanks, each 34 m long by 12 m wide. During the night, the central refrigeration system builds a complete charge of ice on the coils over a 12-h off-peak period. During the daytime, ice is melted to provide the building's base cooling requirements, thereby minimizing the peak demand. The refrigeration system is used during the day to provide any extra required cooling capacity upstream of the ice thermal storage coils. This results in higher refrigeration system efficiency and lower operating costs. Unlike other types of thermal storage units, the ice chiller with consistent low temperature supply can be located downstream from the chillers for highest overall system efficiency. In addition to the thermal storage coils, four large industrial fluid coolers and six heat exchangers on this largest European thermal storage project were also provided.

Detailed information can be found in BAC (1999c).



**Figure 8.10** Thermal storage coils integrated with air-conditioning system (Courtesy of Baltimore Aircoil International N.V.)

## 8.3 Ice-Slurry CTES Case Studies

### 8.3.1 The Stuart C. Siegel Center at Virginia Commonwealth University, VA

During the summer/fall of 1998, a 380-t ice-slurry generating system was installed to cool the Stuart C. Siegel Center, a 190,000-ft<sup>2</sup> basketball arena and athletic complex at Virginia Commonwealth University in Richmond, Virginia. The arena has a seating capacity of 7500 people and the total complex peak design cooling load is 1290t. Engineering and economic evaluations were undertaken and led to the decision to install the slurry CTES system. Ice-slurry storage has two main characteristics that provide the potential for cost savings in HVAC projects. These characteristics are as follows:

- **Ability to provide chilled water at temperatures as low as  $-1.1^{\circ}\text{C}$ .** This characteristic reduces the size, and therefore, the first cost, of chilled water distribution piping, air handlers, heat exchangers, and other components.
- **Ability to produce and store cooling when the cooling load is small and then use the stored cooling when the cooling load peaks.** This characteristic can reduce the peak electrical demand charges and can reduce first cost for many projects depending on the ratio of peak cooling load to average cooling load over a day or week.

These two characteristics played a part in the decision for ice thermal storage in the project discussed here. The chilled water supply temperature is  $1.1^{\circ}\text{C}$  and the return temperature  $11.6^{\circ}\text{C}$ . The low temperature supply water resulted in downsizing of the air-side equipment and offered



additional dehumidification via the variable-volume air-supply system. The design peak cooling load is 1290 t and the peak 24-h design load is 6776 ton-hours. An ice-slurry generator system of 380-t capacity was selected to meet this peak load.

### System Schematic

Figure 8.11 illustrates the operation of an ice-slurry generator and the application to this project. The slurry solution is 7% glycol and has a freeze point of  $-2.22^{\circ}\text{C}$ . The solution is pumped from the bottom of the tank and delivered to the top of the slurry generator. The solution moves through the evaporator with an average temperature of  $-8.33^{\circ}\text{C}$ , which causes crystals to form in the solution as it falls into the tank. The slurry floats and therefore accumulates in the tank as this process continues. The slurry generators and storage tank are located about 30 m away from the building. The ice-slurry storage provides a  $1.1^{\circ}\text{C}$  solution to the building heat exchanger which, in turn, provides  $2.22^{\circ}\text{C}$  supply water to the building air handlers. The outside air units are equipped with variable speed drives that operate to maintain the proper fresh air in the 7500 seat arena. Control of these outside air units is based on levels of occupancy. The outside dampers are set at maximum volumetric flow rate for “event” operation only. During normal occupancy, supply fans are ramped down to 30% speed and outside air dampers are reduced to 10% of full open capacity. During unoccupied periods and in the evenings, the air systems are shut down.

### System Operation

Figure 8.12 illustrates the design load that peaks at 1290 t at hour 13 in a day. Most of this cooling load is due to the need for fresh air for 7500 occupants during a function in the arena. The timing of a major event is arbitrary. Since the total 24-h load is 6776 ton-hours, it was evident that the

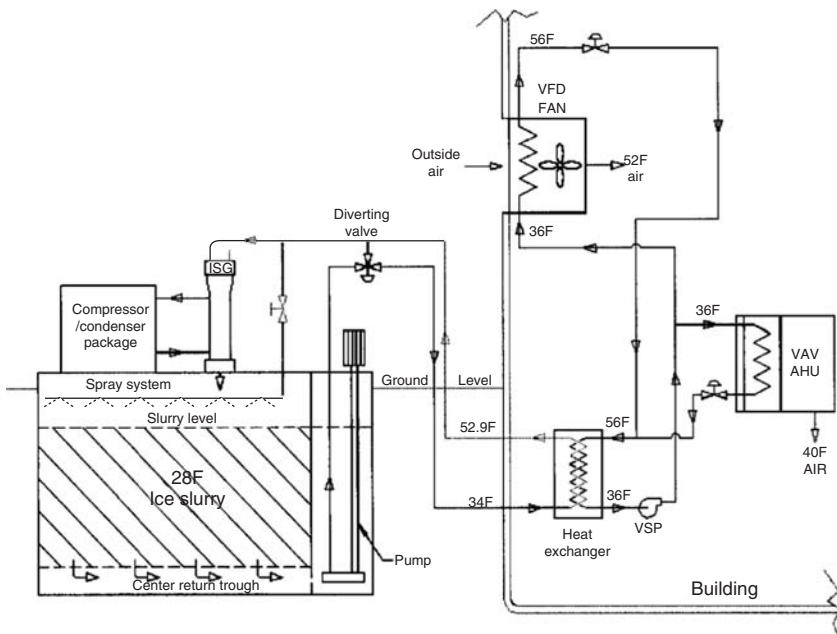


**Figure 8.11** Ice-slurry system for the project (Courtesy of Paul Mueller Company from Proceedings at the IDEA College-University Conference, New Orleans, February 1999)

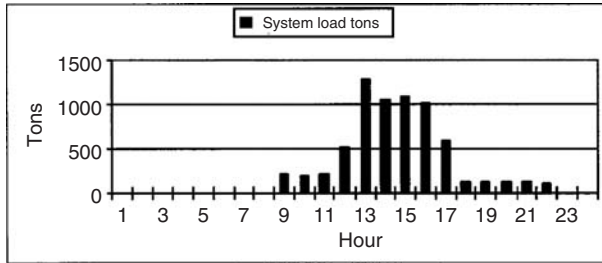


**Figure 8.12** System loads (Courtesy of Paul Mueller Company from Proceedings at the IDEA College-University Conference, New Orleans, February 1999)

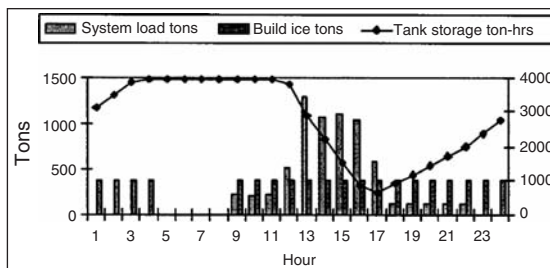


**Figure 8.13** System loads during ice-slurry CTES operation (Courtesy of Paul Mueller Company from Proceedings at the IDEA College-University Conference, New Orleans, February 1999)

load could be spread out over 24 h with a CTES system. This system incorporates with a 380-t slurry generator.

Figure 8.13 illustrates the operation of the slurry system. The tank has 3927 ton-hours of cooling capacity stored at 4:00 a.m. and holds that amount until noon when the cooling load exceeds the capacity of the slurry generator. Over the next 5 h, slurry is melted to meet the cooling load, reducing the storage to about 640 ton-hours of cooling capacity at 17:00. The load is less than 380 t at 18:00, and slurry begins to accumulate in the tank, which attains about 2700 ton-hours of cooling capacity by midnight. The ice generator shuts off at 4:00 a.m. when the tank again is full of ice slurry.

### Economics

The ice system provides annual operating-cost savings of approximately \$75,000 through reduced demand charges. Electrical demand is reduced because of

1. a 380-t ice machine versus a 1290-t chiller,
2. reduced water pump sizes, and
3. smaller fan motors.

The first cost of this ice-slurry system was less than a conventional system because the 1.1 °C supply water permitted the following:

- reduced duct/pipe and insulation sizes,
- reduced refrigeration capacity (and smaller air coils, water pumps, and so on),



- reduced motor sizes, and
- reduced electrical service size.

Compared to a conventional systems with 6.66 °C supply water, significant savings in first cost are realized. For this application, the ice-slurry TES system proved to be an attractive alternative providing both first- and operating-cost savings.

Further information on this project can be found elsewhere (Nelson *et al.*, 1999).

### 8.3.2 A Slurry Ice Rapid Cooling System, Boston, UK

Slurry ice is a crystallized water-based ice solution that can be pumped, and offers a secondary cooling medium for TES while remaining fluid enough to be pumped. It flows like conventional chilled water whilst providing five to six times the cooling capacity.

#### System Description

The installed system consists of an 88 kW remote condensing slurry ice machine and an associated 10 m<sup>3</sup> ice storage tank to satisfy a peak load of 180 kW (Figure 8.14). The ice machine is designed to operate until the tank is full or during rapid cooling periods in order to introduce ice into the cooling circuit. The stored energy over off-peak/low load periods is later utilized to satisfy the short and sharp peak loads. Hence, the installed refrigeration machinery is one-third of the equivalent capacity of a conventional direct cooling system. Harvested fresh vegetables are subject to rapid cooling within the cold storage facility whereby the energy stored during off-peak periods is recovered by circulating solution within the air spray heat exchanger in order to provide 0–1 °C air off-temperatures during the rapid cooling periods.

#### Technical Benefits

- **Cost-effective installation.** Smaller pipework and flexible storage tank, coupled with smaller pump sizes, result in lower initial installation cost.
- **Reduced running cost.** Reduced refrigeration machinery results in reduced maximum demand and availability charges, coupled with night-time low ambient and off-peak electricity prices, offers unmatched overall running cost savings.
- **Quick response.** Fine ice crystals offers good thermal efficiency for the system. Hence, large peak loads can be handled without affecting the system exit temperatures.

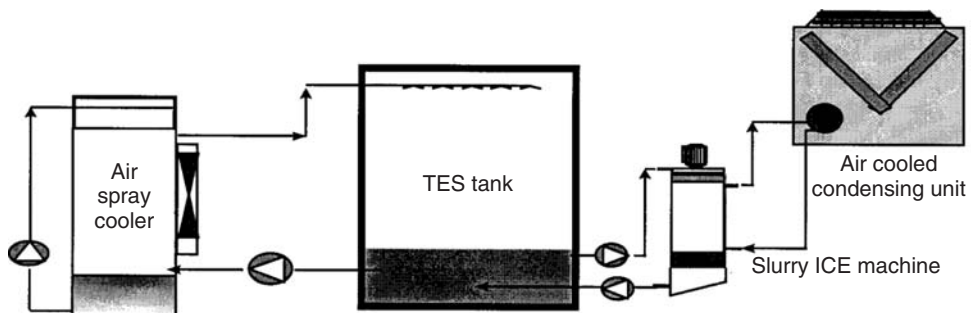


Figure 8.14 The slurry ice system (Courtesy of Environmental Process Systems Ltd)

- **Flexible system.** Any future capacity or change of operational patterns can be easily handled without the need for additional refrigeration machinery.
- **Full standby capability.** The stored energy can be used to operate the process in case of breakdown or regular maintenance shutdowns.
- **Green solution.** Reduced refrigeration machinery leads to reduced refrigerant volume.

Further information can be obtained from EPS (2000).

## 8.4 Chilled Water CTES Case Studies

### 8.4.1 *The Central Chilled Water System at the University of North Carolina, NC*

The Central Chilled-Water System (CCWS) at the University of North Carolina at Chapel Hill (UNC-CH) is responsible for chilling water and pumping it throughout the main campus, where it is used as a heat sink in air-conditioning. Both electric and steam-driven chillers are used to chill the water. Thus electric and steam consumption represents a significant cost. Electricity is purchased from the Duke Power Company on its hourly pricing (HP) rate. Under this plan, the electric rate may change at the top of each hour, but remains constant through the hour. The rates for each day from Tuesday through Saturday are known at 4:00 p.m. on the previous day. Sunday and Monday rates are known on Friday. Steam is produced on campus at the University Cogeneration Facility at a constant rate based on fuel prices. The use of steam allows UNC-CH to generate its own electricity, reducing the amount purchased from Duke Power.

To reduce utility costs, a TES unit is to be installed. With this system, chilled water can be stored for later use, allowing the CCWS to take advantage of lower nightly HP rates and cooling loads. A study was undertaken to assess when and how much chilled water to store in the TES, and when the TES should be discharged in order to take advantage of the HP rates while satisfying university demands for chilled water. The Department of Operations Research at UNC-CH carried out the study, which is described here.

#### **Purpose of the Study**

This study examines the use of a TES by developing a computer-based tool capable of producing optimal cooling strategies. An optimal cooling strategy is an hourly schedule indicating how the TES should be utilized (charged and discharged) in conjunction with existing equipment to satisfy cooling load at minimum overall cost to the university.

Determining such a strategy involves comparing the relative cooling costs with a TES and with chillers. The total cost of providing 1 t of cooling via the TES during a particular hour is the sum of the charging and discharging costs, where the former depends on the utility rates during the hour the TES is charged. The cost of supplying the same cooling ton through electric and absorption chillers depends only on the utility rates during that hour. An optimal strategy ensures the most cost-effective use of the TES.

The optimization tool may be used on a daily basis. In determining the strategies, the program accounts for all current system parameters and attributes, including the following:

- Each chiller has a maximum cooling capacity (given in tons). These capacities, along with pumping constraints, limit the rate at which the TES may be charged.
- Each absorption (steam-driven) chiller must be “ramped” up to capacity. That is, the rate at which steam levels are changed cannot exceed an upper bound.
- Absorption chillers that have been off-line for an extended period must be primed before being turned back on. This leads to the practice of base loading. Absorbers are kept on line, regardless of their cost-effectiveness, to ensure the satisfaction of anticipated high demands.

- The cogeneration facility produces steam at a pressure higher than is needed by the absorption chillers. This excess pressure is used to generate electricity, reducing the amount purchased from Duke Power and altering the overall costs to the university.
- Parameters for the TES suggest that it should be fully charged (discharged) before being discharged (charged).

The tool is designed to aid the CCWS plant operators in determining 32- and 110-h cooling schedules (for weekdays and weekends, respectively) corresponding to periods of known HP rate schedules. However, it may be used over a different horizon provided that the HP rates and cooling loads for each hour are known (or predicted). Furthermore, the tool may be easily modified, allowing for system changes such as the addition or removal of chillers, parameter changes to the TES, and changes in cost calculations.

### Methods and Model Development

The development of the optimization tool was divided into two steps. The first step involved finding a method of predicting cooling loads. This was done through linear regression on historical data provided by the CCWS. It was determined that using wet-bulb temperature predictions allows accurate predictions of cooling demand.

Given estimated demand and known HP rates, a model was developed of the system, which provides a quantitative means of determining optimal chilling strategies. The model uses an operations research technique called *dynamic programming*.

### Analyses

The study examined and compared four options regarding a TES:

1. operation under the current system (without a TES);
2. operation with a 20,000 ton-hour capacity TES running under a standard industry-operating procedure, as suggested by the client. Under this policy, the TES is charged and discharged at constant rates, starting at midnight and noon, respectively;
3. operation with a 20,000 ton-hour capacity TES running according to the policies generated by the optimization tool;
4. as an alternative to a TES, the final option examines the effect of adding two high-efficiency electric chillers.

In addition, for each of the four scenarios above, the benefits were examined of reducing the number of base-loaded absorbers. Three cases were studied:

1. current base loading operations;
2. reducing the number of base-loaded absorbers by the previous step;
3. eliminating the need to base-load absorption chillers.

### Findings

On the basis of 152 days of demand and corresponding HP data from the summer of 1996, the study found that the optimized operating procedure (TES Option 3) results in significant benefits over Options 1, 2, and 4. Furthermore, it was determined that by reducing the number of base-loaded chillers, the CCWS can reduce its costs by up to 30%. Table 8.3 gives the total costs of operating under the different options. The costs cited in Table 8.3 and below are in US dollars.

**Table 8.3** Comparison of total costs (in US\$) for four different options for base loading

Base loading options	1. Current system (No TES)	2. Industry-operating procedure	3. Optimal cooling schedule	4. Two electric chillers
a. Current	1,017,766	999,978	910,710	971,185
b. Current less one	918,245	900,297	821,074	868,318
c. Zero	711,812	702,812	612,506	650,213

Source: UNC-CH (2000).

Several results are worth noting:

- For each base loading option, the optimized operating procedure (TES Option 3) results in the lowest cost to the university.
- Given base loading Option 1, the optimized operating procedure represents a \$107,056 saving over the current operation with no TES. For a 7% interest rate, the present value of the savings over 5 years is \$469,677. (Note that this represents savings during the summer months only.)
- Given base loading Option 2, the optimized operating procedure represents a \$97,171 savings over the current system. The present value of the savings over 5 years is \$426,309.
- Given base loading Option 3, the optimized operating procedure represents a \$98,992 savings over the current system. The present value of the savings over 5 years is \$434,299.
- Combining TES Option 3 (optimization of the TES) with base loading Option 3 (elimination of the need to base-load absorbers) results in a  $1,017,766 - \$612,506 = \$404,260$  (or 39.8%) saving when compared to the current system and base loading practices. Over 5 years, the savings are \$1,777,961.

### Closing Remarks

Given the advantages of the optimized operating procedure (TES Scenario 3), it was recommended that the CCWS plant operators utilize the optimization tool on a daily basis. Following the schedules generated by the tool will result in substantial savings to the university. It was also recommended that the CCWS examine ways of minimizing the number of base-loaded absorption chillers.

The model was developed under two primary restrictions that limit the scope of this study. First, the method of predicting demands was based only on summer data. Secondly, the TES was assumed to have no “dedicated” chillers. That is, the load placed on the current system to charge the TES is divided equally among all operating chillers. A dedicated system involves separating the TES piping system from the main system. Thermal energy is transferred to the main piping system through a heat exchanger. This allows the TES to store colder water, although some energy is lost through heat transfer. Further study is needed to determine an optimal operating policy for the TES over nonsummer months and with dedicated chillers.

Further information on this case study is available from UNC-CH (2000).

### 8.4.2 Chilled Water CTES in a Trigeneration Project for a World Fair (EXPO'98), Lisbon, Portugal

This case study considers a trigeneration (simultaneous generation of electricity, heat, and cold) project, which incorporates CTES, and which was constructed for the World Fair EXPO'98 in Lisbon, Portugal. The project was completed on a fast-track basis in good time, the first distribution of chilled water being achieved nearly 9 months before the opening of EXPO'98. The client was

Parque EXPO'98 and the contractors were Climaespço (Elyo, Climespaço, Gaz de France & RAR Ambiente) and EIG (Entrepose, Ingérop, and GTMH).

### Technical Details

The plant consists of a gas turbine, waste heat boiler, two absorption chillers, two compression chillers, chilled water storage, and auxiliary equipment (Figure 8.15a and 8.15b). The exhaust gases from the gas turbine are reheated by direct combustion in the exhaust duct and then sent to the waste heat boiler to produce steam. An additional boiler produces the extra steam needed during the winter and also acts as a standby unit.

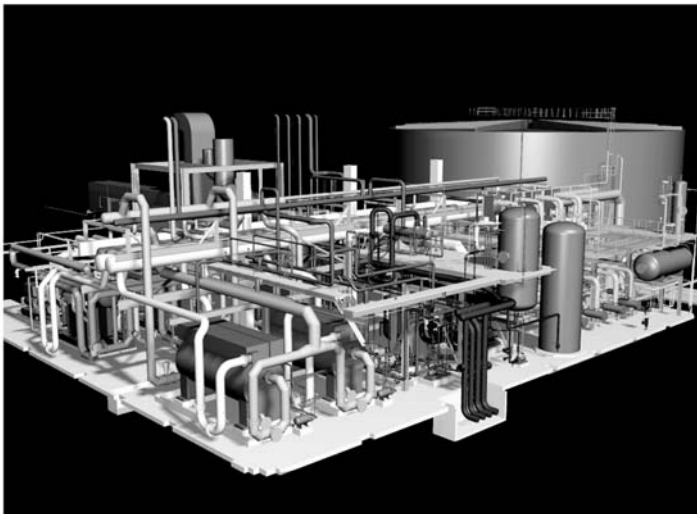
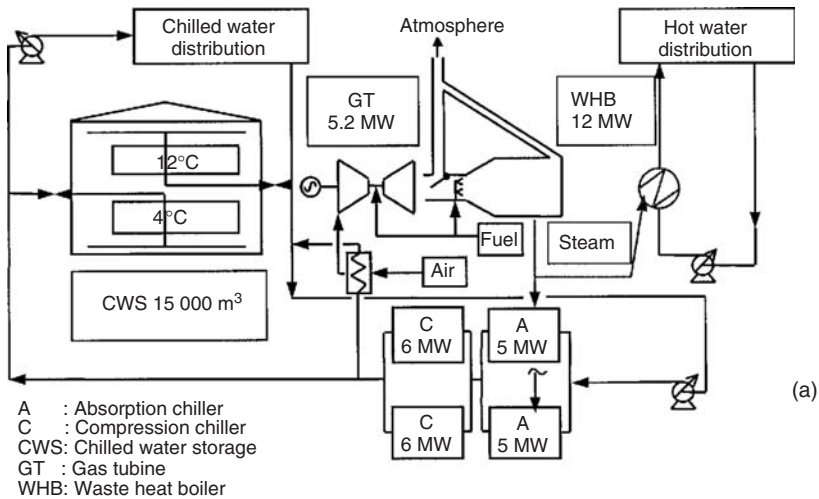


**Figure 8.15** The EXPO'98 trigeneration plant (a) schematic and (b) computerized view (showing large cylindrical TES tank in rear) (Courtesy of Paragon-Litwin)

Steam is supplied for the following purposes:

- for use in a shell-tube exchanger in which water is heated from 65 °C to 100 °C; and
- for use in absorption chillers, providing the first stage of refrigeration from 12 °C down to 8 °C.

Compression chillers then reduce the chilled water temperature from 8 °C to 4 °C. A closed circuit treated water system cools the chiller condensers and the machinery, and the treated water is cooled by river water through a heat exchanger.

Electricity produced by the gas turbine generator is partly utilized within the plant, with the excess being sold to the Energias de Portugal (EDP), the Portuguese national electricity company.

Chilled water thermal storage is provided for peak demands. Pumps for chilled water service (both chiller loop and chilled water distribution) have variable frequency drives.

The chilled and hot water are distributed through two distinct networks to over 40 users throughout the exhibition area, some as far distant as 5 km. Each user has its own plate exchanger and closed circuit system.

### Chilled Water CTES

The chilled water storage is undoubtedly the most significant and innovative concept of the trigeneration plant. Table 8.4(a) describes the capacity and Table 8.4(b) the main equipment of the plant. Apart from its feature as a unique application of trigeneration, it became the largest stratified chilled water thermal storage in Europe when it was installed, having a thermal capacity of approximately 140 MWh (39,807 ton-hours).

With a diameter of 35 m and a height of 17 m, the bottom 6 m of which is below ground, it consists of a cylindrical reinforced concrete tank, cast in situ, having a wall thickness of 45 cm. It is coated internally with a sealant and painted externally. The steel roof is thermally insulated (Figure 8.15b).

The tank is equipped with instrumentation to monitor the system performance and current status. The actual vertical profile of the water temperature is measured by thermocouples. The 26 temperature sensors, at 60-cm intervals, allow the operator to monitor the thermal capacity and to confirm that stratification is maintained. The temperature profiles recorded during the plant operation, both for reduced capacity and for design capacity, have shown that the gravitational separation between the lower zone and warm upper zone appears to be as good as can be expected (for details, see Figures 8.16a and 8.16b).

Designed for both charge and discharge rates of 18 MW<sub>r</sub> (5118 t), the storage depends on effective stratification. The symbol MW<sub>r</sub> is used to denote MW of refrigeration. Chilled water is introduced and withdrawn near the tank bottom, and warm water is withdrawn and introduced from just under the water surface by two piping diffusers. Each diffuser is composed of three octagonal rings of piping with calibrated, equally spaced holes along the top of the straight sections for the upper diffuser and along the bottom for the lower diffuser. During the design, a techno-economic comparison was also made between single-pipe and double-pipe diffusers (Table 8.5). Although

**Table 8.4a** Present and planned future capacity of the trigeneration plant

	Present capacity	Planned capacity
Electricity	5 MWe	5 MWe
Refrigeration (including TES)	40 MW <sub>r</sub> (11,373 t)	60 MW <sub>r</sub> (17,060 t)
Heat	23 MW <sub>th</sub>	44 MW <sub>th</sub>

Source: Dharmadhikari (2000), Dharmadhikari *et al.* (1999, 2000)

**Table 8.4b** Main equipment and their capacities for the trigeneration plant

Equipment	Main characteristics
Gas turbine	Solar Taurus 60 (5.2 MWe)
Waste heat boiler	12 MWth (41 MM Btu/h), 1000 kPa (145 psi) steam
Auxillary boiler	15.3 MWth (52.2 MM Btu/h), 1000 kPa (145 psi) steam
Absorption chillers	2 × 5.1 MW <sub>r</sub> (1450 t) double effect (lithium bromide)
Compression chillers	2 × 5.8 MW <sub>r</sub> (1649 t) ammonia screw compressors
Chilled water storage	Stratified storage, 15,000 m <sup>3</sup> (4 million gallons) concrete cylindrical tank Inner diameter 35 m × 17 m high (bottom 6 m below ground)
Chilled water circuit	Capacity: 21.9 MW <sub>r</sub> (6230 t) Planned extension: 42 MW <sub>r</sub> (11,945 t) Chiller feed pumps: (2 + 1) 1190 m <sup>3</sup> /h (5240 gpm), 270 kPa (39 psi) Variable frequency motors: 132 kW <sub>e</sub> Distribution pumps: (2 + 1) 2050 m <sup>3</sup> /h (9027 gpm), 460 kPa (67 psi) Variable frequency motors: 355 kW <sub>e</sub>
Hot water circuit	Shell-tube heat exchanger: 11.5 MWth (39.2 MM BTU/h) Distribution pumps: (1 + 1) 555 m <sup>3</sup> /h (2444 gpm), 600 kPa (87 psi) Variable frequency motors: 160 kW <sub>e</sub>
Cooling water circuit	4 plate exchangers Cooling water pumps: (2 + 1) 1750 m <sup>3</sup> /h (7706 gpm), 250 kPa (36 psi) Fixed-speed motors: 160 kW <sub>e</sub> River pumps: (2 + 1) 1830 m <sup>3</sup> /h (8058 gpm), 380 kPa (55 psi) Fixed-speed motors: 260 kW <sub>e</sub>

Source: Dharmadhikari (2000), Dharmadhikari *et al.* (1999, 2000).

double-pipe diffusers provided certain advantages, such as higher charge and discharge rates, single-pipe diffusers were selected because of their lower material and labor costs. The inlet Froude number is not well defined for single-pipe diffusers, whereas the Reynolds number does not depend upon single or double pipe, but rather on total length and flow rate. The single-pipe diffusers are designed to keep the inlet Reynolds number below 1200.

### Cost Saving Achieved with TES

The cost of the initial phase of the entire trigeneration plant was approximately US\$40 million. The thermal storage considerably reduced the chiller plant capacity, which would otherwise have been required, giving an estimated capital cost saving of US\$2.5 million (Table 8.6). Decreasing the chiller plant capacity also considerably reduced utility (electricity and steam) consumption and, consequently, loads on the power and steam generation. This resulted in savings in fuel consumption and also a reduction of pollutant emissions (CO<sub>2</sub> by 17,500 t per year and NO<sub>x</sub> by 45 t per year). Considering only the saving in fuel, the estimated reduction in annual operating cost is over US\$1.6 million. In these calculations, no credit is taken for chiller operation during the night in order to charge the thermal storage, which copes with the daytime peak demand (Figure 8.17).

### Other Related Innovations

Throughout the design, a refrigerant was sought that would not adversely affect the environment. Besides its inherent characteristics, including zero ozone depletion, ammonia has the advantages of high thermal capacity and high latent heat of vaporization. The ammonia charge was reduced by minimizing the size of the plate heat exchanger for both the condenser and evaporator, resulting in lighter and more compact chiller packages.

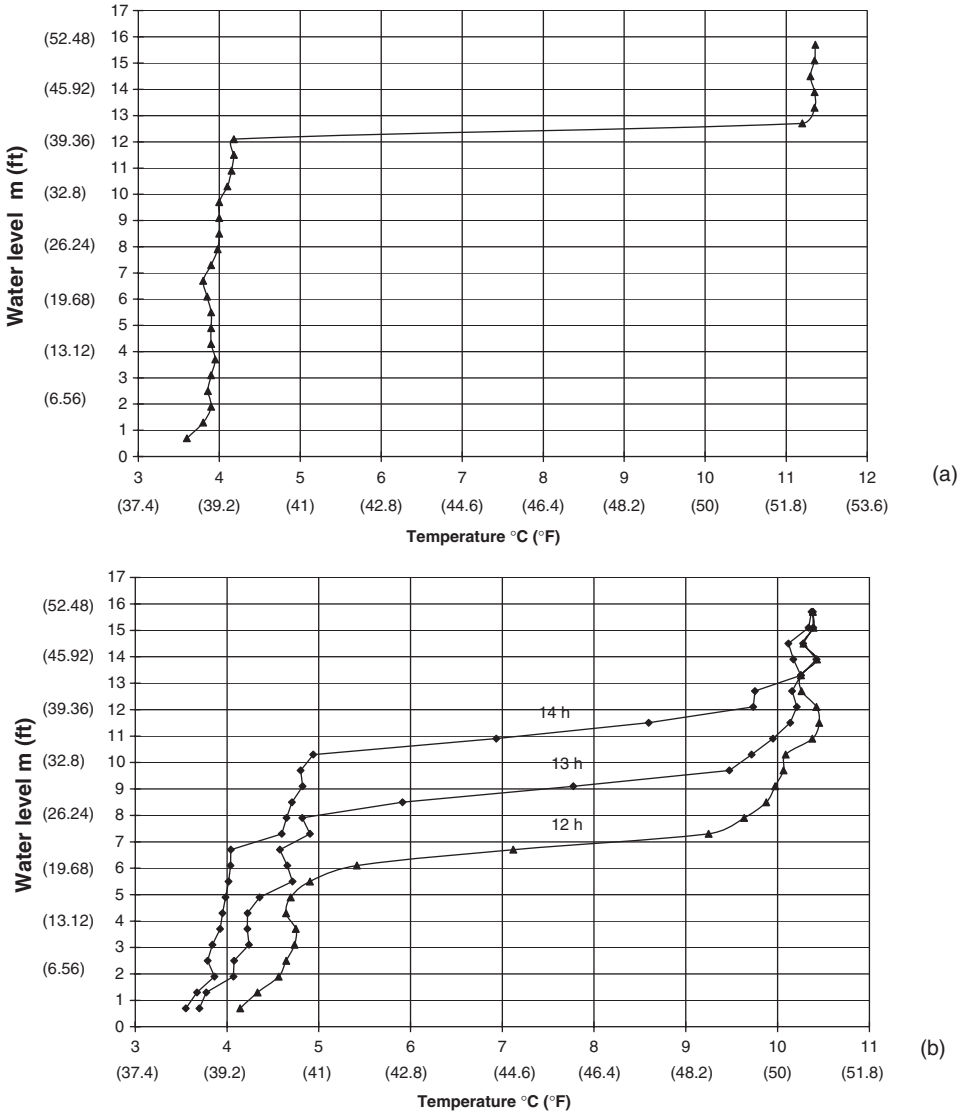


**Figure 8.16** Temperature profiles (a) design case and (b) actual (*Courtesy of Paragon-Litwin*)

A trigeneration plant, by definition, includes a refrigeration product. Thus, a cold source for cooling the turbine inlet air is readily available. For the project, during hot weather, less than 1% of the chilled water is used for the gas-turbine inlet-air cooling, but this measure increases the power output by nearly 17% and reduces the specific fuel consumption by nearly 7%.

The chilled water requirement is met by four chillers, two absorption units, and two compression units. All units are mounted in a series-parallel arrangement, that is, two absorption chillers in parallel, connected in series with two compression chillers in parallel. A bypass is also provided for each group to enhance operational flexibility. This arrangement not only reduced the investment cost but also increased the plant overall efficiency. Furthermore, this arrangement increased flexibility by modulating the operating mode of the plant to energy demands.



**Table 8.5** Techno-economic comparison of diffusers

Expo'98 thermal storage – single-pipe versus double-pipe diffusers

Charge/discharge rate	MWr (tons) m <sup>3</sup> /h (gpm)	Single-pipe			Double pipe		
		Inner	Middle	Outer	Inner	Middle	Outer
Octagon		1200	690	980	1510	870	1230
Reynolds number (flow per unit length over diffuser)	Re						
Relative material and labor costs		100			120		

Source: Dharmadhikari (2000); Dharmadhikari *et al.* (1999, 2000).**Table 8.6** Equipment and capital costs with and without TES

Parameter and unit	With storage	Without storage	Equipment cost reduction (thousand US\$)	
Equipment				
● Chillers	MWr (tons)	20 (5687)	40 (11,373)	1870
– Compression		2 × 5 MWr (1422)	4 × 5 MWr (1422)	
– Absorption		2 × 5 MWr (1422)	4 × 5 MWr (1422)	
● Chilled water storage	m <sup>3</sup> (million gallons)	15,000 (4)	–	(–920)
	MWh (ton-hour)	140 (39,807)	–	
● Gas turbine	MWe	5	8	970
● Waste heat boiler	MWth (MM Btu/h)	12 (41)	20 (68.3)	105
● Pumps				185
– Chiller feed pumps	m <sup>3</sup> /h (gpm)	(2 + 1) × 1100 (4844)	(4 + 1) × 1100 (4844)	
– Cooling water (closed circuit)	m <sup>3</sup> /h (gpm)	(2 + 1) × 1800 (7926)	(4 + 1) × 1800 (7926)	
– Cooling water (open circuit)	m <sup>3</sup> /h (gpm)	(2 + 1) × 1800 (7926)	(4 + 1) × 1800 (7926)	
– Boiler feed water pumps	m <sup>3</sup> /h (gpm)	(1 + 1) × 15 (66)	(1 + 1) × 30 (132)	
● Cooling water exchangers	MWth (MM Btu/h)	8.1 (27.6)	16.2 (55.2)	290
Equipment cost	million US\$	5.6	8.1	
Operating cost (fuel gas)	million US\$/year	1.84	3	
Cost reduction using storage				
● Investment	million US\$	2.5	–	
● Operating cost (fuel gas)	million US\$/year	1.16	–	
Reduction in CO <sub>2</sub> emission	tons/year	17,500	–	
Reduction in NO <sub>x</sub> emission	tons/year	45	–	

Source: Dharmadhikari (2000); Dharmadhikari *et al.* (1999, 2000).

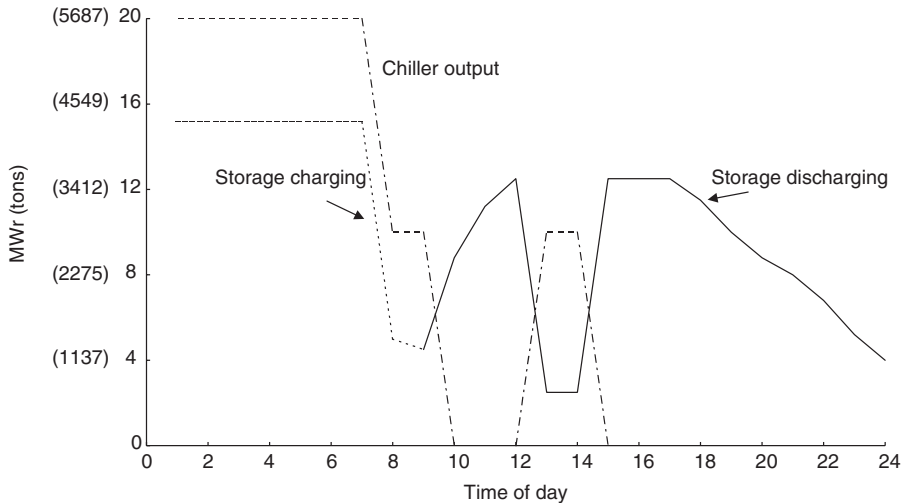


Figure 8.17 TES charging and discharging (Courtesy of Paragon-Litwin)

### Benefits from Centralized System

A centralized trigeneration plant not only helped to reduce investment cost but also contributed to a significant reduction in operating expenses. It achieved an energy saving of 45%, compared to a conventional system in which the chiller plant is installed in each building, resulting in an estimated annual saving of around 6000 TOE (ton oil equivalent). Also, it completely eliminated use of chlorofluorocarbon/ hydrochlorofluorocarbon (CFC/HCFC) refrigerants in individual buildings, and resulted in a reduction of environment pollutants (including CO<sub>2</sub>) by 20,000 tons per year, corresponding to a reduction of more than 54%. Furthermore, there are additional substantial savings in costs related to civil engineering, machine maintenance, and so on.

All connected buildings also receive numerous other benefits, including suppression of noise nuisance, fewer maintenance staff, more space available in the building for rental or sale purposes, and total absence of exhaust gas ducting and chimneys.

Detailed information on this case study can be obtained from Dharmadhikari (2000) and Dharmadhikari *et al.* (1999, 2000).

### 8.4.3 TES at a Federal Facility, TX

The Dallas, Texas Veterans Administration (VA) Medical Center was the first VA medical facility in the United States to use TES technology to reduce operating costs. A partnership with Texas Utilities Electric Company (TU Electric) made implementing this technology possible. The center now shifts a significant portion of its energy demand away from the peak cost period to a lower cost period. Supporting this technology benefits the utility because it relieves pressure to construct new, increasingly more costly power plants. Shifting a large energy demand away from the peak period enables the utility to optimize the use of its generating plants. Thus, TES saves money for both the client and the utility.

### Background

Like most large commercial utility customers, the VA Medical Center's annual electrical costs were based on a rate that is 80% of the highest demand charged during the year. If the facility could find



**Figure 8.18** The VA Medical Center's 12,491 m<sup>3</sup> stratified water storage tank (DOE, 1999)

a way to lower the demand, it could reduce its overall annual expense for electrical service. The system that was selected to reduce demand was a stratified chilled water storage tank (Figure 8.18). The tank provides 24,628 ton-hours of thermal storage. In the summer of 1997, thermal storage reduced peak demand by 2934 kW, lowering annual electricity costs by \$223,650. Installing the system also allowed the utility to reduce its costs by getting more use out of its existing generating plants. The need to build new generating capacity lessened considerably. The hospital can meet cooling requirements by producing chilled water during the period of lowest electric cost, then storing it for use during periods of high electric cost.

### The Project

On February 6, 1996, the center contracted with TU Electric for financial support for the project. It was agreed that TU Electric would build the tank, finance the cost, and let the center pay for the thermal storage on its electric bill. The utilities provided \$500,000 of the total cost of \$2.2 million required for design and installation. Savings resulting from installation of the thermal storage technology will allow the VA to recoup its investment within 7 years.

Initially, a feasibility study was conducted on how to add thermal storage to the existing central plant. This study offered six alternate solutions, each with estimated construction costs, maintenance costs, utility savings, and lifecycle cost analysis. The partners selected a stratified water thermal storage system with a 12,491 m<sup>3</sup> tank at its core, which has 3000 t of chiller capacity for 8 h. (The tank is considerably larger than an olympic-size swimming pool.) The system became operational in the fall of 1996.

The storage tank is filled with chilled water every night. Then every day, from noon until 8:00 p.m., the hospital draws its chilled water from the tank to meet its cooling load, instead of requiring continuous electric service to operate on-site chillers.

As an added benefit, the TES system also doubles the capacity of the hospital's central cooling plant. If the hospital expands, the VA could use the thermal storage system and its existing cooling system at the same time, avoiding additional capital investment.

### Benefits of Utility Contracting

Although TU Electric was involved in about 200 thermal storage systems before this project, this was its first project at a VA facility. It was also TU Electric's first partnership arrangement in

which the utility agreed to design, build, and help find third-party financing for a thermal storage system. The authority for this partnership was existing Federal legislation that allows government to enter into sole-source arrangements with utility companies for services generally available to other customers.

Some important lessons were learned through the project:

- **Participant education.** The Department of Energy's Federal Energy Management Program (FEMP) worked closely with both parties to facilitate this project. A knowledgeable FEMP liaison staff member provided necessary training and support, greatly assisting this project.
- **Quality subcontractor selection.** To improve the project, the utility chose to serve only as the project's prime contractor. TU Electric retained a professional architectural and engineering firm, Carter & Burgess, Inc., of Fort Worth, Texas, to provide design, architecture, and construction management services.

Detailed information on this case and its benefits can be obtained from DOE (1999).

## 8.5 PCM-Based CTES Case Studies

### 8.5.1 *Minato Mirai 21, Yokohama*

Minato Mirai 21 (MM 21) is a new urban area in Yokohama. Mitsubishi Petrochemical Engineering Co. chose a DHC system to provide heating and cooling to the whole district. Use of DHC is a new Japanese policy for protecting the environment. MM 21 DHC includes a Cristopia Energy Systems (latent heat storage (STL) latent CTES) manufactured by Mitsubishi under Cristopia licence. This STL (one of the biggest latent TES system in the world), as shown in Figure 8.19, is the basic component of the system and permits efficient energy management.

#### Technical Data

- Cooling energy stored: 120,000 kWh
- Storage volume: 2200 m<sup>3</sup>
- Storage temperature: 0 °C
- Nodule type: S-00



**Figure 8.19** CTES system located on the roof of the technical building in Minato Mirai 21 (*Courtesy of Cristopia Energy Systems*)

- Number of tanks: 2 (vertical)
- Tank height: 28 m
- Tank diameter: 7.3 m
- Tank volume: 1100 m<sup>3</sup>

### Characteristics

The thermal storage is a Cristopia STL-00-2200, which is composed of two 1100 m<sup>3</sup> vertical tanks filled with S-00 nodules. The nodules are filled with PCM, allowing for thermal phase transition at 0 °C. Cooling energy of 120,000 kWh is stored daily in two 1100 m<sup>3</sup> vertical tanks. The cooling energy is provided by two centrifugal chillers. The height of the tanks is equivalent to a nine-storey building.

### Technical Advantages

The use of CTES in the DHC system yields several technical benefits:

- smaller chiller capacity;
- smaller heat rejection from the plant;
- reduced maintenance;
- increased system efficiency;
- increased system reliability;
- reduced electrical installation.

### Financial Advantages

The use of CTES also provides significant economic benefits such as lower initial investment and significant savings on electricity costs.

Further information on this project can be obtained from Cristopia (2001a).

## 8.5.2 Harp Brewery, Dundalk, Ireland

Harp Brewery in Dundalk, Ireland (Figure 8.20a), produces 1,000,000 hL of lager per year and consumes 12,000,000 kWh of electricity (4,000,000 kWh for the refrigerant plant). In 1992 Harp decided to modernize its refrigeration plant.

The existing system consisted of a wide range of process cooling loads satisfied by two circuits, a high-temperature circuit at -8 °C and a low-temperature circuit at -12 °C. During the design stage, it was decided to install a Cristopia TES System (STL) on the high-temperature circuit. The STL reduces the instantaneous peak refrigeration demand by as much as 45% by shifting 10,000 kWh daily from day to night. The STL reduced the maximum demand by 1 MW and the cooling consumption by 16%.

### Technical Data

- Daily cooling energy consumption: 44,000 kWh
- Maximum cooling demand: 4000 kW
- Cooling energy stored: 10,000 kWh
- Storage temperature: -10.4 °C
- Store type: STL-N10-200 (Figure 8.20b)
- Nodules type: SN.10

- Number of tanks: 2
- Tank diameter: 3 m
- Tank height: 14 m

### Characteristics

To improve the system efficiency and to reduce electrical cost, it was proposed to install a Cristopia STL-N10-200 TES system to shift electrical consumption to off-peak periods and to reduce the peak period electrical demand. To achieve this, an STL-N10-200 was specified storing 10,000 kWh at  $-10^{\circ}\text{C}$  during the night-time off-peak tariff period. The STL also reduces daytime chiller power by 1000 kWe.

The STL-N10-200 is composed of two  $100\text{ m}^3$  vertical tanks filled with SN.10 (77-mm diameter) nodules. The nodules are filled with a PCM allowing thermal storage at  $-10^{\circ}\text{C}$ .

### Technical Advantages

- smaller chiller capacity;
- stable flow temperature;
- reduced electrical supply, by 1000 kWe;
- improved refrigeration efficiency;
- simplified servicing;
- backup at disposal;
- smaller cooling towers.

### Financial Advantages

- reduced cost, as the system with STL costs less than a traditional system with chillers;
- saving on maintenance costs;
- savings due to reduced electrical supply, by 1000 kWe;
- saving on demand charge and energy cost.



(a)



(b)

**Figure 8.20** (a) Two STL-N10-100 systems and (b) Harp Brewery in Dundalk (Courtesy of Cristopia Energy Systems)

### Environmental Advantages

- reduced refrigerant charge (leading to ozone layer protection);
- reduced emission of CO<sub>2</sub>, SO<sub>2</sub>, and N<sub>2</sub>O (avoiding contributions to the greenhouse effect and other environmental impacts).

Further information on this project can be obtained from Cristopia (2001b).

### 8.5.3 Korean Development Bank, Seoul

An office building, occupied by the Korean Development Bank (KDB), is located at Yoido island in the business center of Seoul, South Korea. It is the computer center for Korean and overseas activities. For this building, the KDB chose to use advanced technologies having high performance. The KDB decided to install a Cristopia TES System using STL to reduce nearly 50% of the cooling demand and to make system operation more reliable. In addition to the technical advantages (better backup, reduced maintenance, higher efficiency, and reliability), the KDB anticipated significant operating and maintenance cost savings.

#### Technical Data

- Daily cooling energy consumption: 18,132 kWh
- Maximum cooling demand: 1948 kW
- Energy stored: 10,100 kWh
- Store type: STL-C-184
- Storage temperature: 0 °C
- Nodule type: C-00
- Number of tanks: 4
- Tank diameter: 3.6 m
- Tank length: 5 m

#### Characteristics

The STL system is composed of four 46 m<sup>3</sup> horizontal tanks for a total storage of 10,100 kWh. This capacity represents 55% of the daily cooling consumption, and allows for financial incentives from KEPCO (Korean Electricity Power Co.). Two 566-kW chillers with reciprocating compressors are used in the direct cold production and in the charge mode of the TES system. The control and energy management are achieved using a sophisticated BMS to ensure the highest operating cost savings.

#### Technical Advantages

- smaller chiller capacity (reduced by 47%);
- smaller cooling towers;
- simplified servicing;
- backup at disposal;
- reduced electrical installation.

#### Financial Advantages

- lower initial investment;
- KEPCO incentive for load shifting;
- large savings on electricity costs (energy cost and demand charge).

### Environmental Advantages

- use of refrigerant reduced (leading to ozone layer protection);
- emissions of CO<sub>2</sub>, SO<sub>2</sub>, and N<sub>2</sub>O reduced because of off-peak consumption (mitigating greenhouse effect and other pollution contributions).

Further information on this project can be obtained from Cristopia (2001c).

### 8.5.4 Museum of Sciences and Industry, La Villette, France

At the site of the old Paris slaughterhouse in La Villette Park, France, a modern leisure center was built in 1983, which included (i) the sciences and industry museum, (ii) an audio-visual center, and (iii) the GEODE 3D cinema. The center (Figure 8.21a) is one of the largest science and technology centers in the world, and one of the most innovative (150,000 m<sup>2</sup> of displays, shows, exhibitions). A cooling and heating plant supplies air-conditioning to a distribution network. This plant includes an STL-00-550 (storing 31 MWh) and three 2700 kW chillers.

### Technical Data

- Main AC system type: Air-handling unit
- Building volume: 1,350,000 m<sup>3</sup>
- Daily cooling energy consumption: 163,000 kWh
- Maximum cooling demand: 12,500 kW
- Chiller capacity:
  - Direct mode: 8100 kW (6/12 °C)
  - Charge mode: 4400 kW (−6–2 °C)
- Energy stored: 31,750 kWh
- Volume: 549 m<sup>3</sup>



(a)



(b)

**Figure 8.21** (a) The center and (b) the TES tanks (Courtesy of Cristopia Energy Systems)



- Store type: STL-00-550 (Figure 8.21b)
- Number of tanks: 3
- Tank diameter: 4 m
- Tank height: 18 m

### Characteristics

The STL system is used to reduce 50% of the peak cooling demand. The storage is charged between 22:00 and 7:00 when electricity rates are low. Since 1985, significant operating cost savings have been achieved.

### Technical Advantages

- smaller chiller capacity;
- smaller heat rejection plant;
- reduced maintenance;
- increased system efficiency and reliability;
- increased plant lifetime expectancy.

### Environmental Advantages

- reduced refrigerant charge;
- reduced emissions of CO<sub>2</sub>, SO<sub>2</sub>, and N<sub>2</sub>O.

Further information on this project can be obtained from Cristopia (2001d).

### 8.5.5 Rueil Malmaison Central Kitchen, France

The Rueil Malmaison Central Kitchen is a new modern kitchen using the latest technologies for producing meals and for managing the production process. It supplies 12,000 meals daily to schools in Rueil Malmaison (Parisian suburbs). To meet food hygienic standards, the meals are rapidly cooled leading to high cooling peaks during a relatively short time. During the design stage, it appeared that the use of the STL latent storage had the potential to reduce the system capital cost compared to a classical installation without storage. An STL (Figure 8.22) was used and sized to reduce more than 80% of the peak electrical demand. In addition, the STL permits efficient energy management with a very high reliability and yields savings on operating costs.

### Technical Data

- Daily cooling energy consumption: 440 kWh
- Maximum cooling demand: 139 kW at 1/7 °C
- Energy stored: 440 kWh
- Storage temperature: -10.4 °C
- Store type: STL-N10-10
- Nodules type: SN.10
- Number of tanks: 1
- Tank diameter: 1.6 m
- Tank length: 5.2 m

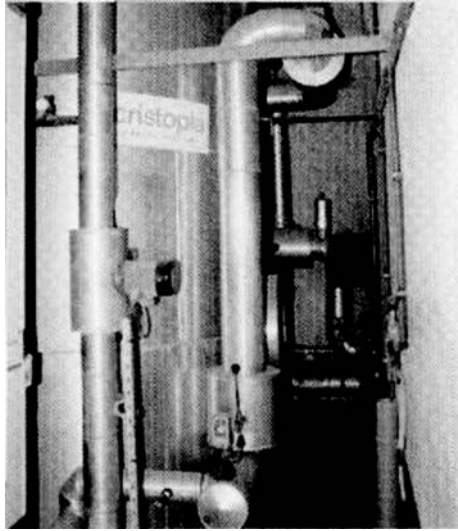


**Figure 8.22** The STL system (*Courtesy of Cristopia Energy Systems*)

### Characteristics

The cooking is done in autoclaves, cooking pots, or streaming water systems at temperatures between 65 °C and 95 °C. The meals are packed in small baskets under vacuum. An initial cooling down to 20 °C is achieved with waste water, and then a second cooling down to 2 °C is achieved with the STL. The meals are then stored in cold rooms. The rapid cooling of food for hygienic reasons introduces high load peaks into the cooling profile. The use of latent CTES helps reduce these peaks.

### Technical Advantages

- smaller chiller capacity;
- smaller heat rejection plant;
- flexible system available for efficient energy management;
- servicing simplified;
- backup at disposal.

### Financial Advantages

The STL system costs less than a more conventional system with chillers, but not TES. Also, the use of CTES leads to lower operating costs (because of reduced demand charges and off-peak electricity consumption) and financial savings associated with the plant's efficiency, life, and maintenance.

### Environmental Advantages

- use of refrigerant reduced;
- emissions of CO<sub>2</sub>, SO<sub>2</sub>, and N<sub>2</sub>O reduced because of off-peak consumption;
- primary fuel consumption of generator power plant reduced.

Further information on this project can be obtained from Cristopia (2001e).

### 8.5.6 The Bangsar District Cooling Plant, Malaysia

The district cooling system supplies chilled water to a district that comprises the Cygal Hotel and the Cygal Towers A&B, the Atlas Towers A to F, Menara Telekom and Wisma Telekom, and Tenaga Head Quarters (TNB) (Figure 8.23a).

#### Objective

To take advantage of the lower electricity tariff during the night, the Cristopia TES System (STL) (Figure 8.23b) is used for storing cold during the night for use during the day. It has enabled the client to greatly reduce the installed cooling capacity and to increase the plant efficiency.

#### Technical Data

- Daily cooling energy consumption: 450,000 kWh
- Maximum cooling demand: 40,000 kW
- Cooling energy stored: 110,000 kWh
- STL storage volume: 1900 m<sup>3</sup>
- Number of tanks: 5

#### Characteristics

The plant consists of five centrifugal chillers (3500 kW each) working in conjunction with five cylindrical STL steel tanks of 380 m<sup>3</sup> (3.80-m diameter, 35-m long). Two conventional water chillers are used for the base load. Each brine chiller operates with one STL and one heat exchanger to provide brine at 3.3 °C at the primary side of the heat exchanger. Each of the five loops operates independently of the others. The chillers and the STLs can be operated singularly and separately or in any combination to meet the demand, and the decision for their operating status during the day is based on the objective of minimizing the use of the chillers and depleting the energy stored.

#### Technical Advantages

- smaller chiller capacity;
- smaller heat rejection plant;



**Figure 8.23** (a) The Bangsar district cooling plant and (b) the STL system (Courtesy of Cristopia Energy Systems)

- reduced maintenance;
- efficient and reliable system;
- increased plant lifetime;
- flexible system available for efficient energy management.

### Financial Advantages

- saving on operating costs (24%), maintenance, demand charge, and off-peak consumption;
- lower initial investment.

Further information on this project can be obtained from Cristopia (2001f).

### 8.5.7 Dairy TES Application Using Eutectic Solutions, Dorset, UK

At a dairy in Dorset, UK, the original system (Figure 8.24) consisted of an ice bank and room cooler circulation system. Following a yoghurt incubation process around 45 °C, the warm return water penetrated an ice block. The ice bank response was very poor. Hence, it took between 6 and 8 h to cool the product. A combination of 7 °C and 10 °C PlusIce modules were applied in a two-phase program on the return leg of the system as a thermal buffer being charged by the ice bank at night. During the rapid cooling process, the stored energy in the PlusIce beams is released back to the return leg, reducing the return temperature back to the ice bank considerably. As a result of this buffer action, the product cooling period is reduced by half, and therefore the client doubled their production capacity with an estimated annual saving of 30%.

### Benefits

- **Maintenance-free installation.** PlusIce has no moving parts, and therefore it is virtually maintenance free.
- **Reduced running cost.** Operating cost savings are provided through reduced refrigeration machinery, which results in reduced maximum and availability charges, coupled with night-time low ambient and off-peak electricity rates.
- **Quick response.** Large peak loads can be handled without affecting the system leaving temperatures.
- **Standby capability.** The stored energy can be used to operate the process in case of breakdown or regular maintenance shutdowns.

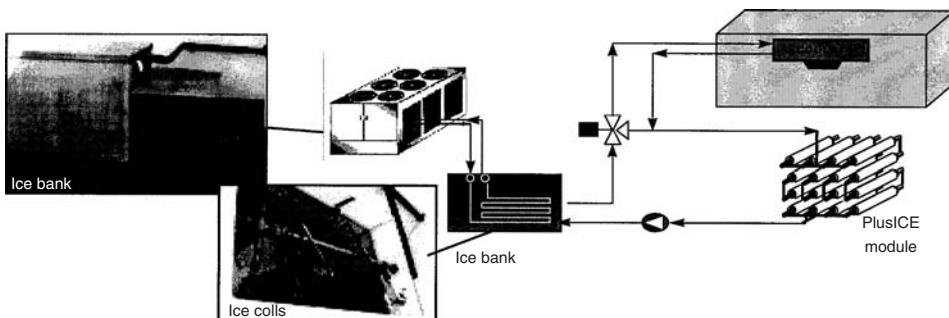


Figure 8.24 TES system using PlusIce modules (Courtesy of Environmental Process Systems Ltd.)

- **Flexibility.** Any future capacity or change of operational patterns can be easily handled by simply adding more beams.
- **Green.** PlusIce using salts has no environmental impact.

Detailed information is available in EPS (2000).

## 8.6 PCM-Based Latent TES for Heating Case Studies

### 8.6.1 Solar Power Tower in Sandia National Laboratories, NM

Solar power towers use solar radiation to heat the working fluid of an electricity generation cycle to high temperatures (see Figures 8.25 and 8.26).

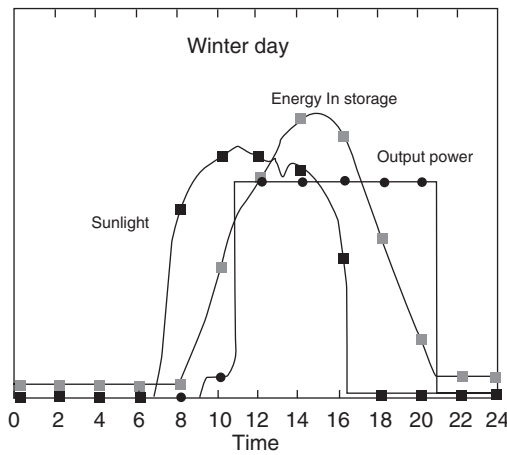


Figure 8.25 Capacity profiles of the solar power tower (Mahoney, 2000)

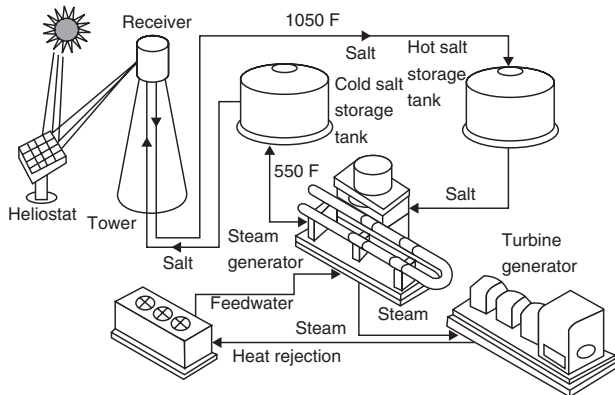


Figure 8.26 Schematic of the solar power tower (Kolb, 2000)

### Desirable Features of Power Towers for Utilities

Because of their practical energy storage, solar power towers (Figure 8.26) have two features that are particularly desirable for utilities: flexible capacity factors and a high degree of dispatchability. Power towers can be designed with annual capacity factors up to 60% and as high as 80% in summer when the days are longer. This means a power tower can operate at capacity for up to 60% of the year without using fossil fuel as a backup, thus being able to deliver power during most peak demands.

Without energy storage, the annual capacity factor of any solar technology is generally limited to about 25%. A solar power tower's high capacity factors are achieved by building the solar portion of the plant with extra heliostats so that during daylight, sufficient energy is collected to power the turbine, while extra energy can be put into the TES system. At night or during extended cloudy periods, the turbine is powered with stored thermal energy. The dispatchability of a solar power tower (its ability to deliver electricity on demand) is illustrated in Figure 8.25, where three different parameters are plotted against the time of day: the intensity of sunlight (insolation), the amount of energy stored in the hot salt tank, and the output power from the turbine generator. In this example, sunrise on a winter day is around 7:00 a.m., and the intensity of sunlight rises quickly to reach its maximum at noon and drops off at sunset around 5:00 p.m.

The solar plant begins collecting energy shortly after sunrise and stores it in the hot salt tank (the level of energy in storage increases during daylight hours). The turbine is brought on-line not at sunrise, but when the power is needed – in this example, at 11:00 a.m. The output power of the plant is constant throughout the day, even though there are fluctuations in the intensity of sunlight. After sunset, the turbine continues to operate on energy from the storage tank; note that the level of energy in storage declines after sunset. The turbine operates continuously until 9:00 p.m. using the thermal energy in storage. In summer when the days are longer, the turbine is able to operate for a larger fraction of each day.

In designing a power tower, the size of the turbine, the fraction of the day it is in operation, and the period when it is operated are flexible. The plant's TES system provides dispatchability, and by adjusting the size of the solar field and the size of the storage tanks, the capacity factor can be tailored to meet the specific needs of a utility.

### Advantages of Using Molten Salt as a Heat Transport and Storage Medium

A variety of fluids were tested to transport the sun's heat, including water, air, oil, and sodium, before molten salt was selected. Molten salt is used in solar power tower systems because it is liquid at atmospheric pressure, it provides an efficient, low-cost medium in which to store thermal energy, its operating temperatures are compatible with today's high-pressure and high-temperature steam turbines, and it is nonflammable and nontoxic. In addition, since molten salt is used in the chemical and metal industries as a heat-transport fluid, experience with molten-salt systems exists for nonsolar applications.

The molten salt is a mixture of 60% sodium nitrate and 40% potassium nitrate, commonly called *saltpeter*. The salt melts at 221.1 °C and is kept liquid at 287.7 °C in an insulated cold storage tank. The salt is then pumped to the top of the tower, where concentrated sunlight heats it in a receiver to 565.5 °C. The receiver is a series of thin-walled stainless steel tubes. The heated salts then flow back down to a second insulated hot storage tank. The size of this tank depends on the requirements of the utility; tanks can be designed with enough capacity to power a turbine from 2 to 12 h. When electricity is needed from the plant, the hot salt is pumped to a conventional steam-generating system to produce superheated steam for a turbine/generator.

The uniqueness of this solar system is in decoupling the collection of solar energy from producing power. Electricity can be generated in periods of inclement weather, or even at night using the stored thermal energy in the hot salt tank. The tanks are well insulated and can store energy for up to a week. As an example of their size, tanks that provide enough thermal storage to power a 100-MW

turbine for 4 h would be about 9.1-m tall and 24.4 m in diameter. Studies show that the two-tank storage system could have an annual efficiency of over 90%.

## 8.7 Sensible TES Case Studies

### 8.7.1 *New TES in Kumamoto, Kyushu*

Wide daily and seasonal fluctuations in power consumption, which have long troubled electricity providers, are a problem. Kumamoto University and Kyushu Electric Power Co. have jointly developed a system for storing electricity obtained during cheaper late-night hours as thermal energy, making it available for climate control during the day, when power grids are often overtaxed. The storage medium for the thermal energy is common dirt, keeping installation costs as well as daytime power consumption down. Electricity providers need sufficient generation capacity to handle peak demand; increased night-time use, by spreading consumption more evenly throughout the day, lowers the number of generators needed and therefore leads to reduced emissions of gases like carbon dioxide.

#### System Description

The thermal storage climate-control system is designed around the use of common soil as the heat storage medium (Figure 8.27). The first such system was installed in spring 1997 in the city of Kumamoto, Kyushu, where it is being used for the climate control of an indoor exercise ground's lounge area. Four layers of flexible 25-mm plastic water pipe, with a total length of 4800 m, are buried up to one meter beneath the earth's surface. Using electricity during late-night hours, when costs are much lower, the system adjusts the temperature of the water running through the pipe, cooling the surrounding earth to 10 °C in the summer and heating it to 45 °C in the winter. This thermal energy is used to cool or heat the lounge during the daytime hours of high power usage.

The system actually uses 20% to 30% more electricity than a standard climate-control system. But by switching its hours of power use from day (8:00 a.m. to 10:00 p.m.) to night (10:00 p.m. to 8:00 a.m.) under a discounted pricing scheme, the exercise ground pays only one-third to one-fourth the normal rate for the electricity it converts into thermal energy.

The TES system occupies about 200 m<sup>2</sup> (the same area as the lounge it is used to heat and cool). A wall of thermal insulation surrounds the earth to a depth of 1.8 m; deeper than this, temperatures remain quite stable, negating the need for an insulating layer at the bottom of the heat storage area. The system has a low installation cost, as its relatively simple structure requires no laying of concrete or other elaborate construction techniques. Moreover, the system occupies no more



**Figure 8.27** The network of water pipes with TES for heating and cooling buildings (JIN, 2000)



area than the space to be heated or cooled (it can be installed directly below the building, solving problems of where to locate the climate-control unit).

### Levelling Peak Electrical Loads

Once generated, electricity cannot be stored economically in large quantities. Power companies must therefore install enough generating capacity to cover the highest peaks of consumption, which occur at midday on the hottest days of summer. Recent years have seen rises in both household and industrial power consumption, and demand has accordingly become more extreme. This system sizing has led to the problems of excess capacity and inefficiency, as some generators are only called into service for those few hours of peak usage during the summer, and lie idle for much of the year. Also, the need for the capacity is forcing power providers to invest in new generating plants that can be costly. Fossil fuel-based power plants have significant environmental impacts. Nuclear power plants can be built almost anywhere, and have low GHG emissions, but antinuclear movements often make the planning of new reactors difficult. So power providers are seeking alternative means to reduce peak demand.

The soil-based thermal storage system, by transferring some demand to night-time hours, is seen as a way to flatten the daytime peaks in electricity consumption and to bring about more constant usage levels. This in turn improves the efficiency of existing power plants and reduces the need for the construction of new capacity. Customers also benefit from lower power costs. Systems using inexpensive electricity to chill water at night and use it to cool a building during the day were first put to use in 1952. Similar systems that freeze the water and then use the transfer of heat as the ice melts for daytime climate control have been on the market since 1995. This latter system proved to be a significant step forward, since ice absorbs 10 times the thermal energy of liquid water for its weight, and its use made possible a size reduction of such cooling systems.

Although these units may have grown smaller, they often require space on a building's roof for installation. They cost between 20% and 30% more to be installed than conventional air-conditioning systems. Moreover, they become a less attractive option for small- to mid-sized buildings where economies of scale cannot be obtained. These factors make a new thermal storage climate-control system, which uses dirt as its medium, advantageous. With its low construction costs and minimal external space requirements, it is seen as likely to contribute to greatly expanded off-peak power consumption by smaller buildings, and to more efficient energy consumption in Japan as a result.

Further information can be found in JIN (2000).

### 8.7.2 *The World's First Passive Annual Heat Storage Home, MT*

Passive annual heat storage (PAHS) is a method of collecting heat in the summer, by passively cooling a home, storing the heat in the earth passively, and then returning that heat to the home in the winter. PAHS includes extensive use of natural heat flow methods, and the arrangement of building materials so as to direct heat from where it is produced to where it is needed, without using machinery.

Use of PAHS has resulted in the creation of homes and other structures that are able to self-maintain an internal temperature that varies only a few degrees up and down from a comfortable average of about 20°C. Such homes have actually been able to collect and save more energy than they need for operation. Such homes have been built and operated successfully in the United States (e.g., in Montana and Alaska), New Zealand, and Europe.

The goal of PAHS is to provide a method of building materials placement and construction organization such that continuously comfortable environments are produced, which are able to extract all of their energy needs from the natural environment without using any commercial energy sources or mechanical devices and without causing disruption to global ecosystems.





**Figure 8.28** The PAHS residence (RMRC, 2000)

As of about 2000, a number of homes around the world had actually achieved full annual heat storage. That is, they collect the heat and cool that the homes need for the winters and summers. They thereby reduce energy consumption and sometimes provide a surplus of energy that is used to provide partial domestic water heating and power to run heat recovery systems for fresh air.

The world's first PAHS home (Figure 8.28) was built in the winter of 1980–1981 in Montana. Through its first summer, the specially insulated earth around it extracted the summer heat from the home, keeping it at a cool  $18.5^{\circ}\text{C}$  on the lower floor and  $23.5^{\circ}\text{C}$  on the second floor ceiling at the dome's zenith. The following winter, the home obtained its heating needs by conduction back into the home. Although the ground gradually cooled off, by April, the home had not dropped below  $19^{\circ}\text{C}$ . This cold climate building met all of its cooling and heating needs throughout the entire year without the aid of either a furnace or air conditioner. The layout of building materials controls temperature naturally on an annual basis. The dome's shape was chosen because of its strength, which is capable of supporting a load of earth over 1.22 m thick. The PAHS method, however, does not require the use of a dome, but can be used with any earth-sheltered shape.

Further information on this project and its applications is available in RMRC (2000).

## 8.8 Other Case Studies

In this section, we include some case studies to illustrate and information on how it is possible to extend TES from small- to macro-scale for various applications. Economic aspects relating to the design, application, and operation of energy conversion systems has brought TES to the forefront. Storage provisions are often required in an energy conversion system when the supply of and demand for thermal energy do not coincide in time. Such TES systems have great practical potential, permitting more effective use of thermal energy equipment and facilitating largescale energy substitutions in an economic manner. The macrosystems considered here demonstrate how a coordinated set of actions are often needed in several parts of the energy system for the maximum potential benefits of TES to be realized.

### 8.8.1 Potential for TES in a Hotel in Bali

Rather than considering an existing TES, this case study considers an investigation to examine the viability of implementing chilled water TES in a hotel in Bali, Indonesia. The primary intent of the exercise is to improve the efficiency of energy resource use at the hotel, but benefits are

also potentially realized that are economic and environmental in nature and that improve energy security. The case study is based on an investigation reported recently by Susila, *et al.* (2009).

Bali is a small province island, with a dry-bulb temperature typically between 21 °C and 24 °C during the day and between 27 °C and 30 °C during the night. Bali is currently connected by a 190-MW Java–Bali undersea electrical power cable from another island. Another 374.8 MW of electrical supply capacity is available from four local diesel power generation units, with the largest and smallest capacities being 130 MW and 80 MW, respectively. Between the years 2000 and 2008, Bali has experienced stable growth in peak-hour electrical demand, averaging 5.7% per year. The gap between peak demand and total capacity has decreased over this time period, and the peak demand was 483 MW in 2008. Hence, the excess capacity was only 7.4%, after accounting for distribution and transmission losses, which are on average 9.5% of input. The growing power demand threatens to exceed supply capacity, and shutdowns due to disruptions or maintenance greatly reduce the reliability of the power system. This situation could harm the tourism industry significantly. Since 2007 Bali has been listed by the state electricity authority and enterprise (PT.PLN/Perusahaan Listrik Negara) as a province that experiences power supply shortages.

Options to improve the situation have been considered. The government has limited resources to build new power generation capacity, and received no response to an invitation to private sector companies to participate in building new power generation systems. The lack of interest is partly due to the fact that the government subsidized electricity price is such that the price to sell electricity (0.05 \$/kWh for households and between 0.05 and 0.1 \$/kWh for the commercial sector) is lower than production cost (normally between 0.08 and 0.14 \$/kWh depending on the type of power generation). Note that the monetary units used throughout this section are 2008 U.S. dollars. Cold TES is an alternative option for reducing peak electrical demand (Roth *et al.*, 2006), which is why it was examined here for a hotel.

### Description of Hotel and its Cooling System

To study the viability of applying chilled water storage (CWS), the NBH (Nusa Dua Beach) hotel, which volunteered to be considered, is examined. This hotel has 401 guest rooms (including in-house rooms), three restaurants, two kitchens, a luxury spa and health-club facility, laundry facilities, and several meeting rooms. The hotel has a total air-conditioned floor space of 22,442 m<sup>2</sup> and a projected land area for gardens and landscaping of 64,500 m<sup>2</sup>. The land area is more than enough to accommodate a CWS facility.

Three unit chillers provide cooling, which is typical of large hotels in Bali, which typically have three or four unit chillers. Two unit chillers each have cooling capacities of 300 t and compressor input power requirements of 147 kW. One standby chiller has a cooling capacity of 280 t and an electrical power input of 2.6 kW along with a liquefied petroleum gas (LPG) burner that consumes fuel at average rate of 40 kg/h. Although during normal operation, only chillers 1 and 2 operate while chiller 3 is mostly in standby mode, when the hotel is full and meeting rooms are used, all chillers are operated to cope with the cooling demand. A schematic of the air-conditioning system is depicted in Figure 8.29, including the option for chilled water TES.

All chillers have similar accessories, that is, an 8.4-kW fan-motor cooling tower, a 13.7-kW cooling tower circulation pump, a 21.8-kW chilled water supply pump, and a 21.8-kW chilled water return pump. All chillers use variable speed drive control (VSD-C) that permits control of compressor operation according to cooling load.

The hotel is observed to have an average cooling load over 24 h of 437 t and a cooling load during peak hours of up to 600 t. The fact that the peak exceeds the average cooling load permits the opportunity for TES. The hourly electrical load of the hotel over a typical day is shown in Figure 8.30. In this figure, the base load without cooling is shown for information. The typical building load with only chiller 1 operating is shown by the middle line. A typical electrical load for the hotel during periods of high cooling loads is shown by the top line in Figure 8.30, where it is seen that chiller 2 is operating to complement the first chiller.

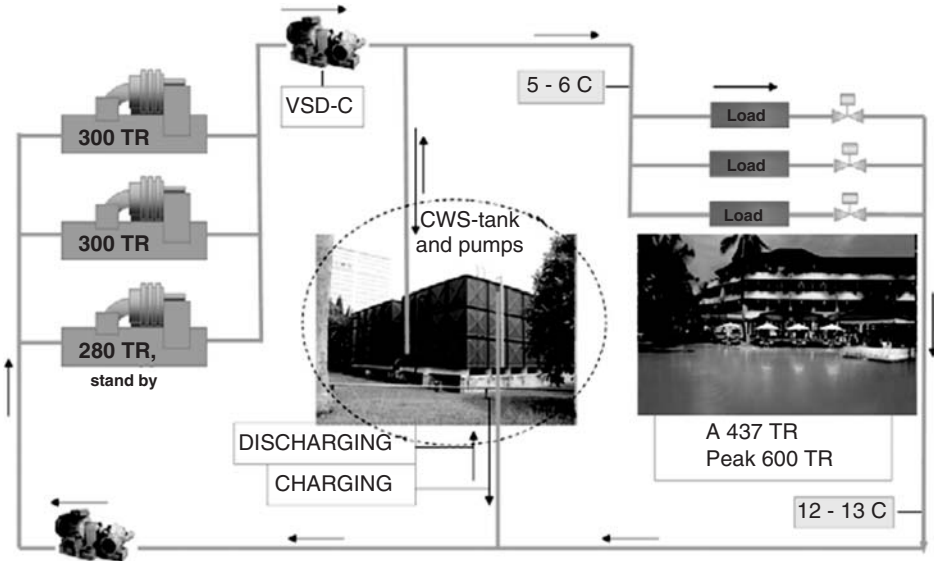


**Figure 8.29** Schematic of the air-conditioning system of the NBH hotel. The center section is included when chilled water TES is applied, and excluded otherwise. TR denotes tons of refrigeration, CWS denotes chilled water storage, and VSD-C denotes variable speed drive control

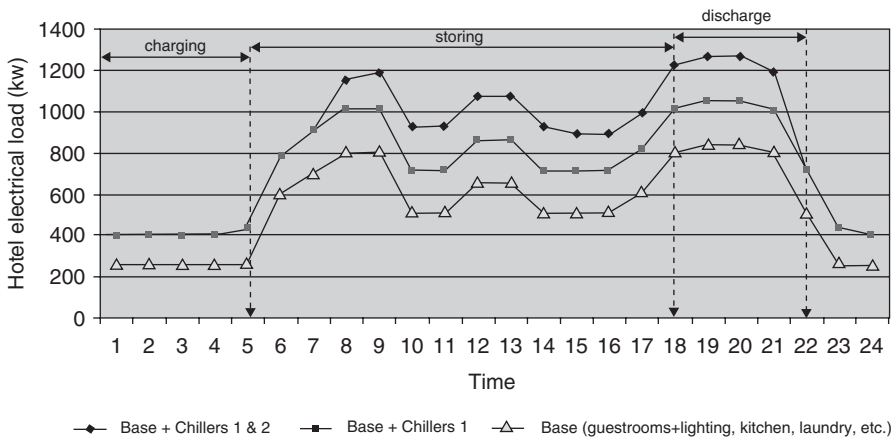


**Figure 8.30** Electrical load for the NBH hotel for several cooling loads (for 70% room occupancy). Possible TES operating phases are shown along the top of the diagram

**Chilled Water TES Scenarios**

Some options exist for using CWS for shifting the electrical load. In the conventional situation, both chillers and their accessories are operating mostly during the peak hours (18:00 to 22:00), during which time they require 425.4 kW of electrical power and consume 1701.6 kWh of electricity.

For the first scenario, an electrical partial load-leveiling strategy is employed using a chilled water TES capable of meeting part of the load (approximately 50%). Here, chiller 2 is turned off

during peak hours (the region in Figure 8.30 labelled “discharge”), but is used to charge one unit CWS tank for 5 h during low-demand hours (midnight until 5:00 in the morning, corresponding to the region in Figure 8.30 labelled “charging”). During charging, chiller 2 consumes 1063.5 kWh of electricity. The CWS circulation pumps operate during discharging to transport cool water from the CWS tank to provide cooling to the hotel. These pumps require 43.6 kW of power and consume 174.4 kWh of electricity during this period.

For the second scenario, full-storage CWS is utilized. Here, both chillers 1 and 2 are turned off during peak hours, and their function is offset by two CWS tank units. In this scenario, 425.4 kW of electrical load (2 chillers at 212.7 kW) and 1811.2 kWh of electricity consumption (2 chillers at 905.6 kWh) are shifted from peak to off-peak hours. As a consequence, there is a new electrical load of 87.2 kW and an electrical consumption of 348.8 kWh because of the operation of both the CWS circulation pumps to transport chilled water during discharging, as well as a new electrical consumption of 2127 kWh at off-peak hours (1 chiller at 212.7 kW over 10 h for charging, from 22:00 until 7:00).

To assess the economics of the TES scenarios, these electrical loads and consumptions, listed in Table 8.7, are multiplied by their associated charge rates. The resulting billing rates are tabulated and compared in Table 8.8. Further, an economic analysis is presented in Table 8.9.

The billing rate (electricity use and associated cost) of the NBH hotel for the conventional (or base) case and the two TES scenarios are provided in Table 8.8. For the conventional case, it can be seen that the costs for load connection, electricity consumption, disincentive, and tax for street lighting represent 17%, 51%, 28%, and 4% of the total electricity bill, respectively. The disincentive charge is applied if the hotel’s load connection (in kW) and electrical consumption (in kWh) during peak hours exceed the threshold amount permitted by the state electricity authority. For peak hours, the threshold for this hotel for load connection is 1090 kW (maximum permitted) and the threshold electrical consumption is 56,250 kWh/month (maximum permitted). The disincentive charge is strongly influenced by the use of chillers to cope with cooling demands during peak hours, that is, 18:00 to 22:00 hours.

Several other important details are observed in Tables 8.7 and 8.8.

- The hotel has a contract load connection from the grid of 3465 kW, but the maximum load connection actually achieved during peak hours is 1480 kW, or 43% of the contract amount. Thus, almost 50% of contract load connection is not utilized but the hotel still has to pay for the entire contracted load connection, leading to unnecessary costs.
- Use of the 50% partial-storage CWS in scenario 1 could reduce the load connection by 169 kW (11.4% of the actual load connection) and electrical consumption by 20,292 kWh/month (15.4% of the actual consumption for the conventional case) during peak hours. Also, this scenario shifts to nonpeak hours an additional electrical consumption of 31,905 kWh/month (5.9% of electrical consumption during nonpeak hours). Therefore, this scenario could potentially reduce the total monthly electricity bill from \$64,250 to \$60,296, for a savings of \$3,954.
- Use of the full-storage CWS in scenario 2 could reduce the load connection by 338 kW (22.8% of the actual load connection) and electrical consumption by 40,548 kWh/month (30.7% of the actual consumption) during peak hours. This scenario also shifts to nonpeak hours an electrical consumption of 63,810 kWh/month (11.8% of nonpeak consumption), and could reduce the total monthly electricity bill by up to \$11,599.

Note that, although both scenarios lead to financial savings, they do not reduce overall electricity consumption. The overall electricity consumption by the hotel is observed, as shown in Table 8.7, to increase by 11,613 kWh/month (31,905 – 20,292) for 50% partial storage and by 23,226 kWh/month (63,810 – 40,584) for full storage. This increase is mainly attributable to the additional consumption of having the CWS circulation pumps operating for longer periods (during

**Table 8.7** Electricity use data for two TES scenarios for the NBH hotel for September 2008 (based on a 70% occupancy rate)

Quantity	Base case	50% partial-storage scenario			Full-storage scenario		
		Value	Change	% change	Value	Change	% change
Contract load connection (kW)	3,465	3,465			3,465		
Actual load connection, peak hours (kW)	1,480	1,311	-169	-11.4	1,142	-338	-22.8
Actual electricity consumption, peak hours (kWh/month)	132,000	111,708	-20,292	-15.4	91,416	-40,584	-30.7
Electricity consumption, nonpeak hours (kWh/month)	540,000	571,905	31,905	5.9	603,810	63,810	11.8

*Note:* Change and percentage change indicate the difference in the value for the scenario relative to the base case.

**Table 8.8** Monthly electricity cost data for two TES scenarios for the NBH hotel for September 2008 (based on a 70% occupancy rate)

Quantity	Base case		50% partial-storage scenario		Full-storage scenario	
	Cost (\$)	Portion of total cost for case (%)	Cost (\$)	Portion of total scenario cost (%)	Cost (\$)	Portion of total scenario cost (%)
Load connection cost	10,932	17	10,932	18	10,932	21
Consumption cost	32,625	51	34,220	57	35,816	68
Disincentive charge	18,154	28	12,793	21	3,916	7
Tax street lighting	2,539	4	2,351	4	1,987	4
Total electricity bill	64,250	100	60,296	100	52,651	100

charging and discharging periods), and to the fact that there is little difference between dry-bulb temperature during peak hours (25–27 °C) when chillers are shut and after midnight (21–24 °C) when chillers are charging the CWS.

For cold TES technology where water is used as the storage medium, we need to calculate the volume of CWS tank required to offset the cooling load of each chiller during discharging. Susila *et al.* (2009) determined the size of CWS tanks to be 757 m<sup>3</sup> for partial storage and 1514 m<sup>3</sup> for full storage.

An economic analysis of the TES scenarios is presented in Table 8.9. For the partial- and full-storage scenarios, respectively, the net present value (NPV) balance at the end of the analysis period is found to be \$213,840 and \$861,526, and the payback period to be 3 years and 2 years. The annual net saving for the full-storage scenario (\$139,200) is determined to be almost three times greater than that for the partial-storage scenario (\$47,448), but the initial capital cost is only two times greater (i.e., \$250,000 versus \$125,000). From an economic perspective, both payback periods are reasonable and worthy of further investigation leading to implementation, but the full-storage scenario appears to be somewhat advantageous.

**Table 8.9** Economic analysis of the use of chilled water TES for the NBH hotel

Quantity	Conventional (base) case	50% partial- storage scenario	Full-storage scenario
<i>Financial and technical parameters</i>			
Annual interest rate to borrow capital (%)	10	10	10
Annual discount rate for incurred savings and costs (%)	8	8	8
Service lifetime (analysis period) (years)	15	15	15
Minimum volume of CWS tank (m <sup>3</sup> )	–	757	1,514
<i>Costs (\$)</i>			
Capital cost for CWS (tank and piping) construction	–	100,000	200,000
Capital cost for CWS circulation pumps	–	25,000	50,000
Annual interest payment on bank loan capital	–	5,000	10,000
Billing rate per month	64,250	60,296	52,651
Billing rate per year	771,000	723,552	631,812
Net billing rate per year due to applying CWS <sup>a</sup>	–	47,448	139,200
Operating, maintenance, and repair cost per year	24,000	26,000	28,000
Incremental operating, maintenance, and repair cost per year due to applying CWS <sup>a</sup>	–	2,000	4,000
Salvage value (10% of capital cost of CWS circulation pumps)	–	2,500	5,000
<i>Net present values (NPVs) (\$)</i>			
NPV of capital cost (bank loan)	–	–125,000	–250,000
NPV of interest payment on capital (bank loan)	–	–106,998	–213,997
NPV of energy savings on billing rate due to applying CWS	–	464,635	1,363,117
NPV of marginal operating, maintenance, and repair cost	–	–19,585	–39,170
NPV of salvage value	–	788	1,576
NPV (overall)	0.0	213,840	861,526
<i>Economic viability</i>			
Payback period (years)	–	3	2

<sup>a</sup>Assumes an annual escalation rate of 2%.

### Extension to Other Hotels in Bali

In a broad sense, if CWS is applied to all 41 hotels in Bali that use chillers for central air-conditioning, the total shifted power demand during peak hours, estimated by prorating the results obtained here for the NBH hotel, would be between 4.0 MW using 50% partial storage and 7.9 MW using full storage. TES would allow the hotels to reduce their energy costs and improve their competitiveness. Reducing peak power demand would also improve the reliability of electrical supply of Bali by reducing the gap between available electrical capacity and electrical power demand during peak periods. This demand shift would allow local diesel power generation units to reduce their operation during peak hours and associated emissions from burning diesel fuel. From an environmental perspective, therefore, TES utilization would permit the hotels to reduce their emissions of CO<sub>2</sub> and other pollutants emitted by diesel generators.

Further information on this study is presented by Susila *et al.* (2009).

### 8.8.2 Integrated TES Community System: Drake Landing Solar Community

As energy costs and concerns and actions regarding environmental harm increase, we are seeing the development of increasing numbers of integrated energy systems, usually with the objective of

improving energy sustainability. Such systems incorporate multiple energy technologies and often involve renewable energy options. In line with this trend, numerous systems incorporating TES are now doing so in conjunction with renewable and other advanced energy technologies.

The Drake Landing Solar Community (DLSC), located in Okotoks, Alberta, Canada (25 km south of Calgary) and completed in March 2006, is a highly cited example of TES used in a community energy system in conjunction with several other sustainable energy technologies, including solar energy, district heating, and heat pumps. In DLSC, 52 low-rise detached homes, located on two streets running east–west, are supplied with space heating and hot water. The average house size is 138 to 151 m<sup>2</sup> (1490 to 1630 ft<sup>2</sup>) based on gross floor area, and each has a detached garage in the back facing a lane. The garages are joined by a roofed breezeway, with the roof structure extending the length of each of the four laneways and providing a platform for the solar collectors. The 52 homes in DLSC are located within a 835-home subdivision.

The DLSC project is intended to demonstrate the feasibility of replacing substantial residential conventional fuel energy use with solar energy, collected during the summer and utilized for space heating during the following winter, in conjunction with seasonal TES.

### Energy System and its Operation

Although complex, the DLSC energy system is illustrated with a simplified schematic in Figure 8.31. The primary components of the system and their operation are described here. Additional details are available elsewhere (McClenahan *et al.*, 2006; Wong *et al.*, 2006; Sibbitt *et al.*, 2007).

Over 800 solar collectors are mounted on top of garages in the DLSC, covering nearly 2300 m<sup>2</sup>. There are four rows of garages with two rows of collectors per garage. A photograph showing one row of houses and garages covered with solar collectors is presented in Figure 8.32. Glycol (a mixture of water and antifreeze) is used as the heat transport fluid for conveying thermal energy from the solar collectors through a network of insulated pipes to the Energy Centre, a 2500 ft<sup>2</sup> building connecting the various distributed systems of the network and containing two short-term storage tanks.

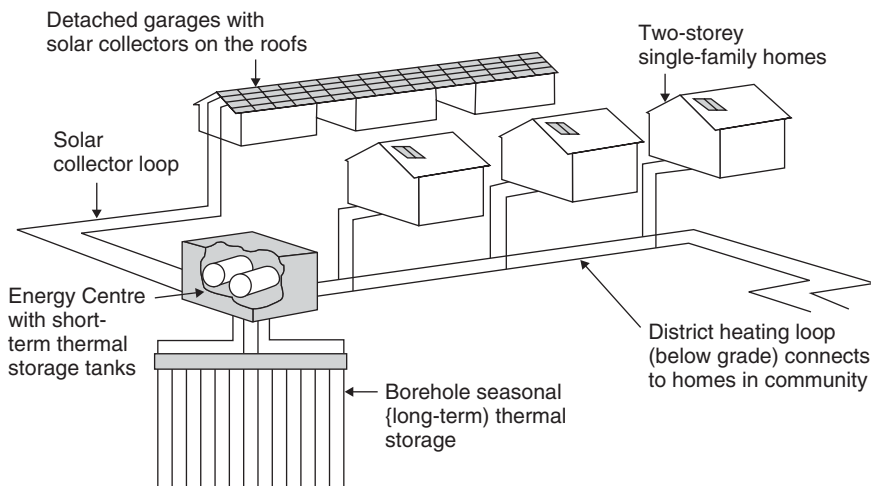


**Figure 8.31** Simplified schematic of the principal energy components in the DLSC (Courtesy of DLSC). Source: “The Drake Landing Solar Community Project – Early Results.” B. Sibbitt, T. Onno, D. McClenahan, J. Thornton, A. Brunger, J. Kokko, B. Wong, Natural Resources Canada, 2007. Reproduced with the permission of the Minister of Natural Resources Canada, 2010.





**Figure 8.32** Photograph of one row of houses and garages covered with solar collectors in the DLSC (Courtesy of DLSC). *Source:* “The Drake Landing Solar Community Project – Early Results.” B. Sibbitt, T. Onno, D. McClenahan, J. Thorton, A. Brunger, J. Kokko, B. Wong, Natural Resources Canada, 2007. Reproduced with the permission of the Minister of Natural Resources Canada, 2010

At the Energy Centre, a heat exchanger transfers thermal energy from the solar collector loop to two 125,000-L steel tanks containing a volume of 240 m<sup>3</sup> of water, which act as short-term storages (see Figure 8.33). Hot water from the tanks can be transferred directly into a district heating network connecting the DLSC homes. During warmer months, hot water from the tanks is circulated to a series of pipes located within boreholes beside the Energy Centre under a corner of a neighborhood park. This borehole thermal energy storage (BTES) stores heat collected in the spring and summer for subsequent use in winter. Covered with a layer of insulation beneath the topsoil, the BTES has 144 boreholes that are 35 m deep and linked in 24 parallel circuits, each with 6 boreholes in series. The six boreholes in series are arranged in a radial pattern (see Figures 8.34 and 8.35). Water flows from the center to the outer edge when charging the BTES with heat, and from the edge toward the center when recovering heat, maintaining the highest temperature near the center. Heat from the pipes is transferred through a series of U-shaped pipes (see Figure 8.34) to the surrounding earth, raising its temperature to a peak of approximately 40–50 °C. During winter, water at approximately 80 °C from the boreholes is transferred by the heat exchanger to the district energy network for circulation to homes. The Energy Centre distribution network has additional auxiliary systems, including a natural gas-fired hot water boiler for peaking requirements during winter and a separate cooling system for the solar collector loop. Pumps for the collector and district heating loops use variable speed drives to reduce electrical power consumption while managing varied thermal power levels.

The short-term TES tanks in the Energy Centre act as a buffer between the collector loop, the district energy loop, and the BTES field, receiving and discharging thermal energy as necessary. The short-term TES tanks support the system operation by being able to receive and discharge heat



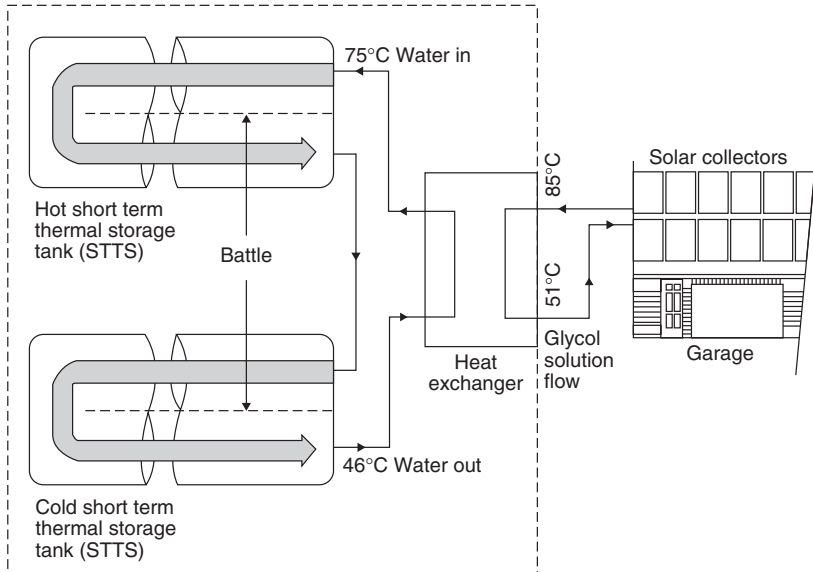


**Figure 8.33** Schematic of the DLSC Energy Centre, showing the heat exchanger, the solar collector loop, and the two short-term storage tanks. Some typical temperatures for the heat transport fluids are shown (Courtesy of DLSC). *Source:* “The Drake Landing Solar Community Project – Early Results.” B. Sibbitt, T. Onno, D. McClenahan, J. Thorton, A. Brunger, J. Kokko, B. Wong, Natural Resources Canada, 2007. Reproduced with the permission of the Minister of Natural Resources Canada, 2010

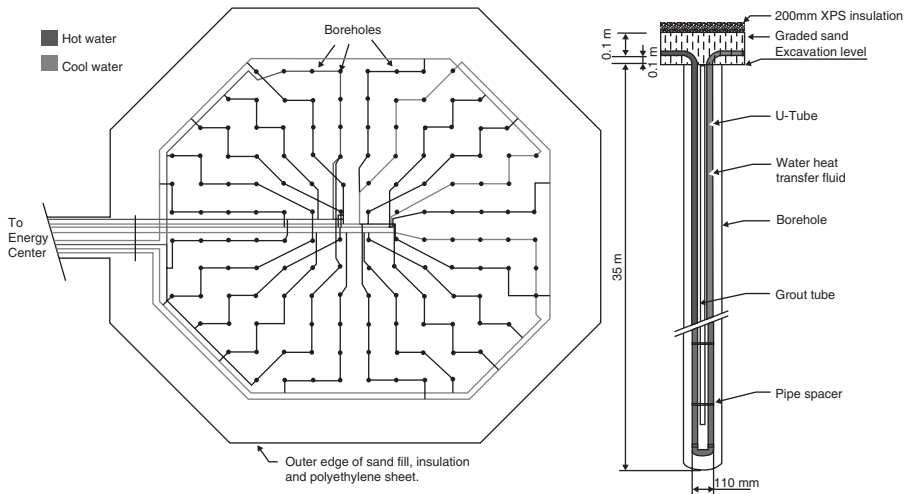


**Figure 8.34** Borehole thermal energy storage at DLSC. Layout of the 144 boreholes in 24 parallel circuits, each with six boreholes joined in series and laid out radially (a); U-shaped pipes that descend in each borehole 35 m (b) (Courtesy of DLSC). *Source:* “The Drake Landing Solar Community Project – Early Results.” B. Sibbitt, T. Onno, D. McClenahan, J. Thorton, A. Brunger, J. Kokko, B. Wong, Natural Resources Canada, 2007. Reproduced with the permission of the Minister of Natural Resources Canada, 2010



**Figure 8.35** Construction photograph of the DLSC borehole thermal energy storage showing piping joining the boreholes in a radial configuration (Courtesy of DLSC). *Source:* “The Drake Landing Solar Community Project – Early Results.” B. Sibbitt, T. Onno, D. McClenahan, J. Thorton, A. Brunger, J. Kokko, B. Wong, Natural Resources Canada, 2007. Reproduced with the permission of the Minister of Natural Resources Canada, 2010

at a much greater rate than the BTES storage, which has a much higher thermal storage capacity. The need for this tandem use of short- and long-term storage can be observed in two main ways:

- During periods of high insolation, the BTES cannot receive energy as quickly as it can be collected, so it is temporarily stored in the short-term TES tanks and subsequently transferred to the BTES at night.
- When heat cannot be discharged from the BTES sufficiently quickly to meet winter peak heating demands, usually in early mornings, the situation reverses. Then heat is continually removed from the BTES and stored in the short-term storage tanks if not immediately needed.

DLSC homes are certified to Natural Resources Canada’s R-2000 standard, incorporating such features as upgraded insulation and heat recovery ventilation. Each home has a low-temperature air handler that blows air across a warm fan coil, where it is heated and then transferred throughout the home via standard air ducts. The integrated air handler and heat recovery ventilator consists of a water–air heat exchanger that provides forced-air heating and fresh air.

Domestic hot water is supplied by a separate two-collector solar energy system, backed up with a high-efficiency gas-fired water heater. A layout of the DLSC energy distribution system is illustrated in Figure 8.36.

### Key Energy Components

The DLSC has five main components:

- **Solar thermal collectors.** During a typical summer day, the approximately 800 single-glazed flat-plate solar panels organized in four rows on the garages generate 1.5 MW of thermal power. The solar panels are linked via an insulated underground pipe carrying a glycol solution to the Energy Centre.

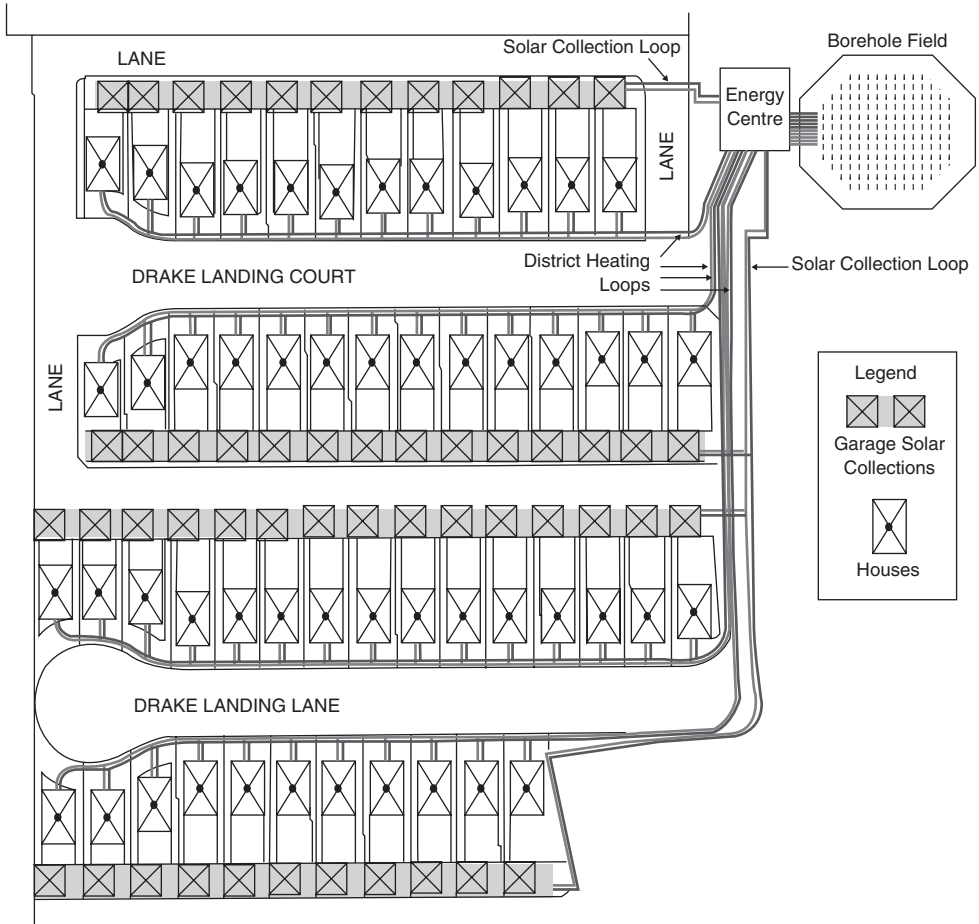


**Figure 8.36** Layout of the DLSC energy distribution system, showing the 52 houses, the Energy Centre, and the borehole thermal energy storage field (Courtesy of DLSC). *Source:* “The Drake Landing Solar Community Project – Early Results.” B. Sibbitt, T. Onno, D. McClenahan, J. Thornton, A. Brunger, J. Kokko, B. Wong. Natural Resources Canada, 2007. Reproduced with the permission of the Minister of Natural Resources Canada, 2010

- Energy Centre.** The solar collector loop, the district heating loop, and the BTES loop pass through the Energy Centre, which contains the two 120 m<sup>3</sup> short-term heat storage tanks, the back-up gas boiler, and most of the mechanical and electrical equipment (pumps, heat exchangers, controls, etc.).
- District heating system.** Heated water is transported from the Energy Centre to the DLSC homes through insulated underground piping. At each home, the heated water passes through an air handler located in the basement, which avoids the need for a conventional furnace, warming air that is then distributed throughout the house via ducting. The network capacity is 4.5 MW and the annual heat demand per house is 50 GJ.
- BTES system.** The underground seasonal BTES system stores large quantities of solar heat collected in summer for winter use. Solar-heated water is pumped to the center of the BTES and its 144 boreholes. The heat transferred to the surrounding soil and rock raises its temperature by the end of summer to about 80 °C.

- **Solar domestic hot water.** Hot water is produced by a self-regulated, separate solar domestic hot water system using rooftop solar panels. Natural gas-based hot water units supplement hot water demands when solar energy is not available and act as backups.

### Benefits

For the homes in DLSC, 90% of heating and 60% of hot water needs are designed to be met using solar energy. Annually, each home uses approximately 110.8 GJ less energy and emits about 5.65 t fewer GHGs than a conventional Canadian home (see Table 8.10). Thus, the DLSC avoids about 260t of GHG emissions annually. Each DLSC home is about 30% more efficient than conventionally built houses and is expected to use 65–70% less natural gas to heat water than a conventional new home.

Note that large seasonal TES systems require a significant time to charge since the storage medium must be heated up to a minimum temperature before any heat can be extracted. Hence, it is anticipated that by the fifth year of operation, the system will reach a 90% solar fraction, defined as the ratio of the amount of energy provided by the solar technologies to the total energy required.

### Economics

The Drake Landing system had an initial start-up capital of \$7 million (Canadian), including \$2 million from federal government agencies, \$2.9 million from the Green Municipal Investment Fund of the Federation of Canadian Municipalities, and \$625,000 from Innovation Program agencies of the government of Alberta. But the cost to repeat this project is estimated to be \$4 million, as those involved in the project feel that the \$7 million project cost included a significant amount

**Table 8.10** Comparison of annual energy use and GHG emissions for a Drake Landing Solar Community home and a conventional (baseline) home, for space and domestic hot water heating

Quantity	Conventional (baseline) home	DLSC home	Reduction for DLSC relative to conventional home <sup>a</sup>
<b>Energy use (GJ)</b>			
• Space heating			
– Natural gas	100	6	94
– Solar energy	0	62	–
– Total	100	68	32
• Water heating			
– Natural gas	26	9	17
– Solar energy	0	9	–
– Total	26	18	8
• Space and water heating			
– Natural gas	126	15	111
– Solar energy	0	71	–
– Total	126	86	40
<b>Greenhouse gas emissions (t)</b>			
• Space heating	5.1	0.3	4.8
• Water heating	1.3	0.5	0.9
• Space and water heating	6.4	0.8	5.7

<sup>a</sup>Savings in rows labelled “Natural gas” reflect reduction in natural gas use for DLSC home with respect to the baseline home. Savings in rows labelled “Total” reflect the reduction in energy required and thus reflect savings because of conservation measures in the DLSC homes.

of one-time research and development expenses that would not be necessary if the project were replicated in another community.

The optimal size for such a community has been estimated based on economies of scale and data for 2008 to be a minimum of 200 to 300 homes. The system would be the same except that more boreholes would be required.

It is noted that the use of a low-temperature hot water system permitted the capital cost of piping to be reduced.

The DLSC houses sold for an average of \$380,000 (in Canadian dollars). DLSC homeowners receive a monthly solar utility bill for heating of \$60 on average.

### 8.8.3 *The Borehole TES System at the University of Ontario Institute of Technology*

A BTES system is utilized at the University of Ontario Institute of Technology (UOIT) in Oshawa, Ontario, Canada. The UOIT campus, which opened in 2003 and is still growing, has about 6000 students. The campus includes seven buildings, most of which are designed to be heated and cooled using ground-source heat pumps (GSHPs) in conjunction with the BTES, with the aim of reducing energy resource use, environmental emissions, and financial costs. Besides being a critical component of the university's heating and cooling system, the borehole TES is used for research and student education.

The borehole TES system at UOIT is one of many types of underground TES that have been used or investigated (Sharma *et al.*, 2009; Sanner *et al.*, 2003). Although some underground TES applications exist in Canada, such as those at Scarborough Centre in Toronto, Carleton University in Ottawa, the Sussex Hospital in New Brunswick, and the Pacific Agricultural Centre in Agassiz, BC (International Energy Agency (IEA), 2009), the UOIT borehole TES is unique in Canada in terms of the number of holes, capacity, and surface area. Also, the UOIT BTES field is the largest and deepest in Canada, and the geothermal well field is one of the largest in North America. Large-scale storage systems, comparable to the UOIT one have been implemented at Stockton College in New Jersey and in Sweden (International Energy Agency (IEA), 2009).

With the UOIT system, energy is upgraded by heat pumps for heating, that is, heat is taken from the ground at low temperature and transferred at a higher temperature to the building. Alternatively, the ground can absorb energy and be increased in temperature using the heat pump in its cooling (reverse) mode. The UOIT facility is an integrated system, in that it combines an energy resource (the ground) with a system to exploit this energy (the heat pump, HVAC, and distribution equipment and related devices) and a specialized interface (ground-based heat exchangers and storages). The UOIT BTES system has 384 boreholes each 213-m deep. The system uses GSHPs to attain the desired temperatures. A glycol solution, encased in polyethylene tubing, circulates through an interconnected, underground network. During the winter, fluid circulating through tubing extended into the wells collects heat from the earth and carries it into the buildings. In summer, the system reverses to extract heat from the building and place it in the ground. Thus, the BTES provides for both heating and cooling on a seasonal basis. The system is illustrated in Figure 8.37.

The design of UOIT system was deemed beneficial in the Canadian context. In Canada, the building sector (commercial, institutional, and residential) accounts for 31% of total secondary energy use and 28% of GHG emissions (Caneta, 2004; Hanova and Dowlatabadi, 2007; Caneta, 2003; Marbek, 1999). Space heating dominates, accounting for 56% of this energy use and a similar proportion of the GHG emissions. Also, the demand for air-conditioning is significant and has in recent decades increased greatly (by 80% since 1990). This increase is likely attributable to increased living standards and higher internal heat gains in buildings, and may become greater in the future because of climate change effects. Air-conditioning is now responsible for peak electrical demand during the summer in many regions in Canada, particularly Ontario.

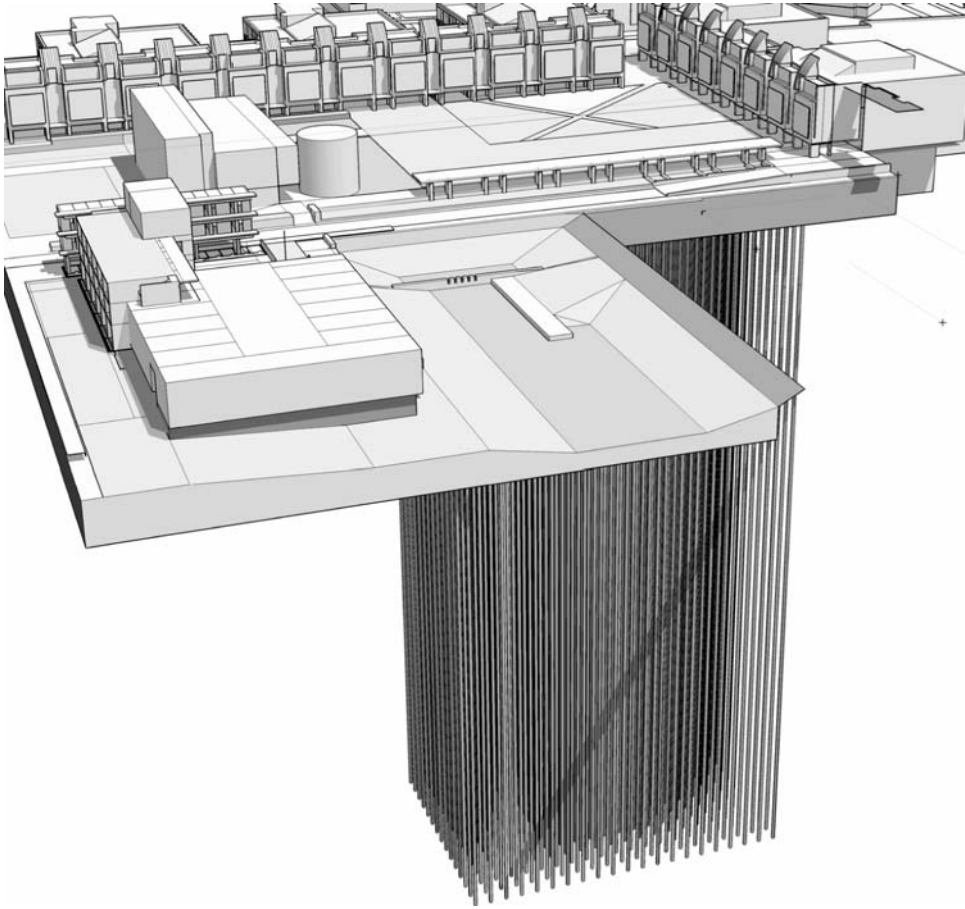


**Figure 8.37** Borehole thermal energy storage system at UOIT, showing boreholes below university buildings

GSHPs have gained significant market shares in countries such as Japan and Sweden, and other countries with similar climatic conditions (Forsen, 2005; Halozan, 2008; Nordell and Ahlstrom, 2007). For instance, there are approximately 300,000 GSHP installed in Sweden with an annual growth rate of 30,000 units. The systems delivered 16% of all space heating in Sweden in 2000 and this percentage was expected to increase to 27% in 2010. The Canadian market remains largely untapped, with only 3150 units installed in 2006 according to a survey by the Canadian GeoExchange Coalition (2007). Research is needed to increase utilization (Marbek, 1999; Spitler, 2005), and several investigations aimed at improving GSHP technical and economic performance and developing alternative configurations were reported at the International Energy Agency's 2008 International Heat Pump Conference (Halozan, 2008).

### Hydrogeology at Site

The hydrogeologic setting at the vicinity of the site has over 40m of unconsolidated overburden deposits overlying shale bedrock, and groundwater resources in the Oshawa area are limited to isolated, thin sand deposits (Beatty and Thompson, 2004). Test drilling programs were carried out to determine the feasibility of thermal storage in the overburden and bedrock formations



at the UOIT site, and in-situ tests were conducted to determine the groundwater and thermal characteristics. It was determined that the overburden comprises layers of glacial till, clay, silt, and silty fine sand, and that no water-bearing sand deposits exist in 44 m of deposits. Two Paleozoic sedimentary bedrock formations were present: 14 m of shale and 142 m of limestone. The limestone formation is almost impermeable and is encountered from 55 m to 200 m below the surface, as shown in Figure 8.38. The background temperature of the geologic formations at the site is 10°C. The homogeneous, nonfractured rock is well suited for TES since little groundwater flow exists to transport thermal energy from the site.

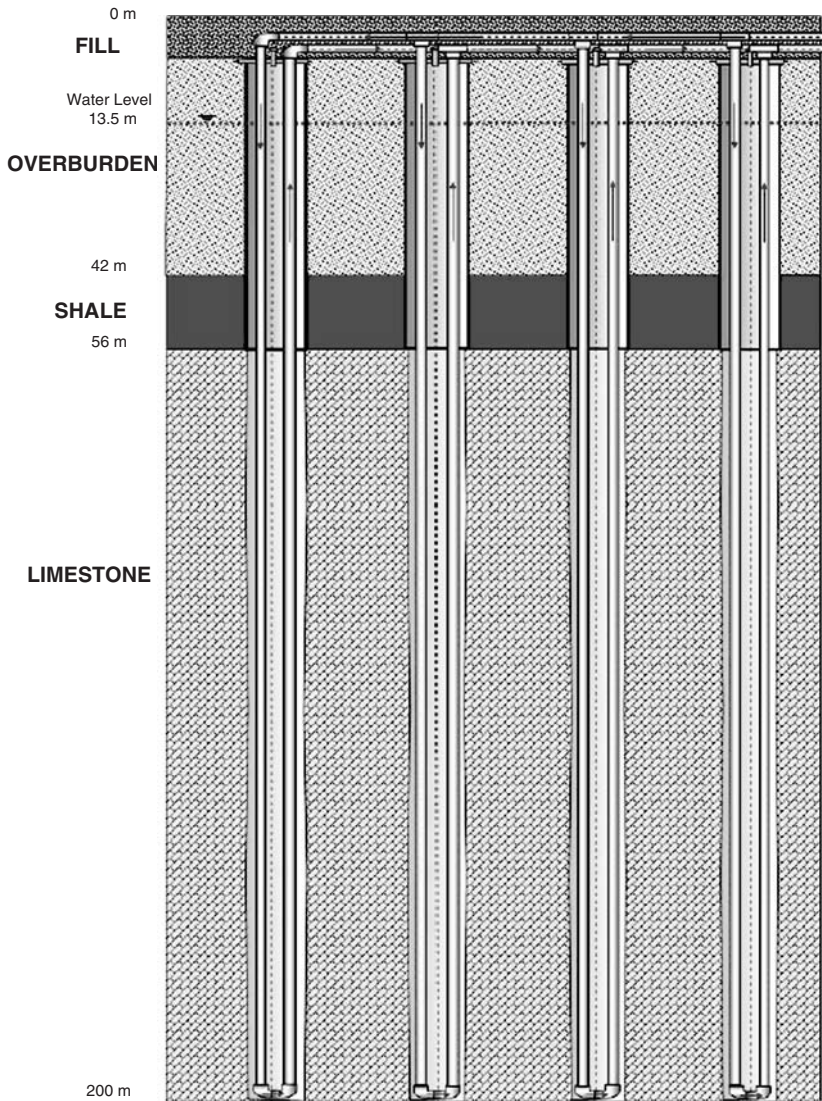


**Figure 8.38** Illustration of four boreholes and the ground composition and geology for the UOIT BTES system

### BTES System

The total cooling load of the campus buildings was anticipated to be about 7000 kW. The thermal conductivity for the geologic media encountered in a test well was found to be about 1.9 W/m K (Beatty and Thompson, 2004). Using the thermal conductivity test results, it was determined that a field of about 370 boreholes, each about 200 m in depth, would be required to meet the energy service needs. In addition, five temperature-monitoring boreholes were installed.

The total drilling length for the project was about 75 km. The borehole drilling was carried out using three drilling rigs, operating 24 h per day. Design changes were made to the borehole heat exchangers (BHEs) as a result of the lack of groundwater flow in the rock. The Swedish practice of water-filled BHEs was utilized instead of the North American practice of grouted BHEs. Water-filled BHEs improve the efficiency of U-tube installation and extend the life of the boreholes.

In the system, over 150 km of polypropylene tubing routes water down the borehole depth. Steel casing was installed in the upper 58 m of each borehole to seal out groundwater in the shallow formations.

A site view during construction of the well field of the BTES system at UOIT, showing the grids of boreholes and piping that interconnect them, is shown in Figure 8.39. Here, uncapped well heads show up as black dots. Ten-centimeter (four-inch) piping runs from the wells into the mechanical corridors that circle the field. The BTES field occupies the central courtyard of the UOIT campus. The field is divided into four quadrants in order to optimize seasonal energy storage. The BHEs are located on a 4.5-m grid and the total field is about 7000 m<sup>2</sup> in area. The BTES field has a volume of approximately 1.4 million m<sup>3</sup>, and contains 1.7 million tonnes of rock and 0.6 million tonnes of overburden.



**Figure 8.39** View of construction of the UOIT borehole thermal energy storage system, showing the grid of borehole headers and interconnecting piping



Start-up of the system occurred during the summer of 2004. Monitoring of the fluid and energy flow in the first few years of operation has been required to optimize the long-term performance of the BTES system. A string of temperature probes in each of the five monitoring wells monitor the thermal store within and outside the BTES field.

### **BTES Field Construction and Borehole Heat Exchanger Installation**

A good description of the construction of the BTES field at UOIT and the installation of the BHEs is provided by Beatty and Thompson (2004), and is drawn on extensively in this subsection.

Before borehole drilling, approximately 2 m of soil was removed to create a level base for the BTES field. A 0.3-m layer of crushed stone was placed over the glacial till soils to provide a working base for the heavy drilling rigs and a drainage layer for precipitation and drilling fluids.

Drilling, using three Ingersoll Rand Model T-90 drilling rigs, was carried out from mid-July to the end of October 2003, on a 24-h per day and 7-day per week basis. Three to four boreholes were drilled daily by six two-person crews working 12-h shifts. Average hourly drilling rates of about 15 m were achieved, using two drilling techniques to accommodate the nature of the site geology:

- Hydraulic mud rotary drilling was used in the upper 56 m of overburden and shale.
- For drilling in the limestone, an air-driven down-the-hole hammer was used, in which high-pressure air is supplied to a drill bit through the drill string to remove the drill cuttings.

Steel casings of 150-mm diameter with threaded couplings were seated about 1.5 m into the limestone bedrock of each borehole. To prevent downward seepage of surface drainage, the surface annulus around each casing was sealed with bentonite grout.

The borehole drilling was inspected daily for stratigraphy and groundwater conditions in the boreholes, and to confirm borehole depths. About 10% of the boreholes were video-logged to evaluate the borehole plumbness and examine the limestone formation for fractures and groundwater seepage. The inspections indicated that the geologic conditions throughout the BTES are homogeneous.

At the completion of drilling, the boreholes were left dry and were ready for the installation of the BHEs. The water level recovery rate was monitored in three of the 200-m deep observation wells, and averaged only about 2 cm per day over a 200-day period. This low value corresponded to the low groundwater flow in the rock, which was consistent with the video-log observations of few fractures or fissures in the limestone.

BHEs are manufactured, installed, and operated in a relatively standardized manner today. In each borehole, a polyethylene U-tube is normally installed through which a heat-transfer fluid circulates, and the main design variations are the type of heat-transfer fluid (water or antifreeze) and the borehole filling material (water or grout). Water-filled boreholes were used in the UOIT system, resulting in several cost savings over conventional U-tubes. U-tube installations lagged drilling operations by about 6 weeks, allowing separate material storage and working areas for each task. The UOIT U-tube, made of high-density polyethylene tubing with a 32-mm inner diameter, was delivered to the UOIT site in large reels of 2100 m rather than the smaller, custom-length reels normally supplied for individual boreholes. The long reels, which were pressurized and sealed with fusion caps, reduced the size of on-site material storage areas and the time required for U-tube installation. The heat exchanger tubing remained sealed until insertion in each borehole.

During U-tube installations, 2-cm-diameter iron sinker bars with a mass of 90 kg were attached to the bottom 20 m of the U-tube to counteract the buoyancy of the tubing in the water-filled borehole. As the 200-m long U-tube assembly was inserted into each dry borehole (see Figure 8.38), the U-tube and the borehole were simultaneously filled with treated water from the local water supply system. Fusion caps were installed on the pipe ends to prevent entry of any surface water or debris. The 370 U-tube installations were done by a four-man crew over 50 days and the U-tube daily installation rate was about 6000 m. A borehole and its U-tube heat exchanger are illustrated in Figure 8.40.

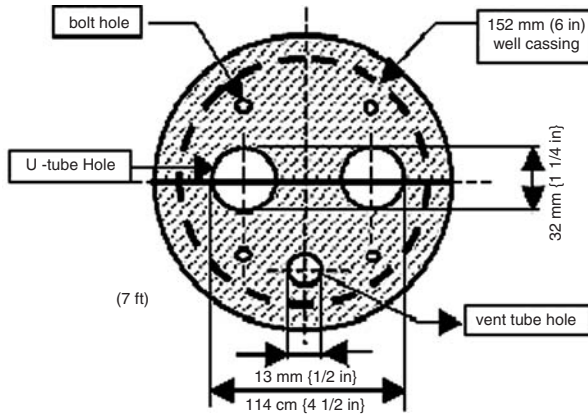


**Figure 8.40** Cross section of borehole and U-tube borehole heat exchanger

After installation, each heat exchanger assembly was pressure tested by pressurizing the water in the U-tube with compressed air to at least 690 kPa and maintaining the pressure for 1 h. The U-tube was deemed leak-free if little pressure was lost at the end of the 1-h test period. Two of the 370 installed U-tubes exhibited excessive pressure loss due to leakage at the U-band fusions and were replaced.

After the heat exchangers were installed and tested, each borehole was topped up with municipal water and an air-tight sanitary well seal was placed on top of the borehole casing. A custom-made steel cap was then installed over the sealed U-tube extensions, to protect against damage from vehicles prior to connecting the U-tubes to the horizontal distribution pipes. After connection of the heat exchanger tubes to the horizontal distribution pipes, the BTES field was backfilled with about 2 m of clean fill. The casings on the six temperature-monitoring wells and one of the heat exchange boreholes were extended up to the final grade level to permit easy access, for future instrumentation and monitoring or other purposes.

### Ground-Source Heat Pump and HVAC System

A GSHP system is the central part of the UOIT mechanical complex, and incorporates the BTES. The university buildings are linked to a central plant by a carefully arranged lattice of wells and transfers that is serviced through a tunnel that circumvents the field.

Chillers are used to pump energy from the buildings into the TES. The chillers are run only in the cooling mode, their primary purpose being cooling. The other heat pump modules assist in this cooling load. Chilled water is supplied from two chillers, each having seven 90-t modules, and two sets of heat pumps with seven 50-t modules each. The 90-t modules are centrifugal units with magnetic bearings that allow for very good part-load performance. The condensing water passes to the BTES field. The field retains the condensing heat for use in the winter (when the heat pumps reverse) and provides low-temperature hot water for the campus. All but a few services use this low-temperature (53 °C) hydronic heat. Each building is hydronically isolated with a heat exchanger, and has an internal distribution system. Supplemental heating is also provided by condensing boilers.

In autumn, energy is reclaimed from the BTES field, and the return water is hot enough to be used in a “free-heating” application (without having to use the heat pumps).

The circulation pumps are installed in banks, with rotating duty cycles. This is to ensure continuous availability even in the case of failures.

All the motors are controlled by the central control system and have variable frequency drives, which electronically control the frequency of the electrical supply and vary the motor rotational speed. The net effect is a pump with continuously variable and controllable flow rates. This approach permits the heat-transfer characteristics for the chillers and heat pumps to be optimized.

Air-handling units condition, filter, and feed the air to the rooms. Air is monitored for temperature, humidity, and CO<sub>2</sub>. The CO<sub>2</sub> concentration is used to meter the amount of outside fresh air required. This outside air is preheated using heat from the exhaust air.

A flow chart for the BTES system is presented in Figure 8.41, and the technical specifications of the chiller and two heat pumps, each having seven modules, are listed in Table 8.11. Further information on UOIT's BTES system can be found elsewhere (Beatty and Thompson, 2004).

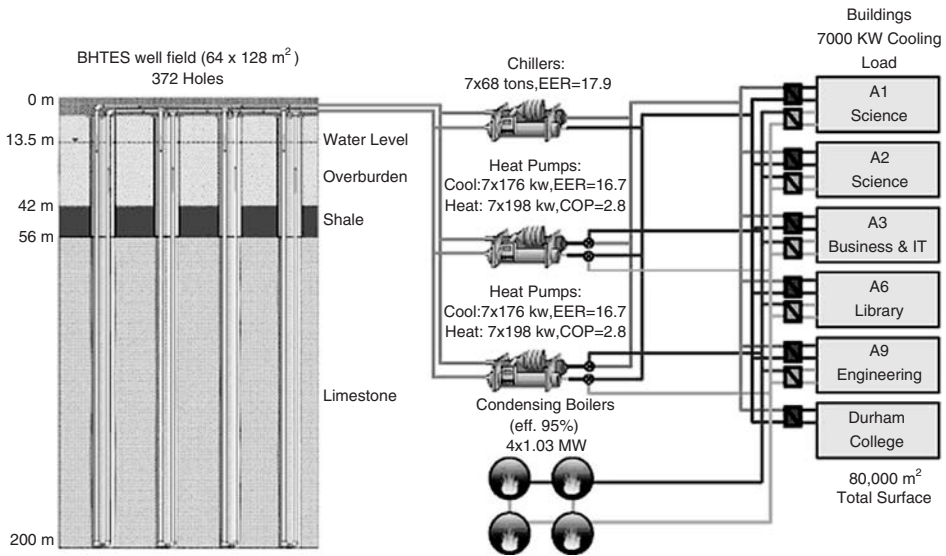


**Figure 8.41** Schematic flow diagram of the BTES and related equipment at UOIT

**Table 8.11** Design values for the heat pumps

Total energy loads (kW)	
● Heating	1386
● Cooling	1236
Temperatures (°C)	
● For heating	
– Load water: entering/leaving water temperatures	41.3/52
– Source water: entering/leaving water temperatures	9.3/5.6
● For cooling	
– Load water: entering/leaving water temperatures	14.4/5.5
– Source water: entering/leaving water temperatures	29.4/35
COP <sub>design</sub>	
● Heating	2.8
● Cooling	4.9

### Efficiency

Historical data are being analyzed to determine the efficiency of the BTES system, but is not yet available. Nonetheless, the behavior of the system heat pumps can be examined by considering three types of COP: conventional, exergetic, and Carnot. Conventional COP (or “energy efficiency”) of the heat pump can be expressed as follows:

$$\text{COP}_{\text{actual}} = \frac{\dot{Q}_h}{\dot{W}_{\text{comp}}}$$

where  $\dot{Q}_h$  is the heating load rate and  $\dot{W}_{\text{comp}}$  is the work input rate to the compressor. The Carnot COP is the maximum heating COP, based on a Carnot (ideal) heat pump system operating between low- and high-temperature reservoirs at  $T_L$  and  $T_H$ , respectively, and is given by

$$\text{COP}_{\text{Carnot}} = \frac{T_H}{T_H - T_L}$$

An exergetic COP (i.e., efficiency ratio) can be written as

$$\text{COP}_{\text{exergetic}} = \frac{\text{COP}_{\text{actual}}}{\text{COP}_{\text{Carnot}}}$$

The variation of these three COPs with the exit temperature of the heat pump (or supply temperature of the heat distribution system) in the heating mode is illustrated in Figure 8.42 for a typical set of conditions. Normally, in heating systems, the supply temperature of the heat distribution network plays a key role in terms of exergy loss. This temperature is determined via an optimization procedure since increasing the supply temperature reduces the investment cost for the distribution system and the electrical energy required for pumping stations, but increases heat losses in the distribution network.

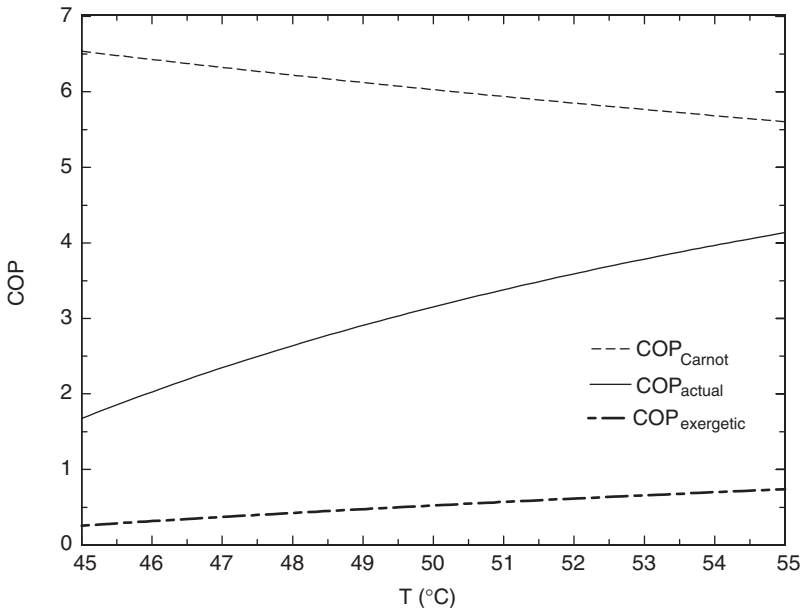


**Figure 8.42** Variation of COP with heat pump supply temperature

It is demonstrated in Figure 8.42 that raising the supply temperature increases the exergy efficiency of the heat pumps and hence the overall system. Other points to be considered in the design include the effect of outdoor conditions on the return temperature of the heat distribution network, the type of users connected to the system, and the characteristics of the heating apparatus. Also, in the heat exchanger design, a certain temperature difference is desired depending on the type of heat exchanger to be used. But, decreasing the supply temperature increases the size of building heating equipment. Oversizing leads not only to increased cost but also to greater exergy destruction because of unnecessarily increased irreversibilities in pumping, pipe friction, and so on.

### **Economics**

The BTES system is designed to be economically beneficial. Annual energy savings are reduced using the BTES system by 40% for heating and 16% for cooling. The simple payback period for the geothermal well field was 7.5 years when the system was designed, while the simple payback period for the high-efficiency HVAC equipment was 3–5 years.

The system also yielded other indirect financial benefits, including the following:

- reduced boiler plant costs;
- reduced use of potable water (23 million liters annually);
- reduced use of chemicals for the treatment of water;
- eliminated costs for roof cooling towers and associated building support.

The main challenge was convincing decision makers that the higher initial capital cost for high-efficiency HVAC equipment and the geothermal field was justified and would be repaid in a reasonable time frame and save the university money thereafter.

### **Other Efficiency Measures**

The BTES system is one of the numerous efficiency and environmental measures installed in the UOIT facilities. Others include green roofs (areas of vegetation planted directly on a roof) that help cool buildings, extend a roof's life by slowing heat-related deterioration of buildings, and mitigate storm-water runoff; surface water retention cisterns; high levels of insulation in walls and windows; solar reflective windows that allow daylight to pass through but filter out solar heat and reduce air-conditioning loads; a high level of building automation that controls HVAC systems as well as lighting, security, fire safety, and other systems; and use of low environmental-impact materials in construction. As a consequence, the energy, environmental, and economic benefits attributable to using of BTES are less than would be the case if BTES were the only efficiency measure applied. Nonetheless, designers determined that it was worthwhile to utilize BTES at UOIT.

## **8.9 Concluding Remarks**

A wide range of case studies drawn from reports in the literature and elsewhere are presented here. Included are CTES systems using chilled water, ice, and PCMs, as well as sensible and latent TES systems for heating capacity. The case studies demonstrate how TES is normally not addressed in an isolated manner, but as a part of the overall energy infrastructure for a facility. The applications represented by these case studies also vary widely, and include institutional facilities, such as government and educational buildings, commercial facilities, industrial plants, and such broader uses as part of a DHC network.

Each TES system and installation has its own advantages and disadvantages. The energy sources represented also vary widely, ranging from conventional fuels to solar energy. The case

studies demonstrate in many different ways how TES is an efficient and effective way of storing thermal energy.

## References

- Abusaa, G. (2000). Combustion turbine inlet air cooling, Lecture Notes, Presented at: Mechanical Engineering Seminar, KFUPM, Dhahran, 31 October.
- BAC (1999a). *Channel Island Power Station Opts for Ice Thermal Storage System*, Project Report, No. PRJ44/99, Baltimore Aircoil Company.
- BAC (1999b). *Thermal Storage is State of the Art, Gulf Construction*, Baltimore Aircoil Company.
- BAC (1999c). *Ice Keeps Alitalia Cool*, Application Leaflet, No. MN-92-10, Baltimore Aircoil Company.
- Beatty, B. and Thompson, J. (2004). 75 km of drilling for thermal energy storage, *Geo-Engineering for the Society and its Environment: Proceedings of the 57th Canadian Geotechnical Conference*, Session 8B, pp. 38–43, Quebec City.
- Canadian GeoExchange Coalition. (2007). Survey of Canadian geexchange industry: 2004-2006, *GeoConneXion Magazine*, December, 10–13.
- Caneta. (2003). *Global Warming Impacts of Ground-Source Heat Pumps Compared to Other Heating and Cooling Systems*. Final Report. Prepared for Renewable and Electrical Energy Division, Natural Resources Canada, by Caneta Research Inc., Mississauga, Ontario.
- Caneta. (2004). *Market, Economic, and Barrier Analysis for Ground Source Heat Pumps in Canada, US, and Europe. Draft Report. Prepared for Renewable and Electrical Division, Natural Resources Canada*, Caneta Research Inc., Mississauga, Ontario.
- Cristopia (2001a). *MM21 in Yokohama (Japan)*, Cristopia Energy Systems, France, <http://www.cristopia.com/english/project/yokohama.html>.
- Cristopia (2001b). *Harp Guinness Subsidiary (Ireland)*, Cristopia Energy Systems, France, <http://www.cristopia.com/english/project/harpguinness.html>.
- Cristopia (2001c). *Korean Development Bank (Korea)*, Cristopia Energy Systems, France, <http://www.cristopia.com/english/project/koreanbank.html>.
- Cristopia (2001d). *Museum of Sciences and Industry: 'La Villette' (France)*, Cristopia Energy Systems, France, <http://www.cristopia.com/english/project/lavillette.html>.
- Cristopia (2001e). *Rueil Malmaison Central Kitchen (France)*, Cristopia Energy Systems, France, <http://www.cristopia.com/english/project/rueil.html>.
- Cristopia (2001f). *Bangsar District Cooling Plant (Malaysia)*, Cristopia Energy Systems, France, <http://www.cristopia.com/english/project/bangsar.html>.
- Dharmadhikari, S. (2000). Une installation de trigénération exemplaire (in French). *Gaz d'aujourd'hui*, 6, 7–12.
- Dharmadhikari, S., Pons, D. and Principaud, F. (1999). Trigeneration for the World Fair Expo'98, *Lisbon, Presented at 20th International Congress of Refrigeration, IIR/IIF*, Sydney.
- Dharmadhikari, S., Pons, D. and Principaud, F. (2000). Contribution of stratified thermal storage to cost-effective trigeneration project, *ASHRAE Transactions* 106 (2), 16–21.
- DOE (1999). *Thermal Energy Storage at a Federal Facility*, The U.S. Department of Energy (DOE) Federal Energy Management Program, DOE/GO-10098-439.
- EPS (2000). *Thermal Energy Storage Systems*, Environmental Process Systems Limited, Berkshire, <http://www.epsltd.co.uk>.
- Forsen, M. (2005). *Heat Pumps – Technology and Environmental Impact (Part 1)*. Report. Swedish Heat Pump Association.
- Hall, A.D., Stover, J.C. and Breisch, R. (1994). Gas turbine inlet-air chilling at a cogeneration facility, *ASHRAE Transactions* 100(Part 1), 595–600.
- Halozan, H. (2008). Ground-source heat pumps and buildings, *Proceedings of the 9th International IEA Heat Pump Conference*, Zurich, Switzerland.
- Hanova, J. and Dowlatabadi, H. (2007). Strategic GHG reduction through the use of ground source heat pump technology, *Environmental Research Letters* 2 (4), 1–8, paper 044001.
- International Energy Agency (IEA). (2009). Energy conservation through energy storage, <http://www.iea-eces.org> (accessed on 14 Aug. 2009).

- JIN (2000). Going Underground, Japan information Network, <http://jin.jcic.or.jp/trends98/honbun/ntj980217.html>.
- Kent, H.S. (1996). *Thermal Energy Storage Increases Research Center's Cooling Capacity*, Technical Report, Levittown, Pennsylvania.
- Kolb, G. (2000). *Desirable Features of Power Tower for Utilities*, Sandia National Laboratories, Albuquerque, [http://www.sandia.gov/Renewable\\_Energy/solarthermal/feature.html](http://www.sandia.gov/Renewable_Energy/solarthermal/feature.html).
- Mahoney, A.R. (2000). *Advantages of Using Molten Salt*, Sandia National Laboratories, Albuquerque, [http://www.sandia.gov/Renewable\\_Energy/solarthermal/salt.html](http://www.sandia.gov/Renewable_Energy/solarthermal/salt.html).
- Marbek. (1999). *Ground Source Heat Pump Market Development Strategy*. Prepared for Natural Resources Canada. Renewable and Electrical Energy Division, by Marbek Resource Consultants Ltd.
- McClenahan, D., Gusdorf, J., Kokko, J., Thornton, J. and Wong, B. (2006). Okotoks: seasonal storage of solar energy for space heat in a new community, ACEEE, 2006 summer study on energy efficiency in buildings, Pacific Grove, CA.
- Nelson, K.P., Pippin, J. and Dunlap, J. (1999). *University Ice Slurry Systems*, Applications Catalog, Paul Mueller Company, Springfield.
- Nordell, B. and Ahlstrom, A.-M. (2007). Freezing problems in borehole heat exchangers, in *Thermal Energy Storage for Sustainable Energy Consumption: Proceedings of the NATO Advanced Study Institute on Thermal Energy Storage for Sustainable Energy Consumption—Fundamentals, Case Studies and Design* (ed. H.O. Paksoy), NATO Science Series II: Mathematics, Physics and Chemistry, Springer, pp. 193–204.
- Palmer, M. (2000). *Case Study in Saudi Arabia, Project Report*, WS Atkins Consultants Limited, Surrey, UK.
- RMRC (2000). *The World's First Passive Annual Heat Storage Home*, Rocky Mountain Research Center (RMRC), Montana, <http://www.rmrc.org/dome1.htm>.
- Roth, K., Zogg, R. and Brodick, J. (2006). Cool thermal energy storage, ASHRAE Journal, September, 94–96.
- Sanner, B., Karytsas, C., Mendrinou, D. and Rybach, L. (2003). Current status of ground source heat pumps and underground thermal energy storage in Europe, *Geothermics* 32 (4-6), 579–588.
- Sharma, A., Tyagi, V.V., Chen, C.R. and Buddhi, D. (2009). Review on thermal energy storage with phase change materials and applications, *Renewable and Sustainable Energy Reviews* 13, 318–345.
- Sibbitt, B., Onno, T., McClenahan, D. *et al.* (2007). The Drake Landing Solar Community project—early results. Canadian Solar Buildings Conference, Calgary, June 10–14.
- Spitler, J.D. (2005). Ground-source heat pump system research—past, present, and future, *International Journal of HVAC&R* 11 (2), 165–167.
- Susila, B., Chirattananon, S., Sorapipatana, C., Rakkwamsuk, P. and Chaiwiwatworakul, P. (2009). A study on energy efficiency of hotels in Bali, *Proceedings of the World Renewable Energy Congress 2009—Asia: 3rd International Conference on Sustainable Energy and Environment*, Bangkok, Thailand, May 19-23, pp. 143–150.
- UNC-CH (2000). A recent operations research public service project, University of North Carolina at Chapel Hill, <http://www.unc.edu/depts/or/dp/or350/bradford.htm>
- Wong, W.P., McClung, J.L., Snijders, A.L., Kokko, J.P., McClenahan, D. and Thornton, J. (2006). First large-scale solar seasonal borehole thermal energy storage in Canada, Ecostock 2006 Conference, Stockton, NJ.

## Study Questions/Problems

- 8.1 For a liquid water-based CTES case study in this chapter, explain qualitatively how TES is advantageous. Determine quantitatively the benefits, considering such parameters as efficiency, energy utilization, fuel substitution, load shifting, economics, environment, and so on.
- 8.2 Repeat Problem 8.1, but for an actual liquid water-based CTES system in your jurisdiction or a nearby location.
- 8.3 For an ice-based CTES case study in this chapter, explain qualitatively how TES is advantageous. Determine quantitatively the benefits, considering such parameters as efficiency, energy utilization, fuel substitution, load shifting, economics, environment, and so on.



- 8.4** Repeat Problem 8.3, but for an actual ice-based CTES system in your jurisdiction or a nearby location.
- 8.5** For a heating TES case study in this chapter that uses a short-term storage cycle, explain qualitatively how TES is advantageous. Determine quantitatively the benefits, considering such parameters as efficiency, energy utilization, fuel substitution, load shifting, economics, environment, and so on.
- 8.6** Repeat Problem 8.5, but for an actual heating TES system that uses a short-term storage cycle in your jurisdiction or a nearby location.
- 8.7** For a heating TES case study in this chapter that uses a seasonal storage cycle, explain qualitatively how TES is advantageous. Determine quantitatively the benefits, considering such parameters as efficiency, energy utilization, fuel substitution, load shifting, economics, environment, and so on.
- 8.8** Repeat Problem 8.7, but for an actual heating TES system that uses a seasonal storage cycle in your jurisdiction or a nearby location.
- 8.9** For a case study in this chapter considering TES and cogeneration, explain qualitatively how TES is advantageous. Determine quantitatively the benefits, considering such parameters as efficiency, energy utilization, fuel substitution, load shifting, economics, environment, and so on.
- 8.10** Repeat Problem 8.9, but for an actual TES and cogeneration system in your jurisdiction or a nearby location.
- 8.11** For a PCM-based TES case study in this chapter, explain qualitatively how TES is advantageous. Determine quantitatively the benefits, considering such parameters as efficiency, energy utilization, fuel substitution, load shifting, economics, environment, and so on.
- 8.12** Repeat Problem 8.11, but for an actual PCM-based TES system in your jurisdiction or a nearby location.
- 8.13** For a case study in this chapter that uses a ground-based TES, explain qualitatively how TES is advantageous. Determine quantitatively the benefits, considering such parameters as efficiency, energy utilization, fuel substitution, load shifting, economics, environment, and so on.
- 8.14** Repeat Problem 8.13, but for an actual ground-based TES system in your jurisdiction or a nearby location.
- 8.15** For a TES case study in this chapter that involves solar energy, explain qualitatively how TES is advantageous. Determine quantitatively the benefits, considering such parameters as efficiency, energy utilization, fuel substitution, load shifting, economics, environment, and so on.
- 8.16** Repeat Problem 8.15, but for an actual TES system that uses solar energy in your jurisdiction or a nearby location.
- 8.17** Apply the analysis methodology presented in the feasibility study for the hotel in Bali (Section 8.8.1) to a similar facility in your jurisdiction or a nearby location.
- 8.18** Compare qualitatively the sensible and latent TES case studies in this chapter qualitatively. What are their main quantitative differences?
- 8.19** Explain the differences between ice CTES and ice-slurry CTES systems, using data from the case studies considered in this chapter.
- 8.20** For a trigeneration facility, such as the one in Section 8.4.2, what are the three products? For which products could energy storage be applied? List several possible storage options for each storable product. Describe possible applications of TES for a trigeneration facility.



# 9

## Recent Advances in TES Methods, Technologies, and Applications

### 9.1 Introduction

Much research on thermal energy storage (TES) has been carried out over the last decade or so in academe and industry, leading to innovations in TES systems and their applications, as well as advances in such areas as TES types, materials, control strategies, measurement techniques, and macro- to nano-encapsulation processes. Advances in TES systems include new pumpable slurries and microencapsulated phase change materials (MPCMs), which are of interest for applications ranging from building materials to new textiles that improve human comfort. New operation, control, and simulation strategies are under development for many TES applications. Many of the developments are or can be useful to designers.

Environmental issues such as climate change and concerns regarding future use of fossil fuels are increasingly debated by government agencies and the public. Given society's interest in increasing the efficiency and cost effectiveness of energy producing and consuming systems and reducing their environmental impacts, new thermal systems have been introduced, including advanced cooling and heating methods. These are particularly significant since heating, ventilating, and air-conditioning (HVAC) systems in the residential, commercial, and industrial sectors are responsible for a major portion of energy utilization in many countries. Thermal management investigations of energy systems often facilitate performance improvements.

The role of TES is likely to increase given the ability of the technology to help manage the costs and overall system efficiencies of HVAC systems during peak and nonpeak demand periods. For a cooling plant with a typical TES (Figure 9.1), the times and durations of the peak energy demand and production do not usually coincide. Often the price of electricity and some other energy forms varies during the day and seasonally, usually to encourage efficiency and conservation. Solar thermal systems often require TES for periods ranging from daily to seasonal. Cooling technologies usually require cooling capacities sized for peak electrical energy demands during the hottest daily periods. Suitable heat or cold storage enhances such systems by storing energy produced during off-peak periods for use during peak periods. Such load leveling normally reduces HVAC energy costs by permitting increased operating time at relatively lower and more constant capacities. The energy use by an air-conditioning system with and without a suitable cold TES can differ significantly (see Figure 9.2).

### 9.2 Recent TES Investigations

Many TES types and systems for cooling and heating exist and have been examined. TES performance depends on such criteria as type, size, storage medium and heat-transfer fluid (HTF)

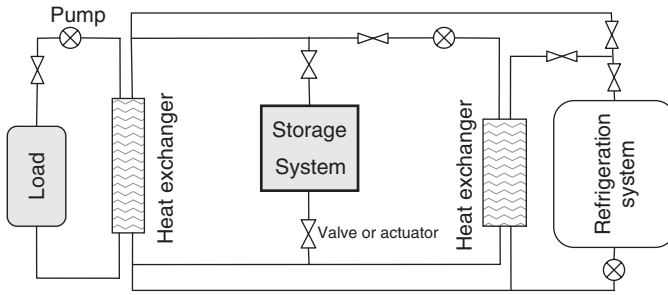


**Figure 9.1** A cooling load serviced by a refrigeration system that incorporates thermal storage

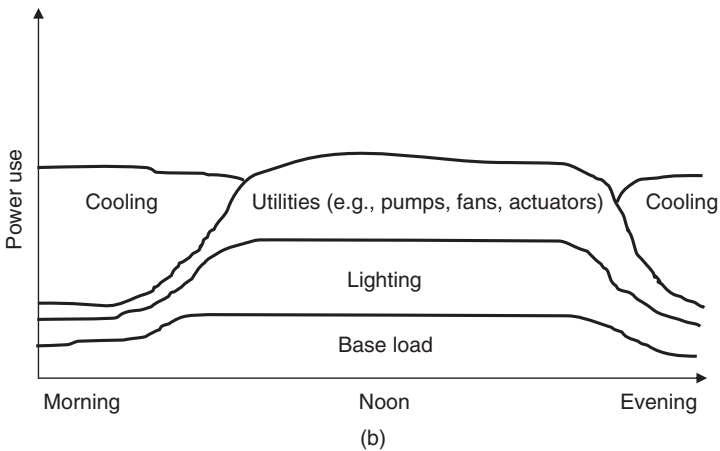
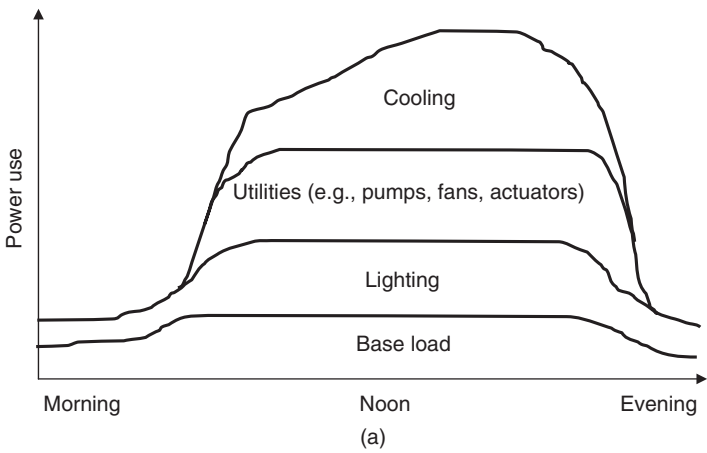


**Figure 9.2** Diurnal variation of electrical power use for a building, illustrating the load leveling capability of cold storage for conventional air-conditioning: (a) with CTES; (b) without CTES

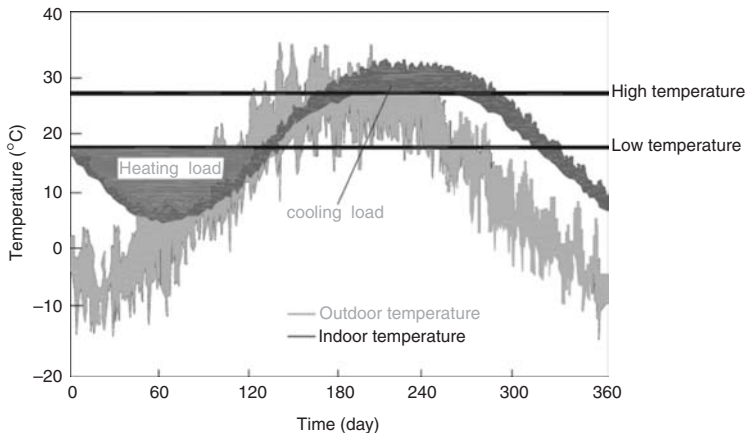


**Figure 9.3** Typical daily variation of indoor and outdoor air temperatures, with heating and cooling load regions identified (modified from Zhang *et al.*, 2007)

materials, ambient temperature, constant or variable working temperatures, and application. Researchers and designers often seek the most effective TES performance parameters for a given heating/cooling facility. The comfort level of buildings can be improved by proper integration of TES with a cooling or heating system.

Thermal storages of various shapes and cross sections filled with phase change material (PCM) capsules have been found attractive for incorporation into heating and/or cooling plants (Cheralathan *et al.*, 2007a). In these storages, an HTF below or above the solidification temperature of the PCM passes through the TES. The capsules vary in shape and size, and are made of such materials as plastics (e.g., polyethylene) and metals, depending on use, demand, and charging/discharging rates. Most PCMs do not have a fixed phase-change temperature, so temperature-dependent enthalpy correlations obtained with calorimetric methods based on nucleation temperatures are often employed (Günther *et al.*, 2007).

Cold thermal energy storage (CTES) can be integrated into an HVAC system actively or passively. Active methods lead to reduced operating costs but are complex, involving components such as pumps, piping distribution lines, heat exchangers, and valves/actuators. Passive methods integrate PCMs with appropriate melting temperatures into building materials such as walls and ceilings, or inside of ducting at suitable locations (e.g., window openings). In some cases, they are used in passive systems to increase heat-transfer rates. Passive systems store cold from night air for daytime cooling, or vice versa. Similarly, passive TES can be used with solar energy, again facilitating effective energy management (Arkar and Medved, 2005). Active and passive cooling/heating can also be utilized together to decrease HVAC energy requirements and operating costs and to improve comfort in indoor living and work spaces (Figure 9.3).

Economic factors play a significant role in the production methods and applications for new TES developments and technological innovations. Also important is thermal management, based on fluid flow, heat transfer, and thermodynamic (including exergy) analysis. These disciplines together enable optimal TES designs within constraints and boundary and environmental conditions (Figure 9.4).

During the past decade, many studies have been carried out on different aspects of TES systems such as PCM and HTF materials, applications, and modeling. Many reviews of these studies have been reported, as outlined in Table 9.1.

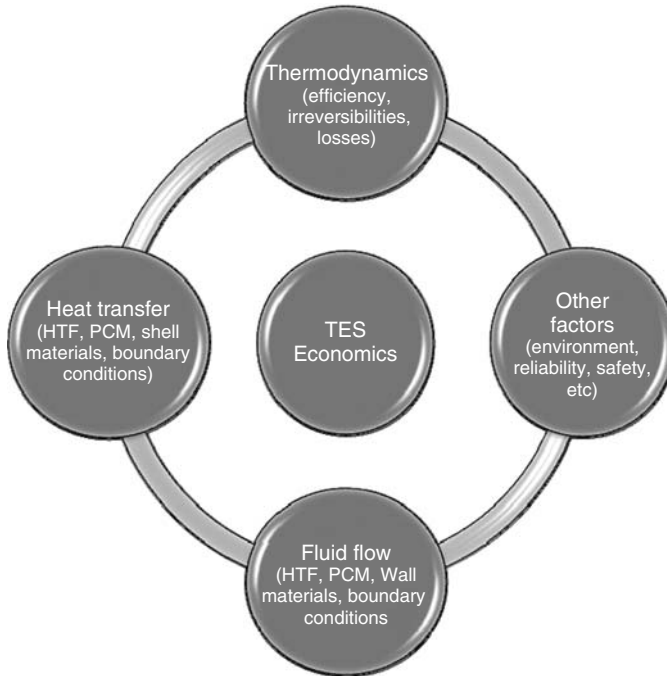


**Figure 9.4** Illustration of the effect on the economics of TES systems and applications of thermofluids and other considerations

### 9.3 Developments in TES Types and Performance

Some of the main aspects of PCMs and HTFs in TES systems are discussed in this section (while integration of thermal storage into HVAC systems is addressed in the next chapter). Important factors affecting storage performance and heating/cooling system operation and efficiency are shown in Figure 9.5.

#### 9.3.1 Developments in PCM/HTF Material Selection

To achieve high efficiencies with TES for various applications, it is necessary to consider thermophysical, environmental, and economic characteristics and criteria. Many of these factors are provided in Table 9.2. Some PCMs do not exhibit a single melting temperature like pure substances. Techniques such as differential scanning calorimeter (DSC) allow evaluation of the temperature–time history of a PCM during heating and cooling. DSC allows the determination of substance properties like melting temperature or range and latent heat. A comprehensive description of DSC method to evaluate the temperature history and properties for ice-slurry melting is reported by Kousksou *et al.* (2006). The melting temperature or range for a latent TES is selected according to the application requirements. This makes latent TES systems more demanding than sensible storages. Higher latent heats of fusion and densities are making some new PCMs more attractive.

PCMs are manufactured under various brand names and others are under development. Some major PCM manufacturers are listed in Table 9.3. The three main groups of PCMs in heating/cooling applications are categorized in Figure 9.6. Various PCMs and their characteristics are summarized in Table 9.4.

**Table 9.1** Recent reviews of investigations of TES systems

Reference	No. papers reviewed	Main topic	Issues covered	Remarks
Verma <i>et al.</i> (2008)	62	Modeling	Mathematical modeling/analysis of latent TES systems with first and second law considerations; review of PCM storage capacities by mass, volume, and energy, and comparison with selected reference material	Recommends comprehensive study of systems with second law to clarify duration of supply/demand heat rates and experimentation to reduce uncertainties of rheological behavior of ice slurries
Regin <i>et al.</i> (2008)	70	PCMs	Types of organic/inorganic, fatty acids and commercial PCMs; macro- and microencapsulation; applications of TES systems	Reviews heat transfer in capsules of varying geometries and packed-bed storage
Zhang <i>et al.</i> (2007)	67	Building applications	TES applications and PCMs for building applications, load shifting, and storing natural cooling by night ventilation	Advantages: reduced diurnal temperature fluctuations, energy use, costs, and difference in peak and nonpeak electrical loads; increased comfort
Kitanovski <i>et al.</i> (2005)	54	Ice slurry	Fine crystalline ice slurry fluid dynamics, empirical and semiempirical friction factors, pressure drops for flow patterns	Identifies need for comprehensive understanding of time behavior of ice slurry, especially for stratified flows
Egolf and Kauffeld (2005)	45	Ice slurry	Ice slurries' properties, applications, and generators	—
Sharma and Sagara (2005)	>250	PCM applications	Measurement techniques; corrosion; thermal cycles and heat-transfer enhancement	Applications for new PCMs with various specifications and advantages/disadvantages for TES applications
Davies (2005)	18	Ice slurry	New applications of pumpable ice slurries; innovative applications for food chilling and freezing	Describes fire fighting using nozzle spray of ice slurry and heat-transfer equipment for special applications (e.g., milk cooling, sensitive semiconductor instrument cooling)
Zalba <i>et al.</i> (2003)	237	PCMs	PCM thermophysical properties, measurement methods, and stability; list of 150 general and 45 commercial PCMs	Describes TES applications for conservation and transportation of sensitive materials (e.g., medicines)

(continued overleaf)

Table 9.1 (continued)

Reference	No. papers reviewed	Main topic	Issues covered	Remarks
Saito (2002)	140	Applications	Load leveling in countries with TES; ice-making systems; simulation and control	Considers sensible and latent TES and static and dynamic ice making
Novo <i>et al.</i> (2010)	>30	Seasonal TES	Techno-economic feasibility of artificial large basins as heat/cold underground TES; aquifer, borehole, cavern, pit, and tank storage	Provides advantages and disadvantages and technical data for underground TES systems in Europe; compares storage media and concepts and their required geological aspects
Xin <i>et al.</i> (2009)	53	Building envelopes	Passive and active TES systems via incorporating PCMs in building envelopes	Describes building-envelope PCM selection for enhancing building thermal performance and design factors: energy storage capacity per area, properties, and economics
Dincer (2002)	–	TES in buildings	Technical and environmental aspects of energy-saving techniques, with energy and exergy design and optimization	Identifies ability of exergy economics to meaningfully assess designs and amendments
Mehling <i>et al.</i> (2007)	–	PCMs in buildings	PCM building applications to reduce daily temperature fluctuations and store free energy (e.g., cold outside night air, solar radiation) or cheaper energy (e.g., nonpeak electricity)	Identifies melting temperature and heat capacity as main design and material selection criteria, and ability of PCMs in buildings to reduce energy storage volume by over 30%
Zhu <i>et al.</i> (2009)	>100	PCM in buildings	Performance and dynamic characteristics of buildings using PCMs for free cooling, active and passive cooling, and peak-load shifting; modeling and simulation with experimental data	Clarifies economic and comfort aspects of using PCMs via dynamic response of building thermal mass, based on various PCM installations
Gil <i>et al.</i> (2010)	>120	Power generation	Organic and inorganic materials for sensible liquid/solid and chemical storage; modeling methods; storage concepts	Identifies the few high-temperature TES installations for power generation in the world and their HTFs
Medrano <i>et al.</i> (2010)	>30	Power generation	Existing and planned active and passive storages; high-temperature TES for power generation	Summarizes materials used in high-temperature solar power generation and their advantages/disadvantages

Agyenim <i>et al.</i> (2010)	>130	Latent TES	PCM types for various temperatures: domestic heating/cooling (0–60 °C), applications <120 °C (e.g., LiBr/H <sub>2</sub> O absorption chiller), and solar high-temperature direct/indirect steam power plants	Identifies need for common testing procedure for PCM thermophysical properties; enhancing PCM heat transfer and conductivity for PCM materials and containers
Kemisarin (2010)	>100	High-temperature PCMs for solar energy	Thermophysical properties of PCMs (metal alloys and metallic salts such as fluorides, chlorides, hydroxides, nitrates, carbonates, vanadates, molybdates) with melting temperatures of 120–1000 °C and chemical compatibilities with containers	Notes importance of reliability and stability over multiple thermal cycles and price in PCM selection, and potential of graphite to improve low thermal conductivity of the salts provided thermal stability can be demonstrated
Singh <i>et al.</i> (2010)	52	Packed-bed TES systems	Storage material, heat-transfer enhancement, flow phenomenon and pressure drop in solar air heater	Considers mainly rocks and pebbles in packed-bed sensible storages
Sharma <i>et al.</i> (2009)	>30	Solar cooker with TES	Thermophysical properties of TES materials, and direct and indirect techniques for solar cookers for late evening cooking	Notes that a high portion of energy consumption (over 35%) in India is for cooking; considers latent TES
Muthusivagami <i>et al.</i> (2010)	~20	Solar cooker with TES	Direct (e.g., concentrating) and indirect solar cookers with 120 °C application temperatures, single and community (multiuser) design concepts, and indoor/outdoor solar cookers	Presents a novel PCM-based storage solar cooker concept
Haller <i>et al.</i> (2009)	>30	Stratification efficiency	Procedures to determine sensible TES stratification efficiency for a complete thermal cycle and efficiency comparisons	Describes need for efficiency determination to reflect heat losses and entropy generation through mixing
Shukla <i>et al.</i> (2009)	–	TES in solar water heater	Types of collectors and storage sensible/latent materials, especially PCMs	Greater PCM latent heat and surface area provide better thermal performance; commercial systems are lacking

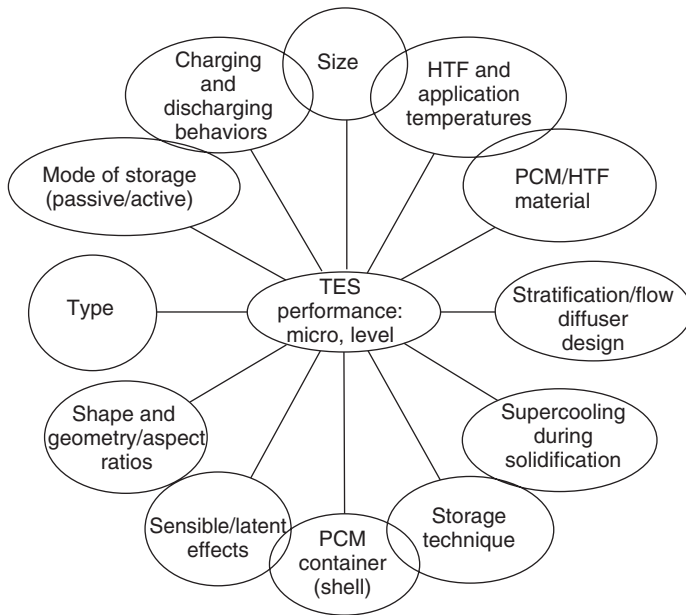


**Figure 9.5** Parameters that affect TES performance at the micro level

**Table 9.2** Selection criteria for PCMs<sup>a</sup>

Factor	Property type	Remarks
Melting point or range	Thermal	Near-water-melting temperature is preferred for active CTES conventional HVAC systems and 15–23 °C for passive cooling/night ventilation systems
Latent heat	Thermal	Substantial latent heat is desirable and a small difference between melting and solidification temperatures increases the system charging efficiency
Thermal stability	Thermal	The ability is desired to repeat over many cycles the same melting/solidification thermal performance during charging/discharging
Thermal conductivity	Thermal	A higher thermal conductivity is preferred, especially for solid PCMs for CTES systems
Supercooling	Thermal	Supercooling can reduce CTES performance during charging
Density/thermal capacity	Physical/Thermal	Higher values are preferred
Flammability	Physical	Lower values are preferred
Physical stability	Chemical	The ability is desired to attain the same performance and exhibit the same chemical properties during many charging/discharging cycles
Environmental impact	Environmental	Lower values are preferred
Toxicity	Environmental	A low value is preferred
Availability and price	Economic	High availability and low price are preferred

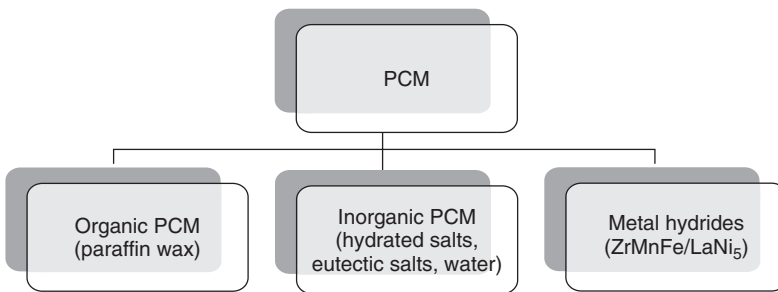
<sup>a</sup>Adapted and extended from Nagano *et al.* (2003).



**Table 9.3** Some of the major PCM manufacturers<sup>a</sup>

Manufacturer	Melting range (°C)	Number of PCMs
EPS Ltd. (www.epsLtd.co.uk)	−114 to 164	61
Rubitherm (www.rubitherm.de)	−3 to 100	29
TEAP (www.teappcm.com)	−50 to 78	22
Cristopia (www.cristopia.com)	−33 to 27	12
Climator (www.climator.com)	−18 to 70	9
Mitsubishi Chemical (www.mfc.co.jp)	9.5 to 118	6
Döerken (www.doerken.de)	−22 to 28	2
Merck (www.merck.de)	N/A	N/A
BASF (www.basf.com)	N/A	N/A

<sup>a</sup>For details see (Agyenim *et al.*, 2010).

**Figure 9.6** Main PCM categories (modified from Nagano *et al.*, 2003)

He and Setterwall (2002) have investigated aspects of technical grade paraffin waxes for CTES systems. Using economic and technical results, these authors suggest the use of CTES to achieve four goals in industrial or urban sectors: reducing cooling-system operating and initial costs, downsizing chilling equipment, adding operational flexibility, and expanding chilling-system capacity. Paraffin waxes are saturated hydrocarbon mixtures of *n*-alkane chains ( $\text{CH}_3-(\text{CH}_2)_n-\text{CH}_3$ ). The crystallization of the  $(\text{CH}_2)_n$  releases heat. The melting temperature and the latent heat of fusion both increase with the chain length. Paraffin waxes are available to meet a variety of melting temperatures, depending on the system operating temperature. Rubitherm (RT) is the brand name of a commercially available wax. RT5 is usually chosen as a PCM for mild-temperature cold storage systems with a melting range of 5–10 °C. Zalba *et al.* (2003) have reviewed 45 commercially available PCMs and over 150 materials that provide a comparative reference for different organic/nonorganic PCMs and a criteria-based PCM classification. Nagano *et al.* (2003) have investigated the thermal behavior of manganese (II) nitrite hexahydrate ( $\text{Mn}(\text{NO}_2)_2 \cdot 6\text{H}_2\text{O}$ ) as a new PCM for CTES systems, and discussed ways to reduce its supercooling with a melting point of 15–25 °C as well as price and safety issues. Roxas-Dimaano and Watanabe (2002a) have investigated a capric–lauric acid mixture (65/35%) with chemical additives to reduce its melting temperature of 18 °C for some CTES applications. Roxas-Dimaano and Watanabe (2002b) have also studied capric and lauric acid based PCMs to assess heat storage performance for CTES.

### 9.3.2 Shape

The shapes of a PCM container (shells or capsule) can have a significant effect on heat-transfer rate and pressure losses of the flowing HTF, which in turn have an important role in the efficiency and

**Table 9.4** Characteristics of selected PCMs for TES systems

Reference	Major investigation	Method and results	Recommendations
Tyagi and Buddhi (2008)	Thermal cycle testing of calcium chloride hexahydrate ( $\text{CaCl}_2 \cdot 6\text{H}_2\text{O}$ ) as a new PCM	Differential scanning calorimeter (DSC) measurement to find melting temperature and latent heat of fusion	Promising material for different cooling/heating applications ( $T_{\text{melt}} \approx 24^\circ\text{C}$ )
Nagano <i>et al.</i> (2003)	Thermal response of manganese (II) nitrate hexahydrate ( $\text{Mn}(\text{NO}_3)_2 \cdot 6\text{H}_2\text{O}$ ) as a new PCM, its price, and safety concerns	Methods to determine PCMs for CTES applications; decreasing supercooling by dissolving small amount of salts; commercial PCMs and additives, and their properties	A promising method with a good melting range ( $15\text{--}25^\circ\text{C}$ ). $\text{MnCl}_2 \cdot 4\text{H}_2\text{O}$ found to be a good nucleating agent
Abraham <i>et al.</i> (2003)	Performance characteristic of metal hydride $\text{ZrMnFe/LaNi}_5$	A new PCM for CTES and some other applications	PCM applications of this metal hydride include deep freezing, ice making, HVAC, and heat pumps
Roxas-Dimaano and Watanabe (2002a)	Capric-lauric acid mixture (65/35%) with chemical additives for CTES applications	DSC is referred to as a standard test to determine the thermal behavior of PCM mixtures	Organic additives such as methyl salicylate, eugenol, and cineole lower the melting temperature from $18^\circ\text{C}$ , increasing suitability for CTES
He and Setterwall (2002)	CTES savings of initial and capital costs with proper PCM	RT5 with a freezing point of $7^\circ\text{C}$ and $158.3\text{ kJ/kg}$ heat of fusion is a cost effective material for CTES systems	Capital cost of new PCMs should be considered before final selection

performance of a TES system. Several investigations have been reported of PCM container shapes and their impact on a TES system. Bony and Citherlet (2007) performed a numerical simulation for three PCM capsule shapes (cylinder, sphere, and thick plate) submerged in a water storage tank to extend the capabilities of TRNSYS, a transient simulation software package developed by the University of Wisconsin. TRNSYS includes weather data and thermal and electrical system modules which can be connected to simulate equipment arrangements. Hysteresis and supercooling effects have been added for both vertical and horizontal tank configurations. Vyshak and Jilani (2007) have investigated the phase-change time (melting) for a PCM in three vessels (cylinder, rectangular cube, and cylindrical shell), which have the same volume and external surface exposure to a HTF. Different inlet HTF temperatures were also considered. It is found that the cylindrical shell needs the least amount of time for charging, for a fixed storage energy, and that it is the most sensitive shape to the HTF inlet temperature.

### 9.3.3 Nano- to Macro-Size Storage Media or PCM Particles and Capsules

Thermal storage medium sizes usually vary from some cubic centimeters to some cubic meters depending on the application for heating or cooling purposes. Many studies based on the size of the storage medium, PCM, or storage container have been reported on TES systems. Mawire *et al.* (2010) investigated the pebble glass bed as a rapid sensible thermal storage for cooking and heating in solar concentric systems. Data from experiments on these PCM sizes have been compared with packed-bed/gas (e.g., air) simulations. Oil and pebble average temperatures (100–300 °C) have been found for different charging rates. The charging flow rate depends on the volumetric heat-transfer coefficient, and a relation has been found experimentally among HTF mean velocity, average pebble diameter, and volumetric heat-transfer rate. As water is not a good choice for storage temperatures above 100 °C (unless expensive pressurizing is added), oils have been utilized in solar collector systems for heating purposes. Mawire and McPherson (2009) simulated and verified experimentally a sandy pebble/oil TES system for a variable heat source, determining the axial temperature distribution for the system. Sandy pebbles can also be used as sensible storage media for cooking with an oil HTF. Rady (2009a) studied the performance of granular bed pebbles in the 1–3 mm diameter range. DSC and temperature history (*T*-history) methods have been used to determine phase-transition characteristics (melting point, latent heat, and total heat energy capacity) considering granular (pebble) PCM particles. In another study, Mawire *et al.* (2009) investigated three pebble materials (silica, glass and alumina), and determined the ratio of total exergy to the total energy stored and the thermal stratification performance. Silica exhibited better thermal stratification and alumina demonstrated the highest total stored exergy to energy ratio variations over the duration of the experiment, and initially charged the most rapidly.

PCM size has a significant effect on heat transfer rates between PCMs and HTFs, and affects the HTF pressure drop. PCM particle (or capsule) size also affects the total heat capacity of a flowing fluid in which tiny PCM particles are dispersed as a secondary refrigerant. As these factors affect the performance of a plant integrated with a TES system, the impact of PCM size is evident. Microcapsules can be created for some PCMs, allowing them to be part of the HTF (e.g., pumpable encapsulated PCM slurries). In such instances, PCM particles or capsules vary in size from some nanometers to a couple of millimeters.

Various factors should be considered in developing a new microencapsulated PCM (Özonur *et al.*, 2006):

- particle size profile (spectrum);
- mean particle size;
- surface characteristics and morphology of the particles (or capsules);
- phase-transition temperature (range);

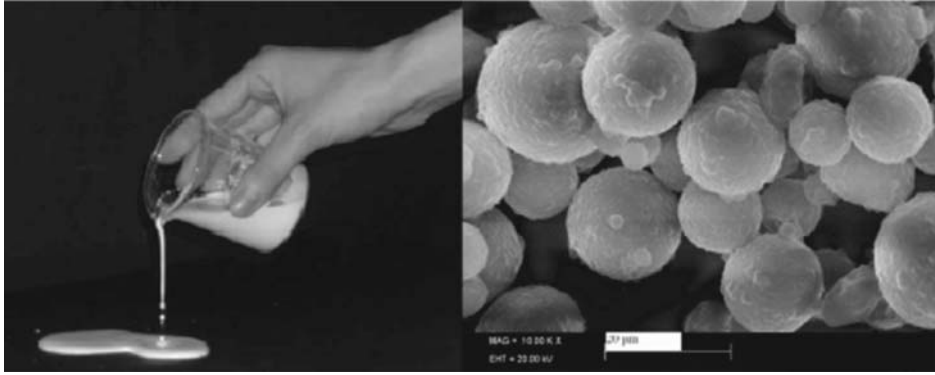


**Figure 9.7** Flowing microencapsulated PCM as a phase-change slurry (Wang *et al.*, 2008a)

- chemical nature (shell and PCM core material specifications);
- stability;
- thermal and mechanical cycling reliability and durability (e.g., during melting/freezing or continuous pumping);
- volumetric change during thermal cycles.

The heat-transfer interface between a HTF and PCM can be increased by reducing PCM particles' (or capsules') sizes and mixing them into the HTF homogeneously, thereby creating a phase-change slurry as the secondary refrigerant (Figure 9.7). Such slurries can be produced by a coacervation process, in which a microsize droplet (1  $\mu\text{m}$  to 1 mm diameter depending on the agitation/mixing process) of an organic substance such as oil or paraffin wax is held by hydrophobic forces from a surrounding liquid. MPCM slurries have different applications from functional thermoregulated fibers (used in textile industries), solar energy, and heat-transfer enhancement to various material usages in agriculture, biology, and building industries (Su *et al.*, 2005). DSC and other measurement procedures have recently been suggested for evaluating MPCM thermal properties and their durability. Table 9.5 shows several innovative MPCMs and their recent uses, especially as pumpable phase-change slurries.

The procedures required before introducing a new MPCM into an industrial application have been described (Alvarado *et al.*, 2007).

The many physical and chemical steps and procedures to produce MCPMs can be categorized on the basis of the following production methods:

- coacervation (chemical) (Özonur *et al.*, 2006) and solvent evaporation–precipitation (physical) (Salaün *et al.*, 2010),
- blending and comparison molding (Li *et al.*, 2009a),
- interfacial polycondensation (Zhang and Wang, 2009),
- phase separation (Yang *et al.*, 2009).

Most MPCMs are prepared through a multistep technique that can be illustratively summarized as follows:

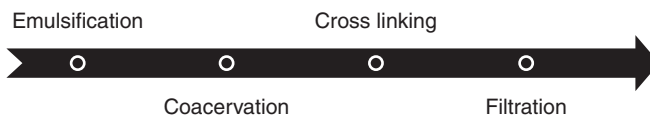


**Table 9.5** Some innovative microencapsulated PCMs

Reference	PCM	Application	Remarks
Chen <i>et al.</i> (2008)	Industrial-grade 1-bromohexadecane (C <sub>16</sub> H <sub>33</sub> Br)	Secondary refrigerant	Water-based MPCM slurry; 15.8% heat-transfer enhancement over water, reducing pump power for same heat transfer
Wang <i>et al.</i> (2008a)	Hexadecane (C <sub>16</sub> H <sub>34</sub> ) particles and pure water	Evaporative cooling system	Water-based MPCM slurry; chiller energy saving for five climates; melting temperature 18.1 °C; latent heat 224 kJ/kg
Alvavado <i>et al.</i> (2007)	<i>n</i> -Tetradecane and 1% gelatin	Secondary refrigerant	PCM is encapsulated through coacervation; heat transfer is enhanced
Sarier and Onder (2007)	Four polymerized polyurea-formaldehyde microcapsules containing different waxes	Thermally enhanced textiles and fabrics for cold weather and physical activity conditions	Provides a thermal barrier in which ambient heat is absorbed by the outer layer, and skin temperature is maintained constant by the inner layer in cold weather
Su <i>et al.</i> (2005)	Melamine-formaldehyde polymer core; styrene maleic anhydride copolymer solid dispersant, and nonionic surfactant emulsifier	Reducing supercooling for CTES applications	Latent heat of fusion of 225.5 kJ/kg and 24 °C melting temperature; 5–10 μm average diameter microcapsules, with smooth and compact globular surface
Gschwander <i>et al.</i> (2005)	Water-based microencapsulated paraffin phase-change slurry	Suitable for small temperature differences above 0 °C	Stability and durability of the slurry and micro-PCM particles tested for conditions like continuous pumping
Özonur <i>et al.</i> (2006)	Natural coco fatty acid mixture	Building materials (passive TES)	Manufactured by coacervation with a capsule wall; structural integrity maintained after 50 freeze/melt cycles; gelatin/gum arabic found to be the best capsule wall material
Salatin <i>et al.</i> (2010)	A hydrated salt (sodium phosphate dodecahydrate)	Textile fabrics	Physical method (solvent evaporation/precipitation from interfacial polymerization) to prepare microcapsules from organic solvents and cellulose acetate butyrate crosslinked by methylene disocyanate as coating polymer
Sari <i>et al.</i> (2009)	<i>n</i> -Octacosane in polymethylmethacrylate microcapsules	Pumpable water-based secondary refrigerant (MPCM slurry)	Good thermal reliability over multiple thermal cycles with a melting/freezing temperature range of 50.6–53.2 °C and a latent heat range of 86.4–88.5 kJ/kg

(continued overleaf)

Table 9.5 (continued)

Reference	PCM	Application	Remarks
Li <i>et al.</i> (2009a)	Microencapsulated paraffin, high-density polyethylene wood flour supporting material	Form-stable building materials	Micro-mist graphite dispersion enhances thermal conductivity by 17.7%; PCM leakage is prevented by the shell and the matrix materials; stable for more than 100 thermal cycles
Fang <i>et al.</i> (2009)	Nano-encapsulated <i>n</i> -tetradecane. Micro-/nano-capsules of organic oil compounds	Heat-transfer enhancement	NaCl additive improves thermal stability; nano-capsules of 100 nm, with 100–130 kJ/kg latent heat (maximum 134.16 kJ/kg) at 5–9 °C phase transition temperature
Yang <i>et al.</i> (2009)	<i>n</i> -Teradecane with different shell materials	Building materials	Shell materials: acrylonitrile–styrene copolymer (best), acrylonitrile–styrene–butadiene copolymer and polycarbonate; particle sizes < 1 μm, latent heat > 100 kJ/kg
Zhang and Wang (2009)	<i>n</i> -Octadecane with polyurea shells containing soft segments	Thermo-regulating fibers, fabrics, textiles, foam, and building materials	18–36 °C phase-change temperature range is suitable for comfortable fabrics
Li <i>et al.</i> (2010)	Paraffin/silicon dioxide (SiO <sub>2</sub> ) composites	Waste heat recovery, solar heating systems	SiO <sub>2</sub> supporting material for shape-stabilized PCM with a melting/freezing temperature of 57.07/58.10 °C and latent heat of 59.66/139.59 kJ/kg
Sari <i>et al.</i> (2010)	<i>n</i> -Heptadecane with transparent acrylic polymer shell of polymethyl methacrylate	TES systems	Melting/freezing temperature range is 18.2–18.4 °C and latent heat range is 81.5–84.2 kJ/kg
Fang <i>et al.</i> (2010)	Paraffin encapsulated by gelatin and acacia shell	Heat TES systems	Capsule size of 81 μm with a melting/freezing temperature of 52.05–59.68 °C and latent heat range of 121.59–141.03 kJ/kg
Huang <i>et al.</i> (2009)	Pumpable paraffin/water emulsions	Comfort cooling/secondary refrigerant	Temperature range is 0–20 °C; tested for mechanical and thermal stability; 30–50 wt% paraffin is suitable for CTES
Chaiyasat <i>et al.</i> (2008)	<i>n</i> -Hexadecane encapsulated in crosslinked polymer shells	Heat TES systems	Water formation in capsules during solidification (15 °C) penetrates capsules and affects thermal properties

Here, an aqueous solution is emulsified by stirring and adding emulsifiers, and a surfactant material is added during stirring. Emulsifiers have different ends (hydrophobic and hydrophilic segments). A polymer shell is added to the solution to cover the small PCM particles surrounded by emulsifier molecules. The MPCM is ready after filtration.

### 9.3.4 Recent Advances in TES Types and Storage Techniques

Over the past two decades, new types of TES have been introduced for various applications and situations, incorporating production and storage techniques. Many practical advanced TES types and their production techniques are described in this section.

#### Sensible Solid TES for Solar Parabolic Trough Power Plants

Laing *et al.* (2006) investigated the use of a synthetic oil HTF and a solid storage medium with a capacity of 350 kWh at 390 °C as a TES for a solar parabolic trough power generation plant. A tubular heat exchanger is integrated in concrete and ceramic, with densities of 2750 and 3500 kg/m<sup>3</sup> and heat capacities of 916 and 866 J/kg K, respectively. Ceramic has been shown to be a 35% more conductive storage medium with 20% more heat capacity (Figure 9.8a). The performance of the system (Figure 9.8b) based on the heat exchanger design (e.g., number of tubes or tube diameter) has been evaluated numerically. Both storage materials are found to be suitable as PCMs but the concrete is less expensive.

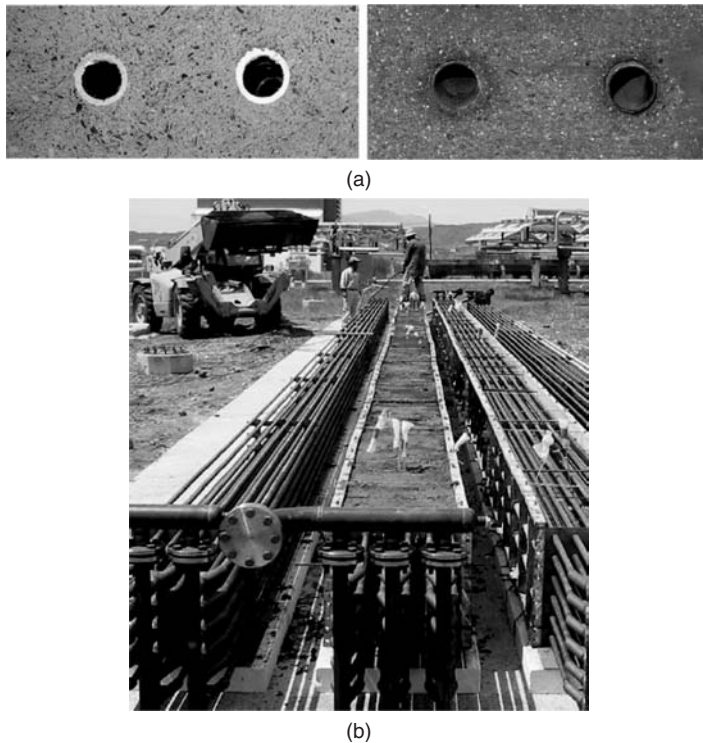


**Figure 9.8** (a) Tube heat exchangers inserted in high-temperature concrete (left) and ceramic (right); (b) concrete-sensible TES system with distribution tubes and heat-transfer fluid collectors (Laing *et al.*, 2006)



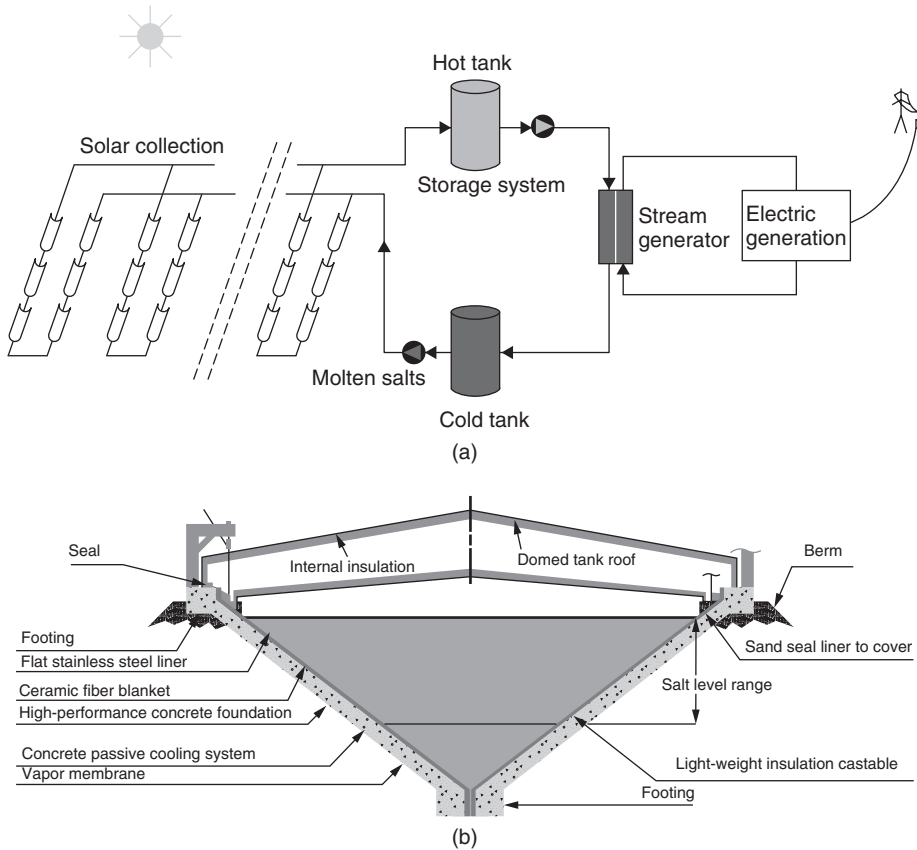


**Figure 9.9** (a) Schematic of a parabolic-trough solar steam generating and salt thermal storage and (b) conical concrete salt storage system (modified from Salomoni *et al.*, 2008)

Salomoni *et al.* (2008) have investigated an innovative concrete storage tank for molten salt in a two-tank storage solar power plant in Barstow, California. The hot tank is partially buried in the ground to store molten nitrate salt at  $565^{\circ}\text{C}$  (Figure 9.9). The concrete durability for exposure over long periods to high temperatures has been investigated numerically.

### Ice Slurries to Microencapsulated PCM Slurries

Ice slurry is a high-density energy carrier that is used in some TES systems. The slurry is usually made from a water-based (aqueous) emulsion that is cooled to generate ice particles in different sizes within the heat-transfer medium. Various additives, emulsifiers, and depressants are added to these HTFs. Two main types of ice-slurry generators exist: static and dynamic. Some of the main measures to enhance ice-slurry generation involve the use of (Stamatiou *et al.*, 2005):

- direct contact systems to reduce heat exchange barriers. A refrigerant directly evaporating in a slurry feed solution (as an evaporator) provides enhanced mixing and heat transfer;
- periodic ice removal, typically using mechanical methods like ice-crushing, scraping, or brushing;



- supercooling, which can disperse the locations where ice crystal nucleation is initiated via such techniques as ultrasound waves, mechanical shocks, or other nuclei seeding methods;
- depressants, such as alcohols (e.g., ethanol), mixed in the water.

At the triple point, ice crystal growth is initiated by any vapor formation in pure water, whereas at the adiabatic condition of this fast phenomenon, heat extraction from the water forms the crystals. This phenomenon causes ice adhesion to the heat exchanger walls in the case of pure water. Depressants are more volatile than water, allowing them to be used as additives to prevent ice formation on heat exchanger walls. Special coatings on the slurry side of a heat exchanger wall can also prevent ice adhesion. In order to study the physics of ice-slurry generating methods, a substantial knowledge of crystal growth and nucleation is needed.

A static ice maker that freezes ethylene glycol on an inclined polyvinyl-chloride (PVC) plate submerged in a brine solution has been studied experimentally by Hirata *et al.* (2002). The PVC plate is cooled by another lower copper plate. The ice crystals grow and join, slide along the plate, and are removed by buoyancy forces. A larger inclination allows ice sheet production rather than individual crystal growth and easier removal. Another static ice maker has been investigated experimentally by Hirata *et al.* (2004) for freezing an ethylene glycol solution on a vertical, cooled PVC plate. Greater ice crystal formation is observed for vertical rather than horizontal plates submerged in brine and cooled by an adjacent conductive plate. Hirata *et al.* (2003) also investigated ice formation around vertical cylinders and its removal, using numerical simulation and experimental verification. The crystal growth rate in all cases depends on the heat-transfer rates to the plates and to the brine through the external surface. Higher cooling rates may cause ice adhesion to the surface. Cylinder length is an important design factor, since ice removal is easier for shorter lengths. Stirring of the brine facilitates ice removal. Transport equations have been solved numerically to model ice crystal growth on a vertical wall in contact with water (Ismail and Radwan, 2003), showing that the wall Nusselt number (which is an indicator of heat transfer) depends on the Stefan number (which reflects ice crystal concentration).

On the basis of a review of rheology, flow behavior, and heat transfer for ice slurries as a secondary refrigerant, Ayel *et al.* (2003) listed ice-slurry rheological behavior according to flow type (Newtonian/non-Newtonian). A comprehensive pressure drop analysis is presented for horizontal pipes, and heat-transfer measurements are reviewed. Vane-in-cup rheometers are used to measure ice-slurry shear-stress rate variation to better measure viscosity. The significance is identified of flow regime (Figure 9.10) on the heat transfer coefficient in slurry flows, and heat exchanger geometry modification is utilized to enhance heat-transfer rates. Oda *et al.* (2004) presented a dynamic ice-slurry maker based on a water–oil mixture and a silane coupler (a surfactant) as an additive to produce an emulsion. The mixture is cooled in a fluoroplastic tube (e.g., perfluoroalkoxy or

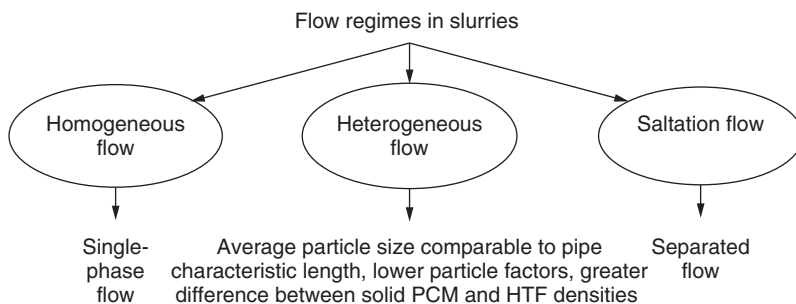


**Figure 9.10** Flow types in slurry suspensions (adapted from Ayel *et al.*, 2003)

polytetrafluoroethylene (PTFE)) to produce ice slurry continuously for storage. The concept demonstrated better heat transfer and production rates and reduced ice adhesion to the heat exchanger wall compared with methods using PVC tubes or ethylene glycol aqueous mixtures.

Yamada *et al.* (2002) proposed a slush-ice production method, in which ice slurry is produced in a rotating cooled tube submerged in a brine mixture. An auxiliary oscillatory rotation is added to the tube to enhance ice removal. The production performance has been evaluated numerically and experimentally by introducing an ice packing factor (IPF), which is the ratio of total ice mass to initial solution mass, and considering the effects of brine initial concentration, angular acceleration, rotation angle for the cooled tube, and oscillating tube motion. Higher values of angular acceleration, rotation angle, and solution concentration result in more convenient ice separation and a higher IPF.

A dynamic ice-slurry production method has been presented by Chibana *et al.* (2002) for a water/silicone oil emulsion flowing in a spiral tube heat exchanger. The effects of brine flow rate and temperature and wall conductivity on production performance are assessed. For continuous slurry production conditions, ice adhesion (choking) was avoided. A silane-coupler agent ( $\gamma$ -aminopropyltriethoxysilane:  $\text{NH}_2\text{C}_3\text{H}_6\text{Si}(\text{C}_2\text{H}_5\text{O})_3$ ) was used to make the emulsion. The thermal resistance of the tube can be altered to improve the refrigerator coefficient of performance (COP) and the slurry production rate, with a smaller tube thickness recommended. For high thermal resistance tubes, ice-slurry production can be achieved for low Reynolds numbers and high heat removal fluxes.

Bellas *et al.* (2002) experimentally investigated the melting heat transfer and pressure drop of an ice slurry (5% aqueous propylene mixture) flowing in a plate heat exchanger. Decreasing the flow rate or ice fraction reduces the pressure drop. Heat transfer is 30% greater than that for a single-phase liquid flow, and can increase further at higher flow rates. Ice fraction, ice crystal size, Reynolds number, and flow geometry influence the total heat transfer. To increase IPF without ice adhesion to the cooling walls, Matsumoto *et al.* (2002) proposed two additives, an amino group ( $\text{NH}_2$ ) and a silanol group ( $\text{SiOH}$ ), for a water/oil mixture. A decrease in freezing point evaluated with a DSC method showed that the ice in the slurry is a compound of the ice additive and not pure water. These authors also used numerical modeling and experimental verification to assess unsteady homogeneous ice-slurry behavior and to assess the effect of antifreeze additive mass fraction and cooling rate on slurry production. Matsumoto *et al.* (2004) proposed a continuous ice-slurry generation method using a 10% silicon oil aqueous mixture emulsified by adding a small amount of silane coupler (i.e., 4% by weight  $\gamma$ -aminopropyltriethoxysilane). Larger ice particles are produced (2.2–3.5 mm) than with conventional ice-slurry generation methods. Ice particle size can be increased by decreasing supercooling and cooling rate. Matsumoto *et al.* (2006) subsequently proposed operating conditions to improve the performance of the method.

A direct contact evaporator is another device for ice-slurry production. Kiatsiriroat *et al.* (2003) experimentally investigated heat transfer with a lumped method in a water tank that acts as a direct contact evaporator, and into which a refrigerant (R12/R22) is injected. Dimensionless heat-transfer correlations involving Stanton, Prandtl, and Stephan numbers and pressure ratio are obtained, and indicate that the proposed method achieves a high heat-transfer rate. Wijesundera *et al.* (2004) investigated the same ice-slurry production method using direct contact of water with refrigerant Fluorinert (FC-84). Production performance heat-transfer rates have been analyzed for this inert coolant, which has a higher density and lower freezing point than water, by varying the position of the coolant nozzle in the water tank (from top to bottom) and the spray pattern (vertical/inclined). Thongwik *et al.* (2008) numerically and experimentally investigated ice-slurry production by direct injection of carbon dioxide at a range of temperatures ( $-15$  to  $-60^\circ\text{C}$ ) into water, and obtained high energy efficiencies and heat-transfer rates. To avoid nozzle blockage, ice slurry is produced rather than pure ice by adding oil to the water tank, for an appropriate water/oil mixture composition (Figure 9.11).

Hong *et al.* (2004) experimentally demonstrated for an ice-slurry production method that high concentrations yield smaller particles and higher supercooling degrees, and ice adhesion to the wall

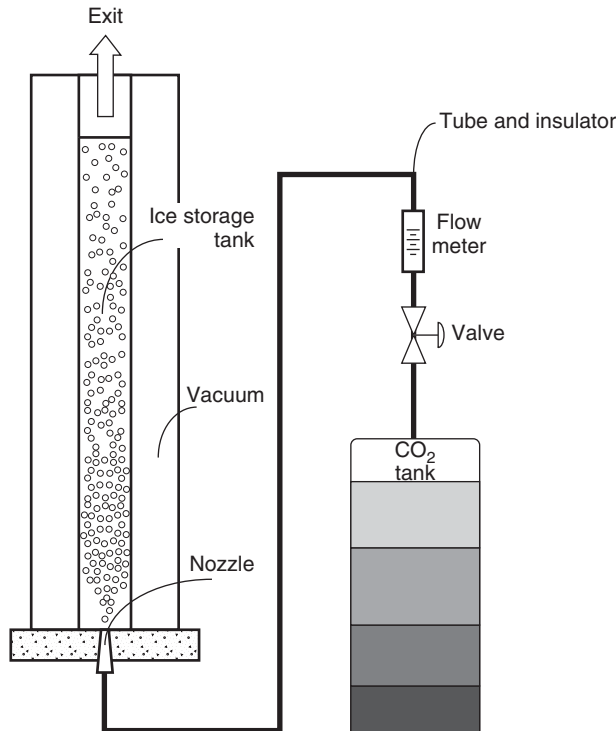


**Figure 9.11** Experimental system for direct contact (water/CO<sub>2</sub>) ice production (modified from Thongwik *et al.*, 2008)

can be prevented by appropriate stirring power or other agitation and particle size as well as use of an additive.

Ostwald phenomena (ripening, agglomeration, and attrition) change the size distribution of ice crystals during long storing periods. Attrition leads to the formation of secondary particles when stresses become sufficiently large to cause the original crystal to break apart, as a result of the actions of impellers and pumps or wall shear stress (friction). Over time, crystals tend to merge as a result of surface tension, but such agglomeration can be inhibited by agitation (Stamatiou *et al.*, 2005). These factors affect the performance and efficiency of ice-slurry CTES systems, and it is generally desirable to avoid their detrimental effects by not storing slurries for long durations. Pronk *et al.* (2005b) modeled Ostwald ripening in an ice-slurry storage tank through crystal growth kinetics, and obtained numerically and validated experimentally ice crystal size distribution.

Various dynamic ice-slurry production techniques exist, and most continuous ice-slurry generation methods have been reviewed by Stamatiou *et al.* (2005), especially those with moving parts such as scraper blades or orbital rods and also fluidized-bed ice-slurry generators (Figures 9.12 and 9.13).

Thermal and physical characteristics and behaviors of ice slurries have been studied recently (Matsumoto and Suzuki, 2007; Ionescu *et al.*, 2007; Rached *et al.*, 2007; Niezgodna-Żelasko and Żelasko, 2007; Pronk *et al.*, 2005a; Egolf *et al.*, 2005), especially those that significantly affect the performance of CTES systems: pressure drop, deposition velocity, flow behavior and type, and thermal conductivity. Deposition velocity is defined in slurry flows when a moving bed appears in an internal (e.g., pipe) flow, and is the velocity at which ice particles move on the top of the main transport fluid and appear separated.

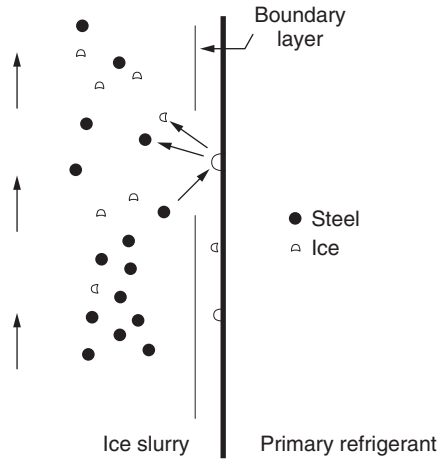


Figure 9.12 Ice removal in a fluidized bed system (Stamatiou *et al.*, 2005)

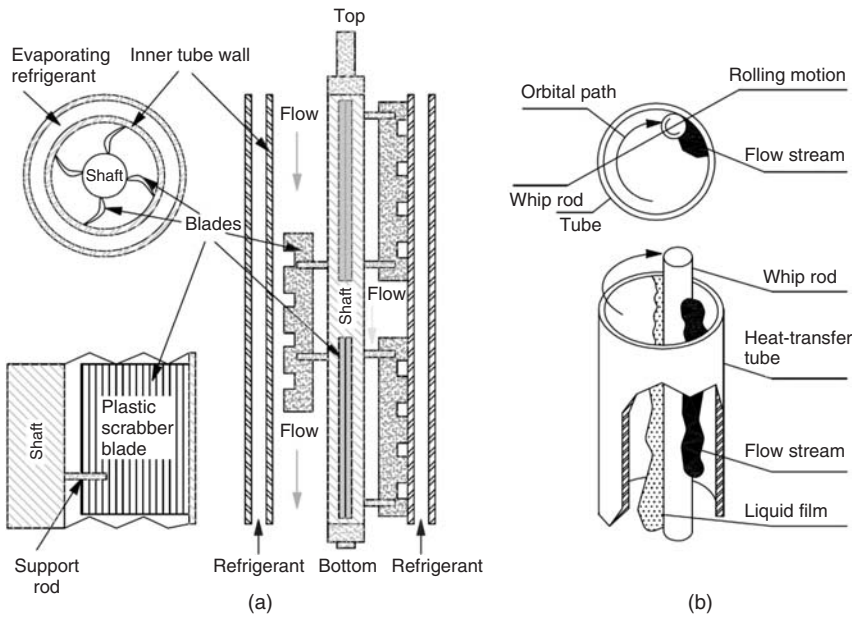
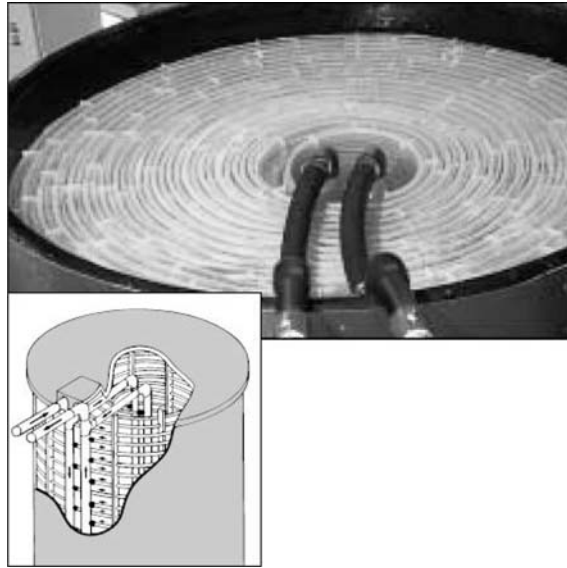


Figure 9.13 Two types of ice-slurry generators: (a) scraped-surface and (b) orbital-rod (modified from Stamatiou *et al.*, 2005)

**Ice-on-Coil**

Ice-on-coil ice production for CTES systems was developed decades ago and has been relatively popular for many years. In such systems, heat exchanger tubes are exposed to water or an alternate PCM (Figure 9.14). The HTF inside the tubes, in straight or spiral bundles or in other configurations, exchanges heat with the water in which the tubes are submerged. Ice-on-coil systems include a chiller, valves and actuators, heat exchangers and pumps.



**Figure 9.14** A typical ice-on-coil ice-storage tank (Courtesy of Calmac Manufacturing Corp.) (Calmac, 2010)

Many aspects of ice storage on tubes with or without fins have been examined. Soltan and Ardehali (2003) investigated numerically water solidification around a tube and the performance of an ice-on-coil TES system. The solidification rate and front are determined with a finite difference method, and the ice thickness on the coil is found to affect the TES system performance and safety. Shi *et al.* (2005) incorporate a resistance–capacitance circuit to measure ice layer thickness on an ice-on-coil storage tank. This method exploits the difference in ice/water permeability and resistivity values. Shi *et al.* demonstrate potential industrial applications with experimental and analytical models, and show that the method constitutes a good sensor for the accumulation of ice on a plate or around a tube ice TES, which is required to determine the IPF.

### Encapsulated PCMs and Packed-Bed Tanks

Encapsulated PCMs and packed-bed tanks are attractive and innovative cold storage systems. Many capsule and tank shapes, and capsule shell and tank wall materials, are available commercially, and a wide range of industrial and domestic applications are reported (Cryogel, 2010). Investigations have been carried out to determine optimum operating conditions, procedures, and strategies. To better understand the dynamic behavior of a packed-bed storage tank, single PCM-filled capsules (usually spherical) during charging and discharging have been examined, as have tanks filled with capsules.

Koizumi (2004) studied the unsteady behavior of an isothermal sphere numerically and verified the results experimentally using micro-foil heat flow sensors. The heat transfer and flow patterns for the capsule are determined for two flow directions: opposing and in line with natural convection. Partitioning within the capsules with copper plates increases the heat-transfer rate from the inner shell wall to the PCM, reducing melting times. Eames and Adref (2002) provide semiempirical expressions for the ice fraction inside a sphere during charging and discharging. The ice mass fraction in a capsule is evaluated by sensing the internal pressure, yielding a dimensionless relation between the solid–liquid interface (solid PCM radius) and time. At least 90% of the total energy is charged or discharged during 70% of the time needed to fully charge a capsule. Discharging the capsule fully is advantageous for performance. Reducing HTF temperature increases charging rate,

but this effect is diminished by ice thickening during charging because of increased ice layer thermal resistivity. Smaller capsule diameters attain higher charging rates and performance. An empirical relation for unsteady growth in ice thickness in a capsule was subsequently developed by Adref and Eames (2002). Chan and Tan (2006) experimentally investigate *n*-hexadecane solidification in a spherical capsule, and observe a high solidification rate at the beginning of the process followed by a declining rate of phase change. Voids can appear within the capsule during phase change, causing an irregular phase front and an eccentric PCM shape. PCM solidification time for cylindrical and spherical capsules has been numerically investigated (Bilir and İken, 2005).

Cheralathan *et al.* (2007b) experimentally investigate the effect of inlet temperature and porosity of a CTES tank filled with spherical PCM capsules, considering a range of inlet HTF temperatures and porosities so as to determine optimum operation parameters. The tank is integrated with the evaporator of a vapor compression refrigerator. Raising evaporator temperature is seen to increase chiller energy consumption.

## 9.4 Micro- and Macro-Level Advances in TES Systems and Applications

Recent advances in TES systems and their applications have been reported at the “micro” level, where thermophysical properties, phenomena, and characteristics that affect performance are considered (some of which have been covered in sections 9.3.1–9.3.4), and the “macro” level, which examines design criteria and their effect on TES performance and integration in energy systems (e.g., refrigeration systems). This section describes micro and the macro advances, focusing on cold TES. Enhancements of understanding of TES behavior and functions are identified, as are common phenomena encountered in technology and applications.

## 9.5 Micro-Level Advances in TES Systems

### 9.5.1 Modeling Methods

Modeling of an engineering system involves application of conservation laws and other scientific relations. The system is often taken to be bounded by a control volume (CV), across which interactions can occur with the surrounding (see Figure 9.15). The CV can include a small portion of a system to a device or system of devices. In the finite CV method in computational fluid dynamics (CFD), the governing equations (mass, momentum, and energy balances) are discretized, creating a grid of CVs across a region. Each CV is represented by a node having mean intensive properties such as temperature and pressure according to mass and energy interactions with the surroundings and neighboring nodes.

Ismail and Henriques (2002) numerically analyzed a transient one-dimensional model of a TES tank by dividing it into axial layers with thicknesses equal to or greater than a TES capsule diameter. El Omari and Dumas (2004) developed a CFD code based on an enthalpic model to simulate charging of one and two capsules filled with a PCM (water) exposed to an external flow below the PCM melting temperature, and investigated the effect of having the first capsule downstream of the second on crystallization. The two-dimensional Navier–Stokes equations have been solved using the FLUENT CFD package, considering the Boussinesq approximation to incorporate natural convection. Supercooling phenomenon has been considered in the method to permit prediction of the solidification front and PCM crystallization duration within the capsule(s).

Kousksou *et al.* (2005) have considered a two-dimensional porous medium model to simulate a storage tank in vertical and horizontal positions. Natural convection is taken into account in a two-dimensional HTF momentum equation and solved with mass and energy balances. Heat transfer between the PCM and the HTF enters the energy balance as a source term. The total resistance incorporates the capsule skin resistance and ice layer conductive resistance and the overall

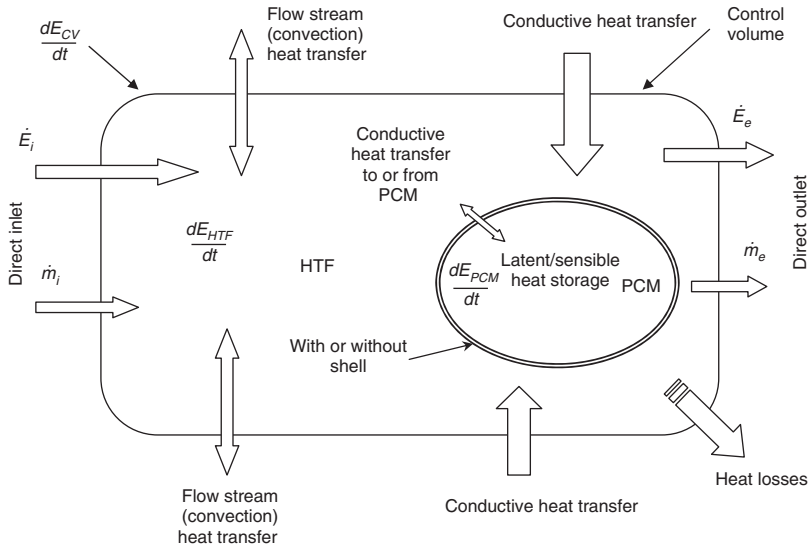


**Figure 9.15** Model showing heat and mass transfers for a control volume surrounding a flowing (or still) HTF and PCM inside a storage tank (modified from Bony and Citherlet (2007))

convective heat-transfer coefficient between the flowing fluid and the capsule. The latter coefficient is available as a Nusselt number based on constant porosity and HTF velocity. The nucleation law is invoked through a probability function related to the nodal liquid PCM temperature. Furthermore, the effects of capsule size, porosity, and length on TES charging period have been investigated numerically, for a fixed tank volume (Kousksou *et al.*, 2008). Decreasing capsule size increases the heat-transfer rate, but porosity does not remain constant. Increasing the porosity increases the heat-transfer rate but reduces the total latent cold storage by decreasing the PCM mass in the tank. Selection of an appropriate capsule diameter size enhances the performance of a CTES tank design.

Recent numerical and experimental methods applied to various CTES systems are summarized in Table 9.6.

### 9.5.2 Contact Melting Driven by Temperature and Pressure Differences

Contact melting is usually thought to be driven by a temperature difference ( $\Delta T$ ). But changes in the density of a solid PCM during charging or discharging and buoyancy lead to a force that can move the solid PCM to the shell and cause pressure-difference ( $\Delta P$ )-driven contact melting. Further, the ice-melting temperature decreases with increasing pressure. In some cases,  $\Delta P$ -driven ice melting may result from the excess pressure that a PCM exerts on a heating/cooling object or wall/shell.

The effect of PCM capsule swelling due to density changes during phase change on melting process has been analyzed numerically based on a mathematical approximation model of contact melting (Wilchinsky *et al.*, 2002). A closed-form expression is reported for modeling the evolution of the shape of PCM-filled elastic capsules having cylindrical and spherical shapes (Figure 9.16). In the model, the density of the solid PCM is higher than that of the liquid PCM, causing capsule deformation and consequently a slower melting rate. A higher melting rate is observed for spherical capsules as they have greater surface-to-volume ratios (by about 1.5 times) than cylinders. Flattening of the contact surface due to melting and density differences between the solid and liquid PCM causes a pressure drop on the solid PCM, which is at the bottom of the capsule. Consequently, the contact over a large area is decreased. Shell dimensions and materials



Table 9.6 Recent micro-level numerical and experimental methods applied to TES systems

Reference	PCM type	Method and results	Mode	Remarks	PCM/HTF
Elsayed (2007)	Capsule	Numerical; enthalpy and finite difference methods	Discharge	Periodic (cyclic) temperature of HTF	Water/ ethylene glycol
Bony and Citherlet (2007)	Capsule	Numerical and experimental; enthalpy method	Discharge heat storage	Hysteresis and supercooling phenomena examined for three capsule shapes	
Guzman and Braga (2005)	Capsule	Experimental	Charging	Capsule material: acrylic, PVC, brass, aluminum	Water/ water-alcohol
Ismail <i>et al.</i> (2003)	Capsule	Numerical and experimental ice thickening history in capsule; finite difference approach with moving grid scheme	Charging	Pyrex, copper, and aluminum capsule shells exposed to natural convection in constant-temperature tank; supercooling experimental results; equal solid and liquid densities	Water/ water-ethanol
Eames and Adref (2002)	Capsule	Experimental	Charging/ discharging	Deionized water (filling 80% of capsule volume) in glass capsule shell	Water
Adref and Eames (2002)	Capsule	Experimental	Charging/ discharging	90% of discharging occurs in 70% of spherical-capsule discharge time	Water
Assis <i>et al.</i> (2007)	Capsule	Unsteady numerical/experimental; relation between mean Nu and phase-change temperature with Fo, Ste, St, and Gr found with dimensional analysis	Melting	Convection in liquid PCM; volumetric expansion during phase change; different liquid/solid PCM densities; contact melting	Paraffin wax
Teke and Ulusarslan (2007)	Capsule (train)	Numerical, experimental, and dimensional analyses; $\Delta P$ across pipes filled with cylindrical and spherical capsules	N/A	Dimensionless pressure gradients of spherical capsule train (number) found for $Re > 1.5 \times 10^5$ ; capsules move nearly axially with no wall contact and pressure drop equal to homogeneous flow values	Solid capsules/water
Ulusarslan and Teke (2006)	Capsule (train)	Experimental; pressure drop for higher velocities tends to that for homogeneous water across pipe	N/A	$1.2 \times 10^4 > Re > 1.5 \times 10^5$	Solid capsules/water
Niezgoda-Zelasko and Zalewski (2006a)	Ice slurry	Numerical; experimental verification of pressure drop and velocity distribution	–	Bingham and mixture model for laminar flow; RNG $k-\epsilon$ model for turbulent flow	–



Niezgoda-Żelasko and Zalewski (2006b)	Ice slurry	Experimental and analytical models for pressure drop across pipe	–	Bingham model for horizontal pipe flow; mass fraction and flow velocity for laminar to turbulent flow obtained	–
Lee and Sharma (2006)	Ice slurry	Experimental; heat-transfer coefficient and rate during melting in a heat exchanger vs. slurry mass flux; effect of ice fraction is not significant at high slurry mass flux	Charging	Ice slurry melting in a tube-in-tube heat exchanger; 6.5% ethylene glycol–water mixture, ice mass fraction (0–25%), slurry mass flux (800–3500 kg/m <sup>2</sup> s); sharp increase in heat transfer rate for low mass flux (<1500 kg/m <sup>2</sup> s) and ice fraction > 15%	–
Niezgoda-Żelasko (2006)	Ice slurry	Experimental; heat transfer for horizontal tubes; dimensional analysis for local heat-transfer coefficient (laminar to turbulent flow)	Charging	Modeling Bingham fluid; enthalpy–porosity model; varying thermal conductivity for moving slurry in Fluent	–
Lee <i>et al.</i> (2006)	Ice slurry	Experimental; horizontal pipe slurry flow	Discharging	6.5% Ethylene glycol–water mixture; ice mass fraction (0–25%) and slurry mass flux (800–3500 kg/m <sup>2</sup> s); sharp change in heat transfer rate at 10% ice fraction	–
Ermiš <i>et al.</i> (2007)	Ice-on-coil	Artificial neural network; evaluation of total stored energy	Charging	Different Re numbers and inlet temperatures considered; experimental data used in numerical model for verification	Water/ethyl alcohol
Kayansayan and Acar (2006)	Ice-on-coil	Axisymmetric and 2D numerical CV method; effect of fin density and size on system dynamic performance	Charging	Finned tube; numerical results verified experimentally	Water
Shi <i>et al.</i> (2005)	Ice-on-coil	Analytical and experimental; IPF measurement based on permeability and resistivity of ice/water difference	Charging	Resistance–capacitance sensor (circuit) used to predict ice front on a coil	Water
Soltan and Ardehali (2003)	Ice-on-coil	Numerical simulation (transient FDM algorithm); prediction of time required for water solidification and ice accumulation	Charging	2609 s duration for solidification of 10 mm of ice around a 20-mm diameter pipe	Water
Cheralathan <i>et al.</i> (2007a)	Packed-bed tank	Numerical and experimental	Charging	Sensible heat storage	Water/ethylene glycol–water

(continued overleaf)

Table 9.6 (continued)

Reference	PCM type	Method and results	Mode	Remarks	PCM/HTF
Benmansour <i>et al.</i> (2006)	Packed-bed tank	Numerical and experimental methods	Charging	Sensible heat storage	Paraffin wax/air
Kouksou <i>et al.</i> (2005)	Packed-bed tank	Numerical; porous medium assumption; vertical tank exhibits superior performance	Charging	Supercooling; vertical/horizontal tank position; time-varying inlet temperature	Water
Ismail and Henríquez (2002)	Packed-bed tank	Finite difference and moving grid scheme in capsules	Charging/ discharging	Acrylic, PVC, copper, and aluminum spherical shells; 30% ethylene glycol by volume	Water/ water-ethylene glycol
Halawa <i>et al.</i> (2005)	Thin PCM slabs	Numerical; varying wall temperature model; three main design parameters: appropriate inlet and outlet temperatures, PCM melting point, and HTF flow rate	Charging/ discharging	Sensible/latent energy storage in parallel thin PCM slabs exposed to air flow	CaCl <sub>2</sub> ·6H <sub>2</sub> O/air
Nallusamy <i>et al.</i> (2006)	Packed bed	Experimental – total and instantaneous heat storage and TES efficiency evaluated	Charging/ discharging	Spherical paraffin capsules in cylindrical hot water tank reduced tank size in a solar heating system to provide daily hot water	Paraffin/water
Rady (2009b)	Packed bed	Mathematical/experimental granular Rubitherm GR27/GR41 with mixing ratios of 0.8–1.0	Charging	Mixing rates of granular materials investigated for better performance	Rubitherm/air
Regin <i>et al.</i> (2008)	Packed bed	Numerical enthalpy method; effects of the Stefan number (inlet HTF temperature), mass flow rate, and phase transition temperature for spherical capsule size	Charging/ discharging	Solar water-heating tank applications	Paraffin wax/water
Bédécarrats <i>et al.</i> (2009)	Packed bed	Experimental; lower HTF temperature and higher mass flow rate increase energy storage	Charging/ discharging	Nucleating agent added to PCM; supercooling affects performance	Water/mono-ethylene glycol–water solution

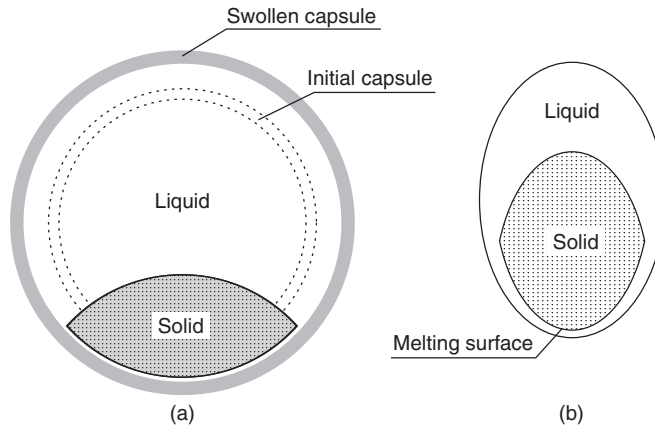


**Figure 9.16** Contact melting for PCM capsules, with both solid and liquid phases visible in each capsule: (a) spherical/cylindrical (modified from Wilchinsky *et al.*, 2002); (b) elliptical (modified from Fomin and Wilchinsky, 2002)

are restricted by the dynamic behavior and must be set by manufacturers to avoid ruptures. Similarly, Fomin and Wilchinsky (2002) investigated contact melting for an elliptical capsule, including relevant characteristic scales and nondimensional parameters. The numerical results, confirmed by dimensional analysis, suggest that aspect ratio affects the melting rate, with increasing capsule elongation raising phase changing rates.

Chen *et al.* (2005b) investigated contact melting of ice on the external surface of a horizontal elliptical cylinder, and compared  $\Delta P$ -driven versus  $\Delta T$ -driven melting. Analytical solutions for the two melting processes are developed and compared for a fixed temperature difference between the ice and the elliptical cylinder. The melting rate for the  $\Delta P$ -driven process is smaller than that for the  $\Delta T$ -driven one. Using an analytical film theory formulation, Chen *et al.* (2008) investigate PCM contact melting around a horizontal cylinder, and obtain the solid thickness and displacement rate as well as the pressure distribution inside the liquid boundary of the cylinder.

### 9.5.3 Supercooling, Superheating, and Hysteresis

The phenomenon of supercooling occurs only during PCM solidification, and inhibits energy release from a heat TES while delaying the latent heat storage in cold processes. Supercooling requires the use of more energy during charging, and reduces energy recovery during discharging compared to the recovery for a constant melting temperature. Supercooling, which is also dependent on PCM size and quantity, thus detracts from the performance for some PCMs.

The temperature–time relations for the solidification of a pure substance (water) under normal conditions and with supercooling in a capsule are compared in Figure 9.17. Supercooling is seen to cause dendritic ice formation in the capsule after the metastable sensible storage period ends by a crystallization initiation process. As the first ice nucleus forms on the surface, the remaining water absorbs heat and the temperature rises to the melting temperature. Then, an ice layer forms in a rapid adiabatic process. The ice layer thickness in the capsule is increased because of increased heat absorption from the surrounding heat-transport fluid.

Günther *et al.* (2007) propose a novel algorithm to model supercooling for salt hydrates using a one-dimensional conduction analysis. An expression is derived for enthalpy on the basis of the temperature and phase of individual nodes. The phase is treated as liquid until crystallization is initiated by nucleation. Phase change commences when the temperature falls below the nucleation temperature or from direct contact with a solid node. A simple step function is used to model

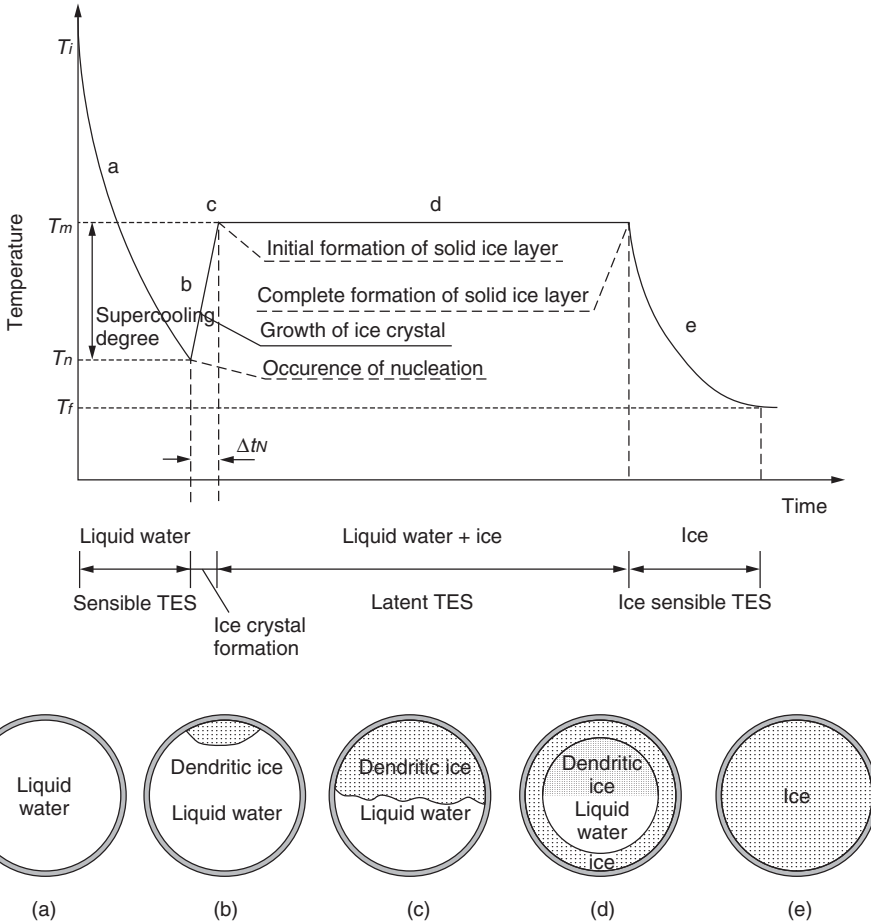


**Figure 9.17** Supercooling during water solidification in a spherical capsule (modified from Chen *et al.*, 2000)

supercooling phenomenon, which is suitable for low supercooling degrees (difference between nucleation and melting temperatures). The results are verified experimentally.

As a result of encapsulated PCM supercooling in different locations of a tank, the TES requires supplementary cooling and therefore greater refrigeration power. A similar effect is not observed during melting (cold TES discharging). The nature of the phenomenon is erratic and is usually described by probability functions. Supercooling degrees are usually included in PCM data sheets (Ismail and Henríquez, 2002). Recent advances in supercooling for CTES applications are reviewed in Table 9.7. In ice-slurry applications, the degree of supercooling depends on the ice-slurry velocity, heat flux, solute concentration, ice fraction, and ice crystal size.

Superheating can occur in the TES system. Heat-transfer rate and pressure drop are primary design factors for ice-slurry melting heat exchangers, but a superheating degree occurs when the ice-slurry liquid temperature exceeds its equilibrium temperature. In some cases, the slurry is superheated during discharging, and consequently, the slurry outlet temperature is raised considerably, resulting in a smaller difference between the cooling fluid and ice-slurry temperatures and a decreased heat exchanger capacity. Pronk *et al.* (2008) showed experimentally that superheating in such heat exchangers depends on slurry crystal size and solute concentration, with higher values decreasing superheating degree.

**Table 9.7** Some recent advances in understanding supercooling in cold TES systems

Reference	Type	Method	Remarks
Matsumoto <i>et al.</i> (2008)	Ice slurry	Experimental	70–80% water/silicone oil emulsion (and small amount of amino-group emulsifier) ice-slurry production through voltage and ultrasonic wave applications; dissolution propagation method to decrease supercooling; reducing ice-slurry adhesion
Günther <i>et al.</i> (2007)	PCM	Numerical	Modeling PCM supercooling with a 1D algorithm and phase parameter that uses neighboring solid nodes as solidification initiators
Matsumoto <i>et al.</i> (2007)	Ice slurry	Experimental	Effects of composition viscosity, size of ice nuclei, and time on propagation rate and maximum supercooling degree of a water/oil slurry
Alvarado <i>et al.</i> (2007)	Microencapsulated PCM slurry	Experimental	Nucleating agent selection to prevent supercooling and applications to MPCM slurries
Kitanovski <i>et al.</i> (2005)	Ice slurry	Review	Supercooling-based ice-slurry production
Milón Guzman and Braga (2005)	Cylindrical capsule	Experimental	Water supercooling in a cylindrical capsule (acrylic, PVC, brass, aluminum) in a constant-temperature bath; nucleation probabilities as a function of HTF temperature, which increases supercooling; nucleation more pronounced in high-conductivity shells
El Omari and Dumas (2004)	Spherical capsule	Numerical	Natural convection for low HTF flow velocity (<10 mm/s); initial ice thickness due to supercooling is usually small (2% internal radius) as supercooling degree is usually small (<10 K)
Teraoka <i>et al.</i> (2002)	Crystal growth	Experimental	Dendrite ice is thinner for higher concentrations and crystal growth depends on solution concentration and supercooling degree for water–ethylene glycol solutions
Chen <i>et al.</i> (2000)	Packed-bed tank	Experimental	Total net energy transferred by the inlet/outlet flows can be stored in an encapsulated tank only if HTF temperatures are lower than the 100% nucleation probability temperature
Braga <i>et al.</i> (2009)	Cylindrical capsule	Experimental	Water supercooling in a horizontal cylindrical capsule (aluminum, bronze, acrylic) in a constant-temperature bath with vertical upward flow; internal capsule wall heat-transfer rate increases with decreasing diameter and increasing conductivity and depends on angular distribution of HTF temperature

The phenomenon of hysteresis in TES applications is defined as the delay in PCM solidification during charging. Unlike supercooling, hysteresis is not affected by the presence of solid particles or surfaces (Bony and Citherlet, 2007). Accounting for hysteresis can improve PCM modeling accuracy.

### 9.5.4 Geometry and Performance Optimization

Geometry and configuration are significant performance factors in cold TES. Bejan *et al.* (1995) indicate that heat transfer, fluid flow, and thermodynamics define an optimum shape in engineering or natural systems, and the relation between shape configuration optimization in an engineering problem with energy and exergy optimization methods. The constructal law describes possible optimum shapes and configurations in simple tree-shape distribution systems (networks) with the least amount of irreversibility. Zamfirescu and Bejan (2005) propose a tree-shape structure as a CTES based on constructal law. An optimized shape structure is proposed, considering ice production on parallel plates and parallel cylinders with constraints regarding temperature difference, pressure drop, storage time, and material type. An optimal ice production per unit volume function is developed. Bejan *et al.* (1995) present a TES optimization methodology based on first and second law analyses and economic considerations, noting that the proper geometry for a CTES affects system performance and can be optimized.

### 9.5.5 Other Micro-Level Phenomena Affecting TES Performance

Factors other than those considered above also affect CTES performance. Some are general while others apply to specific storage types. For ice-slurry systems, for example, important performance factors for a CTES and the system into which it is integrated include deposition velocity, pressure drop, brine type and concentration, ice mass fraction, flow type and behavior, application temperature, inlet temperature (Guilpart *et al.*, 2006; Rached *et al.*, 2007), attrition, agglomeration, Ostwald ripening, generator type, additive materials (emulsifiers or depressants) (Matsumoto *et al.*, 2002), choking, ice adhesion to internal pipe or heat exchanger coating, and heat-transfer rate. Significant performance factors for tanks filled with encapsulated PCM include porosity, velocity distribution, sphericity, apparent specific heat (dynamic heat capacity), tank wall heat loss, capsule thickness and material properties (especially conductivity), HTF inlet temperature, capsule skin texture, and aspect ratios (tank to capsule diameter or tank diameter to length).

Research on these factors has been reported in diverse areas, including heat transfer, fluid flow, and other deterministic phenomena on performance. Several dimensionless parameters important to such research on CTES systems follow:

- particle Reynolds number,  $Re_p = Ud_p/(1 - \varepsilon)v$ , where  $U$  denotes the mean fluid velocity and  $d_p$  the particle (capsule) diameter (Çarpinlioğlu and Özahi, 2008);
- sphericity,  $\Phi = \pi^{1/3}(6V_p)^{2/3}/A_p$ , where  $V_p$  and  $A_p$  denote, respectively, the total particle (capsule) volume and surface area (Çarpinlioğlu and Özahi, 2008);
- IPF, which denotes the ratio of ice mass  $m_{ice} (= \Delta V \rho_{ice} \rho_w / (\rho_w - \rho_{ice}))$  to the total ice-slurry mass, where  $\Delta V$  is the total volume change of the ice slurry during freezing. This factor is sometimes expressed on a volume basis;
- porosity  $\varepsilon$ , which is the volume fraction filled by fluid in a porous solid matrix. The porosity determines the maximum HTF volume surrounding a PCM in some of CTES applications, while the interaction of these materials determines the heat-transfer rate, pressure drop, and other factors that affect CTES performance.

The porosity in annular packed beds has been assessed numerically (du Toit, 2008). The results agree well with experimental data and several empirical correlations for local porosity. Götz *et al.*

(2002) utilized magnetic resonance imaging to visualize the 3D porosity and velocity distributions around cylindrical and spherical capsules packed in a container, identifying high porosity near the wall and stagnation points in the domain.

Inlet and outlet diffuser shapes and configurations affect TES designs. Chung *et al.* (2008) determine numerically the impact of such design factors as diffuser configuration, Reynolds and Froude numbers, and diffuser to tank cross-section area ratio on performance of TES systems. They consider a rectangular sensible stratified storage tank and propose an optimum diffuser design based on system efficiency. The Reynolds number is seen to have a significant effect on performance, while the effect of the Froude number is negligible. For a PCM storage used in a refrigerated compartment on a truck, Simard and Lacroix (2003) investigate the effect of frosting on performance, for various air flow velocities and relative humidities.

Additives to the main PCM or HTF materials can affect the performance of CTES systems. Water/oil (W/O) emulsions are usually made from water and oil emulsified by additives, while oil/water (O/W) emulsions are often prepared with ultrasonic mixing techniques. Water-based (70, 80, and 90%) ice slurries with oil additives emulsified by amino-group-modified silicone oil have been studied by Matsumoto *et al.* (2006). The hydrophobic property of the additive leads to no freezing point depression, while the emulsion electrical resistance determines the structure of the emulsions (W/O or O/W). W/O emulsions are recommended for superior ice-slurry production performance.

An assessment of the effect of temperature on the performance of CTESs using organic and inorganic ice slurries indicates the need to select the solute type and concentration according to the application type and temperature (Guilpart *et al.*, 2006).

Niezgoda-Zelasko and Zelasko (2008) experimentally investigated the heat transfer rate of ice slurry flowing in tubes with circular, rectangle, and slit rectangle cross sections, and determined the Nusselt number for laminar and turbulent flows. When ice slurry is generated in an insulated tank without mixing, the ice particles rise to the surface because of buoyancy forces. When the tank is not sufficiently sealed to prevent the infiltration of outside moist air, the ice particles join with the freezing moisture and create sheets of ice particles on the top of the tank, causing problems since the mushy material is difficult to be pumped and used as a secondary refrigerant. To prevent this phenomenon, Egolf *et al.* (2008) proposed a method to make stratified particles in a CTES tank using a pump mounted on the top of the tank to circulate the ice particles. Using a pump rather than a mixer is experimentally found to reduce energy consumption.

Two additional significant microlevel phenomena follow:

- Pressure drops across a tank or tubes used as heat exchangers (PCM/HTF interaction) directly affect CTES performance, as they necessitate additional pumping power to circulate the HTF during charging and discharging. Çarpınlioğlu and Özahi (2008) investigate some of main parameters affecting the pressure drop for a turbulent air flow through round particles, considering a range of sphericity ( $0.55 < \Phi < 1.00$ ), porosity ( $0.36 < \varepsilon < 0.56$ ) and particle Reynolds number ( $675 < Re_p < 7772$ ). The pressure drop is found to be a function of porosity, sphericity, particle diameter, container length, and particle Reynolds number.
- Varying (or cyclic) HTF inlet temperatures affects charging or discharging for CTES systems. Elsayed (2007) investigated the effect of the aforementioned inlet condition during discharging (ice melting) for a single rectangular capsule on two performance indicators: heat transfer efficiency and stored energy. The energy stored for a cyclic HTF inlet temperature is shown to be equal to the stored energy if the HTF flow is at the mean temperature of the cyclic variations.

### 9.5.6 Developments in Stratification Analysis

Stratified TES tanks often exhibit superior performance to nonstratified tanks, especially in low HTF flow heating systems. The level of TES stratification is decreased by HTF mixing, due to natural

**Table 9.8** Recent developments in stratification analysis

Reference	Stratification cause/effect	Analysis and results	Method
Rosen <i>et al.</i> (2004)	Exergy storage enhancement via stratification	Storage capacity increased	Thermodynamic analysis
Altuntop <i>et al.</i> (2006)	Inlet water velocity	Obtaining greater stratification/internal circulation increases with increasing inlet water flux	Numerical; data validation
Panthalookaran <i>et al.</i> (2007)	Aspect ratio, containment shape and size for four tanks	Hot water seasonal storage; higher efficiency for higher aspect ratios	Thermodynamic analysis
Arias <i>et al.</i> (2008)	Selecting more or less of nodes	Sensible packed-bed TES; sensitivity of daily storage simulations to number of nodes in domain	Numerical
Jack and Wrobel (2009)	Conduction losses to environment	Energy and exergy analyses; determine optimum charging time	Thermodynamic optimization
Haller <i>et al.</i> (2009)	Entropy change with heat losses and generation with mixing	Qualitative efficiency; more meaningful results obtained when entropy change is considered	Review
Göppert <i>et al.</i> (2009)	Inlet diffuser (angle) design	Reduced suction in inlet diffuser; reduced mixing improves designs	Numerical
Panthalookaran <i>et al.</i> (2008)	Axial, radial, and conical diffuser shapes, and flow guides	Performance enhancement by proper diffuser/flow guide designs; conical diffuser with smaller angle exhibits greatest efficiency	–

or forced convection or by heat diffusion by conduction. Recent developments in stratification analysis are summarized in Table 9.8. Haller *et al.* (2009) reviewed and compared methods to determine the stratification efficiency of a TES during a complete thermal cycle. Only one method considers entropy generation, which provides a more meaningful interpretation of efficiency than energy analysis.

## 9.6 Macro-Level Advances in TES Systems and Applications

Macro-level parameters important to CTES system's overall performance are discussed. When thermal storage is integrated into a HVAC system, the efficiencies of the additional equipment dictate new operating conditions that must be understood in designs. For instance, the installation and operation under different strategies (e.g., proper cycling of a chiller and storage duration) depend on many parameters. Many important deterministic performance parameters at the macro level are shown in Figure 9.18 and discussed in subsequent sections.

### 9.6.1 Mode of Cooling/Heating: Passive or Active

Building energy consumption accounts for about 40% of the energy used in Europe, which constitutes a developed and industrial region. Passive conservation methods, including the use of



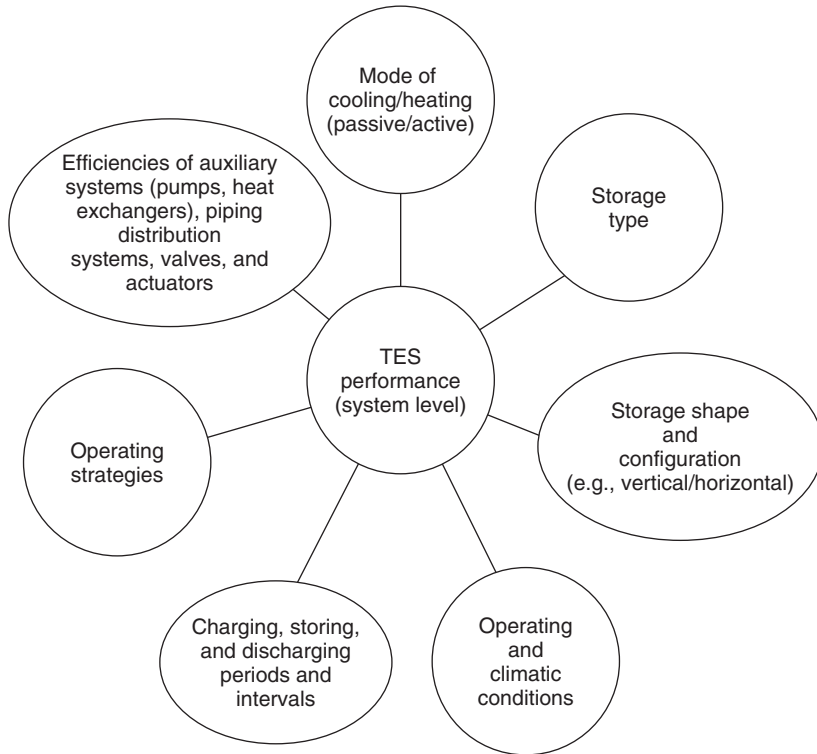


**Figure 9.18** Macrolevel parameters that affect TES performance

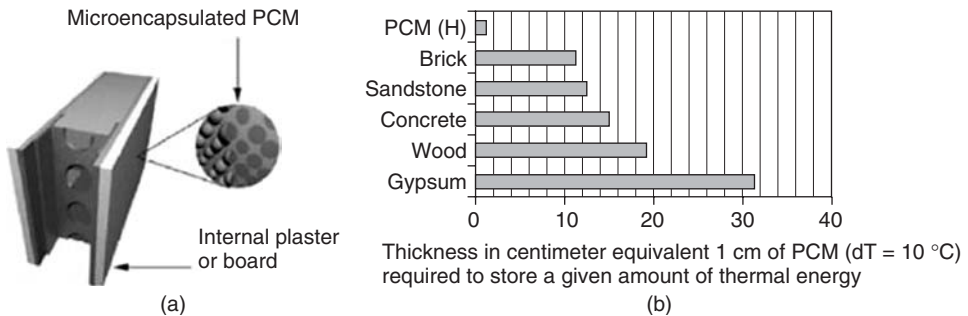


**Figure 9.19** (a) MPCM integration into building materials and (b) comparison of wall thicknesses for a fixed thermal energy storage capacity (modified from Mehling *et al.*, 2007)

renewable energy sources, can help reduce energy consumption. Low-temperature night-time ambient air can be used for cooling, reducing building cooling loads. Latent energy storage with PCMs, typically mixtures of materials, stabilizers, and thickening and nucleating agents, is beneficial for some buildings (Arkar and Medved, 2007). Figure 9.19 shows a typical integration of PCM into building materials. The storage capacity of a building can be enhanced by the use of MPCMs, which enable designers to use less material and obtain lighter structures.

Design factors and criteria to be assessed in the industrial-scale manufacturing of building materials incorporating PCMs include appropriate phase-transition temperature, apparent specific heat in the transition-temperature interval, thermal conductivity, mechanical properties, and stability. The preparation method and material composition and thermophysical properties also need to be considered. The storage material should retain its structure even during multiple thermal (melting/freezing) cycles. The use of PCMs in building materials has some drawbacks, for which solutions are being investigated, including low thermal conductivities, varying thermal properties over multiple thermal cycles, and potential leakage or frosting. Approaches under investigation to mitigate these drawbacks involve dispersing high-conductivity materials (e.g., graphite) into the PCM, filling high-conductivity matrices with liquid paraffin, and utilization of micro- or nanoencapsulated PCMs.

Some of the techniques to determine thermophysical and thermomechanical properties of such building composites are as follows (Fang *et al.*, 2009; Özonur *et al.*, 2006; Li *et al.*, 2009):

- Fourier transform infrared spectroscopy;
- visualization with optical or scanning electron microscopes;
- DSC;
- thermal gravimetric analysis.

Özonur *et al.* (2006) investigated microcapsules composed of inexpensive natural coco fatty acid mixture PCMs with different shell materials. This PCM material can be used in porous construction materials (e.g., plasterboards) or as an additive to cladding materials (e.g., plaster). The facts that the PCM may leak from the surface and that humidity can affect hydrate PCMs pose potential concerns. Diffusion of a low-viscosity liquid PCM through construction/building materials may occur when there is no microencapsulation process.

Li *et al.* (2009b) introduced a novel PCM for TES applications such as radiant electrical floor heating, using microencapsulated paraffin as the base material and high-density polyethylene/wood flour composite as its structural matrix. These two parts comprise a form-stable PCM for passive building purposes, which helps builders utilize a low-cost material to regulate room temperature during days and nights. The PCM material exhibits appropriate design characteristics for use in building materials. Alkan *et al.* (2009) propose another form-stable paraffin/polypropylene composite, which is prepared through paraffin dispersion into a polymer matrix and which demonstrates promising thermomechanical properties for solar heating applications. Zhen-guo *et al.* (2006) experimentally compared floor-radiant and fan-coil heating systems, and found that the former achieves a more stable room temperature range within comfort levels, even with outdoor temperature fluctuations. Zeng *et al.* (2010) investigate a solar water-heating floor system integrated with a shape-stabilized PCM (75% paraffin and 25% polyethylene as a supporting material) to reduce or eliminate the use of hot water tank reservoirs. Requiring less building space and using light-weight materials, the system provides a constant and stable floor temperature and a heat flux with 50% less room-temperature fluctuations. A typical floor-heating system integrated with a PCM using hot water as an HTF is shown in Figure 9.20.

Quanying *et al.* (2008) investigated over 80 mixture ratios to determine if they possess an adequate phase-change temperature and latent heat for building-envelope applications. By considering various composition ratios for two PCM material types, one of which is *n*-heptadecane, *n*-octadecane, *n*-eicosane, paraffin no. 46 and 48, or liquid paraffin, the authors generate a selection guide for designers and manufacturers. Some novel PCMs used in passive TES systems in the building sector are summarized in Table 9.9.

Yanbing *et al.* (2003) numerically investigated a night-ventilation passive system of packed-PCM-staggered air ducts, and verified the results experimentally. The system increases thermal comfort using latent TES in a building by decreasing cooling loads.

Typical active and passive uses of PCMs as CTES systems are shown in Figure 9.21. The passive cooling systems may have a fan or use free convection. The PCM can be incorporated into many room structures (walls, floors, ceiling, roof, windows). Thermal energy is absorbed from the

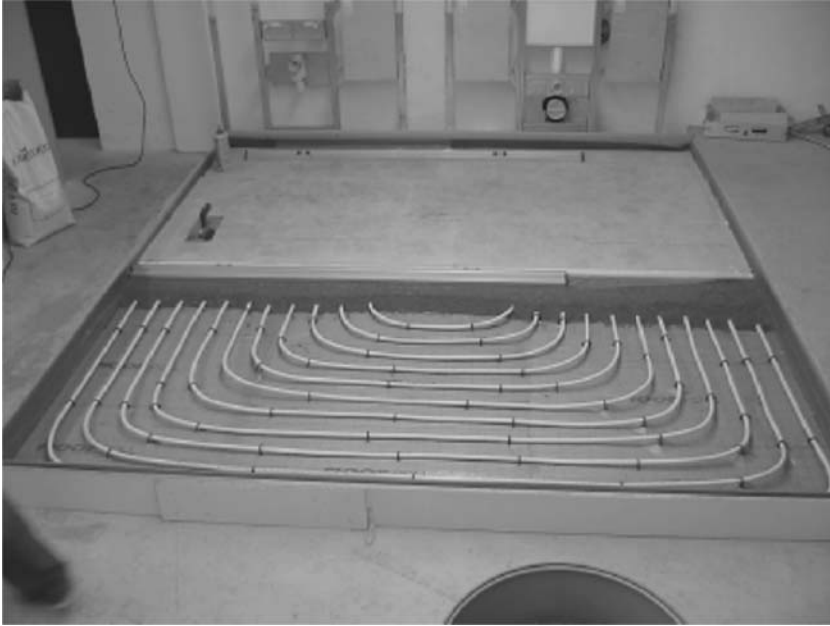


**Figure 9.20** Floor-heating system with an integrated PCM (Rubitherm) storage using hot water as a heat supply (Mehling *et al.*, 2007)

**Table 9.9** Novel PCMs used in building sector to provide passive TES

Reference	Core/shell or matrix PCM	Application	Properties and remarks
Alkan <i>et al.</i> (2009)	Paraffin/polypropylene composite	Form-stable building material for passive solar heating	Melting temperature: 44.77–45.52 °C Crystallization temperature: 53.55–54.80 °C Latent heat: 136.16–136.59 kJ/kg
Sari and Karaipekli (2009)	Palmitic acid/expanded graphite	Form-stable building material	Melting/freezing temperature: 60.88–60.81 °C Latent heat: 148.36–149.66 kJ/kg Reliability test: >3000 cycles
Li <i>et al.</i> (2009b)	Paraffin and polyethylene–wood flour composite	Form-stable PCM plate for floor heating	Melting/freezing temperature: 12–25 °C Latent heat: 27.6–28.2 kJ/kg
Liu and Awbi (2009)	DuPont™ Energain™ microencapsulated boards	Boards used in natural convection	Melting temperature: 21.7 °C (according to technical data sheet)
Xin <i>et al.</i> (2009)	Mostly paraffin and crystalline hydrate	Building envelopes	Range of $\rho c < 4.0 \text{ MJ/m}^3 \text{ K}$ ; suitable for passive TES
Özonur <i>et al.</i> (2006)	Natural coco fatty acid mixtures/gum Arabic, gelatin powder, melamine, formaldehyde, urea, and $\beta$ -naphthol	Building materials/greenhouse	Melting temperature range: 29–31 °C Reliability test >50 cycles

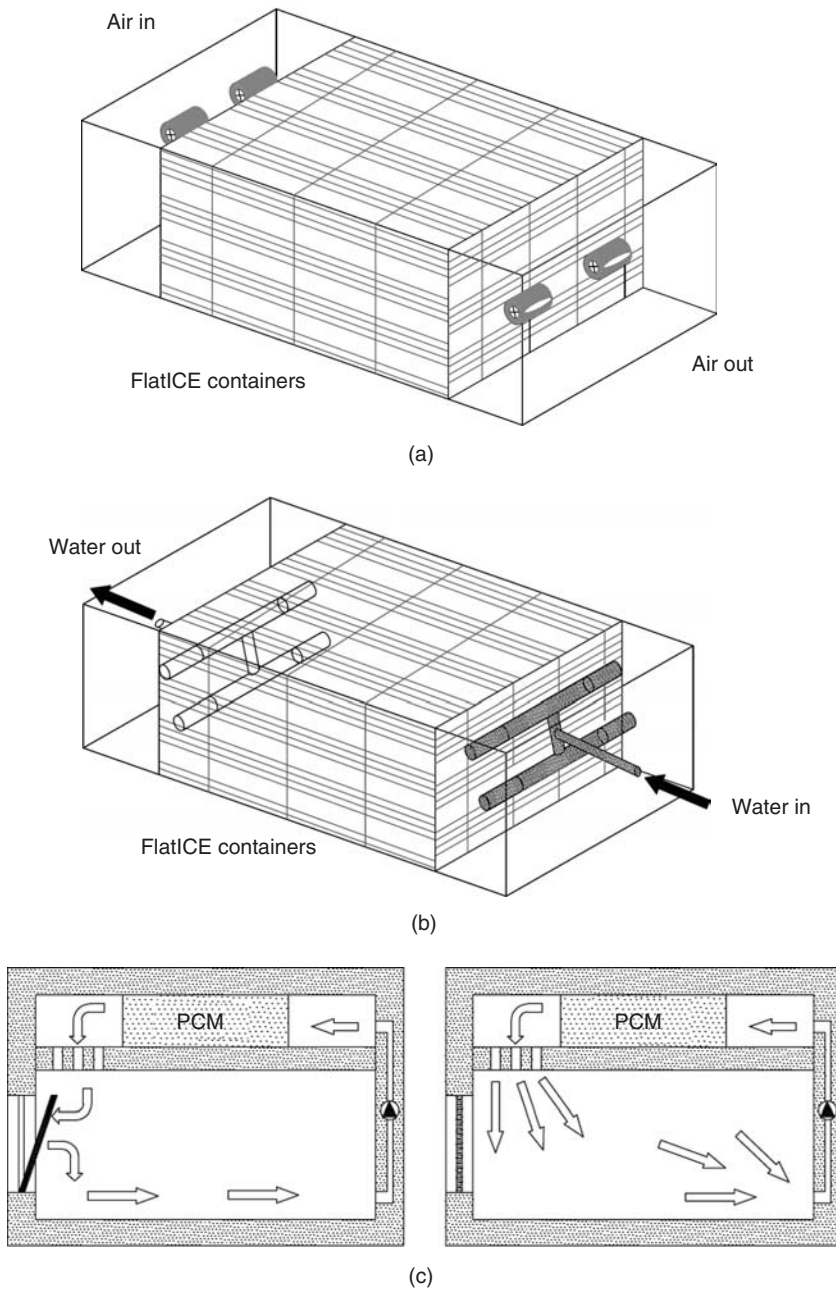


**Figure 9.21** (a) Active environmental system for air cooling; (b) active environmental system for water cooling; (c) passive cooling system, showing charging at night (left) and space cooling during the day (right) (modified from Stritih and Butala, 2007)

indoor air during the day to charge the solid PCM, cooling the room. Paraffin waxes are usually good PCM candidates (Roxas-Dimaano and Watanabe, 2002a; Zhang *et al.*, 2007), but numerous PCM compounds are available commercially. Mixtures of different materials can achieve the proper melting temperature for various applications. Knowledge of the dependence of the heat capacity on temperature is needed, as melting usually takes place over a temperature range.

An important performance factor in the design of passive cooling systems using latent TES is the appropriate PCM melting point. Arkar and Medved (2007) numerically assess the performance of a vertical cylinder filled with spherical PCM capsules by examining the output temperature. They found a suitable melting temperature range for varying inlet air temperatures during typical operating conditions, and recommend a PCM weight per ventilating air flow rate for climate conditions in continental Europe. Two main parameters affect the overall performance of the system: PCM melting temperature and the tank length to capsule diameter aspect ratio ( $L/d$ ). The software package TRNSYS is used to predict the indoor temperature during free cooling, yielding results that agree well with data from an experimental prototype heat exchanger. A variable heat capacity  $c(T)$  can be used for PCM mixtures in the market, for cooling load calculations. For real installations, the total PCM weight is a significant design criterion that can be decreased by use of a suitable mixture, which has an appropriate heat capacity variation. Roxas-Dimaano and Watanabe (2002b) proposed a PCM for passive cooling with a mixture of capric-lauric acids (65/35%) and a melting temperature of 18–19.5°C.

Recent developments in PCM use in building envelopes for space cooling have been reviewed by Zhang *et al.* (2007). These authors investigate the ability to store solar power during winter days and reject heat during summer nights, so as to reduce diurnal indoor temperature fluctuations and help HVAC systems provide better comfort. Some building panel manufacturers propose using microsize PCMs to enhance the thermophysical properties of the walls, floors, or ceilings in new efficient buildings. PCMs with a melting point close to the average required room temperature are recommended for panels, provided they do not introduce problems related to flammability, stability, and cost.

Medina *et al.* (2008) developed a new insulating wall incorporating a PCM and insulation. The PCM acts as a capacitor, receiving and rejecting large quantities of energy as it changes phase. Structural insulated panels can incorporate PCMs to create a distributed thermal mass. Such walls have been tested under actual daily temperature variations, demonstrating their abilities to be good insulators and to provide a stable room temperature through a heat flux reduction. Several organic and inorganic PCMs are mentioned that are good candidates for this application, demonstrating appropriate melting temperatures and latent heats. Possible installation locations for such building materials for several cooling/heating applications have been described (Zhang *et al.*, 2007) and are illustrated in Figure 9.22.

Stritih and Butala (2007) numerically assessed and experimentally verified several paraffins, eutectics, and blends for floor- and ceiling-free cooling. Ventilation occurs during cooler night times and a PCM with a proper melting temperature incorporated in the air duct permits the provision of cooler day-time room temperatures. HVAC energy consumption during warm days is thereby reduced. Arkar *et al.* (2007) presented a fan/duct model for night ventilation of a room, providing fresh air and a cool environment. Using TRNSYS to assess the building thermal response and experimental data for verification, a method is recommended for reducing the mechanical ventilation for buildings. A typical duct design in which a PCM has been integrated for free cooling is shown in Figure 9.23.

Medved and Arkar (2008) numerically and experimentally examined the use of latent TES for free cooling for a range of climate conditions and suggest an optimal latent TES based on the ratio of PCM mass and ventilation-air volume flow rate. An optimum PCM melting temperature is also suggested, approximately equal to the average ambient air temperature for the hottest month, in order to provide a free-cooling potential, which is proportional to the average daily amplitude of the ambient temperature fluctuations. For the climatic conditions analyzed, the PCM with the widest phase-change temperature range (12 K) has been found to be the most efficient. The optimal

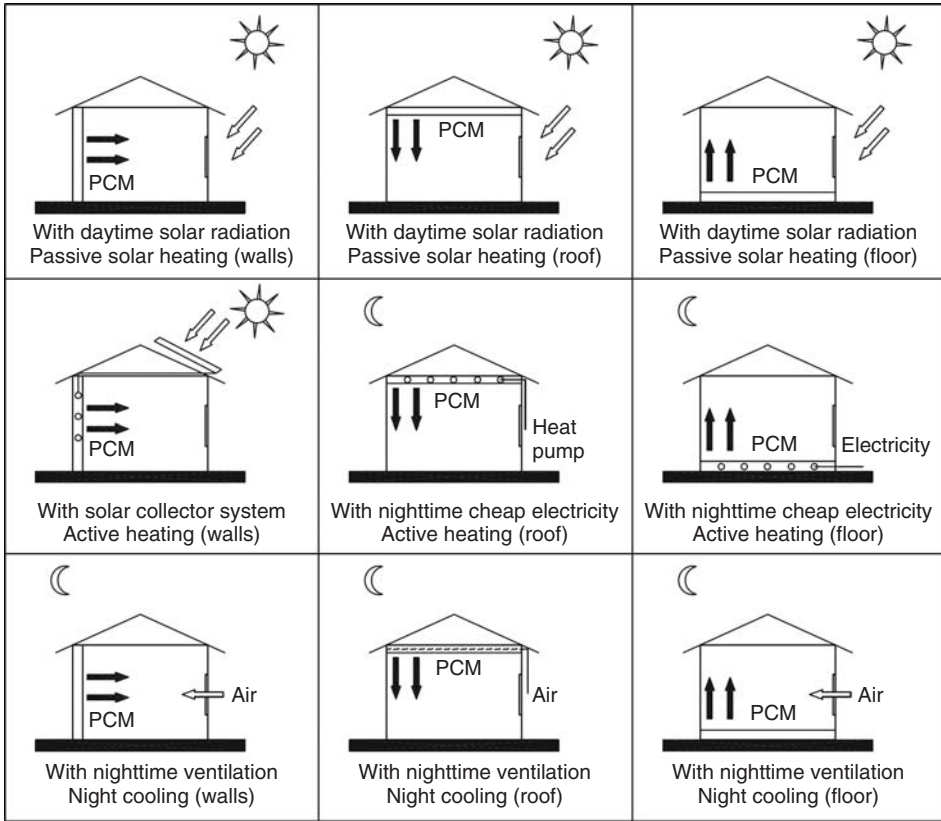


**Figure 9.22** Possible PCM installations for several building envelopes and applications (modified from Zhang *et al.*, 2007)

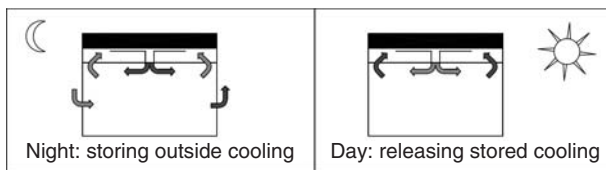


**Figure 9.23** Free cooling by storing coolness during the night and using it for space cooling during the day (modified from Mehling *et al.*, 2007)

PCM mass for the free cooling of a room is found to be 1–1.5 kg per m<sup>3</sup>/h of fresh ventilation air. Recent advances in passive cooling are reviewed in Table 9.10.

### 9.6.2 Operating Strategies and Installation Configurations

Many operating strategies and installation configurations can be used to integrate TES and a typical heating/cooling system. Some of the main strategies are depicted in Figure 9.24. With the chiller-priority control strategy, chillers operate as often as possible during peak hours, and excess building

Table 9.10 Recent developments in passive heating/cooling TES methods and applications

Reference	PCM	Remarks	Approach/model
Medina <i>et al.</i> (2008)	Noncorrosive and nontoxic paraffin	New insulating wall in which PCM-filled tubes are inserted, increasing the thermal barrier effect	Experimental
Medved and Arkar (2008)	Paraffin RT 20	Average daily temperature for the hottest month is optimum PCM melting temperature for free cooling; optimal PCM mass is 1.0–1.5 kg per m <sup>3</sup> /h of fresh ventilating air	Numerical and experimental
Arkar and Medved (2007)	Paraffin RT 20	PCM melting point is 20–22 °C; 4.6 kg/m <sup>2</sup> for PCM for continental European climate and five volume changes per hour ventilation air exchange, with variable radial porosity (2D unsteady porous media model using effective heat capacity), velocity, and ambient temperature	Numerical (TRNSYS)
Stritih and Butala (2007)	Paraffin, eutectics, and other compounds	Ceiling and floor free-cooling systems	Numerical and experimental
Zhang <i>et al.</i> (2007)	PCMs used in building panels	Building panels with a PCM having a melting point of average room temperature are useful for stabilizing room temperature during day, increasing comfort, and decreasing HVAC capacity	—
Arkar <i>et al.</i> (2007)	Paraffin RT 20	Night ventilation for free cooling using latent TES allows reduction in mechanical ventilation system capacity	Numerical (TRNSYS)
Hed and Bellander (2006)	PCMs with variable $c(T)$	Design of low-weight PCM duct for passive cooling should consider heat capacity variation with temperature of PCM	Numerical
Yanbing <i>et al.</i> (2003)	Newly developed fatty acid	Use of this PCM in air ducts verified to allow night ventilation cooling	Numerical and experimental
Roxas-Dimaano and Watanabe (2002b)	Capric–lauric acid mixture (65/35%)	New PCM for passive cooling with a melting temperature of 18–19.5 °C	Experimental
Heim (2010)	PCM–gypsum composite	Solar heating applications; utilize effective heat capacity and control volume method with variable thermal properties	Numerical
Benli and Durmuş (2009)	CaCl <sub>2</sub> ·6H <sub>2</sub> O	Greenhouse heating integrated with solar energy system, which charges the PCM, provides 3–4 h energy for greenhouse	Experimental
Sharma <i>et al.</i> (2009)	Various	Solar cooker applications of PCMs	Review



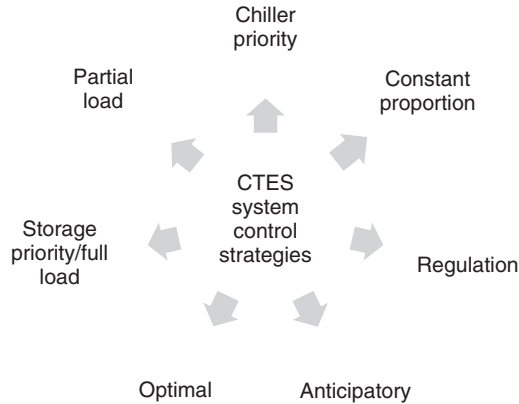


**Figure 9.24** Types of control strategies for CTES systems (modified from Henze *et al.*, 2003; Ihm *et al.*, 2004; LeBreux *et al.*, 2009; Lemort, 2006)

cooling load is provided by charging storage tanks during off-peak hours. The HTF flow rate is set to use the storage to compensate when the load exceeds the chiller capacity. The main advantage of the chiller-priority strategy is that it permits the chiller to operate at a constant capacity over the entire process. A drawback of this strategy is that it could lead to nonoptimal use of ice storage. For the constant-proportion strategy, a constant fraction of the building cooling load during peak hours is met by CTES, while for the storage priority (full-load) strategy, most of the cooling load is satisfied by the storage system (Figure 9.25) (Lemort, 2006).

Although real-time control strategies do not exist, Henze *et al.* (2003) investigated three conventional control strategies (chiller priority, constant proportion, and storage priority) for an ice-storage system, and proposed an optimum strategy based on minimization of total operating cost. The study considered three types of ice-storage systems (ice-on-coil, internal, and external melting dynamic ice harvesters) and three types of vapor-compression chillers (centrifugal, reciprocating, and screw driver).

With the anticipatory strategy, a fuzzy logic procedure is used with a controller to simultaneously address the stored energy and the supplied energy from a source (e.g., solar heat or electricity) and to incorporate information on the expected energy supply, accounting for weather forecasts. With the regulation strategy, a supplementary energy source (e.g., electricity) is usually needed. A proportional-integral-derivative (PID) controller regulates the temperature of a designated area (e.g., room) to a set point using a fan to adjust the air flow (LeBreux *et al.*, 2009). Zhao *et al.* (2008) optimized a seasonal underground borehole TES according to operational strategies, and propose a strategy to decrease heat losses and increase thermal energy utilization from the system during discharging.

Ihm *et al.* (2004) integrated a TES model for typical storage strategies with EnergyPlus, a whole-building thermal simulation program for performance analysis of TES that can accommodate various control strategies and operating conditions. Two ice TES systems (external melt ice-on-coil and ice harvester) were modeled using the building load and system thermodynamics (BLAST) program.

Various installation arrangements are possible for CTES in HVAC systems, two of which are shown in Figure 9.26. Different storage types can be used in each arrangement, although performance varies with their run-time patterns. Operating strategy and installation configuration affect the overall performance of the CTES systems. Numerous recent investigations of operating strategies and their influence on system performance are summarized in Table 9.11.



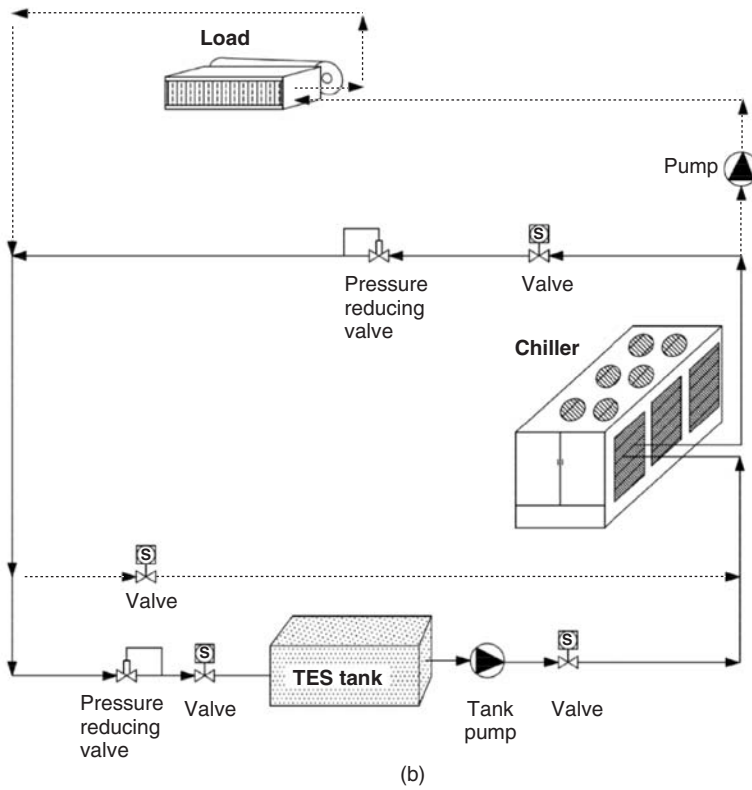
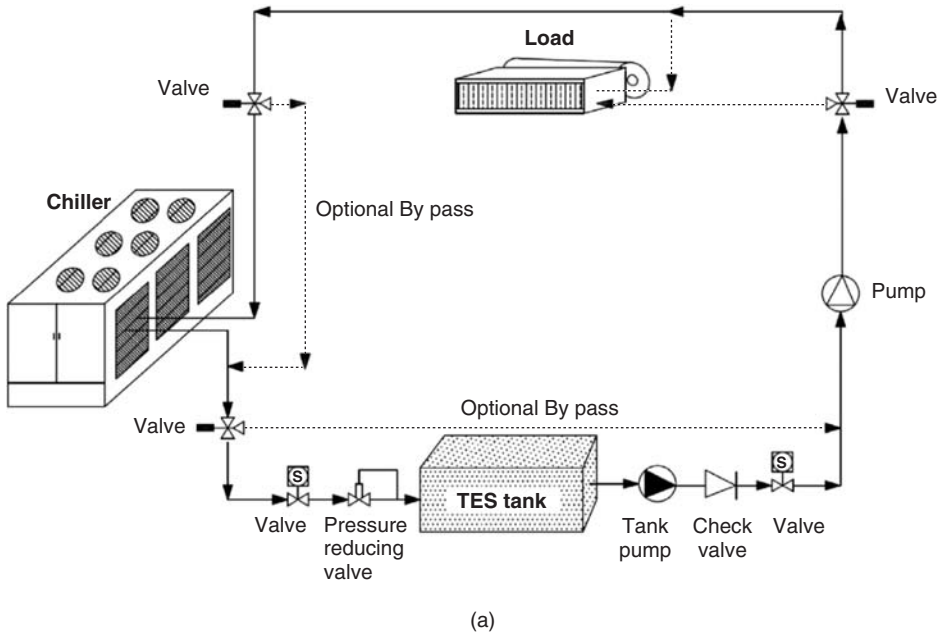


**Figure 9.25** Two operating strategies: (a) full-load storage priority; (b) partial-load (modified from *Environmental Process Systems*, 2010)

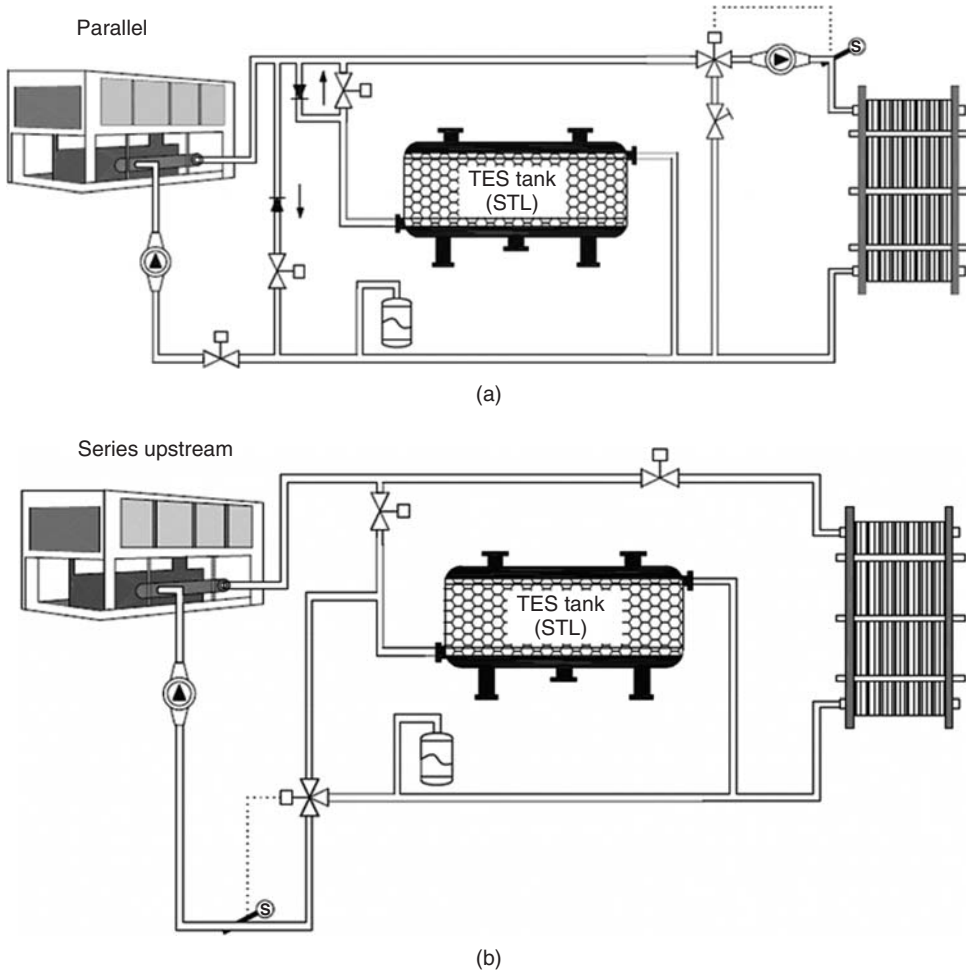


**Figure 9.26** Two configurations for TES in HVAC systems: (a) parallel; (b) series (modified from Cristopia Energy Systems, 2010)

### 9.6.3 Modeling, Control, Programming, and Optimization Methods

Various dynamic modeling procedures are available to simulate the real-time behavior of cooling/heating units incorporating CTES, with numerical methods usually requiring experimental verification. Thermal storage dynamic simulation software (TSTORS) for HVAC systems, EnergyPlus, BLAST and TRNSYS are among the software codes to simulate CTES systems and their integration into refrigeration or HVAC plants. Some of the codes can consider different control strategies and installation configurations. TSTORS, which is under development at Tsinghua University, is designed to perform feasibility studies according to different control strategies for ice-storage systems and balance economic and financial factors (Zhu and Zhang, 2000).

Dynamic programming permits the solution of complicated and multistage decision-making problems by finding an optimal strategy (Jaluria, 2008). Optimum chiller and ice-storage capacities can be determined for different operating conditions with dynamic programming. A dynamic programming algorithm has been utilized by Chen *et al.* (2005a) to optimize the performance of an

**Table 9.11** Investigations of operating strategies for TES systems

Reference	TES type	Investigation method	Remarks
Lemort (2006)	Ice capsule	Numerical with Engineering Equation Solver (EES) using experimental data at 15-min intervals	Three charge and discharge control strategies (chiller-priority, constant-proportion, load limiting) compared for operating costs; ice-storage systems reduce operating costs even if energy consumption increases
Chen <i>et al.</i> (2005a)	Ice-on-coil	Dynamic programming	Optimized strategy according to least life-cycle cost and highest ice-storage efficiency
Guilpart <i>et al.</i> (2005)	Ice slurry	Review of strategies by on/off pump and valve actuators	Plugging risk in ice-storage generators at some operating conditions (temperature $> -3/-4^{\circ}\text{C}$ and high solute concentration)
Ihm <i>et al.</i> (2004)	Ice-on-coil, internal-external ice harvester	Numerical using EnergyPlus and BLAST algorithms	Strategy presented to minimize operating cost for three types of ice-storage systems, based on a comparison of chiller-priority, constant-proportion, and storage-priority control strategies
Henze <i>et al.</i> (2003)	Ice storage	Numerical simulation, for various ice storage and cooling loads	Chiller size found for a combined mode of full and partial load; 28% reduction of chiller size achievable depending on peak period characteristics
LeBreux <i>et al.</i> (2009)	Hybrid solar-electrical TES	Numerical/experimental	Ability of anticipatory and regulation strategies to enhance performance is investigated
Zhao <i>et al.</i> (2008)	Seasonal underground borehole	Numerical	Strategy proposed for better thermal performance during discharging

ice-storage air-conditioning system, including the storage tank, a screw-type chiller, and auxiliary equipment, and simultaneously to minimize its life cycle (operating and energy) cost. The power consumption of the chiller and auxiliary equipment, and heat-transfer rates in the ice-storage tank are provided in manufacturer's data sheets. The objective functions are the initial and operation costs, and the constraints are the performance of the chiller and ice-storage tank. A numerical simulation determined the optimum chiller and ice-storage tank capacities, which were then used to find such design criteria as life-cycle cost and payback period. Two control strategies are considered: chiller priority and ice-storage priority. Use of chiller priority with a lower power consumption coefficient reduces energy costs. Enhanced chiller performance has been reported using the chiller-priority mode, but a higher heat-transfer efficiency can be achieved with the ice-storage priority mode. The former provides a higher chilled-water inlet temperature and the latter a better heat-transfer efficiency for the ice-storage tank. Under the same ice discharge condition, the ice-storage priority mode requires less ice storage. For regular cooling loads, ice priority yields a lower life-cycle cost and payback period than chiller priority.

Henze *et al.* (2003) presented a performance-improvement guideline for ice-storage systems in different types of buildings, consisting of a conventional compression chiller and associated auxiliaries. To determine an optimum strategy, three control priorities are compared. Chiller priority

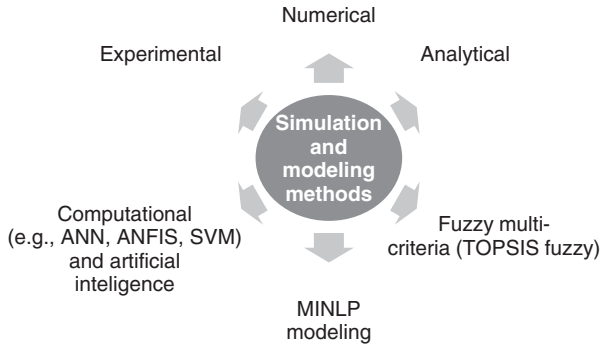


**Figure 9.27** Simulation and modeling methods used for TES systems

(direct cooling with no storage phase), constant proportion, and storage priority are the load-shifting patterns in the study. Although one of the main reasons to use TES is reduced utility cost and energy consumption or peak-demand charges, only one of these is considered in most cases; the approach of Henze *et al.* (2003) defines an optimal strategy to reduce both of these costs. Rate-based load-shifting incentives can constitute another reason for owners to use TES, and in this study the optimal control strategy is also developed for locations with lower energy-use incentives, which serve to decrease energy consumption. The results enable owners to determine if a new or retrofit ice-storage system is advantageous in their circumstances. In the investigation, 360 combinations of ice-storage systems, chiller types, building types, weather conditions, and cooling rates were considered for charging and discharging. For many cases, the peak demand reduction with storage-priority control is observed to be near optimal.

Definition of a mathematical model is one of the first steps in TES simulation. Halasz *et al.* (2009) developed a mathematical model for computer simulation of an ice-on-coil storage system, considering several operating strategies and system arrangements. Multi-period mixed-integer nonlinear programming (MINLP) has been used to simulate combined heat and power plants for district heating networks (Tveit *et al.*, 2009), with global optimum (thermal and financial) conditions sought. Some of simulation and modeling procedures used in TES applications are shown in Figure 9.27.

Cavallaro (2010) suggests a fuzzy multicriteria method called TOPSIS (technique for order performance by similarity to ideal solution) to evaluate HTFs for molten salt TES systems for solar power plants. The method determines a suitable and feasible molten salt for the system, and obtains a solution near to the ideal one. As we are often considering multi-criteria problems, fuzzy sets are good choices for performance analysis. By maximizing benefit criteria and minimizing cost criteria, a near-optimal solution is found. The method can help determine innovative solutions for antifreeze systems via less expensive solar systems operating with molten salts that are more environmentally benign than other HTFs. The method involves the following steps, the most important of which are choosing criteria such as investment, operation, and maintenance costs:

- generating alternative systems and subsystems;
- choosing objective criteria (e.g., costs and expenses);
- defining and weighting rating variables;
- defining the fuzzy decision matrix;
- matrix normalization;
- constructing the normalized fuzzy decision matrix.

To assess a typical flat plate solar collector incorporating a PCM for hot water applications, Varol *et al.* (2010) investigate the following prediction computing methods: artificial neural network (ANN), adaptive-network-based fuzzy inference system (ANFIS) and support vector machines

(SVM). The predicted results are verified with experimental data. These methods consist of a well-defined layered architectural structure (e.g., nodes, neurons, and networks) and training parameters used through learning rules. By providing predicted input values for such multi-criteria problems, the performance of the overall system can be determined.

LeBreux *et al.* (2009) investigate anticipatory and regulation control strategies for a hybrid solar/electrical TES system, which stores both solar and electrical energies for heating purposes when one or both are inexpensive (during off-peak periods). Optimization determines the preferred storing durations based on solar radiation and atmospheric air temperature. Electrical power consumption is reduced significantly using these strategies, which are particularly promising for new TES applications. Fuzzy logic and free forward controllers are the main tools for overcoming input disturbance effects on system performance; common PID controllers tend to overpredict the necessary room temperature.

### 9.6.4 Measurement and Visualization Methods

Numerous measurement and visualization techniques have been used in TES system analyses while others are under development. Heat transfer and fluid flow measuring devices and sensors are generally useful in TES studies. This section focuses on new and innovative methods for TES systems.

For packed beds consisting of cylindrical capsules, Götz *et al.* (2002) proposed magnetic resonance imaging (MRI) for measuring important parameters, including porosity and velocity distributions, wall effects on these distributions, and the total HTF volume in the tank. Among such measurement techniques as hot-wire and laser-Doppler anemometry, a nuclear magnetic resonance (NMR) method has been utilized to determine axial and angular variations of the aforementioned parameters and, subsequently, to represent the velocity vector at each point in a domain. Revankar and Croy (2007) visually examined with a photographic method the void distribution in PCM capsules during freezing, utilizing transparent capsules of various shapes (e.g., sphere, torus, and flat plate). The results reveal that, for some PCM/capsule combinations, performance changes over several thermal cycles as a result of appearance of voids in the PCM, with a direct effect on melting.

Castellón *et al.* (2008) investigated two heat-flux DSC methods for finding the enthalpy–temperature relation of PCMs through dynamic and step procedures. In these methods, the variation of the heat capacity of a sample with temperature is found and the correlation is then integrated to determine the enthalpy–temperature relation. A dynamic procedure is used to obtain the melting enthalpy of the PCMs for constant heating/cooling rates, while a step procedure is used to bring the sample/measurement system to thermal equilibrium by providing constant temperature intervals during the test. The temperature values are maintained by varying the sample heating/cooling rates. The method appears to reduce experimental uncertainty. A typical industrial DSC measurement system is shown in Figure 9.28.

With a DSC and heating rates versus temperature for a sample, it is possible to determine its melting temperature and latent heat of fusion through graphical/numerical estimation (e.g., integration). As depicted in Figure 9.29, the melting temperature is the intersection of the line connecting the two local peaks and the line with the highest slope tangent to the curve that represents melting. Tests are carried out for a fixed heating rate (degree Celsius per minute). The area of the curve confined by the melting portion can be used to calculate the latent heat of fusion.

The T-history method is another technique to measure heat capacity and the enthalpy–temperature relation for PCMs. In this technique, a sample material (e.g., distilled water) and a PCM specimen at the same temperature are exposed to a constant ambient temperature. The temperature histories of both materials are recorded during a cooling down, and used with known values of the selected sample (water) to calculate the apparent liquid and solid heat capacities, the latent heat, and the melting/solidification temperatures (Rady *et al.*, 2010).

Some of measurement and visualization methods used for TES systems are summarized in Figure 9.30.



**Figure 9.28** A typical industrial DSC measurement system (courtesy of TA Instruments, 2010)

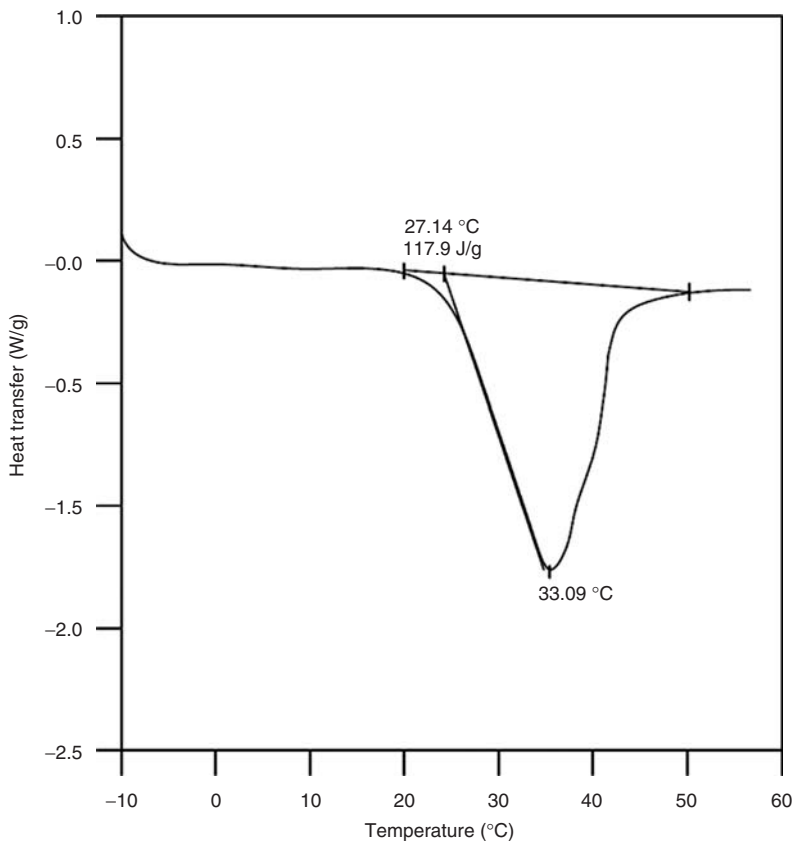


**Figure 9.29** A typical measurement of melting temperature and latent heat of fusion with a DSC measurement system (modified from Tyagi and Buddhi, 2008)

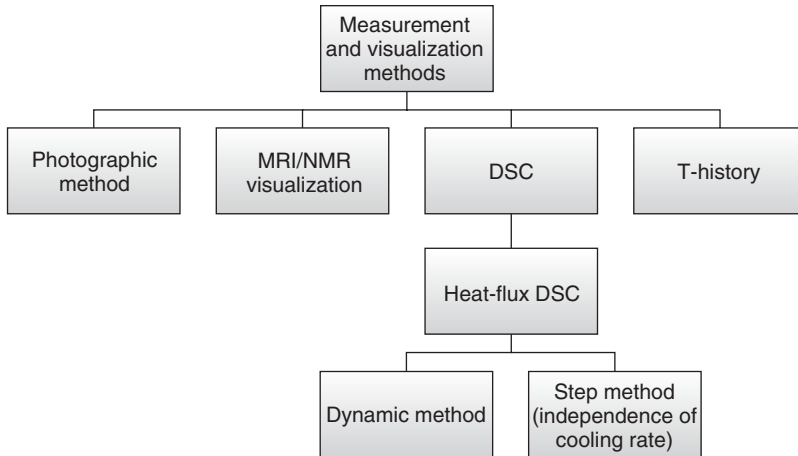


**Figure 9.30** Summary of measurement and visualization methods for TES systems (modified from Castellón *et al.*, 2008; Götz *et al.*, 2002; Rady *et al.*, 2010; Revankar and Croy, 2007)

### 9.6.5 Auxiliaries

Many pieces of auxiliary equipment, such as pumps, fittings, valves, actuators, piping and working fluid distribution systems, and heat exchangers, are included in an integrated TES/HVAC system. Sometimes these auxiliaries can affect the behavior and performance of the integrated system.

Operating characteristics for three types of pumps (centrifugal, single-channel, and screw) have been studied for ice-slurry applications by Frei and Huber (2005), considering three rotational speeds and a range of ice fractions. The centrifugal pump, which is generally less expensive, works well for ice fractions up to 25%, while the other two pump types perform better for greater ice fractions. The performance of multistage centrifugal pumps for ice slurries with ice concentration of 0–30 wt% have been analyzed experimentally (Nørgaard *et al.*, 2005), demonstrating a decrease in pump performance with increasing viscosity (ice fraction). The variation with ice fraction and flow rate of the pressure loss coefficient for various fittings (e.g., elbows, bends, contractions, tees) as well as straight pipes and heat exchangers indicates that the reduction in pressure is more dependent on flow rate than ice fraction.

Heat exchangers are one of the most important components in TES designs, and can be in the form of a tank filled with PCM capsules or a heat exchanger with a slurry on one side. The “superheating degree” is the temperature to which a fluid increases above its equilibrium temperature (if it does so). Pronk *et al.* (2008) investigate superheating as the driving force of melting in heat exchangers working with ice slurries as a secondary refrigerant. They also study the dependence of superheating on operating conditions, the most significant of which are ice fraction, ice-slurry’s bulk velocity, wall heat flux, crystal size, and solution concentration. Higher superheating degrees in heat exchangers can reduce performance, by increasing the average ice-slurry temperature and thereby reducing the heat-transfer rate between it and the cooling fluid from which heat is being drawn. Consequently, the capacity of the heat exchanger decreases, hindering TES system performance. The superheating degree of the heat exchanger outlet fluid increases with increasing average ice crystal size, wall heat flux, solute concentration, and decreasing ice fraction. Tube-in-tube heat exchangers with lower hydraulic diameters have higher superheating degrees according to the relation in this work (Pronk *et al.*, 2008). It is important to understand the effect of these parameters as well as pressure drop and heat transfer in the HTF flow on heat exchanger performance in TES systems.



## 9.7 Performance Enhancement Techniques

Various techniques are available to increase TES performance, depending on the type, application, HTF, and storage medium. Most techniques increase heat-transfer rates between the storage medium and the HTF. Some recent and innovative TES performance enhancement techniques and their effects are summarized in Table 9.12, described in subsequent sections and summarized in Figure 9.31.

Inaba *et al.* (2005) reviewed different antifreeze proteins, their substitutes, and types of surfactants as additives for preventing agglomeration and ice crystal growth in water (and for drag reduction). An important factor when using additives is freezing temperature depression. Some of them cause a decrease in the phase-change temperature and a consequent decrease in CTES performance.

One of the most widely used enhancement techniques for increasing the performance of TES systems is increasing overall PCM conductivity, which increases the heat-transfer rate and consequently decreases charging and discharging durations. Conductivity enhancement can be achieved by dispersing highly conductive small particles (e.g., graphite) in a PCM, adding fins and using a highly porous PCM-filled conductive material.

A numerical and analytical investigation by Shiina and Inagaki (2005) of the melting time of capsules filled with PCMs ( $\text{H}_2\text{O}$ , octadecane,  $\text{Li}_2\text{CO}_3$ , and  $\text{NaCl}$ ) in a porous metal (copper, aluminum, and carbon steel) showed that the highly porous ( $\sim 0.9$ ) metal medium allows the best PCM performance. The best conductive PCM/porous metal combination offers better discharging performance.

### 9.7.1 Conductivity-Enhancing Techniques

Recently developed enhancement techniques for thermal conductivity that are used in industries or are under development are summarized in Figure 9.32. Thermal conductivity enhancement has been achieved using a porous copper screen mesh around a cooling tube, increasing the ice growth rate (by 50–90% based on volume at steady state) for an ice-on-tube CTES system (Kazmierczak and Nirmalanandhan, 2006). A graphite matrix filled with paraffin to enhance the conductivity of the latent TES for a night-ventilation TES system reduced response times for charging and discharging periods (Marín *et al.*, 2005). In this case, thicker paraffin plates can be used as the PCM and fan power consumption decreases without significant change in response during charging and discharging. One drawback of these porous matrices is a decrease in the thermal storage capacity of the whole PCM. So, the conductivity reduction should be carefully examined for new applications and matrix materials. Mesalhy *et al.* (2005) examined the thermal response of a PCM in a cylindrical thick shell. Use of a highly conductive solid matrix with a high porosity is recommended to increase the phase-change time for TES systems.

### 9.7.2 Thermal Batteries

Thermal batteries involve the integration of TES and heat pipes. Huang *et al.* (2007) modified a previously developed novel idea for using a passive control method experimentally in ice-storage systems (Alawadhi, 2008). A closed finned and modified two-phase thermosyphon is used in a compact water/ice CTES system and, to increase the heat transfer rate, the heat pipes (parallel finned tubes) are placed in series (Figure 9.33a). Heat pipes are tubes filled with a refrigerant, which can be installed vertically or inclined between cold and hot sources, absorbing heat at one end (refrigerant evaporation) and rejecting heat at the other (refrigerant condensation). Advantages of these systems include fast responding; elimination of the piping system, circulation pumps, valves, and actuators; more rapid heat transfer (even compared to finned heat pipes); and dynamic response in more limited spaces. These systems can be utilized for charging and/or discharging, even for low values of input cooling or heating power. The refrigerant condenses on the tube as a low-temperature fluid flows through the charging double-pipe heat exchanger section (Figure 9.33b). The condensing



Table 9.12 Recent performance enhancement techniques for TES systems

Reference	Storage type	Enhancement technique	Effects	Remarks
Zhang <i>et al.</i> (2008)	Dynamic vertical ice-slurry generator	Bubbling device	Reduced ice adhesion to cooling wall	Air bubbling rates and coolant inlet temperature can be optimized to improve performance
Mesalhy <i>et al.</i> (2005)	PCM in concentric cylinders	Using high conductive porous matrix	Increased thermal conductivity	Numerical analysis of highly conductive porous matrix filled with PCM in a thick cylindrical shell
Matsumoto <i>et al.</i> (2007)	Ice slurry	Using optimum solution concentration	Reduced ice adhesion to heat exchanger wall	Water/oil emulsion is a good PCM; concentrations found for some additive oils
Marin <i>et al.</i> (2005)	TES	Porous graphite matrix embedded in core paraffin	Increased thermal conductivity	HTF (air) and PCM (paraffin-graphite)
Lamberg and Sirén (2003a)	Internal semi-infinite fins in a PCM	Internal fins in a PCM	Increased heat-transfer rate within PCM	Analytical results verified experimentally
Lamberg and Sirén (2003b)	Flat fins in a PCM	Internal fins in a PCM	Increased heat transfer rate within PCM	Fins enhance solidification when conduction is dominant heat-transfer mode; analytical results verified experimentally
Lamberg (2004)	PCM with an internal fin	Increasing PCM thermal conductance	Increased heat transfer rate within PCM	Simplified analytical model and numerical approach
Kazmierczak and Nirmalanandhan (2006)	External ice-on-tube	Porous copper mesh wound on cooling tube	Increased overall porous PCM conductivity	50–90% increment in ice generation
Huang <i>et al.</i> (2007)	Ice storage	Thermal battery as a subcooler	Enhanced heat transfer via two-phase closed thermosyphon	28% more cooling capacity and 8% higher COP
Henze <i>et al.</i> (2003)	Ice storage	Optimization strategy	Simulation to reduce operational costs	Accounts for storage type, chiller compressors, building type, and control strategy
Erek <i>et al.</i> (2005)	Ice storage	External finned tube	Increased heat-transfer rate within medium	Effects of Re for HTF, fin spacing, and diameter investigated numerically and experimentally
Chieh <i>et al.</i> (2008)	Ice storage	Thermal battery as a subcooler	Enhanced heat transfer via two-phase closed thermosyphon	Experimental and theoretical models; ratio identified of heating pipes clearance distance to outer pipe diameter

(continued overleaf)

Table 9.12 (continued)

Reference	Storage type	Enhancement technique	Effects	Remarks
Alawadhi (2008)	Cold water	Triangular corrugated fins inserted into storage medium	Increased heat-transfer rate within medium via higher conductance	Proper aspect ratio ( $>0.75$ ) for triangular fins greatly improves charging
Akgin <i>et al.</i> (2008)	Novel tube-in-shell storage configuration	Consistent geometry design with phase change	Improved performance during charging/discharging	Effect of Re and Ste for HTF on charging/discharging investigated
Agyenim <i>et al.</i> (2009)	Shell and tube	HTF multi-tube array in PCM-filled horizontal cylindrical shell	Radial 2D convection is dominant for HTF; radial conduction in shell is the highest during phase change	Natural convection details needed to determine phase-change front; erythritol used as PCM with melting point of $117.7^\circ\text{C}$ and latent heat of $33.9.8\text{ kJ/kg}$
Zhong <i>et al.</i> (2010a)	Graphite foam and Wood's alloy	Graphite foam infiltrated with Wood's alloy (50B <sub>4</sub> /27Ph/13Sn/10Cd)	Thermal conductivity doubled and thermal expansion reduced	No significant change in the latent heat; applications include solar energy and electronic device thermal management
Zhong <i>et al.</i> (2010b)	Paraffin/graphite	Compressed expanded natural graphite (CENG) in paraffin	Conductivity increased 28–100 times; anisotropic structure and texture lower natural convection	Different density storage matrices used; linear relation identified between (i) thermal conductivity and density and (ii) latent heat and graphite/paraffin mass ratio
Zhang <i>et al.</i> (2010)	High-density polyethylene/paraffin	Expanded graphite matrix and flame retardant material	Thermal conductivity increased and flammability reduced	Composite PCM maintains shape even during melting, expanding potential applications
Azzouz <i>et al.</i> (2009)	PCM integration with evaporator	Refrigerator COP enhancement	COP increased 10–30%	Various PCM thicknesses, ambient temperatures, and thermal loads; 1–3 h operation without PCM and 5–9 h with PCM
Zurigat <i>et al.</i> (2006)	Ice or chilled water	Gas turbine inlet air cooling to enhance turbine efficiency	Storage not recommended for considered weather/location	Installed in warm regions; technical feasibility of seasonal, partial, or full storage is case/location dependent
Wang <i>et al.</i> (2009)	Form-stable polyethylene glycol/silicadioxide (SiO <sub>2</sub> )	Adding $\beta$ -aluminum nitride powder to organic PCM	Increased thermal conductivity (0.3847 to 0.7661 W/m K)	Although composite PCM latent heat decreases, value is maintained in most latent TES applications

Lai and Hui (2009)	Heat (water)/cold TES	Trigeneration TES integration	Strategies based on daily demands	Feasibility study; flexibility necessary for integration
de Marchi Neto <i>et al.</i> (2009)	Hot water-stratified tank	Waste heat of refrigerator condenser heats water	Comfort increased	Experimental; no significant effect on refrigerator COP
Mazman <i>et al.</i> (2008)	Palmitic/lauric acid (80/20) and stearic-myristic (80/20)	Stainless steel, copper pieces or graphite/PCM composition	Enhanced thermal conductivity to increase melting/freezing rate	1.3–1.8 times faster phase change; better results for copper
Agyenim <i>et al.</i> (2009)	Finned double-tube heat exchanger	Circular/longitudinal fins	Reduced subcooling and increased heat-transfer rate	PCM (erythritol) melts at 117.7 °C; better performance for longitudinal fins
Sari and Karaipekli (2007)	Form-stable PCM	Expanded graphite with <i>n</i> -docosane paraffin	Increased thermal conductivity	2–10% expanded graphite used; impregnation used to insert liquid paraffin

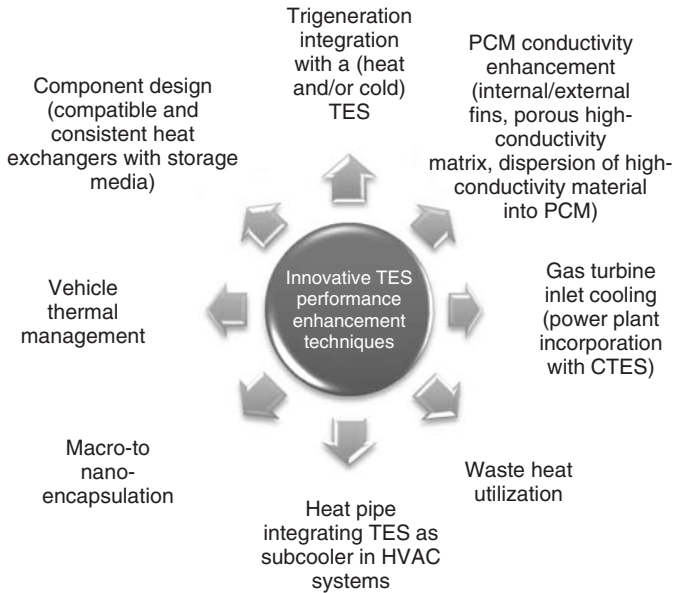


**Figure 9.31** Some of the innovative TES performance enhancement techniques and their applications

refrigerant falling from the wall absorbs thermal energy from the water tank and consequently makes water solidification possible by further heat removal from the exterior surface and through fins. Simultaneously, the refrigerant evaporates inside the thermosyphon. The ice-storage system can function in three modes (charging, discharging, charging/discharging). The system has computer monitoring and data collection, and is controlled by valve actuators. The system supplies subcooled refrigerant for the plate heat exchanger by using the ice-storage system and provides increased cooling capability and a higher COP for the refrigeration unit. The three operating modes of the storage system facilitate passive control of the unit.

Tardy and Sami (2009) assessed with a mathematical model the enhanced HVAC thermal performance obtained by integrating a heat pipe into a TES. One end of a bundle of heat pipes is inserted in a CTES and subjected to an air flow that is cooled at the other end. The thermal behavior is investigated experimentally under various conditions, to develop a better understanding of thermal behavior of heat pipes as part of cooling TES systems. One of the main advantages of such TES systems is their ability to function in a limited space with a rapid thermal response. Hsiao *et al.* (2009) investigated experimentally an HVAC performance enhancement technique using TES as a subcooler. Since the compressor operates under constant frequency, the integration improves the COP of the overall system.

### 9.7.3 Other Techniques

One of the drawbacks of dynamic ice-slurry generators is ice adhesion to the heat exchanger wall. Zhang *et al.* (2008) proposed a bubbling system to reduce ice adhesion in a continuous ice maker. An air compressor is installed on a test vertical ice generator unit to produce bubbles in the solution that agitate it and prevent adhesion. Factors affecting performance include air bubbling rate, coolant inlet temperature, and additive concentrations in the solution. Ice-slurry production methods require proper amounts of emulsifier and additives to the water to avoid ice adhesion to cooling walls.

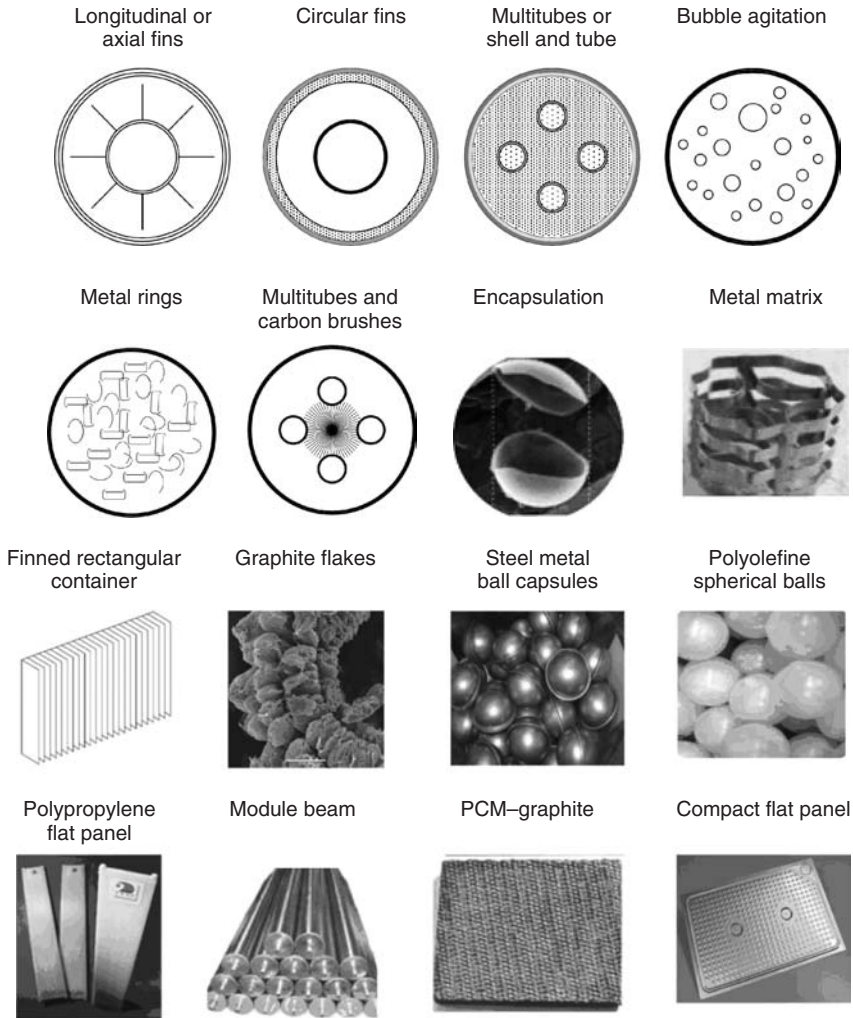


**Figure 9.32** Some recent enhancement methods for PCM thermal conductivity (modified from Agyenim *et al.*, 2010)

A consistent geometry for a PCM storage container improves TES performance in some cases (Akgün *et al.*, 2008). Heat transfer and fluid flow analyses help better understand the thermal performance of the system and relevant design factors.

## 9.8 Innovative Applications of TES Systems

Many innovative applications of TES using PCMs and other substances exist in the industrial sector or are undergoing research and development. Various recently proposed TES applications are summarized in Table 9.1 and depicted in Figure 9.34, include the integration of refrigeration system's cooling components with a PCM to reduce temperature variations, cooling innovations for personal digital assistants and large-scale integrated electrical circuits, the integration of subcooler

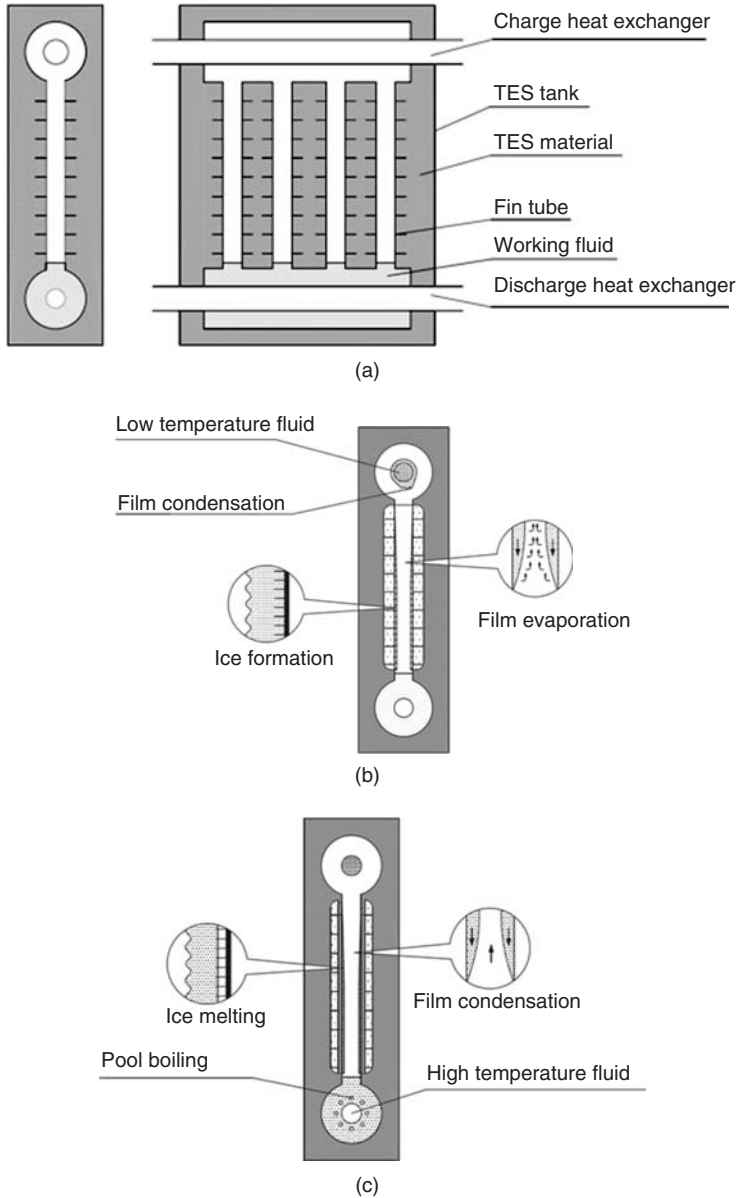


**Figure 9.33** A typical finned thermosyphon as a thermal battery: (a) submerged in a water tank; (b) in charging mode; (c) in discharging mode (modified from Huang *et al.*, 2007)

heat exchangers with refrigeration systems to enhance gas turbine inlet-air cooling in warm environments, and the integration of PCMs with wall or partitioning materials to provide a more constant temperature and enhance comfort.

New applications of TES systems in remote and dry areas have been reported for still water production and desalination of brackish water (Fang *et al.*, 2009). Murugavel *et al.* (2010) used sensible TES, consisting of solid materials such as quartzite rock, red brick pieces, and cement

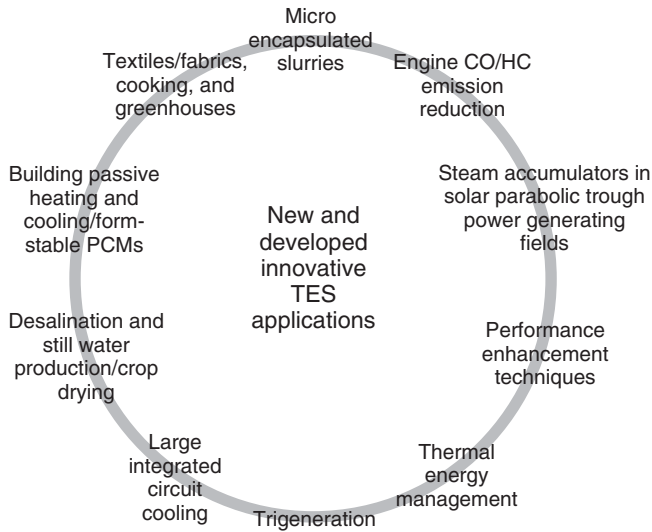


**Figure 9.34** Some new and developed innovative TES applications

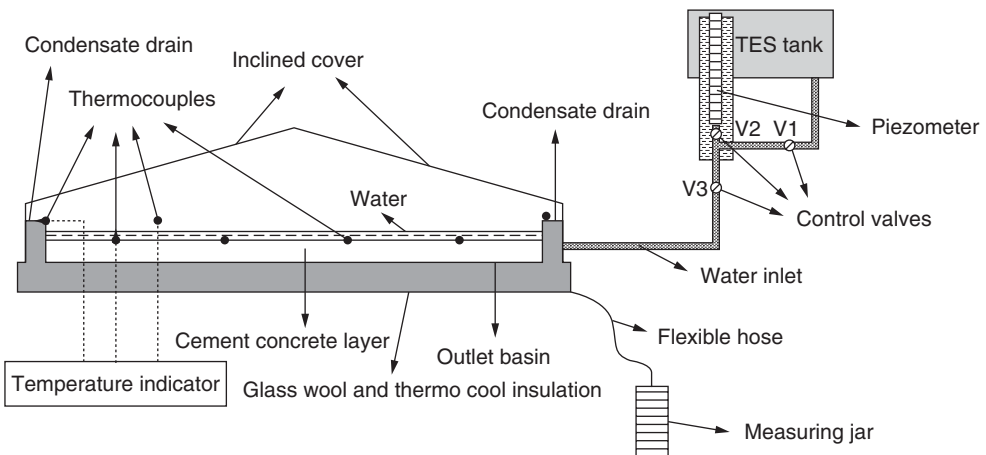


**Figure 9.35** Double-slope solar-based water production system (modified from Murugavel *et al.*, 2010)

concrete pieces, in a portable solar water-producing system (Figure 9.35). It consists of a sealed compartment as single basin double slope with two inclined sheets of glass, which receives the solar radiation. Water vapor is generated by direct contact of salty water with some solid sensible heat storages inside the system. Pure water condenses on the glass sheets and is drained on both sides. The production rate depends on the water/glass and atmosphere temperature difference, and a minimum basin depth exists that yields maximum productivity.

El-Sebaï *et al.* (2009) investigated numerically a desalination system integrating a PCM, producing a transient mathematical model of the desalination process, and examining production performance on daily and overnight bases. An analysis of the effect of several parameters (e.g., PCM mass, time of season, water mass) on productivity and efficiency showed that the use of stearic

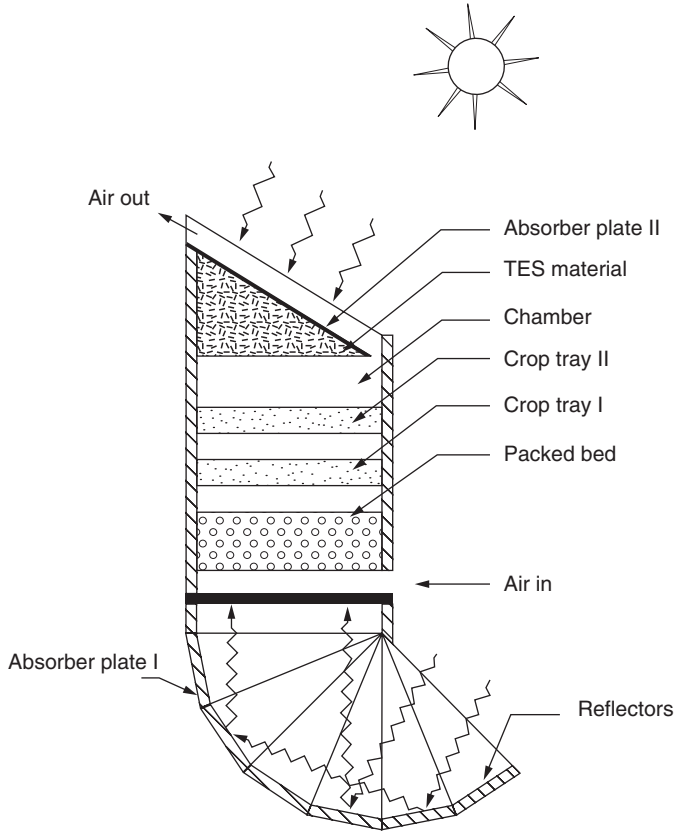


**Figure 9.36** Solar crop dryer using natural convection and incorporating a packed-bed TES (modified from Jain, 2007)

acid as the PCM almost doubled the system water production per unit area. Muthusivagami *et al.* (2010) review solar cookers and crop dryers with and without thermal storage. The performance of a crop dryer incorporating a packed-bed (porous plates of pebbles) TES and natural convection has been investigated (Figure 9.36), as has the relation between crop temperature and moisture content with drying rate (Jain, 2007). Utilizing TES reduces the temperature fluctuations during drying even if solar radiation intensity varies, and permits use during nonsunny hours.

A novel and efficient reflux heat-transfer storage that operates at high temperatures is proposed for use in a combined evaporation/condensation process in order to facilitate constant steam production for a 12-MW solar power plant (Adinberg *et al.*, 2010). Steam accumulators (Figure 9.37a) are used in some solar power plants with parabolic trough collectors; steam/water or oil is utilized as the heat transport material in the direct steam generation fields, reaching temperatures exceeding  $400^{\circ}\text{C}$  at a pressure of 100 bar (Steinmann and Eck, 2006). To achieve the highest volumetric energy capacity, the steam accumulators store saturated water at high pressures instead of as superheated vapor and are capable of a sensible heat storage capacity of  $20\text{--}30\text{ kWh/m}^3$ . Steam is obtained during discharge by lowering the pressure. Disadvantages of using steam accumulators as a storage include nondelivery of steam at constant pressure and high costs. But integrating TES with a steam accumulator (Figures 9.37b and 9.37c) maintains a constant-pressure output during a longer period and also decreases thermomechanical stresses in the main component of the power generating plant (Figure 9.38).



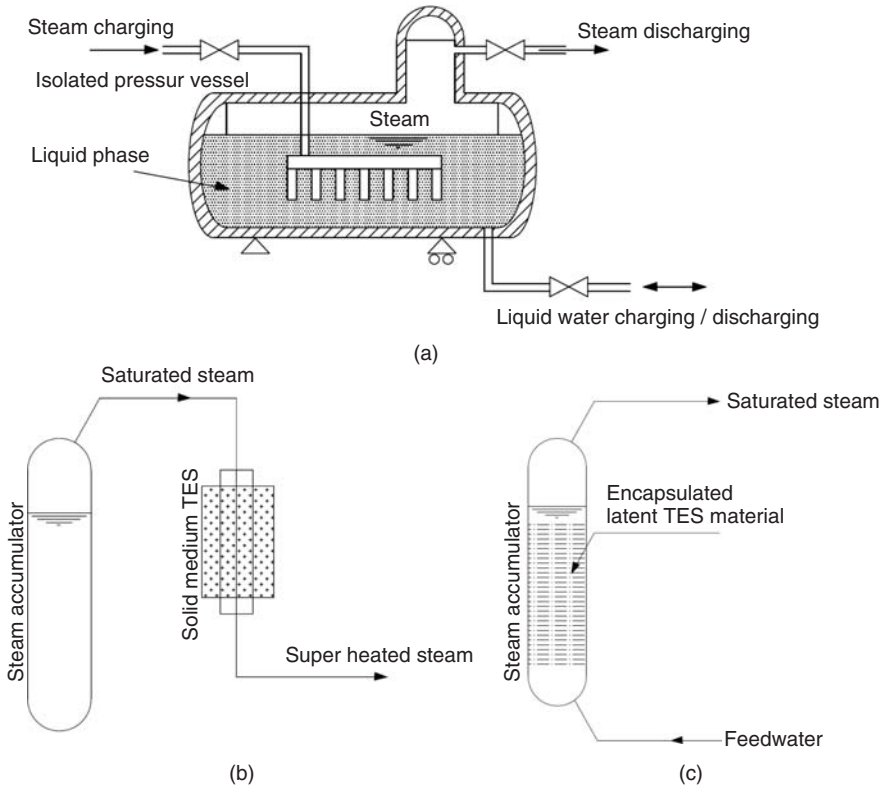


**Figure 9.37** (a) Sliding-pressure steam accumulator; (b) integration of sensible TES with the accumulator; (c) integration of latent TES with the accumulator (modified from Steinmann and Eck, 2006)

In some countries, where hydroelectric power is utilized, pumped storage is used when electricity is not required or for economic reasons if a two-tariff policy exists for generation during peak and nonpeak hours (Crampes and Moreaux, 2010). As an alternative to pumped storage, Desrues *et al.* (2010) propose a high-temperature TES system with charging and discharging cycles of a Brayton heat pump and heat engines, as depicted in Figure 9.39. This novel system avoids the geological constraints associated with pumped storage and the need for elevation differences.

Gumus (2009) proposed integrating a thermal storage PCM with internal combustion engines to eliminate or reduce CO and HC emissions during engine cold starts in cold weather. The performance requires careful thermal management, which depends on such parameters as engine temperature increment during charging/discharging, environmental conditions ( $T$  and  $P$ ), and required preheating time. Some of the PCMs considered for use in vehicle thermal management via TES are listed with their properties in Table 9.13.

Storing waste heat in a PCM for thermal management and performance enhancement also has been investigated experimentally by Kauranen *et al.* (2010). The TES is part of an exhaust-gas heat recovery system for a diesel engine, and is particularly beneficial when the engine has many periods of idling. Tests of the designed heat exchanger (Figure 9.40) demonstrated reductions in fuel consumption and emissions.

Innovative integrations of TES with trigeneration systems for buildings (Table 9.14) have been proposed recently (Lai and Hui, 2009, 2010). An example of such an integrated system for cooling and heating applications is shown in Figure 9.41. The economic feasibility depends on

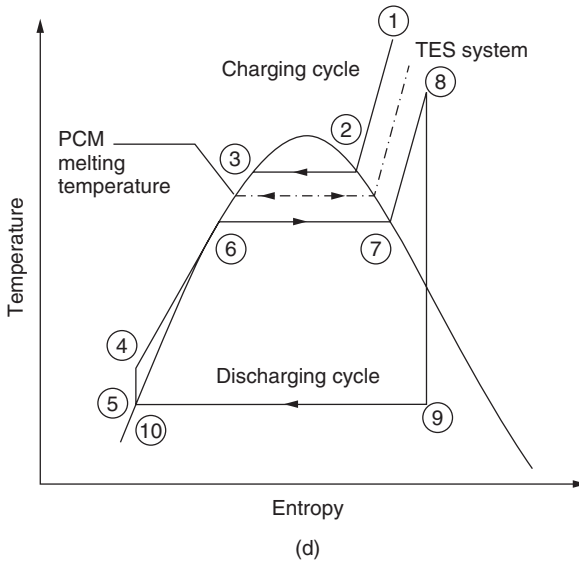
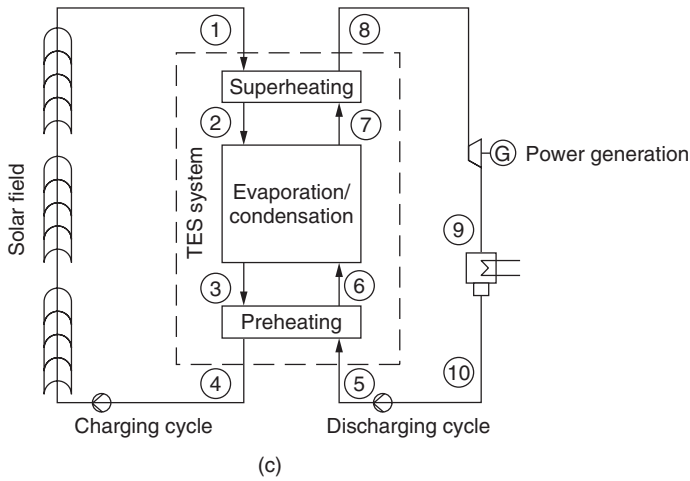
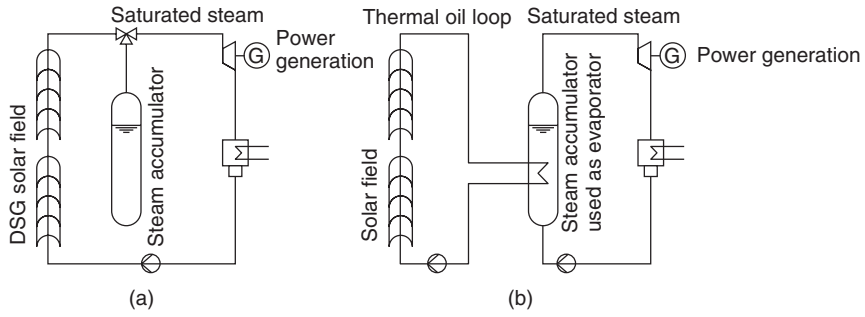


**Figure 9.38** Solar power plant using (a) steam and (b) oil as heat transport medium in collectors (Steinmann and Eck, 2006). Use of TES in a power production (c) and the corresponding  $T-s$  diagram (d) (Modified from Tamme *et al.*, 2008)

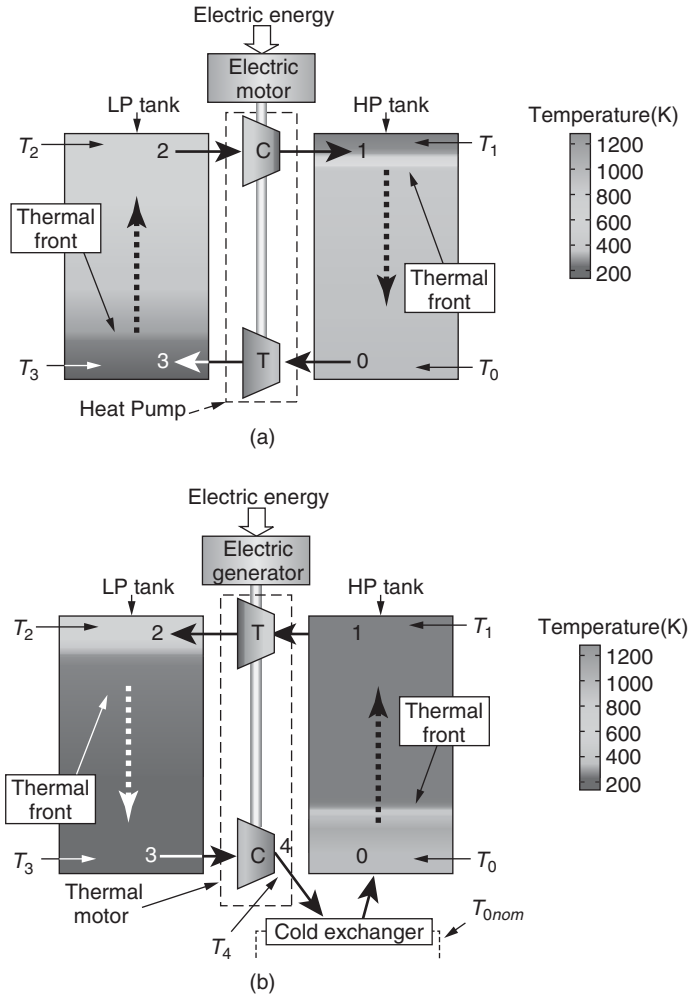


**Figure 9.39** Electricity storage using TES (modified from Desrues *et al.*, 2010). (a) Charging by the supply of energy to the Brayton heat pump; (b) discharging by generating electricity with a Brayton heat engine

**Table 9.13** PCMs used in vehicle thermal management systems (Gumus, 2009)

PCM	Melting temperature (°C)	Heat of fusion (kJ/kg)	Thermal conductivity (W/m K)	Density (kg/m <sup>3</sup> )
Na <sub>2</sub> CO <sub>3</sub> ·10H <sub>2</sub> O	32–36	246.5	N/A	1442
Na <sub>2</sub> SO <sub>4</sub> ·10H <sub>2</sub> O	32.4	254	0.544	1458
Ba(OH) <sub>2</sub> ·8H <sub>2</sub> O	48	265.7	0.653	1937
NaOH·H <sub>2</sub> O	58	N/A	N/A	N/A
NaOH	64.3	227.6	N/A	1690
NaNO <sub>3</sub>	307	172	0.5	2260
KNO <sub>3</sub>	333	266	0.5	2110
LiCl/KCl (58.7/41.3%)	352.7	251.5	N/A	1880
KOH	380	149	0.5	2044



**Figure 9.40** Heat recovery system for exhaust gases from a diesel engine. The heat exchanger and its casing work as a latent TES (Kauranen *et al.*, 2010)

heating/cooling load demands and the cost of the TES and its integration into the system. In jurisdictions where electricity tariffs differ during peak and nonpeak periods, trigeneration systems can be made economically more advantageous by incorporating TES for cooling and/or heating, thereby adding flexibility to the system. Detailed techno-economic assessments for a given case are necessary to determine the feasibility.

## 9.9 Advanced Applications of Exergy Methods

Energy analysis provides one view of system efficiency, focusing on heat transfer and losses, but neglects second-law factors such as entropy generation and exergy. Exergy analysis is a particularly beneficial complement to energy analysis.

Bouزيد *et al.* (2008) investigated analytically the entropy generation in a fully developed, laminar ice-slurry flow, utilizing a non-Newtonian power-law model for the slurry flow. The relation is described between entropy generation and three main parameters: ice mass fraction and two dimensionless groups. Increasing ice mass fraction flattens the velocity profile and increases entropy generation in the slurry flow.

MacPhee and Dincer (2009) modeled a CTES consisting of ice capsules in a horizontal cylindrical tank for two different temperature distributions (linear and quadratic), and applied first and second law analyses. Fully developed plug flow is also considered with a mean porosity at steady state, as is one- and two-dimensional conduction. The HTF temperature distribution and wall heat leakage are determined, and radial conduction is observed to be more important than axial conduction.

Exergy analyses of refrigeration and HVAC systems incorporating TES identify component irreversibilities and facilitate efforts to improve performance from manufacturing through to operation by the implementation of efficient techniques. Rosen and Dincer (2003) investigated with exergy analysis performance issues for sensible cold storage and identified meaningful measures to improve

Table 9.14 Selected applications of TES systems

Reference	TES application	Innovative aspects	Remarks
Azzouz <i>et al.</i> (2008)	PCM in vapor compression domestic refrigerator to enhance performance	Adding thermal inertia to evaporator increases evaporator temperature and system efficiency	5–30% efficiency losses due to compressor cycling caused by refrigerant displacement, which can be reduced
Yin <i>et al.</i> (2008)	Rapid response cooling for large-scale integrated circuit/electronic chips	Using paraffin in expanded graphite; required storage period is reduced by 65.3% and discharge period by 26.2%	Highest conductivity achieved: 4.676 W/m K
Wang <i>et al.</i> (2008b)	Potential PCM heat sink for personal digital assistants and notebooks	Extruded aluminum sink embedded with suitable PCM to enhance the overall performance	Important parameters: PCM volume fraction, temperature difference, aspect ratio, and PCM properties
Kandasamy <i>et al.</i> (2008)	Electronic PCM-based heat sink	Improved cooling performance	Experimental and numerical investigation
Evans <i>et al.</i> (2008)	Pipeline cleaning	1D numerical model for heat and mass transfers with melting solved and verified experimentally	4.75% NaCl aqueous solution utilized, with ice mass fraction of 18–24%
Wang <i>et al.</i> (2007a)	PCM heat exchanger in a HVAC system	PCM heat exchanger used as precondenser to improve overall COP	PCMs usually act like capacitors for dampening temperature variations of refrigeration compartment, but this precondenser provides subcooled refrigerant
Wang <i>et al.</i> (2007b)	PCM used for energy saving and control of refrigeration system	Mathematical model solved for dynamic behavior of refrigeration with a PCM heat exchanger as subcooler	Higher COP achieved by the integration
Wang <i>et al.</i> (2007c)	PCM used for energy saving and control of refrigeration system	Shell-and-tube PCM heat exchanger used at several locations in refrigeration system as subcooler	Higher COP achieved by the integration
Carbonari <i>et al.</i> (2006)	Prefabricated walls with PCM	Insulating wall	Numerical/experimental study; heat flux reduced through wall during warm summer days
Sebzali and Rubin (2006)	Cool TES for building of a medical clinic	Operating strategies tested to reduce electrical demand and/or energy consumption	Chiller capacity required is larger for full storage and smaller for partial storage
Ameri <i>et al.</i> (2005)	Gas turbine performance improvement	Inlet air-cooling of combustion turbines located in warm environments using chilled water/ice storage	Turbine capacity increased by 13.6% by lowering its inlet air temperature

(continued overleaf)

Table 9.14 (continued)

Reference	TES application	Innovative aspects	Remarks
Bellas and Tassou (2005)	Present and potential future applications of ice slurry	Future applications: ice pigging (internal cleaning of vessels), medical, artificial snow, transport refrigerant, fire fighting	Review article; considers comfort cooling, food processing, and preservation (fish industry, dairy products)
Simard and Lacroix (2003)	Truck refrigerated compartment with temperature lower than 265 K	Frost model added to storage system	Mathematical model of a system of PCM parallel plates, with experimental validation; HTF is warm, moist air
Lai and Hui (2009)	Trigeneration units	Feasibility and flexibility of TES integration with trigeneration systems for buildings	Heating/cooling loads affect techno-economic feasibility of TES integration
Lai and Hui (2010)	Trigeneration units	Integration of CTES with trigeneration for residential buildings	TES inclusion can improve trigeneration economics, especially if peak and nonpeak electricity costs differ

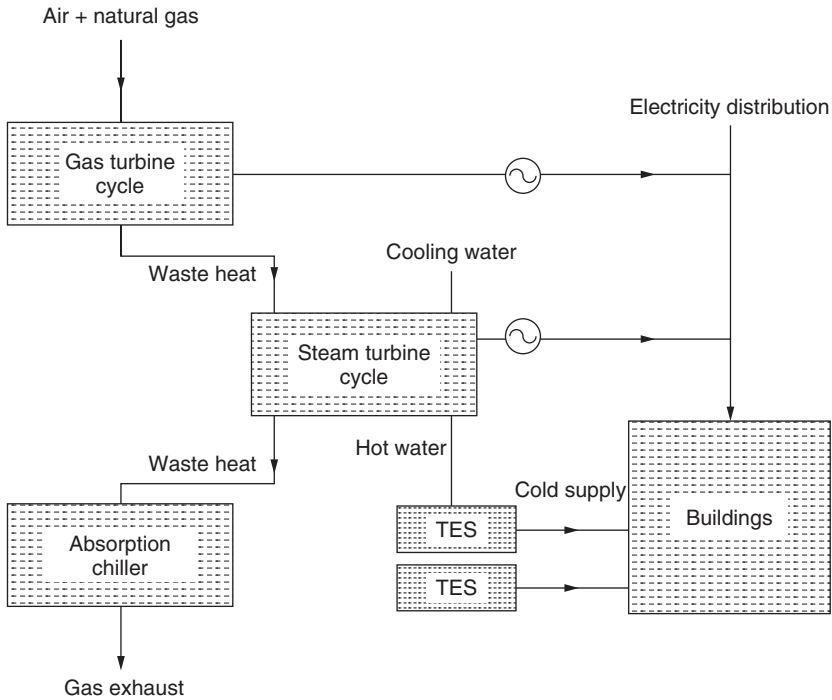


**Figure 9.41** Typical integration of TES systems with a trigeneration unit (modified from Lai and Hui, 2009)

energy management and reduce losses. TES system performance is enhanced by exploiting the advantage of thermal stratification within the storage, avoiding mixing and using more efficient pumps. Bakan *et al.* (2008) determined for an ethylene-glycol-sensible CTES in a 350,000 kg tank that the chiller COP depends significantly on storage and ambient temperature, HTF mass flow rate and heat losses, and mildly on ambient temperature.

A response-based energy efficiency of the charging and discharging periods accounting for outlet temperatures is determined by Yamaha *et al.* (2008) for two CTES systems: ice-on-coil and dynamic-type ice generator. For the ice-on-coil storage system, the IPF is the most important performance parameter, while inlet HTF temperature and mixing also have an effect.

## 9.10 Illustrative Examples

To illustrate the recent advances in TES methods, technologies, and applications discussed in this chapter, three examples are presented: use of effectiveness as a measure of merit, the application of a thermal battery ice storage in an HVAC system, and artificial neural networks in TES.

### 9.10.1 Use of Effectiveness to Complement TES Energy and Exergy Efficiencies

The use of effectiveness as a measure of merit to complement efficiency in TES energy and exergy analyses is described. The two measures together provide greater insights into performance efficiency than efficiency alone.

To illustrate, we focus on TES systems that comprise a shell-and-tube-type latent heat storage system for its charging process. Many investigations suggest the shell-and-tube-type heat exchanger as promising for latent heat storage, as it provides high efficiency while being compact. For instance, Erekan and Ezan (2007) examined the effect of flow parameters on energy stored for different configurations, while Trp (2005) and Trp *et al.* (2006) developed a model using an enthalpy formulation for external melt on tube.

### Effectiveness and Efficiency for TES

For evaluating TES systems, a dimensionless effectiveness measure was introduced (Erekan and Dincer, 2009), where

$$\text{Effectiveness} = \frac{\text{Useful output}}{\text{Maximum output}} \quad (9.1)$$

The energy effectiveness of a TES system  $\varepsilon_{En}$  is defined as the ratio of actual total energy stored to the maximum energy that can be stored. Maximum energy storage is achieved when the final state of the system is equal to the temperature of inlet. Hence,

$$\varepsilon_{En} = \frac{\Delta E_{sys,t}}{\Delta E_{sys,max}} = \frac{E_{sys,t} - E_{sys,i}}{E_{sys,t \rightarrow \infty} - E_{sys,i}} \quad (9.2)$$

Correspondingly, the exergy effectiveness of a TES system  $\varepsilon_{Ex}$  is defined as the ratio of actual total exergy stored to the maximum exergy that can be stored. The exergy effectiveness can be expressed as

$$\varepsilon_{Ex} = \frac{\Delta Ex_{sys,t}}{\Delta Ex_{sys,max}} = \frac{Ex_{sys,t} - Ex_{sys,i}}{Ex_{sys,t \rightarrow \infty} - Ex_{sys,i}} \quad (9.3)$$

It is instructive to contrast these effectiveness measures with the more common efficiencies. In general, efficiency is often expressed as follows:

$$\text{Efficiency} = \frac{\text{Useful output}}{\text{Input}} \quad (9.4)$$

The energy efficiency  $\eta$  of a TES is the ratio of the energy recovered from the TES to the energy input:

$$\eta = \frac{\text{Energy recovered}}{\text{Energy delivered}} \quad (9.5)$$

Similarly, the TES exergy efficiency  $\psi$  is the ratio of the exergy recovered to that input:

$$\psi = \frac{\text{Exergy recovered}}{\text{Exergy delivered}} \quad (9.6)$$

### Illustration

As an illustration, we consider the shell-and-tube latent heat storage unit, modeled as shown in Figure 9.42. The PCM fills the annular space around the tube, of inner radius  $r_o$  and outer radius  $r_{inf}$ , while HTF flows inside the tube. The tube wall has inside and outside radii of  $r_i$  and  $r_o$ , respectively. The rate of heat gain from the surroundings is evaluated as

$$\dot{Q}_{gain} = UA(T_0 - T_{PCM}) \quad (9.7)$$



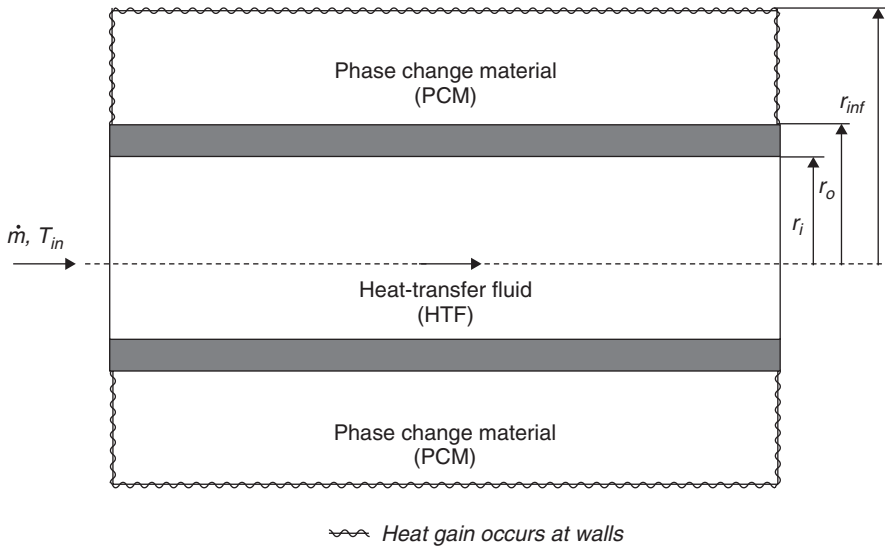


**Figure 9.42** Model of a latent TES system

where  $U$  is the experimentally determined overall heat-transfer coefficient,  $A$  is the heat transfer area, and  $T_0$  and  $T_{PCM}$  are the temperatures of the surroundings and the PCM near the wall, respectively. The thermophysical properties of the PCM, tube wall, and HTF (see Table 9.15) are taken to be independent of temperature, but the properties of the PCM differ in the solid and liquid phases. Initially, the overall system is set to an initial temperature, which is higher than the melting temperature of PCM. An analysis of the system is described by Erekan and Dincer (2009). Two

**Table 9.15a** Properties of heat transfer fluid at several temperatures

Temperature, $T$ (°C)	Density, $\rho$ (kg/m <sup>3</sup> )	Specific heat, $c$ (J/kg K)	Thermal conductivity, $k$ (W/m K)	Thermal diffusivity, $\alpha$ (m <sup>2</sup> /s)	Dynamic viscosity, $\mu$ (Pa s)
-10	838.594	2252.917	–	$1.053 \times 10^{-7}$	0.0030
-15	842.940	2208.537	0.199	$1.069 \times 10^{-7}$	0.0034
-20	847.286	2148.665	–	$1.093 \times 10^{-7}$	0.0038

**Table 9.15b** Properties of tube wall and phase change material

Material	Phase	Density, $\rho$ (kg/m <sup>3</sup> )	Specific heat, $c$ (J/kg K)	Thermal conductivity, $k$ (W/m K)	Thermal diffusivity, $\alpha$ (m <sup>2</sup> /s)	Latent heat (J/m <sup>3</sup> )
Tube wall	Solid	8800	420	52	$1.407 \times 10^{-5}$	–
PCM (water)	Liquid	999.8	4217	0.561	$1.33 \times 10^{-7}$	$333.5 \times 10^6$
	Solid	916.8	2040	2.2	–	–

dimensionless dimensions are utilized:

$$R = \frac{r}{D}$$

$$X = \frac{x}{D}$$

The Fourier and Reynolds numbers are also used, where

$$Fo = \frac{\alpha_f t}{D^2}$$

$$Re_f = \frac{4\dot{m}}{\pi D \mu_f}$$

In this illustration, the thermal behavior of a cold latent TES system is described only for the charging process. Heat infiltration losses are accounted for. While the energy delivered to the TES is equivalent to the energy supplied by the HTF, the energy recovered is the total energy stored during the charging process. The energy efficiency of the TES charging process is

$$\eta = \frac{\Delta E_{sys,t}}{E_{HTF}} \quad (9.8)$$

where  $E$  denotes the internal energy and

$$\Delta E_{sys,t} = E_{sys,t} - E_{sys,i} = \iiint_V \rho(u - u_i) dV \quad (9.9)$$

$$E_{HTF} = \dot{m} \int_{t=0}^t (h_{out} - h_{in}) dt \quad (9.10)$$

We can determine the corresponding exergy efficiency as follows:

$$\psi = \frac{\Delta E_{x,sys,t}}{E_{x,HTF}} = \frac{\iiint_V \rho [(u(t) - u_i) - T_0 (s(t) - s_i)] dV}{\dot{m} \int_{t=0}^t (\varepsilon_{out} - \varepsilon_{in}) dt} \quad (9.11)$$

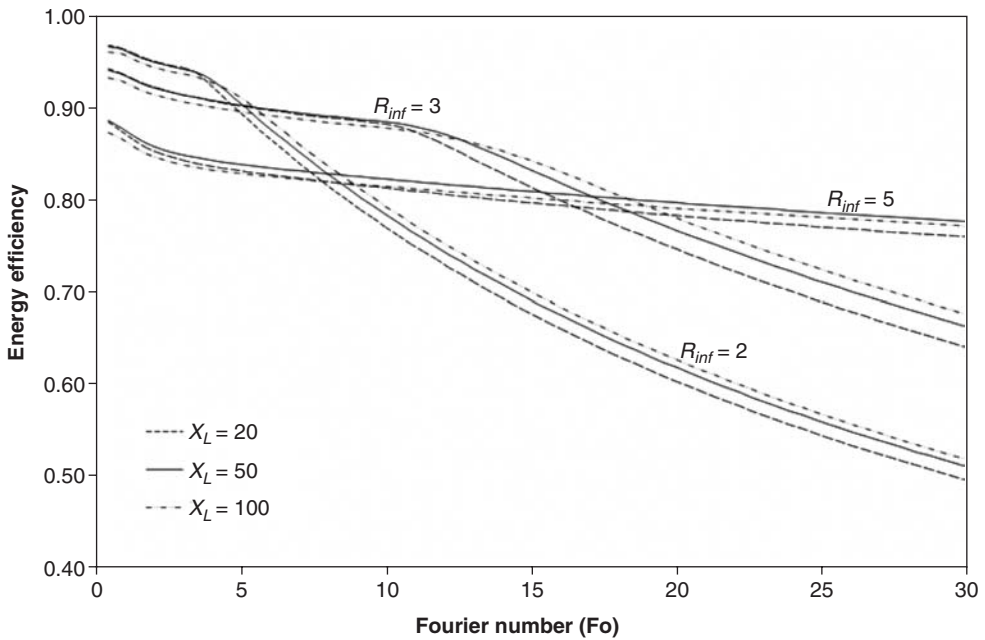
where  $\Delta E_{x,sys}$  denotes the exergy accumulation in the system, and  $E_{x,HTF}$  denotes the flow exergy of the HTF. Also,  $\varepsilon$  denotes specific flow exergy  $[(h - h_0) - T_0 (s - s_0)]$  and  $\iiint_V$  denotes the triple integral for  $V$  in three-dimensional space.

The numerical model used in this study has been experimentally validated by Erek and Ezan (2007). That work included a series of 81 parametric studies performed to assess the overall thermal behavior of the TES unit by varying the design and operating parameters in Table 9.16.

First, we examine the behavior of the efficiencies, on energy and exergy bases. The time-dependent variation of energy efficiency, defined earlier as the ratio of energy stored to energy supplied by the HTF, is shown in Figure 9.43 for several design parameters and  $Re = 1000$  and  $T_{in} = -15^\circ\text{C}$ . This case ends when complete solidification occurs and the charging process finishes. It is observed that the energy efficiency increases as shell radius decreases because of reduced heat gain during charging. After solidification, however, the energy efficiency decreases as the shell radius and the length of the TES decrease. Since heat loss continues but no additional energy is stored, the energy efficiency decreases in this period. The variation in energy efficiency with the Fourier number is shown in Figure 9.44 for several operating parameters with  $R_{inf} = 3$  and  $X_L = 100$ . The most important operating parameter affecting energy efficiency is the HTF inlet temperature, and energy efficiency increases as this temperature increases.

**Table 9.16** Design and operating parameters considered

Parameter	Material, quantity, or value(s)
Element	
PCM	Water
HTF	Ethyl alcohol
Pipe wall	Bronze
Dimensionless dimensions	
Inner radius of pipe	0.50
Outer radius of pipe	0.75
Shell radius, $R_{inf}$	2, 3, 5
Pipe length, $X_L$	20, 50, 100
Reynolds number, Re	500, 1000, 2000
Temperatures ( $^{\circ}\text{C}$ )	
Inlet temperature of HTF, $T_{in}$	-10, -15, -20
Initial temperature of TES, $T_i$	0.3
Environment temperature, $T_o$	16.85

**Figure 9.43** Variation of energy efficiency with several design parameters for  $\text{Re} = 1000$  and  $T_{in} = -15^{\circ}\text{C}$ 

The variation of exergy efficiency, defined as the ratio of the exergy stored in the TES to the exergy supplied by the HTF, with several design parameters is shown in Figure 9.45 for  $\text{Re} = 100$  and  $X_L = 100$ . Since exergy is a measure of energy quality, exergy efficiencies are more significant than energy efficiencies. Irreversibilities mainly due to heat transfers across finite temperature differences, between the environment and the PCM and between the PCM and the HTF, destroy some of the input exergy. The exergy efficiency increases as the shell radius decreases and the TES length increases until solidification is completed. The exergy efficiency decreases with time because

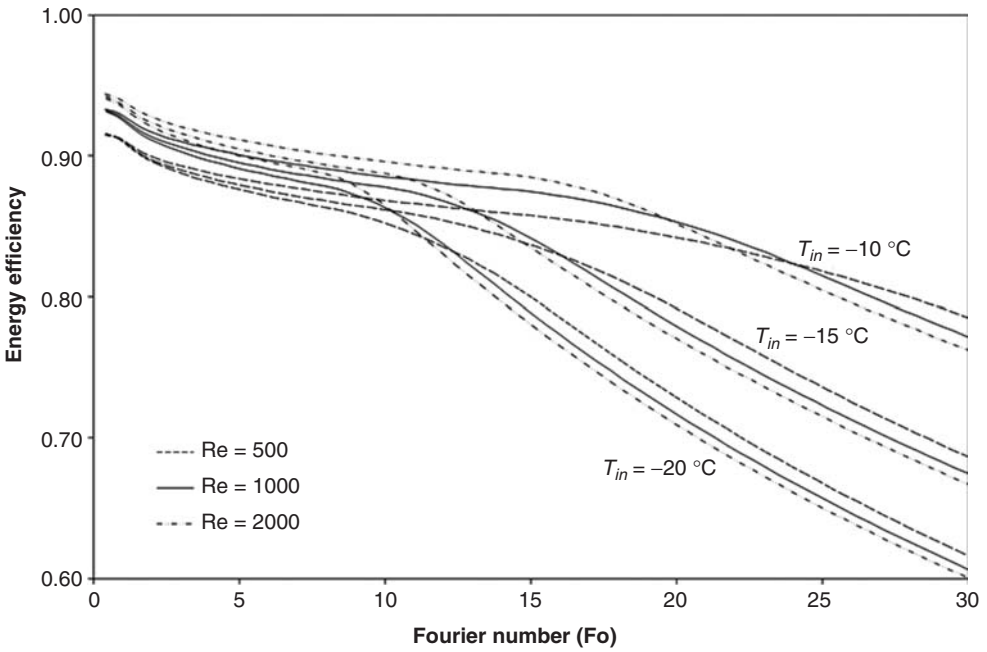


Figure 9.44 Variation of energy efficiency with several operating parameters for  $R_{inf} = 3$  and  $X_L = 100$

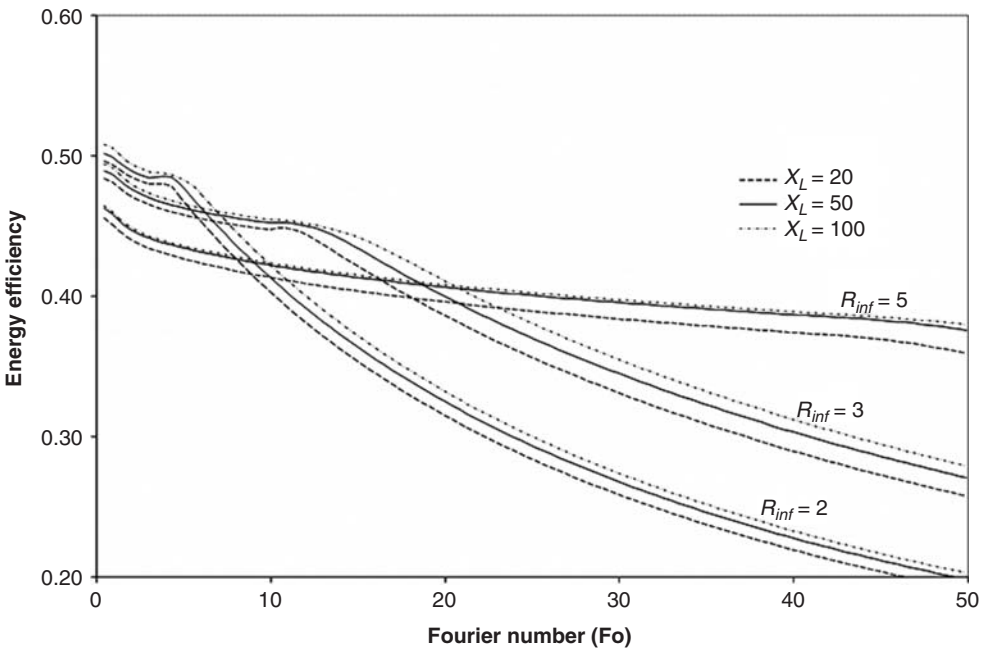
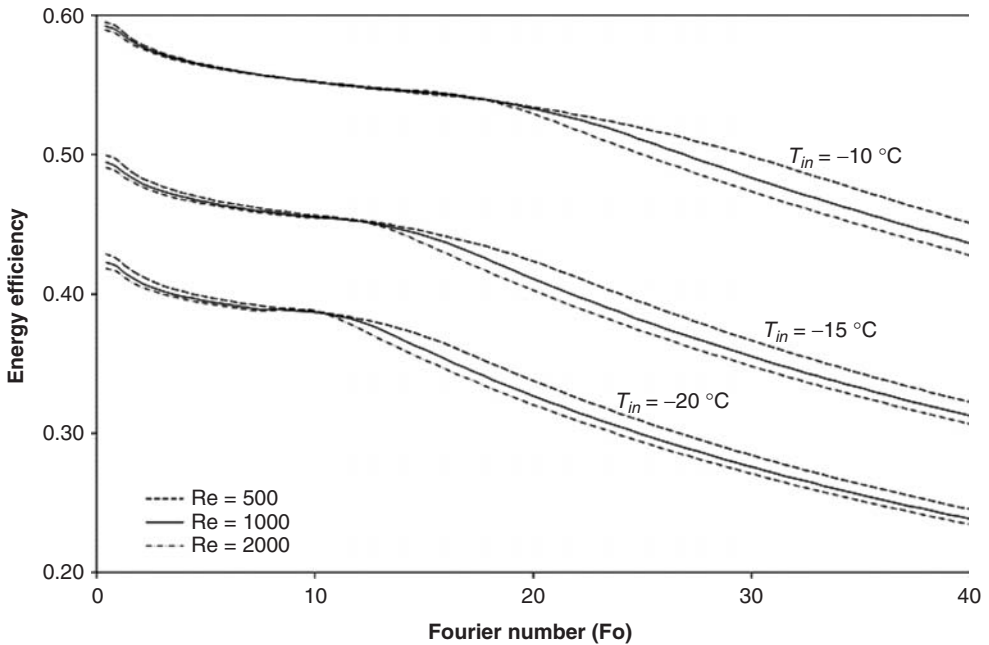


Figure 9.45 Variation of exergy efficiency with several design parameters for  $Re = 1000$  and  $T_{in} = -15\text{ °C}$



**Figure 9.46** Variation of exergy efficiency with several operating parameters for  $R_{inf} = 3$  and  $X_L = 100$

of heat gain. If heat gain is not considered, the exergy efficiency remains fixed after solidification. The effect of operating parameters on the exergy efficiency for  $R_{inf} = 3$  and  $X_L = 100$  is shown in Figure 9.46, where it is observed that the exergy efficiency decreases as HTF inlet temperature decreases and that the effect of Reynolds number is much less significant.

Now, we consider the effectiveness measures. The effect of design parameters on energy effectiveness is shown in Figure 9.47 for  $Re = 1000$  and  $T_{in} = -15^\circ\text{C}$ . It is observed that the charging time decreases as the shell radius decreases, and that the effect of TES system length becomes more significant as the shell radius increases. The effect of operating parameters on the energy effectiveness is illustrated in Figure 9.48 for  $R_{inf} = 3$  and  $X_L = 100$ . The energy effectiveness increases, or charging time decreases, as Reynolds number increases and HTF inlet temperature decreases, since heat transfer increases with increasing Reynolds number and decreasing inlet temperature.

The effect of shell radius and TES length on the exergy effectiveness is illustrated in Figure 9.49 for  $Re = 1000$  and  $T_{in} = -15^\circ\text{C}$ . A similarity between energy and exergy effectiveness measures is observed, mainly since the storage behaviors of energy and exergy are similar in the TES system considered. The variation of exergy effectiveness with the Fourier number for several Reynolds numbers and inlet temperatures is presented in Figure 9.50 for  $R_{inf} = 3$  and  $X_L = 100$ . As anticipated, the exergy effectiveness increases and the required charging period decreases with HTF inlet temperature and increasing Reynolds number.

The insights described here support the contention that energy and exergy effectiveness measures are important parameters for assessing TES systems during charging and, more generally, other processes.

### Closure for Illustrative Example

The results show that energy and exergy effectiveness measures are significant parameters for the assessment of TES systems, and provide useful complements to the corresponding efficiency

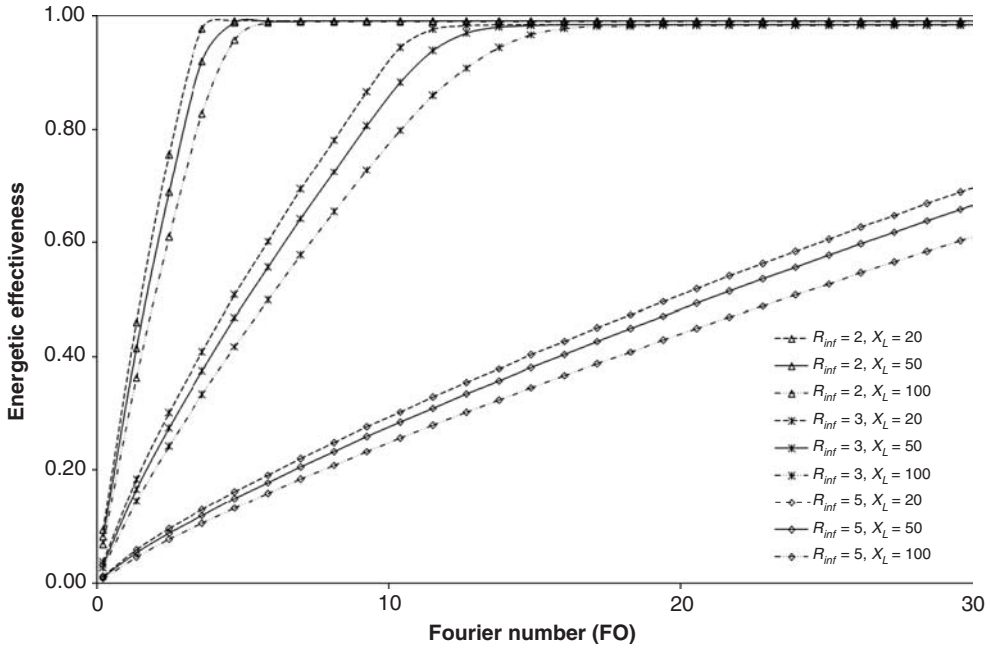


Figure 9.47 Variation of energy effectiveness with several design parameters for  $Re = 1000$  and  $T_{in} = -15^\circ C$

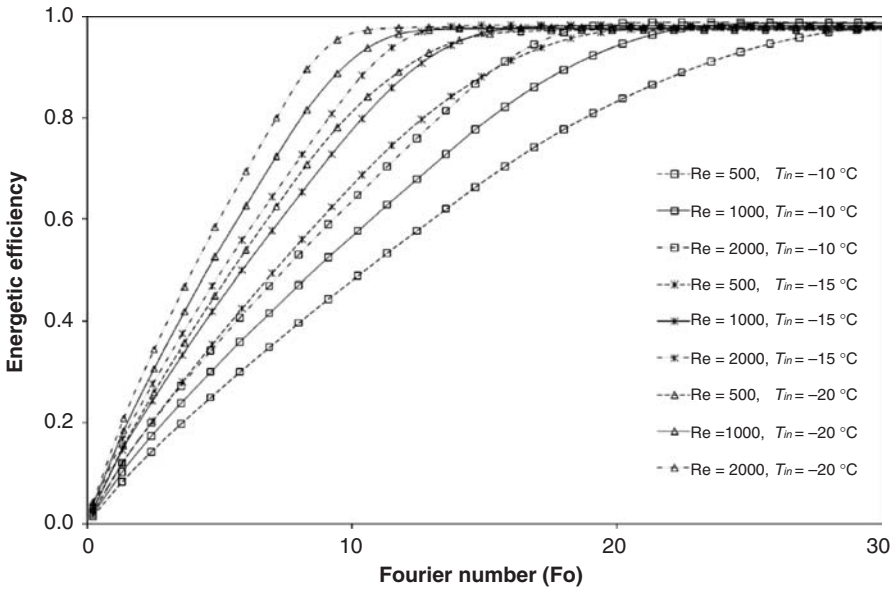


Figure 9.48 Variation of energy effectiveness with several operating parameters for  $R_{inf} = 3$  and  $X_L = 100$

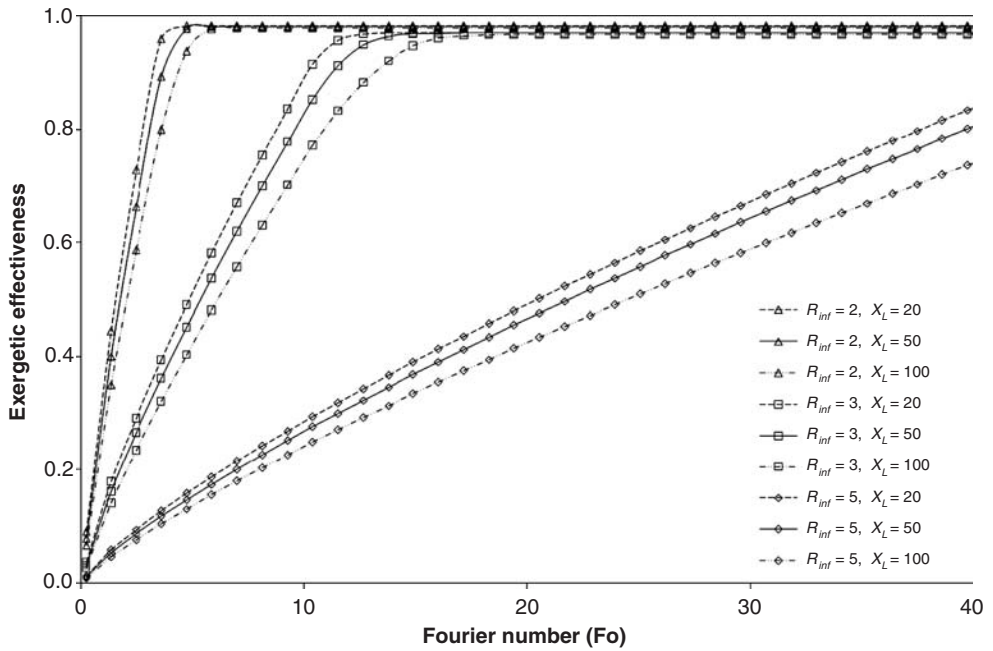


Figure 9.49 Variation of exergy effectiveness with several design parameters for  $Re = 1000$  and  $T_{in} = -15\text{ }^\circ\text{C}$

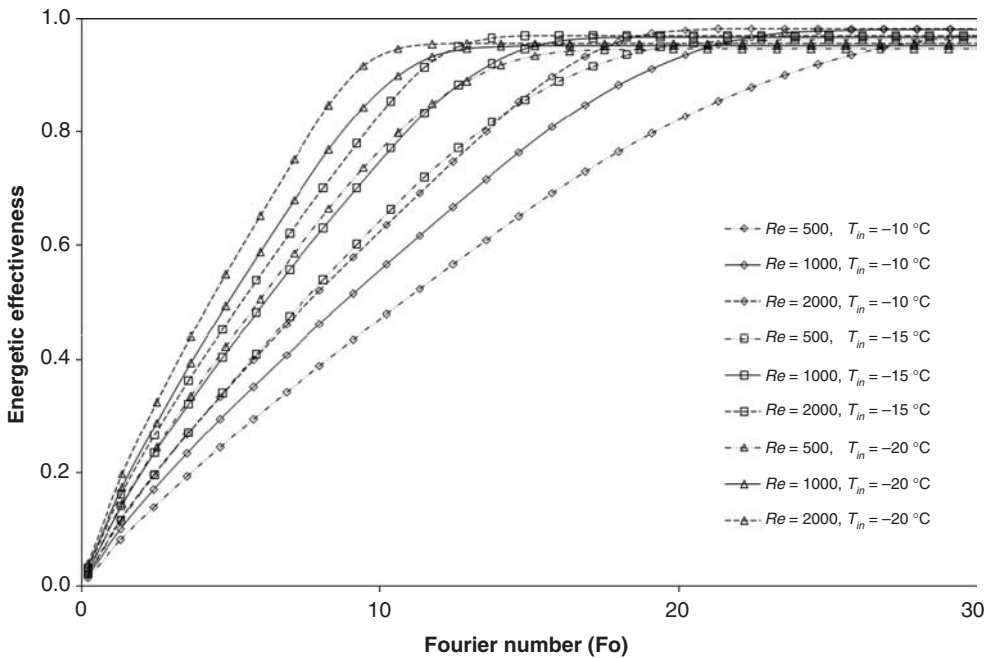


Figure 9.50 Variation of exergy effectiveness with several operating parameters for  $R_{inf} = 3$  and  $X_L = 100$

measures. Effectiveness parameters demonstrate how effectively the system functions and are sometimes useful in optimization activities.

### 9.10.2 Thermal Battery Ice-Storage System

A thermal battery ice-storage system has been proposed by Huang *et al.* (2007), along with an application in air-conditioning systems. The thermal battery stores and transfers thermal energy, and includes a thermal reservoir maintained at or near its melting temperature, which acts as a latent TES. It also includes a thermal conductor between the thermal reservoir and the external fluid or substance, and a means for recharging the reservoir to maintain it at its melting temperature.

A thermal battery that includes a TES tank and a two-phase thermosyphon has been experimentally investigated (Huang *et al.*, 2007). The thermosyphon consists of three main parts: parallel-finned tubes placed vertically inside the tank, and charging and discharging heat exchangers of a double-pipe type located at the upper and lower regions of the energy storage tank, respectively. The thermosyphon contains a working fluid (R-22 in this case) while the thermal energy reservoir medium is water.

A thermal battery with its main components is shown in Figure 9.33a. This design aims to overcome two drawbacks of conventional TES systems. First, there is no requirement for a pump or valve to control the flow direction. Second, the system does not rely on the system piping to charge or discharge energy, as both operation modes can be accomplished simultaneously.

#### Operation

There are three modes of operation for the thermal battery. Its charging and discharging modes are illustrated in Figure 9.33b and c, respectively.

- **Charging.** A cooling fluid passes through the charging heat exchanger at the top of the battery. Heat is transferred from the stored water to the working fluid inside the thermosyphon, causing it to evaporate and the water to solidify. The evaporated fluid flows upward because of buoyant forces. When the vapor reaches the charging heat exchanger, heat is transferred to the cooling fluid and the vapor condenses. The condensed vapor flows along the wall of the finned tube where it undergoes film evaporation to form ice again.
- **Discharging.** The hot fluid passes through the discharging heat exchanger at the bottom of the thermal battery, and heat is transferred from the hot fluid to the working fluid in the thermosyphon, causing it to evaporate. The evaporated fluid flows upward and undergoes film condensation at the inner wall of the finned tubes. The condensed vapor flows down to the discharge heat exchanger. This process results in indirect heat transfer from the stored ice to the hot fluid.
- **Simultaneous charging and discharging.** Cold and hot fluids pass through the charging and discharging heat exchangers, respectively. The cold fluid causes charging of the battery while the hot fluid causes discharging. If the energy supply rate to the battery is greater than the energy discharge rate, ice is formed and energy is stored in the battery. If the energy discharge rate is greater than the supply rate, ice is melted and energy is released from the battery. If energy supply and discharge occur at the same rate, energy is transferred via the working fluid directly from the cold to the hot fluid.

#### Integration into Air-Conditioning Systems

The thermal battery can be integrated into an air-conditioning system to function in two main ways: (i) to cool return water from cooling coils by passing it through the discharge heat exchanger and (ii) to cool the discharged refrigerant from the condenser and act as a subcooler. The latter method was adopted by Huang *et al.* (2007) and is described here.



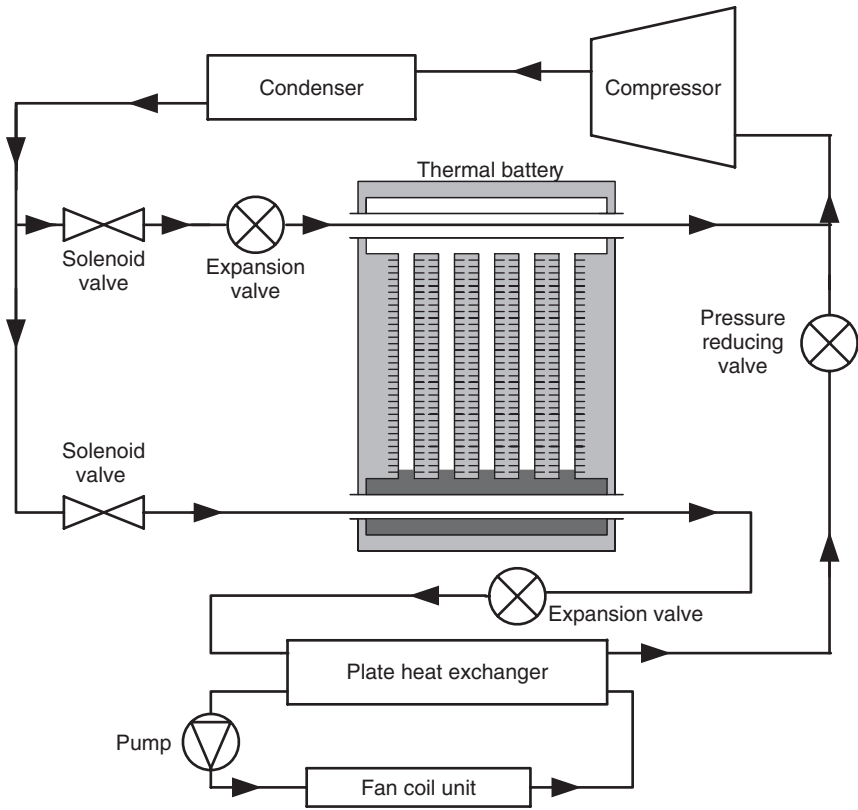


**Figure 9.51** Integration of a thermal battery into an air-conditioning system

Figure 9.51 shows a possible integration into an air-conditioning system, where the thermal battery acts as a subcooler for the discharged refrigerant from the condenser. The system consists of a refrigeration unit (indoor), consisting of a pump, a fan coil, and the thermal battery. The thermal battery is integrated into the refrigeration cycle by connecting the liquid line (condenser outlet) to both the charging and discharging heat-exchanger inlets. The outlet of the thermal battery is connected to the compressor of the charging heat exchanger outlet and to the evaporator of the discharging heat exchanger outlet. Three additional components are needed for the refrigeration cycle: an extra solenoid valve, an expansion valve at the inlet of the charging heat exchanger, and a pressure-reducing valve on the suction line, which lowers the pressure of the suction gas from the evaporator pressure to that of the charging heat exchanger.

Hence, this system is self-regulating and does not need any form of control for the refrigerant flow. The expansion valves act as actuators for controlling the refrigerant flow through the cycle, to regulate the refrigerant flow depending on the load.

The overall cycle observed by the system is shown in Figure 9.52 on a  $P-h$  diagram. When the cycle is in charging mode, all refrigerant is circulated through the thermal battery and the cycle operates as a refrigeration cycle between the condensing pressure and the charging heat exchanger pressure. This mode can be seen in Figure 9.52 as the cycle 1, 2, 3, 4, and 5, noting that points 5 and 1 are the same when operating in charging mode. No refrigerant is allowed to pass through the evaporator. When operating in the discharge mode, the cycle also operates as a refrigeration cycle, but this time the low pressure becomes the pressure of the evaporator. The cycle in this mode is shown in Figure 9.52 as cycle 1, 2, 3, 6, 7, 8, and 9, noting that points 9

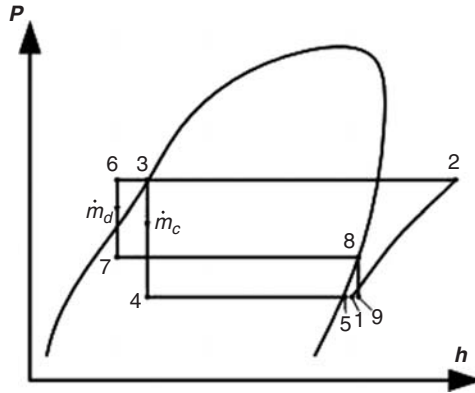


**Figure 9.52** System pressure  $P$  versus enthalpy  $h$  diagram with a thermal battery

and 1 are the same at the charge heat exchanger pressure. Again the refrigerant is not allowed to circulate through the charging heat exchanger. When operating simultaneously, a fraction of the refrigerant passes through the charging cycle and the remainder through the discharge cycle. In this instance, point 1 becomes the point of mixing both streams from points 9 and 5. When the system operates in the simultaneous charging and discharging mode, the refrigerant passes through all system components, with the refrigerant fractions flowing through the charging heat exchanger and the evaporator controlled by the cooling load. As the cooling load increases, more refrigerant passes through the evaporator and less through the charging heat exchanger. We can see that the compressor always has to compress the refrigerant from the lower pressure, the charging heat exchanger pressure, to the condensing pressure regardless of the cycle operation mode. This is a weakness of the cycle since there will always be the same compressor power input. The reason for this is the pressure-reducing valve installed in the suction line, which always lowers the refrigerant pressure from the evaporator pressure to the charge heat exchanger pressure.

### Assessment

The performance of the system in Figure 9.51 has been investigated experimentally. The behavior of the energy storage material in the thermal battery for several charging temperatures has been examined, as has the overall system performance with the thermal battery in simultaneous charging and discharging modes of operation. The ice fraction in the thermal battery can be observed visually during experiments.

A performance assessment of the thermal battery shows that the total cooling capacity of the system is

$$\dot{Q}_a = \dot{Q}_b + \dot{Q}_1 \quad (9.12)$$

where  $\dot{Q}_a$  is the cooling capacity provided by the overall cycle,  $\dot{Q}_b$  is the cold storage rate in the thermal battery, and  $\dot{Q}_1$  is the cooling load on the fan coil unit. The cold storage rate in the thermal battery can be expressed as

$$\dot{Q}_b = \frac{1}{\Delta t} \left\{ \left[ \sum_{n=10}^{12} M_n C_p \Delta T_{n,t} \right] + (m_{s,t+\Delta t} - m_{s,t}) h_e \right\} \quad (9.13)$$

where the first term in the braces represents the sensible cooling rate and the second term the latent cooling rate. The cooling load on the fan coil unit can be found with the difference in water

temperature between the inlet and exit as

$$\dot{Q}_1 = \dot{m}_w(T_{wi} - T_{wo}) \quad (9.14)$$

### Performance

First we consider the performance of the thermal battery, focusing on the charging operation. The behavior of water in the thermal battery varies with charging temperature. The water was cooled sensibly from 21 to 0 °C (sensible cooling), and then ice formed (latent cooling). The water exhibited supercooling, as ice did not start to form at 0 °C. The vertical temperature distribution with time in the thermal battery for a charging temperature of  $-5\text{ }^\circ\text{C}$  is shown in Figure 9.53. For a charging temperature of  $-5\text{ }^\circ\text{C}$ , no ice was formed and the water became supercooled. The behavior varies with charging temperature. For a charging temperature of  $-9\text{ }^\circ\text{C}$ , for instance, the water supercools to its nucleation temperature (around  $-6\text{ }^\circ\text{C}$ ) and then ice starts forming at a temperature of 0 °C. After all the water freezes, the ice is cooled sensibly to the charging temperature. The ice fraction can be determined as a function of time and charging temperature, but it is noted that no ice is formed for a charging temperature of  $-5\text{ }^\circ\text{C}$ .

Next we consider the performance of the system with a thermal battery. The performance of the total system is examined with the water in the thermal battery initially at 24 °C, based on experimental data. Simultaneous charging and discharging of the thermal battery is assumed. Little ice is formed between 8:00 am and 6:00 pm because of the high fan coil cooling capacity required. Latent energy is stored when cooling is not required at the fan coil unit. System performance characteristics are illustrated for component energy transfer rates in Figure 9.54 and for COP in Figure 9.55.

### Energy and Exergy Assessments

The charging and discharging processes for the thermal battery can be assessed as part of a system. In the charging process, the system operates as a refrigeration cycle with the evaporator acting as the charging heat exchanger. Charging occurs when there is no cooling load on the fan coil unit. The discharge heat exchanger acts as a refrigerant subcooler, and can be viewed as an extension of the condenser in the thermal battery discharge process. Assessment from energy and exergy perspectives can be carried out for the overall process and its subprocesses.

As an example, energy and exergy assessments are considered for a discharging process. The temperature of the reference environment is taken to be 25 °C and the pressure 100 kPa.

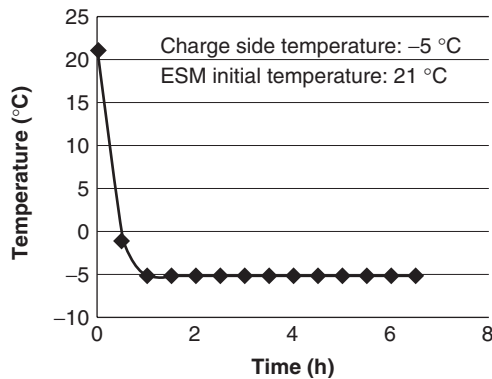


**Figure 9.53** Temperature distribution in the thermal battery for a  $-5\text{ }^\circ\text{C}$  charging temperature. ESM denotes energy storage module

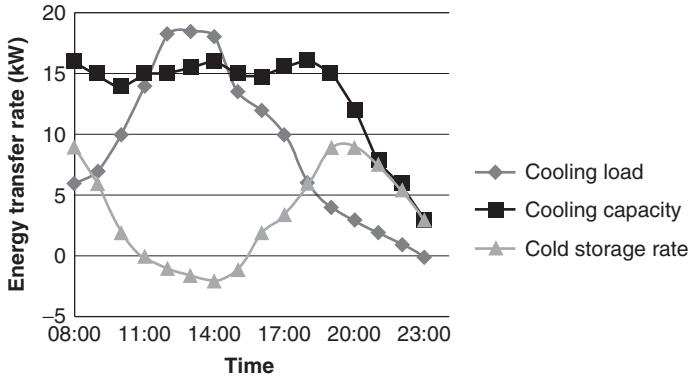


Figure 9.54 Variation of energy transfer rate with time for selected system components

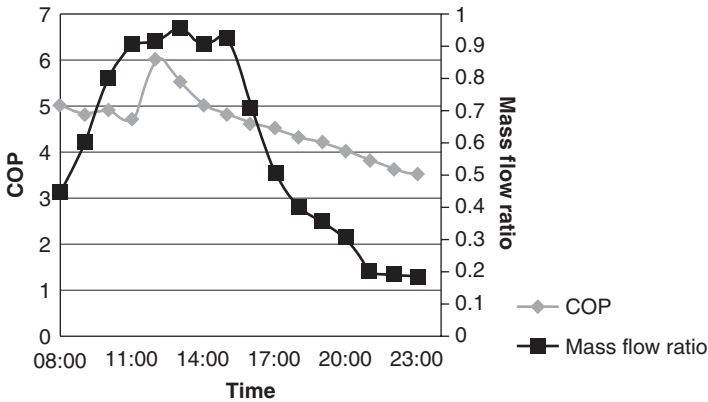
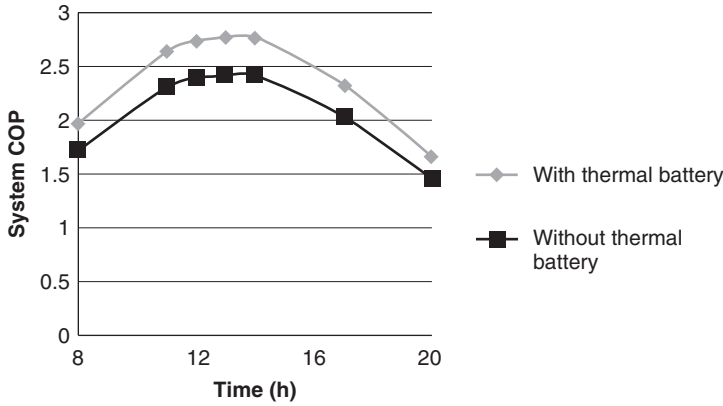


Figure 9.55 Variation of COP and refrigerant mass flow ratio with time

Discharging occurs when the system provides cooling to the chilled water in the fan-coil loop. During this process, all the refrigerant is passed through the discharging heat exchanger. Various parameters can be modified, including condensing temperature, evaporating temperature, refrigerant mass flow rate, the storage water temperature in the thermal battery, and the amount of subcooling provided by the thermal battery. During discharging, the thermal battery can be viewed as an extension of the condenser that supplies further subcooling to the refrigerant. The advantage of the thermal battery in the subcooling application over other methods of subcooling is that, due to its low temperature, it provides significantly more subcooling to the refrigerant. The net effect is a notable increase in system capacity. Conventional subcooling methods provide up to 6–10 °C of refrigerant subcooling, but with the thermal battery this figure increases because of the high temperature difference between the refrigerant exiting from the condenser and the thermal battery temperature. Hence, 15 °C of refrigerant subcooling is considered here.

Two systems are considered: one with and one without a thermal battery. The manner in which the two systems respond to the change in cooling load demand with time is assessed. The performance of the systems in terms of the cooling load it supplies over time, when operating with and without a thermal battery, indicates that a system with a thermal battery can supply a greater cooling load



**Figure 9.56** Variation of system COP over a day, for systems with and without a thermal battery

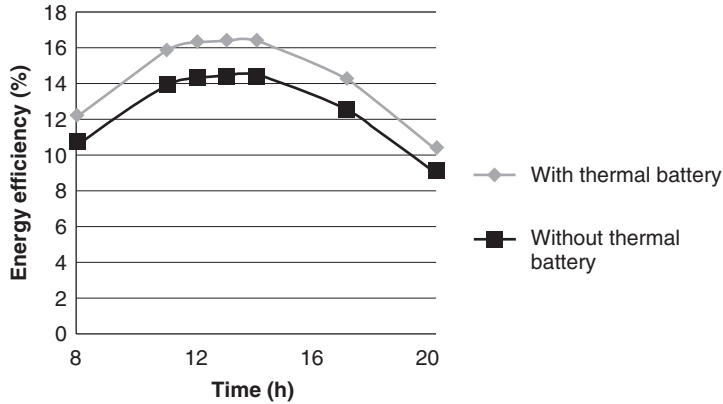


**Figure 9.57** Variation of system exergy efficiency over a day, for systems with and without a thermal battery

at all times. In fact, a system operating with a thermal battery is able to provide a maximum peak load 14% greater than that of the system without a thermal battery. Next, measures of merit are considered. The variation in energy efficiency (in terms of COP) for the systems during the day is illustrated in Figure 9.56, where the system COP is clearly observed to increase when the system operates with a thermal battery (by 15% on average over the operational period). Similarly, the variation in exergy efficiency for the systems during the day is illustrated in Figure 9.57, where the system exergy efficiency is observed to increase when operating with a thermal battery (by an average of around 14%). The benefits demonstrated here indicate that a thermal battery can be beneficially applied in air-conditioning systems.

In general, the use of a thermal battery in an air-conditioning system was found to enable a 28% greater cooling effect than the maximum rated cooling capacity of the system without the thermal battery. Also, the overall system achieves high COPs (up to 6.1) during discharging but has low values (as low as 3.1) during charging because of the greater compressor work required. Note that the integrated part-load operational performance over the period of operation is needed to better understand thermal battery and its behavior.

### 9.10.3 Use of Artificial Neural Networks in TES

Artificial neural networks (ANNs) are nonlinear mapping systems whose structures are based on principles inspired by the biological nervous systems of humans. An ANN consists of a large number of simple processors linked by weighted connections. By analogy, the processing units are called *neurons*. Neural networks provide a fundamentally different approach from numerical solution methods to forecast future behavior. This technique has been applied in various scientific disciplines and has yielded encouraging results in many areas of system modeling, for example, Massie (2002), Yang *et al.* (2005), Ben-Nakhi and Mahmoud (2004), Abbassi and Bahar (2005), Lecoeuche *et al.* (2005), Diaz *et al.* (2001), and Pacheco-Vega *et al.* (2001).

Although analytical and numerical methods have been employed for thermal modeling of TES systems, ANN methods have only begun to be applied. In this section, the use of ANNs is examined for TES applications, based on an investigation reported by Ermis *et al.* (2007). For simplicity, we focus on a particular TES process for latent storage. In other words, we use ANNs to predict the total thermal energy stored in a TES system. Experimental data are utilized with the ANN approach, in which heat transfer is examined during phase change in a finned-tube latent storage. The ANN results are compared with numerical and experimental predictions.

The ANN approach allows predictions even when data for heat transfer are lacking. ANN can consequently provide a useful tool for heat-transfer analysis during such two-phase heat-transfer processes, as it can avoid the costs and challenges of experimental work.

#### Artificial Neural Network Approach

The ANN approach is described here. The neuron is a basic processor in neural networks. Each neuron has one output, based on the characteristic of the neuron activation, and can receive multiple inputs from other neurons. An artificial neuron is modeled as a multi-input nonlinear process with weighted interconnections. The back-propagation algorithm is considered to be the most suitable method for training multilayer feed-forward networks (Reed and Marks, 1999; Rojas, 1996; Haykin, 1999; Fausett, 1994) and involves the following steps:

1. Provide a training pattern and propagate it through the network to obtain the outputs.
2. Initialize all weights and thresholds, by setting all weights and thresholds to small random values. Usually the training sets are normalized to values between  $-0.9$  and  $0.9$  during processing.
3. Calculate the net input to the  $j$ th node in the hidden layer:

$$net_j = \sum_{i=1}^n w_{ij}x_i - \theta_j \quad (9.15)$$

Here,  $i$  denotes the input node,  $j$  denotes the hidden-layer node,  $x$  is the input,  $w_{ij}$  is the weighting value for the connection from the  $i$ th input node to the  $j$ th hidden-layer node, and  $\theta_j$  is the threshold between the input and hidden layers.

4. Calculate the output of the  $j$ th node in the hidden layer:

$$h_j = f_h \left( \sum_{i=1}^n w_{ij}x_i - \theta_j \right) \quad (9.16)$$

$$f_h(x) = \frac{1}{1 + e^{-\lambda_h x}} \quad (9.17)$$

Here,  $h_j$  is the vector of hidden-layer neurons,  $f_h$  is a logistic sigmoid activation function from the input layer to the hidden layer, and  $\lambda_h$  is a variable that controls the slope of the sigmoidal function.

5. Calculate the net input to the  $k$ th node in the hidden layer:

$$net_k = \sum_j w_{kj}x_j - \theta_k \quad (9.18)$$

Here,  $k$  represents the output layer,  $w_{kj}$  is the weight for the connection from the  $j$ th hidden-layer node to the  $k$ th output layer, and  $\theta_k$  is the threshold connecting the hidden and output layers.

6. Calculate the output of the  $k$ th node in the output layer:

$$y_k = f_k \left( \sum_j w_{kj}x_j - \theta_k \right) \quad (9.19)$$

$$f_k(x) = \frac{1}{1 + e^{-\lambda_k x}} \quad (9.20)$$

Here,  $y_k$  is the output of the output-layer neurons,  $f_k$  is a logistic sigmoid activation function from the hidden layer to the output layer, and  $\lambda_k$  is a variable that controls the slope of the sigmoid functional.

7. Calculate errors: The output-layer error between the target and the observed output is

$$\begin{aligned} \delta_k &= -(d_k - y_k) f'_k \\ f'_k &= y_k(1 - y_k) \text{ for sigmoid function} \end{aligned} \quad (9.21)$$

Here,  $\delta_k$  is the vector of errors for each output neuron and  $d_k$  is the target activation of the output layer.  $\delta_k$  depends only on the error  $(d_k - y_k)$  and  $f'_k$  is the local slope of the node activation function for the output nodes. Similarly, the hidden-layer error is

$$\begin{aligned} \delta_j &= f'_h \sum_{k=1}^n w_{kj} \delta_k \\ f'_h &= h_j(1 - h_j) \text{ for sigmoid function} \end{aligned} \quad (9.22)$$

where  $\delta_j$  is the vector of errors for each hidden-layer neuron,  $\delta_j$  is a weighted sum of the all nodes and  $f'_h$  is the local slope of the node activation function for hidden nodes.

8. Adjust the weights and thresholds in the output layer:

$$w_{kj}^{(t+1)} = w_{kj}^{(t)} + \alpha \delta_k h_j + \eta \left( w_{kj}^{(t)} - w_{kj}^{(t-1)} \right) \quad (9.23)$$

$$\theta_k^{(t+1)} = \theta_k^{(t)} + \alpha \delta_k \quad (9.24)$$

Here,  $\alpha$  is the learning rate,  $\eta$  is the momentum factor, and  $t$  is the time period. The learning rate and the momentum factor are used to allow the previous weight change to influence the weight change in time period  $t$ . These calculation steps are repeated until the output layer error is within the desired tolerance for each pattern and neuron.

## Numerical and Experimental Data

As noted earlier, numerical and experimental data are utilized as part of the ANN approach. The numerical analysis of the system is developed on the basis of the simplified model for the finned-tube heat storage unit shown in Figure 9.58. The numerical analysis is described by Ermis *et al.* (2007), and the experimental unit and procedure by Ereke *et al.* (2005).

Experimental data are obtained from the test unit shown in Figure 9.59, which has three main parts: flow system, heat-transfer test section, and temperature measurement system. The heat-transfer

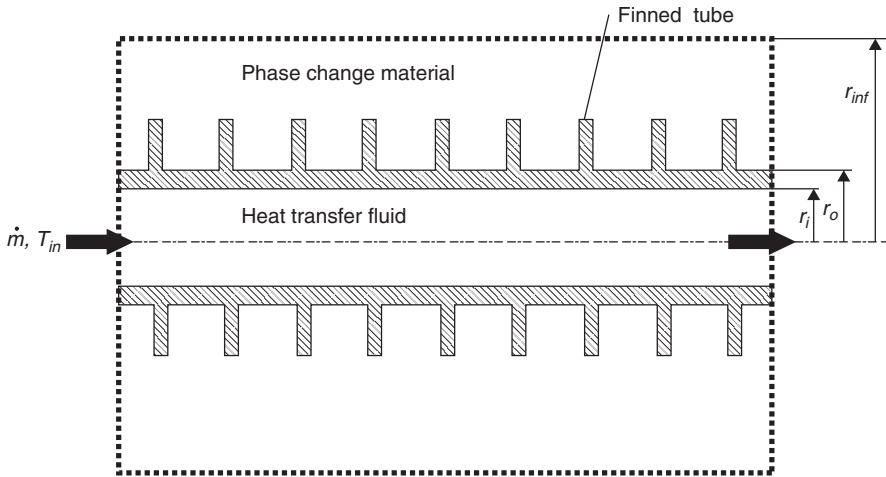
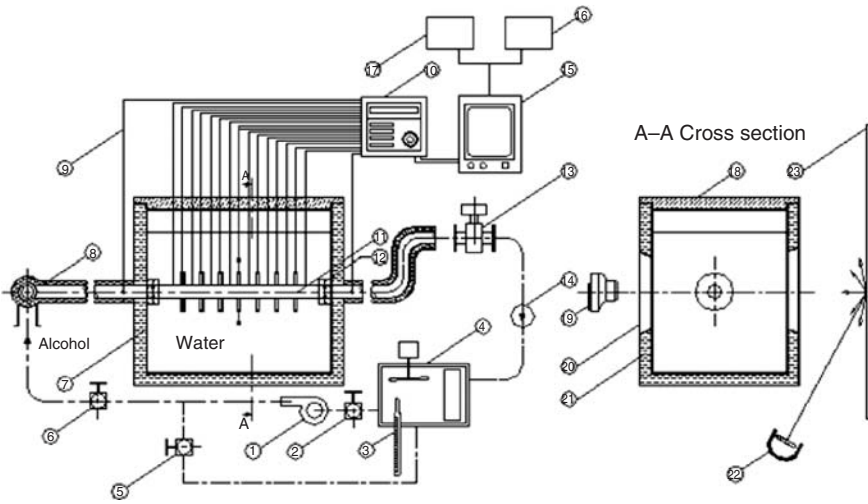


**Figure 9.58** Cross section of finned tube used in experiments, showing inlet heat-transfer fluid mass flow rate and temperature, and radii related to the finned tube



1: Constant temperature bath; 2: main valve; 3: thermometer; 4: alcohol circulation pump; 5: recirculation valve; 6: flow adjustment valve; 7: energy storage tank; 8: connecting pipe; 9: thermocouple extension wires; 10: data logger; 11: finned tube; 12: fittings; 13: flow meter; 14: check valve; 15: PC computer; 16: monitor; 17: disc drive; 18: tank top cover; 19: digital camera; 20: plexiglass view window; 21: insulation; 22: light source; 23: white screen

**Figure 9.59** Experimental test system and its components (Erek *et al.*, 2005)

test section consists of an energy storage tank in the shape of a rectangular solid (420 mm in width, 570 mm in length, and 500 mm in height) and a finned tube around which is a PCM. A digital camera is used to visualize the solidification fronts around the finned tube and data are transmitted to a computer. To reduce heat losses, the tank base is covered with a 50-mm layer of styrofoam insulation and the side walls and top with 30 mm of styrofoam. The finned tubes are cylinders made of bronze (87.2% Cu, 6.57% Sn, 4.13% Zn, and 1.97% Pb), with a length of 570 mm and



**Table 9.17** Characteristics of tubes used in experiments

Tube type	Fin details			Heat-transfer area (m <sup>2</sup> )
	Number	Diameter (mm)	Spacing (mm)	
1 (bare tube)	–	–	–	0.0942
2	7	54	65.0	0.1650
3	7	64	65.0	0.1936
4	11	54	40.0	0.2060
5	11	64	40.0	0.2513
6	15	54	27.5	0.2505
7	15	64	27.5	0.3139

inner and outer radii of 10 and 15 mm, respectively. The finned portion of the tube has a length of 440 mm, and the fin thickness is 3 mm. Other tube dimensions are listed in Table 9.17. The flow system contains a HTF reservoir, a constant-temperature circulating bath, a variable-speed pump, a flow meter, and a hydrodynamic entry section. The hydrodynamic entry section length chosen (approximately 240 tube diameters or 6500 mm) is sufficiently long to ensure fully developed flow for the HTF at the inlet of the energy storage unit. Ethyl alcohol (CH<sub>3</sub>–CH<sub>2</sub>OH) is used as the HTF to assure liquid behavior over the experimental temperature range. Thermocouples are embedded in the midsections of the fin tip and the fin base. Water is used as the PCM and preliminarily cooled to a temperature of 0.3 °C. Tests are performed at three inlet temperatures (–10, –15, and –20 °C) and six Reynolds numbers between 500 and 7000.

### Application of the ANN Approach to TES

The feed-forward neural network has become the most popular among the various types of a neural networks, and the back-propagation network is the most common technique for a feed-forward neural network since a mathematically strict learning scheme exists to train the network and ensure mapping between inputs and outputs. Here, an ANN is used to predict the heat transfer in a PCM heat storage around a finned tube, and a feed-forward back-propagation method is used for the training and learning processes. A C++ computer code is developed to solve the ANN algorithm. Neural networks need a range of input and output values, which should be between 0.1 and 0.9, in line with restrictions for the sigmoid function.

Experimental and required data are normalized as follows:

$$\frac{\text{Actual data} - \text{Minimum data}}{\text{Maximum data} - \text{Minimum data}} \times (\text{High data} - \text{Low data}) + \text{Low data} \quad (9.25)$$

where minimum and maximum refer to the annual minimum and maximum data values, respectively, while high and low refer to the maximum normalized data value (0.9) and the minimum normalized data value (0.1), respectively, as commonly preferred (Nasr *et al.*, 2003).

A three-layer feed-forward back-propagation neural network for heat storage is developed as shown in Figure 9.60. There are four network input parameters: heat-transfer area, Reynolds number, inlet temperature of HTF, and time. The output term is stored thermal energy. The weights, biases, and hidden node numbers are altered to minimize the error between output values and the current data. To obtain error convergence, the configurations of the ANN are set by selecting the number of hidden layers and nodes, and the learning rate and momentum coefficient. The 240 cases corresponding to the experimental data set are divided into two data groups. The first data group consists of 200 sets (83% of all data) used for training the network and the second data group consists of 40 sets used to verify the ANN model. Data for the first group are selected randomly

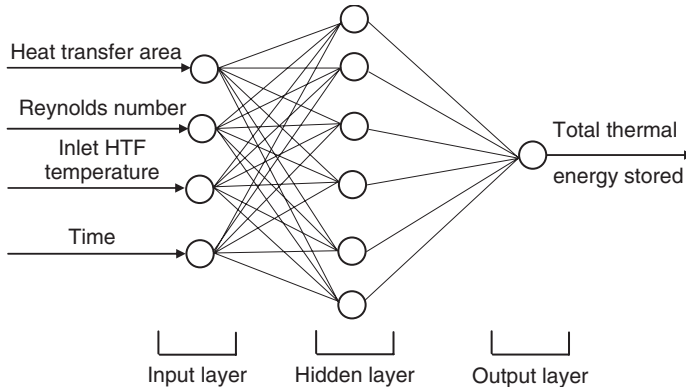


**Figure 9.60** Three-layer feed-forward back-propagation neural network for thermal analysis

for the second tube type from the experimental tubes. The learning process is performed using the first, third, fourth, fifth, sixth, seventh, and bare tube types (see Table 9.17).

The ANN approach is utilized for stored thermal energy by using the four inputs, one output, and three different nodes (8, 13, and 18 in the hidden layer). In the algorithm, the learning rates and momentum coefficients are 0.6 for learning processes, in which 400,000 iterations are used to obtain good fits.

The three error parameters used to compare the performance of the various ANN configurations are consistent with those recommended by Sablani *et al.* (2005). Specifically, the performance of various ANN configurations is compared using the absolute mean relative error (AMRE), the standard deviation (SD) in the relative error, and the absolute fraction of variance ( $R^2$ ) as follows:

$$\text{AMRE} = \frac{1}{n} \sum_{i=1}^n \text{ABS}(B) \quad (9.26)$$

$$\text{SD} = \sqrt{\frac{\sum_{i=1}^n (B - \bar{B})^2}{n - 1}} \quad (9.27)$$

$$R^2 = 1 - \left[ \frac{\sum_{i=1}^n (y_i - a_i)^2}{\sum_{i=1}^n (a_i)^2} \right] \quad (9.28)$$

where  $y_i$  is the prediction value,  $a_i$  is the experimental value,  $n$  is the number of data values, and  $B = (y_i - a_i)/a_i$ .

### Results for ANN Approach

Table 9.18 lists the prediction errors (AMRE, SD in the relative errors, and absolute fraction of variance) for the ANN configurations for stored thermal energy in the learning process, including 200 experimental data for the training data set. The 13 nodes of the hidden configuration appear to be the best selection, based on the resulting prediction errors in Table 9.18. Figure 9.61 shows a plot of the predicted versus desired output values of stored thermal energy using the optimal neural network in the learning process.

**Table 9.18** Prediction errors associated with the ANN configuration for stored thermal energy in the learning process

No. of neurons in hidden layer	AMRE (%)	SD (%)	$R^2$
8	6.7181	7.8695	0.9917
13	6.6384	7.7835	0.9919
18	6.6562	8.0609	0.9918

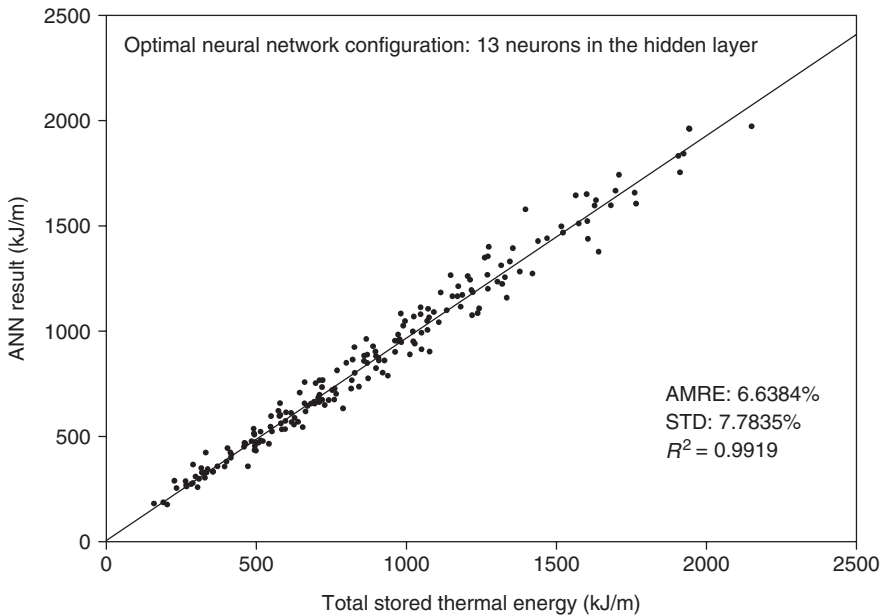


**Figure 9.61** Comparison of stored thermal energy predicted with the ANN approach and actual values

The network performance with various neuron numbers in the hidden layer is presented in Figure 9.62. It is seen that the optimum neuron numbers are 13 in the hidden layer for 400,000 iteration cycles. The ANN results are also compared with the experimental and numerical results for total stored thermal energy in the tube type-2 for the various experimental conditions in Table 9.19. To compare the ANN and numerical models, 13 of hidden numbers, 0.6 of the learning rates, and momentum coefficients are used in the model. The results of this comparison are assessed using the prediction errors. The ANN approach is observed to have an average AMRE of 5.58%, an average SD of 0.01791, and an average  $R^2$  of 0.9950, while the numerical model has corresponding values of 14.99%, 0.00887, and 0.9664 respectively.

The results for the ANN approach are compared with the numerical and experimental data for the total stored thermal energy in Figure 9.63 at  $Re = 500, 1000,$  and  $2000,$  and in Figure 9.64 for  $Re$  values of  $3000, 5000,$  and  $7000,$  at an inlet temperature of  $-15^\circ\text{C}.$  In these figures, the ANN prediction has an average AMRE of 13.74%, compared to the numerical model prediction, which has a corresponding value of 4.62%, in comparison with experimental results for a laminar flow regime at  $Re = 500.$  Table 9.20 also shows the average AMRE values, to facilitate comparisons

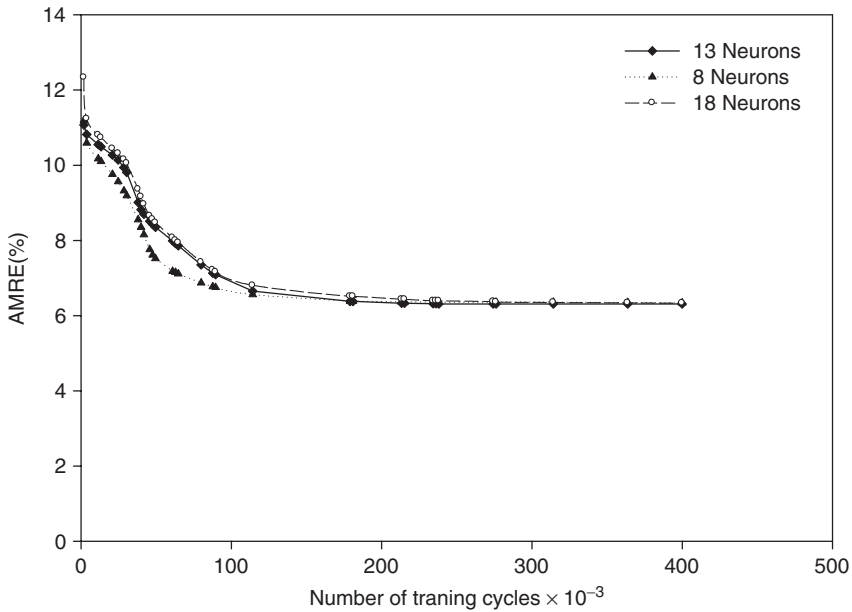


**Figure 9.62** Variation of network performance in terms of AMRE with training cycles, for several numbers of neurons in the hidden layer

between the ANN and numerical approaches for the tube type-2 for various Reynolds numbers, at an inlet HTF temperature of  $-15^{\circ}\text{C}$ . This table basically shows that the ANN provides better results and achieves better agreement with experimental data, although this is in part because the ANN approach uses some experimental data. Also the ANN and numerical approaches are compared with experimental data for the total stored thermal energy at  $\text{Re} = 500$  and  $5000$ , for an inlet HTF temperature of  $-20^{\circ}\text{C}$  in Figure 9.65 and  $-10^{\circ}\text{C}$  in Figure 9.66. Although these figures demonstrate that both ANN and numerical results are close to the experimental data at  $\text{Re} = 500$ , the ANN approach provides better agreement than the numerical model at  $\text{Re} = 5000$  for both HTF inlet temperatures.

A validation of the ANN model, which is an important step in ensuring the reliability of results, is reported by Ermis *et al.* (2007). Overall, the ANN approach appears to be a promising tool for thermal analysis of both latent and sensible TES systems.

## 9.11 Future Outlook for TES

Many new applications of TES systems are anticipated to evolve to improve thermal management for thermal systems, including enhanced waste heat/cold recovery, electrical circuit cooling, energy management in electrical and fuel cell vehicles, and photovoltaic battery cooling.

Energy-use reduction and performance optimization of engineering systems are likely to remain significant concerns for TES systems and their utilization in industry. Thermodynamics, particularly second-law considerations, will become increasingly important in assessing and improving efficiency, with exergy destruction being a significant measure of merit for meaningfully quantifying the entropy generating in a TES-based system and its components. Research will almost certainly continue on improving the performance and efficiency of thermal systems incorporating TES, and on developing improved materials, storage configurations, and operational strategies, especially where relevant to industry.

**Table 9.19** Total stored energy parameters predicted by ANN and numerical models for various experimental conditions (tube type 2)

Experiment conditions			Total stored energy parameters								
Reynolds number	Inlet temperature (°C)	Time (min)	Experimental results (kJ/m)	Numerical model				ANN Model			
				Results (kJ/m)	AMRE (%)	SD (%)	R <sup>2</sup>	Results (kJ/m)	AMRE (%)	SD (%)	R <sup>2</sup>
500	-10	30	184.72	183.13	0.86	0.02646	0.9999	174.93	5.30	0.00477	0.9972
		60	348.28	349.15	0.25	0.02442	1.0000	326.61	6.22	0.00624	0.9961
		90	496.21	505.22	1.82	0.02157	0.9997	454.48	8.41	0.00975	0.9929
		120	644.92	654.10	1.42	0.02229	0.9998	557.67	13.53	0.01795	0.9817
	-15	30	281.03	267.98	4.64	0.03336	0.9978	255.76	8.99	0.01068	0.9919
		60	533.82	506.09	5.19	0.03437	0.9973	468.27	12.28	0.01595	0.9849
		90	770.76	727.77	5.58	0.03507	0.9969	650.29	15.63	0.02131	0.9756
		120	971.42	938.28	3.41	0.03111	0.9988	796.08	18.05	0.02519	0.9674
	-20	30	346.69	340.94	1.66	0.02791	0.9997	328.45	5.26	0.00471	0.9972
		60	664.86	639.45	3.82	0.03186	0.9985	607.28	8.66	0.01015	0.9925
		90	928.16	915.99	1.31	0.02728	0.9998	866.35	6.66	0.00695	0.9956
		120	1187.49	1178.18	0.78	0.02632	0.9999	1092.37	8.01	0.00911	0.9936
1000	-15	30	275.53	321.12	16.54	0.00532	0.9726	279.67	1.50	0.00612	0.9998
		60	531.71	597.38	12.35	0.00233	0.9847	515.91	2.97	0.00104	0.9991
		90	762.73	850.74	11.54	0.00382	0.9867	719.56	5.66	0.00535	0.9968
		120	966.93	1089.26	12.65	0.00179	0.9840	886.39	8.33	0.00962	0.9931
2000	-15	30	312.89	372.40	19.02	0.00984	0.9638	334.69	6.97	0.01488	0.9951
		60	590.57	682.67	15.60	0.00359	0.9757	609.05	3.13	0.00873	0.9990
		90	843.77	963.42	14.18	0.00101	0.9799	850.18	0.76	0.00493	0.9999
		120	1063.06	1225.94	15.32	0.00309	0.9765	1053.49	0.90	0.00227	0.9999
3000	-15	30	416.75	478.83	14.90	0.00231	0.9778	397.67	4.58	0.00362	0.9979
		60	730.25	831.83	13.91	0.00051	0.9806	698.33	4.37	0.00328	0.9981
		90	1018.75	1139.24	11.83	0.00329	0.9860	965.57	5.22	0.00464	0.9973
		120	1281.75	1421.37	10.89	0.00500	0.9881	1195.62	6.72	0.00705	0.9955
5000	-10	30	319.40	461.56	44.51	0.05638	0.8019	357.72	12.00	0.02293	0.9856
		60	570.66	770.15	34.96	0.03894	0.8778	620.70	8.77	0.01776	0.9923
		90	789.07	1035.13	31.18	0.03205	0.9028	849.99	7.72	0.01608	0.9940
		120	984.29	1272.47	29.28	0.02857	0.9143	1054.57	7.14	0.01515	0.9949
	-15	30	472.04	619.36	31.21	0.03209	0.9026	486.44	3.05	0.00860	0.9991
		60	818.17	1030.59	25.96	0.02252	0.9326	831.43	1.62	0.00631	0.9997
		90	1132.52	1380.66	21.91	0.01512	0.9520	1132.18	0.03	0.00367	1.0000
		120	1402.43	1699.08	21.15	0.01373	0.9553	1389.67	0.91	0.00226	0.9999
	-20	30	608.69	752.89	23.69	0.01837	0.9439	613.74	0.83	0.00504	0.9999
		60	1035.99	1246.88	20.36	0.01228	0.9586	1050.49	1.40	0.00596	0.9998
		90	1423.98	1671.69	17.40	0.00687	0.9697	1436.37	0.87	0.00511	0.9999
		120	1758.65	2057.08	16.97	0.00610	0.9712	1741.06	1.00	0.00211	0.9999
7000	-15	30	553.10	688.11	24.41	0.01968	0.9404	578.88	4.66	0.01118	0.9978
		60	927.21	1121.72	20.98	0.01342	0.9560	956.41	3.15	0.00876	0.9990
		90	1254.21	1488.61	18.69	0.00924	0.9651	1275.41	1.69	0.00642	0.9997
		120	1548.99	1821.52	17.59	0.00724	0.9690	1543.57	0.35	0.00315	1.0000
Mean					14.99	0.01791	0.9664	-	5.58	0.00887	0.9950

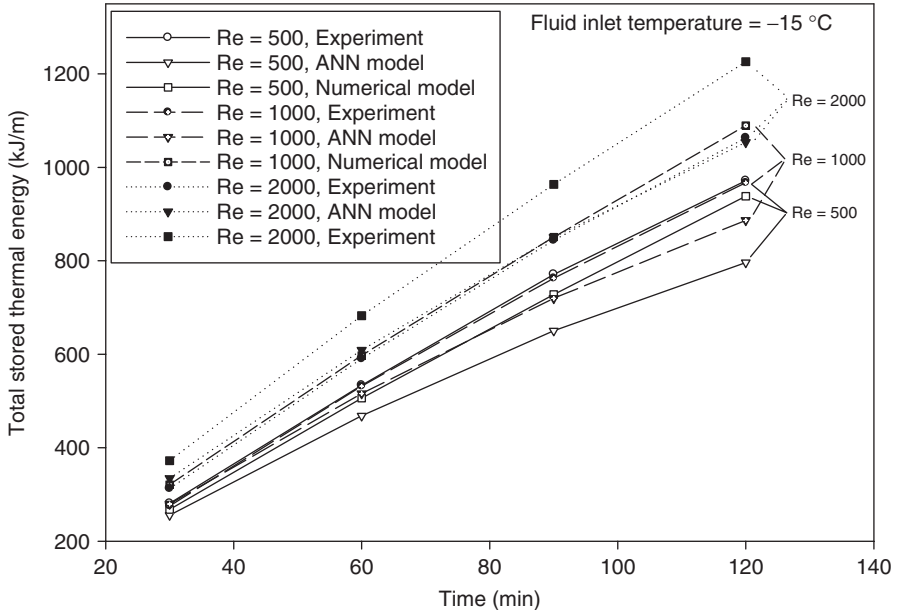


**Figure 9.63** Variation of total stored thermal energy with time, using the ANN approach, the numerical model, and experimental data, for Re = 500, 1000, and 2000 and a HTF inlet temperature of -15 °C

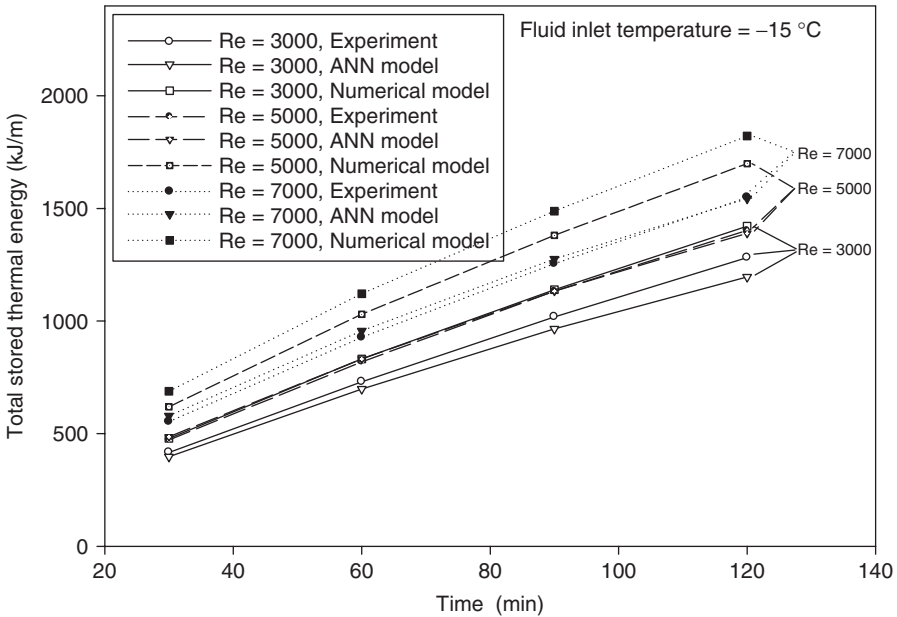


**Figure 9.64** Variation of total stored thermal energy with time, using the ANN approach, the numerical model, and experimental data, for Re = 3000, 5000, and 7000 and a HTF inlet temperature of -15 °C

**Table 9.20** Comparison of mean AMRE values (in %) for ANN approach and numerical model for various Reynolds numbers (tube type 2 and HTF inlet temperature =  $-15^{\circ}\text{C}$ )

Approach	Reynolds number					
	500	1000	2000	3000	5000	7000
ANN approach	13.74	4.62	2.94	5.22	1.40	2.46
Numerical model	4.71	13.27	16.03	12.88	25.06	20.42

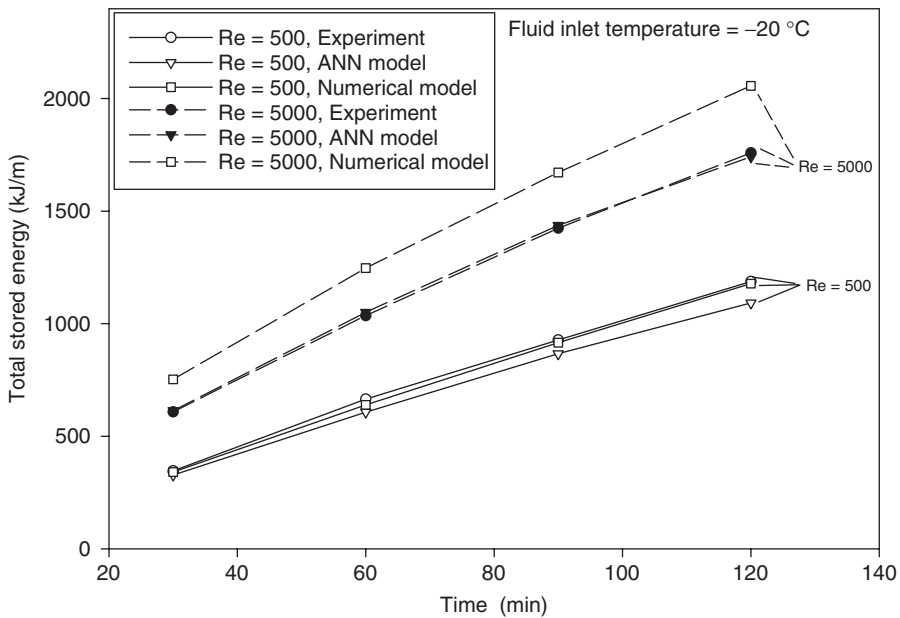


**Figure 9.65** Variation of total stored thermal energy with time, using the ANN approach, the numerical model, and experimental data, for  $\text{Re} = 500$  and  $5000$  and a HTF inlet temperature of  $-20^{\circ}\text{C}$

The use of TES systems as thermal capacitors in refrigeration or HVAC plants will likely facilitate enhanced energy utilization. To design TES systems better, improved understanding is needed of the behaviors of such parameters as velocity, temperature, and pressure. Reliance on numerical approaches to quantify these and other parameters like temperature, in thermodynamic analysis, optimization, and design can be expected to increase. A description of the dynamic behavior of the thermal systems incorporating TES, obtained via simulation and experimentation, will become increasingly necessary to develop enhanced operational strategies and applications.

It will remain important to select a TES type that is appropriate to the application and environmental conditions. Comprehensive design methodologies based on relevant criteria, including thermodynamics, economics, environmental impact, and other factors, will likely be increasingly needed.

Although much of the material covered in this chapter focuses on TES components and microlevel considerations for charging and discharging under steady conditions, broader macrolevel considerations like thermoeconomic analyses of TES systems and their incorporation in HVAC will be needed. This knowledge can help enhance operation strategies and installation configurations and

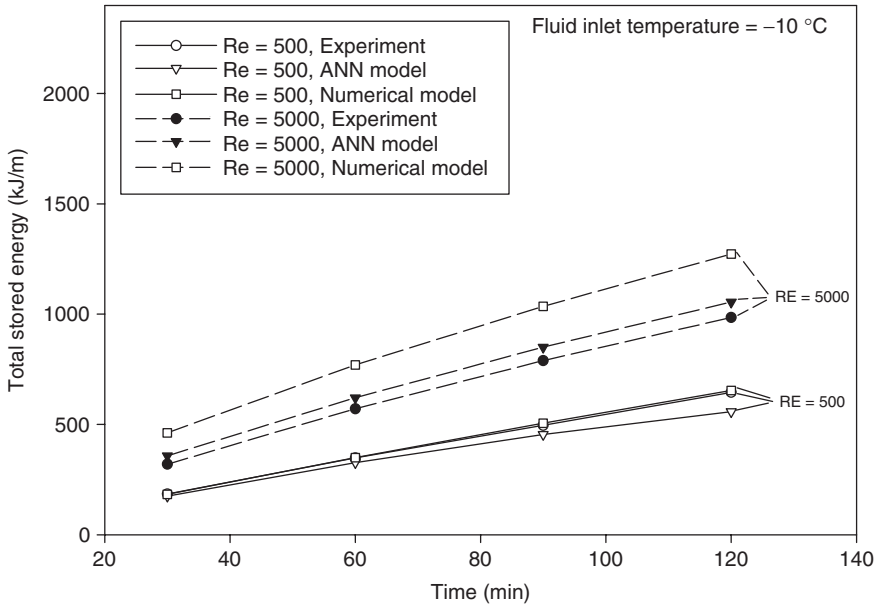


**Figure 9.66** Variation of total stored thermal energy with time, using the ANN approach, the numerical model, and experimental data, for  $Re = 500$  and  $5000$  and a HTF inlet temperature of  $-10^{\circ}\text{C}$

facilitate optimization. Efforts are likely to expand to reduce internal and external exergy losses due to irreversibilities during TES charging, storing, and discharging. Comprehensive studies on relevant parameters and systems will become increasingly important to assist future design efforts.

Improved technology transfer between researchers and designers involved with TES will remain important to ensure that researchers understand industry needs and that industry is aware of new TES developments.

### Nomenclature

$A$	area ( $\text{m}^2$ )
AMRE	absolute mean relative error
$a_i$	experimental value
$B$	variable
$c$	specific heat ( $\text{J/g K}$ )
COP	coefficient of performance
$D$	diameter (m)
$d$	capsule diameter (m)
$d_k$	target activation of output layer
$E$	energy (J)
$Ex$	exergy (J)
Fo	Fourier number
$f$	logistic sigmoid activation function
$f_h$	logistic sigmoid activation function from input layer to hidden layer
$f_k$	logistic sigmoid activation function from hidden layer to output layer
$f'_h$	local slope of the node activation function for hidden nodes
$f'_k$	local slope of node activation function for output nodes



$h$	specific enthalpy (J/kg); vector of hidden-layer neurons
$h_e$	latent heat of water (kJ/kg)
$k$	thermal conductivity (W/m K)
$L$	length (m)
$M$	mass of energy storage material (kg)
$m$	mass (kg)
$n$	data number
$\dot{Q}_a$	cooling capacity (kW)
$\dot{Q}_b$	cold storage rate (kW)
$\dot{Q}_1$	cooling load (kW)
$R$	dimensionless radial distance
$r$	radius, radial distance (m)
$R^2$	absolute fraction of variance
Re	Reynolds number
$s$	specific entropy (J/kg K)
SD	standard deviation
$T$	temperature ( $^{\circ}\text{C}$ )
$t$	time (s)
$U$	overall heat transfer coefficient (W/m <sup>2</sup> K); velocity (m/s)
$u$	specific internal energy (J/kg); velocity (m/s)
$V$	volume (m <sup>3</sup> )
$w_{ij}$	weight connecting $i$ th input node to $j$ th hidden-layer node
$w_{kj}$	weight connecting $j$ th hidden layer node to $k$ th output layer
$X$	dimensionless length
$x$	longitudinal distance (m); multiple inputs
$y$	output
$y_i$	prediction value

### *Greek symbols*

$\alpha$	thermal diffusivity (m <sup>2</sup> /s); learning rate
$\delta_j$	vector of errors for each hidden-layer neuron
$\delta_k$	vector of errors for each output neuron
$\varepsilon$	porosity; effectiveness
$\theta_j$	threshold between the input and hidden layers
$\eta$	energy efficiency; momentum factor
$\lambda$	variable controlling slope of sigmoid function
$\mu$	dynamic viscosity (N s/m <sup>2</sup> )
$\rho$	density (kg/m <sup>3</sup> )
$\Phi$	sphericity
$\psi$	exergy efficiency

### *Subscripts*

,	partial derivative
–	mean
$d$	discharge heat exchanger
$En$	energy
$Ex$	exergy
$f$	transfer fluid
$h$	hidden layer

<i>i</i>	node number; initial; inside
<i>ice</i>	ice
<i>in</i>	inlet
<i>inf</i>	outside of tank
<i>j</i>	hidden-layer node
<i>k</i>	output layer node
<i>l</i>	cooling load
<i>n</i>	data number
<i>o</i>	outside
<i>out</i>	outlet
<i>p</i>	particle
<i>sys</i>	system
<i>t</i>	time
<i>w</i>	water

### Acronyms

ANFIS	Adaptive-network-based fuzzy inference system
ANN	Artificial neural network
BLAST	Building load analysis and system thermodynamics
CTES	Cold thermal energy storage
DSC	Differential scanning calorimeter (calorimetry)
HTF	Heat transfer fluid
HVAC	Heating, ventilating, and air-conditioning
IPF	Ice packing factor
MINLP	Multi-period mixed-integer nonlinear programming
MPCM	Microencapsulated phase change material
O/W	Oil in water emulsion
PCM	Phase change material
PTFE	Polytetrafluoroethylene
PVC	Polyvinyl chloride
RT	Rubitherm
SVM	Support vector machines
TES	Thermal energy storage
TOPSIS	Technique for order performance by similarity to ideal solution
TRNSYS	Transient Energy System Simulation Tool
W/O	Water in oil emulsion

### References

- Abbassi, A. and Bahar, L. (2005). Application of neural network for the modeling and control of evaporative condenser cooling load, *Applied Thermal Engineering* 25, 3176–3186.
- Abraham, K., Maiya, M.P. and Murthy, S.S. (2003). Analysis of a metal hydride cold storage module, *International Journal of Hydrogen Energy* 28, 419–427.
- Adinberg, R., Zvegilsky, D. and Epstein, M. (2010). Heat transfer efficient thermal energy storage for steam generation, *Energy Conversion and Management* 51, 9–15.
- Adref, K.T. and Eames, I.W. (2002). Experiments on charging and discharging of spherical thermal (ice) storage elements, *International Journal of Energy Research* 26, 949–964.
- Agyenim, F., Eames, P. and Smyth, M. (2009). A comparison of heat transfer enhancement in a medium temperature thermal energy storage heat exchanger using fins, *Solar Energy* 83, 1509–1520.
- Agyenim, F., Hewitt, N., Eames, P. and Smyth, M. (2010). A review of materials, heat transfer and phase change problem formulation for latent heat thermal energy storage systems (LHTESS), *Renewable and Sustainable Energy Reviews* 14, 615–628.

- Akgün, M., Aydın, O. and Kaygusuz, K. (2008). Thermal energy performance of paraffin in a novel tube-in-shell system, *Applied Thermal Engineering* 28, 405–413.
- Alawadhi, E.M. (2008). Numerical analysis of a cool-thermal storage system with a thermal conductivity enhancer operating under a freezing condition, *Energy* 33, 796–803.
- Alkan, C., Kaya, K. and Sari, A. (2009). Preparation, thermal properties and thermal reliability of form-stable paraffin/polypropylene composite for thermal energy storage, *Journal of Polymers and the Environment* 17, 254–258.
- Altuntop, N., Kilik, Z., Ozceyhan, V. and Kincay, O. (2006). Effect of water inlet velocity on thermal stratification in a mantled hot water storage tank, *International Journal of Energy Research* 30, 163–176.
- Alvarado, J.L., Marsh, C., Sohn, C., Phetteplace, G. and Newell, T. (2007). Thermal performance of microencapsulated phase change material slurry in turbulent flow under constant heat flux, *International Journal of Heat and Mass Transfer* 50, 1938–1952.
- Ameri, M., Hejazi, S.H. and Montaser, K. (2005). Performance and economic of the thermal energy storage systems to enhance the peaking capacity of the gas turbines, *Applied Thermal Engineering* 25, 241–251.
- Arias, D.A., McMahan, A.C. and Klein, S.A. (2008). Sensitivity of long-term performance simulations of solar energy systems to the degree of stratification in the thermal storage unit, *International Journal of Energy Research* 32, 242–254.
- Arkar, C. and Medved, S. (2005). Influence of accuracy of thermal property data of a phase change material on the result of a numerical model of a packed bed latent heat storage with spheres, *Thermochimica Acta* 438, 192–201.
- Arkar, C. and Medved, S. (2007). Free cooling of a building using PCM heat storage integrated into the ventilation system, *Solar Energy* 81, 1078–1087.
- Arkar, C., Vidrih, B. and Medved, S. (2007). Efficiency of free cooling using latent heat storage integrated into the ventilation system of a low energy building, *International Journal of Refrigeration* 30, 134–143.
- Assis, E., Katsman, L., Ziskind, G. and Letan, R. (2007). Numerical and experimental study of melting in a spherical shell, *International Journal of Heat and Mass Transfer* 50, 1790–1804.
- Ayel, V., Lottin, O. and Peerhossaini, H. (2003). Rheology, flow behaviour and heat transfer of ice slurries: a review of the state of the art, *International Journal of Refrigeration* 26, 95–107.
- Azzouz, K., Leducq, D. and Gobin, D. (2008). Performance enhancement of a household refrigerator by addition of latent heat storage, *International Journal of Refrigeration* 31, 892–901.
- Azzouz, K., Leducq, D. and Gobin, D. (2009). Enhancing the performance of household refrigerators with latent heat storage: an experimental investigation, *International Journal of Refrigeration* 32, 1634–1644.
- Bakan, K., Dincer, I. and Rosen, M.A. (2008). Exergoeconomic analysis of glycol cold thermal energy storage systems, *International Journal of Energy Research* 32, 215–225.
- Bédécarrats, J.P., Castaing-Lasvignottes, J., Strub, F. and Dumas, J.P. (2009). Study of a phase change energy storage using spherical capsules. Part I: Experimental results, *Energy Conversion and Management* 50, 2527–2536.
- Bejan, A., Tsatsaronis, G. and Moran, M. (1995). *Thermal Design and Optimization*, Wiley-Interscience.
- Bellas, J., Chaer, I. and Tassou, S.A. (2002). Heat transfer and pressure drop of ice slurries in plate heat exchangers, *Applied Thermal Engineering* 22, 721–732.
- Bellas, I. and Tassou, S.A. (2005). Present and future applications of ice slurries, *International Journal of Refrigeration* 28, 115–121.
- Benli, H. and Durmuş, A. (2009). Performance analysis of a latent heat storage system with phase change material for new designed solar collectors in greenhouse heating, *Solar Energy* 83, 2109–2119.
- Benmansour, A., Hamdan, M.A. and Bengueuddach, A. (2006). Experimental and numerical investigation of solid particles thermal energy storage unit, *Applied Thermal Engineering* 26, 513–518.
- Ben-Nakhi, A.E. and Mahmoud, M.A. (2004). Cooling load prediction for buildings using general regression neural networks, *Energy Conversion and Management* 45, 2127–2141.
- Bilir, L. and İken, Z. (2005). Total solidification time of a liquid phase change material enclosed in cylindrical/spherical containers, *Applied Thermal Engineering* 25, 1488–1502.
- Bony, J. and Citherlet, S. (2007). Numerical model and experimental validation of heat storage with phase change materials, *Energy and Buildings* 39, 1065–1072.
- Bouaid, N., Saouli, S. and Aiboud-Saouli, S. (2008). Entropy generation in ice-slurry pipe flow, *International Journal of Refrigeration* 31, 1453–1457.

- Braga, S.L., Guzmán, J.J.M. and Pacheco, H.G.J. (2009). A study of cooling rate of the supercooled water inside of cylindrical capsules, *International Journal of Refrigeration* 32, 953–959.
- Calmac. (2010). A Technical Introduction to Cool Storage Commercial Application. accessed on 17 March. <http://www.calmac.com/downloads/calmacte.pdf>.
- Carbonari, A., De Grassi, M., Di Perna, C. and Principi, P. (2006). Numerical and experimental analyses of PCM containing sandwich panels for prefabricated walls, *Energy and Buildings* 38, 472–483.
- Çarpınlioğlu, M.Ö. and Özahi, E. (2008). A simplified correlation for fixed bed pressure drop, *Powder Technology* 187, 94–101.
- Castellón1, C., Günther, E., Mehling, H., Hiebler, S. and Cabeza, L.F. (2008). Determination of the enthalpy of PCM as a function of temperature using a heat-flux DSC-A study of different measurement procedures and their accuracy, *International Journal of Energy Research* 32, 1258–1265.
- Cavallaro, F. (2010). Fuzzy TOPSIS approach for assessing thermal-energy storage in concentrated solar power (CSP) systems, *Applied Energy* 87, 496–503.
- Chaiyasat, P., Ogino, Y., Suzuki, T. and Okubo, M. (2008). Influence of water domain formed in hexadecane core inside cross-linked capsule particle on thermal properties for heat storage application, *Colloid and Polymer Science* 286, 753–759.
- Chan, C.W. and Tan, F.L. (2006). Solidification inside a sphere - an experimental study, *International Communications in Heat and Mass Transfer* 33, 335–341.
- Chen, S., Chen, C., Tin, C., Lee, T. and Ke, M. (2000). An experimental investigation of cold storage in an encapsulated thermal storage tank, *Experimental Thermal and Fluid Science* 23, 133–144.
- Chen, H., Wang, D.W.P. and Chen, S. (2005a). Optimization of an ice-storage air conditioning system using dynamic programming method, *Applied Thermal Engineering* 25, 461–472.
- Chen, W., Li, H., Gao, M., Liu, Z. and Sun, F. (2005b). The pressure melting of ice around a horizontal elliptical cylinder, *Heat Mass Transfer* 42, 138–143.
- Chen, B., Wang, X., Zeng, R. *et al.* (2008). An experimental study of convective heat transfer with microencapsulated phase change material suspension: Laminar flow in a circular tube under constant heat flux, *Experimental Thermal and Fluid Science* 32, 1638–1646.
- Chen, W., Zhao, Y., Sun, F., Chen, Z. and Gong, M. (2008). Analysis of  $\Delta T$  driven contact melting of phase change material around a horizontal cylinder, *Energy Conversion and Management* 49, 1002–1007.
- Cheralathan, M., Velraj, R. and Renganarayanan, S. (2007a). Effect of porosity and the inlet heat transfer fluid temperature variation on the performance of cool thermal energy storage system, *Heat Mass Transfer* 43, 833–842.
- Cheralathan, M., Velraj, R. and Renganarayanan, S. (2007b). Performance analysis on industrial refrigeration system integrated with encapsulated PCM-based cool thermal energy storage system, *International Journal of Energy Research* 31, 1398–1413.
- Chibana, K., Kang, C., Okada, M., Matsumoto, K. and Kawagoe, T. (2002). Continuous formation of slurry ice by cooling water–oil emulsion in a tube, *International Journal of Refrigeration* 25, 259–266.
- Chieh, J., Lin, S. and Chen, S. (2004). Thermal performance of cold storage in thermal battery for air conditioning, *International Journal of Refrigeration* 27, 120–128.
- Chung, J.D., Cho, S.H., Tae, C.S. and Yoo, H. (2008). The effect of diffuser configuration on thermal stratification in a rectangular storage tank, *Renewable Energy* 33, 2236–2245.
- Crampes, C. and Moreaux, M. (2010). Pumped storage and cost saving, *Energy Economics* 32, 325–333.
- Cristopia Energy Systems. (2010). Thermal Energy Storage, accessed on 17 March. <http://www.cristopia.com/english/products/-documentation.html>
- Cryogel (2010). System Operation, accessed on 17 March. [http://www.cryogel.com/-thermal\\_storage-\\_operation-.htm](http://www.cryogel.com/-thermal_storage-_operation-.htm)
- Davies, T.W. (2005). Slurry ice as a heat transfer fluid with a large number of application domains, *International Journal of Refrigeration* 28, 108–114.
- Desrués, T., Ruer, J., Marty, P. and Fourmigué, J.F. (2010). A thermal energy storage process for large scale electric applications, *Applied Thermal Engineering* 30, 425–432.
- Diaz, G., Sen, M., Yang, K.T. and McClain, R.L. (2001). Dynamic prediction and control of heat exchangers using artificial neural networks, *International Journal of Heat and Mass Transfer* 44, 1671–1679.
- Dincer, I. (2002). On thermal energy storage systems and applications in buildings, *Energy and Buildings* 34, 377–388.

- Eames, I.W. and Adref, K.T. (2002). Freezing and melting of water in spherical enclosures of the type used in thermal (ice) storage systems, *Applied Thermal Engineering* 22, 733–745.
- Egolf, P.W. and Kauffeld, M. (2005). From physical properties of ice slurries to industrial ice slurry applications, *International Journal of Refrigeration* 28, 4–12.
- Egolf, P.W., Kitanovski, A., Ata-Caesar, D. et al. (2005). Thermodynamics and heat transfer of ice slurries, *International Journal of Refrigeration* 28, 51–59.
- Egolf, P.W., Kitanovski, A., Ata-Caesar, D., Vuarroz D. and Meili, F. (2008). Cold storage with ice slurries, *International Journal of Energy Research* 32, 187–203.
- El Omari, K. and Dumas, J.P. (2004). Crystallization of supercooled spherical nodules in a flow, *International Journal of Thermal Sciences* 43, 1171–1180.
- Elsayed, A.O. (2007). Numerical study of ice melting inside rectangular capsule under cyclic temperature of heat transfer fluid, *Energy Conversion and Management* 48, 124–130.
- El-Sebaei, A.A., Al-Ghamdi, A.A., Al-Hazmi, F.S. and Faidah, A.S. (2009). Thermal performance of a single basin solar still with PCM as a storage medium, *Applied Energy* 86, 1187–1195.
- Environmental Process Systems. (2010). FlatICE™ Phase Change Material Thermal Energy Storage Systems, accessed on 17 March. <http://www.pcmproducts.net/files/flatice.pdf>
- Erek, A. and Dincer, I. (2009). A new approach to energy and exergy analyses of latent heat storage unit. *Heat Transfer Engineering* 30 (6), 505–515.
- Erek, A. and Ezan, M.A. (2007). Experimental and numerical study on charging processes of an ice-on-coil thermal energy storage system, *International Journal of Energy Research* 31, 158–176.
- Erek, A., Ylken, Z. and Acar, M.A. (2005). Experimental and numerical investigation of thermal energy storage with a finned tube, *International Journal of Energy Research* 29, 283–301.
- Ermis, K., Erek, A. and Dincer, I. (2007). Heat transfer analysis of phase change process in a finned-tube thermal energy storage system using artificial neural network, *International Journal of Heat and Mass Transfer* 50, 3163–3175.
- Evans, T.S., Quarini, G.L. and Shire, G.S.F. (2008). Investigation into the transportation and melting of thick ice slurries in pipes, *International Journal of Refrigeration* 31, 145–151.
- Fang, G., Li, H., Liu, X. and Wu, S. (2010). Experimental investigation of performances of microcapsule phase change material for thermal energy storage, *Chemical Engineering & Technology* 33, 227–230.
- Fang, G., Li, H., Yang, F., Liu, X. and Wu, S. (2009). Preparation and characterization of nano-encapsulated n-tetradecane as phase change material for thermal energy storage, *Chemical Engineering Journal* 153, 217–221.
- Fausett, L. (1994). *Fundamentals of Neural Networks: Architecture Algorithms and Applications*, Prentice Hall, Englewood Cliffs, NJ.
- Fomin, S.A. and Wilchinsky, A.V. (2002). Shape-factor effect on melting in an elliptic capsule, *International Journal of Heat and Mass Transfer* 45, 3045–3054.
- Frei, B. and Huber, H. (2005). Characteristics of different pump types operating with ice slurry, *International Journal of Refrigeration* 28, 92–97.
- Gil, A., Medrano, M., Martorell, I. et al. (2010). State of the art on high temperature thermal energy storage for power generation. Part 1: concepts, materials and modellization, *Renewable and Sustainable Energy Reviews* 14, 31–55.
- Göppert, S., Lohse, R., Urbaneck, T., Schirmer, U., Platzer, B. and Steinert, P. (2009). New computation method for stratification pipes of solar storage tanks, *Solar Energy* 83, 1578–1587.
- Götz, J., Zick, K., Heinen, C. and König, T. (2002). Visualisation of flow processes in packed beds with NMR imaging: determination of the local porosity, velocity vector and local dispersion coefficients, *Chemical Engineering and Processing* 41, 611–629.
- Gschwander, S., Schossig, P. and Henning, P. (2005). Micro-encapsulated paraffin in phase-change slurries, *Solar Energy Materials and Solar Cells* 89, 307–315.
- Günther, E., Mehling, H. and Hiebler, S. (2007). Modeling of subcooling and solidification of phase change materials, *Modelling and Simulation in Materials Science and Engineering* 15, 879–892.
- Guilpart, J., Stamatou, E., Delahaye, A. and Fournaison, L. (2006). Comparison of the performance of different ice slurry types depending on the application temperature, *International Journal of Refrigeration* 29, 781–788.
- Guilpart, J., Stamatou, E. and Fournaison, L. (2005). The control of ice slurry systems: an overview, *International Journal of Refrigeration* 28, 98–107.

- Gumus, M. (2009). Reducing cold-start emission from internal combustion engines by means of thermal energy storage system, *Applied Thermal Engineering* 29, 652–660.
- Guzman, J.J.M. and Braga, S.L. (2005). Supercooling water in cylindrical capsules, *International Journal of Thermophysics* 26, 1781–1802.
- Halasz, B., Grozdek, M. and Soldo, V. (2009). Development of computer program for simulation of an ice bank system operation, Part I: mathematical modelling, *International Journal of Refrigeration* 32, 1323–1335.
- Halawa, E., Bruno, F. and Saman, W. (2005). Numerical analysis of a PCM thermal storage system with varying wall temperature, *Energy Conversion and Management* 46, 2592–2604.
- Haller, M.Y., Cruickshank, C.A., Streicher, W., Harrison, S.J., Andersen, E. and Furbo, S. (2009). Methods to determine stratification efficiency of thermal energy storage processes—Review and theoretical comparison, *Solar Energy* 83, 1847–1860.
- Haykin, S. (1999). *Neural Networks: A Comprehensive Foundation*, Prentice Hall, New Jersey.
- He, B. and Setterwall, F. (2002). Technical grade paraffin waxes as phase change materials for cool thermal storage and cool storage systems capital cost estimation, *Energy Conversion and Management* 43, 1709–1723.
- Hed, G. and Bellander, R. (2006). Mathematical modelling of PCM air heat exchanger, *Energy and Buildings* 38, 82–89.
- Heim, D. (2010). Isothermal storage of solar energy in building construction, *Renewable Energy* 35, 788–796.
- Henze, G.P., Krarti, M. and Brandemuehl, M.J. (2003). Guidelines for improved performance of ice storage systems, *Energy and Buildings* 35, 111–127.
- Hirata, T., Ishikawa, M. and Yamada, K. (2002). Crystal ice formation of solution and its removal phenomena on inclined cooled plate, *International Journal of Refrigeration* 25, 190–198.
- Hirata, T., Matsuzaki, Y. and Ishikawa, M. (2004). Ice formation of aqueous solution and its removal phenomena on vertical cooled plate, *International Journal of Refrigeration* 27, 511–519.
- Hirata, T., Nishi, T. and Ishikawa, M. (2003). Ice formation of aqueous solution and its removal phenomena around vertical cooled cylinder, *International Journal of Refrigeration* 26, 189–196.
- Hong, H., Peck, J.H. and Kang, C. (2004). Ice adhesion of an aqueous solution including a surfactant with stirring on cooling wall: ethylene glycol – a silane coupling agent aqueous solution, *International Journal of Refrigeration* 27, 985–992.
- Hsiao, M., Cheng, C., Huang, M. and Chen, S. (2009). Performance enhancement of a subcooled cold storage air conditioning system, *Energy Conversion and Management* 50, 2992–2998.
- Huang, M.C., Chen, B.R., Hsiao, M.J. and Chen, S.L. (2007). Application of thermal battery in the ice storage air conditioning system as a subcooler, *International Journal of Refrigeration* 30, 245–253.
- Huang, L., Petermann, M. and Doetsch, C. (2009). Evaluation of paraffin/water emulsion as a phase change slurry for cooling applications, *Energy* 34, 1145–1155.
- Ihm, P., Krarti, M. and Henze, G.P. (2004). Development of a thermal energy storage model for EnergyPlus, *Energy and Buildings* 36, 807–814.
- Inaba, H., Inada, T., Horibe, A., Suzuki, H. and Usui, H. (2005). Preventing agglomeration and growth of ice particles in water with suitable additives, *International Journal of Refrigeration* 28, 20–26.
- Ionescu, C., Haberschill, P., Kiss, I. and Lallemand, A. (2007). Local and global heat transfer coefficients of a stabilised ice slurry in laminar and transitional flows, *International Journal of Refrigeration* 30, 970–977.
- Ismail, K.A.R. and Henríquez, J.R. (2002). Numerical and experimental study of spherical capsules packed bed latent heat storage system, *Applied Thermal Engineering* 22, 1705–1716.
- Ismail, K.A.R., Henríquez, J.R. and da Silva, T.M. (2003). A parametric study on ice formation inside a spherical capsule, *International Journal of Thermal Sciences*, 42, 881–887.
- Ismail, K.A.R. and Radwan, M.M. (2003). Modeling of ice crystal growth in laminar falling films for the production of pumpable ice slurries, *Energy Conversion and Management* 44, 65–84.
- Jack, M.W. and Wrobel, J. (2009). Thermodynamic optimization of a stratified thermal storage device, *Applied Thermal Engineering* 29, 2344–2349.
- Jain, D. (2007). Modeling the performance of the reversed absorber with packed bed thermal storage natural convection solar crop dryer, *Journal of Food Engineering* 78, 637–647.
- Jaluria, Y. (2008). *Design and Optimization of the Thermal Systems*, CRC Press.
- Kandasamy, R., Wang, X. and Mujumdar, A.S. (2008). Transient cooling of electronics using phase change material (PCM)-based heat sinks, *Applied Thermal Engineering* 28, 1047–1057.



- Kauranen, P., Elonen, T., Wikström, L., Heikkinen, J. and Laurikko, J. (2010). Temperature optimisation of a diesel engine using exhaust gas heat recovery and thermal energy storage (diesel engine with thermal energy storage), *Applied Thermal Engineering* 30, 631–638.
- Kayansayan, N. and Acar, M.A. (2006). Ice formation around a finned-tube heat exchanger for cold thermal energy storage, *International Journal of Thermal Sciences* 45, 405–418.
- Kazmierczak, M.J. and Nirmalanandhan, V. (2006). Heat transfer augmentation for external ice-on-tube TES systems using porous copper mesh to increase volumetric ice production, *International Journal of Refrigeration* 29, 1020–1033.
- Kenisarin, M.M. (2010). High-temperature phase change materials for thermal energy storage, *Renewable and Sustainable Energy Reviews* 14, 955–970.
- Kiatsiriroat, T., Vithayasai, S., Vorayos, N., Nuntaphan, A. and Vorayos, N. (2003). Heat transfer prediction for a direct contact ice thermal energy storage, *Energy Conversion and Management* 44, 497–508.
- Kitanovski, A., Vuarnoz, D., Ata-Caesar, D., Egolf, P.W., Hansen, T.M. and Doetsch, C. (2005). The fluid dynamics of ice slurry, *International Journal of Refrigeration* 28, 37–50.
- Koizumi, H. (2004). Time and spatial heat transfer performance around an isothermally heated sphere placed in a uniform, downwardly directed flow (in relation to the enhancement of latent heat storage rate in a spherical capsule), *Applied Thermal Engineering* 24, 2583–2600.
- Kousksou, T., Bédécarrats, J.P., Dumas, J.P. and Mimet, A. (2005). Dynamic modelling of the storage of an encapsulated ice tank, *Applied Thermal Engineering* 25, 1534–1548.
- Kousksou, T., Bédécarrats, J.P., Strub, F. and Castaing-Lasvignottes, J. (2008). Numerical simulation of fluid flow and heat transfer in a phase change thermal energy storage, *International Journal of Energy Technology and Policy* 6, 143–158.
- Kousksou, T., Jamil, A., Zeraouli, Y. and Dumas, J.P. (2006). DSC study and computer modelling of the melting process in ice slurry, *Thermochimica Acta* 448, 123–129.
- Lai, S.M. and Hui, C.W. (2009). Feasibility and flexibility for a trigeneration system, *Energy* 34, 1693–1704.
- Lai, S.M. and Hui, C.W. (2010). Integration of trigeneration system and thermal storage under demand uncertainties, *Applied Energy* 87, 2868–2880.
- Laing, D., Steinmann, W., Tamme, R. and Richter, C. (2006). Solid media thermal storage for parabolic trough power plants, *Solar Energy* 80, 1283–1289.
- Lamberg, P. (2004). Approximate analytical model for two-phase solidification problem in a finned phase-change material storage, *Applied Energy* 77, 131–152.
- Lamberg, P. and Sirén, K. (2003a). Analytical model for melting in a semi-infinite PCM storage with an internal fin, *Heat and Mass Transfer* 39, 167–176.
- Lamberg, P. and Sirén, K. (2003b). Approximate analytical model for solidification in a finite PCM storage with internal fins, *Applied Mathematical Modelling* 27, 491–513.
- LeBreux, M., Lacroix, M. and Lachiver, G. (2009). Control of a hybrid solar/electric thermal energy storage system, *International Journal of Thermal Sciences* 48, 645–654.
- Lecoeuche, S., Lalot, T.S. and Desmet, B. (2005). Modelling a non-stationary single tube heat exchanger using multiple coupled local neural networks, *International Communications in Heat and Mass Transfer* 32, 913–922.
- Lee, D.W. and Sharma, A. (2006). Melting of ice slurry in a tube-in-tube heat exchanger, *International Journal of Energy Research* 30, 1013–1021.
- Lee, D.W., Yoon, E.S., Joo, M.C. and Sharma, A. (2006). Heat transfer characteristics of the ice slurry at melting process in a tube flow, *International Journal of Refrigeration* 29, 451–455.
- Lemort, V. (2006). A numerical comparison of control strategies applied to an existing ice storage system, *Energy Conversion and Management* 47, 3619–3631.
- Li, H., Fang, G. and Liu, X. (2010). Synthesis of shape-stabilized paraffin/silicon dioxide composites as phase change material for thermal energy storage, *Journal of Materials Science* 45, 1672–1676.
- Li, J., Xue, P., Ding, W., Han, J. and Sun, G. (2009a). Micro-encapsulated paraffin/high-density polyethylene/wood flour composite as form-stable phase change material for thermal energy storage, *Solar Energy Materials and Solar Cells* 93, 1761–1767.
- Li, J., Xue, P., He, H., Ding, W. and Han, J. (2009b). Preparation and application effects of a novel form-stable phase change material as the thermal storage layer of an electric floor heating system, *Energy and Buildings* 41, 871–880.

- Liu, H. and Awbi, H.B. (2009). Performance of phase change material boards under natural convection, *Building and Environment* 44, 1788–1793.
- MacPhee, D. and Dincer, I. (2009). Thermal modeling of a packed bed thermal energy storage system, *Applied Thermal Engineering* 29, 695–705.
- de Marchi Neto, I., Padilha, A. and Scalon, V.L. (2009). Refrigerator COP with thermal storage, *Applied Thermal Engineering* 29, 2358–2364.
- Marfn, J.M., Zalba, B., Luisa Cabeza, F. and Mehling, H. (2005). Improvement of a thermal energy storage using plates with paraffin–graphite composite, *International Journal of Heat and Mass Transfer* 48, 2561–2570.
- Massie, D.D. (2002). Optimization of a building’s cooling plant for operating cost and energy use, *International Journal of Thermal Sciences* 41, 1121–1129.
- Matsumoto, K., Namiki, Y., Okada, M., Kawagoe, T., Nakagawa, S. and Kang, C. (2004). Continuous ice slurry formation using a functional fluid for ice storage, *International Journal of Refrigeration* 27, 73–81.
- Matsumoto, K., Oikawa, K., Okada, M., Teraoka, Y. and Kawagoe, T. (2006). Study on high performance ice slurry formed by cooling emulsion in ice storage (discussion on adaptability of emulsion to thermal storage material), *International Journal of Refrigeration* 29, 1010–1019.
- Matsumoto, K., Sakae, K., Oikawa, K., Okada, M., Teraoka, Y. and Kawagoe, T. (2007). Study on formation of high performance ice slurry by W/O emulsion in ice storage (discussion on characteristics of propagation of supercooling dissolution), *International Journal of Refrigeration* 30, 1300–1308.
- Matsumoto, K., Sakae, K., Yamauchi, H. and Teraoka, Y. (2008). Formation of high performance ice slurry by W/O emulsion in ice storage (effective method to propagate supercooling dissolution), *International Journal of Refrigeration* 31, 832–840.
- Matsumoto, K., Shiokawa, Y., Okada, M., Kawagoe, T. and Kang, C. (2002). Ice storage system using water–oil mixture discussion about influence of additive on ice formation process, *International Journal of Refrigeration* 25, 11–18.
- Matsumoto, K. and Suzuki, T. (2007). Measurement of thermal conductivity of ice slurry made from solution by transient line heat-source technique (analytical discussion on influence of latent heat of fusion), *International Journal of Refrigeration* 30, 187–194.
- Matsumoto, K., Suzuki, Y., Okada, M., Teraoka, Y. and Kawagoe, T. (2006). *International Journal of Refrigeration* 29, 1208–1217.
- Mawire, A. and McPherson, M. (2009). Experimental and simulated temperature distribution of an oil-pebble bed thermal energy storage system with a variable heat source, *Applied Thermal Engineering* 29, 1086–1095.
- Mawire, A., McPherson, M., van den Heetkamp, R.R.J. and Mlatho, S.J.P. (2009). Simulated performance of storage materials for pebble bed thermal energy storage (TES) systems, *Applied Energy* 86, 1246–1252.
- Mawire, A., McPherson, M., van den Heetkamp, R.R.J. and Taole, S.H. (2010). Experimental volumetric heat transfer characteristics between oil and glass pebbles in a small glass tube storage, *Energy* 35, 1256–1263.
- Mazman, M., Cabeza, L.F., Mehling, H., Paksoy, H.Ö. and Evliya, H. (2008). Heat transfer enhancement of fatty acids when used as PCMs in thermal energy storage, *International Journal of Energy Research* 32, 135–143.
- Medina, M.A., King, J.B. and Zhang, M. (2008). On the heat transfer rate reduction of structural insulated panels (SIPs) outfitted with phase change materials (PCMs), *Energy* 33, 667–678.
- Medrano, M., Gil, A., Martorell, I., Potau, X. and Cabeza, L. F. (2010). State of the art on high-temperature thermal energy storage for power generation. Part 2: case studies, *Renewable and Sustainable Energy Reviews* 14, 56–72.
- Medved, S. and Arkar, C. (2008). Correlation between the local climate and the free-cooling potential of latent heat storage, *Energy and Buildings* 40, 429–437.
- Mehling, H., Cabeza, L.F. and Yamaha, M. (2007) Application of PCM for heating and cooling in buildings, in *Thermal Energy Storage for Sustainable Energy Consumption* (Ed. H. O. Paksoy), Springer, pp. 323–348.
- Mesalhy, O., Lafdi, K., Elgafy, A. and Bowman, K. (2005). Numerical study for enhancing the thermal conductivity of phase change material (PCM) storage using high thermal conductivity porous matrix, *Energy Conversion and Management* 46, 847–867.
- Murugavel, K.K., Sivakumar, S., Ahamed, J.R., Chockalingam, K.K.S.K. and Srithar, K. (2010). Single basin double slope solar still with minimum basin depth and energy storing materials, *Applied Energy* 87, 514–523.
- Muthusivagami, R.M., Velraj, R. and Sethumadhavan, R. (2010). Solar cookers with and without thermal storage-A review, *Renewable and Sustainable Energy Reviews* 14, 691–701.



- Nagano, K., Mochida, T., Takeda, S., Domański, R. and Rebow, M. (2003). Thermal characteristics of manganese (II) nitrate hexahydrate as a phase change material for cooling systems, *Applied Thermal Engineering* 23, 229–241.
- Nallusamy, N., Sampath, S. and Velraj, R. (2006). Study on performance of a packed bed latent heat thermal energy storage unit integrated with solar water heating system, *Journal of Zhejiang University – Science A*, 7, 1422–1430.
- Nasr, G.E., Badr, E.A. and Joun, C. (2003). Backpropagation neural networks for modeling gasoline consumption, *Energy Conversion and Management*, 44, 893–905.
- Nieżgoda-Żelasko, B. (2006). Heat transfer of ice slurry flows in tubes, *International Journal of Refrigeration* 29, 437–450.
- Nieżgoda-Żelasko, B. and Zalewski, W. (2006a). Momentum transfer of ice slurry flows in tubes, modeling, *International Journal of Refrigeration* 29, 429–436.
- Nieżgoda-Żelasko, B. and Zalewski, W. (2006b). Momentum transfer of ice slurry flows in tubes, experimental investigations, *International Journal of Refrigeration*, 29, 418–428.
- Nieżgoda-Żelasko, B. and Żelasko, J. (2007). Generalized non-Newtonian flow of ice-slurry, *Chemical Engineering and Processing* 46, 895–904.
- Nieżgoda-Żelasko, B. and Żelasko, J. (2008). Melting of ice slurry under forced convection conditions in tubes, *Experimental Thermal and Fluid Science* 32, 1597–1608.
- Nørsgaard, E., Sørensen, T.A., Hansen, T.M. and Kauffeld, M. (2005). Performance of components of ice slurry systems: pumps, plate heat exchangers, and fittings, *International Journal of Refrigeration* 28, 83–91.
- Novo, A.V., Bayon, J.R., Castro-Fresno, D. and Rodriguez-Hernandez, J. (2010). Review of seasonal heat storage in large basins: water tanks and gravel-water pits, *Applied Energy* 87, 390–397.
- Oda, Y., Okada, M., Nakagawa, S., Matsumoto, K. and Kawagoe, T. (2004). Continuous ice formation in a tube by using water-oil emulsion for dynamic-type ice-making cold thermal energy storage, *International Journal of Refrigeration* 27, 353–359.
- Özönur, Y., Mazman, M., Paksoy, H.Ö. and Evliya, H. (2006). Microencapsulation of coco fatty acid mixture for thermal energy storage with phase change material, *International Journal of Energy Research* 30, 741–749.
- Pacheco-Vega, A., Sen, M., Yang, K.T. and McClain, R.L. (2001). Neural network analysis of fin-tube refrigerating heat exchanger with limited experimental data, *International Journal of Heat and Mass Transfer* 44, 763–770.
- Panthalookaran, V., Heidemann, W. and Müller-Steinhagen, H. (2007). A new method of characterization for stratified thermal energy stores, *Solar Energy* 81, 1043–1054.
- Panthalookaran, V., Heidemann, W. and Müller-Steinhagen H. (2008). The effects of momentum diffusers and flow guides on the efficiency of stratified hot water seasonal heat stores, *International Journal of Energy Research* 32, 911–925.
- Pronk, P., Hansen, T.M., Infante Ferreira, C.A. and Witkamp, G.J. (2005a). Time-dependent behavior of different ice slurries during storage, *International Journal of Refrigeration* 28, 27–36.
- Pronk, P., Infante Ferreira, C.A. and Witkamp, G.J. (2005b). A dynamic model of Ostwald ripening in ice suspensions, *Journal of Crystal Growth* 275, 1355–1361.
- Pronk, P., Infante Ferreira, C.A. and Witkamp, G.J. (2008). Superheating of ice slurry in melting heat exchangers, *International Journal of Refrigeration* 31, 911–920.
- Quanying, Y., Chen, L. and Lin, Z. (2008). Experimental study on the thermal storage performance and preparation of paraffin mixtures used in the phase change wall, *Solar Energy Materials and Solar Cells* 92, 1526–1532.
- Rached, W., Sicard, F., Lafargue, A. and Thorel, D. (2007). Ice slurry: pressure drop and deposition velocity, *International Journal of Refrigeration* 30, 1393–1400.
- Rady, M. (2009a). Granular phase change materials for thermal energy storage: experiments and numerical simulations, *Applied Thermal Engineering* 29, 3149–3159.
- Rady, M. (2009b). Thermal performance of packed bed thermal energy storage units using multiple granular phase change composites, *Applied Energy* 86, 2704–2720.
- Rady, M.A., Arquis, E. and Le Bot, C. (2010). Characterization of granular phase changing composites for thermal energy storage using the T-history method, *International Journal of Energy Research* 34, 333–344.
- Reed, R.D. and Marks, R.J. (1999). *Neural Smithing: Supervised Learning in Feedforward Artificial Neural Networks*, MIT Press, London.

- Regin, A.F., Solanki, S.C. and Saini, J.S. (2008). Heat transfer characteristics of thermal energy storage system using PCM capsules: a review, *Renewable and Sustainable Energy Reviews* 12, 2438–2458.
- Revankar, S.T. and Croy, T. (2007). Visualization study of the shrinkage void distribution in thermal energy storage capsules of different geometry, *Experimental Thermal and Fluid Science* 31, 181–189.
- Rojas, R. (1996). *Neural Networks*, Springer-Verlag, Berlin.
- Rosen, M.A. and Dincer, I. (2003). Exergy methods for assessing and comparing thermal storage systems, *International Journal of Energy Research* 27, 415–430.
- Rosen, M.A., Tang, R. and Dincer, I. (2004). Effect of stratification on energy and exergy capacities in thermal storage systems, *International Journal of Energy Research* 28, 177–193.
- Roxas-Dimaano, M.N. and Watanabe, T. (2002a). The capric and lauric acid mixture with chemical additives as latent heat storage materials for cooling application, *Energy* 27, 869–888.
- Roxas-Dimaano, M.N. and Watanabe, T. (2002b). Performance investigation of the capric and lauric acid mixture as latent heat energy storage for a cooling system, *Solar Energy* 72, 205–215.
- Sablani, S.S., Kacimov, A., Perret, J., Mujumdar, A.S. and Campo, A. (2005). Non-iterative estimation of heat transfer coefficients using artificial neural network models, *International Journal of Heat and Mass Transfer* 48, 665–679.
- Saito, A. (2002). Recent advances in research on cold thermal energy storage, *International Journal of Refrigeration* 25, 177–189.
- Salaün, F., Devaux, E., Bourbigot, S. and Rumeau, P. (2010). Influence of the solvent on the microencapsulation of an hydrated salt, *Carbohydrate Polymers* 79, 964–974.
- Salomoni, V.A., Majorana, C.E., Giannuzzi, G.M. and Miliozzi, A. (2008). Thermal-fluid flow within innovative heat storage concrete systems for solar power plants, *International Journal of Numerical Methods for Heat and Fluid Flow* 18, 969–999.
- Sari, A. and Karaipekli, A. (2007). Thermal conductivity and latent heat thermal energy storage characteristics of paraffin/expanded graphite composite as phase change material, *Applied Thermal Engineering* 27, 1271–1277.
- Sari, A. and Karaipekli, A. (2009). Preparation, thermal properties and thermal reliability of palmitic acid/expanded graphite composite as form-stable PCM for thermal energy storage, *Solar Energy Materials and Solar Cells* 93, 571–576.
- Sari, A., Alkan, C. and Karaipekli, A. (2010). Preparation, characterization and thermal properties of PMMA/n-heptadecane microcapsules as novel solid-liquid microPCM for thermal energy storage, *Applied Energy* 87, 1529–1534.
- Sari, A., Alkan, C., Karaipekli, A. and Uzun, O. (2009). Microencapsulated n-octacosane as phase change material for thermal energy storage, *Solar Energy* 83, 1757–1763.
- Sarier, N. and Onder, E. (2007). The manufacture of microencapsulated phase change materials suitable for the design of thermally enhanced fabrics, *Thermochimica Acta* 452, 149–160.
- Sebzali, M.J. and Rubini, P.A. (2006). Analysis of ice cool thermal storage for a clinic building in Kuwait, *Energy Conversion and Management* 47, 3417–3434.
- Sharma, A., Chen, C.R., Murty, V.V.S. and Shukla, A. (2009). Solar cooker with latent heat storage systems: a review, *Renewable and Sustainable Energy Reviews* 13, 1599–1605.
- Sharma, S.D. and Sagara, K. (2005). Latent heat storage materials and systems: a review, *International Journal of Green Energy* 2, 1–56.
- Shi, W., Wang, B. and Li, X. (2005). A measurement method of ice layer thickness based on resistance-capacitance circuit for closed loop external melt ice storage tank, *Applied Thermal Engineering* 25, 1697–1707.
- Shiina, Y. and Inagaki, T. (2005). Study on the efficiency of effective thermal conductivities on melting characteristics of latent heat storage capsules, *International Journal of Heat and Mass Transfer* 48, 373–383.
- Shukla, A., Buddhi, D. and Sawhney, R.L. (2009). Solar water heaters with phase change material thermal energy storage medium: a review, *Renewable and Sustainable Energy Reviews* 13, 2119–2125.
- Simard, A.P. and Lacroix, M. (2003). Study of the thermal behavior of a latent heat cold storage unit operating under frosting conditions, *Energy Conversion and Management* 44, 1605–1624.
- Singh, H., Saini, R.P. and Saini, J.S. (2010). A review on packed bed solar energy storage systems, *Renewable and Sustainable Energy Reviews* 14, 1059–1069.

- Soltan, B.K. and Ardehali, M.M. (2003). Numerical simulation of water solidification phenomenon for ice-on-coil thermal energy storage application, *Energy Conversion and Management* 44, 85–92.
- Stamatiou, E., Meewisse, J.W. and Kawaji, M. (2005). Ice slurry generation involving moving parts, *International Journal of Refrigeration* 28, 60–72.
- Steinmann, W. and Eck, M. (2006). Buffer storage for direct steam generation, *Solar Energy* 80, 1277–1282.
- Stritih, U. and Butala, V. (2007). Energy saving in building with PCM cold storage, *International Journal of Energy Research* 31, 1532–1544.
- Su, J., Ren, L. and Wang, L. (2005). Preparation and mechanical properties of thermal energy storage micro-capsules, *Colloid and Polymer Science* 284, 224–228.
- TA Instrumentation. (2010). Accessed on 17 March. <http://www.tainstruments.com>
- Tamme, R., Bauer, T., Buschle, J., Laing, D., Müller–Steinhagen, H. and Steinmann, W. (2008). Latent heat storage above 120°C for applications in the industrial process heat sector and solar power generation, *International Journal of Energy Research* 32, 264–271.
- Tardy, F. and Sami, S.M. (2009). Thermal analysis of heat pipes during thermal storage, *Applied Thermal Engineering* 29, 329–333.
- Teke, I. and Ulusarslan, D. (2007). Mathematical expression of pressure gradient in the flow of spherical capsules less dense than water, *International Journal of Multiphase Flow* 33, 658–674.
- Teraoka, Y., Saito, A. and Okawa, S. (2002). Ice crystal growth in supercooled solution, *International Journal of Refrigeration* 25, 218–225.
- Thongwik, S., Vorayos, N., Kiatsiriroat, T. and Nuntaphan, A. (2008). Thermal analysis of slurry ice production system using direct contact heat transfer of carbon dioxide and water mixture, *International Communications in Heat and Mass Transfer* 35, 756–761.
- du Toit, C.G. (2008). Radial variation in porosity in annular packed beds, *Nuclear Engineering and Design* 238, 3073–3079.
- Trp, A. (2005). An experimental and numerical investigation of heat transfer during technical grade paraffin melting and solidification in a shell-and-tube latent thermal energy storage unit, *Solar Energy* 79, 648–660.
- Trp, A., Lenic, K. and Frankovic, B. (2006). Analysis of the influence of operating conditions and geometric parameters on heat transfer in water-paraffin shell-and-tube latent thermal energy storage unit, *Applied Thermal Engineering* 26, 1830–1839.
- Tveit, T., Savola, T., Gebremedhin, A. and Fogelholm, C. (2009). Multi-period MINLP model for optimising operation and structural changes to CHP plants in district heating networks with long-term thermal storage, *Energy Conversion and Management* 50, 639–647.
- Tyagi, V.V. and Buddhi, D. (2008). Thermal cycle testing of calcium chloride hexahydrate as a possible PCM for latent heat storage, *Solar Energy Materials and Solar Cells* 92, 891–899.
- Ulusarslan, D. and Teke, I. (2006). An experimental determination of pressure drops in the flow of low density spherical capsule train inside horizontal pipes, *Experimental Thermal and Fluid Science* 30, 233–241.
- Varol, Y., Koca, A., Oztop, H.F. and Avci, E. (2010). Forecasting of thermal energy storage performance of phase change material in a solar collector using soft computing techniques, *Expert Systems with Applications* 37, 2724–2732.
- Verma, P., Varun and Singal, S.K. (2008). Review of mathematical modeling on latent heat thermal energy storage systems using phase-change material, *Renewable and Sustainable Energy Reviews* 12, 999–1031.
- Vyshak, N.R. and Jilani, G. (2007). Numerical analysis of latent heat thermal energy storage system, *Energy Conversion and Management* 48, 2161–2168.
- Wang, F., Maidment, G., Missenden, J. and Tozer, R. (2007a). The novel use of phase change materials in refrigeration plant. Part 1: experimental investigation, *Applied Thermal Engineering* 27, 2893–2901.
- Wang, F., Maidment, G., Missenden, J. and Tozer, R. (2007b). The novel use of phase change materials in refrigeration plant. Part 2: dynamic simulation model for the combined system, *Applied Thermal Engineering* 27, 2902–2910.
- Wang, F., Maidment, G., Missenden, J. and Tozer, R. (2007c). The novel use of phase change materials in refrigeration plant. Part 3: PCM for control and energy savings, *Applied Thermal Engineering* 27, 2911–2918.
- Wang, X., Niu, J. and van Paassen, A.H.C. (2008a). Raising evaporative cooling potentials using combined cooled ceiling and MPCM slurry storage, *Energy and Buildings* 40, 1691–1698.

- Wang, X., Yap, C. and Mujumdar, A.S. (2008b). A parametric study of phase change material (PCM)-based heat sinks, *International Journal of Thermal Sciences* 47, 1055–1068.
- Wang, W., Yang, X., Fang, Y., Ding, J. and Yan, J. (2009). Enhanced thermal conductivity and thermal performance of form-stable composite phase change materials by using b-Aluminum nitride, *Applied Energy* 86, 1196–1200.
- Wijesundera, N.E., Hawlader, M.N.A., Andy, C.W.B. and Kamal Hossain, M. (2004). Ice-slurry production using direct contact heat transfer, *International Journal of Refrigeration* 27, 511–519.
- Wilchinsky, A.V., Fomin, S.A. and Hashida, T. (2002). Contact melting inside an elastic capsule, *International Journal of Heat and Mass Transfer* 45, 4097–4106.
- Xin, W., YinPing, Z., Wei, X., RuoLang, Z., QunLi, Z. and HongFa, D. (2009). Review on thermal performance of phase change energy storage building envelope, *Chinese Science Bulletin* 54, 920–928.
- Yamada, M., Fukusako, S. and Kawabe, H. (2002). A quantitative evaluation of the production performance of ice slurry by the oscillatory moving cooled wall method, *International Journal of Refrigeration* 25, 199–207.
- Yamaha, M., Nakahara, N. and Chiba, R. (2008). Studies on thermal characteristics of ice thermal storage tank and a methodology for estimation of tank efficiency, *International Journal of Energy Research* 32, 226–241.
- Yanbing, K., Yi, J. and Yinping, Z. (2003). Modeling and experimental study on an innovative passive cooling system-NVP system, *Energy and Buildings* 35, 417–425.
- Yang, J., Rivard, H. and Zmeureanu, R. (2005). On-line building energy prediction using adaptive artificial neural networks, *Energy and Buildings* 37, 1250–1259.
- Yang, R., Zhang, Y., Wang, X., Zhang, Y. and Zhang, Q. (2009). Preparation of n-tetradecane-containing microcapsules with different shell materials by phase separation method, *Solar Energy Materials and Solar Cells* 93, 1817–1822.
- Yin, H., Gao, X., Ding, J. and Zhang, Z. (2008). Experimental research on heat transfer mechanism of heat sink with composite phase change materials, *Energy Conversion and Management* 49, 1740–1746.
- Zalba, B., Marín, J.M., Cabeza, L.F. and Mehling, H. (2003). Review on thermal energy storage with phase change: materials, heat transfer analysis and applications, *Applied Thermal Engineering* 23, 251–283.
- Zamfirescu, C. and Bejan, A. (2005). Tree-shaped structures for cold storage, *International Journal of Refrigeration* 28, 231–241.
- Zeng, R., Wang, X., Xiao, W., Zhang, Y., Zhang, Q. and Di, H. (2010). Thermal performance of phase change material energy storage floor for active solar water-heating system, *Frontiers of Energy and Power Engineering in China*, 4(2), 185–191.
- Zhang, P., Hu, Y., Song, L., Ni, J., Xing, W. and Wang, J. (2010). Effect of expanded graphite on properties of high-density polyethylene/ paraffin composite with intumescent flame retardant as a shape-stabilized phase change material, *Solar Energy Materials and Solar Cells* 94, 360–365.
- Zhang, X.J., Qiu, L.M., Zhang, P., Liu, L. and Gan, Z.H. (2008). Performance improvement of vertical ice slurry generator by using bubbling device, *Energy Conversion and Management* 49, 83–88.
- Zhang, H. and Wang, X. (2009). Synthesis and properties of microencapsulated n-octadecane with polyurea shells containing different soft segments for heat energy storage and thermal regulation, *Solar Energy Materials and Solar Cells* 93, 1366–1376.
- Zhang, Y., Zhou, G., Lin, K., Zhang, Q. and Di, D. (2007). Application of latent heat thermal energy storage in buildings: state-of-the-art and outlook, *Building and Environment* 42, 2197–2209.
- Zhao, J., Chen, Y. and Li, X. (2008). Optimization for operating modes based on simulation of seasonal underground thermal energy storage, *Frontiers of Energy and Power Engineering in China* 2, 298–301.
- Zhen-guo, L., Su-yun, Z., Xiang-zhao, F. and Yong, W. (2006). Investigation of floor heating with thermal storage, *Journal of Central South University of Technology* 13, 399–403.
- Zhong, Y., Guo, Q., Li, S., Shi, J. and Liu, L. (2010a). Thermal and mechanical properties of graphite foam/Wood's alloy composite for thermal energy storage, *Carbon* 48, 1689–1692.
- Zhong, Y., Li, S., Wei, X. *et al.* (2010b). Heat transfer enhancement of paraffin wax using compressed expanded natural graphite for thermal energy storage, *Carbon* 48, 300–304.
- Zhu, N., Ma, Z. and Wang, S. (2009). Dynamic characteristics and energy performance of buildings using phase change materials: a review, *Energy Conversion and Management* 50, 3169–3181.
- Zhu, Y. and Zhang, Y. (2000). Dynamic modeling of encapsulated ice tank for HVAC system simulation, *HVAC R&D Research* 6 (3).
- Zurigat, Y.H., Dawoud, B. and Bortmany, J. (2006). On the technical feasibility of gas turbine inlet air utilizing thermal energy storage, *International Journal of Energy Research* 30, 291–305.

## Study Questions/Problems

- 9.1 Review the new developments and advances in this chapter relating to TES *methods*, including such activities as modeling, analysis, optimization, and design, and list in rank order the three that you feel are the most important or significant. Explain and justify your selection, with quantitative as well as qualitative arguments.
- 9.2 Review the new developments and advances in this chapter relating to TES *technology and systems*, including new devices and system integrations, and list in rank order the three that you feel are the most important or significant. Explain and justify your selection, with quantitative as well as qualitative arguments.
- 9.3 Review the new developments and advances in this chapter relating to TES *applications*, including utilization of TES in building systems, industry, and power generation, and list in rank order the three that you feel are the most important or significant. Explain and justify your selection, with quantitative as well as qualitative arguments.
- 9.4 Investigate new developments and advances in TES *methods* that are not included in this chapter, and list three that you feel are important or significant. Use sources such as journals, conference proceedings, web sources, and industry communications. Explain and justify your selection, with quantitative as well as qualitative arguments.
- 9.5 Investigate new developments and advances in TES *technology and systems* that are not included in this chapter, and list three that you feel are important or significant. Use sources such as journals, conference proceedings, web sources, and industry communications. Explain and justify your selection, with quantitative as well as qualitative arguments.
- 9.6 Investigate new developments and advances in TES *applications* that are not included in this chapter, and list three that you feel are important or significant. Use sources such as journals, conference proceedings, web sources, and industry communications. Explain and justify your selection, with quantitative as well as qualitative arguments.
- 9.7 Locate a TES facility in the area where you live, and carry out an analysis to determine the advantages and benefits of implementing one of the advances in TES described in this chapter. Consider advantages and benefits such as increased efficiency, enhanced economics, and reduced environmental impact.



# Appendix A

## Conversion Factors

**Table A.1** Conversion factors for commonly used quantities

Quantity	SI to English	English to SI
Area	$1 \text{ m}^2 = 10.764 \text{ ft}^2$ $= 1550.0 \text{ in}^2$	$1 \text{ ft}^2 = 0.00929 \text{ m}^2$ $1 \text{ in}^2 = 6.452 \times 10^{-4} \text{ m}^2$
Density	$1 \text{ kg/m}^3 = 0.06243 \text{ lb}_m/\text{ft}^3$	$1 \text{ lb}_m/\text{ft}^3 = 16.018 \text{ kg/m}^3$ $1 \text{ slug/ft}^3 = 515.379 \text{ kg/m}^3$
Energy	$1 \text{ J} = 9.4787 \times 10^{-4} \text{ Btu}$	$1 \text{ Btu} = 1055.056 \text{ J}$ $1 \text{ cal} = 4.1868 \text{ J}$ $1 \text{ lb}_f \cdot \text{ft} = 1.3558 \text{ J}$ $1 \text{ hp} \cdot \text{h} = 2.685 \times 10^6 \text{ J}$
Energy per unit mass	$1 \text{ J/kg} = 4.2995 \times 10^{-4} \text{ Btu/lb}_m$	$1 \text{ Btu/lb}_m = 2326 \text{ J/kg}$
Force	$1 \text{ N} = 0.22481 \text{ lb}_f$	$1 \text{ lb}_f = 4.448 \text{ N}$ $1 \text{ pdl} = 0.1382 \text{ N}$
Gravitation	$g = 9.80665 \text{ m/s}^2$	$g = 32.17405 \text{ ft/s}^2$
Heat flux	$1 \text{ W/m}^2 = 0.3171 \text{ Btu/h} \cdot \text{ft}^2$	$1 \text{ Btu/h} \cdot \text{ft}^2 = 3.1525 \text{ W/m}^2$ $1 \text{ kcal/h} \cdot \text{m}^2 = 1.163 \text{ W/m}^2$ $1 \text{ cal/s} \cdot \text{cm}^2 = 41870.0 \text{ W/m}^2$
Heat generation (volum.)	$1 \text{ W/m}^3 = 0.09665 \text{ Btu/h} \cdot \text{ft}^3$	$1 \text{ Btu/h} \cdot \text{ft}^3 = 10.343 \text{ W/m}^3$
Heat transfer coefficient	$1 \text{ W/m}^2 \cdot \text{K} = 0.1761 \text{ Btu/ft}^2 \cdot ^\circ\text{F}$	$1 \text{ Btu/h} \cdot \text{ft}^2 \cdot ^\circ\text{F} = 5.678 \text{ W/m}^2 \cdot \text{K}$ $1 \text{ kcal/h} \cdot \text{m}^2 \cdot ^\circ\text{C} = 1.163 \text{ W/m}^2 \cdot \text{K}$ $1 \text{ cal/s} \cdot \text{m}^2 \cdot ^\circ\text{C} = 41870.0 \text{ W/m}^2 \cdot \text{K}$
Heat transfer rate	$1 \text{ W} = 3.4123 \text{ Btu/h}$	$1 \text{ Btu/h} = 0.2931 \text{ W}$
Length	$1 \text{ m} = 3.2808 \text{ ft}$ $= 39.370 \text{ in}$ $1 \text{ km} = 0.621371 \text{ mi}$	$1 \text{ ft} = 0.3048 \text{ m}$ $1 \text{ in} = 2.54 \text{ cm} = 0.0254 \text{ m}$ $1 \text{ mi} = 1.609344 \text{ km}$ $1 \text{ yd} = 0.9144 \text{ m}$
Mass	$1 \text{ kg} = 2.2046 \text{ lb}_m$ $1 \text{ ton (metric)} = 1000 \text{ kg}$ $1 \text{ grain} = 6.47989 \times 10^{-5} \text{ kg}$	$1 \text{ lb}_m = 0.4536 \text{ kg}$ $1 \text{ slug} = 14.594 \text{ kg}$

(continued overleaf)

Table A.1 (continued)

Quantity	SI to English	English to SI
Mass flow rate	1 kg/s = 7936.6 lb <sub>m</sub> /h = 2.2046 lb <sub>m</sub> /s	1 lb <sub>m</sub> /h = 0.000126 kg/s 1 lb <sub>m</sub> /s = 0.4536 kg/s
Power	1 W = 1 J/s = 3.4123 Btu/h = 0.737562 lb <sub>f</sub> ·ft/s 1 hp (metric) = 0.735499 kW 1 ton of refrig. = 3.51685 kW	1 Btu/h = 0.2931 W 1 Btu/s = 1055.1 W 1 lb <sub>f</sub> ·ft/s = 1.3558 W 1 hp <sup>UK</sup> = 745.7 W
Pressure and stress (Pa = N/m <sup>2</sup> )	1 Pa = 0.020886 lb <sub>f</sub> /ft <sup>2</sup> = 1.4504 × 10 <sup>-4</sup> lb <sub>f</sub> /in <sup>2</sup> = 4.015 × 10 <sup>-3</sup> in water = 2.953 × 10 <sup>-4</sup> in Hg	1 lb <sub>f</sub> /ft <sup>2</sup> = 47.88 Pa 1 lb <sub>f</sub> /in <sup>2</sup> = 1 psi = 6894.8 Pa 1 stand. atm. = 1.0133 × 10 <sup>5</sup> Pa 1 bar = 1 × 10 <sup>5</sup> Pa
Specific heat	1 J/kg·K = 2.3886 × 10 <sup>-4</sup> Btu/lb <sub>m</sub> ·°F	1 Btu/lb <sub>m</sub> ·°F = 4187 J/kg·K 1 lb <sub>f</sub> /ft = 14.594 N/m
Surface tension	1 N/m = 0.06852 lb <sub>f</sub> /ft	1 dyn/cm = 1 × 10 <sup>-3</sup> N/m T(°R) = 1.8 T(K)
Temperature	T(K) = T(°C) + 273.15 = T(°R)/1.8 = [T(°F) + 459.67]/1.8 T(°C) = [T(°F) - 32]/1.8	= T(°F) + 459.67 = 1.8 T(°C) + 32 = 1.8[T(K) - 273.15] + 32 1 °R = 1 °F = 1 K/1.8 = 1 °C/1.8
Temperature difference	1 K = 1 °C = 1.8 °R = 1.8 °F	1 Btu/h·ft·°F = 1.731 W/m·K
Thermal conductivity	1 W/m·K = 0.57782 Btu/h·ft·°F	1 kcal/h·m·°C = 1.163 W/m·K 1 cal/s·cm·°C = 418.7 W/m·K
Thermal diffusivity	1 m <sup>2</sup> /s = 10.7639 ft <sup>2</sup> /s	1 ft <sup>2</sup> /s = 0.0929 m <sup>2</sup> /s 1 ft <sup>2</sup> /h = 2.581 × 10 <sup>-5</sup> m <sup>2</sup> /s
Thermal resistance	1 K/W = 0.52750 °F·h/Btu	1 °F·h/Btu = 1.8958 K/W
Velocity	1 m/s = 3.2808 ft/s 1 km/s = 0.62137 mi/h	1 ft/s = 0.3048 m/s 1 ft/min = 5.08 × 10 <sup>-3</sup> m/s
Viscosity (dynamic) (kg/m·s = N·s/m <sup>2</sup> )	1 kg/m·s = 0.672 lb <sub>m</sub> /ft·s = 2419.1 lb <sub>m</sub> /fh·h	1 lb <sub>m</sub> /ft·s = 1.4881 kg/m·s 1 lb <sub>m</sub> /ft·h = 4.133 × 10 <sup>-4</sup> kg/m·s 1 centipoise(cP) = 10 <sup>-2</sup> poise = 1 × 10 <sup>-3</sup> kg/m·s
Viscosity (kinematic)	1 m <sup>2</sup> /s = 10.7639 ft <sup>2</sup> /s = 1 × 10 <sup>4</sup> stokes	1 ft <sup>2</sup> /s = 0.0929 m <sup>2</sup> /s 1 ft <sup>2</sup> /h = 2.581 × 10 <sup>-5</sup> m <sup>2</sup> /s 1 stoke = 1 cm <sup>2</sup> /s
Volume	1 m <sup>3</sup> = 35.3134 ft <sup>3</sup> 1 L = 1 dm <sup>3</sup> = 0.001 m <sup>3</sup>	1 ft <sup>3</sup> = 0.02832 m <sup>3</sup> 1 in <sup>3</sup> = 1.6387 × 10 <sup>-5</sup> m <sup>3</sup> 1 gal <sup>US</sup> = 0.003785 m <sup>3</sup> 1 gal <sup>UK</sup> = 0.004546 m <sup>3</sup>
Volumetric flow rate	1 m <sup>3</sup> /s = 35.3134 ft <sup>3</sup> /s = 1.2713 × 10 <sup>3</sup> ft <sup>3</sup> /h	1 ft <sup>3</sup> /s = 2.8317 × 10 <sup>-2</sup> m <sup>3</sup> /s 1 ft <sup>3</sup> /min = 4.72 × 10 <sup>-4</sup> m <sup>3</sup> /s 1 ft <sup>3</sup> /h = 7.8658 × 10 <sup>-6</sup> m <sup>3</sup> /s 1 gal <sup>US</sup> /min = 6.309 × 10 <sup>-5</sup> m <sup>3</sup> /s



# Appendix B

## Thermophysical Properties

**Table B.1** Thermophysical properties of pure water at atmospheric pressure

T(°C)	$\rho(\text{kg/m}^3)$	$\mu \times 10^3(\text{kg/m}\cdot\text{s})$	$\nu \times 10^6(\text{m}^2/\text{s})$	k(W/m·K)	$\beta \times 10^5(1/\text{K})$	$c_p(\text{J/kg}\cdot\text{K})$	Pr
0	999.84	1.7531	1.7533	0.5687	-6.8140	4209.3	12.976
5	999.96	1.5012	1.5013	0.5780	1.5980	4201.0	10.911
10	999.70	1.2995	1.2999	0.5869	8.7900	4194.1	9.2860
15	999.10	1.1360	1.1370	0.5953	15.073	4188.5	7.9910
20	998.20	1.0017	1.0035	0.6034	20.661	4184.1	6.9460
25	997.07	0.8904	0.8930	0.6110	20.570	4180.9	6.0930
30	995.65	0.7972	0.8007	0.6182	30.314	4178.8	5.3880
35	994.30	0.7185	0.7228	0.6251	34.571	4177.7	4.8020
40	992.21	0.6517	0.6565	0.6351	38.530	4177.6	4.3090
45	990.22	0.5939	0.5997	0.6376	42.260	4178.3	3.8920
50	988.04	0.5442	0.5507	0.6432	45.780	4179.7	3.5350
60	983.19	0.4631	0.4710	0.6535	52.330	4184.8	2.9650
70	977.76	0.4004	0.4095	0.6623	58.400	4192.0	2.5340
80	971.79	0.3509	0.3611	0.6698	64.130	4200.1	2.2010
90	965.31	0.3113	0.3225	0.6759	69.620	4210.7	1.9390
100	958.35	0.2789	0.2911	0.6807	75.000	4221.0	1.7290

Source: D.J. Kukulka, *Thermodynamic and Transport Properties of Pure and Saline Water*, MSc Thesis, State University of New York at Buffalo (1981).

**Table B.2** Thermophysical properties of air at atmospheric pressure

T(K)	$\rho$ (kg/m <sup>3</sup> )	$c_p$ (J/kg·K)	$\mu \times 10^7$ (kg/m·s)	$\nu \times 10^6$ (m <sup>2</sup> /s)	$k \times 10^3$ (W/m·K)	$a \times 10^6$ (m <sup>2</sup> /s)	Pr
200	1.7458	1.007	132.5	7.59	18.10	10.30	0.737
250	1.3947	1.006	159.6	11.44	22.30	15.90	0.720
300	1.1614	1.007	184.6	15.89	26.30	22.50	0.707
350	0.9950	1.009	208.2	20.92	30.00	29.90	0.700
400	0.8711	1.014	230.1	26.41	33.80	38.30	0.690
450	0.7740	1.021	250.7	32.39	37.30	47.20	0.686
500	0.6964	1.030	270.1	38.79	40.70	56.70	0.684
550	0.6329	1.040	288.4	45.57	43.90	66.70	0.683
600	0.5804	1.051	305.8	52.69	46.90	76.90	0.685
650	0.5356	1.063	322.5	60.21	49.70	87.30	0.690
700	0.4975	1.075	338.8	68.10	52.40	98.00	0.695
750	0.4643	1.087	354.6	76.37	54.90	109.00	0.702
800	0.4354	1.099	369.8	84.93	57.30	120.00	0.709
850	0.4097	1.110	384.3	93.80	59.60	131.00	0.716
900	0.3868	1.121	398.1	102.90	62.00	143.00	0.720
950	0.3666	1.131	411.3	112.20	64.30	155.00	0.723

Source: I. Dincer, *Heat Transfer in Food Cooling Applications*, Taylor & Francis, Washington, DC. (1997); and C. Borgnakke and R.E. Sonntag, *Thermodynamic and Transport Properties*, Wiley, New York (1997).

**Table B.3** Thermophysical properties of ammonia (NH<sub>3</sub>) gas at atmospheric pressure

T(K)	$\rho$ (kg/m <sup>3</sup> )	$c_p$ (J/kg·K)	$\mu \times 10^7$ (kg/m·s)	$\nu \times 10^6$ (m <sup>2</sup> /s)	$k \times 10^3$ (W/m·K)	$a \times 10^6$ (m <sup>2</sup> /s)	Pr
300	0.6994	2.158	101.5	14.70	24.70	16.66	0.887
320	0.6468	2.170	109.0	16.90	27.20	19.40	0.870
340	0.6059	2.192	116.5	19.20	29.30	22.10	0.872
360	0.5716	2.221	124.0	21.70	31.60	24.90	0.870
380	0.5410	2.254	131.0	24.20	34.00	27.90	0.869
400	0.5136	2.287	138.0	26.90	37.00	31.50	0.853
420	0.4888	2.322	145.0	29.70	40.40	35.60	0.833
440	0.4664	2.357	152.5	32.70	43.50	39.60	0.826
460	0.4460	2.393	159.0	35.70	46.30	43.40	0.822
480	0.4273	2.430	166.5	39.00	49.20	47.40	0.822
500	0.4101	2.467	173.0	42.20	52.50	51.90	0.813
520	0.3942	2.504	180.0	45.70	54.50	55.20	0.827
540	0.3795	2.540	186.5	49.10	57.50	59.70	0.824
560	0.3708	2.577	193.5	52.00	60.60	63.40	0.827
580	0.3533	2.613	199.5	56.50	63.68	69.10	0.817

Source: I. Dincer, *Heat Transfer in Food Cooling Applications*, Taylor & Francis, Washington, DC. (1997); and C. Borgnakke and R.E. Sonntag, *Thermodynamic and Transport Properties*, Wiley, New York (1997).

**Table B.4** Thermophysical properties of carbon dioxide (CO<sub>2</sub>) gas at atmospheric pressure

T(K)	$\rho$ (kg/m <sup>3</sup> )	$c_p$ (J/kg·K)	$\mu \times 10^7$ (kg/m·s)	$\nu \times 10^6$ (m <sup>2</sup> /s)	$k \times 10^3$ (W/m·K)	$a \times 10^6$ (m <sup>2</sup> /s)	Pr
280	1.9022	0.830	140.0	7.36	15.20	9.63	0.765
300	1.7730	0.851	149.0	8.40	16.55	11.00	0.766
320	1.6609	0.872	156.0	9.39	18.05	12.50	0.754
340	1.5618	0.891	165.0	10.60	19.70	14.20	0.746
360	1.4743	0.908	173.0	11.70	21.20	15.80	0.741
380	1.3961	0.926	181.0	13.00	22.75	17.60	0.737
400	1.3257	0.942	190.0	14.30	24.30	19.50	0.737
450	1.1782	0.981	210.0	17.80	28.20	24.50	0.728
500	1.0594	1.020	231.0	21.80	32.50	30.10	0.725
550	0.9625	1.050	251.0	26.10	36.60	36.20	0.721
600	0.8826	1.080	270.0	30.60	40.70	42.70	0.717
650	0.8143	1.100	288.0	35.40	44.50	49.70	0.712
700	0.7564	1.130	305.0	40.30	48.10	56.30	0.717
750	0.7057	1.150	321.0	45.50	51.70	63.70	0.714
800	0.6614	1.170	337.0	51.00	55.10	71.20	0.716

Source: I. Dincer, *Heat Transfer in Food Cooling Applications*, Taylor & Francis, Washington, DC. (1997); and C. Borgnakke and R.E. Sonntag, *Thermodynamic and Transport Properties*, Wiley, New York (1997).

**Table B.5** Thermophysical properties of hydrogen (H<sub>2</sub>) gas at atmospheric pressure

T(K)	$\rho$ (kg/m <sup>3</sup> )	$c_p$ (J/kg·K)	$\mu \times 10^7$ (kg/m·s)	$\nu \times 10^6$ (m <sup>2</sup> /s)	$k \times 10^3$ (W/m·K)	$a \times 10^6$ (m <sup>2</sup> /s)	Pr
100	0.2425	11.23	42.1	17.40	67.00	24.60	0.707
150	0.1615	12.60	56.0	34.70	101.00	49.60	0.699
200	0.1211	13.54	68.1	56.20	131.00	79.90	0.704
250	0.0969	14.06	78.9	81.40	157.00	115.00	0.707
300	0.0808	14.31	89.6	111.00	183.00	158.00	0.701
350	0.0692	14.43	98.8	143.00	204.00	204.00	0.700
400	0.0606	14.48	108.2	179.00	226.00	258.00	0.695
450	0.0538	14.50	117.2	218.00	247.00	316.00	0.689
500	0.0485	14.52	126.4	261.00	266.00	378.00	0.691
550	0.0440	14.53	134.3	305.00	285.00	445.00	0.685
600	0.0404	14.55	142.4	352.00	305.00	519.00	0.678
700	0.0346	14.61	157.8	456.00	342.00	676.00	0.675
800	0.0303	14.70	172.4	569.00	378.00	849.00	0.670
900	0.0269	14.83	186.5	692.00	412.00	1030.00	0.671

Source: I. Dincer, *Heat Transfer in Food Cooling Applications*, Taylor & Francis, Washington, DC. (1997); and C. Borgnakke and R.E. Sonntag, *Thermodynamic and Transport Properties*, Wiley, New York (1997).

**Table B.6** Thermophysical properties of oxygen (O<sub>2</sub>) gas at atmospheric pressure

T(K)	$\rho$ (kg/m <sup>3</sup> )	$c_p$ (J/kg·K)	$\mu \times 10^7$ (kg/m·s)	$\nu \times 10^6$ (m <sup>2</sup> /s)	$k \times 10^3$ (W/m·K)	$a \times 10^6$ (m <sup>2</sup> /s)	Pr
100	3.9450	0.962	76.4	1.94	9.25	2.44	0.796
150	2.5850	0.921	114.8	4.44	13.80	5.80	0.766
200	1.9300	0.915	147.5	7.64	18.30	10.40	0.737
250	1.5420	0.915	178.6	11.58	22.60	16.00	0.723
300	1.2840	0.920	207.2	16.14	26.80	22.70	0.711
350	1.1000	0.929	233.5	21.23	29.60	29.00	0.733
400	0.9620	0.942	258.2	26.84	33.00	36.40	0.737
450	0.8554	0.956	281.4	32.90	36.30	44.40	0.741
500	0.7698	0.972	303.3	39.40	41.20	55.10	0.716
550	0.6998	0.988	324.0	46.30	44.10	63.80	0.726
600	0.6414	1.003	343.7	53.59	47.30	73.50	0.729
700	0.5498	1.031	380.8	69.26	52.80	93.10	0.744
800	0.4810	1.054	415.2	86.32	58.90	116.00	0.743
900	0.4275	1.074	447.2	104.60	64.90	141.00	0.740

Source: I. Dincer, *Heat Transfer in Food Cooling Applications*, Taylor & Francis, Washington, DC. (1997); and C. Borgnakke and R.E. Sonntag, *Thermodynamic and Transport Properties*, Wiley, New York (1997).

**Table B.7** Thermophysical properties of water vapor (steam) gas at atmospheric pressure

T(K)	$\rho$ (kg/m <sup>3</sup> )	$c_p$ (J/kg·K)	$\mu \times 10^7$ (kg/m·s)	$\nu \times 10^6$ (m <sup>2</sup> /s)	$k \times 10^3$ (W/m·K)	$a \times 10^6$ (m <sup>2</sup> /s)	Pr
380	0.5863	2.060	127.1	21.68	24.60	20.40	1.060
400	0.5542	2.014	134.4	24.25	26.10	23.40	1.040
450	0.4902	1.980	152.5	31.11	29.90	30.80	1.010
500	0.4405	1.985	170.4	38.68	33.90	38.80	0.998
550	0.4005	1.997	188.4	47.04	37.90	47.40	0.993
600	0.3652	2.026	206.7	56.60	42.20	57.00	0.993
650	0.3380	2.056	224.7	66.48	46.40	66.80	0.996
700	0.3140	2.085	242.6	77.26	50.50	77.10	1.000
750	0.2931	2.119	260.4	88.84	54.90	88.40	1.000
800	0.2739	2.152	278.6	101.70	59.20	100.00	1.010
850	0.2579	2.186	296.9	115.10	63.70	113.00	1.020

Source: I. Dincer, *Heat Transfer in Food Cooling Applications*, Taylor & Francis, Washington, DC. (1997); and C. Borgnakke and R.E. Sonntag, *Thermodynamic and Transport Properties*, Wiley, New York (1997).

**Table B.8** Thermophysical properties of some solid materials

Composition	T (K)	$\rho$ (kg/m <sup>3</sup> )	k (W/m·K)	$c_p$ (J/kg·K)
Aluminum	273–673	2720	204–250	895
Asphalt	300	2115	0.0662	920
Bakelite	300	1300	1.4	1465
Brass (70% Cu + 30% Zn)	373–573	8520	104–147	380
Carborundum	872	–	18.5	–
Chrome brick	473	3010	2.3	835
	823	–	2.5	–
Diatomaceous silica, fired	478	–	0.25	–
Fire clay brick	478	2645	1.0	960
	922	–	1.5	–
Bronze (75% Cu + 25% Sn)	273–373	8670	26.0	340
Clay	300	1460	1.3	880
Coal (anthracite)	300	1350	0.26	1260
Concrete (stone mix)	300	2300	1.4	880
Constantan (60% Cu + 40% Ni)	273–373	8920	22–26	420
Copper	273–873	8950	385–350	380
Cotton	300	80	0.06	1300
Glass				
Plate (soda lime)	300	2500	1.4	750
Pyrex	300	2225	1.4	835
Ice	253	–	2.03	1945
	273	920	1.88	2040
Iron (C $\approx$ 4% cast)	273–1273	7260	52–35	420
Iron (C $\approx$ 0.5% wrought)	273–1273	7850	59–35	460
Lead	273–573	–	–	–
Leather (sole)	300	998	0.159	–
Magnesium	273–573	1750	171–157	1010
Mercury	273–573	13400	8–10	125
Molybdenum	273–1273	10220	125–99	251
Nickel	273–673	8900	93–59	450
Paper	300	930	0.18	1340
Paraffin	300	900	0.24	2890
Platinum	273–1273	21400	70–75	240
Rock				
Granite, Barre	300	2630	2.79	775
Limestone, Salem	300	2320	2.15	810
Marble, Halston	300	2680	2.80	830
Rubber, vulcanized				
Soft	300	1100	0.13	2010
Sandstone, Berea	300	2150	2.90	745
Hard	300	1190	0.16	–
Sand	300	1515	0.27	800
Silver	273–673	10520	410–360	230
Soil	300	2050	0.52	1840
Steel (C $\approx$ 1%)	273–1273	7800	43–28	470
Steel (Cr $\approx$ 1%)	273–1273	7860	62–33	460
Steel (18% Cr + 8% Ni)	273–1273	7810	16–26	460

*(continued overleaf)*

Table B.8 (continued)

Composition	T (K)	$\rho$ (kg/m <sup>3</sup> )	k (W/m·K)	$c_p$ (J/kg·K)
Snow	273	110	0.049	–
Teflon	300	2200	0.35	–
Tin	273–473	7300	65–57	230
Tissue, human				
Skin	300	–	0.37	–
Fat layer (adipose)	300	–	0.2	–
Muscle	300	–	0.41	–
Tungsten	273–1273	19350	166–76	130
Wood, cross grain				
Fir	300	415	0.11	2720
Oak	300	545	0.17	2385
Yellow pine	300	640	0.15	2805
White pine	300	435	0.11	–
Wood, radial				
Fir	300	420	0.14	2720
Oak	300	545	0.19	2385
Zinc	273–673	7140	112–93	380

Source: I. Dincer, *Heat Transfer in Food Cooling Applications*, Taylor & Francis, Washington, DC. (1997); and F.P. Incropera and D.P. DeWitt, *Fundamentals of Heat and Mass Transfer*, Wiley, New York (1998).

# Appendix C

## Glossary

All terms in this section follow standard industry definitions that were adapted from ARI Standard 900 (1998). These definitions are of importance in practice and are intended to provide clarity.

**Ambient Air.** The air in the space surrounding a thermal energy storage device, or outside air.

**Ambient Heat Load.** The thermal load (typically expressed in tons (kW)) imposed on a storage device due to heat gain.

**Build Period.** The operating period of a thermal storage generator during which ice is produced.

**Charge Fluid.** The heat transfer fluid used to remove heat from a thermal storage device or generator during the charge or build period, or to add heat to a heat storage.

**Charge Period.** The period of time during which energy (heat) is removed from a cold storage or added to a heat storage.

**Charge Rate.** The rate (typically expressed in tons (kW)) at which energy (heat) is removed from or added to a storage device during the charge period.

**Discharge Fluid.** The heat transfer fluid used to add heat to the thermal storage device.

**Discharge Period/Cycle.** The period of time when energy (heat) is added to the storage device.

**Discharge Rate.** The rate (typically expressed in tons (kW)) at which energy (heat) is added to the storage device during the discharge period.

**Fouling Factor.** A thermal resistance included in heat transfer calculations to account for the fouling expected over time on a heat transfer surface.

**Hermetic (Sealed Unit) Compressor.** A motor-compressor assembly contained within a gas-tight casing through which no shaft extends, which uses the refrigerant as the motor coolant.

**Interval.** A time span, such as the period between individual test readings.

**Latent Heat of Fusion.** The change in energy accompanying the conversion of a unit mass of a solid to a liquid at its melting point, at constant pressure and temperature.

**Load Intensity.** The ratio of the instantaneous load imposed upon the storage device to the net usable storage capacity of the unit, typically expressed in tons/ton-hour (kW/kWh).

**Melt Period.** That period of a test during which the ice produced by a thermal storage generator is melted to determine its quality.

**Net Ice-Making Capacity.** The net ice-producing capability of a thermal storage generator operating in a charge mode, typically expressed in tons (kW).

**Net Usable Storage Capacity.** The actual amount of stored cooling that can be supplied from the storage device at or below the specified cooling supply temperature for a given charge and discharge cycle, typically expressed in ton-hour (kWh).

**Nominal Storage Capacity.** A theoretical capacity of the storage device as defined by the storage device manufacturer (which in many cases is greater than the net usable storage capacity).

**Open-Type Compressor.** A refrigerant compressor with a shaft or other moving part extending through its casing to be driven by an outside source of power, thus requiring a shaft seal or equivalent rubbing contact between fixed and moving parts.

**Period.** A time duration during which a storage process occurs; often a period such as the total duty cycle of a thermal storage system is divided for the purpose of analysis and evaluation into 1-hour time segments.

**Phase Change Material (PCM).** A substance that undergoes changes of state while absorbing or rejecting thermal energy, normally at a constant temperature.

**Published Ratings.** Published ratings for thermal storage equipment are the data and methodologies that are used to develop supplier specified data for a specified duty cycle. They may take the form of tables, graphs, or computer programs, as elected by the manufacturer, and are intended to apply to all units of like nominal size and type (identification) produced by the same manufacturer.

**Standard Rating.** A rating based on tests performed at standard rating conditions.

**Mapped Rating(s).** Mapped ratings are ratings falling within certain specified limits, which are provided for products that do not have a standard rating condition. They are based upon tests performed across a range of operating conditions as defined by the product manufacturer.

**Application Rating.** A rating, based on tests, at application rating conditions (other than standard or mapped rating conditions).

**Saturated Evaporator Temperature.** The dew point temperature of the refrigerant at the pressure at the outlet connection of the evaporator.

**Secondary Coolant.** Any liquid cooled by a refrigerant and used for heat transmission without a change in its state. Sometimes referred to as simply “coolant.”

**Thermal Storage Device.** Equipment which stores cooling capacity using sensible and/or latent heat. May consist solely of a storage means or be packaged with one or more components of a mechanical refrigeration package.

**Thermal Storage Equipment.** Any one of, or a combination of, thermal storage devices and/or generators, that may include various other components of a mechanical refrigeration package.

**Thermal Storage Generator.** An assemblage of components packaged by the manufacturer (but not necessarily shipped as one piece) to provide refrigeration to a thermal storage system that includes an evaporator, and may include compressor(s), controls, heat rejection devices, and so on, whose overall performance as a thermal storage generator is rated by the manufacturer.

**Ton-Hour.** A quantity of thermal energy typically used to describe the capacity of a thermal storage device, in tons, absorbed or rejected in 1 hour (3.517 kW).

Source: ARI Standard 900. *Standard for Thermal Storage Equipment Used for Cooling, Air-Conditioning & Refrigeration Institute*, Arlington, Virginia (1998).



# Index

- absolute pressure, 3
- achieving sustainability, 203
- acid rain, 194
- active cooling, 514
- active heating, 514
- advanced applications, 542
- air quality management, 204
- analysis, 270, 316
- applications, 198
- aquifer, 118
- aquifer storage, 118, 272
- artificial neural network, 560
- ASHRAE standards, 104
- ATES, 272
- atmospheric pressure, 3
- auxiliaries, 529
  
- balance equations, 235
- battery, 63
- benefits, 89, 183
- Bernoulli's equation, 23, 26
- biological storage, 75
- Biot number, 32
- borehole, 466, 471
- borehole thermal energy storage, 466, 471
- boundary layer, 29
- Boussinesq model, 344
- Brundtland Commission, 200
- Brundtland Commission's definition, 200
- building applications, 107
  
- capsule, 136
- case study, 204, 225, 277, 304, 349, 369, 376, 413, 414, 432, 436, 446, 455, 457, 459
- challenges, 105
- change of state, 9
- charging efficiency, 263
- charging period, 263
  
- checklist, 94, 95
- chemical criteria, 132
- chemical energy storage, 62
- chemical heat pump storage, 73
- chilled water, 153, 436
- chilled water storage, 153
- closed system, 7, 249, 260, 309
- cogeneration, 89
- cold air, 180
- cold air distribution, 180
- cold storage, 142,
- complex system, 391, 404
- composite wall, 38
- compressed air storage, 57
- compressible flow, 22
- computational fluid dynamics, 335, 337
- computational time ratio, 340, 351, 357
- conceptual issues, 200
- concrete, 114
- conduction, 33, 40
- conduction heat transfer, 33
- conductivity enhancing techniques, 530
- contact melting, 505
- continuity equation, 23
- convection, 34
- convection heat transfer, 34
- conventional systems, 217
- conversion factors, 585
- control, 524
- cooling, 99
- cooling application, 99
- cooling capacity, 186, 221
- correlations, 338
- criteria, 90
- CTES, 142, 219, 432, 436, 446
- cycle, 7
- cylinder, 38
- cylindrical tube, 366

- data acquisition, 316
- deferral, 215
- demand charge, 214
- density, 6
- design aspects, 178
- design consideration, 108, 144
- developments, 486, 513
- discharge, 310
- discharging efficiency, 264, 311
- discharging period, 264
- discretization, 337, 345
- domain, 335, 337, 344
  
- economic aspects, 221
- economic criteria, 133
- economic sustainability, 201
- Eddy viscosity, 47
- effectiveness, 545
- efficiency, 218, 243, 262, 265, 301
- efficiency definitions, 265
- efficiency limitations, 219
- efficiency measure, 260
- electric utility, 184
- electrochemical battery, 63
- encapsulation, 133, 134
- energy, 15, 192, 202, 215
- energy analysis, 233–236, 245, 246, 298
- energy balance, 235, 236, 261, 269, 299
- energy conservation, 217
- energy demand, 52
- energy efficiency, 218, 243, 262, 271, 301, 545
- energy expression, 282
- energy saving, 211, 212, 215, 219, 221
- energy storage, 51, 53
- energy storage methods, 54
- energy storage systems, 51
- energy storage technologies, 80
- energy transfer, 15
- enthalpy, 7, 10, 244
- entropy, 11
- entropy balance, 235, 269
- environment, 192, 202
- environmental criteria, 90
- environmental impact, 191, 198
- environmental limit, 201
- environmental problem, 193
- environmental sustainability, 201
- equation of flow, 23
- equipment purchase, 215
- essential factors, 203
  
- Euler's equation, 26
- eutectic salt, 100, 102, 127
- evacuated solar collector, 125
- evaluation, 90, 246
- example, 257, 266
- exergy, 18, 219
- exergy analysis, 219, 233, 234, 236, 238, 240, 245, 246, 298
- exergy balance, 236, 238, 240, 261, 269, 301
- exergy consumption, 243
- exergy efficiency, 219, 243, 262, 271, 301, 545
- exergy evaluation, 249
- exergy expression, 282
  
- feasibility criteria, 90
- finite element method, 336
- finite volume method, 336
- first law of thermodynamics, 17
- flow equation, 23
- fluid flow, 20, 343, 366
- fluid flow classification, 20
- flywheel, 59
- force, 2
- forced convection, 43, 345
- Fourier number, 32
- Fourier's law of heat conduction, 33
- full storage, 143
- future outlook, 566
  
- general solutions, 198
- geometry, 512
- global climate change, 195
- global sustainability, 201
- global warming, 195
- glossary, 332, 593
- glycol system, 164
- greenhouse effect, 195
- Graetz number, 32
- Grashof number, 32
- grid, 337, 341
  
- heat, 16
- heat generation, 40
- heat transfer, 32, 343, 366
- heat transfer coefficient, 398
- heat transfer fluid, 398
- heating, 99, 215
- heating application, 99
- heating capacity, 185
- heating equipment, 215
- heat pump, 215

- heat pump equipment, 215
- hydrogen, 77
- hydrogen storage, 77
- hydrostorage, 54
- hysteresis, 509
  
- Ice, 158
- ice forming, 174
- ice harvester, 161
- ice-on-pipe, 159
- ice slurry, 432
- ice storage, 158, 554
- ice thickness, 174
- ice thickness control, 174
- ideal gas, 11
- illustration, 186, 272, 404
- illustrative example, 266, 297, 302, 312, 545
- implementation, 217
- implications, 245
- incompressible flow, 22
- increased efficiency, 218
- innovative applications, 535
- installation configuration, 520
- insulation, 316
- integrated system, 469
- interface, 340, 366, 381
- internal energy, 8, 10, 289, 300
- irreversibility, 18
  
- kinetic criterion, 132
  
- laminar flow, 21
- latent heat, 7, 127
- latent heat of fusion, 8
- latent heat storage, 127, 128, 360, 396
- length, 2
- limitations, 218
- load control, 147
- local sustainability, 201
- losses, 247
  
- macro, 493, 504, 512, 514
- magnetic storage, 75
- market consideration, 96
- mass, 2, 7
- mass balance, 235
- mass flow rate, 6
- material selection, 486
- measurement, 527
- mechanical energy storage, 54
- melting, 369, 376
- methods, 83, 109
  
- micro, 493, 504, 512
- modelling, 366, 392, 504, 524
- models, 289
- momentum equation, 25
- monitoring, 147
- motivation, 235
  
- nano, 493, 504, 512
- natural convection, 42, 349
- Navier–Stokes equation, 27
- Newtonian fluid, 23
- Newton’s law of cooling, 35
- no slip, 344, 356, 377
- non-Newtonian fluid, 23
- non-uniform flow, 21
- nucleation, 133
- numerical method, 335
- numerical modeling, 335, 340, 366, 392
- Nusselt number, 32
  
- operating characteristics, 103
- operating strategy, 520
- operational aspects, 128
- operational loading, 143
- optimal discharge period, 309
- optimization, 217
- optimization methods, 524
- organic molecular storage, 55, 71
- other techniques, 534
- ozone layer, 196
  
- packed bed, 338, 388
- paraffin, 135
- partial storage, 143
- passive cooling, 514
- passive heating, 514
- PCM, 129, 446
- Peclet number, 32
- performance enhancement, 530
- performance evaluation, 269
- performance measure, 269
- performance optimization, 512
- period, 143
- phase change material, 129
- planning, 217
- potential improvement, 316
- potential solution, 198
- practical limitations, 218
- Prandtl number, 32
- pressure, 2
- principles, 86
- process, 7

- programming, 524  
 pump work, 309  
 pumped storage, 54  
 pure substance, 11
- quantity, 2
- Radiation, 36  
 radiation heat transfer, 36  
 rational efficiency, 244  
 reference environment, 241, 249  
 reference environment temperature, 249  
 refrigerating, 215  
 refrigerating equipment, 215  
 relaxation, 346  
 reversibility, 18  
 Rayleigh number, 32  
 Reynolds number, 21, 30  
 regional sustainability, 201  
 rock, 114
- seasonal storage, 185, 186  
 seasonal thermal energy storage, 465, 474  
 second law of thermodynamics, 17  
 secondary coolant, 148  
 selection, 148, 179  
 selection aspects, 179  
 sensible heat, 7, 109  
 sensible heat storage, 109, 269, 457  
 shape, 491  
 simulation, 335, 340, 344, 366, 392  
 sizing strategies, 146  
 slip, 344  
 social sustainability, 201  
 solar applications, 105, 106  
 solar collector, 125  
 solar energy, 104, 107, 108  
 solar energy systems, 105  
 solar pond, 124, 314, 315  
 solidification, 376  
 solutions, 199  
 specific enthalpy, 10  
 specific entropy, 11  
 specific internal energy, 10  
 specific volume, 6  
 sphere, 39  
 spherical shell, 376  
 standards, 104  
 Stanton number, 32  
 state, 9  
 state change, 9  
 steady flow, 21  
 Stefan Boltzmann law, 36  
 STL system, 139  
 storage, 248  
 storage duration, 106, 248  
 storage duration criteria, 248  
 storage media, 148  
 storage model, 253  
 storage size, 216  
 storage size limitations, 216  
 storage tank, 111, 152  
 storing efficiency, 263  
 storing period, 253, 263  
 stratification, 248, 281, 289, 293, 513  
 stratified storage, 281, 290  
 stratospheric ozone depletion, 196  
 subprocess, 253  
 subprocess efficiencies, 253  
 supercooling, 509  
 superheating, 509  
 surplus energy, 213  
 sustainability, 199, 201  
 sustainable development, 199, 202, 203  
 system model, 269  
 system of units, 2  
 systems, 198
- tank, 111  
 tank configuration, 111  
 task efficiency, 244  
 technical aspects, 178  
 technical criteria, 133  
 temperature, 4, 269, 284  
 temperature distribution model, 284  
 terminology, 332  
 theoretical limitations, 218  
 thermal batteries, 530, 554  
 thermal energy, 84  
 thermal energy storage, 76, 83, 85, 191, 211, 212  
 thermal engineering, 1  
 thermal exergy, 235, 239  
 thermal load, 216  
 thermal load profiles, 216  
 thermal resistance, 37  
 thermally stratified tanks, 111  
 thermistor, 6  
 thermocline, 289, 294  
 thermocouple, 4

- thermodynamic analysis, 7, 246, 347
- thermodynamic consideration, 246
- thermodynamic criteria, 132
- thermodynamic loss, 247
- thermodynamic optimization, 283
- thermodynamic property, 7
- thermodynamic system, 7
- thermodynamic table, 8
- thermodynamics, 7
- thermometer, 4
- thermophysical properties, 587
- threshold temperature, 273, 277
- time, 2
- time duration, 248
- time step, 340, 342
- time step independence, 342
- tolerance, 335, 345
- trigeneration, 438
- turbulent flow, 21
- types, 105, 152
- uniform flow, 21
- units, 2
- unsteady flow, 21
- UOIT, 471
- vacuum, 3
- vapor, 8
- viscosity, 22
- viscous dissipation, 339, 383
- visualization methods, 527
- volume of fluid model, 366
- volumetric flow rate, 6
- waste energy, 213
- water/rock, 114
- water storage, 147, 149
- work, 16
- working principle, 142
- zeolite, 130